

PHOTOGRAPH THIS SHEET

DTIC File Copy

LEVEL

INVENTORY

DTIC ACCESSION NUMBER

AD-A213210

R/D 5984-EN-02

DOCUMENT IDENTIFICATION

1988  
DATA 45-87-M-0403

This document has been approved  
for public release and sale; its  
distribution is unlimited.

DISTRIBUTION STATEMENT

ACCESSION FOR

NTIS GRA&I ☒

DTIC TAB ☐

UNANNOUNCED ☐

JUSTIFICATION

per form 50

BY

DISTRIBUTION /

AVAILABILITY CODES

DIST

AVAIL AND/OR SPECIAL

A-1

DISTRIBUTION STAMP

DTIC  
ELECTE  
OCT 06 1989  
S E D  
C

DATE ACCESSIONED

DATE RETURNED

REGISTERED OR CERTIFIED NO.

89 10 6 0 13

DATE RECEIVED IN DTIC

PHOTOGRAPH THIS SHEET AND RETURN TO DTIC-FDAC

AD-A213 210

ON LOAN. Please  
return to

US ARMY RESEARCH, DEVELOPMENT & STANDARDIZATION GROUP (UK)  
Box 63  
Portsmouth, UK



Proceedings  
of  
13. Regional Seminar  
on  
Earthquake Engineering

Turkish National Committee  
For  
Earthquake Engineering  
ISTANBUL 1988

## C O N T E N T S

### TOPIC-1. Seismic Hazard, Risk and Vulnerability

- Paper 1-1. B.GOSCHY, Soil-structure interaction considerations in vulnerability analysis.  
Paper 1-2. V.SCHENK, The state-of-the-art in seismic hazard assessment.  
Paper 1-3. G.GRANDORI, Attenuation of macroseismic intensity with epicentral distance and local hazard evaluation.  
Paper 1-4. J.SOLNES The seismicity and earthquake hazard in Iceland

### TOPIC-2. Microzonation

- Paper 2-1. E.SULSTAROVA, Earthquake protection, seismic regionalization, seismic microzoning, design and technical regulation problems in Albania.  
Paper 2-2. J.STUDER, Influence of geology and local topography on the intensity of shaking.  
Paper 2-3. E.ŞAFAK, Discrete time-domain problems for site amplification.  
Paper 2-4. F.K.CHANG, Site-dependent root-mean-square amplification

### TOPIC-3. Strong Motion and Seismicity

- Paper 3-1. G.GRANDORI, Probabilistic interpretation of short term earthquake precursors.  
Paper 3-2. H.SANDI AN Engineer's approach to the scaling of ground motion intensities  
Paper 3-3. V.SCHENK, Analysis of strong ground motions in amplitude domain-review and applications  
Paper 3-4. B.SKIPP, Geological faults and earthquakes codes  
Paper 3-5. F.CHANG, Earthquake response spectral analysis of Franklin Falls Dam, New Hampshire  
Paper 3-6. I.PASKALEVA, A general procedure for estimating earthquake ground motions parameters

### TOPIC-4. Soil Dynamics and Soil-Structure Interaction

- Paper 4-1. M.HAMADA, The effects of liquefaction on buried structures  
Paper 4-2. K.TALAGANOV, Determination of Liquefaction potential by cyclic strain approach  
Paper 4-3. M.ERDİK, Soil-structure interaction effects on strong ground motion.  
Paper 4-4. T.KOBORI, Verification studies on dynamic soil-structure interaction

### TOPIC-5. Rural Housing and Historical Monuments

- Paper 5-1. E.S.GEORGESCU, Present aspects of the aseismic protection of rural buildings in Romania.  
Paper 5-2. D.ANICIC, Earthquake strengthening of the franciscan monastery in rozat  
Paper 5-3. M.TOMAZEVIC, Cultural monuments and old urban nuclei in seismic areas

#### TOPIC-6. Seismic Behavior of Structures

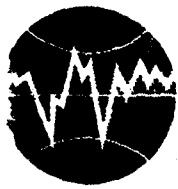
- Paper 6-1. K.KUBO, Incredible seismic damages during past earthquakes.
- Paper 6-2. T.PASKALOV, Simplified method for inelastic deformations in buildings exposed to real seismic effects.
- Paper 6-3. H.SANDI, Framework for a full specification of seismic design conditions.
- Paper 6-4. A.RAVARA, The use of masonry in seismic zones.
- Paper 6-5. C.DYRBYE, Response of Elastic Frames To Seismic Actions
- Paper 6-6. O.FISCHER, Seismic resistance of high and slender structures
- Paper 6-7. A.DUMANOGU, Stochastic analysis of the response of suspension bridges.
- Paper 6-8. E.UZGIDER, M.AYDOGAN, A simple method for the dynamic response of 3-D framed structures subjected to ground motion.
- Paper 6-9. M.IPEK, Approximate considerations of beam stiffnesses in shear walled structures.
- Paper 6-10- C.CONSTANTINESCU, Dynamic tests of large scale models and full scale structures.

#### TIPIC-7. Disaster Prevention

- Paper 7-1. H.SAZANAMI, Regional planning and disaster prevention
- Paper 7-2. Y.OHTA, Dynamic simulation of damages and restoring process of a municipal area in an earthquake: methodology and a proto-type model.
- Paper 7-3. E.GEORGESCU, The experience and existing premises for an efficient response in case of earthquake under conditions of seismic zones in Romania

#### TOPIC-8. CODES

- Paper 8-1. R.G.FLESCH, Principles for the elaboration of national codes-national and international trends.
- Paper 8-2. D.NENOV, Some normative requirements for the design and construction of large-panel buildings in seismic regions.



**TURKISH NATIONAL COMMITTEE FOR  
EARTHQUAKE ENGINEERING**

**THIRTEENTH REGIONAL SEMINAR ON EARTHQUAKE ENGINEERING**

**September 14-24, 1987 - Istanbul - Turkey**

**SOIL-STRUCTURE INTERACTION CONSIDERATIONS  
IN VULNERABILITY ANALYSIS OF STRUCTURES**

**by B. Goschy (Hungary)**

SOIL-STRUCTURE INTERACTION CONSIDERATIONS  
IN VULNERABILITY ANALYSIS OF STRUCTURES

by B. Goschy (Hungary)

Summary

Of primary concern in earthquake-engineering practice is to predict the vulnerability of building structures erected in seismic prone areas. It is intended here, to emphasize the role and importance of actual soil-structure inter-system connectivity in vulnerability analyses, further to harmonize damage evaluation processes with the limit state design philosophy.

The influence of soils of foundation over the seismic response of structural system was found to be considered in earthquake resistant design in two ways as follows:

- by the seismic quality of soils identified as soil profiles and
- by the elastic or plastic support condisitons of a given structure.

The aim of this work is to give quantitative guide-lines to damage probability assessments in correlation with the limit state design strategy.

1. State of the Art.

Design and detailing of basements (foundations) subjected to combined compression and bending is at present based on two assumptions as far as the failure condition is considered.

These are (Figure 1.)

- the failure condition for linear-elastic soils described by

$$\frac{N}{N_u} + \frac{M}{M_u} = 1 \quad (1.1)$$

and

- the failure condition for nonlinear plastic soils described by

$$\frac{4N}{N_u} \left(1 - \frac{N}{N_u}\right) - \frac{M}{M_u} = 0 \quad (1.2)$$

where:

$N_u$  is the ultimate axial force in pure compression,  
and  
 $M_u$  is the ultimate moment in pure bending of the contact area of the basement.

Considering that the elastically or plastically supported structure under earthquake actions suffers displacements of first and second order, structural failure may occur in two different ways:

- material failure in case of stiff structures and/or basements, and
- stability failure in case of slender structures and/or basements. (Figure 1.)

If it is intended to determine the capacity of the basement in terms of seismic coefficients ( $C$ ) or accelerations ( $a = 9,81C \sim 10C$ ) in limit state situations, one starts with the equilibrium condition expressed with the equality

$$M_E = M_B \quad (1.3)$$

where:

- $M_E$  is the external moment at base due to seismic actions,
- $M_B$  is the ultimate moment of the contact area being in combined bending and compression such as derived from Eqs (1.1) and (1.2)

$$M_B = (1 - N/N_u) M_u \quad (1.1/a)$$

in elastic range, and

$$M_B = \frac{4N}{N_u} \left(1 - \frac{N}{N_u}\right) M_u \quad (1.2/b)$$

in plastic range.

The moment at base produced by seismic actions, considering geometric nonlinearity can be written in the form of:

$$M_E = k(T)C \frac{NH}{1 - N/N_c} \quad (1.4)$$

with

- $k(T) = n/T$  is the site dependent dynamic magnification factor,
- $T$  is the natural period of the soil-structure dual system,
- $n$  is the site factor, depending upon the soil profile,
- $N_c$  is the critical (buckling) load of the flexibly supported cantilever structure.

The natural period can be expressed as

$$T = T_s \sqrt{1 + T_F^2 / T_s^2} \quad (1.5)$$

where the period of the elastic structure and of the basement can be obtained from the circular frequencies

$$\omega_s^2 = \frac{30 K_E}{NH^3}; \quad \omega_F^2 = \frac{10 k_f o}{NH^2}$$

On the other hand, the critical load can be deduced from

$$N_c = \frac{N_{cs}}{1 + N_{cs}/N_{cf}} \quad (1.6)$$

with

$$N_{cs} = \frac{2,47 K_E}{H^2} \quad \text{and} \quad N_{cf} = \frac{k_f o}{H}$$

$K_E$  the bending stiffness of the super-structure,  
 $k_f o = C_f I_F = C_f B^3 L / 12$

Physico-mechanical property of the soil under investigation is described by its rotational subgrade, obtained from

$$C_f = 2,2 \frac{E_s}{f \sqrt{A_F}} \quad (\text{kN/m}^3) \quad (1.7)$$

where:

$E_s$  is the modulus of elasticity of the soil,  
 $A_F = BL$  is the contact area,  
 $f$  is the experimental constant ranging between

$$0,30 \leq f \leq 0,45.$$

Introducing these values in Eq (1.3), after some rearrangement the capacity function in terms of seismic coefficient yields [4] :

$$C = \left[ 1 - \left( 1 + \frac{N_u}{N_c} \right) \left( \frac{N}{N_u} \right) + \frac{N_u}{N_c} \left( \frac{N}{N_u} \right)^2 \right] \frac{N_u B}{6 NH} \cdot \frac{1}{k(T)} \quad (1.8)$$

under elastic conditions, and

$$C = \left[ 1 - \left( 1 + \frac{N_u}{N_c} \right) \left( \frac{N}{N_u} \right) + \frac{N_u}{N_c} \left( \frac{N}{N_u} \right)^2 \right] \frac{B}{2H} \cdot \frac{1}{k(T)} \quad (1.9)$$

under plastic conditions.

By representing the graph of functions (1.8) and (1.9), as shown in Figure 3, one can observe the upper bounds of the capacity of the basement, associated with elastic and plastic presumptions over the soil behaviour.

With these premises in mind it is obvious to extend soil-structure interaction analysis over the most appropriate soil model characterized by material nonlinearity.

## 2. Nonlinear soil behaviour

Soils in most of cases have visco-elastic properties simulated in this work by a nonlinear continuous skeleton curve (Figure 4.) following the  $M-\varphi$  interrelationship given as

$$\frac{M}{M_u} = \frac{2\varphi}{\varphi_u} - \left( \frac{\varphi}{\varphi_u} \right)^2 \quad (2.1)$$

where  $\varphi/\varphi_u$  is the rotational ratio of the foundation to the ultimate.

The equilibrium condition (Eq 1.1) than provides the capacity function written as

$$C = \left[ \frac{2\varphi}{\varphi_u} - \left( \frac{\varphi}{\varphi_u} \right)^2 \right] \left( 1 - \frac{N}{N_u} \right) \left[ 1 - \frac{N}{N_u} \left( \frac{N_u}{N_c} \right) \right] \frac{B}{H} \frac{\pi}{n\omega} \quad (2.2)$$

Perturbance sensitivity of the selected model (Figure 2) can be analysed with the help of deterministic or random variables such as:

$$0 \leq \alpha = \varphi/\varphi_u \leq 1,5$$

where  $\alpha > 1$  marks the strength and stiffness degradation process during seismic actions, further

$a = N/N_u$ ;  $b = N_u/N_c \geq 1$  and  $\lambda = H/B \leq 1$  stands for squat (rigid)



whereas  $b = N_u/N_c < 1$  and  $\lambda = H/B > 1$  for slender structural systems.

Perturbance analysis carried out on the one mass model shows that the nonlinear soil behaviour may produce instability situations of the imperfect system prior ultimate capacity is reached (Figure 5), in other words the stability failure anticipates the material failure. In this case the capacity diagram can be broken up into two branches, a stable and an unstable branche. The point of divergency or the peak value of capacity function is obtainable by partial derivations with respect to independent variables.

### 3. Rating of limit states

Present Codes prescribe the limit state strategy by establishing three limit states ( $LS_i$ ;  $i = 1, 2, 3$ ) such as:

- serviceability ( $SLS = LS_{i=1}$ )
- failure (ultimate) ( $FLS = LS_{i=2}$ )
- collapse ( $CLS = LS_{i=3}$ )

limit states.

In possession of capacity diagrams (e.g. Figure 5) one can proceed with partitioning of ordinates  $f/f_u$  into three ranges, limited by values representing limit state situations.

The exploitation tendency of the structure in accordance with defined goals, calles for acceptability criteria quantified as reliability criteria extended over limit situations, - limit states.

Reliability in structural engineering practice is by definition the probability of nonlimit performance, termed as limit states.

The structural reliability referred to a given limit state  $i$  ( $i=1, 2, 3$ ) extended over the full life time  $T_0$  of the structure, is quantified by the reliability (safety) index written as [14]:

$$\beta_i(T_0) = \frac{E(R_i - S_i)}{\sqrt{\text{Var}(R_i + S_i)}} \quad (3.1)$$

where:

$E(R_i - S_i)$  is the difference of mathematical expectations referred to independent random variables in term of capacities ( $R_i$ ) and actions ( $S_i$ ),

$Var(R_i + S_i)$  is the sum of variances of random variables.

The probability that a performance limit state ( $LS_i$ ) is attained during a life span of  $T_0$  can be approximated with the relation [13]:

$$P(LS \leq LS_i; T_0) = 460 \exp[-4,3\beta(T_0)] \quad (3.2)$$

Making use of Eq (3.2) and accepting reliability levels taken from CEB-FIP Recommendations, classification on probability scale can be obtained as shown in Table 1.

Table 1.

$LS_i$	Limit states	Probability	Reliability $\beta_i(T_0=50)$
1	SLS	$\leq 10^{-5}$	$\geq 4,0$
2	FLS	$10^{-4}$	3,5
3	CLS	$10^{-3}$	3,0

Translated into the language of earthquake engineers the reliability index becomes

$$\beta_i(T_0) = \frac{E(a_i - a_{si})}{\sqrt{Var(a_i + a_{si})}} \quad (3.3)$$

with symbols:

$a_i$  is the capacity in term of acceleration taken from partitioned capacity functions,

$a_{si}$  is the site dependent peak acceleration.

Since the calculated capacities are supported by nominal or expected (mean) values, (admitting generally normal distribution low for capacities)  $a_i$  represents a probability level of 50 %.

The "counter" value of the site dependent acceleration  $a_{si}$  aiming to maintain the reliability level adopted for normal statical loadings, has to be derived from

$$a_{si} = a_i - \beta_i(T_0) \sqrt{\text{Var}(a_{si} + a_i)} \quad (3.4)$$

On the other hand the probability of 50 % in occurrence of the site dependent ( $a_{sj}$ ) peak acceleration can be obtained with the help of local Poisson or Gumbel (Type I) probability distribution models.

It is also acceptable to derive the 50 % probability level from the equality

$$P(a \leq a_{sj} ; T_0) = \exp \left( - \frac{T_0}{t_{rj}} \right) = 0,5 \quad (3.5)$$

where:

$t_{rj}$  represents the return period or period of repetition of accelerations at level  $a_{sj}$ .

Finally, the equality

$$a_{si} = a_{sj} \quad (3.6)$$

provides the value of the variance

$$\sqrt{\text{Var}(a_{si} + a_i)}$$

#### 4. Rating of structural damages

Capacity diagrams can also be used to estimate structural damages by scaling  $\alpha = \varphi / \varphi_u$  ordinates into limit state ranges (Figure 6.)

The stable branche of diagrams divided into two parts is suitable to inform about SLS and FLS ranges, whereas the unstable branche indicates the CLS range as listed in Table 2.

Table 2.

Limit states		Specified characteristic values of $\alpha = \varphi / \varphi_u$
1	SLS	$0 < \alpha_s \leq \alpha_F/2$
2	FLS	$\alpha_F/2 < \alpha \leq \alpha_F$
3	CLS	$\alpha > \alpha_F$

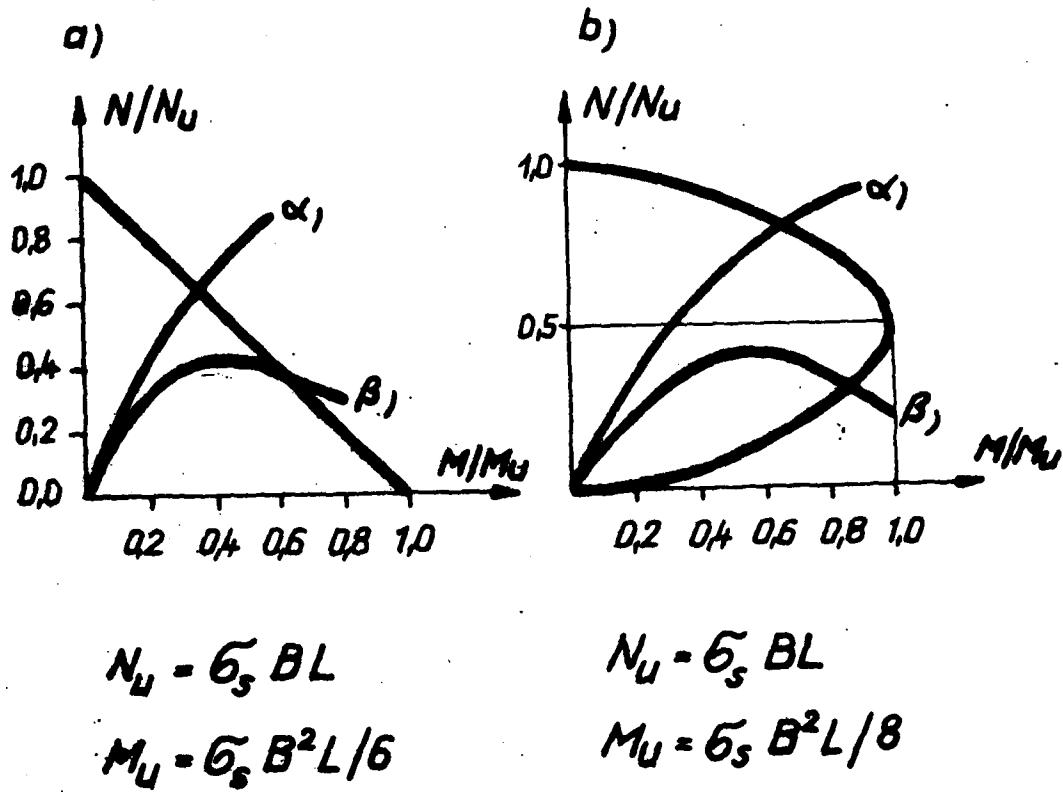
The harmonization of limit state situations with damage rates can be achieved by subdividing limit state ranges into damage degree ( $DD = D_i/D_t$ ) ranges. The suggested damage rating is shown in Table 3.

Table 3.

LS	$\alpha = \varphi / \varphi_u$	$DD = D_i/D_t$ (%)		Description
SLS	$0 < \alpha \leq \alpha_F/4$	I	0 + 2	No damage, minor nonstructural damage
	$\alpha_F/4 < \alpha \leq \alpha_F/2$	II	2 + 10	Minor structural damage
FLS	$\alpha_F/2 < \alpha \leq 3\alpha_F/4$	III	10 + 30	Substantial str. damage
	$3\alpha_F/4 < \alpha \leq \alpha_F$	IV	30 + 50	Major str. damage
CLS	$\alpha > \alpha_F$	V	100	Collapse

5. Conclusions

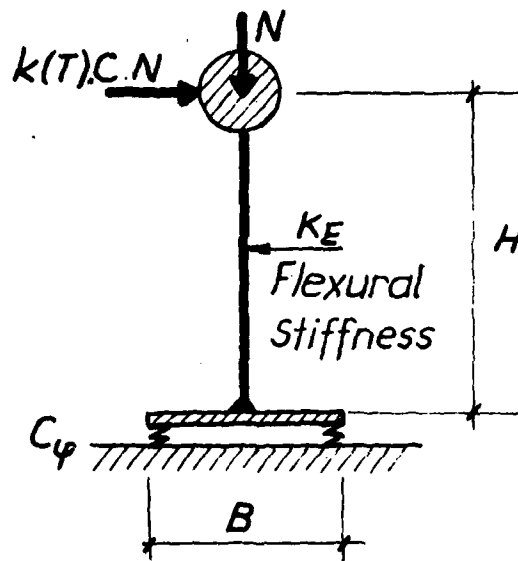
- 5.1 Soft soils require a more detailed analysis of the material nonlinearity of support conditions, whereas slender superstructures involve the account of geometric nonlinearity.  
In both cases the stability failure can occur prior to material failure.
- 5.2 Theories of elasticity and plasticity in soil-structure interaction efficiency are suitable to indicate upper and lower bounds for safe design.
- 5.3 The harmonization of limit design philosophy with damage rate evaluation can be refined on the basis suggested in this work, taking into account scaled limit capacities of structural systems.



**Failure Conditions:**

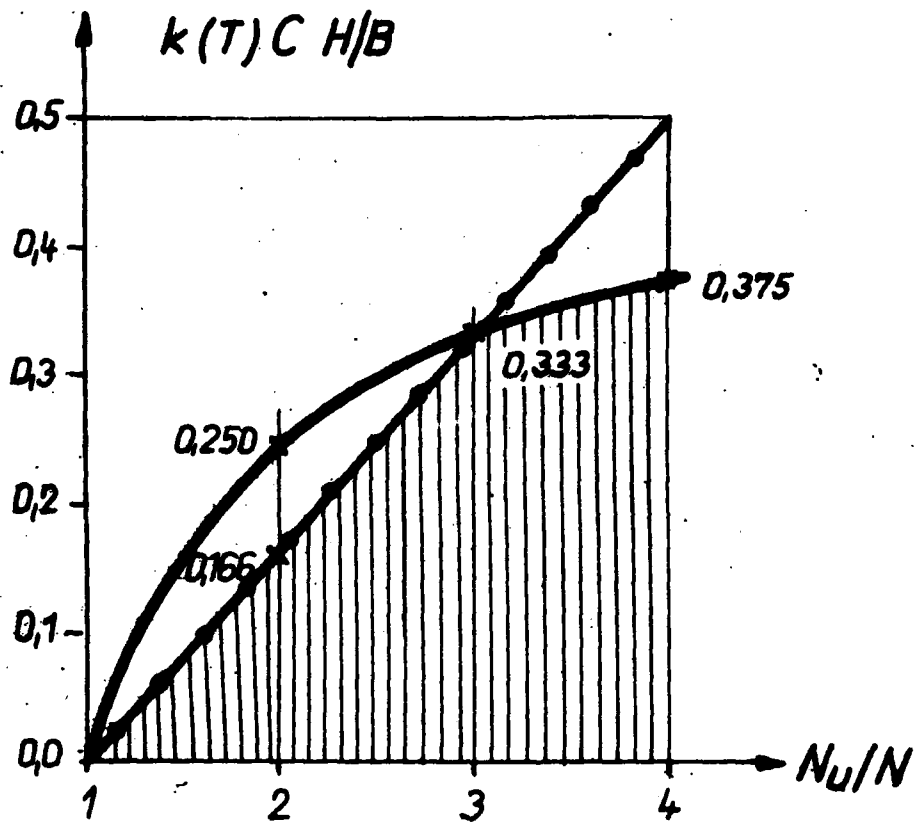
- a) linear elastic soil model
- b) plastic soil model
- $\alpha_1$  material failure
- $\beta_1$  stability failure

Figure: 1



*Model Structure on Flexible  
Support*

*Figure: 2*

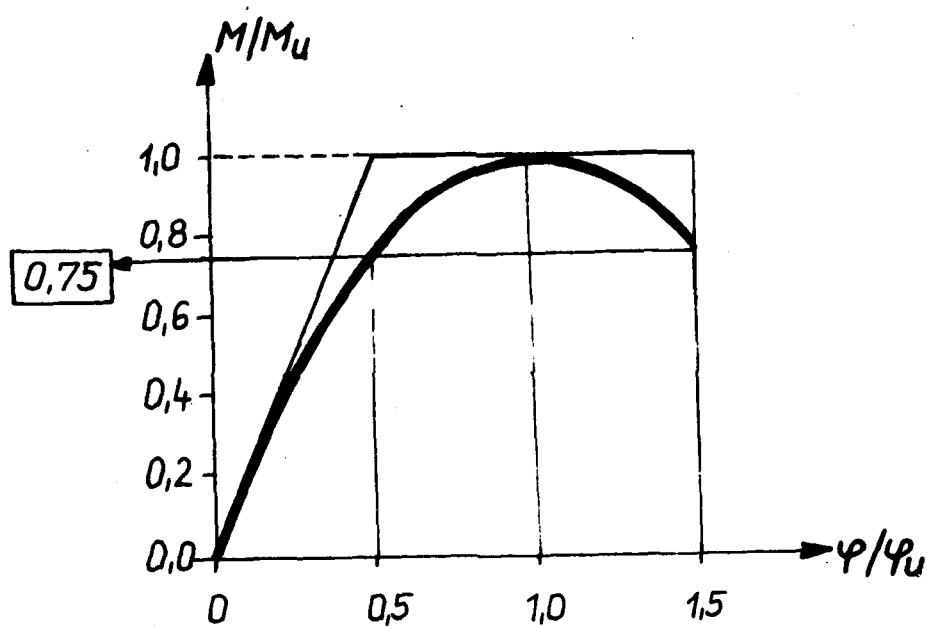


Upper-Bound Diagrams for  
Seismic Zone Factors

- elastic soil behaviour
- plastic soil behaviour

Figure: 3.





*Non-linear Skeleton Curve  
of the Soil*

*Figure: 4 .*

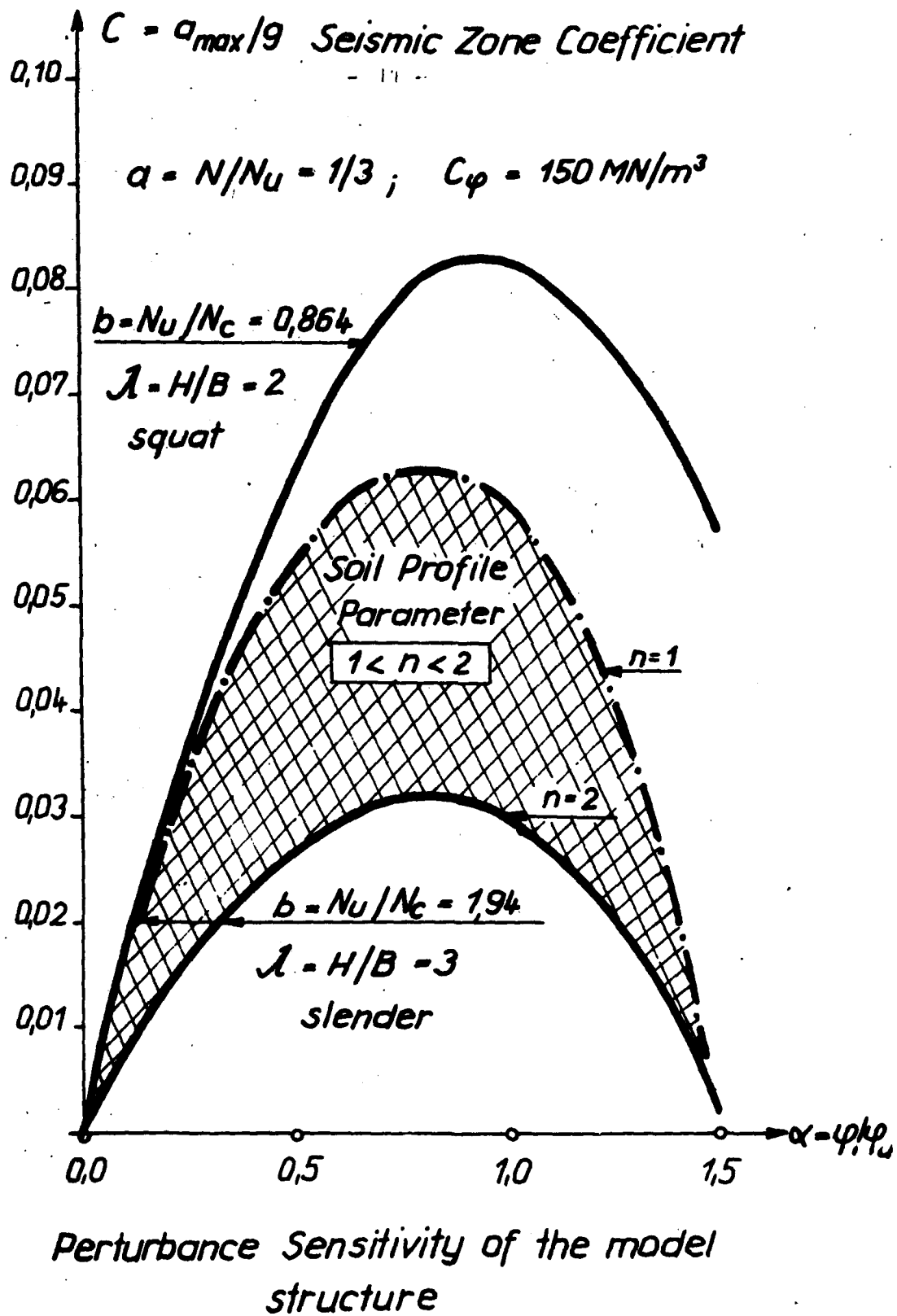
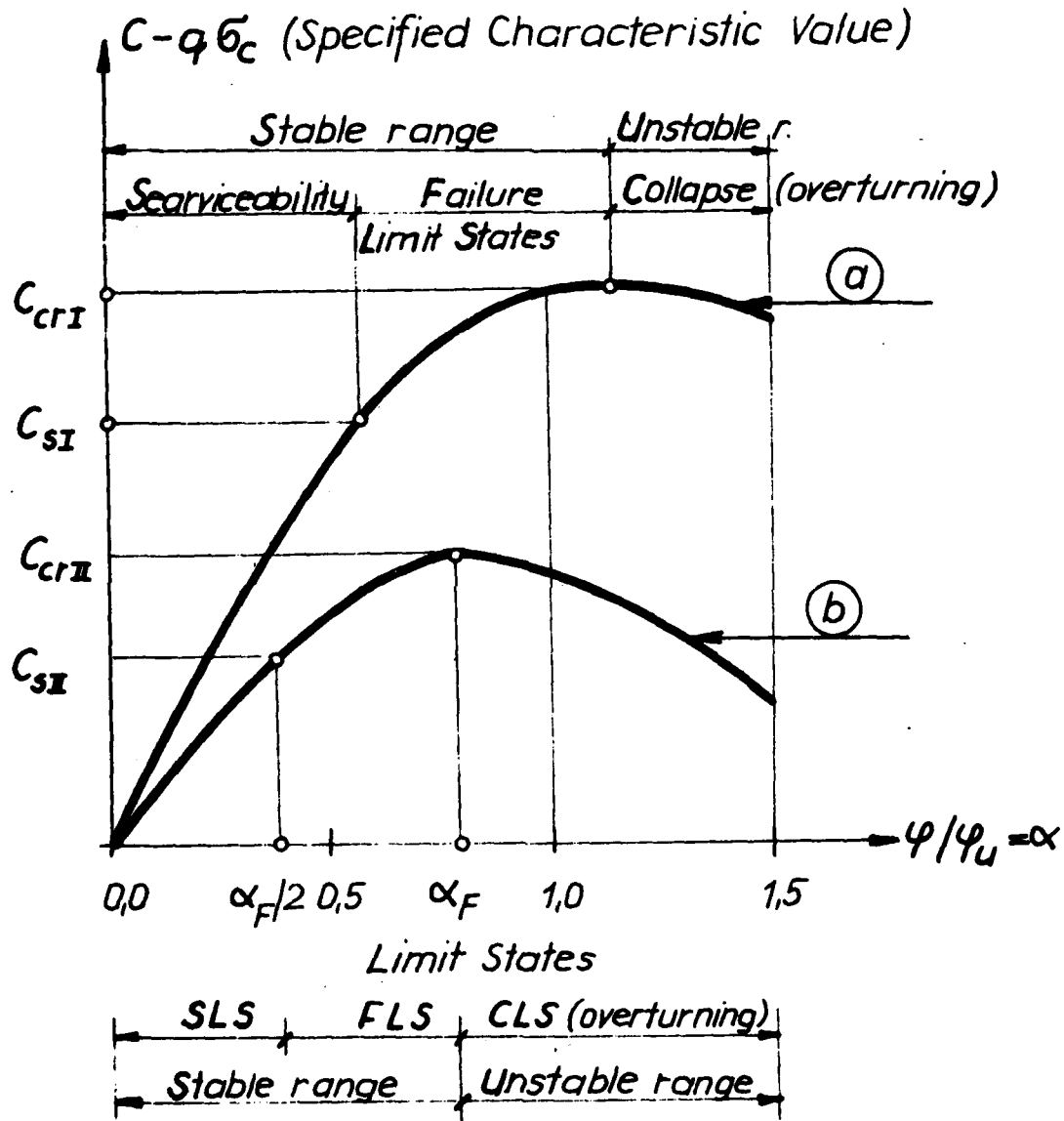


Figure 5

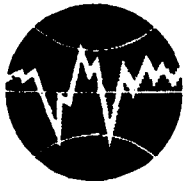


### Limit State Ranges of the Basement

a). rigid soil - structure system

b). flexible (stender) soil-structure system

1. Ambraseys, W.N.; Jackson, I.A.: Earthquake Hazard and Vulnerability in the North-Eastern Mediterranean Desasters Vol. 3. No. 4. 1981.
2. Budiansky, B.: Theory of Buckling and Post-Buckling Behaviour of Elastic Structures. Ad. Appl. Mech 14(1974)
3. Elishakoff, I.: Probabilistic Methods in the Theory of Structures. John Wiley and Sons NY. 1983.
4. Goschy, B.: Vulnerability prediction of Existing Settlements in Seismic Prone Areas. EAEE Paper, Hungarian National Committee 1987.
5. Grandori, G.; Benedetti, D.: On the Choice of Acceptable Seismic Risk. A new approach. Proc. of the 5-th World Conf. on Earthquake Eng., Rome, 1973.
6. Hutchinson, I.W.; Koiter, W.T.; Postbuckling Theory. Appl Mech. Rev. 1970.
7. Koiter, W.T.: On the Stability of elastic equilibrium. AFFDL-TR-70-20, 1970.
8. Lomnitz, C.; Rosenblueth, E.: Seismic Risk and Engineering Decisions. N.Y. Elsevier SP Comp. 1976.
9. Paskaleva, I.: Correlation Between Observed and Predicted Vulnerability. RER Project Bucharest Seminar, 1983.
10. Petrovski, I. et al.: Development of Theoretical Vulnerability and Seismic Risk Models. Proc. of the 8-th Conf. on Earthquake Eng. San Francisco, 1984.
11. Sandi, J.: A Report on Vulnerability Analysis Carried out in the Balkan Region. Proc. of the 8-th Conf. on Earthquake Eng. San Francisco, 1984.
12. Thomson, I.M.T.: Towards a General Statistical Theory of Imperfection-Sensitivity in Elastic Post-Buckling. I.Mech. Phys. Solids 15 (1967)
13. Monograph on Planning and Design of Tall Buildings. Vol CL. ASCE N.Y. 1980.
14. Seismic Design of Concrete Structure. Prepared by CEB. 1987.



**TURKISH NATIONAL COMMITTEE FOR  
EARTHQUAKE ENGINEERING**

**THIRTEENTH REGIONAL SEMINAR ON EARTHQUAKE ENGINEERING**

**September 14-24, 1987 - Istanbul - Turkey**

**THE STATE-OF-THE-ART IN EARTHQUAKE HAZARD ASSESSMENT**

**Vladimír Schenk  
Geop.Inst., Czechosl.Acad.Sci., 14131 Praha**

# THE STATE-OF-THE-ART IN EARTHQUAKE HAZARD ASSESSMENT

Vladimír Schenk  
Geop.Inst., Czechosl.Acad.Sci., 14131 Praha

## ABSTRACT

The earthquake hazard can be expressed in different ways : from simple observed macroseismic fields over the seismostatistical calculations analyzing earthquake occurrences in time and space and assessing their dynamic effects in a certain site or region up to sophisticated seismogeological approaches evaluating the maximum expected earthquake effects on the Earth's surface. Advantages and shortcomings of each method, ways of source regions delineation, testing the quality of input data, their processing to suit the chosen method of hazard assessment, application of mutually dependent or independent earthquakes in the computations, estimates of the maximum expected earthquake magnitude, procedures of the attenuation relationships as well as the extent of respective errors will be presented. Prospects of earthquake hazard assessments and their calculation techniques in the near future will be discussed.

## 1. INTRODUCTION

Human and material losses caused by earthquakes are continuously increasing because of (a) the concentration of population and industry in large urban agglomerations, (b) new settlements in the already density populated areas, and (c) natural growth of population. Even through new construction technologies have been introduced in the recent years and earthquake-resistant structures have become more common, the losses are ever greater. In order to make protection and prevention most effective, the new body of knowledge achieved by geoscientific research has to be applied to hazard assessments, and new and more sophisticated approaches to input data processing have to be adopted. Then immediate applications of such results to earthquake engineering allow us to reduce essentially the losses. From the viewpoint of designers, the requirement is to express the seismic hazard in terms of vibration, especially in the time history of acceleration or its parameters (amplitude, frequency, duration, etc.), and in terms of probability of an earthquake effect occurrence in the future.

## 2. EARTHQUAKE HAZARD REPRESENTATIONS

### 2.1 What do we understand under the term "seismic hazard" ?

The seismic hazard is defined as a probability of occurrence of earthquake effects given in units of a certain dynamic level of vibrations which can be expected in a particular region (or site) within a certain time period. Very often, however, in various

works we come across the term "seismic risk", the meaning of which is frequently confused with the term "seismic hazard". What do we then understand under the seismic risk? The seismic risk is defined as a probability that earthquake consequences (technical, economic or social) will reach or exceed certain values in a region (or site) within a certain exposure time. The final result of the seismic hazard analysis is the determination of the probability of occurrence of a natural phenomenon, while the final result of the seismic risk analysis is a function of the interrelation between that natural phenomenon (in our case earthquake effects) and the total human activity.

In the last two decades, perhaps every seismologist has made a contribution to the solution of the problems of seismic hazard. Apart from a host of most varied results, this vivid interest in representing the seismic hazard has also produced their mutual heterogeneity. For one thing, the heterogeneity is caused by the participation of a great number of seismologists and specialists, and by the quality of input data, for the other. Even though the influence of a subject cannot be neglected, it can be demonstrated that it is the input data that have produced the many variants of seismic hazard representation. We can find such that suit the regions of a higher or lower seismic activity, longer or relatively short observation periods, better or worse seismological reconnaissance of a region, etc. For this reason, in the following part of this paper I will not only concentrate on the general characteristics of seismic hazard representations and the causes of their origin, but also on the possibilities to prevent the differences or to restrict them the least possible measure.

## 2.2 Two-parametric earthquake hazard

If we skip the problem of probability determination from the definition of the seismic hazard, the problem of occurrence of earthquake effects in a certain region within a certain time period remains. Such data can be assumed in a sense as the simplest representation of seismic hazard, because they provide us with the knowledge on occurrences of earthquake effects within a known observation period. Then consequently, they may be designated as the "two-parametric" seismic hazard representation, i.e., they express the relation between earthquake effects and observation time.

There are a lot of materials describing damaging or destructive effects of some historical events without giving any other information. Although these materials often constitute only singular reports, or at best, they are incorporated in the maps of certain earthquake effects, they have to be taken into account and attributed the simplest degree of seismic hazard representation.

It is evident that in the most conservative approach, only observations from the past define the model of future activity. These models naturally assume a stability in the earthquake

energy release processes. According to the reports of observed historical and present earthquake effects, different levels of the two-parametric representation of seismic hazard can be distinguished:

- i) macroseismic field of one earthquake,
- ii) macroseismic field of the earthquake, which is suggested to be close to a maximum expected shock, and
- iii) map of the maximum observed intensities, which is a result of the summation of all macroseismic effects having occurred during a certain period.

The mentioned fields and map can be converted to the level of the maximum expected earthquake (SCHENK 1984) and then other two two-parametric representations of seismic hazard can be obtained:

- iv) macroseismic fields of the maximum expected earthquake effects for given focal zone and
- v) map of the maximum expected macroseismic intensities over the area under interest.

It is well-known that (iii) "maps of the maximum observed intensity" are frequently annexed to many national construction standards and codes, and they provide the basis to introducing respective measures towards increasing the seismic resistance of building structures. In terms of the IAEA recommendation (Safety Guides), they can thus be regarded as the first approximations of "the site design earthquake". Consequently, (v) "the maps of the maximum expected intensity" can be assumed to be the simplest version of the macroseismic effects marked in the IAEA recommendations as "the safe shutdown earthquake".

As in the case of the two-parametric hazard representations, maps of individual dynamic parameters of strong ground motions can be compiled. Though earthquake engineers have not lately focused their interest on one or two wave parameters only, it can be stated that the so far compiled maps are

- vi) map of the maximum iso-accelerations of one earthquake, and
- vii) map of the maximum iso-accelerations, which is the result of the summation of all known maximum acceleration data recorded over the given area during a certain observation period.

Naturally, with the growing number of permanent seismological stations equipped with strong motion recorders, the observation networks in seismoactive regions are becoming denser and therefore it can be expected in the future that not only maps of maximum iso-accelerations but also of maximum iso-velocities and iso-displacements will be compiled. A question arises whether analogous maps can be constructed e.g. for the predominant frequency or the total duration of a vibration, and whether the maps



would be applicable in practice.

As in the previous approach to macroseismic and strong motion data, there are other possible simple representations based on distributions of all events or some events only defined by a certain magnitude level over the studied area :

viii) map of earthquake epicentres ; such a map can be assumed as a seismic zoning map (or map of earthquake source regions) without or with respect of the return period,

ix) maps of the number of events occurred on a given area,

x) maps of the earthquake energy flux released by the given area or space and during a given time period ; such a map is expressed in isolines of energy,

xi) maps of the maximum earthquake magnitudes originated within the area under study.

Since earthquake distributions can be relatively simply connected with a rough assessing of their effects on the Earth's surface, then the mentioned maps can also be included in a certain sense into the group of the two-parametric representations of seismic hazard. Such maps are often called "seismic zoning maps" or "maps of earthquake source regions", which sometimes have or have not any respect to the return period. These zoning maps do not introduce any other additional information and only reflect the surface distribution of observed effects or parameters. Also the procedures of observation smoothing and drawing of isolines are sometimes considerably afflicted with subjective personal judgement. We can see that this approach can hardly be applied in regions of low seismicity. In this case it is necessary to broaden the knowledge on earthquake activity by including other sophisticated aspects (e.g., geological or seismotectonic criteria) to assess both stronger events and events in new places.

The last kind of maps that can be included into the group of two-parametric earthquake hazard maps are those based on the relationship of seismic activity to the tectonic manifestations of the geological units. The knowledge of the motion potential of individual geological blocks and of the orientation of the stress field in the region, or possibly the dependences known for the region between the earthquake magnitude, the fault plane size, the thickness of the seismoactive layer, etc., enable the construction of the map of maximum seismic hazard of the respective area. Unless a part of the above-mentioned dependences is known for the area under study, the dependences established earlier in analogous geological conditions are used in some cases. The reliability of the thus determined maximum seismic hazard obviously depends not only on the quality of the geological and seismotectonic finding on the study area, but very often on the selection of analogous dependences in other areas, which are included in the particular procedure. The resultant maps of seismic hazard have the character of deterministically determined

maximum possible and/or expected earthquakes, and can thus be regarded as a variant of the maps giving "the safe shutdown earthquake".

### 2.3 Three- and more-parametric earthquake hazard

To extend the seismic hazard representations to the probability of earthquake effect occurrence, the statistical analysis and procedures have to be applied. They allow the probability of earthquake occurrences to be assessed not only in time (prediction to the future) but also in size (the maximum expected and/or possible earthquake). Of course, the time stability of earthquake energy release is again assumed.

At present the seismostatistical approach involves three basic steps:

- a) definition of the earthquake source region: its delineation, determination of its seismogenetic regime including an estimate of the maximum possible earthquake,
- b) determination of attenuation functions for strong ground motions and/or macroseismic intensity including the local seismogeological effects (microzoning), and
- c) probabilistic algorithms of hazard calculations.

Steps (a) and (b) are composed of several operations under which the input data for the third (c) step are prepared. It is evident that the accuracy of the data depends first of all on the availability of homogeneous earthquake information from the largest possible time span and on appropriate additional geological, geophysical, geodetic, etc. data. As the questions connected with the preparation of input data for a statistical calculation of the seismic hazard will be discussed later, this paragraph will only treat the third item, i.e. the algorithms of the probabilistic determination of the seismic hazard.

The first attempt to formalize the seismostatistical method of calculation (RIZNICHENKO 1966) was based on determining the probability of earthquake effect occurrence in a site or area from the knowledge of the cumulative distribution of the effects known during a given observation period. RIZNICHENKO denoted the resultant parameter as "shakeability" and defined it as a long-term mean frequency of recurrence of shaking of macroseismic intensity at a particular site. This method of determining seismic hazard can be essentially characterized in the following way: if a particular site is endangered by several earthquake source regions, for which we know e.g. intensity-frequency graphs, after introducing the attenuation between these regions and the site, we can found the recurrence graph of cumulative effects for the site, normalized to a time period of one year. Then the effects corresponding to e.g. the value  $N = 0.1$  are attributed occurrence periodicity once in ten years, the value  $N = 0.01$  occur-

rence periodicity once in a hundred years, etc. The occurrence periodicity, also referred to as "the return period", is thus defined by a reciprocal value of the cumulative frequency of annual occurrence of a particular earthquake effect. If these return periods do not much exceed the range of the observation period, from which the cumulative distribution of effects was compiled, then the obtained results are very close to those we obtain with the use of sophisticated seismostatistical models. But the more the return period exceeds the observation period, the less dependable results we obtain, and it often happens that an author fails to consider this fact and consequently, the hazard assessments are completely false.

Even though the method of determining three-parametric earthquake hazard is greatly simplified, it is frequently used. Its advantage is that it can be easily understood logically and that the results obtained can be verified in a simple way on real data. It is obvious, however, that inferior-quality input data may adversely influence or even devalue the seismic hazard in the same manner as in other statistical approaches as shown later.

Later RIZNICHENKO and SEIDUZOVA (1984) developed this method further and introduced the definition of "spectral" shakeability, in which the level of shaking (intensity) relates to the wave period of given vibrations.

In 1968 CORNELL published the approach which has become the standard methodology of seismic hazard assessment used up to now. It is based on the calculation of the conditional cumulative probability distribution  $F(I)$ , which is the ratio between the number of expected occurrences with  $I \leq I$  and  $M \geq M_{min}$  to the total number of expected occurrences ( $M \geq M_{min}$ ). The distribution is given in the form

$$F(I) = \frac{\sum_{i=1}^j N_i}{\sum_{i=1}^m N_i} \quad (1)$$

where  $N_i$  are the corresponding numbers of occurrence of  $I_{i-1} < I \leq I_i$ ,  $I_i$  being the discrete intensity boundaries ( $i=1,2,...,m$ ;  $j \leq m$ ). The condition requires an occurrence of earthquakes with magnitude  $M$  equal to or greater than some minimum magnitude  $M_{min}$  which has occurred in a given source region.

The average number of events that must occur for an intensity exceeding  $I$  to be attained is defined by the relation

$$R(I) = 1 / (1 - F(I)) \quad (2)$$

The quantity  $R(I)$  is a parameter of engineering interest and is sometimes termed "the return period", however,  $R(I)$  expresses the number of events. On the other hand the return period  $R_y(I)$  expressed in years is given by the ratio between  $R(I)$  and the expected number of events ( $M \geq M_{min}$ ) for one year, i.e.,

$$R_y(I) = R(I) / \sum_{i=1}^m N_i \quad (3)$$

Thus, the  $R_y(I)$  gives the number of occurrences expected at different seismic levels per year. The values of  $F(I)$ ,  $R(I)$  and  $R_y(I)$  are calculated for each level  $I_i$ .

The extreme probability distribution  $F_{\max}(I)$  can be obtained from the cumulative probability distribution  $F(I)$  by invoking several simple assumptions. Then

$$F_{\max,t}(I) = \exp(-t / R_y(I)) \quad (4)$$

Putting the equation in a logarithmic form, we obtain

$$R_y(I) = -t / \ln F_{\max,t}(I) \quad (5)$$

If  $t = R_y(I)$ , i.e. the number of years in the period of interest equals the return period in years, then  $F_{\max,t}(I) = 1 / e \approx 0.37$ .

Thus, this statistical three-parametrical approach of earthquake hazard assessment elaborated by CORNELL allows us to determine

- the return periods  $R_y(I)$  of the given maximum intensity  $I$  at a selected site, which will not be exceeded with the probability  $F_{\max,t}(I)$  in a given number of years  $t$ ,

or

- on the contrary, for the given return periods  $R_y(I)$ , the probabilities  $F_{\max,t}(I)$  that the maximum intensity  $I$  at a selected site will not be exceeded over a given number of years  $t$ .

Of course, there are other authors who modified the procedures mentioned above, compiled different numerical algorithms applied in computer techniques, but the principal steps remain the same.

A widely used computer program is EQRISK compiled by McGUIRE (1976), which is based on Cornell's algorithm of determining seismic hazard. Its advantage is easy manipulation with input data, its disadvantage being a substantial simplification of the medium attenuation characteristics, with only one attenuation law applied to the entire area. This shortcoming can be overcome e.g. by the introduction of elliptic isoseismals into the computation (MAYER-ROSA and MERZ, 1976), etc.

On the basis of Cornell's algorithm, ALGERMISSEN and PERKINS (1976) compiled program RISK4A. Compared with the preceding one, this program is not so easy to operate, but it allows the introduction of particular attenuations of the medium between the source region and the site, and of the computation of the seismic

hazard for arbitrary occurrence probabilities in dependence on the required return period. The original version of this program, allowing the seismic hazard to be determined in particle motions (e.g. accelerations), was modified to be used also for computing macroseismic intensities (SCHENKOVA et al. 1981).

A comparison of the seismic hazard values determined by both the mentioned programs has revealed that the values given by program EQRISK more or less correspond to probabilities  $F_{max,t(1)} = 37\%$  (relation (5)).

There are of course other programs based on Cornell's algorithm to determine seismic hazard, which, apart from maximum values of particle motions, determine e.g. the probable character of seismic vibrations (ANDERSON and TRIFUNAC, 1978) that may appear in a particular site.

All the currently used programs of computing seismic hazard conceived on the basis of Cornell's algorithm assume that the occurrences of earthquakes constitute a Poisson process. Attempts are made to introduce in the calculation model also Bayesian distribution or to use Markov processes, as well as to include the clustering of earthquakes. This activity, however, gives rise to considerable analytical complications. Anyway, in most cases the Poisson process seems to provide useful and adequate information.

Implicit in all the models proposed for seismic hazard evaluation (specifically those based on Cornell's algorithm), is the assumption that the energy released during an earthquake is concentrated at a point, and thus these models will be referred to as "point source" models. While this assumption is acceptable for small earthquakes, it would not be valid for major earthquakes in which the total energy of the shocks is composed of the energy released along the fault slips which could be many tens or hundreds of kilometers long.

This fact conditioned the compilation of computer programs making use of the linear source. DerKIUREGHIAN (1975) closely studied this problem, testing the differences in the use of point and linear sources. McGUIRE (1977) compiled program FRISK, which enables the seismic hazard to be determined with respect to the fault position. In applying these methods, however, we often come across the problem of defining faults in a given region, its continuation down to the depth, and particularly the problems of defining its seismoactive parts. The determination of these parameters invariably depends on the unambiguity of a geological region, and its character is thus strictly deterministic. Since any probabilistic screening of input data is dismissed, this approach may sometimes lead to better results, but cases of false results or even of errors cannot be excluded, either.

### 3. EARTHQUAKE CATALOGUE AND ITS UNCERTAINTIES

A catalogue represents a basic seismological tool to find and deduce other fundamental characteristics describing the parameters of the seismic activity of a given region and allowing us to define seismogenetic zones. It is evident that the homogeneity of its parameters in time and space as well as their uniformity in determination are the guarantee for the subsequent data management and calculation. It means that an earthquake catalogue cannot originate by a simple collection of information from different sources without critical unification.

The present seismological centres and agencies suggest these earthquake parameters to be included in the basic file : date, origin time, geographic coordinates, depth, magnitude (surface- and body -wave, local), epicentral intensity and radii of isoseismals, if the event is macroseismically observed. All parameters should be accompanied by the quality factor. Of course, both instrumental and macroseismic data as well as references (stations, bulletins, isoseismal maps, monographs, reports) are welcomed and advisable. Then such a catalogue can serve research tasks and applications as well.

Many good national and regional catalogues have been compiled during the last two decades, evidently also under the pressure of practical requirements for a sound seismic hazard analysis. In Europe and in the Mediterranean there are prepared such catalogues for Algeria, the Alps, the Balkans, the Caucasus, Central and Eastern Europe, the Iberian Peninsula, Great Britain, the Pyrenean Peninsula, Scandinavia, etc. The USSR catalogue of strong earthquakes (Eds. KONDORSKAYA and SHEBALIN 1977) is remarkable by the serious attempt to indicate the accuracy of parameters by estimates of errors; the catalogue is also interesting by giving different types of magnitudes and all known mean radii of isoseismals.

For hazard assessments, however, a much longer time span of observations is needed than one or two decades. Thus the main difficulty seismologists face is to collect and unify reliable information from the whole historical period. It has to be emphasized that one should not be satisfied with what is easily found in publications describing historical events. They often contain information which was transcribed several times, one author copied it from another, and this gave rise to misprints, errors and translation mistakes. It is highly desirable to search in original documents, which brings not only new data but also eliminates serious mistakes. The work of AMBRASEYS and MELVILLE (1982) on Persia is a typical example of such an effort.

#### 3.1 Coordinates of earthquake origin

As to epicentre geographic coordinates, it is advisable to recompute or at least to check them when we use agency's data from the first half of this century, because of the inadequate

density and distribution of seismic stations at that time. Frequently, so called macroseismic epicentres are more reliable than the instrumental ones from the above mentioned period.

The problem of focal depth in the catalogues is undoubtedly a significant parameter; however, only very dense station networks can guarantee a reliable depth determination. For a majority of events the instrumental depths down to 50-60 km, i.e. in the domain of "normal" or "shallow" earthquakes. Deep phases of P wave permit the depth determination to be more reliable for intermediate and deep shocks.

### 3.2 Earthquake magnitude

It is imperative that every catalogue should contain clearly defined magnitudes. If several magnitudes are used in one catalogue, the conversion formulae and all calibration curves should be presented too. Misleading results can be obtained if earthquakes classified by different types of magnitudes ( $m_b$ ,  $M_s$  or  $M_L$ ) are mixed together and a magnitude-frequency graph is compiled. Consequently, if such data are used in analyses which lead to the standardization and/or time normalization of this recurrence graph, to the maximum possible earthquake determination, to the finding of any energy release pattern, etc., the obtained results are wrong too.

At present, there are many catalogues having a global, regional or national validity. The catalogue by GUTENBERG and RICHTER (1949) covering the first half of the 20th century still remains very useful because of uniform magnitude determination, however, it is complete only above  $M_s = 7$ . The more recent document for the period 1904-1980 is the global catalogue by ABE (1981) completed above  $M_s = 6 \frac{3}{4}$ . In the other global source, the International Seismological Summary (ISS), information is lacking on the size of events, and in bulletins of the International Seismological Centre (ISC), though they have been issued since 1963 with more advanced procedures of parameter determination, for many years only body wave magnitudes  $m_b$  were used for size classification of events. The users have to be aware of the limitations of this scale which saturates at about  $M_s = 6 \frac{1}{2}$  (KANAMORI 1983). Therefore  $m_b$  values are not suitable for statistical studies involving large events. Only since 1981 do the bulletins of ISC and of NEIS regularly contain surface wave magnitudes based on the vertical component of Rayleigh waves, i.e., the situation in the domain of large events has been improved.

### 3.3 Macroseismic data

Macroseismic information, at least the epicentral and maximum observed intensity, is often included in many earthquake catalogues. If the radius of the shaken area and some radii of isoseismals, e.g.  $r_5$  and  $r_3$  recommended as standard, are added in a catalogue, then the first attempt to assess the attenuation law

can be made. It is evident that isoseismal maps are still the main source of information on attenuation if intensity is that quantity defining seismic hazard. The isoseismals also control substantial regional differences in attenuation. Even if different sources indicate that the same macroseismic scale is used, it is advisable to check the values by studying original reports. There are a lot of examples of a very personal use of a scale so that differences between two individual authors can easily amount to two macroseismic grades.

### 3.4 Accuracy of catalogized data

The last very important item is the classification of accuracy of the catalogue parameters mentioned above. There is no recipe for that if a long observation period is covered. Anyway, this information, either in the form of a standard error or by introducing classes should be a part of each earthquake catalogue.

The good-quality catalogized data then serve to provide the valuable information on the seismogenic regime of any area, understanding of the time changes among shock occurrences of the earthquake sequences and probable migrations of individual shocks within those sequences. This information together with the knowledge of the recurrence graphs and the maximum possible earthquakes creates a reliable basis for the seismic hazard calculation.

## 4. STRONG GROUND MOTIONS AND THEIR UNCERTAINTIES

A frequent source of uncertainties are the dependences of strong ground motions on focal parameters or the medium properties. Dependences measured in other sites or regions are often used because actual data on the area under investigation are missing. In their application we should of course observe analogy criteria, and therefore try to utilize only those properties and data that approach the given conditions most. It can be said that all empirical dependences determined from direct observations are often substantially different although e.g. the rock medium is analogous after a geologist's judgement. As yet there is no guideline how to make best analogies and how to identify the deviations having originated in a calculation of seismic hazard due to these inaccuracies or uncertainties in the approximation of the initial physical quantities. For this reason, great emphasis is put on the methods of expert estimates, which involve experience of more specialists, and which then enable the inaccuracies or errors thus originated to be identified.

Another group of uncertainties are the questions connected with the conversion of the resultant values of seismic hazard given in macroseismic intensities to strong ground motions expressed in particle acceleration, velocity and/or displacement.



It has turned out lately that, for purposes of earthquake engineering the most important are not only the peak (maximum) values, which may originate even due to an accidental coincidence of some wave phases or wave groups, but especially, also the so-called effective values of vibration : effective particle motions or effective durations.

The question of determining predominant frequencies play an important role as well : the value of the predominant frequency that should be used in practical problems has not yet been unambiguously defined. As a matter of fact, it cannot be only said that it is the frequency which the maximum spectral amplitude belongs to. The character of the spectrum often allows an "objective" determination of even more such frequencies that may differ mutually. Should we then use two or more frequencies, or a particular frequency band of a given spectrum level, or of the effective values of these frequencies ? These problems will have to be solved in the future.

Likewise, in practice there also appear dependences on the duration of vibrations of a certain amplitude level. The duration is defined by a time interval in which the amplitudes exceeded given level. Unfortunately, we have not yet solved the problem when amplitudes exceed the given level several times in the whole wave pattern : do we then consider the total time period during which a deviation was exceeded, or only those intervals in which it was exceeded ?

## 5. SEISMIC HAZARD ASSESSMENT - PROBLEMS AND IMPROVEMENTS

To understand the present stage in the seismic hazard assessment and the accuracy of its determination, we shall now discuss the individual topics from the viewpoint of their influence on final hazard estimates. Seismic hazard should consider not only the damage potential of elastic ground motion but also, especially in the earthquake source regions, the areas of expected ground deformations and failures including places of fault rupture. In sea and oceanic coastal zones the extent of tsunami hazard has to be taken into account too.

The uncertainties associated with the relationships and parameters that are used as input data are the following ones :

- i) coordinates of the boundaries delimiting source regions,
- ii) cumulative magnitude- or intensity-frequency graphs of individual focal zones,
- iii) maximum possible or expected earthquake in a focal region,
- iv) dependences of seismic wave attenuation on the earthquake magnitude, focal depth, epicentral distance, geological media of the entire region and, especially, on local struc-

tures (geological blocks, subsurface and alluvial layers),

- v) probabilistic and deterministic approaches, seismic hazard outputs and their application to earthquake engineerings.

If possible, these uncertainties are restricted by applying probabilistic approaches in the use of exactly defined statistical quantities, e.g. mean values, quality factors, standard deviations, limits of confidence intervals, etc.

It is obvious that the calculations of the seismic hazard should be made in such a way as to take into account not only the mean values of a certain parameter or dependence, but also the limits of these values ranges, given e.g. by one standard deviation of the value from the mean course to either side, etc. Increased differences of the seismic hazard assessments thus determined with respect to the mean values of the seismic hazard would then indicate "suspicious" combinations of input parameters, which would have to be verified once more, and if necessary, the earlier determined hazard values reinterpreted.

For the definition of earthquake source regions and delineation of their boundaries the information given by earthquake catalogues is not often sufficient and has to be completed by other data related to earthquake occurrence, e.g., information on recent crustal movements as evidenced by geodetic, archeological and neotectonic observations. Recently, traces of active fault movements accompanying the largest earthquakes are found by trenching across faults and by satellite image interpretations. This complex approach contributes substantially to the identification of potential source regions but, unfortunately, does not guarantee that some potential sources remain unknown.

Two possible approaches of seismogenic zone delineation can be found :

I. Subjective approach - an expert's eye-fitting and application of his experience - which uses the following data:

- a) occurrence of great earthquakes - the level, above which we consider the earthquakes to be great depends on the activity of the region under study: e.g.  $M_s > 5$ ,
- b) occurrence of all known earthquake epicentres - planary distribution of epicentres can indicate both seismogenic provinces or areas and seismoactive faults or zones,
- c) correlation of earthquake epicentres with the geological structures of the area - with the use of geological and geophysical data, especially neotectonic data, geodetical and satellite image observations and geodynamic analysis.

II. Objective approach - based on the combination of the previous ("subjective") one together with the results obtained by statistical and other mathematical analyses performed by computer

techniques. The following quantities and procedures can be applied in this approach:

- d) density of earthquake shocks per area - number of event occurrences normalized to a certain area  $[km^2]$ ,
- e) earthquake energy-flux per area - amount of energy released in a certain space  $[km^3]$  or a certain area  $[km^2]$ ,
- f) establishing the differences from the background seismicity pattern - determination of a different seismogenic regime with the help of recurrence graphs,
- g) maximum possible and/or maximum expected earthquake - territory of high earthquake activity can be mapped, e.g., by the extreme value statistics (3rd Gumbel distribution),
- h) multidimensional correlation of geoscientific data by the pattern recognition algorithms

The second step in hazard calculation is to determine the cumulative recurrence graphs  $N(M)$  or  $N(I_0)$  for each region, usually in the form

$$\log N = a - b M \quad (6a)$$

or

$$\log N = a' - b' I_0 \quad (6b)$$

The minimum number of events needed for the compilation of the graphs is between 40 to 100. The coefficients  $b$  or  $b'$ , defining the slope of distribution, varies from region to region, although it is negligible in some areas. Therefore, in such areas sometimes a particular magnitude level is defined to compile of the maps of earthquake activity. Before the standard procedure of the recurrence graphs determination is used, the following items have to be solved:

- a) classification of events: dependent or independent shock,
- b) definition of the background seismicity of region,
- c) cumulative recurrence graphs of the earthquake magnitude or the epicentral intensity - with the use of time normalizing within each magnitude or intensity class.

However, the basic problem is to estimate of maximum possible earthquake in a focal region by probabilistic and deterministic approaches. The upper magnitude threshold, feasible for the region within a defined time interval  $M_{max}$  is the most decisive quantity in the assessment of hazard extremes and can vary from  $M_g = 5$  to  $M_g = 9$ . It can be misleading to determine  $M_{max}$  (or  $I_{max}$ ) by a simple inspection of  $N(M)$  if the observa-

tion period is short. The bending of the  $N(M)$  distribution can be caused simply by the saturation of the magnitude scale used (see Paragraph 3.2). The slope of  $N(M)$  depends

- i) on aftershock series and on character of sequence (e.g. swarm) - problem dependent and independent events,
- ii) on the period of activity or quiescence,
- iii) on earthquake magnitude classes,
- iv) on the character of recurrence graph density, cumulative)

Besides the recurrence graph the other ways can assess the maximum possible earthquake magnitude:

- a) the theory of extreme values (3rd Gumbel distribution),
- b) the Benioff energy-release diagram,
- c) seismotectonic analysis of focal zone - to find relations between earthquake magnitude and seismoactive (or rupture) fault dimensions (length, width, surface),
- d) intensity of recent crustal movements, etc.

Empirical strong motion observations fit approximately a general formula for attenuation law of seismic vibrations in the form

$$\log X = c_1 + c_2 M - c_3 \frac{1}{R} \quad (7)$$

where  $c_1$ ,  $c_2$ , and  $c_3$  are coefficients determined by the least square method,  $M$  is earthquake magnitude,  $R = \sqrt{d^2 + h^2}$  is focal distance and  $X$  is the maximum ground motions (particle acceleration, velocity and displacement). There are two main sources of ground motion data at present: macroseismic observation and strong motion records, mainly accelerograms. Before compiling and using an attenuation function to the seismic hazard calculation following investigation has to be done

- a) corrections and restoration of time history of particle acceleration, velocity and displacement,
- b) dependence of strong ground motions (or macroseismic intensity): on earthquake size (magnitude, energy) and mechanism,  
on distance (epicentral or focal, depth),  
on physical properties of media - composition of the medium and on soil properties at a site.

There are conversion formulae linking macroseismic intensity and particle motions, however, they provide only approximative values because the relationship is complicated and the scatter of experimental data is large.

Attenuation curves of maximum ground motions have been compiled for some earthquake active area. Moreover, they are not suitable for design purposes, and other quantities like the "effective acceleration" are now preferred. The strong motion parameters can be studied in three domains:

- I. Time domain - maximum acceleration, velocity and displacement, duration of seismic vibration,
- II. Amplitude domain - maximum particle motions determine statistically, effective particle motions of seismic vibration, total and effective durations, total kinetic energy and impulse of seismic vibration, total root-mean-square amplitude and duration, and
- III. Frequency domain - spectral particle motion, pseudo-relative and pseudo-absolute particle motions, predominant frequency, absolute and relative spectrum content, spectrum intensity.

It is highly advisable to study azimuthal dependences of macro-seismic intensity and/or strong ground motions, to select suitable type of attenuation law approximation and to assess influence of local seismogeological conditions.

#### 6. CONCLUSION

The existing methods of seismic hazard assessment now in use correspond to the level of knowledge reached so far and the outputs which have not yet reached the required level of accuracy. It is important that the hazard information always contains the indication of the probability level for which it is valid.

Basic principles of all methods are the same, i.e. the integration of seismic effects at a site, however, the algorithms vary according to statistical models. In the future it is desirable to extend present assumptions (Poisson model of earthquake occurrences, point source region) for other statistical models of occurrence (Markov model, Bayesian distribution, clustering etc.). Also the application of "linear" and "plane" source models as well as new quantities and wave parameters, which are more suitable for earthquake engineers should be introduced.

Future improvements in hazard assessment depend mainly on the progress made in accurate estimates of earthquake potential and on better knowledge of propagation of strong ground motion under varying conditions.

#### REFERENCES

- Abe K. (1981): Magnitudes of large shallow earthquakes from 1904 to 1980. Phys. Earth Planet. Inter. 27, 72.

Ambraseys N.N., Melville C.P. (1982): A history of Persian earthquakes. Cambridge Univ. Press.

Algermissen S.T., Perkins D.M. (1976): A probabilistic estimate of maximum acceleration in rock in the contiguous United States. U.S. Geol. Survey Open-File Report 76-416, 45 pp.

Algermissen S.T., Perkins D.M., Thenhaus P.C., Hanson S.L., Bender B.L. (1982): Probabilistic estimates of maximum acceleration and velocity in rock in the contiguous United States. U.S. Geol. Survey Open-File Report 82-1033.

Bune V.I. (Ed.) (1974): Metodicheskie rekomendatsii po seismicheskomu rayonirovaniyu territorii SSSR. Inst. Fiziki Zemli AN SSSR, Moscow, 195 pp.

Cornell C.A. (1968): Engineering seismic risk analysis. Bull. Seis. Soc. Amer. 58, 1583-1606.

Gutenberg B., Richter C.F. (1949): Seismicity of the Earth and associated phenomena. Princeton Univ. Press.

Kanamori H. (1983): Strong motion seismology. Seminar "Evaluation of Seismic Hazards and Decision Making in Earthquake-Resistant Design". EERI Annual Meeting, Reno, Nevada.

Karnik V., Nersisov I.L. (1987): Principles and problems of assessment of seismic hazard. Proc. of the Seminar "On Earthq. Prediction and the Mitigation of Earthquake Losses", Dushanbe.

Keilis-Borok V.I., Kronrod T.K., Molchan G.M. (1973): Algorithm dlya ocenki seismicheskogo riska. In "Vychislitelnye i statisticheskiye metody interpretatsii seismicheskikh dannykh", Nauka, Moscow, 21-43.

Kiureghian A. Der (1975): A line-source model for seismic risk analysis. PhD Thesis, Urbana, Illinois, 134 pp.

Kiureghian A. Der, Ang A.H.S. (1977): A fault-rupture model for seismic risk analysis. Bull. Seis. Soc. Amer. 67, 1173-1194.

Kondorskaya N.V., Shebalin N.V. (Eds.) (1982): New catalogue of strong earthquakes in the USSR from ancient times through 1977. Boulder (Moscow 1977).

Makropoulos K.C., Burton P.W. (1985): Seismic hazard in Greece, I. Magnitude recurrence, II. Ground acceleration. Tectonophysics 117, 205-257, 259-294.

Mayer-Rosa D., Merz H. (1976): Seismic risk maps of Switzerland. Proc. ESC Meeting, Luxemburg.

McGuire R.K. (1976): Fortran computer program for seismic risk analysis, U.S. Geol. Survey Open-File Rept. 76-67, 90 p.

McGuire R.K. (1978): FRISK - Computer program for seismic risk analysis, using faults as earthquake sources, U.S. Geol. Survey Open-File Rept. 78-1007.

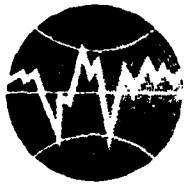
Riznichenko Yu.U. (1966): Raschet sotryasaemosti tochk zemnoy po-verchnosti. Izv.AN SSSR, Fizika Zemli No.5, Nauka, Moscow,

Riznichenko Yu.U., Seiduzova S.S. (1984): Spektral'no-vremennaya kharakteristika seismicheskoy opasnosti. Nauka, Moscow, 180 pp.

Schenk U. (1984): Conversion of observed macroseismic field up to higher intensity level by generalized circular isoseismals. J. Eng. Geol. 20, 153-160.

Schenkova Z., Karnik U. (1987): Earthquake catalogues and hazard assessment. Proc. of the "20th General Assembly of the European Seismol. Commission", Kiel.

Schenkova Z., Schenk U., Karnik U. (1981): Seismic hazard estimate for a low seismicity region - example of Bohemia. PAGEOPH 119, 1077-1092.



**TURKISH NATIONAL COMMITTEE FOR  
EARTHQUAKE ENGINEERING**

**THIRTEENTH REGIONAL SEMINAR ON EARTHQUAKE ENGINEERING**

**September 14-24, 1987 - Istanbul - Turkey**

**On the Attenuation of Macroseismic Intensity with Epicentral  
Distance**

**G. Grandori, F. Perotti, A. Tagliani**

*Dipartimento di Ingegneria Strutturale, Politecnico di Milano, Piazza Leonardo  
da Vinci, 32, Milano, Italy*



## On the Attenuation of Macroseismic Intensity with Epicentral Distance

G. Grandori, F. Perotti, A. Tagliani

*Dipartimento di Ingegneria Strutturale, Politecnico di Milano, Piazza Leonardo da Vinci, 32, Milano, Italy*

### INTRODUCTION

The relation between macroseismic intensity and epicentral distance is widely used in seismic hazard analysis. The attenuation of macroseismic intensity,  $I$ , actually depends both on epicentral distance  $D$  and on hypocentral depth  $h$ . Therefore, if  $h$  is not explicitly taken into account, the relation between  $I$  and  $D$  must refer to earthquakes having hypocentral depths which span a relatively small range.

Many formulas relating  $I$  and  $D$  have been suggested. Most of these are either equivalent to or special cases of the following two formulas [1]:

$$I_0 - I = a_1 + b_1 \ln D + c_1 D, \quad (1)$$

$$\ln I_0 - \ln I = a_2 + b_2 \ln D + c_2 D, \quad (2)$$

where  $I_0$  is the epicentral intensity.

As mentioned in [1], equations (1) and (2) derive from two different hypotheses about the relation between macroseismic intensity and seismic energy density.

As far as the use of the attenuation law in local hazard analysis is concerned, the following alternative procedures are generally applied.

a) Method of homogeneous zones. The method is based on the hypothesis that over the considered zone the mean annual number of earthquakes per unit area,  $\lambda'_0$ , is constant and that the intensity distribution

$$F_{I_0}(1) = F_{I_0}(1_0)$$

is also constant.  $F_{I_0}(1)$  and  $V_0$  are derived from historical data. It is then possible, using the attenuation law, to calculate  $\lambda$  and  $F_I(1)$  at any given site.

b) Merely statistic method. The intensity  $I$  at the site for each historical earthquake is evaluated through the attenuation law. The series of local events so defined is then statistically interpreted in order to derive  $\lambda$  and  $F_I(1)$  at the site.

In the application of formulas (1), (2) and of methods a), b), some difficulties may arise. In this paper such difficulties are discussed and some variants are proposed with particular reference to Italian conditions.

#### PRELIMINARY OBSERVATIONS ABOUT THE ATTENUATION LAW

As mentioned in [1], equations (1) and (2) "are based on the implicit assumption that the seismic energy is radiated from a point source. The equations can be expected to fail where distance is not large compared to the source dimensions".

This limitation is especially important in the evaluation of seismic hazard at a site which is close to, or inside a seismic region; and this is in general the most interesting case from the engineering point of view. Some changes in the structure of formulas (1), (2) seem therefore to be necessary.

Equation (1) implies that attenuation  $I_0 - I$  is independent of  $I_0$ . This is not always true. As mentioned in (1), "inspection of isoseismal maps will suggest that the rate of attenuation of intensity with distance is often more rapid for small than for large earthquakes".

As far as equation (2) is concerned, note that this is equivalent to

$$I_0 - I = I_0 \left[ 1 - \frac{1}{\exp(a_2 + b_2 \ln D + c_2 D)} \right] \quad (3)$$

This means that, according to equation (2), the rate of attenuation of intensity with distance is more rapid for large than for small earthquakes. This may be true in some cases, but as previously mentioned real situations often show an opposite behaviour.

As an example, fig. 1 shows the correlations (1), (2) obtained using the coefficients  $a$ ,  $b$ ,  $c$  that have been defined in [1] for the "Cordilleran Province".

Mean values of equivalent radii  $D_i$  obtained from isoseismal maps of 19 Italian earthquakes are plotted in fig. 2. The hypocentral depths of these earthquakes, evaluated according to Blake's formula [2], range between 10 and 15 km. Fig. 2 shows that, on the average, for the earthquakes here considered the rate of attenuation is more rapid for small than for large earthquake. This kind of behaviour cannot be interpreted by either formula (1) or (2).

#### PROPOSAL OF A VARIANT OF EQUATION (1).

Many variants of equations (1) and (2) have been proposed in order to adapt them to different conditions. We propose here a new variant of equation (1) which shows a very good fitness to the sample of fig. 2.

Assume as starting point the following simplified variant of equation (1):

$$i = I_0 - I = a + b \ln D_i \quad (4)$$

Equation (4) is equivalent to the relations used by Gutenberg and Richter [3] and Cornell [4].

In order to make the rate of attenuation depend on  $I_0$  it is sufficient to introduce  $D_i/D_0$  instead of  $D_i$ :

$$i = I_0 - I = a + b \ln \frac{D_i}{D_0} \quad (5)$$

where  $D_0$  is the equivalent radius of the highest mapped isoseismal line. From equation (5) we obtain

$$D_i = D_0 \alpha e^{i/b} \quad (6)$$

where  $\alpha = e^{-a/b}$ .

Obviously, if  $D_0$  is constant, equation (6) coincides with (5). However, if  $D_0$  depends on  $I_0$  all the radii  $D_i$  depend on  $I_0$  as well.

Assume the ratio  $D_0(I_0=j)/D_0(I_0=j-1)$  to be constant (i.e. independent of  $j$ ) and call  $\phi$  such constant. As a consequence

$$\frac{D_0(I_0=j)}{D_0(I_0=j-1)} = \frac{D_1(I_0=j)}{D_1(I_0=j-1)} = \phi. \quad (7)$$

The constant  $\phi$  is a measure of the more (or less) rapid rate of attenuation of small earthquakes compared with large ones. If  $\phi > 1$  the trend is of the type of fig. 2 while  $\phi < 1$  would correspond to the behaviour represented by formula (2) in fig. 1.

The value of  $\phi$  for a given set of earthquakes can be calculated as the mean value of the ratios  $D_1(I_0=j)/D_1(I_0=j-1)$ . The data of the sample of fig. 2 lead to the mean value  $\phi = 1.36$ .

Observe now that, for  $i \geq 1$ , equation (6) implies that the ratio

$$\psi = \frac{D_{i+1} - D_i}{D_i - D_{i-1}} \quad (8)$$

does not depend either on  $i$  or on  $I_0$ . It is easy to prove that its value is

$$\psi = e^{1/b} \quad (9)$$

The experimental value of  $\psi$  can be calculated as the mean value of the ratios (8). For the sample of fig. 2 we obtain  $\psi(i \geq 1) = 1.58$ .

As to the ratio

$$\psi_0 = \frac{D_1 - D_0}{D_0} \quad (10)$$

taking into account the condition

$$D_1 = D_0 \quad \text{for } i = 0, \quad (11)$$

equation (6) gives

$$\psi_0 = \psi - 1 \quad (12)$$

From a qualitative standpoint, equation (12) is acceptable. In fact the rate of attenuation is more rapid for

small than for large distances. However equation (12) represents too rigid a constraint from a quantitative point of view. For instance, the sample of fig. 2 leads to a mean value  $\psi_0 = 1.07$ , while equation (12) would lead to  $\psi_0 = 0.58$ .

In order to overcome this inconsistency, it is convenient to modify equation (6) by adding a new coefficient:

$$D_i = D_0 \exp^{i/b} + \epsilon \quad (13)$$

The ratio  $\psi$  is given again by equation (9), while the value of  $\psi_0$  can now be adapted to experimental data.

Combining equations (13) and (10) with condition (11) we obtain:

$$D_i = D_0 \left( 1 + \psi_0 \frac{\psi^i - 1}{\psi - 1} \right) \quad (14)$$

i.e.

$$i = I_0 - I = \frac{1}{\ln \psi} \ln \left[ 1 + \frac{\psi - 1}{\psi_0} \left( \frac{D_i}{D_0} - 1 \right) \right] \quad (15)$$

If coefficients  $\psi_0$ ,  $\psi$ ,  $\phi$  are known, equations (7) and (15) completely define the attenuation law, provided that a reference value for  $D_0$  is established. This can be done as follows. Using equation (14) derive from the experimental values  $D_i$  a mean value  $\bar{D}_0$  for each  $I_0$ . Impose then that the reference value of  $D_0$  through equation (7), minimizes the deviations (squared) from the mean values  $\bar{D}_0$ . For the sample of fig. 2 one obtains, in this way,  $D_0 (I_0=10) = 9.3$  km.

In conclusion, the coefficients that define the attenuation law (15), with the help of equation (7), for the sample of fig. 2 are:

$$\psi_0 = 1.07 \quad , \quad \psi = 1.58 \quad , \quad \phi = 1.36 \quad ,$$

$$D_0 (I_0 = 10) = 9.3 \text{ km} \quad .$$

The attenuation law so defined is represented in fig. 3.

Using the data of the same sample, the coefficients of the formulas (1) and (2) have been calculated using the least square method. The results are shown in fig. 4.

#### INFLUENCE OF THE STRUCTURE OF THE ATTENUATION LAW ON THE EVALUATION OF LOCAL HAZARD

Consider a site located at the center of a hypothetical homogeneous seismic zone (fig. 5). The correlation between intensity and return period for this site has been calculated assuming alternatively the attenuation law (1), (2) and (15), with the coefficients derived from the sample of fig. 2. The results are in fig. 6.

The considerable differences clearly point out that the choice of the attenuation law is a crucial step in seismic hazard analysis.

#### ABOUT THE USE OF ATTENUATION LAW IN SEISMIC HAZARD ANALYSIS AT A SITE.

Consider a seismic region with area  $A$ . Suppose that the catalogue of historical earthquakes of the region is given and that for a certain number of the earthquakes the isoseismal map is known. In general for most of the earthquakes only  $I_0$  and epicentral coordinates are known. From the available isoseismal maps an attenuation law can be derived and assumed as suitable for the interpretation of all events

At this point as mentioned in the introduction, two alternative procedures are available in order to define the seismic hazard at a site.

As far as method a) is concerned, the hypothesis

$$F_{I_0}(i) = \text{constant over } A \quad (16)$$

cannot be avoided. In fact the size of a seismic region that can affect a given site is not very large and it is necessary to take all the events of the region into account in order to compute the distribution function  $F_{I_0}(i)$ . We will assume that intensities  $I_0$  comply with hypothesis (16).

As to the spatial distribution of epicenters, if the hypothesis

$$\lambda'_0 = \text{constant over } A \quad (17)$$

is not verified (and this is often the case), the error in the evaluation of the intensity distribution  $F_I(i)$  at the site is rather small. On the contrary, the error in the calculation of  $\lambda$  can be considerable.

As an example, a circular seismic region with radius 95 km has been considered. The distribution  $F_{I_0}(i)$  has been assumed

$$F_{I_0}(i) = 1 - \exp(6.91 - 1.15 I_0) ; I_0 \geq 6$$

and the attenuation law (15) with  $\psi_0 = 1$ ,  $\psi = 1.4$  has been used. For the sake of simplicity a constant value  $D_0 = 8$  km has been adopted.

The evaluation of  $F_I(i)$  and  $\lambda$  at the center of the seismic region has been carried on under two different hypotheses:

- 1)  $\lambda'_0 = \text{constant over the region};$
- 2)  $\lambda'_0 = \text{twice the average value used in 1) in the inner zone with radius 65 km; in this case the value of } \lambda'_0 \text{ in the remaining area has been obtained by imposing the total number } \lambda_0 \text{ of events in the region to be the same as in 1).}$

The maximum difference between the ordinates of  $F_I(i)$  in the two cases is 6%, while the value of  $\lambda$  for the first hypothesis is about 50% of the value corresponding to the second one.

If the merely statistic method b) is used, the actual distribution of epicenters is automatically taken into account, so that the best estimate of  $\lambda$  is obtained. On the other hand, the evaluation of the distribution  $F_I(i)$  becomes uncertain due to the fact that, at the site, the number of events becomes in general very small for the higher intensities.

In conclusion, method a) leads to a good estimate of  $F_I(i)$  but may be unreliable for the calculation of  $\lambda$ . Method b) offers the best estimate of  $\lambda$  but is affected by large uncertainties in the evaluation of  $F_I(i)$ .

Thus, it seems reasonable to adopt a mixed procedure, derive  $F_I(1)$  using method a) and calculate  $\lambda$  through method b).

#### REFERENCES

1. Howell B.F. and Schultz I.R. (1975), Attenuation of Modified Mercalli Intensity with Distance from the Epicenter, Bull. Seism. Soc. Am., Vol. 65, pp. 651-665.
2. Blake A. (1941), On the Estimation of Focal Depth from Macroseismic Data, Bull. Seism. Soc. Am., Vol. 31, pp. 225-231.
3. Gutenberg B. and Richter C.F. (1942), Earthquake Magnitude, Intensity, Energy and Acceleration, Bull. Seism. Soc. Am., Vol., 32, pp. 163-191.
4. Cornell C.A. (1968), Engineering Seismic Risk Analysis, Bull. Seism. Soc. Am., Vol. 58, pp. 1583-1606.



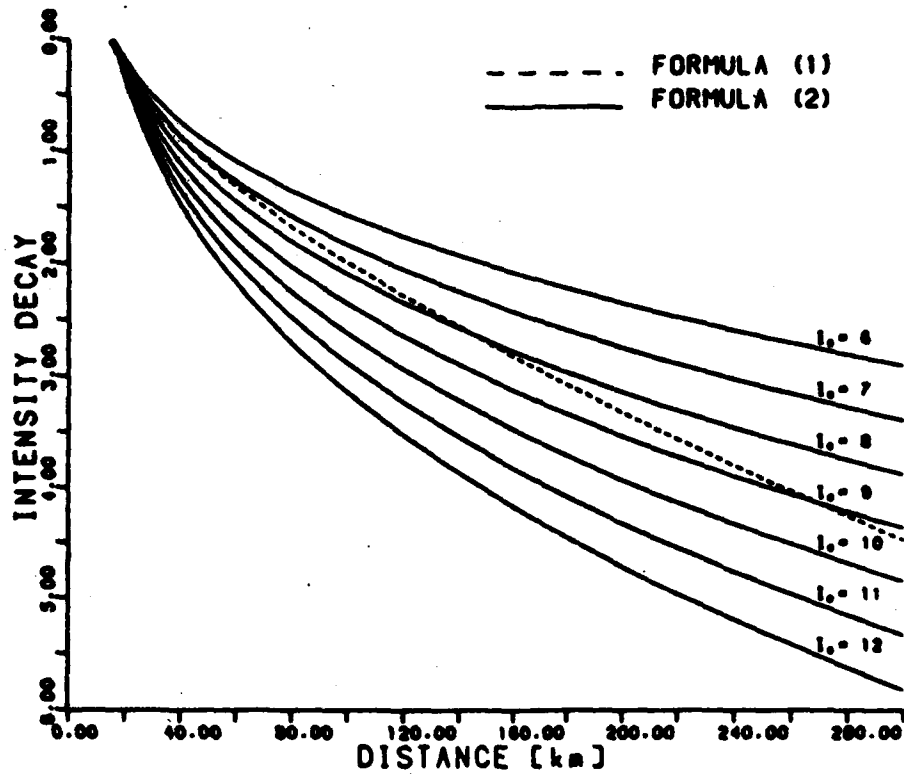


Figure 1. Intensity attenuation with epicentral distance for the "Cordilleran Province" following Ref. [1]

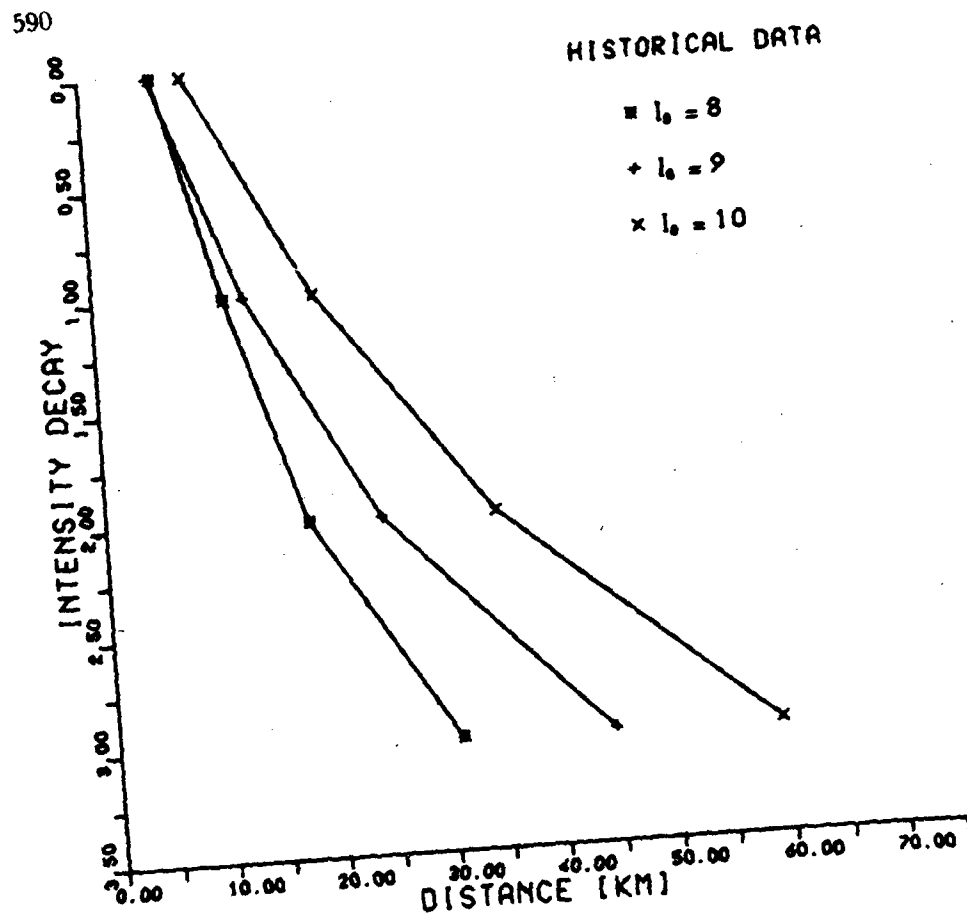


Figure 2. Average intensity attenuation with epicentral distance for 19 Italian earthquakes

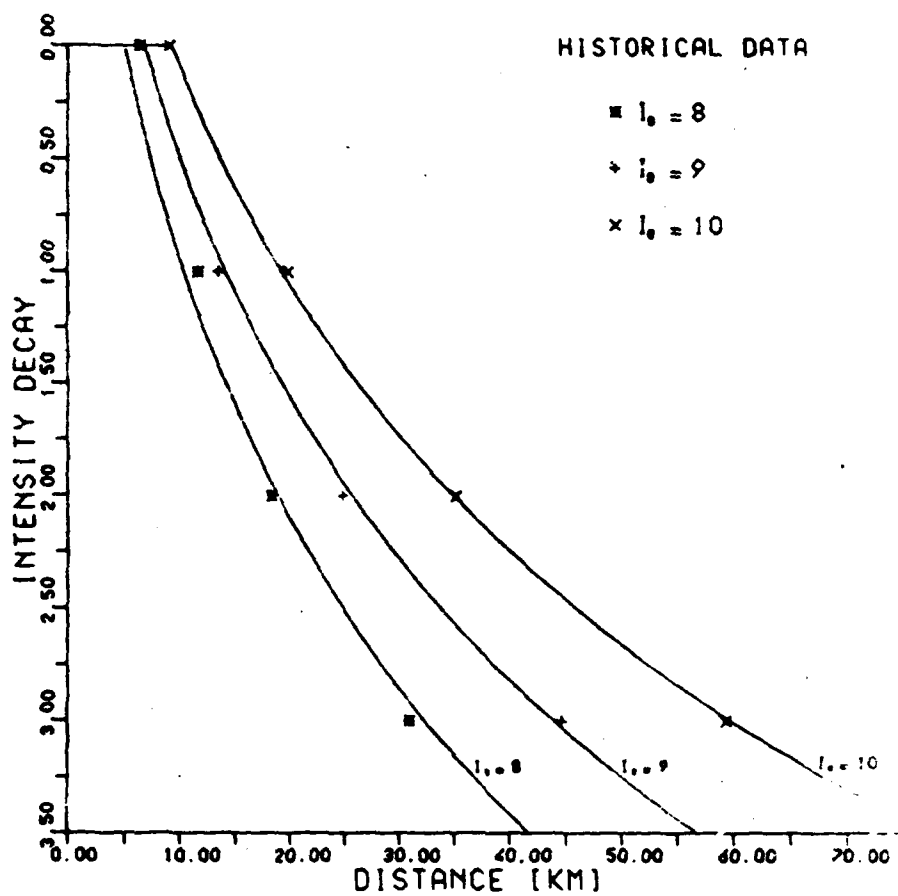


Figure 3. Interpretation of the sample of figure 2 using the proposed law

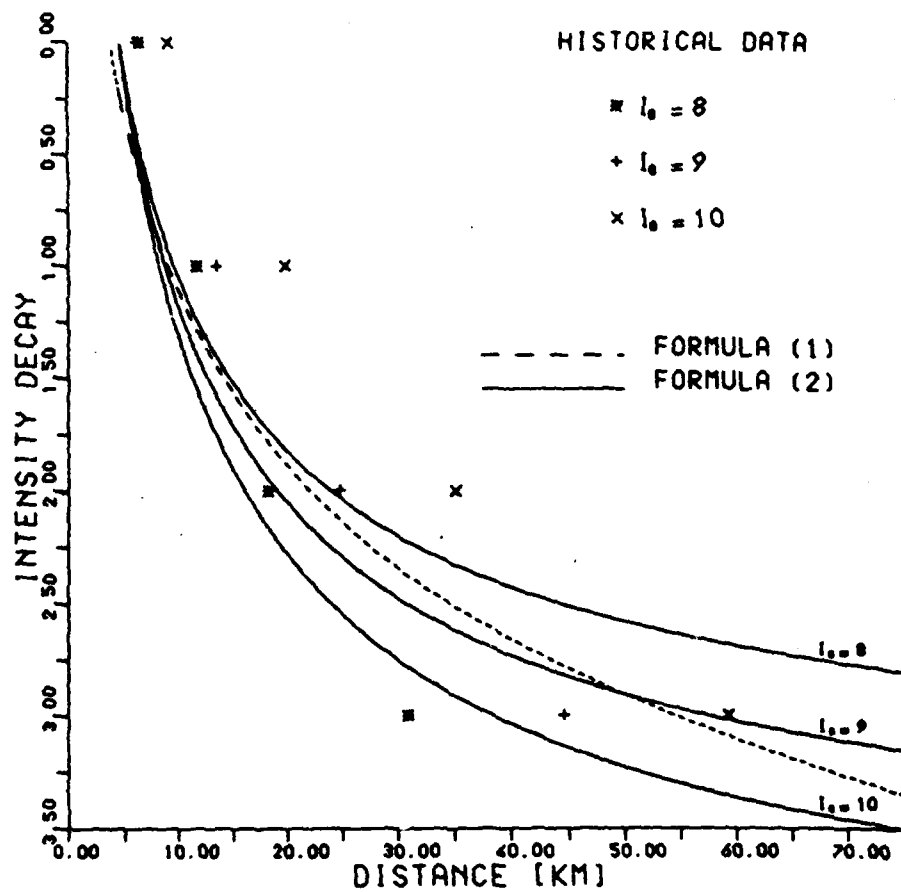


Figure 4. Interpretation of the sample of Figure 2 using formulas (1) and (2)

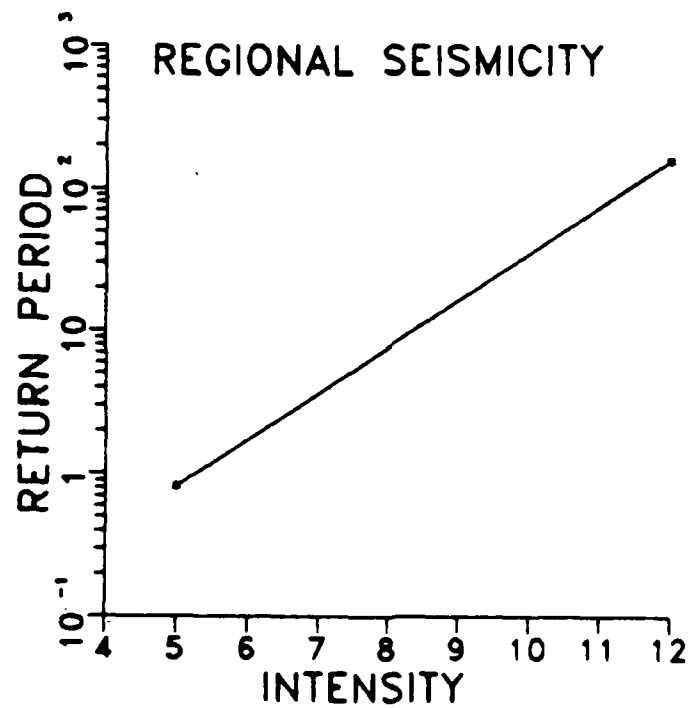
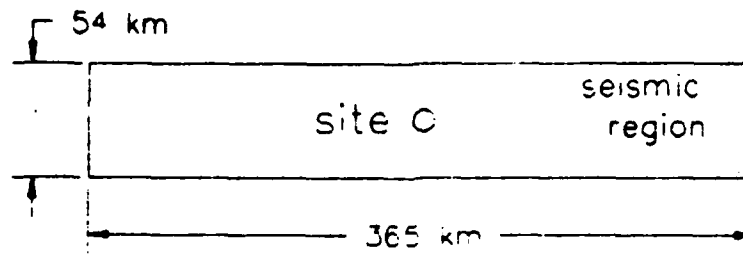


Figure 5. Hypothetical homogeneous seismic region

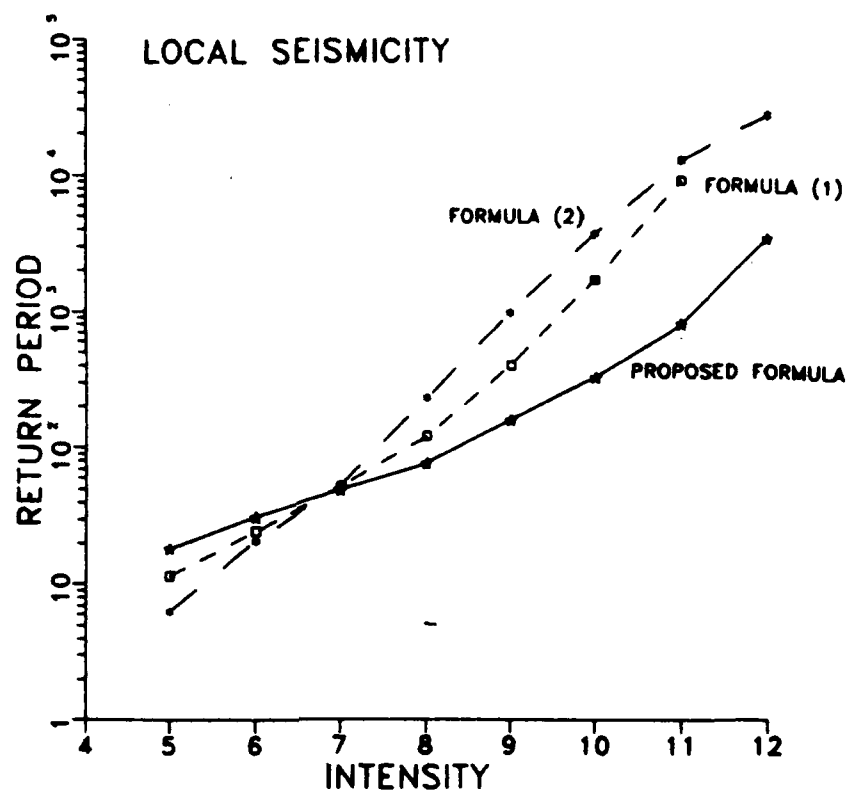
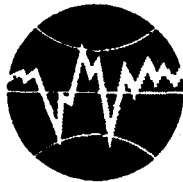


Figure 6. Local seismicity for the site of figure 5 using different attenuation laws



TURKISH NATIONAL COMMITTEE FOR  
EARTHQUAKE ENGINEERING

THIRTEENTH REGIONAL SEMINAR ON EARTHQUAKE ENGINEERING

September 14-24, 1987 - Istanbul - Turkey

THE SEISMICITY AND EARTHQUAKE  
HAZARD IN ICELAND

by

Július Sólnes  
Professor of Civil Engineering,  
University of Iceland

THE SEISMICITY AND EARTHQUAKE  
HAZARD IN ICELAND

by

Július Sólnes  
Professor of Civil Engineering,  
University of Iceland

Engineering Research Institute  
Report no. 85008  
Reykjavík 1985



ISSN 0255-9226

THE SEISMICITY AND EARTHQUAKE  
HAZARD IN ICELAND.

by

Július Sólmes  
Professor of Civil Engineering,  
University of Iceland

## LIST OF CONTENTS

1.0	Introduction.....	1
2.0	The Seismic History of Iceland.....	4
2.1	The South Iceland Seismic Zone.....	5
2.1	The Reykjanes Seismic Zone.....	7
2.3	The North Iceland Seismic Zone.....	9
2.4	Other Areas of Seismic Acticity.....	12
2.5	Minimum Risk Areas.....	13
3.0	Seismic Zoning and Earthquake Risk Map of Iceland.....	13
3.1	Intensity-Acceleration Relations.....	14
3.2	Intensity-Magnitude Relations.....	15
3.3	Earthquake Risk Maps of Iceland.....	16
4.0	Summary and Conclusion.....	17
5.0	Acknowledgements.....	19
6.0	References.....	19

## 1.0 INTRODUCTION

Iceland is located in the North Atlantic Ocean as a super-structural part of the Mid-Atlantic Ridge. The ridge marks the boundary between the North American Plate and the Euro-asian Plate and creates a belt of seismic activity ranging from the Azores in the South and towards Jan Mayen in the North. The boundary approaches Iceland from the southwest along the Reykjanes Ridge and from the north along the Kolbeinsey Ridge, (Fig. 1).

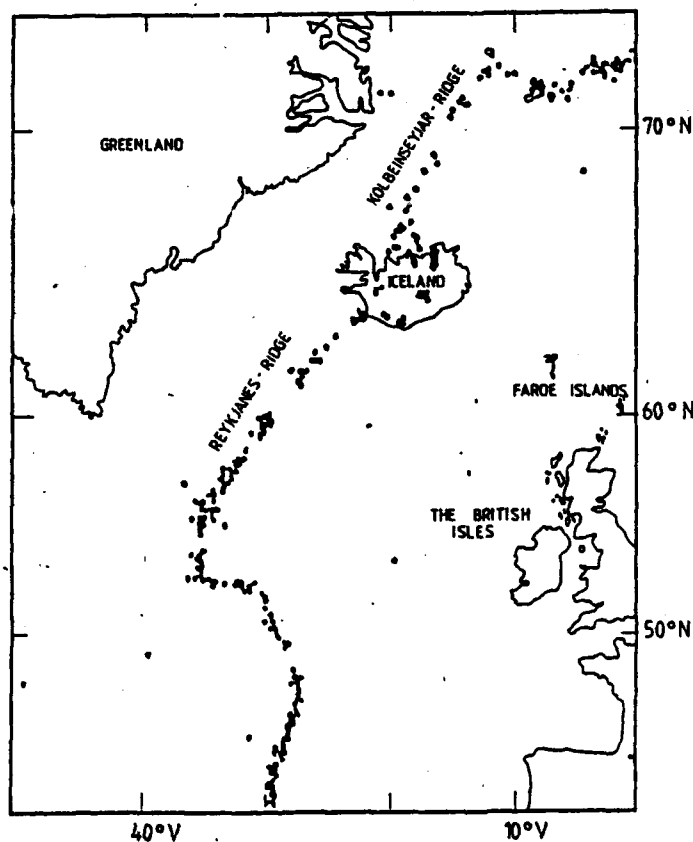


Fig.1 Epicentres of earthquakes on the Mid-Atlantic ridge 1962-1980, /7/.

Across Iceland from southwest to the north, the plate boundary is displaced to the east by two major fracture zones, the South Iceland seismic zone in the lowlands of the south and the Tjörnes fracture zone in the north. The largest earthquakes in Iceland have occurred within these zones and may have exceeded magnitude 7. (The magnitude  $M$  of an earthquake is defined in the usual sense as the amplitude-

logarithm defined by C.F. Richter. It should not be confused with the intensity of an earthquake, I or MMI, which describes the local effects of an earthquake on the Modified Mercalli Scale). The focal mechanism of these earthquakes, which are of tectonic origin, indicates strike-slip faulting with a sense of motion, right-lateral in N-Iceland and left-lateral in SW-Iceland which is consistent with transform fault interpretation of these zones. Both zones, however, lack the clear topographic expression characteristic of fracture zones on the ocean floor, and in neither zone is the transform motion taken up by a single major fault. Outside these two fracture zones an intraplate earthquake zone with clusters of seismic activity is seen in Borgarfjörður in West Iceland. Seismic activity associated with the volcanic zones in Iceland is also evident, /2/, /5/, /7/, /8/\*). In Fig. 2, epicentres of past and recent earthquakes with magnitude 6.0 or above are shown with the year of occurrence.

The volcanic earthquakes rarely exceed magnitude 5 and are mostly related to imminent volcanic activity. In the Western Volcanic Zone which covers the Reykjanes Peninsula, the Thingvellir region, Langjökull and Hofsjökull regions, seismic activity is mostly confined to the Reykjanes Peninsula where tectonic earthquakes at the plate boundary and volcanic follow hand in hand. In other parts, as well as in the Southern Volcanic Zone, which covers the Vestmanna Islands and follows the rift zone across the west part of Vatnajökull, Askja and Krafla areas until Axarfjörður in the north, earthquakes of pure volcanic origin are frequent, (Fig. 3). Thus the South Iceland Seismic Zone bridges the gap between the two volcanic rift zones in South Iceland whereas the North Iceland Seismic Zone touches the volcanic rift zone in Axarfjörður.

The seismic and volcanic activity in Iceland is very well localized and confined to certain clearly indicated regions. Large parts of the Country are outside these zones of geophysical manifestations and have been quiescent for millenniums. The inhabited coast and valleys in East Iceland, the Western fjords and large areas of West and North West Iceland are judged to be minimal or no risk zones.

\*) Numbers within slashes correspond with the list of references at the end.

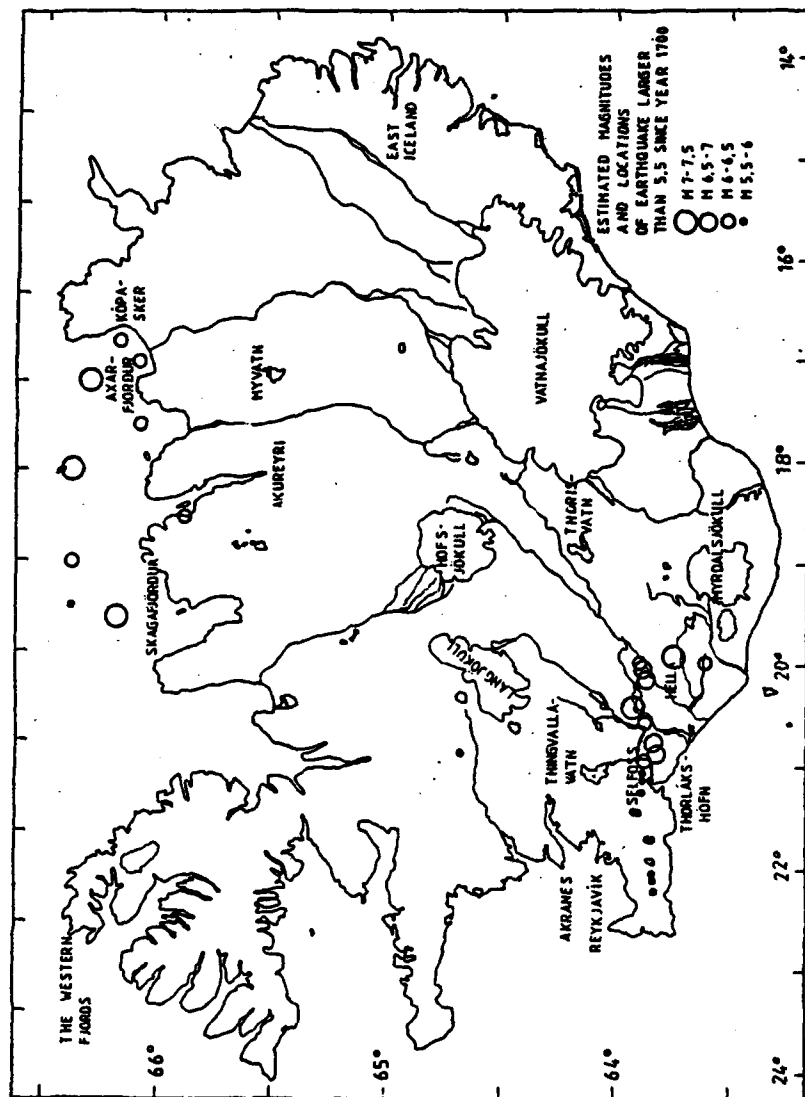


Fig.2 Epicentres of past and recent earthquakes with magnitude 5.5 and above.

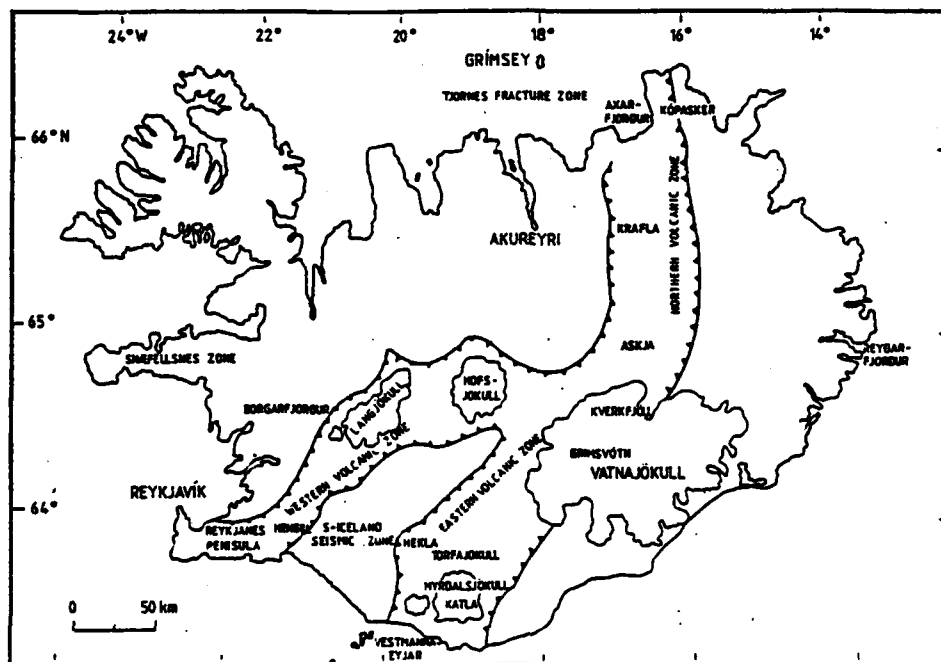


Fig.3 The interrelationship between the volcanic and seismic zones in Iceland.

## 2.0 THE SEISMIC HISTORY OF ICELAND

Since the settlement of Iceland in the late ninth century, seismic activity has been observed in all seismic zones and moderate to strong earthquakes have occurred from time to time. Very strong earthquakes, of the order encountered at the Pacific plate boundaries, are, however, unlikely to take place. Possibly, the strongest earthquake in historic times occurred in the South Iceland Zone on August 14th 1784. Damage to farm houses was severe and three people lost their lives. The magnitude of this earthquake, which was first in a series of violent earthquakes that shook the whole seismic region in the South, has been estimated to be about 7.5, /4/. This by comparison is an order of a magnitude lower than the strongest earthquakes that have occurred in say Japan, California and Chile in recent times.

The past seismic history of a certain region is the best indicator on what to expect in the future. In the following, the earthquake history of the different seismic zones and their character is briefly discussed.

## 2.1 THE SOUTH ICELAND SEISMIC ZONE

Most destructive earthquakes in Iceland since its settlement in the ninth century have occurred within the South Iceland lowlands. Major earthquake sequences have affected the sparsely populated farmlands in historic times with intervals ranging between 45 and 112 years. The earthquake zone extends about 70 km in the E-W direction with almost a perfect E-W alignment of epicentres in a 5-10 km band from the Ölfus region in the West towards Rangárvellir in the East. However, no major E-W striking faults can be found and the destruction zones of individual earthquakes tend to be elongated in the N-S direction as shown in Fig. 4. The distribution of recent microearthquakes indicates that the seismicity is associated with brittle deformation of a 10-20 km wide belt located above an E-W trending zone of aseismic deformation in the lower crust or upper mantle, /7/, /9/.

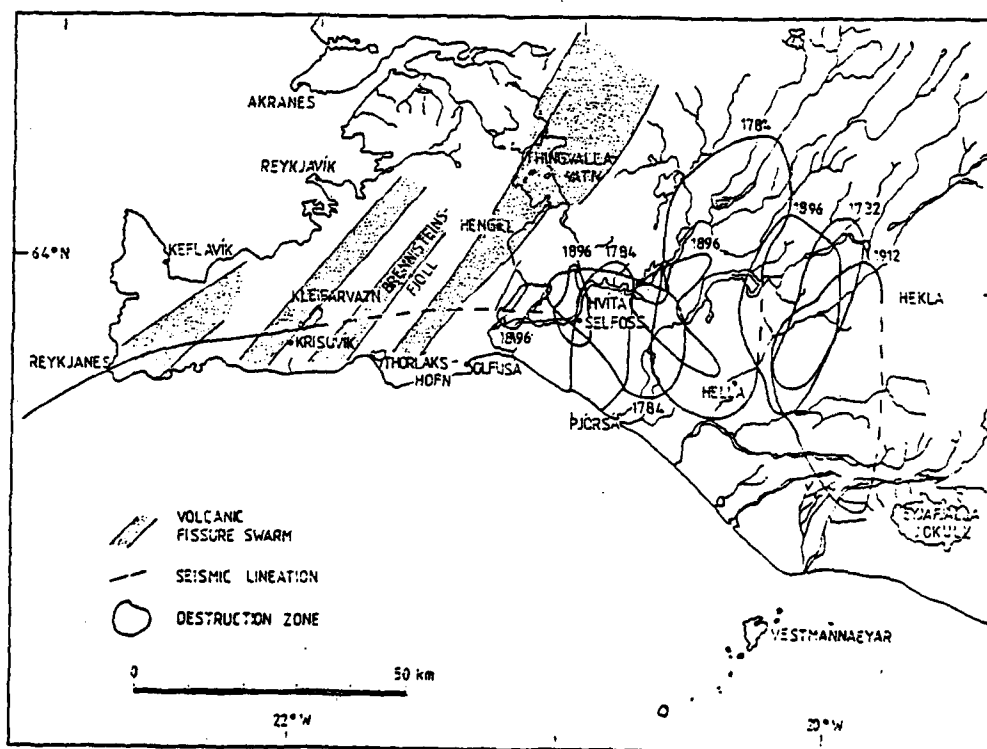


Fig.4 The Reykjanes Peninsula and adjacent South Iceland Seismic Zone. The destruction zones of past historic earthquakes within which more than 50% of the houses collapsed are shown.

The historic earthquakes seem to be grouped in two different categories. In the first category, the whole region is shaken by a sequence of violent earthquakes which usually begins with a strong earthquake in the east part of the Zone followed by big but gradually smaller events moving to the West. The above 1784 earthquake is typical of such a sequence. Other major earthquake sequences in this category have been the 1896 earthquakes which is the last major earthquake sequence in the region, causing widespread damage, 1732-34, 1630-33, 1389-91 and 1339. In all these earthquake episodes severe damage to farm houses in the entire region with several deaths is reported in the annals, /1/. In table 1, a list of all known major earthquakes in the South Iceland Zone in historical times is given with assessed values for maximum intensity and magnitude.

TABLE 1. A list of destructive and large magnitude earthquakes in South Iceland. Assessed values are within parentheses, /1/, /2/, /9/, /11/.

DATE	LOCATION	MAGNITUDE/ Max. Intensity	NOTES
1164	Ölfus/Flói		Damage in Ölfus/Flói, 19 deaths
1182	Whole region?		" extent uncertain, 11 deaths
1211	"		" " 18 "
1294	Rangárvellir		" in Land/Rangárvellir
1300	"		" in Rangárvellir
1308	Whole region?		" extent uncertain, 6 deaths
1339	Whole region		" in most parts of the zone
1370	Ölfus		" in Ölfus, 6 deaths
1389	Rangárvellir		" in Land/Rangárvellir
1391	Flói		" in Ölfus/Flói/Grímsnes, 5 deaths
1510	Rangárvellir		" in Land/Rangárvellir
1546	Whole region?		" in eastern and western parts
May 12 1581	Rangárvellir		" in Rangárvellir
Spring 1597	Ölfus		" in Ölfus
1614	Flói		" in Ölfus/Flói/Grímsnes/Skeið
Nov 1624	Flói		" in Flói
Feb 21 1630	Land		" in Holt/Land/Rangárvellir, 6 deaths
Early 1633	Ölfus		" in Ölfus
March 16 1657	Flói		" in Flói and Fljótshlíð?
Summer 1671	Ölfus		" in Ölfus/Grímsnes, 5 deaths
Jan 28 1706	(64°N, 21° W)	(6-6.5)	" in Ölfus/Flói, 4 deaths
April 1 1725	Rangárvellir		" in Rangárvellir
Summer 1726	"		" " "
Sept 7 1732	(64°, 20°.2)	( 6.5)	" in Hreppar/Land/Rangárvellir
March 21 1734	(64°, 20°.5)	( 6.5)	" in Ölfus/Flói/Grímsnes, 9 deaths
1749	Ölfus		" in Ölfus
1752	"		" " "
1757	Fljótshlíð		" in Fljótshlíð
Sept 9 1766	Ölfus/Holt		" in Ölfus/Holt/Land
Aug 14 1784	(64°.1, 20°.5)	( 7.5)	" in whole region, 3 deaths
June 10 1789	(64°, 21°.5)	(6-6.5)	" in Reykjanes and Ölfus
Feb 21 1829	(64°, 20°)	(6-6.5)	" in Land/Rangárvellir, 1 death
Aug 26 1896	(64°, 20°.2)	(7)	" in whole region, 4 deaths
May 6 1912	(64°, 19°.9)	(7)	" in Land/Rangárvellir/Fljótshlíð,
March 29 1947	64°, 19°.7	5	No damage   1 death
April 1 1955	64°.1, 21°.2	5.5	Slight damage near Soq
Júlí 2 1967	64°, 20°.7	5.0	Slight damage at Brúnastráir

The big earthquake sequences in category 1 seem to occur about once every century, on the average, or more accurately once every 112 years with a probability of 80% or more based upon the historical data. The large interval including the



fifteenth century may be due to the very poor historical records from that time, the so-called historical gap, rather than scarcity of earthquakes.

In the second category, major earthquakes have occurred as a single outstanding event either in the western or the eastern part of the zone. In the eastern part, Rangárvellir and Landssveit, the earthquakes of 1912, 1829, 1726, 1581 belong to this category and in the western part, (Ölfus and Flói), the earthquakes of 1789, 1766, 1752, 1749, 1706, 1671, 1597, 1546 and 1370.

The 1912 earthquake of magnitude 7 is the last major earthquake to have occurred within the zone. It caused damage in a sparsely populated area close to the volcano Hekla in the Eastern Volcanic Zone with one casualty. The seismologist August Sieberg studied the intensity of this earthquake and assessed the maximum intensity at XI on the Mercalli intensity scale.

Smaller earthquakes have occurred in the western part in more recent times such as Oct. 9, 1935 (M=6), April 1, 1955 (M=5.5) and July 27, 1967 (M=5.0). In these earthquakes minor damage of farmhouses near the epicentres was observed.

## 2.2 THE REYKJANES SEISMIC ZONE

The Reykjanes Peninsula which is a transition between the Reykjanes ridge to the west across the western volcanic zone to the South Iceland Seismic Zone is an important region due to its proximity to the industrial and population center of Reykjavík and vicinity.

The mid-Atlantic plate boundary enters Iceland near the tip of Reykjanes and then runs along the peninsula in an easterly direction delineating an area of high seismic activity less than 2 km wide in most places. Reykjanes is also a region of active volcanism which is unusual for a highly active seismic zone. It is believed that within the volcanic areas, the intense heat will generate stress relief in the crust thus minimizing the possibility of high stress concentration earthquakes.

The earthquake activity of this region is mainly concentrated in three different areas, that is on the ridge out of the peninsula, west of Kleifarvatn, (Kleifarlake), and around Brennisteinsfjöll, (Brennisteinsmountains). A fourth concentration of earthquake activity, in the Hengill Area, is at the boundary between the South Iceland Seismic Zone and Reykjanes and can have influence in both zones, Fig 5.

The earthquakes in Reykjanes and Hengill are smaller than the big earthquakes in the South Iceland Zone. The focal depth is mostly at 1-5 km which causes comparatively higher intensity of the shallow Reykjanes earthquakes than the

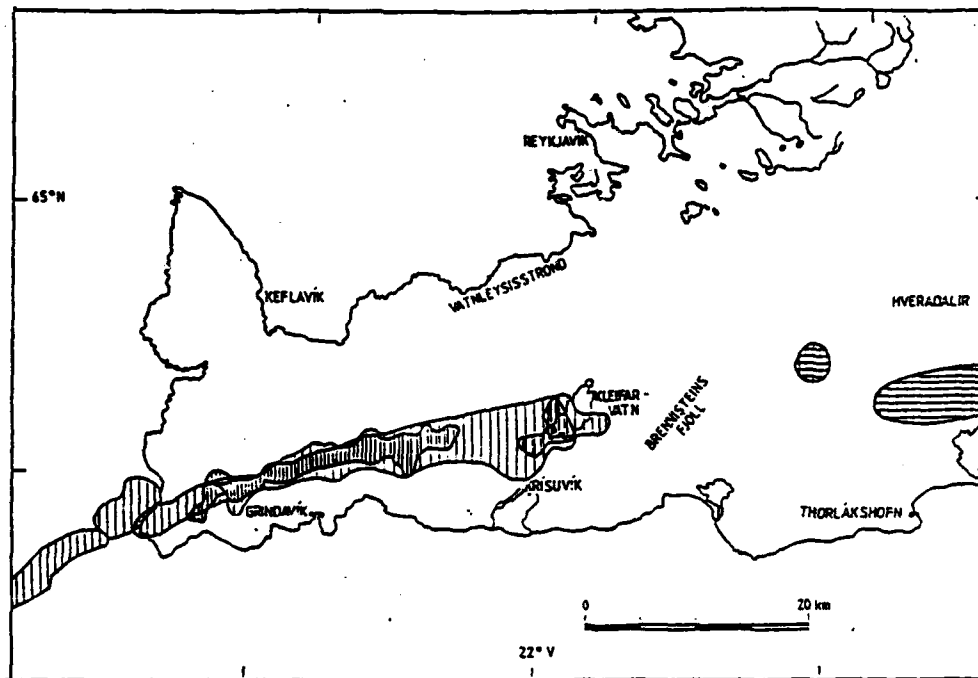


Fig.5 The Reykjanes Peninsula with zones of seismic activity. The hatched areas designate origin of earthquake swarms in 1971-75. The cross-hatched areas show epicentres of earthquakes in Ölfus in the South Iceland Zone.

deeper South Iceland earthquakes. However, due to the volcanism, it is to be expected that the stress concentration in the subterranean heated rock is lowered whereby the energy release in an earthquake is also lowered as has already been mentioned. The fault structures are complex and several seismic lineations or faults can be identified striking obliquely or even transversely to the main zone.

Seismic activity in the Reykjanes zone during this century has been high but concentrated on low magnitude earthquakes. One of the biggest earthquakes in recent times has been the June 1933 earthquake in western Reykjanes (Mw6) with an epicentre south of Keilir which caused some damage at Vigdísarvellir. The intensity of the earthquake was assessed at VI in Grindavík and V in Reykjavík. A similar earthquake occurred in the same region in October 1889 with some damage to farmhouses at Vigdísarvellir, Krísuvík and Vatnsleysuströnd.

In Reykjavík, the earthquake caused a part of the churchgoers to rush out in the midst of a sermon in the Cathedral. In the Brennisteins mountains, two earthquakes have occurred in this century with magnitude about 6. In July 1929, an earthquake of magnitude 6, caused widespread alarm in Reykjavík. Some minor damage occurred such as cracks in concrete walls and ceilings, and in the harbour. The House of Parliament and the old Post Office Building suffered some damage. The intensity of the earthquake was assessed at VI-VII in Reykjavík and at X in the epicentral region. In December 1968, an earthquake of magnitude 6 occurred in the same region. The intensity was lower than that of the 1929 earthquake, about IV-V in Reykjavík where damage was minimal although people there were alarmed.

Near the Hengill area east of Bláfjöll, an earthquake of magnitude 6 occurred in October 1935. Since this area is almost uninhabited, there is little to show except for the Ski-Lodge in Hveradalir where some slight damage occurred.

This easternmost part of Reykjanes Peninsula has not been very well investigated and chronicles relating to this area are rather meagre as is to be expected. However this is the most important source of earthquakes to endanger the Reykjavík area. In Table 2, the number of earthquakes that have been felt in Reykjavík is given grouped according to their intensity on the modified Mercalli scale (MMI), /1/, /9/.

Table 2. Number of earthquakes felt in the Reykjavík Area.

Time Period/MMI Intensity	III	IV	V	VI-VII
1801-1850	8	1	1	0
1851-1900	19	4	5	3
1901-1950	66	19	9	1
1951-1985			3	0

According to Table 2, the earthquake activity in Reykjavík appears to be increasing. This is probably more due to lack of information from the nineteenth and earlier centuries rather than actual increasing seismicity.

### 2.3 THE NORTH ICELAND SEISMIC ZONE

The North Iceland Seismic Zone is a broad zone of faulting and seismicity which connects the southern end of the submarine Kolbeinsey Ridge and the volcanic zone in North Iceland in Axarfjörður. Earthquake epicentres are scattered throughout a region which is about 80 km wide from north to south and 150 km long between Melrakkaslétta in the east to Skagi in the west. A concentration of epicentres is in the northeast corner of the zone whereas the larger magnitude earthquakes may be more frequent in the western part of the area. The seismic character of the zone is of a complex nature and can not be associated with a single fault or a simple plate boundary. Studies of recent earthquakes show

that a considerable part of the seismicity is associated with possibly three different WNW trending lines which originate in the volcanic belt. The sense of motion along these trending lines is right-lateral strike-slip as has been evidenced by two recent focal mechanism solutions, /5/, /7/.

The Grímsey seismic line runs slightly north of Grímsey and joins the Krafla fissure swárm in Axarfjörður, (Fig. 6). It has no clear trace in the topography. Instead, the surface structure is characterized by northerly trending troughs and ridges. In some respects this resembles the structure in SW-Iceland where the epicentral belt lacks clear surface manifestation.

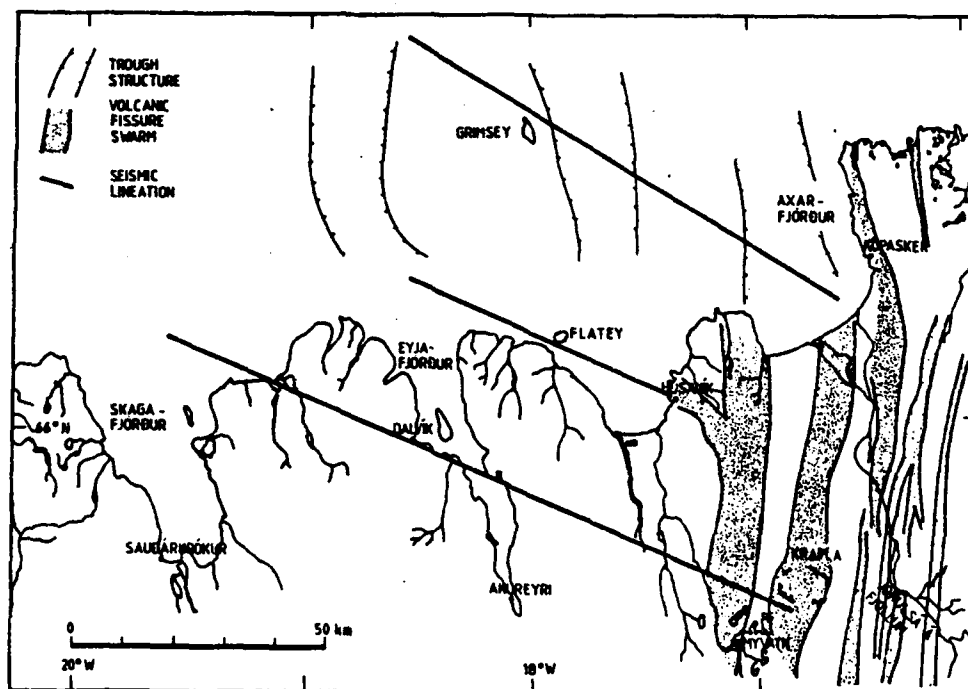


Fig.6 Main tectonic features of the North Iceland Seismic Zone with lines of seismic activity.

The January 13, 1976 Kópasker earthquake of magnitude 6.3, which is the largest, most recent earthquake in Iceland, caused moderate damage in the small fishing village of Kópasker at the eastern end of the Grímsey line. This earthquake is connected with the rifting episode in N-Iceland,

which has been in progress since 1975. The activity has been mostly confined to the Krafla central volcano and its associated fissure swarm. Extensive tensile movements have been observed in the volcanic belt north of Krafla and in Axarfjörður near Kópasker with severe land subsidence.

Amongst other big earthquakes which have occurred along the Grímsey line is the 1910 magnitude 7.3 earthquake, which originated in the ocean straight north of Tjörnes (66.5N, 17.0W). An interesting fact is that few hours later on the same day, a magnitude 5 earthquake occurred west of the toe of Reykjanes. However, no geophysical relationship is between the two earthquakes. Another Kópasker earthquake with magnitude 6, occurred in 1865 and in 1755 a big earthquake (M 7) close to Grímsey caused damage in the Skjálfandi and Eyjafjörður regions.

Along the second seismic line, which runs NWN from Húsavík across Flatey and the mouth of Eyjafjörður, the most destructive earthquake is the 1872 magnitude 6-7 earthquake which caused damage in Húsavík, Flatey and Flateyjardal where several farmhouses were destroyed.

The third speculative seismic line also runs NWN from Krafla across Eyjafjörður near Dalvík and to the mouth of Skagafjörður. On June 2, 1934, a 6, magnitude earthquake occurred near to the small town of Dalvík with considerable damage there. Besides the Kópasker earthquake of 1976, where damage was only slight to moderate, this is the last earthquake to have caused severe damage of houses and buildings in Iceland. The maximum intensity of the earthquake in Dalvík was assessed by the late professor Sigurður Þórarinnsson to be VIII-IX in Dalvík, VIII in Hrísey and upper part of Árskógsströnd. In Akureyri the intensity was assessed V. A very good contemporary description of the extent of damage to different kind of houses and buildings has been given by Sveinbjörn Jónsson, a tradesman and builder. New well-constructed concrete houses showed practically no damage whereas the typical old Icelandic houses of turf, stone and timber fared badly.

Finally, the 1963 magnitude 7 earthquake which occurred in the mouth of Skagafjörður should be mentioned. As is the case with most North Iceland earthquakes, the epicentre was off the coast in the ocean and the land intensity therefore comparatively low. The earthquake caused alarm in Sauðárkrókur where the intensity was VII and some minor damage occurred.

In Table 3, all known earthquakes to have occurred in the North Iceland Seismic Zone are listed. Obviously, earthquakes in North Iceland are rarer than in South Iceland.

TABLE 3. A list of destructive and large magnitude earthquakes in North Iceland. Assessed values are within parentheses. /1/, /2/, /9/, /11/.

DATE	LOCATION	MAGNITUDE/ Max. Intensity	NOTES
	1260		Damage in Skjálfandi region
	1584		" in Eyjafjörður "
Autumn	1618		" in Skjálfandi "
	1624		
Sept 11	1755 (66°.5N, 18°W)	(7-7.5)	" in Skjálfandi and Eyjafjörður
June 11	1838 (66°, 19°)	(6-7)	" in Skjálfandi region
Dec 30	1867		" in Skjálfandi region
April 17	1872 (66°.2, 17°.5)	(6-7)	" in Axarfjörður "
Jan 25	1885 (66°.3, 16°.7)	(6-6.5)	No damage reported
Nov 15	1905 66°, 18°	5.5/VI	Off the coast, no damage
Jan 22	1910 66°, 17°	7.3	" " " "
Aug 23	1921 67°, 18°	6.3	" " " "
June 2	1934 66°, 18°.5	6.3/X	Damage in Dalvík and Eyjafjörður
Oct 23	1936 66°.8, 17°.4	5.4	Off the coast, no damage
March 28	1963 66°.3, 19°.6	7.0	Slight damage in Sauðárkrúkur
Jan 13	1976 66°.3, 16°.5	6.3/IX	Damage in Kópasker and vicinity

#### 2.4 OTHER AREAS OF SEISMIC ACTIVITY

Intraplate earthquakes which originate outside the plate boundaries, that is the seismic zones in North and South Iceland and the volcanic zones, are rather rare in Iceland. Historic records mention seismic activity near Öræfajökull in the Vatnajökull area during the 1727 volcanic eruption there. On May 3rd 1897, a magnitude 5 earthquake occurred on the Vatnsnes peninsula which is to the west of the North Iceland Seismic Zone. This earthquake was felt over a large part of north and northwest Iceland without any significant damage.

Small earthquake swarms have several times been felt locally in Borgarfjörður in the midwestern part of Iceland. Usually, these are very low magnitude earthquakes. In the spring of 1974, one such sequence of earthquakes culminating with a 5.5 magnitude earthquake on June 12th occurred in the upper Borgarfjörður area. The epicentral region was near Sigmundarstaðir in Þverárhlið and extended about 25 km to the east. Another belt of earthquake origins was oriented in a SW-NA direction and intersected the first around the middle. The focal mechanism of these earthquakes indicates a slip-dip motion due to horizontal strain in the crust, /3/.

The largest, June 12th shock, caused slight damage, mostly cracking of poorly built farmhouses, but then the epicentre was well to the east and north of the inhabited areas in Þverárhlið and Hvítársíða. Several landslides occurred, however, as the soil was wet, especially in the northern slopes of Kjarrárdalur.

Finally, earthquakes near the insular shelf margin east of Iceland are known to happen, but damage in such "off the coast" earthquakes has never been reported.

## 2.5 MINIMUM RISK AREAS

As already mentioned, large areas of the Country can be considered to be outside the volcanic and seismic zones whereby the earthquake hazard is quite minimal in these parts. In Reykjavik, the Capital City, the western part from the old town centre, ( "Kvosin"), to and including the small suburban town Seltjarnarnes at the tip of the peninsula is unlikely to experience but small earthquake intensities. Kópavogur, Hafnarfjörður and the eastern part of Reykjavík with Mosfellsveit, however, have to be considered to be within or close to the Reykjanes and the Hengill seismic zones. Precise seismic zoning of the Capital Region, that is Reykjavík and surrounding towns has not yet been attempted but is most certainly overdue. Application of the Icelandic Aseismic Code for Structures, IST 13, /13/, is often subject to severe misunderstanding regarding which earthquake risk zone, ( the code specifies three zones of 25%, 50% and 100% risk ), should be considered for the Capital Region.

The coastal area west of Reykjavík/ Mosfellsveit through Hvalfjörður and lower parts of Mýrarsýsla, ( Akranes and Borgarnes ), is another region with very low expected earthquake intensities. From Snæfellsnes through Dalasýsla including the large region of the western fjords is another low risk zone with no history of earthquakes nor volcanic activity in historic times.

The region from the western fjords across Húnavatnssýslur to and including Blöndós is another low-risk zone with no earthquake history except for the Vatnsnes earthquake of 1897, cf 2.4.

The coastal region beginning at Rifstangi, which is the northern most tip of mainland Iceland, through the entire eastern coast and inhabited area of East Iceland is a minimum risk zone with no earthquake history nor volcanic activity in historic times. The southeastern part of the country is also a minimum risk zone, ( Hornafjörður), until the eastern volcanic zone begins near Kirkjubæjarklaustur and subsequently the South Iceland Seismic Zone.

## 3.0 SEISMIC ZONING AND AN EARTHQUAKE RISK MAP OF ICELAND

Whereas the seismic zones of Iceland are rather clearly and well defined, it is more difficult to evaluate the earthquake hazard in terms of expected intensities or maximum surface acceleration. Basically, the earthquake hazard to civil engineering and other manmade structures can be separated into two categories. Firstly, the faulting and rupturing of the ground in and near the epicentre of an earthquake can incur heavy damage in a structure built across an active fault or hit by surface rupturing. Damage of this kind can only be avoided through microzoning and a

precise geological site investigation prior to site development. Secondly, the earthquake wave motion will induce dynamical vibration response of any structure where ground shaking is severe enough. Permanent damage or even collapse of the structure can be the direct result if the surface acceleration of the earthquake is high and its frequency composition unfavourable to the structure. The main parameter governing the structural response is therefore the maximum surface acceleration of the earthquake ground motion. Since there are no instrumental strong motion records available for past Icelandic earthquakes, evaluation of seismic risk regarding maximum surface acceleration must be reflective, /12/.

The intensity of an earthquake is a measure of its effects as experienced by observers in the struck area. Intensity scales can be related to the maximum surface acceleration through knowledge of the rate of destruction caused by a certain level of acceleration. This is very problematic, however, due to many reasons. In Iceland for instance, the intensity of past earthquakes can be judged to be quite high due to the high rate of destruction. Until the beginning of this century, all houses in the seismic zones were of very poor construction, mostly simple farmhouses of turf and stone, extremely vulnerable and ill-suited to withstand earthquakes. It is therefore quite likely that the damage extent in future earthquakes of the kind which occurred in 1784 and 1896 in South Iceland will be much less. Even if seismologists have tried to take this into consideration when assessing the intensity and magnitude of past earthquakes, it is possible that their effects tend to be overestimated.

### 3.1 INTENSITY-ACCELERATION RELATIONS

Unfortunately, no strong motion accelerograph records have ever been obtained in Icelandic earthquakes. Until recently, no strong motion accelerographs had been installed. A complete strong motion network is now being installed in the South Iceland Seismic Zone and instrumental records throwing light on the surface acceleration in Icelandic earthquakes are eagerly awaited. Several attempts to evaluate the acceleration in Icelandic earthquakes, mostly based on foreign studies, have been made, /9/, /12/. They have to be taken at face value since many unknown factors have yet to be resolved. For instance, where the seismic and volcanic zones intercept like in Reykjanes and in parts of the other seismic zones, it is believed that stress relaxing in the crust takes place due to the intense subterranean heat in the volcanic rocks, thus reducing the acceleration level. Also, it has been observed that the earthquake shear waves, (S-waves), which are mainly responsible for the destruction caused by earthquakes, will propagate badly in the volcanic zones and complete S-wave shadows have been observed. In table 4, a possible connection between the Modified Mercalli Intensities (MMI) and the probable maximum surface



acceleration is given. The surface acceleration is then interpreted as the maximum horizontal component. Usually, the maximum vertical acceleration is about 60-80% of the maximum horizontal value.

Table 4. Modified Mercalli Intensities, and surface accelerations, (1 Gal = 1 cm/s<sup>2</sup> ).

MMI	II	III	IV	V	VI	VII	VIII	IX	X	XI	XII
$\alpha_{max}$	4.8	9	17	32	60	113	214	403	760	>g	>g Gals

The table reflects the fact that human perception of earthquakes will underestimate the acceleration level. It is a well known phenomenon regarding the human senses, that an increase by powers in a physical quantity, (level of acceleration, intensity of light etc.), is perceived as an increase by a constant difference (quotient series vs difference series). This phenomenon is sometimes referred to as the Weber-Fechners law of perception. In mathematical sense this can be described as follows

$$(1) \quad \alpha_{max}(I) = A 10^{\beta I}$$

where A and  $\beta$  are constants, which have been given the values A = 1.35 and  $\beta = 0.275$ .

### 3.2 INTENSITY-MAGNITUDE RELATIONS

Even if the intensity of an earthquake is a more appropriate measure for seismic risk evaluation than the instrumental magnitude, it is often necessary to use the earthquake magnitude as the basic parameter when estimating the earthquake hazard. The following relationship between Modified Mercalli Intensities, I, and the magnitude M of Icelandic earthquakes has been proposed by Halldórsson, /9/.

$$(2) \quad I_0 = 0.33 + 1.24 M$$

where  $I_0$  is the maximum MMI intensity of the earthquake. Based on historic records, the magnitude and intensities have thus been evaluated with the reservations voiced above and are shown in tables 1 and 2. After 1904, which is the beginning of instrumental records in Iceland, the magnitude assessment of Icelandic earthquakes is more or less correct.

### 3.3 EARTHQUAKE RISK MAPS OF ICELAND

Earthquake risk maps can either be based on the maximum expected surface acceleration or the maximum intensities. In both cases such maps should show contour lines with statistical values either based on certain probabilities of occurrence or values with certain average recurrence time. Unfortunately, precise statistical evaluation is made difficult because of lack of reliable data.

In Fig. 7, an attempt is made to draw up such a map of Iceland showing areas of expected maximum earthquake intensities based upon the previous discussion. The recurrence or return period of the values has not been fully established but a 100 years period can be taken as representative. Only intensities above V are considered since maximum intensities lower than V-VI are not likely to cause any damage to civil engineering structures even if sensitive equipment may possibly be endangered.

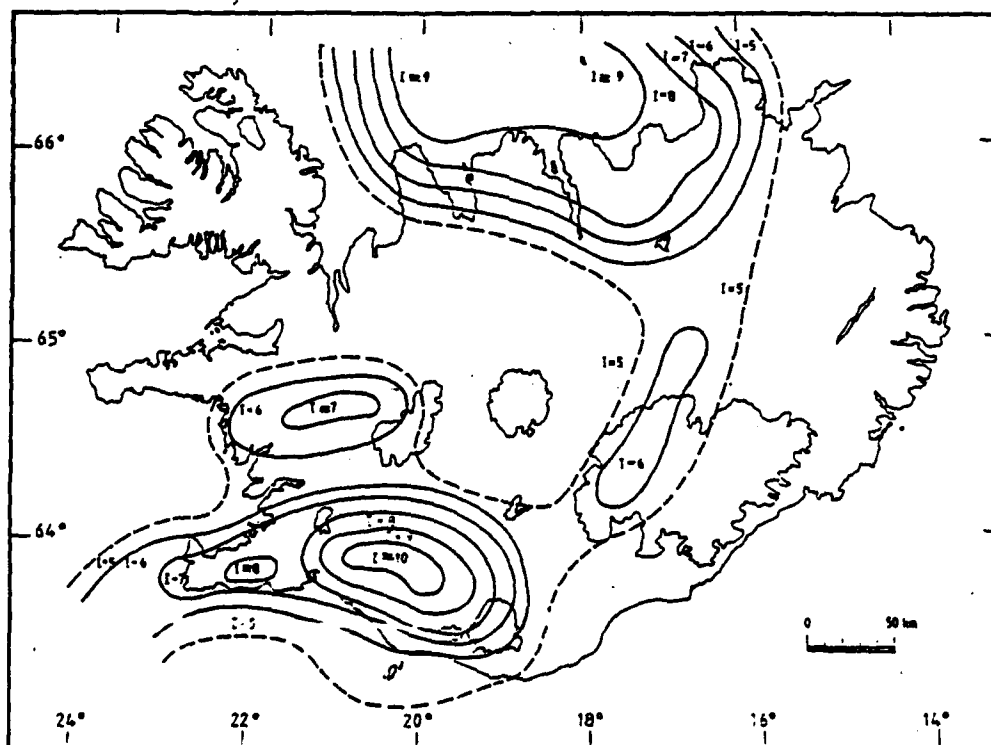


Fig.7 An earthquake risk map of Iceland. Contours of 100 years intensities V and above are shown, (guestimative).

Whereas the contour for intensity VI clearly delineates four different seismic areas, the contour for intensity V marks a single zone of earthquake activity for the whole country. The contours are drawn on a speculative basis but should give a good idea about the seismicity of the country. The inland zone delineated by the contour for intensity VI corresponds to the volcanic activity in the Vatnajökull and Askja regions and as such is without interest considering possible human development.

In Fig. 8, an earthquake zoning map for Iceland is proposed. The map is based on the previous risk map and designates four different risk zones. Firstly, for the parts of the Country outside the contours for intensities V or above, the maximum surface acceleration is put at less than 75 Gals in correspondence with the relationship between acceleration and intensities shown in Table 4. Zone 1 is therefore the minimum risk zone where civil engineering structures are not affected by earthquakes. Only in extreme cases could very sensitive equipment be affected. Zone 2 bears the risk of maximum surface accelerations up to 150 Gal., which is easily accommodated by all well designed structures. Reykjavík and vicinity falls within Zone 2.

Zone 3 covers the centre of the North-Iceland Seismic Zone, that is to the coastline, the central part of the Reykjanes Seismic Zone and most of the South-Iceland Seismic Zone. The maximum surface design acceleration is 150 - 250 Gals which can well be taken care of by properly designed structures. In Zone 4 which covers the central part of the South-Iceland Seismic Zone, the maximum surface acceleration to be expected is 250 Gals and above. Possibly very large accelerations up to 600-750 Gals can be expected in the immediate epicentral region of a major South-Iceland earthquake and extreme care should be taken with the design of all engineered and otherwise structures in Zone 4.

#### 4.0 SUMMARY AND CONCLUSIONS

Based upon historical records and instrumental data which is available for Icelandic earthquakes since 1904, a discussion of the distribution, frequency and magnitude of earthquakes in Iceland is presented. The major earthquake zones in Iceland are defined and each zone described in detail. A list of historic and recent earthquakes is given for both the North-Iceland and the South-Iceland Seismic Zones and various maps show the extent of the seismic zones. The geophysical attributes of Icelandic earthquakes and the volcanism in Iceland is also briefly discussed.

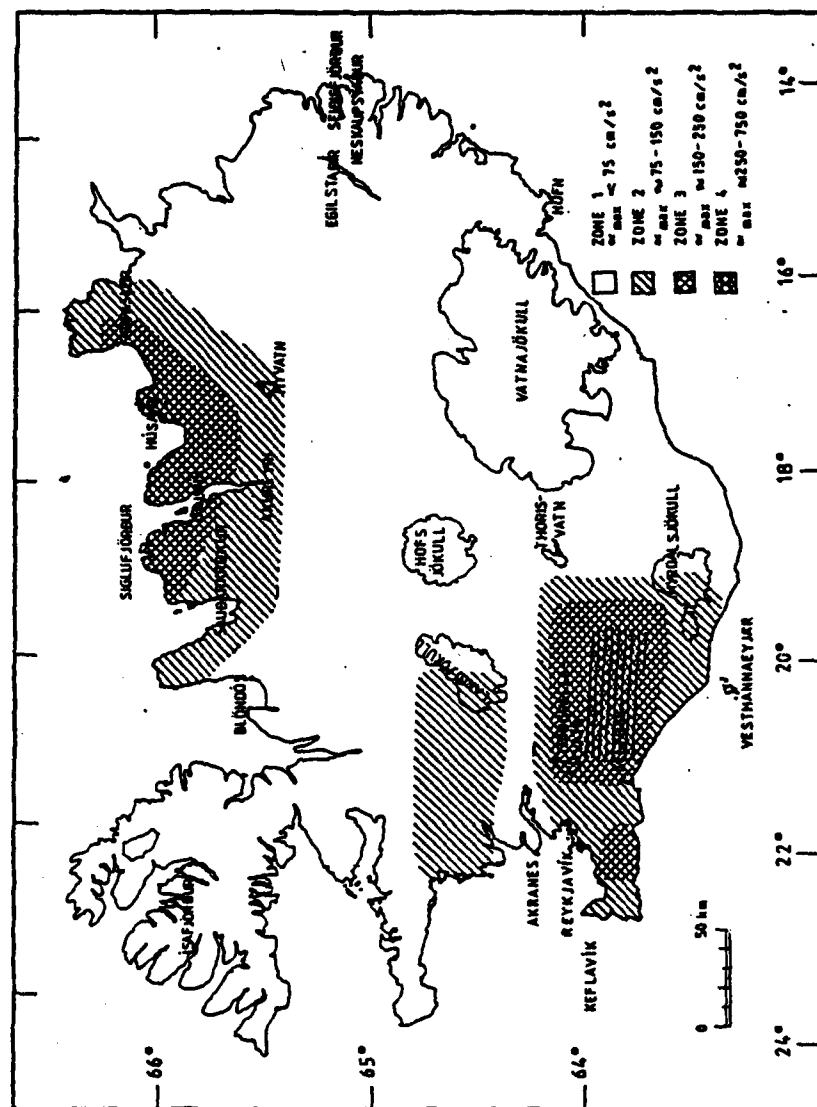


Fig.8 A proposal for an earthquake zoning map of Iceland. Maximum design accelerations are given for each of 4 zones.

Earthquake risk zoning with reference to man-made structures is proposed in terms of a contour map of expected earthquake intensities. At this stage, a complete statistical evaluation of expected values and recurrence is not available, which must be kept in mind when the results are interpreted. Finally an earthquake design zoning map is presented in terms of clearly defined zones with proposed design values for the surface acceleration to be employed.

## 5.0 ACKNOWLEDGEMENTS

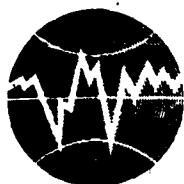
This study has been supported by the Committee on Power-Intensive Industries. Professor Öttar P. Halldórsson has given valuable advice and information for inclusion in the main text. Without his critical remarks and assistance in interpreting the often obscure and meagre data on earthquakes in Iceland, this report would have been less significant.

Ragnar Stefánsson and Páll Halldórsson of the National Meteorological Bureau in Iceland gave valuable information on the distribution and magnitude of past Icelandic earthquakes and information given by Páll Einarsson of the Science Institute of the University of Iceland is also acknowledged.

## 6.0 REFERENCES

- /1/ Tryggvason, E.S., Thoroddsen, S. and Thorarinsson, S., 1959, Report on Earthquake Risk in Iceland, (in Icelandic), Engineers Soc. Iceland, 43, pp 1-9.
- /2/ Tryggvason, E.S., 1973, Seismicity, Earthquake Swarms and Plate Boundaries in the Iceland Region, Bull. Seism. Soc. Amer., 63, pp 1327-1348.
- /3/ Björnsson, S. and Einarsson, P., 1974, Seismicity of Iceland in Geodynamics of Iceland and the North Atlantic Area, Kristjánsson, Leo (ed.), NATO ASI series C, D. Reidel, Dordrecht, Holland.
- /4/ Petersen, G. et al, 1978, A Large Earthquake in South Iceland, Report of a working group to the Civil Defense Authority in Iceland, (in Icelandic), 54 pp.
- /5/ Einarsson, P. and Björnsson, S., 1979, Earthquakes in Iceland, Jökull, 29, pp 37-43.
- /6/ Guðmundsson, G. and Sæmundsson, K., 1980, Statistical Analysis of Damaging Earthquakes and Volcanic Eruptions in Iceland from 1550-1978, Journ. Geophysics, 47, pp 99-109.

- /7/ Björnsson, S. and Einarsson, P., 1980, Earthquakes, (in Icelandic), in Náttúra Íslands, pp 121-155, Almenna bókafélagið, Reykjavík.
- /8/ Einarsson, P. et al, 1981. Seismicity Pattern in the South Iceland Seismic Zone, Earthquake Prediction. An International Review, Maurice Ewing Series 4, A.G.U., pp 141-151.
- /9/ Halldórsson, Páll et al, 1984, Evaluation of Earthquake Risk. A Report to the Committee for Site Selection of Large Industries. 52 pp.
- /10/ Einarsson, Páll, Earthquake Prediction, (in Icelandic), 1985, Náttúrufræðingurinn, 55(1), pp 9-28.
- /11/ Halldórsson, Páll, List of Earthquakes (M r 5) in Iceland 1905- 1955. A personal communication.
- /12/ Sólmes, Júlíus, 1983, Bridges and Earthquakes in South-Iceland, (in Icelandic), Report No. 83002, Engineering Res. Institute, University of Iceland.
- /13/ IST 13, Earthquakes, action and design rules. Icelandic Standards, ( in Icelandic), Iðntæknistofnun Íslands, febrúar 1976.



TURKISH NATIONAL COMMITTEE FOR  
EARTHQUAKE ENGINEERING

THIRTEENTH REGIONAL SEMINAR ON EARTHQUAKE ENGINEERING

September 14-24, 1987 - Istanbul - Turkey

EARTHQUAKE PROTECTION: SEISMIC REGIONALIZATION, SEISMIC  
MICROZONING AND ASEISMIC DESIGN TECHNICAL REGULATIONS  
PROBLEMS IN ALBANIA

Eduard SULSTAROVA  
SEISMOLOGICAL CENTER, TIRANA, ALBANIA

EARTHQUAKE PROTECTION: SEISMIC REGIONALIZATION, SEISMIC  
MICROZONING AND ASEISMIC DESIGN TECHNICAL REGULATIONS  
PROBLEMS IN ALBANIA

Eduard SULSTAROVA  
SEISMOLOGICAL CENTER, TIRANA, ALBANIA

It is presented the general strategy followed in Albania for earthquake protection and are treated the principles and the methodologies applied for the seismic regionalization of PSR of Albania on scale 1:500 000, for the seismic microzoning of the urban areas, for the new aseismic design Technical Regulations and the elimination of the earthquake consequences.

INTRODUCTION

Albania is a country with a high seismic activity, in Europe is the country which is more frequently hit by damage earthquakes, next to Turkey and Greece. The studies have proved that only during this century the earthquakes in Albania and near-by have generated 7.2% of the total energy released by all the shallow earthquakes of Europe for the same period.

At nowadays development, when the density of the population in urban areas is always increasing and when the investments realising or the ones planned to be realised in our country are too high, if we do not take the necessary precautions based on the seismological, seismological-engineering and earthquake-engineering studies against the probable events the damages will be everytime greater. In our country there are taken many measures to reduce the human losses and the material damages that may cause the eventual earthquakes.

The term " earthquake risk " may be defined as the total expected loss of life and property, loss of production and other secondary losses, caused by earthquakes to a community over a given period of time. It is function of the value of the elements at risk (human lives, buildings,



production, facilities, etc.), the vulnerability of these elements to earthquake action, and the probability of occurrence of earthquakes (the earthquake hazard).

By "vulnerability" we mean the probable degree of loss or damage to a given element at a risk due to earthquake ground motion. It cannot be expressed by a single figure, for it is a complex function of the dynamic properties of the building or structure and of the various parameters of ground motion (peak acceleration, peak velocity, displacement, frequency of vibration, duration of shaking etc.). Vulnerability is nevertheless the component of risk over which the greatest degree of control can be exercised, through the choice of construction sites and through appropriate design and construction.

Earthquake hazard is a complex function defining the probability of occurrence, at any given site, and during any given period of time, of earthquake ground motion of various intensities. Earthquake hazard is determined entirely by natural processes going on deep within the Earth's Crust and, at the present time at least, is not susceptible to human influence.

In order to assess accurately, and subsequently to control and reduce the earthquake risk to given community, it is necessary to have reliable information on the three components of risk, that is to say:

1. The value of the elements at risk,
2. The vulnerability of these elements,
3. The earthquake hazard.

#### I. EARTHQUAKE HAZARD IN ALBANIA - SEISMIC REGIONALIZATION

Earthquake hazard assessment is connected with the precision of the time and place occurrence and the strength of the future earthquake as well. Earthquake hazard cannot be changed, but it is nevertheless essential that it be accurately known, in order that the most appropriate

technical-economic measures be taken to reduce the damages that the earthquakes may cause to a point where the overall risk is brought down to an acceptable level for the society; the definition of this level is a task of considerable difficulty.

Assessing the earthquake hazard we have acted this way:

1. Data on the earthquakes of Albania (historical and instrumental)

As a result of many years work we have gathered and examined an ample material of a period of about 2000 years, on the earthquakes of Albania. All the data collected have been computed according to up to date methods, so we might compile the "Catalogue of the Earthquakes in Albania" up till 1970 (Sulstarova, E., Koçiaj, S., 1975) and the catalogue for 1971-1985 (Sulstarova, E., Koçiaj, S., 1986). At the same time we have compiled the album of the isoseismal maps, which contains the isoseismal maps of 160 earthquakes occurred during 1800-1985. The most reliable data, for which exist instrumental recordings and macroseismic information, are those of this century. For the period from 1800-1900, more or less complete data may be considered those of earthquakes of Intensity  $\geq 7$  degrees MSK-64 scale, while for the period before 1800 there are data only for the earthquakes of  $I \geq 8$  degrees MSK-64. For the period 1900-1970 there are complete data of the earthquakes of  $I \geq 6$  degrees, but for latter there are complete data, even for the weak shocks of  $I < 6$  degrees.

This publication provides complete data of the earthquakes ( $T_0$ ,  $\tau$ ,  $\lambda$ ,  $h$ ,  $M_0$ ,  $I_0$ ,) and information, from diverse point of the territory, for the shocks that were felt and the destructive ones.

In our country the seismological network is extended consisted of 13 seismological stations (the master station of Tirana and 12 secondary ones (fig. 1), which from 1975 are able to detect all the events with  $M \geq 2.5$

occurring in our country and near-by. On (fig. 2, 3) there are presented two maps of epicenters of the Albanian earthquakes; as it is seen, Albania is a country with a high seismic activity.

## 2. THE MACROSEISMIC FIELD LEVEL

The observed effect of the earthquakes on the surface is expressed in degrees (I), velocity (cm/sec), or acceleration (cm/sec<sup>2</sup>). In our country in the two latter years, we have set up a strong motion network. At present this network contains 27 accelerographs SMA-1 and 27 seismoscopes WM-II. As, up to the moment, we haven't got any information from this network, we have done the evaluation of the seismic intensity for seismic hazard studies according to MSK-1964 scale. On the basis of the best available data, specially on the earthquakes of which  $\varphi$ ,  $\lambda$ ,  $h$ ,  $M$ , and  $I_0$ , have been defined, we have found the relations between the instrumental and the macroseismic parameters (Sulstarova, E., 1986). Making use the method of the ortodox regression, for the macroseismic field, the following relations are found:

$$I_0 = 1.9M - 3.06 \log h - 0.61; \quad h \leq 10 \text{ km}; \quad 4.0 \leq M \leq 7.5 \quad (1)$$

$$I_0 = 1.75M - 4.55 \log h + 3.45; \quad 10 < h \leq 40 \text{ km}; \quad 4.0 \leq M \leq 7.5; \quad (2)$$

As average for all Albania:

$$I_0 = 2.1M - 4 \log h + 0.44; \quad 4.0 \leq M \leq 7.5 \quad (3)$$

On the basis of this relations we have concluded that in Albania and near-by shakings of 6 degrees MSK-1964 are caused by earthquakes with  $M \geq 4.9$ ; shakings of 7 degrees with  $M \geq 5.5$ , and those of 8 degrees by earthquakes with  $M \geq 6.0$ ; while the ones of 9 degrees by earthquakes with  $M \geq 6.6$ .

The foci of Albanian earthquakes are generally located in the granitic layer, therefore they are shallow foci up to 10-20 km, few earthquakes have depths exceeing 50-70 km.

For mean geological-engineering conditions are found

the relations between the surface outlined by the isoseists with magnitude (M) and the epicentral intensity  $I_0$  and for these surfaces we have found the average expected radius in which shocks with  $h \geq 10\text{km}$ , epicentral intensity  $I_0$  and magnitude (M) in our country are felt or may be felt at different range of intensity as are presented at table 1.

Table Nr. 1

M	$I_0$	Average radius in km						
		9	8	7	6	5	4	3
6.6	9	8	20	42	72	108	152	215
6.0	8	-	8	23	51	85	125	175
5.5	7	-	-	7	30	58	87	135
4.9	6	-	-	-	8	22	40	59

Graphically these quantities are represented on fig. 4.

There are found the coefficients of the attenuation of intensity along and across the extension trend of the structures (the coefficient  $\delta$ ) (Sulstarova, E., 1986).

The above parametres are of a special importance for the studies of the seismic risk and seismic hazard.

Generalizing the isoseismal maps of the strongest earthquakes, from the maximum intensity observed in all inhabited centers, from Albanian earthquakes foci maps (taking into consideration the above relations of the macroseismic field) the map of the maximum observed intensities for the period 1800-1985 was compiled (fig. 5). This map presents the maximum surface effects of the earthquakes in our country.

### 3. DISTRIBUTION IN SPACE AND TIME OF SEISMIC ACTIVITY

In the studies of seismic hazard the final objective is to define the focus, the magnitude and the time of the future event. As, up to the present time, is impossible to acco-

unt for all the processes that take place in an earthquake focus, our efforts are made to determine the average seismic hazard by combining various empiric relations and statistical models or by defining some criteria of the distribution of earthquakes in time and space. Such analysis requires homogeneity of seismological data in space, in time and within energy range. These requirements for our country can be fulfilled if we take into consideration all the events of  $M_0 \geq 6$  degrees MSK-64 for the period 1901-1985.

Frequency distribution of earthquakes as a function of their magnitude has first hand importance in the study of the seismicity of a region. Already is known the law of earthquake recurrence, which is known as the law of Gutenberg-Richter (1954):

$$\log N(M) = a - b M \quad (4)$$

The exponential function of this distribution is considered the law of earthquake recurrences. This relation, which has become very useful in statistical seismology over the last decades, is widely used in our statistical elaborations and in our studies of seismic activity.

Coefficient "a" indicates the level of seismicity of a region and is considered to be the average index of yearly seismic activity, while the coefficient "b" is considered a representative seismotectonic parameter and is directly related with the field of stresses that acts in a given region (Mogi, K., 1962, 1963; Scholz, C. M., 1968). The changes in value of this coefficient in time are used in earthquake prediction.

By the least square method and by the data of the period 1901-1985, the law of earthquake recurrence normed for a period of one year, for our country, was found to be:

$$\log N = 5.74 - 1.09M; \quad 4.6 \leq M \leq 7.0 \quad (5)$$

Whereas using the method of maximum likelihood (Utsu, T., 1965; Aki, K., 1965) the following relation was obtained:

$$\log N = 5.74 - 1.10M; \quad 4.6 \leq M \leq 7.0 \quad (6)$$

As can be seen both methods give more or less the same result. Coefficient  $b = 1.10$  approximates the world value for shallow earthquakes (Utsu, T., 1979) and the value obtained for the shallow earthquakes of Europe,  $b = 1.01$  (Karnik, V., 1979)

The relation  $\log N(M)$  is a linear one and is implied that lower and the upper limit of magnitudes is unlimited. If we take into account that the volume of the rocks in the zone of the earthquake focus, that is subject of a determined field of stresses, is limited then is comprehensible that must exist an upper limit of the magnitude, respectively  $M_{\min}$  and  $M_{\max}$ . For seismic risk analysis we are interested in the upper limit of magnitude,  $M_{\max}$ .

As a matter of fact there exists no reliable deterministic approach for an estimation of the upper bound magnitude value within a certain region. The most popular probabilistic approach is the application of the Gumbel theory of largest value. The advantage of the method is that it uses only extremes within certain intervals (generally every year), thus ignoring the influence of aftershocks and the usual incompleteness of data in the lower magnitude range.

In our country is used the first Gumbel asymptotic distribution and latter his third one; the latter being preferable because it sets an upper magnitude limit and curvature to earthquake data.

In the first Gumbel distribution the probability model of Epstein et al, (1966), have been used. For this model to be applied the supposition must be made that earthquakes are events independent of each other and constitute a Poissonian processes, which for the earthquakes in Albania is ascertained (Sulstarova, E., 1975, 1980). From this model we have obtained the relation:

$$\log N = 3.96 - 0.80M; \quad 4.6 \leq M \leq 7.0 \quad (7)$$

According to the above relations (5, 6, 7) can be found: the average number of earthquakes for every range of magnitudes, the average period of their recurrence (in years) with magnitude greater than  $M$  ( $T_M = \frac{1}{N(M)}$ ), the maximum yearly magnitude which can be observed more frequently ( $\bar{M} = \frac{\log \alpha}{\beta}$ ) and the seismic hazard for all the country as a probability of the occurrence of an earthquake with greater or equal magnitude  $M$ , for  $D$  years according to the following formula:

$$R_D(M) = 1 - \exp(-\alpha D^{-\beta M}) \quad (8)$$

$\alpha$  and  $\beta$  are coefficients found with the method of the least squares and have the respective values:

$$\alpha = 9119,025; \beta = 1.8437; \text{ in formula (7) } a = \frac{\ln \alpha}{\ln(10)};$$

$$b = \frac{\beta}{\ln(10)}$$

By using equation (8) we can see that in our country 7 degree's earthquakes ( $M \geq 5.5$ ) should be expected every 5 years, earthquakes of 8 degrees ( $M \geq 6.0$ ) every 10 years, while 9 degrees' earthquakes ( $M \geq 6.6$ ) every 30 years (probability 80-97%).

The first distribution of extrem values at the upper bound, as mentioned above, is limited. In regard to the fact that for every region must exist an upper  $M_{\max}$ , which is determined by the dimensions and the physico-mechanical properties of the bloc or microplate where is going to generate the future earthquake as well as seismic energy accumulated, recently the third Gumbel asymptotic distribution is used:

$$\Phi_{F(X)}^{III} = \exp \left[ - \left( \frac{\omega - x}{\omega - u} \right)^k \right]; \quad (9)$$

where  $K > 0$ ;  $x \leq \omega$ ;  $u < \omega$ ;  $\omega$  - is the upper magnitude limit;  $K = 1/\lambda$  is the shape parameter,  $u$  - is the characteri-

stic largest value. It follows that:

$$\phi_{F(u)}^{III} = e^{-1}, \quad \phi_{F(\omega)}^{III} = 1.0$$

The three parameters were calculated by the least square method for the data of the period 1901-1985 (Sulstarova, E., Koçiaj, S., 1986); annual intervals were used. The curve of the third asymptotic distribution defined by  $\omega = 7.46$ ,  $\lambda = 0.26$   $k = 3.83$  and  $u = 4.99$  fits the observed data quite well. They can be used for the calculation of some useful quantities, for instance of the return periods or of the largest magnitudes which can be exceeded with a given probability in the future (the interval should not be longer than the observation interval) or of the expected largest magnitude or of the most probable largest (mode) within the next  $n$  years.

The probability of a magnitude to be equal or greater than  $M$  will be:

$$P(M) = 1 - \phi_{F(x)}^{III} \quad (10)$$

The return period of shocks with magnitude equal or greater than a given threshold values is defined as:

$$T = \left( 1 - \phi_{F(x)}^{III} \right)^{-1} \quad (11)$$

The value  $\omega = 7.46$  can be considered as the magnitude of the largest possible event in Albanian area.

When applying the results we must take into account that the Gumbel theory is based on several assumptions:

- the conditions prevailing in the past must be valid in the future;
- the largest events observed in a given interval are independent;
- the behaviour of the future largest events will be similar to that in the past.

According to the algorithm proposed by Rocca et al (1984),



based on the third Gumbel distribution, Koçiaj, S., (1986) prepared a programme and with the data of 1800-1983 has compiled the map of the maximum expected magnitudes (fig. 6). According to this map the maximum expected magnitude is  $M_{\max} = 7.1 - 7.5$

#### 4. GEOLOGICAL CRITERIA OF THE SEISMICITY OF ALBANIA

The period of seismological recordings (historical and instrumental) is relatively short and consequently is difficult to decide for the seismic activity of a country only with the seismological data, and moreover for the strongest probable earthquakes the recurrence period of which is relatively long.

The earthquakes are phenomena accompanying the present geological situation, manifestations of the deep tectonic processes. There is a close connection between the earthquakes and the neotectonic structure which crops up on the surface. The earthquakes lead to new changes in the geological structure, therefore to evaluate the seismic hazard, is indispensable to carry out special geological, geophysical and geodetic studies.

Intending the study of the seismicity in Albania, we have carried out special seismotectonic studies, and widely used the geological and geophysical studies on the geological and tectonic construction of our territory carried out by other specialists.

The geodetic studies on today Earth's Crust movements, in our country, are at their beginning. In some zones of Vlora, Durrës and Shkodra are set up special geodetic networks.

The seismotectonic (Aliaj, Sh., 1980, 1983, 1986), geophysical and earthquakes focal mechanism studies (Sulstarova, E., 1980, 1983, 1986), have indicated that our territory and near-by is divided in some blocks or "microplates" by deep faults with NW and NE extension. The seams that border these "microplates" (longitudinal and transversal deep fault zones) are seismogenetic structural elements. The main cause of seismic activity in these borders is the

collision between the two great plates, the Euroasiatic and African ones. In this process an important role is played by the "Adriatic promontory" of the African plate which, due to its northern motions, <sup>in</sup> our territory and nearby exerts stresses and is responsible of the seismic activity of our country.

Confronting the fault zones with earthquakes generated by them, we have determined the seismoactive deep fault zones in Albania, their expected seismic energy and their respective mechanism (fig. 7) (Sulstarova, E., 1986).

Based on the geological and tectonic structure of our country, on the dimension of the micropates and the seismological data as well, the maximum magnitude of earthquakes in Albania should not exceed  $M_{\max} \approx 7.2$  (Sulstarova, E., 1975, 1983).

#### 5. THE MAP OF THE ZONES OF EARTHQUAKE FOCI OF ALBANIA ON THE BASIS OF SEISMOLOGICAL AND GEOLOGICAL DATA

According to the seismotectonic and seismological data we have compiled the map of the zones of earthquakes in Albania with the respective dimensions and seismic energy (fig. 8) (Sulstarova, E., et al., 1980, 1982).

#### 6. THE MAP OF THE SEISMIC REGIONALIZATION OF THE PSR OF ALBANIA

From the map of the zones of earthquake foci (fig. 8) according to the average radius of the attenuation of intensity from the focal zone, we have compiled the map of seismic regionalization of the PSR of Albania on scale 1: 500 000 (fig. 9).

This map is compiled according to the principle that an earthquake may occur at every point of the focus.

The map of seismic regionalization represents the maximum expected intensity for mean soil conditions

expressed in degrees according to MSK-1964 scale.

For mean soils we have accepted the soils of most inhabited centers of our country (most ordinary soils), where the basic intensity is equal to the maximum intensity observed: thick loose quaternary deposits of deep level of underground waters, below 5 m from the surface of the earth, (sands, fine sands, clay fine, clay gravel). These soils are situated at the field part of the country. In this category we have also included the hard and semi-hard rocks at a relief mean differentiated.

At the seismic map there are distinguished three categories of zones, zones with I-VIII, VII, VI degrees (MSK-64). At some strong focal zones, due to bad soil conditions, the seismic intensity, may attain up to 9 degrees. The seismic map represent the expected seismic hazard in Albania for the 100 future years.

## II. SEISMIC MICROZONING OF URBAN AREAS

As we have mentioned above (part I), seismic zoning provides information for the distribution in space and time of the expected seismic hazard relatively in large zones. Most of the studies carried out in our country and in others, dealing with distribution of the damages by large earthquakes, indicate that large differences in the extend of damage often occur over relatively short distances, that the areas of intensive damage are highly localized and that the amount of damage may change abruptly over distances as short as 0.5 to 1 km. Damages to engineering structures caused by earthquakes is known to depend on some factors, which are: seismological ones - amplitude, frequency, time duration of strong motion, engineering-geological - the concrete soil conditions and constructive - the type of the engineering structures and the building materials. Therefore evaluating the real seismic hazard at an area where is foreseen to build engineering structures

with special economic or political importance or merely for urban planning, it is indispensable to be carried out detailed seismological, engineering-seismological and complex engineering-geological, geophysical studies, called seismic microzoning studies based on the seismic regionalization. Thus, to determine the seismic hazard of an urban area, we have to find the superficial effect that may cause all the earthquake foci of this zone or the seismogenic zones as it is shown at fig. 10.

At our country such studies have begun at 1981, and are realized as presented on flow diagram fig. 11.

1. The seismological, neotectonic (using the microtectonic method) and the seismotectonic studies of the surrounding zone of the site (with a ray that goes to 50 km) on scale 1:500 000

The seismological studies aim to explain the historical and recent activity and its trend at a region subject to our study. From these studies we determine:

- a - Earthquake source mechanism,
- b - maximum expected magnitude,
- c - the attenuation of the energy from earthquake foci to the site,
- d - amplitude and the frequencial content of the representative earthquake (short or long distant),
- e - active fault zones,
- f - from them are selected the accelerograms as input data, which serves to calculate the real seismic hazard.

2. Complex engineering-geological, geophysical and hydrological studies of the site on scale 1:10 000

These studies include: neotectonic, engineering - geological, geomorphologic, hydrogeologic, shallow bore holes, elemetrometric surveying, seismic refraction, electric and accoustic measurments and velocity measurment as well. There are also included in-situ and laboratory tests. From them we made known:

- a - Topographic configuration of the bedrocks,

- b - thicknesses and the kind of the deposits situated on the bedrocks,
- c - physical-mechanical and dynamic properties of the soils of each layer or sublayer,
- d - respective geotechnical models.

3. Engineering-Seismological studies of the site on scale 1:10 000

In these studies there are included: Vs and Vp surface and bore holes measurements, microtremor and small earthquake measurements, analytical studies for the dynamic behaviour of soils, and studies on the damage caused by past earthquakes. These studies aim to evaluate, instrumentally and analytically, the actual influence on the local ground shaking. From them are obtained:

- a - the increase intensity in degrees as regard the etalon ground,
- b - based on the selected representative accelerogram for the bedrocks (we have selected the one recorded during the main shock of April, 15, 1979 earthquake:  $M = 7.2$  at the bedrocks of Ulgini and on the geotectonic models of the urban area, which represent L(W) filters that modify this accelerogram B(W), as it is shown at fig. 12; We could do the analytical evaluation of strong motions by means of acceleration response spectra (SA), the velocity (SV), the displacement (SD) and the Furje spectra (FL).

These results are confronted with the damages caused by earthquakes in the past.

Based as above, we compiled the seismic microzoning maps of some urban areas in different variants. The more important are two:

First variant - is based on the methods taking into account the elastic behaviour of the soils; in this case the evaluation of the seismic intensity is calculated in degrees (MSK-1964 scale).

In this variant the seismic intensity, given by the map of the seismic regionalization for the concrete zone is precised basing on three methods:

- a - on the complex engineering geological method - at this case increase intensity varies  $\pm 1$  degree in regard to the mean soils (as shown on the map of the seismic regionalization) and according to the given geotechnical model.
- b - on acoustic impedance method and to the hydrogeological conditions, (Medvedev, S.V. 1977).
- c - microtremors method, based on the maximum amplitudes and on the predominant periods of the microtremors (Konaf, K., Tanaka, T., 1961, Kanai, K. et al., 1965).

From these three methods we may find the mean value of increase intensity as regard the mean soil condition.

Second variant is based on the methods which take into consideration the nonelastic behaviour of the soils (elasto-plastic behaviour of the soils). These methods are analytical ones. At this case are used such parameters as acceleration, velocity, displacement or their response spectra.

At this present phase, the response spectra are determined by the analytical accelerograms resulting by the computation of the dynamic behavior of the geotechnical models under expected seismic excitation.

Based on the acceleration response spectra, the soils of our threetowns Vlora, Durrës and Shkodra may be divided in three categories.

In the microzoning maps are presented also the geological phenomena which may create undesirable effect during an earthquake as:

- alluvial and deluvial covers,
- active and tectonic faults,
- new archeologic deposits,
- water saturated sand zones, soft clay, mud and torfe where may be created the phenomenon of liquefaction and thixotropy.

### III. SOME CHARECTERISTICS OF THE NEW ASEISMIC DESIGN TECHNICAL REGULATIONS

The first aseismic regulation for constructions based on the static method were adopted in 1952. At 1963, based on the dynamic method, were approved new aseismic design technical regulations which, taking into consideration the engineering analysis of the consequences of the earthquakes, and specially of the one of April 15, 1979, at 1978 and 1981 were revised and had some improvements.

The high rythmes of buildings lay down the necessity to know better the earthquakes action to the structures and to adopt more justifying technical and economical criteria in aseismic design. Based on our experience and the experience of other countries we have compiled a draft aseismic design Technical Regulations.

The purpose of these new Technical Regulations, combining the technical criteria with the economical ones, is, at first, to secure the life of the people and to reduce at the maximum possible the material damages that may be caused by earthquakes. Their aim is that the constructions may resist:

- a - to the earthquakes of a low intensity, which are very frequent in our country, without damages;
- b - to the earthquakes up to 8 degrees, without important structural damages;
- c - to the large earthquakes, without heavy destructions or heavy damages.

In general they aim, at probable events, that the constructions may stand utilizable (without repairs or partial repairs) after them.

From the engineering point of view the aseismic constructions may be realised conceiving such suitable constructions able to absorbe the seismic energy trasmeted through their foundations without distructions or heavy damages. It is aimed to be attained since at architectural treatment making an effort to arrange the building

configuration to be simple, to have the masses and rigidities to be symmetrical and uniformly distributed and to avoid irregular shapes, any abrupt change in elevation plan.

At the new Technical Regulations we have decided for a unique calculation method for various types of constructions based on the modal analysis method.

Parallely to the adoption of the standard design spectra, computations using suitable and sintetic accelerograms will be used.

As regards to the general aspects of the calculations, we have conserved the concept of the direct calculations method of seismic forces at different points (levels) of the analysed structures. The design seismic forces  $S_{ki}$  at the point (level) "k" that corresponding to the  $i^{th}$  mode of the free vibrations of the structure is obtained from the formula:

$$S_{ki} = K_s k_r k_d \psi \beta_i \gamma_k Q_k \quad (12)$$

where:

$Q_k$  - gravitational load concentrated at point (level) k;

$K_s$  - seismic coefficient which is determined taking into account the seismic intensity of the urban area, according to the seismic regionalization or seismic microzoning maps, and the concrete conditions as given at the table nr. 2 below:

THE VALUE OF THE COEFFICIENT  $K_s$

Table Nr. 2

The category of the soil	Seismic intensity in degrees (LEK - 1964 scale)		
	7	8	9
I	0.08	0.14	0.23
II	0.11	0.22	0.35
III	0.14	0.25	0.42



$k_r$  - importance factor, as regard to the importance, the constructions are classiflicated into 5 groups and, according to these groups, the value of this coefficient varies from 0.5 (fifth group) to 1.75 (first group);

$k_d$  - allowed damage factor, the value of which varies from 0.25 to 1.0; 1.0 is the construcion where are not allowed residual deformations;

$\psi$  - which takes into account the material and structure type, the values of which varies from 0.8-1.7 (the factors  $k_d$  and  $\psi$ , which may be compacted in a single one, account for the ductility and damping in the construcion);

$\beta_i$  - dynamic coefficient determined as function of the period of own vibrations of the system,  $T_i$ , and the natyre of fondation soils by curves fig. 14 (as it is seen, we thought to take into consideration the influence of the soils conditions twice: at  $k_g$  and  $\beta_i$ );

$\eta_{ki}$  - coefficient depending on the deformation curve of structure at  $i^{th}$  mode of vibrations and on the point of application of the load  $Q_k$ .

The formula (12), proposed to calculate the seismic forces, allow possible improvements that may be made to its coefficients. Special structures with horizontal member spanning more than 20 m will be calculated considering the vertical seismic action as well. In these cases  $\beta$  is proposed to be taken as 2/3 of its value in the case of the horizontal action.

It is proposed that the combination of modal values be carry out by taking the square root of the sum of the squares of each of the modal values. Also, it is porposed that the combination of design loads, due to the action of the seismic horizontal component (referring to x and y axes) and vertical one (referring to z axis), be carry adding the design loads, due to the seismic action according to one axis with those due to two other ones, reducing the latters by the coefficient  $\lambda \leq 0.3$ .

For all kinds of constructions great importance is attached to the problems and technical structural precautions.

#### IV. ON THE LIQUIDATION OF THE CONSEQUENCES OF THE EARTHQUAKES

Since the liberation of the country on November 29, 1944 the consequences of the earthquakes are completely liquidated, within a short period of time, with the expenses of the state and the contribution of all our society.

Here is an example: The earthquake of April 15, 1979,  $M=7.2$ , the epicenter of which were near our Northwestern border, at Monte Negro (Yugoslavia), in our country rased to the ground or made unfit for use 17122 houses, economic and social-cultural buildings in 551 villages and some towns like Shkodra, Lezha, Shëngjin and Rrëshen. 100 000 inhabitants were left homeless.

For the elimination of the consequences of this earthquake there were involved 25 000 persons, who liquidated completely its consequences for 5 months, on october 1, 1987. Many new villages and many new quarters in the affected towns were set up.

For the liquidation of the consequences of the earthquakes we use to act like this:

- the local state organs with the aid of central ones take immediat measures and give the first help to the affected people;

- a special group of experts as engineers, technicians, etc. is set up, their task being to point out the damages caused in every object and compile the respective documentation;

- the respective Design Institutes set up special working groups, who study and design the objects to be builed and compile the respective projects for the necessary repair. Following the projects, the building materials are to be calculated.

According to the terms defined by the Council of Ministers in the decision for the liquidation of the consequences, the number of the participants in the work is determined, and other necessary planifications are made as well.

A special enterprise, set up for the purpose, takes all the measures for the elimination of the consequences.

#### REFERENCES

- Aki K., (1965), "Maximum likelihood estimate of  $b$  in formula  $\log H = a - b M$  and its confidence limits", Bull. Earthq. Res. Inst. Tokyo Univ., 43, 237-239.
- Aliaj Sh., (1979), "Seismotectonic and the geological criteria of the seismicity of Albania", Thesis, Seismological Center, Tirana, 270p (in Albanian).
- Aliaj Sh., (1983), "The main seismotectonic characteristics of Albania", The earthquake of April 15, 1979; Academy of Sci., Seismological Center - pp 358-384
- Aliaj Sh., (1987), "Seismoactive faults in Albania, Buletin i Shkencave gjeologjike nr. 2 pp 123-135 (in Albanian).
- Bejleri G., Doraci D., (1983), "Conclusions regarding the damage caused by the April 15, 1979 Earthquake and our experience of work for the liquidation of its consequences", The earthquake of April 15, 1979; Academy of Sci. Seismological Center - pp 478-498.
- Epstein B., Lomnitz C., (1966), "A model for occurrence of large earthquakes", Nature, 211, 5052, pp. 954-956.
- Gumbel E. J. (1962), "Statistics of extremes", New York, Columbia University Press.
- Karnik V., (1979), "Large European Earthquakes of the 20<sup>th</sup> century", Tectonophysics, 53, pp 159-169.
- Koçiaj S., (1986), "The seismic hazard of Earth Crust in Albania and its precision in building site" Ph. D. Thesis, Academy of Sci. PSR of Albania, Tirana, pp 270

- Mogi K., (1962), Study of elastic shocks caused by fracture of heterogeneous materials and its relations to earthquake phenomena\*, Bull. Earthq. Res. Inst. Tokyo Univ., 41, 595-614.
- Mogi K., (1963), The fracture of semi-infinite body caused by an inner stress origin, its relations to the earthquake phenomena (second paper), Bull. Earthq. Res. Inst. Tokyo Univ. 40, 125-174.
- (1987), On aseismic calculation of construction Technical Report, Seismological Center, Tirana, p 187 (in Albanian)
- (1983), "The seismic microzoning of Vlora town", Report, Seismological Center, Tirana, (in Albanian).
- (1984), "The seismic microzoning of Burrësi town", Report, seismological Center, Tirana, (in Albanian).
- (1985), "The seismic microzoning of Shkodra town", Report, Seismological Center, Tirana, (in Albanian).
- Roca A., Laper A., Surinach E., (1984), "Application of the Gumbel III law to seismic data from Southern Spain", Engineering geology, vol. 20, nr. 1/2.
- Scholz C.H., (1986), "The frequency-magnitude relation of microfracturing in rock and its relation to earthquake", Bull. Seism. Soc. Am., 58, 319-415.
- Sulstarova E., (1974), "The Albanian Seismicity" Thesis, Academy of Sci., Seismological Center, Tirana, 170p (in Albanian)
- Sulstarova E., Koçiaj S., (1975), "Catalogue of earthquakes of Albania", Academy of Sciences, Seismological Center, Tirana, p. 224 (in Albanian).
- Sulstarova E., Koçiaj S., Aliaj Sh., (1980), "Seismic regionalization of the PSR of Albania", Academy of Sciences, Seismological Center, Tirana, 297p.
- Sulstarova E., Koçiaj S., Aliaj Sh., (1982), "Map of earthquake foci in Albania", Final Report of WG A of UNDP/UNESCO project RER/79/014, Paris UNESCO.
- Sulstarova E., Koçiaj S., (1986), "Catalogue of earthquakes of Albania for the years 1971-1985",

Academy of Sci., Seismological Center, Tirana,  
(in Albanian).

Sulstarova E., (1986), "The focal mechanism of earthquakes  
and tectonic stress field in Albania" Ph. D.,  
Thesis, Academy of Sci. PSR of Albania, pp 228  
(in Albanian).

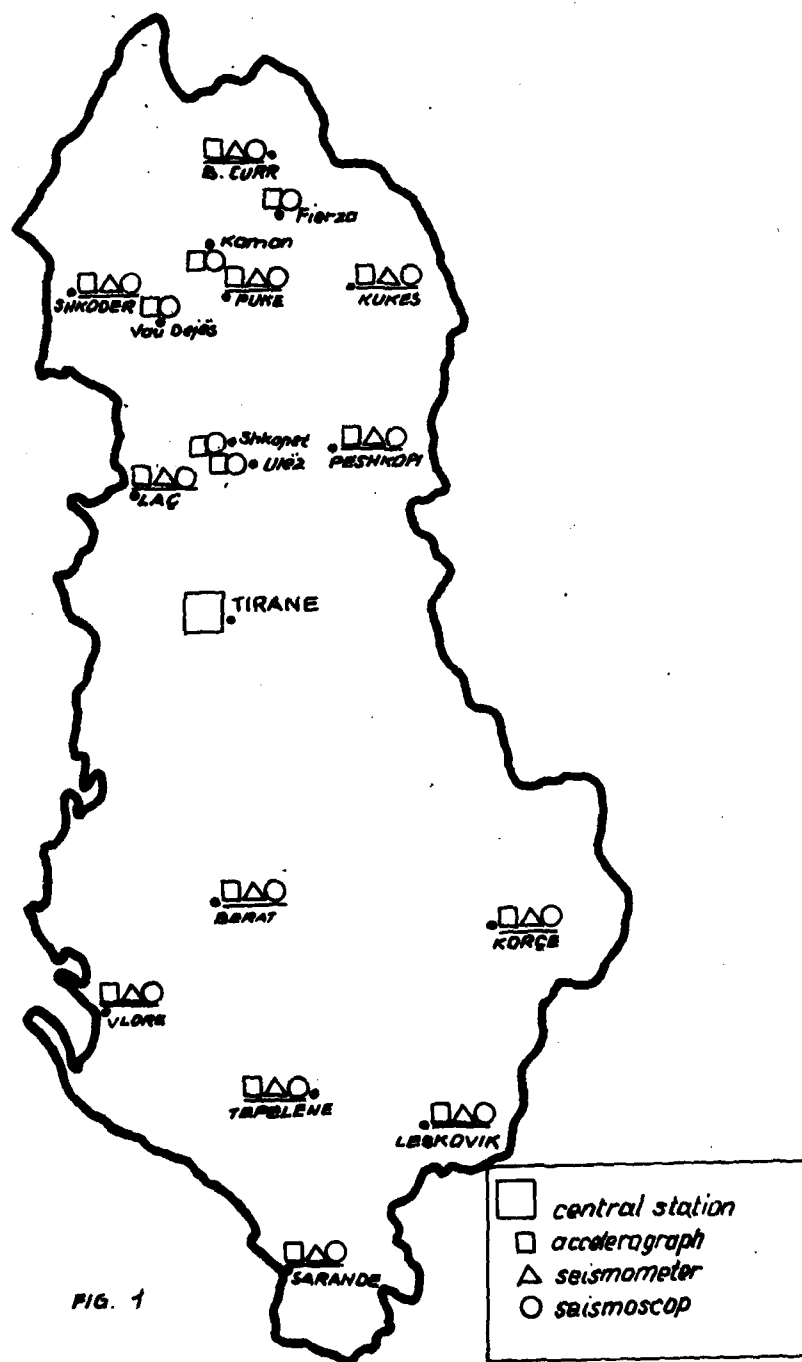
Utsu T., (1965), A method for determining the value of  $b$   
in formula  $\log n = a - b M$  showing the magni-  
tude frequency relation for earthquakes. Geophys.  
Bull. Hokkaido Univ. 13, 89 - 103.

Utsu T., (1971), Aftershocks and earthquake statistics (III).  
J. Fac. Sci. Hokkaido Univ. Geophys. 3, 379-441.

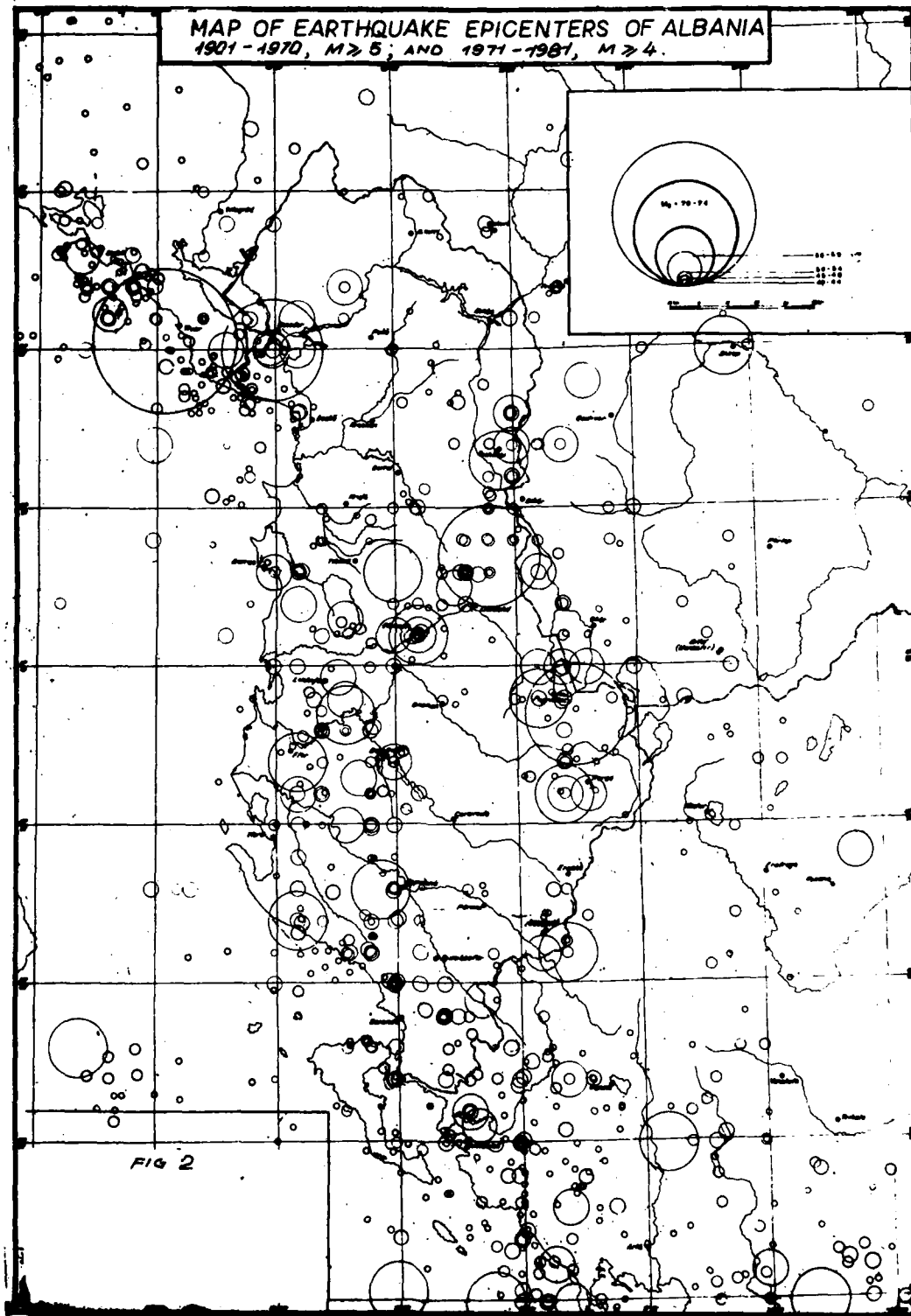
### List of Illustrations

- Fig. 1 - The Seismological and Accelerographic Network of the PSR of Albania.
- Fig. 2 - Map of Earthquake Epicenters of Albania (1901-1970,  $M \geq 5$  and 1971-1981,  $M \geq 4$ )
- Fig. 3 - Map of Earthquake Epicenters of Albania for the Period 1977-1985  $M \geq 2.5 \pm 0.3$
- Fig. 4 - Observed and expected average epicentral radius for which the shocks in  $h=10$  km depth, with a maximum intensity  $I_0$ , are felt or may be felt, with different intensity  $I$ , in Albania and nearby.
- Fig. 5 - Maximum Intensity Observed in Albania for the Period 1800-1980
- Fig. 6 - The Map of the Maximum Magnitudes  $M_{max}$ , the Third Distribution of the Extreme Values According to Data of 1980-1983  $M \geq 5.1$
- Fig. 7 - Fault zones in Albania and Today Tectonic Field According to the Focal Mechanism and Macroseismic Field.
- Fig. 8 - Zones of Earthquake Foci of Albania on the Basis of Seismological and Geological Data.
- Fig. 9 - Map of the Seismic Regionalization of the PSR of Albania
- Fig. 10 - Seismic Hazard Evaluation of a Site
- Fig. 11 - Complex Seismological Engineering Works for the Seismic Microzoning of an Area (block diagrams)
- Fig. 12 - Schematic Illustration for the Evaluation of Strong-Motion at a Site.
- Fig. 13 - The Map of Seismic Microzoning of Shkodra Town
- Fig. 14 - The Curves of Dynamic Coefficient  $\beta$  for Soils of Different Categories

THE SEISMOLOGICAL AND ACCELEROGRAPHIC  
NETWORK OF THE P.S.R. OF ALBANIA



MAP OF EARTHQUAKE EPICENTERS OF ALBANIA  
1901-1970,  $M \geq 5$ ; AND 1971-1981,  $M \geq 4$ .





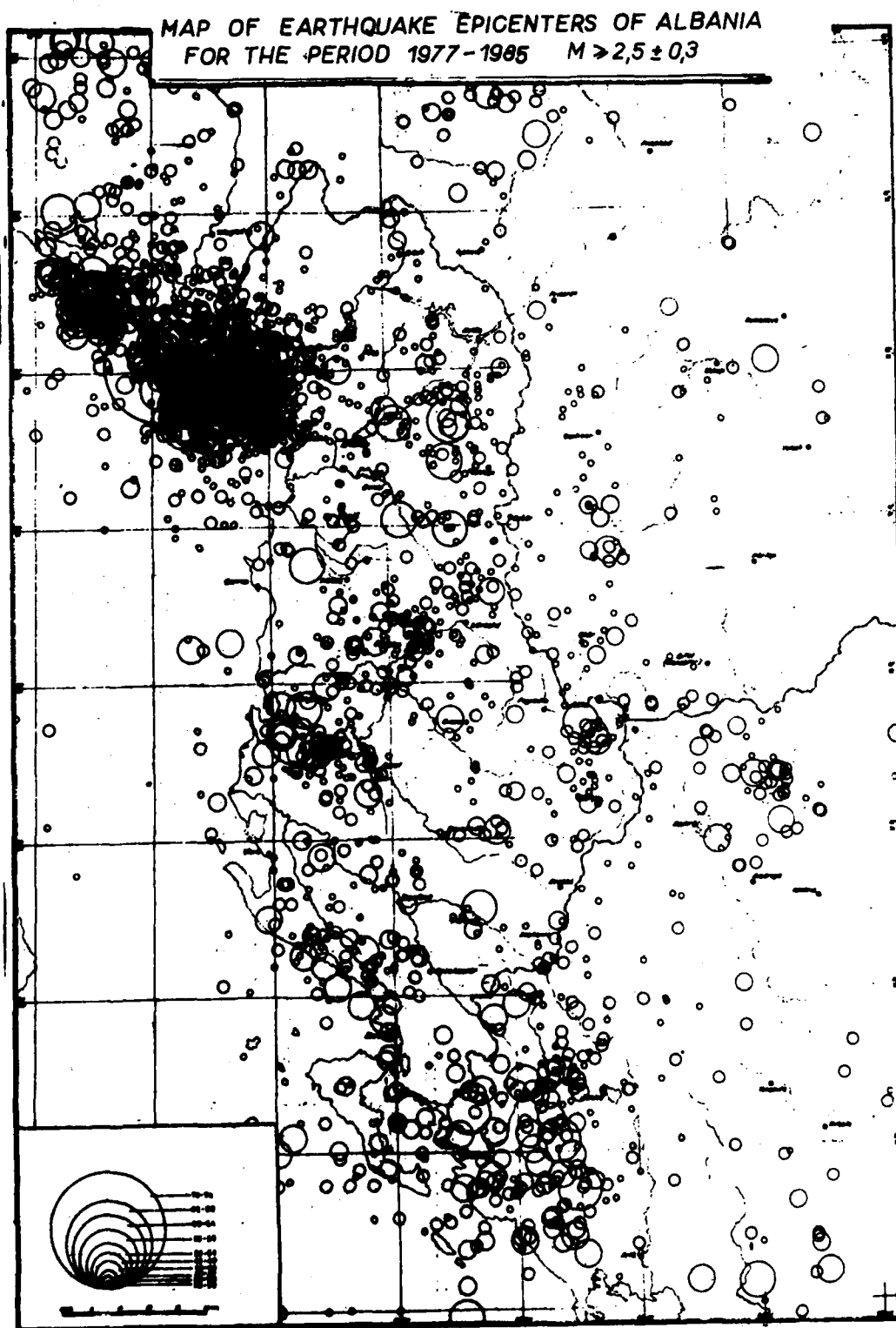


FIG. 3

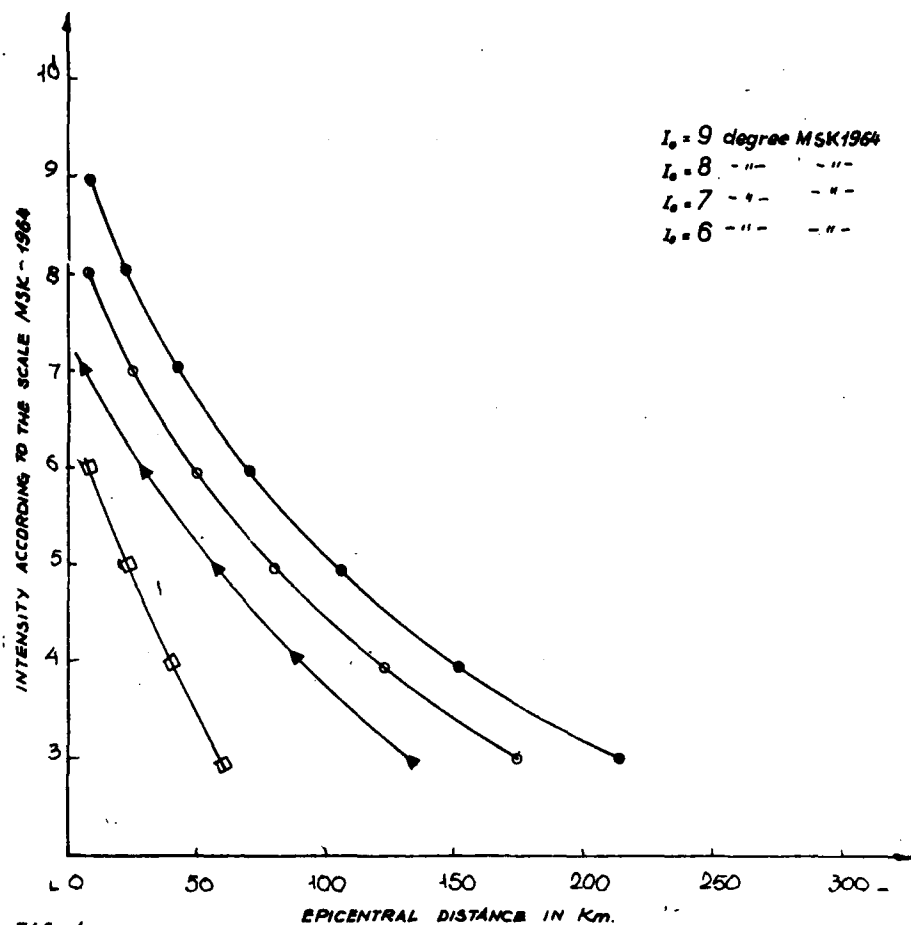
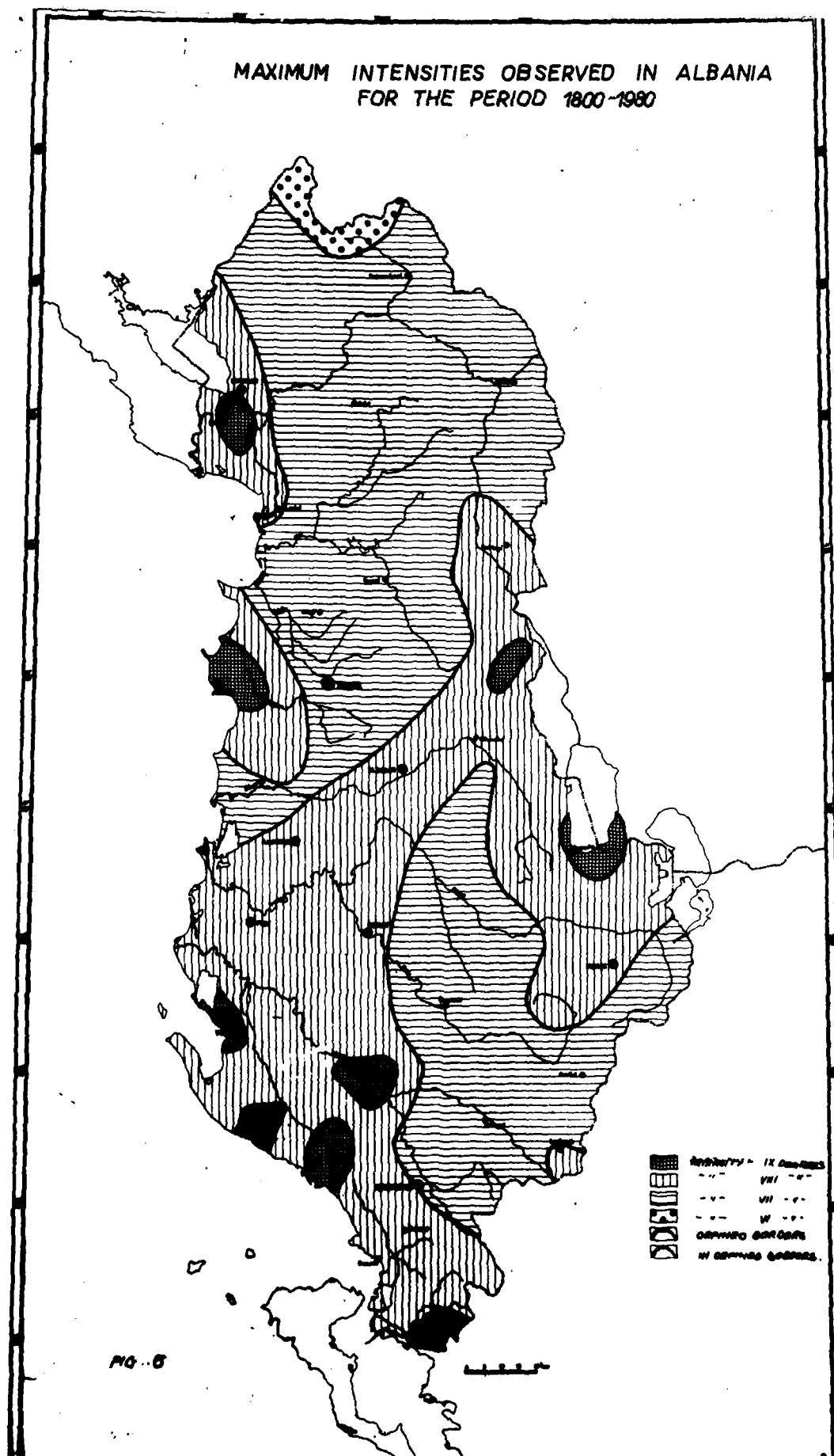


FIG. 4

Observed and expected average epicentral radius for which the shocks in  $h=10$  Km depth, with a maximum intensity  $I_0$  are felt or may be felt, with different intensity  $I$ , in Albania and near-by.

MAXIMUM INTENSITIES OBSERVED IN ALBANIA  
FOR THE PERIOD 1800-1980



THE MAP OF THE MAXIMUM MAGNITUDES ( $M_{max}$ )  
THE THIRD DISTRIBUTION OF THE EXTREME  
VALUES ACCORDING TO THE DATA OF  
1980 - 1983 FOR  $M \geq 5,1$

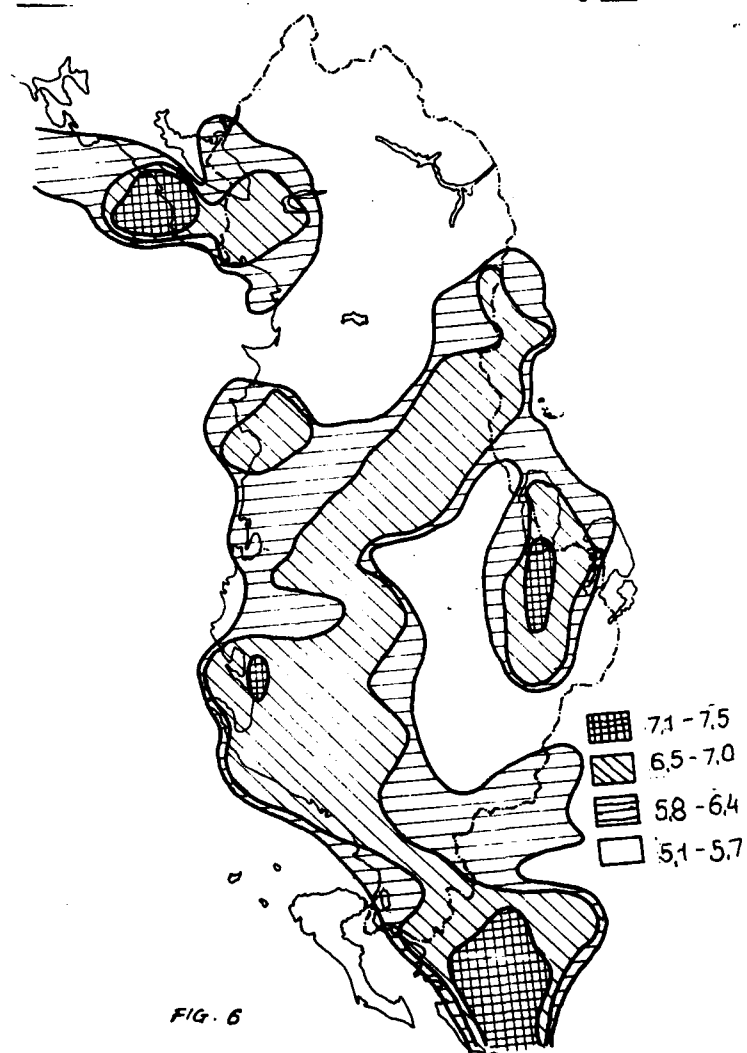


FIG. 6

FAULT ZONES IN ALBANIA AND TODAY TECTONIC  
FIELD ACCORDING TO THE FOCAL MECHANISM  
AND MACROSEISMIC FIELD

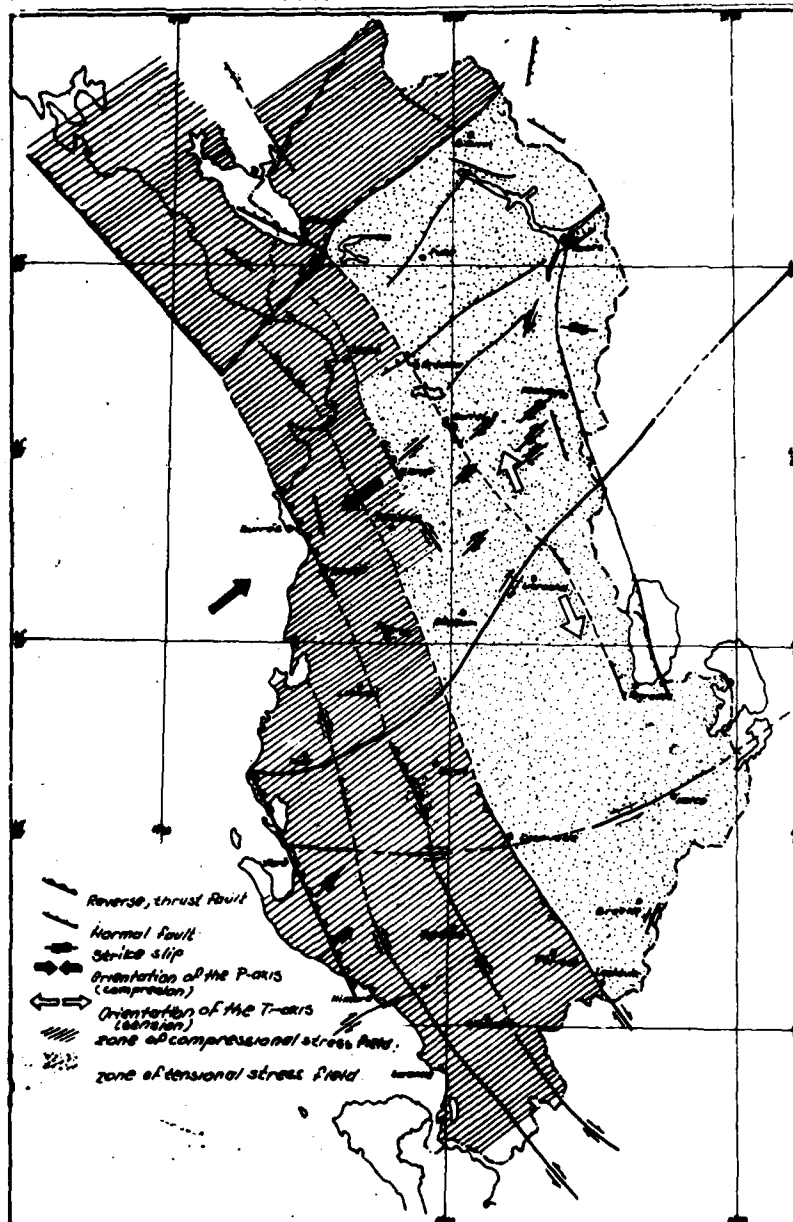


FIG. 7

Fig. 8

ZONES OF EARTHQUAKE FOCI OF ALBANIA ON THE BASIS OF SEISMOLOGICAL AND GEOLOGICAL DATA

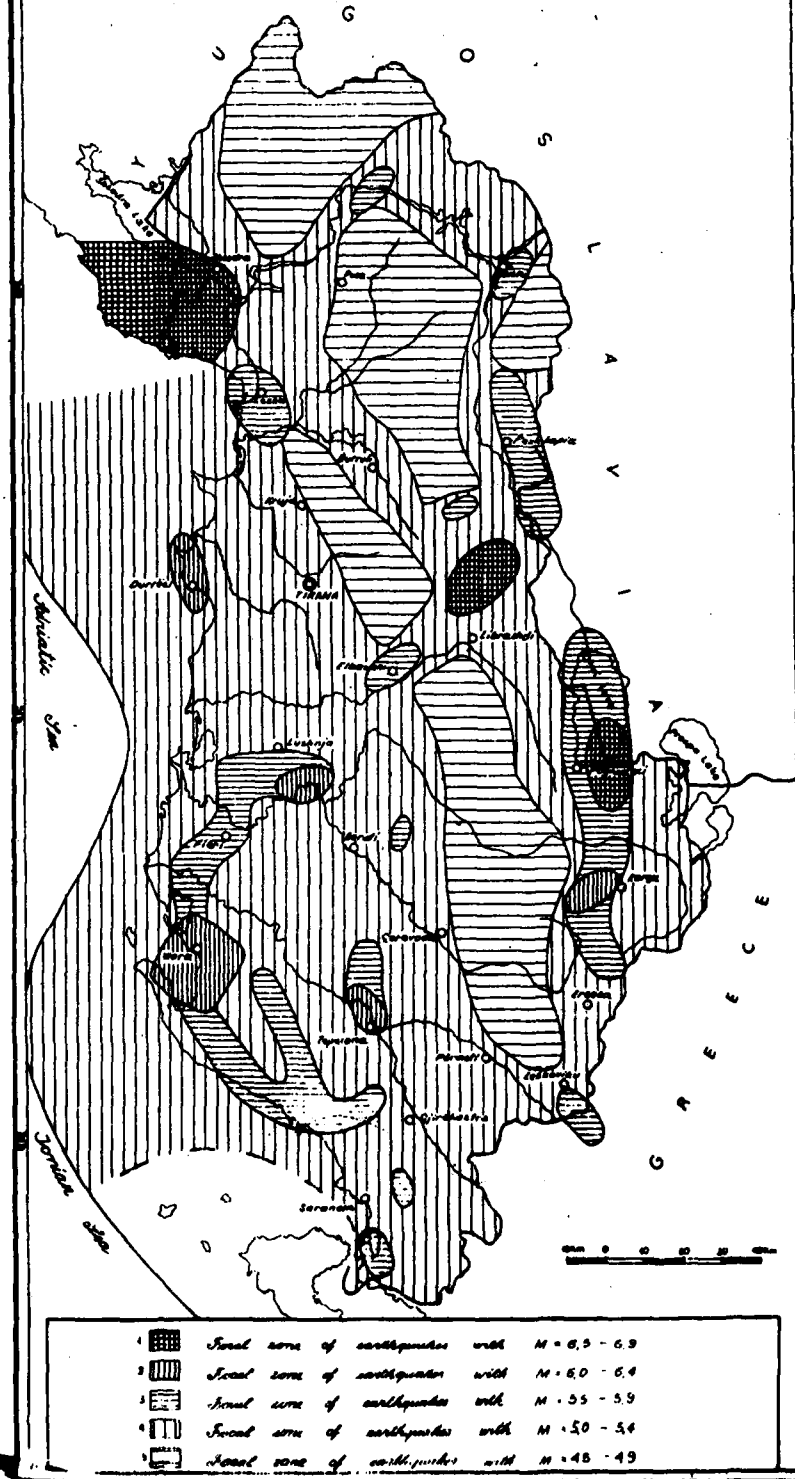
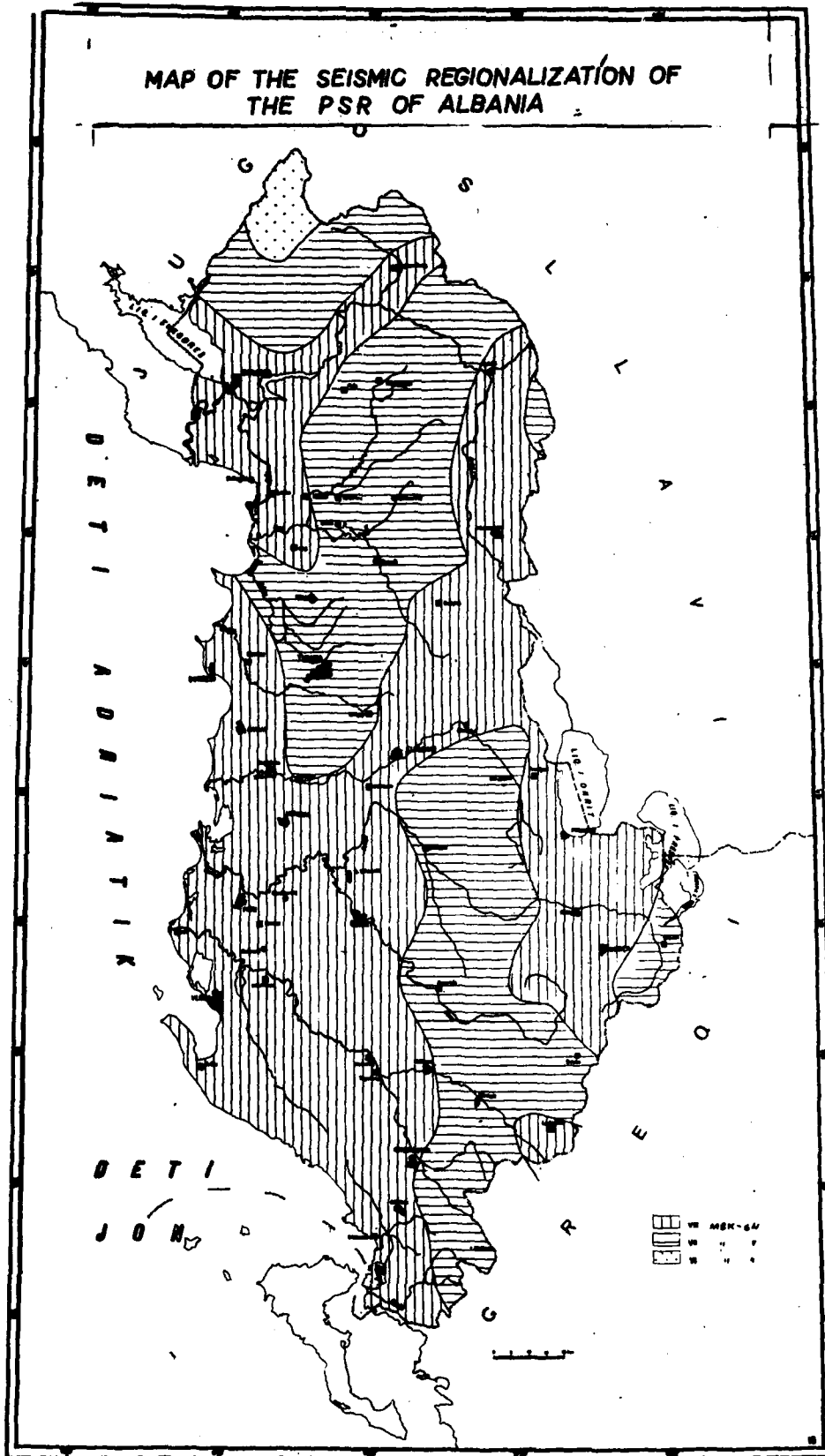


FIG. 9

# MAP OF THE SEISMIC REGIONALIZATION OF THE PSR OF ALBANIA



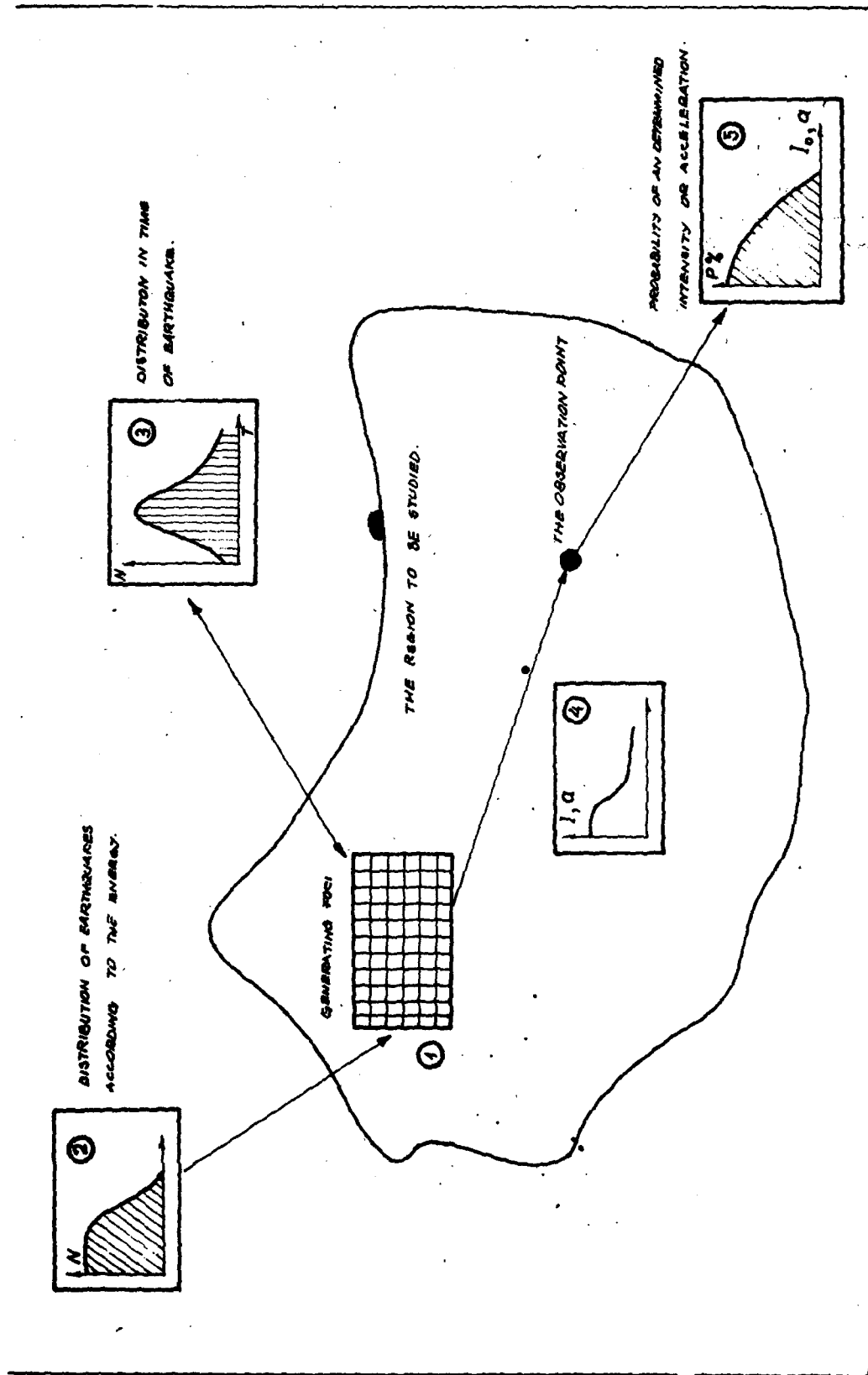
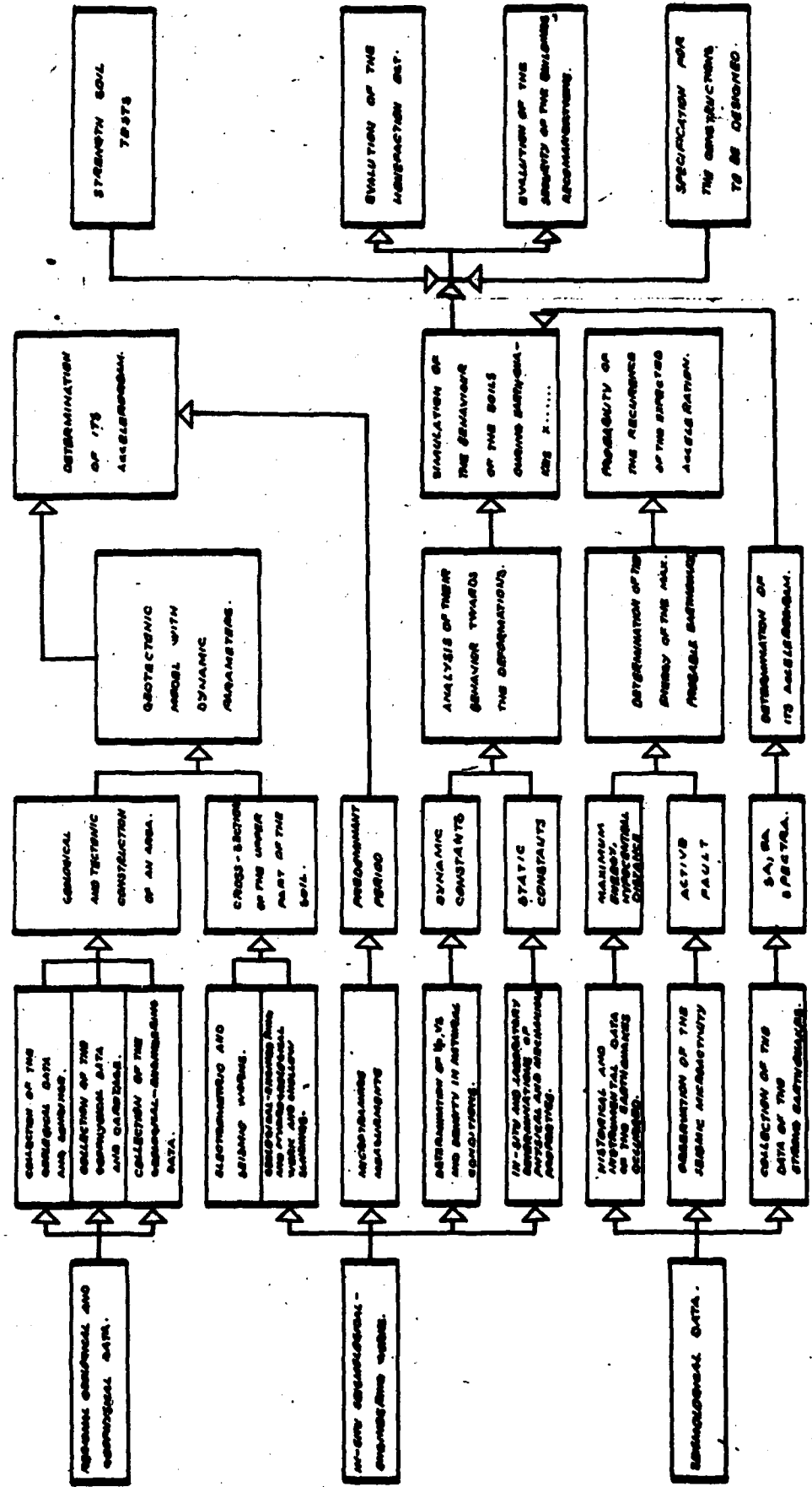


FIG. 10. SEISMIC HAZARD EVALUATION OF A SITE.



COMPLEX SEISMOLOGICAL ENGINEERING WORKS FOR THE SEISMIC MICROZONING OF AN AREA



SCHEMATIC ILLUSTRATION FOR THE EVALUATION  
OF STRONG-MOTION AT THE SITE

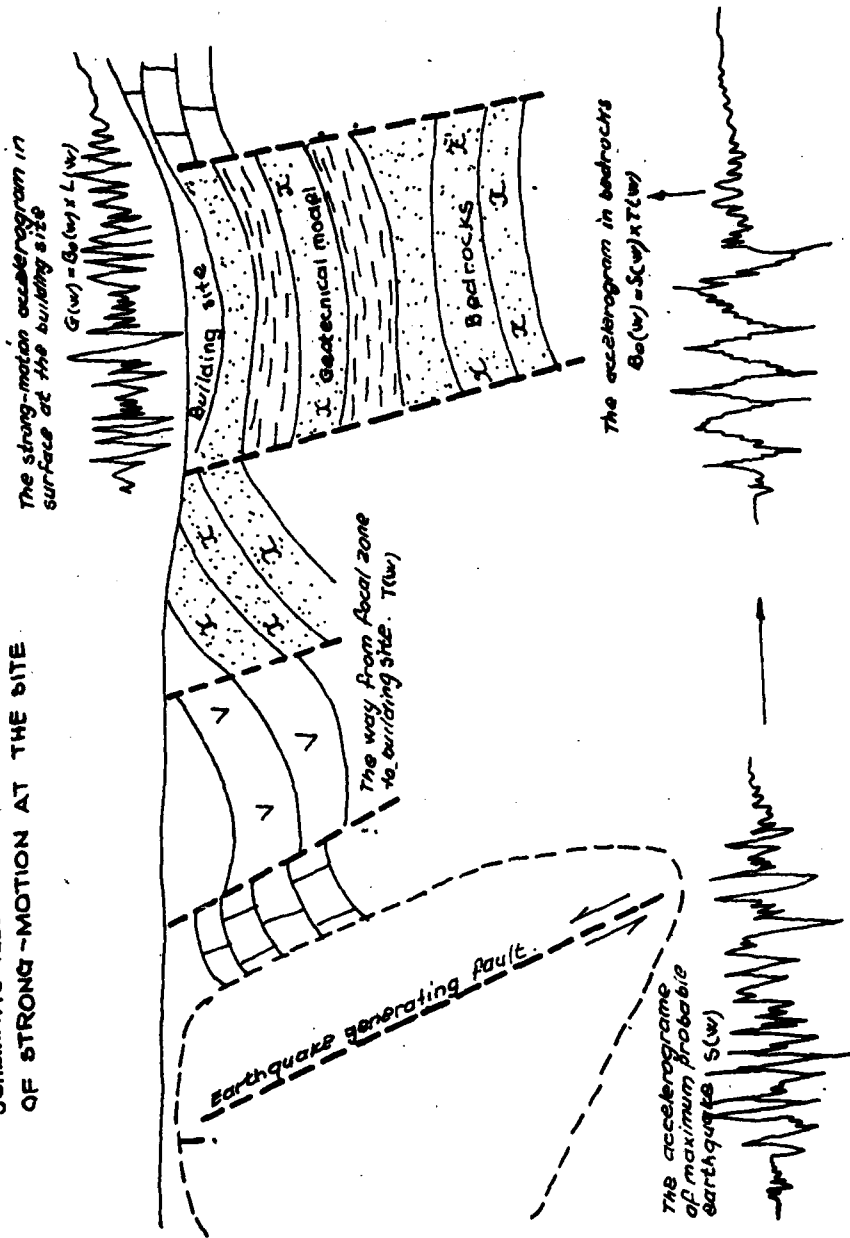
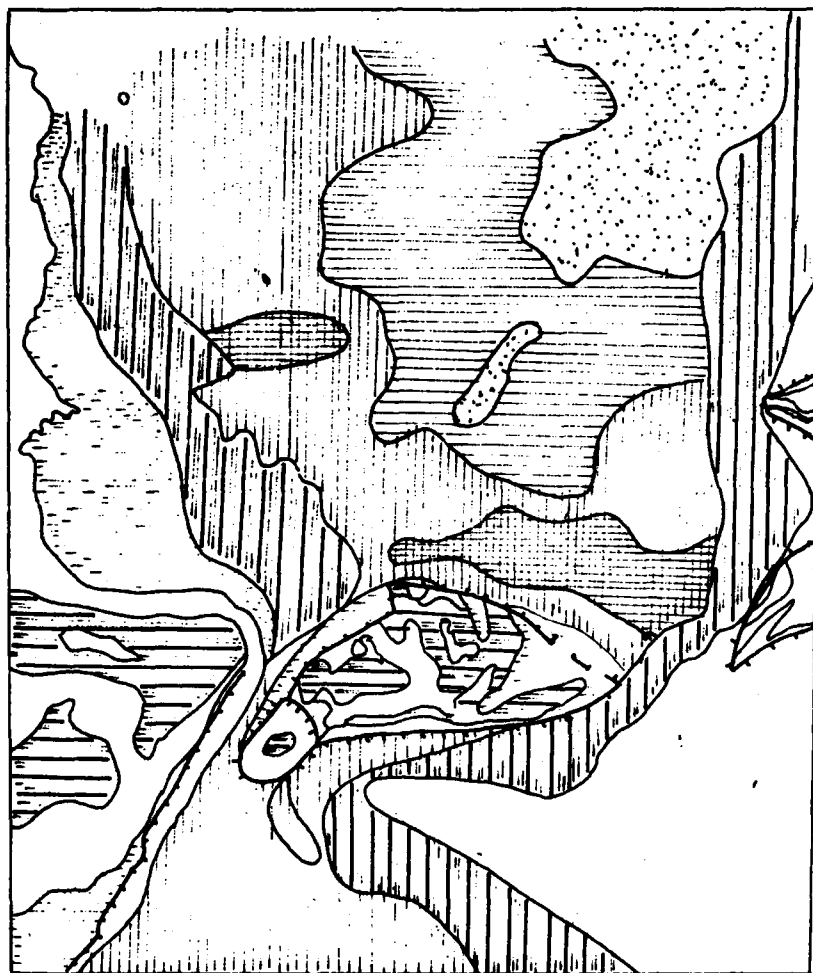


FIG. 12



INTENSITY IN DEGREES, MSK-1964 SCALE.

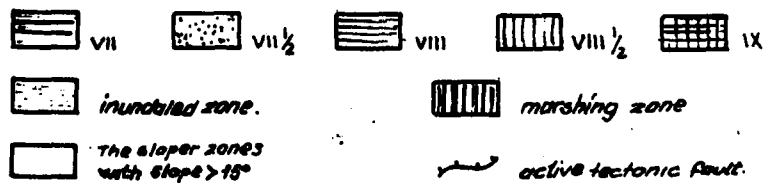
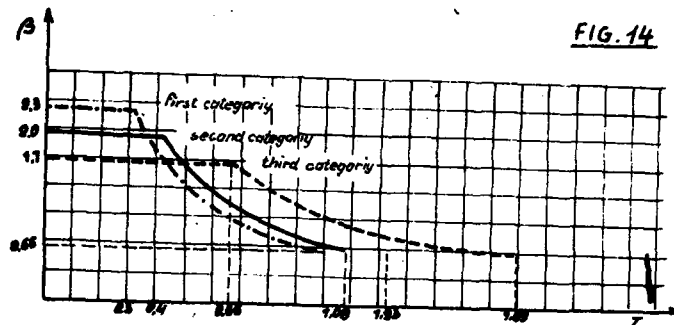
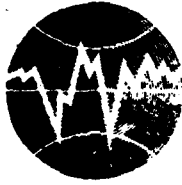


FIG. 13. THE MAP OF SEISMIC MICROZONING  
OF SHKODRA TOWN.



The curves of dynamic coefficient  $\beta$  for soils of different categories.



**TURKISH NATIONAL COMMITTEE FOR  
EARTHQUAKE ENGINEERING**

**THIRTEENTH REGIONAL SEMINAR ON EARTQUAKE ENGINEERING**

**September 14-24, 1987 - Istanbul - Turkey**

**Influence of Geology and Topography on Earthquake Intensity**

**J.A.Studer, Dr.sc.techn., GSS Consulting Engineers Ltd., CH-8032  
Zurich and Lecturer in Civil Engineering, Swiss Federal Institute  
of Technology**

## **Influence of Geology and Topography on Earthquake Intensity**

**J.A.Studer, Dr.sc.techn., GSS Consulting Engineers Ltd., CH-8032  
Zurich and Lecturer in Civil Engineering, Swiss Federal Institute  
of Technology**

### **1. Introduction and Summary**

The widely differing damage observed locally in earthquakes lends weight to the long held assumption that site intensity is greatly influenced by local geology and topography. In the last 20 years, measurements and numerical investigations have given an indication of the extent of this dependence. This contribution gives an overview of the theoretical assumptions involved.

Based on a recent investigation, primarily the influence of the topography will be discussed. The situation today is that although powerful methods of analysis are available, it is still not possible in an actual case to predict easily these site influences.

### **2. Influence of Geology**

The first models to account for the effects of local geology were developed as long as fifties years ago. The simplest model consists of vertically propagating shear waves [1] - see also Fig.1. It is obviously suited to horizontally layered ground. With the introduction of the method of linear equivalent soil properties by Seed and Idriss [2] about 20 years this model gained wide acceptance in practice and is still the most popular one.

In the seventies there followed various methods of nonlinear total stress analysis based on vertically propagating shear waves [3],[4],[5] and for effective stress analysis, e.g. [6]. At the same time there appeared methods of horizontal wave propagation analysis in layered media. In these cases the number of parameters increases rapidly ( body waves with different incident angles, different modes for Rayleigh and Love waves, etc).

One of the main problems in the practical use of all these methods is the difficulty of obtaining, with the present available means, the proportion of energy in each wave type for near surface waves from existing seismological data. In addition, there is the fact that the system of layers is often not horizontal. For these reasons the ground motions cannot be determined accurately using the abovementioned models. Thus in many cases one has to resort to the finite element method. It is then possible to consider besides irregular geometries also nonlinear material behaviour. On the negative side the computer costs are proportionately higher. References [7],[8] give relevant information on currently used material models.

Which of the proposed methods is the best for a particular situation is still a matter of discussion and further research is required. One area where there is work to be done is in the back-analysis of observed earthquake intensities. The post earthquake analysis of the event at the Humboldt Bay power plant [9] does in fact show that such calculations can produce reasonable results.

It should be pointed out that in such complex investigations it is necessary to have the corresponding input data for geometry and material properties. Obtaining this data may be rather expensive. Nevertheless, the finite element method is a useful tool to investigate local geological and topographical effects for important structures. For investigations covering a wider area, on the other hand, as in the case of microzonation, this method is precluded because of the high expenditure and use must be made of the simpler models offering greater ease with regard to parameter studies.

### 3. Influence of Topography

#### 3.1 Overview

Pointers to the influence of topography on seismic intensity are quite old. They were observed even in the last century in the 1873 Southern Italy earthquake, in which damage to villages perched on the hilltops was greater than that for villages located on the valley floors. Such observations of course have to be interpreted cautiously, as in earlier times either for defence or agricultural reasons in many places the villages were primarily built in elevated positions, rather than in the valleys. As a result the older, and thus poorer quality buildings, tend to be found on the hilltops and ridges. Nevertheless there are clear indications of the influence of topography.

Much discussion was generated by the acceleration measurement taken at the rocky abutment of the Pacoima dam during the San Fernando earthquake of 1971. A maximum acceleration of 1.25 g exceeding all previous observations was measured, though the concrete dam itself was not damaged. In order to explain this high value various investigations were carried out by different researchers. One of the best known is that of Boore [10]. The results of his parametric study show that horizontally propagating SH waves normal to the valley axis undergo the greatest amplification in the hilltop situation (see Fig.2). The amplification amounts to double that for horizontal ground. In this way it was possible to correlate the measured value with values recorded on level ground.

#### 3.2 Recent Studies

Here some results of a recent investigation carried out at the Swiss Federal Institute of Technology (Zurich) are reported. Vogt [11] is probably one of the first to study the problem of a valley with layered ground. His study was based on the indirect boundary element method in the frequency domain. He studied the influence of arbitrary prismatic valley shapes on the seismic intensity. The waves were assumed to be normal to the valley axis, while the body waves may have any direction of propagation with respect to the horizontal. The ground may be horizontally layered, enabling the combined effect of topography and layering to be determined. The model also permits the investigation of the influence of Love waves, which would not be possible with a half space model. The basic idea of the analysis is illustrated in Fig.3.

The two dimensional model comprises horizontal layering with linear elastic material properties. Material damping in the soil is considered. The analysis, which is carried out in the frequency domain, consists of the following three steps:

**Step 1 (State F):** A horizontal ground surface is assumed. For a particular wave type and direction of propagation the stresses and displacements can be determined at each point. Both the interface conditions between layers and the stress-free surface condition can be handled exactly.

**Step 2 (State P):** The stress-free boundary condition on the valley surface is generated by means of a number of dynamic loadings. The latter are determined in such a way that the stresses produced at points lying on the ideal valley surface exactly cancel out the values found at these points in step 1.

**Step 3 (Superposition):** In this step the results of the first two steps are superimposed. Since the valley surface is stress-free the region below it can be separated without affecting the stresses or displacements in the rest of the model.

The method outlined here is valid in principle also for three dimensional situations. The computational effort, however, increases prohibitively so that such investigations are only realistic with the new generation of supercomputers.

Vogt investigated the following wave types, geometries and other parameters:

**Wave Types:**

Body waves: SH, SV and P waves

Surface Waves: Rayleigh and Love waves

**Geometry:**

- U valley form with and without layering, and the layer thickness one or two times the valley depth
- Direction of propagation and type of body wave
- Frequency and relationship wavelength to valley width ( $\lambda_1/L$ )
- Direction of propagation and type of surface wave
- Relationship in the case of layering between shear wave velocity of layer and that of half space ( $C_{SL}/C_{SR}$ )
- Ratio of soil density in the layer to that of half space material
- Ratio of soil damping in the layer to that in the half space material
- Poisson's ratio  $\nu = 1/3$ .

Figs.4 to 14 present a selection of the most important results. Their interpretation may be summarised as follows:

- Topography becomes important when the shortest wave lengths are smaller than about twice the dimension of the valley
- The influence of the valley is noticeable to a lateral extent of several times that of the valley width
- The amplification of the seismic intensity strongly depends on:
  - valley geometry
  - layering
  - wavelength ( $\lambda_1$ )
  - angle of incidence ( $\psi$ ) of propagating wave
  - local site
- The greatest amplifications can occur at or near the valley, depending on the parameters
- In many of the cases investigated the valley flanks lie in zones in which the seismic intensity is strongly influenced by topography
- The valley has a shielding (isolation) effect only in a limited number of cases:
  - in homogeneous (non-layered) ground for sloping incident SH waves the amplification in front of the valley is generally greater than behind it; for layered ground, on the other hand, it is possible for greater amplifications to occur behind the valley



- for sloping incident SV, P waves and Rayleigh waves greater amplifications can occur in front of or behind the valley depending on the configuration of the parameters; thus the valley only shields against seismic waves in relatively few cases
- In the case of layered ground the separate effect of the layering on amplifications can be much greater than of the other parameters involved.

The method of analysis employed in the work of Vogt[11] described above, as in most of the previous investigations, assumed elastic material properties. In nature the ground behaviour can be strongly nonlinear, so that at first sight it appears that the results could not be applied directly to the real life situation. However, on the basis of various back-analyses of actual earthquakes (see e.g. [9]) it may be concluded that using equivalent linear soil properties a reasonable approximation to reality can be achieved, provided that the equivalent elastic parameters are properly matched to the corresponding strain level. Observations show that the greatest strains generally occur near to the ground surface. When investigating topographical influences it is usual to consider fairly thick layers, which are relatively stiff, and so the linearized parameters do not deviate greatly from the initial low strain values.

#### 4. Future Prospects

In the last 10 years much progress has been made in the analysis of the effects of geology and topography on earthquake ground motions. Today it is possible to investigate in some detail a particular site configuration. The computer costs, however, can be a limiting factor. Despite this progress the earthquake engineer must be warned against an indiscriminate use of these complex methods in practical situations. In reality they reflect, for the following reasons, an accuracy that does not exist in practice:

- Carrying out the complex computer analysis is justifiable only if the input parameters (earthquake excitation, soil profile, topography and material properties) are accurately known. To obtain these parameters in a particular investigation usually involves excessive expenditure. It is virtually impossible to assess the accuracy, i.e. reliability, of the input data.
- Despite the enhanced methods of modelling available nowadays, for cost reasons it is mostly possible to adopt only 2-dimensional models. True practical situations, of course, tend to be 3-dimensional.
- Again for reasons of costs in such investigations only a limited number of computer runs are possible, i.e. parameter studies are limited.

Consequently, due to inadequate input parameters, such calculations give an exaggerated picture of the real situation. For this reason, in practice it is preferable to apply simpler models allowing parameter studies. It is then easier to estimate the influence of different parameters. This is especially valid for regional studies as in the case of microzonation. However, for the development and assessment of simplified methods of analysis, the more complex methods referred to here are important.

## References

- [1] Kanai, K. (1952) Relation between the nature of the surface layer and the amplitudes of earthquake motions, Bull. Earthquake Research Institute, Vol.30, pp. 31-37.
- [2] Seed, H.B. and Idriss, I.M. (1969) The influence of soil conditions on ground motions during earthquakes, Jnl. Soil Mech. & Fdn. Div., ASCE, Vol.94, SM1
- [3] Streeter, V.L., Wylie, E.B., Richard, F.E., Jnr., (1974) Soil motion computations by characteristics method, Jnl. Geot. Eng. Div., ASCE, Vol.100, GT1
- [4] Idriss, I.M., Dobry, R., Doyle, E.H., and Singh, R.D. (1976) Behaviour of soft clays under earthquake loading conditions, Proc. Offshore Technology Conference, Dallas.
- [5] Taylor, P.W. and Larkin, T.J. (1978) Seismic site response of nonlinear soil media, Jnl. Geot. Eng. Div., ASCE, Vol.104, GT3.
- [6] Finn, W.D.L., Lee, K.W. and Martin, G.R. (1975) An effective stress model for liquefaction, Jnl. Geot. Eng. Div., ASCE, Vol.101, GT6.
- [7] Dungar, R., Pande, G.N. and Studer, J.A. (1982) Editors: Numerical Models in Geomechanics, A.A.Balkema, Rotterdam.
- [8] Dungar, R., and Studer, J.A. (1986) Editors: Geomechanical Modelling in Engineering Practice, A.A.Balkema, Rotterdam.
- [9] Valera, J.E., Seed, H.B., Tsai, C.F. and Lysmer, J. (1977) Seismic soil structure interaction effects at Humboldt Bay power plant, Jnl. Geot. Eng. Div., ASCE, Vol.103, GT10.
- [10] Boore, D.M. (1973) The effect of simple topography on seismic waves, Bull. Seismological Soc. of America, Vol.63, No.5.
- [11] Vogt, R.F. (1987) Einfluss von Tälern auf die seismischen Bodenbewegungen, Dissertation, Inst. für Baustatik und Konstruktion, Swiss Federal Institute of Technology, Zurich

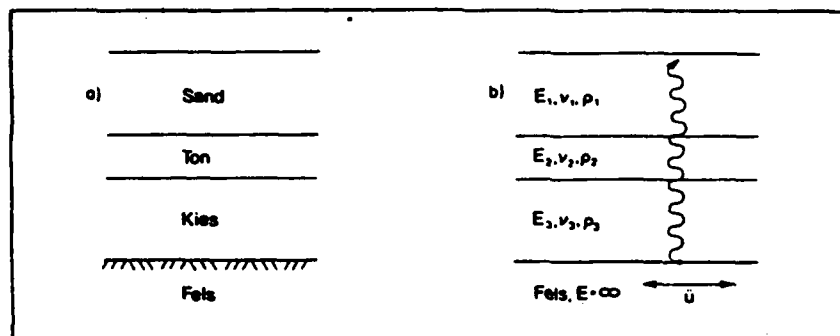


Fig.1 Influence of local geology on seismic intensity - simple model.

a)

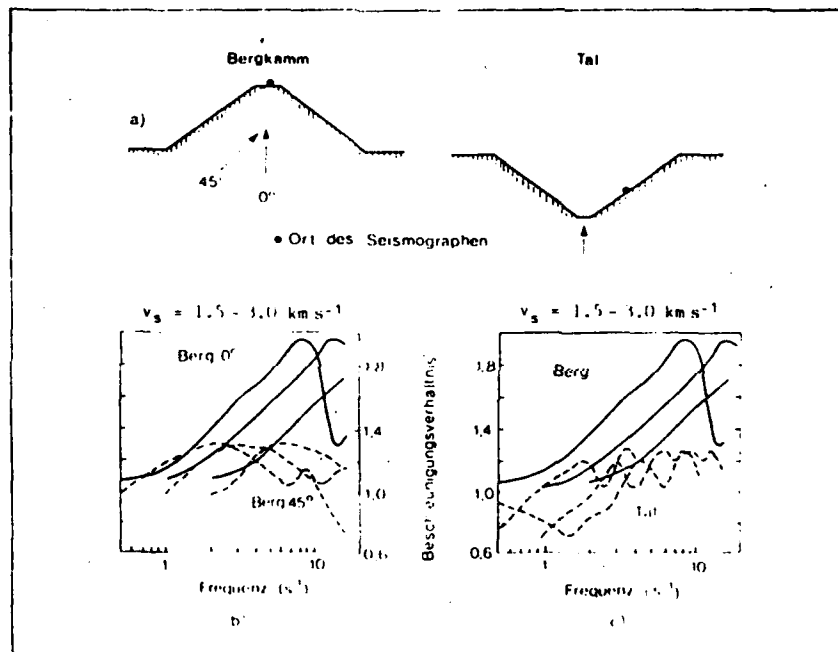


Fig.2 Influence of topography on ground acceleration (after Boore, 1973):  
 (a) geometrical situation (b) influence of angle of incidence  
 (c) influence of valley and ridge situation

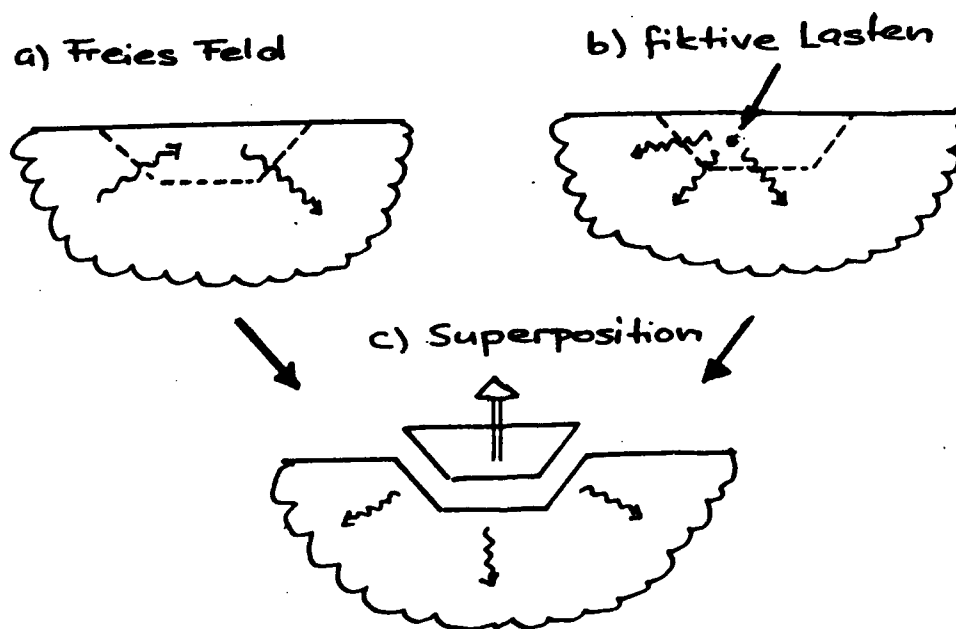


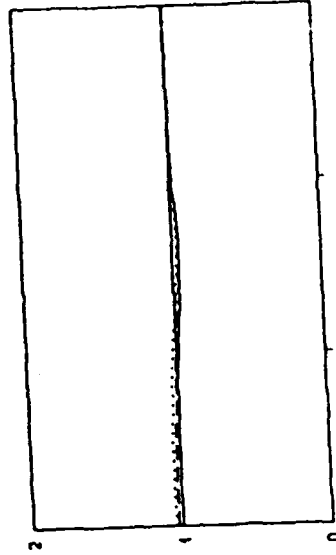
Fig.3 Schematic representation of solution procedure  
 (a) free field (state F) (b) fictitious loading (state P) (c)  
 superposition

SH-Wellen

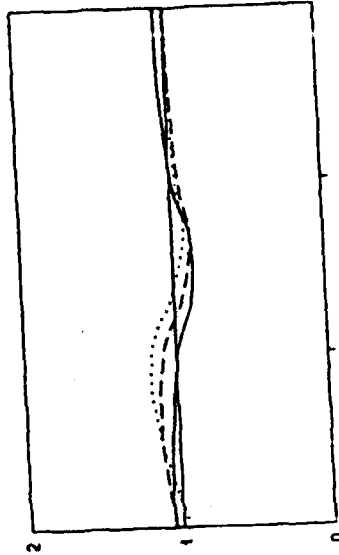


$\psi$

- $\psi = 90^\circ$
- - -  $\psi = 60^\circ$
- .....  $\psi = 30^\circ$



$\lambda_R/L = 8.000$



$\lambda_R/L = 4.000$

Fig. 4a Amplification curves for U-shaped valley in homogeneous ground  
(after Vogt[11])

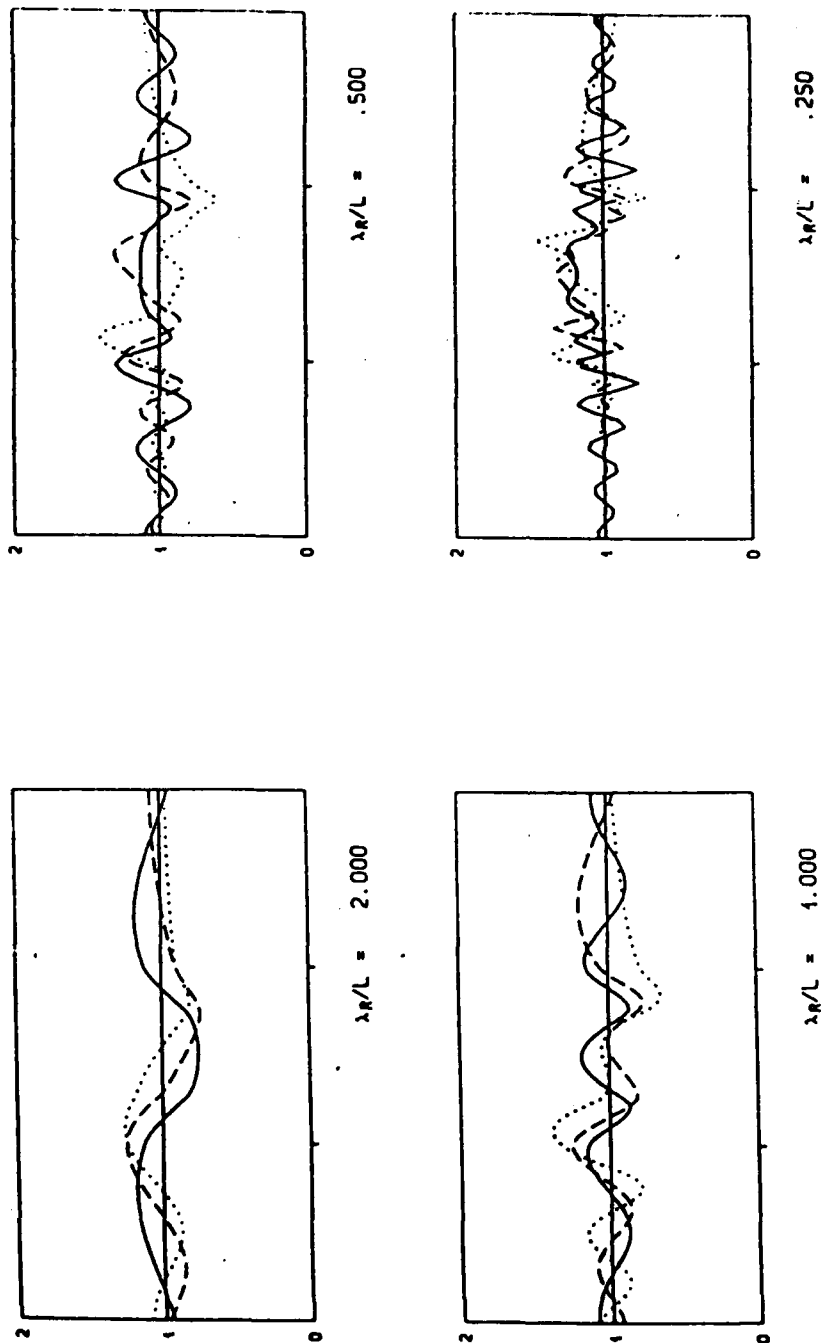
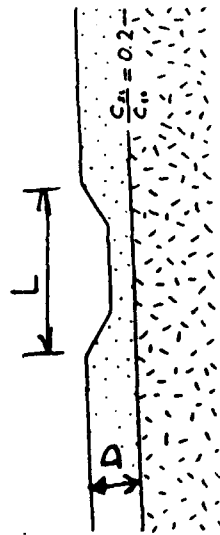


Fig.4b Amplification curves for U-shaped valley in homogeneous ground  
(after Vogt[11])

# SH- & Love-Wellen



-11-

—  $\psi = 90^\circ$

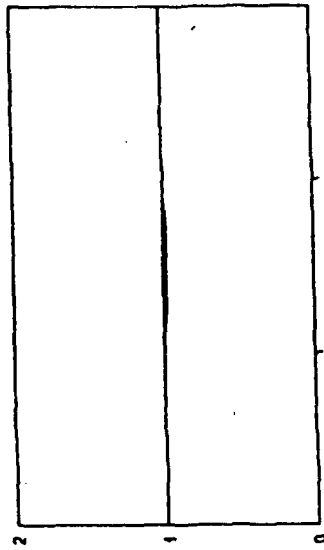
- - -  $\psi = 60^\circ$

.....  $\psi = 30^\circ$

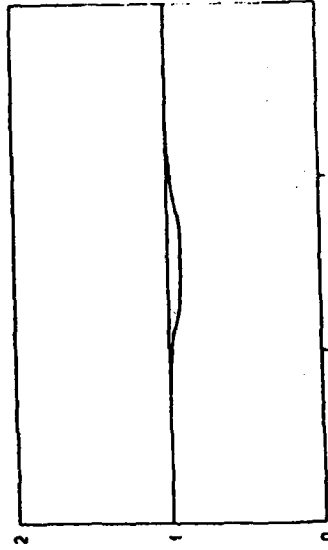
- - - - - Love-Welle mit grösstem  $c_s$

- - - - - Love-Welle mit 2. grösstem  $c_s$

— Love-Welle mit 3. grösstem  $c_s$



$\lambda_L/L = 8.000$      $\lambda_R/L = 40.000$



$\lambda_L/L = 4.000$      $\lambda_R/L = 20.000$

Fig. 5a Amplification curves for U-shaped valley in layered ground:  
 $c_{SL}/c_{SR} = 0.2, D_L = 2 T, (\text{after Vogt [11]})$



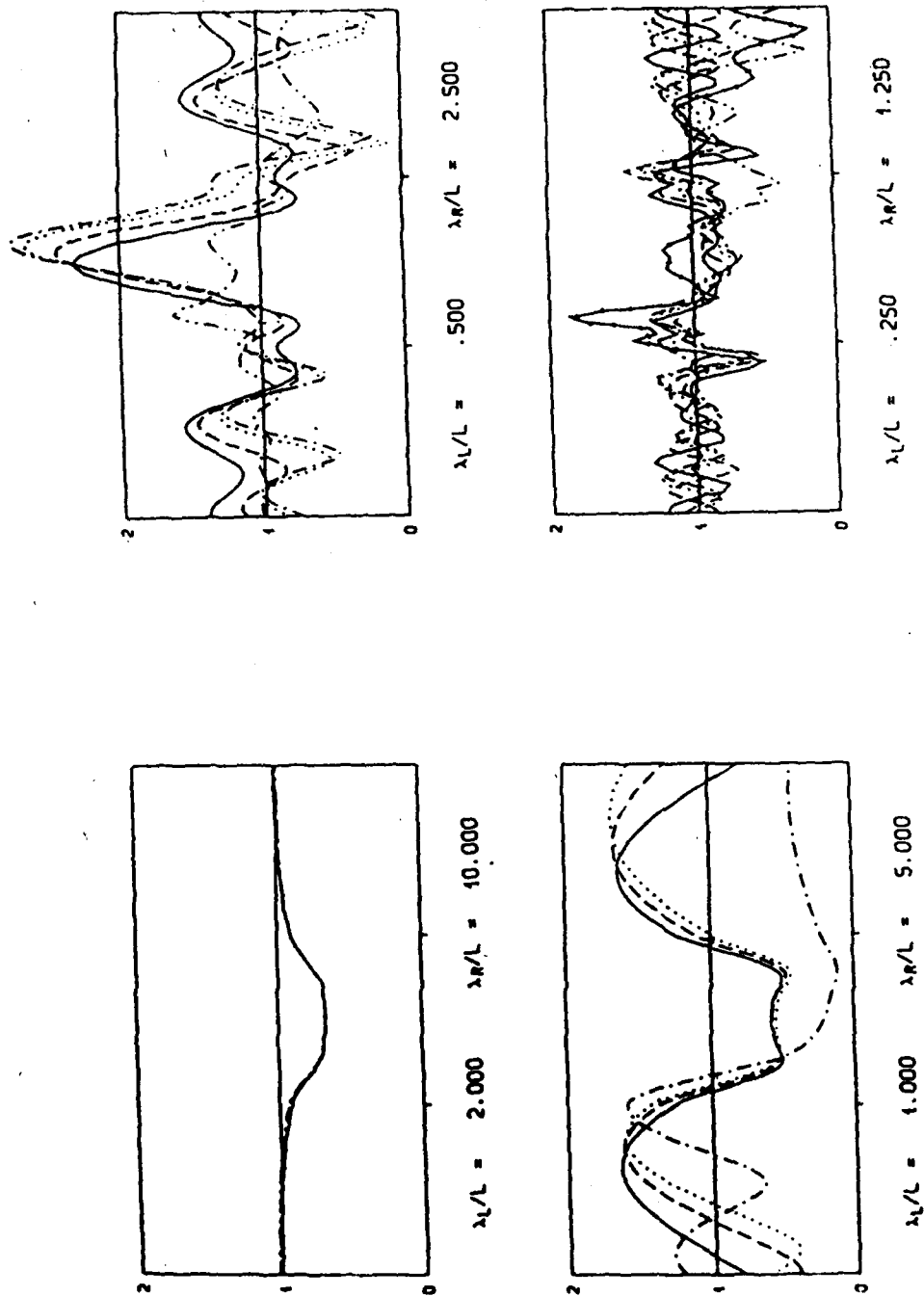
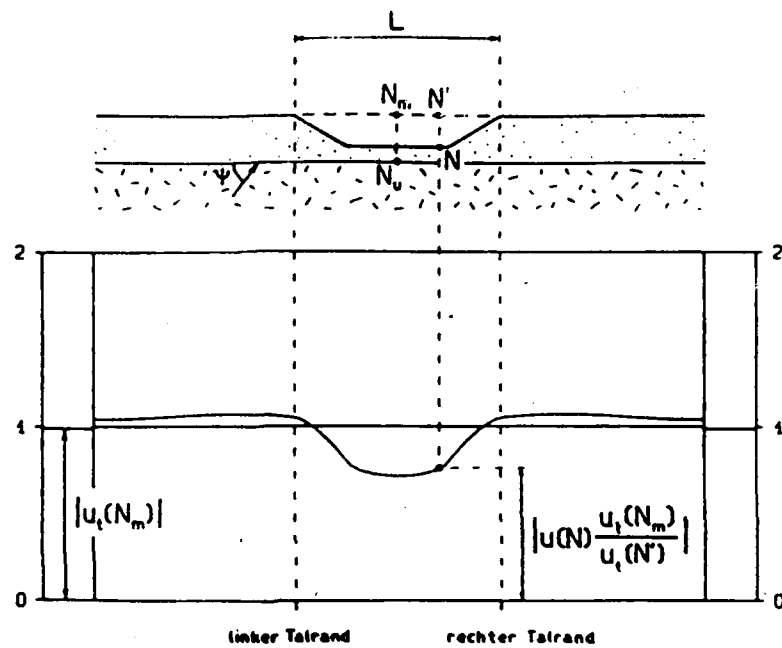


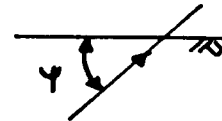
Fig. 5b Amplification curves for U-shaped valley in layered ground:

$c_{SL}/c_{SR} = 0.2, D_L = 2T, (\text{after Vogt(11)})$



#### P and SV Waves

- =  $90^\circ$
- - - =  $60^\circ$
- - - - =  $30^\circ$



#### Rayleigh Waves

- - - - mode with highest velocity
- - - - mode with second highest velocity
- mode with third highest velocity

Fig.6 Legend to the figures 7ff.

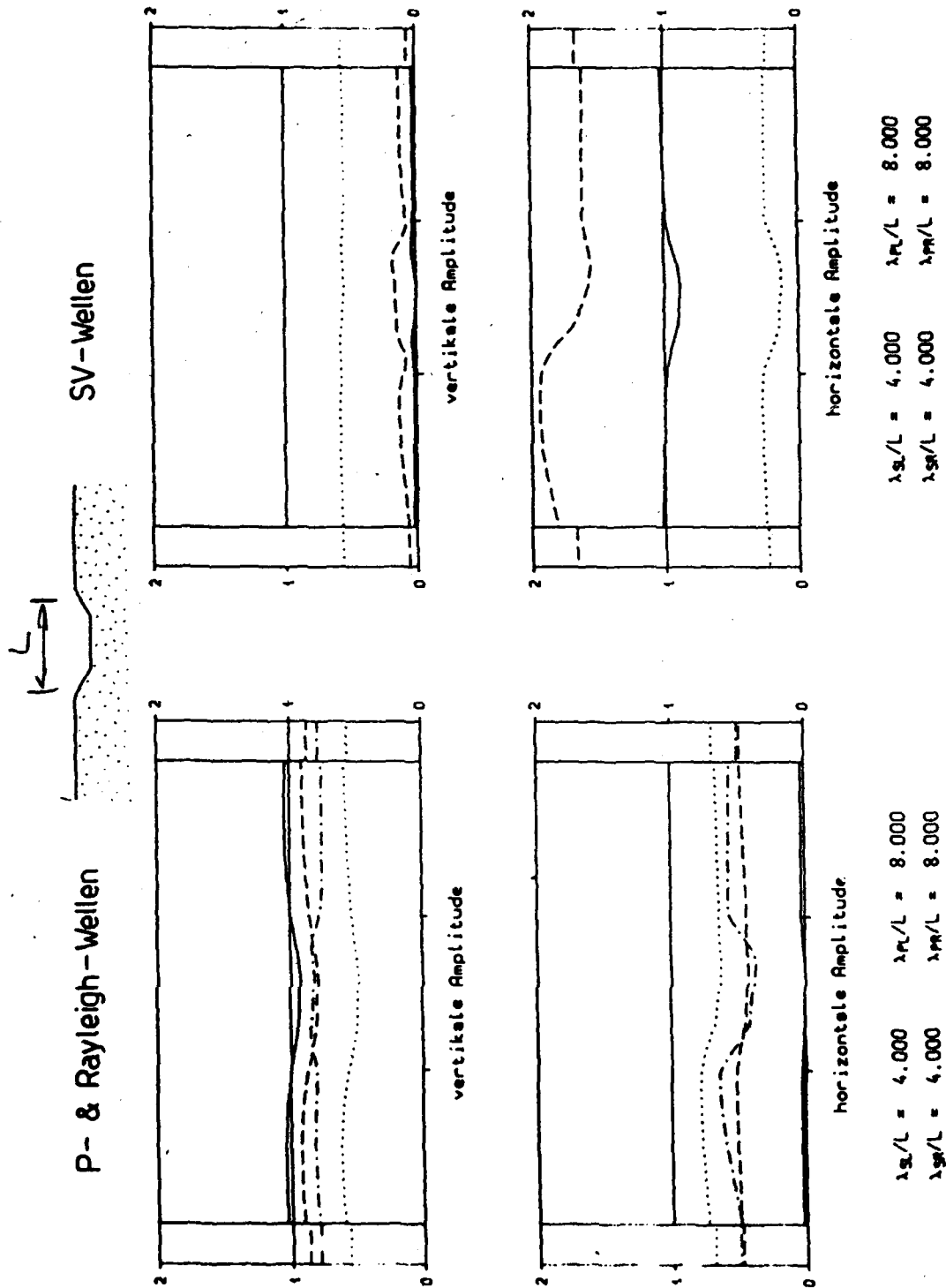


Fig.7 Amplification curves for U-shaped valley in homogeneous ground  
 (after Vogt[11])

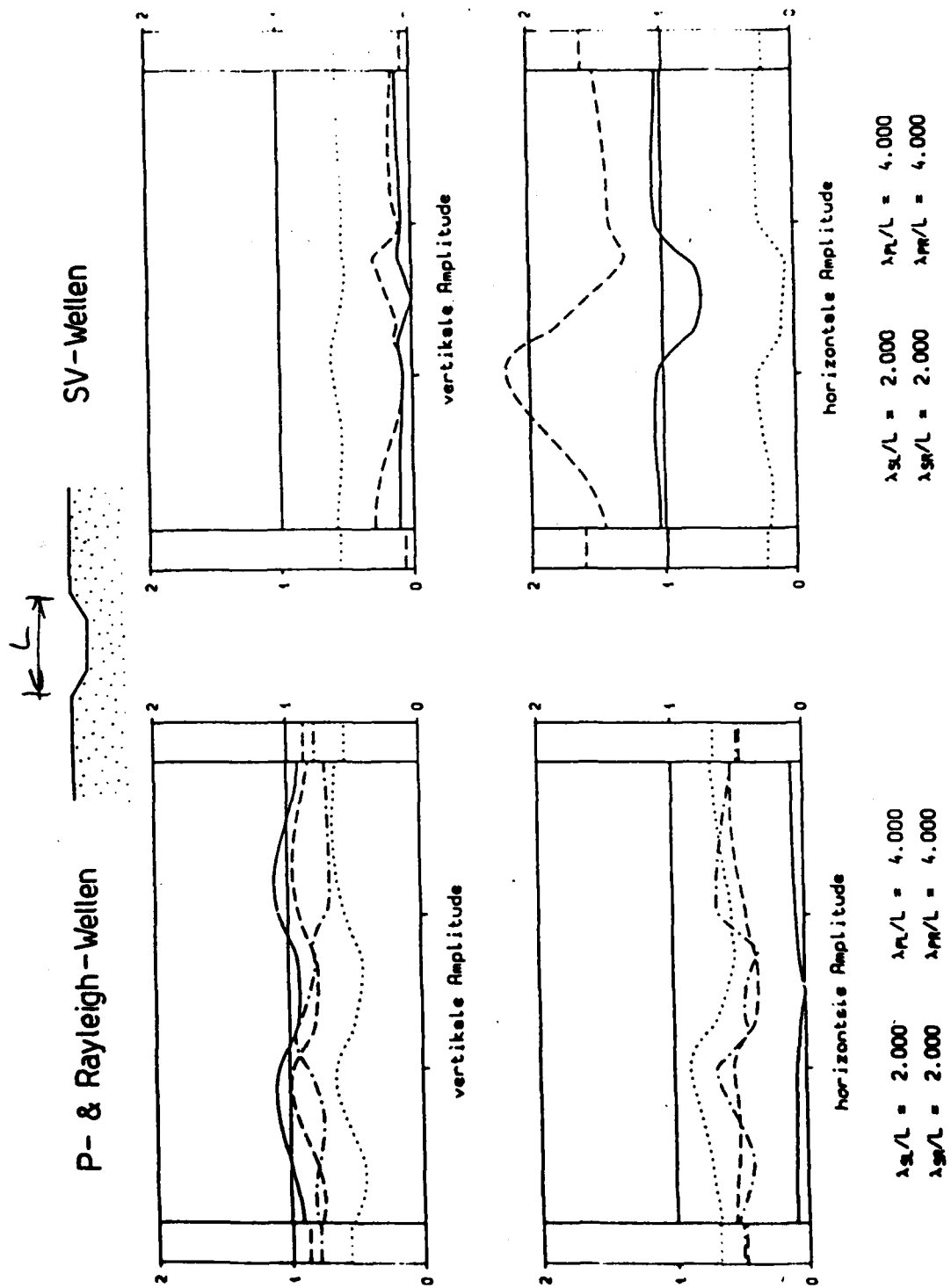
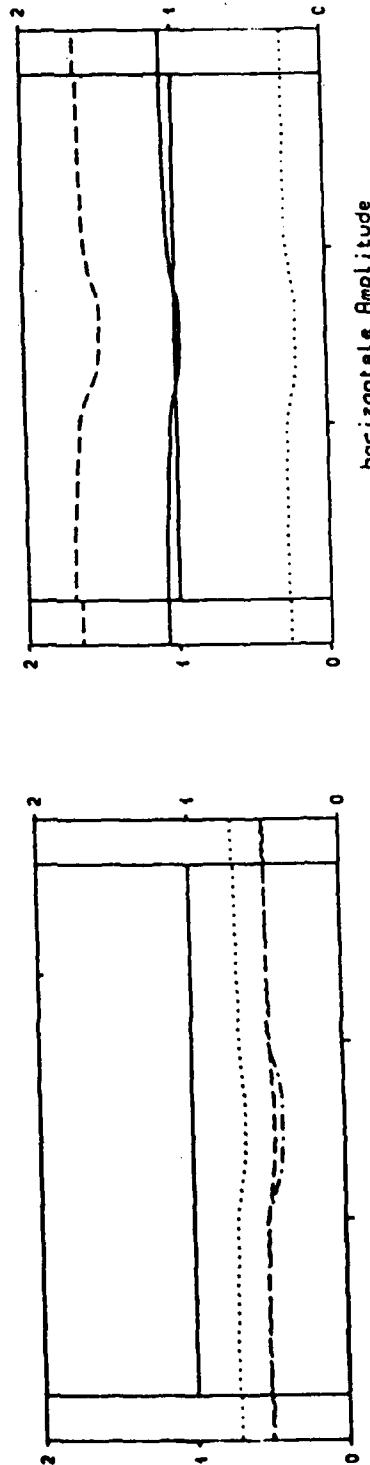
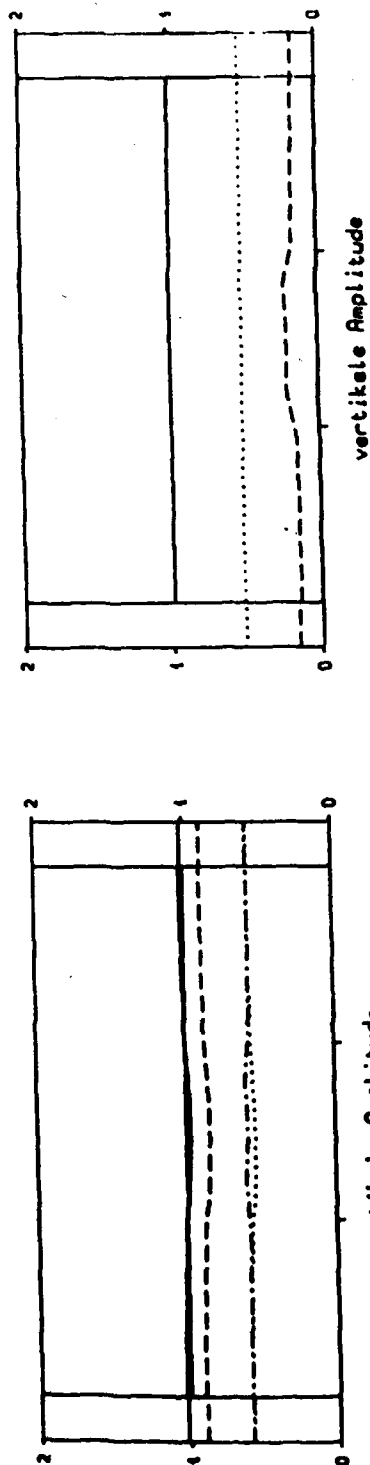


Fig.8 Amplification curves for U-shaped valley in homogeneous ground  
(after Vott1111)

# SV - Wellen



# P- & Rayleigh - Wellen



$\lambda_s/L = 4.000$      $\lambda_R/L = 8.000$   
 $\lambda_{PR}/L = 8.000$      $\lambda_{PR}/L = 16.000$

$\lambda_s/L = 4.000$      $\lambda_R/L = 8.000$   
 $\lambda_{PR}/L = 8.000$      $\lambda_{PR}/L = 16.000$

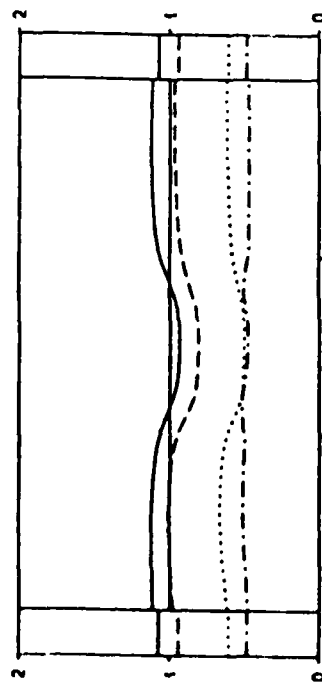
Fig.9 Amplification curves for U-shaped valley in layered ground:

$c_{PL}/c_{PR} = 0.5, D_L = 2T, (\text{after Vogt[11]})$

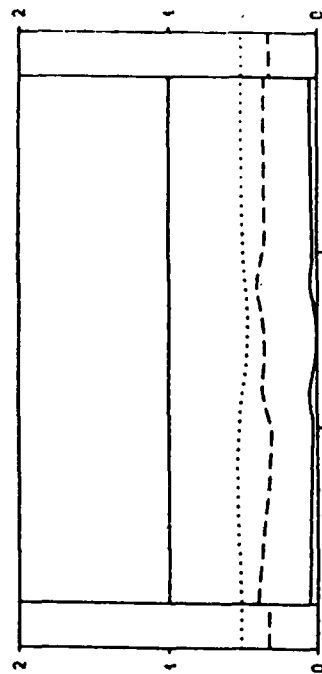
# P- & Rayleigh - Wellen



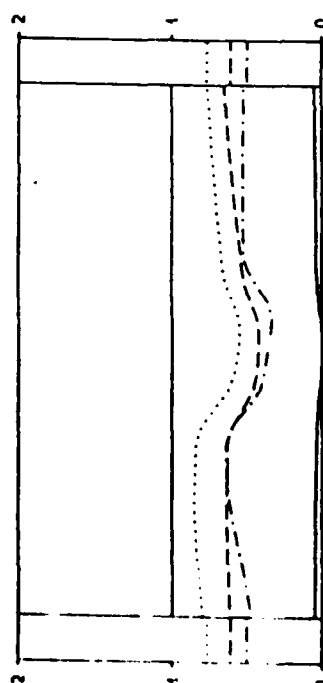
# SV - Wellen



vertikale Amplitude

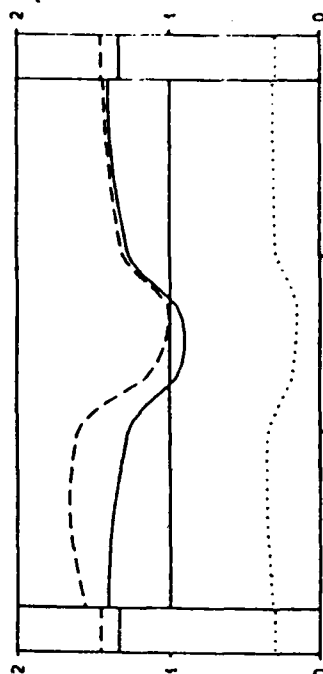


vertikale Amplitude



horizontale Amplitude

$\lambda_s/L = 2.000$      $\lambda_R/L = 4.000$   
 $\lambda_{sp}/L = 4.000$      $\lambda_{RP}/L = 8.000$



horizontale Amplitude

$\lambda_s/L = 2.000$      $\lambda_R/L = 4.000$   
 $\lambda_{sp}/L = 4.000$      $\lambda_{RP}/L = 8.000$

Fig. 10 Amplification curves for U-shaped valley in layered ground:

$c_{01}/c_{00} = 0.5, D_1 = 2T$ , (after Vogt(11))

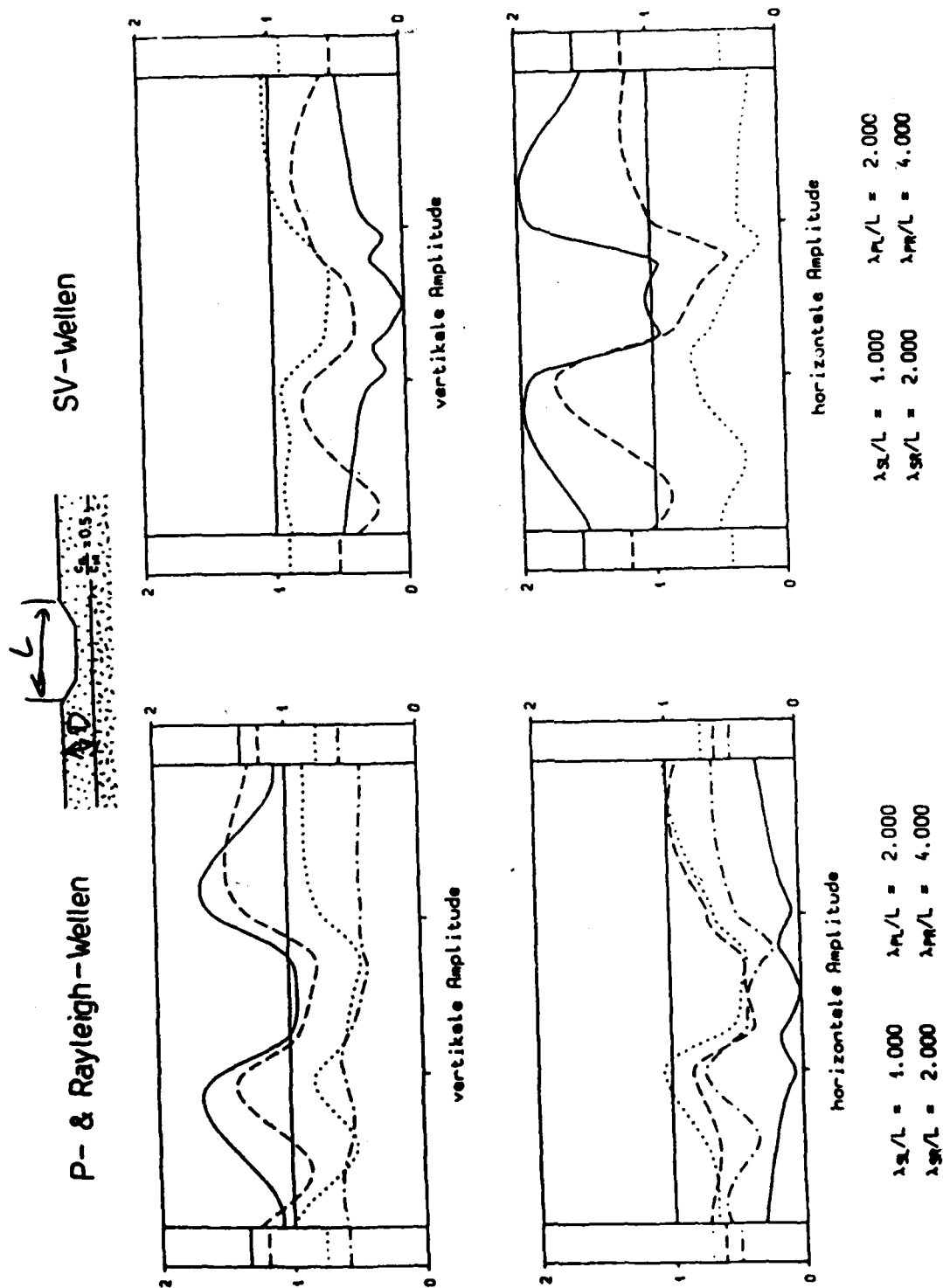
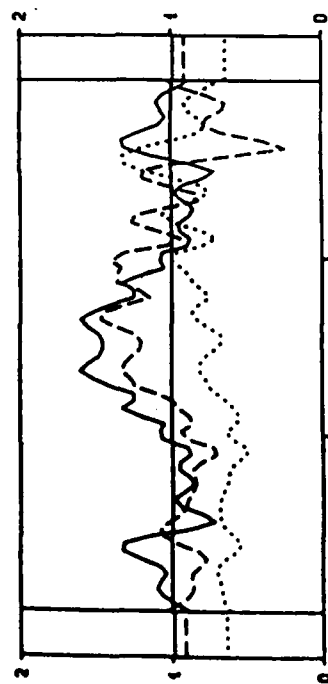


Fig. 1.1 Amplification curves for U-shaped valley in layered ground:  
 $c_{pl}/c_{pr} = 0.5, D_L = 2T$ , (after Vogt[11])

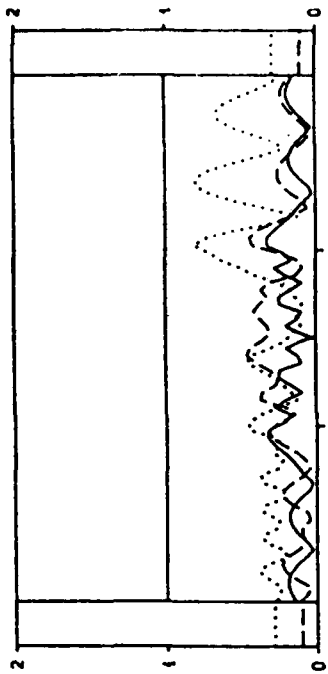
P-Wellen



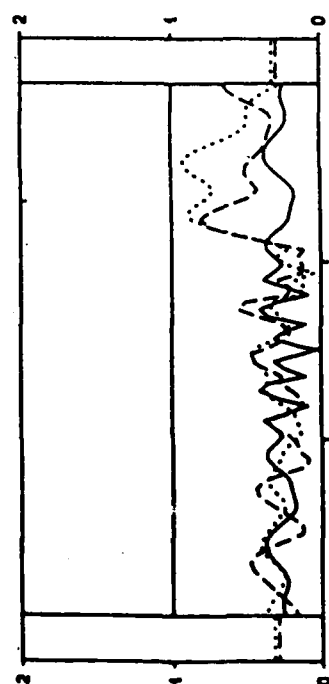
SV-Wellen



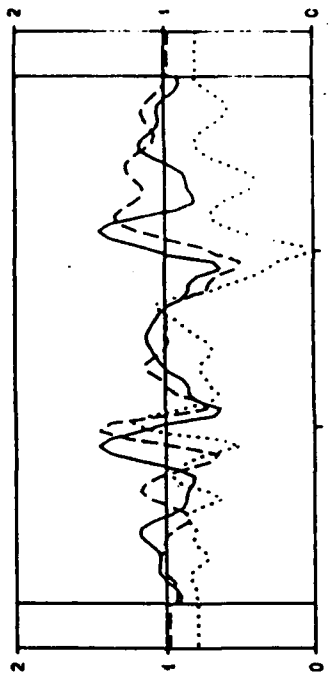
vertikale Amplitude



vertikale Amplitude



horizontale Amplitude



horizontale Amplitude

$\lambda_g/L = .250$      $\lambda_m/L = .500$   
 $\lambda_{sv}/L = .500$      $\lambda_{pr}/L = 1.000$

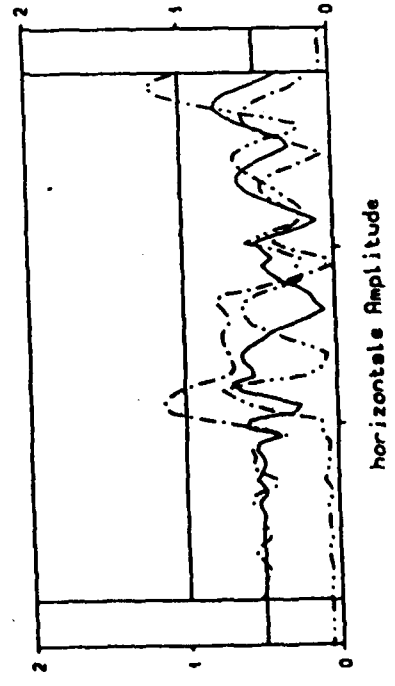
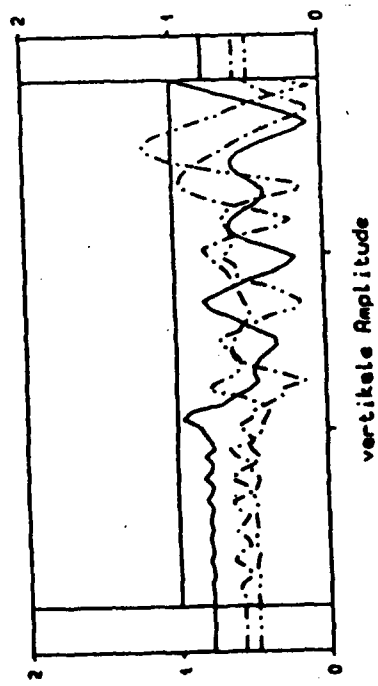
$\lambda_g/L = .250$      $\lambda_m/L = .500$   
 $\lambda_{sv}/L = .500$      $\lambda_{pr}/L = 1.000$

Fig. 1.2 Amplification curves for U-shaped valley in layered ground:  
 $c_{PL}/c_{PR} = 0.5$ ,  $D_L = 2T$ , (after Vogt[11])





Rayleigh - Wellen



$\lambda_g/L = .250$      $\lambda_R/L = .500$   
 $\lambda_g/L = .500$      $\lambda_R/L = 1.000$

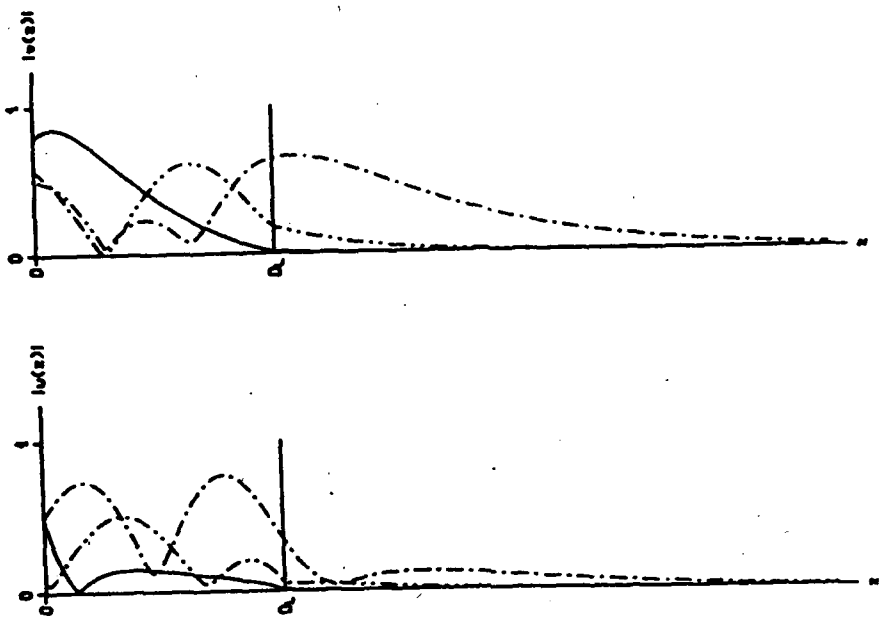
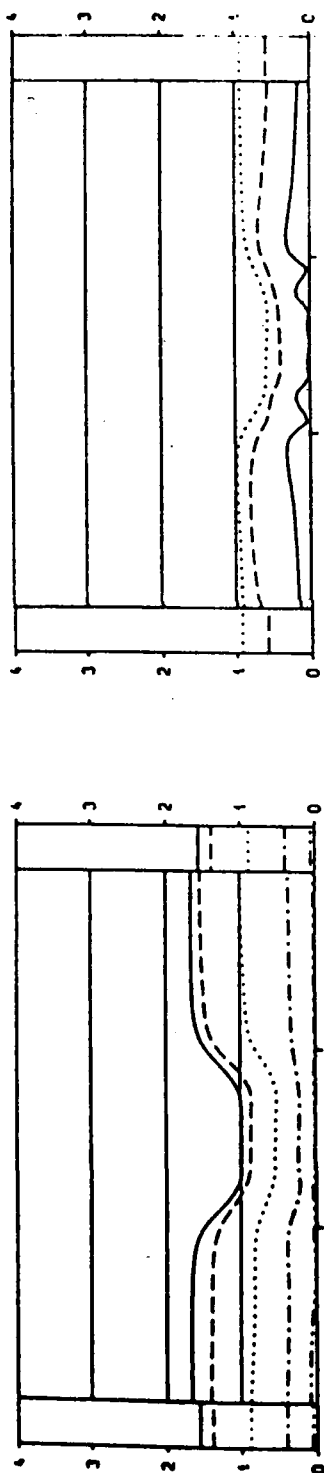


Fig. 13 Amplification curves for U-shaped valley in layered ground:  
 $c_{PR}/c_{PR} = 0.5, D_L = 2T$ , (after Vogt [11])

# P - & Rayleigh - Wellen

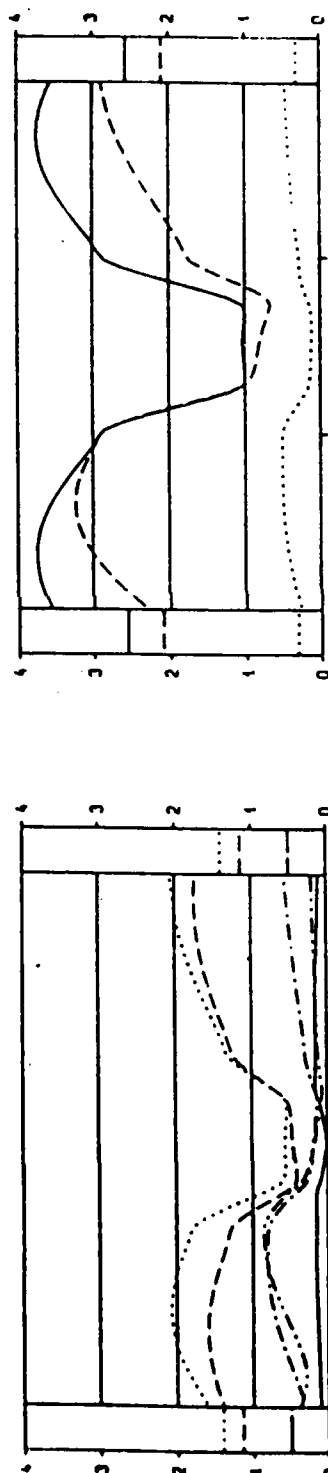


# SV - Wellen



vertikale Amplitude

vertikale Amplitude



horizontale Amplitude

horizontale Amplitude

$\lambda_g/L = 1.000$   $\lambda_{PR}/L = 2.000$   
 $\lambda_{SR}/L = 5.000$   $\lambda_{PR}/L = 10.000$

$\lambda_g/L = 1.000$   $\lambda_{PR}/L = 2.000$   
 $\lambda_{SR}/L = 5.000$   $\lambda_{PR}/L = 10.000$

Fig. 14 Amplification curves for U-shaped valley in layered ground.

$c_{PR}/c_{PR} = 0.5, D_L = 2T, \text{ (after Vogt[11])}$

## DISCRETE-TIME DOMAIN MODELS FOR SITE AMPLIFICATION

Erdal Şafak

U.S. Geological Survey, MS977, Menlo Park, CA 94025, USA.

### SUMMARY

Site amplification has commonly been described in terms of spectral ratios. It can be shown that spectral ratios are very sensitive to signal-to-noise ratios of the records, and contain very large false peaks and valleys. This paper presents an alternate approach for modeling site amplification. The method is based on discrete-time domain filtering and stochastic approximation techniques. It is assumed that the site is a time-varying linear filter of unknown parameters. The input and output of the filter are the rock-site and soil-site recordings, respectively, both contaminated with noise. Knowing the input and output, the parameters of the filter are calculated recursively by using stochastic approximation techniques. The method is applied to a site amplification problem observed during the March 3, 1985 Chile earthquake. The results are compared with those of the standard spectral ratio approach. It is shown that the method presented is far superior to the spectral ratio approach in modeling site amplification.

### INTRODUCTION

Site amplification is an important factor that must be allowed for in earthquake design. Analyses of earthquake recordings have shown that surface motions are significantly altered by the local geology and topography. In general, the alteration is in the form of amplification of the amplitudes at frequencies near the the dominant frequency of the site, and attenuation of the amplitudes at remaining frequencies.

Site amplification has commonly been described in terms of spectral ratios. For a given site, the spectral ratio is defined as the ratio of the Fourier amplitude spectrum of the recorded motion at the site to that recorded at a nearby rock site. Although spectral ratios show the gross characteristics of the site amplification, they are very sensitive to the level of noise existing in the signals, and generally contain very large false peaks and valleys. It can be shown that the standard deviation of the calculated spectral ratio from the exact ratio at a particular frequency is directly proportional to the ratio of the Fourier amplitude of the noise to that of the signal (Rake, 1980; Ljung, 1985). To eliminate the effects of the noise, the usual method is to filter the signals by using band-pass type filters (e.g., Butterworth filter), and to smooth each spectrum before taking their ratio (Rabiner

and Gold, 1975; Robinson, 1967). The magnitude of smoothing varies depending on the noise level in the signal. For low signal to noise ratios, little smoothing does not eliminate the false peaks, while too much smoothing alters the location and magnitude of real peaks. Moreover, irrespective of how accurate they are, the spectral ratios are not easy to model analytically or empirically, especially when there is more than one dominant frequency at the site.

This paper presents an alternate approach to describe site amplification. The technique is based on the concept of optimal filtering and stochastic approximation. It is assumed that the site acts as a time-varying linear filter, whose parameters are initially unknown. The input and output of the filter are the rock-site and soil-site recordings, respectively, both contaminated by noise. The filter parameters are determined from the input and output series based on the criterion that the difference between the recorded output and the filter output is equivalent to white-noise.

The initial development of optimal filtering and stochastic approximation techniques is attributed to Kolmogorov (1941) and Weiner (1949). Today, these techniques are used extensively in various areas in science and engineering, such as analysis of speech and radar signals, guidance systems, automatic control, and econometrics. More on the theory and applications can be found in Jaswinski (1970), Kailath (1976), Kushner and Clark (1978), Ljung and Soderstrom (1983), Goodwin and Sin (1984), Young (1984), and Ljung (1987).

The paper first gives the theoretical derivations for the method. Then, the method is applied to a site amplification problem observed in Chile during the March 3, 1985 earthquake. The results are compared with those of the standard spectral ratio approach.

## THEORY

### 1. System equations in discrete-time domain:

Assume that the site is an unknown linear system with a single input, and a single output, as schematically given in Fig. 1. The input  $x(t)$  is the rock-site record, and the output  $y(t)$  is the soil-site record. The noise  $n(t)$  is assumed to represent the combination of the noise in the input and output, and is unknown. However, it will be assumed that the noise is a stationary random process, such that it can be expressed as a filtered white-noise process. Since site effects are assumed to be linear, the governing equations for the site can be represented by any form of linear equation, such as a differential equation or an integral equation. For discrete systems with zero initial conditions and sufficiently small time interval, it can be shown that any linear equation can be put into a finite difference equation of the following form (Cadzow, 1973):

$$y(t) + a_1 y(t-1) + \cdots + a_{n_a} y(t-n_a) = b_1 x(t-1) + \cdots + b_{n_b} x(t-n_b) +$$

$$e_t + c_1 e(t-1) + \dots + c_{n_c} e(t-n_c) \quad (1)$$

where  $e(t)$  denotes white-noise, the index  $(t-j)$  denotes the discrete time  $(t-jT)$ , and  $T$  is the sampling interval of the time series. It is assumed that the output at time  $t$  is dependent on the input values up to time  $t-1$ , but not the input at time  $t$ . In control theory, the model given by Eq. 1 is known as the ARMAX model, an acronym for the *Stochastic Autoregressive Moving-Average Model With Auxiliary Input*.

For simplicity, let us define the following polynomials in the backward shift operator  $q^{-1}$ :

$$A(q^{-1}) = 1 + a_1 q^{-1} + \dots + a_{n_a} q^{-n_a} \quad (2)$$

$$B(q^{-1}) = b_1 q^{-1} + \dots + b_{n_b} q^{-n_b} \quad (3)$$

$$C(q^{-1}) = 1 + c_1 q^{-1} + \dots + c_{n_c} q^{-n_c} \quad (4)$$

where the backward shift operator is defined as  $q^{-j}y(t) = y(t-j)$ . With these, Eq. 1 becomes

$$A(q^{-1})y(t) = B(q^{-1})x(t) + C(q^{-1})e(t) \quad (5)$$

Eq. 5 can also be written in the frequency domain by taking the  $Z$  transform of both sides in Eq. 1, that is

$$A(z^{-1})Z[y(t)] = B(z^{-1})Z[x(t)] + C(z^{-1})Z[e(t)] \quad (6)$$

where  $A(z^{-1})$ ,  $B(z^{-1})$ , and  $C(z^{-1})$  are polynomials in the complex variable  $z$ , similar to those given by Eqs. 2-4,

$$A(z^{-1}) = 1 + a_1 z^{-1} + \dots + a_{n_a} z^{-n_a} \quad (7)$$

$$B(z^{-1}) = b_1 z^{-1} + \dots + b_{n_b} z^{-n_b} \quad (8)$$

$$C(z^{-1}) = 1 + c_1 z^{-1} + \dots + c_{n_c} z^{-n_c} \quad (9)$$

$Z[y(t)]$  denotes the  $Z$ -transform of  $y(t)$ , defined as  $Z[y(t)] = \sum_{n=0}^{\infty} y(nT) z^{-n}$ , where  $t = nT$ .  $Z[x(t)]$  and  $Z[e(t)]$  are similar. Since  $e(t)$  is white-noise,  $Z[e(t)]$  is constant. The ratios

$$H(z) = \frac{B(z^{-1})}{A(z^{-1})} \quad \text{and} \quad G(z) = \frac{C(z^{-1})}{A(z^{-1})} \quad (10)$$

are the transfer functions for the signal (i.e., for the actual site effect), and for the noise, respectively. The roots of the numerator polynomial  $B(z^{-1})$  of  $H(z)$  are the zeros of the transfer function, whereas the roots of the denominator polynomial  $A(z^{-1})$  are the poles. (The use of the terms poles and zeros come from the observation that if  $H(z)$  is plotted in a three dimensional cartesian coordinate system such that the horizontal axes are the real and imaginary parts of  $z$ , and the vertical axis is  $H(z)$ , the resulting shape looks like a tent, with poles corresponding to the locations where the tent is supported, and the zeros corresponding to the locations where the tent is tied to the ground.) For stable systems (i.e., systems that have bounded output for any bounded input) the poles are in complex conjugate pairs, located inside the unit circle in the complex plane.

The argument  $z$  in  $Z$  transforms can be any complex variable. For  $z = e^{i2\pi fT}$ , where  $f$  is the cyclic frequency and  $i = \sqrt{-1}$ , the  $Z$ -transform becomes equivalent to the Fourier transform. The commonly used spectral ratio,  $S(f)$ , is then calculated as

$$S(f) = \frac{|B(e^{i2\pi fT})|}{|A(e^{i2\pi fT})|} \quad (11)$$

Note that the spectral ratio calculated by Eq. 11 is for the signals only (i.e., after the noise is removed from the records). The impulse response function of the system can be obtained recursively from Eq. 1 by putting  $x(0) = 1$  and  $x(t) = 0$ , for  $t > 0$  with  $e(t) = 0$  for all  $t$ .

## 2. Parallel form realization (modal analysis):

For  $n_b \leq n_a$ ,  $H(z)$  can be put into the following form by using partial fraction expansion (if  $n_b > n_a$ , a polynomial division is required before the partial fraction expansion):

$$H(z) = \sum_{j=1}^{n_b} \frac{q_j}{1 - p_j z^{-1}} \quad (12)$$

where  $p_j$  is the  $j$ 'th complex pole, and  $q_j$  is the corresponding residue of  $H(z)$ . The residue  $q_j$  is calculated by the equation (Tretter, 1976)

$$q_j = \lim_{z \rightarrow p_j} (1 - p_j z^{-1}) H(z) = \frac{b_1 p_j^{-1} + \dots + b_{n_b} p_j^{-n_b}}{\prod_{\substack{k=1 \\ k \neq j}}^{n_a} (1 - p_k p_j^{-1})} \quad (13)$$

If the pairs of terms corresponding to pairs of complex-conjugate poles are combined, then

$$H(z) = \sum_{j=1}^{n_a/2} H_j(z) \quad (14)$$

with

$$H_j(z) = \frac{2\Re(q_j) - 2\Re(q_j \bar{p}_j)z^{-1}}{1 - 2\Re(p_j)z^{-1} + |p_j|^2 z^{-2}} \quad (15)$$

where  $\bar{\cdot}$  and  $\Re$  denote the complex-conjugate and the real part, respectively. The form given by Eq. 12 (or Eq. 14) for  $H(z)$  is known as the parallel form realization, where the filter output  $y(t)$  is modeled as the linear combination of the outputs of second-order filters each subjected to input  $x(t)$ . A schematic of parallel form realization is given in Fig. 2. Each  $H_j(z)$  is equivalent to a simple-damped oscillator, whose damping  $\xi_0$ , and frequency  $f_0$  are given by the equations (Safak, 1987a):

$$\xi_{0j} = \frac{\ln(1/r_j)}{[\phi_j^2 + \ln^2(1/r_j)]^{1/2}} \quad (16)$$

$$f_{0j} = \frac{\ln(1/r_j)}{2\pi \xi_{0j} T} \quad (17)$$

where  $r_j$  and  $\phi_j$  are the modulus and the arguments of the  $j$ 'th pole (or of its complex-conjugate). Thus, each  $H_j(z)$  can be considered as a mode of the system, whose frequency and damping are defined by the denominator of  $H_j(z)$ . The numerator of  $H_j(z)$  gives the weighting factor for that mode.

### 3. System identification:

As the above equations show, once the coefficients  $a_j$ ,  $b_j$ , and  $c_j$  are determined, the dynamic properties of the system (e.g., spectral ratio, modes, impulse response, and noise characteristics) can all be calculated from the transfer function. Estimation of the coefficients is called system identification, and can be accomplished by using stochastic approximation techniques. The reason for using stochastic approach rather than deterministic approach is because of the existence of noise in the records.

By algebraic manipulations, let us first put Eq. 5 into a form such that the white-noise term  $e(t)$  is isolated, as

$$y(t) = \left[1 - \frac{A(q^{-1})}{C(q^{-1})}\right] y(t) + \frac{B(q^{-1})}{C(q^{-1})} x(t) + e(t) \quad (18)$$

It can be shown by simple algebra that the highest order term in the expression  $[1 - A(q^{-1})/C(q^{-1})]$  on the right hand side of Eq. 18 is  $q^{-1}$ . Therefore, the right hand side contains output values only up to time  $t - 1$ . If the output, input, and the parameters of the polynomials  $A(q^{-1})$ ,  $B(q^{-1})$ , and  $C(q^{-1})$  are all known up to time  $t - 1$ , then the best estimate (i.e., the expected value) of the output at time  $t$ ,  $\hat{y}(t)$ , is equal to ( $e_t$  is white-noise, therefore its expected value is zero)

$$\hat{y}(t) = \left[1 - \frac{A(q^{-1})}{C(q^{-1})}\right] y(t) + \frac{B(q^{-1})}{C(q^{-1})} x(t) \quad (19)$$

The error in the estimation, at time  $t$ , is then equal to

$$\varepsilon(t) = y(t) - \hat{y}(t) \quad (20)$$

The total error, assuming a quadratic criterion, can be written

$$V(t) = \sum_{s=1}^t \Gamma(s, t) \varepsilon^2(s) \quad (21)$$

where  $\Gamma(s, t)$  is the weighting factor. The weighting factor is needed to handle time-varying systems, for which  $\Gamma(s, t)$  is selected such that the recent data points have more weights than the earlier ones. It should be noted here that the quadratic criterion is not the only way to measure the total error. Other error criteria, such as absolute value or maximum likelihood, can also be used (for more detail, see Ljung, 1987).

The values of parameters  $a_i$ ,  $b_i$ , and  $c_i$  are obtained from the condition that the criterion function  $V(t)$  is minimum. The minimization of  $V(t)$  is accomplished recursively by using stochastic approximation techniques. There are various algorithms for stochastic approximation. Most of them are based on the Robbins-Monro algorithm (Robbins and Monro, 1951). The texts by Albert and Gardner (1967) and Kushner and Clark (1978) give an extensive evaluation of stochastic approximation techniques. The algorithm used here is the stochastic Gauss-Newton algorithm. With this algorithm, and also using the quadratic error criterion and an exponentially decaying weighting function, the equations for the parameters  $a_j$ ,  $b_j$ , and  $c_j$  can explicitly be derived. The detail of derivations can be found in Şafak (1987a). The final form is given by the following recursive matrix equation:

$$\theta(t) = \theta(t-1) + \gamma(t) R^{-1}(t) \psi(t) \varepsilon(t) \quad (22)$$



The parameters of Eq. 22 are defined as follows:

$\theta^T = (a_1, \dots, a_{n_a}, b_1, \dots, b_{n_b}, c_1, \dots, c_{n_c})$  ( $m = n_a + n_b + n_c$  dimensional vector),

$R^{-1}(t)$  : the Hessian (second derivative) of  $V(t)$  with respect to  $\theta$  ( $m \times m$  dimensional matrix),

$\psi(t)$  : the gradient (first derivative) of  $\hat{y}(t)$  with respect to  $\theta$  ( $m$  dimensional vector), and

$\gamma(t) = 1 / \sum_{s=1}^t \Gamma(s, t)$ , the gain sequence of the recursion.

In order to start the recursion initial values of the parameters need to be specified. It can be shown that for stable systems the effect of initial values diminishes very rapidly with time, thus they can be assumed zero. The method just outlined for parameter estimation is known as the Recursive Prediction Error Method, or the RPEM for short, developed for ARMAX model structure.

#### 4. Model order and validity:

In order to start calculations, first the model order (i.e., values for  $n_a$ ,  $n_b$ , and  $n_c$ ) should be specified. They can be determined by observing the variation of total prediction error (Eq. 21) with different model orders. Initially, the prediction error drops sharply as the model order increases. Then the error becomes insensitive to the model order. In other words, models beyond a certain order do not give any new information about the system. This order is then selected as the model order.

After the model is specified and the coefficients are determined, some checks with regards to the validity of the model need to be made. There are a number of tests available, each with different precision. The simplest one is to visually compare the plots of the calculated transfer function and the spectral ratio (calculated by using Fourier transforms), and see whether there are drastic differences. More precise tests can be made by using the residual time series,  $\varepsilon(t)$  (Eq. 20). In order that the model be valid  $\varepsilon(t)$  should be a white-noise series; therefore, its Fourier amplitude spectrum should be nearly flat, and the autocovariance function should be close to a Delta function. A statistical whiteness test, such as the Chi-Square ( $\chi^2$ ) test, can be used for  $\varepsilon(t)$ . There may be cases where the model is good for the signal, but not so good for the noise (i.e., the  $a_j$  and  $b_j$  terms are estimated correctly, but not the  $c_j$  terms). This usually occurs when the noise signal has different pole locations than the system. In this case, although the residuals do not pass the whiteness test, the model still describes the system transfer function accurately, since the  $c_j$  terms are not used in the calculation of  $H(z)$ . This can be tested by investigating the cross-covariance of residuals  $\varepsilon(t)$  with the input  $x(t)$ . In order that the model be valid, at least for the signal,  $\varepsilon(t)$  should be independent of  $x(t)$ . In other words, the residual

should not contain any information that originates from the input. More on model validity can be found in Ljung (1987) and Bohlin (1987).

### NUMERICAL EXAMPLE

The linear filtering approach presented above was applied to an actual site amplification problem observed during the March 3, 1985, magnitude 7.8, Central Chile Earthquake. The investigations after the earthquake showed that the local geological and topographical site conditions caused large variations in ground motion amplitudes and structural damage (Çelebi, 1986).

To apply the method, two strong motion acceleration records from this earthquake were considered. One of the records is from a rock site, and the other is from an alluvial site. The time history of the records are shown in Fig. 3. The smoothed Fourier amplitude spectra and the spectral ratio (alluvial/rock) are shown in Fig. 4. Although the stations are only five miles apart, there are significant differences in the amplitudes and the frequency contents of the motions.

The first step in the calculations is to synchronize the records. The synchronization used in here is based on the maximum correlation criteria. The correlation  $R_k$  for a time shift  $k$  between input  $x_t$  and output  $y_t$  will be defined as

$$R_k = \sum_{t=1}^N |x_t y_{t+k}| \quad \text{with} \quad k = -N, \dots, N \quad (23)$$

where  $N$  is the smaller of the lengths of the time series  $x_t$  and  $y_t$ . When  $R_k$  is maximum it is assumed that the series are synchronized. In reality there may be situations where the synchronization does not mean maximum correlation, such as systems where the response has a time delay with respect to input. However, the theoretical equations derived above are all based on the assumption that there is no time delay between input and output (i.e., the response to the input is instantaneous). Therefore, the synchronization based on the maximum correlation is appropriate for the formulation, even if it is not the real case.

Next, in order to specify the model order, the variation of error with model order is investigated. The results are plotted in Fig. 5a, b, and c. It was assumed in Figs. 5b and 5c that  $n_b = n_a - 1$ . The reason for this is that if the site amplification can actually be represented by a parallel system (i.e., sum of second order filters), as given by Eqs. 12-17, then theoretically  $n_b$  would be equal to  $n_a - 1$  (Şafak, 1987a). Fig. 5a indicates that  $n_a \geq 12$ . The error is not very sensitive to  $n_b$ , as seen in Fig. 5b; thus,  $n_b = n_a - 1$  is acceptable. Fig. 5c shows that error is minimum for  $n_c = 0$ . This suggests that the noise in the signals is approximately white-noise.

Based on Fig. 5, a model with  $n_a = 12$ ,  $n_b = 11$ , and  $n_c = 0$  is chosen. The parameters were calculated recursively by using Eq. 22. Time variations of parameters  $a_j$  and  $b_j$  are

plotted in Figs. 6a and 6b. The  $a_j$  values are fairly constant beyond three seconds. Recall that the  $a_j$ 's determine the dominant frequencies of the site. The  $b_j$  values show distinct changes at 3-second and 9-second points. They are also fairly constant beyond nine seconds. Note that the scaled values, not the exact values, of  $b_j$ 's are given in Fig. 6b. The reason for large fluctuations at the beginning can be attributed to the source effects. The beginning of constant regions indicate that the rupture process is over.

The amplitude of the transfer function, and its match with the spectral ratio at  $t = 18$  sec. are given in Fig. 7. The match with the spectral ratio seems to be good, except for very low frequencies. This can be attributed to the effects of windowing on Fourier spectra and spectral ratios. The corresponding numerical values for the parameters, pole locations, modal frequencies and dampings, and the weighting factors are given in Table 1. Since  $n_a = 12$ , the model gives the first six modes of the site.

The results of model validity checks on the residuals are given in Fig. 8. Fig. 8a shows the residual time series (Eq. 20), and Fig. 8b shows its Fourier amplitude spectrum. Recall that, for validity, the residual should be white-noise. Although the amplitude spectrum of the residuals is not completely flat, as should for white-noise, it is fairly broad band. It should also be remembered here that the residual plotted represents only a sample function of the random noise process. Theoretically, the ensemble average of residual spectra should be flat. The autocovariance of the residuals are given in Fig. 8c. The straight lines in the figure show the values corresponding to 90-percent confidence levels in  $\chi^2$  distribution test. For model validity, the autocovariance should not cross the straight lines, except at zero lag. However, the calculated autocovariance of the residuals crosses the 90-percentile boundaries at several points. This suggests that the model for the noise is not very good. Fig. 8d gives the cross-covariance of the residuals with the input. The straight lines are the 90-percent confidence limits based on the standard (0,1) normal distribution. The cross-covariance curve crosses the boundaries at one location. The implication of this is that the model order should be increased.

Next, a higher order model with  $n_a = 16$ ,  $n_b = 15$ , and  $n_c = 0$  is tried. The transfer function and its match with the spectral ratio are plotted in Fig. 9, again at  $t = 18$  sec. The corresponding numerical values for the parameters and modal characteristics are given also in Table 1. The residual tests are presented in Fig. 10, which shows slight improvement over the previous model, Fig. 8. The cross-covariance values now are all inside the 90-percentile confidence interval. The auto-covariance curve still exceeds the boundaries at some points, but the amplitudes are smaller than those of the previous model. Thus the model is still not valid for the noise, but it is valid for the signal. In other words, the filter is accurate for site amplification (which is more important from the engineering view point), but not accurate noise. It is possible to identify the noise better

by using different models than the ARMAX model (see Şafak, 1987a).

Further studies on this site, done using different models and records, have shown that (Şafak and Çelebi, 1987): (a) the higher the model order the more detail of the site amplification is obtained up to about 16th order model (i.e., an increase in the model order gives the next significant mode); beyond the 16th order the results become unstable because of the numerical precision and the noise effects, (b) the assumption that the noise is white-noise is appropriate (i.e.,  $n_c = 0$ ), and (c) the amplification characteristics for this site are approximately time invariant.

## SUMMARY AND CONCLUSIONS

A time domain discrete-linear recursive filtering approach is presented to characterize the site amplification. The site is modeled as a finite order linear filter of unknown coefficients, represented by an ARMAX model. The input and output of the filter are the rock-site and soil-site recordings, respectively, both contaminated with noise. The parameters of the filter are determined by using recursive prediction error technique, based on the stochastic approximation theory. The transfer function, modes, and the impulse-response function of the site can all be calculated, once the filter parameters are known.

The theory is applied to an actual site amplification problem observed during the March 3, 1985 Chile earthquake. The results show that the method has several advantages over the commonly used spectral ratio technique. They can be summarized as: (a) filtering of the noise is done over the whole frequency band, which can not be accomplished by band-pass type (e.g., Butterworth type) filters, (b) time-varying characteristics of the site can easily be detected, and (c) site amplification is represented analytically in the form of a simple recursive filter.

The method presented can have various other applications in earthquake engineering and structural dynamics. Applications for modeling spectral shape and source scaling of ground motions are given in Şafak (1987b), whereas applications for system identification in structural dynamics for wind and earthquake excitations are given in Şafak (1987c).

## REFERENCES

- Albert, A.E. and L.A. Gardner (1967). *Stochastic approximation and nonlinear regression*, Research Monograph 42, MIT Press, Cambridge, MA.
- Bohlin, T. (1987). Model validation, *Encyclopedia of Systems and Control* (M. Singh, editor), Pergamon Press, Oxford, England.
- Cadzow, J.E. (1973). *Discrete-time systems*, Prentice-Hall, Englewood Cliffs, NJ.
- Celebi, M. (1986). Seismic site-response experiments following the March 3, 1985 central Chile earthquake, *Open-File Rep.* 86-90, U. S. Geol. Surv., Menlo Park, CA.
- Goodwin G.C. and K.S. Sin (1984). *Adaptive filtering, prediction and control*, Prentice-Hall, Englewood Cliffs, NJ.
- Jaswinski, A.H. (1970). *Stochastic processes and filtering theory*, Academic Press, New York, NY.
- Kailath, T. (1976). *Lectures on linear least-squares estimation*, Springer-Verlag, Wien, West Germany.
- Kolmogorov, A.N. (1941). Interpolation and extrapolation of stationary random sequences, *Bull. Acad. Sci. (USSR)*, translated by the Rand Corp., RM-3090-PR, 1962, Santa Monica, CA.
- Kushner, H.J. and D.S. Clark (1978). *Stochastic approximation methods for constrained and unconstrained systems*, Springer-Verlag, New York, NY.
- Ljung, L. (1985). On the estimation of transfer functions, *Automatica*, vol. 21, pp. 677-696.
- Ljung, L. (1987). *System Identification: Theory for the User*, Prentice-Hall, Englewood Cliffs, NJ.
- Ljung, L. and T. Soderstrom (1983). *Theory and Practice of Recursive Identification*, MIT Press, Cambridge, MA.
- Rabiner, L.E. and B. Gold (1975). *Theory and Application of Digital Signal Processing*, Prentice-Hall, Englewood Cliffs, NJ.
- Rake, H. (1980). Step response and frequency response methods, *Automatica*, vol. 16, pp. 519-526.
- Robbins, H. and S. Monro (1951). A stochastic approximation method, *Annals of Mathematical Statistics*, vol.22, pp. 400-407.
- Robinson, E.A. (1967). *Multichannel Time Series Analysis with Digital Computer Programs*, Holden-Day, San Francisco, CA.
- Safak, E. (1987a). Stochastic filtering, prediction, and control in earthquake engineering, *Open-File Report 87-*, U. S. Geological Survey, Menlo Park, CA.
- Safak, E. (1987b). Optimal-adaptive filters for modeling spectral shape, site amplification, and source scaling, submitted to *Soil Dynamics and Earthquake Engineering*.

Şafak, E. (1987c). System identification by using discrete-linear filters and stochastic approximation techniques, will be submitted to *ASCE Journal of Engineering Mechanics*.

Şafak, E. and M. Çelebi (1987). On identification of site amplification from earthquake records, *proceedings*, Soc. for Exp. Mech., Spring Conf., June 1987, Houston, TX.

Tretter, S.A. (1976). *Introduction to Discrete-Time Signal Processing*, John Wiley and Sons, New York, NY.

Wiener, N. (1949). *The Extrapolation, Interpolation and Smoothing of Stationary Time Series with Engineering Applications*, John Wiley and Sons, New York, NY.

Young, P.C. (1984). *Recursive Estimation and Time Series Analysis*, Springer-Verlag, New York, NY.

TABLE 1

Filter parameters, pole locations, and the corresponding modal frequency, damping, and the weighting factors for the site amplification example (records are from the March 3, 1985 Chilean earthquake).

$n_a = 12, n_b = 11, n_c = 0; t = 18 \text{ sec.}$

$j$	$a_j$	$b_j$	$c_j$	$r_j$	$\phi_j(\text{deg.})$	$f_j$	$\xi_j$	$2\Re(q_j)$	$2\Re(q_j \bar{p}_j)$
0	1.000	0.000	1.000						
1	-4.121	-0.008	0.000	0.928	0.912	7.284	0.082	229.574	80.451
2	9.649	0.030	0.000	0.928	-0.912	7.284	0.082	229.574	80.451
3	-16.660	-0.067	0.000	0.920	1.311	10.453	0.064	1191.369	1052.694
4	23.273	0.115	0.000	0.920	-1.311	10.453	0.064	1191.369	1052.694
5	-27.382	-0.160	0.000	0.944	-1.135	9.044	0.050	436.193	1222.136
6	27.639	0.184	0.000	0.944	1.135	9.044	0.050	436.193	1222.136
7	-24.082	-0.180	0.000	0.948	0.583	4.662	0.091	-262.090	106.185
8	17.982	0.148	0.000	0.948	-0.583	4.662	0.091	-262.090	106.185
9	-11.280	-0.097	0.000	0.927	-1.484	11.826	0.051	-161.601	-557.945
10	5.708	0.046	0.000	0.927	1.484	11.826	0.051	-161.601	-557.945
11	-2.130	-0.015	0.000	0.960	0.183	1.492	0.218	-77.697	129.498
12	0.462	0.000	0.000	0.960	-0.183	1.492	0.218	-77.697	129.498

$n_a = 16, n_b = 15, n_c = 0; t = 18 \text{ sec.}$

$j$	$a_j$	$b_j$	$c_j$	$r_j$	$\phi_j(\text{deg.})$	$f_j$	$\xi_j$	$2\Re(q_j)$	$2\Re(q_j \bar{p}_j)$
0	1.000	0.000	1.000						
1	-4.523	-0.001	0.000	0.933	0.731	5.842	0.094	-171.195	232.077
2	11.793	0.000	0.000	0.933	-0.731	5.842	0.094	-171.195	232.077
3	-22.980	0.006	0.000	0.943	-1.513	12.045	0.039	-2345.374	-2339.097
4	36.880	-0.024	0.000	0.943	1.513	12.045	0.039	-2345.374	-2339.097
5	-51.014	0.056	0.000	0.950	-1.233	9.822	0.042	-1912.515	-1970.833
6	62.412	-0.101	0.000	0.950	1.233	9.822	0.042	-1912.515	-1970.833
7	-68.565	0.147	0.000	0.944	0.502	4.024	0.113	-162.119	44.324
8	68.156	-0.181	0.000	0.944	-0.502	4.024	0.113	-162.119	44.324
9	-61.456	0.194	0.000	0.943	1.346	10.719	0.044	763.469	-100.972
10	50.148	-0.183	0.000	0.943	-1.346	10.719	0.044	763.469	-100.972
11	-36.746	0.147	0.000	0.947	-0.934	7.446	0.058	1321.034	-388.209
12	23.817	-0.102	0.000	0.947	0.934	7.446	0.058	1321.034	-388.209
13	-13.295	0.057	0.000	0.939	1.016	8.099	0.062	-45.058	-712.433
14	6.113	-0.026	0.000	0.939	-1.016	8.099	0.062	-45.058	-712.433
15	-2.096	0.007	0.000	0.980	0.168	1.347	0.119	-6.407	107.599
16	0.421	0.000	0.000	0.980	-0.168	1.347	0.119	-6.407	107.599

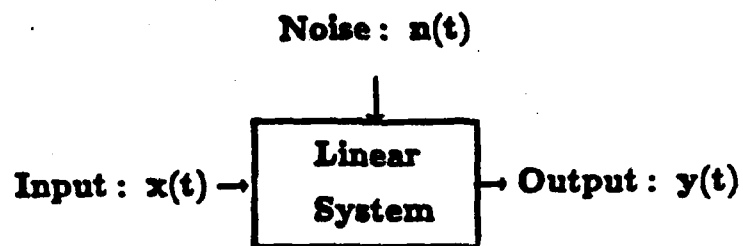


FIG. 1. Schematic of a single-input, single-output system contaminated by noise.

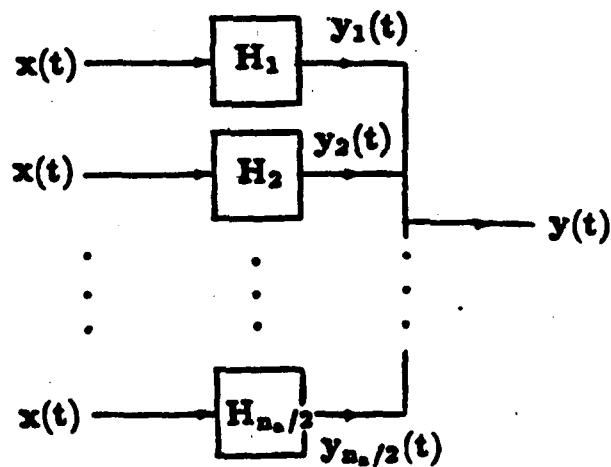
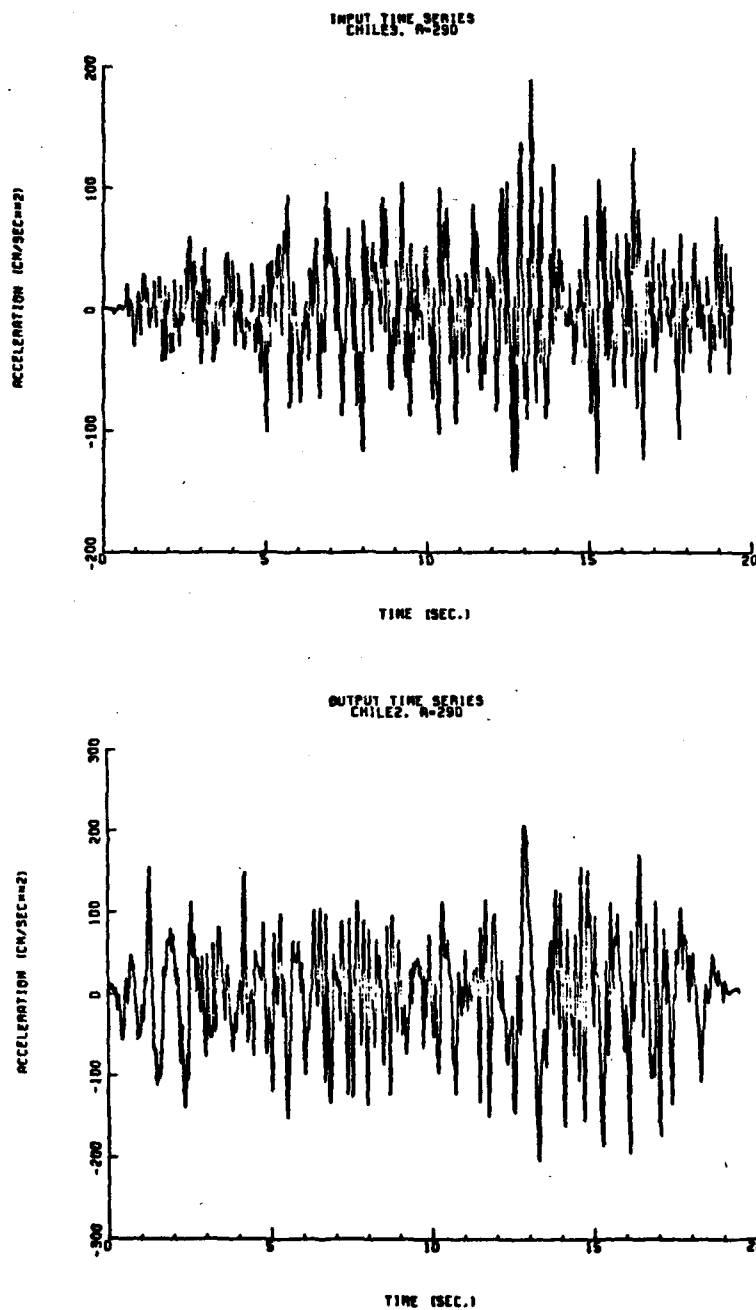
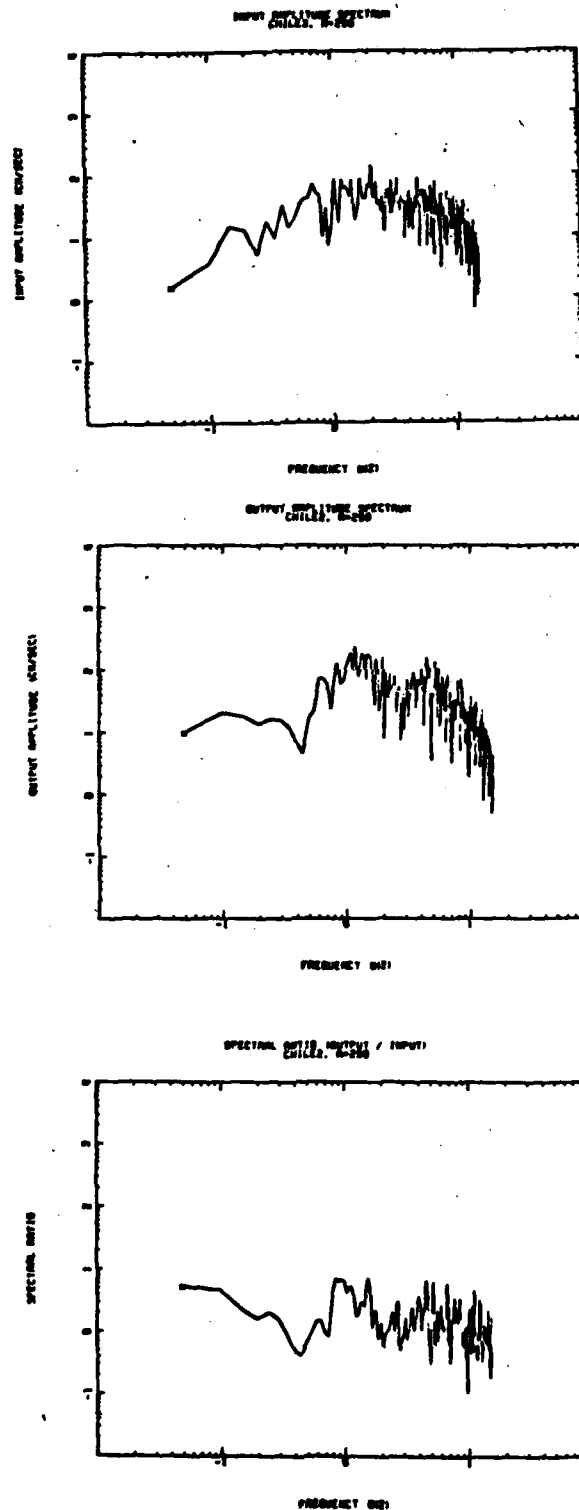


FIG. 2. Schematic of parallel form realization of a single-input single-output linear system.





**FIG. 3.** Input (rock site) and output (soil site) time series for the site amplification example. The records are from the 3 March 1985 Chilean earthquake.



**FIG. 4.** Input (rock site) and output (soil site) Fourier amplitude spectra and the smoothed spectral ratio (soil site/rock site) for the site amplification example. The records are from the 3 March 1985 Chilean earthquake.

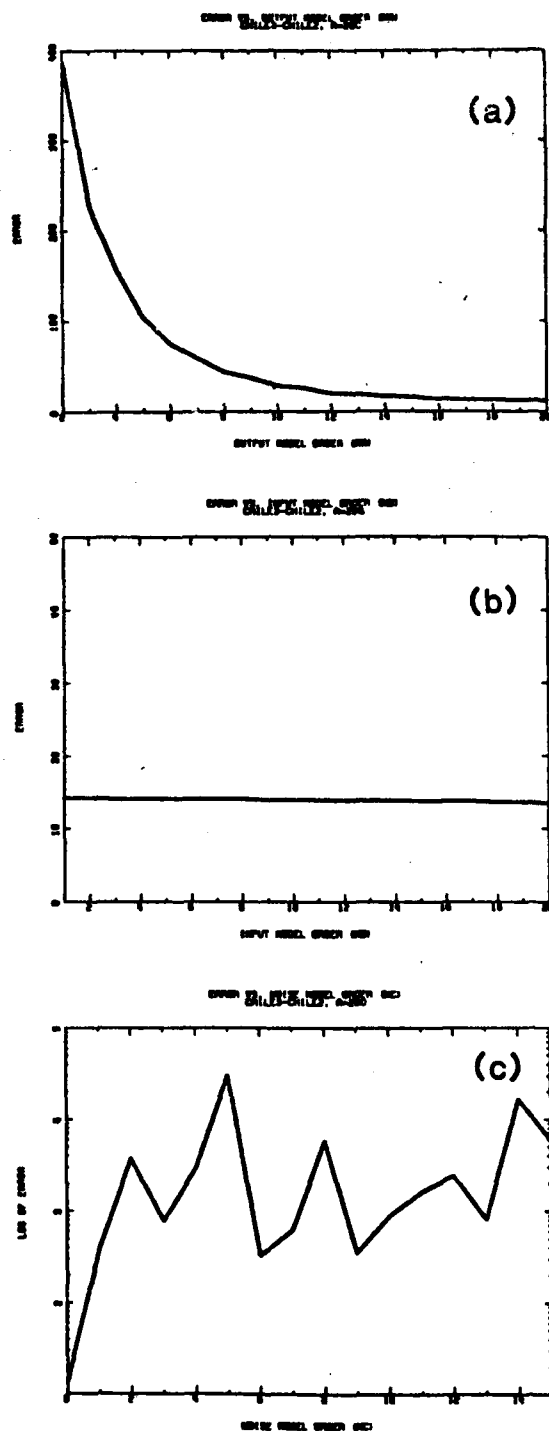
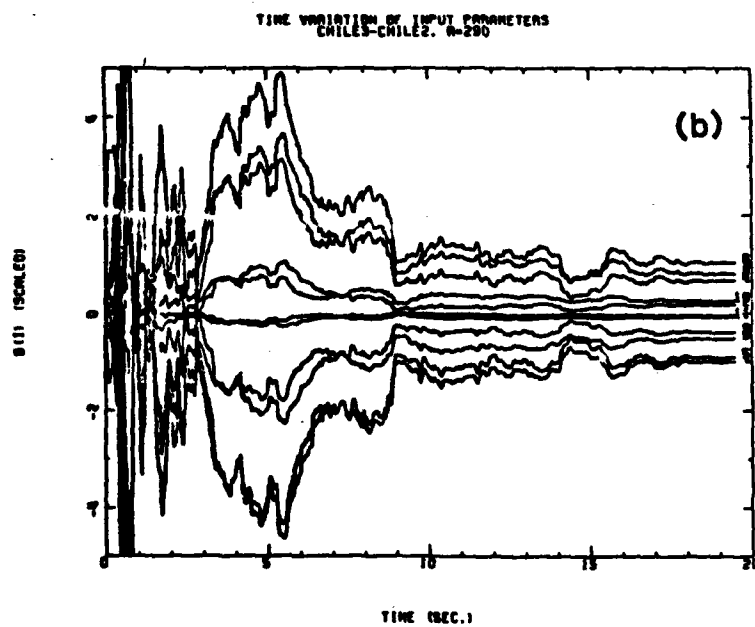
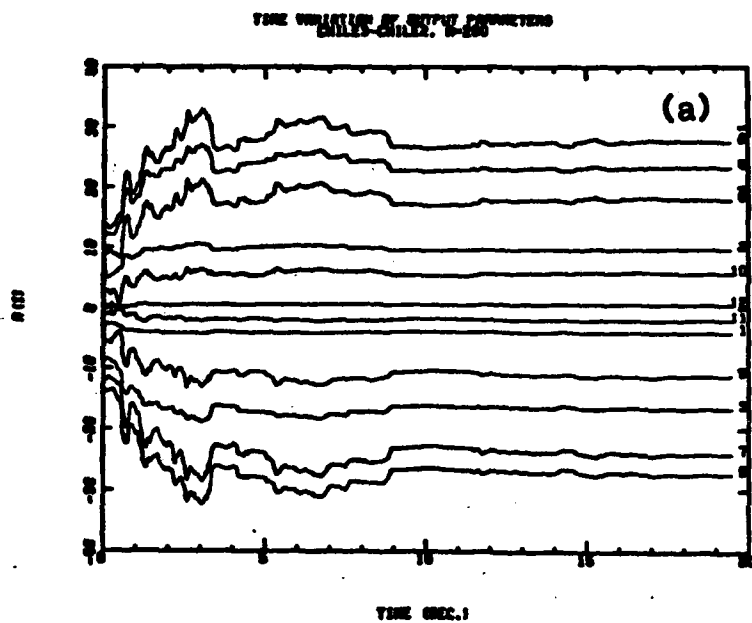
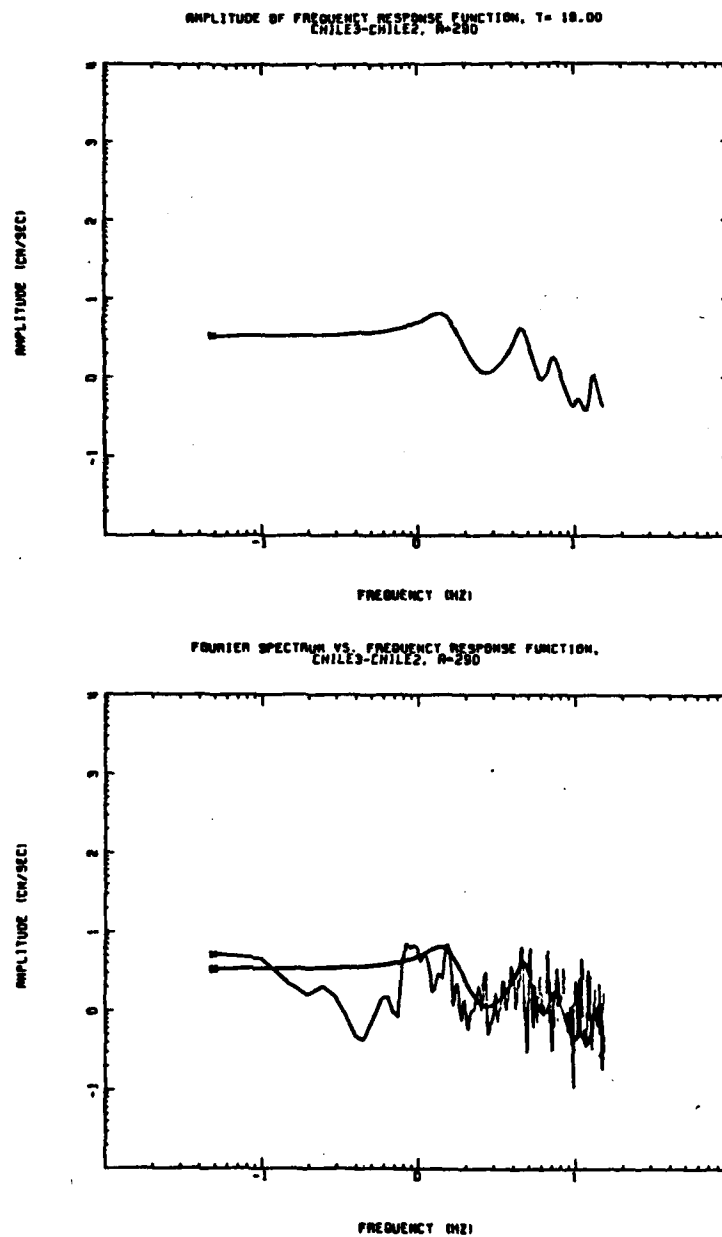


FIG. 5. Model order versus prediction error for the site amplification examples (1985 Chilean earthquake): (a)  $n_a$  vs.  $V(N)$  with  $n_b = n_a - 1$  and  $n_c = 0$ ; (b)  $n_b$  vs.  $V(N)$  with  $n_a = 12$  and  $n_c = 0$ ; (c)  $n_c$  vs.  $V(N)$  with  $n_a = 12$  and  $n_b = 11$ .



**FIG. 6.** Time variation of model parameters for the site amplification example (1985 Chilean earthquake): (a)  $a_j$ ,  $j = 1 \sim 12$ ; (b)  $b_j$ ,  $j = 1 \sim 11$ .



**FIG. 7.** The amplitude of the transfer function for (12-11-0) model for the site amplification example (1985 Chilean earthquake) evaluated at  $t = 18$  sec., and its match with the Fourier amplitude spectrum.

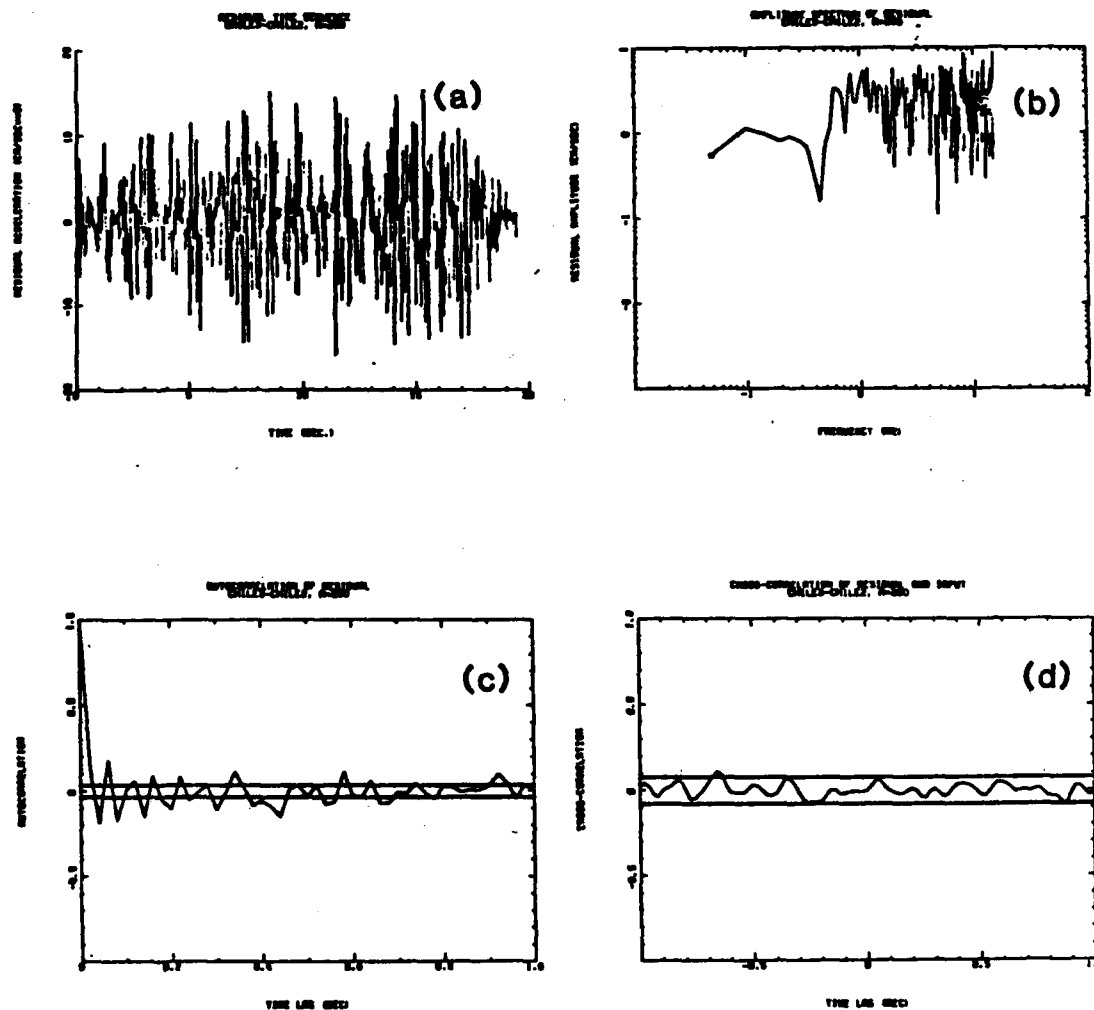


**FIG. 8.** The residual tests for (12-11-0) model for the site amplification example (1985 Chilean earthquake) evaluated at  $t = 18$  sec.: (a) time history of the residual; (b) Fourier amplitude spectrum of the residuals; (c) autocovariance function of the residuals, and the 90-percentile confidence limits for whiteness according to the Chi-square  $\chi^2$  test; (d) cross-covariance function of the residuals with input, and the 90-percentile confidence limits according to (0,1) normal distribution law.

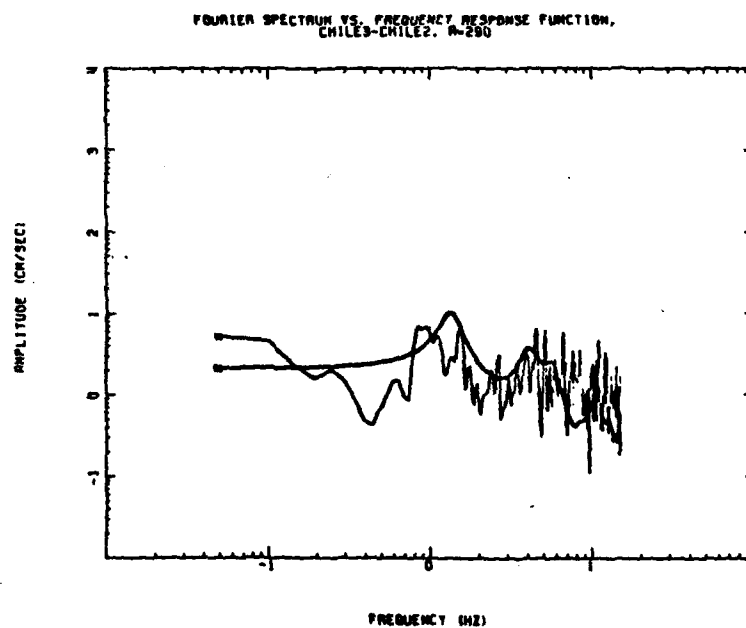
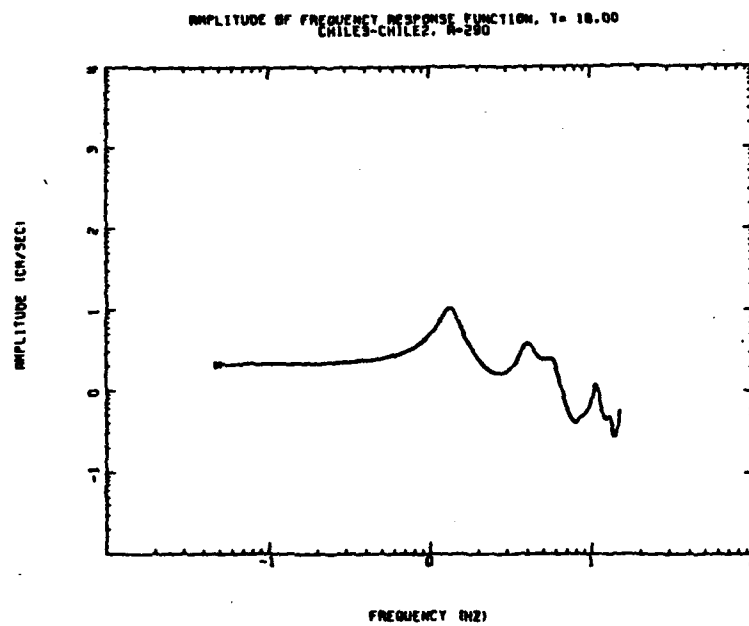


**FIG. 9.** The amplitude of the transfer function for (16-15-0) model for the site amplification example (1985 Chilean earthquake) evaluated at  $t = 18$  sec., and its match with the Fourier amplitude spectrum.

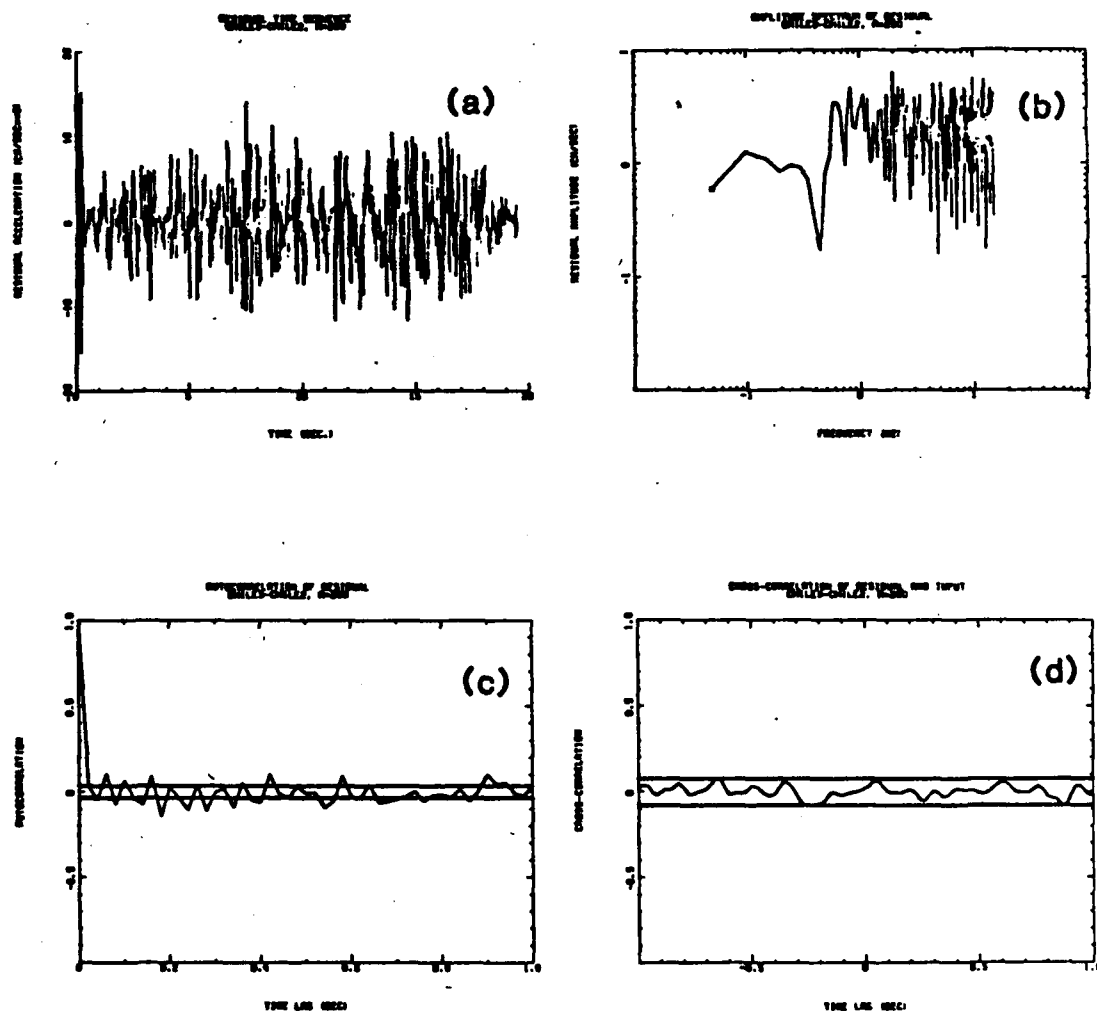
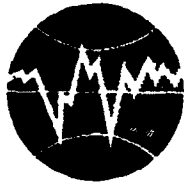


**FIG. 10.** The residual tests for (16-15-0) model for the site amplification example (1985 Chilean earthquake) evaluated at  $t = 18$  sec.: (a) time history of the residual; (b) Fourier amplitude spectrum of the residuals; (c) autocovariance function of the residuals, and the 90-percentile confidence limits for whiteness according to the Chi-square  $\chi^2$  test; (d) cross-covariance function of the residuals with input, and the 90-percentile confidence limits according to (0,1) normal distribution law.





**TURKISH NATIONAL COMMITTEE FOR  
EARTHQUAKE ENGINEERING**

**THIRTEENTH REGIONAL SEMINAR ON EARTHQUAKE ENGINEERING**

**September 14-24, 1987 - Istanbul - Turkey**

**Frank K. Chang**

**US Army Engineer Waterways Experiment Station  
Vicksburg, Mississippi  
U.S.A.**

## SITE DEPENDENT ROOT-MEAN-SQUARE ACCELERATION

F. K. Chang and A. G. Franklin

U. S. Army Engineer Waterways Experiment Station, Corps of Engineers, Vicksburg, Mississippi 39180, U.S.A.

### PURPOSE AND SCOPE

There are unique relationships connecting peak ground acceleration (PGA), root-mean-square acceleration (RMSA), or average acceleration, power spectral density function (PSDF), and duration (record length) of strong-motion earthquake records. The purpose of this study is to determine the site dependence of the PSDF and its scaling factor, which could be correlated with the damage intensity or Modified Mercalli Intensity (MMI), from the above relationships.

Factors affecting the ground motion at a particular site include the source mechanism (nature of fault movement and magnitude of energy release), propagation path characteristics, the direction of the site relative to the fault rupture, and local geological and soil conditions. This study, however, deals only with the influence of local geological and soil conditions on ground motion.

### PREVIOUS WORK

Seed, Ugas, and Lysmer<sup>1</sup> and Kiremidjian and Shah<sup>2</sup> presented similar results of a statistical analysis of the site-dependent response spectral shapes from ground motion accelerograms obtained mostly in the western United States. The analysis shows clear differences in spectral shapes for different soil and geological conditions. Chang and Krinitzsky<sup>3</sup> studied the duration and spectral content of strong-motion records from the western United States according to site conditions and found that the predominant frequencies are in the range of 1.0 to 6.67 Hz and the spectral shape depends on the source spectrum function (magnitude), distance, and geological conditions.

Considering the earthquake ground motion to be random in nature, Arnold<sup>4</sup> and Arnold and Vanmarcke<sup>5</sup> studied the influence

of site azimuth relative to source fault orientation and local soil conditions on earthquake ground motion spectra for the San Fernando, California, earthquake of 9 February 1971 using PSD functions. The result showed that local soil conditions and site azimuth, as well as epicentral distance, can have a significant effect on both the intensity and the frequency content of ground motions. This study demonstrated the potential value of PSD functions as a tool for comparing and studying variations in ground motion characteristics and also showed the great utility of PSD functions as input to random vibration analyses of structural response.

#### POWER SPECTRAL DENSITY FUNCTION (PSDF)

In the application of the random vibration theory of linear systems for evaluation of the effects of variations in ground motion characteristics on structural response to earthquake excitation, the ground motion may be defined in the form of a PSDF. The PSDF,  $G(\omega)$ , is defined as a measure of the ground motion power or energy per unit time as a function of frequency  $\omega$  (Figure 1). Usually, estimates of the PSD are obtained from the squared amplitudes of the Fourier transform, or the squared Fourier amplitude spectrum. In Figure 1,  $A_j$  is the amplitude of the Fourier transform at frequency  $\omega_j$ .

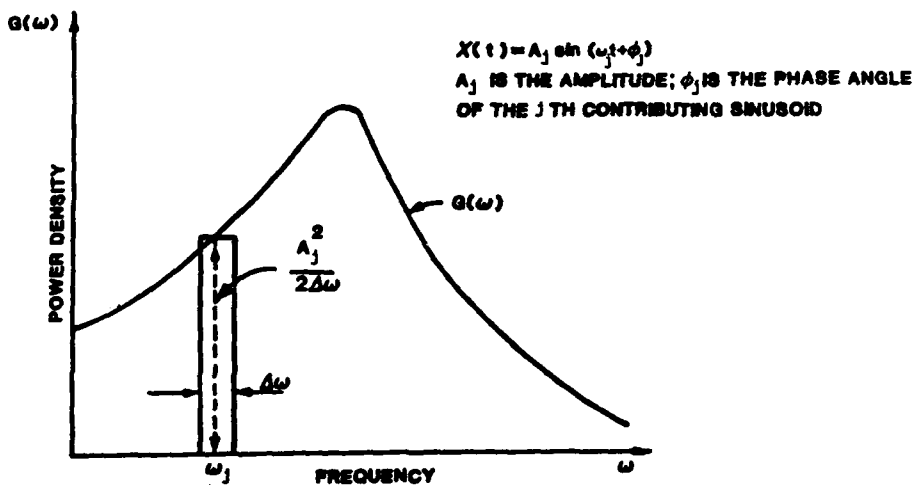


Figure 1. The PSDF  $G(\omega)$

#### FOURIER TRANSFORM

Generally, the given earthquake ground motion function, such as an acceleration versus time plot, can be represented in the time domain as  $a(t)$  and in the frequency domain as  $F(\omega)$ :

$$F(\omega) = \int_0^{t_0} a(t) e^{-i\omega t} dt, \quad i = \sqrt{-1} \quad (1)$$

and

$$a(t) = \frac{1}{\pi} \int_{\omega_1}^{\omega_0} F(\omega) e^{i\omega t} d\omega, \quad i = \sqrt{-1} \quad (2)$$

Equations 1 and 2 are called the Fourier transform pair; i.e.,  $F(\omega)$  is the Fourier integral or Fourier transform of  $a(t)$ , and  $a(t)$  is the inverse Fourier transform of  $F(\omega)$ . The symbols  $t$  and  $t_0$  denote the instant in time and total duration, and  $\omega$ ,  $\omega_1$ , and  $\omega_0$  represent the frequency, lower frequency bound  $\omega_1 = 2\pi/t_0$ , and maximum frequency (in radians per second), respectively. For practical purposes,  $\omega_1$  can usually be taken as zero.

#### TOTAL INTENSITY, AVERAGE POWER, AND PSDF

By Parseval's theorem, the relation between the energy of the motion as expressed in the time domain and in the frequency domain can be represented in the following equations. For a nonperiodic function, the total intensity (total energy) or Arias intensity  $I_0$  delivered by the source is given by

$$I_0 = \int_0^{t_0} |a(t)|^2 dt = \frac{1}{\pi} \int_0^{\omega_0} |F(\omega)|^2 d\omega \quad (3)$$

The mean-square average value is expressed

$$\frac{1}{t_0} \int_0^{t_0} |a(t)|^2 dt = \frac{1}{\pi} \frac{1}{t_0} \int_0^{\omega_0} |F(\omega)|^2 d\omega = \int_0^{\omega_0} G(\omega) d\omega \quad (4)$$

in which  $G(\omega)$  is the energy per unit time (power), or the power spectral density of the function  $a(t)$ . The integrand on the right side of Equation 4 can be written as

$$G(\omega) = \frac{1}{\pi} \frac{1}{S_0} |F(\omega)|^2 \quad (5)$$

if  $S_0$  (duration of strong motion) is substituted for  $t_0$ ,  
and

$$\frac{1}{\pi} \int_0^{\omega_0} |F(\omega)|^2 d\omega = S_0 \int_0^{\omega_0} G(\omega) d\omega$$

The quantity  $|F(\omega)|^2$  is called the power (energy) spectrum or power spectral density function of  $a(t)$  (Hsu<sup>6</sup>). The left side of Equation 4 gives the statistical (PSDF) average power  $\lambda_0^2$  of the function  $a(t)$  over the total duration of the motion  $t_0$ . From Equation 4, also note that  $\lambda_0^2$  is equal to the area under the curve of  $G(\omega)$  in Figure 1. Therefore, the average power can be written as

$$\lambda_0^2 = \int_0^{\omega_0} G(\omega) d\omega \quad (6)$$

A more effective way for dealing with the frequency content of ground motion is through the normalized spectral density function  $G^*(\omega)$ :

$$G^*(\omega) = \frac{1}{\lambda_0^2} G(\omega) \quad (7)$$

If  $G_i^*(\omega)$  is an individual normalized PSD function, the statistical mean NPSD curve will be

$$\bar{G}^*(\omega) = \frac{1}{n} \sum_{i=1}^n G_i^*(\omega), \quad i = 1, 2, \dots, n \quad (8)$$

In practice, curves of  $\bar{G}^*(\omega)$  computed from suites of actual earthquake records show large and irregular fluctuations. To isolate the systematic component from the random variations, frequency smoothing with a "Hanning" window (Blackman and Tukey<sup>7</sup>) was used.

## DATA SELECTION AND SITE CLASSIFICATIONS

A total of 421 horizontal ground accelerograms from 89 earthquakes, mostly in the western United States and Japan (with a few records from Russia, Rumania, and India), were selected for this analysis. Based on the site classifications of Seed, Ugas, and Lysmer<sup>1</sup>, these records have been divided into four groups: (a) 56 records for rock sites, (b) 131 records for stiff soil sites (depth <150 ft), (c) 120 records for deep cohesionless soil sites (depth >250 ft), and (d) 114 records for soft to medium clays with associated strata of sands or gravels. One hundred seventy-three of the 421 records were obtained from the California Institute of Technology<sup>8</sup> Volume II-Corrected Accelerograms (1971-75), and 220 uncorrected records were provided by the Port and Harbour Research Institute, Japan. The digitized Gazli (USSR) and Bucharest (Rumania) records were provided by Dr. A. G. Brady, U. S. Geological Survey. All 421 corrected and uncorrected records were adjusted to zero mean before processing the PSD.

## DEFINITION OF AVERAGE POWER AND AVERAGE ACCELERATION

The main approach used in this study was to determine the normalized mean and the mean plus one standard deviation PSD shape (NPSD) for each group, and the average acceleration  $\lambda$  which is the root-mean-square of the average power  $\lambda^2$  for each raw record. Figure 1 shows  $G(\omega)$ , whose value at  $\omega$  is equal to  $A^2/2\Delta\omega$ , so that  $\lambda^2$  is actually the power or energy density in an accelerogram for a finite frequency band ( $0 \leq f \leq 10$  Hz in this study), and  $A_j$  is the amplitude of the  $j$ th frequency component in centimetres per second squared. The total or average power will become equal to the area under the continuous curve  $G(\omega)$ .

## RECORD LENGTH, INCREMENT FREQUENCY, AND NPSD FUNCTION

The record length and spectral content (spectral amplitude and frequency range) are two basic elements for controlling the spectral intensity. The incremental frequency  $\Delta f$ , used in the PSD computer program, depends on the total record length. Since it is necessary to use the same value for  $\Delta f$  throughout, all accelerograms have been processed to give them a duration of 163.82 sec or 8192 ( $2^{13}$ ) digital points with an equal time interval  $\Delta t$  of 0.02 sec, which gives  $\Delta f = 0.006104$  Hz. Outside the time of the actual record, the amplitudes at extended times were set to zero. In this study, the PSD function  $G(f)$  has been defined to include only the frequency range of 0 to 10 Hz, since this is also the natural frequency-range of many engineering structures, so that

$$\lambda^2 = \int_0^{10 \text{ Hz}} G(f) df \quad (9)$$

Since  $\Delta f$  is 0.006104 Hz, there are 1640 points in the raw PSD function for each accelerogram. The NPSD function is defined as the PSD amplitude divided by the area  $\lambda^2$  under the power density versus frequency curve. This area may also be called the spectral density or spectral intensity.

#### ANALYSIS OF SITE-DEPENDENT PSD SPECTRAL SHAPE

The NPSD functions for the horizontal accelerograms in each group were first determined and then were analyzed statistically to obtain the average NPSD spectra and the average plus one standard deviation ( $\sigma$ ) NPSD spectra (about 84 percentile). Figure 2 present these mean and mean plus one standard deviation NPSD spectra for the four different site conditions. The mean NPSD spectra for the different site conditions are compared in Figure 2a, and the mean plus one standard deviation NPSD spectra are compared in Figure 2b. Both NPSD spectra in Figures 2a and 2b are smoothed 500 times.

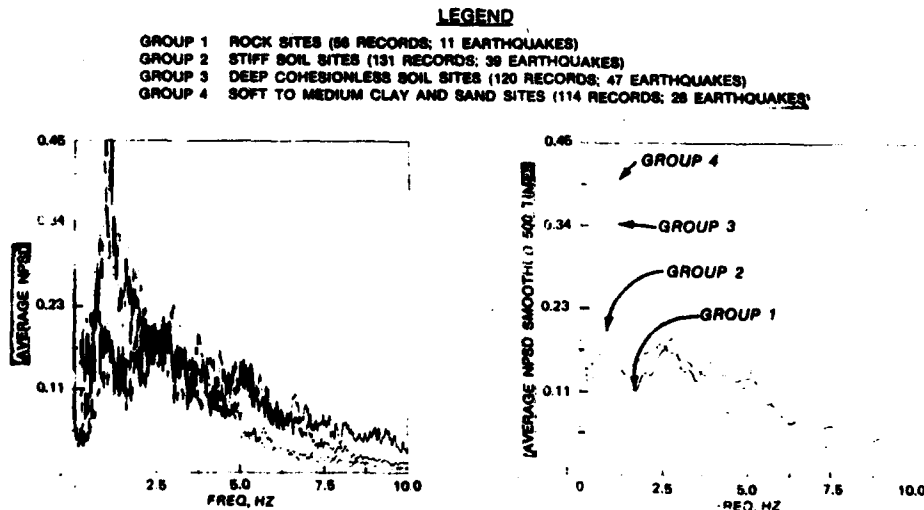


Figure 2a. Comparison of mean NPSD curves of four soil groups, raw (left) and smoothed 500 times (right)

#### LEGEND

GROUP 1 ROCK SITES (88 RECORDS; 11 EARTHQUAKES)  
 GROUP 2 STIFF SOIL SITES (131 RECORDS; 30 EARTHQUAKES)  
 GROUP 3 DEEP COHESIONLESS SOIL SITES (120 RECORDS; 47 EARTHQUAKES)  
 GROUP 4 SOFT TO MEDIUM CLAY AND SAND SITES (114 RECORDS; 28 EARTHQUAKES)

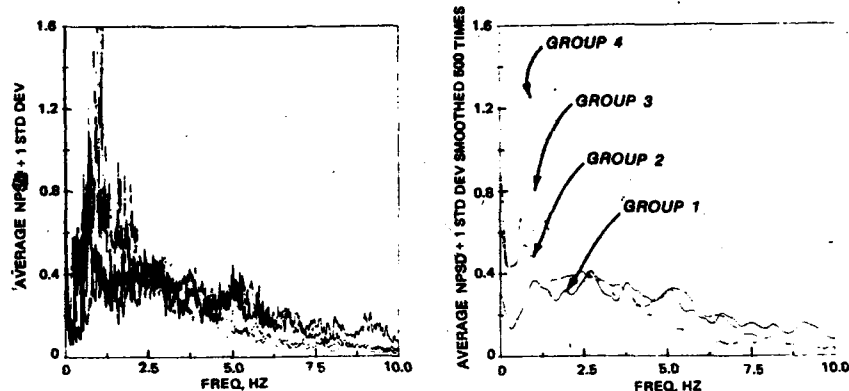


Figure 2b. Comparison of mean +  $\sigma$  NPSD curves of four soil groups, raw (left) and smoothed 500 times (right)

It is clear that the differences in PSD spectral shapes depend on the site conditions. In particular, two categories can be distinguished: sites having soft to medium clays and sands or deep cohesionless soils (>250 ft) are similar and form one category, the soft group; stiff soil and rock sites form another category, the hard group. A dividing line on the frequency axis appears at 2.5 Hz (0.4-sec period). In the frequency range below 2.5 Hz, spectral amplifications for the soft group are much higher than those for the hard group; in the frequency range above 2.5 Hz, spectral simplifications for the hard group are higher than those for the soft group. In the soft group, the energy peaks for the soft to medium clays and sands and the deep cohesionless soils both occur at about the same frequency, 1 Hz, but the amplifications are slightly different (0.4 and 0.35, respectively).

The average NPSD spectrum of the deep cohesionless soil sites has a large hump at 2.8 Hz (0.36-sec period), but the spectrum of the soft to medium clay and sand sites does not. The large amplitude at 0 Hz is believed to be caused by a digitization error, particularly that due to the uncorrected Japanese strong-motion data in the soil site group. For the hard site group, in the frequency range below 2.5 Hz, the spectral amplitude for the stiff soil is higher than that for the rock; but in the frequency range above 2.5 Hz, the spectral amplitude for the rock is slightly higher than that for the stiff soil. The largest energy peaks for the rock sites and the stiff soil sites are at 2.75 Hz (0.36 sec) and 0.8 Hz (1.25 sec), respectively.



# **STATISTICAL CHARACTERISTICS OF THE EARTHQUAKE GROUND MOTIONS**

Table 1 lists the statistical characteristics of the earthquake ground motions.

Table 1

Statistical Characteristics of Earthquake Ground Motion

Condition	Maximum Ground Acceleration, g			Frequencies of Selected Peaks, PSD Hz	Bot. Max. PSD		Average Acceleration, cm/sec <sup>2</sup>		
	Mean	S.D.	Var.		Mean	Mean + σ	Mean	S.D.	Var.
Rock	0.196	0.234	0.054	1.06	0.146	0.369	30.84	38.35	1444.8
				2.75	0.184	0.412			
				3.80	0.160	0.357			
					0.127	0.327			
Stiff soil	0.050	0.384	0.147	1.80	0.190	0.410	12.2	12.2	16.0
				2.45	0.180	0.410			
				5.20	0.127	0.327			
Deep cohesionless soil	0.063	0.272	0.074	1.00	0.350	0.827	11.2	8.3	68.5
				2.80	0.190	0.445			
Soft to medium clay and sand	0.054	0.046	0.002	1.05	0.405	1.315	9.3	8.4	70.5
				4.58	0.089	0.266			

It is apparent from Table 1 that statistical characteristics of the ground motions are strongly site-dependent. The rock sites produce an average maximum ground acceleration of about 0.20 g for the entire suite of 56 records. The rock site group shows the highest maximum acceleration and average acceleration of the four site groups. The PSD function estimates are almost uniform over the peak frequencies of 1.06, 2.75, 3.80, and 5.17 Hz.

The average maximum ground accelerations and PSD spectral intensities (or squared average accelerations) for the other three site groups--stiff soils, deep cohesionless soils, and soft to medium clays and sands--are relatively close together. However, the spreads of the standard deviation of maximum accelerations for the stiff soil and deep cohesionless soil groups are wider than for the soft to medium clays and sand group. This large spread is believed to be caused by the different magnitudes of earthquakes and the different epicentral distances. The group of accelerograms for soft to medium clays and sands shows relatively low ground acceleration but the

highest PSD function estimates at the frequency of 1 Hz among the four groups. One second (1 Hz) is probably near the predominant natural period of sites on soft to medium clays and sands. It seems that the acceleration and the PSD spectral intensity at 1 Hz are roughly in proportion and inverse proportion, respectively, to the degree of stiffness of the site material. In conclusion, the average acceleration or the mean spectral intensity is site-dependent.

#### SITE-DEPENDENT NPSD FUNCTIONS AND SCALING FACTORS

In the previous sections, the four statistical site-dependent NPSD functions of rock, stiff soil, deep cohesionless soil, and soft to medium clay and sand based on the analysis of 421 horizontal ground accelerograms have been established and are shown in Figures 2a and 2b. The scaling factor,  $\lambda^2$  is defined as the area under each PSD,  $G(f)$  versus  $f$ ; its physical meaning in an engineering sense is the average power of spectral intensity. It is logical to use  $\lambda^2$  as the scaling factor of the four NPSD spectra. It is also closely related to the degree of damage to engineering structures. Although earthquake strong ground motions are of primary concern in engineering problems, we used an extended ground motion duration,  $t_o = 163.82$  sec, throughout the analysis. The extended duration was made by adding zeros to the trailing part of the accelerogram.

From Equations (3), (4), and (9), we have

$$\frac{I_o}{t_o} = \int_0^{\omega} G(\omega) d\omega = 2\pi \int_0^{10 \text{ Hz}} G(f) df = 2\pi \cdot \lambda^2 \quad (10)$$

For a given earthquake ground motion

$$I_o = 2\pi \cdot \lambda^2 \cdot t_o = 2\pi \cdot \lambda_o^2 \cdot S_o \quad (11)$$

i.e.

$$\lambda_o^2 = \lambda^2 \cdot (t_o / S_o) \quad (12)$$

where  $\lambda_o^2$  is defined as the scaling factor for the earthquake strong-motion and  $S_o$ , the strong-motion duration for a design earthquake. The total duration  $t_o$  is fixed as 163.82 sec. If the PGA of a design earthquake is known,  $\lambda$  can be determined from the linear relation in the curves of PGA versus  $\lambda$  in Chang's study<sup>9</sup>, or Figure 3 in this paper. Therefore,  $\lambda^2$  can be calculated. Figure 3 presents the mean values obtained from Chang's<sup>9</sup> PGA versus  $\lambda$  plots for the four site groups. They reflect the site-dependency of the average acceleration,  $\lambda$ , or RMSA.

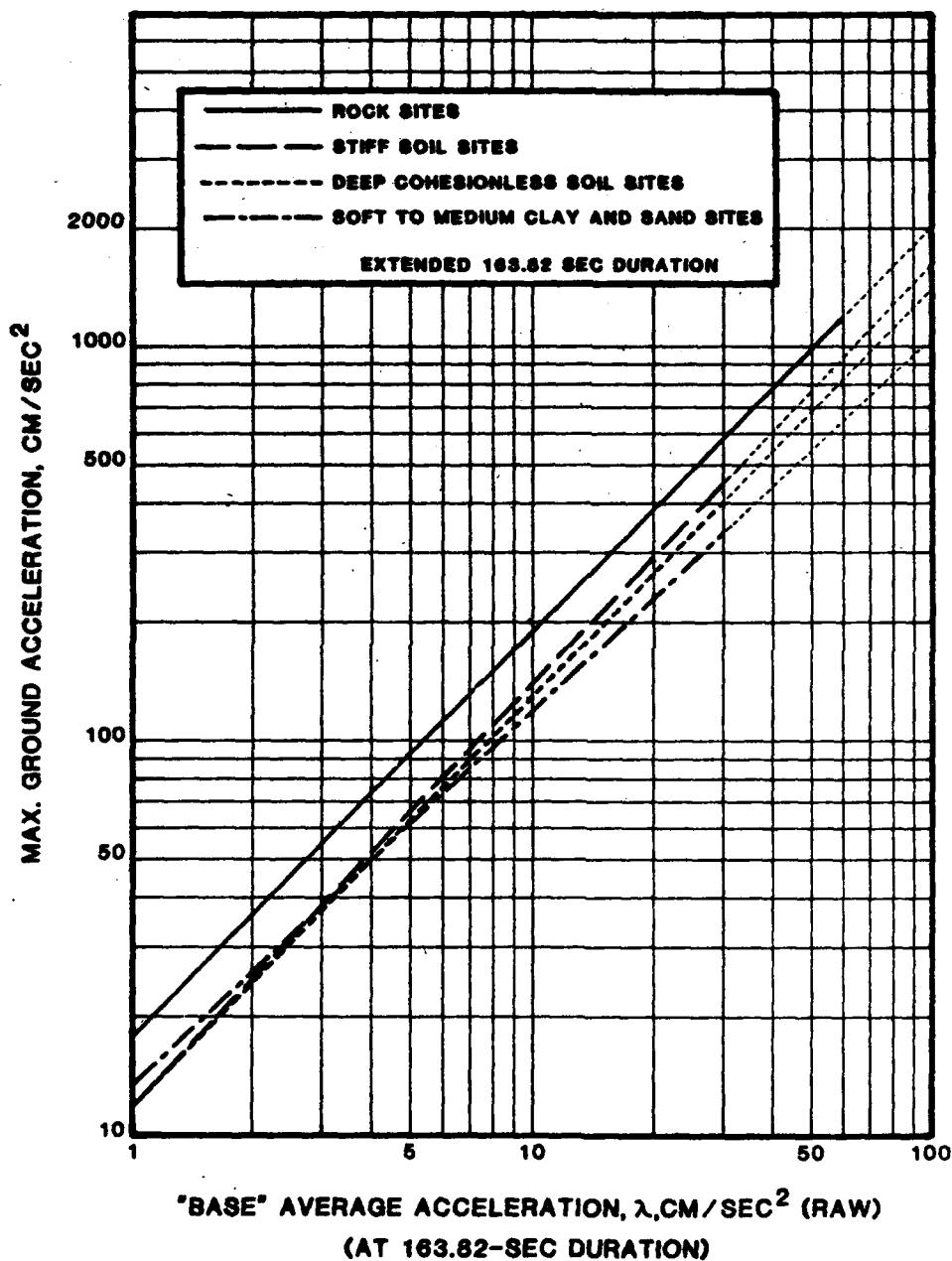


Figure 3. Correlation of maximum ground acceleration (g) versus "base" average acceleration based on extended 163.82-sec duration. Dashed lines show extrapolation beyond existing data

### GENERATION OF EARTHQUAKE ACCELERATION TIME-HISTORY

An important characteristic was found in the study by Chang<sup>9</sup>. The value of  $\lambda$ , or root mean square acceleration (RMSA) for  $t = 163.82$  sec, which was defined as the base average acceleration to distinguish from the RMSA in the strong-motion duration  $S_0$ , was in linear relation with the PGA or  $A_{\max}$ . This is shown in Figure 3. From Equation (1), we have

$$F(\omega) = \int_0^{t_0} a(t)e^{-i\omega t} dt = \int_0^{163.82 \text{ sec}} a(t)e^{-i\omega t} dt \quad (13)$$

Based on Equation (13), if a satisfying statistical results in terms of the Fourier spectrum can be achieved, then using inverse Fourier transform,  $a(t)$  can be derived. This has been demonstrated by Chang, et al.<sup>10</sup>, using the Chang's statistical model of the NPSD,  $G^*(f)$  (Figures 2a and 2b) and the linear relation of PGA versus the average acceleration,  $\lambda$  (Figure 3), with the computer program EQGEN to generate a synthetic earthquake acceleration time-history.

### CORRELATION OF RMSA AND MMI

It will be of much benefit to the engineering community if a quantitative earthquake intensity scale, such as root-mean-square acceleration (RMSA) of the strong-motion duration, can be correlated with the Modified Mercalli Intensity (MMI) (Figure 4 for hard sites and Figure 5 for soft sites).

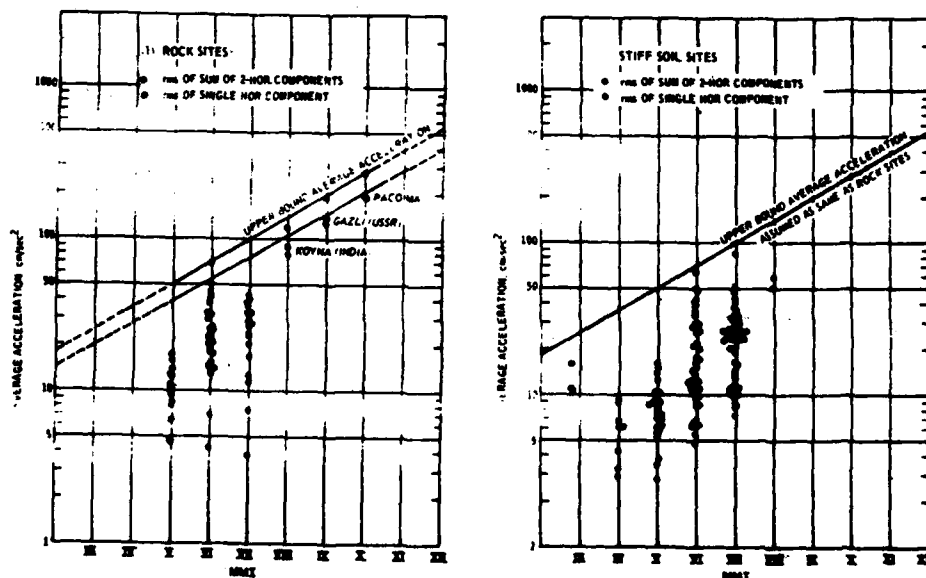


Figure 4. Correlation of upper-bound average acceleration versus MMI - hard sites (rock and stiff soil)

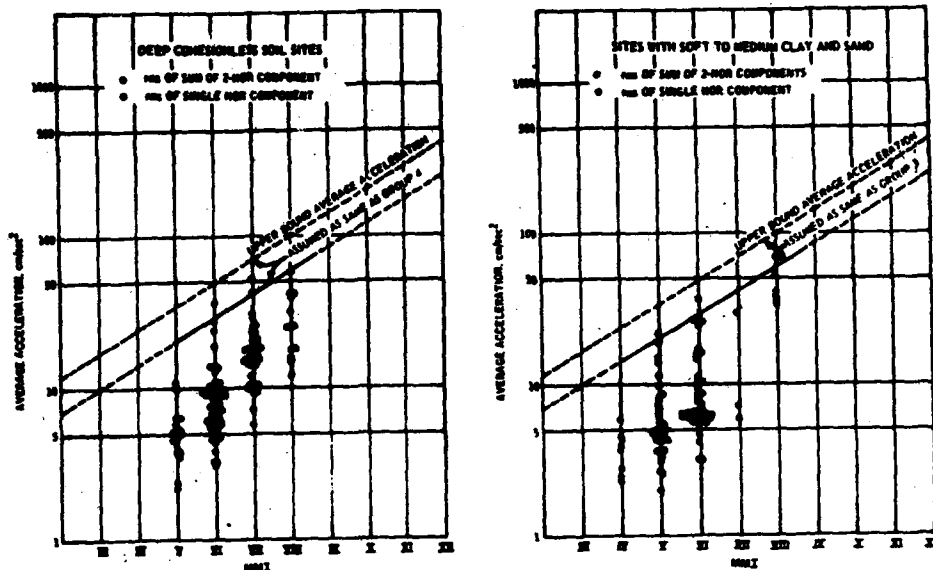


Figure 5. Correlation of upper-bound average acceleration versus MMI - soft sites (deep cohesionless soil and soft to medium clay and sand sites)

Table 2 shows the upper bound of site-dependent RMSA intensity (square root of the sum of two horizontal average powers,  $\lambda_o^2$ ) versus MMI.

Table 2. Correlation of Upper-Bound RMSA versus MMI

Upper bound of the site-dependent RMSA intensity, $\text{cm/sec}^2$ (square root of the sum of 2-horizontal variances, $\lambda_o^2$ )		
MMI	Hard Sites	Soft Sites
XII	400-500	250-400
XI	290-400	200-250
X	200-290	150-200
IX	150-200	100-150
VIII	100-150	70-100
VII	70-100	50-70
VI	50-70	30-50
V	40-50	20-30

To obtain the bounds shown in the above table, the rock and stiff soil sites were combined as hard sites and the deep cohesionless soil and soft soil sites as soft sites. The Pacoima Dam, Karakyr Point (Gazli earthquake), Koyna Dam, and Lake Hughes Array No. 12 sites were located in the epicentral regions and near the faults ( $3 \text{ km} \leq R \leq 20 \text{ km}$ ). They possessed the maximum average accelerations seen and these might be called epicentral average accelerations. It seems from these limited data that the maximum average acceleration at the epicentral region might not be over  $550.0 \text{ cm/sec}^2$ . However, the power  $\lambda^2$  or the average acceleration  $\lambda^2$  is inversely proportional to the duration, i.e., the smaller the duration of strong shaking, the higher the average acceleration or RMSA.

#### CORRELATION OF $I_0$ AND MMI

The correlations of total intensity  $I_0$  with the MMI based on the data of hard sites (Group 1 and 2)<sup>0</sup> and soft sites (Group 3 and 4), are plotted in Figures 6 and 7, respectively. The upper bound line of Figure 6 is established by five earthquakes (San Fernando, Gazli, Parkfield, Koyna, and Tokachi Oki). There are four sites located in the epicentral region, so the values are named as epicentral intensities. The extrapolation from these values, the upper-bound epicentral seismic intensities versus the MMI, are listed as in Table 3 below:

Table 3. Upper-Bound Seismic Epicentral Intensity

MMI	Hard Sites	Soft Sites
	$10^4 (\text{cm}^2/\text{sec}^3)$	$10^4 (\text{cm}^2/\text{sec}^3)$
XII	135-160	120
XI	82-92	70
X	52-54	40
IX	30-34	24
VIII	17-20	14
VII	10-13	8
VI	6-8	5
V	3-5	3
IV	2-3	2

The upper-bound line of Figure 7 indicates that the greatest seismic intensity at soft sites is lower than at hard sites. Also, the rate of attenuation is lower for soft sites than for hard sites. Of course, the upper-bound seismic intensities for both the hard sites (Figure 6) and the soft

sites (Figure 7) are in the near field. The data under the upper-bound line (both Figures 6 and 7) spread widely because of various earthquake magnitudes and distances.

Damage to structures in the epicentral area is generally more severe on soft sites than on hard sites, based on past experience and observations. However, this study showed the seismic total intensity (seismic energy) at soft sites to be lower than at hard sites. Thus, the degree of damage to structures does not correlate with the seismic total intensity in the epicentral region. Furthermore, the predominant frequencies at soft sites are in the range of 0 to 2.5 Hz; the seismic energy in this low-frequency range deserves further investigation as it relates to structural damage.

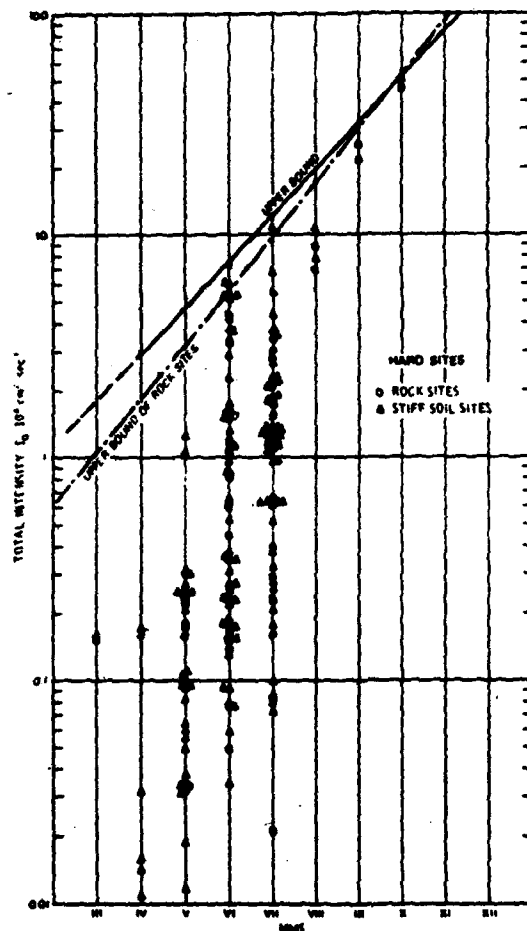


Figure 6. Total seismic intensity  $I_0$  at epicentral region - hard sites

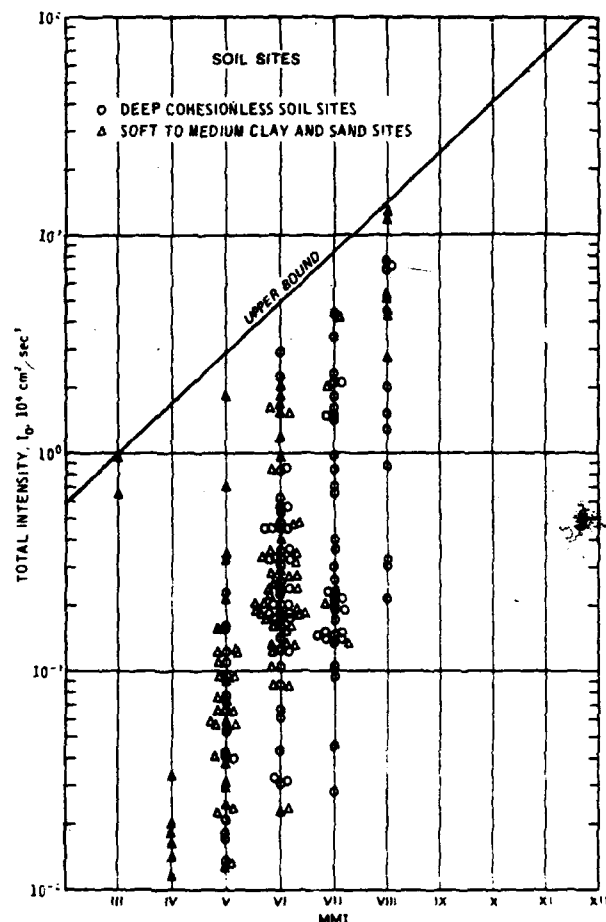


Figure 7. Total seismic intensity  $I_0$  at epicentral region - soft sites

#### CONCLUSIONS

The statistical analysis of 421 accelerograms shows clear differences in spectral shapes for different soil and geological conditions. Within the high-frequency range of 2.5 to 10 Hz, the spectrum for the rock sites contains the highest energy or intensity; the spectrum of the stiff soil sites is slightly lower than for the rock sites; and the spectra of the soft clay and sand sites and the deep cohesionless soil sites are lower still and almost the same. However, in the low-frequency range of 0 to 2.5 Hz, the reverse relation exists: the soft sites indicate the highest energy, the deep cohesionless soil sites are next, the stiff soil sites are third, and finally, the rock sites. Generally, the spectra of rock sites and stiff soil sites of similar characteristics can be classified together as hard sites; the other two site types can be classified together as soft sites.



The site dependence of NPSD spectra have been established by statistical analysis as expected. The most significant finding of the study is the approximate linear correlation of the PGA ( $a_{max}$ ) and base average acceleration for an arbitrary record length of 163.82 sec ( $\lambda$ ). However, the area,  $\lambda_o^2$  under the PSDF curve of a strong-motion duration  $S_o$ , or any record length ( $S_o < 163.82$  sec) can be determined by the following relation:

$$\lambda_o^2 = \lambda^2 \cdot \frac{163.82}{S_o}$$

$\lambda$  can be found from the established charts. If the PGA and  $S_o$  for the design earthquake are given, the scaling factor,  $\lambda_o^2$  for the NPSDF curve can also be obtained. Therefore, the standard NPSD spectrum can be amplified by  $\lambda_o^2$  to become a design PSD spectrum. Furthermore, the design PSD spectrum can be used to generate a design accelerogram with the computer program-EQGEN by Chang, et al.

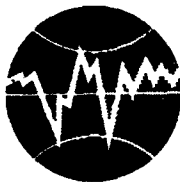
#### ACKNOWLEDGMENT

This study was conducted as part of the work at the U. S. Army Engineer Waterways Experiment Station under the Military Works Program, Project 4A161102AT22, Work Unit 00296, which was monitored for the Office, Chief of Engineers (OCE) by Mr. A. F. Muller.

#### REFERENCES

1. Seed, H. B., Ugas, C., and Lysmer, J. (1976), Site-Dependent Spectra for Earthquake-Resistant Design, Bulletin, Seismological Society of America, Vol. 66, pp. 221-244.
2. Kiremidjian, A. S., and Shah, C. H. (1978), Probabilistic Site-Dependent Response Spectra, Report No. 29, John A. Blume Earthquake Engineering Center, Department of Civil Engineering, Stanford University, Stanford, California.
3. Chang, F. K., and Krinitzsky, E. L. (1977), State-of-the-Art for Assessing Earthquake Hazards in the United States; Duration, Spectral Content, and Predominant Period of Strong-Motion Earthquake Records from Western United States, Miscellaneous Paper S-73-1, Report 8, U. S. Army Engineer Waterways Experiment Station, CE, Vicksburg, Mississippi.
4. Arnold, P. (1975), The Influence of Site Azimuth and Local Soil Conditions on Earthquake Ground Motion Spectra, M.S. thesis, Massachusetts Institute of Technology, Cambridge, Massachusetts.

5. Arnold, P., and Vanmarcke, E. H. (1977), Ground Motion Spectral Content: The Influence of Local Soil Conditions and Site Azimuth, Proceedings, Sixth World Conference on Earthquake Engineering, New Delhi, India, Vol 2, pp. 113-118.
6. Hsu, H. P. (1967), Outline of Fourier Analysis, Simon and Schuster, Inc., New York.
7. Blackman, R. B., and Tukey, J. W. (1958), The Measurement of Power Spectral, Dover Publications, Inc., New York.
8. California Institute of Technology, (1971-1975), Strong-Motion Earthquake Accelerograms; Corrected Accelerograms and Integrated Ground Velocities and Displacements, Vol. 2, Parts A-N, Earthquake Engineering Research Laboratory, Pasadena, California.
9. Chang, F. K. (1981), Site Effects on Power Spectral Densities and Scaling Factors, Miscellaneous Paper GL-81-2, U. S. Army Engineer Waterways Experiment Station, CE, Vicksburg, Mississippi.
10. Chang, N. Y., Huang, M. J., Lien, B. H., and Chang, F. K. (1986), EQGEN-A User-Friendly Artificial Earthquake Simulation Program, Vol. I, pp. 439-450, Proceedings of the Third U. S. National Conference on Earthquake Engineering, Charleston, South Carolina, U.S.A., August 24-28, 1986. Earthquake Engineering Research Institute, El Cerrito, CA.
11. Vanmarcke, E. H., and Lai, S. S. (1977), Strong-Motion Duration and R.M.S. Amplitude of Earthquake Records, Bulletin, Seismological Society of America, Vol. 70, No. 4, pp. 1293-1307.



**TURKISH NATIONAL COMMITTEE FOR  
EARTHQUAKE ENGINEERING**

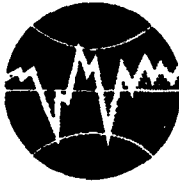
**THIRTEENTH REGIONAL SEMINAR ON EARTQUAKE ENGINEERING**

**September 14-24, 1987 - Istanbul - Turkey**

**DISCRETE-TIME DOMAIN MODELS FOR SITE AMPLIFICATION**

**Erdal Şafak**

**U.S. Geological Survey, MS977, Menlo Park, CA 94025, USA.**



**TURKISH NATIONAL COMMITTEE FOR  
EARTHQUAKE ENGINEERING**

**THIRTEENTH REGIONAL SEMINAR ON EARTHQUAKE ENGINEERING**

**September 14-24, 1987 - Istanbul - Turkey**

**ALARM SYSTEMS BASED ON A PAIR OF SHORT-TERM EARTHQUAKE PRECURSORS**

**by Giuseppe Grandori, Elisa Guagenti and Federico Perotti**

## ALARM SYSTEMS BASED ON A PAIR OF SHORT-TERM EARTHQUAKE PRECURSORS

by Giuseppe Grandori, Elisa Guagenti and Federico Perotti

### ABSTRACT

A statistical analysis of the foreshock-main shock correlation for an Italian seismic zone is here presented. It is found that the probability that a weak shock will be followed within two days by a main shock is of the order of 2 per cent, while the probability that a main shock is preceded by a foreshock is of the order of 50 per cent. These results are quite similar to those found by L. Jones (1985) for Southern California.

The effectiveness of alarm systems based on a pair of short-term earthquake precursors is then analysed. In particular, the analysis shows under what conditions the precursor consisting of potential foreshocks could be combined with another precursor to provide a reasonably effective alarm system.

### INTRODUCTION

Increasing attention has been paid in recent years to the short-term earthquake precursor consisting of weak seismic shocks regarded as potential foreshocks (e.g. Jones, 1985; Kagan and Knopoff, 1987). In Italy, on January 23rd 1985 the zone of Garfagnana (NW of Florence) was evacuated after the occurrence of a potential foreshock.

The statistical analysis for Southern California (Jones, 1985) shows that the probability that a weak shock will be followed within 5 days by an  $M \geq 5.0$  main shock increases with the magnitude of the weak shock from less than 1 per cent at  $M = 3$  to 5 per cent at  $M = 4.5$ .

As far as the Garfagnana seismic warning is concerned, no scientific report has been published as yet. So a statistical analysis of the foreshock-main shock correlation seemed necessary for that zone. In the first of the following sections this analysis will be briefly described.

As will be seen, the results are in good agreement with those obtained by L. Jones for Southern California.

As pointed out by L. Jones, although the hazard level after a potential foreshock is several orders of magnitude above the background rate, "the absolute probability that an earthquake will occur is still quite low". In other words the percentage of false alarms is very high. As a possible way to reduce the expected number of false alarms, L. Jones suggests combining together two or more independent precursors.

The theory of multi-precursor systems has been developed quite extensively over the last few years (Utsu, 1979; Aki, 1981; E. Grandori et al., 1983). In particular a more recent paper (G. Grandori et al., 1984) has shown that the effectiveness of a multi-precursor system does actually depend on a number of factors, and may indeed be smaller than the effectiveness of a system based on the use of only one of the component precursors. So it seemed useful to carry out a detailed analysis of the conditions under which a multi-precursor system could be more effective (if possible, much more effective) than each component precursor. This analysis is contained in the second of the following sections. Both for the sake of simplicity and because it does not seem realistic, nowadays, to assume that more than two precursors are available with statistically documented characteristics, the analysis will be limited to the case of a pair of precursors. This analysis will first use the theory that is already known and that is founded on two main hypotheses. The first is that the two precursors are independent of each other, and the other that the occurrence process of main shocks is a stationary Poisson process. Afterwards, the case of non independent precursors, not so far treated in the literature, will be studied. It will be shown that even a small degree of correlation between precursors reduces drastically the effectiveness of the system.

The last section considers a single precursor, with the assumption that the occurrence process of main shocks is not a stationary Poisson process. In particular it is assumed that the background hazard level depends on the time  $t_0$  elapsed since the preceding earthquake (renewal process). This case can be formally handled (Jones, 1985) by using the

same equations that govern the systems based on two independent precursors. In these equations, the time  $t_0$  plays the role of the second precursor. The advantages and drawbacks of this kind of application will be discussed, with particular attention to the meaning of the independence conditions.

#### FORESHOCK-MAIN SHOCK CORRELATION IN THE GARFAGNANA ZONE

Definitions. Let  $F$  be the precursor,  $E$  the potentially damaging earthquake and  $\Delta t$  the alarm lifetime. If  $F$  occurs, but not  $E$  in the immediately following time interval  $\Delta t$ , this will be called a false alarm.

In order to define the correlation between  $F$  and  $E$ , the following quantities will be assumed:

$p$  is the "probability of false alarm", i.e. the probability that, given  $F$ , there will be no  $E$  within the interval  $\Delta t$ ,

$$p = P(\bar{E}/F) \quad ; \quad (1)$$

$q$  is the "probability of missed alarm", i.e. the probability that in the interval  $\Delta t$  immediately before  $E$  there has been no  $F$ ,

$$q = P(\bar{F}/E) \quad . \quad (2)$$

Finally, let  $P(E)$  be the background probability of the event  $E$ , i.e. the probability of  $E$  in the next interval  $\Delta t$ , evaluated at a given time instant by ignoring any precursors.

$P(E)$  is actually a conditional probability, given all the information provided by the knowledge of the occurrence process at the time instant at which the prediction is performed. Probabilities  $p$  and  $q$  depend on the characteristics of the coupled point process of events  $E$  and  $F$ . In general nor are the values of  $p$  and  $q$  constant in time and they depend on the history of the stochastic process.

Provided that the quantities  $\Delta t$ ,  $p$ ,  $q$ ,  $P(E)$  are known, all the probabilities involved in decision-taking processes can be calculated. In particular, the probability that, given  $F$ , there will be an event  $E$  within  $\Delta t$  is obviously

$$P(E/F) = 1 - p \quad (3)$$

For the sake of completion it is also necessary to allow for the fact that, if  $q > 0$ , there will anyway be unpredicted earthquakes.

A quantity to provide a concise measure of the effectiveness of the alarm system, allowing for both  $p$  and  $q$ , could be defined as follows:

$$U = \frac{s}{f + m} \quad (4)$$

where:

$s$  is the expected number of successes (alarms followed by an event  $E$  within  $\Delta t$ ) over a long period of time in which the system is actually operating;

$f$  and  $m$  are the expected numbers of false and missed alarms over the same period of time.

The effectiveness  $U$  defined by (4) is thus substantially the ratio between the expected number of favorable cases and the expected number of unfavorable cases.

Expression (4) may be suitably modified whenever social, economic or psychological factors make it seem preferable to attribute different relative weights to the successes, the false alarms and the missed alarms. If expression (4) is accepted, the effectiveness  $U$  in stationary conditions can be calculated as a function of  $p$  and  $q$  (G. Grandori et al., 1984):

$$U = \frac{(1-p)(1-q)}{p(1-q) + q(1-p)} \quad (5)$$

The experiment. The events that occurred in the period 1700-1980 in the Garfagnana zone (Fig. 1) were analysed. Seismic shocks of intensity



between 4 and 6 on the MCS scale were considered as potential foreshocks. Potentially damaging earthquakes were taken to have  $I(MCS) \geq 8$ . An alarm lifetime  $\Delta t = 2$  days was assumed, while for the space window a maximum foreshock-main shock distance of 30 km was considered.

Four main shocks (Fig. 2) were not preceded by foreshocks, two by an intensity 4 foreshock, one by an intensity 5 foreshock and one by two foreshocks ( $I = 4$  and  $I = 6$ ).

The following figures were obtained from the catalog of the Italian National Research Council (see Table A):

- the number  $n(E)$  of events with  $I \geq 8$
- the number  $n(F)$  of events with  $4 \leq I \leq 6$
- the number  $n(F|E)$  of events with  $4 \leq I \leq 6$  followed, within 2 days, by an event with  $I \geq 8$ .

In the case of "swarms" of events  $F$ , i.e. when several weak shocks follow each other within an interval of time not greater than one day, only the first shock was computed, but the alarm lifetime was extended to two days after the last shock of the swarm. All shocks in the 3 years following each of the shocks with  $I \geq 8$  were excluded.

The data obtained in this way made it possible to arrive at an estimate of mean values of the probabilities of false alarm and missed alarm over a long time period (see Table A).

The first three lines of the table assume that only weak shocks with  $I = 4$ ,  $I = 5$  or  $I = 6$  respectively are considered. In the fourth line the figures are given for the case of any shock with  $4 \leq I \leq 6$  being considered as a potential foreshock.

TABLE A

	I	n(F)	n(F E)	p	q
GARFAGNANA	4	137	3	0.978	0.62
n(E) = 8	5	81	2	0.975	0.75
	6	27	1	0.963	0.87
	4 ≤ I ≤ 6	210	4	0.981	0.50

Table A shows that the probability of false alarm decreases when the intensity  $I$  of the potential foreshock increases. On the other hand, the probability of missed alarm increases considerably with  $I$ . The most attractive precursor corresponds to the class  $4 \leq I \leq 6$ , for which the probability of false alarm is practically the same as for the other classes, while the probability of missed alarm is considerably smaller.

It is interesting to note that these results are quite similar to those obtained by L. Jones for Southern California. Moreover, it is worth mentioning that the analysis of two other Italian seismic zones (Friuli, North Eastern Italy, and Irpinia, Southern Italy) leads to results that are practically the same. In Table B the average figures obtained from the three zones are presented.

TABLE B

	$I$	$n(F)$	$n(F \cap E)$	$p$	$q$
CARFAGNANA +	4	341	8	0.977	0.69
FRIULI + IRPINIA	5	187	5	0.973	0.81
$n(E) = 26$	6	77	3	0.961	0.88
	$4 \leq I \leq 6$	530	12	0.977	0.54

In conclusion, it seems that the short-term precursor consisting of potential foreshocks has practically the same characteristics in many different regions, namely a high probability of false alarm ( $p = \sim 0.98$ ) and a relatively low probability of missed alarm ( $q = \sim 0.5$ ).

#### ALARM SYSTEMS BASED ON A PAIR OF INDEPENDENT PRECURSORS.

Basic equations. Consider two independent precursors  $F_1$  and  $F_2$ . It should be made clear that the independence of the two precursors does not mean that the two events  $F_1$  and  $F_2$  are statistically independent events. This would be in contradiction to the fact that both are related to events  $E$ . We say that the two precursors are independent if events  $F_1$  and  $F_2$  are correlated to each other only through events  $E$ , with no other

direct correlations. Such a conditional independence of events  $F_1$  and  $F_2$  exists if and only if:

$$P\left(\bigcap_{i=1}^n F_i/E\right) = \prod_{i=1}^n P(F_i/E) \quad (6)$$

$$P\left(\bigcap_{i=1}^n F_i/\bar{E}\right) = \prod_{i=1}^n P(F_i/\bar{E}) \quad (7)$$

If the state of alarm is proclaimed only when the two warning signals overlap, the probability of false alarm  $p^{(2)}$  of the system is given by:

$$p^{(2)} = 1 - \frac{1}{1 + \frac{P(E)}{1-P(E)} \cdot \frac{p_1}{1-p_1} \cdot \frac{p_2}{1-p_2}} \quad (8)$$

If the quantities involved in eq. (8) refer to a finite alarm lifetime  $\Delta t$ , this equation is rigorously valid under the assumption that, when the two signals overlap, they occur together at the beginning of  $\Delta t$ . In general this is obviously only an approximation (G. Grandori et al., 1984). Later on, however, it will be seen that in the specific application suggested by L. Jones (1985) eq. (8) is rigorously valid even for a finite alarm lifetime.

As far as the probability of missed alarm  $q^{(2)}$  is concerned, from eq. (6) one obtains:

$$q^{(2)} = 1 - (1 - q_1)(1 - q_2). \quad (9)$$

**Combination of weak precursors.** A precursor will here be classified as "weak" either if both  $p$  and  $q$  are very high, or if at least one of them is very high. Only weak precursors will be considered here because, obviously, should a strong precursor be available (i.e. with both  $p$  and  $q$  sufficiently small) the problem would be satisfactorily solved by this single precursor.

The examples of Table C show what happens when changing over from a single precursor to a pair of independent precursors. Three types of

precursors are considered (to the left in the table): type a with both  $p$  and  $q$  very high, type b with  $q$  very high and  $p$  relatively low, type c viceversa. To the right the table shows the characteristics of the alarm systems based on a pair of independent precursors, both <sup>of</sup> type a, or both of type b, or both of type c respectively. The value of  $P(E)$  in eq. (8) has been assumed  $P(E) = 0.00025$ . In stationary conditions this value corresponds to a mean interoccurrence time between main shocks  $T(E)=22$  years, with an alarm lifetime  $\Delta t = 2$  days.

The probability of false alarm of the double-precursor system is always extremely small compared to the single precursor. As an obvious counterbalance, the probability of missed alarm is larger than that of the single precursor. In particular, in cases a and b only two in a thousand main shocks would be predicted. The influence of this fact on the effectiveness of the double-precursor system is such that  $U^{(2)}$  is ten times smaller than  $U$  in case a and twenty times smaller in case b.

On the contrary, two precursors of type c provide a much more effective alarm system than the single precursor. Another advantage of

TABLE C

type	SINGLE			PAIR $p_1=p_2=p, q_1=q_2=q$		
	$p$	$q$	$U$	$p^{(2)}$	$q^{(2)}$	$U^{(2)}$
<u>a</u>	0.96	0.96	0.02	0.125	0.998	0.002
<u>b</u>	0.4	0.96	0.04	0.0001	0.998	0.002
<u>c</u>	0.96	0.4	0.04	0.125	0.64	0.52
<u>c</u>	$P(E/F) = 0.04$			$P(E/F_1 \wedge F_2) = 0.875$		
				$P(E/F_1 \wedge \bar{F}_2) = 0.016$		

the combination of two weak precursors of type c shown in the lower part of the table. When one of the precursors occurs, but not the other,

the conditional probability of a main shock,  $P(E/F_1 \wedge F_2)$ , is noticeably smaller than the conditional probability  $P(E/F)$  for a single precursor. This fact gives value to the criterion "proclaim the alarm only when the two signals overlap".

The values of  $U$  and  $U^{(2)}$  of table C have been obtained from eq. (5), and so, in particular, by assigning the same weight to false and missed alarms. It is worth pointing out, however, that to assign different weights to false and missed alarms would hardly change the conclusions regarding cases a and b. In fact, if missed alarms were considered more unfavorable than false alarms, the ratio  $U^{(2)}/U$  would be even smaller, and only if the weight of false alarms is assumed to be much larger than that of missed alarms may  $U^{(2)}$  become comparable with  $U$ . For example in case a, in order to obtain  $U^{(2)} = U$  it would be necessary to assume that the weight of false alarms is 12 times as large as the weight of missed alarms. This does not seem realistic. It is true, in fact, that false alarms give rise to economic damage and to a decrease of confidence in the alarm system. However, a missed alarm means failing in the very aim of an alarm system.

In conclusion, only the combination of weak precursors of type c offers valuable advantages. In other words, an alarm system based on a pair of independent precursors, even if the probability of false alarm of each single precursor is very high, seems to have remarkable interesting characteristics provided that the probability of missed alarm of each precursor is relatively low. As pointed out in the preceding section, potential foreshocks constitute a precursor that does in fact have the properties just mentioned.

Unfortunately, a second precursor, independent of foreshocks, and with similar characteristics, is not available at present. However, the observations contained in this section clarify the way in which it will perhaps be possible in the future to obtain an effective alarm system based on a pair of weak precursors. On the other hand, these observations are a necessary premise for the discussion that will be presented in the last section of the present paper.

It remains to be seen what happens if the precursors are not independent. It is worth discussing the problem first with the help of a numerical example, based on a calculation process that is not rigorous, but that has great heuristic value. The example makes clear in a simple way the role of independence of the two precursors in the calculation of  $p^{(2)}$ . Moreover, it helps the intuitive understanding of the conditions under which the probability of false alarm of the pair of precursors may be very much smaller than that of each component precursor.

A heuristic example. Consider two precursors with the same characteristics, namely

$$p_1 = p_2 = p = 0.9, \quad q_1 = q_2 = q = 0.$$

Suppose, for the moment, that the precursors are independent of each other.

Let the mean interoccurrence time between events E be  $T(E) = 81 \Delta t$ .

Let that precursor  $F_1$  be a natural phenomenon that occurs at sunrise when in the 24 hours following there will be the earthquake E. As a consequence,  $\Delta t = 1$  day. Note that, since  $q = 0$ ,  $F_1$  certainly occurs on the day of the earthquake.

There will be an average of 81 days without strong earthquakes between two events E. At sunrise on some of these days there will be false  $F_1$ . Since, by hypothesis,  $p = 0.9$ , the expected number of days which contain a false  $F_1$  must be 9, so that on average for every 10 alarms 9 will be false. Let the 9 days containing false  $F_1$  have a random distribution over the 81 days without E.

The precursor  $F_2$  has the same characteristics as  $F_1$ , and so, like  $F_1$ , will certainly occur on the day of the earthquake. There are also 9 false  $F_2$  randomly distributed over the 81 days without E, as required by the independence of the precursors. So the number  $k_{12}$  of false  $F_2$  that occur on the 9 days that contain false  $F_1$  (and thus give rise to a false alarm of the system based on the use of both precursors) is:

$$k_{12} = 9 \times \frac{9}{81} = 1 \quad (10)$$

In conclusion, every 82 days there will be on average one successful alarm and one false alarm. The probability of false alarm  $p^{(2)}$  of the double-precursor system is thus

$$p^{(2)} = \frac{k_{12}}{k_{12}+1} = 0.5 \quad (11)$$

However,  $T(E) = 82 \text{ days} = 0.22 \text{ years}$  is a very short interoccurrence time for main shocks. In stationary conditions it corresponds to a background probability  $P(E) = 0.012$ . With the same characteristics of the precursors ( $p = 0.9$  and  $q = 0$ ), if  $T(E)$  is longer and so  $P(E)$  is smaller, the only thing that changes in expression (10) is the denominator, with the results shown in the following table.

$T(E) \text{ years}$	0.22	2.2	22
$P(E)$	0.012	0.0012	0.00012
$p^{(2)}$	0.5	0.1	0.01

The probability of false alarm of the double-precursor system (given  $p$  and  $q$ ) is thus greatly influenced by the value of the background probability  $P(E)$ . This clearly depends on the fact that the smaller the  $P(E)$ , i.e. the greater the  $T(E)$ , the smaller will be the probability of a false  $F_2$  overlapping a false  $F_1$  thus giving rise to a false alarm from the double-precursor system.

It would be easy to show that, in the same way as for eq. (11), it is also possible to arrive at a heuristic proof of eq. (8).

#### THE CASE OF NON INDEPENDENT PRECURSORS

If the two precursors are not independent, eq. (8) is no longer valid. From the Bayes theorem and from the theorem of total probabilities one obtains:

$$P(E/F_1 F_2) = \frac{P(F_1 F_2 | E)}{P(F_1 F_2 | E) + P(F_1 F_2 | \bar{E})} = \frac{1}{1 + \frac{P(F_1) P(\bar{E}/F_1) P(F_2/F_1 \bar{E})}{P(F_1) P(E/F_1) P(F_2/F_1 E)}}$$

i.e.  $1 - p^{(2)} = P(E/F_1 F_2) = \frac{1}{1 + \frac{P(F_2/F_1 \bar{E})}{P(F_2/F_1 E)} \cdot \frac{p_1}{1 - p_1}}$  (12)

In eq. (12) subscripts 1 and 2 can obviously be permuted.

In order to point out the quantitative influence of a possible non independence, let us consider again a particular case defined as follows:

$$p_1 = p_2 = p, \quad q_1 = q_2 = q = 0, \quad T(E) = (r+1)\Delta t.$$

Let  $K$  be the average number of false  $F_1$  (and false  $F_2$ ) in the  $r$  intervals  $\Delta t$  without  $E$ . As  $q = 0$ , then:

$$P(F_2/F_1 E) = 1. \quad (13)$$

Moreover:

$$P(F_2/F_1 \bar{E}) = \frac{K_{12}}{K} \quad (14)$$

where  $K_{12}$ , as in the preceding section, is the average number of false  $F_1 F_2$  in the  $r$  intervals  $\Delta t$  without  $E$ .

Taking into account (13) and (14), eq. (12) becomes:

$$1 - p^{(2)} = \frac{1}{1 + \frac{K_{12}}{K} \cdot \frac{p}{1 - p}} \quad (15)$$

The ratio  $K_{12}/K$  is a measure of the correlation between the two precursors. In the case of independence, eq. (10) holds, so that

$$\frac{K_{12}}{K} = \frac{K}{r}.$$



while in the case of a complete and positive correlation between false alarms  $K_{12}$  coincides with  $K$ . Thus

$$\frac{K}{r} \leq \frac{K_{12}}{K} \leq 1.$$

For example, if  $p = 0.98$ , the values of  $p^{(2)}$  corresponding to different values of the correlation index  $K_{12}/K$  are shown in the following table.

$K_{12}/K$	0.012	0.1	0.5	1
$p^{(2)}$	0.37	0.83	0.96	0.98

The lower limit  $K_{12}/K = 0.012$  coincides with the value of  $K/r$  corresponding to  $T(E) = 22$  years and  $\Delta t = 2$  days. The probability of false alarm  $p^{(2)}$  as a function of  $K_{12}/K$ , for different values of  $p$ , is represented in Fig. 3.

As can be seen, the independence of precursors is of crucial importance: even a small degree of correlation between precursors will drastically reduce the advantage of the double-precursor system, compared with the single precursor, in terms of probability of false alarm.

#### THE CASE OF NON STATIONARY CONDITIONS

Now consider a single precursor  $F_1$  associated with main shocks that follow a renewal process, i.e. with a background probability  $P(E)$  that depends on the time  $t_0$  elapsed since the preceding earthquake. In this case the conditional probability  $P(E/F_1)$  will also depend in general on  $t_0$ . A simple example of a case of this type was developed by the present authors (1984).

L. Jones (1985) essentially suggests considering  $t_0$  as a second precursor. This stimulating suggestion deserves a more detailed analysis.

In order to make clear the role of  $t_0$  as second precursor, it is convenient to consider the beginning of  $\Delta t$  as a random time point and to call  $P(E_r)$  the probability of a main shock within  $\Delta t$ .  $P(E_r)$  coincides

with the "Poissonian" probability  $\Delta t/T(E)$  and is constant in time. Then for the sake of simplicity call  $t_0$  the following event: "the backwards time is included between  $t_0$  and  $t_0+dt$ ". Given these definitions, it is easy to see that the actual background probability  $P(E)$  defined in the previous sections is:

$$P(E) = P(E_r/t_0)$$

The conditional probability  $P(E_r/F_1/t_0)$  can now be derived, again on the basis of the Bayes theorem and of the theorem of total probabilities. If  $F_1$  and  $t_0$  are conditionally independent, one obtains:

$$P(E_r/F_1/t_0) = P(E/F_1) = \frac{1}{1 + \frac{P(E_r)}{1-P(E_r)} \cdot \frac{1-P(E_r/F_1)}{P(E_r/F_1)} \cdot \frac{1-P(E_r/t_0)}{P(E_r/t_0)}} \quad (16)$$

where  $1 - P(E_r/F_1) = \bar{p}_1$  is the average percentage of false alarms. Note that the probability of false alarm  $p_1$  at a given instant  $t_0$  is  $1-P(E/F_1)$ .

If  $P(E_r)$  is very small compared with unity, and in general this is the case, expression (16) depends, from the numerical point of view, only on  $\bar{p}_1$  and on the ratio  $P(E_r/t_0)/P(E_r)$ . In the following table a few examples of  $p_1 = 1 - P(E/F_1)$  for different values of  $\bar{p}_1$  and of  $P(E_r/t_0)/P(E_r)$  are presented.

TABLE D

$P(E_r/t_0)/P(E_r)$	$p_1 = 1 - P(E/F_1)$	
	$\bar{p}_1 = 0.98$	$\bar{p}_1 = 0.96$
1	0.98	0.96
5	0.91	0.83
10	0.83	0.71
20	0.71	0.55

The procedure suggested by L.Jones, expressed by eq. (16), has two main advantages. First, the "precursor"  $t_0$  has probability of missed alarm  $q = 0$ , so that the probability of missed alarm of the double-precursor system coincides with that of  $F_1$ . Second, both the "events"  $F_1$  and  $t_0$  occur at the beginning of  $\Delta t$ , so that eq. (16) is rigorously valid.

However, it must be pointed out that eq. (16), like eq. (8), is valid only for independent precursors. In particular this requires that  $P(F_1/\bar{E}) = P(F_1/\bar{E} \Delta t_0)$ , i.e. the rate of occurrence of events  $F_1$  in the gap between two events  $E$  must be independent of  $t_0$ . In the particular case of foreshocks, this independence should be carefully checked, taking into account that, as pointed out in the preceding section, even a small degree of correlation would drastically increase the probability of false alarm of the system.

Moreover, the numerical examples of Table D show that rather large values of the ratio  $P(E_r/t_0)/P(E_r)$  are necessary in order to obtain a substantial reduction of the probability of false alarm. In other words, the occurrence process of main shocks must be a process with a very strong memory, i.e. main shocks should follow each other in a quasi-periodic sequence.

#### CONCLUSIONS

The short-term earthquake precursor consisting of potential foreshocks in some Italian seismic zones have quite similar characteristics to those found by L.Jones for Southern California, namely a high probability of false alarm ( $p = \sim 0.98$ ) and a relatively small probability of missed alarm ( $q = \sim 0.5$ ). Should a second precursor be ever singled out, independent of the foreshocks, and with similar characteristics, the alarm system made up of the pair of precursors (with the state of alarm proclaimed only when the two warnings overlap) seems to offer much more interesting prospects. In particular, the probability of false alarm would be reduced to values so low that there could be no doubts about the suitability of taking emergency measures should the two warnings overlap.

It is however of crucial importance that the two precursors should be independent. So the problem that arises is how to distinguish, from the various possible short-term precursors, those that from the physical point of view can be judged as independent of the foreshocks. This would be a suitable field in which to concentrate research effort, bearing in mind that the second precursor can be extremely useful even if its probability of false alarm is very high, provided that the probability of missed alarm is relatively small.

If the occurrence process of main shocks is not a stationary Poisson process, and the background probability depends on the time  $t_0$  elapsed since the preceding earthquake, the value of  $t_0$  can be used as a second precursor, with the chief advantage that this particular type of precursor has probability of missed alarm  $q = 0$ . However, careful scrutiny should be applied, in this case, to the independence of the two precursors. Moreover, the combination of foreshocks with  $t_0$  becomes useful only if the ratio between the conditional probability  $P(E_r/t_0)$  and the "Poissonian" probability  $P(E_r)$  is very high.

#### REFERENCES

- Aki, K. (1981). A probabilistic synthesis of precursory phenomena, in Earthquake Prediction, An International Review, Am. Geophys. Union, Washington, D.C., 566-574.
- Grandori, E. and Grandori, G. (1983). Some probabilistic aspects of earthquake prediction, Meccanica, J. of Ital. Assoc. Theoret. Appl. Mech., 18, 246-253.
- Grandori, G., Guagenti E. and Perotti, F. (1984). Some observations on the probabilistic interpretation of short-term earthquake precursors, Earth. Eng. and Struct. Dynamics, 12, 749-760.
- Jones, L. (1985). Foreshocks and Time-dependent Earthquake Hazard assessment in Southern California, Bull. Seism. Soc. Am., 75, 1669-1679.
- Kagan, Y.Y. and Knopoff, L. (1987). Statistical Short-Term Earthquake Prediction, Science, 236, 1563-1567.

Utsu, T. (1979). Calculation of the probability of success of an earthquake prediction (in the case of Izu-Oshima-Kinkai earthquake of 1979), Report of Coordinating Committee for Earthquake Prediction, 21, 1964-1966 (in Japanese).

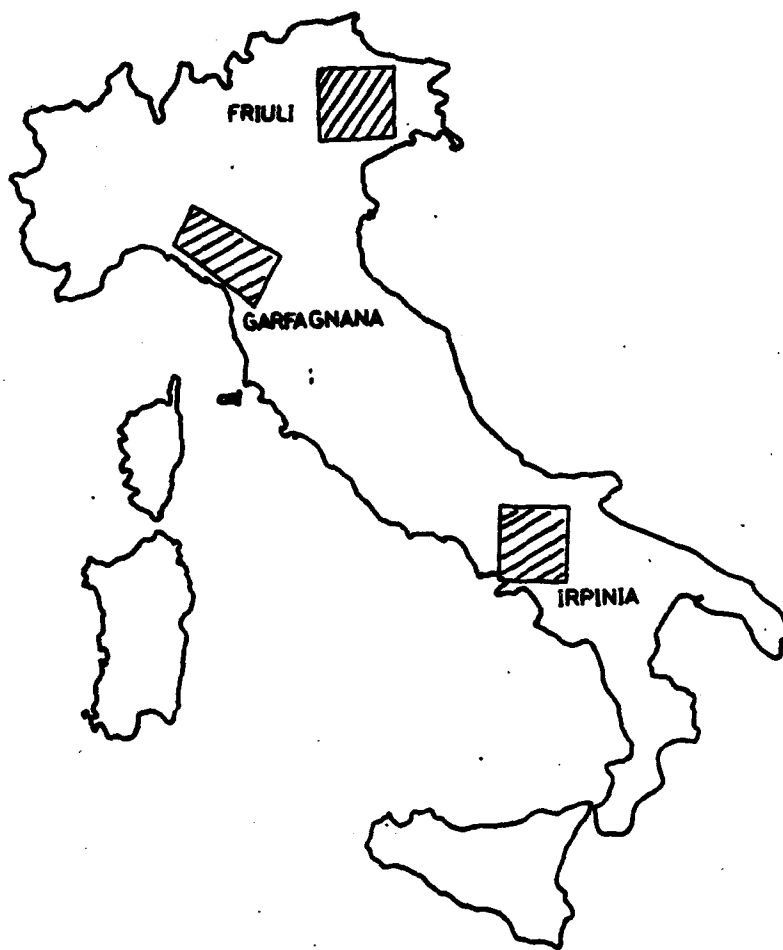
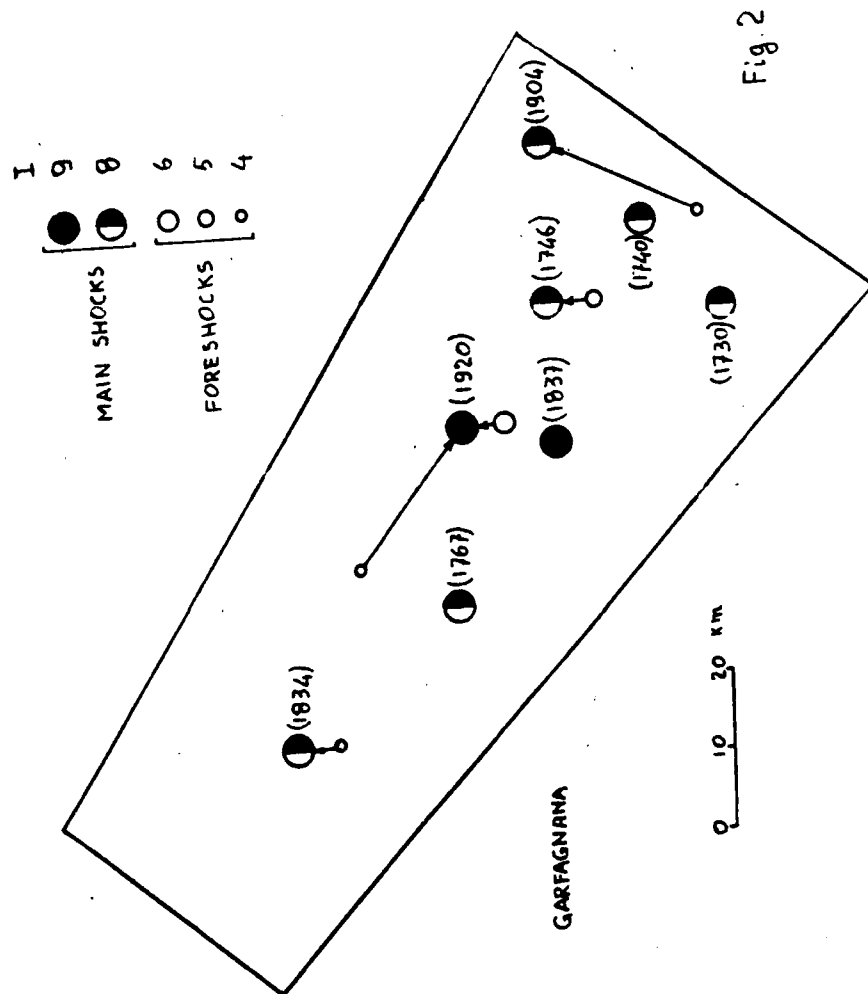


Fig.



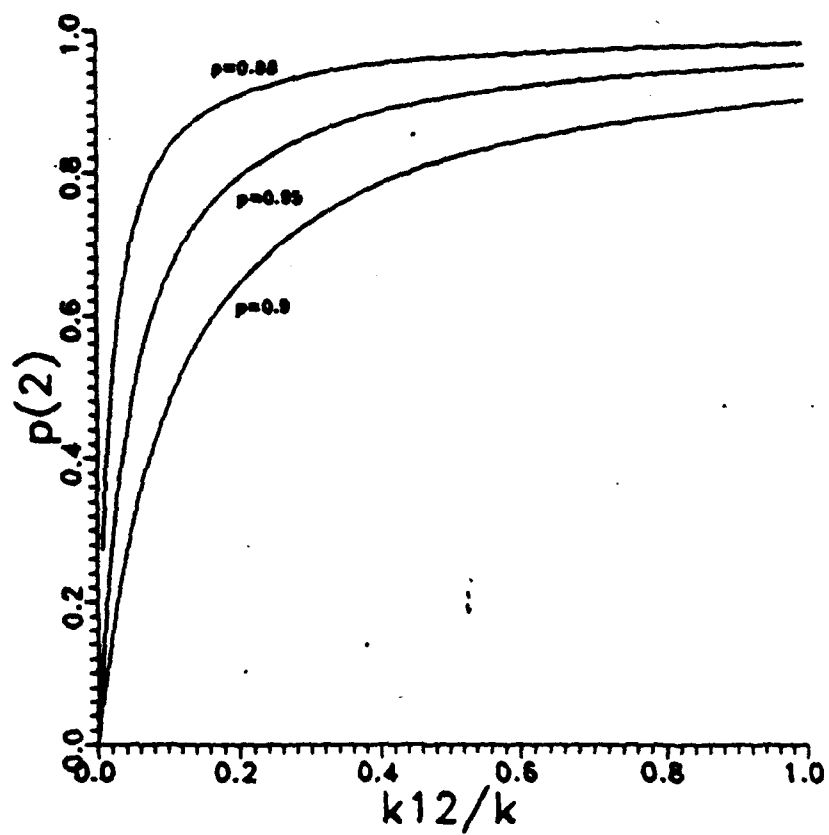


Fig. 3





**TURKISH NATIONAL COMMITTEE FOR  
EARTHQUAKE ENGINEERING**

**THIRTEENTH REGIONAL SEMINAR ON EARTHQUAKE ENGINEERING**

**September 14-24, 1987 - Istanbul - Turkey**

**AN ENGINEER'S APPROACH TO THE SCALING  
OF GROUND MOTION INTENSITIES**

**H.Sandi\***

# AN ENGINEER'S APPROACH TO THE SCALING OF GROUND MOTION INTENSITIES

H.Sandi\*

## ABSTRACT

Recognizing the importance of the concept of seismic intensity, the paper is intended to contribute to a more consistent approach to this concept. The state of the art is discussed, essentially in connection with the MSK scale. An improved approach is proposed, considering instrumental criteria as basic criteria, and macroseismic criteria as derived criteria, to avoid bias raised at present. Two complementary ways of defining instrumental criteria are proposed. The development of macroseismic criteria is related to vulnerability analyses for various classes of structures.

### 1. INTRODUCTION.

The concept of seismic intensity is at present a common concept for seismologists, structural engineers and other specialists, or even non-specialists. Persons working with this concept are recognizing at the same time its importance and some current shortcomings of it. The most important shortcomings that must be emphasized at this place consist of the imperfect definition of the concept, of the fact that the main criteria for intensity estimate are based on vulnerability characteristics which, at their turn, are defined conditionally upon the intensity (building thus a source of bias and tautology), of the lack of satisfactory criteria of this kind connected with earthquake resistant construction, of the non-satisfactory correlation between the macroseismic intensity on one hand and the instrumental criteria on the other hand.

The activities of the fields of engineering seismology and of earthquake engineering require the use of a conceptual and methodological basis free of the shortcomings referred to. This paper is intended to discuss the state of the art of this field, present some proposals for a more consistent approach to the concept of seismic intensity and, accordingly, to the definition of intensity scales and, thus, to contribute to progress in this basic field.

### 2. SOME REMARKS ON THE STATE OF THE ART.

The main reasons to use the concept of intensity are :

- a) the need of quantifying the severities of different, actual, ground motions.
- b) the current limitations in the possibilities of obtaining actual accelerograms, generated by the limited instrumentation density.
- c) the need to relate hazard maps to one, or a few, parameters characterizing ground motions.
- d) the needs raised by the quantification of seismic vulnerability of the various artifacts of man.

The MSK scale [9],[10] is, according to the information available to the author, the most complete and best organized scale of seismic intensity. The intensity is estimated in this frame mainly on the basis of observation of seismic effects upon:

- a) the behaviour of humans and animals ;
- b) the performance of buildings and other artifacts of man;
- c) the effects on landscape and natural environment;

which are referred to as macroseismic criteria.

The most significant criteria are related to the effects of category b), i.e.

---

\*) INCERC (Building Research Institute), Bucharest.

the performance of buildings or other artifacts. The performance of buildings and other works is evaluated having in view three basic coordinates:

- b.1.) the category of buildings or other works, with a view on their resistance to earthquake action;
- b.2.) the degree of damage undergone subsequently to a seismic event;
- b.3.) the proportion of buildings or other works of a definite category (b.1), having undergone the damage degrees referred to under item (b.2).

Instrumental criteria (related to the peak ground acceleration, to the peak ground velocity or to the peak displacement of a standard seismoscope [10]) are used as secondary estimation criteria.

The macroseismic criteria are considered in first place due to two factors:

- a) the availability of much more information of this kind;
- b) the unsufficiently strong correlation of macroseismic data with instrumental criteria (moreover, as it is emphasized further on, the relative nature of the accepted instrumental criteria).

The macroseismic criteria are essentially statements on the vulnerability of structures, presented in a rather qualitative manner. Consider in this connection:

- a) several categories of structures,  $S_i$ ;
- b) a discrete quantification of intensity,  $q_i$  (e.g. integer values of it);
- c) a discrete quantification of damage,  $d_k$  (e.g. given integer values ranging from 0-no damage to 5-collapse [19]). The vulnerability of the class  $S_i$  can be expressed under these circumstances by means of the matrix of conditional probabilities (or frequencies)  $p_{k/i}^{(i)}$ , corresponding from a qualitative viewpoint to the macroseismic criteria. The use of macroseismic criteria as a basis of subsequent vulnerability estimates leads to tautology, since some rather vague data  $p_{k/i}^{(i)}$  are used to derive more accurate data  $p_{k/j}^{(i)}$ . Some more in depth discussion on this subject is given in [15], [16].

Given the problems raised by the current approach to the intensity estimate, some proposals are formulated further on. They are related to the development of instrumental criteria (section 3), to the development of macroseismic criteria (section 4) and to the structure of an improved intensity scale as a whole (section 5).

### 3. DEVELOPMENT OF INSTRUMENTAL CRITERIA.

An attempt is made at this place to develop a convenient system of characteristics and criteria, to lie at the basis of a more consistent intensity scale.

A categorization of instrumental characteristics based on accelerographic records was adopted in [16] in this view. The approach adopted at this place consists of two fairly compatible steps, that rely, both, on the use of proper (corrected) accelerograms:

- a) a first step, aimed primarily to provide on the basis of simple analyses some general data on the intensity and frequency content of ground motion;
- b) a second step, aimed to give a flexible insight into the ground motion characteristics, going up to a desired degree of detail.

The first step consists of the combined use of EPA (effective peak acceleration) and EPV (effective peak velocity) as defined in [23] on the basis of spectral acceleration  $S_a^{(c)}$  and spectral pseudovelocity  $S_{pv}^{(c)}$  for 0.05 critical damping (fig. 3.1.):

$$EPA = S_a^{(c)} / 2.5 \text{ (measured in m/s}^2\text{)} \quad (3.1a)$$

$$EPV = S_{pv}^{(c)} / 2.5 \quad (\text{measured in m/s}) \quad (3.1b)$$

It is possible to define on this basis the corner circular frequency  $\omega_c$ ,

$$\omega_c = EPA/EPV \quad (\text{measured in s}^{-1}) \quad (3.2)$$

Given the quite extensive and classical studies on the destructiveness of steady-state vibration on structures [8], which put to evidence the significance of the product of acceleration and velocity amplitudes, it is proposed to consider for the earthquake motions, which are of transient nature as known, the product of EPA and EPV and to define (for a single direction first), an instrumental intensity given by the expression :

$$I = \log_4(EPA \times EPV) + I_0 = \log_2 EPA - \log_4 \omega_c + I_0 = \log_2 EPV + \log_4 \omega_c + I_0 \quad (3.3)$$

This definition is compatible with the classical ratio 2.0 of increase of instrumental criteria for a unit increase of intensity [10]. Conversely, one can write:

$$EPA = EPV \times \omega_c = 2^{I-I_0} \times \sqrt{\omega_c} = 4^{I-I_0}/EPV \quad (3.4a)$$

$$EPV = EPA / \omega_c = 2^{I-I_0} / \sqrt{\omega_c} = 4^{I-I_0} / EPA \quad (3.4b)$$

A value :

$$I_0 = 8.0 \quad (\text{or VIII}) \quad (3.5)$$

can be conveniently postulated. In case one considers simultaneously the motion along two axes,  $Ox$  and  $Oy$ , the definition (3.3) may be generalized :

$$I = \log_4[(EPA_x \times EPV_x + EPA_y \times EPV_y)/2] + I_0 \quad (3.6)$$

The system of relations (3.2) to (3.6) corresponds to the graphic representation of fig.3.2. In case one wants to use the expression (3.6), for which  $\omega_c$  is no more defined, it appears to be convenient to locate the point corresponding to the value  $I$  (3.6) on a straight segment determined by the couples of points  $(EPA_x, EPV_x)$  and  $(EPA_y, EPV_y)$ .

The use of previous relations is illustrated in table 3.1 and in fig.3.2 for some recent, well known, records.

Table 3.1

No. Earthquake	Record	Direction	EPA (m/s <sup>2</sup> )	EPV (m/s)	$\omega_c$ 1/s	I	PGA (m/s <sup>2</sup> )
1. Romania, 4 March 1977 [2]	INCERC Bucharest	N-S	2.5	(.625)	4.	(8.3)	2.2
2. - " -	- " -	E-W	1.6	(.32)	5.	(7.5)	1.8
3. - " -	- " -	Horiz. plane	-	(1.04)	-	(8.0)	
4. Off the Adriatic Coast, 15 April 1979 [12]	Petrovac, Oliva Hotel	Long.	7	0.6	(11.7)	(9.0)	4.4
5. - " -	Ulcinj, Olympic Hotel	Long.	3.3	0.42	(7.9)	(8.2)	2.6
6. - " -	Bar, Town Assembly Building.	Long.	4	0.64	(6.25)	(8.7)	3.7

No.	Earthquake	Record	Direction	EPA (m/s <sup>2</sup> )	EPV (m/s)	$\omega_c$ 1/s	I	PGA (m/s <sup>2</sup> )
7.	San Fernando, 9 February 1971 [7]	8244 Orion Blvd.1-st floor	W	(2.4)	0.4	6. (8.0)		1.4
8.	- " -	- " -	N	(2.4)	0.4	6. (8.0)		2.7
9.	- " -	445 South Figueroa St.Stat	N 52 W	(1.36)	0.17	8. (6.9)		1.5
10.	- " -	- " -	S 38 W	(1.08)	0.18	6. (6.8)		1.3
11.	- " - [21]	Pacoima Dam	S 74 W	(11.2)	0.75	15. (9.5)		12.5
12.	- " -	- " -	S 16 E	(11.9)	0.7	17. (9.5)		12.4
13.	Mexico City, 19 Sept.1985 [3]	Comm.Transp. Building	N-S	2.8	0.8	(3.5)(8.6)		1.1
14.	- " -	- " -	E-W	4.2	1.3	(3.2)(9.2)		1.8
15.	- " -	UNAM	N-S	0.48	0.13	(3.7)(6.0)		0.35
16.	- " -	- " -	E-W	0.48	0.10	(4.8)(5.8)		0.38

Note: Values under parentheses are derived from (3.2) to (3.6).

The instrumental intensity estimates of table 3.1 are in at least good agreement with macroseismic estimates, while the use of instrumental criteria of [10] would have led in several cases to important gaps. Note the possibility of use of the relations (3.4) for retrodiction of EPA and EPV if estimates on I and  $\omega_c$  are available. Note also, what is more important, that the acceptance of relations (3.3) to (3.6) puts to evidence the relative significance of EPA or EPV (and hence more of PGA and PGV). The representation of fig.3.2 shows that one must go along a straight line  $\omega_c = \text{const.}$  in case one wants to use a (relative) system of values EPA or EPV. For example, the instrumental criteria of the MSK scale correspond to the assumption  $\omega_c = 12.5 \text{ s}^{-1}$ .

The second step consists of the use of the system developed in [13], [14], for which some basic elements are recalled. The absolute velocity of the mass of an SDOF system with undamped natural frequency  $f$  and fraction of critical damping  $n$ , subjected to the component  $i$  of ground motion ( $i=1,2,3$ ) is denoted by  $v_i^{(abs)}(f,n,t)$ . The destructiveness tensor of the ground motion is defined under these conditions by the expression :

$$D_{ij}(f;n) = \int_0^\infty v_i^{(abs)}(f,n,t) v_j^{(abs)}(f,n,t) dt \quad (3.7)$$

(where  $i,j = 1,2,3$  and where it is assumed that there was no disturbance applied to the SDOF system for  $t < 0$ ). The horizontal plane destructiveness is given by the expression :

$$D_{\text{plane}}(f;n) = D_{11}(f;n) + D_{22}(f;n) \quad (3.8)$$

(where  $i = 1,2$  are the indices of the orthogonal, horizontal, axes).

The destructiveness can be averaged over a definite frequency interval. Without specifying the kind of destructiveness by means of any subscript, one can write for the averaged destructiveness  $\bar{D}(f', f''; n)$  the expression

$$\bar{D}(f', f''; n) = \frac{1}{\ln(f''/f')} \int_{f'}^{f''} D(f;n) \frac{df}{f} \quad (3.9)$$

The specific (engineering, horizontal plane) intensity  $I_{\text{plane}}(f)$  is given by an expression :

$$I_{\text{plane}}(f) = \log_4 D_{\text{plane}}(f; 0.5) + I_{\text{plane}}^{(0)} \quad (3.10)$$

where  $I_{\text{plane}}^{(0)}$  is a constant, related to the case of 2-D definition. It is possible to pass in the same way from the averaged destructiveness  $\bar{D}(f', f''; 0.5)$  to the averaged intensity  $\bar{I}_{\text{plane}}(f', f'')$ . The overall intensity is postulated to be an average intensity corresponding to the bounds

$$f' = 0.25 \text{ Hz}; f'' = 16.0 \text{ Hz} \quad (3.11)$$

The use of the tensor  $D_{ij}(f; n)$  makes it possible to define principal axes and destructiveness ellipses for various frequencies ( $f$ ). It is possible to consider also averaging for the principal axes and destructiveness ellipses, starting from the averaged destructiveness tensor. To account for the spectral content of ground motion, using a discretized representation, it is possible to use a sequence of values  $I_{\text{plane}}(f_k)$  for  $f_k = 0.25, 0.5, 1, \dots, 16$  Hz or  $f_k = 0.25, 0.35, 0.5, 0.7, 1, \dots, 16$  Hz or to consider averaged values  $\bar{I}_{\text{plane}}(f_k, f_{k+1})$  related to the sequences referred to.

It appears to be reasonable to adopt a calibration

$$I_{\text{plane}}^{(0)} = 5.5 \text{ (or } \sqrt{1/2}) \quad (3.12)$$

for the constant  $I_{\text{plane}}^{(0)}$  introduced in expression (3.10).

To illustrate the possibilities of this approach on the basis of the record of INCERC-Bucharest of 4 March 1977, for which the absolute acceleration response spectra of horizontal directions are given in fig.3.3a,b, the sequences of specific intensities are reproduced in fig.3.4a, while the sequence of destructiveness ellipses is reproduced in fig.3.4b. The destructiveness ellipses represented are well correlated with the directivity of motion, put to evidence by the damage distribution observed. Note in relation to fig.3.4a that the representation for  $I_{\text{NS}}$  corresponds to the hypothetical case of zero E-S component, using further on the calibration (3.12). The representation for  $I_{\text{EW}}$  corresponds to homologous assumptions.

#### 4. DEVELOPMENT OF MACROSEISMIC CRITERIA

The development of vulnerability-based macroseismic criteria must rely essentially on vulnerability analyses for various categories of structures. Vulnerability analyses require primarily dealing with following problems :

- definition of some categories of buildings or other works,  $S_i$ , including a thorough qualitative description and a quantitative characterization by means of some parameters that are significant from the structural engineering view point and may be relatively easily estimated for existing structures;
- definition of a damage measure or damage degree, that is at the same time easily observable and, if possible, makes sense from the view point of the degree of exhaustion of the resistance to seismic action;
- definition of an appropriate system of quantification of the seismic intensity;
- development of an adequate methodology for deriving the discrete conditional probabilities  $p_{k/j}^{(i)}$  introduced in section 2.

More developments on this subject are given in [17], where conceptual and methodological aspects are discussed, a summary of data available in Europe is

given and the use of the outcome of vulnerability and risk analyses is dealt with.

#### 5. SUGGESTIONS FOR A MORE CONSISTENT APPROACH TO THE DEVELOPMENT OF INTENSITY SCALE.

1. The main body of an up-to-date intensity scale should consist of two parts:  
Part I :instrumental criteria  
Part II:macroseismic criteria

2. The basic criteria for intensity estimation must be postulated in the form of instrumental criteria, to avoid the bias raised by the tautological approach of current scales. It is proposed in this connection to define (at least provisionally) the (instrumental) intensity by means of the couple of expressions (3.3) (or (3.6)) and (3.5), unless a more detailed analysis makes it possible to further refine the expression (3.6) and/or to introduce the influence of the vertical component, which was neglected in previous developments. In order to introduce a more detailed insight into the ground motion characteristics, it is proposed to use, complementarily, the spectral and directional characterization introduced by a set of specific (or averaged) intensities, as provided by the expressions (3.9) or (3.10), together with the provisional calibration (3.12), until a better calibration becomes available.

3. The vulnerability-based (macroseismic) criteria, which represent at present the main body of the intensity scale, should be applied further on extensively (even more extensively than at present), but must be regarded as derived criteria, and not as basic criteria. The development of a satisfactory set of macroseismic criteria must be considered as a dynamic process of cumulation of information and of development of a comprehensive data bank. The statements of the macroseismic part of the intensity scale should make explicit reference to tables containing information of the type  $p_{k,j}^{(i)}$  (section 2), for various categories of structures  $S_i$ .

4. The use of macroseismic criteria should be regarded essentially as a means of approximate, but consistent, completion of information provided by the instrumental data which will be available in a limited quantity in the previsible future.

#### 5. CONCLUDING REMARKS.

1. The concept of seismic intensity represents a necessary tool for various problems of engineering seismology and of earthquake engineering and, consequently, a scale of seismic intensities is equally necessary.

2. The analysis of the state of the art puts to evidence on one hand the use of the concept of seismic intensity but, on the other hand, the current conceptual and methodological shortcomings.

3. The qualitative improvement of the concepts referred to requires a more rigorous and consistent approach. The possible way of removing the current conceptual bias is represented by the definition of seismic intensity primarily on the basis of instrumental parameters. The macroseismic criteria will become under these conditions derived criteria, losing the current position of primary criteria.

4. The system of instrumental parameters lying at the basis of the intensity scale must be flexible, making it possible to determine for a given ground motion more precisely for a 3-D accelerogram) either one single parameter (instrumental intensity), or several parameters, to account for the spectral, directional etc. features of ground motion. Some proposals were developed in this sense in section.

5. The macroseismic criteria should be gradually developed, considering various categories of structures, for which vulnerability characteristics are to be defined and derived. The work in this field should encompass adequate definitions

and descriptions for the categories of structures dealt with, for the (observable) damage and for the intensity of ground motion (providing, of course, the necessary compatibility between the primary definition of instrumental seismic intensity on one hand and the parameters considered in the definition of vulnerability characteristics on the other hand).

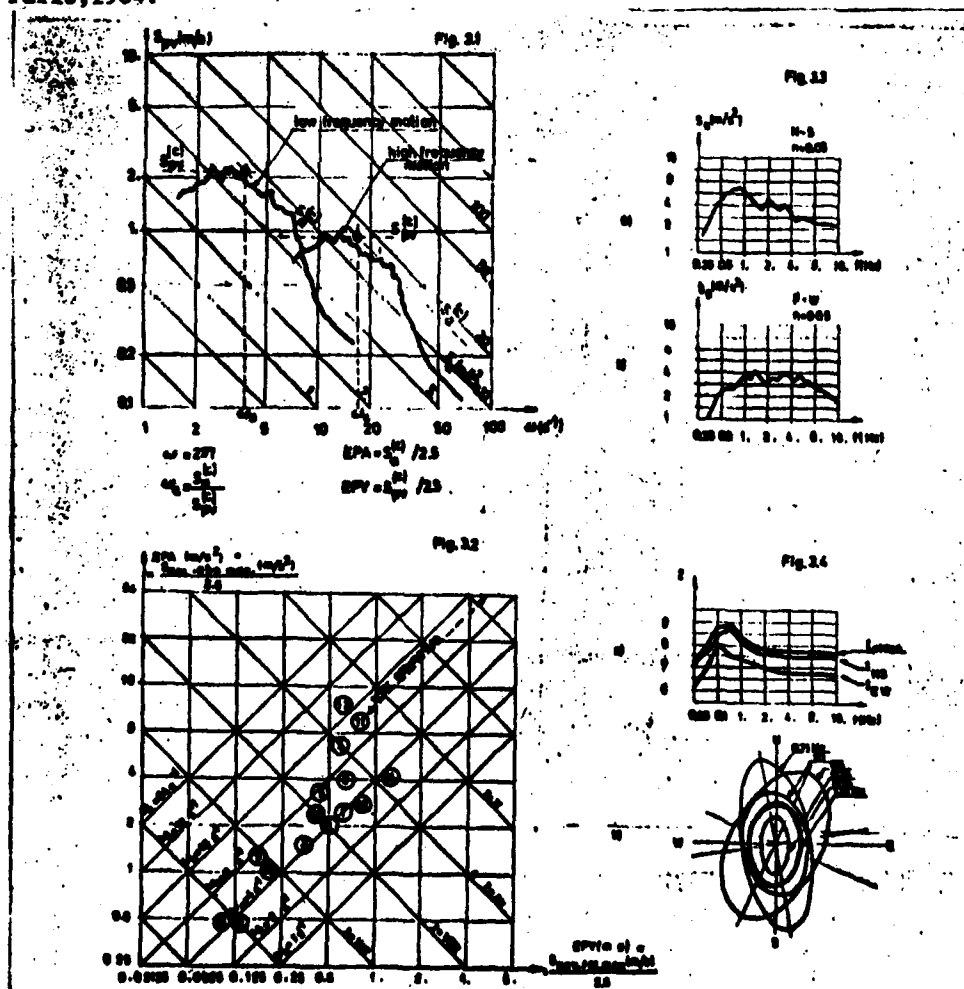
6. The development of a more refined concept of seismic intensity and accordingly of a more refined scale, must be regarded as a long lasting process, requiring sample applications of intermediate results besides a particularly extensive work of gathering of information.

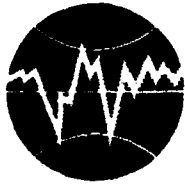
#### REFERENCES

1. A.Arias : A Measure of Earthquake Intensity. In "Seismic Design for Nuclear Power Plants" (editor: R.J.Hansen). The MIT Press, Cambridge, Mass., 1970.
2. St.Balan, V.Cristescu, I.Cornea (editors): The Romania Earthquake of 4 March 1977 (in Romanian). Editura Academiei, Bucharest, 1983.
3. B.Bolt : Lecture on the Mexico, 19 September 1985, Earthquake. Notes taken by C.Radu during the International Symp.on the Analysis of Seismicity and on Seismic Hazard, Liblice, Czechoslovakia, 1985.
4. F.Braga, M.Dolce, D.Liberatore : Influence of Different Assumptions on the Maximum Likelihood Estimation of the Macroseismic Intensities. Proc. 4-th International Conf.on Applications of Statistics and Probabilities in Soil and Structural Engineering (ICASP-4), Firenze, 1983.
5. M.Dolce, D.Liberatore : Modelli statistici per una scala macroseismica : Analisi comparative sui dati del terremoto del 23/11/80. Proc. 2-nd Conf. "L'Ingegneria sismica in Italia", Rapallo, 1984.
6. G.W.Housner : Characteristics of Strong Ground Motion. Chapter 4 in "Earthquake Engineering" (editor : R.L.Wiegel) Prentice Hall, Englewood Cliffs, N.J., 1970.
7. D.E.Hudson : Strong Motion Accelerogram Processing. In vol.III of "San Fernando, California, Earthquake of February 9, 1971" (scientific coordinator: L.M.Murphy). NOAA, US Dept. of Commerce, Washington, D.C., 1973.
8. H.W.Koch : Ermittlung der Wirkung von Bauwerkschwingungen. Z.VDI, vol.95 (1953), no.21.
9. S.V.Medvedev : Engineering Seismology (in Russian). Gosstroyizdat, Moscow, 1962.
10. S.V.Medvedev : Seismic Intensity Scale MSK-70. Publ.Inst.Geophys.Pol.Ac.Sc., A-6, Warsaw, 1977.
11. V.Pérez : Peak Ground Accelerations and their Effects on the Velocity Envelope Response Spectra as a Function of Time, San Fernando Earthquake, February 9, 1971. Proc. 5-th World Conf.on Earthquake Engineering, Rome, 1973.
12. J.Petrovski, T.P. Golov (editors) : The Montenegro, Yugoslavia, Earthquake of April 15, 1979. MHS-80-65, Skopje, 1981.
13. H.Sandi : Measures of Ground Motion. Proc. 65 National Conf.on Earthquake Engineering, Stanford Univ., Palo Alto, Cal., 1979.
14. H.Sandi : Requirements in Characterizing Ground Motions. Proc. 7-th World Conf. on Earthquake Engineering, Istanbul, 1980.
15. H.Sandi : Seismic Vulnerability and Seismic Intensity. Proc. 7-th European Conf. on Earthquake Engineering, Athens, 1982.
16. H.Sandi : Engineering Aspects and Possible Refinements of the Concept of Seismic Intensity. Proc. 12-th Regional Seminar on Earthquake Engineering, Halkidiki, Greece, 1985.



17. H.Sandi : (Working Group coordinator) : Report on "Vulnerability and Risk Analysis for Individual Structures and Systems". Proc.8-th European Conf.on Earthquake Engineering,Lisbon,1986.
18. H.Sandi,G.Serbanescu et al. : Lessons from the Romania Earthquake of 4 March 1977. Proc.6-th European Conf.on Earthquake Engineering, Dubrovnik,1978.
19. N.V.Shabalin : Estimates of Seismic Intensity.In "Scales of Seismic Intensity" and Estimation Methods" (in Russian).Nauka,Moscow,1975.
20. M.D.Trifunac : Envelope Spectrum and Interpretation of Strong Earthquake Ground Motion. Bull.Seismological Society of America, 61,1971.
21. M.D.Trifunac : Analysis of Pacoima Dam Accelerogram.In.vol.III of "San Fernando, California,Earthquake of February 9, 1971." (scientific coordinator:L.M.Murphy). NOAA,US Dept.of Commerce,Washington,D.C.,1973.
22. R.V.Whitman,C.A.Cornell : Design.Chapter 9 in "Seismic Risk and Engineering Decisions" (editors : C.Lomnitz and E.Rosenblueth), Elsevier,Amsterdam-Oxford-New-York,1976.
23. NSF-NBS-ATC. Tentative Provisions for the Development of Seismic Regulations for Buildings. ATC Publications 3-06,1978.
24. UNDP/UNESCO/UNDRO Project RER/79/014 "Earthquake Risk Reduction in the Balkan Region".WG.B : Vulnerability Analyses in the Balkan Region.Final Report.UNESCO, Paris,1984.





**TURKISH NATIONAL COMMITTEE FOR  
EARTHQUAKE ENGINEERING**

**THIRTEENTH REGIONAL SEMINAR ON EARTHQUAKE ENGINEERING**

**September 14-24, 1987 - Istanbul - Turkey**

**ANALYSIS OF STRONG GROUND MOTIONS IN AMPLITUDE DOMAIN  
- REVIEW AND APPLICATIONS**

**Vladimir Schenk  
Geoph.Inst., Czechosl.Acad.Sci., 14131 Praha**

# ANALYSIS OF STRONG GROUND MOTIONS IN AMPLITUDE DOMAIN - REVIEW AND APPLICATIONS

Vladimir Schenk  
Geoph.Inst., Czechosl.Acad.Sci., 14131 Praha

## ABSTRACT

The present analysis extends the current methods of studying the kinematic and dynamic parameters of seismic waves applied in the time and frequency domains to the third amplitude domain. This approach makes it possible to determine the maximum amplitude of vibration, the total values of its duration, energy, impulse, and root-mean-square amplitude, effective amplitudes and durations, which are defined by the probability of amplitude occurrences in the seismic signal. Applications of these quantities in standard seismological practice allow us to calculate the duration magnitude of small and/or local earthquakes in a more effective way, to find the attenuation curves of seismic motions and to estimate the quality factor  $Q$  of a medium, to assess the values of effective amplitudes and durations, which can be applied in the engineering seismology, and to classify ground motions with respect to macroseismic effects. The last application is also successfully used in the selection of analogous strong ground motions for purposes of earthquake engineering.

## 1. INTRODUCTION

A ground motion record is the sum of a seismic signal generated by an earthquake or by any other artificial event, and of seismic noise. The present signal analysis involves the methods of studying the kinematic and dynamic parameters of seismic waves applied in the time and frequency domains. Since recently, most ground motions have been recorded in the digital form, the computer techniques of their analyses can be easily introduced to the common practice. From this viewpoint, the present seismic signal analysis often involves routine spectral processing of the signals and, as presented in this paper, this processing can be also extended to the new amplitude domain.

An attempt to study the frequency of different amplitudes within a certain time period of the ground motion record has already been made by BOLT and ABRAHAMSON (1982). However, only a part of a seismic record with maximum amplitudes exceeding 0.02 and 0.04 g was investigated. Contrary to this approach, SCHENK (1985a) analyzed all digitized amplitudes of a seismic record without any restriction. By using the absolute values of digitized amplitudes and by classifying them according to their magnitudes, a frequency distribution of these amplitudes within a seismic record was obtained. Just like in the study of a seismic wave in the time domain we need the time history of vibrations and in the frequency domain we have to know the amplitude and phase spectra, in analyzing a wave in the amplitude domain we

have the amplitude-frequency distributions (AFD). Since the analysis of seismic waves in the amplitude domain is a new approach in standard processing techniques and, therefore, it is not so widely known, this paper summarizes the results achieved recently. The methodology of AFD calculation and the description of new wave parameters as well as their application to standard seismological and earthquake-engineering practice are discussed.

## 2. THEORETICAL BACKGROUND

A record of seismic particle ground motion consists of various wave types and their phases arriving at the observation place at different times and from different directions. In the first approximation it can thus be presumed that the record is a series of individual seismic signals, whose character can be expressed by a simple vibrating motion described by the differential equation of the second order in the following form

$$\frac{d^2x}{dt^2} + \frac{\delta}{m} \frac{dx}{dt} + \frac{\omega_0^2}{m} x = 0 \quad (1)$$

where  $\delta$  is the constant of proportionality between the medium resistance (proportional to the inner friction of the medium) and the velocity of a particle vibration,  $\omega_0$  is the constant of proportionality giving the magnitude of the force that caused the harmonic motion in direction  $x$ ,  $m$  being the weight of the medium particle. The solution of equation (1) yields the amplitude  $A$  in direction  $x$  at arbitrary time  $t$

$$A = A_0 \cos \omega t \exp(-\beta t) \quad , \quad (2)$$

where  $\beta = \delta / 2m$  is the constant of attenuation of a particle vibration with time,  $\omega = \sqrt{\omega_0^2 - \beta^2}$  is the angular vibration frequency, and  $A_0$  is the angular frequency in time  $t_0$  when the deviation of a particle from its equilibrium position in direction  $x$  was the greatest ( $A = A_0$ ). From relation (2) it ensues that the amplitudes of the vibration motion  $A$  having originated decay with time according to the relation

$$A = A_0 \exp(-\beta t) \quad , \quad (3)$$

where  $\beta$  is referred to as the vibration attenuation of the medium particles.

As relation (3), corresponding to the envelope of absolute values of particle motion amplitudes with time, is a continuous and purely monotonous function over the entire interval of the values of time  $t$ , there is also an inverse function (JARNIK 1955) to this function in the following form

$$t = t_0 \exp(-\beta t) \quad . \quad (4)$$

The inverse function makes it possible to transfer the strong

ground motion analysis from the time domain to the amplitude domain.

In analyzing the wave pattern of particle motions in the amplitude domain, we determine the number of occurrences  $N$  of the sampled amplitudes in individual amplitude classes  $\Delta A$  of a constant size (SCHENK 1985a, 1985b). Relation (3) makes it evident that the decrease of the amplitudes of the vibrating attenuated motion by a constant difference  $\Delta A$  of amplitudes (size of the amplitude class) corresponds to the exponential law, which means that the decrease of the lower vibration amplitudes by the  $\Delta A$  value lasts a longer time period than the same decrease in the range of higher amplitudes. Therefore, we can write

$$t_j - t_i = N \Delta t, \quad (5)$$

where times  $t_j$  and  $t_i$  are those between which amplitude  $A_i$  attenuates to amplitude  $A_j$ ,  $\Delta t$  being the sampling interval of the record. From relation (3) it then follows that

$$|A_j - A_i| = A_0 \exp \{ -\beta (t_j - t_i) \}, \quad (6)$$

and the inverse function to relation (6) can be written in the following form

$$(t_j - t_i) = t_0 \exp ( -\beta |A_j - A_i| ) \quad (7)$$

After taking the logarithm, we obtained the following relation

$$\ln (t_j - t_i) = \ln t_0 - \beta |A_j - A_i|, \quad (8)$$

which after the introduction of relation (5) can be rewritten into the form of the amplitude-frequency distribution of ground motion (SCHENK 1985a)

$$\ln N = \ln N_s - \beta \Delta A, \quad (9)$$

where  $N_s = T_s / \Delta t$  is the total number of the amplitude samples which belong to the investigated seismic signal of an overall duration  $T_s$  and  $\Delta A = |A_j - A_i|$  is the amplitude class in the amplitude-frequency distribution.

### 3. AMPLITUDE-FREQUENCY DISTRIBUTIONS

Let us take a digital ground motion record, e.g. a series of amplitudes  $A$  in times  $t$  during an observation period  $T$ ; the  $\Delta t$  between two successive amplitudes is a sampling interval which has to be constant (Fig. 1). It is obvious that adequate density of digitization is necessary to express the proper character of the motion. Since the goal of our analysis is to find the amplitude-frequency distribution of digitized amplitudes according to their magnitudes, thus the maximum amplitude  $A_{\max}$  defines the upper limit of a set of amplitude classes  $\Delta A$  for which the distribution is to be found and the set of the amplitude classes

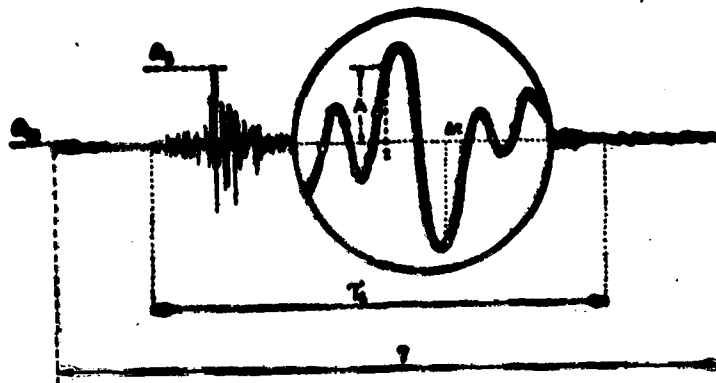


Fig. 1. Ground motion record and quantities of digitalization

is created by simple linear division of this value into the required number of classes. Then by simple statistical assortment of the absolute amplitude values of a seismic record into individual amplitude classes we obtain the density amplitude-frequency distribution (AFD). In conformity with the presumption that the attenuation of the seismic signal amplitudes with time corresponds to the exponential law (see relation (9)), the AFD can be approximated by the exponential dependence. In principle, we distinguish density and cumulative AFD, and we can express it either in dependence on the sequential order of the amplitude class  $K$  in the set or in dependence on the absolute value of the amplitude  $A$  of ground motion.

For density AFD we thus write

$$\log N_i = a_D - b_D(K) \quad [\text{class } K] \quad (10a)$$

or

$$\log N_i = a_D - b_D(A) \quad [\text{amplitude } A] \quad (10b)$$

and for cumulative AFD

$$\log \sum N_i = a_c - b_c(K) \quad [\text{class } K] \quad (11a)$$

or

$$\log \sum N_i = a_c - b_c(A) \quad [\text{amplitude } A] \quad (11b)$$

where  $N_i$  is the number of seismic wave amplitudes that belong to amplitude class  $K$ , index  $i=1,2,\dots,K_{\max}$ , coefficients  $a_D$ ,  $a_c$ ,  $b_D(K)$ ,  $b_D(A)$ ,  $b_c(A)$  and  $b_c(K)$  are determined empirically from the approximation of the central signal part of the respective AFD by the least-square method. Figure 2 shows the AFD of the known accelerogram El Centro 1940, vertical component.

In the approximation of both AFD types, an important role is played by the selection of the range of values  $N_i$  that will characterize the seismic signal sufficiently well. The  $N_i$  values that correspond to the lowest amplitude classes have

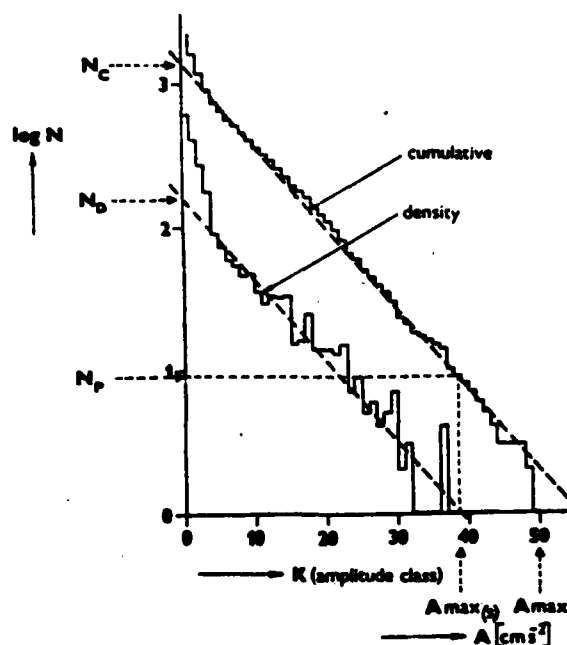


Fig.2. Amplitude-frequency distributions

proved to be affected by seismic noise, while the chaotic ("zig-zag" or "comb-like") character of the  $N_i$  values of the highest amplitude classes is given by the irregular occurrence of random peak amplitudes of the signal, often due to the local seismogeological inhomogeneities of the medium (SCHENK 1985a). For this reason, both marginal parts of the AFD should first be separated from the central part of the distribution, which then provides more or less reliable characteristics of the seismic signal, and only then approximated by relations (10) and (11).

The question of separating the amplitudes of seismic noise from those of the signal and the methods of optimum approximation of amplitude-frequency distributions were solved earlier (SCHENK 1985a). A successful separation of the noise amplitudes from the signal amplitudes generally depends on two ratios:

- i) the signal amplitudes  $A_s$  to the noise amplitudes  $A_n$ , and
- ii) the duration of the entire investigated period  $T$  to the signal duration  $T_s$ .

In some cases, if  $A_s \gg A_n$  and/or  $T = T_s$ , the "noise" part of the AFD does not appear, but sometimes, if  $T > T_s$  or  $A_s$  does not differ from  $A_n$  by more than one order, it is very pronounced especially in the density AFD. To select the "noise" part of the distribution from the whole AFD and to find only its repre-

sentative part for a reliable approximation by relation

$$\log N = a - b A, \quad (12)$$

where  $N$  is the number of amplitudes of the ground motion record which corresponds to the given amplitude class  $A$ , we applied the procedure that follows.

Theoretically, a determination of a suitable range of amplitude classes depends on the ratio between the maximum amplitude of the signal  $A_{\max}$  and the seismic noise amplitudes  $A_n$  (Fig.1). Let us have  $K$  amplitude classes, then the lower limit of the class range, in which the values  $N$ , where index  $i=1,2,\dots,K$ , can be used for the approximation, is

$$K_L = (A_n / A_{\max}) K \quad (13a)$$

and for the upper limit of this range, according to our experience, the value

$$K_U = K - n K_L \quad (13b)$$

can be recommended: coefficient  $n$  is approximately 3 - 3.5 for the density AFD and approximately close to 2 for the cumulative one. Of course, these values have to be determined individually for each record. Therefore, after testing several records (SCHENK 1985a), we can recommend the limits

$$K_L = n_1 K \quad \text{and} \quad K_U = n_2 K \quad (14)$$

for routine processing of strong ground motion records, where  $0.1 \leq n_1 \leq 0.15$  and  $0.65 \leq n_2 \leq 0.75$  for the density AFD and  $0.75 \leq n_2 \leq 0.8$  for the cumulative AFD; these coefficients were checked by visually.

Another way of finding a reliable central part of the AFD is based on the application of a mutual correlation of all values  $N$  of the AFD and by a sequential cutting off its marginal values to find the highest correlation coefficient. Then we assume that the remaining central part of the AFD represents the distribution of the seismic signal.

#### 4. PROPERTIES OF THE "AFD" COEFFICIENTS

The number of amplitude classes does not only determine the character of the AFD, but it mostly affects also the actual course of density distribution. Figure 3 demonstrates examples of the density AFD (thin line) and the cumulative AFD (bold line) of seismic signal, component S90W, recorded at El Centro site during the Imperial Valley earthquake, May 18, 1940, constructed for eight different numbers of  $K_{\max}$  classes. A comparison of the distributions obtained for different values of  $K_{\max}$  has revealed that the parameters of the cumulative AFD of  $a_c$ ,  $b_c(x)$  and  $b_c(A)$  as well as the parameters of the density AFD  $b_D(x)$  and



$b_D(A)$  do not necessarily depend on  $K_{max}$ , while values  $a_D$  directly depend on the maximum number of amplitude classes. In fact it can be written

$$a_D(j) = a_D(i) + \log [K_{max}(i) / K_{max}(j)] \quad (15)$$

where  $K_{max}$  are the maximum numbers of amplitude classes used to forming the AFD,  $a_D(m)$  being the corresponding parameters of the density AFD.

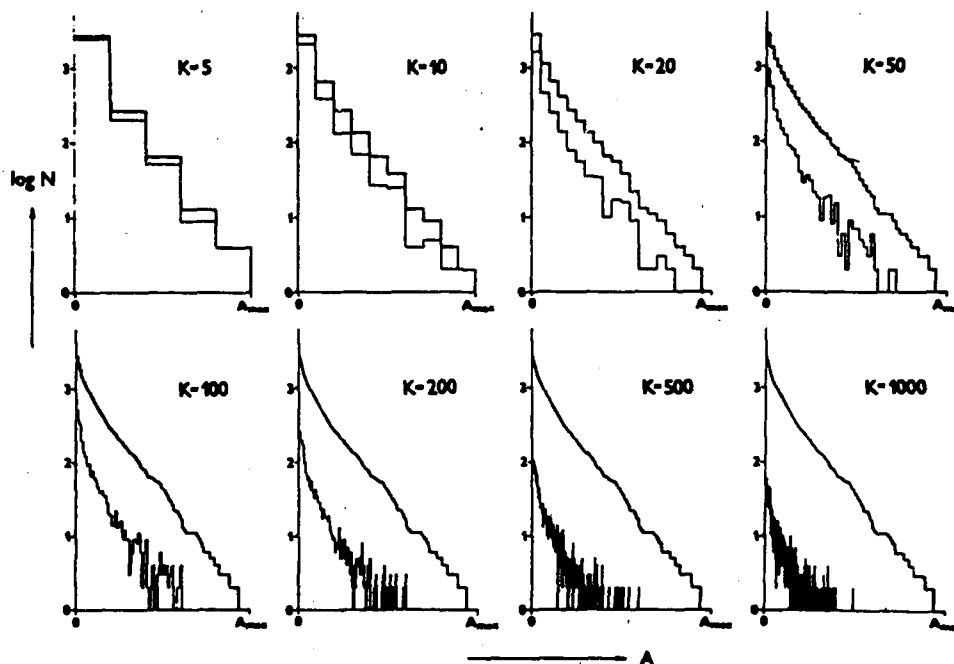


Fig.3. Dependence of density and cumulative AFDs on the  $K_{max}$ .

In principle, different combinations of the density and cumulative AFDs can be made (Fig.3) depending on the values of  $K_{max}$ . It appears that the approximation of the cumulative AFD by relation (11), adherence to this value is not essential since a change of  $K_{max}$  does not affect the course of this distribution very much. From the point of view of the character and the course of the density AFD, however, the maximum number of amplitude classes  $K_{max}$  equal to 50 seems to be the optimum number: the character of the AFDs are quite distinct for an objective approximation by relations (10) and (11). The greater the number of  $K_{max}$  classes, the greater the scatter of  $N$  values in the part of higher amplitudes of the density AFD (see Fig. 3), in other words, a more extensive part of the "zig-zag" values is formed. For this reason, all the following relations in the present paper correspond to the AFDs with  $K_{max} = 50$ . If they are to be modified to another number of amplitude classes, it is necessary to use relation (15).

The other, not less important parameters of the AFD, are parameters  $a$  and  $b$ , which characterize the relationship of the amplitude number in individual amplitude classes. From relations (10) and (11) it follows that these parameters can be expressed in following ways:

- $a_D$  ... corresponding to the density AFDs,
- $a_C$  ... corresponding to the cumulative AFDs,
- $b_D(K)$  ... corresponding to the density AFD constructed in dependence on the number of  $K$  classes,
- $b_D(A)$  ... corresponding to the density AFD constructed in dependence on a physical quantity of a seismic wave amplitude, e. g., on acceleration  $[cm\ s^{-2}]$ , etc.
- $b_C(K)$  ... corresponding to the cumulative AFD constructed in dependence on the number of  $K$  classes and
- $b_C(A)$  ... corresponding to the cumulative AFD constructed in dependence on a physical quantity of a seismic wave amplitude.

A study of the character of parameters  $a$  and  $b$  of the density and cumulative AFDs was performed on a set of accelerograms of five Californian earthquakes (Parkfield  $M=5.5$ , Borrego Mtn.  $M=6.0$ , Imperial Valley  $M=6.4$ , San Fernando  $M=6.5$  and Kern County  $M=7.2$ ), i.e. 163 horizontal and 82 vertical components (SCHENK 1985a,b). The obtained results are summarized under the following items and figures:

- i) the reliability of determining the dependence of the cumulative AFD, and the  $b_C$  values connected with it, is greater than with the density AFD.
- ii) amplitude relations of the density and cumulative AFDs are invariable with the increasing distance from the source and the following approximate relation is valid

$$a_C = a_D + 0.878 \pm 0.269 \quad (16)$$

- iii) the values of coefficients  $a_C$  and  $a_D$  increase with the increasing distance from the source (Figs 4a and 4b).
- iv) between the "b" parameters of the density and cumulative AFD of the same record, the following dependence can be found

$$b_C \approx 1.3 b_D \quad (17)$$

- v) the values of coefficients  $b_C(K)$  and  $b_C(A)$ , and consequently also those of  $b_D(K)$  and  $b_D(A)$ , appear to be independent on the source size,
- vi) coefficients  $b_D(K)$  and  $b_C(K)$  do not change with the distance from the source and it appears that there is no difference in the behaviour of the coefficients that belong to the horizontal or vertical component of a seismic wave (Fig. 5),
- vii) the values of coefficients  $b_D(A)$  and  $b_C(A)$  increase with

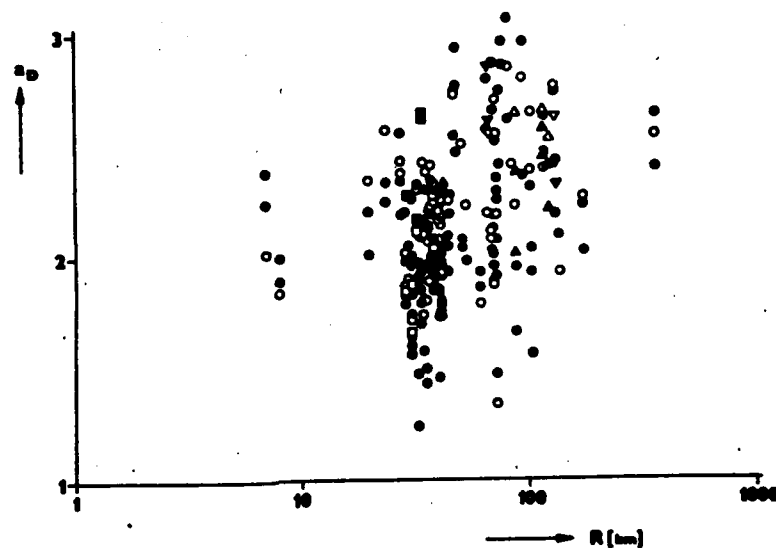


Fig.4a. Dependence of the coefficient  $a_D$  on distance  $R$ .

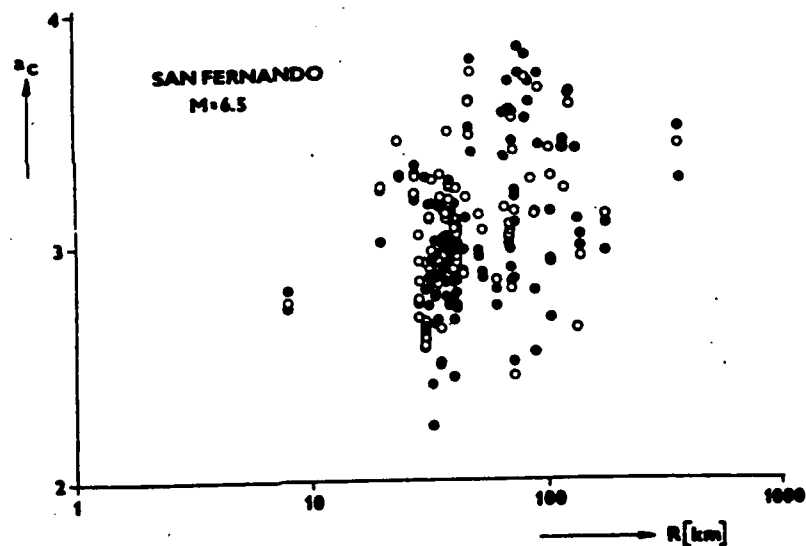


Fig.4b. Dependence of the coefficient  $a_C$  on distance  $R$ .

the increasing distance from the source (Fig.6); for the vertical component we can write

$$\log b_{C(A)} = 1.41 \log R + 3.63 \quad (18a)$$

and for the horizontal one

$$\log b_{C(A)} = 1.41 \log R + 3.89 \quad , \quad (18b)$$

where  $R$  [km] is the distance of the recording site from the earthquake epicentre of a magnitude  $5.5 \leq M \leq 7.2$ .

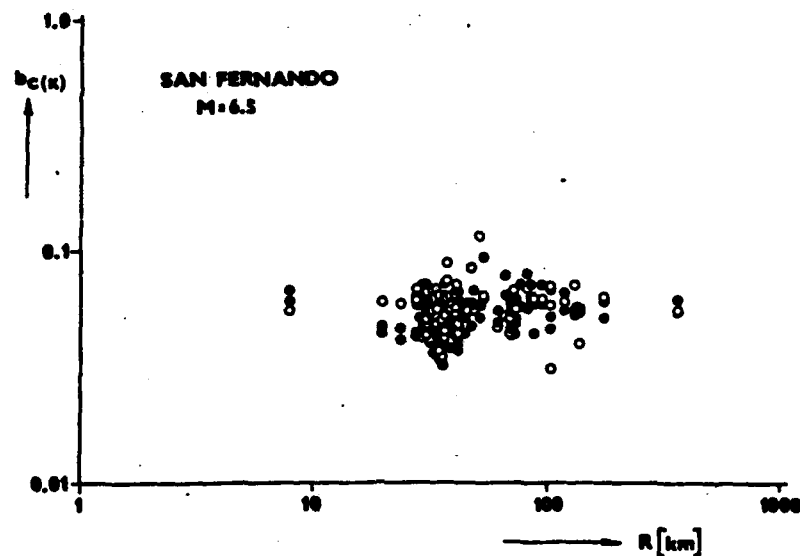


Fig.5. Dependence of the coefficient  $b_C(\kappa)$  on distance  $R$ .

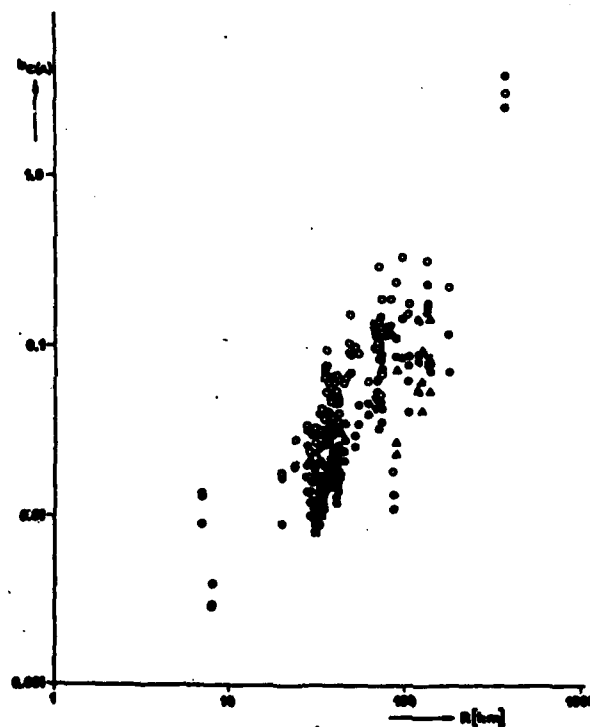


Fig.6. Dependence of the coefficient  $b_C(A)$  on distance  $R$ .

## 5. "STANDARD" AFD

The conditions for the computation of the AFD have to be defined in such a way as to make the values characterizing the ground motion dynamics comparable. As it follows from the previous part of the paper, the AFDs may not be affected only by the differences in the records of seismic waves, but also by the parameters that determine their computation. In standardizing the computation, we have to adhere to the following rules:

- i) keeping an identical sampling interval  $\Delta t$  of a record,
- ii) expressing the record amplitudes in identical physical units of the ground motion and
- iii) preserving the same total number of amplitude classes  $K_{\max}$  in the AFD computation.

A great majority of accelerograms of the world data bank are sampled at  $t = 0.02$  sec (SCHENK and VOJTISEK, 1985) and this value has proved to be sufficient for determining the AFD too (SCHENK 1985a). In the future, the sampling interval 0.02 sec of a seismic record is most likely to be regarded as the standard sampling interval  $\Delta t_{ST}$ .

If a seismic record is sampled at an interval  $\Delta t_x$  different from  $\Delta t_{ST}$ , there occurs a change in the amplitude number of a record, which is also reflected in different numbers of  $N_i$  amplitude occurrences in amplitude classes  $\Delta A_i$ . The shorter the interval  $\Delta t$ , the greater the numbers of  $N_i$ , and thus we can write

$$N_{ST} = N_x (\Delta t_x / \Delta t_{ST}) \quad , \quad (19)$$

where  $N_{ST}$  is the number of seismic ground motion amplitudes contained in the respective amplitude class at sampled interval  $\Delta t_{ST}$  and  $N_x$  is the number of amplitudes if interval  $\Delta t_x$  is used. Thus, the following relations are valid between these AFDs

$$\log N_x = a_x - b_x A \quad , \quad (20a)$$

determined from a seismic record at sampling interval  $\Delta t_x$ , and by an analogous "standard" AFD

$$\log N_{ST} = a_{ST} - b_{ST} A \quad , \quad (20b)$$

determined at sampling interval  $\Delta t_{ST}$ :

$$a_{ST} = a_x + \log (\Delta t_x / \Delta t_{ST}) \quad (21)$$

and

$$b_{ST} = b_x \quad . \quad (22)$$

The other condition that has to be satisfied for standard AFD is giving the amplitudes of seismic ground motion always in the same physical units: for accelerations in  $[cm \ s^{-2}]$ , for velo-

city in  $[cm\ s^{-1}]$  and for displacement in  $[cm]$ . The necessity to satisfy this condition is evident and need not be explained further.

The standardization of the computation of the AFD of a seismic record requires preserving the same maximum number of amplitude classes in each analysis. As mentioned above, a change in the maximum number of amplitude classes also produces a change in the total number of amplitudes  $N$  of each class of the density AFD, and consequently, the computed coefficient  $a$  in relation (10) will always be different: the greater the number of  $K_{max}$  amplitude classes, the smaller the value of coefficient  $a$ .

The experience in computing the density AFD gained by computer processing of a test set of accelerograms (SCHENK 1985a) has shown that for the purposes of routine computations fifty amplitude classes ( $K_{max} = 50$ ) seem to be a sufficient number. For  $K_{max} < 30$ , objective approximation cannot be ensured in all cases, on the other hand, an increasing number of amplitude classes, e.g.  $K_{max} > 100$ , demands not only more computer time, especially what concerns graphical plotting of the AFD, but also a chaotic ("zig-zag") pattern of the density AFD in the range of its highest amplitude classes. For this reason we recommend using a maximum number of 50 amplitude classes as a standard value of  $K_{max}$ . For this value we also defined a criterion to eliminate automatically the lowest and the highest amplitude classes in approximating the central "signal" part of the AFD (SCHENK 1985a).

## 6. AFD GROUND MOTION PARAMETERS

The knowledge of the density and cumulative AFDs enables us to establish new as yet unused parameters of seismic wave motion. In essence it involves three types of data:

- i) data of amplitude character
  - a. statistically determined maximum seismic signal amplitude ( $A_{max}(s)$ ,  $A_{max}(ref)$ ),
  - b. effective seismic signal amplitudes ( $A_{eff}$ ) and
  - c. the total value of the root-mean-square amplitude of the seismic signal ( $RMS$ ),
- ii) data on the energy content of wave motion
  - d. the total kinetic energy carried by the seismic signal ( $E$ ),
  - e. the total impulse of the seismic signal ( $IMP$ ),
- iii) data characterizing the time duration of the signal
  - f. the total duration of the seismic signal ( $T_s$ ), and

g. effective durations of the seismic signal  $\langle T_{eff} \rangle$ .

In this part of the paper a discussion of the relation of these parameters to the earthquake magnitude  $M$ , to the epicentral distance  $R$  and to the macroseismic intensity will be presented.

#### 6.1 Statistically determined maximum amplitude of ground motion.

The density AFD allows a statistical value of the probable maximum amplitude  $A_{max}(s)$  to be determined. This value is defined by the occurrence level of one amplitude digit, i.e.  $N = 1$ . This makes  $A_{max}(s)$  dependent on the entire course of the density AFD of the seismic signal and it may be regarded as a more representative value of the maximum amplitude of the seismic signal than a possible accidental peak amplitude  $\langle A_{max} \rangle$  in the record. From the above mentioned condition it follows that

$$A_{max}(s) = a_p / b_p, \quad (22)$$

where  $a_p$  and  $b_p$  are the coefficients of the density AFD of the signal.

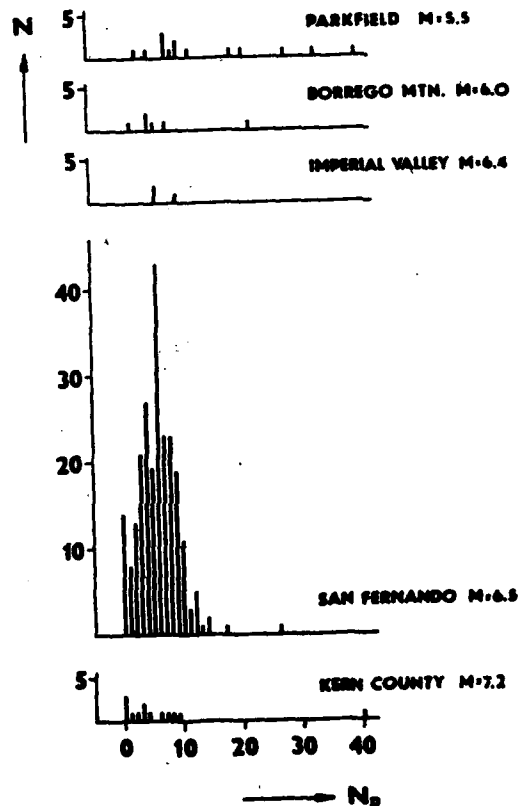


Fig.7. Histogram of the  $N_p$  values in dependence magnitude  $M$ .

From relation (15) it further follows that  $A_{\max}(s)$  is directly dependent also on the maximum number of amplitude classes  $K_{\max}$ . Since value  $K_{\max} = 50$  was used for the analysis of all accelerograms of the five Californian earthquakes mentioned above we observed the number of the highest amplitude digits between  $A_{\max}$  and  $A_{\max}(s)$  that were eliminated in each record. The number of these digits was denoted by the symbol  $N_p$ . Figure 7 presents histograms of the  $N_p$  values in dependence on the earthquake magnitude  $M$ . It appears that in the majority of cases  $N_p \leq 10$ , i.e. of the total number of all the amplitude digits of a record, as a rule containing a few thousand amplitude digits, a maximum of 1% of values is eliminated. This relation can be considered reasonable, for some extreme amplitudes of a record are given by the time superposition of two or more wave groups in a particular site, or by the local seismological inhomogeneities of the site.

If we compare the dependence of the observed peak amplitude  $A_{\max}$  on the epicentral distance  $R$  (Fig.8a) with that of the statistical maximum amplitude  $A_{\max}(s)$  (Fig.8b), we can readily find that the amplitude scatter of the latter dependence is approximately 30 - 40% smaller. Therefore, we believe that the values  $A_{\max}(s)$  will not be so much affected by the random changes of the local seismogeological conditions in the site as the maximum amplitudes of ground motion observed.

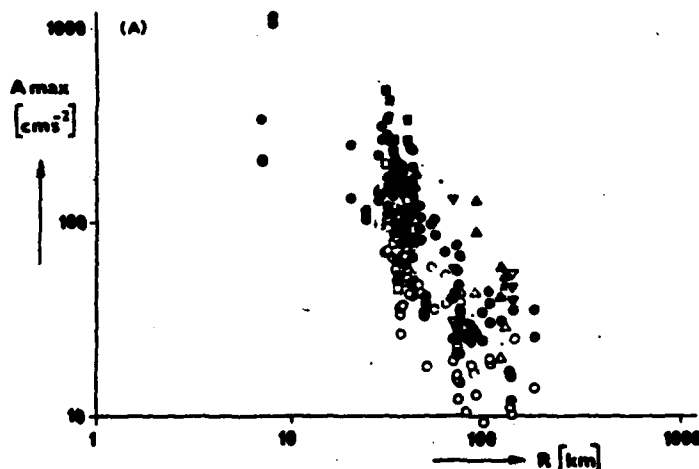


Fig.8a. Dependence of the  $A_{\max}$  value on the epicentral distance  $R$ : empty points - vertical component, full points - horizontal component,  $\square$  - Parkfield  $M=5.5$ ,  $\nabla$  - Borrego Mtn.  $M=6.0$ ,  $\circ$  - Imperial Valley  $M=6.4$ ,  $\bigcirc$  - San Fernando  $M=6.5$  and  $\Delta$  - Kern County  $M=7.2$ .

The relation between the  $A_{\max}$  and  $A_{\max}(s)$  values (Fig.9) shows that the  $A_{\max}(s)$  amplitude is almost always smaller than the  $A_{\max}$  amplitude. We estimate that



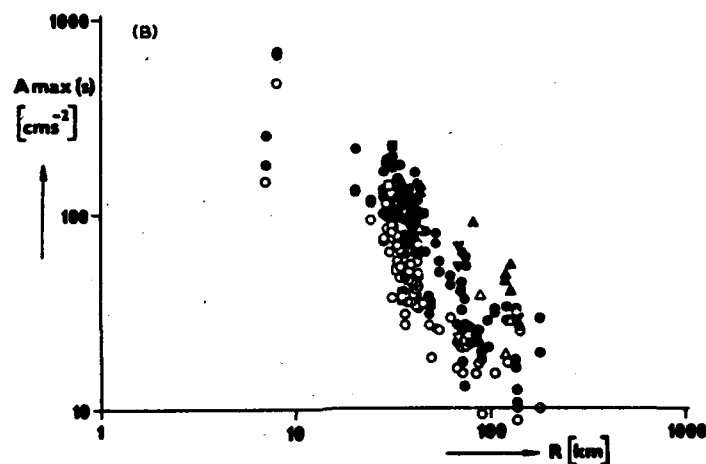


Fig.8b. Dependence of the  $A_{\max}(s)$  value on the epicentral distance  $R$ ; for symbols see Fig.8a.

$$A_{\max} = 1.486 A_{\max}(s) - 0.567 \quad (23)$$

Likewise, the cumulative AFD can be used for finding another statistically determined maximum amplitude of the seismic signal, which is called the "reference" maximum amplitude  $A_{\max}(\text{ref})$  and is given by the relation

$$A_{\max}(\text{ref}) = a_c / b_c \quad (24)$$

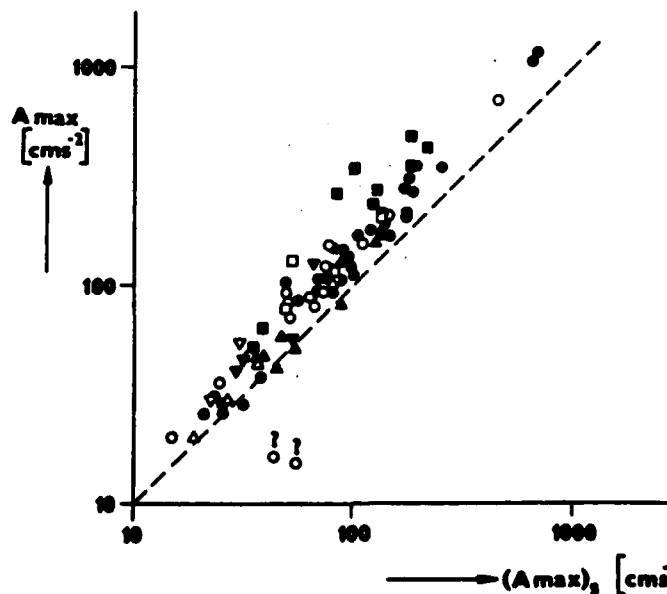


Fig.9. Correlation between the  $A_{\max}$  and the  $A_{\max}(s)$  values; for symbols see Fig.8a.

where  $a$  and  $b$  are now the coefficients of the cumulative AFD (11b). It is clear that  $A_{\max}(\text{ref})$  has no physical meaning, nevertheless we believe it could be applied in some strong motion analysis; for example as any maximum possible amplitude or at least as any pilot value to the  $A_{\max}(s)$  amplitude.

## 6.2 Effective amplitude of ground motion

Under the term effective amplitude we understand such an amplitude level which involves the required number of amplitudes of a ground motion record according to their percentile level  $P$ .

Let us assume a digital ground motion record of a seismic signal consisting, for example, of 100 digit amplitudes and let us try to find an effective amplitude  $A_{\text{eff}}$  involving 98 % of all digit amplitudes. The simplest way would be to neglect the two greatest extreme amplitudes and define an effective amplitude as a value that has to be smaller than the two greatest amplitudes and greater than the other 98 remaining amplitudes. It is understandable that this simplest approach would often be affected by random superposition of different wave groups of ground motions. Thus if we apply the entire signal AFD, we are not using only individual digit amplitudes, excluding seismic noise amplitudes, but the whole amplitude content of the seismic signal.

To determine the effective amplitude  $A_{\text{eff}}$ , the cumulative AFD is used. We extend relation (11b) approximated by this distribution up to the lowest amplitude class and determine the number  $N_c$ , which gives the number of digit amplitudes of the seismic signal in that class, i.e.  $\log N_c = a_c$ . The value  $N_c$  is assumed to be the number of all the digit amplitudes of the seismic signal. Then the effective amplitude  $A_{\text{eff}}$ , which is defined by the percentile level  $P$  [%] of the occurrence of amplitudes in the signal, can be calculated by the following relation

$$A_{\text{eff}}(P) = (a_c + \log P/100) / b_c(A), \quad (25a)$$

where  $a_c$  and  $b_c(A)$  are the coefficients of the cumulative AFD and

$$P \geq 100 / 10^{a_c} \quad (25b)$$

The effective amplitude is limited both from below by zero amplitude, which corresponds to the  $P = 0$  % and eliminates all signal amplitudes, and from above by the  $A_{\max}(s)$  amplitude, which corresponds to the  $P = 100$  % and on the contrary involves all signal amplitudes.

Unfortunately, the dependence of  $A_{\text{eff}}$  on the earthquake magnitude  $M$  could not be estimated due to the small range of  $M$  of the five Californian earthquakes. Consequently, the obtained data allow us to find only a relation between  $A_{\text{eff}}$  [ $\text{cm s}^{-2}$ ] and  $R$  [km] in the form

$$\log A_{eff} = q - k \log R \quad , \quad (2s)$$

where for the horizontal component

$$q = 0.07 P - 3.36 \quad \text{and} \quad k = 0.02 P - 0.52 \quad (26a)$$

and for the vertical component

$$q = 0.07 P - 3.44 \quad \text{and} \quad k = 0.02 P - 0.89 \quad . \quad (26b)$$

It is known that the relations between the peak amplitudes  $A_{max}$  of ground motions and the values of macroseismic intensities of the site  $I_s$ , where those motions were recorded, show a scattering over two orders of values  $A_{max}$  (SHEBALIN 1975, SCHENK and SCHENKOVA 1981, SCHENK 1984). This fact is explained by the influence of the local seismogeological conditions on the site. Since for some sites ground motion records can be directly compared to the observed macroseismic intensities  $I_s$ , we tried to find for these records some dependences between  $A_{eff}$  by means of a different percentile level  $P$ .

26 such records were available, for which the values of  $A_{eff}$  versus  $I_s$  for four percentile levels  $P = 99.5, 98, 95$  and  $90\%$

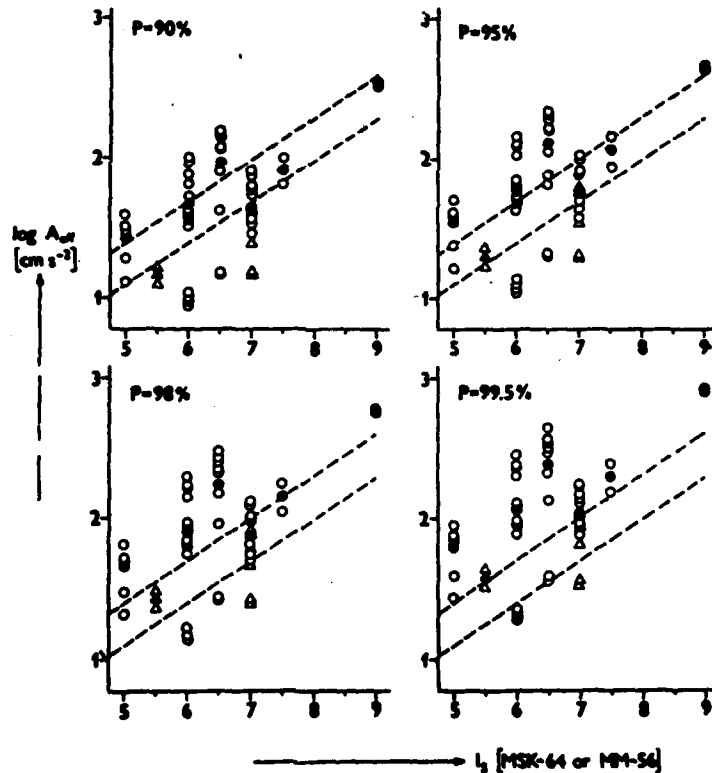


Fig.10a. Correlation between the  $A_{eff}(P)$  of horizontal components and macroseismic intensity  $I_s$ ; full points - mean value, dashed lines - range of accelerations recommended for  $I_s$  in MSK64 Scale.

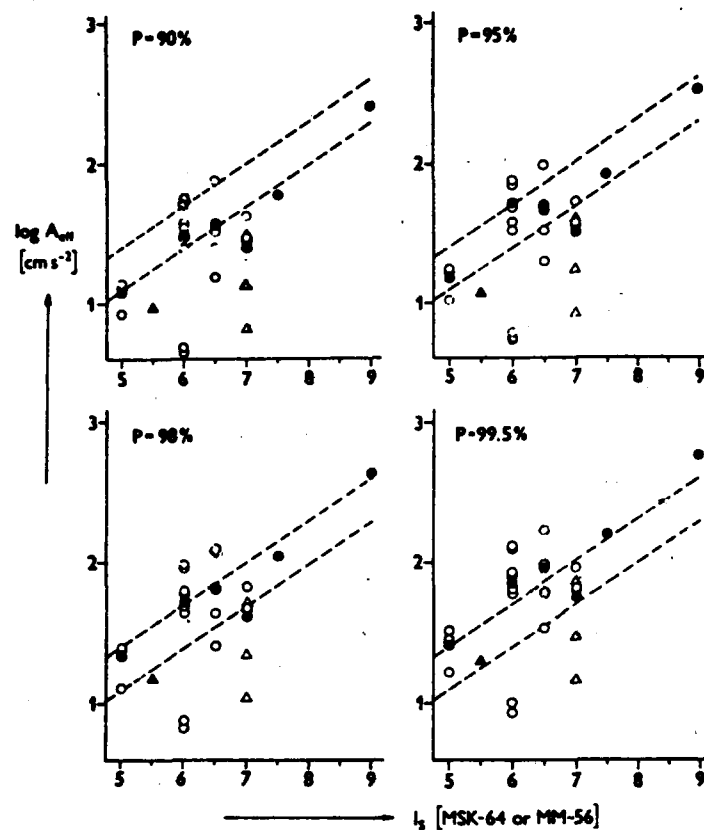


Fig.10b. Correlation between the  $A_{eff}(P)$  of vertical components and macroseismic intensity  $I_s$ ; for symbols see Fig.10a.

were determined (Figs 10). The values  $A_{eff}$  were compared with the acceleration values recommended by the MSK-64 scale for the macroseismic intensities; the upper and lower limits of the values are indicated by dashed lines in the graphs of Fig.10. The most suitable coincidence of the mean values of  $A_{eff}$  (full points) with the recommended values of acceleration for macroseismic intensities  $I_s$  belongs to the percentile level of 90 % for the horizontal component (Fig. 10a) and to 95 % for the vertical component (Fig. 10b). This finding also follows from the fact that the amplitudes of horizontal components are usually greater than those of vertical ones.

To conclude this paragraph, we can emphasize that correlations between the effective values of ground motions and other parameters (in our case with the macroseismic intensity) can probably give more reliable relations than those, which use the peak amplitudes directly measured.

### 6.3 Total root-mean-square amplitude

In a few recent papers (MORTGAT 1979, McCANN and BOORE 1983) the value of "root-mean-square" amplitude RMS of ground motions

is introduced to be a new quantity for an evaluation of seismic vibrations. The RMS amplitude is defined by the following expression (McCANN and BOORE 1983)

$$\text{RMS} = \left[ \frac{1}{t_2 - t_1} \int_{t_1}^{t_2} A^2(t) dt \right]^{1/2}, \quad (27)$$

where values of  $t_1$  and  $t_2$  are integration time limits between those the signal amplitudes  $A(t)$  are used for a calculation of the RMS. The RMS amplitudes are variable with time over the entire seismic signal and, therefore it is clear that the individual time-sequential values of the RMS amplitudes cannot be calculated with the use of the AFD. However, the knowledge of the density AFD of the seismic signal allows us to determine the total RMS amplitude of the signal in the form

$$\text{RMS} = \left\{ \left[ \sum_{i=1}^m A_i N_i \right] / \left[ \left( \sum_{i=1}^m N_i \right) - 1 \right] \right\}^{1/2}, \quad (28)$$

where  $N_i = \left\lfloor 10^{2D - 3D(A)A_i} \right\rfloor$ ,  $A_i = (2i - 1) K_{\max} / 2 A_{\max}$  and the upper limit  $m$  of the summation is defined by following condition: for  $\log N_i \geq 0$  it is  $1 \leq i \leq m$  and for  $\log N_i < 0$  it is  $m < i \leq K_{\max}$ .

A dependence of the total RMS amplitudes, obtained by this process, on the epicentral distance  $R$  is similar to that of the  $A_{\max}(s)$  (Fig. 11). A distinct relation between the total RMS

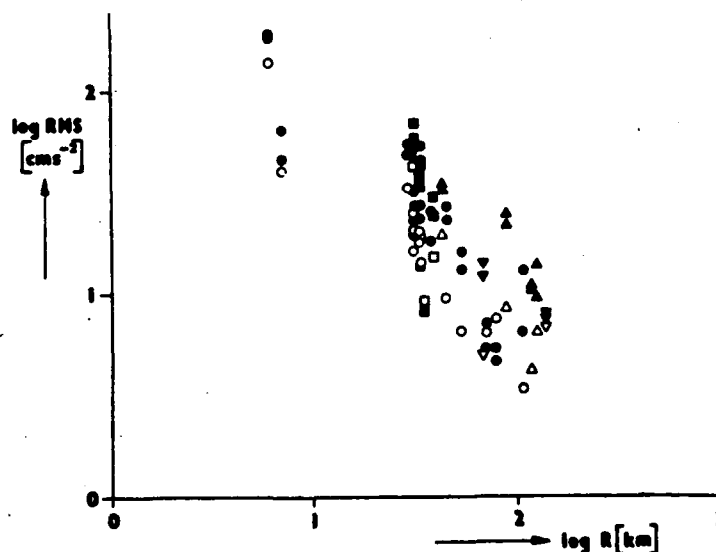


Fig.11. Dependence of the RMS acceleration on the epicentral distance; for symbols see Fig.8a.

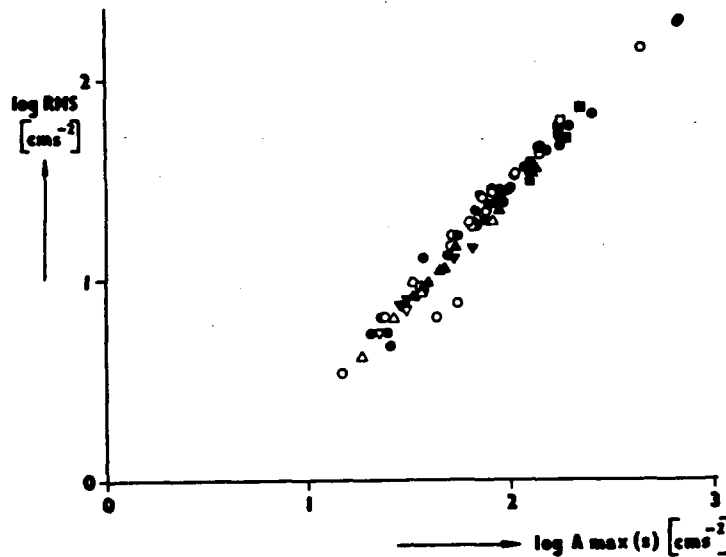


Fig.12. Dependence of the RMS acceleration on the Amax(s) values; for symbols see Fig.8a.

amplitudes of seismic signals and their Amax(s) amplitudes (Fig. 12) explains the similarity mentioned above (see Paragraph 6.1). We estimate that

$$\log \text{RMS} = 1.048 \log \text{Amax}(s) - 0.668 \quad (29)$$

It seems that the total RMS amplitude could become one of the important dynamic parameters of seismic ground motions.

#### 6.4 Total amount of the kinetic energy

The energy the seismic vibrations contains is one of the most important dynamic parameters on which we depend not only for understanding the energy release processes within an earthquake focus but also for assessing the damage caused in the near (or epicentral) zone of the shock. The total amount of the kinetic energy can be determined from the density AFD of the seismic signal in the form

$$E = \left[ (\Delta t / T_s) + 1 \right] \sum_{i=1}^m A_i^2 N_i \quad (30)$$

where  $A_i$  are the amplitude digits of a seismic vibration,  $\Delta t$  is the sampling interval of the vibration,  $T_s$  being the total time duration of the signal (see below).

In order to obtain the energy values in standard physical units [erg or Joule], it is essential that the digitized amplitudes should correspond to the particle velocity.

### 5.5 Total impulse of seismic signal

The next parameter, which characterizes the amount of energy of the seismic signal, is its impulse. Since the impulse corresponds to the changes of particle motion in time, then it can be expressed by the following relation

$$\text{IMPV} = \left[ (\Delta t / \tau_s) + 1 \right] \Delta t \sum_{i=1}^m A_i N_i, \quad (31)$$

where  $A_i$  are amplitudes of particle velocity. If a record of the particle acceleration is available, it holds

$$\text{IMPa} = \text{IMPV} / \Delta t, \quad (32)$$

### 6.6 Total duration of ground motion

The determination of the duration of a seismic signal  $\tau_s$  is related to the problem of its identification within the entire record of seismic vibrations. It is not easy to decide how long the signal code lasts, i.e., to find the termination of the signal in the seismic noise. Therefore, in common practice, the elapsed time between the first and the last amplitude of a given level (e.g. 0.05 g) is taken as a representative period of the duration, referred to as the "bracketed duration" (BOLT 1974).

Using the AFD we can suggest the following way of determining the total duration of the seismic signal. Let us have a cumulative AFD, which was compiled from ground motion amplitudes successively pointed out through the entire record at constant sampling intervals  $\Delta t$ . It is evident that the total number of amplitude digits in the signal coincides with the  $N_c$  value of the lowest amplitude class of the cumulative AFD. We obtain

$$N_c = \left\lfloor 10^{a_c - b_c(A) A/2} \right\rfloor. \quad (33a)$$

Then the total duration of the signal is given in the form

$$\tau_s = (N_c - 1) \Delta t. \quad (33b)$$

If a distribution pattern of the  $\tau_s$  values determined in this way is correlated with the epicentral distance  $R$  [km], we observe their positive dependence (Fig. 13): the greater the epicentral distance, the greater the total duration of a seismic signal. This fact is understandable because with increasing distance the time intervals among the onsets of individual types of seismic waves (P, S, surface) become greater due to different wave velocities. Therefore, the total duration of a signal has to be longer too. For  $R \leq 30$  km this correlation can be roughly expressed in the form

$$\log \tau_s = 1.05 \pm 0.59 \quad (34a)$$

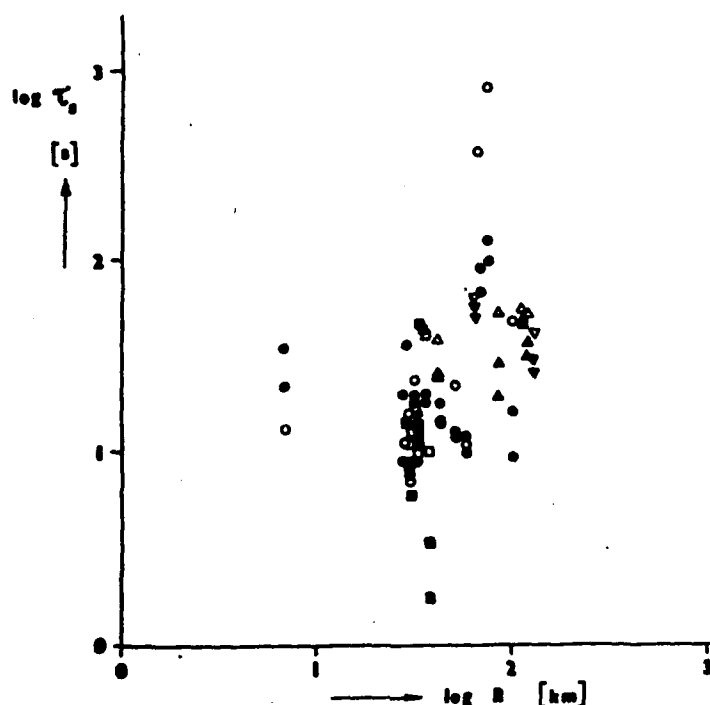


Fig.13. Dependence of the  $T_s$  value on the epicentral distance  $R$ ; for symbols see Fig.8a.

and for  $R > 30$  km

$$\log T_s = 1.19 \log R - (0.71 \pm 0.61) \quad (34b)$$

The dependence between the total signal duration  $T_s$  and the  $A_{\max}(s)$  amplitude of ground motion shows an opposite pattern (Fig. 14): the greater the signal duration  $T_s$ , the smaller the amplitude  $A_{\max}(s)$ . We estimate that

$$\log T_s = (3.19 \pm 0.36) - (1.05 \pm 0.04) \log A_{\max}(s) \quad (35)$$

This fact is obvious, because if the distance is greater, the  $T_s$  values are also greater (Fig. 13) and simultaneously the maximum amplitudes become smaller (Fig. 14). The significant character of this dependence evidences that the attenuation of the amplitudes of the signal wave pattern is more dependent on the distribution of seismic energy into various kinds of wave groups and types, and on their expanding space propagation than on the actual decrease of the energy caused by the material properties of the geological media.

#### 6.7 Effective duration of ground motion

Likewise, the same method can be used to determine the effective "bracketed" duration for different levels of amplitudes. Under the term effective duration we understand the sum of time periods during which the amplitudes of the signal exceed a



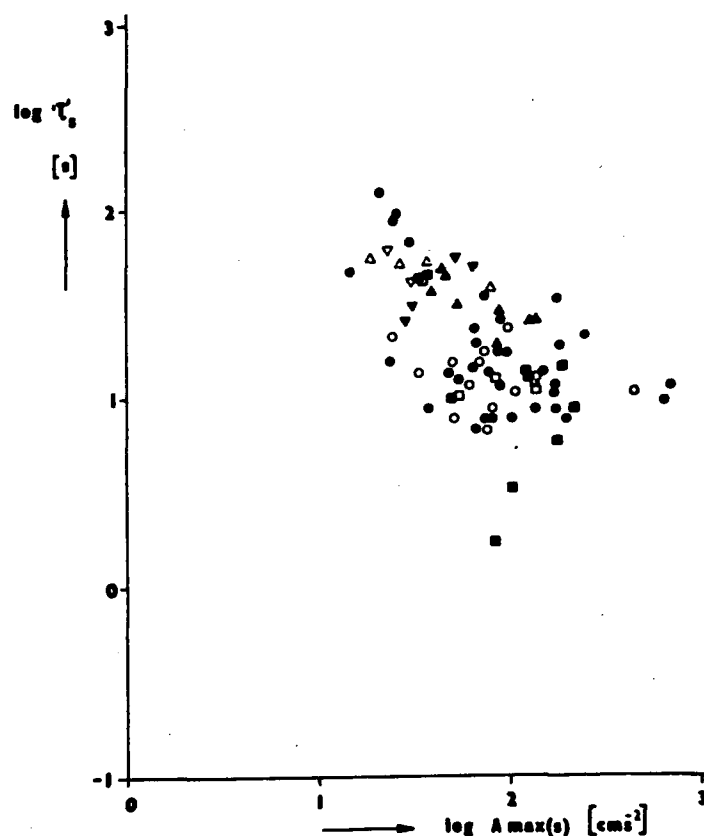


Fig.14. Dependence of the  $T_s$  value on the  $A_{\max}(s)$  value; for symbols see Fig.8a.

given effective amplitude level  $A_{\text{eff}}$ . Since the cumulative AFD of a seismic signal is approximated by relation (11b), the effective amplitude level  $A_{\text{eff}}$  determines the total number of amplitudes greater than  $A_{\text{eff}}$  by expression

$$N_{\text{eff}} = \left\lfloor 10^{a_c - b_c(A) A_{\text{eff}}} \right\rfloor. \quad (37a)$$

The effective duration, bracketed by the  $A_{\text{eff}}$  value, is then

$$T_{\text{eff}} = (N_{\text{eff}} - 1) \Delta t. \quad (37b)$$

In this way, the effective duration  $T_{\text{eff}}$  for the  $A_{\text{eff}}$  values given in absolute units of ground motions (acceleration, velocity or displacement) can be calculated. We analyzed the set of accelerograms of those five Californian earthquakes to determine the dependence of  $T_{\text{eff}}$  versus the  $A_{\max}(s)$  amplitudes for the following levels of  $A_{\text{eff}}$ : 5, 10, 20, 40, 65, 100 and 200  $\text{cm s}^{-2}$  (Fig.15). For  $A_{\text{eff}} = 0 \text{ cm s}^{-2}$ , the  $T_{\text{eff}}$  value becomes the  $T_s$  value.

Figure 18 shows the way the distribution pattern of dependence  $T_{\text{eff}}$  on  $A_{\max}(s)$  changes with increasing effective amplitudes  $A_{\text{eff}}$ : the above described character of the dependence

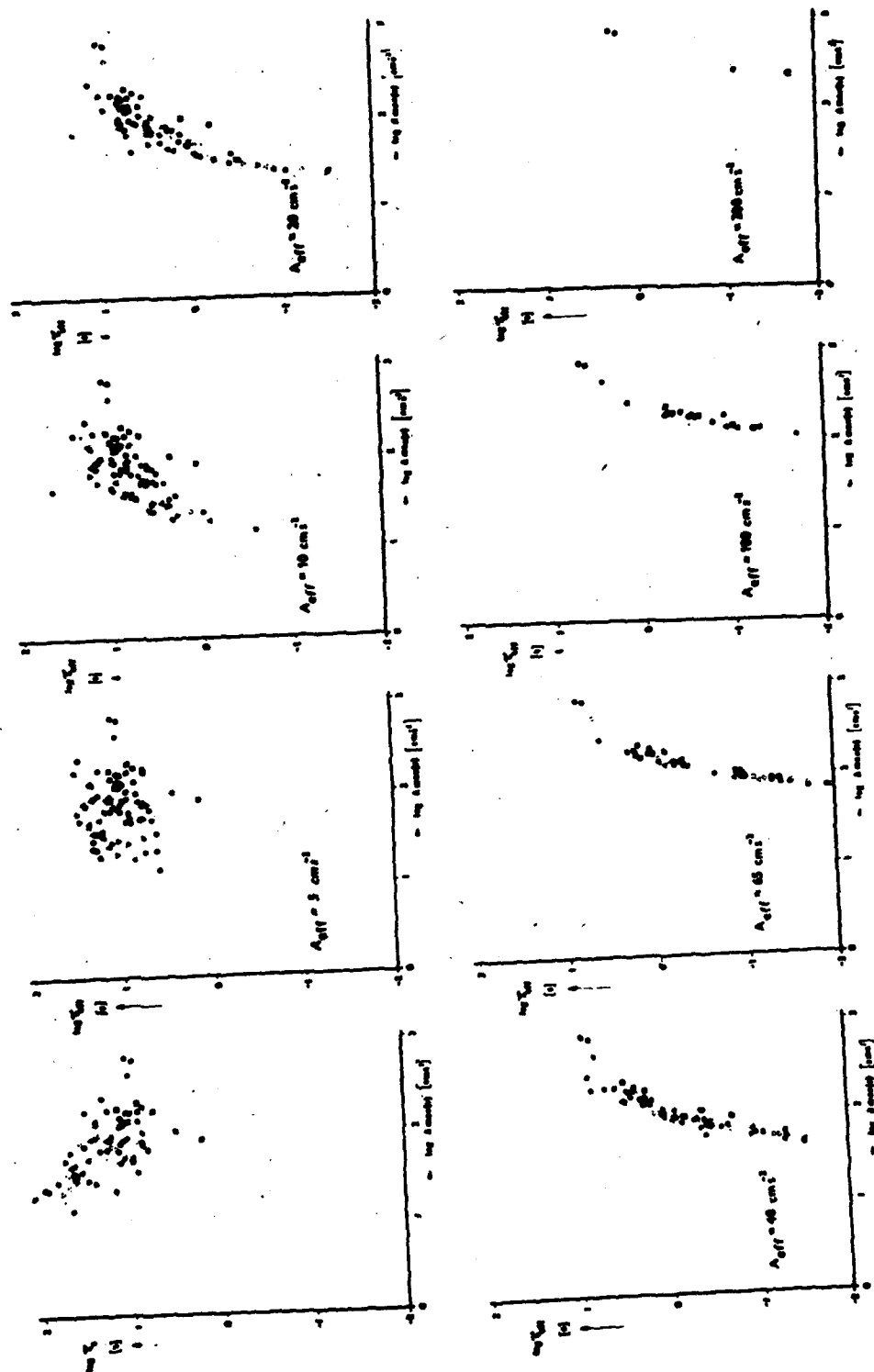


Fig. 18: Dependence of the  $\log T_{eff}$  values on the  $\log A_{max}(s)$  value for different  $A_{eff}$  values for symbols see Fig. 8a.

$T_s$  versus  $A_{max}(s)$  gradually assumes (for  $A_{eff} = 5 \text{ cm s}^{-2}$ ) an opposite character (for  $A_{eff} = 10 \text{ cm s}^{-2}$ ), which becomes more pronounced for  $A_{eff} = 20 \text{ cm s}^{-2}$ . This change of the dependence  $T_{eff}$  versus  $A_{max}(s)$  can easily be explained by the AFD of the seismic signal: the greater the value of  $A_{max}(s)$ , the higher the number of effective amplitudes of a certain level, e.g., in accordance with (36b), longer effective duration  $T_{eff}$ .

## 7. CLASSIFICATION OF GROUND MOTIONS ACCORDING TO MACROSEISMIC EFFECTS

### 7.1 Significance of the parameters for record classification according to macroseismic intensity

The parameters described in Paragraph 6 were determined for the accelerograms of the Californian earthquakes and statistically analyzed. The statistical analysis was performed for vertical and horizontal components separately and for three macroseismic classes (Table 1.). Each component was considered to be one object characterized by a vector of the parameters.

Table 1	macroseismic class		
	class 1	class 2	class 3
	$I \geq 7^0$	$I = 6^0$	$I \leq 5^0$
vertical component	47	29	11
horizontal component	95	58	26

The multidimensional dispersional analysis can be used under the assumption that inside each macroseismic class the vectors of the parameters are normally distributed with respect to the mean vector of this class and that the covariation matrixes of the vectors of the three macroseismic classes are equal (AHRENS and LAUTER 1981). The parameters characterizing amplitude and energy quantities (see Paragraphs 6.1, 6.2, 6.4, 6.5) and peak amplitude  $A_{max}$  were taken in the logarithmic form to make their distributions inside the classes closer to the normal ones.

The mean values of the parameters, e.g., the components of the mean vector together with their standard deviations, were determined separately for vertical and for horizontal components of acceleration (Table 2). Applying the F-statistics (AHRENS and LAUTER 1981) to these mean values, one can find that the mean vectors of all the three macroseismic classes differ with a confidence level of 0.01. Table 3a contains the coefficients of correlation of the parameters of vertical components, Table 3b of horizontal components.

Table 2.

vertical component							
Parameter	class 1		class 2		class 3		D
	Mean	S.D.	Mean	S.D.	Mean	S.D.	
RMS	.82	.14	.73	.15	.72	.15	.11
E	3.63	.57	3.27	.58	2.92	.48	.21
IMP	.03	.27	-.16	.30	-.21	.31	.13
Ae80	2.32	.27	2.04	.33	1.79	.20	.48
Ae90	2.44	.30	2.24	.29	1.95	.19	.37
Ae95	2.56	.28	2.36	.30	2.06	.19	.38
Ae98	2.65	.28	2.46	.31	2.15	.19	.36
Ae99	2.70	.29	2.51	.31	2.20	.19	.35
taus	34.35	21.39	28.67	26.10	36.74	28.30	.02
te05	31.59	18.33	24.60	19.45	29.93	21.94	.03
te10	29.21	15.97	21.36	14.91	24.52	17.13	.06
te20	25.27	12.67	16.61	9.94	16.74	10.71	.15
te40	19.52	9.44	11.08	6.93	8.33	4.94	.34
te65	14.68	7.80	7.50	5.61	3.86	2.66	.42
te100	10.31	6.46	4.85	4.30	1.52	1.46	.40
logF	1.11	.22	1.12	.22	1.10	.22	.00
Amax	2.82	.29	2.66	.33	2.30	.21	.35
aD	2.14	.29	2.03	.37	2.08	.33	.03
bD	-.01	.01	-.01	.01	-.01	.01	.16
aC	3.16	.27	3.01	.36	3.19	.24	.06
bC	-.01	.01	-.01	.01	-.02	.01	.20
bDK	-.05	.01	-.05	.01	-.05	.01	.04
bCK	-.06	.01	-.06	.01	-.06	.01	.03
As	2.74	.29	2.56	.32	2.25	.20	.34
Aref	2.84	.30	2.67	.32	2.34	.19	.33
horizontal component							
Parameter	class 1		class 2		class 3		D
	Mean	S.D.	Mean	S.D.	Mean	S.D.	
RMS	.95	.15	.85	.15	.82	.16	.14
E	4.22	.53	3.77	.62	3.39	.57	.31
IMP	.28	.28	.09	.30	.01	.33	.14
Ae80	2.58	.30	2.32	.34	2.02	.27	.44
Ae90	2.75	.27	2.48	.38	2.19	.26	.44
Ae95	2.87	.27	2.64	.31	2.31	.26	.50
Ae98	2.97	.27	2.75	.32	2.40	.26	.49
Ae99	3.02	.27	2.81	.32	2.45	.27	.47
taus	28.74	19.07	24.24	24.52	29.72	25.97	.01
te05	27.70	17.94	22.58	21.87	26.10	21.74	.01
te10	26.74	16.93	21.08	19.58	23.03	18.37	.02
te20	25.00	15.20	18.48	15.89	18.18	13.45	.05
te40	22.04	12.61	14.52	11.11	11.88	7.96	.14
te65	19.05	10.50	11.13	7.96	7.49	5.10	.27
te100	15.76	8.82	8.12	5.93	4.35	3.71	.39
logF	-.26	11.73	.39	6.41	2.11	6.88	.01
Amax	3.14	.28	2.96	.35	2.59	.28	.38
aD	2.03	.28	1.95	.40	2.06	.33	.02
bD	.00	.00	.00	.00	-.01	.01	.34
aC	3.08	.27	2.91	.38	3.07	.28	.06
bC	.00	.00	.00	.00	-.01	.01	.35
bDK	-.05	.01	-.05	.01	-.05	.01	.03
bCK	-.06	.01	-.06	.01	-.06	.01	.04
As	3.06	.28	2.85	.33	2.49	.27	.47
Aref	3.17	.28	2.98	.33	2.60	.27	.46

# Correlation Matrix of the Parameters of Vertical Components

27

## Correlation Matrix of the Parameters of Horizontal Components

[illegible]

Now we are going to estimate the way each parameter can contribute to the classification of vertical and horizontal components into the three macroseismic classes given above. The statistical quantity "distance"  $D$  of each parameter was introduced to this evaluation (AHRENS and LAUTER 1981); the higher the  $D$ , the more informative the parameter for the classification. For example, the Amax of vertical and horizontal components are less informative than Aeff(80) and Teff(100).

After the statistical analysis of the parameters, the pattern recognition algorithms were introduced to solve the inverse problem: a classification of the accelerogram, which is described by the 25 parameters of each of its components according to macroseismic effects. We used the following algorithms:

- i) MAH - the Mahalanobis distance
- ii) FACT - the estimate of F-statistics (unbiased estimate of Mahalanobis distance)
- iii) APR - the estimate with regards to "a priori" probabilities of classes
- iv) DCOR - the estimate with regard to different covariations in classes, and
- v) DAPR - the estimate with regard to all these possible distinctions between classes.

Table 4.

Pattern Recognition Algorithm	Percentage of Failures in the Classification			
	Horizontal Component		Vertical Component	
	I	II	I	II
FACT	24.7	3.1	24.0	2.1
MAH	24.2	3.1	25.0	2.1
DCOR	23.7	10.3	19.8	33.3
APR	25.3	3.1	22.9	2.1
DAPR	22.7	10.3	19.8	33.3

I - objects referred to the adjacent class

II - objects referred to the opposite class

The inaccuracy of different pattern recognition algorithms applied in the process of classification is given in Table 4. The Mahalanobis algorithm gives the most effective classification for the horizontal component, while the "a priori" probabilities algorithm gives the most effective classification for the vertical component. Table 4 also shows that the pattern recognition algorithms allow us to classify successfully three out of four acceleration components, the vertical or horizontal ones.

## 7.2 "Destructive" and "Save" records

An attempt at establishing the characteristics of the object belonging to the first ( $I \geq 7$  MSK) and the third ( $I \leq 5$  MSK) classes is made. These characteristics are determined by the CORA-3 algorithm of pattern recognition (GELFAND et al. 1976). This algorithm uses binary vectors, i.e., 0 and 1, to detect the characteristic features (traits) of vectors in each of the two given macroseismic classes. Each parameter is coded by 0 if higher than the corresponding thresholds and by 1 if smaller than this threshold. An example of the thresholds for some more informative parameters of vertical and horizontal components is presented in Table 5. By using the CORA-3 algorithm eight parameters were finally selected as the most informative for the classification of vertical and horizontal components of acceleration. It is also necessary to point out that two horizontal components of the same accelerograms create a single vector consisting of the maximum values, which were always elected from two values of the same parameter. The advantage of that approach was discussed in GVI-SHIANI et al. (1987) and therefore we apply it too.

The necessary criteria for a classification of accelerograms into the "destructive" class ( $I \geq 7$  MSK) are the following:

### A. for vertical components

1.  $T_{eff}(65) > 8$  sec,
2.  $T_s > 28.53$  sec,  $A_{eff}(80) > 93$  cm/sec<sup>2</sup>,
3.  $A_{eff}(80) > 92$  cm/sec<sup>2</sup>,  $RMS < 7$  cm/sec<sup>2</sup>,
4.  $b_c(A) < 0.01019$ ,  $T_s < 28.53$  sec,  $RMS < 7$  cm/sec<sup>2</sup>,

### B. for horizontal components

1.  $T_{eff}(100) > 8$  sec,  $T_{eff}(65) > 18.65$  sec,
2.  $T_{eff}(100) > 8$  sec,  $E < 15000$ ,
3.  $b_c(A) < 0.0025$ .

Likewise, to classify the accelerograms into the "save" class ( $I \leq 5$  MSK), the following conditions have to be satisfied:

### A. for vertical components

1.  $T_{eff}(65) < 8$  sec,  $A_{eff}(80) < 92$  cm/sec<sup>2</sup>,  $b_c(A) > 0.01019$
2.  $T_{eff}(65) < 8$  sec,  $A_{eff}(80) < 92$  cm/sec<sup>2</sup>,  $T_s > 28.53$  sec
3.  $T_{eff}(65) < 8$  sec,  $RMS > 7$  cm/sec<sup>2</sup>,



Table 5.

Parameter	Vertical Component	Horizontal Component
$a_c$	3.15	2.98
$b_c(A)$	0.01019	0.00250
$b_D(A)$	0.00999	0.00210
$A_{\max}(s)$	300	1146
$A_{\max}(\text{ref})$	450	1255
$A_{\text{eff}}(80)$	92	260
$A_{\text{eff}}(90)$	150	524
$A_{\text{eff}}(98)$	300	650
RMS	7.0	12.4
E	3500	15000
IMP	1.5	2.0
(s)	28.53	38.0
$\tau_{\text{eff}}(65)$	8.0	18.65
$\tau_{\text{eff}}(100)$	4.5	8.0

B. for horizontal components

1.  $\tau_{\text{eff}}(65) < 18.65 \text{ sec}$ ,  $\tau_{\text{eff}}(100) < 8 \text{ sec}$ ,  $b_c(A) > 0.0025$
2.  $\tau_{\text{eff}}(65) < 18.65 \text{ sec}$ ,  $E > 15000$ ,  $A_{\max}(\text{ref}) < 1255 \text{ cm/sec}^2$

### 8. ATTENUATION COEFFICIENTS OF THE GROUND MOTIONS

Let us have a digitized seismic signal, whose amplitude envelope is attenuated exponentially according to relation (3). Unlike the formerly used AFDs, i.e. a distribution with a constant amplitude class, for calculating the attenuation of the seismic vibrations it has proved more effective to select nonlinear amplitude distribution so that for the limits of the  $i$ -th amplitude class it should hold

$$A_i = A_{\max} \exp(-\beta t_i) \quad (37a)$$

and

$$A_{i+1} = A_{\max} \exp(-\beta t_{i+1}) \quad (37b),$$

where  $t_{i+1} - t_i = \tau$  is the constant time, during which the signal will be attenuated from amplitude  $A_i$  to amplitude  $A_{i+1}$ . From these relations it follows that contrary to the previous practices, indexes  $i$  in amplitude classes will be numbered in

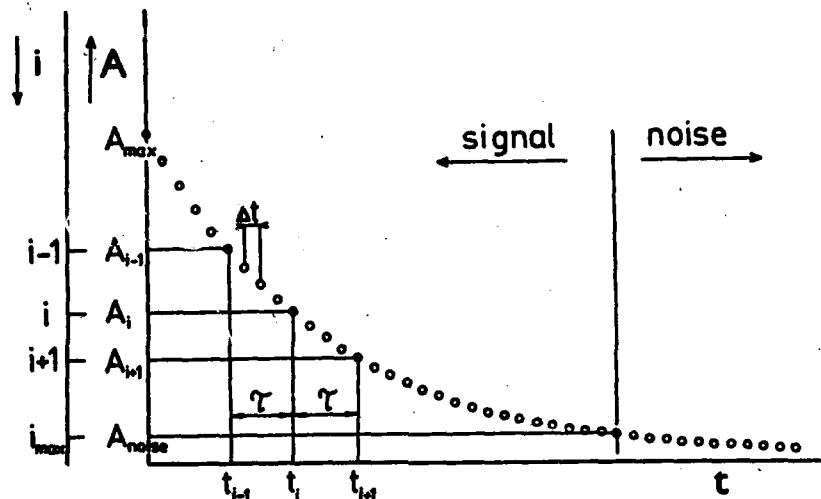


Fig.16. Amplitude classes of the nonlinear AFD

the upward order, beginning with the class of a maximum amplitude and ending with the class of amplitudes close above the boundary of seismic noise. Inserting relation (37) into (3), we get

$$\tau = (\ln A_{i+1} - \ln A_i) / \beta \quad (38)$$

The number of amplitude samples in the  $i$ -th class is then given by (Fig.16)

$$N_i = \tau / \Delta t = (\ln (A_{i+1} / A_i)) / \beta \Delta t \quad (39)$$

where  $\Delta t$  is the constant sampling interval. Relation (39) makes it evident that with a constant ratio of the boundary amplitudes of the new-created amplitude nonlinear AFD, the number of samples in these classes will be constant and in indirect proportion to the attenuation coefficient  $\beta$  of the seismic signal.

As pointed out above, relation (39) is valid under the assumption that all signal samples belong to the exponentially attenuated envelope of amplitudes (3). This assumption is obviously not satisfied since, in addition to the samples on the envelope or in its close proximity, the signal also comprises the samples lying below the envelope and constituting the "content" of the signal. If, however, the signal is a periodical one, we can show that the envelope can not be approximated by the signal extremes but also by any other samples within one period range. Relation (39) will also hold for this envelope, only the absolute amplitude of the signal will be lower. It means that for each class the contributions of the lower envelopes will be constant too, but in accordance with the conditions given by relations (37), it will become manifest only in the higher classes. From all the above stated facts it thus ensues that for the

900 SOUTH FREMONT AVENUE, ALHAMBRA  
BASEMENT, COMP DOWN

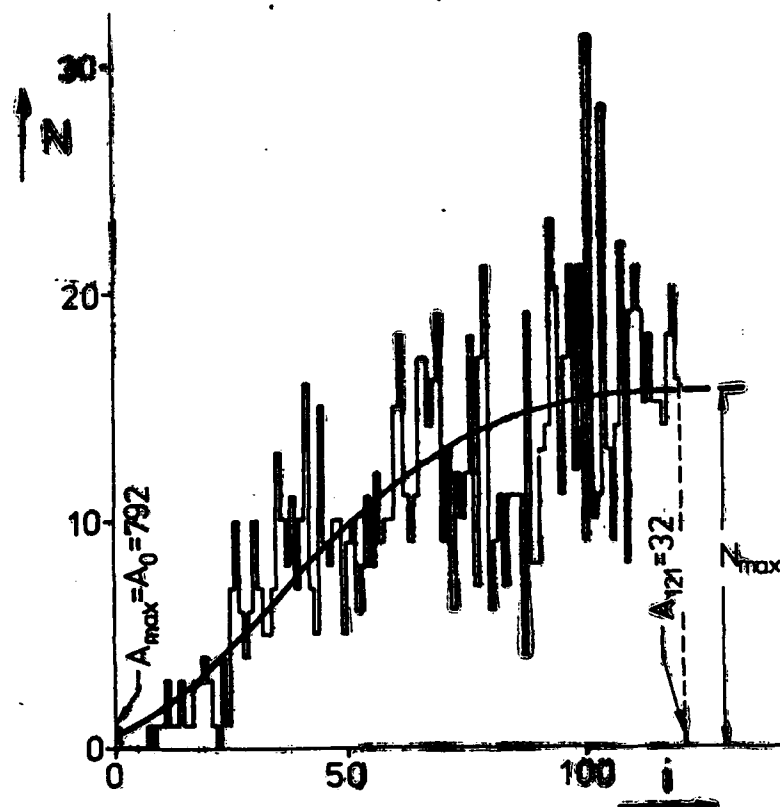


Fig.17. Approximation of a real signal by the relation (41)

periodical signal, which is attenuated according to the exponential law (3), we can write

$$\beta = \lim_{N \rightarrow \infty} \ln (A_{i+1} / A_i) / N_i \Delta t \quad (41)$$

This relation can already be used for digitized seismic signals to determine attenuation coefficient.

Due to the fact that the new logarithmic AFD is not terminated in higher amplitude classes because the amplitudes that belong to them continuously in pass into seismic noise amplitudes, in determining the coefficients  $\beta$  of real seismic records, it is necessary to define the maximum value of index  $i$ . This index is determined from relation (37b) in such a way as to exclude the classes containing seismic noise amplitudes from processing. The nonlinear logarithmic AFD is then unambiguously defined by index  $i_{max}$ .

In order to determine the value of the occurrence frequency of amplitudes in the particular logarithmic amplitude classes, in the set of  $N$  values we approximate by the least-square method the function

$$N(i) = a_1 \exp 2 (a_2 i - a_3) , \quad (42)$$

the value of the curve maximum being considered the limit (40). In analytically defined signals, also other approximations were tested to determine the limit (40); in the end, relation (41) proved to be the most convenient. Figure 17 is an example of such an approximation in a real signal in order to determine the coefficient by the above-mentioned methodology.

The calculation of the quality factor  $Q$ , which characterizes the attenuation properties of a rock medium, is given by the relation

$$Q = T f / \beta , \quad (43)$$

where  $f$  is the predominant frequency of the seismic signal. It is obvious that this relation has a correct validity for the signal of harmonic wave motion, for real seismic signals its validity is only approximate. Frequency  $f$  can be determined by means of the Fourier spectrum or from the frequency distribution of the signal half-periods (SCHENK 1987). The latter method is based on the same principle as the determination of the AFD.

## 9. CONCLUSION

An analysis of a seismic record in the amplitude domain does not only enable us to obtain new parameters characterizing seismic vibration, but also contributes to the classification of seismic wave motion. The introduction of this analysis to routine seismic interpretation procedures together with the analysis of waves in the time and frequency domains extend the present possibilities of studying dynamic parameters and contributes to their more objective and more general evaluation.

These new-defined dynamic parameters can be expected to find a wide application in the methods of earthquake engineering, in particular the values of the statistically determined maximum amplitude, of the effective amplitudes and durations of the seismic signal. A treatment of the records in the amplitude domain has revealed that some parameters change with the earthquake magnitude or with the epicentral distance as opposed to some that remain invariant. The knowledge of the parameters in the near-field of the earthquake, together with the known dependences of the amplitude-frequency distributions and of spectra of seismic waves, contribute to classifying strong ground motions recorded up to now and to selecting more objectively analogous motions (accelerograms, etc.) that express the seismic hazard in a form suitable for the design of earthquake resistant structures.

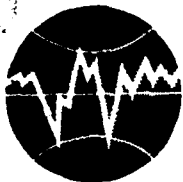
## REFERENCES

- Ahrens H., Läuter J. (1981): Mehrdimensionale Varianzanalyse. Akademie-Verlag, Berlin.
- Bolt B.A. (1974): Duration of strong ground motion. Proc. 5th World Conf. Earthq. Engng, Rome, vol. 1, 1304-1313.
- Bolt B.A., Abrahamson N.A. (1982): New attenuation relations for peak and expected accelerations of strong ground motion. Bull. Seis. Soc. Amer. 72, 2307-2322.
- Gelfand I.M. et al. (1976): Pattern recognition applied to earthquake epicentres in California. Phys. Earth Planet. Inter. 11, 227-283.
- Gvishiani A.D., Mostinskiy A.Z., Shebalin P.N., Tumarkin A.G., Zhizhin M.N. (1987): Classification of strong-motion records by algorithms of pattern recognition. In "Problems of Geophysical Informatics", Inst. Phys. Earth, Acad. Sci. of the USSR, Moscow.
- Jarník V. (1955): Diferencialni počet I., NCSAV, Praha.
- McCann M.W., Boore D.M. (1983): Variability in ground motions: root mean square acceleration and peak acceleration for the 1971 San Fernando, California, earthquake. Bull. Seis. Soc. Amer. 73, 615-632.
- Mortgat C.P. (1979): A probabilistic definition of effective acceleration. Proc. 2nd U.S. Nat. Conf. Earthq. Eng., Berkeley, 743-752.
- Schenk V. (1984): Relations between ground motions and earthquake magnitude, focal distance and epicentral intensity. J. Engng Geol. 20, 143-151.
- Schenk V. (1985a): Amplitude-frequency distribution of strong ground motion. Phys. Earth Planet. Inter. 38, 144-161.
- Schenk V. (1985b): Analysis of strong ground motion amplitudes in time domain. Proc. "3rd Intern. Symp. on the Analysis of Seismicity and on Seismic Risk", Geoph. Inst., Czechosl. Acad. Sci., Praha, 328-339.
- Schenk V. (1987): Determination of quality factor Q by strong ground motion analysis in amplitude domain. Proc. 20th General Assembly of the European Seismol. Comm., Kiel, in press.
- Schenk V., Mantlik F., Vojtisek D., Gvishiani A.D., Filimonov M. B., Tumarkin A.G., Zhizhin M.N. (1987): Macroseismic intensity classification of strong motion records by pattern recognition algorithms. Proc. 20th General Assembly of the European Seismol. Comm., Kiel, in press.

Schenk V., Schenkova Z. (1981): Relation between intensity and ground motion parameters - review and generalization. Gerlands Beitr. Geophysik, Leipzig 90, 247-254.

Schenk V., Vojtisek D. (1985): A project of strong ground motion computer file. Proc. "3rd Intern. Symp. on the Analysis of Seismicity and on Seismic Risk", Geoph.Inst., Czechosl.Acad.Sci., Praha, 347-354.

Shebalin N.V. (1975): Ob ocenke seismicheskoy intensivnosti (On a seismic intensity estimation). In "Seismicheskaya shkala i metody izmereniya seismicheskoy intensivnosti", Nauka, Moscow, 87-109.



**TURKISH NATIONAL COMMITTEE FOR  
EARTHQUAKE ENGINEERING**

**THIRTEENTH REGIONAL SEMINAR ON EARTQUAKE ENGINEERING**

**September 14-24, 1987 - Istanbul - Turkey**

**GEOLOGICAL FAULTS  
AND  
EARTHQUAKE CODES**

**BRYAN O SKIPP  
(SOIL MECHANICS ASSOCIATES, U.K.)**

**EUROPEAN ASSOCIATION OF EARTHQUAKE ENGINEERING  
TURKISH NATIONAL COMMITTEE ON EARTHQUAKE ENGINEERING  
THIRTEENTH EUROPEAN SEMINAR**

**GEOLOGICAL FAULTS  
AND  
EARTHQUAKE CODES**

**BRYAN O SKIPP  
(SOIL MECHANICS ASSOCIATES, U.K.)**

**ISTANBUL  
SEPTEMBER 14-24 1987**



## THIRTEENTH EUROPEAN SEMINAR ON EARTHQUAKE ENGINEERING

### GEOLOGICAL FAULTS AND EARTHQUAKE CODES

#### 1 INTRODUCTION

It is accepted that earthquakes take place on faults but not on all faults with equal likelihood. Whether or not, in a particular setting, a known fault contributes significantly to the seismic hazard is a matter of prime concern in engineering seismology and a theme of much current research. With the increasing capability of numerical hazard modelling, especially when a logic tree formulation is adopted, there is an increasing tendency, if not a temptation, to model faults sources explicitly even where the assignation of the necessary parameters to them is little more than constrained guesswork.

It is not surprising therefore to see in recent 'general' earthquake codes (viz Draft, ISO/DIS 3010.2) and EC8 reference being made to 'active' faults and the restrictions on the siting of important buildings which their proven presence imposes.

In many regions crustal faults are ubiquitous so that the mean distance to the outcrop may be small ( $<1$  km). The chance of siting away from a fault is therefore small for a major construction project or urban development.

The significance of faults so labelled 'active' is well established when it comes to the siting of NPP's dams, LNG facilities (see Meehan 1984) but the incursion of the category into general earthquake codes has wide ranging implications and warrants a brief review of the concept of 'activity', how it can be recognised and what impact on a hazard calculations such recognition may have.

The lecture will review the extent to which 'faults' as such are dealt with or referred to in general earthquake codes and a number of specialised regulatory documents. The 'scientific' basis of a rational concept of

'activity' will be discussed, leading to a set of 'pointers' aiding decisions regarding the incorporation of faults in hazard calculations. Recent advances in geological techniques for the dating of 'last movement' will be referred to. Attention will be drawn to some fundamental limitations in the extent to which a full picture of fault activity can be developed.

## 2 CURRENT CODE AND REGULATORY POSITION

Of the 34 earthquake codes collected in the World List (1984) only a handful specifically refer to faults, usually in very general terms recommending that active ones be avoided. The Draft Eurocode 8 goes further in that it requires that "Buildings belonging to classes I and II according to section 15.31 should not be built within  $\geq$  m from a distance of potentially active fault (to be specified by the competent national authority)".

The issue is also touched upon in regulations in Italy (Seismic act p 64 1974 and p 741 1981) and California. It is however from the power industry with its large dams, nuclear facilities, LNG storage, that the most detailed guidance has emanated.

Faults have been seen as having the potential for surface rupture as well as constituting sites for earthquakes and so affecting the shaking hazard. The most influential document has been the United States Nuclear Regulatory Commission's Rules and Regulations part 100. Reactor Site Criteria NUREG 100A and the derivative but not entirely identical International Atomic Energy Agency Safety Guide no 50-SG-S1 1979. The subject is also touched upon in the American national Standard Criteria and Guidelines for Assessing Capability for Surface Faulting at Nuclear Power Station Sites (1982) and the Draft International Standards Organisation's DIS 6258-Nuclear Power Plants-Design against seismic hazards 1983. Although the nuclear industry has been to the fore front in these matters other agencies have been drawn in.

The formal and detailed listing of criteria which label a fault as 'capable' in the USNRC sense, that is, capable of rupturing at the

surface (implicitly a co-seismic rupture) were developed with the US West Coast settings in mind and have been subject to critical appraisal since the late 70's (Minogue 1979, EPRI 1986). The limitations of the USNRC approach from a 'scientific' point of view will be considered later.

In Japan, for nuclear installations, faults are classified according to deformation rates and on this basis participate in a seismotectonic (deterministic) hazard calculation.

This lecture will not go into details as to the calculation procedures prescribed in the foregoing guides but will concentrate upon the problem of defining and identifying 'activity'.

It is instructive however to examine more closely the provisions of the various regulations in order to uncover any consistent basis for the criteria adopted.

USNRC NUREG 100 A

The full designation of this influential document is:

Title 10 Chapter 1, Code of Federal Regulations-Energy  
Reactor Site Criteria  
Part 100

The date of the text use in the following discussion is May 31 1984/

Appendix A entitled 'Seismic and Geologic Siting Criteria for Nuclear Power Plants'. It consists of six sections:

- I Purpose
- II Scope
- III Definitions
- IV Required Investigations
- V Seismic and Geologic Design Bases
- VI Application to Engineering Design

In Section III dealing with Definitions, subsections (e) to (k) appertain to faults:

(e) A 'fault' is a tectonic structure along with differential slippage of the adjacent earth materials has occurred parallel to the fracture plane, it is distinct from other types of ground disruption such as landslides, fissures and craters. A fault may have gouge or breccia between its two walls and includes any associated monoclinial flexure or other similar geologic structural feature.

(f) 'Surface faulting' is differential ground displacement at or near the surface caused directly by fault movement and is distinct from non tectonic types of ground disruptions such as landslides fissures and craters.

(g) A 'capable fault' is a fault which has exhibited one or more of the following characteristics:

- 1) Movement at or near the ground surface at least once within the past 35000 years or movement of a recurring nature with the past 500000 years.
- 2) Macro-seismicity instrumentally determined with records of sufficient precision to demonstrate a direct relationship with the fault.
- 3) A structural relationship to a capable fault according to the characteristics (1) or (2) of this paragraph such that a movement on one could reasonably be expected to be accompanied by a movement on the other.

In some cases the geologic evidence of past activity at or near the ground surface along a particular fault may be obscured at a particular site. This might occur, for example, at a site having a deep overburden. For these cases evidence may exist elsewhere along the fault from which an evaluation of its characteristics in the vicinity of the site can

reasonably be based. Such evidence shall be used in determining whether the fault is a capable fault within this definition.

Notwithstanding the foregoing paragraphs II (g) (1), (2) and (3), structural association of a fault with geologic features which are geologically old (at least pre-Quaternary) such as many of those found in the Eastern region of the United States shall, in the absence of conflicting evidence demonstrate that the fault is not capable within this definition.

(k) The 'control width' of a fault is the maximum width of the zone containing all faults which can be inferred to have experienced differential movement during Quaternary times and which join or can reasonably be inferred to join the main fault trace measured within ten miles along the fault trend in both directions from the point of nearest approach to the site (see Fig 1 of this Appendix).

Section IV of the regulations goes on to give in detail the required investigation for surface faults and calls for determination of the capability or otherwise of all faults over 1000 ft any part of which is within 5 miles of the site. A Table 1 (of Appendix A in the NUREG) gives a minimum length of fault versus distance which is to be considered for possible capability.

It calls for the listing of all historical earthquakes which can reasonably be associated with capable faults greater than 1000 ft long any part of which is within 5 miles of the site together with date of occurrence magnitude intensity and a plot of epicentral region. For such faults the epicentres are to be correlated with capable faults over 1000 ft long any part of which is within 5 miles of the site. In considering these small fault within 5 mile from the site the length, the relationship to regional tectonics, the history nature and especially Quaternary movement associated with any one earthquake has to be estimated.

Section V part b deals with the determination of the need to design for surface faulting and lays down the distances to be closely investigated as

function of the so called control width of a fault expressed as multiplier times the control width depending on the largest potential earthquake which can be associated with the fault. For a magnitude between 5,5 and 6,4 the width of zone requiring detailed fault investigation is twice the control width as described in a Figure 1 of the (NUREG) document.

Section VI treats the application to engineering design and where a power plant is to be located within the zone requiring detailed investigation and requires extensive data to justify an approach not explicitly taking surface displacement into account.

It is clear that all faults greater than 1000 ft long near the site have to be closely examined and their date of last movement established. There are however no guides as to what could be construed as a 'reasonable association' of an epicentre with a fault.

There would also appear to be room for interpretation of II g (3) in geologically old areas. The regulations are however backed up by the USNRC Standard Review Plan which calls for 'redundant methods and techniques' to be used in demonstrating non capability and emphasises that no plant has ever been built on a capable fault and that is is doubtful if one can design for surface or near surface displacement.

From the exegesis given above it is clear that the designation 'capable' refers specifically to the likelihood of ground surface rupture and although not explicitly defined it is implied that the ground movement of concern is what is generally called 'co-seismic'.

ANSI-ANS 2.7 1982 Criteria and Guidelines for Assessing Capability for Surface Faulting at Nuclear Power Plant Sites

This document is really USNRC 100A presented in the style an American National Standard. It does however give a definition : "A capable fault as used in these guidelines is one capable of surface rupture but which may or may not generate an earthquake". It then uses as its primary criteria those same ones presented in 100A.

Fault is defined as a rupture or zone of rock fracture along which there has been displacement included are growth faults, excluded are the effects of surface processes. It may be noted that a seismic displacement is now recognised.

The standard goes on to define the usage of 'may' 'should' and 'shall' according to the usual code conventions and then lists the procedures which may be followed in order to establish whether or not a fault is to be regarded as 'capable'.

Other reference to surface faults in US regulatory practice are listed by Bonilla (1982) and reproduced here as Table 1.

Draft International Standard ISO/DIS 6258 1983; Nuclear power plants design against seismic hazards.

This document presents an extensive set of definitions and those of particular relevance are as follows:

- 2.1.10 inactive fault: A fault showing no signs of recent geological movement or of significant seismic activity.
- 2.1.11 active fault: A fault presenting any proper significant seismic activity or any potential of proper seismic activity whether or not existence of recent geologic movement related to it can be proven.
- 2.1.12 capable fault (fault capable of seismic activity): A fault which has significant potential for relative displacement at or near the ground surface.
- 2.1.13 surface faulting: The cracks or off-sets on the ground surface caused by the movement of a fault at or beneath the ground surface.
- 2.1.18 earthquake prone structure: geologic structures likely to bring about earthquakes.

The French Approach-Basic Safety Regulations, Regulation No 1.2c  
(Provisional operation from October 1981)

Faults enter the French methodology as 'seismogenic accidents' defined as a 'fault resulting in one or more earth tremors'. It is recognised that such faults are rare outside active areas and the term is regarded as synonymous with the 'capable fault' of international usage. An elaborate set of diagnostics is not included in the regulations.

The Japanese Approach

In the estimate of hazard for nuclear facilities the Japanese recognise two main categories of faults; those generating the maximum design earthquake and those generating the extreme design earthquake.

The first category is further subdivided into faults with a historical record of earthquakes, Class A faults with evidence of movement in the past 10,000 years or associated event with a return period of less than 10,000 years and faults with significant microtremor activity.

The second category is divided into first faults of class A and second, faults of classes B and C having evidence of movement within the last 50,000 years or associated events with a return period of less than 50,000 years.

The classification of fault activity, following Matsuda (1975) is based on geomorphological criteria reduced to deformation rates:

Deformation rate mm/yr

Class A	1.0
Class B	0.1
Class B	0.1



### 3 CLASSIFICATION OF FAULT ACTIVITY-non regulatory sources

From the foregoing discussion it is evident that clear scientific framework is not explicit in regulatory provisions or criteria although the recognition of the concept of what may be called the Current Tectonic Regime (CTR) can be discerned in some approaches.

The general literature does contain a number of helpful classification schemes, Ambraseys and Jackson 1984 recognise faults which are; 'Active', 'Potentially Active', of 'Uncertain Activity' and 'Inactive' based upon mainly geological evidence or lack of evidence for recent movement. They properly draw attention to the need to appreciate the uncertainty of earthquake location before using seismological data to label a fault as active. The Sub-Committee on European Earthquake Geotechnical problems of the International Society of Soil Mechanics and Foundation Engineering has suggested that faults may be divided into:-

- a) Seismogenic (rare) with recent movements
- b) Only recent movements
- c) No movements in neotectonic epoch

Recently there has been increasing awareness that logic tree formulation enables subjective judgements on activity of a particular feature to be rationally handled within a probabilistic hazard model. A notable advance has been made in the EPRI NP-4726 report 'seismic Hazard Methodology for the Eastern United States (1986). In this report a 'candidate tectonic features' which may be seismic sources are pinpointed by a suite of experts having regard to a diversity of 'tectonic hypotheses' (Table 2) with the constraint that they be judged capable of sustaining a moderate to large earthquake. A tectonic feature is defined as a "large scale geologic structure or element of the earth's crust, perhaps manifested only as a geophysical anomaly". In this sense a candidate feature, for the purposes of hazard modelling, may not be a specific fault. It has to be recognised that although every earthquake is on a fault until the location and status of a potential source can be identified the expedient of a 'area' source has to be maintained. The EPRI procedure follows the

route of developing matrices (which refer specifically to eastern USA) relating to various characteristics - spatial association of the feature with seismicity, geometry of the feature relative to stress orientation and or sense of slip, date of last brittle slip movement on the feature, (see Fig 1).

From these matrices the probability that any one of them or any combination participates in a hazard model is quantified. Thereafter the appropriate seismotectonic parameters have to be selected and logic tree formulation permits a distribution of each parameter to be incorporated.

Embedded in these procedures are the judgements of experts which permit the compilation of the matrices.

#### 4 WHAT IS AN ACTIVE FAULT?

An 'active fault' is most sensibly defined as a fault which has acted as the locus of movement within the duration of the (CTR).

Geological studies from many different tectonic regions have shown that once a fault has move it tends to be the locus of continuing movement within the same tectonic regime. (Schwartz and Coppersmith, 1984). It is also revealed by the numerous individual displacements that are required to explain the offset of large faults. The phenomenon of earthquake recurrence demonstrates that a fault provides a preferred zone on which strain energy is repeatedly released. The period from one significant fault movement until its recurrence was termed by Reid (1910) the 'Seismic Cycle'.

It follows from the definition given above that the geological time-scale over which observations must be collected to prove or disprove fault activity is that over which the current tectonic regime (CTR) has been in existence.

Theoretically, the CTR can be considered as being defined by the boundary conditions of deformation existing around a given volume of crust or

lithosphere. The base of this volume can be considered to be at the level where brittle behaviour ceases, either in the lower crust or at the base of the lithosphere. Laterally, the volume should ideally span between tectonic plate boundaries. However, as a result of intraplate deformation and the fact that coherent conditions in reality do not exist throughout an individual plate, it is preferable to consider a sub-plate scale. In any case, the boundary conditions cannot be measured directly and instead the determination of the CTR must be based on the manifestations of deformation within the volume, most importantly from observations of internal stress and strain. By definition, the CTR has been in operation for as long as the current configuration of required stress and strain has existed. There is no a priori definition for this period, and it must be estimated by careful analysis of local geological and tectonic data.

One important measure of strain within a region is provided by fault movement and as the recurrence of individual fault movements (and the concept of characteristic earthquakes) suggests cyclic behaviour, implicit in any understanding of the duration of a CTR is the need to assess the period of this cycle.

The 'Average Seismic Cycle' (ASC) of many faults in a crustal province of consistent strain, is the minimum period over which observations would have to be collected to ensure that a complete pattern of earthquakes had been recorded. The duration of its individual seismic cycle defines the history over which an individual fault should strictly be studied in order to decide whether it is or is not active within the CTR. In practice however it may be necessary to use the ASC.

Thus the study of active faulting in any particular region must address a time period which is longer than the average seismic cycle (ASC) yet within the duration of the current tectonic regime (CTR). As, in general, the duration of the ASC is difficult to determine and as observations of earthquake recurrence suggest a range of earthquake return periods for the same fault, the ASC should not be relied upon to better than an order of magnitude even where its duration can be quantified. In practice, the duration of the CTR is more robust, more reliable and, particularly in intraplate areas, always to be preferred.

The 'Extinct' fault-an ideal scientific definition.

Faults that have not been active in the CTR are effectively 'extinct'.

Extinct faults were active in some previous tectonic regime, but as they are not zones of movement within the current tectonic regime, their presence is of no consequence. In the case of healed faults, their constituent mineralogy makes them mechanically continuous with the rocks they displace. Whilst they are currently frozen or immobilised this does not discount the possibility that, in some future tectonic regime, these faults could become reactivated.

There are two important circumstances in which a fault may move without precedent in the CTR. (N.B. a fault is not, until it moves, an 'active' fault). Because such circumstances undermine the philosophy of using past data to evaluate future hazard levels they must be considered:

- 1 The ASC has not not been completed within the duration of the CTR, in low strain regions where the ASC would be of extremely long duration (intraplate areas) and the plate tectonic boundary conditions could alter before the seismic cycle is complete, and in a region where there are very rapid changes in tectonics regime precluding a full development of earthquakes on individual faults.

The best demonstration that the CTR has prevailed for a period which is longer than the duration of the ASC is provided by evidence that currently active faults have experienced multiple movements within the CTR.

- 2 Internal deformation is not steady-state, but shows evolutionary properties. The simple seismic cycle model of the replication and recurrence of fault movements can only be an approximation because each fault movement changes the state of the crust. When such changes feedback sufficiently to modify the configuration of faulting, evolutionary rather than cyclical tectonics is manifest.

There is also the question of the creation of new faults. Evidence from many tectonic and experimental studies, however, suggest that deformation everywhere involves the preferential reactivation of existing crustal faults, except when the crust is suffering severe deformation, in particular around plate boundaries.

#### Problems in labelling fault as 'active'

As discussed above, an active fault can only be discriminated by evidence of movement within the CTR. Such evidence exists in two distinct forms: surface displacement and seismicity. It is important to recognise that an 'active' fault defined by movement observed from geological data is not always homologous with an 'active' fault defined by movement observed from seismological data.

#### Seismological evidence for fault activity

As any sudden episode of fault-rupture generates a seismic event, where an earthquake can be proved to have originated along a fault, that fault is deemed to be active.

However, the subsurface location of both earthquakes and faults presents great difficulties. No general formula can be proposed by which the elements of a proof of association and hence of fault activity, can be quantified. It is necessary to assess the nature of the available data.

The most important parameters to consider are:

- i) the accuracy with which the fault itself can be located.
- ii) the accuracy with which the earthquake hypocentre can be located.
- iii) the size of the rupture area (and hence the likelihood that the earthquake must have occurred along a significant fault).

- iv) the seismological evidence concerning the orientation of the causative fault and its style of movement.

The parameters are now considered in turn.

Only for a well-mapped crustal fault, of known hade, can the subsurface fault location be determined with accuracy. For many crustal faults there exists an inevitable imprecision in mapping their subsurface course, must particularly where crustal structure is complex.

The precision with which an earthquake main seismic hypocentre can be located reflects the availability of local data, and at its best is rarely better than 5.0 km.

It is, therefore, very rarely possible from macroseismic evidence alone to gain sufficient precision to confidently attribute an earthquake to a known fault.

For instrumentally determined hypocentres unknown crustal velocities prevent the accurate location of events for any circumstance except that in which the event is surrounded by nearby seismic recorders. Even with a local network, precision is ultimately dependent on the degree of heterogeneity of crustal velocities, and locational accuracies more precise than 0.5 km are probably rare. However the numerical stability and confidence in such hypocentre location is now capable of evaluation by computer programs.

As only big fault movements pass through to the surface, only the larger crustal faults outcrop and can be identified from surface observations. Most smaller earthquakes could occur on small crustal faults that do not outcrop. Clearly the larger the earthquake and the larger the rupture area, the greater the probability that the earthquake occurred on a fault known from surface outcrop.

The probability that a small earthquake originated on a known (and therefore large) crustal fault is hard to quantify. Using the assumption that the gradient of the regional earthquake recurrence relationship (the b-value) reflects the actual fractal dimension of failure surface of different sizes within the crust (King, 1983), comparative calculations can be carried out. For example, if the chance of a magnitude 6.5 earthquake occurring on a known fault is taken as unity, for a magnitude 4.5 earthquake this probability will be only 1%. Application of the statistics of line search for mineral bodies would indicate a greater probability but within the same order.

Some of the most important evidence for an association of seismic events with faults, comes from information on source orientation and location contained within the seismological data.

Thus if the orientation of one of the focal planes of a well-constrained double-couple source mechanism (requiring seismograms obtained from a good azimuthal spread of seismic instruments) corresponds with the orientation of a known fault at that location, then evidence for fault activity becomes fortified.

Furthermore if the hypocentres of many events, as in swarms or aftershocks, define a single plane, then an active fault may also be presumed even one that was not previously known.

It is very rare to gain seismological proof that a fault has produced earthquakes within the period of monitoring. The degree of 'proof' required depends on whether a rigorous proof required by a scientific argument, or whether in a hazard model, the probability of fault activity can itself be incorporated.

#### Geological evidence for fault activity

Where fault movement has passed through to the surface and can be dated as having occurred within the current tectonic regime, the geological definition of an active fault is explicit. As most

crustal faults are chiefly known from surface observations, they must, by definition, at some period have been active faults on which movements were large enough to outcrop. Therefore current activity on the same crustal fault should be reflected by continued surface displacement. Hence surface geological observations can hope to discriminate active crustal faults. However, where the surface manifestation of the underlying crustal fault movements is complex surface geological evidence must be used with care.

As only the largest fault ruptures are generally associated with surface fault displacement geological evidence for fault activity only records the largest earthquakes. This has important implications for the estimation of fault activity rates from geological data.

The time-scales for determining whether a fault is or is not active in those regions close to plate boundaries and involved in fairly rapid crustal deformation referred to in Section 2 have not been explicitly founded on a model of the ASC and the CTR. The time-scales previously employed for designating fault activity are conservative with regard to the ASC, these same time-scales have often been inappropriately exported to intraplate regions.

As described above the US NRC definition on geological grounds of a 'capable fault' focuses on one movement in the last 35,000 years or more than one in 5000,000 years. This effectively requires that the length of the ASC is in the first instance less than 35,000, and in the second less than 250,000 years. As a single movement in 500,000 years does not make a fault 'capable', in a region where the ASC is longer than 250,000 years and the CTR longer than 500,000 years a fault can be designated as 'not capable' but may still be active and therefore be able to generating a major earthquake. Therefore, away from regions of active deformation in which the ASC is shorter than 35,000 years, the US NRC definitions of fault capability are inappropriate, are not necessarily conservation as has been a common misconception.



The IAEA definition on geological grounds of fault capability requires evidence of movement in the 'late Quaternary' which implies that the ASC is probably less than  $10^5$  years. Until seismic cycles for intraplate regions are ascertained directly, such an assumption cannot be confirmed as valid.

In California the geological definition for designating a fault as 'active' has generally been chosen as movement in the Holocene. The period of 10,000 years is probably conservative for the ASC in California, but may not be appropriate for all active faults even there. In Japan the understanding of the significance of the ASC is implicit in the discrimination between faults with a return period of less than 10,000 years, and those with a return period between 10,000 and 50,000 years.

The assessment of the time period by which faults are differentiated as active or extinct should not be constrained by the limitations implicit in the duration of the historical record of earthquakes, or by the limitations implicit in some dating techniques. It is exactly such limitations that are imposed in some regulatory definitions of a 'capable' fault. Such definitions cannot be scientifically justified and this is why, in the absence of the direct measure of the duration of local seismic cycles, the definition of an extinct fault is preferably based on the whole geological time period over which the CTR has existed, so laying a burden upon geological studies.

Therefore, in studying a fault, great attention should be paid to identifying and dating the oldest geological formation which is not offset: in particular an overlying deposit, igneous intrusion, or vein material. If a fault can be shown not to have moved within the CTR it can be considered extinct as shown in Table 3.

If a fault can be shown unequivocally to have been the locus of movement within the CTR using either seismological or geological evidence then, as previously discussed, it must be regarded as active, again as shown in Table 3.

There are many faults which, for lack of evidence, cannot be proved to be definitely active or definitely extinct. Away from plate boundaries the time span of historical seismicity forms only a small fraction of the average seismic cycle and the locational imprecision of historical earthquakes almost invariably hinders any association of earthquakes with particular faults. In addition, evidence of surface fault displacements and non-intersected formations may have been obliterated by erosion.

A third category of faults is therefore required (see Table 3) in which activity remains unproven. Such a category contains faults of all descriptions ranging from those that are probably active, although such activity cannot be proven, to those that are probably, but not demonstrably, extinct.

As has already been remarked, geological and seismological evidence of fault activity are different in nature. It is necessary therefore to consider separately those types of observations (see Table 1) that affect the status of an unproven fault.

#### Seismological observations

For one or more earthquakes to be assigned to a known fault with sufficient confidence to define the fault as active the position of both the fault and the earthquakes must be known with great accuracy. Ideally there should also be agreement between the orientation of the fault and one of the two nodal planes of the focal mechanism. In practice, hypocentral locations cannot be sufficiently precise unless they are obtained from nearby instrumental records and local crustal velocities are well-constrained. In addition reliable fault place solutions required not only high quality data but also a suitable disposition of the local instrumentation.

In almost all other cases earthquake macrocentres, epicentres and hypocentres are not known with sufficient precision to define a known fault as being active. The only circumstance in which there is a strong argument for an imprecisely located earthquake having occurred on a specific known fault is when the earthquake is so large that there is no others known fault large enough.

#### Geological observations

As Table 3 shows, only geological evidence can prove a fault to be extinct. An extinct fault is one that can be shown not to have moved within the duration of the CTR or within a period which is larger than the longest such cycle if it can be ascertained.

For a fault to be proved to be active by geological data it must penetrate and displace material younger than the CTR.

For the majority of faults, which cannot be definitely categorised as active or extinct (see Table 3) some discussion is necessary of the nature of the geological evidence available for assessment within the range 'probably active' to 'probably extinct'.

A significant vertical component of fault displacement at the surface produces a fault-scarp which degrades with time. The rate of erosion is dependent on the nature of its constituent materials and the effects of the agents of erosion, including wind, rain and man. In some arid areas of western USA fault-scarps have been dated according to their state of preservation. As a result of the depredations of the Ice Age, over much of Europe and North America and the whole of Britain, any fault scarp that can be shown unequivocally to have resulted from movement and not from differential erosion is a positive demonstration of an active fault. However, the absence of a fault-scarp cannot be taken as conclusive evidence that a fault is extinct.

It is common to find that faults lie parallel to one another within a given region. Within any prevailing tectonic regime, and in particular within the CTR, where one fault is reactivated others with the same orientation may be active. Hence, if it is possible to prove that one of a set of faults is either active or extinct, then this is a strong argument that other analogous parallel faults, share a similar status.

Faults which have undergone multiple reactivation since the last major orogenic episode have demonstrated their vulnerability through geological time placing them under suspicion of being active.

Seismotectonic arguments as to whether a fault is active can be raised on the basis of the faults orientation and movement history with respect to the CTR and this is an important diagnostic in the EPRI 1986 study. In view of the uncertainties in determining the stress tensor over an appropriate volume of crust and the uncertainties in the fault constitutive relations, the most robust statement based on crustal stress is the likely low vulnerability of a strike slip fault normal to the direction of principal compression.

It will be seen from this discussion that the use of Table 3 requires judgement. The implication of this judgement with respect to hazard modelling decisions is discussed in more detail later. The ideal categories of 'active' and 'extinct' must now be understood in terms of the decisions and procedures flowing from such categorisation. Table 4 shows a system to guide decisions on whether or not to include a fault as a discrete source in a model for hazard in the UK.

#### Non-tectonic fault movement

While all displacement observed on a surface fault reflects movement along that fault, there are important implications as to the depth at which that movement was initiated. The removal of some material, whether by natural processes or through fluid or solid extraction,

can cause subsidence to become concentrated along the zone of weakness provided by the fault.

## 5 ASSESSING FAULT ACTIVITY

In order to assess either the ground rupture or the ground motion hazard it is necessary to attribute rates of seismic energy release to all significantly located faults which are in the active state. It may also be necessary to attempt to assess similar parameters for some other faults which, whilst not definitely active, cannot be proved to be extinct. The methods by which 'fault activity rates' can be assessed and the problems that exist, particularly in intraplate areas, are discussed now.

### Fault activity

The complete pattern of individual coseismic displacements along an active fault or some section of an active fault provides a recurrence relationship describing the frequency of various sizes of earthquakes. This is commonly expressed in the same form as the recurrence relation for the seismicity of a zone, viz:

$$\log N = a - bM$$

Because the underlying processes are not clearly understood (in particular the association of all events with a unique planar fault, this representation is not as confidently established for individual active faults as it is for zonal seismicity. A simple relationship of this form is however usually assumed in current seismic hazard assessment methods. The constants which have to be derived from the available geological and seismological data concerning the fault under consideration.

### Seismological versus geological data

Seismological observations, as recorded during the relatively short time periods of recent instrumental monitoring or through history,

generally can only provide the 'lower end' of the recurrence relationship. Only at some plate boundaries, where the seismic cycle may lie within the historical record, is it likely to be possible to retrieve the recurrence relationship for most magnitudes from seismicity alone.

Geological observations of active faults can only provide the 'upper end' of the magnitude recurrence relationship ie knowledge of those earthquakes large enough to have caused surface rupture.

The observational domains of geological, historical, instrumental and microseismic data are illustrated in Fig 2, a plot which shares the same axes as conventional earthquake recurrence relationships. From this plot it can be seen that seismological and geological data only overlap, and can therefore only fully define the recurrence relationship, in the case of faults with very high activity rates as at plate boundaries. For faults with very low activity rates there is no possibility of obtaining direct complete seismological evidence of recurrence rates for magnitudes below the sensitivity of geological data. In such cases, the assessment of activity rates has to be made from geological evidence alone.

#### Fault activity rates from geological data

At their simplest, geological data provide a measure of total fault displacement within a known time period which can be converted into a slip-rate - see below. Fault offsets can also sometimes indicate the size of individual displacement events but they can give no insight into b-values relevant to all sizes of earthquakes on the fault.

Studies of individual displacement events on large active faults in regions of active tectonics in Western America have revealed the phenomenon of 'characteristic earthquakes'. The existence of a 'single size' event at high magnitudes means that the magnitude frequency recurrence relationship is not linear but shows a marked change in gradient (or b-value) from estimated values around 1.0 for

low magnitudes, as retrieved from seismological data, to about 0.2-0.4 for high magnitudes (see Fig 3). This has important implications for any extrapolation of recurrence relationships.

#### Maximum magnitude

The global empirical database on fault movements in major earthquakes allows direct assessment to be made of the dimensions of faults and fault movements related to earthquake size. From such relationships the upper bound magnitude earthquake that could occur on a specific active fault of known length can be estimated.

#### Slip-rate

The cumulative displacement which has occurred on an active fault within the duration of the current tectonic regime divided by the time period over which it has occurred provides an average annual slip-rate. This slip-rate not only indicates greater or lesser scales of fault movement but can be manipulated to estimate earthquake recurrence relationships. In making this conversion it is necessary to invoke a model of earthquake generation with numerous assumptions.

The simplest assumption is that the slip-rate represents series of repeated earthquakes of the same maximum size (Slemmons, 1977). The apportionment of the total displacement between recurrences of different sized earthquakes must also reflect current understanding as to which earthquakes produce surface displacement.

An alternative method employs the concept of seismic moment. With an estimate of the rigidity of the surrounding rock and of the rupture area, it is possible to convert slip-rate to cumulative moment release rate (or seismic moment rate). A seismic moment rate can then be partitioned into a magnitude recurrence relation according to some assumed model, exponential magnitude distribution is usually used.

### Recurrence relationship

The recurrence relation derived by either of these methods is very sensitive to the maximum magnitude of earthquake taken to occur on a given active fault. Maximum magnitude must be estimated from the dimensions of the particular fault or fault segment and from the size of past displacements. Once maximum magnitude has been assigned, the choice between an exponential model and a characteristic earthquake model has important implications, in particular for the rate of occurrence of moderate magnitude earthquakes. (Schwartz and Coppersmith, 1986).

### Problems

Particular problems exist when using geological data for estimating fault activity rates in two specific cases:

- i) Where a fault is proven active on seismological grounds alone (see Table 3), with no geological indications of rate of movement, and insufficient seismological data to provide recurrence intervals.
- ii) Where a fault is proven active in geological grounds (see Table 3) by virtue of what may have been a single displacement.

In both cases, whilst the maximum earthquake can be assessed from the length of the fault there is no possibility of directly calculating a slip-rate. However upper bounds for this slip-rate may be estimated from such information as the average slip-rate of faults within the CTR or from the absence of indicators which would be available had a particular slip-rate been exceeded.

### The problem of active faults with low activity rates

Fig 4 shows idealised linear recurrence relationships for a set of individual active fault superimposed against the observational



domains appearing on Fig 2. The individual lines represent active faults with slip-rates which vary by orders of magnitude. Each fault has been pegged to the same single value of upper bound (or characteristic) magnitude and has an assumed simple single b-value equal to 1.0.

Fig 4 demonstrates that, within intraplate area where the recurrence interval of major earthquakes on individual active faults is very long, direct seismological observations of even low magnitude earthquake recurrence may form such a small dataset that no simple seismic recurrence pattern can be retrieved. At best, seismological data may only provide minimum rates of seismic activity that faults have not exceeded. Thus commonly there is not direct way of deriving the b-value of the fault. Therefore, a b-value has to be imported, either from other well-studied active faults in the same region or from better established fault b-values obtained in areas of high seismicity.

Fig 4 also shows that, while the period of recorded seismicity may be too short to provide useful information on earthquake recurrence relationships for individual faults, geological evidence can provide important information on high magnitude recurrence relationships even for a fault with a low activity rate. However, in comparison with faults subject to more rapid deformation, problems arise with the survival of evidence for long-term fault movements. Excepting in extensional regimes, in which sedimentation accompanies fault movement, evidence likely to be destroyed in a long seismic cycle environment.

Where such evidence has survived, it may prove possible to find instance of repeated fault displacement with which to prove or disprove a characteristic earthquake recurrence relationship. For a fault of prolonged seismic cycle, questions as to whether a recurrence relationship is exponential or involves characteristic earthquakes, may be critical as moderate magnitude earthquakes may form a most important component of the short-term hazard.

#### Activity rates for unproven faults

In such cases, if none of the methods described above can be used to elucidate an activity rate, there is no alternative but to estimate activity rates by analogy with other faults in the region.

For small surface faults representing secondary deformation relating to major crustal faults, while there is generally no reason to consider them as seismic sources in their own right, estimates of potential 'activity' rate, may be needed in considering the ground rupture hazard. Secondary faults move as the result of movement on neighbouring crustal faults. The probability of their displacement therefore cannot be more than the probability of a major earthquake involving ground rupture along the neighbouring crustal fault. The connections to the crustal fault and the past pattern of interrelated movements must be recognised in determining the 'linkage factor', i.e. the probability that a major earthquake on the crustal fault will produce displacements on the secondary or sympathetic fault.

#### Conclusion

Calculating activity rates for faults in the intraplate environment presents many problems because of the paucity of relevant data. Commonly the recurrence relationship can only be considered as lying within a possible range, bounded only by some upper and lower values, as defined from available seismological and geological constraints.

For the majority of faults, whose state remains unproven, the uncertainty inherent in the recurrence relationship means that their contribution to ground motion hazard is most appropriately accommodated within a volume seismic source model. Activity rates for such faults only become critical for those passing through or close to the site of interest, in particular because of their possible implications for the ground hazard rupture hazard.

## 5 DATING OF FAULTS

The dating of last movement of a fault becomes a critical item in the classification procedure and a dated history of coseismic fault movement becomes a valuable source of information from which to estimate the fault activity rate. Both absolute and relative dating methods have their place. There have been considerable advances in the techniques (especially in direct dating of fault rocks and gauges themselves) available. In Table 4 the methods in current use, together with a number at a very early stage of development are listed.

Only very recently have direct methods of dating been applied to fault rocks themselves. Electrom Spin Resonance dating of the quartz veins formed in association with faulting has been used by Fukuchi et al 1986, and tested on both faulted and sedimentary rocks in the Western USA. Thermoluminescence (McKeever 1985) is promising technique which is being used to date sediments and may have application in the dating of syntectonic vein material. Attempts to date fault gauge using Rubidium/Strontium and Potassium/Argon methods are currently underway.

The general dating of Quaternary sediments is receiving much attention and many contracts are being let by the USGS in this field (USGS Open File Report 87-23).

A note also be made of the rapid advances in satellite geodesy (Geosatellite Positioning Systems, (GPS) which may soon become exploitable by engineering seismologists.

## 6 INCLUDING FAULTS IN A MODEL

### Decisions from Table 4

Just as the EPRI matrices are expressed in terms of a probability, it is possible to develop a provisional weighting procedure for Table 4. The questions implicit in the statement within the 'unproven' category are of a different nature. Questions i to v if answered in the affirmative

would tend towards labelling a fault as 'extinct' but questions vi to ix if so answered would tend towards labelling the fault as 'active'. Furthermore there are combinations of answers which are impossible and others which necessarily equivalent to a 'proven' category. It should also be noted that no other combination of the unproven category may constitute an equivalence to the two defined 'proven' categories of Table 4.

Staying within these constraints a preliminary weighting system has been devised which enables a probability to be assigned to all combinations of questions iii to viii (Figs). Such procedures have to be 'calibrated' against expert opinion for the region under consideration.

#### Faults and area sources

The inclusion of fault sources within hazard models together with area sources has been common commercial practice for some time (McGuire 1978) and now programmes are available which enable this to be done in a Bayesian logic tree formulation (Mortgat and Shah 1974, Kulkarni et al 1984, PML 1985). Clearly as more activity can be allocated to specific faults it has to be transferred from the 'area' sources and the 'background'. This may be done crudely where a fault is of low activity even though its 'b' value may not match that of the other sources. Problems arise where significant activity can be ascribed to the fault with a typically lower 'b' value.

### 7 CONCLUSIONS

In stipulating that active faults be identified and avoided draft EC8 is imposing a formidable task on the geologists and seismologists who must advise the competent national authorities. The experience of those who have undertaken the same task for nuclear facilities, gas storage, dams and reservoirs must be cautiously exploited. Each site study may involve a number of man years with the main effort being concentrated on a relatively small area. It is crucial that an agreed set of definitions be established and that a procedure for decision making in the probably dominant 'unproven' category be agreed upon in the varied seismotectonic climate of Europe.

#### ACKNOWLEDGEMENT

Much of the work upon which the lecture is based has been undertaken by the Seismic Hazard Working Party (SHWP) of the CEEB and in particular by the lecturer's colleagues on the SHWP; D J Mallard, I E Higginbottom, R Muir-Wood, W Aspinall, G Woo and D Papastamatiou. The views expressed are not necessarily those of the SHWP or the CEEB.

#### REFERENCES

- AMBRASEYS N N, J JACKSON : 1984 : Engineering Seismology in Ground Movements. ed P Attwell, R Taylor. Surrey University Press.
- AMERICAN NATIONAL STANDARDS : 1982 : Criteria and Guidance for Assessing Feasibility of Surface Faulting at Nuclear Power Plants. ANSI/ANS 2.7. 1982.
- BONILLA M G : 1982 : Evaluation of potential surface faulting and other tectonic deformations USGS OF 820732.
- CENTRAL DEPARTMENT OF SAFETY OF NUCLEAR INSTALLATIONS : 1981 : Basic Safety Regulations, Regulation No 1.2c. (Provisional operation Oct 1981). Ministry of Industry, Industrial Quality and Safety Division. French Republic.
- EPRI : 1986 : 'Seismic hazard methodology for the Central and Eastern United States, EPRI.NP.4726 Vol 1-3.
- FUKUCHI T, M IMAI AND K SHIMOKAWA : 1986 : ESR dating of fault movement using various defects in quartz; the case in Western Fossu Magna, Japan. Earth Planet Sci Lett., 78, 121-128.
- INTERNATIONAL ASSOCIATION OF EARTHQUAKE ENGINEERING : 1984 : Earthquake Resistant Regulations. A World List - 1984, Tokyo, July 1984.
- INTERNATIONAL ATOMIC ENERGY AGENCY : 1979 : Earthquake and associated topics in relation to nuclear power plant siting. IAEA Safety Series, Guide No 50-54-51, 1979.
- INTERNATIONAL STANDARDS ORGANISATION : 1983: Draft International Standard ISO/DIS 6258. Nuclear power plant - design against seismic hazards. ISO 1983.
- KING G : 1983 : The accumulation of large strains in the upper lithosphere of the Earth and other solids by self similar fault systems : the geometric origin of b-value. Page oph Vol 121, 761-815.

- KULKARNI R B, R R YOUNG and K J COPPERSMITH : 1984 : Assessment of confidence intervals for result of seismic hazard analysis, Proc 8th WCEE, San Francisco, 1.1, pp 203-270.
- MCGUIRE R K : 1978 : Computer programme for seismic risk analysis using faults as earthquake sources. US Dept of the International, Geological Survey, Open File Report pp 78-1007, 1978.
- MCKEEVER S W S : 1985 : Thermoluminescence of Solids Cambridge Solid State Science Series 1985.
- MATSUDA T : Magnitude and recurrence interval of earthquakes from a fault (in Japanese), Zisin, Journal of the Seismological Society of Japan, 28,3, pp 269-283.
- MEEHAN, R L : 1984 : The Atom and the Fault, MIT p 161.
- MINOGUE R B : 1979 : Identification of issues pertaining to seismic and geologic siting regulation policy, and practice for nuclear power plant. Information Report SECY-79-300 USNRC.
- MORTGAT C P and H C Shah : 1987 : A Bayesian model for seismic hazard mapping, BSSA 69, 4, pp 1237-1251.
- PRINCIPIA MECHANICA LIMITED : 1985 : 'PRISK Manual, Report prepared for CEB.
- REID, H F : 1910 : The mechanics of the earthquake, the California Earthquake of April 18 1906. Report of the State Investigates Commission, Vol 2, Carnegie Inst of Washington, Washington DC.
- SLEMMONS D B : 1977 : State of the art for assessing earthquake hazards in the United States, Report 6, Faults and earthquake magnitude. US Corps of Engineers, Waterways Experiment Station, Misc Paper 8-73-1, p 129.
- SCHWARTZ D P and K J COPPERSMITH : 1984 : Fault behaviour and characteristic earthquakes : examples from the Wasatch and San Andreas Faults, Journal Geophys Res. 89, pp 5681-5698.
- UNITED STATES REGULATORY COMMISSION : 1984 : Code of Federal Regulations Reactor Site Criteria, NUREG Part 100, 31 May 1984.
- UTSU T : 1965 : Quoted in ALCI (1965) maximum likelihood estimate of b in the formula  $\log N=a-bM$  and its confidence limits. Bull ERI 43, pp 237-239.

# Current Guidelines and Criteria for Assessment of Faults

Agency	Facility	Fault Terminology	Activity Criteria	Remarks	Reference
Nuclear Regulatory Commission	Nuclear power plants.	Capable fault.	1. Movement at least once in past 35,000 yr, or 2. Recurring movement in past 500,000 yr, or 3. Macroseismicity, or 4. Structural relation to another capable fault.	Specific guidance on assessment.	U.S. Atomic Energy Commission, 1973; U.S. Nuclear Regulatory Commission, 1975a, 1978a, 1978b.
Corps of Engineers	Dams	Capable fault	1, 3, and 4 as above. Macroseismicity is magnitude 3.5 or greater.	General guidance on assessment. Refers to 1974 state-of-the-art paper.	U.S. Department of the Army, 1977.
Department of Transportation	LNG (liquefied natural gas facilities)	Surface faulting	Storage facility cannot be located at a site, unless specifically approved, if a) surface faulting can be predicted but displacement not exceeding 30 inches cannot be assured, or b) future surface displacement cannot be predicted but cumulative displacement of a Quaternary fault within one mile of the tank exceeds 60 inches.	General guidance on assessment.	U.S. Department of Transportation, 1980.
Veterans Administration	Hospitals	Active fault	Movement in past 10,000 yr.	General guidance on assessment. Interim requirements	U.S. Veterans Administration, 1973.
Environmental Protection Agency	Hazardous waste facilities	Holocene fault	Displacement in Holocene time	Specific guidance on assessment.	U.S. Environmental Protection Agency, 1981.
State of California	Structures for human occupancy	Active fault	Surface displacement in Holocene time	Specific guidance on assessment.	Alquist-Priolo Special Studies Zones Act of 1972 (Hart, 1980).

from Bonilla, 1982

TABLE 2

TECTONIC "HYPOTHESES" CONSIDERED INITIALLY  
TO DEFINE DATA NEEDS

Reactivation of Failed Rifts  
Isostasy  
Reactivation of Decollement  
Reactivation of Mesozoic Rifts  
Epeirogenic Structures  
Deep-Seated Structural Boundaries  
Onshore Extensions of Oceanic Fracture Zones  
Block Tectonics  
Intrusives  
Thermal Expansion/Contraction  
Structural Intersections  
Induced Seismicity  
Growth Faults  
Eastern Piedmont Ductile Shear Zones  
Cenozoic Reverse Faults  
Areas of Intensive Jointing/Fracturing  
Initiation of New Faults  
Random  
Unknown

From EPRI 1986



TABLE 3

STATE	EVIDENCE
EXTINCT	(i) FAULT DOES NOT DISPLACE MATERIALS OR STRUCTURES PREDATING THE CURRENT TECTONIC REGIME
	(ii) FAULT DOES NOT DISPLACE MATERIAL OF AGE GREATER THAN THE LENGTH OF THE LONGEST 'SEISMIC CYCLE' OF FAULTS WITHIN THE REGION
	(iii) THE MINERALOGY OF <u>MECHANICALLY CONTINUOUS</u> FAULT GOUGE IS INCOMPATIBLE WITH THE CURRENT STRESS/TEMPERATURE REGIME
(UNPROVEN)	(iv) FAULT IS A SMALL SECONDARY FRACTURE
	(v) FAULT DOES NOT DISPLACE MATERIALS OR STRUCTURES YOUNGER THAN THE 'AVERAGE SEISMIC CYCLE'
	(vi) FAULT STYLE AND ORIENTATION MAKES DISPLACEMENT UNLIKELY IN CURRENT TECTONIC REGIME
	(vii) FAULT SHOWS APPARENT GEOGRAPHICAL ASSOCIATION WITH UNCERTAINLY LOCATED EARTHQUAKE
	(viii) FAULT HAS BEEN ACTIVE UNDER A VARIETY OF DIFFERENT TECTONIC REGIMES
	(ix) FAULT HAS A CLOSE ANALOGUE PROVED ACTIVE
ACTIVE	(x) FAULT HAS APPROPRIATE DIMENSIONS AND IS UNIQUELY IMPLICATED BY A WELL-LOCATED LARGE EARTHQUAKE(S)
	(xi) FAULT IS THE LOCUS OF WELL-CONSTRAINED EARTHQUAKE HYPOCENTRE(S)
	(xii) FAULT DISPLACES MATERIAL YOUNGER THAN THE DURATION OF THE CURRENT TECTONIC REGIME

CRITERIA FOR ACTIVE FAULTING

TABLE 4

STATE	EVIDENCE	DECISION
EXTINCT	(i) FAULT DOES NOT DISPLACE PRE-PLIO-QUATERNARY MATERIALS OR STRUCTURES	NO
	(ii) THE MINERALOGY OF <u>MECHANICALLY CONTINUOUS</u> FAULT GOUGE IS INCOMPATIBLE WITH THE CURRENT STRESS/TEMPERATURE REGIME	NO
(UNPROVEN)	(iii) FAULT IS A SMALL SECONDARY FRACTURE	NO
	(iv) FAULT DOES NOT DISPLACE LATE QUATERNARY MATERIALS OR STRUCTURES	NO
	(v) FAULT STYLE AND ORIENTATION MAKES DISPLACEMENT UNLIKELY IN CURRENT TECTONIC REGIME	NO
	(vi) FAULT SHOWS GEOGRAPHICAL ASSOCIATION WITH SMALL MACROSEISMIC EARTHQUAKE OR INSTRUMENTAL EARTHQUAKE LOCATED BY REGIONAL NETWORK	NO UNLESS THE FAULT IS THE UNIQUE CANDIDATE AT THE APPROPRIATE DEPTH
	(vii) FAULT HAS UNDERGONE MULTIPLE POST-VARISCAN REACTIVATION	YES/NO DEPENDING ON LOCAL DETAILS
	(viii) FAULT HAS A CLOSE ANALOGUE PROVED ACTIVE	YES/NO DEPENDING ON LOCAL DETAILS
ACTIVE	(ix) FAULT HAS APPROPRIATE DIMENSIONS AND IS UNIQUELY IMPLICATED BY A WELL-LOCATED LARGE EARTHQUAKE(S)	YES
	(x) FAULT COINCIDES WITH ACCURATELY LOCATED HYPOCENTRE(S) FROM LOCAL NETWORK AND IS CONSISTENT WITH PARAMETERS FROM WELL-CONSTRAINED FOCAL MECHANISM(S)	YES
	(xi) FAULT DISPLACES GROUND SURFACE OR LATE QUATERNARY DEPOSITS AND/OR STRUCTURES	YES

N.B. These are theoretical decisions. Whether or not a fault is actually modelled depends on its location with respect to the site of interest (see text).

TABLE 5

GEOCHRONOLOGICAL TECHNIQUES after Colman and Pierce 1979TABLE

<u>METHOD</u>	<u>APL</u>	<u>OPT. RES</u>	<u>BASIS OF METHOD</u>
		$10^2 10^3 10^4 10^5 10^6$	
Historical	1-3*****		Preserved records, oral
Dendro- chronology	2 *****		Old trees and environment sensitivity preserved. Earth quake stress may be observed
Varves <sup>Ⓢ</sup>	1 *****		Direct counting and overlap
Carbon 14 <sup>Ⓢ</sup>	1-3 *****		Needs non contaminated carbon. Quantulus (β) requires gms, tandem mass accelerator (TAMS) requires sub-milligrams.
Uranium series <sup>Ⓢ2</sup>	..*****		Corals, molluscs, bone carbon. High precision mass spectrometry permits small samples and error 10% of radiocarbon dating. Errors due to lack of closed system. #.
Potassium <sup>Ⓢ</sup> Argon	1 *****		Requires K bearing feldspars, error due to loss of argon or excess or contamination
Fission track <sup>Ⓢ</sup> 2.....	*****		Intense damage when fission fragment passes through non opaque minerals such as apatite and zircon. Track stable <50 #
Uranium trend	4.....*****		Based on open system migration of daughter products in calibrates system ( <sup>234</sup> U, <sup>230</sup> Th )
Thermo luminescence <sup>Ⓢ</sup>	4 .....*****		Based on displacement of electrons

TABLE 5 contd.

			by $\alpha, \beta, \gamma$ . Clock set by exposure to light of feldspars, quartz carbonate	#
Electron spin@ 2	.....*****		Electrons trapped at defect site in quartz give signal in electron spin resonance spectrum (ESR). Zero set by cataclasis.	#
Cosmogenic isotopes@	1 ? ? ? ? ?		Analogous to $^{14}\text{C}$ dating with atmospheric isotopes. eg $^{10}\text{Be}$ , $^{26}\text{Al}$ . Accelerator mass spectrometry (AMS) needed to measure very small ratios relative to their stable isotopes. Observation of slow migration in soils eg penetration of meteoric water in gouges.	#
Amino acid@	2 .....***** 4		Based on L-D conversion of protein amino acids after death of organism. Relative dating (aminostratigraphy) Requires shells or skeletal material.	
Obsidian hydration	1*****		Hydrated layer on crack or surface formed at event.	
Tephra	1 .....		Progressive filling of bubbles in ash	
Lichenometry	1-3****		Stable rock surface for lichen growth needed. Errors due to climate differences	
Pedogenesis@	4.....*****		Development of soil properties with time Best when all other agents constant.	
Rock weathering	2 ...*****		Thickness of weathering rinds. Sonic velocity methods being developed. Precision varies with feature being studied. Useful in humid to sub humid conditions.	
Rock varnish	1.....		Calibrated ratio of minor cations in varnish [(K+Ca)/T <sub>1</sub> ] Best in arid and semi arid environments	

TABLE 5 contd.

Landform	3.....	Depends on climate and lithology. Includes degradation rates for fault scarps. Limited in glaciated regions.
Deposition	2 .....	Depends on calibration. Variable.
Geomorphology Incision rate	3 .....	Assumes rate of deformation constant needs calibration.
Deformation <sup>⊗</sup>	2.....	Fabric analysis, fluid inclusions palaeothermometry, inference on depth of burial and subsequent exhumation. Calcite twinning, quartz clarity.

Key : \* Optimal range within about 10%

1, 2, 3, 4 - seldom applicable to nearly always applicable.

⊗ - possible use in UK

# - possible use in direct dating of gouge

Brittle Slip on a Feature (Most recent age)	Special Association with Seismicity						FIG 1
	Moderate-to-Large Earthquakes		Small Earthquakes Only		No Seismicity		
	Geometry Relative to Stress/Sense of Slip						
	Favorable	Unfavorable	Favorable	Unfavorable	Favorable	Unfavorable	
Pleistocene Holocene Slip	1.0	0.9	0.8	0.7	0.5	0.4	
Cretaceous- Tertiary Slip	0.7	0.5	0.5	0.3	0.2	0.1	
Pre-Cretaceous Slip or No Brittle Slip	0.4	0.3	0.1	0.05	0	0	

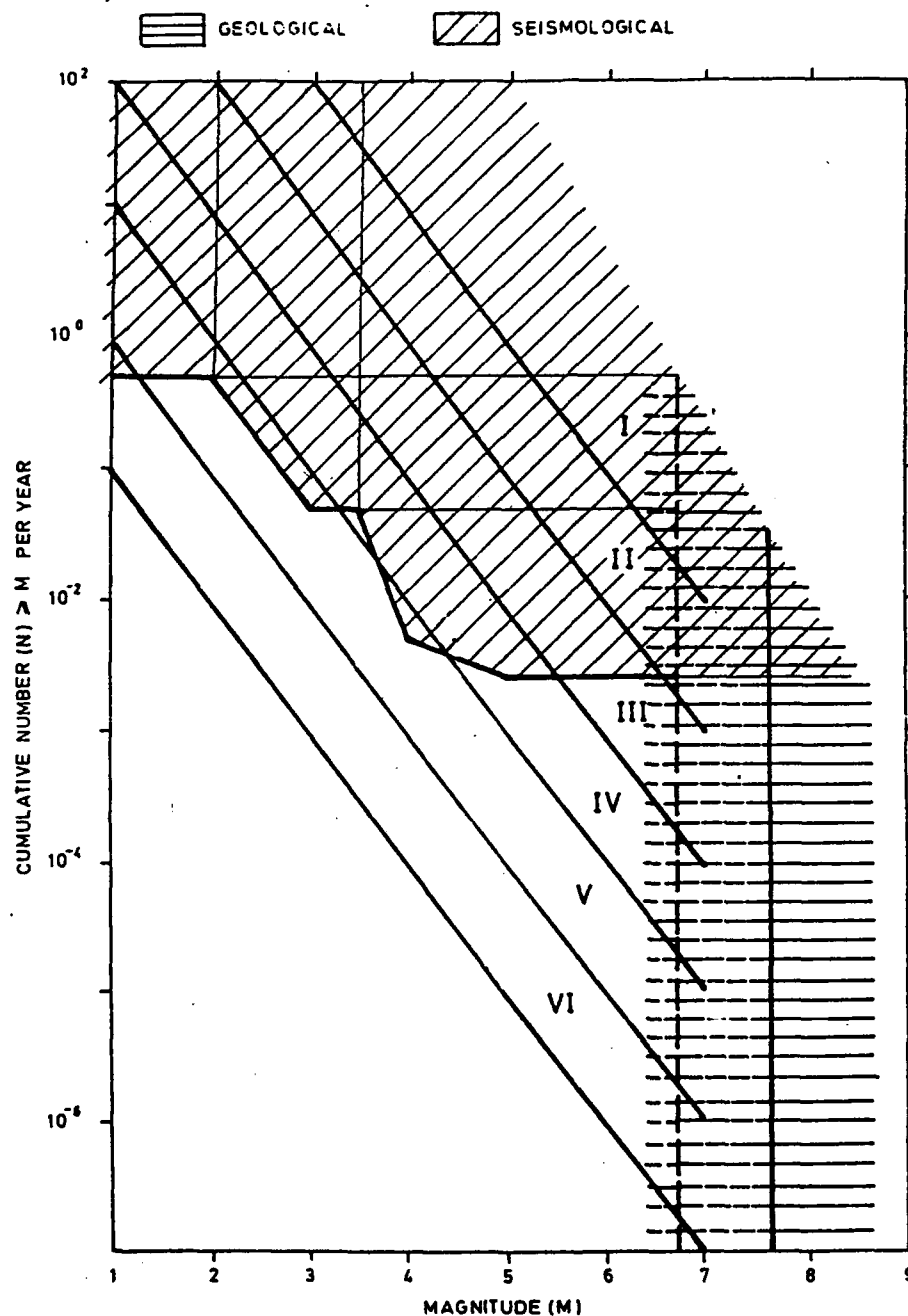
Geometry Relative to Stress/Sense of Slip	Spatial Association with Seismicity		
	Moderate-to-Large Earthquakes	Small Earthquakes Only	No Seismicity
Favorable	1.0	0.5	0.1
Unfavorable	0.8	0.3	0

Matrix of physical characteristics for example evaluation.

Physical Characteristic	Probability that the Given Feature Exhibits a Given Level of Each Characteristic		
	Feature #A	Feature #B	Feature #C
1. Spatial association with seismicity			
1. Moderate-to-large earthquakes	0.3	0.1	0.2
2. Small earthquakes only	0.2	0.5	0.1
3. No seismicity	0.5	0.4	0.7
	$\Sigma = 1.0$	1.0	1.0
2. Geometry of feature relative to stress orientation and/or sense of slip			
1. Favorable geometry/sense of slip	0.3	0.3	0.1
2. Unfavorable geometry/sense of slip	0.7	0.7	0.9
	$\Sigma = 1.0$	1.0	1.0
3. Brittle slip on a feature			
1. Pleistocene-Holocene slip	0	—	0.1
2. Cretaceous-Tertiary slip	0.1	—	0.9
3. Pre-Cretaceous slip or no brittle slip	0.9	—	0
	$\Sigma = 1.0$	—	1.0

Example feature characteristics assessment.

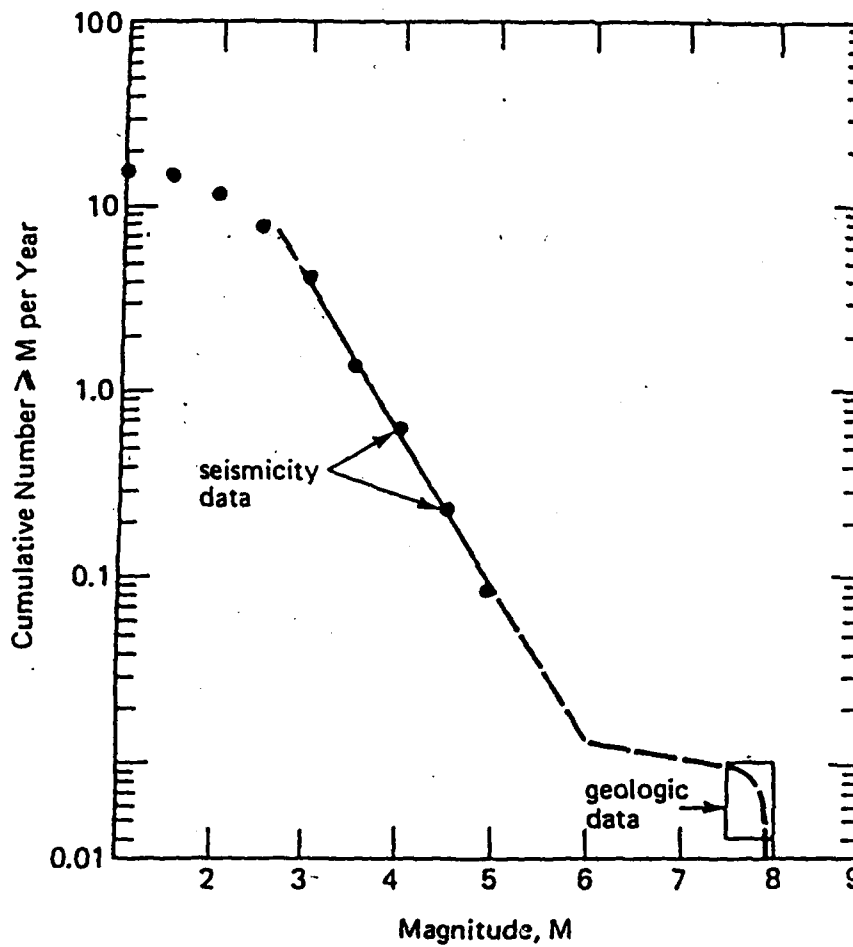
FIG 2



FAULT ACTIVITY RELATED TO OBSERVATIONAL DOMAINS

- |     |                               |                  |
|-----|-------------------------------|------------------|
| I   | = - $5 \times 10^1$ mm / YEAR | } PLATE BOUNDARY |
| II  | = - $5 \times 10^0$ mm / YEAR |                  |
| III | = - $5 \times 10^1$ mm / YEAR | } HIGH ACTIVITY  |
| IV  | = - $5 \times 10^2$ mm / YEAR |                  |
| V   | = - $5 \times 10^3$ mm / YEAR | } LOW ACTIVITY   |
| VI  | = - $5 \times 10^4$ mm / YEAR |                  |
|     |                               | } INTRAPLATE     |

FIG 3

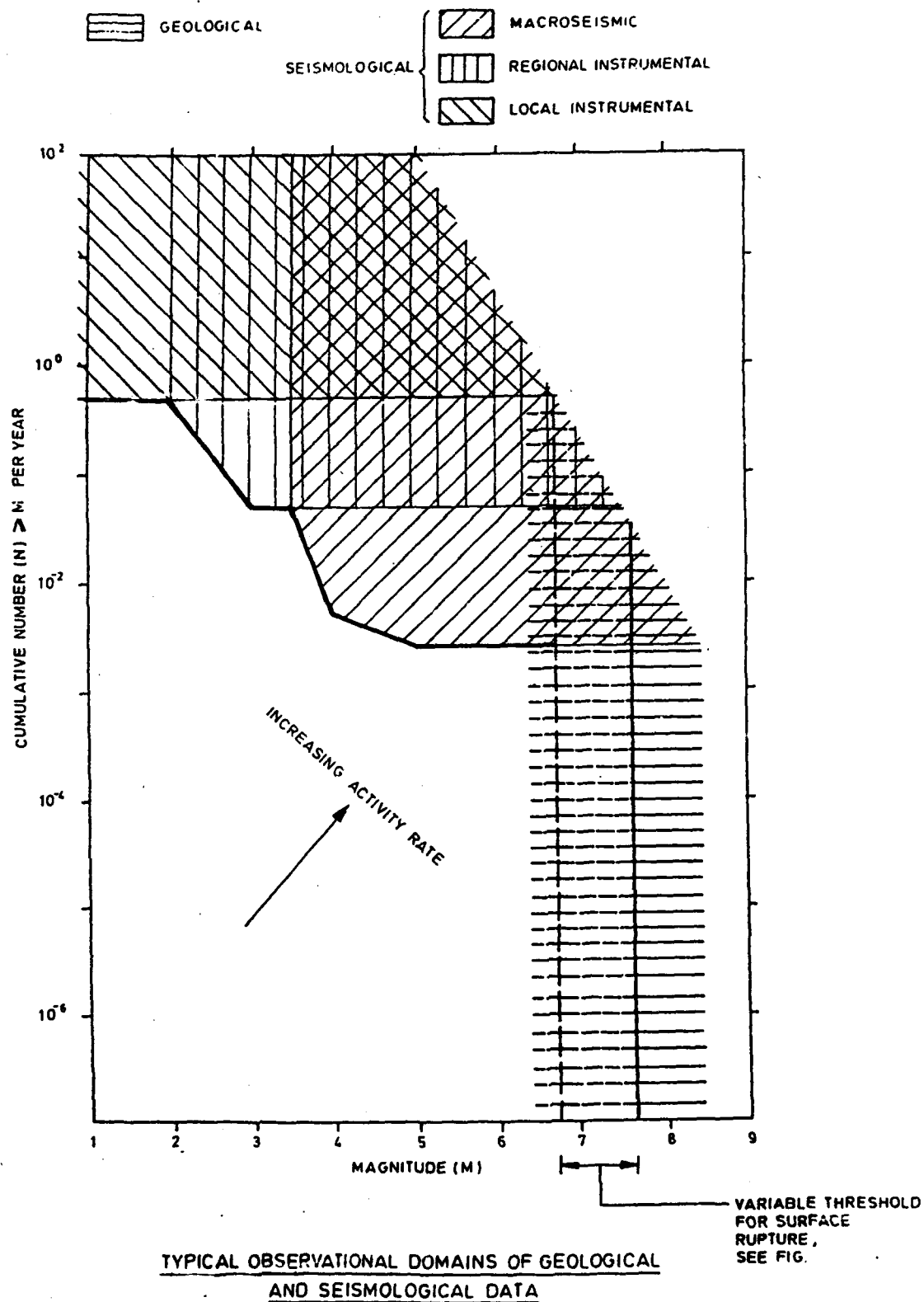


DIAGRAMMATIC CUMULATIVE FREQUENCY-  
MAGNITUDE RECURRENCE RELATIONSHIP  
FOR AN INDIVIDUAL FAULT OR FAULT SEGMENT

(FROM SCHWARTZ AND COPPERSMITH, 1984)



FIG 4

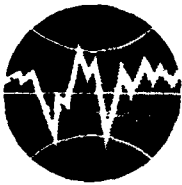


N.B. THERE WILL BE REGIONAL VARIATIONS IN LENGTH AND SENSITIVITY OF THE SEISMOLOGICAL RECORD AND IN THE SURVIVAL OF THE GEOLOGICAL RECORD

- 3 : Fault is a small secondary feature
- 4 : Fault does not displace late Quaternary materials or structures
- 5 : Fault style and orientation makes displacement unlikely in current tectonic regime
- 6 : Fault shows morphological association with small accretionistic earthquakes or instrumental earthquakes located by regional network
- 7 : Fault has undergone multiple post-Variscan reactivation
- 8 : Fault has a close analogue proved active

SCORES 1	QUEST.OM	YES	?	NO	PROBABILITIES 1	SCORE	PROBABILITY
2	20	0.0	0.0	1.0	-50.0	10X	
3	20	0.0	0.0	0.0	-6.0	10X	
4	10	1.0	0.0	1.0	0.0	50X	
5	20	0.0	0.0	0.0	11.0	90X	
7	20	0.0	0.0	0.0	50.0	90X	

[illegible]



**TURKISH NATIONAL COMMITTEE FOR  
EARTHQUAKE ENGINEERING**

**THIRTEENTH REGIONAL SEMINAR ON EARTQUAKE ENGINEERING**

**September 14-24, 1987 - Istanbul - Turkey**

**EARTHQUAKE RESPONSE SPECTRAL ANALYSIS OF  
FRANKLIN FALLS DAM, NEW HAMPSHIRE**

**by**

**Frank K. Chang\***

**Lecture Notes**  
**for**  
**The 13th Regional Seminar on Earthquake Engineering**  
**1987**

**EARTHQUAKE RESPONSE SPECTRAL ANALYSIS OF  
FRANKLIN FALLS DAM, NEW HAMPSHIRE**

**by**  
**Frank K. Chang**

**US Army Engineer Waterways Experiment Station  
Vicksburg, Mississippi  
U.S.A.**

# EARTHQUAKE RESPONSE SPECTRAL ANALYSIS OF FRANKLIN FALLS DAM, NEW HAMPSHIRE

by

Frank K. Chang\*

## ABSTRACT

During the New Hampshire earthquake of 18 January 1982 ( $M = 4.7$ ) which occurred at latitude  $43.5^\circ$  N, longitude  $71.6^\circ$  W, three records were obtained on crest, abutment, and downstream sites at the Franklin Falls Dam about 8 km from the epicenter. The transverse component of the accelerograph located on the right abutment recorded a peak acceleration of 0.55 g, which is the highest acceleration ever recorded in the eastern United States. The purposes of this report were to study the seismic response of the dam as shown by response spectra on crest, abutment, and downstream sites; and to determine the natural periods of foundation and dam from the amplitude ratios (amplification factor) of the response spectra.

## INTRODUCTION

At 19:14:42 EST on 18 January 1982 or 00:13:42 UT on 19 January 1982, an earthquake of Richter magnitude 4.7 occurred at latitude  $43.5^\circ$  N, longitude  $71.6^\circ$  W in New Hampshire. The focal depth was estimated to be between 4.5 and 8.0 km by the Weston Observatory and US Geological Survey, respectively. A typical comment by people at Laconia, Franklin, and Tilton Northfield areas was, "The whole building shook and rumbled." The earthquake was felt in most of New England and parts of New York for about 20 seconds during the night. The Franklin Falls Dam (Fig. 1) is at a distance of 8 km from the epicenter.

A total of 36 accelerograms were recorded at five Corps of Engineers (CE) dams: Franklin Falls Dam (FFD, epicentral distance, 8 km), Union Village Dam (UVD, e.d., 60 km), North Hartland Dam (NHD, e.d., 61 km), North Springfield Dam (NSD, e.d., 76 km), Ball Mountain Dam (BMD, e.d., 103 km); and at the White River Junction (WRJ, e.d., 60 km), Veterans Administration (VA) Hospital. However, the accelerographs at Townsend Dam, Surry Dam, and at the Manchester VA Hospital were not triggered. The locations of these sites and the epicenter are shown in Fig. 2.

\* Research Geophysicist, Geotechnical Laboratory, US Army Engineer Waterways Experiment Station, P.O. Box 631, Vicksburg, Mississippi 39180-0631

## PURPOSE

An earlier report by Chang (1983) discusses the corrections of baseline and instrument for the 36 accelerograms, the integration of particle velocity and displacement, the analysis of maximum acceleration, velocity, displacement, and spectrum intensity, and the study of the attenuation rate of these four parameters with distance for various site conditions. The purpose of this report is to analyze the observed spectral response at crest, right abutment, and free field downstream of the Franklin Falls Dam.

## DESCRIPTION AND GEOLOGICAL ENVIRONMENT OF THE FRANKLIN FALLS DAM

The Franklin Falls Dam, located about 4 kilometers north of Franklin, New Hampshire, is one of the flood control reservoirs for the Merrimack River Basin. The dam is of rolled earth fill with dumped rock shell and toe, 1,740 feet (530 m) long, with a maximum height of 136 feet (41.45 m) and containing about 3,300,000 cubic yards of earth and rock fill. A 550-foot (168 m) spillway and 732 square feet ( $68 \text{ m}^2$ ) of gate-controlled outlet conduits involving 95,000 cubic yards or 72,600 cubic meters of concrete were constructed in open cut rock.

At the Franklin Falls Dam site, the Pemigewasset Valley has a flat bottom U-shaped cross-section lying entirely on glacial deposits. The right abutment of the bedrock is a solid, unweathered rock varying between micaceous gneiss and granular mica schist, with numerous but minor veins of coarse granite. The left abutment is a steep overburden slope rising more than 150 feet (45 m) at an angle of 34 degrees.

## THE ACCELEROGRAMS

Nine accelerograms were recorded on three accelerographs at downstream field, right abutment, and crest sites of the Franklin Falls Dam. The uncorrected and corrected strong-motion parameters of Franklin Falls Dam are listed in Table 1. After the instrument and baseline corrections, the nine corrected accelerograms were integrated to obtain velocity and displacement records (Fig. 3 - Fig. 5). Next, the absolute acceleration response spectrum, relative velocity response spectrum and relative displacement spectrum for each component were calculated and plotted (Fig. 6 - 14).

## CHARACTERISTICS OF RESPONSE SPECTRA

### Absolute Acceleration Response Spectrum

Figures 6a to 14a show that the highest peak spectral acceleration is always in the frequency range ( $\geq 10 \text{ Hz}$ ) of compression (P) waves; the secondary of peak amplitudes is in shear (S) waves

( $2 \text{ Hz} < f < 10 \text{ Hz}$ ). The surface (R or L) waves ( $f < 2 \text{ Hz}$ ) appear as very small peak amplitudes, often not easily recognized. The spectral amplitude approaches zero as the period increases.

#### Relative Spectrum Response Velocity

As in the case of absolute acceleration response, the compression waves usually show the highest spectral amplitudes, though the shear waves contain more energy (Fig. 6b to 14b). However, when the resonant period of the S-wave appears, the amplitudes of compression and other waves will be comparatively reduced, as demonstrated in the longitudinal component (L) of the downstream station (Fig. 12b to 14b), where the shear wave resonant period of 0.4 sec (2.5 Hz) becomes the largest amplitude on the relative velocity response spectrum. The 0.4 sec period is the natural period of the alluvial deposit at the toe or foundation of the Franklin Falls Dam. This resonant period of 0.4 sec appears again on the L-component of the crest recording station (Fig. 9b). It is noted that the amplification factor of the L-component of the accelerograph on the crest caused by the height of dam is less than or equal to one (Table 1). The amplitude of the relative response velocity approaches the base velocity (peak ground velocity) at period between 1 and 4 sec (Fig. 6b - 14b).

#### Relative Spectrum Response Displacement

The surface waves or the long period waves (Love and Rayleigh waves) are the dominant waves in the relative displacement response spectrum (Fig. 6c - 14c). When the resonant period appears in the shear waves, the displacement amplitudes of compression and other higher mode shear waves are reduced rapidly, as demonstrated in the L- and T-components of the downstream station or 2.5 Hz on L-component (Fig. 12c), and 2.2 Hz on T-component (Fig. 14c), respectively. However, the response surface waves of the large periods in the displacement spectrum contain more energy than the shear and compression waves. The compression waves are almost nonexistent in the displacement spectrum.

#### Damping Ratios and Undamped Periods of the Response Spectra

In the engineering design, the response spectral curves for 0, 2, 5, 10, and 20 percent critical damping are usually computed and plotted for absolute acceleration, relative velocity, and relative displacement, (Fig. 6 to 14), respectively, or in the form of tripartite graphs of pseudo velocity versus undamped natural period, in addition to a comparison of the relative velocity response spectrum of zero damping with the Fourier amplitude spectrum. Usually spectra for 2, 5, 10, or 20 percent critical damping that are computed for design purposes is a function of the capability of the structure to dissipate energy without deforming beyond some accepted level. When the damping value increases, the maximum amplitude and irregularity of the response spectrum will decrease. Thus, the numbers of peaks are reduced. However, the distinguished normal mode and higher modes will be persistently preserved, especially the resonant amplitude. Sometimes, the fundamental period increases with the increase in damping. Damping actually functions as a low-pass filter, filtering out some or all of the high-frequency responses. In soils, the amount of damping is dependent upon the intensity of ground shaking so that the material

damping increases with an increase in ground shaking intensity. At 20 percent damping, which for a structure is usually considered high or overdamped, spectra have very few distinguishable peaks.

#### NATURAL FREQUENCIES (PERIODS) OF THE FOUNDATION SOILS

Table 2 summarizes the characteristics of the response spectra of 5% damping for L, V and T components including peak spectral amplitudes of acceleration, relative velocity, relative displacement, and major frequencies at the crest, right abutment, and downstream free field sites, pictured from fig. 6 - 14. The amplification factors (ratios) of crest to abutment, crest to downstream free field, and downstream free field to abutment are also listed.

The accelerograph at the right abutment is located on rock. The peak amplitudes of the compressional (p) or dilatational waves in the frequency range of above 10 Hz on the absolute acceleration response spectrum are much larger on the rock site than on the soil site, such that 14.3 Hz, 12.5 Hz, 11.8 Hz; 14.3 Hz, 12.5 Hz, 11.8 Hz; and 20.0 Hz, 12.5 Hz appear on the longitudinal, transverse, and vertical components, respectively. The criterion used for choosing, major peak frequencies, is based on the large peak amplitude in the p and s wave groups from the absolute acceleration and relative velocity response spectra. The transverse component shows the highest amplitudes on all predominant frequencies (>10 Hz) among the three components.

At the downstream free field site, the main frequency (2.5 Hz) of the shear wave dominates the longitudinal (L) component (Fig. 12). This is believed to be the natural or resonant frequency of the soil foundation for the L-component, because it is not evident on the spectra of the L-component on the rock site (abutment). Also, the peaks of the five response spectra of 0, 2, 5, 10, and 20 percent critical damping are found to be in phase. The 2.5 Hz is also shown as the predominant frequency (distinguished peak) on the spectra (a, v, and d) of the L-component on the crest of the dam; however, the five peaks (approx. 2.5 Hz) of 0, 2, 5, 10, and 20 percent damping spectra are not exactly in phase as shown in Fig. 9. It was also observed that the natural periods shown on the two spectra of 10 and 20 percent damping were larger than the natural periods shown on the spectra for 0, 2, and 5 percent damping. Furthermore, the spectral amplitude at 2.5 Hz of the L component on the crest is somewhat less than the amplitude of the L component at the downstream site due to the attenuation of energy. Even though these are the facts we can not say that the 2.5 Hz is not the natural frequency of the combined dam-foundation system. After a detailed examination of the response spectral frequencies on the curves of 10 and 20% damping (Fig. 9b) of the L-component on the crest, we found an interference of two other frequencies of 2.65 Hz and 2.29 Hz. Because both frequencies are so close to 2.5 Hz; when the damping ratio is increasing in the response spectrum, the shape of the spectrum becomes more flat. Thus, the fundamental period will be slightly shifted to the right. This is due to the natural characteristics of the undamped single degree of freedom system, which is a viscously damped, simple oscillator subjected to the base motion. The largest spectral amplitude ratios of downstream free field to abutment for the L, V, and T components are at 2.5, 3.3,



and 2.2 Hz, respectively. Therefore, these are believed to be the natural frequencies of the foundation for these components.

#### NATURAL FREQUENCY (PERIOD) OF THE DAM

##### Analysis of Response Spectra

By comparing the shear wave spectral amplitude ratios or amplification factors from 2.0 to 7.0 Hz of the acceleration, velocity, and displacement response spectra of the L, V, and T components on the crest to those at the abutment and downstream sites, one finds the largest spectral amplitude ratios on the L, V, and T components at 2.5, 4.0, and 2.2 Hz, respectively. Although the 2.5 Hz peak of the longitudinal component has the largest spectral amplitude on the crest, it is still less than the spectral amplitude at 2.5 Hz of the L-component at the foundation. This was possibly caused by a higher rate of energy dissipation for the longitudinal component of the dam's vibration or by a higher material damping which was caused by the stronger ground-shaking intensity for the L-component. The highest peak spectral amplitude at 2.5 Hz on the L-component has to be the fundamental mode (natural period) for the L-component of the dam. The second highest acceleration spectral amplitude ratio, 2.7, of crest to abutment on the L-component is at 4.0 Hz. This indicates that 4.0 Hz is the second natural frequency for the L component of the dam since it is much higher than the amplitude ratio 1.7 of downstream to abutment. The natural frequency (first mode) for the V component is 4.0 Hz; this frequency shows the largest spectral amplitude ratio on both crest to abutment and crest to downstream. For the T component 2.2 Hz is the natural frequency for both foundation and dam; the resonant spectral amplitude on the crest is much higher than on the foundation (downstream site). In conclusion, the natural frequencies of the Franklin Falls Dam are 2.5 Hz, 4.0 Hz, and 2.2 Hz for L, V, and T components, respectively.

##### Shear Beam Method

Gazetas (1981a, b, and 1982) formulated the natural periods for longitudinal and vertical deformations of an earth dam based on the generalized homogeneous equations:

$$T_{n, h} = \frac{2.57}{n} \frac{H}{\bar{V}} ; n = 1, 2, 3, \dots \quad (1)$$

where

$T_{n, h}$  = the natural period for longitudinal deformations

H = the height of the dam

$\bar{V}$  = the average S-wave velocity of the dam;

and

$$T_{n, v} = \sqrt{\lambda} T_{n, h} ; n = 1, 2, 3, \dots \quad (2)$$

where

$T_{n,v}$  = the natural period for vertical deformations

$$\lambda = \frac{1 - \nu}{2} \quad (3)$$

$\nu$  = Poisson's ratio

The average height of the Franklin Falls Dam is about 40 m, and the observed natural period of the L-component is 0.4 sec. Then, substituting these two parameters into Equation 1, we obtain 257 m/sec as an estimate of the average shear wave velocity in the dam.

If the average Poisson's ratio of the Franklin Falls Dam is assumed to be 0.3, then in Equation 3,  $\lambda = 0.35$  and  $\sqrt{\lambda} = 0.5916$ ; therefore, substituting this in Equation 2, we have

$$T_{1,v} = 0.5916 \times T_{1,h} \quad (n = 1, \text{ normal mode of V-component})$$

Since  $T_{1,h} = 0.4$  sec for the L-component, then

$$\begin{aligned} T_{1,v} &= 0.5916 \times 0.4 \\ &= 0.24 \text{ sec (4.1 hz)} \end{aligned}$$

Hence, the calculated natural period, 0.24 sec (4.1 Hz) of V-component based on the assumed  $\nu = 0.3$  is generally in agreement with the observed natural period, 0.25 sec (4 Hz) of V-component of the Franklin Falls Dam.

Therefore, based on the measured natural period of the horizontal component and average height of the dam, the average shear velocity and Poisson's ratio of the dam can be estimated. A useful check on this analysis could be made by comparing the estimated values with the results of actual field measurement, so far not available.

#### ACKNOWLEDGMENTS

This paper was based on the original analysis of the data provided by the U.S. Army Engineer Division, New England and was sponsored by the U.S. Nuclear Regulatory Commission (NRC) under Inter-agency Agreement NRC-03-82-107, Permission by NRC and the Office of the Chief of Engineers for the publication of this paper is appreciated.

#### REFERENCES

- [1] Chang, P. K., 1983. "Analysis of Strong-Motion Data from the New Hampshire Earthquake of 18 January 1982," NUREG/CR-3327, U.S. Nuclear Regulatory Commission.

- [2] Gazetas, G. 1981a. "A New Dynamic Model for Earth Dams Evaluated through Case Histories," Soil and Foundations, 21(1):67-78.
- [3] Gazetas, G. 1981b. "Vertical Oscillation of Earth and Rockfill Dams: Analysis and Field Observation," Soils and Foundations, 21(4):265.
- [4] Gazetas, G. 1982. "Shear Vibrations of Vertically Inhomogeneous Earth Dams," International Journal of Numerical and Analytical Methods in Geomechanics, 6:219.

Table 1

## The Uncorrected and Corrected Strong-Motion Parameters of Franklin Falls Dam

Site Location	Azimuth of Component	Uncorrected Accelerations cm/sec	Maximum Accelerations (a), cm/sec	Corrected		
				Maximum Velocity (V) cm/sec	Maximum Displacement (d) cm	Velocity Spectrum Intensity 5%, $\xi$
Downstream	L-225°	111.68 (21 Hz)	140.70 (0.143 g)	2.03	0.16	9.53
	Up	208.34 (21 Hz)	271.00 (0.276 g)	1.73	0.08	7.29
	T-135°	267.94 (16 Hz)	377.86 (0.385 g)	2.87	0.17	13.23
Right Abutment	L-45°	282.52 (14 Hz)	287.70 (0.293 g)	2.68	0.25	13.08
	Up	171.89 (20 Hz)	172.89 (0.176 g)	1.86	0.41	11.61
	T-315°	565.05 (14 Hz)	539.96 (0.550 g)	5.59	0.43	22.39
Crest	L-45°	102.79 (11.4 Hz)	123.96 (0.126 g)	2.67	0.36	12.09
	Up	111.38 (11.4 Hz)	114.31 (0.116 g)	2.89	0.47	13.15
	T-315°	243.46 (14 Hz)	306.83 (0.312 g)	4.06	0.33	17.12

Table 2  
 Analysis of Peak Response Spectra (5% Damping) of the Franklin Falls Dam  
 New Hampshire Earthquake of January 18, 1962

Instrument Component	Peak Frequency Hz	Right Abutment			Downstream (Toe)			Center Crest			Cit. Crest/Ret. Abutment			Cit. Crest/Downstream			Donatrum/Ret. Abutment		
		a	v	d	a	v	d	a	v	d	a	v	d	a	v	d	a	v	d
		cm/sec <sup>2</sup>	cm/sec	cm	cm/sec <sup>2</sup>	cm/sec	cm	cm/sec <sup>2</sup>	cm/sec	cm	cm/sec <sup>2</sup>	cm/sec	cm	cm/sec <sup>2</sup>	cm/sec	cm	cm/sec <sup>2</sup>	cm/sec	cm
L	20.0	700.120	4.930	0.041	523.591	3.969	0.030	289.322	1.825	0.017	0.413	0.424	0.415	0.553	0.527	0.567	0.748	0.805	0.732
	18.2	616.117	4.595	0.039	509.827	4.088	0.032	295.691	2.091	0.019	0.480	0.497	0.487	0.580	0.446	0.594	0.827	0.899	0.821
	14.3	1228.955	13.273	0.147	223.574	2.654	0.027	309.033	2.814	0.037	0.251	0.212	0.252	1.382	1.060	1.370	0.182	0.200	0.184
	12.5	1096.469	13.569	0.155	236.147	2.608	0.033	353.712	3.696	0.050	0.322	0.272	0.322	1.498	1.417	1.515	0.215	0.192	0.213
	11.8	909.465	11.990	0.146	218.600	2.652	0.035	343.421	4.022	0.055	0.377	0.335	0.377	1.571	1.516	1.571	0.240	0.221	0.240
	11.4	694.302	10.574	0.126	171.982	2.458	0.031	306.149	3.945	0.056	0.441	0.373	0.444	1.780	1.605	1.806	0.248	0.232	0.246
	5.0	73.416	3.964	0.073	69.049	2.379	0.069	117.300	3.963	0.118	1.598	0.999	1.616	1.699	1.666	1.710	0.940	0.600	0.945
	4.0	37.863	3.280	0.058	65.877	2.613	0.104	101.553	3.614	0.160	2.682	1.102	2.759	1.541	1.383	1.538	1.739	0.797	1.793
	3.3	40.077	3.453	0.089	94.333	4.158	0.213	72.384	4.060	0.164	1.806	1.176	1.843	0.767	0.976	0.770	2.354	1.204	2.393
	2.5	26.954	3.431	0.106	100.155	6.578	0.403	97.510	6.227	0.393	3.618	1.815	3.707	0.973	0.947	0.975	3.716	1.917	3.802
V	20.0	475.210	3.354	0.028	413.681	2.955	0.024	252.146	1.736	0.016	0.530	0.517	0.571	0.609	0.608	0.666	0.870	0.851	0.857
	12.5	364.140	4.087	0.052	474.064	5.931	0.067	385.332	4.440	0.062	1.058	1.058	1.192	0.813	0.749	0.925	1.302	1.451	1.228
	5.0	59.493	2.547	0.060	48.531	2.914	0.049	123.625	3.357	0.125	2.078	1.318	2.083	2.547	1.152	2.551	0.816	1.144	0.817
	4.0	75.268	3.829	0.118	40.574	2.157	0.063	194.679	8.100	0.307	2.586	2.115	2.601	4.798	3.755	4.873	0.539	0.563	0.534
	3.3	67.317	4.561	0.152	40.375	2.714	0.092	170.444	9.106	0.387	2.532	1.996	2.546	4.221	3.355	4.206	0.559	0.595	0.605
	2.5	46.843	3.419	0.186	27.303	2.480	0.109	63.943	5.473	0.257	1.365	1.600	1.382	2.342	2.207	2.358	0.583	0.725	0.586
	0.57	5.304	3.286	0.409	1.842	1.721	0.128	6.149	2.829	0.475	1.159	0.861	1.161	3.338	1.644	3.711	0.347	0.524	0.313
	0.40	5.350	3.148	0.442	1.459	1.564	0.229	3.557	3.243	0.559	0.665	1.030	0.664	2.438	2.073	2.441	0.273	0.497	0.272
	14.3	1981.993	20.884	0.238	797.950	8.776	0.096	905.729	10.112	0.109	0.457	0.484	0.458	1.135	1.132	1.135	0.403	0.420	0.403
	12.5	1893.661	22.628	0.269	827.043	10.177	0.117	767.950	9.874	0.108	0.406	0.436	0.401	0.928	0.976	0.923	0.437	0.447	0.435
T	11.8	1861.172	23.571	0.301	816.506	10.753	0.132	703.095	9.451	0.113	0.378	0.401	0.375	0.861	0.879	0.856	0.439	0.456	0.438
	11.1	1436.281	21.786	0.280	621.746	9.832	0.122	602.112	8.792	0.117	0.419	0.404	0.418	0.968	0.994	0.959	0.433	0.451	0.436
	5.0	104.690	7.207	0.104	179.701	5.086	0.181	142.594	5.392	0.142	1.362	0.748	1.365	0.793	1.060	0.784	1.716	0.706	1.740
	4.0	101.779	8.289	0.159	116.633	5.634	0.182	177.926	6.917	0.280	1.748	0.834	1.761	1.525	1.228	1.538	1.146	0.679	1.145
	3.3	75.890	8.778	0.169	97.103	7.405	0.220	149.457	9.595	0.339	1.969	1.093	2.006	1.539	1.296	1.541	1.279	0.844	1.302
	2.5	45.714	5.928	0.176	86.298	5.300	0.147	129.676	8.100	0.523	2.837	1.366	2.971	1.503	1.528	1.507	1.888	0.894	1.971
	2.2	31.176	5.709	0.149	71.207	5.344	0.163	113.709	8.737	0.580	3.624	1.530	3.893	1.597	1.576	1.598	2.269	0.971	2.436
	0.4	4.185	5.050	0.655	1.553	2.903	0.195	4.740	4.086	0.670	1.133	0.809	1.023	3.052	1.407	3.436	0.371	0.575	0.298

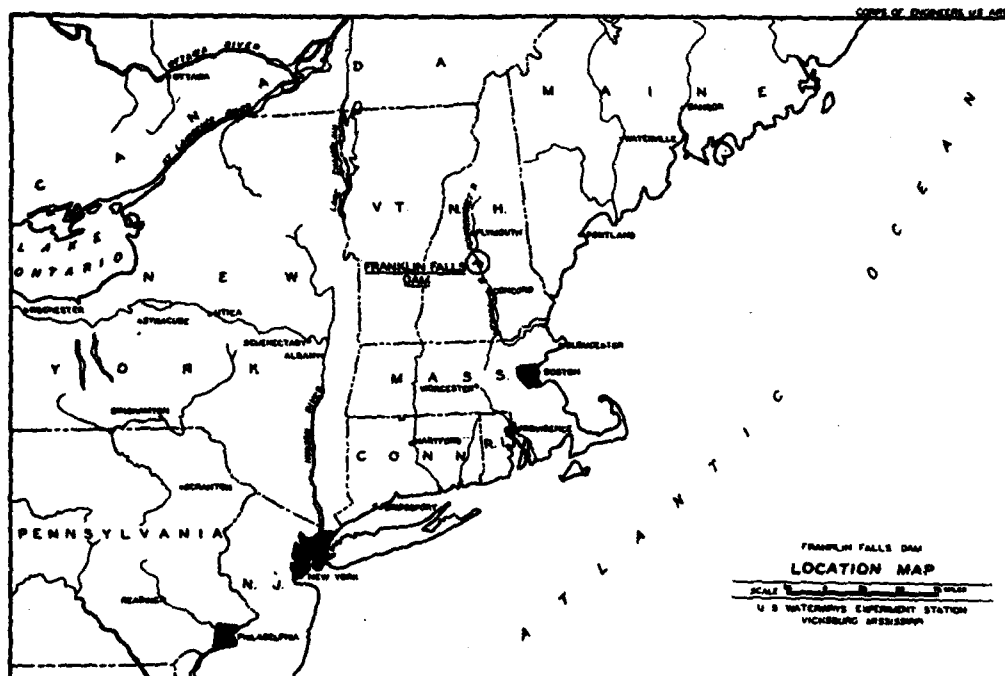


Figure 1. Location of the Franklin Falls Dam

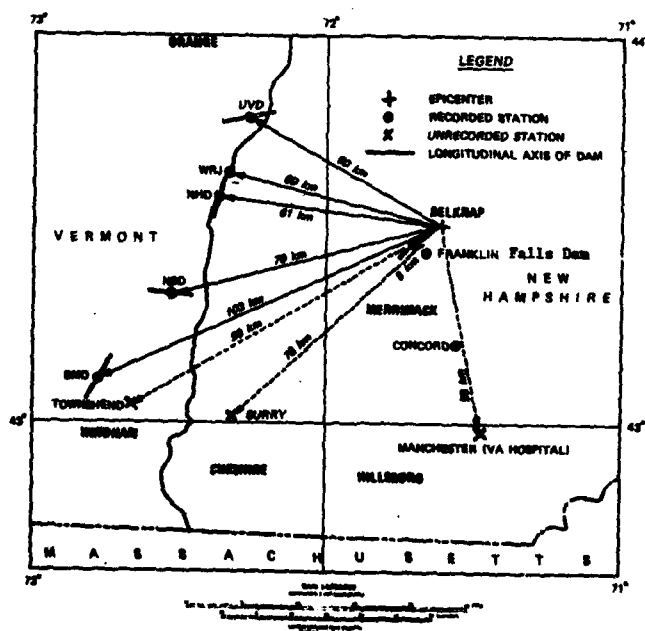


Figure 2. Locations of epicenter and recording stations

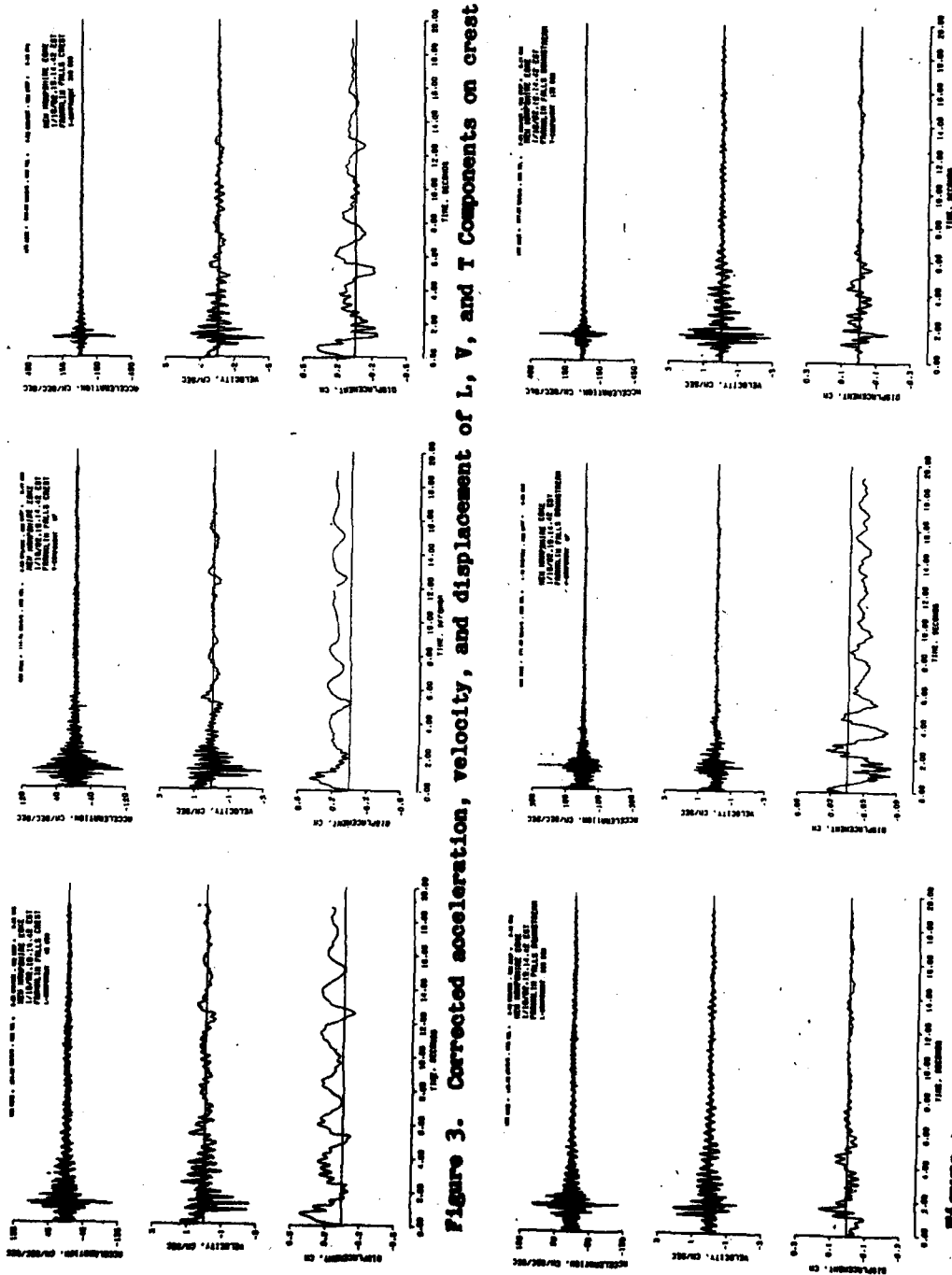


Figure 3. Corrected acceleration, velocity, and displacement of L, V, and T Components on crest

Figure 4. Corrected acceleration, velocity, and displacement of L, V, and T Components on Downstream Free Field

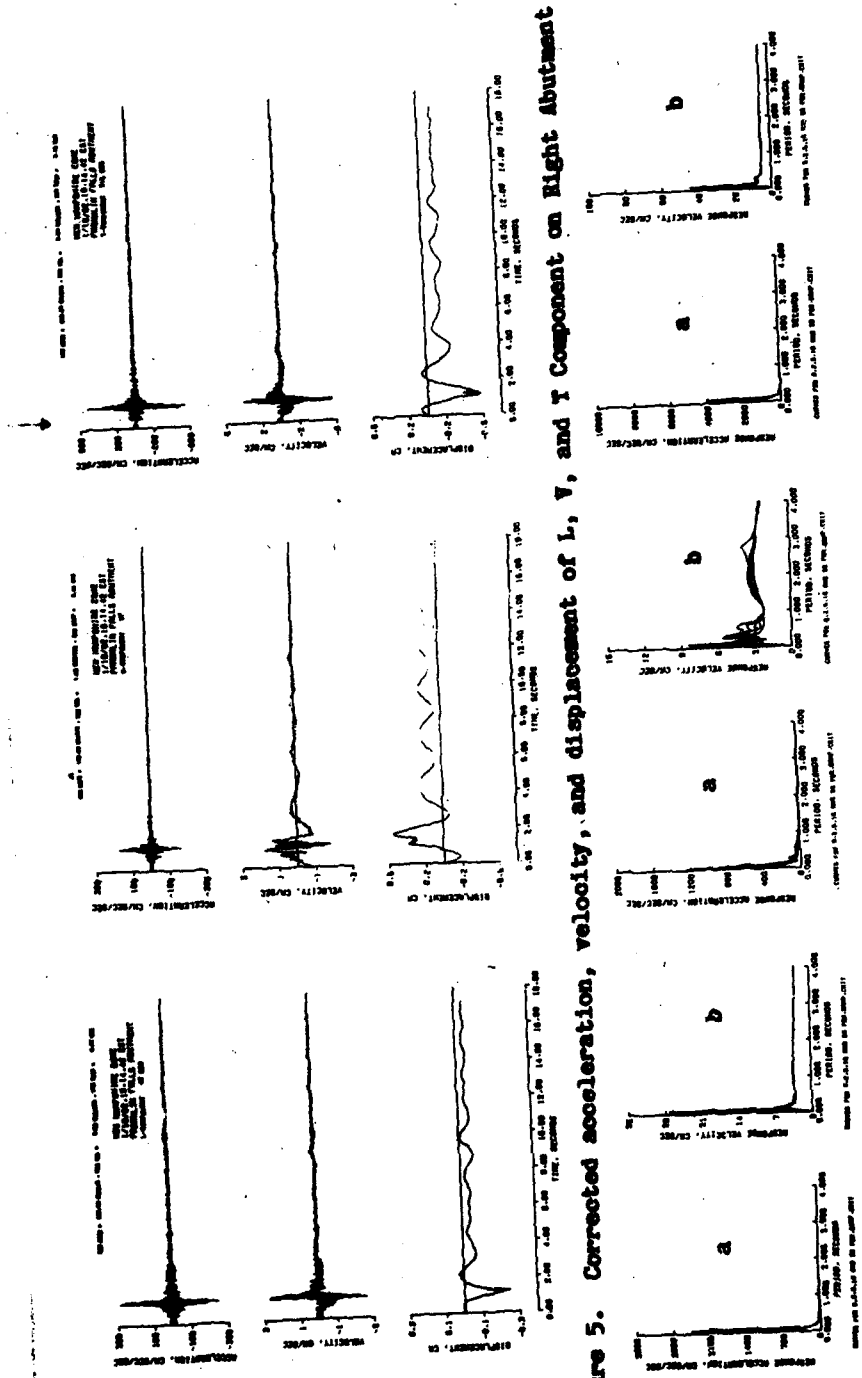


Figure 5. Corrected acceleration, velocity, and displacement of L, V, and T Component on Right Abutment

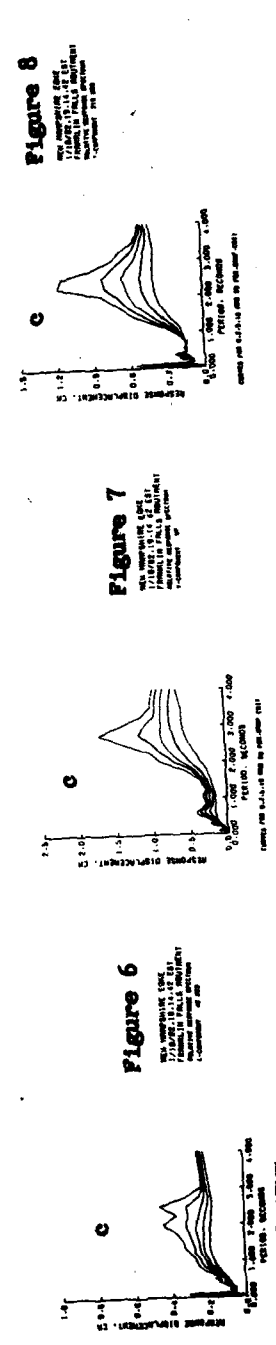
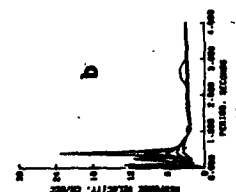
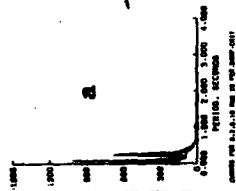
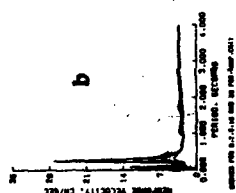
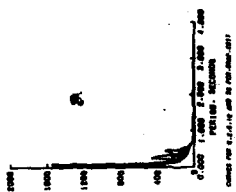
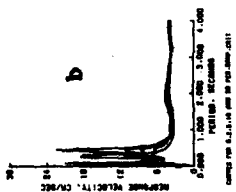


Figure 6

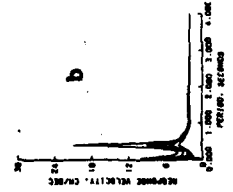
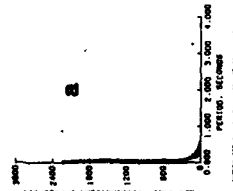
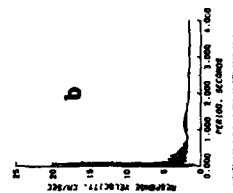
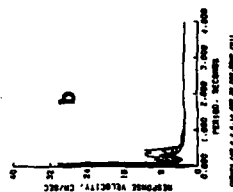
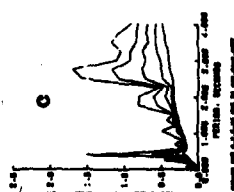
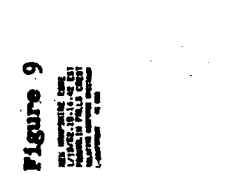
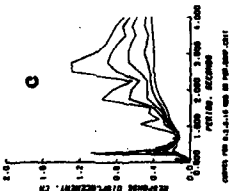
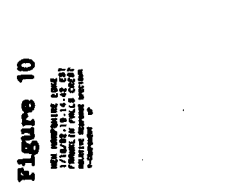
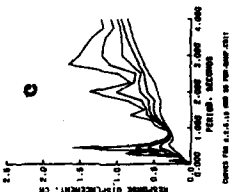
Figure 7

Figure 8





**Figure 9**  
NON-RESPONSE TIME  
PERIOD: 0.114 SECS  
VELOCITY: 18.0 CM/SEC  
ACCELERATION: 900 CM/SEC/SEC  
PERIOD: 0.114 SECS



**Figure 11**  
NON-RESPONSE TIME  
PERIOD: 0.114 SECS  
VELOCITY: 18.0 CM/SEC  
ACCELERATION: 900 CM/SEC/SEC  
PERIOD: 0.114 SECS

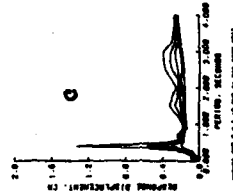
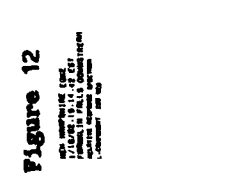
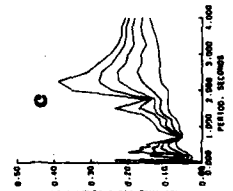
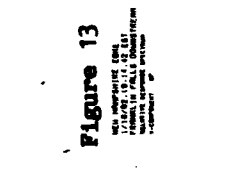
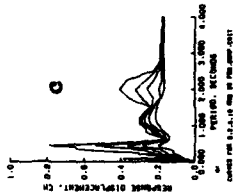


**Figure 12**  
NON-RESPONSE TIME  
PERIOD: 0.114 SECS  
VELOCITY: 18.0 CM/SEC  
ACCELERATION: 900 CM/SEC/SEC  
PERIOD: 0.114 SECS

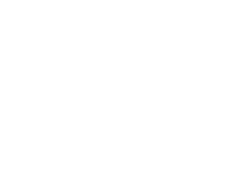
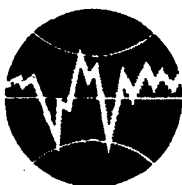


**Figure 13**  
NON-RESPONSE TIME  
PERIOD: 0.114 SECS  
VELOCITY: 18.0 CM/SEC  
ACCELERATION: 900 CM/SEC/SEC  
PERIOD: 0.114 SECS



**TURKISH NATIONAL COMMITTEE FOR  
EARTHQUAKE ENGINEERING**

**THIRTEENTH REGIONAL SEMINAR ON EARTHQUAKE ENGINEERING**

**September 14-24, 1987 - Istanbul - Turkey**

**A GENERAL PROCEDURE FOR ESTIMATING EARTHQUAKE  
GROUND MOTIONS PARAMETERS**

**I. Paskaleva**

# **A GENERAL PROCEDURE FOR ESTIMATING EARTHQUAKE GROUND MOTIONS PARAMETERS**

**I. Paskaleva**

## **1. Introduction**

The specification of earthquake ground motion characteristics for an engineering design application requires a careful evaluation of the best available earth sciences and engineering data. From this information, models are developed to estimate ground motion parameters in terms of the seismotectonic province where the earthquake is expected to occur and the frequency-dependent effects of the earthquake's source and wave propagation path. Adequate data and fundamental knowledge of the earthquake physical processes are the keys for attaining a high level of precision.

Specification of earthquake ground motion characteristics is needed for a wide variety of engineering designs applications.

These applications include:

- Siting and design of nuclear power plants, hospitals, dams, schools, life line systems
- City and land-use planning
- Disaster preparedness
- Building codes

The purpose of these pages is to describe a general procedure that can be adapted to any application of interest.

The technical considerations that are involved in defining the seismic input for various applications have been described by a number of investigators.

A general procedure based on these considerations is shown in Fig. 1 and corresponds to the following steps:

a) Specification of the location and magnitude of likely earthquakes on the basis of the historical seismicity and the seismotectonic features of the area.

b) Specification of the site intensity, as measured by peak ground acceleration. Modified Mercalli Intensity, or some other ground-motion parameters.

c) Specification of the details of the earthquake ground motion in terms of a response spectrum and/or artificial time history.

Each step requires a careful evaluation of the best available ground motion, earth sciences, and engineering data and development of statistical and analytical models for application at the size of interest.

## 2. Physical parameters on ground motion

It is now well known that the ground motions produced by earthquakes are a complex function of the tectonic province where the earthquake occurs, the earthquake source mechanism, the source-site separation, and the geometry and physical properties of the geologic structures traversed by the propagating body and surface waves. The following physical parameters are the most important:

a) Seismicity parameters: seismic source zones, recurrence rates, upper bound magnitude [1]

b) Source parameters: epicenter, focal depth, fault type and rupture length, magnitude, seismic moment, stress drop and effective stress and epicentral intensity [2]

c) Path parameters: the attenuating effects of the earth's crust and mantle on propagating seismic waves [3]

d) Local site parameters: strain level, soil/rock acoustic impedance contrasts and soil thickness and geometry

We shall analyze these four items separately.

2.1. Seismicity parameters

- source zone

The main parameters of source zone are three coordinates  $\lambda$ ,  $\varphi$ ,  $h$  (depth) and magnitude  $M$ . The source can be considered as point, linear, or volume. The effect of the observation site is described by the seismic intensity  $I_1$ . In the simplest case it is supposed that intensity depends only on magnitude  $M$  and the hypocentral distance  $R_1$

$$I_i = bM - g(R_i)$$

$g(R_1)$  - a function which does not take into account the azimuthal effects.

The above equation determines the so called macroseismic field, i.e. a part of the earth surface encircling the epicentre where are or can be observed macroseismic effects. This relation is used in order to check the data which should be included in a catalogue.

- recurrence rates

The law of earthquake recurrence  $N(M)$ , i.e. with mean frequency of earthquake occurrence with magnitude  $M$  and seismic activity  $A$  for the whole region of the observed seismicity and not only for the maximal events. The two-dimensional distribution  $N(M, A)$  is a generalization of the ordinary one-dimensional distribution  $N(M)$

- a law of the earthquake recurrence, Fig. 2.

- upper bound magnitude

$M_{\max}$  of recurrence rates gives the maximal (observed or possible) magnitude for the region under consideration as a whole. The

recurrence rate does not give any possibility to answer the question where in the region  $M_{\max}$  can occur. This possibility is given by the relation  $M_{\max} = M_{\max}(A)$ , Fig. 3, which can conventionally be called a "law of the maximal earthquakes".

## 2.2. Source parameters

From the source parameters enumerated in the beginning we shall consider only those that are closely related with the earthquake value:

- epicenter - by definition the hypocenter (or the focus) is a point below the ground surface where earthquake-location calculations indicate that the rupture originated. The epicenter is the vertical projection of the hypocenter on the ground surface. The energy center is the geometrical center of the ruptured zone of the fault. For cases where the rupture surface is of appreciable size, the seismic waves most affecting a site may originate from points on the rupture surface closer to the site than the hypocenter. This could lead to large errors in the usage of point distances, and for this reason, seismologists and engineers have proposed the use of line or surface distances in that zone.

- seismic energy - (E) - this is the energy of the seismic waves radiated from the source. The founder of this notion is B. Galitsin (1915). In essence it is: In the point of observation the energy density of the surface seismic waves passing through a unit length is determined. The density is integrated along the entire front with a center in the source like a "point" source of seismic radiation with a circular symmetry. Taking also into account the absorption of the waves, as a result the source energy is obtained. This simple scheme is complicated by the need to have in mind the

medium inhomogeneity.

- magnitude - this is a conventional index about the energy released in the source, independent of the place of observation. The magnitude is usually determined by the recorded amplitude for a given earthquake at a given distance as written by the standard type of instrument, and ( $A_0$ ) which is the amplitude selected as a standard for a particular earthquake

$$M = \lg A/A_0$$

For local earthquakes  $A$  and  $A_0$  are measured in millimeters (mm) and the standard instrument is the Wood-Anderson torsion-seismograph which has a natural period of 0.8 sec, a damping factor of 80% of critical and static magnification of 2800. A magnitude determined in this way designates the local magnitude  $M_L$ . For purposes of determining magnitudes for teleseisms, Gutenberg and Richter devised the surface wave magnitude  $M_s$ , and the body wave magnitude  $M_b$ . The local magnitude  $M_L$  is determined at a period of 0.8 sec, the body wave magnitude  $M_b$  is determined at long period body waves (usually between 1-5 sec) and  $M_s$  at a period of 20 sec.

Seismologists still make great efforts to coordinate the different magnitude scales and the formation of an unified scale. The lack of success is because of the many factors on which each magnitude depends. The most relevant to many engineering applications is local magnitude  $M_L$ , determined within the period range of the greatest engineering interest [5]. Besides the advantages of the magnitude approach for determining the earthquake intensity it also has some disadvantages, one of which was already mentioned, but the second disadvantage of the magnitude is its scalar character:

Earthquake is a complex of events referring both to source and to its occurrence on surface. In order to understand an earthquake this complex of composing events should be modeled. The models should be more complex depending on the differentiating data which should be obtained. The disadvantages of the scalar approach refer not only to the magnitude but also to the seismic energy in the source, the maximal accelerations, velocities, displacements, etc.

- seismic moment -  $M_0$ . Another parameter referring to the source again in a simple scalar treatment is the seismic moment  $M_0$ . The physical sense of  $M_0$  is the potential work, i.e. the possible energy which should be spent for overcoming the friction force at the surface of faulting for displacing the banks at a mean distance  $D$  if the surface density of these forces is equal to the shear module  $\mu$ .

The parameters of the source are:

source length - length of faulting  $L$  or  $R$ .

width of source -  $W$ , area of faulting  $S=LW$  in the case of a rectangle and in the case of an ellipse  $S = \pi (L/2)(W/2)$ . Taking into account that the width of the actual faultings in their middle part as a rule are bigger than at the end, it is sensible to assume a variant ellipse and the seismic moment is recorded

$$M_0 = \mu \pi R_0^2 D = \frac{\mu S}{4} L W D \quad (1)$$

Whence a connection between the radius of the circular faulting  $R_0$ , the length  $L$  and width  $W$  of the source

$$(2R_0)^2 = L W \quad (2)$$

From equations (1) and (2) naturally arises the question which of these parameters should be taken as initial and be determined by correlation fields and which should be determined by (1)



and (2). It is necessary to check the results with other correlation fields in order to avoid evident contradictions with the available data.

The aim is to introduce less ambiguities with respect to the models and it is natural to select as initial parameters such which are determined by observations as magnitude  $M$  and the seismic moment  $M_0$ . It can also be started with  $L$  and  $D$  which in some cases permit direct measurements.

For the determination of the correlation between the source length and the magnitude  $M$  after different authors, Fig. 4, and averaged by a relation given by Riznichenko [6] follows

$$\lg L [\text{km}] \pm 0.5 = -0.88 + 0.37 M$$

A correlation and displacement  $D$  along the fault and the magnitude  $M$  after Chinnery [7] is given in Fig. 5. Selecting a confidential interval 68% the relation can be written as follows:

$$\lg D [\text{cm}] \pm 0.4 = -3.2 + 0.76 M$$

It is expedient to follow the series of source parameters determination as below:

1. A correlation between  $M$  and  $M_0$   $\text{din.cm} = \text{erg} = 10^{-7} D$

$$\lg M_0 \pm 0.6 = 15 - 4 + 1.6M \quad \text{Fig. 6}$$

After which the parameters  $R_s$  and  $W$  are determined

$$R_s = \sqrt{M_0 / \mu \pi D}$$

$$W = 2\mu^2 / L$$

If it is assumed that  $\mu = 3 \cdot 10^{11} \text{ din/cm}^2$  and the above correlations for  $M_0$ ,  $L$  and  $D$ , it is obtained:

$$\lg R_s [\text{km}] = -1.67 + 0.42 M$$

$$\lg W [\text{km}] = -1.86 + 0.47 M$$

- stress drop  $\Delta\sigma$  can be determined if  $M_0$  is known as well as the geometry of the faulting surface. At a circular faulting with a radius  $R$ , the stress drop is determined [8] :

$$\Delta\sigma = 7/16 (M_0 / R^3)$$

In the case of a rectangular faulting

$$\Delta\sigma = \frac{(2M_0/3\pi)(4/L^2 + 3/W^2)}{(L^2 + W^2)^{3/2}}$$

At equal areas of faulting  $\pi R_c = LW$  the first formula gives  $\Delta\sigma$  about twice larger than the ones by the second formula which is within the boundaries of precision when determining such values.

$\Delta\sigma$  increases with depth, Fig.7. The increase of stress drop with depth  $h$  at one and the same magnitude  $M$  and moment  $M_0$  is connected with the small area of faulting, small displacements and big friction under the conditions of a big hydrostatic pressure.

### 2.3. Path parameters

Propagation path effect is a term used to refer to the transmission of seismic energy from the source region to the vicinity of the site. The primary effects are associated with the loss of energy as the seismic waves propagate away from the source region. There are two types of damping that contribute to the loss of energy:

- geometric attenuation that results from reduction in energy density as the wave front propagates away from the fault surface;
- internal damping due to frictional heat losses.

The type and amount of attenuation of seismic ground motion depends on many factors, such as the site of the event, the type of fault mechanism, transmission path, distance and local soil

condition of the site. The commonly used empirical attenuation relationship incorporates some of these parameters but generally leaves out important variables such as the azimuth between the source and the site, and the parameters that identify the fault rupture mechanism.

A commonly used empirical attenuation function is

$$PGA = f(M, R, b_1, b_2, b_3, c)$$

where  $R$  - distance from the source to the site

$b_1, b_2, b_3$  - regression constants which depend on the type of data, site condition, transmission path

$c$  - saturation effect depending on magnitude.

Esteve and Rosenblueth [9] after considering data from earthquakes, the propagation of elastic waves and the definition of magnitude, proposed the following general formula:

$$PGA = \frac{b_1 \exp b_2 M}{f(R)^{b_3}}$$

where  $f(R)$  is a function of hypocentral distance and has been considered to modify  $R$ , for better fitting data, obtained at short epicentral distances. Now seismic wave field at distances greater than source sites has been studied rather well. Even a selective analysis of rather limited data concerning ground motions near seismic sources, surface faults, aftershock fields and space distribution of seismic effect demonstrates insufficient validity of accepted theoretical models. Real quantitative seismic models can be compiled only on the basis of experimental data concerning the sizes and geometry of sources, character of rupture propagation in the earth crust material peculiarities of generation and space distribution of short period vibrations near real extent sources.

The curves of peak ground accelerations with distance from fault R are shown in Fig. 8. This figure demonstrates a weak dependence of PGA on source sizes and magnitudes in nearfield zones. While rupture propagating in the non-homogeneous earth crust material the increase of intensity of high frequency radiation occurs (the possibility of vibrations accelerations on account of the local soil surface conditions should be rejected) owing to the destruction of solid barriers or great local friction [10]. The reason of occurrence of a vibrational type of seismic motion near a fault can be explained by irregular faulting. Intensity of high frequency vibrations increases when source complicity increases too. The amplitude level of vibrations depends on the level of stress with rupture starting. The amplitude of ground accelerations and the attenuation of PGA with distance are higher for thrust and overthrust than for strike-slip type faulting, Fig. 9. The dependence amplitude of PGA on magnitude for fixed distances R from surface fault area are shown in Fig. 9.

#### 2.4. Local site influence

Multilayers ground deposit can be considered as multichannels filter with frequency response depending on the ratio between wave length  $\lambda$  and layer thickness H. The ground deposit influence on elastic vibrations in the interval of length of waves  $H \pm \lambda \leq 20-30H$ . The model of horizontal layers is not valid for the description of the behaviour of soil deposits with a curvilinear lower boundary of the mountain valley type. Values of amplification of amplitude vibrations  $V_a$  and that of time duration  $dt$  considerably depends on seismic contrast described by ratios  $p_0 V_0 / p_1 V_1$ , more than on geometry of valley [12].

$$V_a \approx (0.6 \div 0.8) \rho_s V_s / \rho_v V_v$$

$$\delta t \approx (1 \div 1.30) \sqrt{\rho_s V_s / \rho_v V_v}$$

$$K_s \approx (1 \div 1.30) \rho_s V_s / \rho_v V_v$$

where  $\rho_s V_s$  is the rigidity of rocky basement  $\rho_v V_v$  is the rigidity of valley ground,  $K_s$  is a spectral amplification. These characteristics can be used for the forecast of behaviour of valley and seismic microzonation.

The inelastic behaviour of soft ground during strong earthquakes are observed often in the epicentral zones. A weak increase of amplitudes and time duration of short period vibrations of soft grounds comparatively with solid grounds can be greatly explained by an inelastic behaviour of soft grounds.

By the strong wave propagation through porous water saturated sediments the growth of effective stress and liquefaction of loose uncohesive grounds occur. The value of liquefaction threshold depends on dimensions of grains, density, level of water saturation and thickness of loose soil layer.

A summary of the effect of each physical parameter on ground motion, its uncertainty and functional dependence is given in Table 1.

### 3. Summary of current design practice

Current earthquake-resistant design practice uses the following basic engineering parameters: duration, peak values, predominant period, spectral curves, time histories.

#### 3.1. Duration

In spite of the vital importance of this parameter in the dynamic analysis of a nonlinear system no single definition has yet been generally adopted. The duration of an earthquake increases with magnitude, and for a given value of  $M$  decreases with the fo-

cal distance and thickness of the soil deposit.

Several definitions of the concept of duration as a function of the parameters of instrumental recordings have evolved in recent years. Due to the lack of agreement on the concept of duration during the last decade some researchers have investigated on the use of more consistent definitions related to the "effective duration" which corresponds to the zone of almost linear increase of areas intensity

$$I_a = \pi/2g \int_0^{t_{\text{dur}}} a^2(t) dt$$

where  $t_{\text{dur}}$  - recording time, Fig. 10. This duration characterizes that part of the accelerogram in which the level of shaking is constant and in general is smaller than the significant duration.

3.2. Peak ground acceleration  $a_{\text{max}}$  is still the most widely used parameter for seismic design of structures as a measure of the lateral forces on a structure for high frequency systems. In the design practice it is assumed that the PGA in the two horizontal durations are equal and that the max vertical acceleration is at least 2/3 (two thirds) of PGA in horizontal duration.

The ratio  $R_a$  of mean PGA on different sites and on rock estimated by different authors [13, 14] shows that the amplification factor  $R_a$  increases with the epicentral distance regardless of the type of soil, Fig. 11. In the near field it seems that there is no variation of PGA with magnitude.

3.3. Peak ground velocity -  $v_{\text{max}}$  is a parameter useful to characterize the dynamic behaviour of intermediate period structures, neither very rigid nor very flexible, for which PGA and PG

displacements are better indicators. To estimate the  $v_{max}$  for a given local subsurface conditions there are less relationships available than in the case of accelerations. Fig. 12 displays graphically the criteria proposed by Ambraseys and Esteva and Villaverde in this regard.

3.4. Peak ground displacement -  $d_{max}$ . This parameter is rarely reported in the literature. On the basis of 187 accelerograms Trifunac and Bready proposed a relationship as follows:

$$\lg d_{max} = M + \lg D_0(R) - \lg d_0(M)$$

where  $D_0(R)$  and  $d_0(M)$  are soil-dependent functions. Peak displacements are most affected by local subsurface conditions.

3.5. Predominant period -  $T_p$  - this is the period at which acceleration reaches its maximum value. It is normally obtained from the response spectrum. Fig. 13 shows motions in rock. It is seen that the predominant period increases with the distance to the energy center and the magnitude. At soft sites the period increases with the thickness of the alluvium, due to the low-pass filtering effect exerted by the soil over the transmission of the waves.

### 3.6. Spectral curves

Site-independent earthquake response spectra are used in most design applications. These smooth broad-band spectra have control points that are based on statistical analysis of actual response spectra derived from representative accelerograms. These spectra represent the mean-plus-1 $\sigma$  level of the data sample and are considered to be applicable for most sites because of the conservatism and the wide range of seismological, geologic and local

soil conditions represented in the data sample. The exceptions are sites which are relatively close to the epicenter of a design earthquake and sites which have physical characteristics that could significantly affect the spectral composition of the ground motion. In these two cases, appropriate site-dependent response spectra are developed, *Fig. 44*.

### 3.7. Design time histories

Time histories of acceleration, velocity and displacement are typically used to analyze the dynamic response characteristics of important structure (nuclear power plants, dams). At the present time, no truly adequate model exists for analytically computing the acceleration time histories for arbitrary source-site configurations. Therefore, current design practice requires that the design time history produce a response spectrum that exceeds the smooth design response spectrum at all frequencies and account for the maximum ground shaking parameters (PGA and duration of shaking).

## 4. Conclusions and research trends for the future

There is little doubt that the current empirical techniques for defining earthquake ground motions will be refined and improved in the future as improved data bases evolve, as fundamental knowledge of basic earthquake effects increases, and as capability to model (analytically and probabilistically) improves. The "ideal" data base [11] should contain the following information about the site and the region surrounding it:

### A) Seismicity parameters

For all reported earthquakes there should be prepared: a location map, a catalogue with the information about epicenters,



focal depth, source mechanism and dimensions, magnitude, stress drop, seismic moment, and rupture velocity, recurrence relations for the region and for well-defined seismic source zones within the region.

B. Seismotectonic information

Maps with seismotectonic provinces and locations of capable faults. Information about each province as - geometry, type of movement, temporal history of each fault, and the correlation with historic and instrumental epicenters.

C. Seismic attenuation function

Isoseismal maps of significant historic earthquakes accuracy in the region.

Attenuation of intensity or PGA with distance and magnitude and their statistical distribution.

Frequency-dependent distance scaling relations and their statistical distribution.

D. Earthquake ground motion parameters

Ensembles of strong ground motion records sufficient for calibrating the near field ground motion with respect to intermediate and far-field ground motions which may affect the region.

E. Local ground response

Strong ground motion records at surface and subsurface locations for a wide range of input ground motion strain levels.

Information on the static and dynamic properties of the near-surface soils and rock formations like shear wave velocities, bulk densities and water saturation.

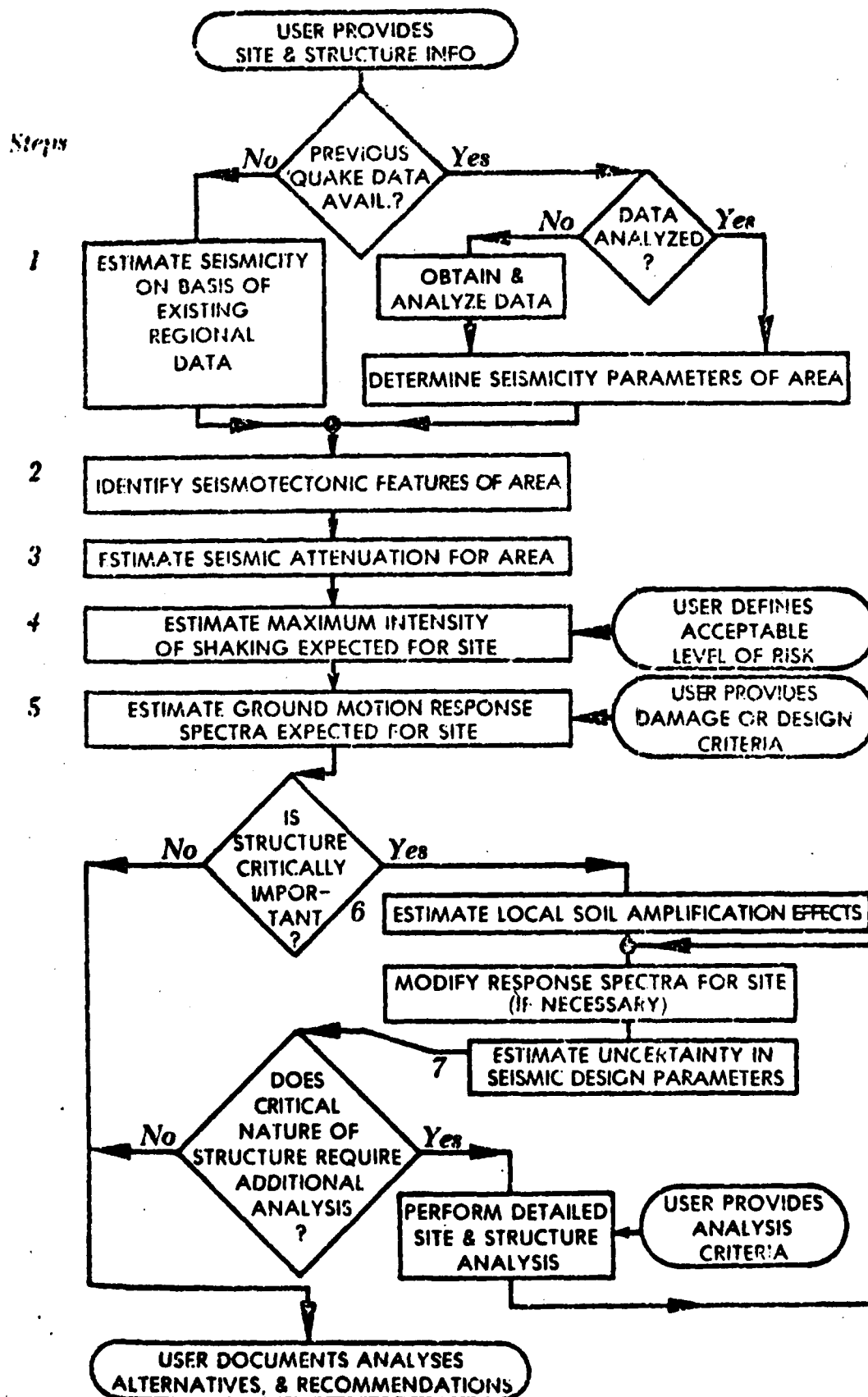
## REFERENCES

1. Hays W.W. Algrmissen S.T. Espinosa A.P. Perkins D.M. and Rinehart W.A. Guidelines for developing design earthquake response spectra. U.S. Army Construction Eng. Research Lab. Tech. Rept. M-114, 1975.
2. Thatcher W. and Hanks T.C. Source parameters of Southern California Earthquakes, Jour. Geophys. Research, v. 78, 1973.
3. Seed H.B. Murarka R. Lysmer J. and Idriss I.M. Relationships of  $\max$  acceleration velocity, distance from source, and local site conditions for moderately strong earthquakes. Seismol. Soc. America Bull., v. 66, 1976.
4. Seed H.B. Ugas C. and Lysmer J. Site dependent spectra for earthquake resistant design. Seismol. Soc. America Bull. v. 66, 1976
5. Kanamori H. and Jennings P.C. (1978) Determination of Local Magnitude  $M_L$  from strong Motion Accelerograms Bull. of Seismol. Soc. of America, vol. 68, No 3, April.
6. Rizinichenko, Y.V. Izbrany trudy Problemy seismologii, Izd. "Nauka", Moskva 1985.
7. Chinnery M.A. Earthquake magnitude and source parameters. Bull. seismol. Soc. Amer. 1969, vol. 59, No 5.
8. Haskell N.A. Total energy and energy spectral density of elastic waves radiation from propagating faults BSSA 1964, vol. 54, No 6
9. Esteve L. and P. Rosenblueth (1964) Espectos de temblores a distancias moderadas y grandes, Boll. Soc. Mex.
10. Shtenberg V.V. On the problem of earthquake source, fault displacement and seismic radiation. Engineering seismology Problems 1984, No 25, Moscow "Nauka".

11. Hays W.W. et al. Guidelines for developing design earthquake response spectra U.S. Army Construction Eng. Research Lab. Tech. Rept. M-114, 1975.
12. Shteinberg V.V. On the soft ground motion by strong earthquakes. Dokl. Acad. Sci. USSR, 1984, v. 275, No 2.
13. Trifunac, M.D. and Brady A.G. (1976) Correlation of Peak Acceleration, Velocity and Displacement with Earthquake Magnitude, Distance and Site conditions, International Journal of Earthquake Engineering and Structural Dynamics, vol. 4, No 5, July-September.
14. Idriss I.M. 1978 Characteristics of Earthquake Ground Motions, Specialty Conference on Earthquake Engineering and Soil Dynamics ASCE, Pasadena, California, June.

Table 1 The uncertainty in physical parameters that affect ground motion

PHYSICAL PARAMETER	EFFECT ON GROUND MOTION	UNCERTAINTY AND FUNCTIONAL DEPENDENCE
<b>SEISMICITY PARAMETERS</b>		
SEISMIC SOURCE ZONE	ZONE SHAPE AFFECTS GROUND MOTION LEVEL	NOT KNOWN. FUNCTION OF SEISMICITY RECORD, GEOLOGIC AND TECTONIC HISTORY
RECURRENT RATE (b)	AFFECTS UPPER BOUND EARTHQUAKE	$\bar{b} = 0.45$ IN EASTERN U.S. WHERE $1.0 \text{ N} = a - bL$ $\sigma = 1(N)$
UPPER BOUND MAGNITUDE	ESTABLISHES GROUND MOTION DESIGN LEVELS	NOT KNOWN. FUNCTION OF COMPLETENESS AND LENGTH OF SEISMICITY RECORD AND GEOLOGIC DATA ON FAULT RUPTURE
<b>SOURCE PARAMETERS</b>		
EPICENTER	ESTABLISHES LOCATION OF DESIGN EARTHQUAKE	BEST LOCATION ACCURACY IS 1 KM; WORST IS 50 KM. FUNCTION OF REGIONAL VELOCITY MODEL AND INSTRUMENT LOCATIONS
FOCAL DEPTH	AFFECTS PARTITION OF BODY/SURFACE WAVE ENERGY	BEST LOCATION ACCURACY IS 2 KM; WORST IS 50 KM. FUNCTION OF REGIONAL VELOCITY MODEL AND INSTRUMENT LOCATIONS
MAGNITUDE ( $m_b, M_L, M_s$ )	AFFECTS LOW FREQUENCIES; GROUND MOTION SCALING	BEST ACCURACY IS 0.1 UNIT; WORST IS $> 1$ UNIT. FUNCTION OF INSTRUMENTS AND SITE CALIBRATION
SEISMIC MOMENT ( $M_0$ )	AFFECTS LOW FREQUENCIES, ESPECIALLY FOR GREAT EARTHQUAKES	$\log M_0 \sim 3/2 M_s$ until $M_0 \approx 10^{26} \text{ dyne cm}$ . $M_0 = 21.9 + 3 M_s$ WITH $1 \sigma \approx 2$ . FUNCTION OF INSTRUMENT DYNAMIC RANGE.
STRESS DROP ( $\Delta\sigma$ ) AND EFFECTIVE STRESS	AFFECTS HIGH FREQUENCIES, PEAK ACCELERATION	$\Delta\sigma$ HAS A LOG-NORMAL DISTRIBUTION. EARTHQUAKES EXHIBIT A CONSTANT AVERAGE STRESS DROP OF ABOUT 10 MPAS WITH $2\sigma \approx 10$ . FUNCTION OF MOMENT DETERMINATION
FAULT LENGTH (L)	AFFECTS MAGNITUDE AND MOMENT	$M = 1.7(5 \pm 1) 243 \log L, \sigma = 0.93$
EPICENTRAL INTENSITY ( $I_0$ )	AFFECTS SITE ACCELERATION ( $a_h$ AND $a_v$ )	$\log a_h = 0.24 I_{0M} + 0.29, 1\sigma \approx 0.19$ $\log a_v = 0.20 I_{0M} - 0.40, 1\sigma \approx 0.53$ } WORLDWIDE DATA
<b>PATH PARAMETERS</b>		
RATE OF ATTENUATION OF SEISMIC ENERGY WITH DISTANCE	ESTABLISHES PEAK GROUND MOTION VALUES AT SITE AND FREQUENCY DEPENDENT SIGNATURE	NOT WELL DEFINED BECAUSE OF LIMITATIONS ON DATA SAMPLE. $1\sigma$ FOR PEAK ACCELERATION VS DISTANCE RELATION IS 2.01 FOR WORLDWIDE DATA, 1.42 FOR THE SAN FERNANDO EARTHQUAKE. $1\sigma$ FOR PEAK VELOCITY VS DISTANCE IS 1.5 FOR MODERATE U.S. EARTHQUAKES.  $1\sigma$ FOR FREQUENCY DEPENDENT ATTENUATION OF SPECTRAL VELOCITY RANGES FROM 1.1 TO 2.22 FOR A GENERAL AREA AND 1.56 TO 1.40 FOR A CALIBRATED AREA ON THE BASIS OF NUCLEAR EXPLOSION DATA.  THE STATISTICAL DISTRIBUTION FOR MAX INTENSITY ATTENUATION IS NOT KNOWN
<b>LOCAL GROUND RESPONSE</b>		
SOIL/ROCK ACOUSTIC IMPEDANCE ( $\rho\beta$ ) CONTRAST	AFFECTS AMPLITUDE LEVEL OF GROUND MOTION	NOT WELL DEFINED. PHYSICAL PROPERTIES DEPEND ON GEOPHYSICAL AND LABORATORY MEASUREMENTS. GROUND MOTION DATA SAMPLE FOR PATH ROCK AND SOIL CLASSIFICATION IS SMALL.
SOIL THICKNESSES AND GEOMETRY	AFFECTS DOMINANT FREQUENCY, DURATION, PEAK/AVG RATIO, DOWNSHIFT RATIO	NOT WELL DEFINED. DEPENDS ON GEOPHYSICAL, GEOLOGIC, ENGINEER AND GROUND MOTION DATA.
STRAIN LEVEL	DETERMINES IF GROUND RESPONSE IS LINEAR OR NONLINEAR	NOT WELL DEFINED BECAUSE OF LIMITATIONS OF THE GROUND MOTION DATA SAMPLE, ESPECIALLY CLOSE TO THE FAULT.
MEAN GROUND RESPONSE	DETERMINES AVERAGE RESPONSE BETWEEN TWO SITES	REPEATABLE WITH $1\sigma = 1.0$ FOR NUCLEAR EXPLOSION AND 1.50 FOR EARTHQUAKE AFTERSHOCKS.



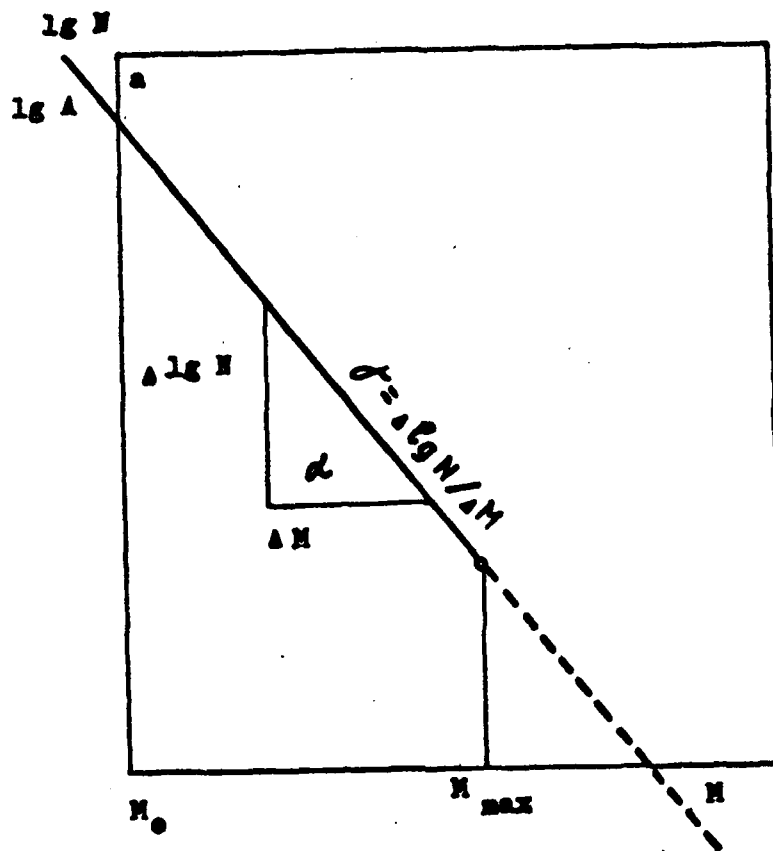


Fig. 2

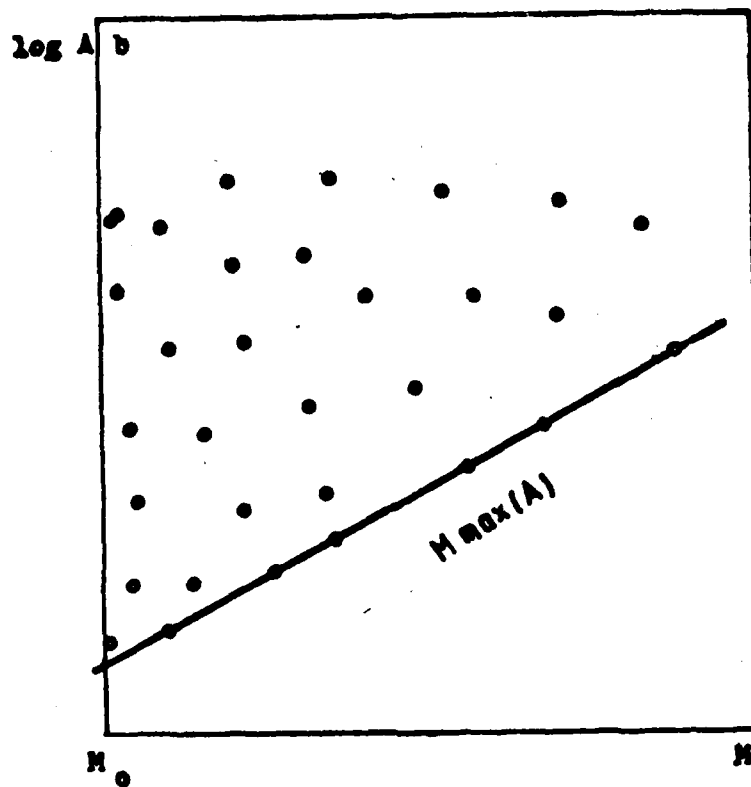
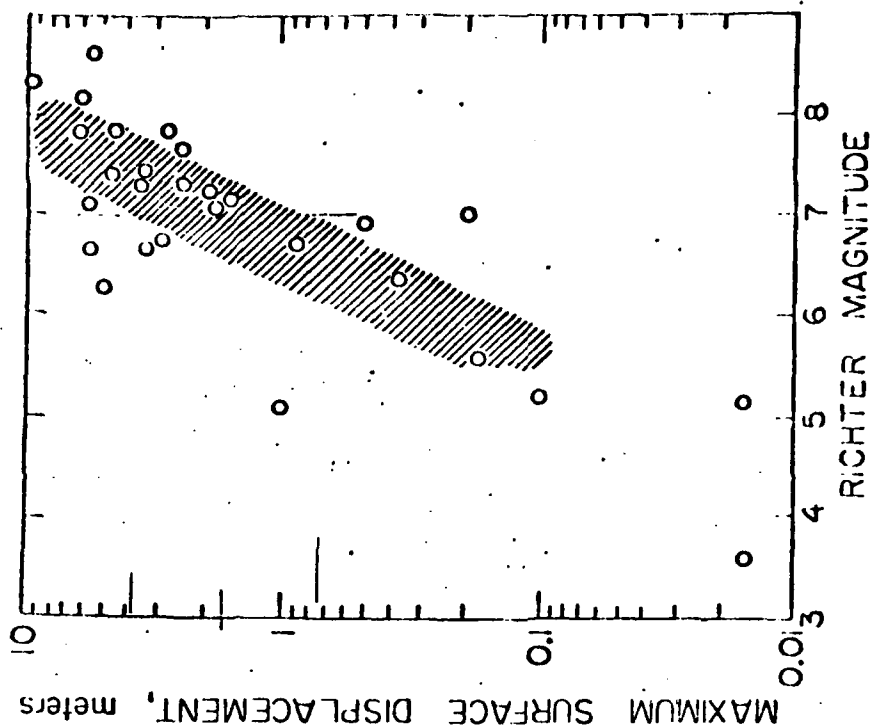
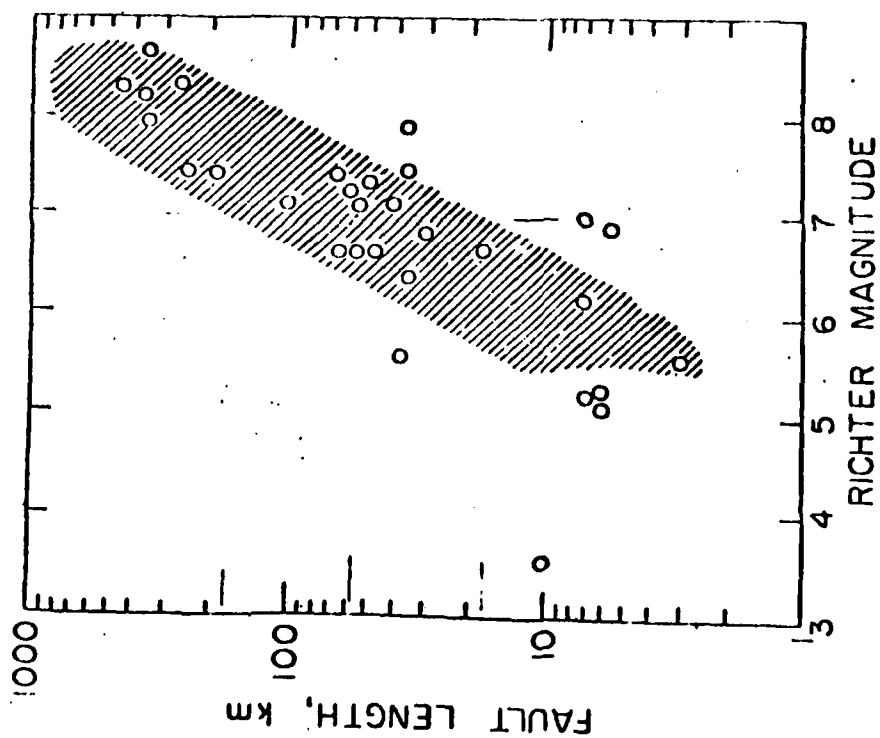


Fig. 3



FAULT LENGTHS AND SURFACE DISPLACEMENTS  
HORIZONTAL STRIKE-SLIP FAULTS, WORLD-WIDE DATA  
(SLEMMONS, 1977)

FIGURE 4, 5

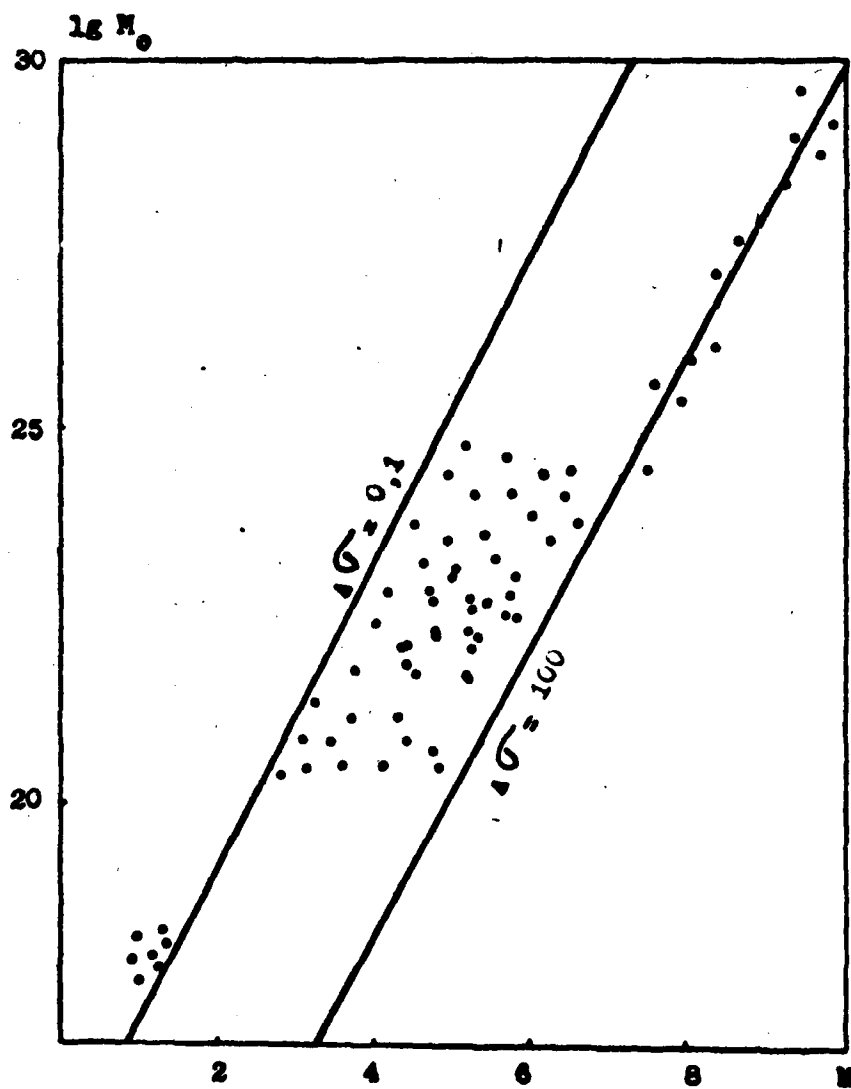


Fig. 6



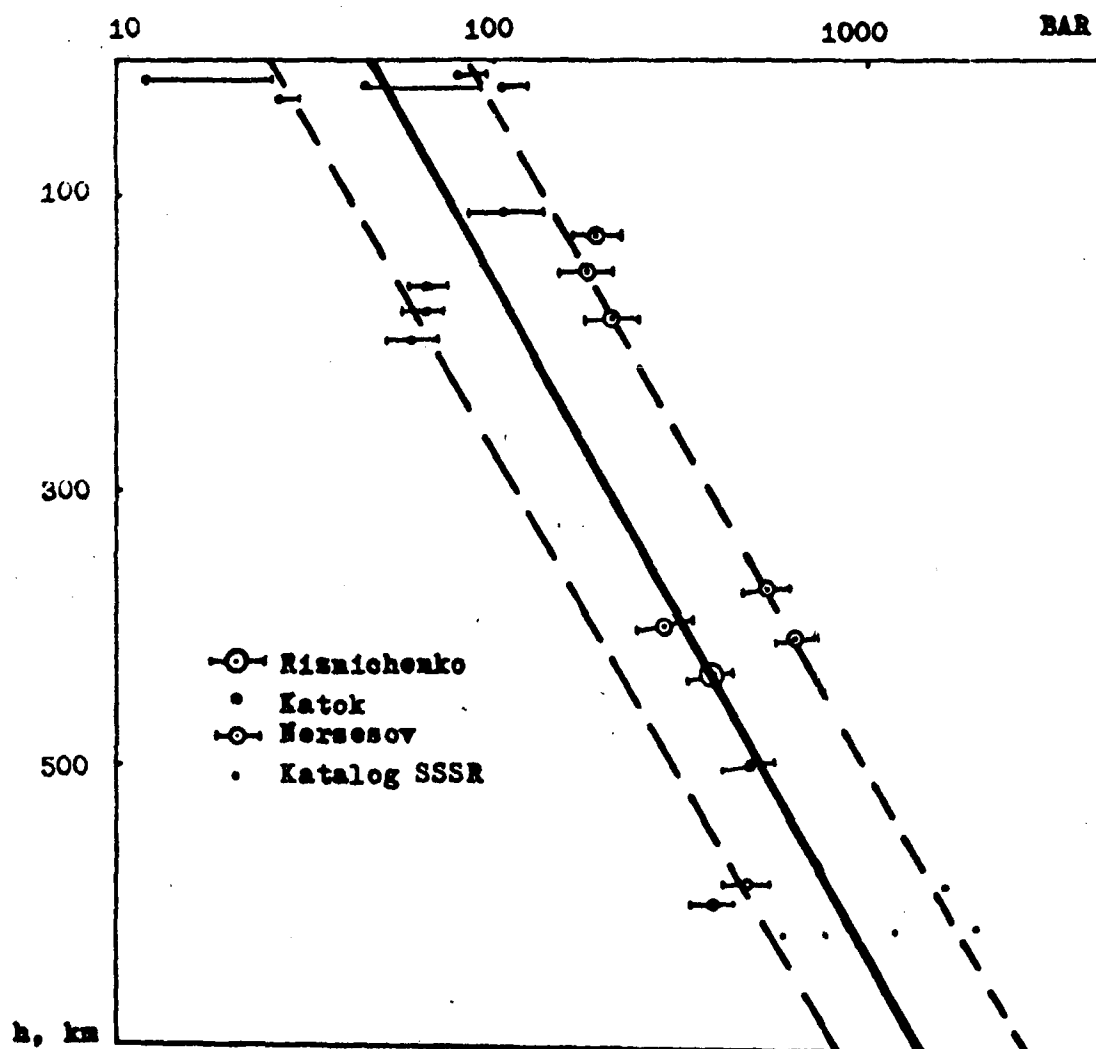


Fig. 7

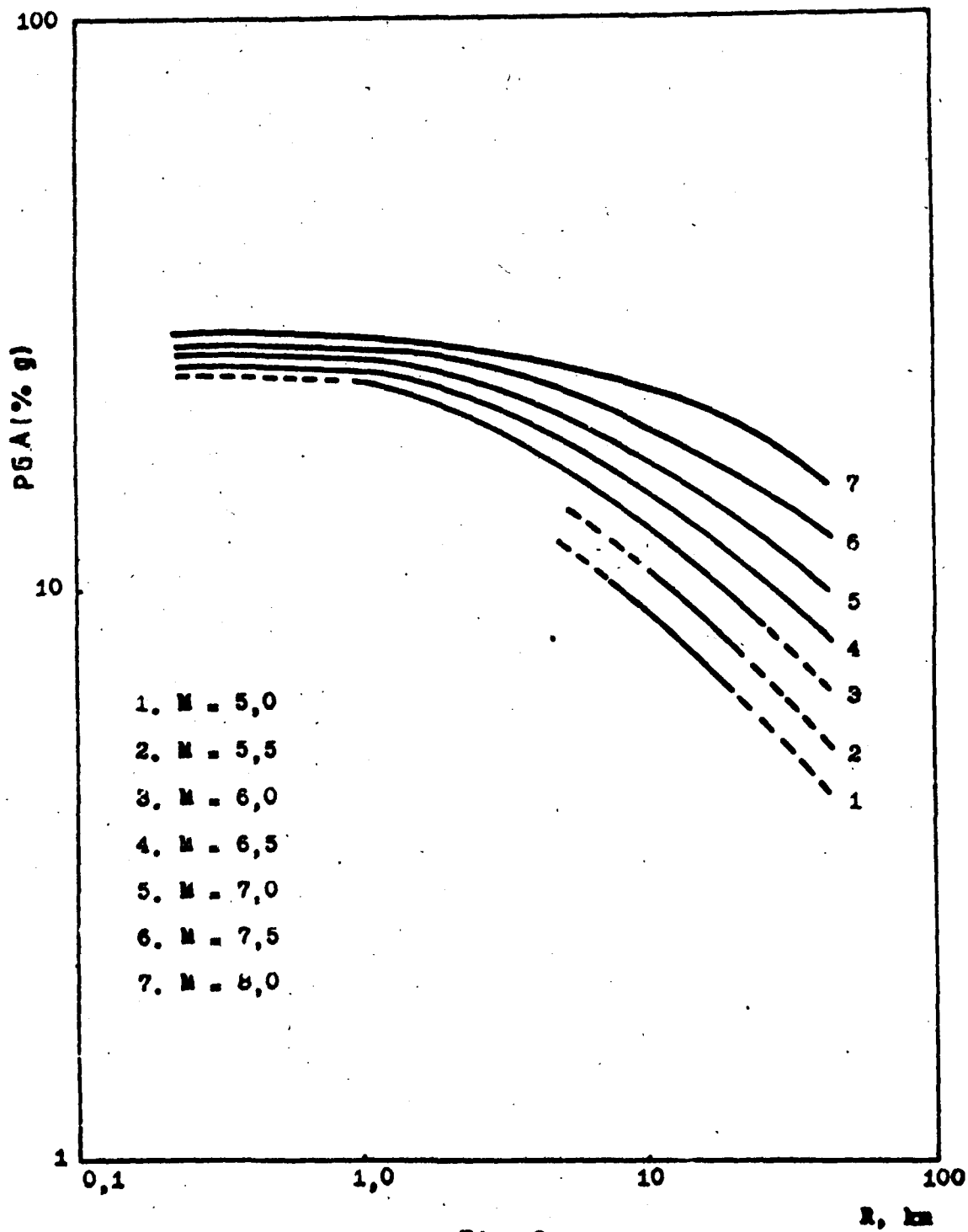


Fig. 8

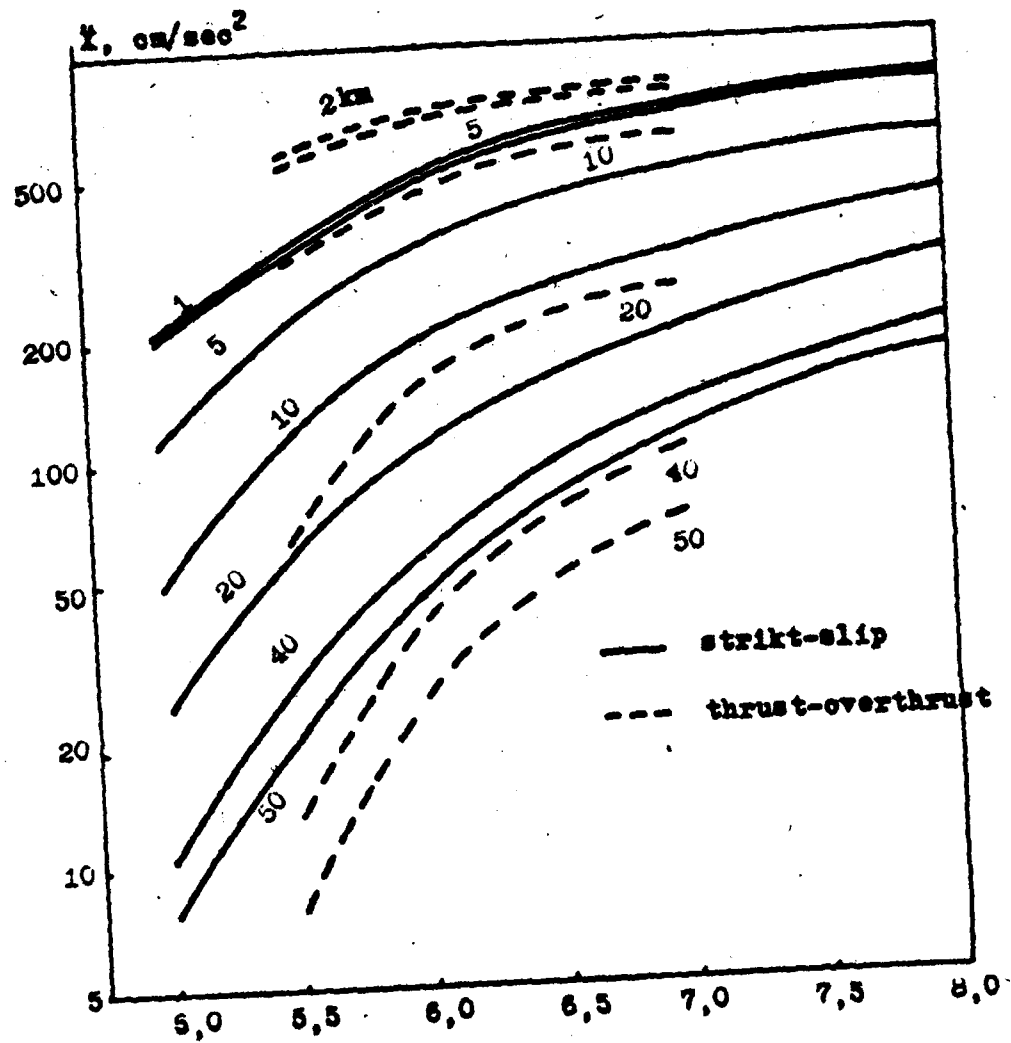
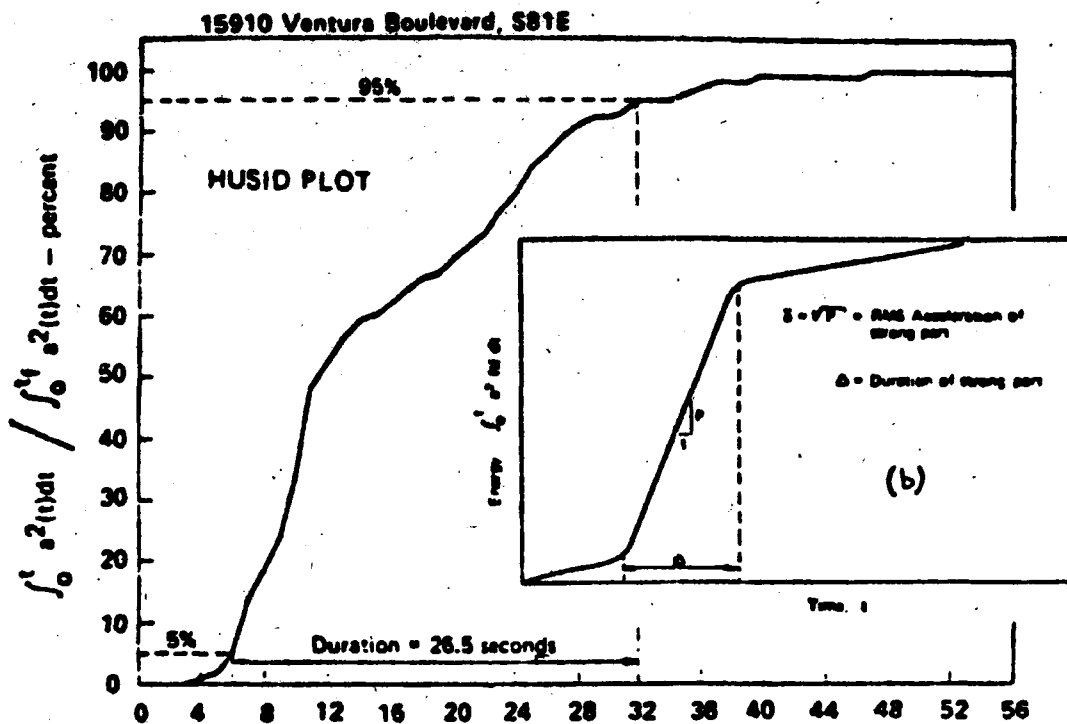


Fig. 9



(a)

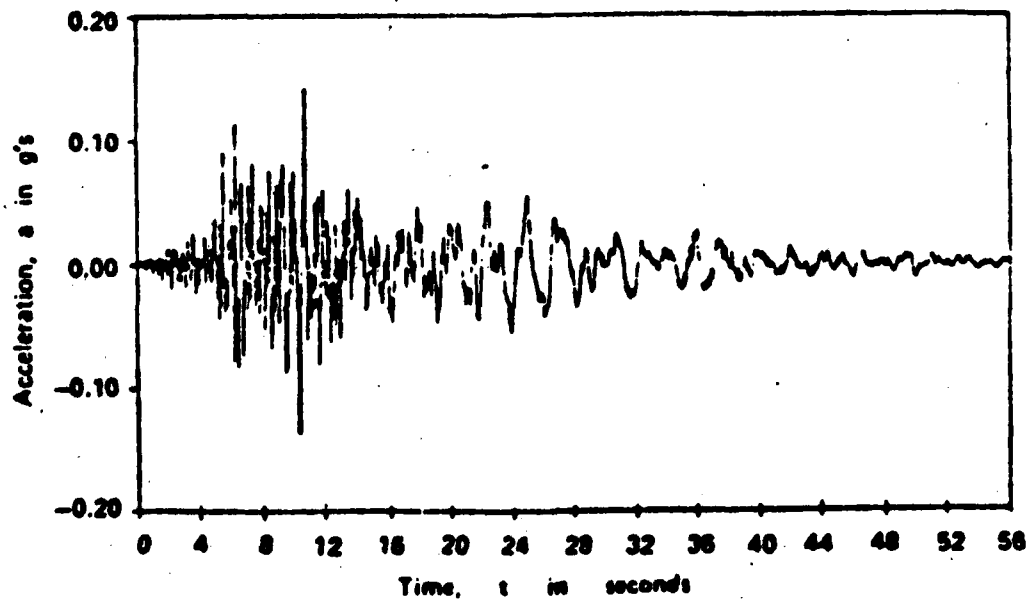


Fig.10, TYPICAL HUSID PLOT, AND DURATION AS DEFINED BY TRIFUNAC AND BRADY (1975)

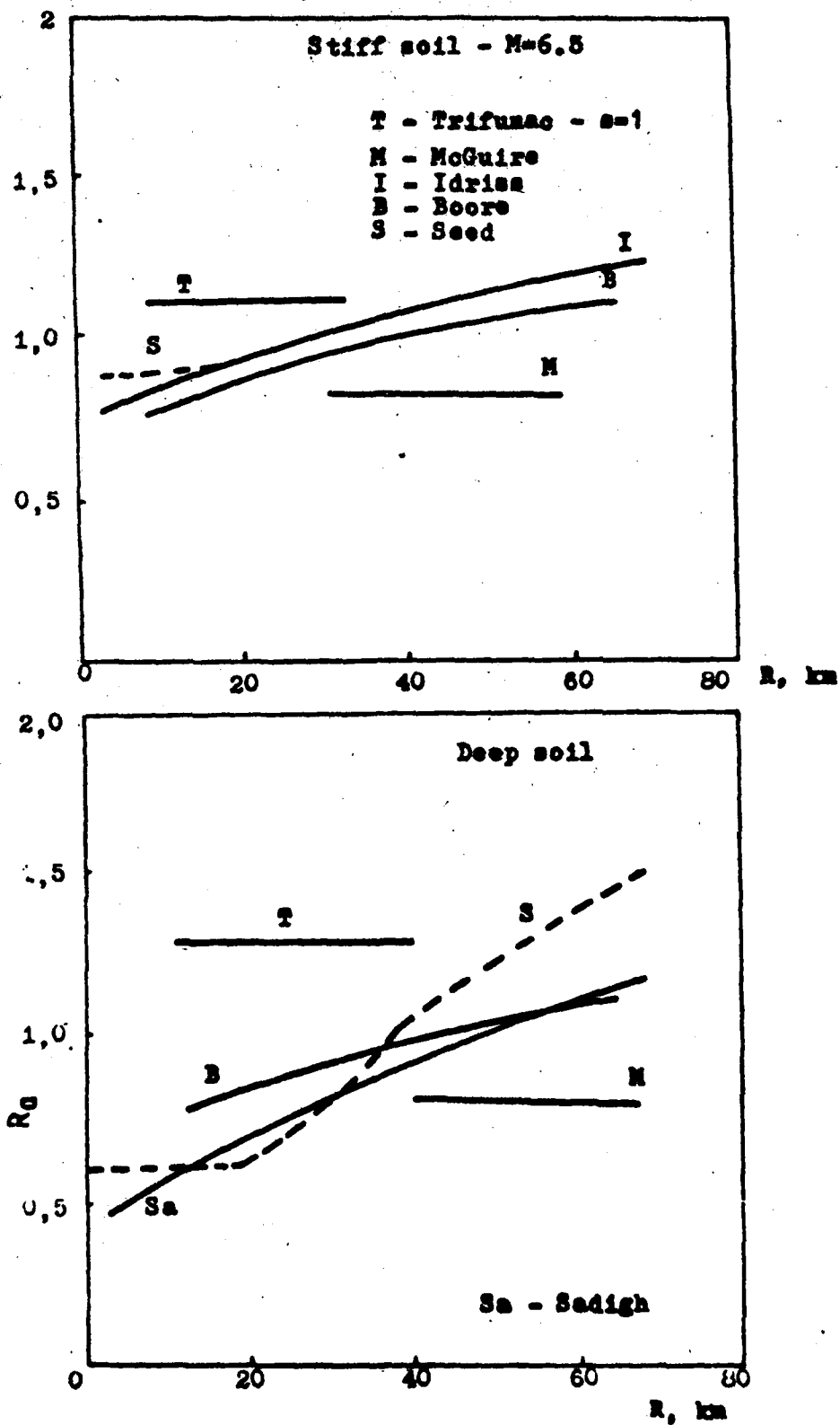


Fig. 11

Ratio  $R_a$  of PGA on soil sites vs PGA on rock sites

— AMBRASEYS (1973)  
 - - - ESTEVA and VILLAVARDE (1973)

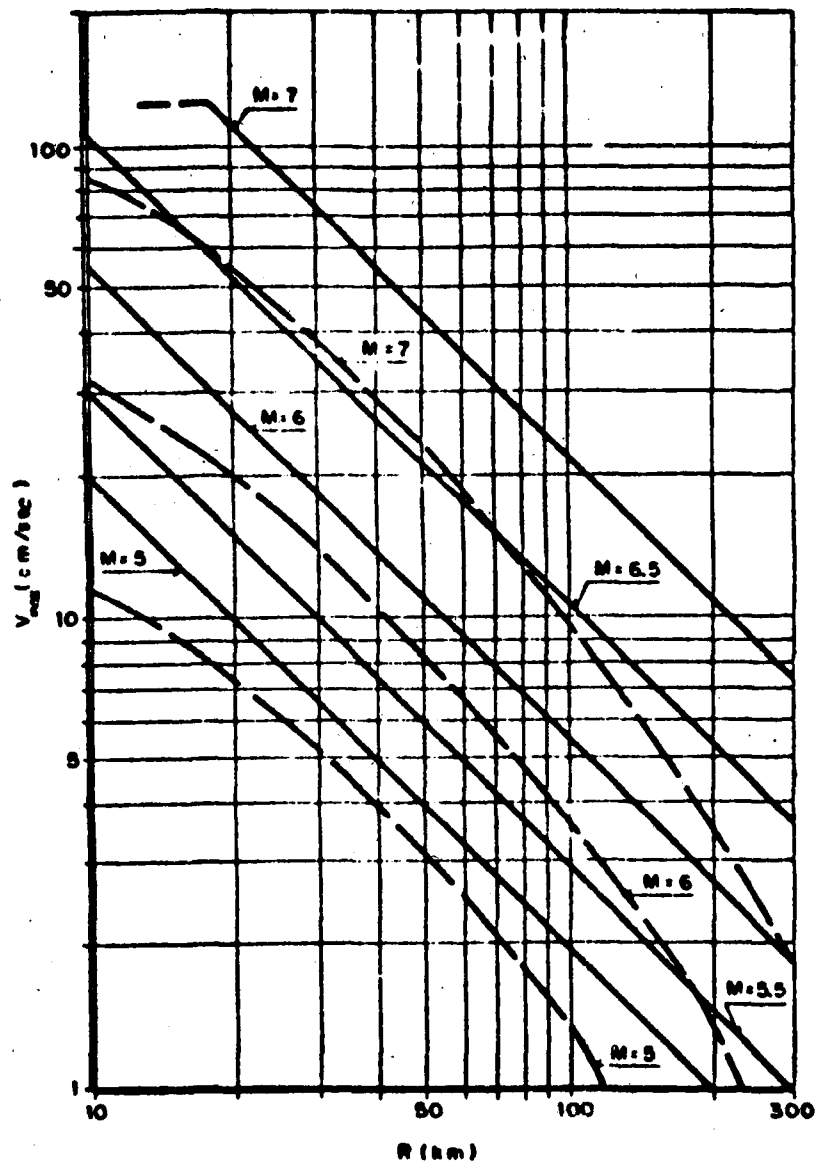


Figure 12

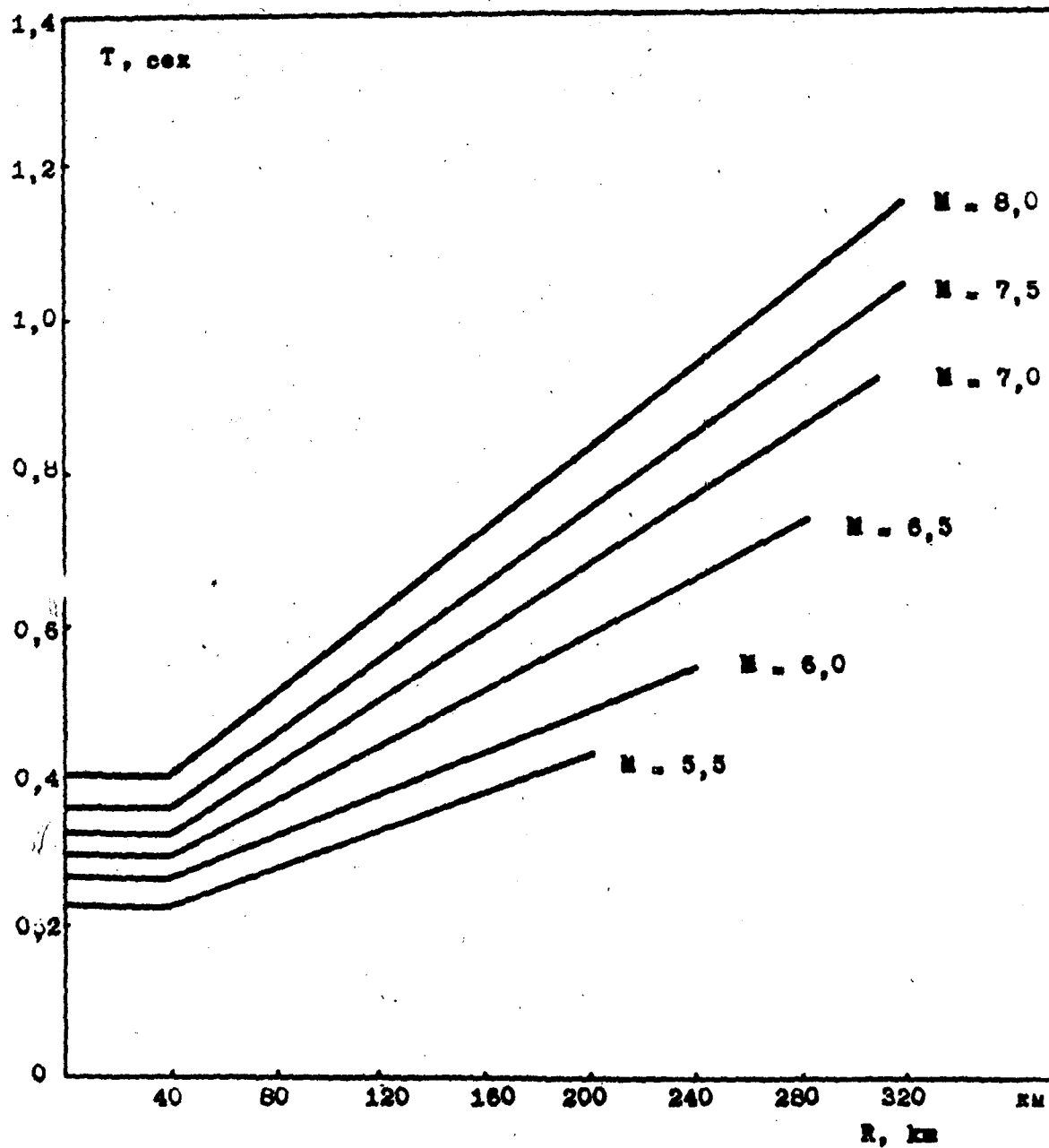
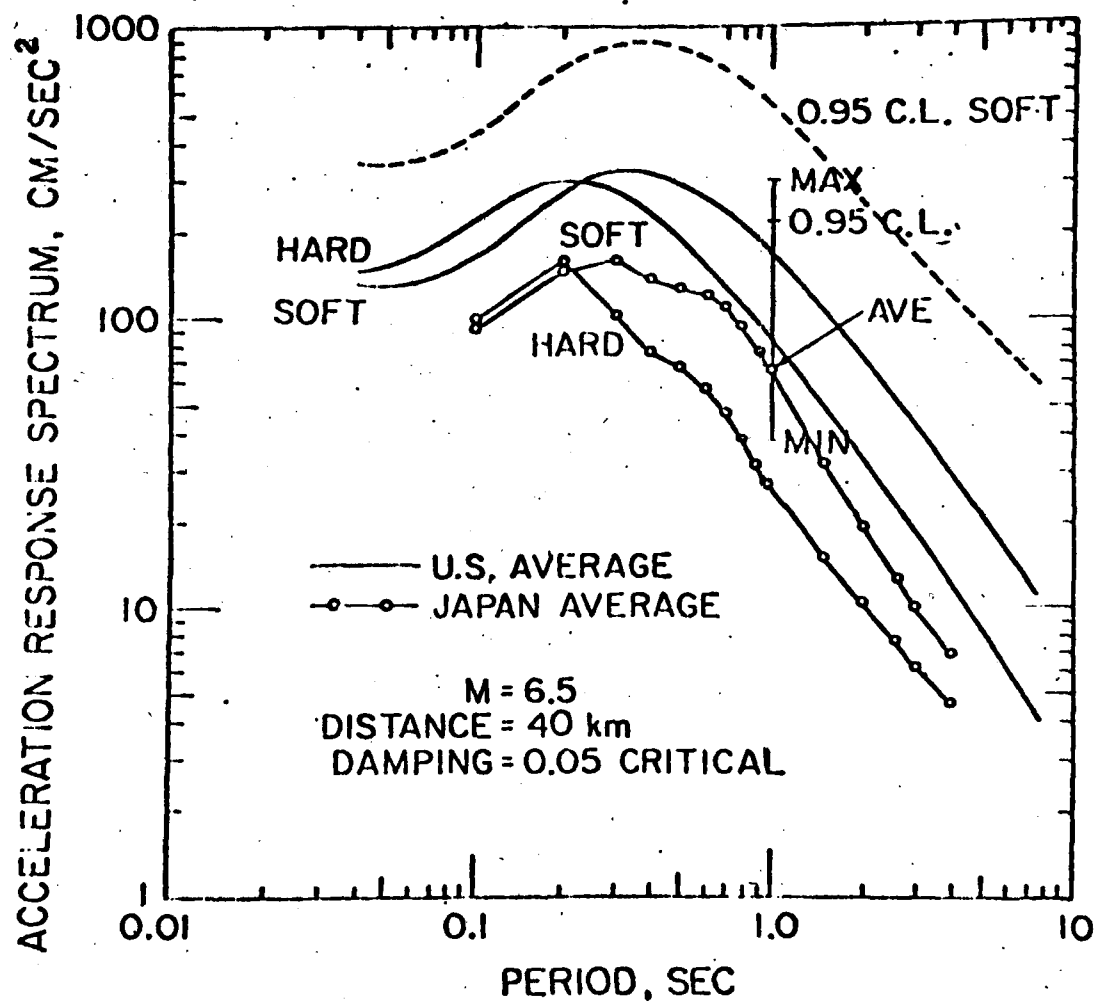


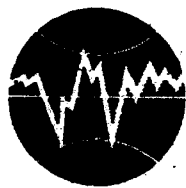
Fig. 13



AVERAGE ACCELERATION RESPONSE SPECTRUM  
AMPLITUDES FOR U.S. AND JAPANESE EARTHQUAKES

FIGURE 14





**TURKISH NATIONAL COMMITTEE FOR  
EARTHQUAKE ENGINEERING**

**THIRTEENTH REGIONAL SEMINAR ON EARTHQUAKE ENGINEERING**

**September 14-24, 1987 - Istanbul - Turkey**

**LECTURE NOTES**

**"EFFECT OF LIQUEFACTION ON BURIED STRUCTURES"**

**By**

**M. HAMADA**

**In**

**Istanbul, Turkey**

**SEPTEMBER 14-24, 1987**

## EFFECTS OF LIQUEFACTION ON BURIED STRUCTURES

### 1. INTRODUCTION

During large earthquakes in the past, the liquefaction of sandy ground has been one of the main causes of damage to various types of structures such as bridges, embankments, buildings, houses and lifeline facilities. Since 1964, when both the Niigata earthquake devastated Niigata City, particularly because of soil liquefaction, and the Alaska earthquake caused a vast area along the Pacific coast near Valdez City to slip into the sea due to liquefaction, the effect of liquefaction has been recognized as one of the most important factors to consider in designing earthquake resistant structures and numerous pertinent studies have been conducted on the mechanism of such liquefaction. Particularly, the factors which influence the occurrence of liquefaction, such as the grain size of the soil, the water level, and the intensity of the earthquake, have been analyzed.

Based on the result of these studies it has become possible to predict the probability of liquefaction. Some practical methods for the prediction of liquefaction were proposed and have been applied to planning measures to reduce earthquake hazards in urban areas. It can be said that at this time we can predict the areas of liquefaction and its degree with a certain level of accuracy by determining the soil conditions and expected intensity of the earthquake motion. To reduce earthquake hazards in areas which have a high probability of liquefaction, various kinds of countermeasures have been adopted, such as flexible joints for buried pipelines, gravel drainage around manholes, strengthening of foundations of buildings, etc.

These countermeasures are thought to have a considerable effect in reducing damage due to liquefaction. However, the effects have not been evaluated quantitatively, the reason being that the behavior of the liquefied soil layer and its effects on the deformation and behavior of structures have not been investigated enough.

Actually, it seems very difficult to discuss the behavior of the liquefied layers and their effects quantitatively, but investigating these problems is essential for establishing really useful countermeasures against liquefaction. And so, my lecture shall focus on the liquefaction-induced effects on structures, especially on the buried facilities of urban lifelines.

### 2. EFFECTS OF LIQUEFACTION ON STRUCTURES

The damage to structures caused by liquefaction includes the following:

- (i) Settlement and tilting of structures due to reduction in the bearing capacity of the foundation soil.
- (ii) Floating of underground structures in the liquefied soil layer due to buoyancy.
- (iii) Failure of retaining walls, quaywalls, etc., due to large increases in earth pressure.

- (iv) Failure of earth structures such as embankments due to decreases in the strengths of sandy soil materials.
- (v) Damage due to permanent ground displacement such as lateral spreading, slippage and cracks.

Structural damage due to permanent ground displacement, which was observed during two earthquakes in Japan, the 1964 Niigata quake and the 1983 Nihonkai-Chubu earthquake is discussed precisely in "3. PERMANENT GROUND DISPLACEMENT AND ITS RESULTANT DAMAGE."

In this chapter, the first four types of damage by liquefaction will be outlined using some actual examples.

#### Settlement and tilting

The liquefied soil layer loses a great deal of its bearing capacity because of increases in the pore water pressure. Structures and facilities without piles or caissons, which are not founded on a stable soil layer, may sink and/or incline due to the decrease of the bearing capacity. Photograph 1 shows a typical example of this type of damage, a four-story building without piles that collapsed, as a result of the 1964 Niigata earthquake. Photograph 2 shows another example, tilted water tank due to liquefaction and the spouted sand can be found around its foundation.

Most residential houses and lightweight facilities are directly based on the ground surface without piles and so many cases of damage have been reported in the liquefied area during past large earthquakes. However if structures are supported on stable foundations such as piles or caissons, damage either is very light or does not occur.

Photograph 3 shows an example of an undamaged frame for an above-ground pipeline with foundation piles in a liquefied area, where some sand volcanoes can be seen.

#### Floating of underground structures

Photograph 4 shows a floating sewage tank caused by the 1983 Nihonkai-Chubu earthquake. If the apparent unit weight of underground structures is less than that of the liquefied soil, around 1.7 to 1.8 t/m<sup>3</sup>, the structures will be caused to float by the buoyancy of the liquefied soil. During past earthquakes it was reported that numerous manholes of sewage lines and buried cables of electric and telecommunication floated up. As countermeasures against such floating, the improvement of the surrounding ground, gravel drainage and the weighting of structures have been proposed.

#### Failure of retaining walls and quaywalls due to increases in earth pressure

Many cases of failure of retaining walls and quaywalls due to liquefaction of the back-filled materials have been reported. Photograph 5 is an example of collapsed quaywalls in Akita harbour during the 1983 Nihonkai-Chubu earthquake. The quaywalls, which were constructed of steel sheet piles, completely collapsed. Some volcanoes and boiling sand can be found behind the concrete apron. Generally, in the practical design of quaywalls, the stability is examined by considering the

active earth pressure as an external force on the landward side, as well, as the passive earth pressure on the seaward side. If the backfill material on the landward side is liquefied, the earth pressure increases largely from the value of the active earth pressure. The coefficient of active earth pressure is generally below 0.5 but that of the liquefied soil layer is about 1.0. In some cases, to prevent liquefaction, backfill material with a high permeability such as gravel is used and/or the compaction is conducted insufficiently.

#### Failure of earth structures

Photographs 6 and 7 show typical examples of failure of embankments for roads and railways, respectively, caused by the 1983 Nihonkai-Chubu earthquake. Failure of earth structures such as embankments is the most common damage due to liquefaction. The decrease of the effective stress by an increase of the pore water pressure results in a great loss of the strength by the soil.

### **3. LIQUEFACTION-INDUCED PERMANENT GROUND DISPLACEMENT AND ITS RESULTANT DAMAGE**

Recently, large permanent ground displacement caused by liquefaction has been recognized as one of the main factors governing damage to structures during past earthquakes, in addition to the four types of damage.

During the 1964 Niigata earthquake, a large area along the Shinano River slipped toward the river with a horizontal magnitude above 8 m. Also, during the 1983 Nihonkai-Chubu earthquake a residential area on a sand dune slope with a slight gradient below 3% suffered lateral spreading with a magnitude of 5 m. Furthermore, in the United States, some instances of large permanent ground displacement have been reported. During the 1971 San Fernando earthquake, a gently sloped ground surface in the vicinity of the upper Van Norman Lake slid 2 to 3 m toward the lake due to the liquefaction of a loose, silty sand layer. Another example of permanent ground displacement was reported in a reclaimed area of San Francisco during the 1906 San Francisco earthquake.

From the examinations into the damage to structures in the liquefied area during these earthquakes, it can be assumed that a considerable part of the damage was caused by large permanent ground displacement. Therefore, in the earthquake resistant design of structures on and in ground with a high probability to be liquefied, it is necessary to take large permanent ground displacements into consideration in addition to the effects of liquefaction mentioned in Chapter 2.

In this chapter, some examples of permanent ground displacement during two earthquakes in Japan and their resultant damage to foundation piles, etc., shall be outlined.

#### Permanent ground displacement and its resultant damage during the 1964 Niigata earthquake

On June 16, 1964, the Niigata earthquake, with a magnitude of 7.5 occurred in the Japan Sea about 50 km off Niigata City. In the area along the Shinano River in Niigata City, buildings, bridges, oil storage tanks, lifeline facilities, etc., were extensively damaged by soil liquefaction.

The permanent ground displacement was measured by comparing two aerial surveys using photographs taken before and after the earthquake. The ground displacement can be measured by subtracting the coordinates obtained by the post-earthquake survey from those of the pre-earthquake survey.

The point where ground displacement were measured were selected at the sites of manholes, cadastral boundary stones and corners of drainage channels, which are fixed on the ground surface and which can be found in both pre- and post-earthquake photographs. The accuracy of the measurement was estimated as  $\pm 72$  cm in the horizontal direction.

Figure 1 shows the horizontal vectors of the permanent ground displacements along with the ground failures, such as sand boiling, and cracks. The permanent ground displacement is large along the Shinano River, with a maximum displacement of above 8 m in the proximity of the Hakusan power substation and on the left bank near the Bandai Bridge. The directions of the horizontal vectors of the displacements are almost perpendicular to the river.

The results, shown in Figure 1, show that the river width was greatly reduced by the earthquake. To verify this fact, an aerial photograph survey was performed, paying attention to the river widths before and after the earthquake. The width reduction was obtained by subtracting the river width measured from the aerial photograph taken in 1975, by which time the revetment had been completely restored, from that measured from the aerial photograph taken before the earthquake.

Figure 2 shows the reduction of the river width. Between the Bandai Bridge and the Yachiyo Bridge, where large permanent ground displacements occurred on both banks, the river width was reduced by 16 to 23.

Photograph 8 shows the left bank of the Bandai Bridge before and after the earthquake. Photo (a) was taken in 1962, two years before the earthquake, while photo (b) was taken in 1971, by which time the embankment had been completely restored. By comparing these photographs, it can be seen that the embankment, which was straight before the earthquake, became curved at the bridge abutment after the earthquake. This shows that in the vicinity of the abutment, the permanent ground displacements were reduced because of the high rigidity of the Bandai Bridge, a stone masonry arch bridge.

Kawamura, et al reported on the damage to the RC piles of a building (shown as N Bldg. in Figure 1) located north of Niigata Railway Station, which were found when the foundation was excavated for construction of the basement in 1985, about twenty years after the earthquake.

As shown in Figure 3 and Photograph 9, the piles were found to be broken at two positions, 2.5 to 3.5 m from the upper end and 2.0 to 3.0 m from the bottom. From the damage, the horizontal deformation of the pile was estimated to be 1.0 to 1.2 m, as shown in Figure 2.

The magnitude of the permanent ground displacement in this area is 1 to 2 m as shown in Figure 1, and coincides well with the pile deformation. Furthermore, the direction of the ground displacement vector is southeasterly, that is, toward the Niigata Railway Station, and is almost the same as that of the pile deformation shown in Figure 2. Therefore,

it can be assumed that the permanent ground displacements were the cause of the damage to the piles.

Figure 4 shows one example of subsurface soil condition along the section line C-C' shown in Figure 1 and liquefied layers estimated by the Factor of Liquefaction Resistance  $F_L$  proposed by Tatsuoka et al. The soil layer with  $F_L$  less than 1.0 was considered to have been liquefied.

As mentioned previously, large permanent ground displacements toward the river occurred on both banks. From the soil profile in this area (Figure (a)), the depth of the liquefied layer increases suddenly toward the river center and the lower boundary face of the liquefied layer is sloped. It can be assumed that the magnitude of the permanent ground displacements depended on the thickness and the inclination of the liquefied layer and also on the topographical condition of the existing revetment.

About 300 m from the river toward Niigata Railway Station, permanent ground displacements of 1 to 2 m occurred in the direction away from the river (as shown in Figure (b)). The ground surface in this area is flat, but the lower boundary face of the liquefied layer is estimated to be sloped with a small gradient of 2-3% toward Niigata Station. For this reason, the permanent ground displacements in this area were in the direction away from the river.

#### Permanent ground displacement during the 1983 Nihonkai-Chubu earthquake

The Nihonkai-Chubu earthquake, with a magnitude of 7.7, occurred in the Japan Sea about 90 km west of Aomori Prefecture on May 26, 1983, causing severe damage to the coastal area of the northern part of the main island.

Figure 6 shows one example of permanent ground displacement measured by using aerial photographs taken before and after the earthquake in the northern part of Noshiro City, where most of the urban area is built on sand dunes along the Japan Sea coast and the alluvial plane of the Yoneshiro River. Houses, buildings and lifeline facilities sustained severe damage, especially because of liquefaction.

The method of measurement is almost the same as in the case of the Niigata earthquake. The accuracy of the measurement was estimated within  $\pm 7$  cm in the horizontal direction.

As shown in Figure 5, permanent ground displacements were dominant in the west side of the Noshiro-Oga Road, which is gently sloped, and forms the transition area between the sand dunes and the alluvial plane. The displacement started from halfway down the sand dune, Sunadome Hill, and extended for about 800 m in a northerly or northeasterly direction. The maximum horizontal displacement in the northern area reached about 3 m, in the graveyard of Aoba-cho. The directions of the displacement are almost perpendicular to the cracks on the ground surface. Photograph 10 shows one example of cracks in the road leading to the graveyard in Aoba-cho, where the maximum horizontal displacement was 3.0 m.

On the other hand, the permanent ground displacements in the east side of the Noshiro-Oga Road, which is mostly flat and is located on the alluvial plane, were very small, at less than 1.0 m.

Figure 6 shows one example of the subsurface soil conditions along a section line, shown in Figure 4 (7-7'), and the estimated liquefied soil layers. The liquefied soil layers were estimated by calculating the Factor of Liquefaction Resistance  $F_L$ . From the figure it was found that a liquefied layer with a thickness of 2-5 m exists under the slightly sloped ground surface. Near the toe of the slope where the liquefied layers become thinner and the ground surface is flat, the permanent ground displacements become smaller. Therefore, the gradient of the ground surface and the thickness of the liquefied layer can be considered as influential factors acting on the magnitude of the displacement.

#### Factors Influential to the Magnitude of Permanent Ground Displacement

The types of permanent ground displacements caused by soil liquefaction during the 1964 Niigata and 1983 Nihonkai-Chubu earthquakes can be summarized as shown in Figure 7. Case A depicts the type of the displacements that occurred in Noshiro City; the ground surface is slightly inclined and the liquefied layer exists along the surface. Cases B and C depict the types found in Niigata City. Case B shows that the ground surface is flat on the land but has an abrupt vertical discontinuity at revetments of the river, and the lower boundary face of the liquefied layer is inclined towards the river center. Case C was found in the area around the Niigata Railway Station where the ground surface is almost horizontal but the lower boundary face of the liquefied layer is inclined.

Figure 8 shows that the correlation of the magnitude of the permanent ground displacement with the thickness of the liquefied layer is comparatively high. The result shown in Figure 7, which includes the data from the 1971 San Fernando earthquake in the U.S.A., suggest that the thickness is one of the factors governing the magnitude of permanent ground displacements.

Figure 9 shows the relationship between the ground surface gradient and the magnitudes of the permanent ground displacements. Although there are some contradictions among the data obtained from the three earthquakes, it can be concluded that the larger the gradient of the ground surface, the larger the magnitudes of the permanent ground displacements.

Figure 10 shows the relationship between the gradient of the liquefied layer's lower boundary face and the magnitude of the permanent ground displacements. In the case of the Niigata earthquake, the magnitude of displacement shows some correlation with the gradient, but no apparent correlation can be found for the Nihonkai-Chubu earthquake (shown as Noshiro in the figure). The reason for this may be due to the fact that most of the liquefied layer's lower boundary face in Noshiro is nearly horizontal and the magnitude of the displacements were mainly governed by the gradient of the ground surface.

Based on the study of the influential factors to the magnitude of the permanent ground displacement, the following regression formula was obtained:

$$D = 0.75 \cdot \sqrt{H} \cdot \sqrt{\theta}$$

Figure 11 shows a comparison between the permanent ground displacements estimated by the above formula and the measured values. Most of the data are within the two dotted lines in the figure which show the range in which the estimated displacements are 1/2 to twice the measured values.

#### 4. COUNTERMEASURES AGAINST LIQUEFACTION

The countermeasures, which have been adopted practically, is classified into following two categories:

- (i) Prevention of occurrence of liquefaction
- (ii) Reduction of effect of liquefaction on structures

##### Prevention of occurrence of liquefaction

The countermeasures for the first category can be grouped as follows by the principles of preventing liquefaction from occurring.

- (a) Increase the density of soil
- (b) Replace sandy soil
- (c) Soil solidification
- (d) Lower the ground water level
- (e) Dissipate pore water pressure
- (f) Prevent shearing deformation and lateral spreading of soil layer.

Among the above-mentioned countermeasures, the most popular method is by increasing the soil density. Various ways of increasing soil density have been developed, such as the sand compaction method, the vibroflotation method, the dynamic compaction method, etc., and they have been employed in actual constructions. The sand compaction method is generally adopted in Japan because of its effectiveness and reasonable cost.

##### Reduction of effect of liquefaction

As mentioned in Chapter 2, the main effects of liquefaction on structures are settlement and tilting due to reduction in the bearing capacity, floating due to buoyancy, damage due to increasing earth pressure, damage due to lateral spreading and permanent ground displacement.

As regards underground structures such as buried pipes, manholes and in tanks, damage due to floating and settlement were reported during past large earthquakes. To reduce this kind of damage following countermeasures can be considered:

- (i) Use of flexible joints for buried pipes
- (ii) Dissipate water pressure around manholes by means of gravel drainage.

Various kinds of flexible joints have been developed and have already been adopted in actual constructions. These joints may show high



effectiveness in reducing the damage due to settlement, rising-up, as well as permanent ground displacement.

The drainage by gravel around the manhole have recently been recognized as one of effective countermeasures. In order to confirm its efficiency some experimental studies using shaking tables are being conducted. Figure 12 shows one example of the idea of gravel drainage for manhole. Similar countermeasures have been used for the common conduit for electricity, telecommunication, water and sewage.

#### REFERENCES

Hamada M., Yasuda S., Isoyama R. and Emoto K.: A Study on Liquefaction Induced Permanent Ground Displacements. Association for the Development of Earthquake Prediction, Tokyo, Japan, Nov., 1986

Noshiro City: The 1983 (May 26) Nihonkai-Chubu Earthquake; A Document of the Hazard Experienced in Noshiro City, 1984 (in Japanese).

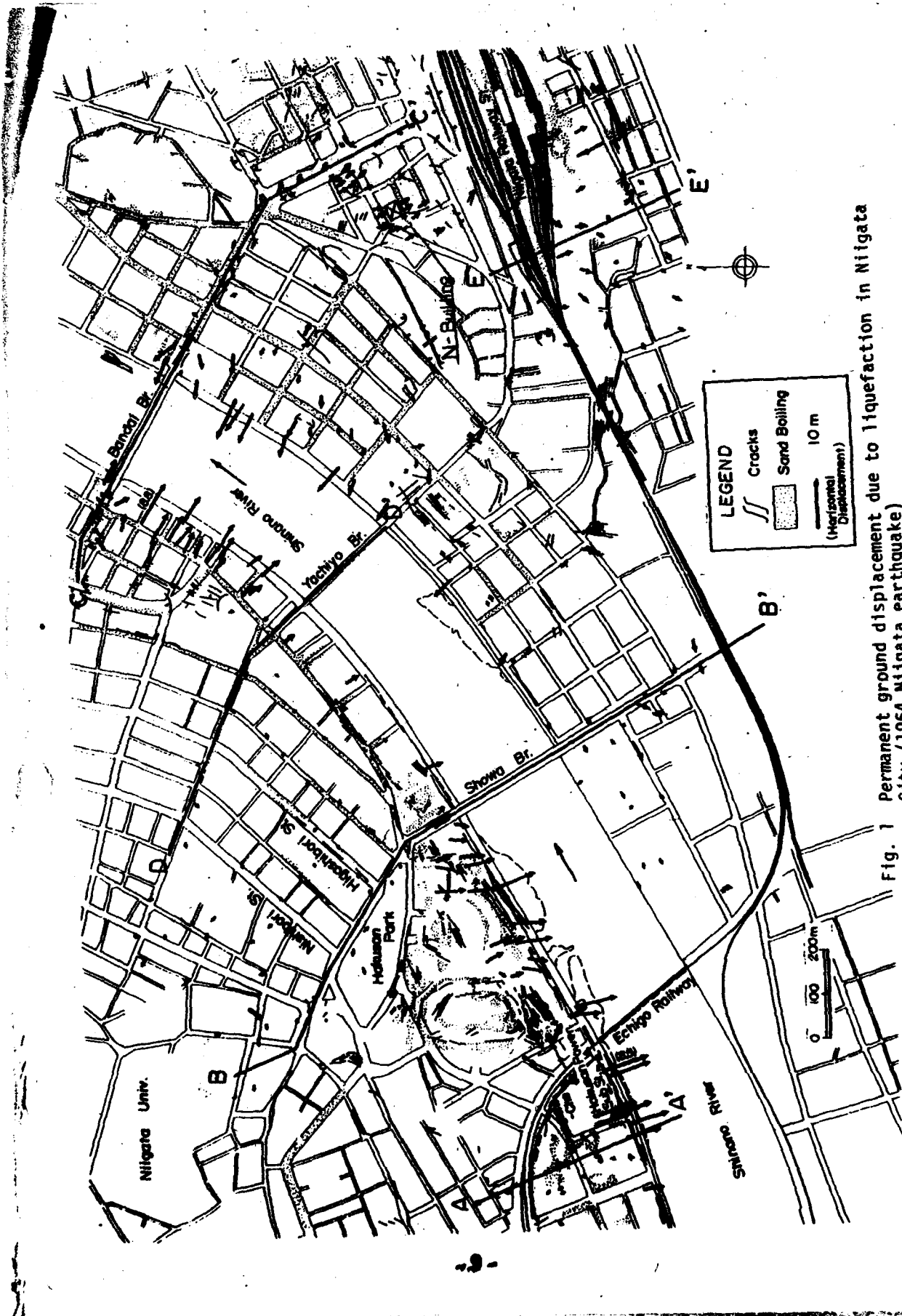
Iwasaki T., Tatsuoka F., Tokida K., and Yasuda S.: A Practical Method for Assessing Soil Liquefaction Potential Based on Case Studies at Various Sites in Japan, Proceedings of the Fifth Japan Earthquake Engineering Symposium, 1978 (in Japanese)

Niigata University, et al: Map of Ground Failure during the 1964 Niigata Earthquake, 1964.

Youd T.L.: Landslides in the Vicinity of the Van Norman Lakes, U.S. Department of Commerce, The San Fernando, California Earthquake of February 9, 1971, Geological Survey Professional Paper 733, 1971.

O'Rourke T.D. and Tawfik M.S.: Effects of Lateral Spreading on Buried Pipelines during the 1971 San Fernando Earthquake, PVP-Vol. 77, Earthquake Behavior and Safety of Oil and Gas Storage Facilities, Buried Pipelines and Equipment, ASME, 1983.

Kawamura S., Nishizawa T., and Wada H.: Damage to Piles due to Liquefaction Found by Excavation Twenty Years after Earthquake, Nikkei Architecture, 1985 (in Japanese).





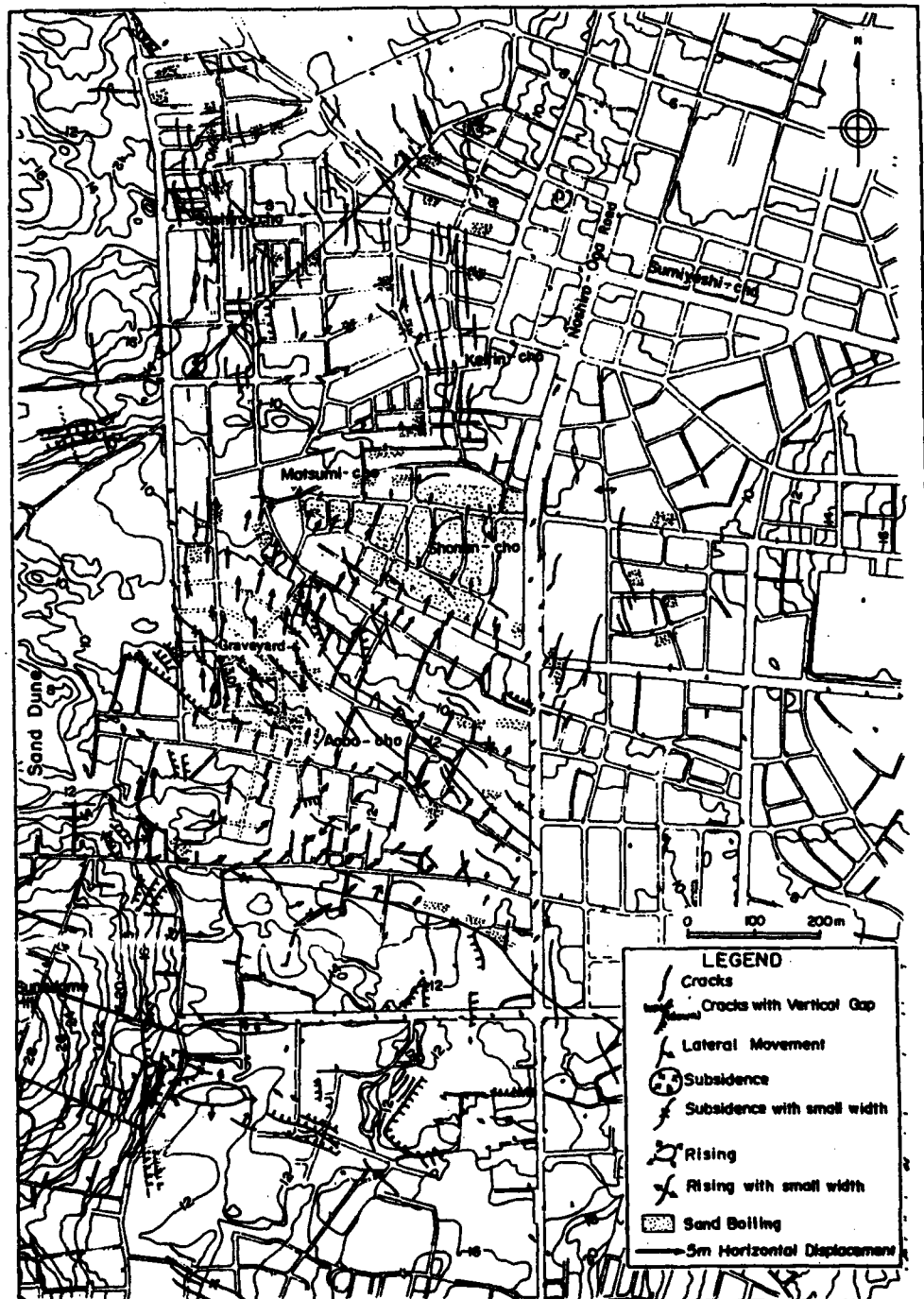


Fig. 5 Permanent ground displacement in northern part of Noshiro City (1983 Nihonkai-Chubu earthquake)

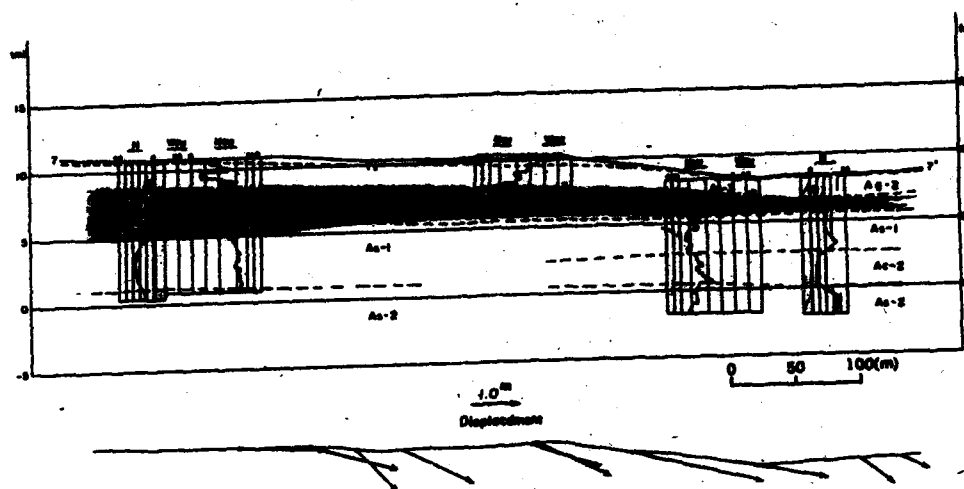
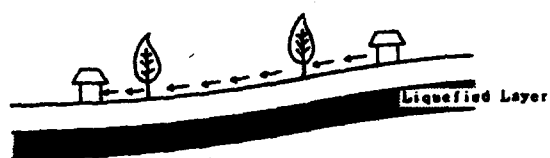
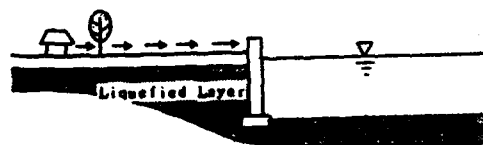


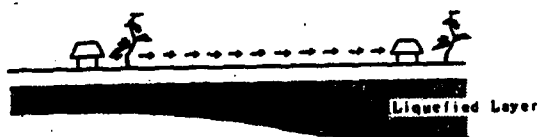
Fig. 6 Soil profile and estimated liquefied layers



CASE A



CASE B



CASE C

Fig. 7 Types of permanent ground displacement

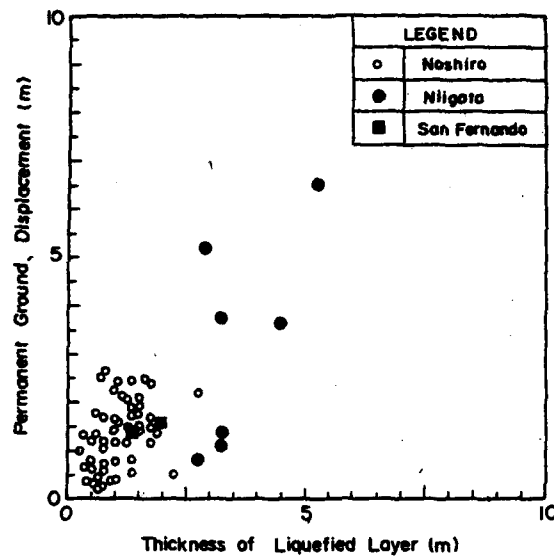


Fig. 8 Relationship between the magnitude of permanent ground displacement and the thickness of liquefied layer

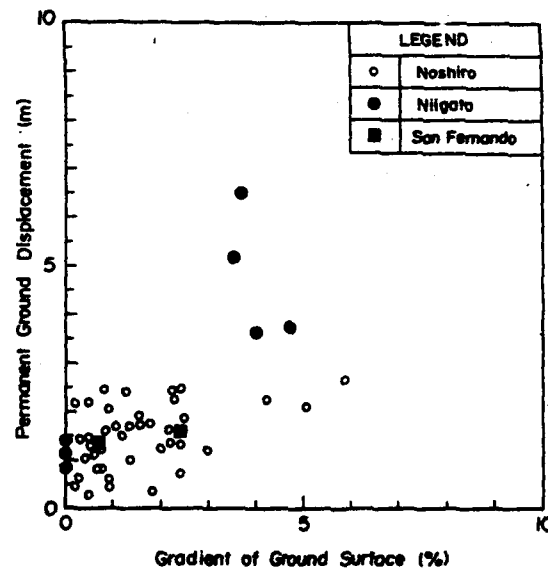


Fig. 9 Relationship between the gradient of ground surface and the magnitude of permanent ground displacement

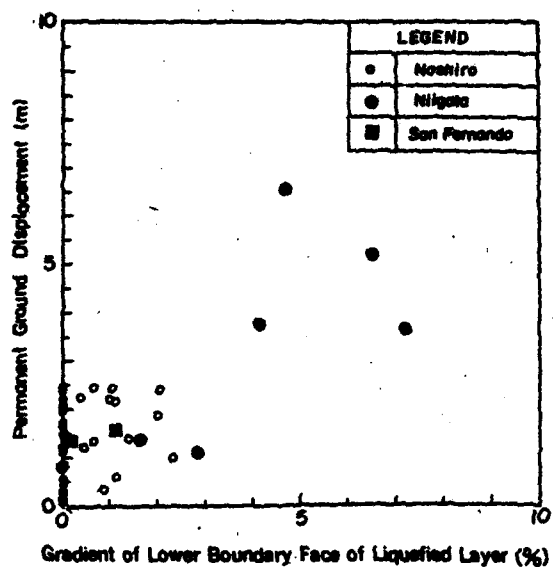


Fig. 10 Relationship between the gradient of lower boundary face of liquefied layer and the magnitude of permanent ground displacement

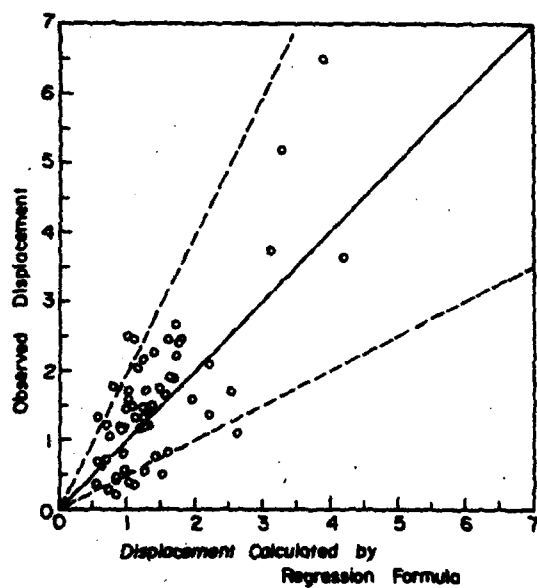


Fig. 11 Comparison of the displacement estimated by regression formula with the observed displacement

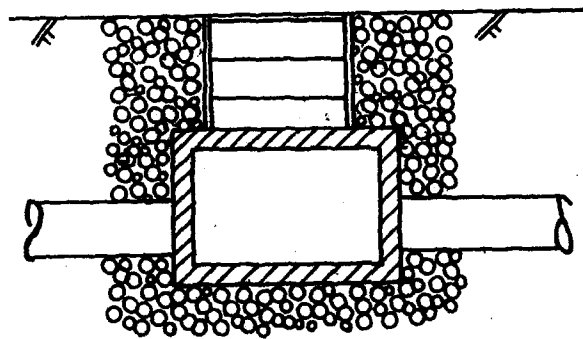


Fig. 12 Gravel drainage around manhole



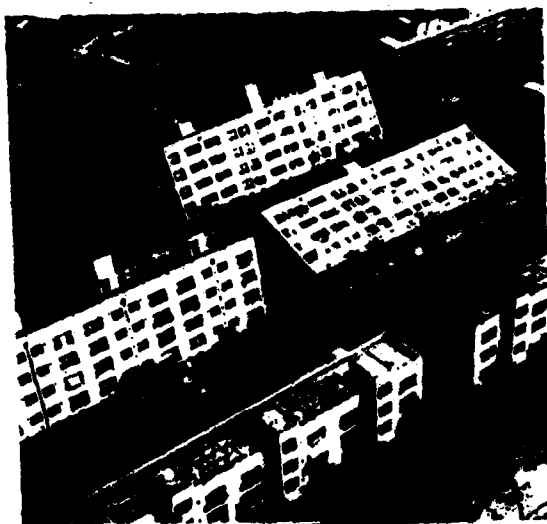


Photo 1 Collapsed R.C. building due to liquefaction  
(1964 Niigata earthquake)

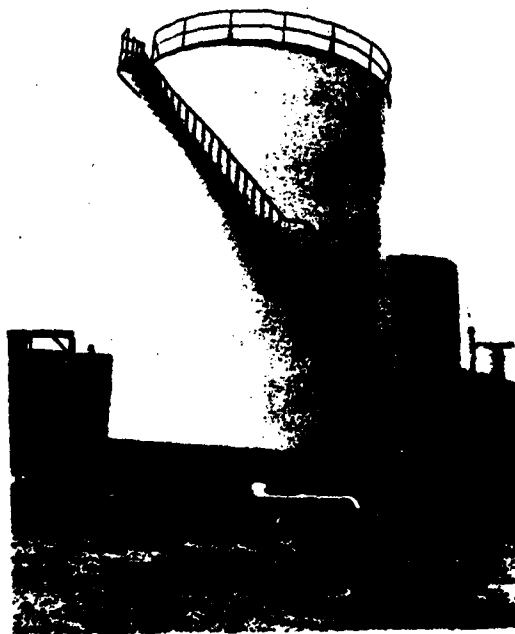


Photo 2 Tilted water tank (1983 Nihonkai-Chubu earthquake)

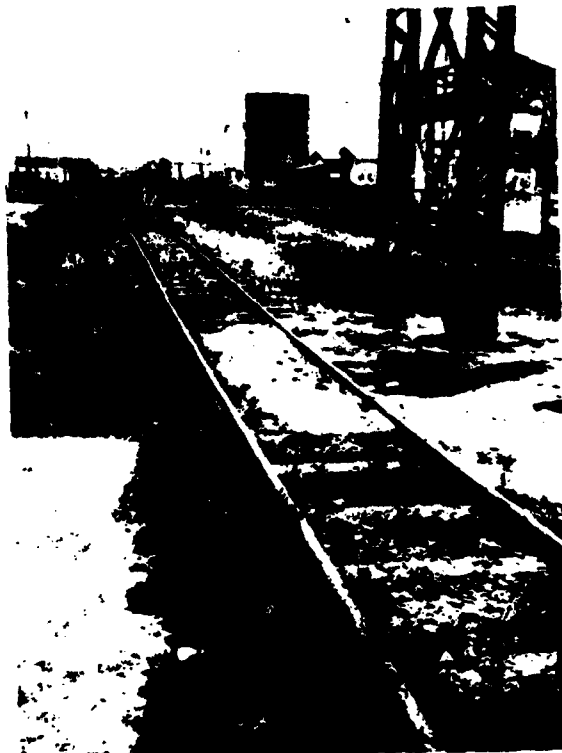


Photo 3 Undamaged steel frame with foundation piles  
(1983 Nihonkai-Chubu earthquake)

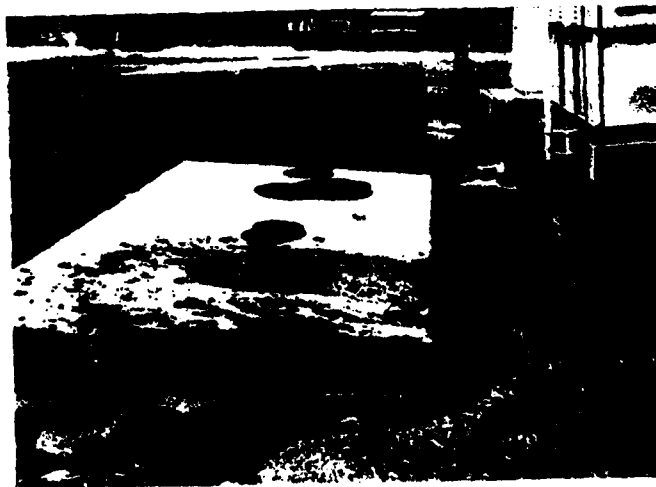


Photo 4 Lift-up of inground sewage tank  
(1983 Nihonkai-Chubu earthquake)



Photo 5 Collapsed quay wall (1983 Nihonkai-Chubu earthquake)



Photo 6 Failure of road embankment (1983 Nihonkai-Chubu earthquake)

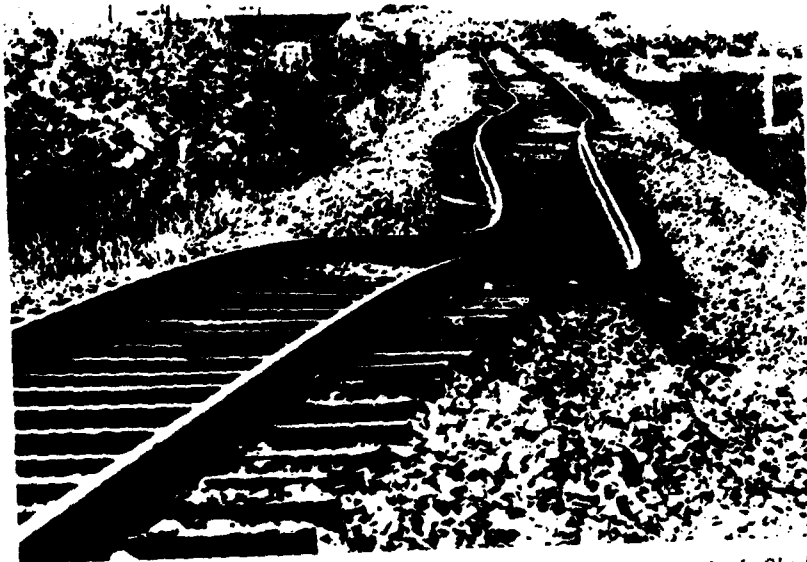


Photo 7 Failure of railway embankment (1983 Nihonkai-Chubu earthquake)



(A) Before the earthquake



(B) After the earthquake

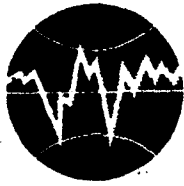
Photo 8 Left bank of Bandai Bridge



Photo 9 Damage to RC pile



Photo 10 Cracks with subsidence on road



**TURKISH NATIONAL COMMITTEE FOR  
EARTHQUAKE ENGINEERING**

**THIRTEENTH REGIONAL SEMINAR ON EARTQUAKE ENGINEERING**

**September 14-24, 1987 - Istanbul - Turkey**

**DETERMINATION OF LIQUEFACTION POTENTIAL BY CYCLIC STRAIN APPROACH**

**Kosta TALAGANOV<sup>1)</sup>**

## DETERMINATION OF LIQUEFACTION POTENTIAL BY CYCLIC STRAIN APPROACH

Kosta TALAGANOV<sup>1)</sup>

### ABSTRACT

The report presents the results of the investigations carried out for definition of the liquefaction potential of soils of level site by cyclic strain and of the dynamic response of soils in which the increase of pore water pressure is possible. The approach with cyclic strains is a new and less investigated aspect of the liquefaction phenomenon.

The investigations consist of experimental, analytical and application part. The experimental part consists of laboratory testing of sand models subjected to cyclic strains. The analytical part comprises analysis of the experimental results and establishment of a function of the liquefaction parameters and the dynamic response of saturated soils in which the increase of the pore pressure is possible. Within this part, models and methods for analysis of the nonlinear dynamic response of soils have been developed. In the application part, performing a comparative analysis of the dynamic response of models at sites of the Montenegro coast, where liquefaction was observed during the earthquake of April 15, 1979, a verification of the developed methodology for analysis of the nonlinear dynamic response of soils was carried out.

---

<sup>1)</sup> Professor, Institute of Earthquake Engineering and Engineering Seismology (IZIIS), University "Kiril and Metodij", Skopje, Yugoslavia.

## 1. INTRODUCTION

The vibratory ground motions caused by earthquakes may cause a loss of soil strength resulting in serious damage. Typical forms are settlement and tilting of buildings and civil engineering structures. Disastrous yielding of soil mass in coastal areas and dams are also observed, as well as landslides, failure of slopes and other hazards.

The process leading to such loss of strength or stiffness is called soil liquefaction. It is a phenomenon associated primarily, but not exclusively, with saturated cohesionless soils /8/.

Almost no earthquake has happened in the world which had not been accompanied by liquefaction /12/. Table T.1.1. gives a list of well-known past earthquakes accompanied by liquefaction.

While the early investigations of this phenomenon were apparently motivated by the dramatic occurrence of liquefaction during the earthquakes in Niigata and Alaska in 1964, the impetus for prompting the study of liquefaction has been supplied incessantly by a series of large earthquakes that have occurred since then throughout the seismically active regions of the world /22/.

For the last two decades after 1964, a great advance has been made in the recognition of the liquefaction phenomenon and the development of the technology for mitigation of the risk associated with this phenomenon. However, many of its aspects are still to be investigated /8/.

The results of the investigations prove that this phenomenon is mainly characteristic for the cohesionless water-saturated sandy soil masses. Dynamic excitation due to earthquakes, mainly shear waves, result in relative displacement of soil grains and a tendency of volume change. In conditions of water-saturation and impossibility of fast drainage, this tendency cannot be realized in the form of volume change. Thus, it is manifested in the form of pore pressure increase as a result of the transfer of the gravity loads from the soil structure to pore water. This process may induce the state of  $(\sigma' = 0)$ , when practically a total reduction in initial effective stresses takes place in soil, which practically means loss of strength. Such a state is globally defined as initial liquefaction occurrence and, depending upon the possibilities of preserving this state and the consequences expressed through the strain level, it further obtains different forms and definitions. This process is illustrated in Fig. 1.1.

The laws of pore pressure increase ( $u$ ), reduction in soil strength and development of shear strains are the basic parameters explaining and defining the process initiating the state of  $(\sigma' = 0)$ .

In the investigations performed so far, these laws have been defined on the basis of shear stresses ( $\tau$ ) as an expression of the dynamic excitation and dynamic soil strength. The number of equivalent cycles ( $N$ ) having amplitude ( $\tau$ ) are representing the excitation energy or its potential. The concept of the dimensionless stress ratio

$$R_\tau = \tau / \sigma'_0$$

simplifying these laws has also been developed. Typical laws of occurrence of  $(\sigma' = 0)$  expressed through  $(R_\tau)$  and  $(N)$ , obtained by laboratory testing of sands are presented in Fig. 1.2. As can be observed, these



**Table T.1.1. A list of known recent earthquakes accompanied by  
liquefaction**

Earthquake	Year	Magnitude	Reference
ALASKA, USA	1964	8.4	KEEFER 1981 /25/
NIIGATA, Japan	1964	7.5	SEED, IDRIS 1967/38/
CARACAS, Venezuela	1967		DOBRY, 1982 /12/
TOKACHI-OKI, Japan	1968	7.9	ISHIHARA, 1985 /22/
PERU	1970	7.8	KEEFER, 1981 /25/
MADANG, New Guinea	1970	7.0	KEEFER, 1981 /25/
SAN FERNANDO, USA	1971	6.5	SEED et al. 1975 /12/
HAICHENG, China	1974		SHENGCONG, TATSUOKA, 1984 /45/
GUATEMALA	1976	7.6	SEED et al. 1979 /25/
FRIULI, Italy	1976	6.5	SIRO, WYLLIE, 1979 /25/
TANGSHAN, China	1976	7.7-7.9	SHENGCONG, TATSUOKA, 1984 /45/
SAN JUAN, Argentina	1977	7.2-7.4	DOBRY, 1982 /12/
VRANCEA, Rumania	1977	7.2	PERLEA, 1984 /45/
MIYAGI-KEN-OKI, Japan	1978	7.4	IWASAKI, TOKIDA, 1978/25/
MONTENEGRO, Yugoslavia	1979	7.2	TALAGANOV, 1980 /42/
IMPERIAL VALLEY, USA	1979		YOUD, 1983 /45/
MAMMOTH LAKES, USA	1980	6.0	KEEFER, 1981 /25/
NIHONKAI-CHUBU, Japan	1983	7.7	ISHIHARA, 1985 /22/

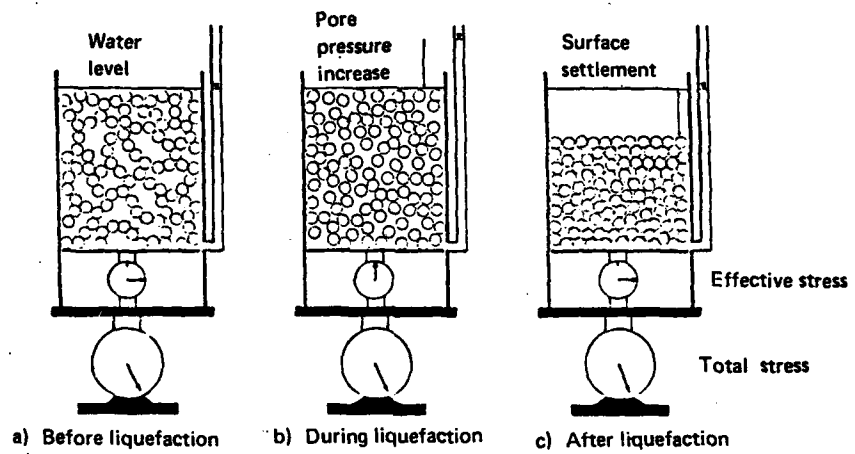


Fig. 1.1. Liquefaction mechanism of water saturated cohesionless materials (Ishihara 1985/22/)

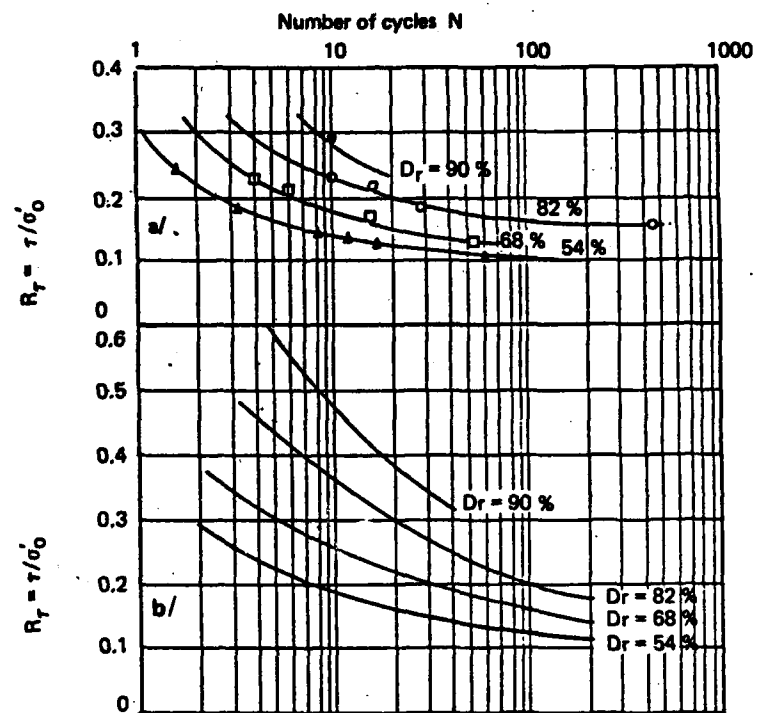


Fig. 1.2. Typical results of laboratory testing by cyclic shear stress: relationships between  $(\tau/\sigma'_0)$  and  $(N)$  for different  $(D_r)$  and pore pressure of 100% (a), i.e., shear strains  $\pm 5\%$  (b) (Seed 1979/40/)

laws are influenced by the relative density of sands ( $D_r$ ) to a great extent. However, a large number of other factors are also influencing these laws like the geological conditions of soil evolution, its history, the grain size distribution characteristics, the initial stress state, etc.

Although some investigations have been made even before the earthquake of Niigata of 1964, the actual development has begun after this earthquake. A large number of scientists have contributed to the explanation of the liquefaction phenomenon by using the concept of ( $\tau$ ) and ( $R_f$ ). The first investigations were carried out by Seed and collaborators 1966 /37/, 1967 /38/, 1968 /32/, 1971 /39/. Further development was especially associated with the investigations performed by Seed et al. 1979 /40/, 1981 /41/, and Ishihara et al. 1977 /17/, 1978 /18/, 1980 /20/, 1981 /21/. As it is impossible to review all the investigators, only the latest State-of-the-Art papers by Yoshimi et al. 1977 /46/, Finn 1981 /15/ and Ishihara 1985 /22/ will be mentioned.

The definition of the critical porosity distinguishing sands liable to liquefaction and those in which only cyclic mobility may occur has also contributed to the explanation of the liquefaction phenomenon. This approach, which is based on behaviour of sands under static loads, has especially been investigated by Casagrande 1971 /4/ and Castro 1975 /5/.

The presented approaches associated with the recognition of the process which leads to liquefaction occurrence are considered to be conventional. However, for the last few years, another aspect of the investigation of this process has been developed. It is the cyclic shear strain ( $\gamma$ ) approach. Although little experience has been acquired considering this approach, it initiates the possibilities for definition of the liquefaction parameters. The need of investigations using this approach has been supported by the results obtained during the investigations carried out by Dobry et al. 1981 /11/, 1982 /12/, 1985 /8/. This approach is suggested to be necessary for further investigations given under /8/.

The dynamic response of soil in which pore pressure increase is possible and the process of this increase initiating liquefaction are fundamental aspects of soil liquefaction. The investigations of these aspects by using the cyclic shear strain approach are the main goals of the investigations presented herein.

## 2. LABORATORY TESTS

The laboratory tests of soils have been very important stage in the investigation of the liquefaction phenomenon. The result of these tests is the experimental definition of the liquefaction parameters as dependent upon the characteristics of both models and the dynamic excitation.

This phenomenon has extensively been investigated by using different laboratory equipment; however, the dynamic excitation with controlled shear stresses has mainly been used. On the basis of the obtained results, corresponding methods have been developed aimed at determination of the liquefaction potential in soils.

Based on the data available in the literature in this field, only few and partial tests applying dynamic excitation with controlled

shear strains have been carried out. Thus, different opinions and recommendations on the needs of such tests and the advantages they offer have been presented /8, 11, 12/.

According to the investigation concept presented herewith, laboratory tests of sands under dynamic excitations with cyclic shear strains represent a basis for development of methods of analysis for the liquefaction potential in sands.

## 2.1. Tested Materials

Laboratory tests have been carried out on samples made of sands taken from the surface at two sites in the Montenegro coast. The sites are Bijela and Baošić. During the Montenegro earthquake of April 15, 1979, typical liquefaction was observed at these sites. In the liquefaction process, the sand from the depth was thrown out on the site surface /42, 43/.

The grain size distribution curves of sands have been shown in Fig. 2.1.1.

## 2.2. Laboratory Equipment and Investigation Procedures

Laboratory tests have been accomplished by using laboratory equipment with a direct dynamic shear loading (Dynamic Simple Shear Device - DSSD) in the Soil Dynamic Laboratory at IZIIS - Skopje.

The equipment has possibilities for direct applying of cyclic shear stresses and strains. The dynamic excitation was applied to the sample in such a way as to simulate the excitation of actual ground conditions under shear waves due to an earthquake. The strain range is very wide and it practically covers the strains of interest. It ranges from approximately ( $10^{-4}\%$ ) to almost (5%). Taking into account the options and possibilities, it can be concluded that the dynamic stress-strain state can successfully be simulated with this equipment.

The sand samples are built in and tested as dry ones. The tests for investigation of conditions for liquefaction occurrence are carried out for the case of a constant sample volume. As a result of given dynamic excitation, the dynamic response of the model is obtained, which results in a change in the grain structure and a simultaneous decrease in the initial vertical stress ( $\sigma'_{10}$ ). The decrease of ( $\sigma'_{10}$ ) is proportional to the increase of the pore pressure ( $u$ ) in saturated models. According to this concept, the dynamic behaviour of the water saturated soil medium is related to the behaviour of the solid structure, that is the soil grains. As an approach, it is used in many investigations and especially in /14/ and /27/.

The stress-strain state of the model is shown in Fig. 2.2.1.

The investigation procedure comprises three basic stages:

- The first stage includes preparation of samples for testing. In this stage, samples were built in by dry compaction, using a wooden hammer up to the planned initial relative density, taking into account that after the consolidation, the expected planned final relative density ( $D_r$ ) is obtained.

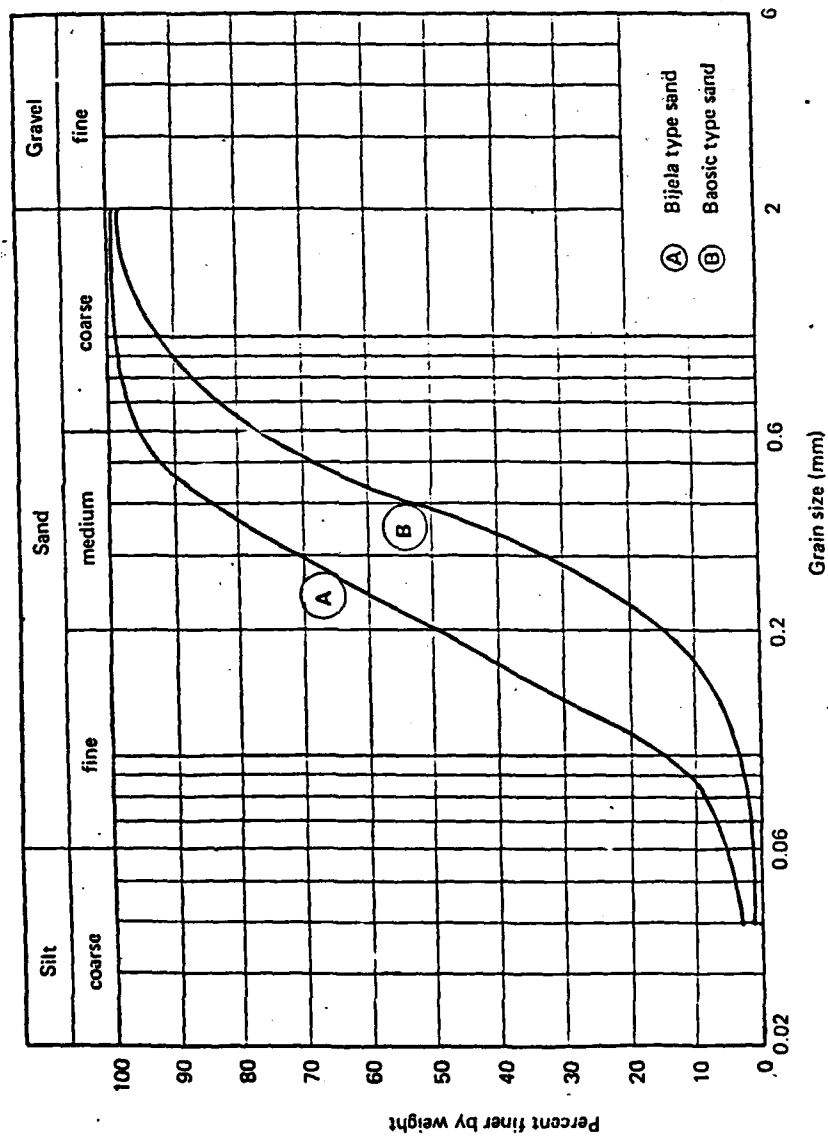


Fig. 2.1.1.1. Grain size distribution curves of sand, types Bijela and Baosic

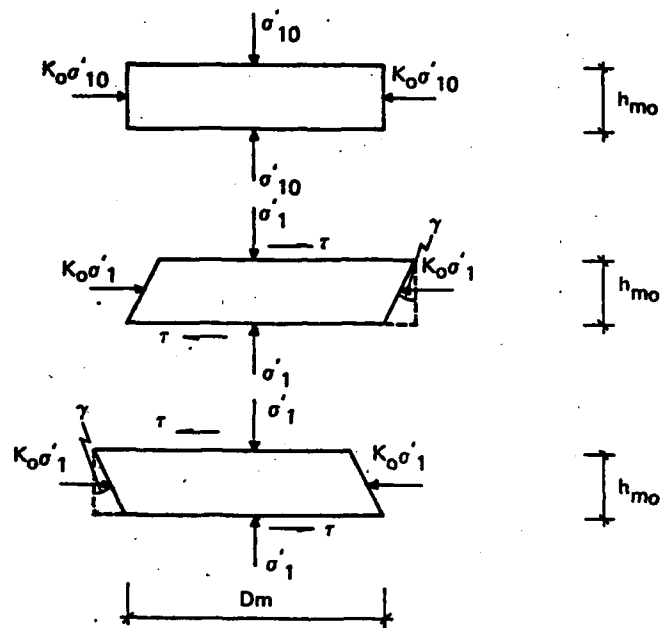


Fig. 2.2.1. Stress-strain state of the model tested by cyclic simple shear apparatus under constant volume

- The second stage comprises the consolidation of the samples under static loads. The samples are consolidated with planned initial stress ( $\sigma'_{10}$ ). Stresses were gradually applied with parallel observation of the vertical settlements. The process continued after the application of the full value of ( $\sigma'_{10}$ ), practically up to the end of the vertical settlements. To this state corresponds the final relative density ( $D_r$ ). A range of ( $D_r$ ) from (40-45%) to (80-85%) was applied. The stresses ( $\sigma'_{10}$ ) have values of (100), (200) and (300 kN/m<sup>2</sup>).
- The third stage represents the direct dynamic testing.

Tests were carried out applying series of cyclic shear strains ( $\gamma$ ) under the conditions of constant volume. Strains have been applied in the range of (0.2%) to (2%), respectively. Certain number of tests were carried out applying strains smaller than (0.2%). At the same time, both observed and recorded were the shear stresses ( $\tau$ ) which correspond to the applied strains ( $\gamma$ ) as well as the decrease of ( $\sigma'_{10}$ ). Also, the nonlinear relationships ( $\tau/\gamma$ ) have directly been recorded.

### 2.3. Results with Cyclic Strains ( $\gamma$ )

For each tested sample, the following results have been obtained by applying cyclic strains:

- time history of shear stresses ( $\tau/N$ );
- time history of cyclic strains ( $\gamma/N$ );
- time history of decrease in effective stresses, ( $\sigma'_1/N$ ), that is in the increase of the pore pressure ( $u/N$ ),
- time history of nonlinear relationships ( $(\tau/\gamma)/N$ ).

In the results, the time is represented through the number of cycles ( $N$ ).

### 3. ANALYSIS OF LABORATORY RESULTS AND DEFINITION OF ANALYTICAL RELATIONSHIPS OF LIQUEFACTION PARAMETERS AS STRAIN DEPENDENT

From the laboratory tests, many data about the behaviour and the response of the tested sand models under the applied cyclic excitation with controlled shear strains have been obtained. These results define the occurrence and development of the pore pressure, the nonlinear stress-strain relationships under cyclic shears and their transformation due to pore pressure development, that is the decrease of the dynamic shear moduli. The results define also the decrease in shear stresses in the case of excitation with controlled cyclic strains.

A special reference was given to the occurrence and development of the pore pressure, the occurrence of ( $\sigma'_1=0$ ) and the decrease in the dynamic shear moduli. Based on the results, the analytical relationships between these parameters and the shear strain level, and the duration expressed through the number of the applied cycles, have been defined.



### 3.1. Relationships for Liquefaction Occurrence

Due to the effects of the cyclic excitation with controlled shear strains in dry sand models, in the case of a constant volume, a decrease in the initial stresses takes place. According to the concept of the applied methodology and laboratory equipment, as shown in Chapter 2, the decreasing of stresses is directly proportional and equal to the occurrence and development of the pore pressure.

Fig. 3.1.1. shows a typical series of cyclic strains ( $\gamma$ ) and the corresponding decreasing of vertical stresses. It can be seen that within the frames of a half-cycle ( $n$ ), the vertical stress is not a constant one, but cyclic. Its frequency is two times larger than the frequency of ( $\gamma$ ). The minimum values are obtained for ( $\gamma=0$ ), while the maximum ones -when ( $\gamma$ ) reaches its extreme values.

Let us denote the following parameters:

- $(\sigma'_1)$  - envelope effective vertical stress, which is minimum during one half-cycle ( $n$ )
- $(\sigma'_{1r})$  - residual effective vertical stress, which is maximum during ( $n$ )
- $(\Delta\sigma'_1)$  - variation of the effective vertical stress during ( $n$ ),

as shown in Fig. 3.1.1.

Applying ( $\gamma$ ) and increasing ( $N$ ), both  $(\sigma'_1)$  and  $(\sigma'_{1r})$  decrease intensively at the beginning and then at a slower rate.  $(\Delta\sigma'_1)$  varies with the increase of ( $N$ ). By excluding the first semi-cycle,  $(\Delta\sigma'_1)$  generally decreases with the increase of ( $N$ ).

However, since ( $u$ ) is proportional to  $(\sigma'_1)$ , these properties will be studied in more details in Section 3.2. We will consider at this stage the characteristic case when  $(\sigma'_1)$ , which decreases gradually, is completely reduced to the value of:

$$\sigma'_1 = 0 \quad (3.1.1)$$

The state when  $(\sigma'_1=0)$  corresponds to the occurrence of an excessive pore pressure which equals the initial effective stress  $(\sigma'_{10})$  and which is also defined as occurrence of ( $u$ ) of (100%):

$$u = \sigma'_{10} \quad (3.1.2)$$

$$(u/\sigma'_{10}) \cdot 100 = 100\% \text{ for } u = \sigma'_{10}$$

The state when  $(\sigma'_1=0)$  starts for the purpose of these tests is defined as initial liquefaction. The behaviour of soil from the moment when the state  $(\sigma'_1=0)$  is reached and further on, depends upon the soil characteristics and characteristics of the dynamic excitation which result from that state as well as upon the total stresses and the characteristics of the soil profile. Generally, this behaviour is related to the soil density and the residual strength of soil. From that viewpoint, in loose soils, the  $(\sigma'_1=0)$  state might result in true liquefaction with occurrence of enormous strains and "yielding", while in more dense sands, the  $(\sigma'_1=0)$  state might result in occurrence of limited strains or cyclic mobility. Since soil behaviour after  $(\sigma'_1=0)$  state depends upon the reduced strength of soil, that is upon the  $(\tau/\gamma)$  properties, this problem will be considered in more detail in Section 3.3.

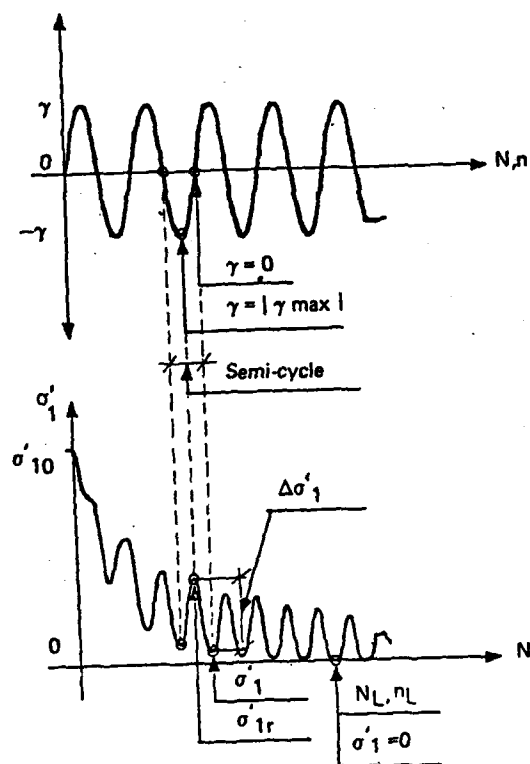


Fig. 3.1.1. Decrease of the effective vertical stress and definition for  $(\sigma'_1)$ ,  $(\sigma'_{1r})$ ,  $(\Delta \sigma'_1)$ ,  $(N_L)$ , and  $(n_L)$

The representative number of cycles with defined ( $\gamma$ ) corresponds to the state ( $\sigma'_1=0$ ), as follows:

$$N \approx N_L \quad (3.1.3)$$

where:

$N_L$  - is the number of cycles for occurrence of initial liquefaction or for ( $\sigma'_1=0$ ) state or for a pore pressure ratio of (100%).

A definition for ( $\sigma'_1=0$ ) and ( $N_L$ ) has been given in Fig. 3.1.1.

( $N_L$ ) is a function of ( $\gamma$ ) and in the case of cyclic excitations, together with ( $\gamma$ ), it is the main parameter for definition of the relationship for occurrence of ( $\sigma'_1=0$ ). During the analysis of the test results, it was concluded that if ( $\gamma$ ) and ( $N_L$ ) are jointly represented in the log-normal coordinates, certain regularity has been established and can be used as a basis for establishment of the ( $\sigma'_1=0$ ) relationship.

The experimental results interpreted in this way have been shown in Fig. 3.1.2. They show the relation between the occurrence of ( $\sigma'_1=0$ ) and the amplitudes of cyclic strains and the influence of the applied cycles. Tests were accomplished with ( $\gamma$ ) from (0.2%) to (2%). They show that the increase of strain amplitudes results in the decrease of number of cycles which causes the occurrence of ( $\sigma'_1=0$ ).

The results shown in this chapter refer to two types of sand models, from Bijela and Baošić, with a relative density of ( $D_r$ ) from (40%) to (85%), respectively, consolidated under stresses ( $\sigma'_{10}$ ) of (100), (200) and (300 kN/m<sup>2</sup>). The larger number of models are made of sand of Bijela type, a total of (34) models, while (8) are of Baošić type. A total of (36) models are of ( $\sigma'_{10}=100$  kN/m<sup>2</sup>), while (6) are of ( $\sigma'_{10}=200$  kN/m<sup>2</sup>) and ( $\sigma'_{10}=300$  kN/m<sup>2</sup>).

Any more expressive difference in the behaviour of the models has not been observed nor a tendency for grouping or classification in the presented results. They lead to conclusion that the shear strains control dominantly the occurrence of ( $\sigma'_1=0$ ), while the influence of ( $D_r$ ), ( $\sigma'_{10}$ ) and the type of sand, Bijela and Baošić, is not emphasized.

It is evident that there is certain uncertainty involved in the obtained results. However, in the evaluation of this uncertainty we should take into account the behaviour of ( $\sigma'_1$ ) close to the occurrence of ( $\sigma'_1=0$ ). This behaviour is shown in Fig. 3.1.1. The convergence of ( $\sigma'_1$ ) to ( $\sigma'_1=0$ ) for ( $\gamma \leq 1.0\%$ ) is almost asymptotical. In that domain, the range of more cycles leads to rather small change in ( $\sigma'_1$ ), which can be expressed by unit percents. Thus, the difference in the obtained number of cycles for equal ( $\gamma$ ) is mainly due to uncertainty involved in the determination of ( $N_L$ ).

Some other interpretation of results is introduced by taking into account the level in which ( $\sigma'_1$ ) decreases more rapidly. Therefore, the following characteristic level has been adopted:

$$\sigma'_1 \approx 0.10 \sigma'_{10} \quad (3.1.4)$$

A pore pressure of (90%) corresponds to that level:

$$u/\sigma'_{10} = 0.90 \quad (3.1.5)$$

and a number of cycles

$$N = N_{0.9} \quad (3.1.6)$$

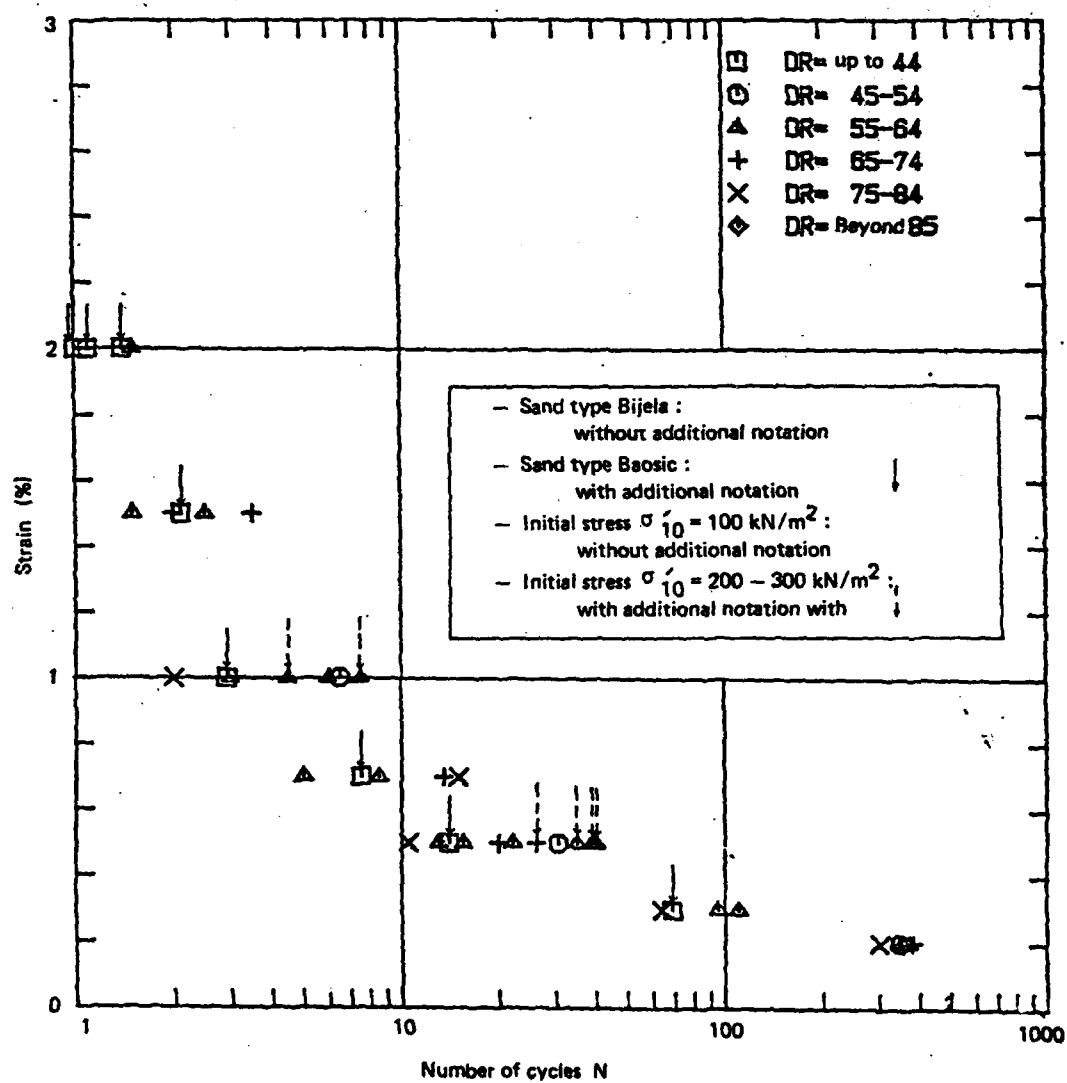


Fig. 3.1.2. Relationship of strain amplitude - number of cycles for occurrence of 100% pore pressure ratio

The results interpreted in this way are shown in Fig. 3.1.3. It is estimated that the uncertainty involved in the values of  $(N_{0.9})$  compared to the values of  $(N_L)$  is considerably decreased.

The results of Fig. 3.1.3. for the occurrence of  $(\sigma'_1=0.10\sigma'_{10})$  support even more the assumption for a dominant influence of  $(\gamma)$  and the smaller influence of  $(D_r)$ ,  $(\sigma'_{10})$  and the type of the tested models.

In order to explain the small influence of  $(D_r)$ ,  $(\sigma'_{10})$  and the type of the tested sands upon the occurrence of  $(\sigma'_1=0)$ , as evaluated from the presented results, an analysis of the maximum shear stresses  $(\tau)$ , which have been applied in the first semi-cycle, has been made. It was found that there are significant variations of  $(\tau)$  for equal  $(\gamma)$ .

The results lead to a conclusion that equal strains  $(\gamma)$  cause different shear stresses  $(\tau)$ , proportional to the strength characteristics of models. This provides the physical explanation about the insignificant influence of  $(D_r)$ ,  $(\sigma'_{10})$  and the type of the tested sands upon the occurrence of  $(\sigma'_1=0)$ .

Taking into account the characteristics of the results and the corresponding estimations, it has been adopted for the purpose of further analysis that the occurrence of  $(\sigma'_1=0)$  has dominantly been controlled by  $(\gamma)$  and  $(N_L)$ .

The results shown in Fig. 3.1.2. show some regularity in the relationship between the strain amplitude  $(\gamma)$  and the number of cycles  $(N_L)$  for the occurrence of  $(\sigma'_1=0)$ . The relative uniformness (regularity) obtained provides the possibility for establishment of a common analytical relationship between  $(\gamma)$  and  $(N_L)$ . For this purpose, a regression analysis of the results with an assumed function has been carried out:

$$\begin{aligned} Y &= Ae^{B \ln(X)} \\ Y &= \gamma \\ X &= N_L \end{aligned} \quad (3.1.7)$$

Within this regression analysis, the constants  $(A)$  and  $(B)$  of the function (3.1.7) have been determined,

$$\begin{aligned} A &= 1.9838 \\ B &= -0.4126 \\ Y &= 1.9838e^{-0.4126 \ln(X)} \end{aligned} \quad (3.1.8)$$

based on the least squares mean values.

The function (3.1.8) together with the experimental results has been shown in Fig. 3.1.4. It defines the conditions for occurrence of  $(\sigma'_1=0)$  in a way which is rather simple. It is simple because of the dominant influence of  $(\gamma)$ . As such, it can be taken as a basis for mathematical model formulation for analysis of the soil liquefaction potential.

It should be taken into account that the definition of the unique (common) function (3.1.8) is based on the small  $(D_r)$  and  $(\sigma'_{10})$  effect and the type of the two tested sands, opposite to the dominant influence of  $(\gamma)$  and the physical explanation about different  $(\tau)$  levels for equal  $(\gamma)$  proportional to strength of sands. The effects of other soil properties which have not been investigated, can have some influence from their part. The effects of sands with large variety of grain size properties can also have their influence upon the conditions of occurrence

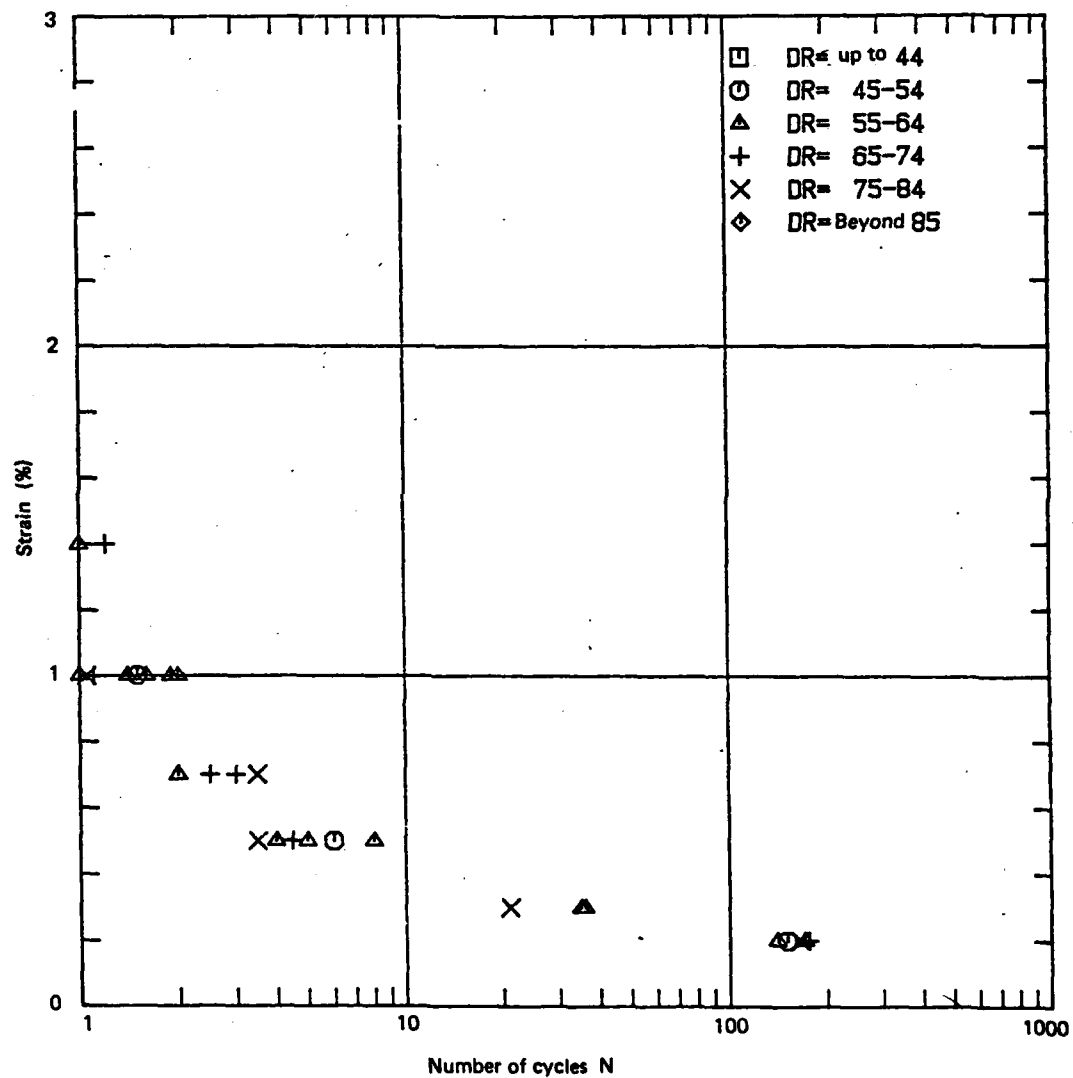


Fig. 3.1.3. Relationship between strain amplitude and the number of cycles for occurrence of 90% pore pressure ratio

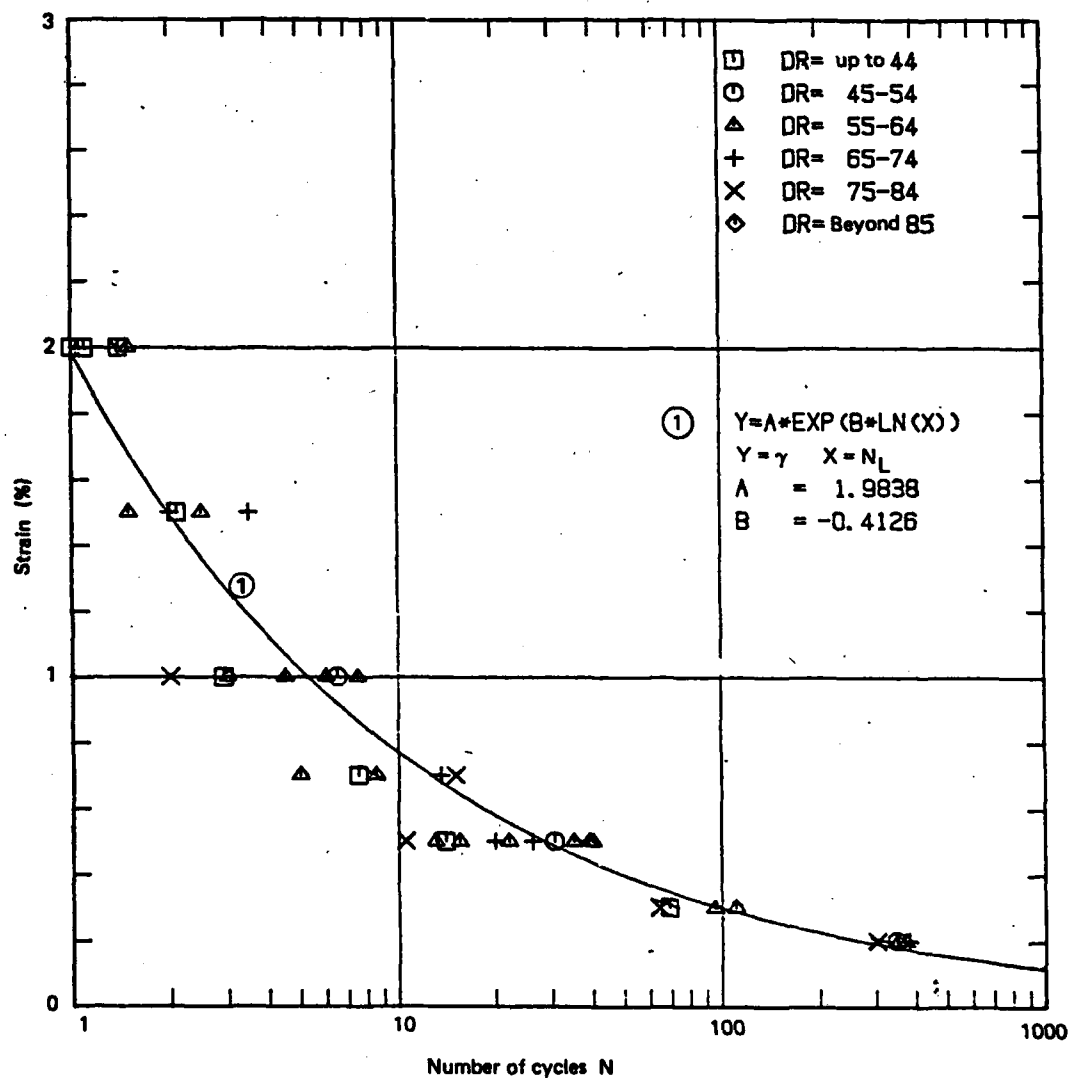


Fig. 3.1.4. Relationship between strain amplitude - number of cycles for occurrence of 100% pore pressure ratio

of ( $\sigma'_1=0$ ). Besides, attention should be paid that the function (3.1.8) has been determined based on the behaviour of sands with ( $D_r$ ) from (40%) to (80%). These tests do not include very loose and very dense sands in which some effects can also be expected.

### 3.2. Relationships for the Pore Pressure Increase

Following the above presented concept of testing, using the above described laboratory equipment, the equivalent increase of the pore pressure is proportional to the decreasing of ( $\sigma'_{10}$ ).

The increasing of the pore pressure is not constant in the frames of one semi-cycle ( $n$ ). It has cyclic features with frequency two times larger than the frequency of ( $\gamma$ ). It obtains its maximum value for ( $\gamma=0$ ), and the minimum when ( $\gamma$ ) reaches its extreme values.

Let us denote by:

- ( $u$ ) - envelope maximum value of the pore pressure in one semi-cycle ( $n$ )
- ( $u_r$ ) - residual, minimum value of the pore pressure during ( $n$ )
- ( $\Delta u$ ) - pore pressure variation during ( $n$ ).

These characteristics and definitions are shown in Fig. 3.2.1.

Increase of the pore pressure has been observed in all tests, at the beginning of excitation applying the first cycle of shear strains.

The smallest strain under which pore pressure has occurred is:

$$\gamma_{min}^* = 0.01\% \quad (3.2.1)$$

A cyclic strain under which a considerable pore pressure develops is ( $\gamma=0.1\%$ ). However, in spite of the long-lasting excitation, a pore pressure of (100%) has not been achieved.

The smallest cyclic strain under which pore pressure of (100%) develops is ( $\gamma=0.2\%$ ).

A general characteristic of the pore pressure development is that at the beginning of the excitation it increases very intensively, while after it reaches an average amount of (80) - (90%), it increases slowly. This was observed in all the tests.

Other characteristic is the variation of intensity ( $\Delta u$ ) during each cycle separately. The same is observed in the presented record of the above-mentioned figures. It can be concluded from these results that the maximum ratio of ( $\Delta u$ ) depends upon the model density and the strain amplitude. ( $\Delta u$ ) increases with the increase in density and the increase of ( $\gamma$ ). Also, ( $\Delta u$ ) is larger in the beginning, and then it decreases converging to the state of ( $u=\sigma'_{10}$ ).

The physical explanation of the presence of ( $\Delta u$ ) is related to the model tendencies for compaction and dilatancy during each semi-cycle, which are evident and present in the obtained results. These tendencies are especially evident in the nonlinear ( $\tau/\gamma$ ) relationships, which will be referred to at a later stage.



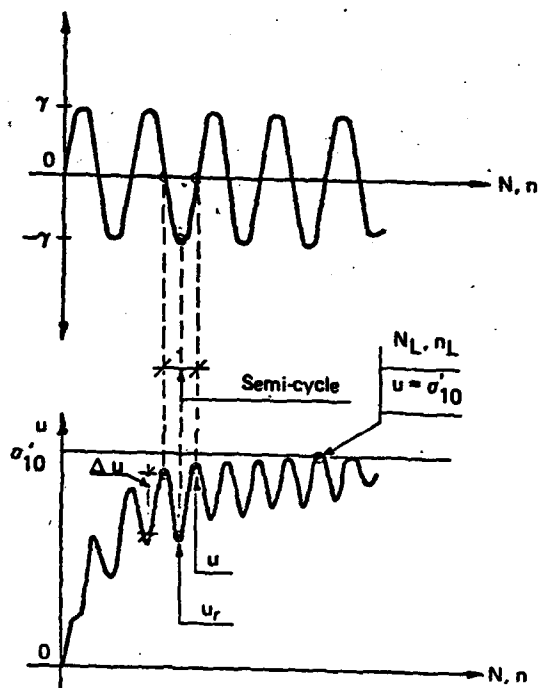


Fig. 3.2.1. Increase of the pore pressure and definitions of  $(u)$ ,  $(u_r)$ ,  $(\Delta u)$ ,  $(N_L)$  and  $(n_L)$

In the semi-cycles when the stage of  $(u=\sigma'_{10})$  has been reached,  $(\Delta u)$  has still finite value. It means that  $(u_r < \sigma'_{10})$ , that is,  $(\sigma'_{1r})$  has a finite value, too. So, a conclusion is made that in the semi-cycle when a state of  $(u=\sigma'_{10})$  is reached, the soil retains some residual strength. Since  $(\Delta u)$  increases with the increase of  $(D_r)$ , the residual strength increases, respectively.

In order to check the regularity of pore pressure development and obtain an analytical expression between  $(u)$ ,  $(N)$  and  $(\gamma)$ , a detailed analysis of (22) representative records of  $(u)$  has been made. These records have been obtained of models having different  $(D_r)$  with different amplitudes of cyclic strains  $(\gamma)$ .

The envelopes of  $(u)$  records have been analysed, which means maximum values in each semi-cycle. The analysed records which have been interpreted as  $(u/\sigma'_{10})$  and  $(N)$  relationships have been shown in Fig. 3.2.2. Since they refer to different  $(\gamma)$ , they look differently, sharing in common the property of a fast increase at the beginning and a slow, almost asymptotic at the end, before  $(u=\sigma'_{10})$  is reached.

It has been noticed during the analysis that if cycles of each record are normalized by dividing with  $(N_L)$  and the record is presented in the coordinate system  $(u/\sigma'_{10})$  and  $(N/N_L)$ , in which  $(N/N_L)$  reaches the value of (0) to (1), this situation changes. The curves presented in this way become similar with tendency of convergence towards one common curve. In this way, they become directly independent of  $(\gamma)$ , but indirectly through  $(N_L)$ . They are shown in Fig. 3.2.3.

In this way, the normalized records  $(u/\sigma'_{10})$  are used in the regression analysis in order to find a suitable analytical expression for them. The regression analysis was carried out using the assumed function:

$$\begin{aligned} Y &= X(A + BX)/(C + DX) \\ Y &= u/\sigma'_{10} \\ X &= N/N_L \end{aligned} \quad (3.2.2)$$

With the regression analysis the constants A, B, C and D of the function (3.2.2) have been determined.

$$\begin{aligned} A &= 1.0357 \\ B &= 0.0547 \\ C &= 0.0357 \\ D &= 1.0547 \end{aligned} \quad (3.2.3)$$

$$Y = X(1.0357 + 0.0547X)/(0.0357 + 1.0547X)$$

The function (3.2.3) together with the data of the normalized records  $(u/\sigma'_{10})/(N/N_L)$  is shown in Fig. 3.2.3. It can be seen that the curve (3.2.3) shows a good correlation with the data.

The function (3.2.3), as common for all the values of  $(\gamma)$ , defines the increase of the pore pressure in a uniform way. The influence of  $(\gamma)$  has been incorporated in directly through  $(N_L)$ . It is defined on the basis of the dominant influence of  $(\gamma)$ . In this sense the function is also general, similar to the previous function (3.1.8). Together with this, it can be taken as a basis for mathematical model development for analysis of the liquefaction potential.

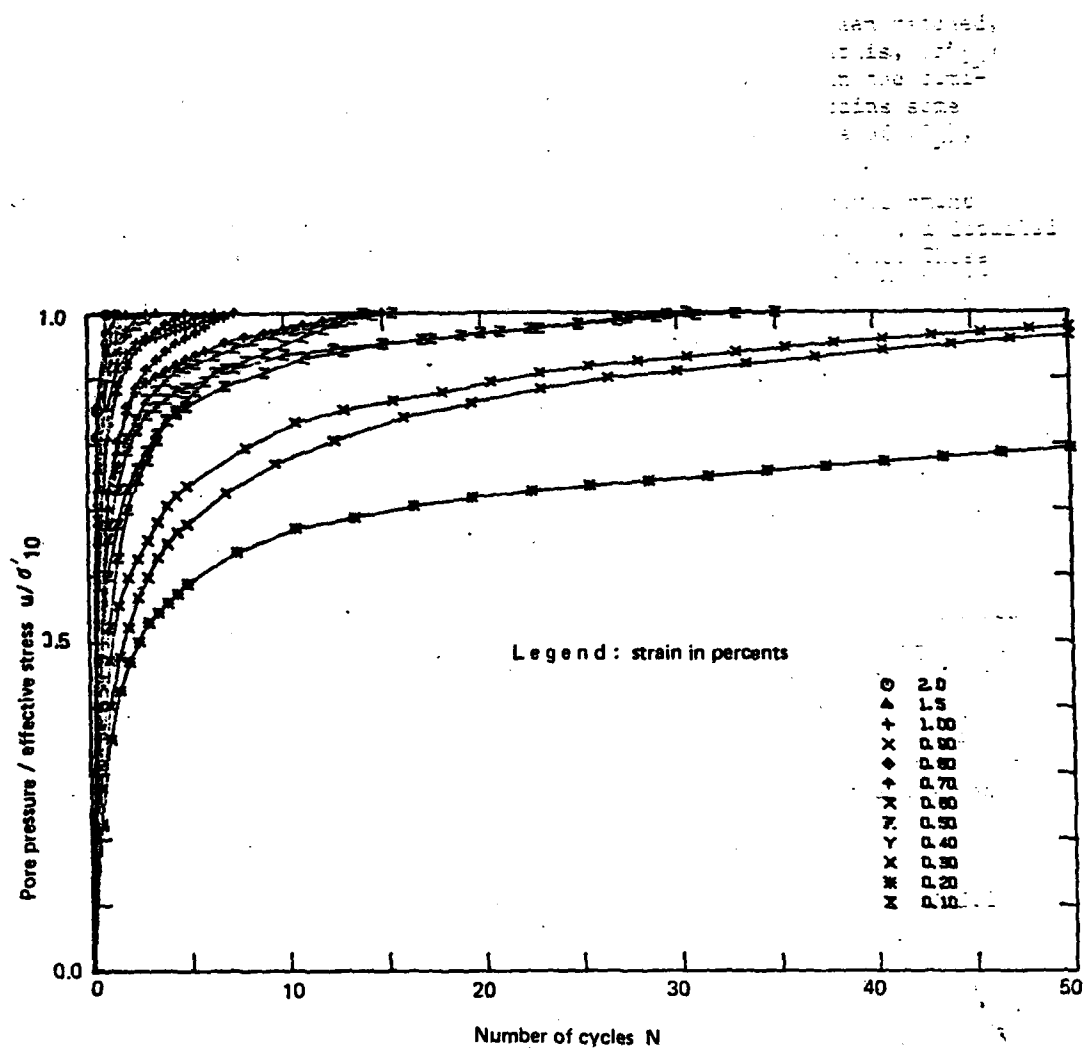


Fig. 3.2.2. Increase of the pore pressure depending upon the strain level and the number of cycles ( $N$ )

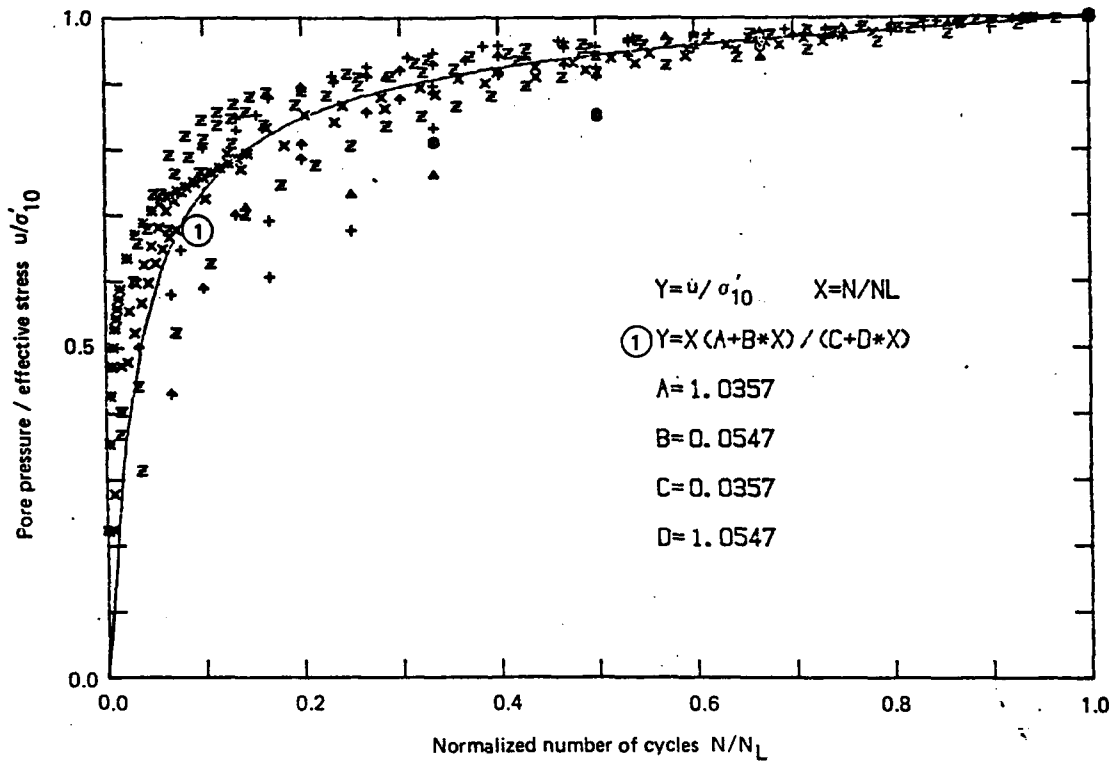


Fig. 3.2.3. Increase of the pore pressure depending upon the strain level and the number of cycles ( $N$ ) divided by the number of cycles for liquefaction occurrence ( $N_L$ )

### 3.3. Relationships for the Decrease of Shear Moduli

Due to the excitation under cyclic strains and decrease of  $(\sigma'_{10})$ , a transformation of strength characteristics takes place in the models. It can be observed through the records of shear stresses  $(\tau)$  and the records of the nonlinear  $(\tau/\gamma)$  relationships.

Representative record has been shown in Fig. 3.3.1. The record has been obtained with excitation  $(\gamma=1\%)$ , in model with  $(D_r)$  equal to  $(40\%)$ . In order to complete the picture, the decrease of  $(\sigma'_{10})$ , that is the increase of  $(u)$  have been presented.

It is evident from the records that a decrease of  $(\tau)$  takes place in the model, following the decrease of  $(\sigma'_{10})$ . The decrease of  $(\tau)$  is more evident on the  $(\tau/\gamma)$  curves showing that the same strain with amplitude  $(\gamma=1\%)$  causes smaller stresses  $(\tau)$  going from a cycle to a cycle. Accordingly, a "rotation" of the curves towards the  $(\gamma)$  axis takes place.

Another property can be defined as a change in the  $(\tau)$  and  $(\gamma)$  relationship during one semi-cycle  $(n)$ , and also during the excitation. This is even more expressed under smaller strains due to the slower convergence towards  $(\sigma'_{10}=0)$  state. Thus, Fig. 3.3.2 shows the  $(\tau/\gamma)$  curve of the same model with  $(D_r)$  equal to  $(40\%)$ , however for  $(\gamma=0.5)$ .

These properties can be best interpreted through the shear moduli. If the moduli are analysed between the extreme values of  $(\gamma)$  from  $(\gamma_{min})$  to  $(\gamma_{max})$ , it can be seen that in the first semi-cycles  $(n)$  the moduli decrease permanently in respect to the initial maximum value. However, in the next semi-cycles, an increase in the vicinity of  $|\gamma_{max}|$  is observed besides this decrease. It means that during one semi-cycle there are both tendencies for compaction and for dilatancy. This reflects in the presence of  $(\Delta\sigma'_1)$  during one semi-cycle.

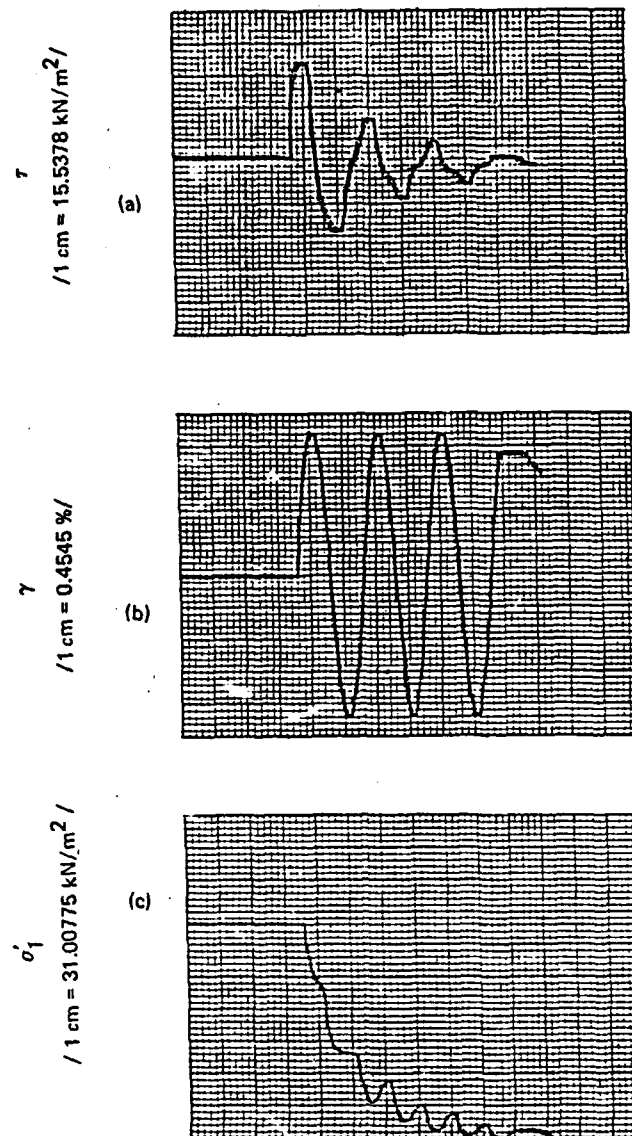
Let us denote with:

- $G_0$  - initial maximum shear modulus of the model, which corresponds to the hysteresis loop, without increase of  $(u)$ , in respect to  $(\gamma_{min})$  under loading and in respect to  $(\gamma_{max})$  under unloading conditions
- $G$  - maximum modulus of any curve  $(\tau/\gamma)$  in conditions of an increased  $(u)$  and in respect to  $(\gamma_{min})$  under loading, that is in respect to  $(\gamma_{max})$  under unloading conditions. Since it is dependent on  $(n)$  it is denoted by  $G(n)$ .

These definitions have been shown in Fig. 3.3.3.

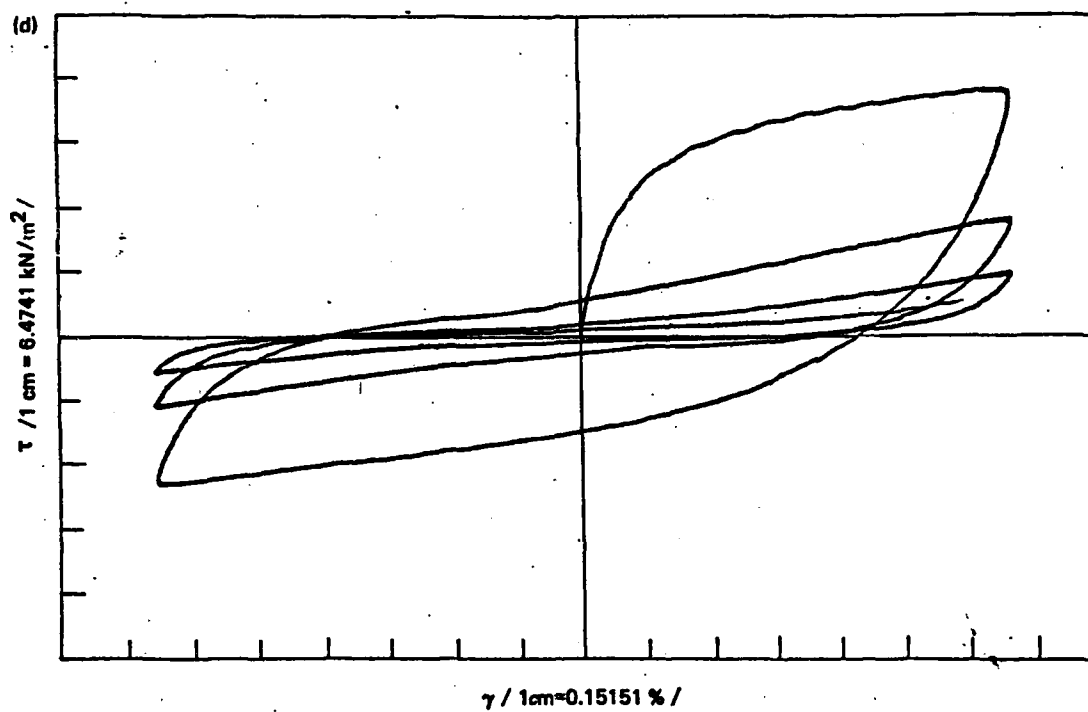
From the presented  $(\tau/\gamma)$  curves, it can be seen that the  $(G)$  moduli permanently decrease so that the final values of  $(\tau)$  in the following semi-cycles are smaller than the preceding ones. It means that although there are both tendencies of compaction and dilatancy in each semi-cycle, the tendency of compaction is prevailing throughout.

A special reference should be given to the behaviour immediately after  $(\sigma'_{10}=0)$  is reached. As shown on the records, it is obvious that in the models, besides the considerable reduction, there is some residual strength. This is due to the fact that in the first semi-cycle, after  $(u=\sigma'_{10})$  is reached,  $(\sigma'_{1r})$  preserves its finite value. The analysis of moduli in the semi-cycles  $(n_L)$  and  $(n_L+1)$  show that they vary as follows: the maximum values which correspond to the extreme strains  $(\gamma_{min})$  and  $(\gamma_{max})$  decrease going to  $(\gamma=0)$ ; for  $(\gamma=0)$  the moduli have



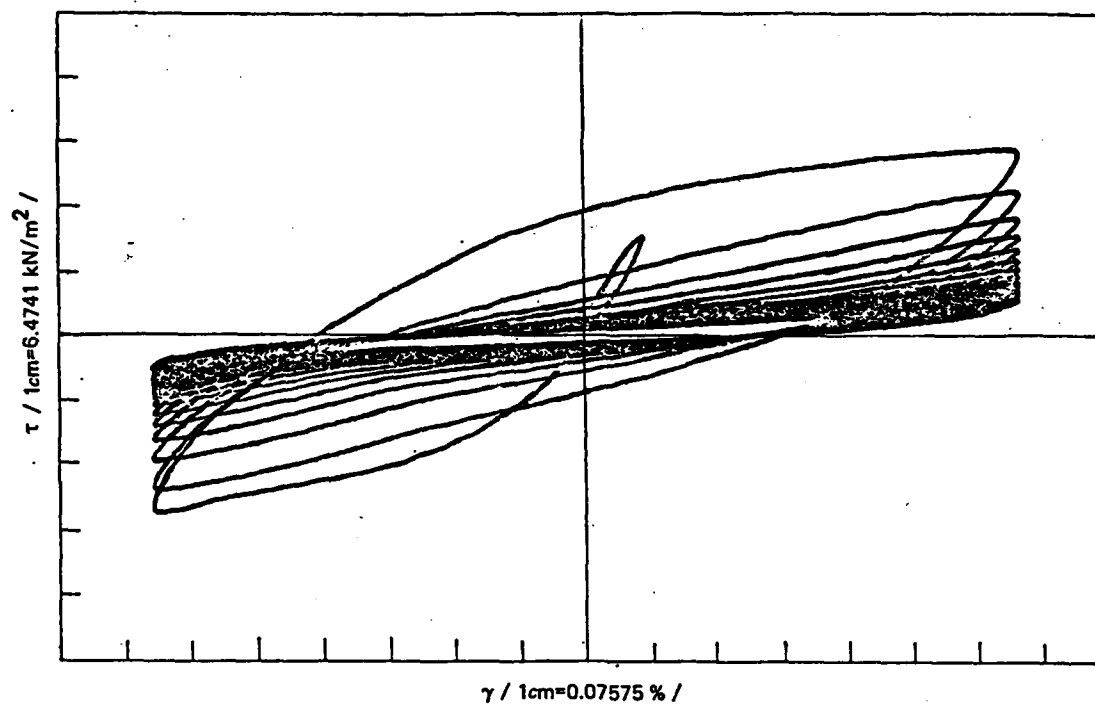
Test	Sand type	Dr (%)	$\gamma$ (%)	$\sigma'_{10}(\text{kN/m}^2)$
1.8-1.1	Baotic	40	1	100

Fig. 3.3.1./1 Representative results from tests under cyclic shear strains with ( $\gamma=1\%$ )  
 a) time history of shear stresses ( $\tau$ )  
 b) time history of cyclic strains ( $\gamma$ )  
 c) time history of vertical stresses ( $\sigma'_1$ )



Test	Sand type	Dr (%)	$\gamma$ (%)	$\sigma'_{10}(\text{kN/m}^2)$
1.B-1.1	Basic	40	1	100

Fig. 3.3.1./2 Representative results from tests under cyclic shear strains with ( $\gamma=1\%$ )  
d) time history of nonlinear relationships ( $\tau/\gamma$ )



Test	Sand type	Dr (%)	$\gamma$ (%)	$\sigma_{10}$ (kN/m <sup>2</sup> )
0.5B-1.1	Basic	40	0.5	10n

Fig. 3.3.2. Representative results from tests under cyclic shear strains with ( $\gamma=0.5\%$ )  
- time history of nonlinear relationships ( $\tau/\gamma$ )



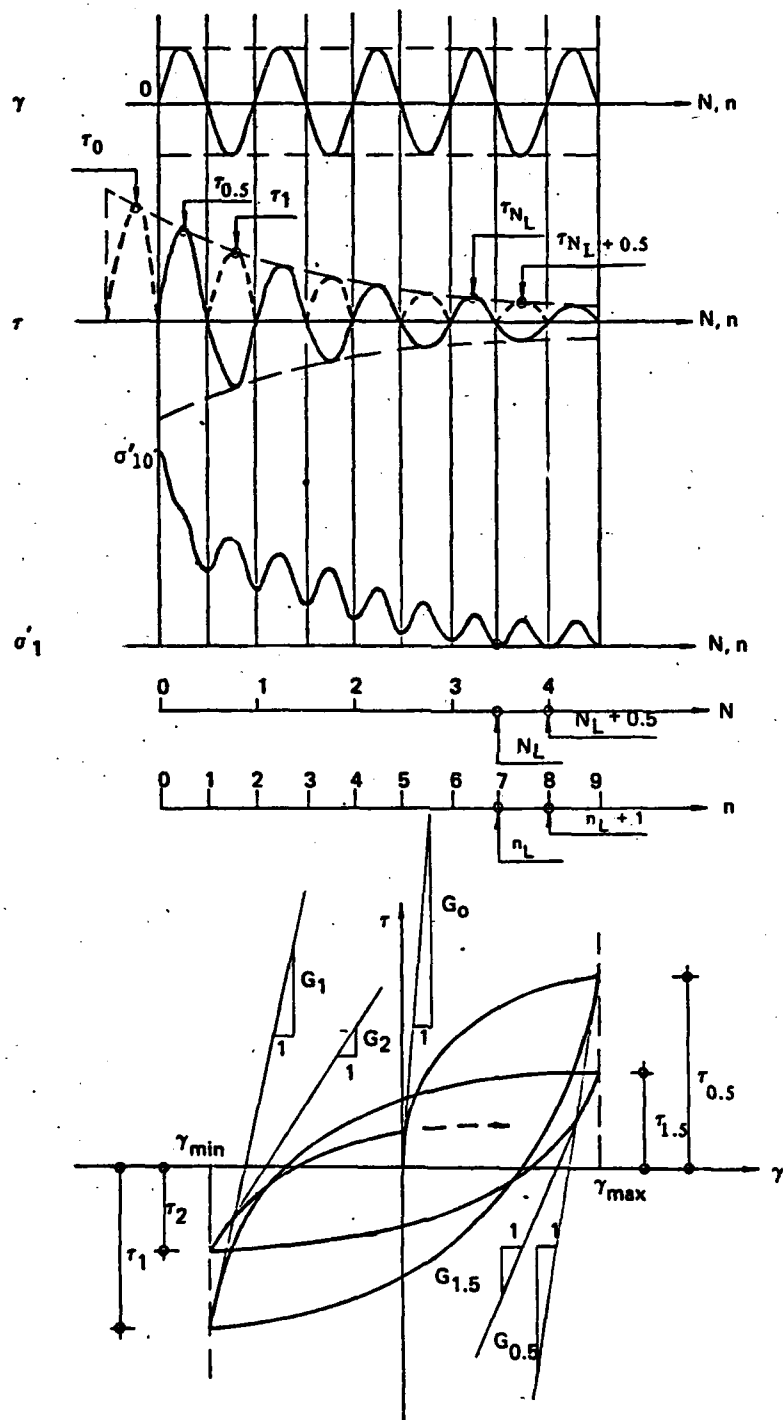


Fig. 3.3.3. Characteristics of the decrease in ( $\tau$ ) and the shear moduli due to the decrease in ( $\sigma'_1$ ) and definitions for ( $G_0$ ) and ( $G$ )

practically the value of (0); while going away from ( $\gamma=0$ ), they increase again. This behaviour follows the change of ( $\sigma'_1$ ) and of the pore pressure between ( $u_p$ ) and ( $u$ ).

As seen from the results, there are differences in the values of ( $\tau$ ) and ( $G$ ), in the semi-cycles ( $n_L+1$ ) after ( $\sigma'_1=0$ ) is reached. This difference shows that by increasing ( $D_p$ ) the residual strength of models increases, too. It complies with the above observed increase of ( $\Delta u$ ) with the increase of ( $D_p$ ). This difference is in the same time the main characteristic of the behaviour between the less and more compacted models.

The decreasing of ( $\tau$ ) and ( $G$ ) with the increase of ( $N$ ), i.e., ( $n$ ), has been shown in Fig. 3.3.3. From the preceding discussion on the properties of the ( $\tau/\gamma$ ) curves, it appears that the decrease of ( $G$ ) can be considered as proportional to the decrease of ( $\tau$ ):

$$\frac{G_0}{G(N)} = \frac{\tau_0}{\tau(N)} \quad (3.3.1)$$

The equation (3.3.1) is an approximation, however, it can be accepted for the purpose of simplicity of further analysis.

On this basis, an interpretation of the records of ( $\tau$ ) and the curves ( $\tau/\gamma$ ) has been accomplished. Analysing the results, time histories of the change of ( $G$ ) from ( $G_0$ ) to ( $G(N_L+0.5)$ ) have been obtained. Representative time histories in a form of a ratio between ( $G/G_0$ ) as dependent upon ( $N$ ) have been shown in Figs. 3.3.4 and 3.3.5. The results in Fig. 3.3.4 refer to models having ( $D_p$ ) from (40%) to (55-56%). It can be seen that the residual moduli ( $G(N+0.5)$ ) are (10-15%) of the initial ( $G_0$ ). In Fig. 3.3.5 are shown the results of models with ( $D_p$ ) from (60%) to (70%). The residual moduli ( $G(N_L+0.5)$ ) for them are (20-25%) of ( $G_0$ ).

During the analysis, it was seen that if the number of cycles of each record is normalized by dividing it with ( $N_L+0.5$ ) and records are presented as ( $G/G_0$ ) relationship, dependent upon ( $N/(N_L+0.5)$ ) they become similar. Also a tendency of convergence towards one common curve is observed. In this way, the results interpreted from Figs. 3.3.4 and 3.3.5 are in a form as shown in Figs. 3.3.6 and 3.3.7.

The normalized records ( $G/G_0$ ) have been used for the regression analysis in order to find suitable analytical expressions for them. The regression analysis has been carried out assuming the function:

$$\begin{aligned} Y &= 1 - X(A + BX)/(C + DX) \\ Y &= G/G_0 \\ X &= N/(N_L + 0.5) \end{aligned} \quad (3.3.2)$$

The regression analysis defines the constants of the function (3.3.2). For the data shown in Fig. 3.3.6 for models with ( $D_p$ ) of (40%) to (55-56%), the following values have been obtained:

$$\begin{aligned} A &= 1.1218 \\ B &= 0.1143 \\ C &= 0.1400 \\ D &= 1.2809 \end{aligned} \quad (3.3.3)$$

$$Y = 1 - X(1.1218 + 0.1143X)/(0.1400 + 1.2809X)$$

The function (3.3.3) for ( $X=1$ ) gets a value of ( $Y=0.13$ ).

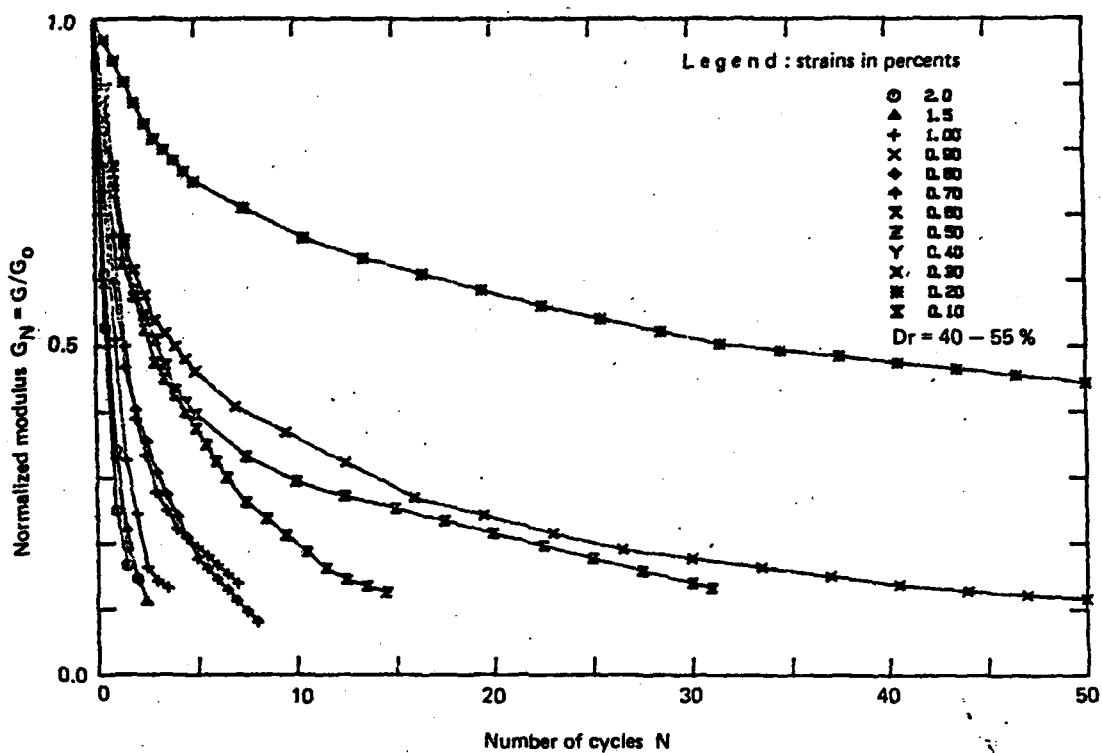


Fig. 3.3.4. Change in the modulus ( $G$ ) depending upon the strain level and the number of cycles ( $N$ )

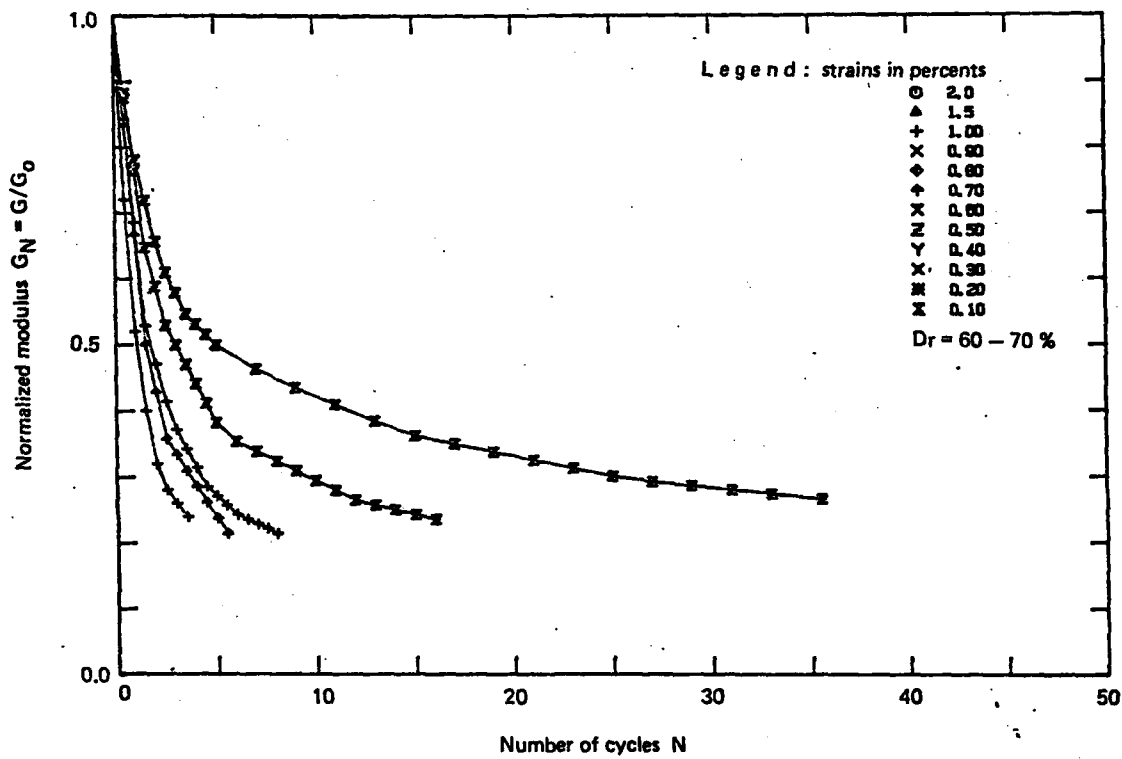


Fig. 3.3.5. Change in the modulus ( $G$ ) depending upon the strain level and the number of cycles ( $N$ )

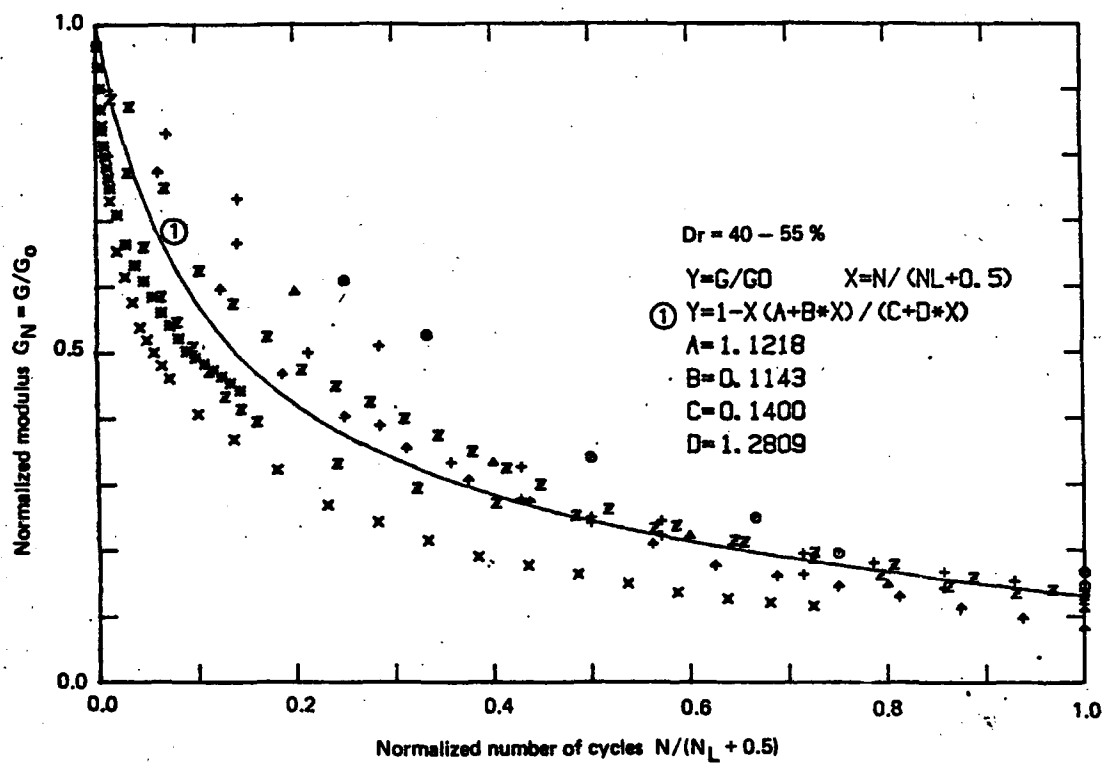


Fig. 3.3.6. Change in the modulus ( $G$ ) depending upon the strain level and the number of cycles ( $N$ ) divided by the cycles for occurrence of liquefaction ( $N_L$ )

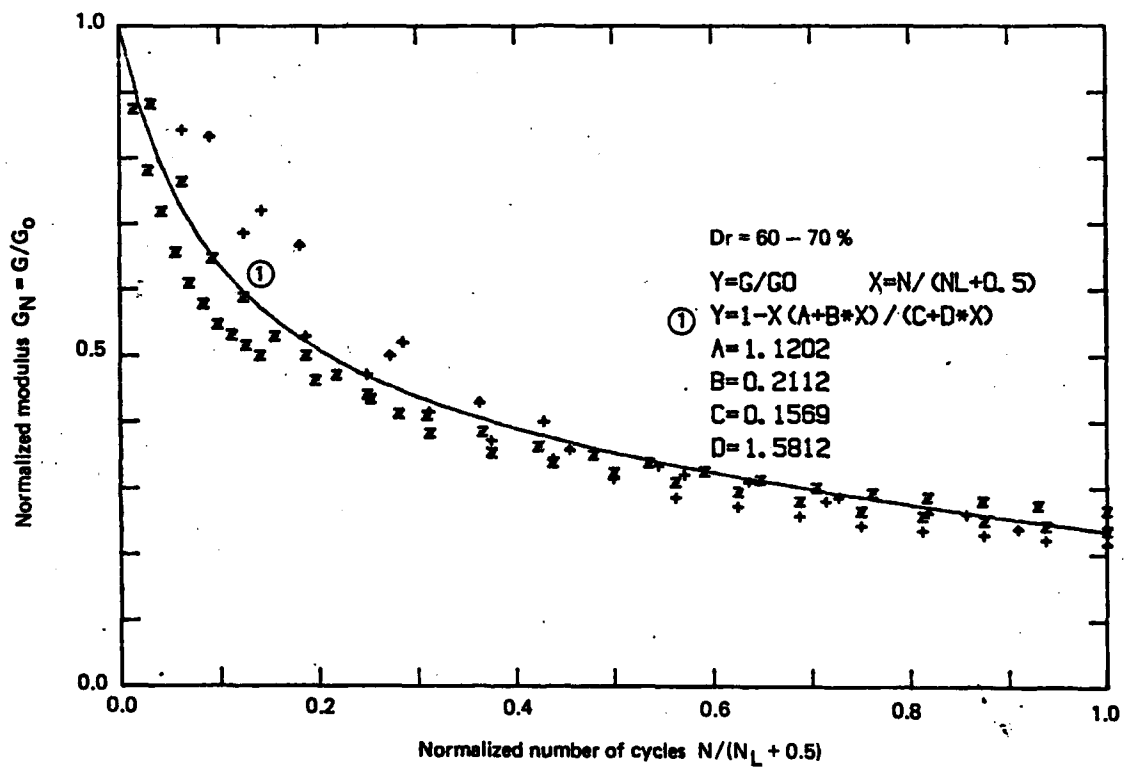


Fig. 3.3.7. Change in the modulus ( $G$ ) depending upon the strain level and the number of cycles ( $N$ ) divided by the cycles for occurrence of liquefaction ( $N_L$ )

For the data given in Fig. 3.3.7, which are for models with ( $D_r$ ) of (60%) to (70%), the following values have been obtained:

$$\begin{aligned} A &= 1.1202 \\ B &= 0.2112 \\ C &= 0.1569 \\ D &= 1.5812 \\ Y &= 1 - X(1.1202 + 0.2112X)/(0.1569 + 1.5812X) \end{aligned} \quad (3.3.4)$$

The function (3.3.4) for ( $X=1$ ) has the value of ( $Y=0.234$ ).

The functions (3.3.3) and (3.3.4) have been shown in Figs. 3.3.6 and 3.3.7, respectively. They define in a rather simple way the decrease of the initial soil moduli due to pore pressure development. During their definition, certain approximation has been introduced by neglecting the ( $\gamma$ ) effect. This effect is present in the results in a form of variation of ( $\Delta u$ ) as dependent upon ( $\gamma$ ), however, it has not been expressed significantly.

It appears from the function (3.3.3) and (3.3.4) and the obtained results that the residual strength of the soil expressed through the moduli ( $G(N_L+0.5)$ ) in the cycle ( $N_L+0.5$ ), immediately after the occurrence of liquefaction, is present and varies with ( $D_r$ ). From a viewpoint of analysis of the soil behaviour after the ( $\sigma'_1=0$ ) is reached and the differences in the behaviour between more and less compacted soils, of special importance is the residual strength immediately after the initial liquefaction is achieved. Therefore, analysis of the results of all the experiments is made. The results of this analysis are shown in Fig. 3.3.8. They give the relationship between ( $D_r$ ) and ( $G(N_L+0.5)/G_0$ ). In the range of the tested values of ( $D_r$ ) of (40%) to (85%), the following correlation relationship taken as the simplest, and linear is as follows:

$$\begin{aligned} Y &= A + BX \\ Y &= G(N_L + 0.5)/G_0 \text{ in \%} \\ X &= (D_r) \text{ in \%} \\ A &= -6.68 \\ B &= 0.43 \\ Y &= -6.68 + 0.43X \end{aligned} \quad (3.3.5)$$

If it is assumed that the obtained simple linear function (3.3.5) can apply to very loose sands, it is obtained:

$$\begin{aligned} Y &= 0 & X &= 15.53\% \\ G(N_L+0.5) &= 0 & D_r &= 15\% \end{aligned} \quad (3.3.6)$$

A conclusion follows from (3.3.6) that for ( $D_r=15\%$ ), after the state ( $\sigma'_1=0$ ) is reached, a full reduction in the soil strength takes place. It means that when the ( $\sigma'_1=0$ ) state is reached, the state of true liquefaction takes place at the same time.

A special reference should be given to the question of further soil behaviour after ( $\sigma'_1=0$ ) is reached. For the definition of this behaviour, several experiments have been carried out in which the

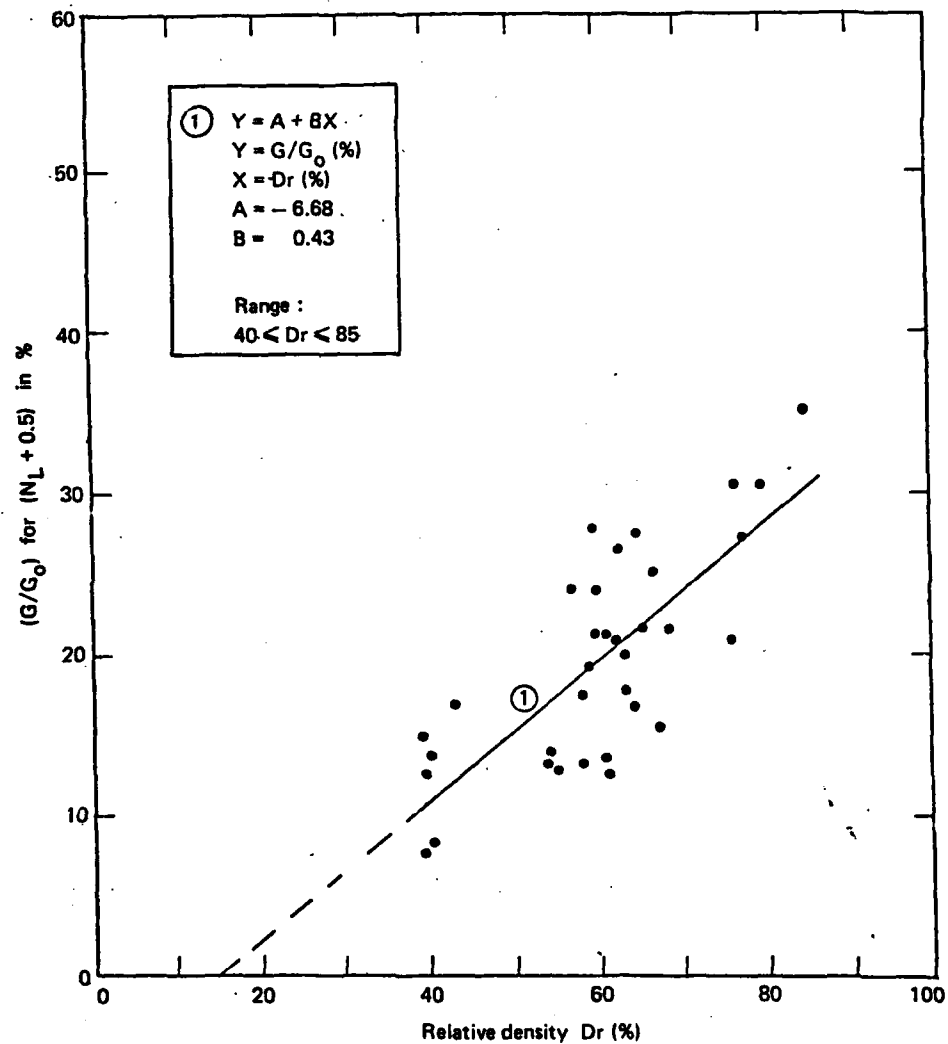


Fig. 3.3.8. Relationship between the normalized modulus  $((G_{NL}+0.5)/G_0)$  and  $(D_r)$



excitation of models continued after  $(\sigma'_{1i}=0)$  was reached. The representative records of  $(\tau)$ ,  $(\gamma)$ ,  $(\sigma'_{1i})$  and  $(u)$  and of the curves  $(\tau/\gamma)$  have been shown in Fig. 3.3.9. It can be seen that even after  $(\sigma'_{1i}=0)$ ,  $(\tau)$  continues to decrease. This decrease is followed by the decreasing of  $(\sigma'_{1pr})$  and  $(\Delta u)$ , and increasing of  $(u_p)$ , while the state  $(\sigma'_{1i}=0)$  continuously is maintained. Accordingly, the curves  $(\tau/\gamma)$  continue rotating towards the  $(\gamma)$  axis. A conclusion follows that  $(G(N_L+0.5))$  as a residual modulus in the  $(N_L+0.5)$  cycle is not a minimum one, but it continues decreasing. Finally, after a larger number of applied cycles,  $(\sigma'_{1i})$  and  $(\sigma'_{1pr})$  become equal with total reduction of  $(\Delta u)$  and complete drop in the strength of the model.

Having in mind this behaviour, it was adopted that the functions (3.3.3) and (3.3.4) apply even after  $(N/(N_L+0.5))$ . Interesting data are obtained in this case. Thus, the function (3.3.3) gets a value of (0) for  $(X=2)$ :

$$\begin{aligned} Y &= 1 - X(1.1218 + 0.1143X)/(0.1400 + 1.2809X) \\ X &= 2 \\ Y &= 0.0 \quad (3.3.7) \\ X &= N/(N_L + 0.5) \\ Y &= G/G_0 \end{aligned}$$

Based on (3.3.7), a conclusion can be made that if for reaching  $(\sigma'_{1i}=0)$  the  $(N_L)$  number of cycles is necessary in which a residual modulus  $(G(N_L+0.5))$  is obtained, then, for complete strength reduction of the model practically (2) times larger number of cycles is necessary for sands with  $(D_r)$  of (40%) to (55-56%).

Similarly, it follows from the function (3.3.4) that:

$$\begin{aligned} Y &= 1 - X(1.1202 + 0.2112X)/(0.1569 + 1.5812X) \\ X &= 2.48 \\ Y &= 0.0 \quad (3.3.8) \\ X &= N/(N_L + 0.5) \\ Y &= G/G_0 \end{aligned}$$

Based on (3.3.8), the conclusion for sands with  $(D_r)$  from (60%) to (70%) would be that a complete strength reduction would take place under (2.5) times larger number of cycles in respect to  $(N_L)$ .

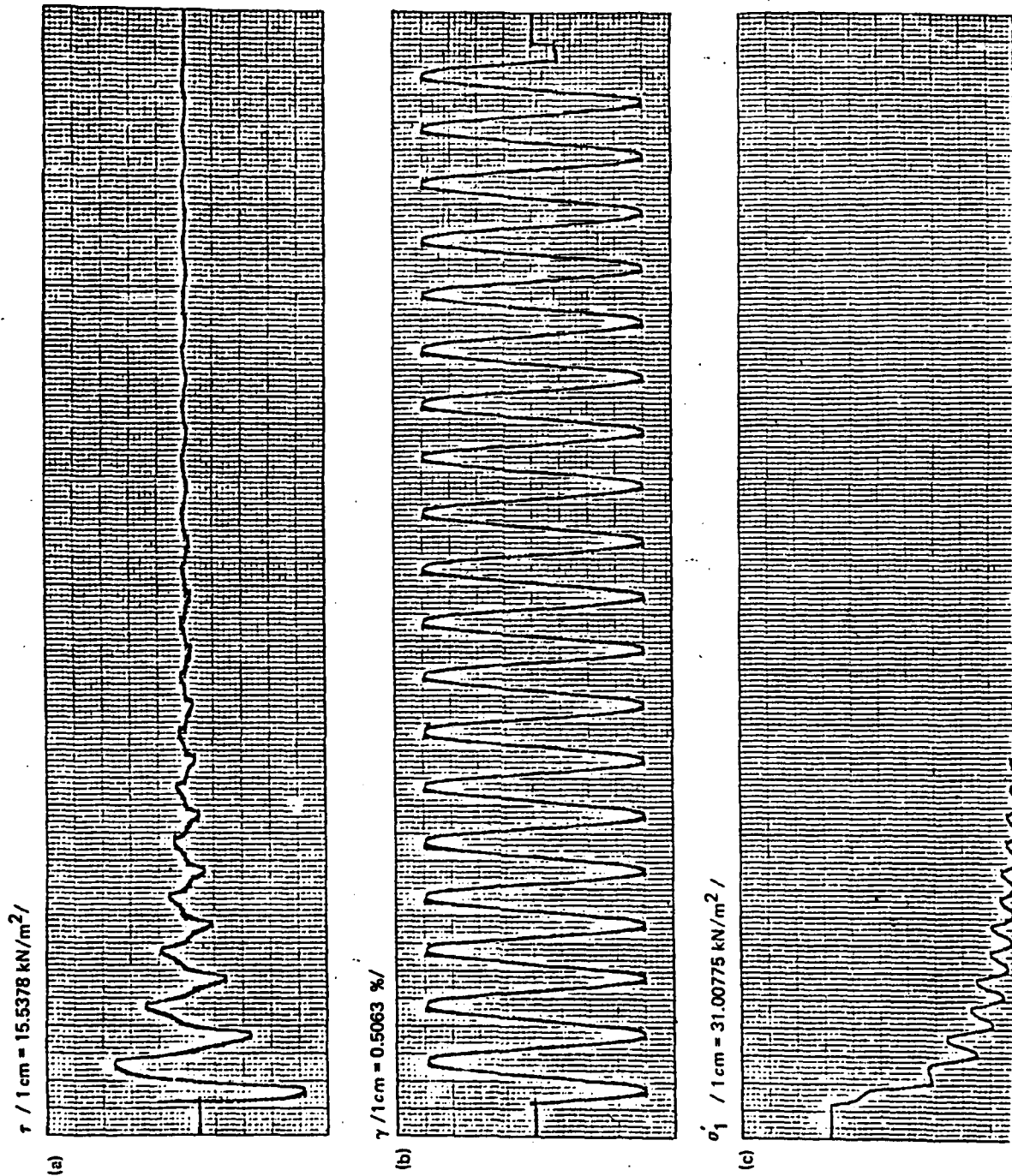
The functions (3.3.3), (3.3.4) and (3.3.5) can be used as a basis for establishment of more relationships for the decrease of  $(G)$  in correlation with  $(G(N_L+0.5))$  and  $(D_r)$ .

Therefore, the  $(G/G_0)$  relationships have been defined for a wider range of  $(D_r)$  values. The same is presented in Table T.3.3.1.

The same analytical expression (3.3.2) has been adopted for definition of  $(G/G_0)$  for the wider range of  $(D_r)$  due to its suitability for correlation with the experimental results.

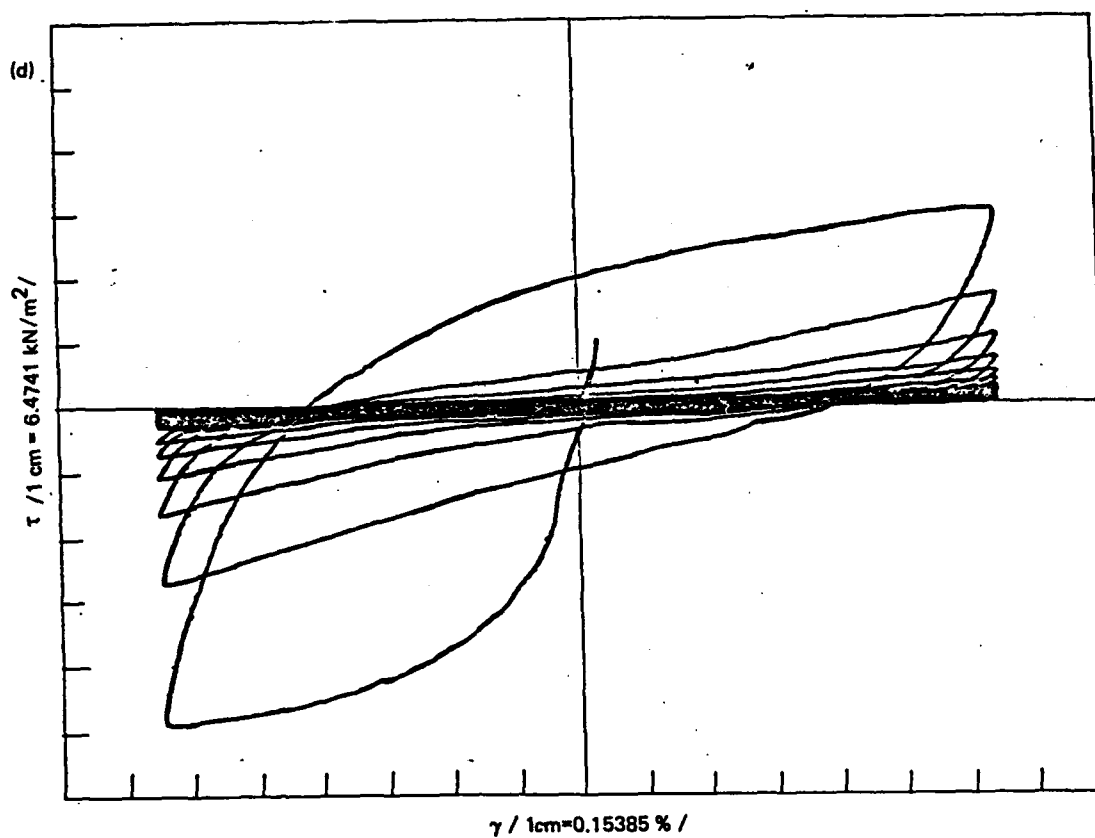
In this way, the problem is reduced to determination of coefficients (A), (B), (C) and (D).

In  $(D_r)$  range up to (90%), the coefficients (A), (B), (C) and (D) have been defined for (8) functions (3.3.2). The coefficients have been determined on the basis of the characteristics of functions (3.3.3) and (3.3.4) yielding the relationship between the decrease in  $(G/G_0)$



Test	Sand type	Dr (%)	$\gamma$ (%)	$\sigma'_{10} (\text{kN/m}^2)$
Additional test	Baotic	39	1	100

Fig. 3.3.9./1 Representative results from tests under cyclic shear strains with ( $\gamma=1\%$ )  
a) time history of shear stress ( $\tau$ )  
b) time history of cyclic strains ( $\gamma$ )  
c) time history of vertical stresses ( $\sigma'_1$ )



Test	Sand type	Dr (%)	$\gamma$ (%)	$\sigma'_{10}(\text{kN/m}^2)$
Additional test	Baotic	39	.1	100

Fig. 3.3.9./2 Representative results of tests under cyclic shear strains with ( $\gamma=1\%$ )  
d) time history of nonlinear relationships ( $\tau/\gamma$ )

Table T.3.3.1. Constants (A), (B), (C) and (D) of function of decrease of (G) depending on (N) for different relative densities ( $D_r$ )

Number	Function	Range of $D_r$	Function coefficients $Y = 1 - X(A + BX) / (C + DX)$ $Y = G/G_0 \quad X = N/(N_L + 0.5)$				$G(N_L + 0.5)/G_0$	$N_{LL}/(N_L + 0.5)$
			A	B	C	D		
1	3.3.2/1	$\leq 20$	1.0798	0.1137	0.0798	1.1137	0.0	1.0
2	3.3.2/2	21-30	1.1163	0.0682	0.1212	1.1135	0.0407	1.3131
3	3.3.2/3	31-40	1.1156	0.0950	0.1262	1.1950	0.0837	1.6438
4	3.3.2/4	41-50	1.1209	0.1137	0.1384	1.2753	0.1267	1.9746
5	3.3.2/5	51-60	1.1303	0.1290	0.1569	1.3598	0.1697	2.3054
6	3.3.2/6	61-70	1.1427	0.1436	0.1813	1.4526	0.2127	2.6361
7	3.3.2/7	71-80	1.1589	0.1581	0.2135	1.5559	0.2557	2.9669
8	3.3.2/8	81-90	1.1799	0.1730	0.2566	1.6726	0.2987	3.2977

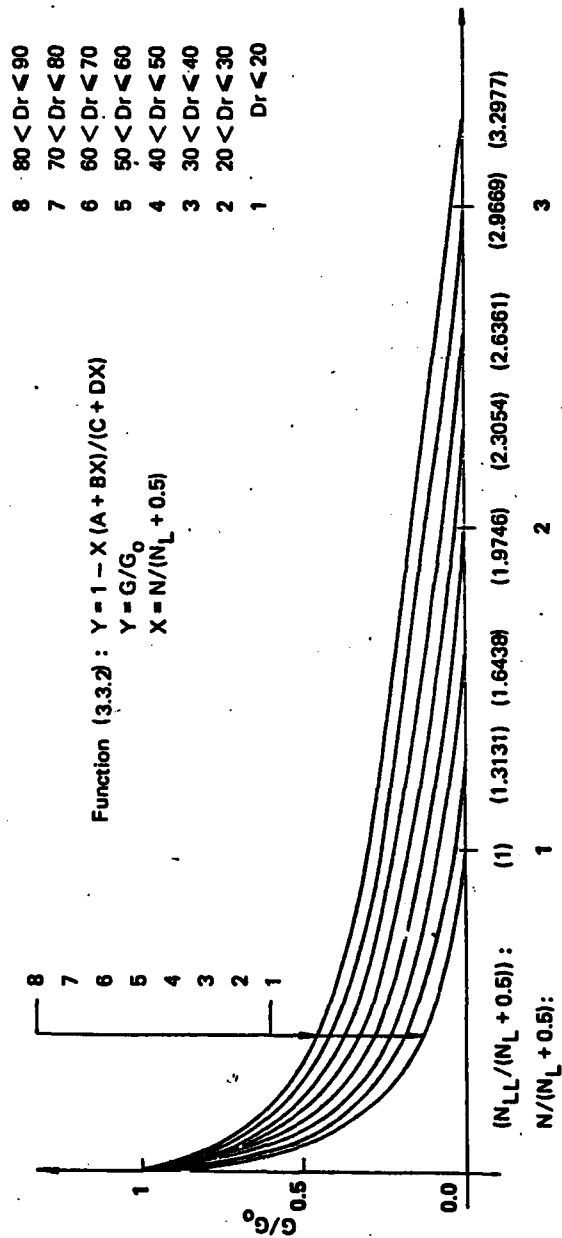


Fig. 3.3.10. Function of decrease in initial moduli ( $G$ ) depending on the number of cycles ( $N$ ), for different relative densities ( $D_r$ )

and  $(N/(N_L+0.5))$  determined by statistic processing of a number of experimental results, and on the basis of function (3.3.5) yielding the relationship between  $(G(N_L+0.5))$  and  $(D_r)$ . The obtained coefficients are presented in Table T.3.3.1. They have been used for definition of functions (3.3.2/1) to (3.3.3/8).

Functions (3.3.2/1) to (3.3.2/8) are presented graphically in Fig. 3.3.10.

Function (3.3.2/1) refers to very loose sands with  $(D_r)$  up to (20%). It acquires the value of (0) for  $(X=N/(N_L+0.5))$ . This means that total reduction in strength takes place if  $(\sigma'_1=0)$  is achieved in very loose sands having  $(D_r < 20\%)$ .

For the other functions (3.3.2/2) to (3.3.2/8), the value of  $(Y=G(N_L+0.5)/G_0 > 0)$  is obtained for  $(X=1)$ . This means that total reduction in strength is not taking place if  $(\sigma'_1=0)$ . Modulus  $(G(N_L+0.5))$  corresponds to this state. However, the elongation of the dynamic excitation beyond  $(\sigma'_1=0)$  induces continuation in the  $(G(N_L+0.5))$  decrease. If, on the basis of experimental results, it is adopted that the same relationships as those up to state  $(\sigma'_1=0)$  hold for this decrease, the characteristic number of cycles  $(N_{LL})$  for the occurrence of total reduction of  $(G)$  can be defined:

$$Y = 1 - X(A + BX)/(C + DX) = 0$$

$$Y = G/G_0$$

(3.3.9)

$$X = X_{LL} = N_{LL}/(N_L + 0.5)$$

where:

$N_{LL}$  - number of cycles for total reduction of  $(G)$ .

The  $(N_{LL})$  values have been defined for functions (3.3.2/2) to (3.3.2/8) and are given in Table T.3.3.1 in the form of  $(N_{LL}/(N_L+0.5))$  relationships.  $(N_{LL}=(N_L+0.5))$  for function (3.3.2/1). The  $(N_{LL})$  values are presented in Fig. 3.3.10.

The obtained results lead to the conclusion that the necessary number of cycles for total reduction in strength of sands, depending on their relative density, is more than (3) times the number initiating liquefaction occurrence for the very dense sands.

#### 4. RESPONSE ANALYSIS OF SOIL SUBJECTED TO DYNAMIC EXCITATIONS RESULTING IN PORE PRESSURE INCREASE

The response analyses of water-saturated cohesionless soil exposed to dynamic excitation inducing pore pressure increase is the complex aspect of the liquefaction problem. The complexity of this aspect results from the fact that the problem of determination of dynamic response of soil which is already very complicated is even aggravated due to the effect of pore pressure increase.

The response of soil excited by strong motions is basically a nonlinear problem. Strong earthquakes cause considerable shear strains in soil, which are even beyond the range of  $(10^{-5}-10^{-2} \%)$ . Soil behaviour in such conditions is characterized by a pronounced nonlinearity. In the conditions of pore pressure increase, this nonlinear behaviour acquires a new dimension, transformation of the nonlinear properties during the dynamic excitation.

For the last years, a considerable progress has been made considering the development of solutions and methodologies for the analysis of the nonlinear dynamic response of soil. As the problem is rather complicated, the solutions are associated with certain simplifications regarding the geometry of soil and the characteristics of the dynamic excitation. These achievements have been used as a starting point in the investigations presented herein, directed towards finding solutions and methodology for analysis of the dynamic response of soil, which is characterized by nonlinear behaviour and the possibility of transformation of the initial nonlinear characteristics due to the pore pressure increase.

The transformation of the initial nonlinear characteristics has been investigated on the basis of the results of laboratory testing and defining the relationships of pore pressure increase, liquefaction occurrence, shear moduli decrease and transformation of the  $(\tau/\gamma)$  relationships, as strain dependent.

#### 4.1. Nonlinear Dynamic Response of Soil

The problems associated with the dynamic response of soil involve determination of motions and their time and spatial variations within the frames of soil medium, induced by a known motion at some point or level at the base, the inside or the surface of the soil. The solutions of the problem are still under development, so that further investigations are needed. For the time being, dynamic response can be determined by introducing simplifications regarding the excitation (in case of earthquakes), as well as the geometry and the characteristics of the soil (Lysmer 1978 /26/).

The earthquake excitation basically includes body waves which propagate vertically or at some angle from the elastic half-space and horizontally propagating surface waves. However, considering the effects in the soil, most methods for analysis of soil response include simplification of vertically propagating shear waves according to the concept of Kanai (1952), Lysmer (1978 /26/). The predominant effect of the vertically propagating shear waves is mostly expressed in the horizontally layered soil. These conditions are most commonly considered from the viewpoint of liquefaction phenomenon. The solutions where the remaining possible waves are considered as an excitation are associated with wider simplifications especially regarding the material properties of soil and are generally in frequency domain. Taking this into account, as well as the predominant influence of shear waves on pore pressure generation, these investigations have been oriented towards finding solutions to dynamic response of soil excited by vertically propagating shear waves.

As to the geometry, the prevailing solutions are associated with the horizontally layered soil when it is possible to apply one-dimensional soil models. The solutions considering two-dimensional and three-dimensional models are associated with simplifications, which are basically reduced to application of linear and equivalent linear models of soil material properties and solutions to the equations of motion in frequency domain. From the viewpoint of problems connected with the liquefaction phenomenon, these solutions are still not satisfying the requirements set. This refers primarily to consideration of the nonlinear soil properties and response analysis in time domain.

The one-dimensional model of soil may belong to the class of continuum or discrete models. The equation of motion for the continuum models is:

$$G \frac{\partial^2 u}{\partial y^2} + \mu \frac{\partial^3 u}{\partial y^2 \partial t} + \rho \frac{\partial^2 u}{\partial t^2} = p(t) \quad (4.1.1)$$

where:

- (G) - shear modulus
- ( $\mu$ ) - viscosity coefficient
- ( $\rho$ ) - mass density
- ( $u(y, t)$ ) - relative displacement
- ( $p(t)$ ) - excitation at time ( $t$ )

The equation of motion for the discretized soil model is the following:

$$M\ddot{U} + C\dot{U} + KU = P \quad (4.1.2)$$

where:

- M - mass matrix
- C - damping matrix
- K - stiffness matrix
- U,  $\dot{U}$ ,  $\ddot{U}$  - displacement, velocity and acceleration vectors
- P - excitation vector

As to the soil properties, linear, equivalent linear and lately nonlinear models have been developed. However, the behaviour of soil during strong earthquakes is nonlinear. Hence, linear models are representing only a rough approximation to the soil material properties.

A considerable progress has been made by application of the equivalent linear material properties, Seed and Idriss 1970 /45/, Hardin and Drnevich 1972 /45/, using equivalent linear model. This model represents the first approximation to the nonlinear models. Applying the iterative procedure, this model makes possible to coordinate the equivalent moduli and material dampings with the developed strains. For the strains developed under strong excitation, this means high reduction of initial elastic moduli and considerable increase of material damping.

Finally, the application of the nonlinear models makes possible to simulate the true nature of the material behaviour of soil during strong dynamic excitations. Several constitutive laws have been defined according to the concept of Massing (1927), Chen and Joyner (1974) /7/, expressed through the following hypotheses:

- Damping is of the hysteretic nature and is independent on the rate of strain;
- The nonlinearity of the material is of plastic nature. The stiffness of the material is independent of the history of the loading as it returns to its maximum at each change of the loading direction;
- Under harmonic loading of constant amplitude, the hysteretic damping provides steady-state response after few cycles.

On these bases, two classes of models to be applied in modeling of material properties of soil have been distinguished: the Ramberg-Osgood models (Yoshimi, Richart et al. 1977 /46/, Hardin and Drnevich 1972 /45/, Streeter et al. 1974 /45/, Finn et al. 1977 /14/, Ishihara and Towhata 1980 /19/) and the Davidenkova models (Martin and Seed 1978 /28/).



Strains are functions of stresses according to Ramberg-Osgood model given by the following loading and unloading relationships:

- Loading

$$\frac{d\gamma}{d\tau} = \frac{1}{G_0} |1 + F(\tau - \tau_{min})| \quad (4.1.3)$$

- Unloading

$$\frac{d\gamma}{d\tau} = \frac{1}{G_0} |1 + F(\tau_{max} - \tau)| \quad (4.1.4)$$

where ( $G_0$ ) is shear modulus for low strains, while ( $F$ ) is a nonlinearity function.

On the contrary, Davidenkov model considers stresses as functions of strains and is given by the following relationships:

- Loading

$$\frac{d\tau}{d\gamma} = G_0 |1 - F(\gamma - \gamma_{min})| \quad (4.1.5)$$

- Unloading

$$\frac{d\tau}{d\gamma} = G_0 |1 - F(\gamma_{max} - \gamma)| \quad (4.1.6)$$

Applying the nonlinear soil models, the equations of motion for both the continuum and the discrete system (4.1.1, 4.1.2) are solved by direct integration in time domain. The integration is performed in successive time intervals selected to provide stability and accuracy of the solution. The structural properties of the system are assumed to be constant within each time step. This practically means application of the equivalent linear integration operator (Martin 1975 /45/).

Several methods have been developed for analysis of the nonlinear soil response by continuum models (Equation 4.1.1) and models with discretization of the soil profile (Equation 4.2.1). The solutions are provided by applying the method of characteristics, finite differences, concentrated masses and finite elements. As it is impossible to mention all authors, only the references referring to solutions and methods /8, 26/ will be mentioned. These solutions are known as solutions by total stresses.

Some of the solutions to the nonlinear dynamic response have been developed further in order to take into account the effect of pore pressure increase. Such solutions are given by Finn et al. 1977 /13/, Liou 1976 /45/, Ishihara et al. 1980 /19/, Martin and Seed 1978 /28, 30/. They are known as solutions by effective stresses.

An analysis of the known solutions to the nonlinear soil response has been performed in order to use the experience gathered so far and select the most suitable method which will serve as a starting point in solving dynamic response by transformation of the initial nonlinear soil characteristics. Generally speaking, most of the solutions could have been used for this purpose. However, priority has been given to Martin's method (1975 /45/) applied in the computer programme MASH /28/ taking into account the investigations discussed in Chapters 2 and 3, where liquefaction parameters are defined by cyclic strains.

The suitability of this method lies mainly in the applied model of the material properties of soil. The Martin-Davidenkov model belongs to the class of models where stresses are expressed as functions of shear strains (Equations 4.1.5 and 4.1.6) so that the defined liquefaction parameters can directly be introduced as dependent upon shear strains.

#### 4.2. Nonlinear Dynamic response Applying the Martin-Davidenkov Model and Direct Integration with Cubic Inertia Method

The solution of the nonlinear dynamic response by application of Martin-Davidenkov model and direct integration with cubic inertia method refers to horizontally layered soil medium excited by vertically propagating shear waves (Martin and Seed 1978 /28/).

The soil medium is discretized by one-dimensional finite elements. The general equation of motion for the discrete system is given by (4.1.2). It can also be presented as follows:

$$M\ddot{U} = P - C\dot{U} - KU \quad (4.2.1)$$

##### 4.2.1. Solution of Equations of Motion

The method from the class of algorithms with inertia forces known as integration method with cubic inertia force (Arguris et al. 1973 /2/, 1973 /3/) has been selected among the possible methods for direct integration of equations of motion (4.2.1).

According to the class of inertia algorithms, the variation of the relative inertia force, from the general equation of motion (4.2.1)

$$R = M\ddot{U} \quad (4.2.2)$$

at the time step of the integration ( $\Delta t$ ), is approximated by some function, the general form of which is given by:

$$R = f(R_0, R_1, \dot{R}_0, \dot{R}_1, \ddot{R}_0, \ddot{R}_1, \dots) \quad (4.2.3)$$

The indices (0) refer to the inertial force and its derivatives at time ( $t_0$ ), at the beginning of time step ( $\Delta t$ ), while (1) are associated with the end of this step, at time ( $t_1 = t_0 + \Delta t$ ). The simplest approximation with (4.2.3) is to consider constant inertial force, while linear variation at interval ( $\Delta t$ ) will be considered in the following approximation:

$$\begin{aligned} R &= sR_1 + (1 - s) R_0 \\ t &= s\Delta t, \quad 0 \leq s \leq 1 \end{aligned} \quad (4.2.4)$$

The exactness is improved with the increase of the order of approximation. On the basis of the performed analyses of the influence of the approximation order, /2, 28/ Martin applied approximation of third order as sufficiently exact. The solution by this approximation is known as cubic inertia method, or Arguris' method.

The main assumption of this method is that the relative inertia force varies as cubic function of time at the integration time step. The cubic function is defined by four constants as well as the values of inertia force ( $R$ ) at the beginning and the end of time step and its derivatives ( $\dot{R}$ ):

$$\dot{R} = H_{00}\dot{R}_0 + H_{10}\dot{R}_0 + H_{01}\dot{R}_1 + H_{11}\dot{R}_1 \quad (4.2.5)$$

In (4.2.5),  $(H_{00})$ ,  $(H_{10})$ ,  $(H_{01})$  and  $(H_{11})$  are Hermitian polynomial of third order:

$$\begin{aligned} H_{00} &= 1 - 3s^2 + 2s^3 \\ H_{10} &= (s - 2s^2 + s^3) \Delta t \\ H_{01} &= 3s^2 - 2s^3 \\ H_{11} &= (-s^2 + s^3) \Delta t \\ t &= s\Delta t, \quad 0 \leq s \leq 1 \end{aligned} \quad (4.2.6)$$

Considering (4.2.5) and (4.2.6), the increments of relative velocity and relative displacement at time step  $(\Delta t)$  are obtained by two successive integrations of equation (4.2.2) over time.

$$M\Delta\dot{U} = \frac{\Delta t}{12} (6R_0 + \Delta t\dot{R}_0 + 6R_1 - \Delta t\dot{R}_1) \quad (4.2.7)$$

$$M\Delta U = M\dot{U}_0\Delta t + \frac{\Delta t^2}{60} (21R_0 + 3\Delta t\dot{R}_0 + 9R_1 - 2\Delta t\dot{R}_1) \quad (4.2.8)$$

where:

$$\Delta\dot{U} = \dot{U}_1 - \dot{U}_0 \quad (4.2.9)$$

$$\Delta U = U_1 - U_0 \quad (4.2.10)$$

Equations (4.2.7) and (4.2.8) are the main equations of the algorithm. They determine displacement and velocity at the end of the time step  $(\Delta t)$  as well as stresses and internal forces. The iterative procedure makes possible to bring into accordance the inertial, internal and excitation forces.

In the solution, the equation of motion at some level  $(i)$  of the system is of the following type:

$$m_i \ddot{u}_i + \tau_i - \tau_{i-1} = -m_i \ddot{u}_b \quad (4.2.11)$$

where:

- $m_i$  - concentrated mass at level  $(i)$
- $\tau_i$  - stress in element  $(i)$ , immediately below level  $(i)$
- $\tau_{i-1}$  - stress in element  $(i-1)$ , immediately above level  $(i)$
- $\ddot{u}_i$  - relative acceleration in respect to the base
- $\ddot{u}_b$  - acceleration at the base

Based on the performed analyses, Martin 1975 /45/ concluded that the direct integration by cubic inertia method is accurate and stable for the condition  $(\Delta t/T \leq 0.5)$ , where  $T$  = natural period of the system (1978 /28/).

#### 4.2.2. Martin-Davidenkov Model

A nonlinear model, which has especially been developed as a constituent part of the response analysis methodology has been applied in modeling of the behaviour of soil medium.

The nonlinear model defined as Martin-Davidenkov model /28/ has been developed on the basis of Davidenkov model given by the general equations (4.1.5) and (4.1.6).

For symmetrical hysteretic relationship, it is the following:

$$\gamma_{min} = -\gamma_{max} \quad (4.2.12)$$

so that by substituting ( $\gamma = \gamma_{max}$ ), i.e. ( $\gamma = \gamma_{min}$ ), the following expression is obtained for the tangent modulus, immediately before changing the loading direction:

$$\frac{d\tau}{d\gamma} = G_0 |1 - F(2\gamma_{max})| \quad (4.2.13)$$

By integration of (4.2.13) for the family of values ( $\gamma_{max}$ ), the following is obtained:

$$\tau = \int_0^{\gamma} G_0 |1 - F(2\eta)| d\eta = G_0 \gamma |1 - \frac{1}{\gamma} \int_0^{\gamma} F(2\eta) d\eta| \quad (4.2.14)$$

that is,

$$\tau = G^* \gamma \quad (4.2.15)$$

with

$$G^* = G_0 |1 - \frac{1}{\gamma} \int_0^{\gamma} F(2\eta) d\eta| \quad (4.2.16)$$

According to definition, ( $G^*$ ) is a secant modulus in respect to strain ( $\gamma$ ).

Defining a new function ( $H(\gamma)$ ):

$$H(\gamma) = \frac{1}{\gamma} \int_0^{\gamma} F(2\eta) d\eta \quad (4.2.17)$$

the following expression is obtained for ( $G^*$ ):

$$G^* = G_0 |1 - H(\gamma)| \quad (4.2.18)$$

The secant modulus ( $G^*$ ) is defined on the basis of experimental results. Accordingly, function ( $H(\gamma)$ ) reflecting the nonlinearity of ( $G^*$ ) is defined in the same way. Martin defines ( $H(\gamma)$ ) function by the following expression

$$H(\gamma) = \left| \frac{|\gamma/\gamma_0|^{2B}}{1 + |\gamma/\gamma_0|^{2B}} \right|^A \quad (4.2.19)$$

where

$\gamma_0$  - reference strain  
 $A, B$  - parameters defined on the basis of experimental results.

Differentiating (4.2.17), the following expression is obtained for ( $F$ ):

$$F(2\gamma) = H(\gamma) + \gamma \frac{dH(\gamma)}{d\gamma} \quad (4.2.20)$$

Considering expression (4.2.19), the following is obtained:

$$F(\gamma) = |1 + 2AB + |\gamma/2\gamma_0|^{2B}| \frac{|\gamma/2\gamma_0|^{2AB}}{|1 + |\gamma/2\gamma_0|^{2B}|^{A+1}} \quad (4.2.21)$$

The basic equations of the Martin-Davidenkov model have been obtained from the main equations (4.1.5) and (4.1.6) of the Davidenkov's model. The integration form of (4.1.5) and (4.1.6) is the following:

$$\tau - \tau_{min} = \int_{\gamma_{min}}^{\gamma} G_0 |1 - F(\xi - \gamma_{min})| d\xi \quad (4.2.22)$$

$$\tau - \tau_{max} = \int_{\gamma_{max}}^{\gamma} G_0 |1 - F(\gamma_{max} - \xi)| d\xi \quad (4.2.23)$$

Substituting:

$$2\eta = \xi - \gamma_{min}, \quad 2d\eta = d\xi, \quad \eta \in |0, \frac{\gamma - \gamma_{min}}{2}|$$

that is,

$$2\eta = \gamma_{max} - \xi, \quad 2d\eta = -d\xi, \quad \eta \in |0, \frac{\gamma_{max} - \gamma}{2}|$$

it is obtained

$$\tau - \tau_{min} = G_0 |\gamma - \gamma_{min}| \left| 1 - \frac{2}{\gamma - \gamma_{min}} \int_0^{\frac{\gamma - \gamma_{min}}{2}} F(2\eta) d\eta \right| \quad (4.2.24)$$

$$\tau - \tau_{max} = -G_0 |\gamma_{max} - \gamma| \left| 1 - \frac{2}{\gamma_{max} - \gamma} \int_0^{\frac{\gamma_{max} - \gamma}{2}} F(2\eta) d\eta \right| \quad (4.2.25)$$

Applying (4.2.17), the following basic expressions are obtained:

• for loading

$$\tau - \tau_{min} = G_0 |\gamma - \gamma_{min}| \left| 1 - H\left(\frac{\gamma - \gamma_{min}}{2}\right) \right| \quad (4.2.26)$$

• for unloading

$$\tau - \tau_{max} = -G_0 |\gamma_{max} - \gamma| \left| 1 - H\left(\frac{\gamma_{max} - \gamma}{2}\right) \right| \quad (4.2.27)$$

Using the results of laboratory testing of moduli ( $G$ ) and damping ( $D$ ), Martin (1975 /45/) defined the ( $\gamma_0$ ), ( $A$ ) and ( $B$ ) parameters for sands and clays, respectively. The results of the tests performed by Seed and Idriss (1970) have also been used. The following values have been obtained for sands:

$$A = 0.9, \quad B = 0.413, \quad \gamma_0 = 3.16 \cdot 10^{-4} \quad (4.2.28)$$

and clays:

$$A = 0.2, \quad B = 0.5, \quad \gamma_0 = 5 \cdot 10^{-3} \quad (4.2.29)$$

#### 4.3. Model of the Initial Soil Properties Transformation

According to Martin-Davidenkov model, the ( $\tau/\gamma$ ) nonlinear relationships have been obtained by functions (4.2.26) and (4.2.27). In these functions, ( $G_0$ ) occurs as a characteristic constant representing the initial, maximum shear modulus. Nonlinearity is considered by function ( $H(\gamma)$ ) given in equation (4.2.19). Stresses ( $\tau$ ) are determined by functions (4.2.26) and (4.2.27) in the range from ( $\gamma_{min}$ ) to ( $\gamma_{max}$ ) during loading, i.e. from ( $\gamma_{max}$ ) to ( $\gamma_{min}$ ) during unloading.

This model is successfully applied when initial soil properties are considered to be constant during the dynamic excitation.

These are the conditions when dynamic excitation induces neither special effect due to loading nor variation of effective stresses, which is even more important.

However, the nonlinear relationships ( $\tau/\gamma$ ) do not remain unvariable in case of water-saturated sands under the conditions of pore pressure generation and variation of effective stresses. For the strain range of ( $\gamma_{min}$ ) to ( $\gamma_{max}$ ), they vary from cycle to cycle, transforming themselves as a result of the decrease in strength. Typical examples of such a transformation are presented in the figures in Chapter 3.

Analysing the experimental results of these investigations, it has been concluded that the maximum initial modulus ( $G_0$ ) does not remain unchanged throughout cyclic loading. It degrades proportionally to the decrease of effective stresses, as discussed under Item 3.3. On the basis of this, it has been estimated that modeling under the discussed conditions can be performed by a model in which modulus ( $G$ ) will also be a variable parameter. The variation of ( $G$ ) is in function of the number of cycles ( $N$ ), i.e., the semi-cycles ( $n$ ). This concept is presented in Fig. 4.3.1.

Taking Martin-Davidenkov model as a starting point, the model based on the upper stated concept is considered by the following mathematical expressions:

$$\tau(n) - \tau_{min}(n-1) = G(n-1) |\gamma - \gamma_{min}| \left| 1 - H\left(\frac{\gamma - \gamma_{min}}{2}\right) \right| \quad (4.3.1)$$

$$\tau(n+1) - \tau_{max}(n) = -G(n) |\gamma_{max} - \gamma| \left| 1 - H\left(\frac{\gamma_{max} - \gamma}{2}\right) \right| \quad (4.3.2)$$

Functions (4.3.1) and (4.3.2) referring to loading and unloading, respectively, define stresses ( $\tau(n)$ ) and ( $\tau(n+1)$ ) in strain range of ( $\gamma_{min} - \gamma_{max}$ ) at semi-cycles ( $n$ ) and ( $n+1$ ). The extreme stresses ( $\tau_{min}(n-1)$ ) and ( $\tau_{max}(n)$ ) occur as functions of ( $n$ ), however, being defined at the previous excitation semi-cycle, they appear as constants during the current semi-cycle. The initial modulus ( $G(n-1)$ ), i.e., ( $G(n)$ ) occurs also as a function of ( $n$ ) and is practically the parameter defining the transformation of the nonlinear curves. It is also defined in the previous semi-cycle and occurs as constant in the current one. Hence, definition of the model is reduced to definition of the ( $G(n)$ ) function.

The bases for definition of the ( $G(n)$ ) function are given by the investigations presented in Chapter 3, Item 3.3.

The complicated behaviour of soil under the conditions of variable initial characteristics due to pore pressure increase and decrease of effective stresses has been interpreted mathematically by the defined model of nonlinear relationship ( $\tau/\gamma$ ) and transformation of the initial characteristics. The nonlinear relationship ( $\tau/\gamma$ ) of the model varied proportionally to the variation of the initial modulus ( $G$ ), which occurs as a parameter governing transformation. The model is defined on the basis of experimental nonlinear relationships.

#### 4.4. Model for a Dynamic Response Analysis of Soil with Included Pore Pressure Increase

A model for dynamic response analysis of soil with included pore pressure increase has been defined on the basis of results of the previously discussed investigations. The model is presented in Fig. 4.4.1.

The model includes the following relationships:

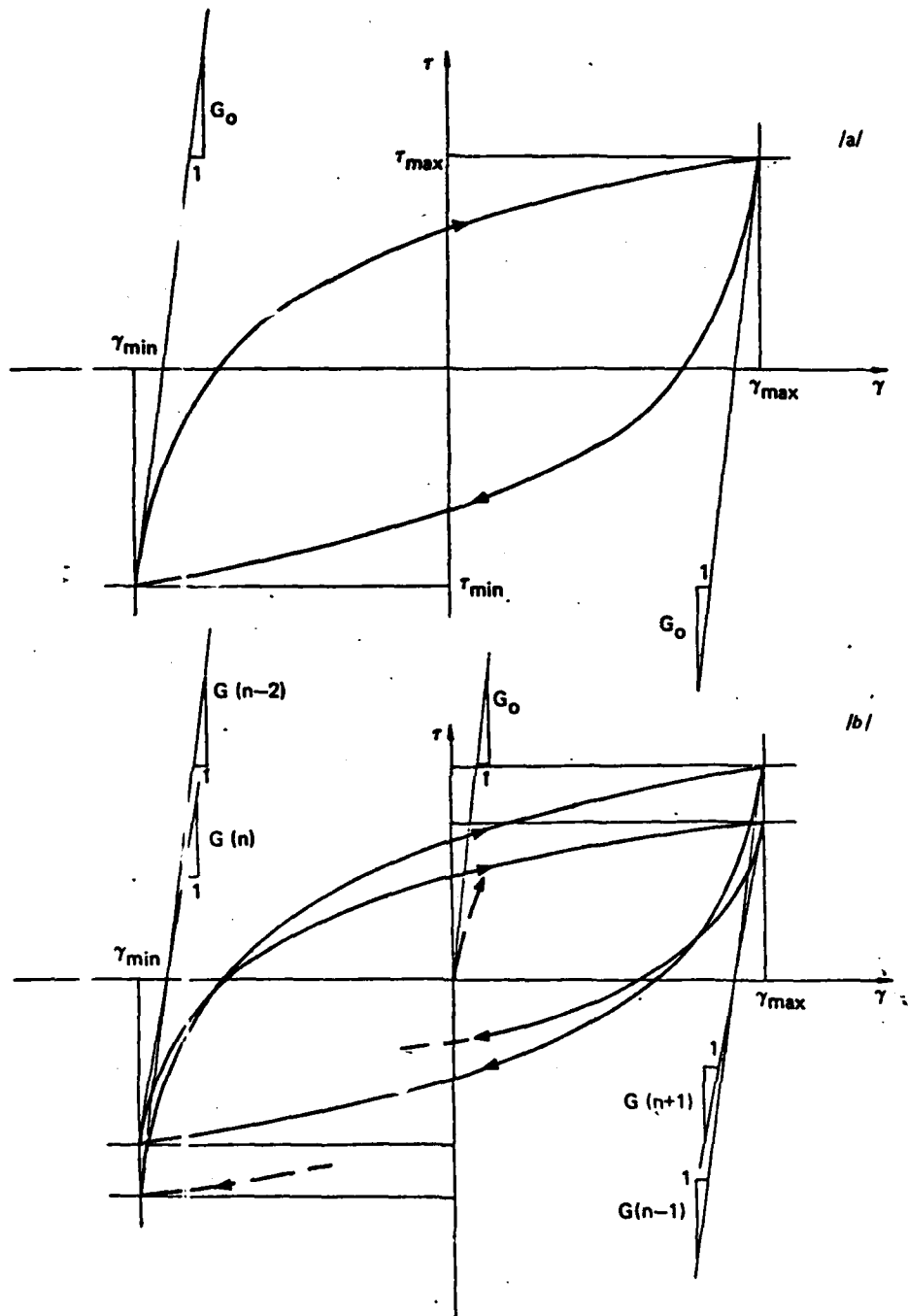


Fig. 4.3.1. Model of nonlinear relationship ( $\tau/\gamma$ ):  
 a) with constant initial properties  
 b) with transformation of initial properties

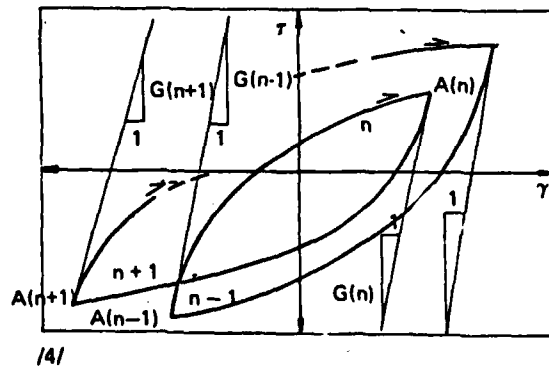
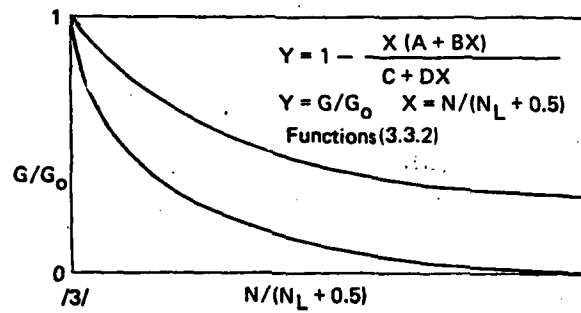
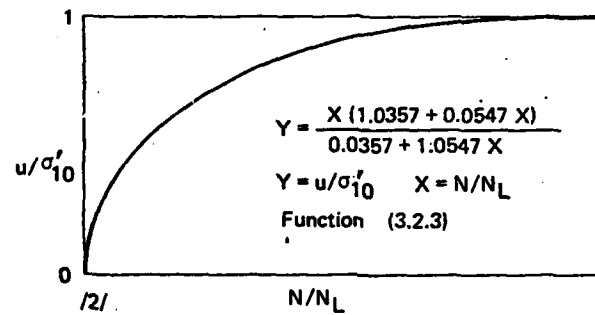
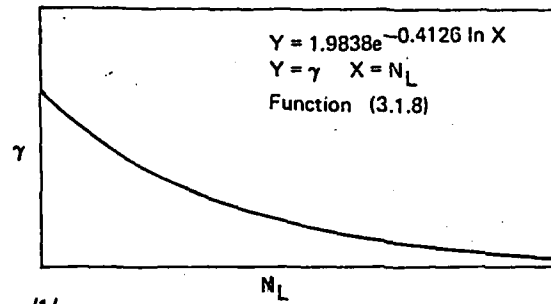


Fig. 4.4.1. Model for dynamic response analysis under increased pore pressure conditions



1. Relationship between shear strain amplitude and number of cycles/semi-cycles for occurrence of pore pressure of (100%);
2. Pore pressure increase function;
3. Maximum shear moduli decrease functions; and
4. Transformation model for the nonlinear relationships ( $\tau/\gamma$ ).

The relationship between ( $\gamma$ ) and ( $N$ ) for the occurrence of ( $u=\sigma'_1$ ) presented in Fig.4.4.1.1 has been defined by the investigations in Chapter 3, Item 3.1. It is given by function (3.1.8) and is directly applied in the model.

The increase function of ( $u$ ) is presented in Fig. 4.4.1.2. It is defined by the investigations in Chapter 3, Item 3.2 and is given by (3.2.3). It is also directly applied in the model.

The decrease functions of the maximum, initial shear moduli have been defined in Chapter 3, Item 3.3. They are given by (3.3.2/1) to (3.3.2/8), directly applied in the model and presented in Fig. 4.4.1.3.

The transformation model of the nonlinear relationships ( $\tau/\gamma$ ) is presented in Fig. 4.4.1.4. It has been defined on the basis of functions (4.3.1) and (4.3.2) and is given by:

$$\tau(n) - \tau_{min}(n-1) = G(n-1) \left| \gamma(n) - \gamma_{min}(n-1) \right| \left| 1 - H\left(\frac{\gamma(n) - \gamma_{min}(n-1)}{2}\right) \right| \quad (4.4.1)$$

$$\tau(n+1) - \tau_{max}(n) = -G(n) \left| \gamma_{max}(n) - \gamma(n+1) \right| \left| 1 - H\left(\frac{\gamma_{max}(n) - \gamma(n+1)}{2}\right) \right| \quad (4.4.2)$$

Functions (4.4.1) and (4.4.2) define stresses ( $\tau(n)$ ) and ( $\tau(n+1)$ ), at semi-cycles ( $n$ ) and ( $n+1$ ), depending upon strains ( $\gamma(n)$ ) and ( $\gamma(n+1)$ ), respectively. In order that they be defined, it is necessary to define previously the initial, extreme points with arbitrary, non-uniform extreme strains ( $\gamma_{min}(n-1)$ ), i.e., ( $\gamma_{max}(n)$ ). In this way, the model includes strain range of ( $\gamma_{min}$ ) to ( $\gamma_{max}$ ) which varies from semi-cycle to semi-cycle in accordance with the effects of the dynamic excitation. The initial moduli ( $G(n-1)$ ) and ( $G(n)$ ) vary in accordance with functions (3.3.2/1) to (3.3.2/8).

At semi-cycle ( $n$ ), the ( $\tau(n)/\gamma(n)$ ) relationship is defined by (4.4.1) and (4.4.2) and parameters ( $G(n-1)$ ), ( $\tau_{min}(n-1)$ ) and ( $\gamma_{min}(n-1)$ ), that is, alternatively by ( $\tau_{max}(n-1)$ ) and ( $\gamma_{max}(n-1)$ ), which are defined at the preceding semi-cycle. At the semi-cycle ( $n$ ), the extreme point in the nonlinear relationship ( $A(n)$ ) is determined by the coordinates ( $\tau_{max}(n), \gamma_{max}(n)$ ) or ( $\tau_{min}(n), \gamma_{min}(n)$ ), alternatively.

The extreme points ( $A(n-1)$ ) from the preceding semi-cycle and ( $A(n)$ ) define the cyclic shear strain amplitude at the semi-cycle:

$$|2\gamma_r(n)| = |\gamma_A(n) - \gamma_A(n-1)| \quad (4.4.3)$$

where:

- $\gamma_r(n)$  - cyclic shear strain amplitude at semi-cycle ( $n$ );
- $\gamma_A(n-1)$  - strain at the extreme point of the nonlinear curve during the preceding semi-cycle;
- $\gamma_A(n)$  - strain at the extreme point of the nonlinear curve during the analysed semi-cycle.

The amplitude ( $\gamma_r$ ) defines the effects of the semi-cycle ( $n$ ) upon the increase of ( $u$ ) and decrease of ( $G$ ). Proportionally to ( $\gamma_r(n)$ ), the equivalent number of cycles ( $N_L(n)$ ) for the occurrence of ( $u=\sigma'_1$ ) (Fig. 4.4.1.1) is obtained from function (3.1.8).

The increase in the excessive pore pressure ( $\Delta u(n)$ ) is obtained from function (3.2.3) (Fig. 4.4.1.2), while functions (3.3.2/1) to (3.3.2/8) yield the reduction of the initial modulus ( $\Delta G(n)$ ). Modulus ( $G(n)$ ) is defined by reduction ( $\Delta G(n)$ ). The determination of ( $G(n)$ ), ( $\tau_{max}(n)$ ) and ( $\gamma_{max}(n)$ ) or ( $\tau_{min}(n)$ ) and ( $\gamma_{min}(n)$ ), alternatively, makes possible to define the ( $\tau(n+1)/\gamma(n+1)$ ) relationship in the following semi-cycle.

On these bases the computer program KOLID was developed.

## 5. CASE STUDIES

In order to verify the developed methodology for dynamic response analysis of soil medium under the conditions of pore pressure increase and the computer programme KOLID, dynamic analysis of 3 models of soil, in which liquefaction took place during the April 15, 1979 Montenegro earthquake, has been performed. A model of soil in which no liquefaction has been observed due to the mentioned earthquake has also been analysed.

The accelerograms obtained at the earthquake epicenter area in the vicinity of the analysed sites have been used as dynamic excitation in the analyses.

For the applied acceleration time histories, the following time histories of response parameters have been obtained by the analysis: pore pressure, accelerations, strains, stresses, nonlinear relationships ( $\tau/\gamma$ ) and displacements in the elements of models at different depths. The acceleration time histories response spectra have also been determined. These parameters have been determined without consideration of the pore pressure increase or analysing the total stresses ( $T_0$ ), or with consideration of the pore pressure increase or analysis by using the effective stresses (EF).

The response of the elements in which liquefaction, i.e., considerable pore pressure increase occurs as well as the response at the surface of the models are of special importance for the comparative analysis of the dynamic response of models with the behaviour of soil media at the sites during the earthquake of April 15, 1979. The response parameters of these elements were studied in details.

As an example, characteristic results obtained for the model (GTM1) for Bijela site are given here.

This model, representing the average characteristics of the site, is considered by 6 finite elements in the analysis.

The profile to which the model refers is characterized by a high level of underground water and sands susceptible to liquefaction, especially at depth of 6 to 14 m. Element (5) with ( $V_{80}=150$  m/s) and ( $D_r=40\%$ ) at depth of (11.5-13.8m) appears as element, which practically controls the behaviour of the whole model under the conditions of pore pressure increase. Therefore, the response of this element will be considered separately further in the text.

For an excitation by the componental time history (Herceg Novi NS) registered near the site during the earthquake with ( $a_{max}=0.23g$ ) there is very high increase of ( $u$ ) in element (5) having the maximum value of:

$$(u/\sigma'_{10})_5 = 0.89217$$

initiating a state which is very close to initial liquefaction.

The componental time history (Herceg Novi WE) also registered at the same time as the NS component with ( $a_{max}=0.26g$ ) induces also very high increase in ( $u$ ) having maximum value of:

$$(u/\sigma'_{10})_5 = 0.93601$$

which is even closer to the initial liquefaction.

However, the equivalent summarized time history (Herceg Novi NS+WE) induces increase of ( $u$ ) in element (5) having maximum value of:

$$(u/\sigma'_{10}) = 1.00$$

which corresponds to initial liquefaction. The time history of ( $u$ ) is presented in Fig. 5.3.1.

The behaviour of element (5) in such conditions can be estimated by comparative analysis of some dynamic response parameters with total stresses (TO) and effective stresses (EF) presented in Figs. 5.3.2 to 5.3.7. The comparative analysis proves that pore pressure development results in the following:

- Considerable increase of strains in the element (Figs. 5.3.2 and 5.3.3);
- At ( $u=\sigma'_{10}$ ), stresses ( $\tau$ ) decrease considerably until total reduction in strength and liquefaction takes place (Figs. 5.3.4 and 5.3.5);
- During the excitation, the nonlinear relationships ( $\tau/\gamma$ ) in the element are characterized by decrease in ( $\tau$ ) and increase in ( $\gamma$ ) as a result of the increase in ( $u$ ) and "rotation" towards the ( $\gamma$ ) axis which reflects the transformation of the initial soil properties and liquefaction occurrence (Figs. 5.3.6 and 5.3.7).

As a result of the liquefaction occurring in element (5), element (1), the behaviour of which is presented in Figs. 5.3.8 and 5.3.9, is characterized by the following:

- Reduction of accelerations immediately after ( $u=\sigma'_{10}$ ) is achieved in element (5) (Figs. 5.3.8 and 5.3.9); and
- Increase in horizontal displacements.

The presented soil behaviour modeled by (GTM1) and presented by the dynamic response parameters of elements (5) and (1) corresponds to the behaviour of soil medium at the Bijela site characterized by liquefaction occurrence during the earthquake of April 15, 1979.

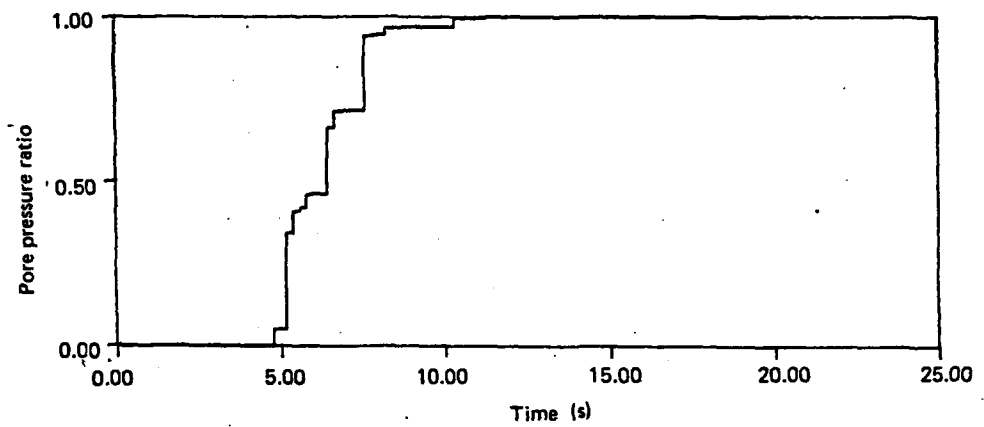


Fig. 5.3.1. Pore pressure time history in element No. 5 for model GTM1 - Bijela, Herceg Novi NS+WE (0.33 g) KOLID-EF

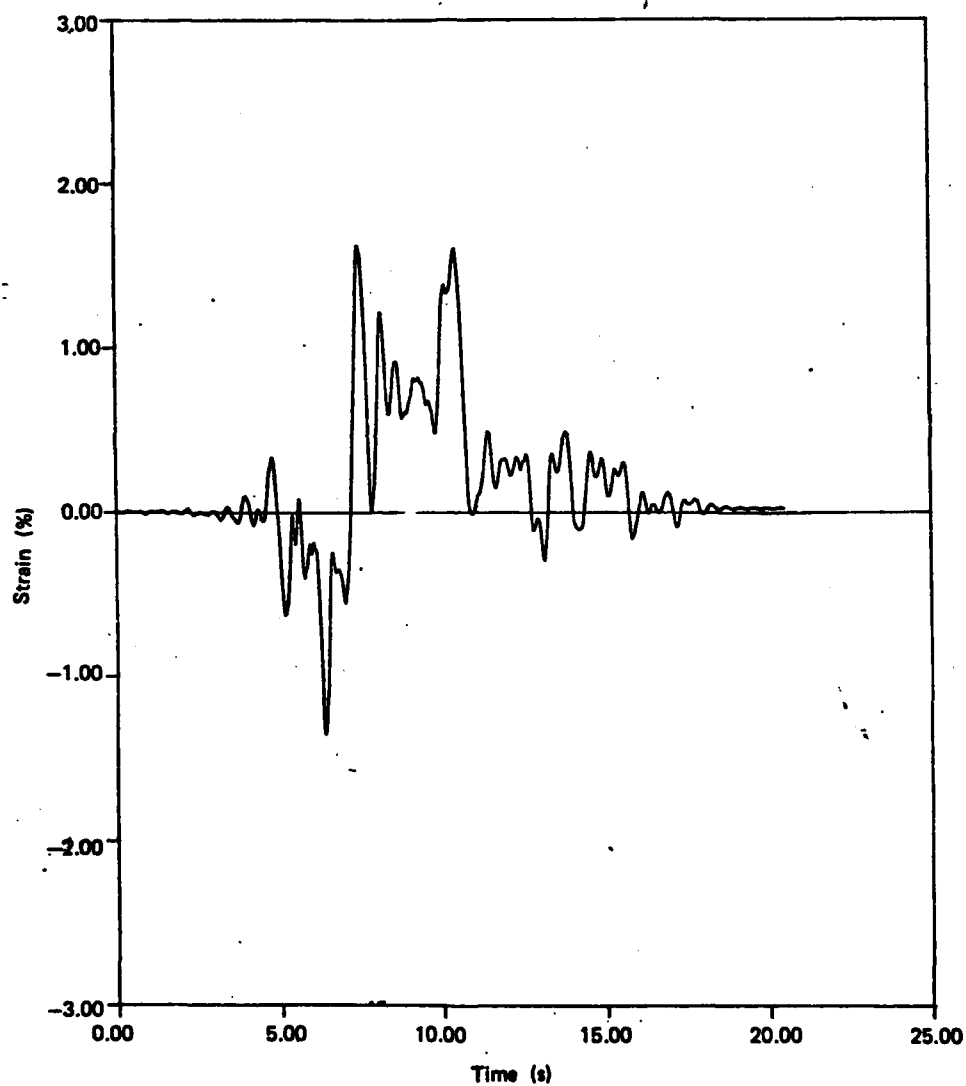


Fig. 5.3.2. Time history of strain (X) in element No. 5 for model GTM1 - Bijela, Herceg Novi NS+WE (0.33 g) KOLID-TO

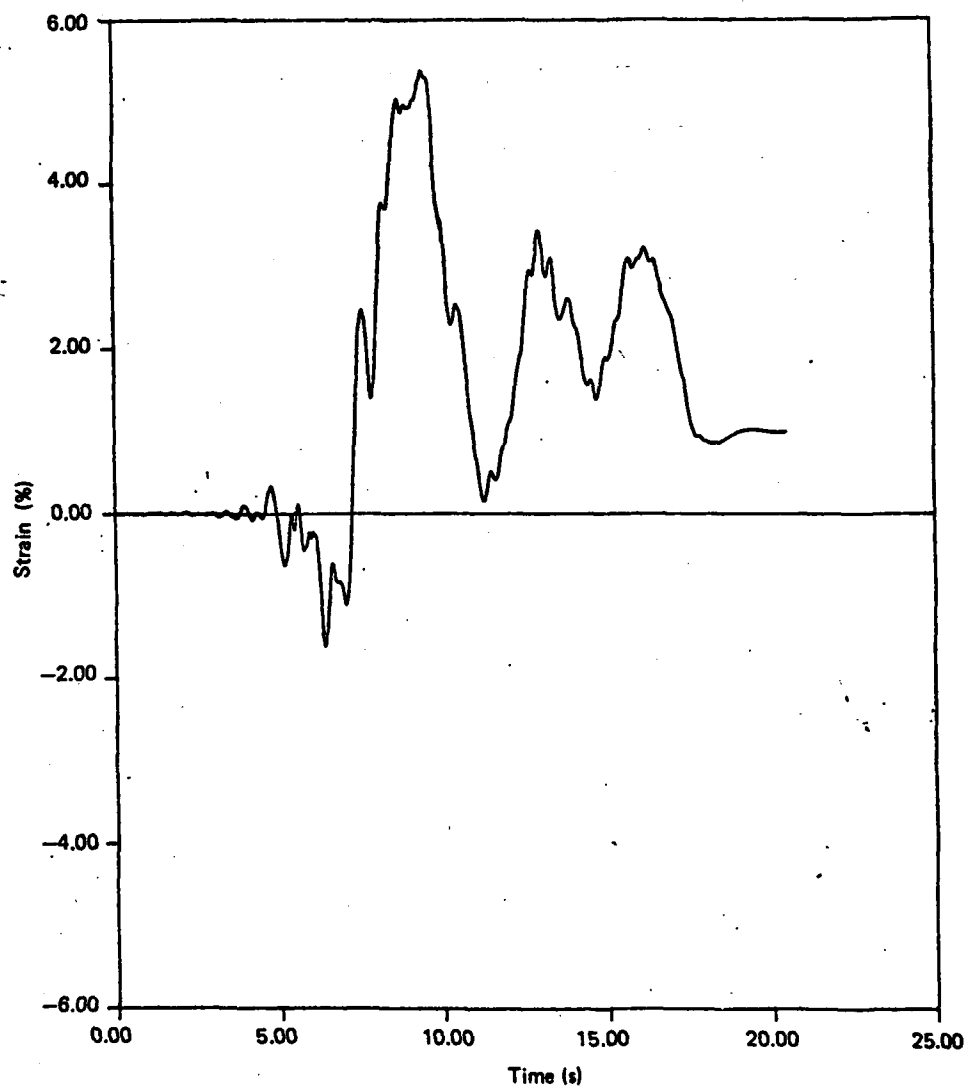


Fig. 5.3.3. Time history of strain (%) in element No. 5 for model GTM1 - Bijela, Herceg Novi NS+WE (0.33 g) KOLID-EF

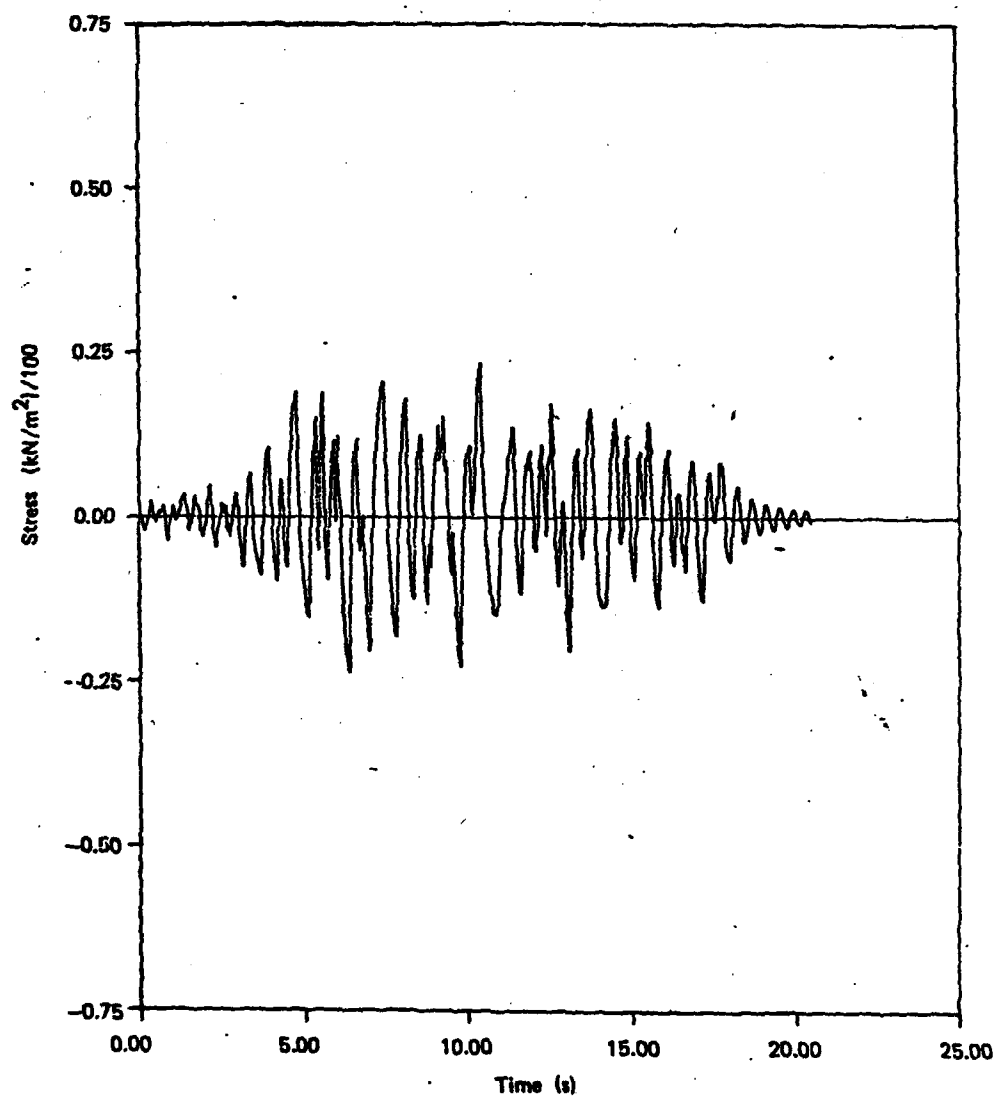


Fig. 5.3.4. Time history of stress  $(kN/m^2)/100$  in element No. 5 for model GTM1 - Bijela, Herceg Novi NS+WE (0.33 g) KOLID-TO

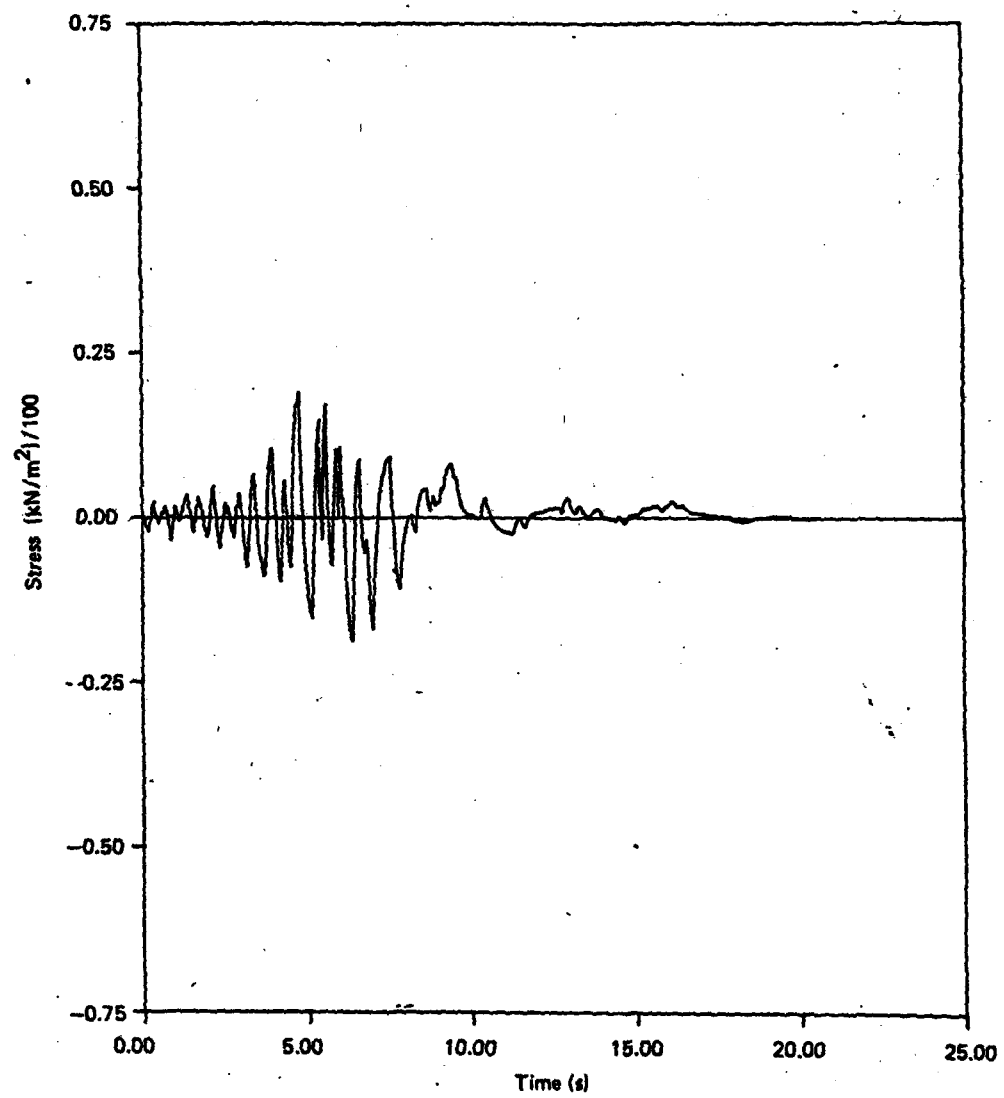


Fig. 5.3.5. Time history of stress  $(\text{kN/m}^2)/100$  in element No. 5 for model GTM1 - Bijela, Herceg Novi NS+WE (0.33 g) KOLID-EF



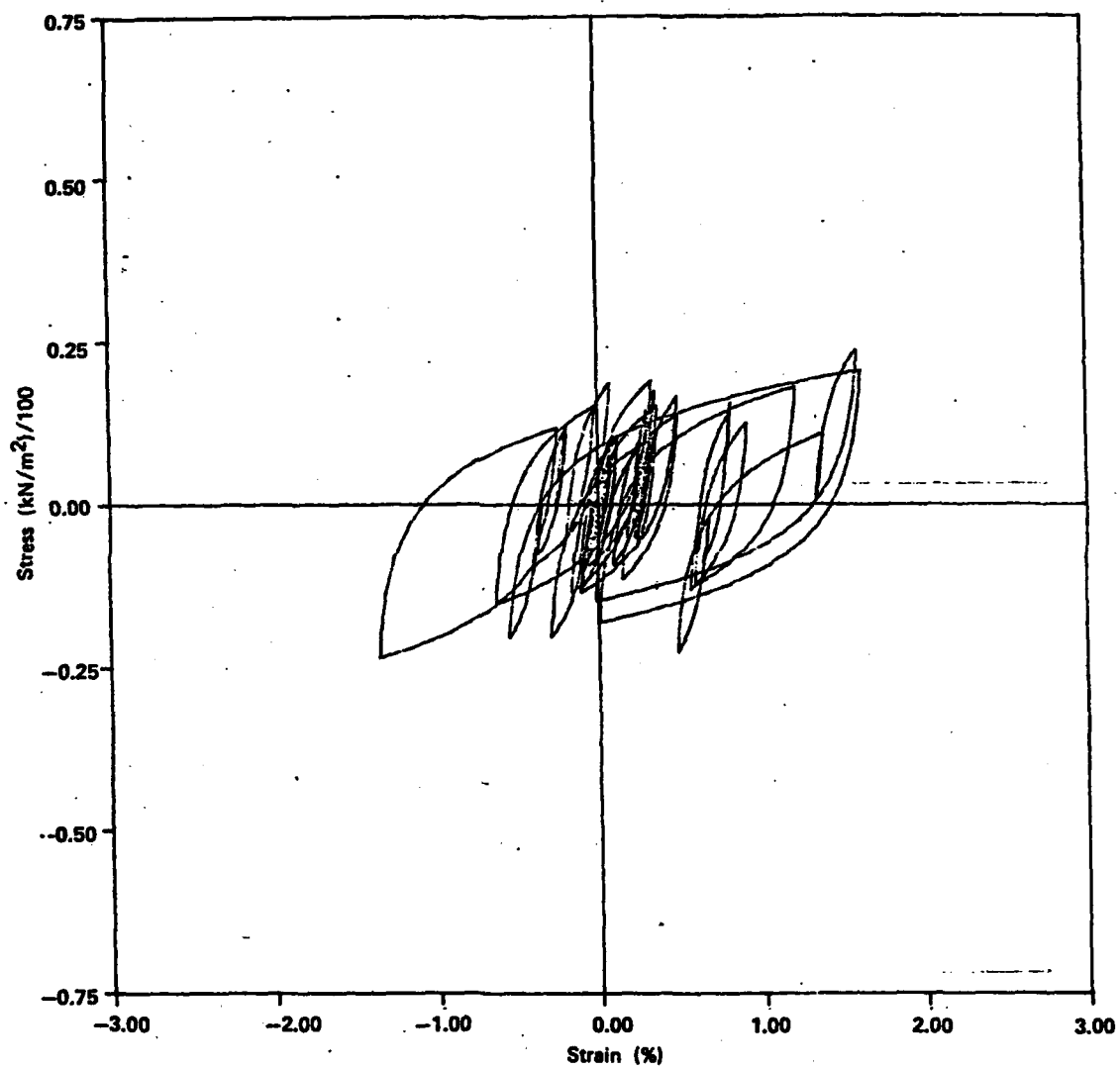


Fig. 5.3.6. Stress-strain relationship of element No. 5 for model GTM1 - Bijela, Herceg Novi NS+WE (0.33 g) KOLID-TO

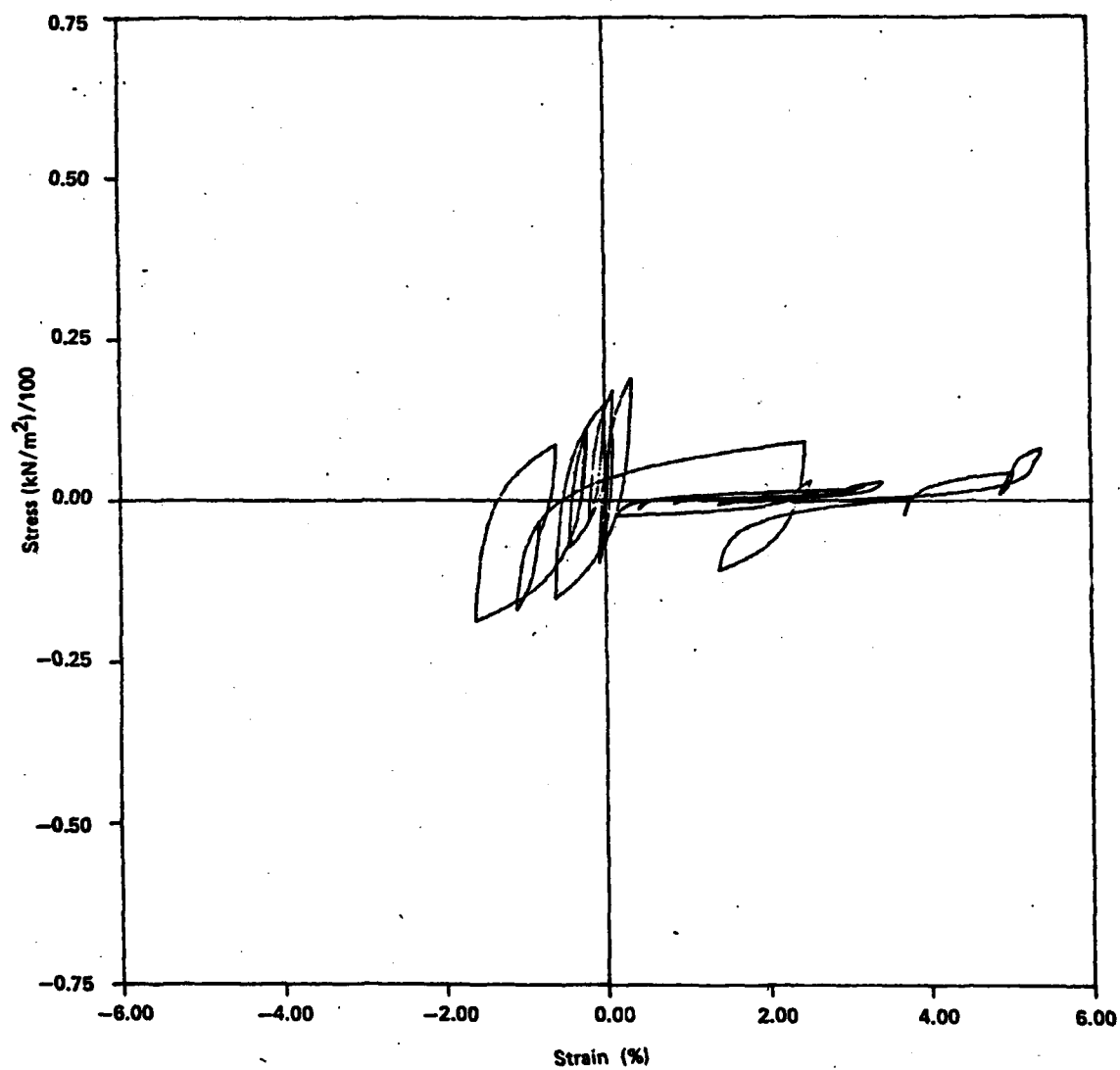


Fig. 5.3.7. Stress-strain relationship of element No. 5 for model GTM1 - Bijela, Herceg Novi NS+WE (0.33 g) KOLID-EF

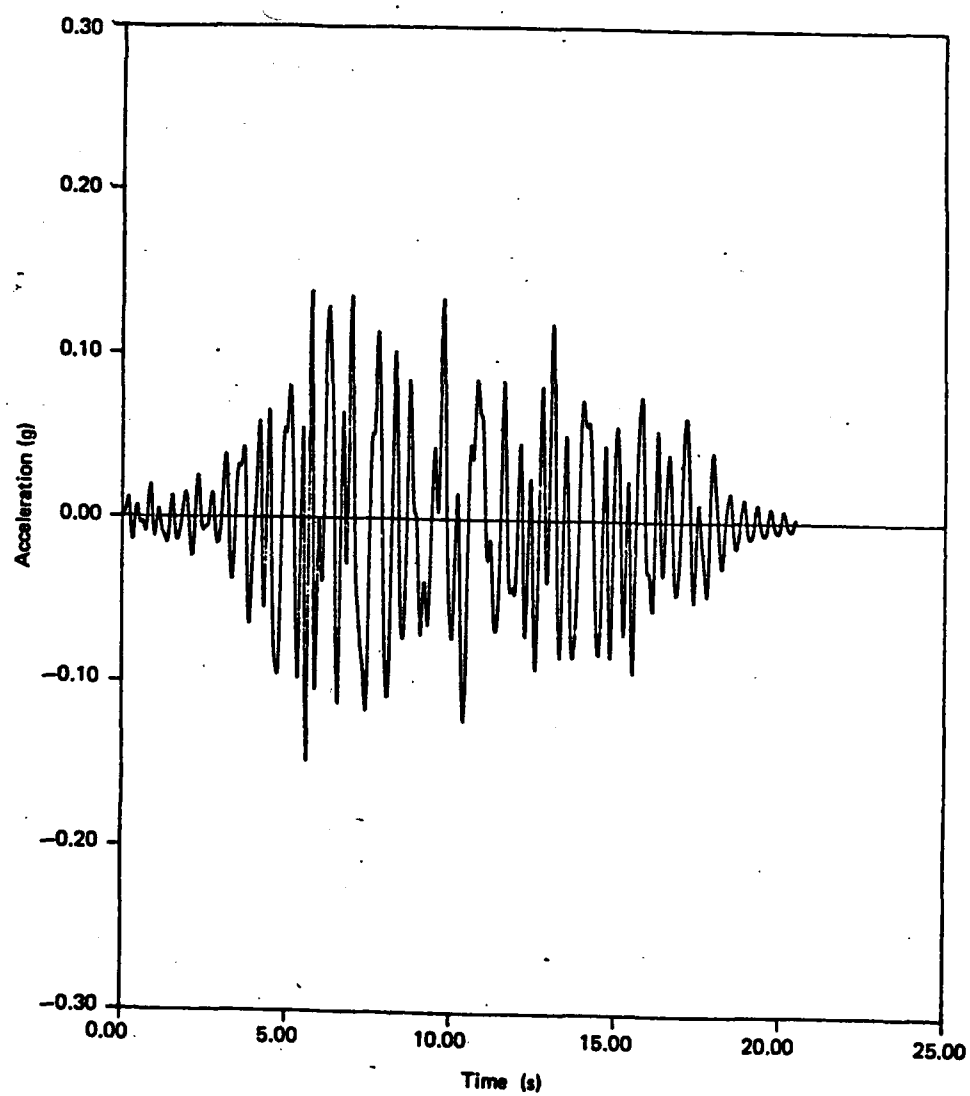


Fig. 5.3.8. Time history of acceleration ( $g$ ) in element No. 1 for  
model GTM1 - Bijela, Herceg Novi NS+WE (0.33 g) KOLID-TO

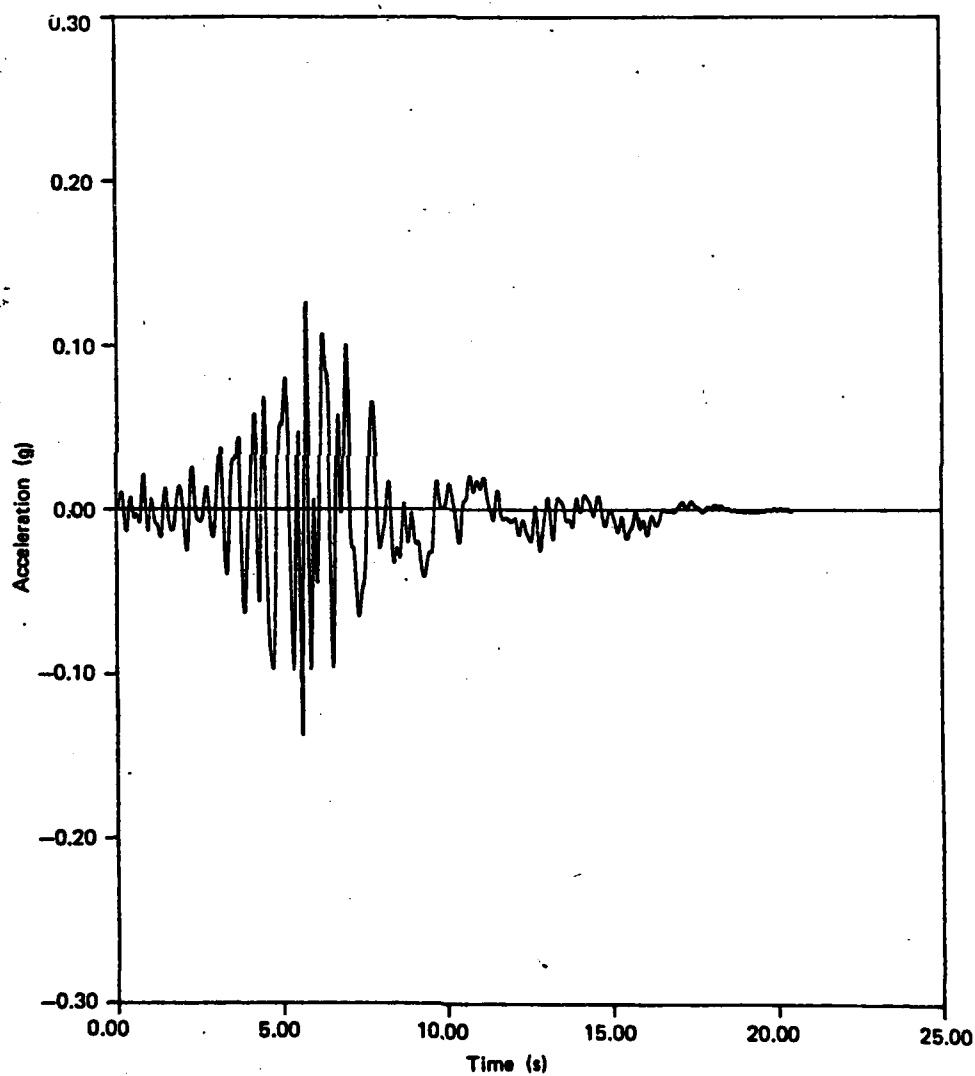


Fig. 5.3.9. Time history acceleration (g) in element No. 1 for model GTM1 - Bijela, Herceg Novi NS+WE (0.33 g) KOLID-EF

## 6. CONCLUSIONS

The soil liquefaction phenomenon under strong earthquakes is a complex problem comprising more aspects. The main aspects deal with investigations of the process leading to the occurrence of ( $\sigma'_v = 0$ ) and the parameters of this process such as the increase of ( $u$ ), decrease of ( $G$ ) and transformation of the nonlinear ( $\tau/\gamma$ ) relationship, as well as the dynamic response and the behaviour of soil. These aspects have been investigated in this report applying the approach with cyclic strains.

A number of conclusions came out of the obtained results, the most significant being listed as follows:

- The cyclic shear strains can represent adequately the liquefaction parameters. Compared to the cyclic shear stresses, this representation is simpler one since, opposite to the dominant influence of strains which in fact controls the liquefaction parameters, all other investigated influences appeared to be less important.
- The dynamic response of the soil subjected to intensive earthquake motion is a nonlinear problem. In the case of an increased pore pressure, the nonlinear dynamic response is dominantly controlled by the transformation effects of the initial nonlinear soil properties, especially when the ( $\sigma'_v = 0$ ) state is reached.
- The liquefaction parameters defined applying the cyclic strain approach enable that considerably simpler models be formulated for the response analysis in the case of an increased ( $u$ ).

It is believed that the investigations of the problems related to the liquefaction phenomenon should include the cyclic strain approach, besides the other methods and procedures, as a starting point in definition of the adequate solutions.

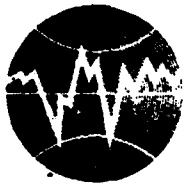
# REFERENCES

1. Ang A.H-S., Tang W.H., (1975), "Probability Concepts in Engineering Planning and Design, Volume I - Basic Principles", John Wiley and Sons, Inc.
2. Argyris J.H., Dune P.C., Angelopoulos T., (1973), "Dynamic Response by Large Step Integration", Journal of Earthquake Engineering and Structural Dynamics, Vol. 2, USA.
3. Argyris J.H., Dune P.C., Angelopoulos T., (1973), "Non-linear oscillations Using the Finite Element Technique", Journal of Computer Methods in Applied Mechanics and Engineering, Vol. 2.
4. Casagrande A., (1971), "On Liquefaction Phenomena", Geotechnique, Vol. 21, No. 3, London, England.
5. Castro G., (1975), "Liquefaction and Cyclic Mobility of Saturated Sands", Journal of the Geotechnical Engineering Division, ASCE, 101, GT6, USA.
6. Castro G., Poulos S.J., (1977), "Factors Affecting Liquefaction and Cyclic Mobility", Journal of the Geotechnical Engineering Division, ASCE, 103, GT6, USA.
7. Chen A.T.F., Joyner W.B., (1974), "Multi-Linear Analysis for Ground Motions Studies of Layered Systems", United States Department of the Interior, Geological Survey, March.
8. Committee on Earthquake Engineering, Commission on Engineering and Technical Systems, National Research Council, (1985), "Liquefaction of Soils During Earthquakes", National Academy Press, Washington, D.C., USA.
9. Dames and Moore, (1981), "Manual for the Operation of the Cyclic Simple Shear Apparatus", Dames and Moore, "The Limes", 123 Nortlake High Street, London.
10. De Alba P., Sees H.B., Chan C.K., (1976), "Sand Liquefaction in Large-Scale Simple Shear Tests", Journal of the Geotechnical Engineering Division, ASCE, Vol. 102, No. GT6, USA.
11. Dobry R., Stokoe K.H., Ladd R.S., Youd T.L., (1981), "Liquefaction Susceptibility From S-Wave Velocity", Institut Testing to Evaluate Liquefaction Susceptibility, ASCE, October 27, St. Louis, Missouri, USA.
12. Dobry R., Ladd R.S., Yokel F.Y., Chung R.M. Powell D., (1982), "Prediction of Pore Water Pressure Buildup and Liquefaction of Sands During Earthquake by the Cyclic Strain Method", NBS Building Science Serie 138, US Government Printing Office, July, Washington, USA.
13. Finn W.D.L., Lee K.W., Martin G.R., (1977), "An Effective Stress Model for Liquefaction", Journal of the Geotechnical Engineering Division, ASCE, Vol. 103, No. GT6, USA.
14. Finn W.D.L., Void Y.P., (1977), "Liquefaction Potential from Drained Constant Volume Cyclic Simple Shear Tests", Sixth World Conference on Earthquake Engineering, New Delhy, India.
15. Finn W.D.L., (1981), "Liquefaction Potential: Developments Since 1976", Presented at the International Conference on Recent Advances in Geotechnical Earthquake Engineering and Soil Dynamics, April 26 - May 3, St. Louis, USA.

16. Florin V.A., Ivanov P.L., (1961), "Liquefaction of Saturated Sandy Soils", Proceedings, 5th International Conference on Soil Mechanics and Foundation Engineering, Paris, France.
17. Ishihara K., (1977), "Pore Water Pressure Response and Liquefaction of Sand Deposits During Earthquake", Proceedings of DMSR 77 /Karlsruhe/ 5-16 September, Vol. 2.
18. Ishihara K., Okada S., (1978), "Effects of Stress History on Cyclic Behavior of Sand", Soils and Foundations, Vol. 18, No. 4, Japan.
19. Ishihara K., Towhata I., (1980), "One-Dimensional Soil Response Analysis during Earthquake Based on Effective Stress Method", Journal on the Faculty of Engineering, The University of Tokyo, Vol. 35, No. 4, Japan.
20. Ishihara K., Yamazaki F., (1980), "Cyclic Simple Shear Tests on Saturated Sand in Multi-Directional Loading", Soils and Foundations, Vol. 20, No. 1, Japan.
21. Ishihara K., Shimizu K., Yamada Y., (1981), "Pore Water Pressures Measured in Sand Deposits During an Earthquake", Soils and Foundations, Vol. 21, No. 4, Japan.
22. Ishihara K., (1985), "Stability of Natural Deposits During Earthquakes", Proceedings of the Eleventh International Conference on Soil Mechanics and Foundation Engineering, A.A. Balkema Publishers, Rotterdam, Netherlands.
23. Iwasaki T., Arakawa T., Tokisa K., Kameda T., (1982), "Estimation Procedure of Liquefaction Potential and its Application to Earthquake Resistant Design", Fourteenth Joint Meeting US-Japan, Panel on Wind and Seismic Effects, U.J.N.R. Washington D.C., USA.
24. Joyner W.B., Chen A.T.F., (1975), "Calculation of Nonlinear Ground Response in Earthquake", Bulletin of the Seismological Society of America, Vol. 65, No. 5.
25. Keefe D.K., Tannaci N.E., (1981), "Bibliography on Landslides, Soil Liquefaction, and Related Ground Failures in Selected Historic Earthquake", Department of the Interior USGS, Open File Report 81-572.
26. Lysmer J., (1978), "Analytical Procedures in Soil Dynamics", Earthquake Engineering Research Center, Report No. UCB/EERC-78/29, University of California, Berkeley, USA.
27. Martin G.R., Finn W.D.L., Seed H.B., (1975), "Fundamentals of Liquefaction Under Cyclic Loading", Journal of the Geotechnical Engineering Division, ASCE, Vol. 101, No. GT5, USA.
28. Martin P.P., Seed H.B., (1978), "MASH A Computer Program for the Non-Linear Analysis of Vertically Propagating Shear Waves in Horizontally Layered Deposits", Earthquake Engineering Research Center, Report No. UCB/EERC-78/23, University of California, Berkeley, USA.
29. Martin P.P., Seed H.B., (1978), "APPOLLO-A Computer Program for the Analysis of Pore Pressure Generation and Dissipation in Horizontal Soil Layers during Cyclic or Earthquake Loading", Earthquake Engineering Research Center, Report No. UCB/EERC-78/21, University of California, Berkeley, USA.
30. Martin P.P., Seed H.B., (1979), "Simplified Procedure for Effective Stress Analysis of Ground Response", Journal of the Geotechnical Engineering Division, ASCE, Vol. 105, No. GT6, USA.

31. McGuire R.K., Tatsuoka F., Iwasaki T., Tokida K., (1978), "Probabilistic Procedures for Assessing Soil Liquefaction Potential", Journal of Research, Volum 19, Public Works Research Institute, Tokyo, Japan.
32. Peacock W.H., Seed H.B., (1968), "Sand Liquefaction Under Cyclic Loading Simple Shear Conditions", Journal of the Soil Mechanics and Foundations Division, ASCE, Vol. 94, No. SM3, USA.
33. Pires J.E.A., Wen Y.K., Ang A.H-S., (1983), "Stochastic Analysis of Liquefaction Under Earthquake Loading", University of Illinois at Urbana-Champaign, Report No. UILU-ENG-83-2005, Urbana, Illinois, USA.
34. Richart F.E., Jr., Hall J.R. Woods R.D., (1970), "Vibrations of Soils and Foundations", Prentice-Hall, Inc., 1970.
35. Саваремслоо Е.Ф. (1972), "Сейсмические Волны", Издательство "Недра" Москва.
36. Schnabel P.B., Lysmer J., Seed H.B., (1972), "SHAKE: A Computer Program for Earthquake Response Analysis of Horizontally Layered Sites", Earthquake Engineering Research Center, Report No. EERC 72-12, University of California, Berkeley, USA.
37. Seed H.B., Lee K.L., (1966), "Liquefaction of Saturated Sand During Cyclic Loading", Journal of the Soil Mechanics and Foundations Division, ASCE, No. SM6, USA.
38. Seed H.B., Idriss I.M., (1967), "Analysis of Soil Liquefaction: Niigata Earthquake", Journal of the Mechanics and Foundations Division, ASCE, Vol. 93, No. SM3, USA.
39. Seed H.B., Idriss M.I., (1971), "Simplified Procedure for Evaluating Soil Liquefaction Potential", Journal of Soil Mechanics and Foundations Division, ASCE, Vol. 97, No. SM9, USA.
40. Seed H.B., (1979), "Soil Liquefaction and Cyclic Mobility Evaluation for Level Ground during Earthquake", Journal of the Geotechnical Engineering Division, Proceedings of the ASCE, Vol. 105, No. GT2, February, USA.
41. Seed H.B., Idriss I.M., (1981), "Evaluation of Liquefaction Potential of Sand Deposits Based on Observations of Performance in Previous Earthquakes", Institue Testing to Evaluate Liquefaction Susceptibility ASCE, October 26-31, St. Louis, Missouri, USA.
42. Talaganov K., Mihailov V., Bogoevski T., (1980), "Analysis of Soil Liquefaction During 1979 Montenegro Earthquake", Seventh World Conference on Earthquake Engineering, Vol. 3, Istanbul, Turkey.
43. Talaganov K., Petrovski J., Mihailov V., (1981), "Soil Liquefaction Seismic Risk Analysis Based on Post 1979 Earthquake Observations in Montenegro", International Conference on Recent Advances in Geotechnical Earthquake Engineering and Soil Dynamics, Vol. II, St. Louis, USA.
44. Talaganov K., (1986), "Determination of Liquefaction Potential by Cyclic Strain Aproch" Proceedings of the Eight European Conference on Earthquake Engineering, Lisboa, Portugal.
45. Talaganov K., (1986), "Determination of Liquefaction Potential of Level Site by Cyclic Strain", Institute of Earthquake Engineering and Engineering Seismology, Report IZIIS 86-129, Skopje, Jugoslavia.





**TURKISH NATIONAL COMMITTEE FOR  
EARTHQUAKE ENGINEERING**

**THIRTEENTH REGIONAL SEMINAR ON EARTQUAKE ENGINEERING**

**September 14-24, 1987 - Istanbul - Turkey**

**LECTURE NOTES  
ON  
SOIL STRUCTURE INTERACTION  
EFFECTS ON STRONG GROUND MOTION**

**Mustafa Erdik**

## INTRODUCTION

Dynamic interaction of soils and structures during dynamic excitation or earthquakes are of concern for the design of structures and foundations and also for the proper interpretation of the strong motion data recorded on the ground floor or basements of structures. It is well known that, under certain conditions, soil structure interaction effects may cause significant difference between the basement and free-field motions. In fact, it has recently been shown that (Werner and Agbabian, 1984) the motions indicated by the El-Centro record of the 1940 Imperial Valley Earthquake, which has a world-wide use as free-field seismic input for the design of structures, may be up to 100% below that of free field for frequencies above 1.5 Hz.

Through the use of finite element procedures the soil-structure interaction problem can be analysed in one step as a site-response problem in the frequency domain (Lysmer et al., 1975), or in the time domain (Bayo and Wilson, 1983). However a better physical understanding of the problem can be gained and the cases, where the interaction effects can be substantial, can be identified by breaking the total problem into separate parts dealing with the structure, soil and interface conditions. This is known as the sub-structure approach.

In this paper a three-degree-of-freedom (3-D.O.F.) model for the soil-structure interaction problem will be studied on the basis of the sub-structure approach and the results will be applied to obtain the transfer function between the free field ground and structure-ground level motions during an earthquake.

## SUB-STRUCTURE FORMULATION

The sub-structure formulation is essentially based on the determination of the total motions by superposing the free-field and interaction motions obtained on the basis of separate analysis. The formulation given here follows that given by Gutierrez and Chopra (1978) and Kausel et al., (1978).

The structure-soil system is treated as two sub-structures shown in Fig.1. The compatibility of the displacements and the forces are satisfied by assigning the same displacements but opposite forces at the structure-soil interface.

The equations of motion for the finite element model of the structure alone can be written as :

$$[M_c]\{\ddot{r}_c\} + [C_c]\{\dot{r}_c\} + [K_c]\{r_c\} = \{R_c\} - [M_c]\{a\} \quad (1)$$

$$\text{or} \quad [M_c] \begin{Bmatrix} \ddot{r}_s \\ \ddot{r}_b \end{Bmatrix} + [C_c] \begin{Bmatrix} \dot{r}_s \\ \dot{r}_b \end{Bmatrix} + [K_c] \begin{Bmatrix} r_s \\ r_b \end{Bmatrix} = \begin{Bmatrix} 0 \\ R_b \end{Bmatrix} - [M_c]\{a\} \quad (2)$$

where :

$\{r_c\}$ : vector of relative displacements (with respect to the free-field displacements at the structure-soil interface) at the degrees-of freedom (D.O.F.) associated with the structure

$\{r_s\}$ : vector of relative displacements at the D.O.F. associated with the structure less those associated with the interface

$\{r_b\}$ : vector of relative displacements at the D.O.F. associated with the interface

$\{R_b\}$ : vector of forces due to soil-structure interaction at the D.O.F. associated with the interface

$\{a\}$  : is a vector related to the free-field accelerations at the D.O.F. associated with the interface and to the pseudo-static deformations at the D.O.F. associated with the structure (less those associated with the interface)

and  $[M_c]$ ,  $[C_c]$  and  $[K_c]$  are respectively the mass, damping and stiffness matrices.

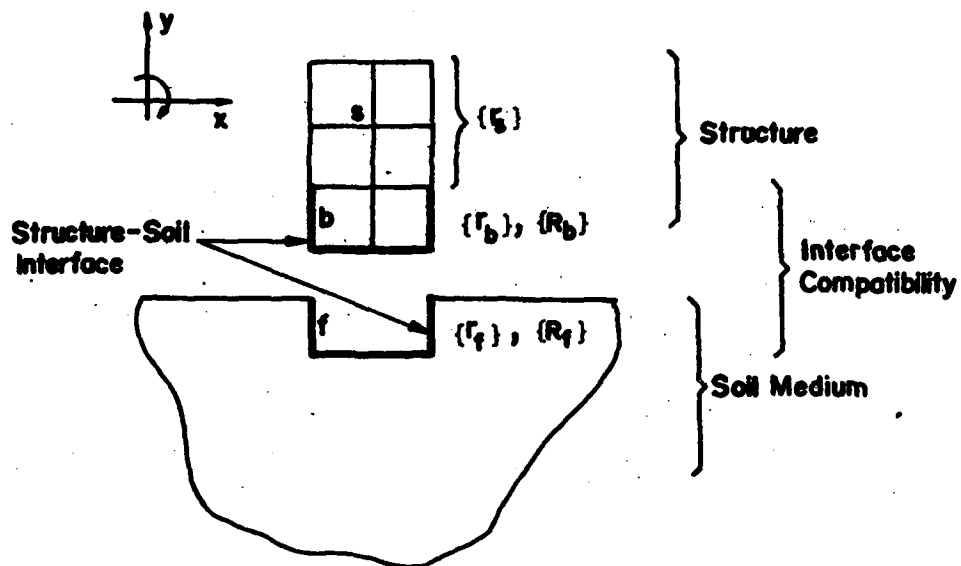


Figure 1. Substructure Representation of the Structure - Soil System .

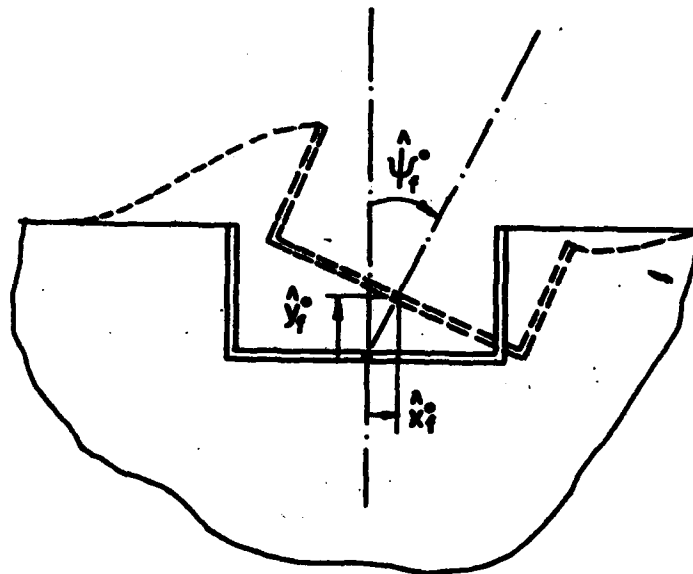


Figure 2. Planar Rigid Body Motion at the Structure-Soil Interface.

The vector  $\{a\}$  can be expressed in terms of the free-field accelerations at the D.O.F. associated with the structure-soil interface  $\{\ddot{r}_f^0\}$  through the use of pseudo-static influence coefficient vector,  $[V]$ , (Clough and Penzien, 1975).

$$\{a\} = [V] \{\ddot{r}_f^0\} \quad (3)$$

Where the superscript "o" identifies free-field quantities. In the frequency-domain Eqn.2 can be given as :

$$\left[ -\omega^2 [M_c] + i\omega [C_c] + [K_c] \right] \begin{Bmatrix} \bar{r}_s \\ \bar{r}_b \end{Bmatrix} = \begin{Bmatrix} 0 \\ \bar{R}_b \end{Bmatrix} - [P_c] \{\bar{r}_f^0\} \quad (4)$$

where  $\omega$  is the excitation frequency,  $\{\bar{r}_c\}$ ,  $\{\bar{r}_b\}$ ,  $\{\bar{R}_b\}$  and  $\{\bar{r}_f^0\}$  are the Fourier Transforms of the respective time-domain quantities, and  $[P_c]$  is given by :

$$[P_c] = [M_c] [V] \quad (5)$$

For the soil substructure the relationship between the forces and the displacements at the D.O.F. associated with the interface can be given in terms of the so-called impedance matrix ( $[S_f]$ ),

$$\{\bar{R}_f\} = [S_f] \{\bar{r}_f\} \quad (6a)$$

or through compatibility relationships

$$\{\bar{R}_b\} = -[S_f] \{\bar{r}_b\} \quad (6b)$$

Substituting Eqn.6b in Eqn.4 and re-arranging one can obtain :

$$\left[ -\omega^2 [M_c] + i\omega [C_c] + [K_c] + \begin{bmatrix} 0 & 0 \\ 0 & [S_f] \end{bmatrix} \right] \begin{Bmatrix} \bar{r}_s \\ \bar{r}_b \end{Bmatrix} = -[P_c] \{\bar{r}_f^0\} \quad (7)$$

Solution of Eqn.7 requires first, the analysis of the soil substructure to obtain the free-field earthquake accelerations at the interface nodes  $\{\bar{r}_f^0\}$  under the existing seismic regime, and second, the determination of the impedance matrix  $[S_f]$ . The former analysis is also known as the "scatter" or "kinematic interaction" problem. In general both of these analysis require discrete, finite-element type treatment. However for simple geometries and other restrictive assumptions closed form solutions have been developed.

Assuming planar rigid-body motion at the structure-soil interface  $\{\bar{r}_f^o\}$  can be expressed as :

$$\{\bar{r}_f^o\} = \begin{Bmatrix} \bar{x}_f^o \\ \bar{y}_f^o \\ \bar{\psi}_f^o \end{Bmatrix} = \begin{Bmatrix} \bar{x}_b^o \\ \bar{y}_b^o \\ \bar{\psi}_b^o \end{Bmatrix} \quad (8)$$

Where  $\bar{x}_b^o$ ,  $\bar{y}_b^o$  and  $\bar{\psi}_b^o$  are the free-field displacements at the rigid interface respectively along the x, y and  $\psi$  directions as shown in Fig.2. Assuming that the equations of motion for the vertical response can be de-coupled for separate treatment, from that of the lateral-rocking  $\{\bar{r}_f^o\}$  will be :

$$\{\bar{r}_f^o\} = \begin{Bmatrix} \bar{x}_b^o \\ \bar{\psi}_b^o \end{Bmatrix} \quad (9)$$

For a lumped-mass model of the structure with one lateral degree-of-freedom at each node, as indicated in Fig.3, the matrices in Eqn.7 can be derived and rearranged as follows :

$$[M_c] = \begin{bmatrix} [M_s] & [M_s]\{I\} & [M_s]\{h\} \\ \{I\}^T [M_s] & \{I\}^T [M_s]\{I\} + m_b & \{I\}^T [M_s]\{h\} \\ \{h\}^T [M_s] & \{I\}^T [M_s]\{h\} & \{I\}^T [M_s]\{I\} + I_t \end{bmatrix} \quad (10)$$

$$[C_c] = \begin{bmatrix} [C_s] & 0 & 0 \\ 0 & 0 & 0 \\ 0 & 0 & 0 \end{bmatrix} ; \quad [K_c] = \begin{bmatrix} [K_s] & 0 & 0 \\ 0 & 0 & 0 \\ 0 & 0 & 0 \end{bmatrix} \quad (11)$$

$$[P_c] = \begin{bmatrix} [M_s]\{I\} & [M_s]\{h\} \\ \{I\}^T [M_s]\{I\} + m_b & \{I\}^T [M_s]\{h\} \\ \{I\}^T [M_s]\{h\} & \{I\}^T [M_s]\{I\} + I_t \end{bmatrix} \quad (12)$$

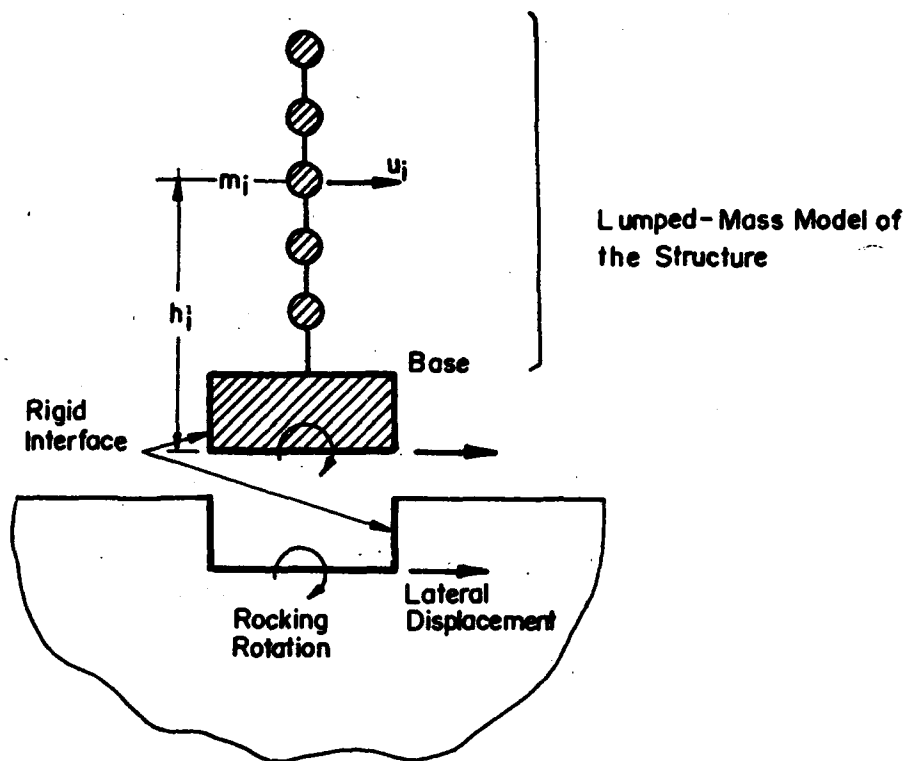


**Figure 3. Soil-Structure Interaction Model Structure Modeled With Lumped Masses and Rigid Base**

where  $[M_s]$ ,  $[C_s]$  and  $[K_s]$  are the conventional mass, damping and stiffness matrices for the structure obtained on the basis of fixed base assumption,  $\{I\}$  is the unit vector,  $\{h\}$  is the vector of vertical distances of the structural nodes from the interface,  $m_b$  is the mass of the base of the structure and  $I_c$  is the sum of the moments of inertia of the lumped masses about their own centroidal axis of rocking and the of the base mass about the axis of rocking at the interface level.

The displacement vector becomes :

$$\begin{Bmatrix} \hat{r}_s \\ \hat{r}_b \end{Bmatrix} = \begin{Bmatrix} \hat{u} \\ \hat{x}_b \\ \hat{\psi}_b \end{Bmatrix} \quad (13)$$

where  $\{\hat{u}\}$  is the vector of relative lateral displacements at the lumped masses and  $\hat{x}_b$  and  $\hat{\psi}_b$  are respectively the base relative lateral displacement and rocking angle.

For proportional damping assumption in the structure, where the so-called Rayleigh condition:

$$[C_c] = \alpha_1 [M_c] + \alpha_2 [K_c] \quad (14)$$

is satisfied, it follows that the modal damping ratios  $\xi_i$  of the  $i$ th fixed base structural mode are related to  $\alpha_1$  and  $\alpha_2$  by the following equation

$$\xi_i = \frac{\alpha_1}{2\omega_i} + \frac{\alpha_2 \omega_i}{2} \quad (15)$$

Where  $\omega_i$  is the natural circular frequency associated with the  $i$ th. fixed-base normal mode of vibration. In practice  $\alpha_1$  and  $\alpha_2$  are chosen in such a way that the damping ratios agree for the first two modes of the structure. It is also a common practice to assume only stiffness proportional damping, yielding:

$$[C_c] = \alpha_2 [K_c] = \frac{2\xi_1}{\omega} [K_c] \quad (16)$$

Thus Eqn.7 can be written as :

$$\left[ \omega^2 [M_c] + (1+2i\xi_1) [K_c] + \begin{bmatrix} 0 & 0 \\ 0 & [s_f] \end{bmatrix} \right] \begin{Bmatrix} \hat{r}_s \\ \hat{r}_b \end{Bmatrix} = -[P_c] \{\hat{r}_f^0\} \quad (17)$$



### Foundation Impedance Matrix

Impedance matrices for simplified cases can be evaluated through analytical and numerical procedures and can be given in closed form expressions. The harmonic forced vibration of a massless rigid cylindrical foundation in a homogenous soil halfspace has been studied by several researchers (Richart et al., 1970). In general the impedance matrix of such a foundation is of the following form:

$$\begin{Bmatrix} \hat{F}_b \\ \hat{M}_b \end{Bmatrix} = [S_f] \begin{Bmatrix} \hat{x}_b \\ \hat{\psi}_b \end{Bmatrix}; \quad [S_f] = \begin{bmatrix} K_{xx} & K_{x\psi} \\ K_{\psi x} & K_{\psi\psi} \end{bmatrix} \quad (18)$$

Where  $\hat{F}_b$ ,  $\hat{M}_b$ ,  $\hat{x}_b$  and  $\hat{\psi}_b$  are respectively the amplitudes of harmonic force and moment and the corresponding lateral translation and rocking rotation at the base of the foundation. The complex stiffnesses functions:  $K_{xx}$ ,  $K_{x\psi}$ ,  $K_{\psi x}$ , and  $K_{\psi\psi}$  can be given by (Kausel et al., 1978):

$$K_{xx} = \bar{K}_{xx} (k_{11} + i a_o c_{11}) (1 + 2i\beta) \quad (19)$$

$$K_{\psi x} = K_{x\psi} = \bar{K}_{x\psi} (k_{12} + i a_o c_{12}) (1 + 2i\beta) \quad (20)$$

$$K_{\psi\psi} = \bar{K}_{\psi\psi} (k_{22} + i a_o c_{22}) (1 + 2i\beta) \quad (21)$$

Where  $i = \sqrt{-1}$ ,  $a_o = \omega R/V_s$  is the normalized frequency,  $R$  is the radius of the foundation and  $V_s$  is the shear wave velocity.  $\bar{K}_{xx}$ ,  $\bar{K}_{x\psi}$ ,  $\bar{K}_{\psi\psi}$ , are the static (i.e.  $\omega=0$ ) stiffnesses,  $k_{ij}$ ,  $c_{ij}$  are the frequency dependent coefficients and  $\beta$  is the hysteretic damping ratio of the soil media.  $\bar{K}_{xx}$ ,  $\bar{K}_{x\psi}$ ,  $\bar{K}_{\psi\psi}$ ,  $k_{ij}$  and  $c_{ij}$  have been provided by several authors (e.g. Johnson et al, 1975; Richard et al. 1970; Veletsos and Wei, 1971; Kausel et al., 1978; ATC, 1978) as a function of  $G$  (Shear modulus),  $E$ (depth of embedment),  $H$ (depth to bedrock), Poisson's ratio),  $R$  and  $\omega$ .

The coefficients  $k_{ij}$  and  $c_{ij}$  are provided as plots against  $a_o$  in Fig.4 after Veletsos and Wei (1971).

Kausel et al. (1978) provides the following approximate expressions for the static stiffnesses :

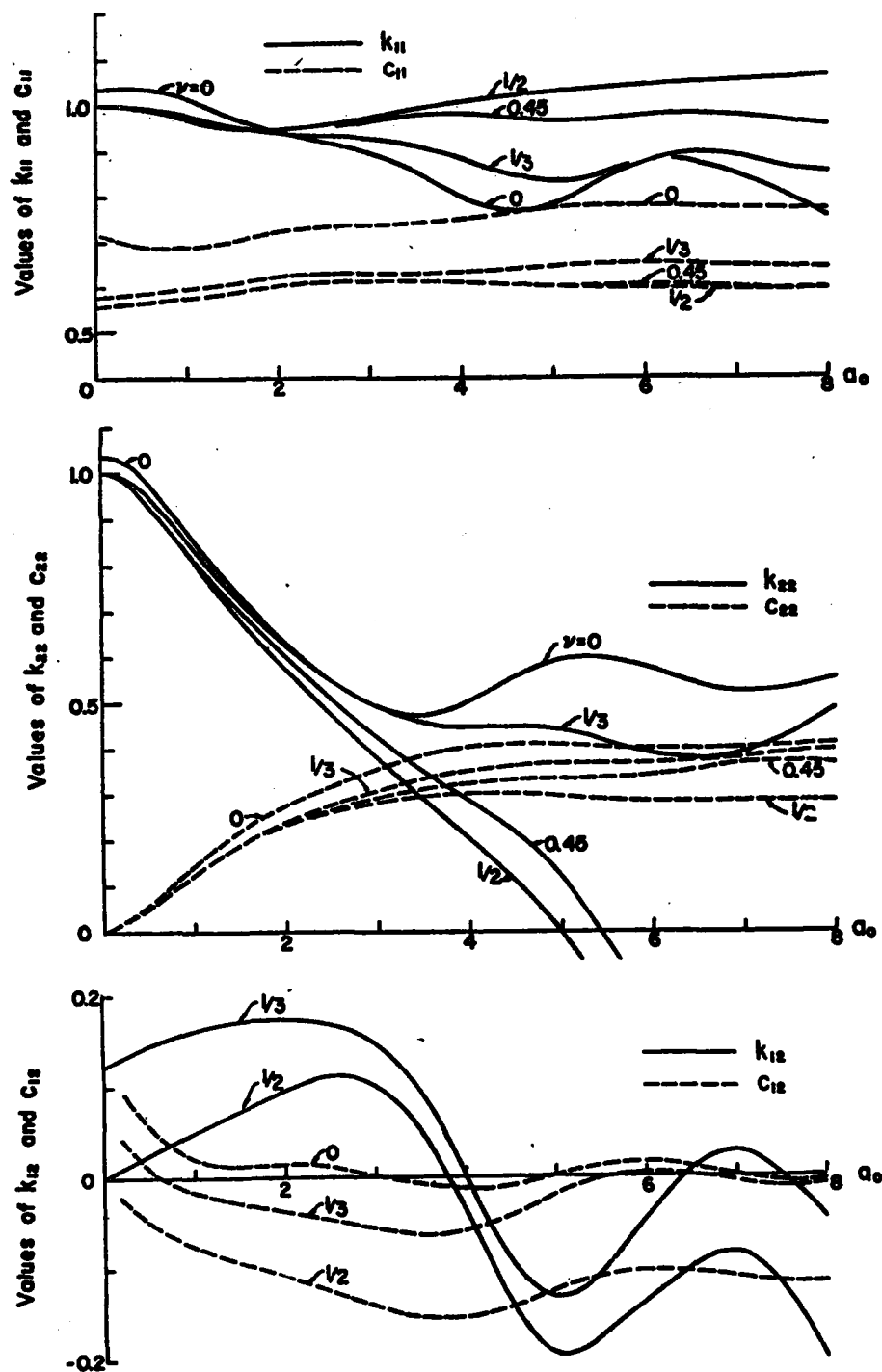


Figure 4. Half-space Impedance Function Coefficients (After Veletsos and Wei, 1971)

$$\bar{K}_{xx} = \frac{8GR}{2-\nu} \left(1 + \frac{1}{2} \frac{R}{H}\right) \left(1 + \frac{2E}{3R}\right) \left(1 + \frac{5}{4} \frac{E}{H}\right) \quad (22)$$

$$\bar{K}_{x\psi} = \bar{K}_{xx} R \left(\frac{2}{5} \frac{E}{R} - 0.003\right) \quad (23)$$

$$\bar{K}_{\psi\psi} = \frac{8GR^3}{3(1-\nu)} \left(1 + \frac{1}{6} \frac{R}{H}\right) \left(1 + 2\frac{E}{R}\right) \left(1 + 0.71 \frac{E}{H}\right) \quad (24)$$

These expressions are also included in ATC(1978).

For foundations that are different from a circle in plan, the effective radius can be defined for the translational motion as  $\sqrt{A_o/\pi}$  and for the rocking motion as  $\sqrt[4]{4I_o/\pi}$  where  $A_o$  is the area of the foundation and  $I_o$  is the area moment of inertia of the foundation about the centroidal rocking axis (ATC, 1978).

The first column of the complex impedance matrix in Eq.17 defines the set of forces and moments which are needed to displace the rigid foundation laterally by a unit amount without rocking, and the second column defines the set of forces and moments required to rock the disk by a unit amount without translation. The real parts of these quantities represent force quantities in phase with the motion, whereas the imaginary parts represent force components which are  $90^\circ$  out of phase as shown in the following equation.

$$\begin{Bmatrix} \bar{F}_b \\ \bar{M}_b \end{Bmatrix} = \begin{bmatrix} \text{Re}(K_{xx}) & \text{Re}(K_{x\psi}) \\ \text{Re}(K_{\psi x}) & \text{Re}(K_{\psi\psi}) \end{bmatrix} \begin{Bmatrix} \bar{x}_b \\ \bar{\psi}_b \end{Bmatrix} + \begin{bmatrix} \text{Im}(K_{xx}) & \text{Im}(K_{x\psi}) \\ \text{Im}(K_{\psi x}) & \text{Im}(K_{\psi\psi}) \end{bmatrix} \begin{Bmatrix} \bar{x}_b \\ \bar{\psi}_b \end{Bmatrix} \quad (25)$$

It is convenient to think of the forces represented by real parts of Eqn.25 as being due to a set of linear springs, and of the forces represented by imaginary parts as being due to a series of dashpots (Veletsos and Wei, 1971). In this representation the spring elements account for the combined effect of restraining action of the supporting medium and the inertia forces, whereas the dashpots account for the effect of energy dissipation by radiation as given by the following time-domain equation.

$$\begin{Bmatrix} F_b \\ M_b \end{Bmatrix} = \begin{bmatrix} k_{xx} & k_{x\psi} \\ k_{\psi x} & k_{\psi\psi} \end{bmatrix} \begin{Bmatrix} x_b \\ \psi_b \end{Bmatrix} + \begin{bmatrix} c_{xx} & c_{x\psi} \\ c_{\psi x} & c_{\psi\psi} \end{bmatrix} \begin{Bmatrix} \dot{x}_b \\ \dot{\psi}_b \end{Bmatrix} \quad (26)$$

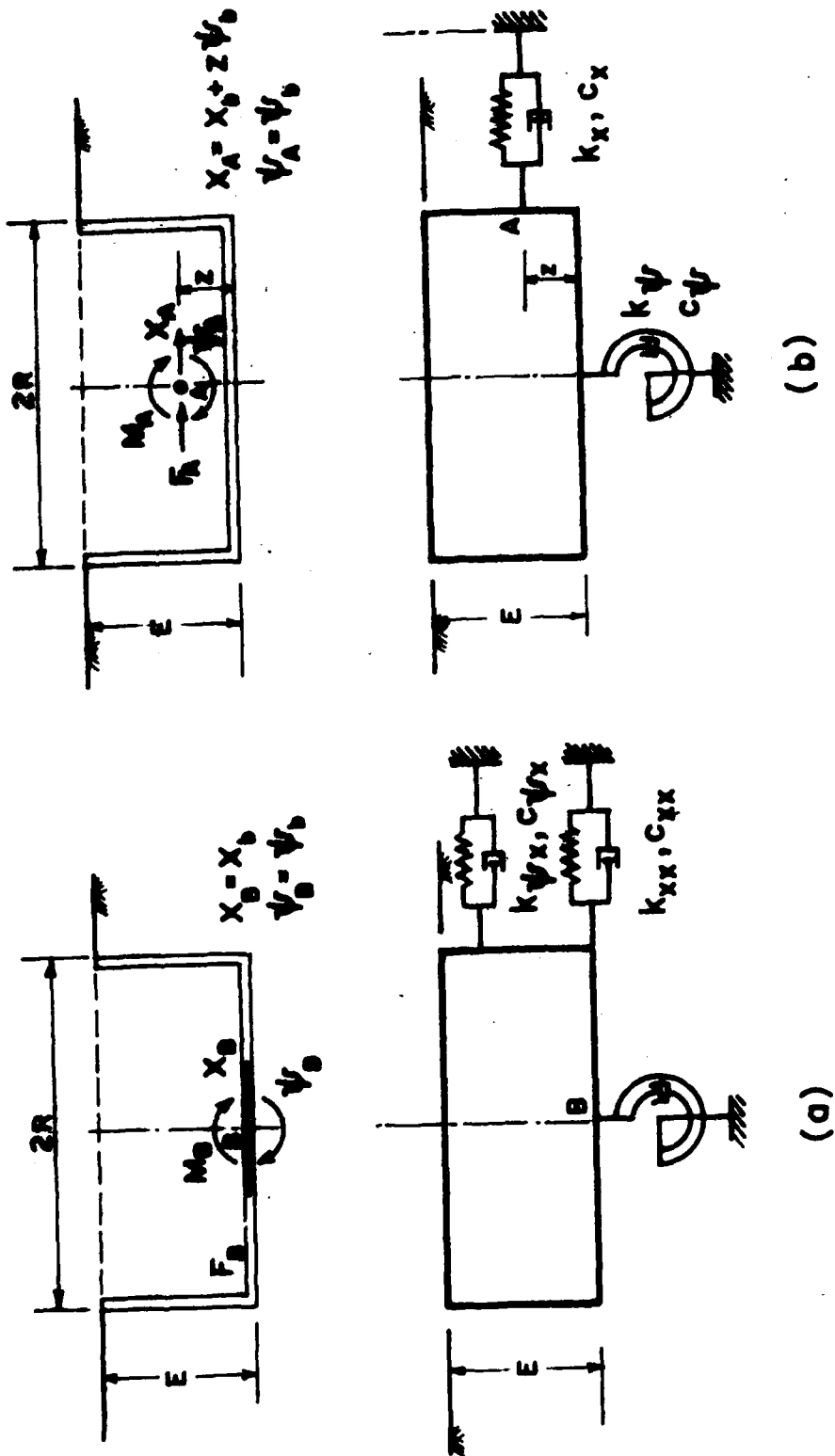


Figure 5. Coupled and Uncoupled Foundation Models.

The first matrix of Eqn.26 will be referred to as the foundation stiffness matrix and the second matrix will be referred to as the foundation damping matrix. The stiffness and damping coefficients respectively constitute the elements of these matrices. On the basis of these stiffness and damping coefficients, the foundation of the structure can be modeled by springs and dashpots in coupled and in uncoupled models as indicated in Fig.5. The stiffness and damping matrices for the uncoupled foundation models can be given as follows :

$$\begin{Bmatrix} F_B \\ M_B \end{Bmatrix} = \begin{bmatrix} k_{xx} & k_{x\psi} \\ k_{\psi x} & k_{\psi\psi} \end{bmatrix} \begin{Bmatrix} x_b \\ \psi_b \end{Bmatrix} + \begin{bmatrix} c_{xx} & c_{x\psi} \\ c_{\psi x} & c_{\psi\psi} \end{bmatrix} \begin{Bmatrix} \dot{x}_b \\ \dot{\psi}_b \end{Bmatrix} \quad (27a)$$

$$\begin{Bmatrix} F_A \\ M_B \end{Bmatrix} = \begin{bmatrix} k_x & 0 \\ 0 & k_\psi \end{bmatrix} \begin{Bmatrix} x_b + z\psi_b \\ \psi_b \end{Bmatrix} + \begin{bmatrix} c_x & 0 \\ 0 & c_\psi \end{bmatrix} \begin{Bmatrix} \dot{x}_b + z\dot{\psi}_b \\ \dot{\psi}_b \end{Bmatrix} \quad (27b)$$

The uncoupled stiffness coefficients  $k_x$  and  $k_\psi$  of the uncoupled model can be determined on the basis of the equilibrium of forces and moments:

$$F_A = F_B \quad \text{and} \quad M_B = M_A + F_B \cdot z \quad (28)$$

Yielding :

$$k_x = K_{xx} \quad \text{and} \quad k_\psi = k_{\psi\psi} - k_{xx} z^2 \quad (29)$$

and

$$c_x = c_{xx} \quad \text{and} \quad c_\psi = c_{\psi\psi} - c_{xx} z^2 \quad (30)$$

$$\text{where } z = k_{x\psi}/k_{xx} \quad (31)$$

Practical findings indicate that  $z$  can be taken to be equal to  $E/3$ , where  $E$  is the depth of embedment.

## KINEMATIC INTERACTION

In several applications of the soil-structure interaction problem the kinematic interaction is either neglected or treated on an approximate basis. For example in the lumped mass formulation of the soil-structure interaction problem adopted in Masao et al. (1980) the kinematic interaction is approximated by assigning the free-field values of the displacements obtained at the foundation level of the structure as input motions to the model as indicated in Fig.6. In the lumped mass model used by Hall et al. (1975), shown in Fig.7 the kinematic interaction is accounted through the use of masses  $m_1$  and  $m_2$ , representing the free field soil inertia and the springs  $K_1$  and  $K_2$ .

The motion of the rigid-massless cylindrical foundation in a uniform soil media has been investigated through theoretical and experimental means. Kausel et al. (1978) has reported the results of a theoretical investigation of the problem, for a foundation located in a homogenous layer overlying a half space, for different embedment layer thickness values, assuming vertically propagating SH-waves. The findings indicate that the translation of the rigid-massless foundation is similar to the free-field translation at the embedment depth in the low frequency regions. However it is smoother in the higher frequency regions and does not show any pronounced absence of the certain frequency components. The transfer function between the translation at the embedment depth of the rigid-massless foundation and the free-field ground-translation (control motion) is approximated by:

$$|T_x| = \frac{|\bar{x}_b^o|}{|\bar{x}_g^o|} = \begin{cases} \cos\left(\frac{\pi}{2} \frac{f}{f_1}\right) & \text{for } f < 0.7 f_1 \\ 0.453 & \text{for } f > 0.7 f_1 \end{cases} \quad (32)$$

Where  $\bar{x}_b^o$  and  $\bar{x}_g^o$  are respectively the Fourier Transforms of the free-field lateral motions at the bottom of the rigid-massless foundation and at the free ground surface and  $f_1$  is the shear beam fundamental modal frequency of the soil column with thickness equal to the embedment depth ( $E$ ), and shear wave propagation velocity is equal to  $V_s$ .

$$f_1 = \frac{V_s}{4E} \quad (33)$$

Eqn. 10 can also be written as :

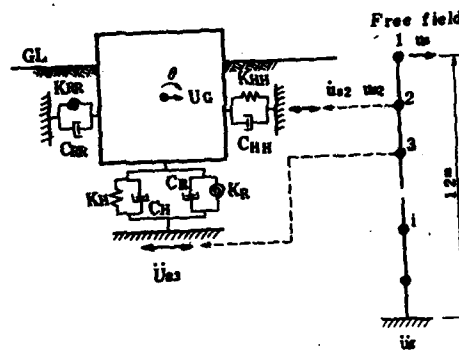


Figure 6. Lumped Parameter Model of Masao et al.,(1980)

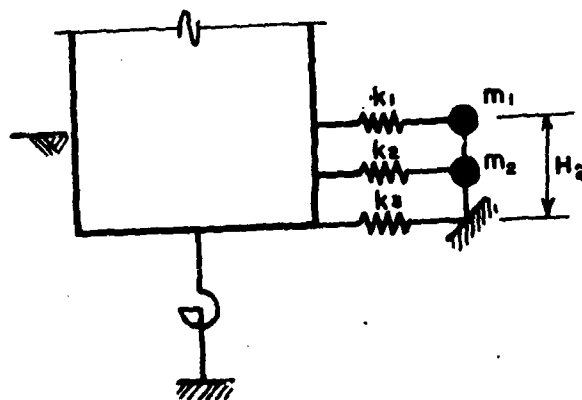


Figure 7. Lumped Parameter Model of Hall et al.,(1975)

$$\frac{|\bar{x}_b^o|}{|\bar{x}_g^o|} = \begin{cases} \cos\left(\frac{\omega E}{V_s}\right) & \text{for } \frac{\omega E}{V_s} < 1 \\ 0.453 & \text{for } \frac{\omega E}{V_s} > 1 \end{cases} \quad (34)$$

As it has been reported in Kausel et al.(1978) the rocking motion experienced by the massless-rigid cylindrical foundation is found to be related to the difference of the free-field displacements between the two locations of the soil corresponding to the top and bottom levels of the foundation divided by the embedment depth. The transfer function between the Fourier Transform of the rocking motion of the rigid-massless foundation ( $\bar{\psi}_b^o R$ ) and the Fourier transform of the free-field lateral ground motion (control motion) ( $\bar{x}_g^o$ ) is approximated by :

$$|T_\psi| = \frac{|\bar{\psi}_b^o R|}{|\bar{x}_g^o|} = \begin{cases} 0.257 \left(1 - \cos \frac{\pi}{2} \frac{f}{f_1}\right) & \text{for } f < f_1 \\ 0.257 & \text{for } f > f_1 \end{cases} \quad (35)$$

or expressed differently, by :

$$\frac{|\bar{\psi}_b^o R|}{|\bar{x}_g^o|} = \begin{cases} 0.257 \left(1 - \cos \frac{\omega E}{V_s}\right) & \frac{\omega E}{V_s} < 1 \\ 0.257 & \frac{\omega E}{V_s} > 1 \end{cases} \quad (36)$$

It has been noted that the rotational component may significantly decrease in foundations with flexible walls.

Ishii et al.(1984) has proposed the following empirical expression for the transfer function given in Eqn.32 and 34.

$$\frac{|\bar{x}_b^o|}{|\bar{x}_g^o|} = \begin{cases} \frac{\tilde{f}}{\pi f} \sin\left(\frac{\pi f}{\tilde{f}}\right) & \text{for } f < 0.71 \tilde{f} \\ 0.35 & \text{for } f > 0.71 \tilde{f} \end{cases} \quad (37)$$

$$\tilde{f} = \frac{1.408}{2.19\left(\frac{E}{V_s}\right) + 0.117}$$

Eqns.32, 36 and 37 behave essentially as low-pass filters.



## STRUCTURAL CONSIDERATIONS

The overturning moment and the base shear created by the inertial forces of the structure are the main contributors to the soil-structure interaction phenomena. Both the base overturning moment and the shear are controlled by the first mode vibration behavior of the structure and the contribution of the higher modes can be assumed to be negligible for most engineering structures. Within the range of parameters that are of interest for the earthquake resistant design of structures the soil-structure interaction affects substantially only the response components associated with the fundamental mode of the structure. Accordingly the use of only the first fixed base mode shape of the structure is common in engineering practice for the assessment of the soil structure effects (ATC, 1978). The higher modes of the structure are not essentially effected by the soil-structure interaction since the base overturning moment and the shear in these modes are comparatively quite low.

The representation of the structural matrices by the generalized fundamental mode characteristics can be found in structural dynamics books (e.g. Clough and Penzien, 1975). With such a representation the  $[M_c]$ ,  $[K_c]$  and  $[P_c]$  matrices of Eqn. 10, 11, 12 and 16 can be given as follows:

$$[M_c] = \begin{bmatrix} \bar{m} & \bar{m} & \bar{m}(\bar{h}+E) \\ \bar{m} & \bar{m}+m_b & \bar{m}(\bar{h}+E) \\ \bar{m}(\bar{h}+E) & \bar{m}(\bar{h}+E) & \bar{m}(\bar{h}+E)^2 + I_t \end{bmatrix} \quad (38)$$

$$[K_c] = \begin{bmatrix} \bar{k} & 0 & 0 \\ 0 & 0 & 0 \\ 0 & 0 & 0 \end{bmatrix} \quad (39)$$

$$[P_c] = \begin{bmatrix} \bar{m} & \bar{m}(\bar{h}+E) \\ \bar{m}+m_b & \bar{m}(\bar{h}+E) \\ \bar{m}(\bar{h}+E) & \bar{m}(\bar{h}+E)^2 + I_t \end{bmatrix} \quad (40)$$

In these matrices  $E$  is the depth of embedment of the base and the first mode effective mass,  $\bar{m}$ , height,  $\bar{h}$ , and stiffness,  $\bar{k}$ , can be given in terms of the fixed base fundamental mode shape  $\{\phi_1\}$  and frequency  $\omega_1$  by the following equations :

$$\bar{m} = \frac{(\{\phi_1\}^T [M_s] \{I\})^2}{\{\phi_1\}^T [M_s] \{\phi_1\}} \quad (41)$$

$$\bar{h} = \frac{\{h\}^T [M_s] \{\phi_1\}}{\{\phi_1\}^T [M] \{I\}} \quad (42)$$

$$\bar{k} = \bar{m} \omega_1^2 \quad (43)$$

For uniform building type structures  $\bar{m}$  can be taken equal to the 70% of the total mass of the super-structure and  $\bar{h}$  can be taken equal to the 70% of the height of the super-structure (ATC, 1978).

The displacement vector of Eqn.7 will have the following shape :

$$\begin{Bmatrix} \hat{r}_s \\ \hat{r}_b \end{Bmatrix} = \begin{Bmatrix} \hat{u}_1 \\ \frac{(\hat{x}_b^0)A}{\hat{\psi}_b} \end{Bmatrix} \quad (44)$$

Where  $\hat{u}_1$  is the relative generalized first mode displacement of the super-structure with respects to the base,  $\hat{x}_b$  is the relative lateral displacement of the base with respect to the free-field base displacement,  $\hat{x}_b^0$ , and  $\hat{\psi}_b$  is the relative base rocking angle (rotation) of the base with respect to the free field base rocking angle (rotation),  $\hat{\psi}_b^0$ .

Soil-structure interaction models of this type are called three-degree-of-freedom models (two D.O.F. at the base, one at the super structure). Such a model is indicated in Fig.8.

Through re-arranging and normalizing the frequency domain equation of motion for such a 3. D.O.F. system can be given as follows :

$$\begin{bmatrix}
 \left[ -1 + \left( \frac{\omega_1}{\omega} \right)^2 + 2i\xi_1 \left( \frac{\omega_1}{\omega} \right) \right] & -1 & -\frac{h_c}{R} \\
 -1 & \left[ -1 - \left( \frac{m_b}{\bar{m}} \right) + \frac{k_x + i\omega c_x}{\bar{m} \omega^2} \right] & -\frac{h_c}{R} \\
 -\frac{h_c}{R} & -\frac{h_c}{R} & \left[ -\left( \frac{h_c}{R} \right)^2 - \frac{I_t}{\bar{m} R^2} + \frac{k_\psi + i\omega c_\psi}{\bar{m} R^2 \omega^2} \right]
 \end{bmatrix}
 \begin{Bmatrix}
 \hat{u}_1 \\
 (\hat{x}_b)_A \\
 R\hat{\psi}_b
 \end{Bmatrix} =$$

$$= - \begin{Bmatrix} 1 \\ 1 + \frac{m_b}{\bar{m}} \\ \left( \frac{h_c}{R} \right) \end{Bmatrix} (\hat{x}_b^0)_A + - \begin{Bmatrix} \left( \frac{h_c}{R} \right) \\ \left( \frac{h_c}{R} \right) \\ \left( \frac{h_c}{R} \right)^2 + \frac{I_t}{\bar{m} R^2} \end{Bmatrix} \hat{\psi}_b^0 \quad (45)$$

Where  $h_c = E + \bar{h}$ ,  $\omega_1$  and  $\xi_1$  are respectively the first mode frequency and damping ratio of the fixed base structure, and  $(\hat{x}_b^0)_A$  can be determined in terms of the free-field rigid body motion components of the foundation.

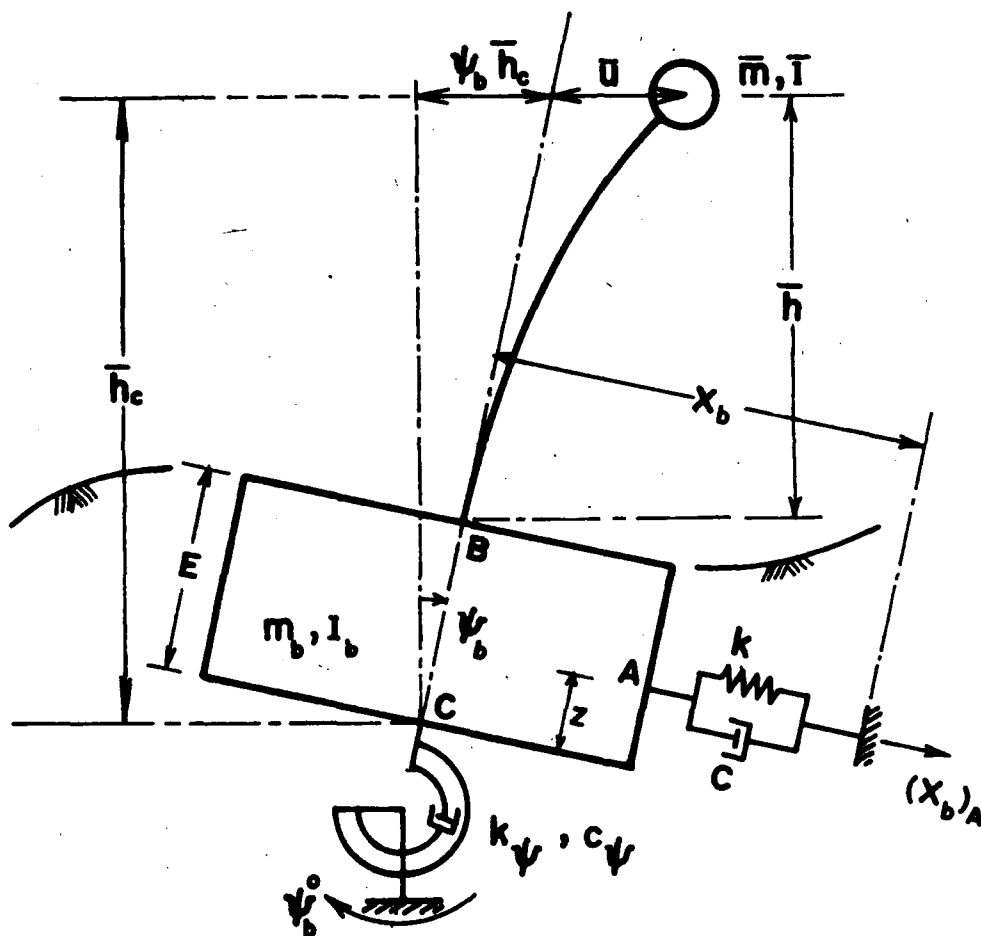


Figure 8. Three-Degree-of-Freedom Lumped-Mass-Spring Model

## NON-DIMENSIONAL PARAMETERS

The non-dimensional parameters for the solution of the set of equations given by Eqn.45 can be determined to be as follows for an embedded structure on a homogenous half space. (Başaran, 1985):

$$\text{Transfer Function : } TF = |\hat{x}_B| / |\hat{x}_g|$$

Where  $\hat{x}_B$  and  $\hat{x}_g$  are respectively the Fourier Transforms of absolute lateral displacements at the ground level of the structure (Point B of Fig.8) and at the free field ground level.

$$\text{Non-dimensional Frequency : } A_0 = \frac{\omega R}{V_s}$$

Where  $V_s$  is the shear wave propagation velocity of the homogenous half-space.

$$\text{Non-dimensional First Mode Frequency : } A_1 = \frac{\omega_1 R}{V_s}$$

Where  $\omega_1$  is the first mode vibration frequency of the fixed base super structure.

$$\text{Mass Ratio : } M_1 = m_b / \bar{m}$$

$$\text{Non-dimensional Height : } N_3 = \bar{h}_c / R$$

$$\text{Non-dimensional Embedment : } N_5 = E / R$$

$$\text{Structure Damping Factor : } \xi_1$$

$$\text{Poisson's Ratio of the Half-Space : } \nu$$

$$\text{Relative Density Ratio : } N_2 = \omega / \rho$$

where  $\omega$  is the gross density of the structure (i.e. mass divided by gross volume) and  $\rho$  is the density of the half-space.  $N_2$  is defined in a similar way in ATC-3-06 (1978). an average value of  $N_2 = 0.15$  is suggested for practical applications.

Figures 9, 10 and 11 depict the behaviour of the transfer function  $TF = \hat{x}_B / \hat{x}_g$  for different values of these non-dimensional parameters as indicated on each figure. As it can be assessed the motion at the ground level of the structure can be up to 80% above or below of that of the motion

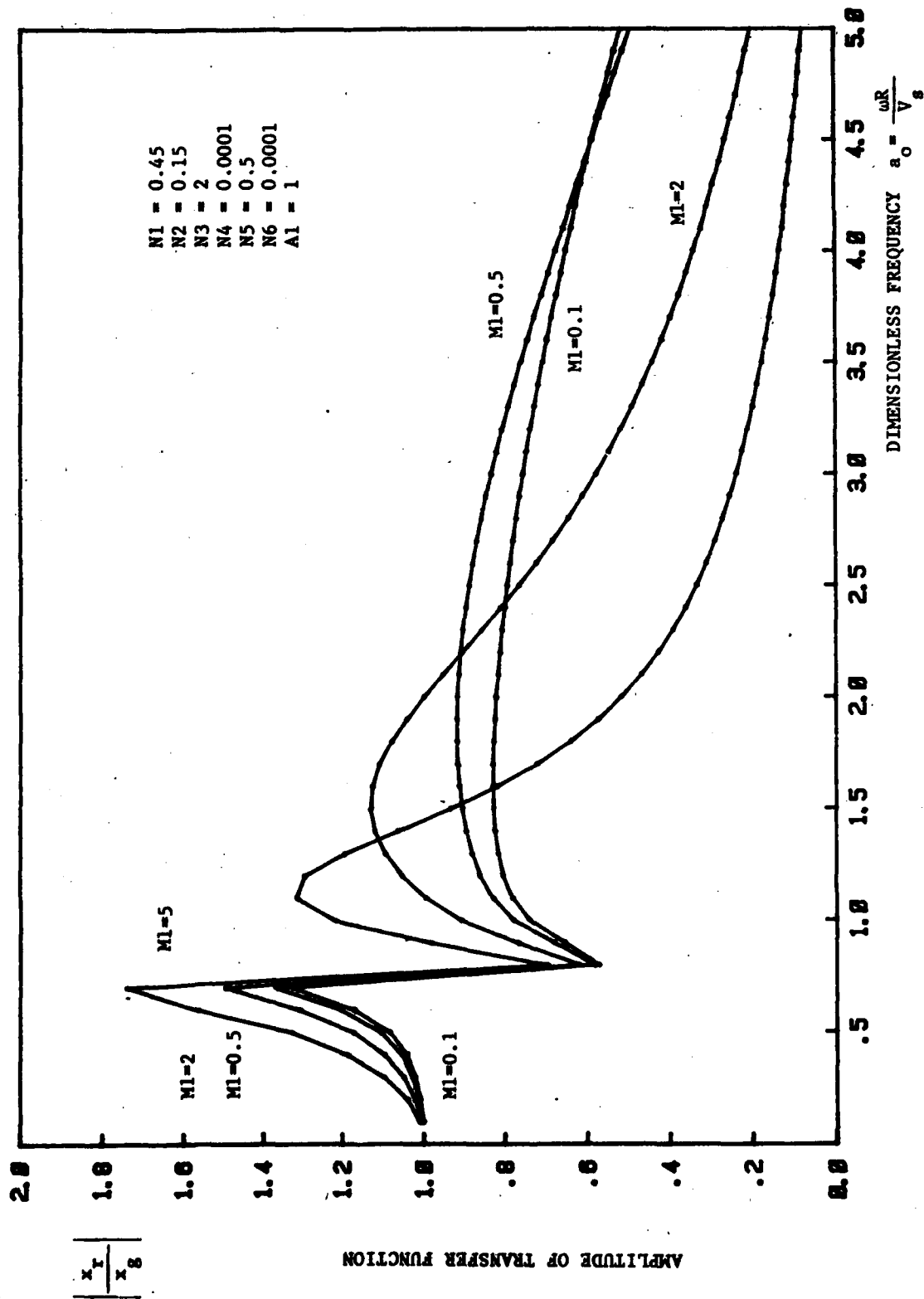


Figure 9. Transfer Function Between Structural and Free Field Motions

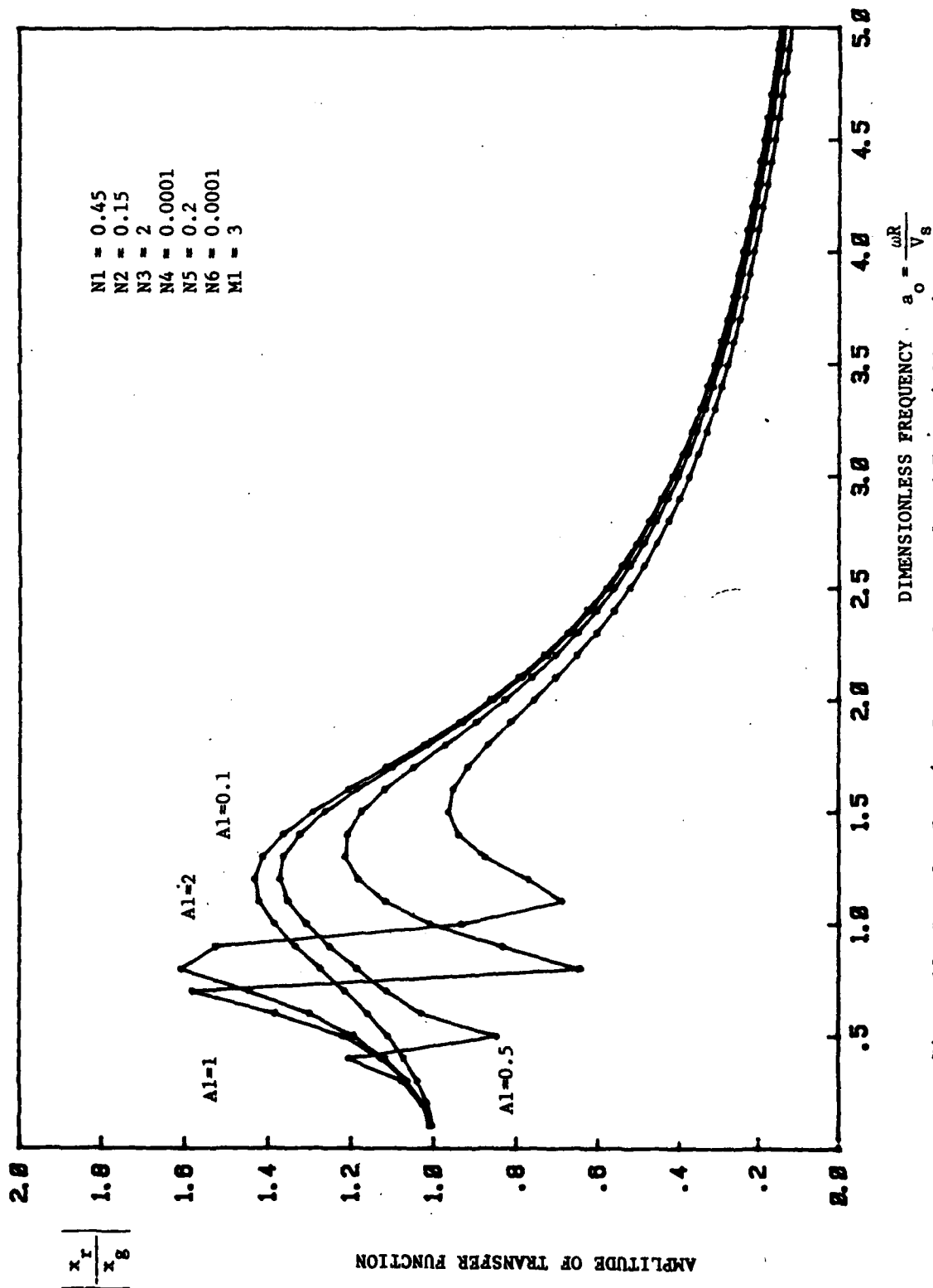


Figure 10. Transfer Function Between Structural and Free Field Motions

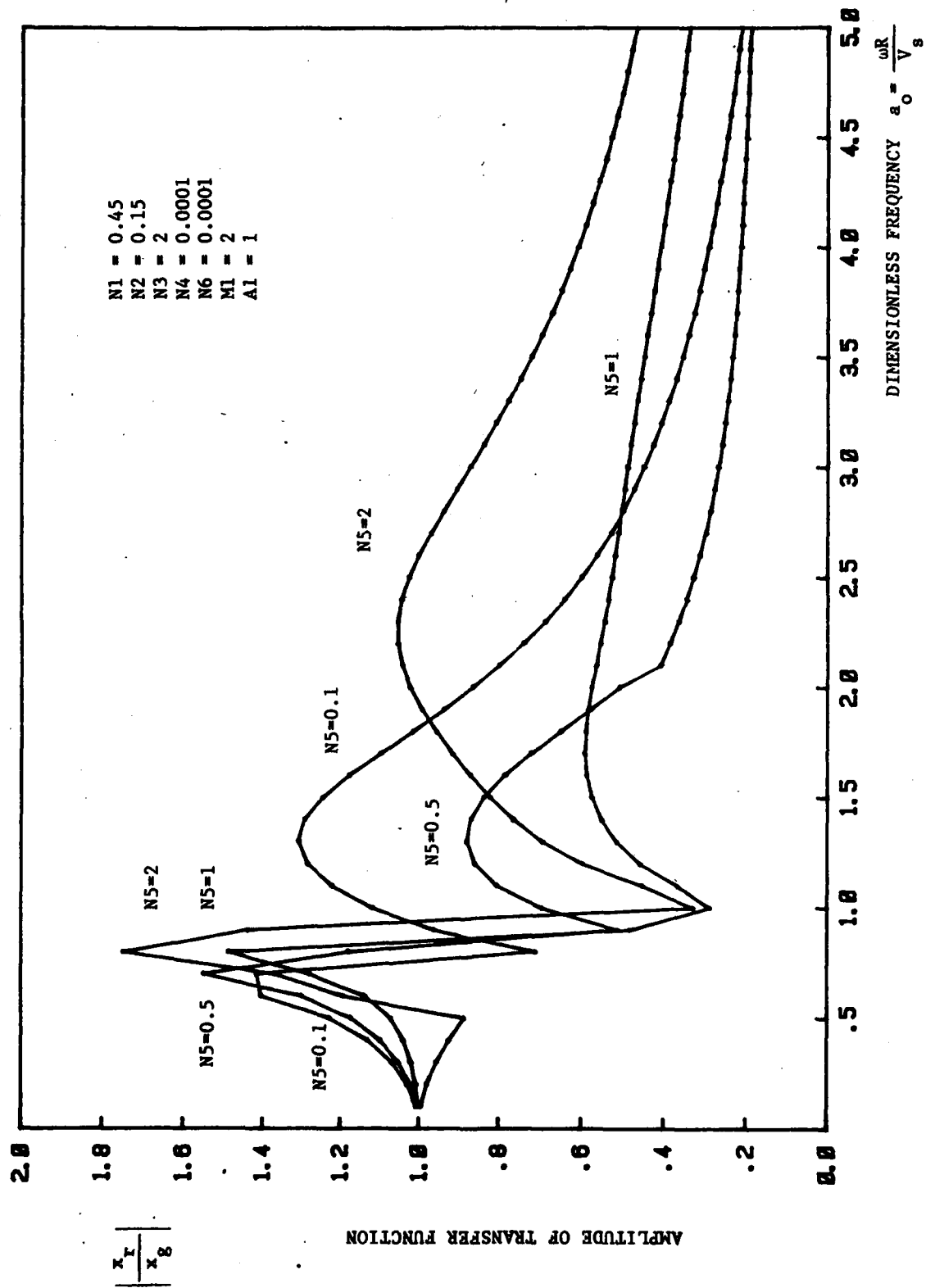


Figure 11. Transfer Function Between Structural and Free Field Motions



recorded in the free field ground level depending on the frequency range. For typical accelerograph stations utilized in the United States as indicated in Figure 12 (Crouse, 1983) one can determine the dimensionless parameters to be :  $M_1 = 2-4$ ,  $A_1 = 1-2$ ,  $N_2 = 0.15$ ,  $N_3 = 1.25$ ,  $N_5 = 0.3$  and  $v = 0.45$ . The transfer function between the motions at the accelerograph location and the free field are indicated in Figure 13 on the basis of these non-dimensional parameters. As it can be seen the recorded motion may be about 50% above or under the free field motion depending on the frequency range. Similar findings have been reported by Crouse (1983) and Crouse et.al.(1984).

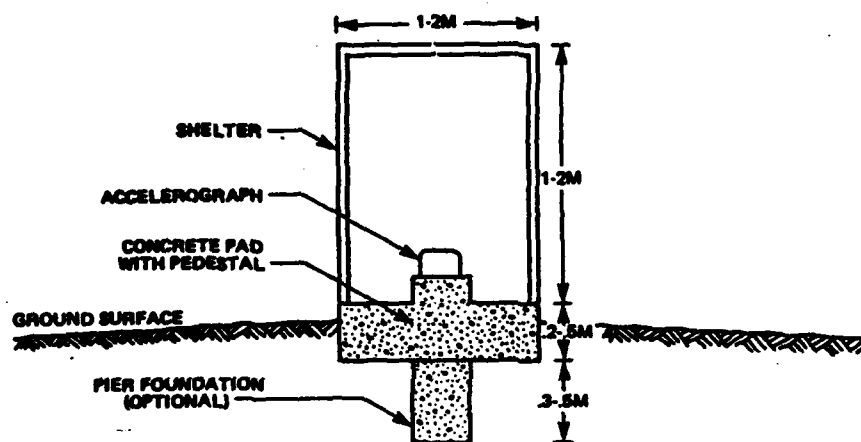


Figure 12. Typical Accelerograph Station (After Crouse, 1983)

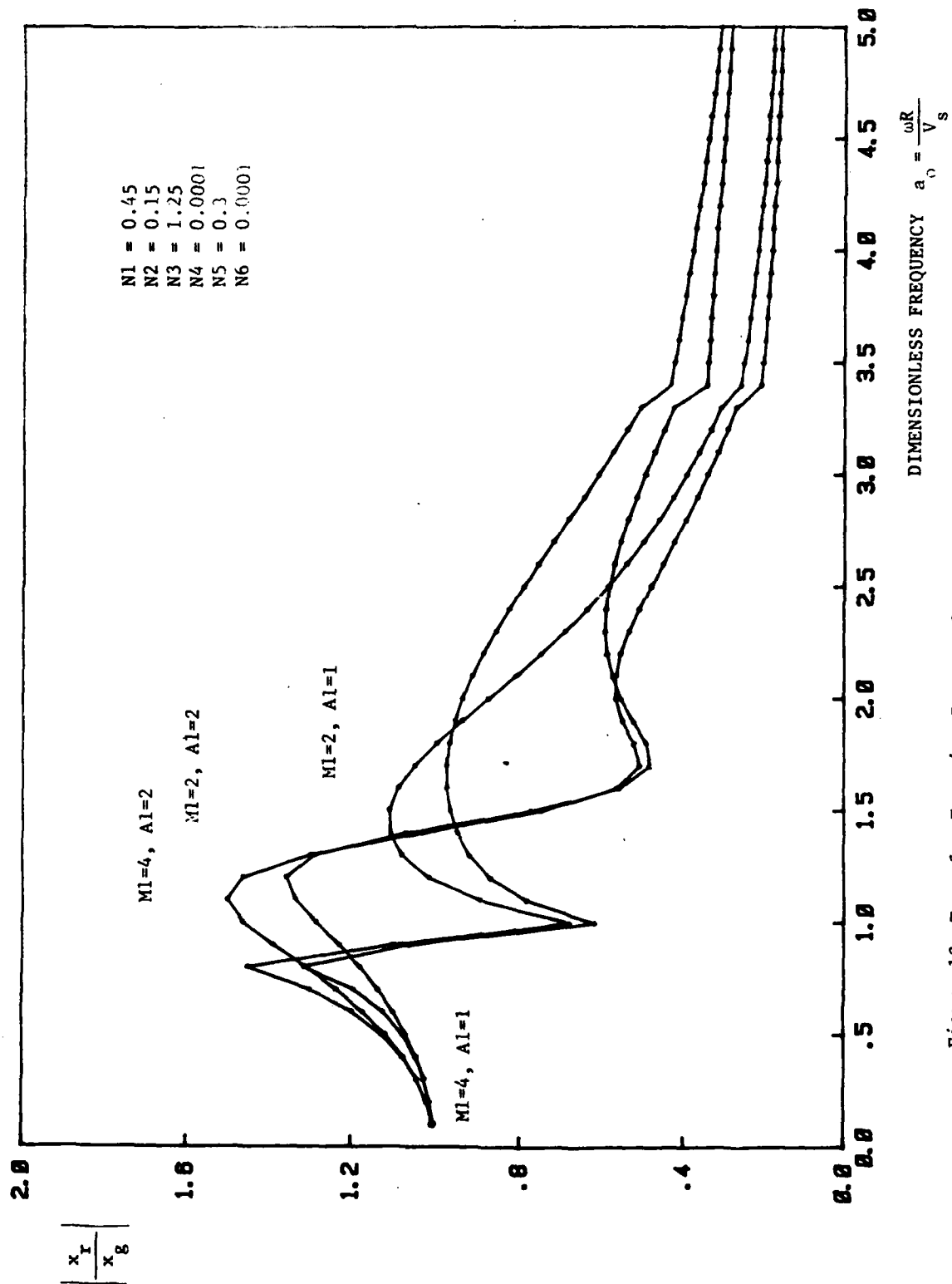
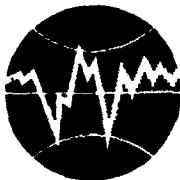


Figure 13. Transfer Function Between Structural and Free Field Motions

## REFERENCES

- ATC-3-06 (1978), Tentative Provisions for the Development of Seismic Regulations for Buildings, Applied Technology Council, U.S. Government Printing Office, Washington, 1978.
- Basaran, C.(1985), Effects of Soil-Structure Interaction on Strong Ground Motion, M.S. Thesis, Dept. of Civil Engineering, Middle East Technical University, Ankara, Turkey.
- Bayo, E. and E.L.Wilson (1983), Numerical Techniques for the Evaluation Soil-Structure Interaction Effects in the Time Domain, Report No: EERC-83/04, Earthq. Engrg. Res.Center, Univ.of Cal., Berkeley, CA.
- Clough, R.W. and J.Penzien (1975), Dynamics of Structures Mc.Graw Hill Book Co., 1975.
- Crouse, C.B.(1983), Soil-Structure Interaction Effects at Accelerograph Stations, Proc. of Conference XXII- a Workshop on "Site-Specific Effects of Soil and Rock on Ground Motion and the Implications for Earthquake-Resistant Design", U.S.G.S., Reston, Virginia, USA.
- Crouse, C.B., G.C.Liang and G.R.Martin (1984), Amplification of Earthquake Motions Recorded at an Accelerograph Station, Proc. 8th. World Conf. on Earthq.Engrg., San Francisco, CA., USA.
- Gutierrez, J.A. and A.K.Chopra (1978), A Substructure Method for Earthquake Analysis of Structures Including Structure-Soil Interaction, Earthq. Engrg. and Struct. Dyn., v.6, pp.51-69.
- Hall, J.R.Jr., J.F.Kissenpfenning and P.C.Rizzo (1975), Continuum and Finite Element Analyses for Soil-Structure Interaction Analysis of Deeply Embedded Foundations, Proc. 3rd. Int.Conf. on Struct. Mech. in Reactor Technology, London.
- Ishii, K., T.Itoh and J.Suhara (1984), Kinematic Interaction of Soil-Structure System Based on Observed Data, Proc. 8th. World Conf. on Earthq. Engrg. San Francisco, California, USA.
- Johnson, G.R., P.P. Christiano and H.I.Epstein (1975), Stiffness Coefficients for Embedded Foundations, Proc. ASCE, Vol.101, No.GT8, Aug.1975.

- Kausel, E., R.V. Whitman, J.P. Morray and F. Elsabee (1978), The Spring Method for Embedded Foundations, Nucl. Engrg. and Des., 48, pp. 377-392.
- Lysmer, J., T. Udaka, C. Tsai and H.B. Seed (1975), "FLUSH-A Computer Program for Approximate 3-D Analysis of Soil-Structure Interaction Problems", Report No: EERC 75-30, Earthq. Engrg. Res. Center, Univ. of Cal., Berkeley, CA.
- Masao, T. et al., (1980), Earthquake Response of Nuclear Reactor Buildings Deeply Embedded in Soil, Nucl. Engrg. and Des., 58, 393-403.
- Richart, F.E. Jr., J.R. Hall and R.D. Woods (1970), Vibration of Soils and Foundations, Prentice Hall, New Jersey, 1970.
- Veletsos, A.S. and Y.T. Wei (1971), Lateral and Rocking Vibration of Footings, Proc. ASCE, SM9, September, 1971.
- Werner, S.D. and M.S. Agbabian (1984), Soil/Structure Interaction Effects at El-Centro, California Terminal Substation Building, Proc. 8th. World Conference on Earthq. Engrg., San Francisco, CA.
- Wong, H.L. and J.E. Luco (1985), Tables of Impedance Functions For Square Foundations on Layered Media, Soil Dynamics and Earthquake Engineering, v.4, pp. 64-81.



**TURKISH NATIONAL COMMITTEE FOR  
EARTHQUAKE ENGINEERING**

**THIRTEENTH REGIONAL SEMINAR ON EARTHQUAKE ENGINEERING**

**September 14-24, 1987 - Istanbul - Turkey**

**VERIFICATION STUDIES ON DYNAMIC SOIL-STRUCTURE INTERACTION**

**Takuji KOBORI**

## VERIFICATION STUDIES ON DYNAMIC SOIL-STRUCTURE INTERACTION

Takuji KOBORI

### SUMMARY

At the time of an earthquake, the building and ground vibrate while they are influencing each other. This effect is called dynamic soil structure interaction, and recognized that is very important for the seismic design of particular structure such as nuclear power plant. Recently, as a lot of sophisticated methods and theorem for this problem has been proposed, and also computer hardware is advancing, this effect becomes to be comprehended with enough accuracy. However, it might also be important matter to verify always those methods by adequate experimental study.

This paper describes basic overview of dynamic soil structure interaction and its verification studies among recent works. And moreover, one of further advanced study and the other problems for dynamic soil structure interaction are introduced.

### 1. Basic Overview of Soil Structure Interaction

#### 1.1 What is Dynamic Soil Structure Interaction

The foundation of a building normally supports the dead weight and the live load of the building, and it has the role of transmitting these loads to the ground. However, at the time of an earthquake, it transmits the ground motion to the building, and at the same time it has the role of resisting the building vibrations and transmitting them to the ground. In other words, the ground and the building influence each other via the foundation, and this is called the Soil Structure Interaction (hereafter abbreviated SSI), and especially the interaction at the time of an earthquake is called the dynamic SSI.

The degree of influence by the dynamic SSI onto the building is decided by the stiffness of the ground, the rigidity and the natural frequency of the building, and the foundation type. Fig.1-1 shows the building foundation types. In the case of the raft foundation of (a), the dynamic SSI takes place via the bottom surface of the foundation, and in the case of the pile foundation of (b), it also takes place via the piles. When the basement exists, the foundation is embedded deeply. As in the case of (c), the dynamic interaction takes place not only via the bottom surface, but also via the side walls surfaces, and when this further is supported by piles, as in case (d), dynamic SSI also takes place via the piles. As the amount of contact area between the ground and the foundation increases sequentially in the order from (a) to (d), the influence of the dynamic SSI becomes stronger and more complicated.

Let us now take a look at the influences between building and ground at the time of an earthquake. In order to show this, the wave propagation during an earthquake as shown in Fig.1-2 shall be considered for the raft foundation of (a). When the seismic waves  $E_0$  generated by the earthquake reach the bottom surface of the foundation of the building, they are divided into the waves entering into the

building and being propagated upwards in the building and the waves being reflected back into the ground. The former ones are called the transmission waves, while the latter ones are called the reflection waves. The transmission waves entering into the building travel towards the top of the building while subjecting the building to vibrate, and then they are reflected at the top and travel back down to the foundation. Here, something occurs which is very important for consideration of the dynamic SSI. When the waves reflected at the top of the building and travelling downwards (F1 in the figure) reach the foundation, a part of them is transmitted into the ground, while the rest is reflected again and once more starts to move upwards through the building. The former waves, escaping into the ground, are called radiation waves. When the amount of these radiation waves is small, the earthquake waves once transmitted into the building continue to remain in the building, the building vibration continue for a long time, and the apparent vibration condition becomes the same as with the small damping of buildings. The damping caused by escape of the earthquake waves, which have been transmitted into the building, back into the ground is called radiation damping.

## 1.2 In Regard to Radiation

The seismic waves escaping back into the ground after once having entered into a building are called radiation waves, and it has been shown that these waves cause radiation damping. Let us now take a look at what kind of waves these radiation waves are. When the building foundation is forced to vibrate vertically, a stress called contact earth pressure is caused at the boundary between the bottom surface of the foundation and the ground. The distribution of this contact earth pressure over the bottom surface of the foundation is called the contact earth pressure distribution, and depending on foundation rigidity, soil type, and soil nonlinearity, the three distributions shown in Fig.1-3 - rigid, uniform, and parabolic distribution - generally can be considered. When a part of the contact earth pressure is picked out and acted onto the ground, the vertical displacement of the ground surface is shown in Fig.1-4. The first displacement peak is reached at the point P at a distance of 10m from the force application point, and the next peaks occur at the points S and R. With increasing distance from the point of force application, these peaks appear at an increasingly later time, and it can be seen that these peaks are propagated at a certain velocity.

When the occurrence times of these peaks are connected by straight lines and the propagation velocity is obtained from the inclination of these lines, it can be found that the propagation velocity for the peak P is 2450m/sec, that for the peak S is 1000m/sec, and that for the peak R is 920m/sec. It was known that the seismic waves include P waves, S waves, and Rayleigh waves called surface waves, and in the same way, these peaks correspond to the P waves, the S waves, and the Rayleigh waves. A look at the amplitude shows that the Rayleigh waves have a large amplitude, so that it can be seen that a large part of the applied force is transmitted by the Rayleigh waves. In the case of a homogeneous ground, the relation of these waves' propagation velocity is decided readily only by the Poisson's ratio of the ground as shown in Fig.1-5. The Poisson's ratio of the ground is normally in the range from 0.4 to 0.5, and in this



case, the propagation velocity of the Rayleigh waves is about 10% lower than that of the S waves.

Fig.1-4 shows the vibrations of the ground surface with force application at only one point of the ground surface, but when the contact earth pressure is distributed over the bottom surface of the foundation as shown in Fig.3, waves as shown in Fig.1-4 are transmitted into the ground from the various contact earth pressure parts, and the composite form of these waves becomes the radiation wave. The vibration energy to the ground by P waves, S waves, and Rayleigh waves, and in the case of a homogeneous ground, the energy distribution ratio for these waves is 7%, 26%, and 67% respectively for P, S, and Rayleigh waves, so that the calculation shows that more than one half of the energy is radiated by the Rayleigh waves. The above explanations in regard to the radiation waves apply for a homogeneous ground, and when the ground is layered, the waves transmitted from the building will be reflected at the layer boundaries and will return to the building, so that the entire matter becomes still more complicated.

### 1.3 Vibration of the Foundation on the Ground Surface

Next, the foundation vibration shall be considered for the case that vibration force is applied at the top of the foundation on the ground surface. Fig.1-6 shows a square foundation with a width of 20m and a height of 10m on the homogeneous ground for an S wave velocity  $V_{sg}$  of 250m/sec, a Poisson's ratio  $\nu$  of 0.4, and a unit volumetric weight  $\gamma$  of 1.8t/m<sup>3</sup>. For simplification, it shall be assumed that the foundation is not deformed locally and that there are no shape changes during the vibration (this is called a rigid body). When the sinusoidal excitation in horizontal direction, the horizontal displacement  $U$  and the rotation  $\phi$  can be found at the foundation bottom. Contact earth pressure resisting this displacement  $U$  and rotation  $\phi$  of the bottom surface is generated at the boundary between the bottom surface of the foundation and the ground surface, and the above mentioned radiation waves are transmitted to the ground by this contact earth pressures. When the ground resisting the displacement  $U$  and the rotation  $\phi$  are represented as spring and dashpot, Fig.1-7 is obtained.  $KH$  is the spring value of the ground resistance in regard to the horizontal displacement  $U$ , and  $CH$  is the dashpot of coefficient absorbing energy proportional to the velocity of the displacement  $U$  as the energy dissipated into the ground by the radiation waves.  $KR$  and  $CR$  are the same values as mentioned above in regard to the rotation  $\phi$ . Fig.1-8 and Fig.1-9 show the calculation results for  $KH$ ,  $CH$ ,  $KR$ , and  $CR$  under the condition that the ground and the bottom surface of the foundation are in contact with each other. The horizontal spring value  $KH$  and the dashpot coefficient (damping factor)  $CH$  are in about constant in regard to the vibration frequency, but  $KR$  and  $CR$  related to the rotation change. Especially the damping coefficient  $CR$  in regard to the rotation shows the characteristic of increasing with the frequency. Fig.1-10 shows the horizontal displacement  $U_f$  of the foundation top of the rigid foundation shown in Fig.1-6, normalized by the exciting force  $P$ , and this type of curve is called a resonance curve.  $\gamma$  in the figure indicates the unit volumetric weight of the foundation, and when  $\gamma$  becomes smaller, i.e. when the foundation becomes lighter, the peak frequencies (resonance frequencies) of the

resonance curve become higher, and it can be seen that the vibration amplitude  $U_f$  becomes smaller.

#### 1.4 In Regard to the Effect of Embedding

Let us now consider the dynamic SSI when the foundation is embedded because of a basement etc. Fig.1-11 shows the resonance curve for the displacement of the center of gravity of the test object before and after the space around the test object is refilled with sand as shown in Fig.1-11 in order to investigate the effect of embedding. It can be seen that the resonance frequency is increased by embedding, and the resonance curve near the peak is not sharp, but rather rounded. The damping factor  $h$  is used in vibration mechanics to express the degree of sharpness of this resonance curve, and this  $h$  is increased from 5.7% to 6.3% by embedding.

Let us now consider the meaning of this. Before embedding, the radiation waves were transmitted from the bottom surface of the test object, but after refilling, they also are put out from the side walls of the test object, so that the entire damping is increased, and the resonance frequency increases because the sides restraint by the ground increased.

#### 1.5 Coupled System of Building and Ground

When the forces are applied to the building by an earthquake or by means of a excitor etc., the building vibrates while the building and the ground are influencing each other. This system is called the coupled system of building and ground. Naturally, this coupled system is connected by the dynamic SSI treated above. Let us now investigate the influence of the dynamic SSI onto the coupled system.

Fig.1-12(a) shows an example for a building with a basement. This building is represented in simplified form by the spring  $K$  connecting the mass point and the basement and the dashpot  $C$ , as shown in (b). When the basement is fixed, the natural frequency of the building is 2Hz and the damping factor  $h$  is 5%. The basement shall be a rigid body with a unit volumetric mass of  $0.5t/m^3$ , and the ground shall be homogeneous.

Fig.1-13 shows the result of the calculation for the resonance curve of the horizontal displacement of the building top with horizontal excitation of the top of the building, when the basement embedding depth is changed. As already stated above, the natural frequency of the building itself with fixed basement is 2Hz, but the resonance frequency shown in this figure is considerably lower than 2Hz. This resonance frequency is called the resonance frequency of the coupled system of building and ground in earthquake engineering, and in comparison with the natural frequency of the building when the foundation is fixed, i.e. when it does not move, this frequency is always lower. With increasing embedding of the basement, the resonance frequency of the coupled system increase and the amplitude shows a decreasing tendency. This is caused by the increased restraint effect and radiation damping because of embedding as already stated above.

Next, the vibration of the coupled system at the time of an earthquake shall be considered. Fig.1-14 shows the behavior of a building with a basement during an earthquake. For simplification, the earthquake waves are assumed as sinusoidal waves with the frequency

f Hz and with displacement only in horizontal direction, and they shall be brought in from below at a right angle to the ground surface. As shown in the same figure, the amplitude of the seismic waves amplifies when the seismic waves approach the ground surface. The earthquake input into the building via the basement takes place not only via the bottom surface, but also via the side walls. While the input from the bottom surface becomes smaller as the ground vibration amplitude decreases with increasing depth of the basement, the input from the walls increases with the increasing wall surface in contact with the ground. When the basement has a high rigidity in comparison to the ground, this input from the walls becomes an input averaging the deformation of the ground. Next, the earthquake input which has entered into the building vibrates the building, and the vibration energy escapes from the basement bottom surface and the side walls as radiation waves.

An earthquake response analysis is carried out using substructure method shown in Fig.1-15. Fig.1-16 shows the analysis results for vibration of the coupled system of building and ground during an earthquake with the same conditions as for Fig.1-13. The vertical axis shows the vibration amplitude ratio between the building top and the ground surface, while the horizontal axis shows the frequency of the seismic waves. The vibration amplitude of the building decreases with increasing embedding depth of the basement, and as shown by the calculation examples, it can be seen that the vibrations at the time of an earthquake decrease with increasing basement depth.

## 2.Verification Studies on Dynamic Soil-Structure Interaction

The basic overview of SSI is discussed in previous section. It might be understood that the study on SSI problem is well-developed theoretically. Now, let us take a look at some examples for the dynamic SSI effect in order to get more precise comprehension, there are many helpful investigations by the experimental approach to verify those theorem.

In this section, two examples among recent experimental studies are shown.

### Example 1

Among the models of response analysis for embedded structures, two mathematical models have been adopted in Japan. Namely, one is the lattice model, and the other one is the sway-rocking model. Considering computational costs and applicability, the latter might be more practical and useful. Of course, this sway-rocking model requires a careful approximation of the spring values.

This example proposes a proper evaluation method for the soil springs of an embedded structure which are valid for the earthquake response analyses.

#### 2.1 Outline of Tests

The tests results, which are used in this study, were obtained on two reactor buildings are shown in Fig.2-1. Plant A has a deep embedment of 45 meters, while Plant B has a relatively shallow

embedment. In particular, the embedment expands into the underlying firm rock for Plant A. The forced vibration tests of both plants were carried out by sinusoidal excitation. These forces were generated by an excitor which was installed on the refuelling floor. Only the results obtained by a horizontal excitation parallel to the adjacent turbine building are investigated.

## 2.2 Evaluation Methods for Soil Springs and Structure

Many evaluation methods for soil springs have been proposed so far. Among them, the following four methods are chosen to be examined.

Method A; In this method, the side soil springs  $K_u$ ,  $K_\theta$  and the base soil springs  $K_H$  and  $K_R$  can be independently evaluated. The side springs are calculated from Novak's theory, while the base springs from Kobori's theory.

Method B; This method is applied to Plant A only. As this plant is also embedded into the underlying firm rock, the soil springs due to this portion are calculated by the Boundary Element Method. The other springs are derived from Method A.

Method C; This method is the Thin-Layered Method which has been developed by Tajimi.

Method D; In this method, the Axisymmetric Finite Element Method is applied. Viscous damping accounts for the infinite energy transmission at the boundaries.

The structure is modelled corresponding the evaluation methods for soil springs mentioned above. All the underground structures are modelled into a lumped mass system in method A. Only the basement of rock portion is assumed as rigid in method B but the other portion is treated as same as the method A. All of the underground structure are assumed as rigid in method C and D. Fig.2-2 shows these resulting models.

## 2.3 Resonance Curve

Fig.2-3 and Fig.2-4 show the resonance curves of Plants A and B on two levels of the structure.

Fig.2-3 represents the results of Plant A, it found that the resonance curve has no peaks and this feature is expressed well by all methods. However, there is the difference in amplitude among all the methods in the upper level.

Fig.2-4 which represents the results of Plant B, shows that the analytical results have good agreement with the test ones on the upper level, while the amplitude is overestimated on the base level. Moreover, the resonance frequency is somewhat underestimated by method A, and method D displays wavy results due to the fact that the wave radiation damping is not exactly evaluated at the mesh boundaries of this axisymmetric finite element method.

## 2.4 Conclusion

As it is mentioned above, we could get almost the same results by using any of the four methods and good agreement with the test results. However, a portion of the underground structures in method B,

and all of them in methods C and D must be as assumed rigid because it is difficult to divide the soil springs as treated in method A. Furthermore, method A requires far less computational time.

Therefore, we think method A in which the side soil springs  $K_u$  and  $K_\phi$ , and the base soil springs  $K_H$  and  $K_R$  are evaluated independently in Fig.2-2 is the most convenient method for practical seismic design analyses.

### Example 2

It is well known that the vibration characteristics of a structure adjacent to the other structures are different from those of an isolated structure. These differences are caused by dynamic interaction between the adjoining structures through the soil. This kind of interaction has been termed the Dynamic Cross Interaction (DCI).

This example describes the simulation analysis of the forced vibration tests on an actual nuclear reactor building and on its adjacent turbine building by the method in which the DCI effect is taken into account.

### 2.5 Outline of Forced Vibration Tests

Fig.2-5 shows the cross section and site layout of the objective nuclear reactor building and turbine building.

The reactor building (hereafter called R/B) is a large reinforced concrete structure, which has overall plan dimensions of about 80m square at the lower level, an underground depth of 18.5m, an above ground height of 58.0m and a total weight of about 300,000 tons. The turbine building (hereafter called T/B) is also a reinforced concrete structure which has overall plan dimensions of 66m x 110m and is set on almost the same ground level as the R/B. Total weight of the T/B is about 280,000 tons. There is an interval of 10cm between the two buildings.

### 2.6 Development of Analytical Method

The buildings are modelled by a detailed multi-stick lumped mass system taking into account not only the fundamental resonance mode but also the local vibration mode in the upper portion of the buildings.

The DCI soil springs are estimated as the coupling impedance matrices under the assumptions as follows;

- 1) The impedance matrix of the supporting soil, and that of the surface layered soil and back filling soil are evaluated independently.
- 2) Three-dimensional BEM with Green's functions derived from surface point exciting solutions, is used to model the supporting soil which is assumed to be a uniform half space. The coupling impedance matrix between the R/B and the T/B (8 x 8 matrix for horizontal, vertical, rotational, and torsional directions) is conducted under the assumption that each basement slab is rigid (as shown in Fig.2-6 (a)).
- 3) Two-dimensional plane strain BEM is applied to the surface layered soil and the backfilling soil. The coupling impedance matrix between the R/B and the T/B (4 x 4 matrix for horizontal

and torsional directions) is evaluated similarly under the assumption that each building is rigid at each embedded level (as shown in Fig.2-6 (b)).

The total model is a multi-stick lumped mass system of buildings combined with the two kinds of the DCI springs (as shown in Fig.2-6 (c)).

## 2.7 Test Results

Only the forced vibration tests and simulation analyses in the E-W direction as shown in Fig.2-5 are dealt, because the effects of DCI can be considered to be larger than another one. Fig.2-7 shows the resonance and phase lag curves of representative measuring points.

Major findings obtained from the test results are as follows;

- 1) Fundamental resonance frequency of the R/B is 2.5Hz, and damping factor evaluated by the half power method is about 30%.
- 2) Horizontal vibration energy transmitted from the R/B to the T/B predominates at the natural frequency of the T/B (about 3.0Hz).
- 3) The phase lag of the R/B increases as the measuring point approaches the basement slab, and furthermore, the higher the measuring point on the T/B is, the larger its phase lag becomes. This shows that the energy transmission from the R/B to the T/B is mainly through the supporting soil.
- 4) The local vibration mode in the upper portion of the R/B predominates at about 7.0Hz and 10.0Hz, while that of the T/B is at 5.0Hz. They cause the energy absorption effects which decrease the response amplitude at the other levels.

## 2.8 Analytical Results

The results of simulation analyses, i.e. the resonance curves and phase lag curves at the refueling floor (GL 38.5m) and the 2nd floor (GL 6.0m) on the R/B are shown in Fig.2-8. Similarly, Fig.2-9 shows those of the representative measuring points on the T/B.

The analytical values generally correspond closely with the experimental values in amplitude and phase lag. In particular, the local vibration mode at about 5.0Hz on the roof on the T/B is well accounted for. It should be noted that the difference between the case 1 (coupled) and case 2 (isolated) is very small.

## 2.9 Conclusion

The simulation analyses of forced vibration tests on the R/B are executed with a model taking into account the DCI between the R/B and the adjacent T/B, and the embedment of buildings.

These results lead to the concluding remarks as follows;

- 1) The results of the simulation analyses are in excellent agreement with the test results not only on the R/B but also on the T/B.
- 2) It may be concluded that the proposed analytical methods using BEM are efficient to evaluate the dynamic coupling vibration problem through soil between embedded structures.
- 3) For forced vibration tests on the R/B, the influence of the adjacent T/B on the response of R/B is relatively small and it is possible to ignore the existence of the T/B in the case

simulation analyses of the R/B.

### 3. Further Advanced Study

Two examples of verification study are introduced above. They might help you to comprehend what the dynamic SSI is, and to realize the theorem are verified very well. These methods are precise enough for practical problems, but the more detailed analysis is sometimes required. One of the advanced methods which is valid for such request is shown in this section.

The soil-structure interaction plays an important role in the earthquake response of massive and large structures such as nuclear reactor buildings and many studies pertaining to this subject have been reported in the past. However, especially in cases of embedded structure in spite of a need of the precise analysis up to high frequency range, the past analytical methods are still insufficient to investigate the 3-dimensional dynamic response characteristics taking into account the complicated configuration of the structure, backfilling soil and the semi-infinity of the 3-D soil medium.

Therefore, the analytical method has been developed using a 3-dimensional hybrid model taking into account the advantage of BEM and FEM in order to evaluate the effect of dynamic SSI of the case of an actual embedded reactor building and have investigated its dynamic response characteristics up to high frequency range.

This section describes the dynamic response analysis of a typical BWR reactor building as a comparative study between two different embedment depths in elastic half space.

#### 3.1 Outline of Analytical Method

The earthquake response analysis is based on substructure method where the soil-structure interaction system is divided into two domains as shown in Fig.3-1. One is the domain composed of the building and the back filling soil which are modelled by finite elements, and the other is the half space soil domain by boundary elements, and the displacement and traction of elements contacting each other are adjusted, the transfer function of each point of the building to the control point is obtained. Then earthquake response analysis is carried out easily by using algorithm of Fast Fourier Transform.

#### 3.2 The Subject of Analysis

Fig.3-1 shows the BWR (MARK-I) type reactor building of subject matter herein. The basement is square shaped 75m x 75m with 5m depth and the building is 65m high from the bottom of the basement to top. The main structural components are the shield wall, the inner wall and the outer wall.

And as an analytical case, two different embedment depths in elastic half-space soil medium with a shear wave velocity of 1000m/sec are taken into account. In Case 1, the building is embedded 20m deep with surrounding back filling soil, and a 1/4 analytical model of the finite elements with 212 nodal points and about 270 elements, and the boundary elements with 40 elements are used. While, in Case 2 only the

basement of the building is embedded without any backfilling soil.

Damping factors of the building and backfilling soil are 5% and 10% as complex damping respectively.

The incident wave to the hybrid model is taken into account as a vertically propagating SH wave and controlled by the free field surface. The sinusoidal wave and EL CENTRO (1940 NS) earthquake wave with the maximum acceleration of 100gal are used as the motion of the free field surface.

### 3.3 Analytical Results

**Acceleration Transfer Function:** Fig.3-2 and Fig.3-3 show the acceleration transfer functions of main points at the refueling floor and the basement respectively.

From these figures, the following findings are pointed out.

- 1) Fundamental resonance frequency is almost the same in both cases but acceleration amplification factor decrease in all frequency range in Case 1 in comparison with Case 2.
- 2) At the refueling floor, two points in the inner wall (15 & 22) indicate the same behavior in all frequency range, but the other two points (17 & 23) show different behavior from the aforementioned points in the inner wall, furthermore in high frequency range beyond 8Hz, not only the shear deflection but also the axial deflection are generated. These behavior are observed to be almost the same in both cases although the quantity is different.
- 3) At the basement in Case 1, acceleration amplification factor to free field surface is less than 1.0 in all frequency ranges and the difference of each point is remarkable in frequency range beyond 8Hz. While in Case 2 acceleration amplification factor is larger than that in Case 1 and behavior of each points are almost same up to about 12Hz.

**Maximum Earthquake Responses Acceleration:** Fig.3-4 shows the maximum acceleration distribution in two vertical sections in view of comparison with both cases. Solid line and chained line show the results for Case 1 and Case 2 respectively.

From these figures, the following findings are pointed out.

- 1) Although little difference is found at the lower parts, there is a distinct difference at the upper part above the 3rd floor and the maximum acceleration in Case 1 is 25%-30% smaller than that of Case 2.
- 2) The maximum response acceleration of the shield wall is larger than those of the inner wall with regard to both horizontal and rotational motions.
- 3) At the upper parts above the refueling floor such as the roof slab and the perpendicular inner wall, the amplification factor shows increase due to local vibration effect.

**Floor Response Spectra;** Figs.3-5(a) and (b) show acceleration response spectra at shown points of the 5th floor in comparison with both cases.

From these figures, it is found that spectral values decrease with the increase of embedment depth and that the floor response spectra are different, especially remarkable in the short period range even at the same floor level.



### 3.4 Concluding Remarks

Concluding remarks in this study are as follows;

- (1) As the results of comparative study, it is confirmed that the earthquake response intensity such as maximum acceleration and floor response up to high frequency range decrease with the increase of embedment depth when 3-dimensional soil-structure interaction effects are taken into account.
- (2) It is confirmed that difference of behavior due to the position is significant even at the same floor level, especially in high frequency range, therefore it is necessary to take into account the shear and axial deflections of the slab in the modeling of the building up to high frequency range.

### 4. Other Problems

The overview of soil structure interaction problems and its applicability verified by some experimental studies are mentioned above. It is found that the recent procedure is well-proved and lead to adequate results. However, needless to say, they should be advanced by further study such as introduced in previous section corresponding to the state of the art.

In this section, a couple of issue that should be investigated further and adopted into the practical procedure are described.

#### 4.1 Nonlinear Problems for Soil

In the seismic design of important structure against the most severe earthquake capable to occur, the dynamic analyses should be executed in consideration with the nonlinear characteristics of building structure. In such cases, it is easily supposed that not only the building but also the soil may show strong nonlinear behavior.

There are many nonlinear phenomena in SSI, and they could be classified these two nonlinear problems.

- 1) Material nonlinear the soil possesses by nature
- 2) Geometric nonlinear such as separation from side wall or structure uplift from the underlying soil.

For the former problem, the direct method is effective to treat the material nonlinearity of soil. Fig.4-1 shows this type of model discretized by FEM or FDM specially. Proper nonlinearity such as plastic theorem-based yield condition and hardening rule is given to each element, and nonlinear dynamic response can be obtained by means of step by step time integration. Due to recent study in this matter, the response value of structure decreases when the material nonlinearity is considered.

For the second problem, direct method mentioned above is also applicable. Fig.4-2 shows an example of separation analysis result by FDM. This method has an advantage that the combined analysis with material nonlinear is possible.

Here is another approach for this problem that is time domain substructure method using Green's function and impulse response function. This method needs excessive computational time, but that has more exactness theoretically.

## 4.2 Pile Foundation

In section 1, it is explained that the effect of dynamic SSI is decided by the foundation type, and in the case of the pile foundation, dynamic SSI takes place via the piles, so the influence of them becomes more complicated.

Once, as simple evaluation, Chang's equation etc. was adopted for the horizontal soil spring, and this method is practically helpful. But this method is valid only for static analysis, because frequency dependency investigated in section 2 can not be represented by this method, and furthermore when the piles are closely spaced, the effect of pile group (i.e. pile soil pile interaction.) become so strong that the more precise evaluation become necessary.

He is one of the methods based on elastic wave propagation theory. The ground surface motion at the points apart particular distance from the force applied point at ground surface is investigated in section 1. The similar procedure is available for pile spring evaluation. The relation between cylindrical force or circular force applied in the ground, corresponding to the traction at side surface and pile bottom respectively, and the displacement at the arbitrary point in the ground can be expressed by some integral equations, and then by solving them, the pile spring for any pile arrangement can be obtained.

## 4.3 Dynamic Analysis According to Site Condition

In order to calculate the soil springs theoretically, it is convenient to assume or idealize that the ground is homogeneous half space or consisting of horizontally lying strata although there are topography and irregularity such as mountains and winding strata. We discussed dynamic SSI problems only for homogeneous ground in section 1. This assumption leads enough good results practically, but in the case that more precise investigation is required, the topography and irregularity should be taken into the analytical model.

Usually, boundary element method or finite element method shown in Fig.4-3 are adopted. The former method has advantage for making a model of topography and infinity, but it is not suitable for internal ground irregularity. On the other hand, the latter method is effective to treat the internal irregularity, but there is a little difficulties to set the boundary condition. A combined analysis as described in section 3 is also possible, the advantage of each method are available in this case. The most proper method should be chosen according to site condition.

## 5. Conclusion

The study on the dynamic SSI problems has started about 50 years ago, and many researchers have achieved fruitful results from theoretical and experimental approach. Consequently, the effect of dynamic SSI can be understood with sufficient accuracy in nowadays. In other words, we can simulate the dynamic response behavior of most type of soil and structure system, but needless to say, the complicated procedure such as mentioned in chapter 3 is not always necessary to investigate them. It is the most important point for

engineers to realize what kind of SSI governs each type of soil and structure interaction system, and to establish the best analytical method for them.

#### References

- 1) Kobori T.; "Dynamic Response of Rectangular Foundation on an Elastic Space.", Proceedings of First Japan Earthquake Engineering Symposium, 1962
- 2) Reissner E.; "Stationäre, Axialsymmetrische, durch eine Schüttelnde Masse Erregte Schwingungen eines Homogenen Elastischen Halbraumes, Ingenieur-Archiv", Vol.7, 1936
- 3) Wolf J.P.; "Dynamic Soil-Structure Interaction", Prentice-Hall, 1985
- 4) Richard F.E., Hall R.J., and Woods R.D.; "Vibrations of Soil and Foundations", Prentice Hall, 1970
- 5) Hijikata K., Uchiyama S., Miura K. et al.; "Dynamic Soil Structure Stiffness of Embedded Reactor Buildings", 9th SMIRT, 1987
- 6) Novak M., Nogami T., and Aboul-Ella F.; "Dynamic Soil Reactions for Plane Strain Case", The Journal of the Engineering Mechanics Division, ASCE, 1977
- 7) Tajimi H.; "A Contribution to Theoretical Prediction of Dynamic Stiffness of Surface Foundations" 7th WCEE, 1980
- 8) Yamashita T., Tanaka H., Miura K. et al.; "Study on the Interaction through the Soil between Adjacent Embedded Structures", 9th SMIRT, 1987
- 9) Motosaka M., Kamata M. et al.; "3-Dimensional Earthquake Response Analysis of Embedded Reactor Building using Hybrid Model of Boundary Elements and Finite Elements", First Japan National Symposium on Boundary Element Method, 1987
- 10) Yamada A., Miura K. et al.; "Effect of Nonlinear Soil Property on Earthquake Response of Reactor Building", (to be appeared 9th WCEE, 1988)
- 11) Kobori T., Minai R., and Baba K.; "Dynamic Behavior of Pile under Earthquake Type Loading", Internal. Conf. on Recent Advances in Geotechnical Earthquake Engineering and Soil Dynamics (RAGEESD), 1981
- 12) Chapel F., Crepel J.M. et al.; "3-D Analysis of a Group of Piles in a Multilayered Soil Submitted to a Seismic Field - Comparisons with Experiments", Fifth International Conference on Numerical Methods in Geomechanics, 1985

- 13) Masuda K., Sasaki F., and Urao K.; "Simulation Analysis of Forced Vibration Test for Actual Pile Foundation by Thin Layer Method", Reliability and Robustness of Engineering Software Conference, 1987
- 14) Sen R., Davies T.G., and Banerjee P.K.; "Dynamic Analysis of Piles and Pile Groups Embedded in Homogeneous Soils", Earthquake Engineering and Structural Dynamics, 1985
- 15) Kasai Y., Yahata K. et al.; "Model Studies on the Effect of Topographic Irregularity and Geological Inhomogeneity in Dynamic Behaviors of Ground", 9th SMIRT, 1987

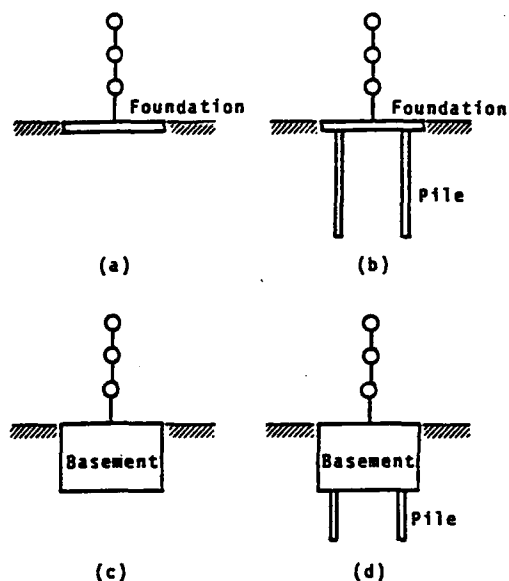


Fig. 1-1 Foundation Type

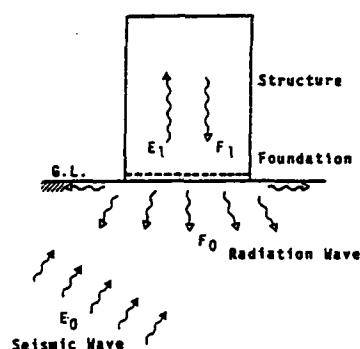


Fig. 1-2 Seismic Wave Propagation in Soil-Structure System

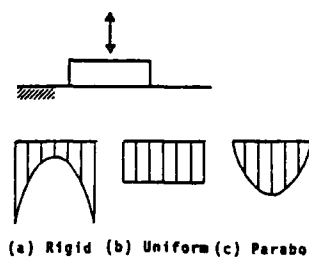


Fig. 1-3 Contact Earth Pressure Distribution

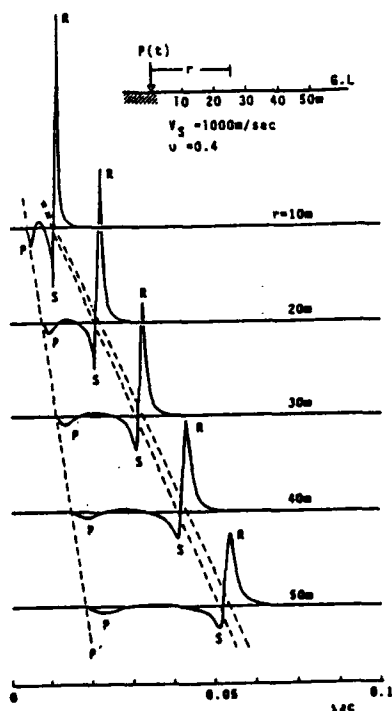


Fig. 1-4 Vertical Displacement due to Impulse Force

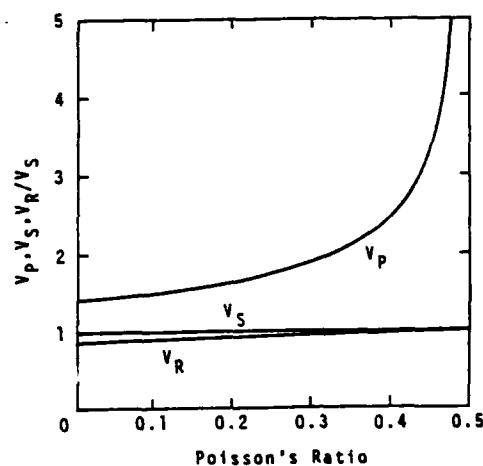


Fig. 1-5 Velocity of P, S, R-Wave Type

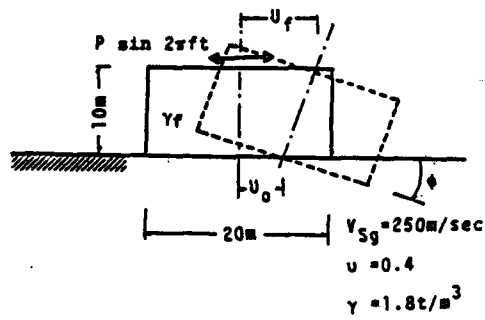


Fig.1-6 Vibration of Foundation on Ground Surface

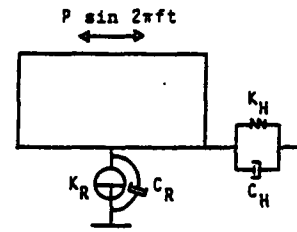


Fig.1-7 Modelling of Foundation

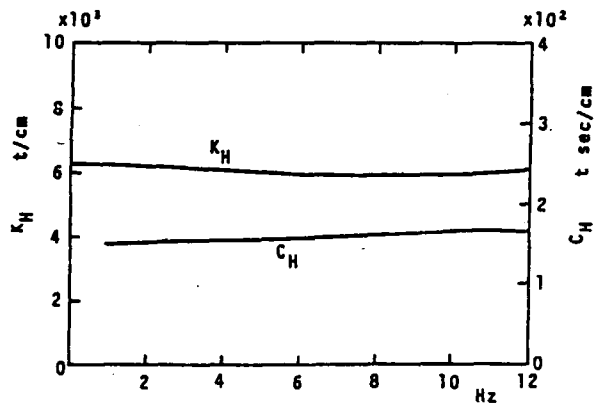


Fig.1-8 Horizontal Soil Spring

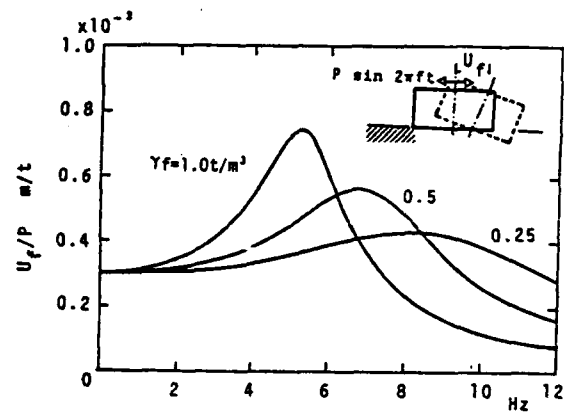


Fig.1-10 Resonance Curve at Foundation Top

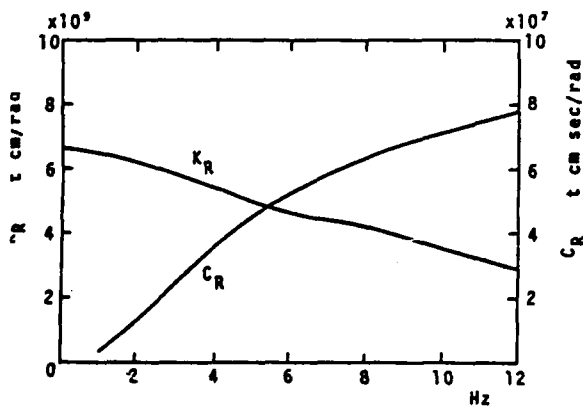


Fig.1-9 Rocking Soil Spring

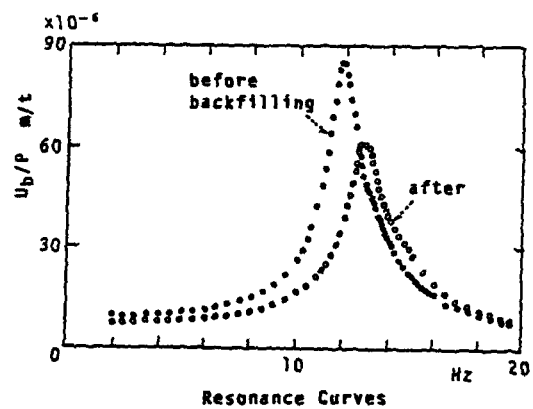
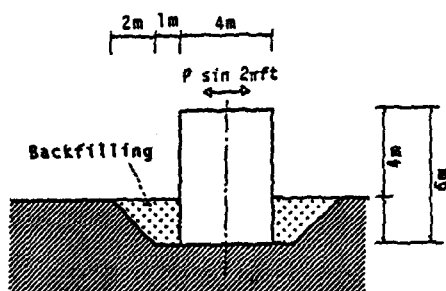


Fig.1-11 Test on Embedment Effects

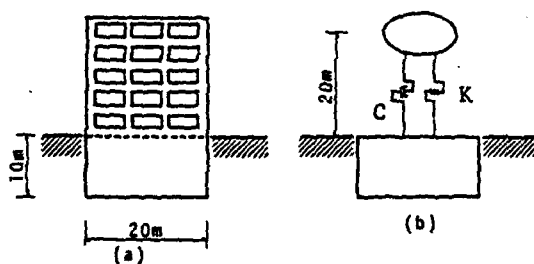


Fig.1-12 Structure with Basement

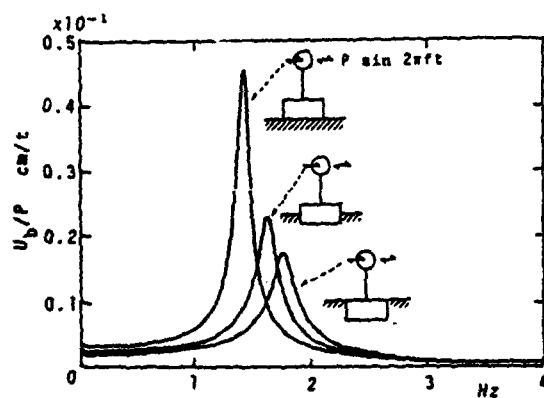


Fig.1-13 Resonance Curve

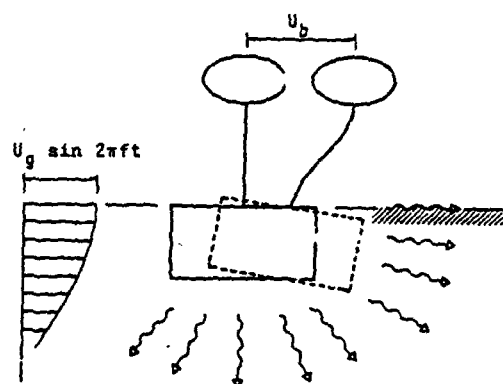


Fig.1-14 Vibration of Structure with Basement during Earthquake

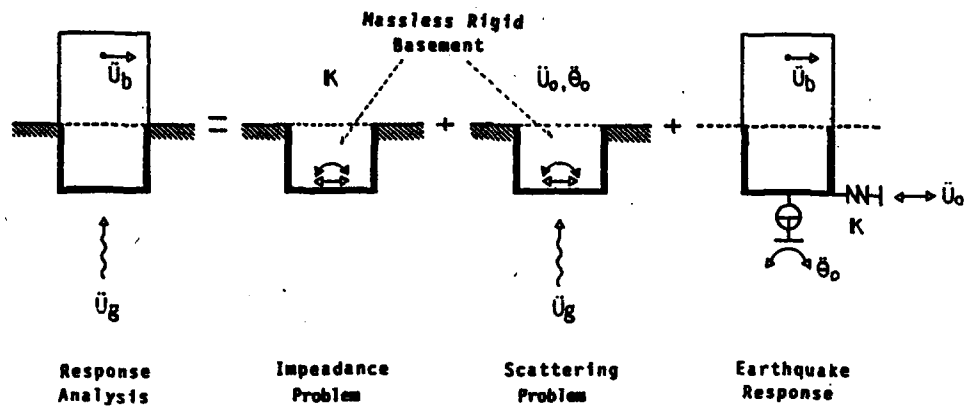


Fig. 1-15 Substructure Method for an Earthquake Response Analysis

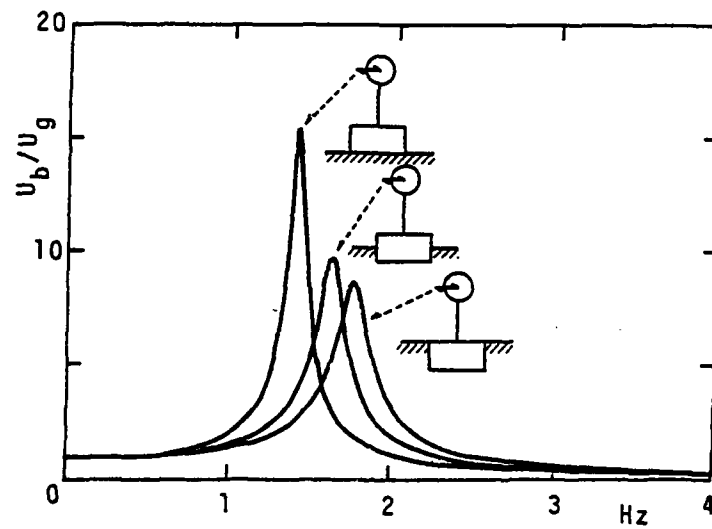


Fig. 1-16 Resonance Curves



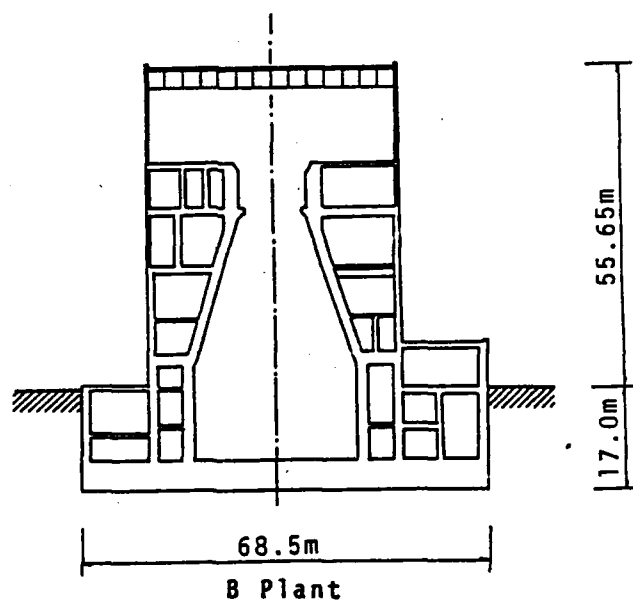
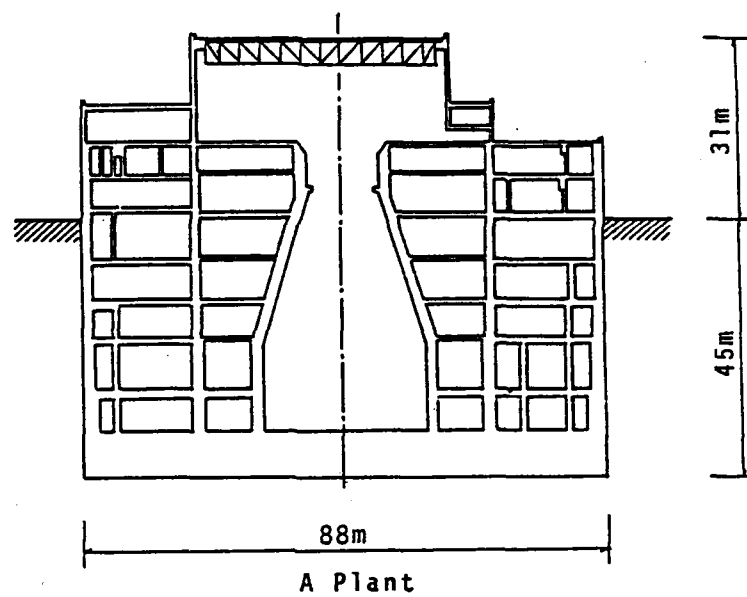
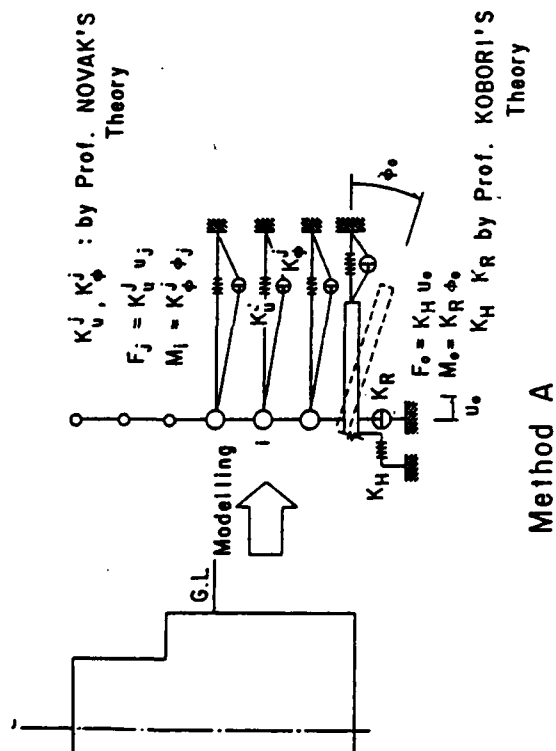


Fig.2-1 Nuclear Power Plant with Embedment



Thin-Layered Method  
by Prof. TAJIMI

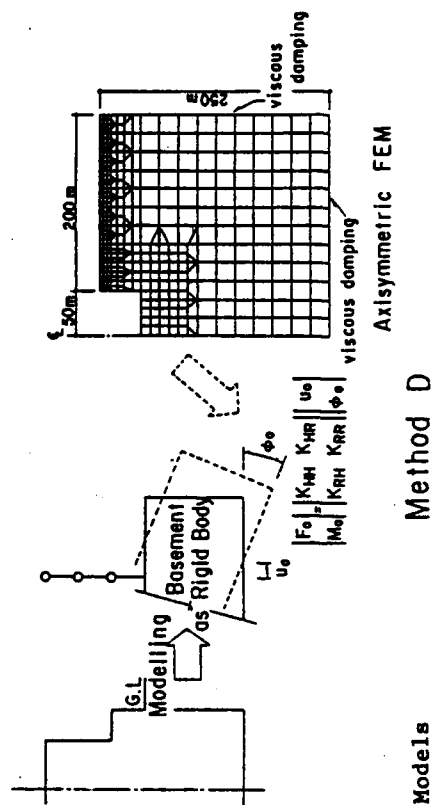
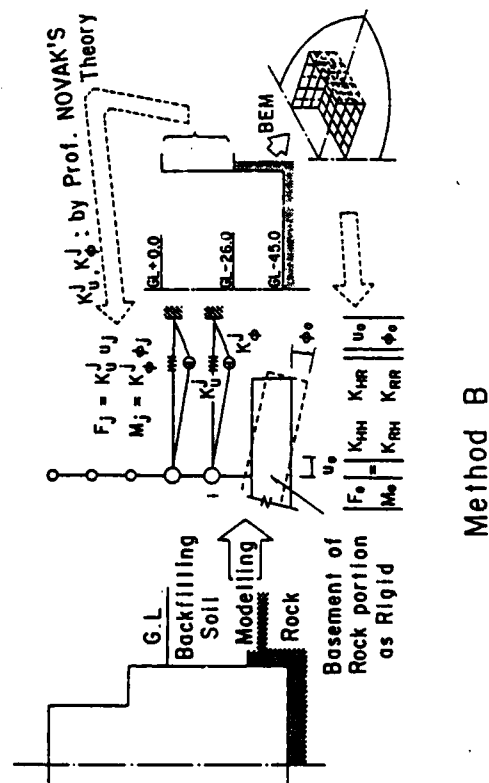
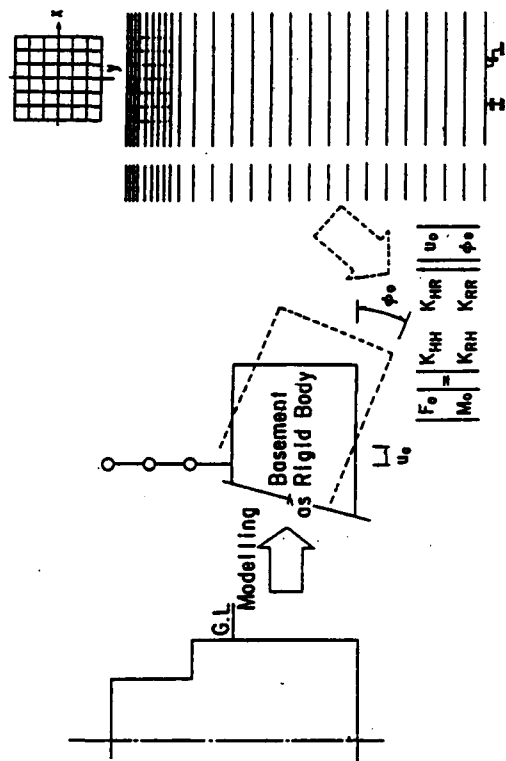


Fig.2-2 Analytical Models

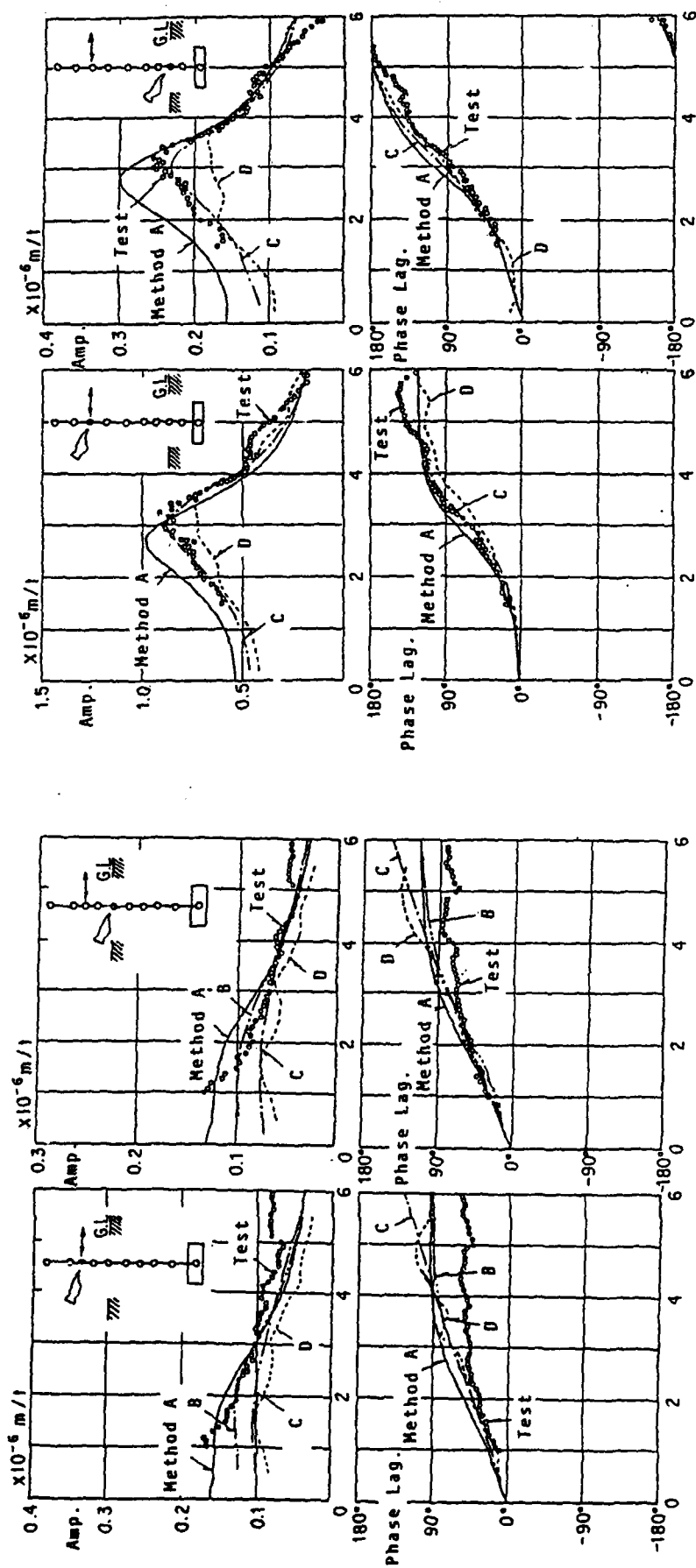


Fig.2-3 Resonance Curves (A Plant)

Fig.2-4 Resonance Curves (B Plant)

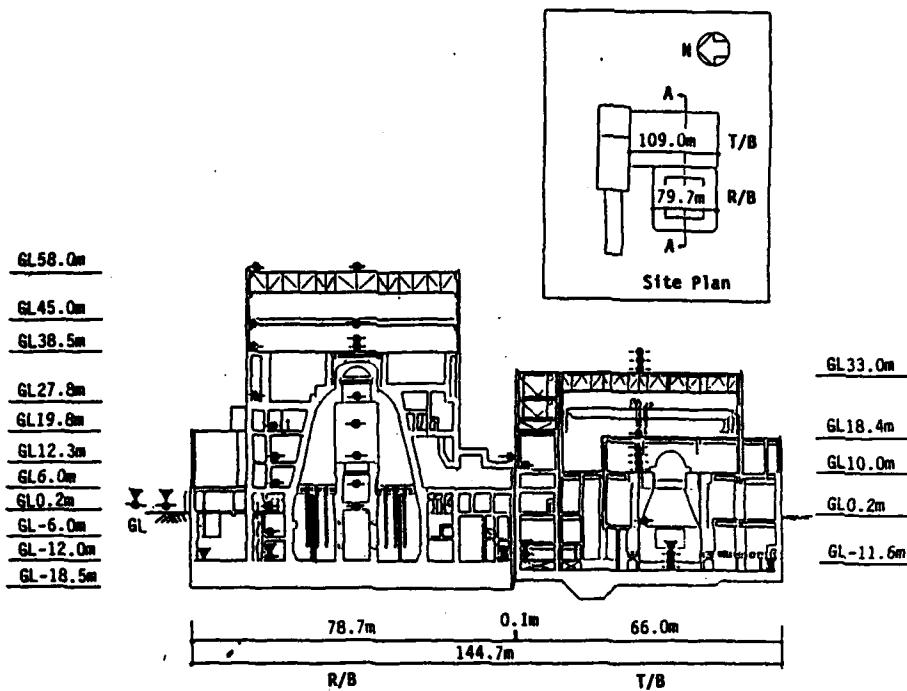


Fig.2-5 A-A Cross Section  
(Showing the Location of all Measuring Points for EW Direction)

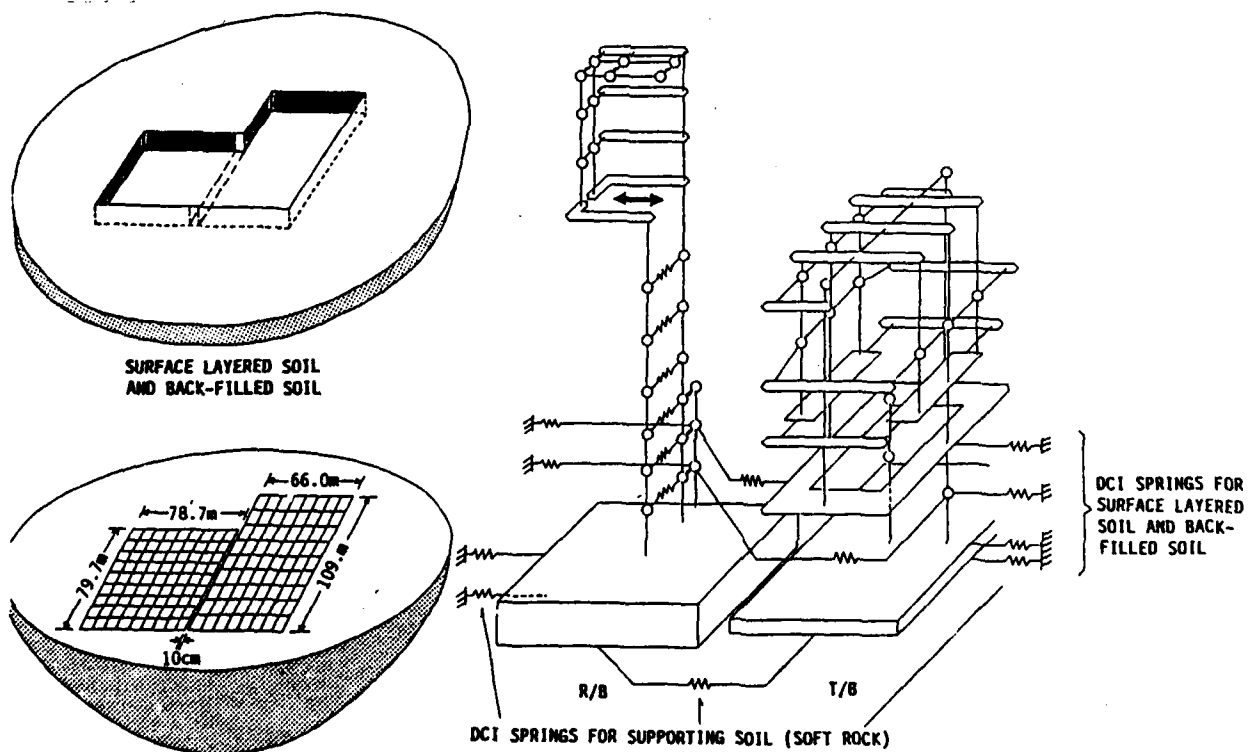


Fig.2-6 Analytical Model  
(Multi-Sticks Lumped Mass Model with DCI Springs)

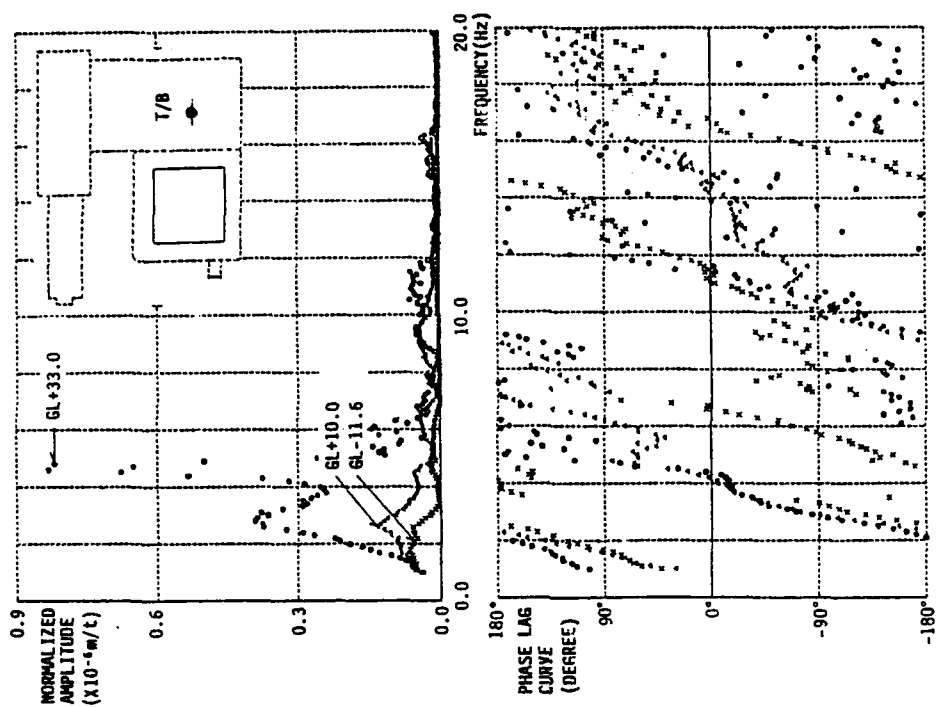
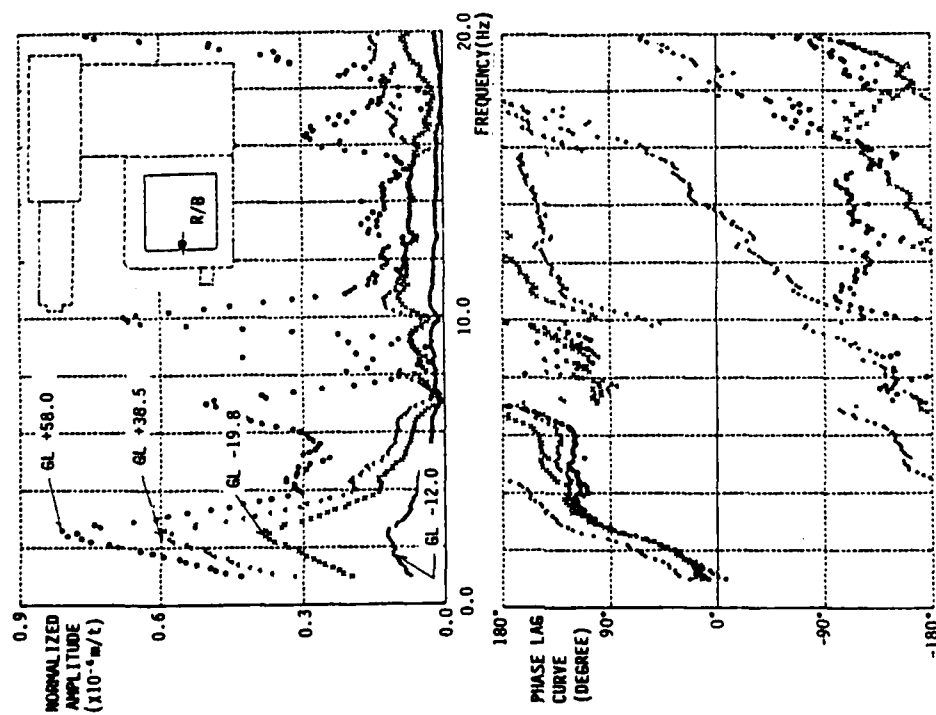
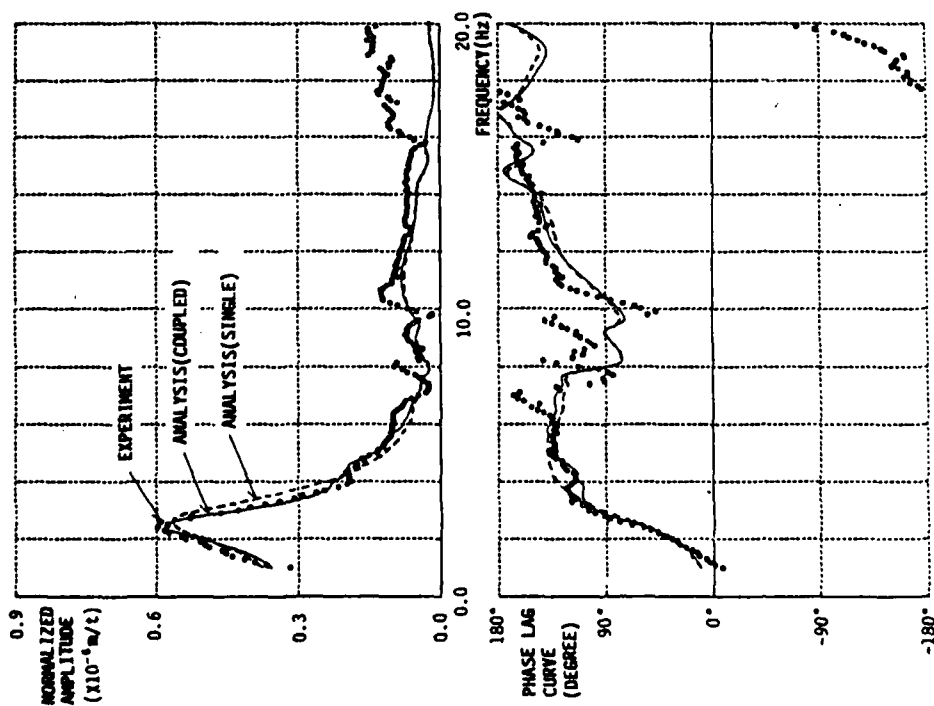
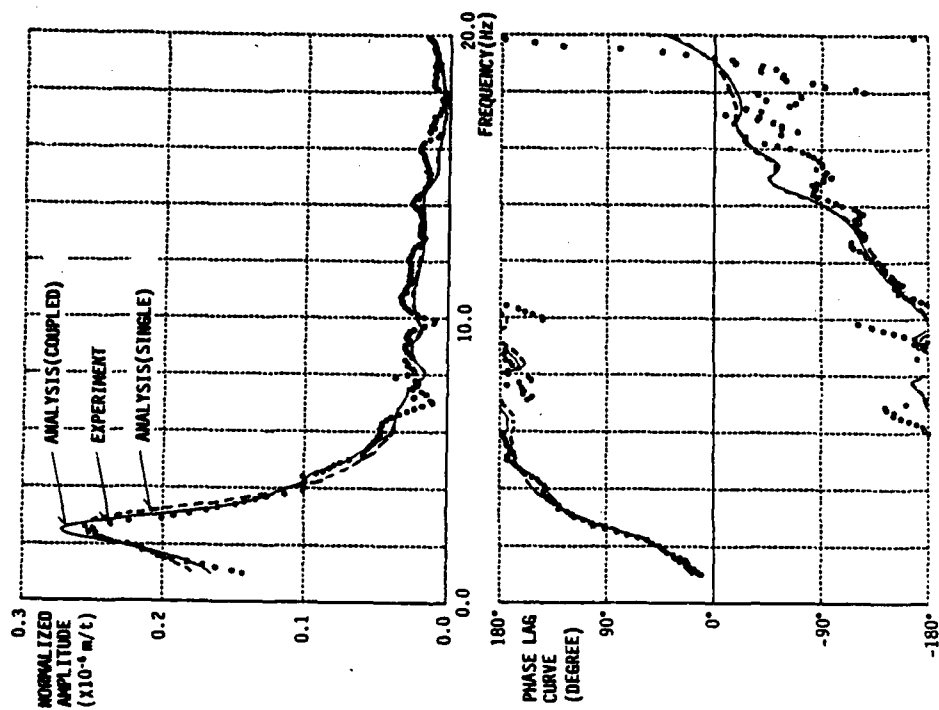


Fig.2-7 Test Results

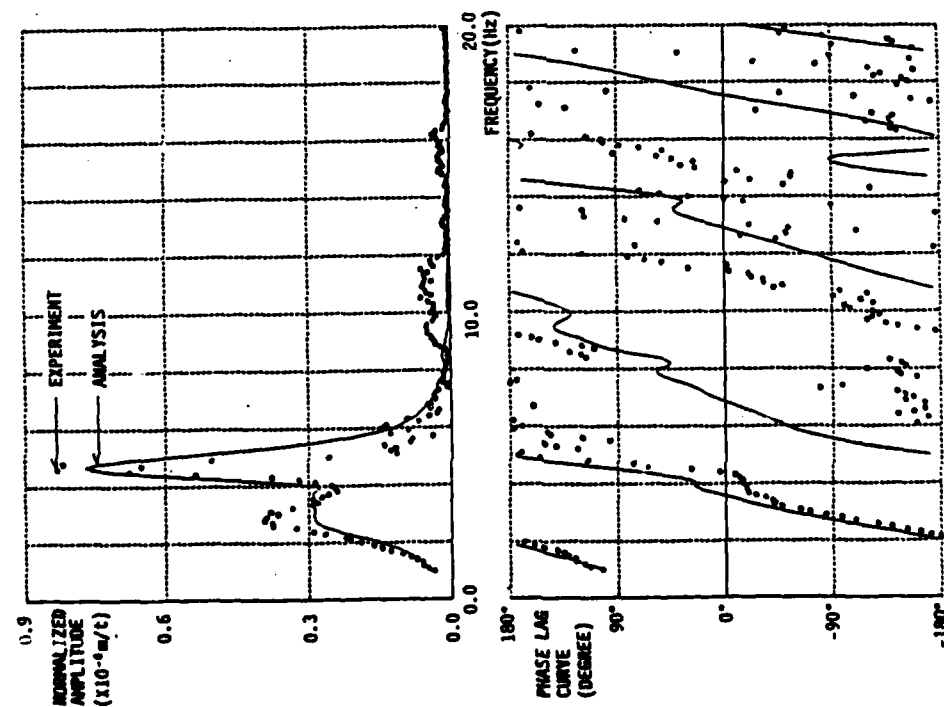


RESULT OF SIMULATION ANALYSIS  
FOR THE REFUELING FLOOR (GL 38.5m) OF R/B

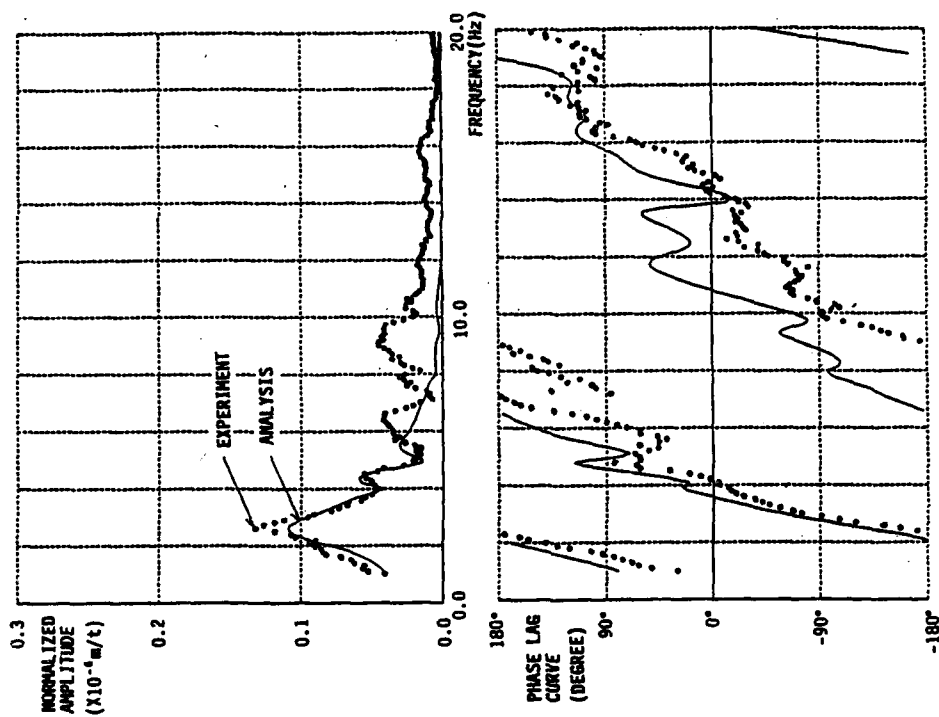


RESULT OF SIMULATION ANALYSIS  
FOR THE 2ND FLOOR (GL 6.0m) OF R/B

Fig.2-8 Result of Simulation Analysis

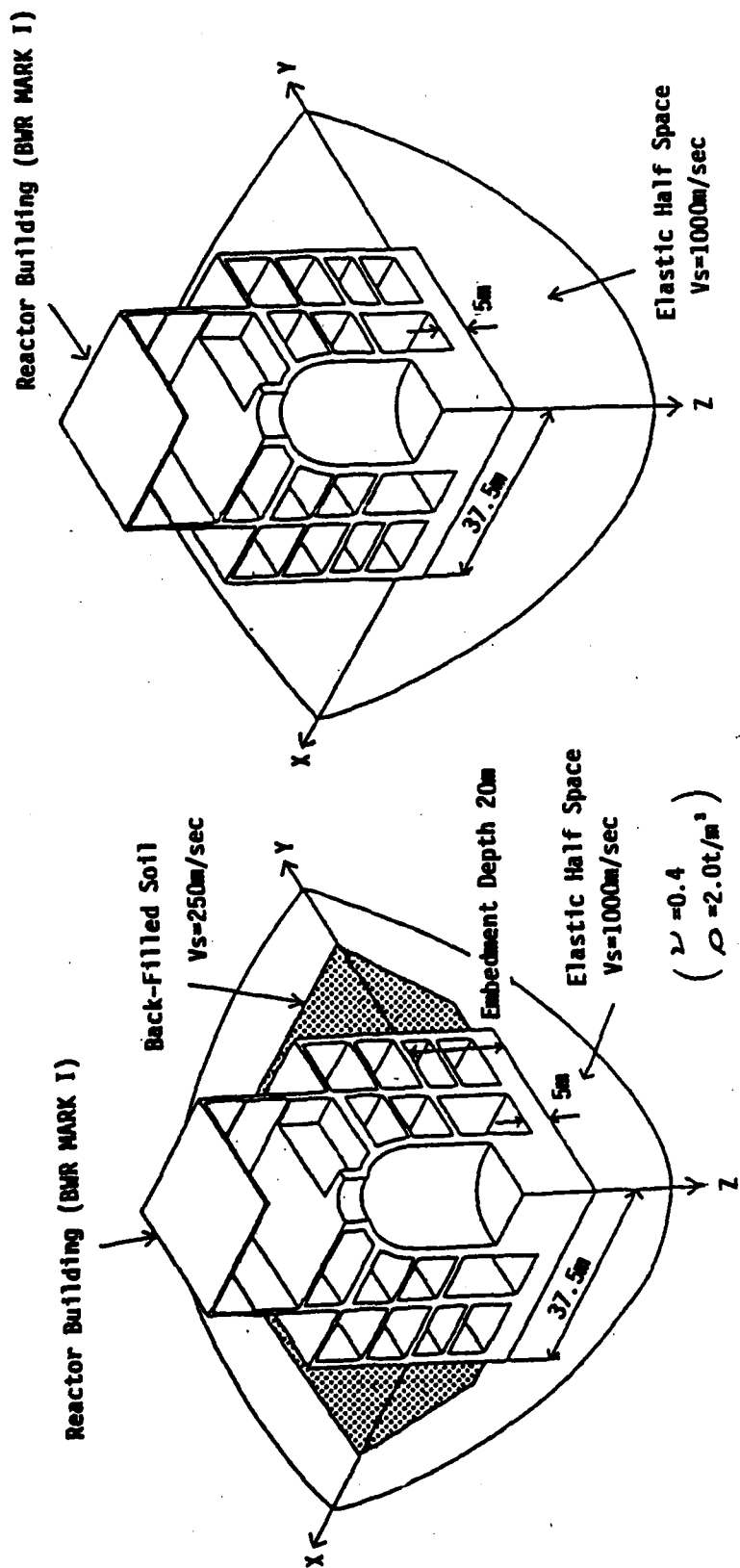


RESULT OF SIMULATION ANALYSIS  
FOR THE ROOF (GL 33.0m) OF T/8



RESULT OF SIMULATION ANALYSIS  
FOR THE 2ND FLOOR (GL 10.0m) OF T/8

Fig.2-9 Result of Simulation Analysis



(a) Case 1

(b) Case 2

Fig.3-1 Reactor Building for Analysis



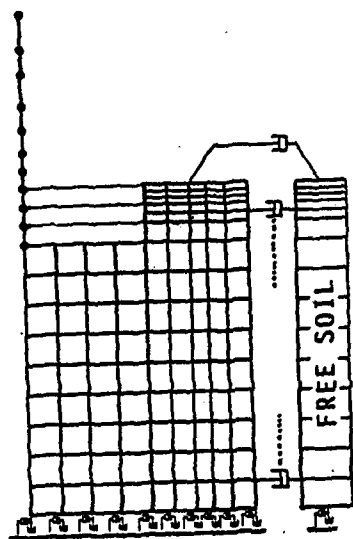


Fig. 4-1 FEM Model

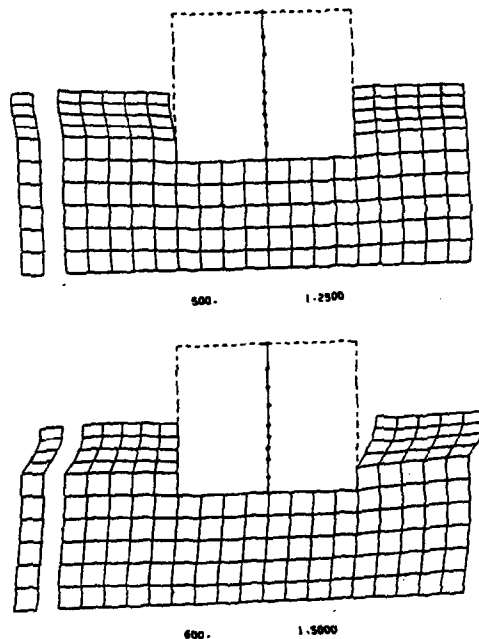


Fig. 4-2 Snapshot of Separation Analysis

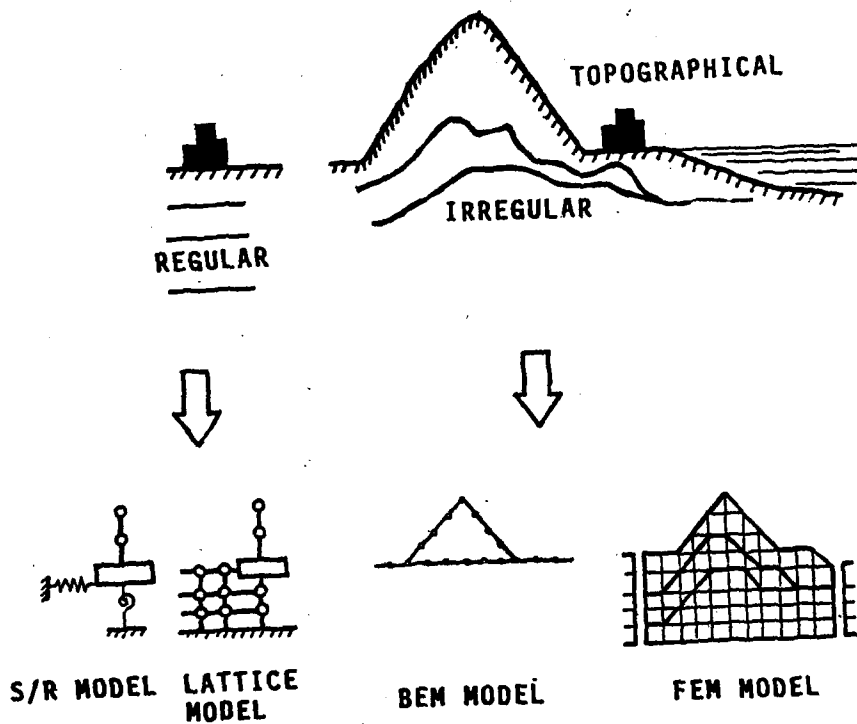


Fig. 4-3 Dynamic Analysis According to Site Condition

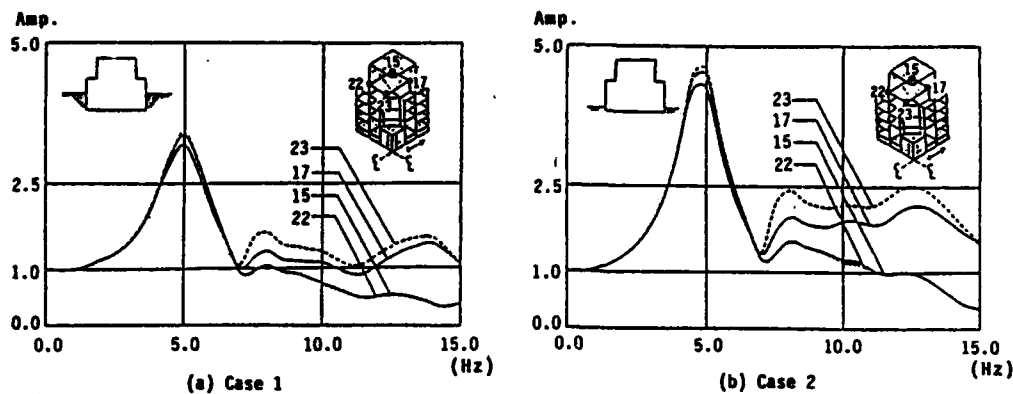


Fig.3-2 Acceleration Transfer Function of Main Points  
at the Refueling Floor to Free Field Surface

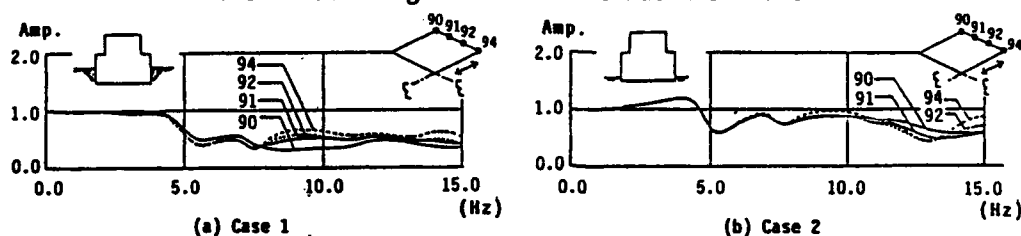


Fig.3-3 Acceleration Transfer Function of Main Points  
at the Basement to Free Field Surface

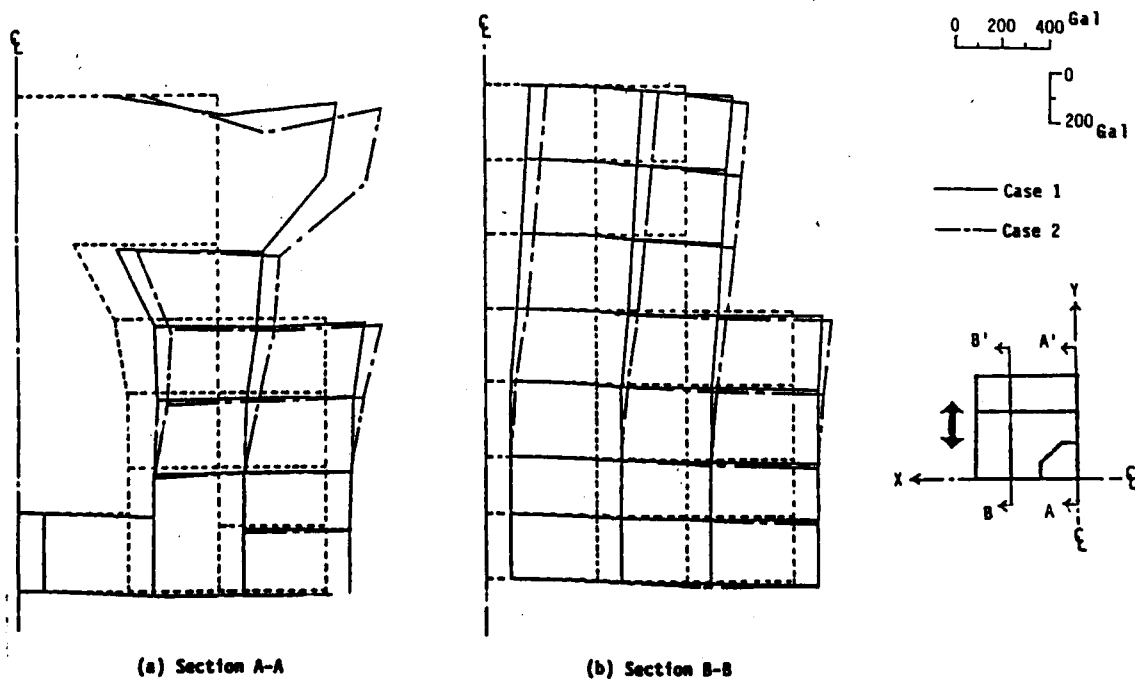


Fig.3-4 Maximum Acceleration Distribution in Vertical Section

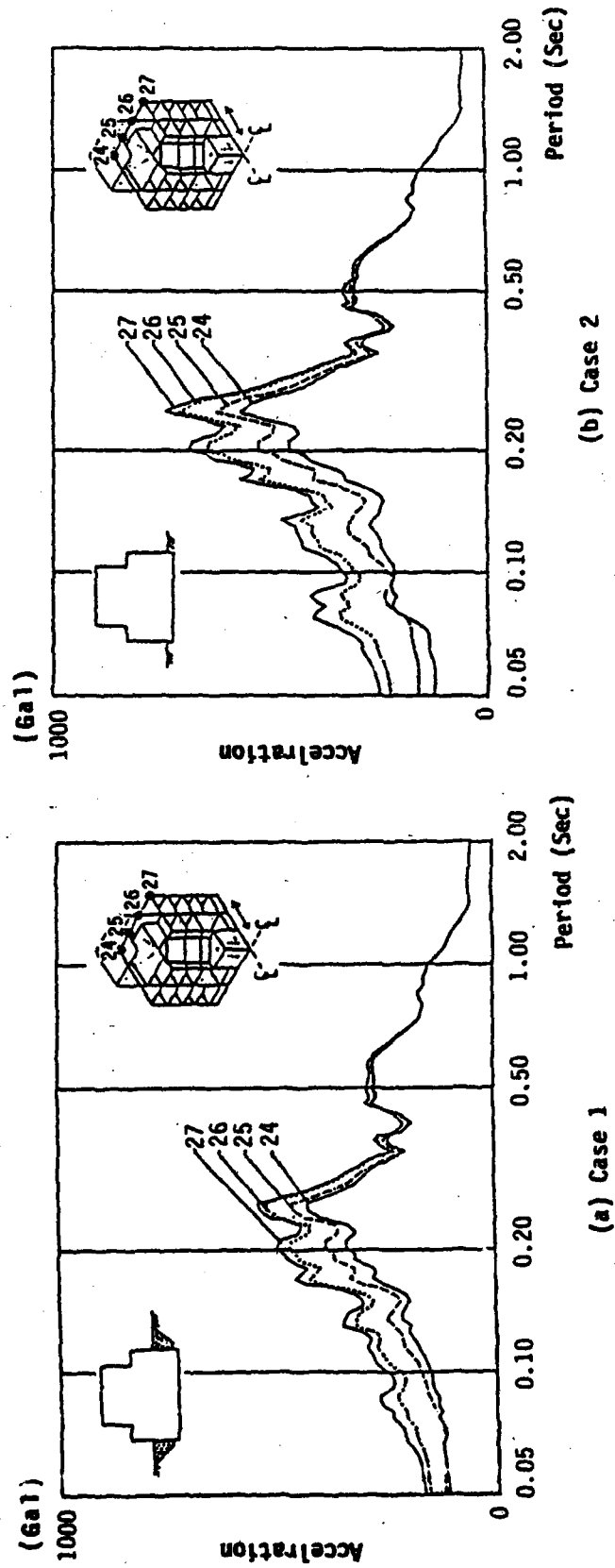


Fig.3-5 Acceleration Response Spectra at Some Points of the 5th Floor  
(FL.33m, Damping=0.05)



**TURKISH NATIONAL COMMITTEE FOR  
EARTHQUAKE ENGINEERING**

**THIRTEENTH REGIONAL SEMINAR ON EARTHQUAKE ENGINEERING**

**September 14-24, 1987 - Istanbul - Turkey**

**Eng. Emil-Sever Georgescu**

**Structural Engineer  
Scientific Researcher**

**Earthquake Engineering and Structural Dynamics Division  
INCERC, Bucharest, ROMANIA**

MINISTRY OF INDUSTRIAL CONSTRUCTION  
CENTRAL INSTITUTE FOR RESEARCH, DESIGN AND GUIDANCE IN  
CIVIL ENGINEERING - ICCPDC  
BUILDING RESEARCH INSTITUTE  
INCERC

THE EXPERIENCE AND EXISTING PREMISES FOR AN EFFICIENT  
RESPONSE IN CASE OF EARTHQUAKE UNDER THE CONDITIONS  
OF SEISMIC ZONES IN ROMANIA

Eng. Emil-Sever Georgescu  
Structural Engineer  
Scientific Researcher  
Earthquake Engineering and Structural Dynamics Division  
INCERC, Bucharest, ROMANIA

Paper prepared for the Session 8 of the 13th Regional  
Seminar of Earthquake Engineering organized by the Turkish  
National Committee on Earthquake Engineering

14 - 24 September 1987  
Istanbul - ATAKÖY  
TURKEY

THE EXPERIENCE AND EXISTING PREMISES FOR AN EFFICIENT  
RESPONSE IN CASE OF EARTHQUAKE UNDER THE CONDITIONS  
OF SEISMIC ZONES IN ROMANIA

Eng. Emil-Sever Georgescu x)

ABSTRACT

The paper deals with the following aspects:

- the meaning of the "aseismic protection" notion in a wide and complex meaning in the frame of UNDRO terminology (1979) used in the study on seismic risk;
- the notion "earthquake response" with reference to the previous earthquakes experienced in our country and in the world;
- the present situation of legislation, codes and undergone actions well-known in the world, concerning the efficient society response in case of earthquakes and the experience gained in our country from the previous earthquakes;
- the use of seismic prediction for planning the earthquake response;
- seismic hazard and risk factors under the conditions of seismic zones in our country;
- elements subjected to seismic risk in our country in urban and rural areas (constructions, population, vital social and economical function, life-lines a.s.o.);
- aseismic design recommendations, the assessment of existing buildings, aseismic resistance and of the strengthening-repairing works in our country;
- legislation concerning the post-seismic emergency intervention and aspects of pre-seismic planning under the seismic conditions of our country;
- the nature and type of aseismic preparedness and protection operations and the required intervention actions in case of earthquake in our country and the existing premises in the field;
- conclusions on the required research programme with a view to take efficient measures in the frame of the integrated national programme for protection, aseismic preparedness and interventions in case of earthquakes in our country.

1. THE ASEISMIC PROTECTION

Romania is encountered among the countries with a severe seismicity, especially in the Vrancea zone. The aseismic protection of buildings has been applied for 40 years and during this time the Romanian seismology and earthquake engineering has gained experience and gathered scientific data.

In a broader sense the aseismic protection means the enlargement of classical seismological and earthquake engineering fields. Thus, besides the aseismic design protection, efficient measures should be provided in order to avoid the

negative effects of earthquakes for the whole society that represent a system with interconnected components. As the age and resistance of components are variable it has been taken into account that even the temporary components out of function due to the earthquake could lead (even with no physical damages noticeable in all fields) to a disorder in the functioning of the society assembly, with a lot of social, economic and cultural losses. In this context, the aseismic protection of a new objective is a construction described by the regulations in force.

The meaning of the term "Complex protection" refers to the state-of-the-art of the existent system and consequently the anticipation of the vulnerable points of the social and economic system as compared with the seismic action and the early drawing up of all the necessary correction measures. Legal and specialized recommendations for this matter have been drawn up only in several countries. The purpose of this preparedness is to avoid and considerably reduce the disastrous losses and disturbances providing an efficient social reply in case of earthquakes.

The UNDRO terminology (1979) is given below in order to use a unitary language; several developments and new specifications drawn-up in the frame of the Balkanic Project RER/79/014 are used too.

The Seismic Hazard represents the expected succession in a probabilistic sense, for a specific time period, of the seismic actions of certain intensities; the seismic hazard depends not only upon the characteristics of the source but also upon the ground conditions of the analysed zone. The seismic hazard maps shows the zones and the probabilities for the return periods.

The Seismic Vulnerability shows the anticipated distribution of noticeable physical seismic damages underwent by a type of structure due to a seismic incident action, conditioned by the intensity of the seismic action; the seismic vulnerability represents an intrinsic characteristic of a certain type of structure as compared with the seismic action; the loss degree is represented on a scale from / 0 (no loss) up to 1 (total loss).

The Specific Risk represents the anticipated distribution of seismic damages underwent by a certain type of structure due to the succession of the expected seismic actions for a determined period of time when the structure is permanently exposed to seismic hazard and depending upon the hazard and vulnerability.

The Elements at Risk (Exposed to Risk) represents the material and cultural values, as well as the human activities, that could be affected (disturbed, damaged) by the earthquake or by the seismic damages of a certain structure. They are characterized by the seismic exposure degree and by the distribution of anticipated losses, conditioned by the degree of the possible damage of the structure under consideration (constructions, population, social, economical and cultural activities exposed to risk in a given zone).

The Seismic Risk represents the anticipated distribution of losses of various kinds with reference to people, the ma-

terial and cultural values as well as the human activities, taking into account the exposure degree of elements at risk for a determined time period. The risk is got by the convolution of hazard, vulnerability and elements at risk.

"Disaster" is a nonstandardized term that is used both for natural phenomena and for serious accidents and their consequences. This explanation refers to the earthquakes because the causes and destructive effects occur almost simultaneously so that people call them the same term even if the situation changed during the last decades at the same time with the evolution of the aseismic protection measures.

There are indeed natural phenomena, even strong motions, that do not cause disasters if the zone struck by the earthquake is unbuild and uninhabited or if the zone is inhabited but efficient aseismic protection measures are going to be applied. That is why the present tendency is to call disaster the severe effects of some natural phenomena (including earthquakes) only if these lead to massive life losses, to destroyed localities, to disturbances of social, economic and cultural life, to serious secondary effects a.s.o.

Using the UNDR0 terminology, the seismic hazard cannot be reduced but the vulnerability of structures and endowments the exposure degree of elements at risk, the specific risk and the seismic risk could be reduced all these referring to the anticipated total losses, in order to avoid disasters.

## 2. THE EARTHQUAKE PREPAREDNESS

### 2.1. The Evolution of Concerns

The social, economical and cultural development of the human society in a seismic zone gradually leads to an increased number of constructions, endowments, settlements and activities performed on this territory.

Their vulnerability depends upon the knowledge degree of the zone seismic hazard and the real aseismic protection measures for each element apart exposed to risk and for their assembly according to the social and economical policy of the country. The experience of previous earthquakes occurred in the 20th century underlined a number of anticipating preparedness requirements for an efficient response to earthquake.

As a result of the previous earthquakes the following examples of concerns are given below:

- 1906 - San Francisco, USA - the aseismic design protection, lifelines protection (for preventing the fire, for running water, for the gas and electricity system and for the communication systems a.s.o.);
- 1923 - Kanto, Japan - fire protection for the wooden buildings in urban zones;
- 1933 - Long Beach, California, USA - the specific aseismic protection of school buildings;
- 1964 - Alaska, USA - the necessity of organizations for postseismic intervention, of an anticipated specialized preparedness, of the site conditions study;
- 1964 - Niigata, Japan - showed the danger of placing the oil storage tanks in the neighbourhood of a big town and the consequences of neglecting the local ground conditions (liquefaction);



- 1971 - San Fernando - USA- underlined the vulnerability of hospital buildings. In California a new legislation concerning the disaster prevention measures in case of earthquakes was adopted;

- 1972 - Managua, Nicaragua - underlined the possible disaster effect in a town without lifelines and adequate emergency endowment where no aseismic urban measures were taken;

- 1975 - Haicheng, China - the first earthquake scientifically predicted on a long, medium, short and imminent term, with attentively prepared evacuation measures and a massive reduction of human life losses and partially of economical losses;

- 1976 - Tansan, China - showed the catastrophic effect of an underestimation of the territory seismicity of the lack of seismic urban measures and the importance of the scientific prediction/6/;

- 1977 - Vrancea, Romania - shows the difference between the serious damage of nonaseismic designed old, high, urban buildings and the good behaviour of buildings designed according to the recent recommendations, especially precast buildings;

- underlined the necessity of instrumental seismic recordings;

- proved the importance of social, economic and human resources for the rehabilitation after the earthquake, under the state control in an adequate time period;

- studies performed on the seismic vulnerability and aseismic protection in a broader sense in our country, too.

1978 - Japan - "Law on the large scale countermeasures in case of earthquakes" were adopted; a seismological temporal evolution and earthquake preparedness in Tokai zone was established/7/, based on the hypothesis of a scientific prediction publicly announced.

1976-1981 - Italy and Greece initiate governmental organizations for the earthquake intervention preparedness, prevention of seismic losses, aseismic education, seismic prediction studies a.s.o.

1983 - Erzurum, Turkey - urgent measures for a temporal lodging of inhabitants in rural zones destroyed by the earthquake. Within one year the zone is rebuilt with modern structures. Aseismic education measures were taken by video cassettes, publications, seminars /8/.

1986 - moderate-severe earthquakes in Vrancea zones, Romania and Veliko-Tirnov, Bulgaria.

During the period September-December 1986, the negative effect of the lack of education and technical and scientific information about earthquakes influenced the psychology of the most sensitive inhabitants.

Generally as a result of the foregoing facts it has been noticed an upward evolution of the people's concern, at present, the aseismic protection as compared with the earthquake effects, has a complex and direct character and is proportional to the number and character of the elements at risk, respectively proportional to the social and economical developing level of the respective countries.

## 2.2. Legislations, codes and experience

The synthetic situation on a world scale is as follows:

Japan: there is a complex legislation for prevention and control measures of the disastrous effects of natural phenomena and accidents, including also those for the earthquakes, occurred in 1961 and applied and controlled by the government. Since 1978 the provisions of a special law for the earthquake preparedness have been applied for the Tokai zone for an earthquake with  $M=8$  that is expected to be publicly predicted and announced in due time, according to the continuous instrumental recordings.

All over the country each year on the 1st of September exercises for the disaster prevention are performed, especially in big cities and the intensified observations zones. Yearly 2.8 billion dollars are allotted for the preparation of earthquake countermeasures /7/.

China: there are legislations and state organisms that regulate the disaster prevention, including the seismic ones. Officially, the use of seismic prediction is considered as an efficient method to avoid or reduce losses, although the general application is not yet possible.

USA: there is the federal legislation concerning the prevention and avoidance of disasters. In California State specific laws and measures have been applied and legislated for earthquakes. For a local usage there is a relative independence with respect to the character and wide application of such measures. Engineering studies have been performed for the estimation of seismic risk for several urban cities such as Los Angeles and San Francisco /9/.

Greece: earthquake protection and preparedness are controlled by the governmental organizations - EPPO (1983) with wide coordination research tasks.

Italy: Ministry for the Coordination of Civil Protection that cooperate with the regional and local organizations in performing the analysis of the vulnerability of towns with old building stock and the intervention in case of earthquake (1976-1980).

France: the planning for the disaster prevention is organized through the ORSEC plan that stipulates the conjugated intervention of all technical and social organizations and ministries involved in case of natural disaster or public accidents /3/.

Turkey: the intervention disaster works are organized by the civil, central, military and local governmental organizations and technical and social organizations and ministries. The earthquake represents one of the frequent intervention field /10/.

USSR: aseismic protection is achieved first by a compulsory application of the seismic design code for buildings, of the code construction provisions drawn-up under the state scientific control. The seismic zoning map of 1981 has a probabilistic meaning. Prediction seismic studies were performed in many active zones. When major post-seismic effects occurred the specialized state organizations applied rapid and efficient measures.

Romania: the aseismic protection is compulsory applied in the building design based on a periodically revised codes. The construction works are performed by the state enterprises

under a specialized technical control. To remove the March 4th 1977 earthquake effects, a rapid and efficient intervention was initiated for the saving, recovery, repairing and strengthening works of vulnerable buildings, built before 1940. There is a legislation concerning the central and local organization for the intervention in case of natural disasters and experience concerning the repairing, strengthening and reconstruction works after the earthquake. The continuous development of high technology, industries and society imposes the enlarging of the directions for improving the earthquake preparedness in all field losses could appear.

x x  
x

In many other countries on a world scale the earthquake response is regulated by the civil protection law or by the general legislation concerning disasters. It has been established that it is not only the legislation or the organizing schemes that condition the response efficiency, but the way the practical cooperation between the involved local and central authorities is achieved, the ratio between the existing sources and those effectively applied, the social and economical conditions of the destroyed country, the dimension of zones subjected to risk, the general level of understanding the earthquake engineering problems by the citizens, authorities, technical staff, the severe authorized and specialized control and the rapidity of intervention works a.s.o. /3/.

### 3. GENERAL SEISMIC RISK AND HAZARD FACTORS FOR THE ROMANIAN TERRITORY

#### 3.1. Seismic Hazard

For the Romanian territory the most important seismic source is Vrancea zone placed at the curvature of the Carpathians Mountains. The earthquakes occur at an intermediate depth of 100 ... 150 km with medium magnitudes  $M=7$  Richter, 2-3 times a century. The strongest earthquakes with  $M=7$  causes seismic motions with VII-VIII MSK intensities on almost half of the country territory. Other local or external sources of the territory generates VII-VIII MSK intensities less often than once a century.

The spectral composition underlined by INCERC recording of the March 4th, 1977 earthquake with  $M=7.2$ , shows relatively long predominant periods (over 1 sec.) especially in zones with thick sedimentary layers affected by the intermediate earthquakes.

The recordings of August 31st 1986 Vrancea earthquake ( $M=6.8$ ) showed the relative short oscillations predominant period (0.2 ... 0.5 s) /21/.

The known elements concerning the historic periodicity of earthquakes on the territory are not synthesized on a seismic hazard map in a probabilistic way required for the evaluation of convolution in the risk analysis.

#### 3.2. Seismic Risk

The seismic events that caused human and material losses occurred in 1940 and 1977. In 1940 almost 500 life losses

were recorded. In 1977, 1570 people were killed; 11.300 injured people, 32.900 damaged and collapsed buildings, the total economic losses value was 2 billion dollars /12/.

In 1940 only one, fourteen storey reinforced concrete building collapsed in Bucharest, on the other hand, in the epicentral zone and the rest of the country many low buildings were destroyed.

In 1977 28 buildings collapsed in Bucharest (all buildings built before 1940). All these were 6-12 storied buildings with vertical reinforced concrete, masonry elements and beams that were not frame joints. Almost 400 hundred buildings in Bucharest were included in this category (buildings damaged in 1940 and inadequately checked after the earthquake). It has been established the character of the strong motion effects combined with the ageing, corrosion and over-stressing effects etc./12/.

From the buildings designed and built according to the aseismic design codes drawn-up between 1950-1977, three partial collapses were recorded and others damaged due to the fact that the design seismic forces and the spectral coefficient included in that codes were very much different from the real requirements underlined by March 4th 1977 earthquake recording. Nevertheless, the damage ratio underlines the positive role of the aseismic design. The high-rise frame structures were much more damaged, and out of the high bearing wall structures almost 30% were damaged and only two cases of partial collapse were recorded. The cost of the repairing and strengthening works was very high increasing the value of the direct losses.

### 3.3. The Seismic Prediction For The Future Activity Of The Vrancea Earthquake

The Vrancea seismic focus is persistent and isolated, and although there is not a full agreement between the researchers, it has been considered that a subduction process may be present in the zone /12/.

Enescu, Mărza and Zamărcă (1974) showed that there is a regular random scheme for the occurrence of Vrancea earthquakes consisting in three peaks of seismic activity in each century. The maximum values occur at the years of 1-10, 30-42 and 70-90 each century. The conclusion proves that an earthquake will be possible to occur with  $L = VIII-IX$  between 1978-1990 (in fact the event occurred in 1977) and similar events may be expected between  $2004 \pm 4$  years and again in  $2040 \pm 5$  years /17,20/. Other studies were performed concerning the long time prediction of Vrancea earthquakes. After 1977, Mărza showed for the first time *a posteriori*, six types of seismic quiescence schemes (seismic gaps) that preceded Vrancea earthquakes with  $M > 5$ .

The seismic event of August 31st, 1986, although occurred at the usual time interval of earthquakes with  $M \approx 7$ , does not change the occurrence periodicity of strong motions similar to the March 4th 1977 Vrancea earthquake. The time interval left (that has to be appreciated in a probabilistic sense) till the future strong motion round the year 2000, must be used for taking measures for the preparedness seismic response.

Meanwhile the developing seismology research on the short

term and imminent earthquake prediction could lead to valid results for Vrancea zone, too.

Supposing that this event could occur in the near future and that the scientific and instrumental basis could exist for the prognosis of a future seismic event, the lack of information and society preparedness would probably be a source of social and economical negative effects, if sometimes news about a coming event spread over a human community from unknown sources.

That is why the prediction research must be rationally used at this stage, first of all to space out usefully the preparedness measures by informing the population, the specialists and administrative personnel about the scientific progress in the field and about the probabilistic limitations of this matter. As a conclusion, the seismic prediction elements known up to now justify the complex aseismic protection measures for removing the main risk factors till the future Vrancea strong motion.

#### 3.4. The Elements At Seismic Risk In Urban And Rural Zones In Romania

Romania has a population of 22.6 million inhabitants, a surface of 237.500 km<sup>2</sup> and is administratively organized in 40 counties and the Municipality of Bucharest. After a brief analysis of the seismic zoning map, only in six counties the expected intensities do not exceed the seismic degree of VI MSK, the other 34 counties and the Municipality of Bucharest could be struck by VII-IX MSK intensities. Generally, 50% of the territory is struck by Vrancea earthquakes; in that zone there are localities with various social and economical activities that potentially may suffer the negative effects of an earthquake. These effects could occur due to the violence of the seismic motion, to the existence of old non-aseismically designed buildings or buildings built according to the codes based on former, reduced code seismic forces.

With respect to provide the general complex aseismic protection, a full analysis should be performed on the number and resistance characteristics of the social and economical elements subjected to seismic risk in the foregoing zones. This is a huge and long time work and requires a lot of information and computation data and sometimes because of lack of data, it requires only general estimations. This paper presents only a few data that have been published and that underlines the need of detailed evaluations for various fields. According to the data included in the statistical annual book /13/ the following can be stated:

- a number of 23 counties and the Municipality of Bucharest, most of them placed in VII-IX MSK intensity zones, comprises 70% of the total fixed funds (endowments) of the social-economical units all over the country, that achieve 69% of the industrial production of the country. Almost all kinds of industries are represented there;

- in neighborhood of Vrancea seismogenetic zone, the density of the inhabitants is 1.5-2 times higher than the average for the whole country; 59% of the whole country population live in seismic zones;

- twenty-nine towns (with more than 10,000 inhabitants)

and the city of Bucharest are placed in VII<sup>1/2</sup> - IX MSK degree intensity zones, including three out of six big towns of the country with 200-300 thousand inhabitants, 10 county capitals and Bucharest, the capital of the country. These 30 towns include 38.53% of the urban population of the country or 18.98% of the whole population. Moreover, 58 towns out of which 13 are county capitals (26.11% of the urban population or 12.86% of the whole country population, namely almost 3 million inhabitants) are located in VII MSK seismic intensity zones.

In all, 51.46% of towns with more than 10,000 inhabitants are placed in VII-IX seismic intensity zones and comprises 64.65% of the urban population or 31.87% of the whole country population.

- the building stock comprises both structures built before 1940 (November 10th, 1940 Vrancea earthquake led to the use of the first official temporary aseismic design code) and relatively new industrial, agrozootechnical, roads, bridges, dams constructions as well as residential buildings and special works, all of them aseismically designed according to the aseismic design codes in force during their construction. The detailed analysis will point evident other characteristics, too.

In general, the big and historical cities are endowed with residential, social and public and economic building stock that is older and more vulnerable at seismic motions.

Noteworthy is the fact that during the period 1951-1983 more than 9 million buildings were built in the country, out of which 2.2 million in the rural areas. The previous earthquake did not cause disastrous effects in rural areas. Other elements subjected to seismic risk must be similarly analyzed taking into account the following specifications:

- the agricultural system is industrialized, provided with an irrigation system, silos, agricultural machine stations, zootechnical halls that were vulnerable at earthquakes in certain cases. To avoid large disturbances in the agricultural and zootechnical production their construction of all types should be tested and aseismically protected, according to the norms in force;

- the commerce and the producing cooperative system are endowed with older vulnerable buildings that due to their damage can stop the supply with goods that are necessary for the emergency stage;

- schools should be specifically analysed both with respect to the aseismic protection of students and to the fact that only through schools the aseismic education of people concerning the behaviour and natural reaction of citizens could be performed;

- hospitals are the first to be analysed in order to be kept in operation during an earthquake and to support the rehabilitation efforts.

The 24 counties that are located in areas with a very severe seismicity are endowed with almost 133 thousands of hospitals beds. These hospital units will be used for emergency medical assistance after an earthquake whenever necessary, but nevertheless, their buildings should be thoroughly tested and provided with independent running water pipes, power station and drugs.

- the cultural and art institutions, the mass media, means should be analysed and protected and kept in proper operation conditions and used after the earthquake at the psychological rehabilitation of the inhabitants and for their proper information;

- very important networks (lifelines) are numerous in the seismic zones of the country.

Magistral power lines railways and very important national roads, highways, some of them being unique, are passing through the Vrancea epicentral zone.

The vulnerability of the lifelines is caused by their weakest point, for example the damage of a bridge could stop the whole undamaged road network when there is no other round about road and consequently the goods and food supply in that zone is stopped. In this respect the critical points of the detailed analysis should be considered with reference to: power stations, power transformer stations, pumping stations, road bridges and railway bridges, telephone exchange and radio transmissions, roundhouses and sheds, and large garages, etc. Under the conditions of automation and the use of electronic systems in the national economy, the protection of new computation systems and processing computers represents a new field of concerns.

The immediate intervention systems - ambulance, firemen brigade, guards, order, recovery, demolishing and urgent strengthening works, the road traffic control - should be analysed and kept in proper operation conditions after the main seismic motion in any season, day or night and having available independent food supplies (water, electricity, communications, and victuals a.s.o.).

The military units and other military and civil organizations, that have specific functions in case of disasters should analyse and organize their work priorly according to special criteria.

#### 4. LEGISLATION, CODES AND PROPOSALS CONCERNING THE ASEISMIC PROTECTION AND EFFICIENT EARTHQUAKE PREPAREDNESS IN ROMANIA

##### 4.1. The experience of March 4th 1977 earthquake

As a consequence of the 1970 and 1975 floods there was an experience of natural disaster, in Romania in 1977, concerning the mustering of all technical, economical and administrative resources, ambulance service and supports given to the victims of disaster, rehabilitation of a locality a.s.o. Naturally, the seismic effects have their own character, and in 1977 the main specific element was the damages in several big towns (Bucharest, Craiova, Ploiesti, Iasi) where the old building stock was richly represented. The postearthquake intervention was very well coordinated at the central and local level, joining all available forces (very often volunteers), the repairing of the damaged zones being very fast done as compared with the international experience. The necessity state was declared by a presidential decree on March 4th, 1977. During the following week the political and governmental organizations joined for meeting every day; the President of Romania, Comrade Nicolae Ceausescu, visited daily the places of the collapsed buildings where people tried to

rescue the victims from under the debris, and efficient measures were taken for providing shelter, food and support to the victims of the earthquakes. On March 8th the schools and universities started their activity again and was published the decision of the Communist Party and Government concerning the ways of financial and material support (money, goods, clothes, new permanent dwellings) for the victims of the disaster. On March 10th, the necessity state ceased on the Romanian territory and on March 15th it ceased in Bucharest, too.

The rescuing operations from under the debris though very fast, continued till all victims were found; in Bucharest many persons were rescued alive from under the debris after considerably long time intervals such as a six year old girl who was rescued after 62 hours, a 22 year old woman after 128 hours, an old woman after 188 hours and a 19 year old boy after 251 hours from under the debris in a basement.

In Bucharest the strengthening and repairing works for the first urgency lasted for 2-3 months and the modern reconstruction of the Zimnicea town center, 80% destroyed, needed several months for building precast structures.

Under these conditions experience was gained on the strengthening and repairing works of various type of structures with reference to the intervention in case of earthquake, to the temporary lodging of the disaster victims etc. The 1977 intervention experience was specifically introduced in the legislation of 1977 and 1978.

#### 4.2. Juridical Framework And The Codes In Force After 1977

The aseismic protection of new buildings has been provided for the last 40 years by the aseismic design, execution and in service survey according to laws and standard codes and technical institutions under the control of the State organizations. Law nr.8/1977 refers to the providing of the in service safety, the operation and quality of structures and Code P.100/1981 concerns the aseismic design of residential buildings, social and cultural, agrozootechnical and industrial constructions/14/. The seismic zoning in force (STAS 11100/1/1977) takes into account the intensity of 1977 earthquake and the historical data for a period of about 500 years.

The preparedness and execution of earthquake intervention are established by the Law of Civil Defense (1976) with additions included in Decree 430/1978 of the State Council, concerning several measures for the civil defense and further on detailed by the Decree of the State Council no.140/1978 concerning the organizing activities for the preparedness, limitation and removing of the large proportion disaster/14/.

According to the Constitution of the Socialist Republic of Romania in such cases a decree is to be proclaimed and declared the "necessity state", in the afflicted area as it was done in 1977.

The suggested measures refer both to the preparedness actions (the inventory and providing the intervention equipment and supply with whatever is necessary for that possible intervention) and the real intervention actions for life rescuing rehabilitation, urgent supplies, providing the operation of the lifelines of public importance, medical assis-



tance for the disaster victims etc. /14/.

This system of juridic regulations stipulates obligations and specific actions for the state, civil, military and community organizations under the leadership of the Defense Council of the SRR and respectively of the guidance of local defense councils and of the ministries, enterprises and institutions on the afflicted territory.

#### 4.3. Character And Nature Of The Preparedness, Aseismic Protection And Intervention Actions In Case Of Earthquakes Considered Necessary In Romania

Based on the experience gained in our country in 1977 and on the information got on a world scale, a list of logical successive operations may be drawn up with a view to assess the level of the seismic risk and to work out measures for an efficient response at a future earthquake. Practically speaking, for some of these there is not enough experience, methods and data, so that the priority research requirements must be mentioned for each intervention action apart /2,3,4, 19/:

##### Preparatory and organizing actions

- it has to be established the dimension of the zone under analysis (county, part of the county, town, rural zone - economic, industrial area, agricultural and industrial zone.);

- a task group has to be organized consisting in seismologists, geologists, structural designers, earthquake engineering researchers, university staff, central and local administration staff, representatives of the industries and other activities specific in that zone, all of them will cooperate or work independently, according to the case.

##### Study and research actions

- the hypothesis of a seismic event, with a significant importance for the zone, is chosen (in specific cases 1-2 hypothesis could be chosen for additional seismic motions caused for various sources) assessing their return periods.  
Note: Up to the present moment such a study was performed for site studies for the nuclear power stations. To analyse sites for common structures, simplified methods could be used with a proper precision degree with no requirements for an additional number of data, difficult to be obtained at present;

- the basic seismic intensity is chosen, considering the transmission of seismic motion coming from the site source under medium ground conditions;

Note: for Vrancea earthquake there is the March 4th 1977 recording got at INCERC-Bucharest and almost 40 recordings of the August 31st 1986 earthquake. It is necessary to process these data for getting sets of artificial accelerograms and spectra for other sites etc. For preliminary estimations only intensities on the zoning map could be used;

- a method is to be established for analysing the influence of the general and local ground conditions with respect to the seismic intensities and to the characteristics of the site movement and the results are depicted on maps.

Note: this survey requires geological and local geotechnical data, drillings, site dynamic measurements, detailed calculation- etc. for which there is experience only from the studies on nuclear power stations. Simplified methods are required for being applied on the usual building sites.

- it has to be estimated what are the specific effects that may occur on the relief on the built or unbuilt area under the foregoing conditions and taking into account the existence of certain faults, grounds prone to liquefaction etc;

Note: during the preliminary stages the effects could be approximated based on the experience of the previous earthquakes in zones with similar ground conditions;

- a distribution of construction on zones is achieved according to intensity zones according to the type, age, state and several general resistance characteristics of the localities (zones taking into account aggravating or relieving factors;

Note: a checking list has to be worked out for the new constructions that can point out the selective groups of similar constructions, typified and eventually designed according to the same aseismic design code (e.g. editions 1963, 1970, 1978) existent in the zone;

- the aseismic resistance of existing structures is assessed as compared with the level required for the present codes;

Note: the action is very important. There are various Romanian assessing methods; INCERC has recently worked out a project of technical instructions for this matter with an unitary approach;

- for constructions designed according to the well-known codes, the computed level of the relative aseismic safety of constructions and endowments is assessed comparing the initial seismic coefficient with the real one stipulated by the codes for the seismic zone, type of structure and the respective importance degree;

Note: this method is suggested by INCERC and speaking about Romania it takes into account that the seismic zoning under went several changes in 1963 and 1977 and the seismic calculation code P.13/1963 was revised in 1970, and then was strongly influenced by the calculations following the March 4th 1977 earthquake for the editions P100/1978 and P100/1981, concerning the increase of the seismic coefficients and the changing of the  $\beta$  dynamic coefficient. This method is simply to be applied with a view to establish the priorities of a further detailed analysis;

- the long-term degradation or in service degradation levels can be assessed and the possible reductions of the initial level is applied;

Note: it is necessary to establish (according to the in-service behaviour analysis of various types of constructions in various surrounding environments) the ratio of this time degradation using graphs or coefficients.

- it has to be established for each area apart, with an expected intensity, the number of exposed elements (such as constructions) that could be damaged especially because of the relative safety level as compared with the codes in force and the exposed population;

Note: the correct evaluation would imply a convolution of the hazard, vulnerability and elements at risk, for which we do not have at the moment enough data;

- the number of damaging cases is a computation instrument that should be probabilistically analysed due to the

random character of the seismic motion. There is not a computation method yet, and the experience of the previous earthquakes is to be taken into account in proportion to the types of constructions and endowments;

- a similar assessment is to be performed on the safety level of the special important networks taking into account the critical points and it must be established the site and the necessary round roads (by-pass);

Note: Less information and computation methods are available in this field. Few recent studies belong to INCERC special lists, namely Dr. M. Sandi /22/.

- the possibility of a chain-occurrence of certain negative phenomena is possible in all fields of the social and economical life of the zone/surveyed localities and specific points are located;

Note: the experience of the previous earthquakes does not provide enough information for Romania but this does not exclude the analysis of the future possibilities starting from hypotheses proved as true by the experience of other countries;

- the structure distribution, physical condition of the endowment, of the intervention departments, have to be analysed in case of earthquake, and all these are compared with the intervention requirements as it is revealed by the analyses performed for each field apart and described at the foregoing paragraphs;

Note: when the information about the intervention requirements are not convincing or are no longer existent, the comparison will be performed with one or more hypotheses of possible effects under the specific conditions of the zone/or of the surveyed locality.

- an analysis is to be performed on the social-professional and age structure of the population in the zone /locality, the interaction with the damage and possible effects when earthquake occurs in the zone, the possible reaction and the need for people education and information for the following intervention stages in the zone or for the future seismic events;

Note: various hypotheses of seismic events will be taken into account e.g. a working day, a holiday, hot-cold season, day-night with the implications of the daily movement (running to and fro) to the urban localities (suttle work, commuters).

#### Planning and intervention works

- an inventory is done of the intervention works that can start immediately as well as of the studies and researches necessary to clear up certain aspects and the necessary funds and resources are evaluated;

- it has to be nominated the administrative organizations that are in charge according to the legal regulations in force and the coordinating authority;

- the necessary funds and resources are requested and introduced in the budget expense plan of the in-charge authorities;

- a plan including specific measures is to be worked out nominating persons in charge of various intervention actions for removing the hazard, the dangerous elements, the necessary studies and researches, and terms of accomplishments;

Note: this plan leads to the cooperation between specialists, research, design, building and administrative institutes and enterprises and requires important funds. The distribution and establishing of priorities is a task of high responsibility, as well as the accomplishing of measures within periods useful to the reduction of the seismic risk.

- the earthquake intervention plans are worked out (territorial and social-economical plans), starting with a steady state in the hypothesis of occurring a seismic event in the zone, till the measures for improving the situation are approved by the authorized organizations and are spread for accomplishment to the institutes involved and for information to other authorized administrative institutions and for the people's information. The plans must stick to the legislation concerning the avoidance of the effects of the natural disasters and they have to be correlated with the plans for the civil defense including them in the legal periodical actions and exercises as well as the activities of other attending organizations (Red Cross, Patriotic Guards, Civil Defense etc.).

Note: at present there are no detailed examples for such a plan although the March 4th 1977 earthquake experience may be easily transferred into the required operational documents (plans) with the legislation of this field as a general guide.

At the beginning, plans have to be worked out with a more general character, their detailing will follow the development of inventory studies of the elements at risk and their assessment as a consequence of the moderate earthquake effects that may occur during that period.

At the beginning it is very important to raise the interest of specialists, administrators, and the involved institutions by synthetic and clear reports about the state-of-the-art, with examples from their own experience and from the international one.

## 5. CONCLUSIONS

### 5.1. Premises For The Practical Implementation Of The Suggested Operations For An Efficient Response At Earthquake

The results got from the previous chapters are as follows: follows:

- the specific seismicity of the Vrancea zone is characterized by periodical events according to the already known statistical regularities;

- following the example of USSR and Bulgaria etc., it is necessary that the present data concerning the seismicity of the country should be compiled in the form of the seismic hazard maps in order to obtain probabilistic evaluations at a higher level;

- the reaction and intervention experience during the March 4th 1977 was possible and lessons can be used in the future;

- legislation concerning the applied measures in case of natural disaster and concerning the civil defense provides the juridical and organizing framework for the preparedness of the earthquake response; the political-economical and social organization of the country is favourable to the po-

sitive joint reaction.

- there are several well-known technical and scientific operations useful for establishing the number of elements at risk, pilot applications and inventories on categories of elements at seismic risk that are necessary with a view to get the required experience and to know the intervention priorities. In this respect, in the field of dwelling constructions of high importance is to adopt unitary evaluation instructions for the aseismic resistance of the existing buildings with a view to suggest an intervention decision adequate from the technical and economical viewpoint. It is necessary to continue the studies and the theoretical and applicative developments about the seismic risk assessment.

- there are proper design codes, standards and instructions for the new buildings, but for the strengthening and repairing works there is a lack of computation and assessing structures in case they are damaged.

- specialists in the field, administrative staff and the population should be given more detailed information with respect to the earthquake engineering preparedness;

- there is a number of large towns in the seismic areas next to which important industrial platforms have been built. This increase of endowments in which the technological and natural phenomena may combine in an unfavourable way (such as the corrosion effect, the possibility of releasing of dangerous substances in case of earthquake, of blocking the railway and road joints) justifies the performing of priority studies and intervention plans in case of earthquake.

## 5.2. The Proper Framework For The Suggested Measures

Starting with the existing favourable premises and with a view to provide an efficient response of the whole Romanian social-economical system at future strong earthquakes, several measures are necessary in order to obtain a full aseismic protection. These measures should be achieved gradually through an Integrated National Programme For Preparedness, Aseismic Education and Intervention In Case Of Earthquake that could be applied by the social and economical institutions that could be a useful guide especially to the administration staff and to the specialists and population as well. Studies in this field have been recently started under the guidance of ICCPDC-INCERC. As a consequence of several specific elements analysis, the suggested measures will be regulated by instructions, codes or decision documents of the authorized organizations specialized on fields and coordinated on a local, territorial, domain and national level. The national program will include both direct applicable measures and researches that prove scientifically the measures on domains when at present there is a lack of data, intervention measures or experience.

According to the implementation periods, measures, and operations the followings will be divided as such:

- permanent measures;
- periodical measures (including measures for a scientifically prognosticable earthquake, if the development of seismology makes possible progress specifically to the territorial seismicity) and measures during the intensified seismic activities;

- emergency measures;
- measures for the rehabilitation and reconstruction period

The implementation of plans and measures at various levels will be performed gradually at the same time with the gathering of data and establishing the responsibilities and the required resources.

#### BIBLIOGRAPHY

1. x x x Natural Disasters and Vulnerability Analysis. UNDRO Report of Expert Group Meetings, 1979
2. SANDI, H. A Report on Vulnerability Analyses Carried Out In The Balkan Region. Vol. VII, 8th WCEE San Francisco, USA, 1984.
3. x x x Aspects relatifs a la planification prealable. Prevention et attenuation des catastrophes. Vol 11. Le point des connaissances actuelles. Nations Unies - UNDRO, New York, 1986.
4. VAN ESSCHE, L. Planning and management for disaster mitigation in urban areas. Earthquake risk reduction. UNDRO Seminar on Earthquake Prediction and Mitigation of Earthquake Losses, USSR, Dushanbe, October 1986, Geneve 1987.
5. ZHAOCHENG, Z. Predictia cutremurelor Haicheng si Tangshan in China. UNDRO Seminar on Earthquake Prediction and Mitigation of Earthquake Losses USSR, Dushanbe, October 1986, Geneve 1987
6. SHAOXIANG, D. Chinese policies of earthquake disaster prevention, MURCEP, Beijing, China.
7. BERTERO, V. V. The Anticipated Tokai Earthquake, Japanese Prediction and Preparedness Activities. Publication No. 84-05 FERI, California, USA.
8. CETINKALE, Y. After an Earthquake. Seminar of Turkish National Committee on Earthquake Engineering. September 1985, Istanbul, Turkey.
9. ARNOLD, C. Planning Against Earthquake In The United States and Japan. Earthquake Spectra, Vol. I, No. 1, Nov. 1984
10. OHTA, Y. A Comprehensive Study On Earthquake Disaster In Turkey In View Of Seismic Risk Reduction- Hokkaido University, Sapporo, Japan, 1983.
11. x x x Proceedings of the UNDRO Seminar on Earthquake Prediction and Mitigation of Earthquake Losses USSR, Dushanbe, October 1986, Geneve 1987.
12. BALAN, St. Cutremurul de pamint din Romania de la 4 martie 1977  
CRISTESCU, V.  
CORNEA, I. Ed. Academiei RSR, 1982.
- 13.

13. x x x Anuarul statistic 1986  
Direcția Centrală de Statistică  
București 1986
14. x x x Legea 8/1977; Legea 2/1976 - Decretele Consiliului de Stat al RSR nr.140/1978 și nr. 430/1978 publicate în Buletinul Oficial al RSR
15. GEORGESCU, S.E. Preliminary study on a Romanian earthquake preparedness programme for Bucharest  
Proc. 8-th ECEE, Lisbon, Portugal, 1986
16. GEORGESCU, S.E. Premises of an Romanian Earthquake Preparedness Programme In Bucharest  
Seminar of Turkish National Committee on Earthquake Engineering, Sept. 1985, Istanbul
17. CONSTANTINESCU, L. Cutremurele de Vrancea în cadru științific și tehnologic  
ENESCU, D.  
Ed. Academiei RSR, București, 1985
18. GEORGESCU, S.E. State of the art of the earthquake behaviour specific to several types of traditional new rural buildings in Southern Romania  
Proc. 8th ECEE, Lisbon, Portugal, 1986
19. GEORGESCU, S.E. Studiu pentru programul național integrat de protecție, pregătire antiseismică și intervenție în caz de cutremur. Referat INCERC faza 1/1987 la contractul 416/87  
SANDI, H.
20. GEORGESCU, S.E. Implications of long-term, mid term, short-term and imminent earthquake predictions on earthquake preparedness programme for Bucharest, Romania.  
UNDRO Seminar on Earthquake Prediction and Mitigation of Earthquake Losses, Dushanbe, USSR, October 1986, Geneve 1987.
21. x x x Studii asupra formelor de manifestare și efectelor cutremurului din 30/31 august 1986. Referat INCERC-ISC, iunie 1987.
22. SANDI, H. Risk Analysis For Structures And Lifelines  
Lecture, 10th Regional Seminar On Earthquake Engineering, Skopje, 1983.

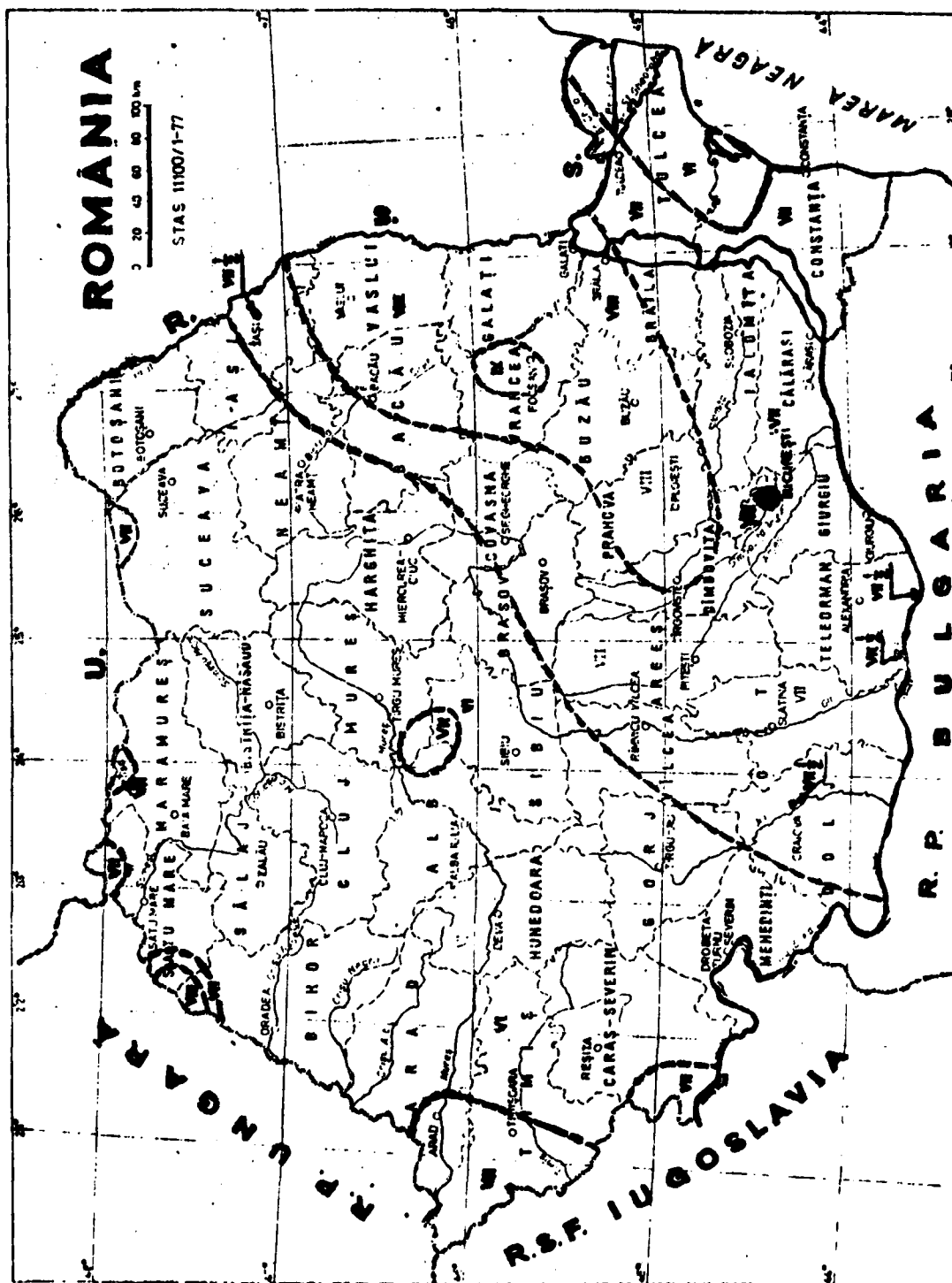


Fig. 1. Seismic zoning of Romania and territorial distribution of expected intensities (MSK degrees) in the 40 counties.



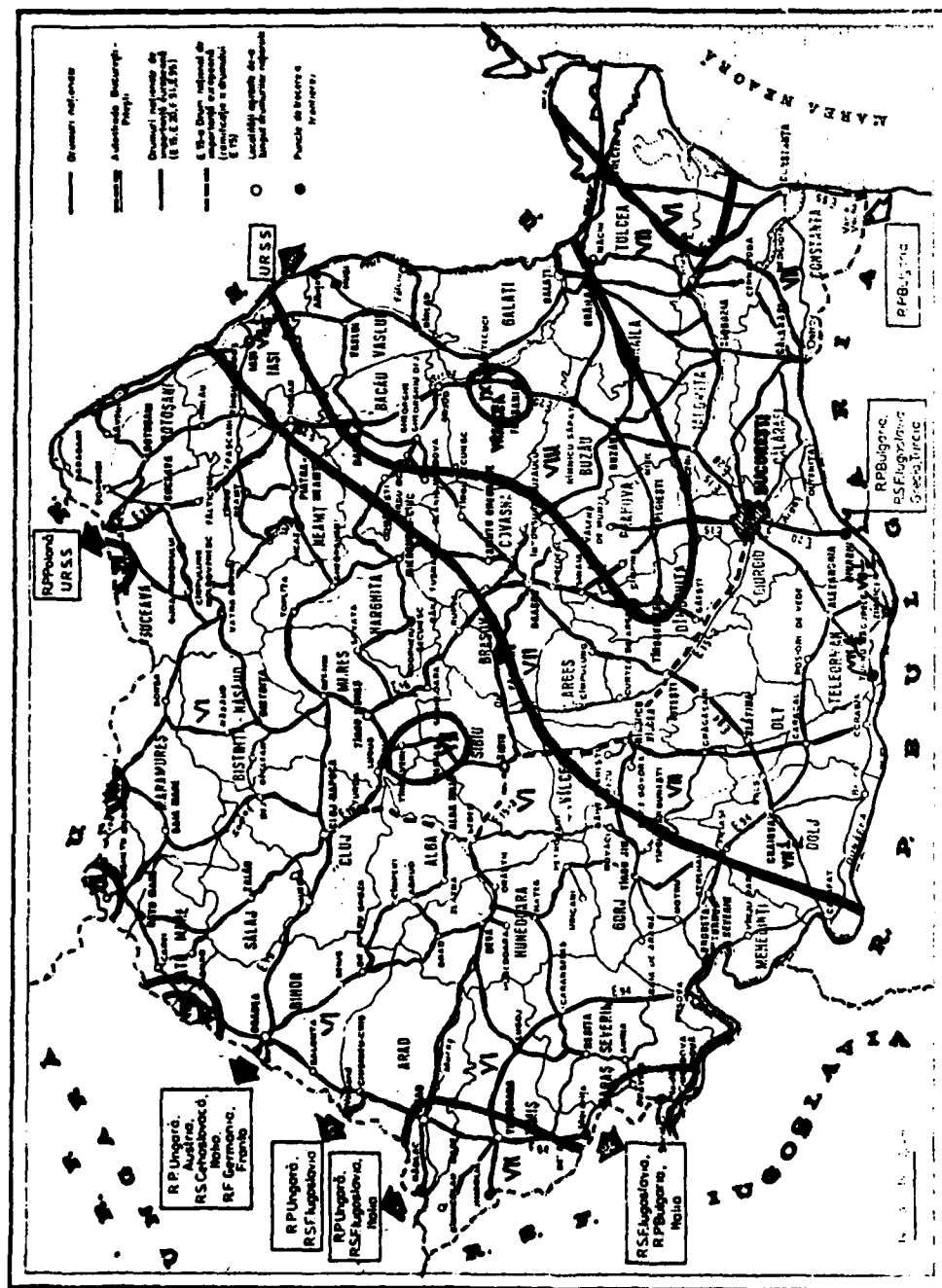


Fig.2. Seismic zoning of Romania and the exposure of the existing highways and roads network to the expected intensities (MSK degrees).



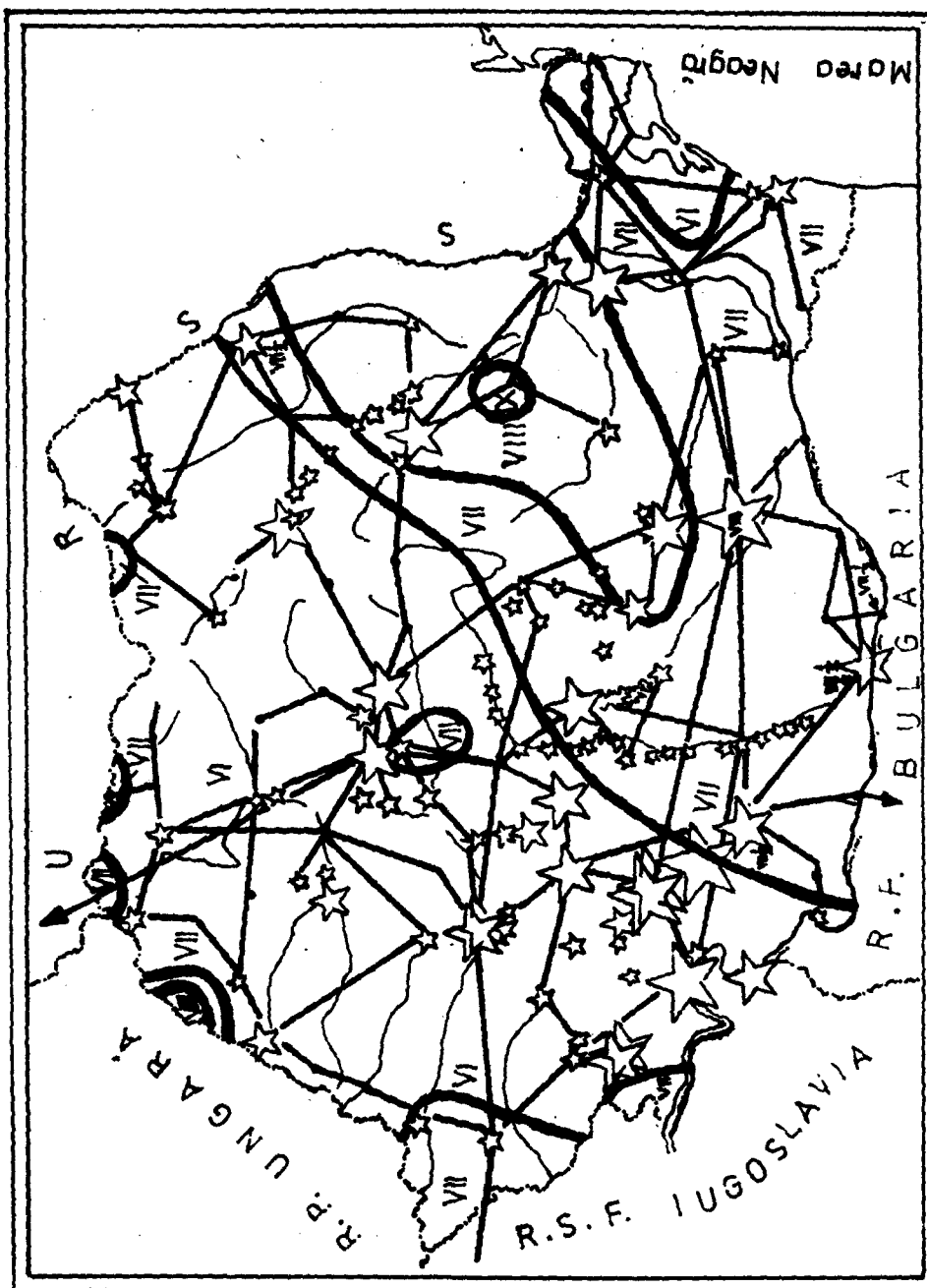
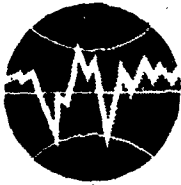


Fig.4. Seismic zoning of Romania and the exposure of the existing national power supply network and power stations to the expected intensities (MSK degrees)



**TURKISH NATIONAL COMMITTEE FOR  
EARTHQUAKE ENGINEERING**

**THIRTEENTH REGIONAL SEMINAR ON EARTQUAKE ENGINEERING**

**September 14-24, 1987 - Istanbul - Turkey**

**EARTHQUAKE STRENGTHENING OF THE FRANCISCAN  
MONASTERY IN ROZAT (DUBROVNIK)**

**by  
Dražen Aničić**

## EARTHQUAKE STRENGTHENING OF THE FRANCISCAN MONASTERY IN ROŽAT (DUBROVNIK)

by  
Dražen Aničić

### SUMMARY.

The 1979 earthquake, the epicentre of which was in Montenegro, damaged several hundreds of old stone buildings in the Dubrovnik area.

The article reviews the earthquake strengthening of the Franciscan monastery of Rožat near Dubrovnik. The reinforcement included the monastery itself, the church and the 30 m belfry. The foundations were strengthened by a reinforced concrete beam-and-stringer grid. The wooden floor structures were replaced by solid reinforced concrete slabs. All the walls were strengthened by shotcrete linings applied on one or on both sides. A number of new concrete walls were added in order to provide for structural stiffening. The belfry is attached to the building, and the cantilevered part was substantially reduced.

The effort has shown the choice of structural interventions to be as important as earthquake desing.

### Historical Survey

*Omnes morimur et quasi aque delabimur in terra que non revertuntur*  
(We all die and like the waters sink irreversibly into the earth)  
(Inscription on the stone plate in monastery cloister, dated 1543.)

The Franciscan monastery in Rožat (Rijeka Dubrovačka near Dubrovnik) was founded by decision of the Dubrovnik Senate in 1393. Because of its dilapidated condition the original building was torn down and a new monastery built in 1585. The latter has been preserved to date, and includes the church with a belfry, and the monastery proper with a cloister. The monastery was built after a Renaissance plan, although some Gothic details and the Gothic plan of the church are related to the original structure. The 1667 earthquake destroyed the church almost completely, and partly damaged the monastery which could not be used for a time. Repairs of the monastery were completed in 1704 with the exception of one wing of the cloister. The reconstruction retained fully the original layout of the ground storey, as well as all the original details. This makes the monastery one of the rare examples where - although the reconstruction took place during the Baroque - the original details were fully respected. Today the monastery is a historical monument of category "0" and it was included into the first group of nine pilot structures envisioned for reconstruction within the scope of the programme covering monuments damaged by the 1979 earthquake. The preliminary surveys and design were completed in 1981, while actual work started in 1983 and was completed in 1985. Part of the monastery will continue to be used for its original purpose, while two wings will accommodate a research institutions.

---

Dražen Aničić, Assoc. Professor, Institute of Civil Engineering, Faculty of C.E. Sciences, University of Zagreb, P.O.Box 165, 41000 Zagreb, Yugoslavia

### Definition of Seismic Parameters

The definition of seismic parameters implies the determination of earthquake intensity and magnitude, epicentral zone distance, earthquake return period, maximum anticipated acceleration, and acceleration anticipated over a certain period (e.g., 200 years). The seismic parameters were determined for the old part of Dubrovnik within the scope of the seismic microzoning project. No special seismologic surveys were carried out for the site of the monastery (which is at about 4 km from the city), and the parameters established for the old city were used instead. Maximum earthquake intensity was found to amount to  $I=100$  (MCS scale), and the corresponding magnitude to  $M=7.0$ . The depth of the earthquake focus is  $h=15$  km, and epicentral distance  $D=10$  km. The maximum anticipated acceleration is  $a_{max}=0.75$  g. Such an earthquake is likely to occur once in 750 years with a 50% chance. No attempt was made to protect the building for such a long period. The adopted acceptable level of protection assumed an earthquake of  $I=90$  MCS likely to occur once in 210 years with a 50% chance. The acceleration for such an earthquake is  $a=0.375$  g, rounded off, for reasons of possible seismic amplification to  $a=0.400$  g because the structure is founded on a stratum of alluvium 10 m thick.

### Geotechnical Surveys

Four test pits were driven next to the foundations, and three boreholes to bedrock next to the structure, in order to determine the form and depth of the foundations, and foundation soil composition. The surveys indicated that the load-bearing walls were supported by foundation strips made of stone bound by lime-clay mortar the compr. strength of which was estimated at  $300-400$  N/cm<sup>2</sup>. The depth of the foundations could not be established because of ground water close to the surface (0.5-1.0 m). Trial borings established bedrock at the depth of 8.5-12.0 m from the surface, overlaid by roughly horizontal strata of high plasticity clay (CH), gravel-clay (GC), medium plasticity clay (Cl) and the fill, in that order. The natural compaction of the material was tested by a standard penetration test. Laboratory tests were performed on undisturbed samples, and the permissible soil loading was determined, for vertical loading, as  $p=19$  N/cm<sup>2</sup> for a foundation depth of 2.0 m.

### Engineering Surveys

Several boreholes were driven in the walls and floors in order to assess the strength of the existing load-bearing structure. As established, the walls are built of semi-dressed limestone bound with lime mortar. Typical stone block sizes are  $23 \times 28 \times 25$  and  $21 \times 30 \times 25$  cm, while the mortar joints are 0.5-3.0 cm thick. The thickness of the walls is 50, 60, 75, 80 and 95 cm. The thicker walls include three courses. The central course is made of broken stone with lime mortar, and is well filled, i.e., with negligible voids. Most of the walls (with the exception of external surfaces) are rendered with low quality mortar. Assessments of the quality of masonry, and their comparison with tests carried out in situ on similar buildings, warrant the anticipated magnitude of the ultimate main tensile stress, at the moment of wall collapse due to the action of vertical and horizontal forces, of  $R_n=18$  N/cm<sup>2</sup>.

Examination of the building disclosed 1-4 cm cracks in the load-bearing walls, particularly along the joints of vertical walls. The cracks are due to earlier earthquakes and uneven soil subsidence.

The floor structures in the building consist of wooden beams spaced too much in relation to the span (730 cm) and load, mainly worn out by the acti-

on of time and moisture, with permanent deflections of several centimeters. Floor beams are supported by the longitudinal secondary beam which rests in turn on small stone cantivelers protruding from the wall. This detail, typical of old stone buildings, is markedly disadvantageous because there is practically no connection between the floor structures and the walls. The cloister, the sacristy and the altar space are vaulted by groined and cloister vaults, made of stone of low bulk weight ( $1.5 \text{ t/m}^3$ ), i.e., porous limestone of organic origin (tufa). Dangerous longitudinal cracks were discovered at the crowns of the stone vaults. The vaults were replaced on two out of three existing sides of the square cloister. The columns in the cloister presented cracks at their bases, while the ties which held them against the walls were completely worn out by corrosion.

Before reconstruction, the belfry presented a 35 cm deviation from the vertical, due to earlier permanent deformations in the soil. The top of the belfry, strengthened by horizontal ties at an earlier date, was also affected by the 1979 earthquake: the columns of the biforium were displaced, and the octagonal tambour and "cap" (in the form of an octagonal pyramid) were cracked.

#### Principles Underlying Earthquake Strengthening of Masonry Buildings

The basic shortcoming of old masonry buildings is the poor connection of the walls so that each wall behaves independently under the action of earthquake forces. The walls bend in a direction perpendicular to their plane, and are separated from the floor beams which thereby easily lose their support and collapse. Forged iron ties, used to connect the walls in the past, improved the behaviour of masonry buildings during an earthquake; their effect, however, depends on their condition (corrosion!), and on the gap between the wall and the key of the tie. State of the art approaches to the strengthening of old masonry buildings require the connection of walls by horizontally rigid floor structures so that each wall is forced to transfer the forces in its own plane.

Because of the geometrical relations prevailing in buildings the walls are mainly subjected to shear deformations. The failure of a wall unit subjected to permanent vertical and variable horizontal loads occurs when the tensile strength of the wall is reached and when diagonal cracks begin to develop. Such a failure is sudden and brittle, while the level of forces at which it occurs depends on wall quality. The ultimate force causing failure can easily be computed if the mechanical properties of masonry and the vertical load are known. If the anticipated seismic forces exceed the load-bearing capacity of the wall, it should be strengthened. This can be done by grouting - provided the approach is feasible. The provision of reinforced concrete or reinforced gunite linings is considerably better. The lining, being made of high grade material, improves the ultimate strength of the wall, while the reinforcement makes it ductile after cracks have begun to develop. New structural units can also be added as required, e.g., brick, stone or concrete walls.

The provision of seismic joints dividing a building having an irregular plan into several smaller and simple parts will result in a satisfactory building behaviour during an earthquake which can be covered by computation. This can easily be achieved in the construction of new buildings. Inasmuch as existing buildings are concerned, joints can be provided, although this may pose considerable engineering difficulties, but often this will not be possible (e.g., when two parts of a building share one wall).

The strengthening of the foundations by a reinforced concrete beam-and-stringer grid is aimed at achieving synchronous building oscillation during an earthquake. New foundations, therefore, do not improve the capability of

vertical force transfer; instead, they provide for a good connection of existing, masonry foundation strips in a single horizontal plane, like monolithic floor structures at higher building levels.

All these principles were applied in the earthquake strengthening of the Franciscan monastery in Rožat, Dubrovnik (see Figures 1-4).

#### Earthquake Strengthening of the Monastery Building, the Church and the Belfry

The strengthening concept was developed following the establishment of seismic parameters, and geotechnical and structural surveys. The plan of the building(s) is very regular. The complex could not be divided into parts (monastery - church - belfry) because of common walls. It was accordingly decided to provide for a sound three-dimensional connection of the entire structure. At foundation level the design provided for reinforced concrete strips laid next and fixed to the existing foundation strips. This was achieved in two ways: if the quality of the existing stone foundations was poor, new foundation strips were placed on either side of the old foundation and connected by cutting through the latter at selected points.

If the old foundations were of good quality and the mortar was petrified, they were connected to the new foundations by steel anchors sunk into the old foundations and sealed with epoxy resin. The anchors were also protected from corrosion.

Two wooden floors (above the ground and first storeys) were replaced by 20 cm reinforced concrete slabs. Along the supports the floor slabs were connected to the walls by  $1020/m^1$  steel anchors. The existing roof structure was replaced by a new structure.

Wherever possible with respect to conservation requirements the stone walls were strengthened by 5 cm of reinforced gunite. At points where cross walls - meant to connect the longitudinal walls - were lacking new 15 cm reinforced concrete walls were provided for. The church could not be internally gunited because of its ornaments; a new floor slab was not feasible either, and the church was accordingly strengthened by two tie beams above the walls. Transversally the tie beams were connected by 4 steel ties and wooden floor beams fixed by bolts to the tie beams.

Particular attention was paid to the belfry. Its lower part is an integral part of the church. It was decided, therefore, to treat the upper, free part as a cantilever fixed to the building at the point where the belfry enters the body of the church. The cantilevered part was protected from toppling by four tie columns invisible to the observer. Tensile forces are assumed by the tie column reinforcement, and compressive forces by the stone and concrete segments of the cross section. The transversal force is transferred at the anticipated fixing point of two walls situated at a right angle, i.e., the external wall of the church and the internal wall of the north - east monastery wing. The strengthening of the latter involved a reinforced concrete cantilever wall masked by a bilateral stone lining. The upper part of the belfry, which had suffered considerable damage in the earthquake, was dismantled. The stone columns and the windows were rebuilt, while the octagonal tambour and the pyramid were poured in concrete. Decorative stone mouldings were anchored in the concrete by copper anchors and epoxy resin.

#### Seismic Calculation

According to Yugoslav seismic regulations, monuments of culture situated in the 9th seismic zone must be calculated by the method of equivalent



static forces for the force level  $S=K \times G$ , where the overall seismic coefficient,  $K=0.30$ , is determined as the product of the coefficients  $K=K_0 \times K_s \times K_p \times K_d = 1.5 \times 0.10 \times 2.0 \times 1.0 = 0.30$ .  $K_0$  is the importance factor,  $K_s$  the seismic coefficient,  $K_p$  the plasticity and damping coefficient, and  $K_d$  the dynamic coefficient. The magnitude  $K_p=2.0$  refers to masonry structures where a non-ductile failure is anticipated. If the wall is strengthened by reinforced concrete linings which may provide for a better ductile behaviour, one may assume  $K_p=1.3$ , and the overall seismic coefficient will then be  $K=0.20$ .

The building of the monastery was designed for this load level. A stone wall strengthened by a gunite lining on one or both sides is a composite consisting of two materials of different mechanical properties. The distribution of the external force,  $S$ , to the stone wall (indexes "k") and to the concrete wall (indexes "b") is obtained from the condition of equal strain of the wall unit - cantilever, fixed at the top and at the bottom and subjected to the action of the horizontal force.

$$S = S_k + S_b$$

$$\Delta_k = \Delta_b$$

$$\Delta_k = \frac{1.2 S_k H}{G_k \cdot F_k} + \frac{S_k \cdot H^3}{12 E_k J_k}$$

$$\Delta_b = \frac{1.2 S_b H}{G_b F_b} + \frac{S_b H^3}{12 E_b J_b}$$

Following transformation these expressions yield

$$S_b = S \cdot \frac{1}{1+F \cdot \delta}$$

$$S_k = S \cdot \frac{1}{1 + \frac{1}{F \cdot \delta}}, \text{ where}$$

$$F = F_k / F_b$$

$$\delta = \frac{G_k}{G_b} \cdot \frac{1 + \gamma \cdot \alpha}{1 + \gamma \cdot \beta}$$

$$\gamma = (H/d)^2$$

$$\alpha = \frac{G_b}{E_b}$$

$$\beta = \frac{G_k}{E_k}$$

These dependences are shown for some common relations between material constants and masonry geometry in Figure 5. The magnitude "beta" can be determined experimentally for a specific case.

The distribution is significant for the elastic stage. After the ultimate tensile strength of the masonry and concrete lining has been reached, the entire transversal force is transferred by the reinforcement. The reinforcement is applied as a welded mat with the identical vertical and horizontal wire spacing and with identical wire cross sections in either direction. The quantity of reinforcement is governed by the condition whereby the ultimate force of nonreinforced masonry should be assumed by the reinforcement, the coefficient being  $K=1.3$  with respect to failure. The other formal condition to be satisfied is  $f_a \geq 0.15\%$ .

Because of the great length of low monastery walls, the influence of the bending moment has been neglected, and so has that of torsion.

The belfry was designed for an equivalent seismic load,  $S=0.30 G$ . The bending moments are transferred by the reinforcement of the new tie columns, and transversal forces by the existing stone structure.

#### Implementation of Strengthening

All the parties involved in the monastery strengthening project (the investor, architect, structural engineer, conservator, and contractor) faced

numerous problems during its implementation. The problems were the outcome of the following:

- Inaccuracies in the survey of the actual condition. Thus, the right angles shown in the blueprints turned out to be different in reality; considerable differences were also established between the level reference lines for floors, the cloister rail, column bases and the roof cornice.
- The quality of the material hidden beneath the mortar often proved to be surprisingly poor. Some of it, at the ground floor, was disintegrated by moisture. The removal of plaster revealed old cracks in load-bearing walls.
- The dismantling of the upper part of the belfry and of two cloister wings required great care, the numbering of each piece, and a logical sequence of piece storage because of later assembly. Fissured stone mouldings had to be repaired with epoxy resin to which a stone-coloured filler was added.
- The removal of limestone deposits and fine cleaning of the capitals, columns and arches required the services of specialist stone-masons.
- The purpose of part of the structure intended for secular use was not defined as the work started; the finishing work and installations were not defined either.
- Archeological excavations in the cloister slowed down the work of the contractors, and affected rainwater drainage from the cloister. In accordance with a later decision the garden in the cloister was replaced by a stone-paved area.
- The contractor was not specifically qualified for work on a historical monument and his team had only standard building construction experience. Hence his frequent decision-making uncertainty and requests for solutions to be provided by other parties.
- The conservators took a long time to take a stand on specific issues arising during reconstruction, and slowed down the progress of the work.

#### CONCLUSION

The seismic reconstruction of cultural monuments requires special care and attention. In addition to structural requirements, architectural and conservation considerations also have to be observed. The seismic calculation serves as an orientation, the essential contribution being made by engineering design meant to transform the existing load-bearing system into a system capable of assuming seismic loads. Project implementation must be preceded by thorough surveys. Actual reconstruction work must be monitored continuously so that all changes and adjustments can be made without unnecessary delays.

#### REFERENCES

1. Aničić, D., Final Design for the Engineered Reconstruction of the Rožat Monastery, Rep. 21-1762/81, Civil Engineering Institute, Zagreb, 1981.
2. Badurina, A., The Franciscan Monastery in Rijeka Dubrovačka - History and Actual Condition, Centre for Historical Sciences, Zagreb, 1981.
3. Aničić, D., Earthquake Strengthening of Cultural Monuments in Dubrovnik, Cultural Heritage of the Balkans and Seismic Problems, Vol. 10, Montenegrin Academy of Arts and Sciences, Titograd 1983, pp 199-208.

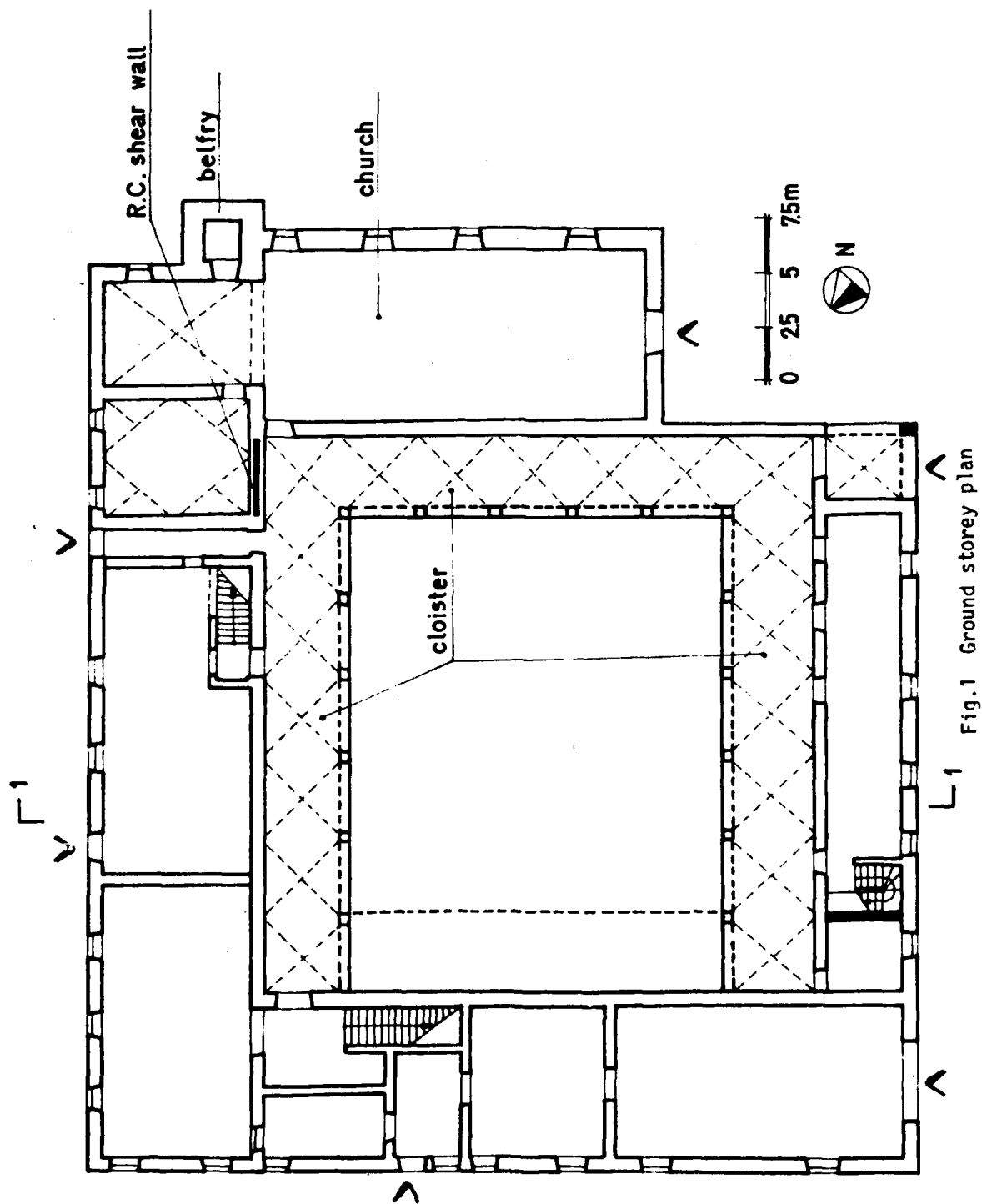


Fig.1 Ground storey plan

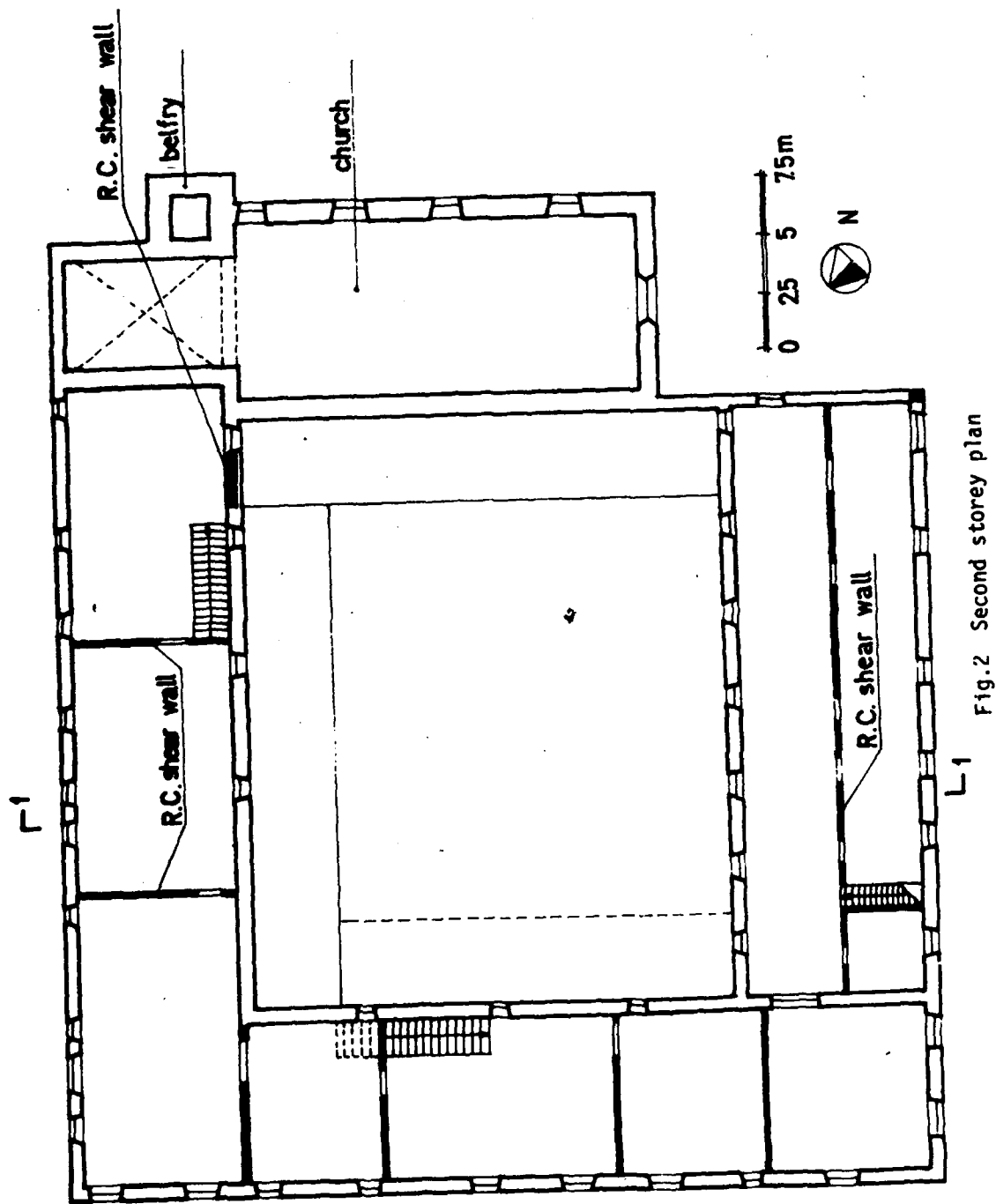


Fig.2 Second storey plan

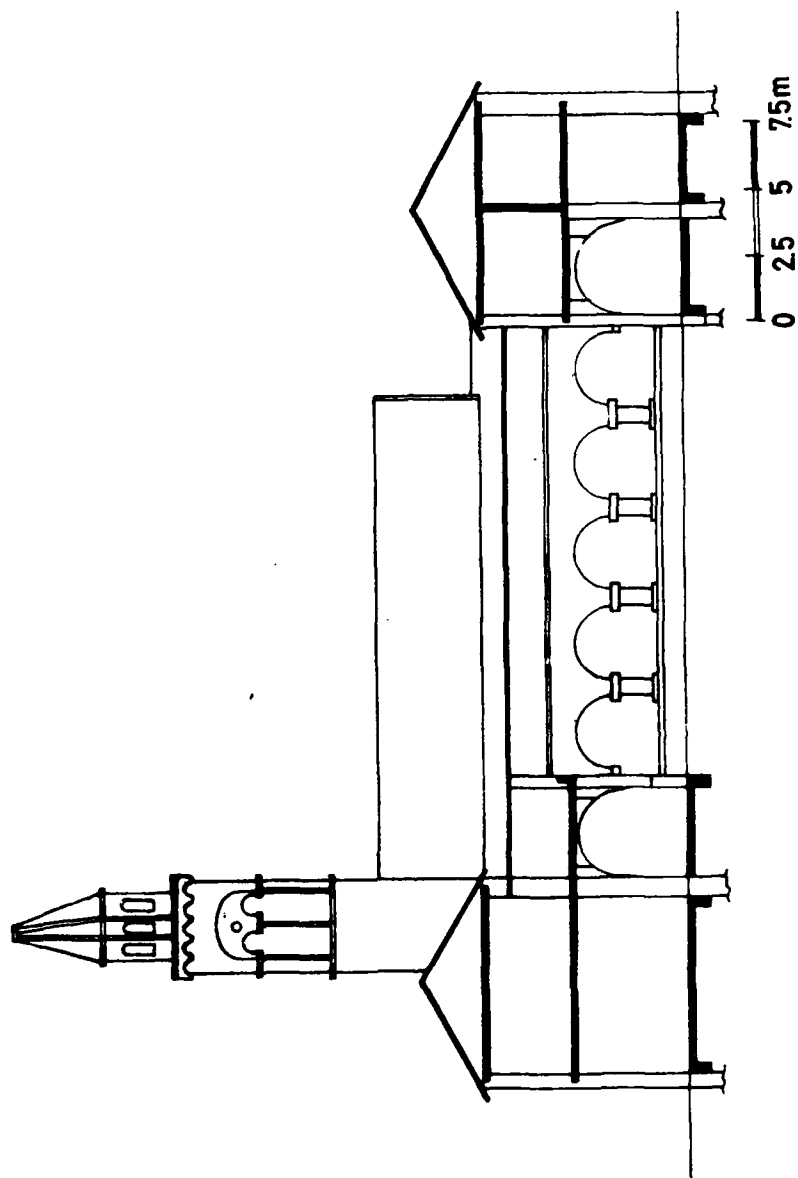


Fig.3 Longitudinal section 1-1

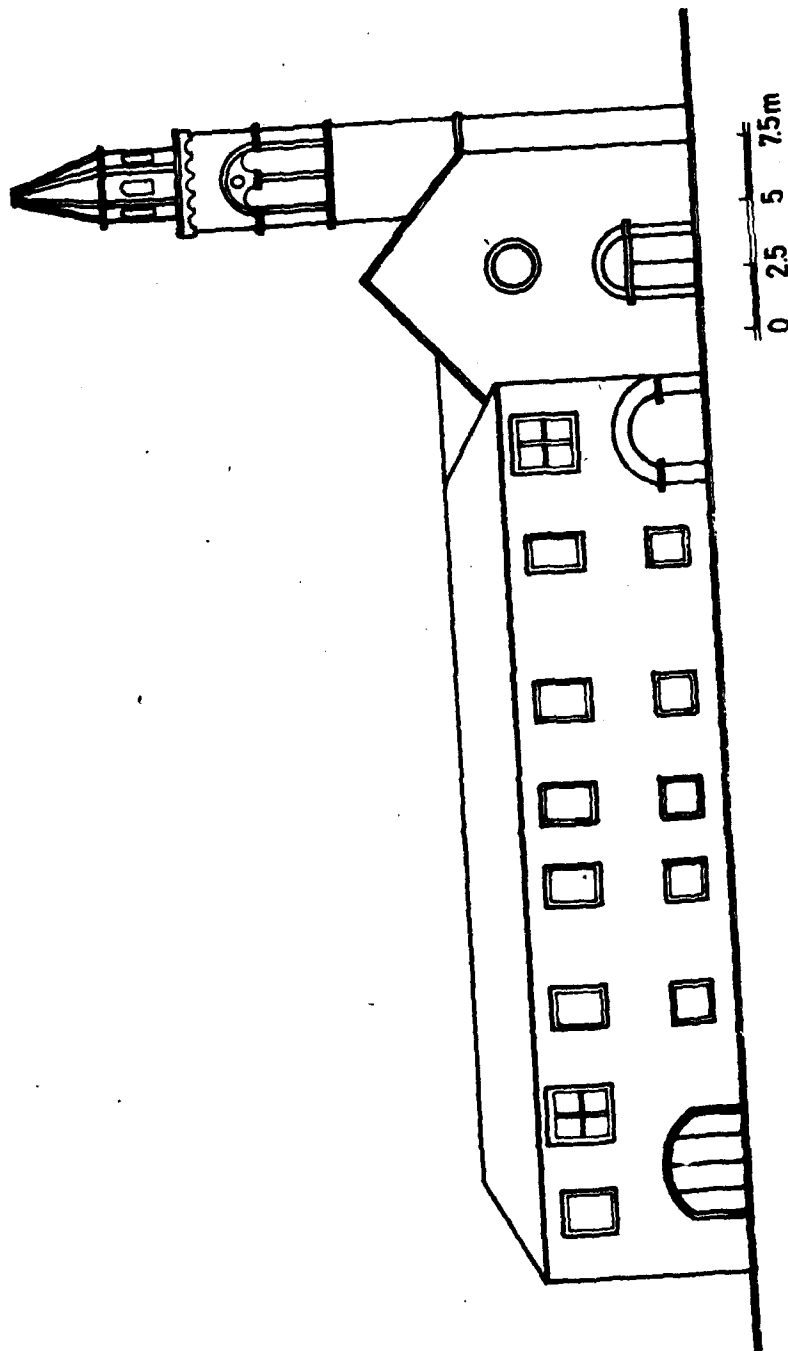


Fig.4 South-West Front View

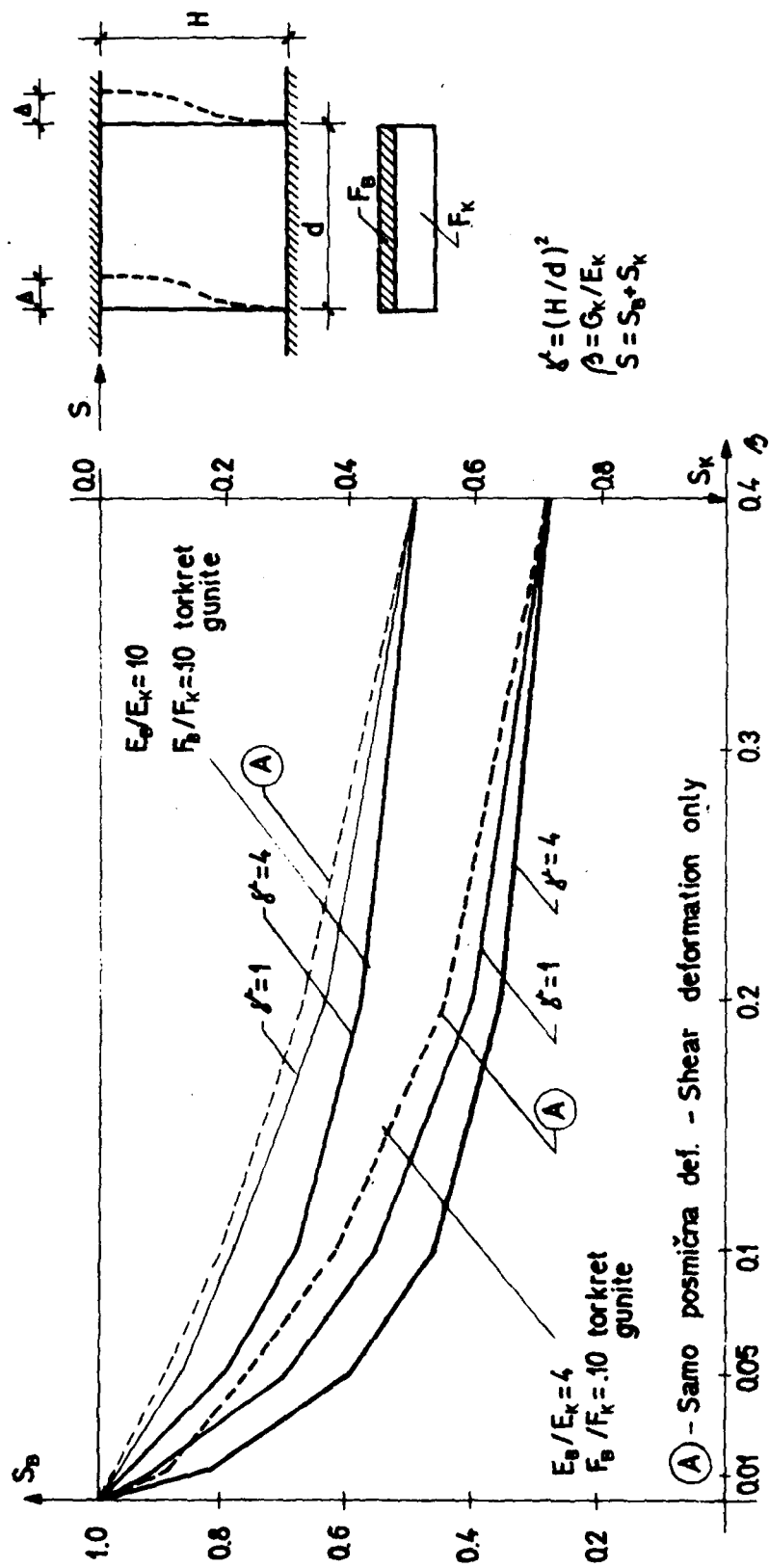
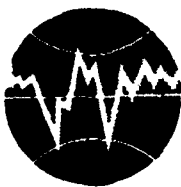


Fig.5 Distribution of Horizontal Force in the Stone Masonry Wall Strengthened by Gunite



**TURKISH NATIONAL COMMITTEE FOR  
EARTHQUAKE ENGINEERING**

**THIRTEENTH REGIONAL SEMINAR ON EARTHQUAKE ENGINEERING**

**September 14-24, 1987 - Istanbul - Turkey**

**CULTURAL MONUMENTS AND OLD URBAN NUCLEI  
IN SEISMIC AREAS**

**by  
Miha Tomažević and  
Dražen Aničić**



## CULTURAL MONUMENTS AND OLD URBAN NUCLEI IN SEISMIC AREAS

by  
Miha Tomažević and  
Dražen Aničić

### SUMMARY

Old masonry buildings and cultural monuments are jeopardized by earthquakes more than modern structures. The community is interested, for a variety of reasons, in saving such buildings, the evidence of its cultural identity, for future generations.

The paper presents the authors' research in the field of earthquake resistance of masonry buildings. The need for preliminary building surveys, experimental evidence on mechanical wall material properties, and interdisciplinary team-work is emphasized. The behaviour of earthquake strengthened and non-strengthened buildings is discussed along with the engineering steps for improving earthquake resistance. Parameter analyses have shown that most old buildings can be strengthened for earthquake forces to a level of publicly acceptable seismic risk.

### INTRODUCTION

Seismic areas with a past record of seven-plus (MCS) earthquakes account for three-fourths of Yugoslav territory (Table 1). Strong earthquakes which have hit this area have brought about the destruction of a number of ancient and medieval settlements, some of which have since been abandoned, while others, following reconstruction, still serve the original purpose. Over the past twenty-odd years, a period of more pronounced seismic activity in Yugoslavia, earthquakes have also hit cultural monuments, and old urban and rural complexes, evidence of national cultural identity. Thus, many monuments have been completely destroyed although the methods of monument strengthening are known.

Old buildings are subject to damage due to the action of strong earthquakes for three reasons: first, old settlements are laid out along, or close to, active tectonic faults where earthquake action is usually the strongest. Second, such buildings have a low earthquake resistance. Although the layout of load-bearing walls, in terms of plan, is mainly adequate, and although such buildings do not exceed five storeys, their weakness is to be found in an inadequate connection of the walls, rather low quality of material, and multiple reconstructions during the life of the building. All this, along with poor maintenance, makes the earthquake a factor which enhances all shortcomings at once. The third reason is related to foundation soil which may show a tendency to subsidence, sliding or liquefaction during an earthquake; along with inadequate foundations, this may severely jeopardize the building.

One of the questions which is regularly raised when the reconstruction of old settlements and individual cultural monuments is concerned is the following: after the earthquake, can old damaged buildings be strengthened so as to be capable of "surviving" future earthquakes without major consequences? This point is associated with two follow-up questions: Can dwellers of old buildings enjoy the same degree of earthquake protection as dwellers of new buildings erected on the basis of state-of-the-art earthquake engineer-

Miha Tomažević, C.E., Ph.D., Senior Consultant, Institute for the Study of Materials and Structures, Dimičeva 12, 61000 Ljubljana

Dražen Aničić, C.E., Ph.D., Associate Professor, Institute of Civil Engineering, Faculty of C.E. Sciences, University of Zagreb, Rakušina 1, 41000 Zagreb

ing knowledge? How to strengthen existing buildings for the action of a future earthquake?

The experience acquired after the 1976 Friuli earthquake, which affected both Yugoslav and Italian territory, has shown that "cosmetic" repairs of damage, based on the hypothesis that there would be no more earthquakes, are useless and a waste of time and money. After-shocks or a new earthquake again lay bare the shortcomings of such buildings, and damage it severely or destroy it. When reconstructing a cultural monument or an urban complex earthquake safety must be observed along with architectural and conservation considerations. If only the latter are taken into account, we shall be reduced to the role of helpless observers of severe damage wrought by a new earthquake.

According to the Law on the Protection of Cultural Monuments of the Socialist Republic of Croatia (24), the category of cultural monuments includes "all stationary and mobile assets, and groups of assets, which, because of their archeological, historical, sociological, ethnographic, artistic, architectural, town planning, engineering, and generally scientific or cultural value, are of significance to the community."

Like all other artefacts, monuments also suffer from gradual wear and destruction over time. The underlying causes may be attributed to human activity or to the action of natural forces.

All modern communities try to save their cultural monuments and protect them from deterioration because they are part and parcel of their national identity. Accordingly, the protection of monuments may not be discussed in market and economic terms. There is no way of accurately determining the monetary value of an old building. The same holds good for any attempt to determine the higher value of a reconstructed building. Reconstructions always yield new archeological, historical, art and other knowledge, and every reconstruction project, therefore, marks not only a step forward in the application of engineering techniques but also contributes to other levels of knowledge. Major cultural monuments are invaluable because their loss cannot be made up for.

Present-day monument protection practices are based on principles laid down in a number of documents adopted over the past fifty years (8), such as the Athens Charter (1931), the Italian Charter (1932), the Venetian Charter (1964), the Amsterdam Declaration (1975), etc. The UNESCO has also adopted a number of conventions on cultural monuments, e.g. the Hague Convention on the Protection of Cultural Treasures in Case of Armed Conflict (1954), the Convention on Prohibiting and Preventing the Illicit Import, Export and Transfer of Cultural Assets (Paris, 1970), and the Convention on the Protection of the World Cultural and Natural Heritage (Paris, 1972). The principles governing protection and applied in these documents are based on cultural-historical and artistic rather than on design and engineering criteria. They discuss concepts such as conservation, restoration, consolidation, anastylosis (the reconstruction of a monument from its parts), renovation, the need to preserve the historical environment and authenticity. Structural engineering is only a tool for the achievement of cultural and historical goals.

#### RECONSTRUCTION AND SOCIO-ECONOMIC CONSIDERATIONS

The reconstruction of monuments and old urban nuclei is aimed primarily at their preservation and the improvement of living conditions of their inhabitants. Housing standards being generally low in old buildings, the introduction of new facilities (water supply, heating, electrical and gas supply installations, bathrooms, protection from humidity and heat) tend to improve such standards. At the same time the monumental value of the building has to be preserved, and parts of it made accessible to the public.

Estimates and experience have shown the cost of reconstruction of an old building to be equal to the cost of construction of a new building. In other words, the reconstruction of old buildings implies major public expenditures. This is why reconstruction is considered primarily in cases when old buildings and towns are to be revitalized, and cultural and historical complexes thus protected from deterioration.

Protection from earthquake action is part of the broader scope of old building reconstruction. Absolute seismic safety cannot be achieved, whether the building is old or new, and the level of acceptable seismic risk is discussed accordingly. The community should be aware of the fact that cultural monuments also have a limited life, that they also "die" and that an earthquake is only one of the factors contributing to the process. The degree of damage on a building strengthened for earthquake action is inversely proportional to the investment into such strengthening, whereby the latter depends on the economic potential and willingness of the community. This is what makes seismic risk not only an engineering but also an economic category.

The publicly acceptable level of seismic risk is reflected by building construction codes and regulations. Yugoslav regulations for building construction in seismic areas make no mention whatsoever of old buildings. The previous, 1964 seismic code included a provision (paragraph 8) regarding the subject under consideration. Because of its clarity, it is as applicable today as it was twenty years ago: "if substantial changes are made in the load-bearing structure the building shall meet the requirements laid down in the regulations in all respects; if no substantial changes of the load-bearing structure are being envisaged, evidence shall be provided that the earthquake resistance of the building following its reconstruction shall be at least equal to its earthquake resistance prior to such reconstruction". In the case of old buildings, earthquake resistance can also be improved by structural improvements of a more limited scope, e.g., by connecting the walls with ties, by adding tie beams at wall top level, or by reconstructing the roof structure, even if the building as a whole need not meet, after such operations, the formal requirements of the regulations (storey height, wall layout, floor structures, etc.). Such decisions do not rest only with the design engineers but also with the bodies representing the interests of the community (municipal building construction boards, monument conservation departments, etc.). Such partial interventions equate the degree of seismic risk for new and old parts of a settlement.

Interest in the reconstruction of old urban complexes first developed, for a variety of reasons, in countries situated in non-seismic areas (Poland, West Germany, Austria), to become subsequently a world-wide movement. A number of old urban and rural complexes have also been reconstructed in Yugoslavia (Skopje, Baš-Čaršija in Sarajevo, Breginj, Ljubljana, Varaždin, Kotor, Budva, Dubrovnik). In recent years the Yugoslav community has been paying considerable attention to earthquake resistance of old buildings, as reported at several national and international meetings (1, 2, 3, 8, 11, 13, 14, 15, 19, 20, 21). The international UNDP-UNIDO Project, Building Construction Under Seismic Conditions in the Balkan Region, also involved the preparation of a manual for protecting cultural monuments and urban complexes from earthquakes which included contributions by Yugoslav experts as well (18).

#### PRELIMINARY SURVEYS

In structural engineering terms the strengthening of a cultural monument is based, in principle, on maintaining or achieving safety with regard to the action of external forces affecting the monument. Whereas a new

building is being "shaped" during design, a monument presents an already finished form requiring the definition of its safety, its weak points, and strengthening points and methods. In most cases monuments are built of materials of unknown physico-mechanical properties, implying that the characteristics of materials used in the calculations are not sufficiently reliable. The inner structure of the material of which the monument is built may be affected by the action of natural forces or by human action but need not be externally visible to the observer. This is why the design of strengthening for a monument necessitates extensive preliminary surveys (2), (4), (13), required to appreciate the current load-bearing scheme of the monument, to assess and test the quality of materials, to record the damage (cracks, subsidence, wear), and to obtain an idea of the required strengthening steps. The implementation of such preliminary surveys is often hindered by the use of the structure and by the lack of a substitute space for its functioning and its users. A strengthening design based on inadequate surveys will suffer numerous changes during actual work.

Surveys related to the historical and archeological aspects of the monument are of special significance. In terms of space and time they may be performed either simultaneously with structural surveys or separately in consideration of the different objectives. Such surveys will expand the scope of knowledge of the monument and thereby influence design work. This part of overall survey work involves the participation of experts of different backgrounds (art historians, archeologists, restoration specialists), each with a specific vision of the future function and appearance of the monument.

Preliminary surveys also include the architectural survey of the actual condition. The plans produced by such a survey may provide data on geometrical relations within the structure and serve therefore as the basis for strengthening design.

#### CLASSIFICATION OF RECONSTRUCTION METHODS AND DAMAGE

The scope of reconstruction of a monument may vary depending upon the requirements, future function and available funding (11), (12).

Repairs are considered to include all actions which do not involve the load-bearing units of the structure, and refer to correcting external defects on non-load-bearing units. This category would thus include repairs of damaged partition walls, claddings, facings, facades, wall and ceiling plaster, and all installations. In addition to the esthetic impression such repairs also produce a positive psychological effect on the staff and users of the monument. In terms of improving earthquake resistance, however, the effect of repairs is nil.

Reconstructions imply operations involving the damaged load-bearing system and focused on re-establishing strength, stiffness and overall safety conditions such as prevailed prior to damage.

Strengthening implies the reconstruction of the load-bearing system meant to improve its load-bearing capacity by available methods to the level provided for in current requirements (e.g. building construction codes).

The term "remedial steps" covers all the three categories listed above and includes, in addition to structural work, architectural and cultural-historical reconstruction aspects.

The following three categories of work have to be implemented during reconstruction and strengthening of a monument:

- reconstruction or strengthening of individual load-bearing units (walls, columns, floors, foundations);
- reconstruction or strengthening of connections (joints) between units;

- reconstruction or strengthening of three-dimensional stiffness meant to improve the overall strength of the monument and providing for the redistribution of external impacts to individual load-bearing units.

The classification of damage may be local - referring to individual load-bearing units, and general - referring to the monument as a whole. Both local and general damage classifications are an integral part of survey work within the scope of long-term planned renovation.

Local damage may be harmless, i.e., it need not require substantial interventions; or dangerous. In the latter case provisional strengthening steps are required without any delay. The record of damage should preferably include the estimated underlying cause because its elimination will constitute one of the objectives of the renovation effort.

The classification of damage involving the assessment of the overall condition of the monument is usually performed after a major earthquake affecting a region and a considerable number of monumental assets. By using a standard methodology (23) applying to all types of buildings, damaged monuments are divided into 6 categories marked green, yellow or red. The categorization of damage is equally applicable to "ordinary" buildings and to monuments. The form for damage recording is not covered by (23); however, following the 1979 Montenegro earthquake a form has been introduced for recording damage to monuments which can also be used for other buildings. The overall classification of damage is performed visually by a commission.

#### MONUMENT RENOVATION - A TEAM EFFORT

The process of monument renovation involves at least four groups of experts advocating different interests.

The interest of the investor - the present or future user, or the organization entrusted with the renovation project - is focused on achieving the maximum effect in terms of future function and benefit at a minimum cost. In Yugoslavia such organizations lack the required specific expertise and, therefore, engage the services of experts for monument renovation.

The architect is responsible for adjusting the building to modern standards of its use. He will be involved in the definition of the design brief in cooperation with the investor, in the coordination of the requirements of all participants in the renovation process, and in the preparation of the preliminary and final design. The work of the architect is limited by the existing bulk and by the constraints imposed by engineering, conservation and regulatory requirements.

The structural engineer is responsible for strengthening the load-bearing structure of the building by using knowledge of its resistance (as obtained by the preliminary surveys) and applying the loads imposed by its new function. All strengthening and new structural units must be agreed with the architect and the conservator.

The conservator is responsible for protecting all values vital to the existence of the monument. He shall endeavour to analyze and report all new aspects unveiled by preliminary surveys, and provide conservation guidelines indicating - to the architect and structural engineer - all units which must not be altered as well as those where changes are permissible to a greater or lesser extent (evaluation of the monument in conservation terms). The conservation effort combines a number of concerns related to archeology, history of art, restoration, paintings and frescoes, ethnology, environmental protection, etc.

The coordination of the views of these four groups of experts is essential to the renovation design and to the actual renovation of the monument. Team work is required in order to arrive at a generally acceptable solution. The success of the team will hinge upon the competence of the experts involved, the clarity of their views, their knowledge of state of the art methods, and sufficient flexibility with regard to the requirements of other members of the team. Owing to many of their features monuments are not easily reconciled to current regulations. Any forceful adjustment of the monument to be renovated to such regulations may also destroy its value. This is why departures from regulations reducing safety should be distinguished from departures related to the comfort of use.

#### BEHAVIOUR OF OLD MASONRY BUILDINGS DURING AN EARTHQUAKE

Knowledge of the shortcomings of old buildings and of their behaviour during an earthquake is required in order to appreciate the principles of their earthquake strengthening (5,6,7).

A masonry building is basically a space frame, box-type structure. If the building is to behave three-dimensionally during an earthquake, some requirements have to be met with regard to the horizontal layout of its walls and their connections. Damage observed after the earthquake and tests of masonry building models on shaking tables have shown that the oscillation of the building as a whole depends substantially on the level of wall connection at floor level.

In buildings with unconnected walls, and wooden floor structures which are just laid and not connected to the walls, the walls will separate and cracks will develop along vertical joints. The cracks are due to the bending of the walls outside their own plane, and to the inadequate tensile and shear strength of the vertical wall joint along the two orthogonal axes. The oscillation of the walls is not harmonious, and external walls often collapse (Fig. 1a,b).

If the walls are connected, during an earthquake they have to oscillate together, harmoniously. The behaviour of the building is better, although the influence of wall bending (outside their own plane) is still considerable because of the wooden floors (Fig. 1c).

The inherent seismic resistance of the building will be used to full advantage only by connecting the walls with ties and solid floors. The walls will then oscillate harmoniously, while the influence of wall bending will be reduced to the minimum because the walls will now be supported along all the four edges (Fig. 1d). The forces of inertia which develop during an earthquake deform the building. The window piers, which transfer all the forces, are the most susceptible. The most frequent damage suffered by window piers are X-cracks due to the action of main tensile forces. When the tensile bending strength is exceeded, cracks will develop around the openings and wall joints (Fig. 2).

The period of the basic oscillation mode of masonry buildings, which are markedly stiff structures, is regularly less than 0.3 and, therefore, falls within the highest acceleration spectrum values of most earthquakes recorded so far.

Detailed analyses of the behaviour of masonry building models tested on the shaking table (6,7) indicate a markedly nonlinear behaviour, a substantial increase of the base period of oscillation, and the capability of energy absorption when structural steps providing for ductility are applied (tie beams or columns, horizontal reinforcement).

## ENGINEERING STEPS FOR INCREASING THE EARTHQUAKE RESISTANCE OF OLD MASONRY BUILDINGS

If the principles of old building behaviour during an earthquake are known, one can decide which engineering action to take in order to improve the earthquake resistance of such buildings. The decision will depend on the configuration of the building, on the quality of the material of which it was built, on the desired level of earthquake protection, and on the location of the building with respect to the possible epicentre. The decision regarding the strengthening approach will require computation with inputs based on experimentally established mechanical properties of the materials (masonry).

The experimental part of the effort may be performed either in the field or in the laboratory. Knowledge of actual mechanical properties of the material(s) will reduce the required intervention to a reasonable scope and, at the same time, take advantage of the available load-bearing capacity of the existing structure. Such "engineering surveys" will not be conducted for each building but, rather, on types of masonry typical of a number of buildings within the urban nuclei. Similarly, the envisioned strengthening steps will be checked experimentally, in the laboratory, only once (e.g., the effect of crack grouting, guniting, reinforcement, etc.), and the results will be used in design.

The detailed presentation of all available steps for the strengthening of old buildings would be beyond the scope of this paper. This has already been done in a number of earlier papers (9), (10), (22), etc. Generally speaking, one should analyze the shortcomings of individual structural parts of the building with respect to the action of earthquake forces, and select an acceptable strengthening method.

Thus, foundations can be strengthened by reinforced concrete strips laid along the existing masonry foundations, so as to create, already at foundation level, a grillage providing for the synchronous movement of individual parts of the building and constituting the groundwork of a "rigid box" into which we want to turn the strengthened building.

As far as walls are concerned, vertical continuity should be established first. Walls which were obviously removed during the use life of the building should be rebuilt, and all unnecessary openings and weak points which reduce the earthquake resistance of the masonry walled up. Walls should next be connected so as to take advantage of their load-bearing capacity in their own plane. This can be achieved by incorporating steel ties on top or underneath the mortar, by anchoring wooden beams to the walls (by steel ties), by increasing the stiffness of wooden floors through the incorporation of cross bracing or bilateral wooden formwork placed at an angle, by providing a new, monolithic floor structure above or instead of the wooden floor, etc. Several methods, some of which have not been fully checked experimentally, are available for wall strengthening. Cracks in a brick wall can be grouted with a cement suspension, although this does not substantially increase the load-bearing capacity with respect to horizontal forces. The walls can bilaterally be strengthened by cement mortar (3 cm) with reinforcement, or gunite (5-7 cm) and reinforcement; the wall load-bearing capacity for the action of horizontal forces can be improved by vertical prestressing (5,14,19).

Roof structures are improved so that they no longer transfer horizontal forces to the walls; if worn out, they are replaced by new wooden structures.

## MATHEMATICAL ANALYSES

The direct result of experimental and analytical work is the mathematical method for checking the earthquake resistance of masonry buildings developed at ZRMK, Ljubljana (17). Essentially, the computation is based on the

limit state method and uses the SREMB program (Seismic Resistance of Masonry Buildings), taking into consideration experimentally established material properties. Following the 1976 Friuli earthquake, Italian regional authorities have adopted the method as mandatory in the design of masonry building reconstruction. A similar program adapted for a microcomputer (e.g., SHARP PC-1500 with a 11.5 kb core store) has been developed by the Civil Engineering Institute, Zagreb, and applied to several cases in Montenegro (16).

Table 2 reviews the results of parameter analyses concerning the earthquake resistance of old masonry buildings, performed in order to highlight their possible earthquake strengthening. The computation has considered experimentally established values for mechanical properties of walls, divided into four categories:

- Category I - three-course wall, undressed stone, lean lime mortar mixed with clay; not plastered.
- Category II - three-course wall, undressed stone, lime mortar with clean sand; not plastered.
- Category III - three-course wall, roughly dressed stone, lime mortar with clean sand; plastered with cement-lime mortar.
- Category IV - three-course wall, roughly dressed stone, lime mortar with clean sand; plastered with cement-lime mortar. Grouted after earthquake damage.

In Table 2 the earthquake resistance of the building is expressed in terms of the ratio of the ultimate horizontal force which the building can transfer at the moment of collapse to the building weight. i.e.,

$$K_s = H_u/G$$

If the actual seismic load affecting a building during an earthquake is taken into account, it becomes clear why old buildings suffer damage already during earthquakes of moderate intensity (degree VI and VII), and are severely damaged or demolished by strong earthquakes (degree VIII and IX). Table 2 also warrants the conclusion that strengthening steps can improve the earthquake resistance of old buildings to the point of obtaining a satisfactory resistance even during the strongest earthquakes.

#### CONCLUSION

Cultural monuments and old urban nuclei are jeopardized by possible earthquake effects more than modern buildings. The community is interested in their reconstruction and preservation for future generations owing to a variety of reasons. Past studies have provided knowledge of the behaviour of such assets during earthquakes, established the basic mechanical properties of the material, and developed a number of computation methods. Thanks to such efforts even old buildings can be new protected from earthquake effects to the level of risk publicly accepted for other buildings.

The reconstruction of cultural monuments and old urban nuclei is a long-term national effort, and in the future it will require the involvement of numerous experts. The structural engineers will also provide a contribution to the effort.

#### REFERENCES

1. Aničić, D., Earthquake Strengthening of Cultural Monuments in Dubrovnik. In: Cultural Heritage in the Balkans and Seismic Problems, Montenegrin Academy of Sciences and Arts, book 10, pp 199-208, Titograd, 1983.



2. Aničić,D., Morić,D., Zaninović,V., Ultimate Main Tensile Stress of Stone and Brick Walls, First Congress of the Society of Croatian Structural Engineers, Plitvice Lakes, Oct. 18-19, 1984.
3. Aničić,D., Steinman,V., Earthquake Strengthening of the Rector's Palace in Dubrovnik. In: Cultural Heritage of the Balkans and Seismic Problems, Montenegrin Academy of Sciences and Arts, book 10, pp 209-224, Titograd 1983.
4. Aničić,D., Steinman,V., Tensile Strength of Masonry Walls as a Factor of Earthquake Resistance of Masonry Buildings, Third International CIB Symposium on Wall Structures, Varšava, 5-7.6.1984.
5. Benedetti,D., Benzoni,G., Petrini,V., Experimental Evaluation of Seismic Provisions for Stone Masonry Buildings, Proceedings, 8-WCEE, San Francisco, 1984.
6. Benedetti,D., Castoldi,A., Dynamic and Static Experimental Analysis of Stone Masonry Buildings, Proceedings, 7-ECEE, Athens, 1982.
7. Benedetti,D., Tomažević,M., Sulla verifica sismica di costruzioni in muratura, Ingegneria sismica, No.10, Bologna, 1984.
8. Borković,A., Protection of the Stone Structures of Cultural Monuments from Earthquake Action - the Dubrovnik Case. Master's thesis, Civil Engineering Institute, University of Zagreb, 1984.
9. Guidelines for Earthquake Resistant Non-engineered Construction, International Association for Earthquake Engineering, 1980.
10. Lizzi,F., The Static Restoration of Monuments, Sagep Publisher, Genova 1982.
11. Meeting on Building Reconstruction, Maribor, 15-16.9.1983., Vol.1-2, SGITJ, DGIT Maribor
12. Second Seminar on Construction in Seismic Regions, Lisbon, 12-16.10.1981. United Nations, Economic Commission for Europe
13. Sheppard,P., In-situ Test of the Shear Strength and Deformability of an 18th Century Stone-and-brick Masonry Wall, 7-IBMaC, Melbourne, 1985.
14. Sheppard,P., Orožen-Adamič,M., Knez,M., Possible Revitalization of Masonry Housing from the Standpoint of Earthquake Safety - Basic Considerations, ZRMK, Ljubljana, 1984.
15. Sheppard,P., Tomažević,M., Possible Revitalization of Masonry Housing from the Standpoint of Earthquake Safety - Basic Considerations, ZRMK, Ljubljana, 1984.
16. Srkoč,M., Masonry Building Design for Earthquake Action, Earthquake Engineering Seminar, DGIT/DPGH, Zagreb, 1985.
17. Tomažević,M., Calculation of Earthquake Resistance of Masonry Buildings, Gradbeni vestnik, Ljubljana, No 9, 1980.
18. Tomažević,M., Assessment of Earthquake Resistance, Strengthening and Repair of Cultural and Historical Monuments and Urban Nuclei, National input report, UNDP-UNIDO project RER/79/015, Istanbul, 1982.
19. Tomažević,M., Sheppard,P., The Strengthening of Stone-masonry Buildings for Revitalization in Seismic Regions, Proceedings, 7-ECEE, Athens, 1982.
20. Tomažević,M., Revitalization of Stone Masonry Buildings from the Standpoint of Earthquake Protection, Gradbeni vestnik, br.4-5, Ljubljana, 1983.
21. Tomažević,M., Problems in Earthquake Strengthening of Old Centres, Meeting on Building Reconstruction, Maribor, 1983.

22. Turnšek,V., Terčelj,S., Sheppard,P., Tomažević,M., The Seismic Resistance of Stone-Masonry Walls and Buildings, Proceedings, 6-ECEE, Dubrovnik,1978.
23. Standard Methodology for the Assessment of Damage Caused by Natural Disasters - Instructions, Official Gazette of Yugoslavia, No. 17, 1979.
24. Law on the Protection of Cultural Monuments, National Gazette of S.R. Croatia, No 7, 1967.

TABLE 1. Areas of Yugoslav seismic zones  
Source: Provisional seismic map of Yugoslavia (Off. Gazette, 49, 1982)

Intensity, MCS Scale	Area in sq.km.	Area in %
5 <sup>0</sup>	5000	1.9
6 <sup>0</sup>	66900	25.2
7 <sup>0</sup>	125650	47.3
8 <sup>0</sup>	51600	19.5
9 <sup>0</sup>	15050	5.7
10 <sup>0</sup>	1000	0.4
===== 265200* =====		100.0 =====

\* including the Adriatic Sea within the line connecting the main islands

TABLE 2. Earthquake resistance of old masonry buildings\*

Wall type	Storey number	Current condition		Strengthened condition	
		Advantage- ous plan	Disadvanta- geous plan	Advantage- ous plan	Disadvanta- geous plan
Brick wall	2	0.19			
	3	0.15			
	4	0.13			
	5	0.12			
Stone wall category I	1	0.16	0.12	0.41	0.30
	2	0.10	0.08	0.25	0.18
	3	0.08	0.06	0.19	0.14
Stone wall category II	1	0.20	0.15	0.72	0.53
	2	0.13	0.10	0.41	0.30
	3	0.10	0.08	0.30	0.22
Stone wall category III	1	0.41	0.30	0.80	0.59
	2	0.25	0.18	0.45	0.33
	3	0.19	0.14	0.33	0.24
Stone wall category IV (grouted)	1			1.45	1.08
	2			0.78	0.58
	3			0.56	0.41

\*) expressed as part of gravity acceleration ( $g=9.81 \text{ m/sec}^2$ )

Actual accelerations:

7<sup>0</sup> MCS      0.05 to 0.10 g  
8<sup>0</sup> MCS      0.10 to 0.20 g  
9<sup>0</sup> MCS      0.20 to 0.40 g

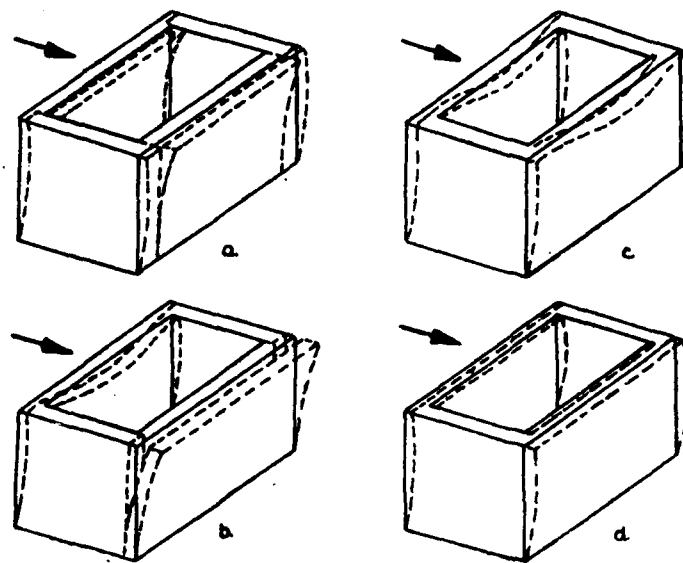
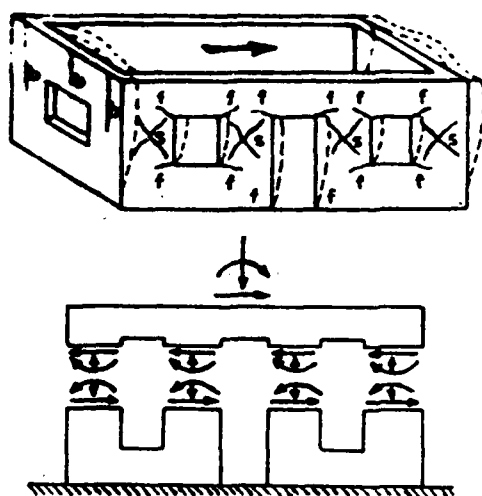
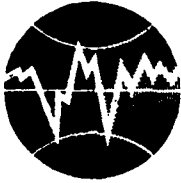


Fig.1 Displacements of a Masonry Building Depending on Wall Connection



- b - cracks due to deflection outside the wall plane
- s - cracks due to main tensile stresses
- f - cracks due to deflection

Fig.2 Mechanism of Masonry Building Collapse



**TURKISH NATIONAL COMMITTEE FOR  
EARTHQUAKE ENGINEERING**

**THIRTEENTH REGIONAL SEMINAR ON EARTQUAKE ENGINEERING**

**September 14-24, 1987 - Istanbul - Turkey**

**The Incredible Seismic Damages to Structures  
During Past Earthquakes**

**K. Kubo**

## The Incredible Seismic Damages to Structures During Past Earthquakes

K. Kubo

### Summary

It is said that earthquake engineering started in 1891, when the strong NOBI Earthquake of M-8.4 attacked the central part of Japan. Until the NOBI Earthquake, no attention was being paid to earthquake-proof construction in most parts of the world. Since 1891, great strides have been made in this field through various efforts of scientists and engineers. There are some seismic damages, however, that cannot be explained even by the advanced knowledge of earthquake engineering, although most seismic damage can be solved theoretically as well as practically. The writer considers that the incredible damages are the blind points of earthquake engineering, and that they are the important research items for future earthquake engineering.

### Introduction

Due to great advancement in earthquake engineering worldwide, some of the seismic damages to structures can be theoretically analyzed and be the source of revision of aseismic codes. These kinds of seismic damages can be prevented from future earthquakes. On the other hand, there are several other earthquake damages which cannot be easily explained, and for which there are few design procedures appropriate for their prevention. The latter damages belong to today's topic, "The Incredible Seismic Damages."

For convenience, the incredible seismic damages will be divided into two groups, Group I and Group II. The mechanism of damage in Group I cannot be easily clarified and therefore there is no way of eliminating seismic failures of this kind. Damage mechanism of the second group is clearly understood, but there is as yet no appropriate or authorized design procedures.

### Structural Damages of Group I

#### a) Performance of Electric Power Transmission Towers:

Before the Izu-Peninsula Earthquake (M=6.9), 1974 occurred, the concrete transmission pole was standing on the cantilever. When the earthquake struck, the impact partially crushed the pole to near ground level. After the earthquake, the pole shifted horizontally and was again standing in the upright position as shown in Slide-1. In this case, the pole was supported by a hinged bearing, and therefore the pole was not a statically stable structure, although it will not overturn. The pole was located near the epicenter.

#### b) Horizontal Movement of RC Girders:

At the time of Fukui Earthquake (M=7.3), 1948, the T-beam reinforced concrete girders shifted horizontally as shown in Slide-2. There was tar paper between the girder and the bridge pier. Among the 13 simply-supported girders, 4 spans shifted horizontally, and

eventually, 2 of them fell down, and the other 2 spans overhanged as shown in Slide-2.

c) Failure of Girder Support:

In the case of Ebino Earthquake ( $M=5.7$ ), 1968, the narrow steel plate connecting the prestressed concrete girders with the bridge pier was broken off from horizontal cracking. This failure cannot be explained unless we consider the large vertical impact acting on the girder. The failure shown in Slide-3 may be similar to the failure pattern mentioned above. Compressive stress caused by the vertical impact, in this case, must have been much larger than the compressive stress due to dead load of the girder.

d) Gate Frame Structure of Maruoka Castle:

Fukui Earthquake, 1948,<sup>1)</sup> overturned the wooden frame of the castle gate of Maruoka castle without any trace of scratching on the pivot hole of the wooden column. Taking into account the existence of the shear steel plate stretching out from the column foundation, the castle gate jumped up nearly higher than the top of the steel plate as shown in Slide-4. This phenomenon is just incredible.

e) Masonry Shrine Gate:

This kind of structure is generally constructed on a footing foundation, and heavy girders are set on top of the structure, whose columns are made of stone, which is a brittle material. Based on these three aspects, it can be concluded that the masonry shrine gate is of very poor structure from the viewpoint of earthquake engineering. The shrine gate in Slide-5 was located near the epicenter of Izu-Peninsula Earthquake, 1974, but the damage to it was very slight - almost no damage.

Structural Damages of Group II

a) Damage to the Banyu Bridge:

This bridge<sup>2)</sup> is located at the estuary of Banyu River to the Sagami Bay, which was the epicenter of the Kanto Earthquake. At the time of the test, it was still under construction. According to the design specification for bridges, substructures, including the bridge piers, had sufficient strength to resist any seismic load acting on the superstructures and substructures. In this case, there was no girder as shown in Slide-6, and the mass of frame of the substructure was not very large, but there were many cracks at the beam-column joints. This damage was caused by the relative movement of the foundation of this bridge caused by ground movement due to liquefaction of sandy ground. There is no clear or authorized design measures for structures against such large ground movement.

b) Failure of the Overpath Bridge:

Measurement of the span length after the Niigata Earthquake,<sup>3)</sup> 1964, revealed that it had become longer by more than 50 cm than the design span. This was the main reason why the main span shown in Slide-7 fell down. A question was raised: Why did the span elongate? This question was answered when the concrete piles of the

bridge foundation were picked up during reconstruction work. Concrete piles were bent as if they had sustained horizontal thrust force applied about their central part. It was clear that horizontal ground movement due to liquefaction was the thrusting force that pushed the concrete piles. This is a similar problem/as a) of this section, that needs to be researched.

c) Opening of Concrete Slab at Juvenile Hall:

Concrete slab of the Juvenile Hall<sup>4)</sup> was broken by the San Fernando Earthquake, 1971, as shown in Slide-8. It was difficult to understand, just after the earthquake, as to why they were broken. Later it was elucidated that this breakage was caused by the ground sliding along the liquefied sand layer of 2-3% slope. Half of the concrete slab of the Juvenile Hall was on the now liquefied ground, and the other half was on the moving ground. The maximum displacement of the landslide reached 1.5 m.

d) Damage to Joseph Jensen Filtration Plant:

The side walls of the in-ground filtration plant<sup>4)</sup> was strongly pushed by an unknown lateral force as shown in Slide-9. This happened at the time of the San Fernando Earthquake, 1971. The lateral force was caused by ground movement sliding along a thin layer of liquefied sand and this force became so great that it demolished the reinforced concrete wall of the filtration plant. Estimation of this lateral force is not easy from the present knowledge of earthquake engineering.

e) Behavior of Arch Bridges:

From observations after the Kanto, Skopje, and Niigata Earthquakes, it can be concluded that an arch bridge shows very good performance during earthquakes and damage sustained by it is very slight. For instance, seismic design coefficient of the Bandai Bridge<sup>3)</sup> in Niigata city in Slide-10 was zero, but it withstood earthquakes better than any other type of bridge in the Niigata area. What is the most appropriate seismic design coefficient for an arch bridge?

f) Underground Structures Crossing Fault:

According to data obtained from past earthquakes, buried pipes show high seismic damage ratio, which is defined by the number of collapsed pipes per unit length of buried pipe near its crossing point with fault. Protection of buried pipes at subway tunnels against fault is now a new research item, and several countermeasure proposals have already been published, but not authorized. Slide-11 shows the damage to a sewage concrete pipeline deformed by the Tanshan Earthquake in 1976.

Concluding Remarks

The writer cited only a few of the incredible seismic damages. More and more incredible damages will probably be reported around the world. They are just the blind points of earthquake engineering. Turkish as well as Chinese engineers may have had similar experience in seismic damage which are very special and incredible. The writer is of the opinion that it may be worthwhile to investigate incredible

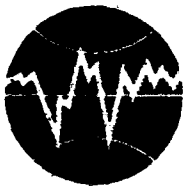


seismic damages, and hopes that this study will provide a new way to advance the progress of earthquake engineering.

In order to collect various data on seismic damages which are difficult to understand, international cooperative work is necessary because many countries have their own special incredible seismic damages.

#### REFERENCES

1. Fukui Earthquake Damage Investigation Committee, Japan Science Council, "Report on Seismic Damages to Civil Engineering Structures," 1950.
2. Seismic Damage Investigation Committee, Japan Society of Civil Engineers, "Report on Seismic Damages by Kanto Earthquake 1923," 1926.
3. Japan Society of Civil Engineers, "Report on Seismic Damages by Niigata Earthquake 1964," 1966.
4. U.S. Department of Commerce, "San Fernando, California Earthquake of February 9, 1979," 1973.



**TURKISH NATIONAL COMMITTEE FOR  
EARTHQUAKE ENGINEERING**

**THIRTEENTH REGIONAL SEMINAR ON EARTHQUAKE ENGINEERING**

**September 14-24, 1987 - Istanbul - Turkey**

**SIMPLIFIED METHOD FOR DETERMINATION OF INELASTIC  
DEFORMATIONS IN BUILDINGS EXPOSED TO REAL SEISMIC  
EFFECTS**

**Dr. Trifun PASKALOV, Professor**

Institute of Earthquake Engineering and Engineering Seismology  
University "Kiril and Metodij" - Skopje, Yugoslavia

SIMPLIFIED METHOD FOR DETERMINATION OF INELASTIC  
DEFORMATIONS IN BUILDINGS EXPOSED TO REAL SEISMIC  
EFFECTS

Dr. Trifun PASKALOV, Professor

Skopje, May 1987

## FOREWORD

The idea for this work appeared on the occasion of the lecture titled "Practical Methods for Considering the Nonlinear Deformations during Seismic Effects", which was given by Acad. Prof. Dr. Schio Germanovich Napetvaridze from Tbilisi, USSR, for the participants to the Course on Low-Cost Housing Construction in Seismic Regions, held in November 1986. On the other hand, there has been a permanent need of explaining the inelastic behaviour of buildings when exposed to intensive seismic effects, to the engineers-designers in a simplified manner, understandable for their level of knowledge of the principles of linear and nonlinear structural dynamics.

The work consists of only one chapter, in which the first part is a sublimated analytical approach for solving the problem, and the second one is an illustrative example, through which the derived methodology has been applied on a twelve-floor reinforced-concrete building constructed with frames and diaphragms as bearing elements.

In this work, the author does not intend to eliminate the exact method for determination of the inelastic response of these buildings through direct solving of the equation of motion, but only to give an evaluation of the kind and size of the inelastic deformations when there is a lack of appropriate computer programs for performance of more refined calculations.

The Author

## SIMPLIFIED METHOD FOR DETERMINATION OF INELASTIC DEFORMATIONS IN BUILDING CONSTRUCTION STRUCTURES EXPOSED TO REAL SEISMIC EFFECTS

Seismic stability of structures is a primary obligation of the human lives protection and reduction of damage due to the effects of major earthquakes. For this purpose, countries exposed to effects of different earthquakes provide preventive protection by strict application of requirements specified in their technical codes in the field of civil engineering. Thus, in the Socialist Federal Republic of Yugoslavia, protection of building structures is provided by application of the requirements in the "Book of Regulations for the Technical Normatives for Design and Construction of Building Structures in Seismic Regions" - Official Register of SFRY No. 49/82 and No. 29/83 (2)\*. According to this Book of Regulations, in some cases, if not categorized structures or typified structures constructed in series are concerned, besides the application of the simplified statical method of earthquake engineering, calculation should be performed of the dynamic nonlinear response of the structural systems, paying attention to the elasto-plastic features of the built-in materials. This is regulated by Articles No. 2, 6, 7, 8, 39 and 40 of the above-mentioned Book of Regulations (2). It is the application of these regulations that brings about confusion among engineers-designers, because this subject material is not included in regular studies at most of the civil engineering departments in the country. This fact induced the author of this work to try and in the simplest way simplify the procedure for determining the nonlinear response of the systems with one or more degrees of freedom, by direct application of the assumptions from the linear spectral theory of earthquake engineering. The methodology suggested here is based on the concept of balance of the deformation energy in the normal elastic-plastic systems with that of the equivalent elastic systems, where theoretically, elastic limit does not exist. The procedure itself is considered to be rather simple, to enable quick and efficient analysis without the use of the modern computer technique, which is not excluded, but, on the contrary, is very suitable with respect to elaboration of appropriate computer program. The only difficulty from the mathematical point of view

\*Numbers in brackets indicate the listed literature.

arises when solving the eigen values of the considered structure in order to solve the periods and shapes of free vibrations, which are taken into account in these analyses. This part of the calculation is not included here, and it may be referred to in two previous papers by the same author (3,4) where detailed description of this procedure can be found.

# 1. Practical Methods for Considering Nonlinear Deformations during Seismic Effects

The basic concept consists of approximate replacement of a multi-mass linear system of a building or a structure (Fig. 1a) by a single-degree-of-freedom system (Fig. 1b), taking the nonlinear structural deformation into consideration in order to make more economical use of strength reserves of the structural elements.

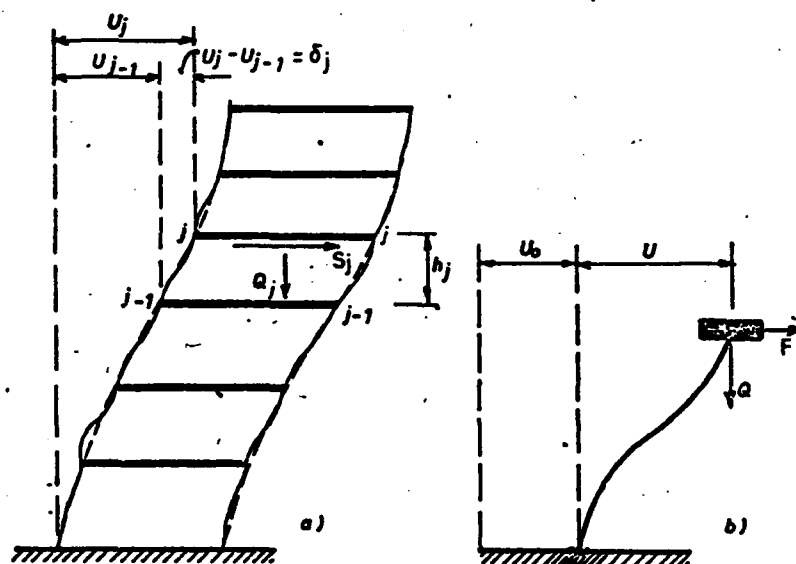


Fig. 1. Multi- and Single-Degree-of-Freedom Systems

For simpler calculations, the "force-displacement" diagram of the single-degree-of-freedom system presented in Fig. 1b is allowed to be simplified in the form of the Prandtl's diagram (Fig. 2).

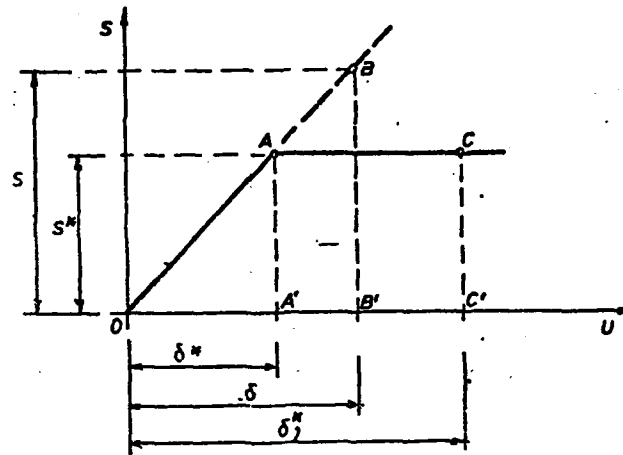


Fig. 2 "Force-Displacement" Diagram of the Prandle's Type

The notations in the above figure are:

$F^*$  and  $U^*$  - boundary elastic force corresponding to the elastic displacement of a single-mass system.

$K$  - system rigidity, obtained as

$$K = F^*/U^* = \operatorname{tg} \alpha \quad \dots (1)$$

$U_1^*$  - entire horizontal structural displacement, obtained as

$$U_1^* = U^* + \Delta U^* \quad \dots (2)$$

where  $\Delta U^*$  is the residual (permanent) displacement.

$F$  and  $U$  - horizontal seismic force and corresponding displacement to occur if the system behaves elastically for any deformation value.

$$F = K \cdot U \quad \dots (3)$$

On the other hand, the potential energy of the deformed elastic system is equal to the triangle  $OBB'$  area and according to (3) is:

$$E = F \cdot U / 2 = F^2 / (2K) \quad \dots (4)$$

The potential energy of the real system in the elastic deformation range is equal to the  $OAA'$  triangle, and according to (1) is:

$$E^* = F^* \cdot U^* / 2 = F^{*2} / (2K) \quad \dots (5)$$

The irretrievable energy after the development of plastic deformations is equal to the triangle A'ACC' area, and it is obtained as

$$E_1^* = F^* (U_1^* - U^*) = F^* U^* \left( \frac{U_1^*}{U^*} - 1 \right) \quad \dots (6)$$

or, respecting the relation in (1) it is obtained that

$$E_1^* = F^{*2} (\mu - 1) / K \quad \dots (7)$$

where  $\mu = U_1^* / U^*$  is the structural ductility coefficient.

From the energy balance, it is obtained

$$E = E^* + E_1^*$$

or, respecting the relations in (4), (5) and (7),

$$F^2 = F^{*2} + 2F^{*2} (\mu - 1)$$

is obtained, i.e.

$$F^* = F / (2\mu - 1)^{1/2} \quad \dots (8)$$

It should be emphasized that for  $\mu > 1$   $F$  is always greater than  $F^*$  and thus, if for example  $\mu = 4$ ,  $F^* = 0.38 F$ . Equation (8) points to the fact that there is a possibility that plastic deformations develop in the structure, the building will be exposed to significantly weaker force compared with the one that would be obtained if the linear theory of earthquake engineering was applied.

Equation (8) may be used with sufficient accuracy in linear multi degree-of-freedom systems as well, which predominantly suffer shear deformations (Shear-Type Structures). For example, the structure presented in Fig. 1a is of this type. The only difference is that instead of  $F$  and  $F^*$  forces (Fig. 1b), the corresponding transverse  $S_j$  and  $S_j^*$  forces occur (Fig. 1a).

According to the spectral theory of earthquake engineering, it is known that the horizontal elastic displacements of the "j"-th transversal cross-section of the structure are:

$$U_{ij} = a_0 \beta(T_i) \phi_{ij} \gamma_i T_i^2 / (2\pi)^2 \quad \dots (9)$$



with the following notations:

"i" - number of the normal mode shape

$a_0$  - peak foundation acceleration

$\beta(T_i)$  - dynamics coefficient, depending on the natural vibrations period,  $T_i$ , in the "i"-th mode shape, and on the structural properties for elastic energy dissipation

$\phi_{ij}$  - ordinate of the normalized "i"-th mode shape to vibrations in the "j"-th structural cross-section

$\gamma_i$  - factor of "i"-th mode participation in the overall system behaviour, obtained as

$$\gamma_i = \{\phi\}_i^T |M| \{1\} / \{\phi\}_i^T |M| \{\phi\}_i = \sum_{j=1}^N m_j \phi_{ij} / \sum_{j=1}^N m_j \phi_{ij}^2 \quad \dots (10)$$

$\{\phi\}_i$  - vector of the normalized "i"-th mode shape

$|M|$  - inertial matrix of the system

$m_j$  - concentrated mass in the "j"-th cross-section

$N$  - definite number of degrees of freedom.

By analogy to the expression (9), the displacement of the "j"-th cross-section of the system, for the same "i"-th vibration mode, is:

$$U_{ij-1} = a_0 \beta(T_i) \cdot T_i^2 \cdot \gamma_i \phi_{ij-1} / (4\pi^2) \quad \dots (11)$$

On the other hand, the transverse force which would be generated in this cross-section according to the assumptions in the structural theory, would be:

$$S_{ij} = K_j (U_{ij} - U_{ij-1}) = K_j \delta_{ij} \quad \dots (12)$$

where:

$S_{ij}$  - transverse elastic force on the "j"-th floor at the "i"-th vibration mode

$\delta_{ij}$  - relative interstory elastic drift.

Because expression (12), through relations (9) and (11), defines the maximum values of the transverse forces, the total transverse force at the "j"-th floor with presence of more vibration modes will be determined as a mean square value of the corresponding transverse forces, or

$$S_j = \frac{a_0 K_j}{4\pi^2} \left\{ \sum_{i=1}^n [\beta(T_i) \cdot T_i^2 \cdot \gamma_i (\phi_{ij} - \phi_{ij-1})]^2 \right\}^{1/2} \quad \dots (13)$$

where  $K_j$  - rigidity of the "j"-th floor (layer)

$n$  - number of calculated mode shapes.

The analogy between Equations (3) and (13) enables application of the procedure for single-degree-of-freedom systems, as it was earlier stated, which is:

$$S_j^* = S_j / (2\mu_j - 1)^{1/2} \quad \dots (14)$$

where the ductility coefficient, by analogy with (7) and (8), depends upon the structural type and the material of the "j"-th structural element.

The residual displacement of the simplified model (Fig. 1b), according to (2) and respecting (8), is determined through

$$\Delta U^* = (\mu - 1) U^* = (\mu - 1) \frac{F^*}{K} \quad \dots (15)$$

Now, if according to Equation (9) and Fig. 1b the seismic force (of a single-mass system) is determined, it will be obtained that

$$F = \frac{a_0}{g} Q\beta(T) \quad \dots (16)$$

which gives expression (15) for obtaining the residual floor displacement the following form:

$$\Delta U^* = \frac{(\mu - 1)}{(2\mu - 1)^{1/2}} \frac{a_0}{4\pi^2} \beta(T) \cdot T^2 \quad \dots (17)$$

where, according to (1)

$$U^* = F^* / K ; \quad K = \frac{Q}{g} \omega^2 = \frac{Q}{g} \frac{4\pi^2}{T^2}$$

In the above expressions "Q" represents mass weight, and "g" is acceleration due to gravity.

By analogy to Equation (15) and respecting (14), for the multi-mass (multi-degree-of-freedom - Fig. 1a) system, it may be written

$$\Delta \delta_j^* = \frac{(\mu_j - 1)}{(2\mu_j - 1)^{1/2}} \frac{S_j}{K_j} \quad \dots (18)$$

where the value of the transverse force "S<sub>j</sub>" is determined according to expression (13). On the other hand, building codes in many countries restrict the residual floor deformations "ΔU\*" through defined ductility coefficients "μ". Now, respecting expression (13), the residual displacement of the "j"-th floor obtains the following final form:

$$\Delta \delta_j^* = \frac{a_0}{4\pi^2} \frac{(\mu_j - 1)}{(2\mu_j - 1)^{1/2}} \left\{ \sum_{i=1}^n [\beta(T_i) T_i^2 \gamma_i (\phi_{ij} - \phi_{ij-1})]^2 \right\}^{1/2} \quad \dots (19)$$

The diagram of deformation of the building structures without strengthening (of the Prandtl's type) is not the only one possible. It is often in accordance with test data of reinforced-concrete elements with relatively low percentage of reinforcement, or elements of light-reinforcement masonry.

For the structural elements of different materials, the deformation diagrams may have different form. However, most of them can be adopted in the forms presented in Fig. 3, diagram with strength increasing (Fig. 4a) or reducing (Fig. 3b).

For both cases of increasing or reducing the strength, the derivations are performed through energies balance, as it was done earlier. Here, for easier derivation, strength reducing in the post-elastic range is accepted as an elastic rigidity relation

$$K_1 = \operatorname{tg} \alpha_1 = r K = -r \operatorname{tg} \alpha \quad \dots (19)$$

where "r" may be positive (Fig. 3a) or negative (Fig. 3b).

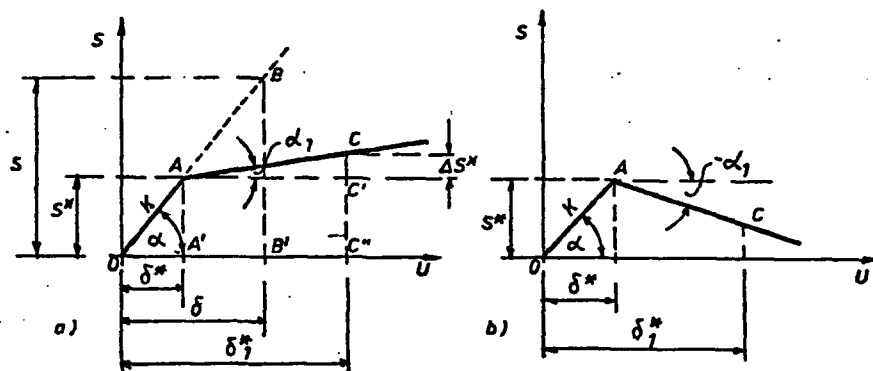


Fig. 3. Force-Displacement Relationship with Increased or Reduced Stiffness

$$E = \frac{1}{2} F \cdot U = \frac{1}{2} \frac{F^2}{K} \quad \dots (20)$$

$$E^* = \frac{1}{2} F^* \cdot U^* = \frac{1}{2} \frac{F^{*2}}{K} \quad \dots (21)$$

$$E_1^* = (U_1^* - U^*) F^* + (U_1^* - U^*) r K (U_1^* - U^*)$$

$$E_1^* = (\mu - 1) F^* U^* + (\mu - 1)^2 r F^* U^*$$

$$E_1^* = (\mu - 1) [1 + r(\mu - 1)] \frac{F^{*2}}{K} \quad \dots (22)$$

Applying the energy balance,  $E = E^* + E_1^*$ , it is obtained

$$F^2 = F^{*2} \{1 + 2(\mu - 1) [1 + r(\mu - 1)]\}$$

$$F^* = F / \{1 + 2(\mu - 1) [1 + r(\mu - 1)]\}^{1/2} \quad \dots (23)$$

Now, if the residual displacement of single-mass system (Fig. 1) is to be determined, expression (15) should be used, being valid here as well. Respecting (23) and (16), it is obtained

$$\Delta U^* = \frac{a_0}{4\pi^2} \frac{(\mu - 1)}{\{1 + 2(\mu - 1) [1 + r(\mu - 1)]\}^{1/2}} \beta(T) \cdot T^2 \quad \dots (24)$$

and for the multi-mass system (Fig. 1a)

$$\Delta \delta_j^* = \frac{a_0}{4\pi^2} \frac{(\mu_j - 1)}{\{1 + 2(\mu_j - 1) [1 + r_j(\mu_j - 1)]\}^{1/2}} \left\{ \sum_{i=1}^n [\beta(T_i) T_i^2 \gamma_i (\phi_{ij} - \phi_{ij-1})] \right\}^{1/2} \quad \dots (25)$$

For  $r = 0$ , expressions (23), (24) and (25) become identical with (8), (17) and (19), which is kind of proof that the first ones represent only special cases of the latter. On the other hand, it is evident that for  $r = 0$ , expression (25) gives higher value than (19), and for  $r < 0$  lower, which is physically logical.

Equation (24) or (25) are suitable for estimation of the maximum residual deformations, both for the single- and multi-degree-of-freedom systems. But, for this purpose, the actual ductility coefficients " $\mu$ " should be determined. This may be done using expression (23), which will give a new expression for determining the ductility coefficient as a function of the seismic force " $F$ " (16) and yield force " $F^*$ ", i.e. the transverse force " $S_j$ " (13) and the yield force " $S_j^*$ ".

$$\mu_j = 1 + \frac{\{1 + 2r_j[(S_j/S_j^*)^2 - 1]\}^{1/2} - 1}{2r_j} \quad \dots (26)$$

The proposed procedure for estimation of the maximum residual deformations may be illustrated on a practical example of a building of twelve floor levels. The example refers to the same building observed under "Practical Example, Computation for a Building Having GF+11 Storeys", presented in Reference (4).

The characteristic plan of the building is shown in Fig. 4, and the vertical cross-section in Fig. 5.

It is obvious from the plan that if the building vibrates in the transverse cross-section, four identical frames (R) and four identical diaphragms (D) appear to be vertical bearing elements. The inertial and rigidity characteristics, and the dynamic properties of the building have been previously determined, and they are directly used. All masses are approximated as one as follows:  $m_1 = m_2 = m = 2.95 \text{ kNcm}^{-1} \text{sec}^2$ .

After solving the eigen-value problem of the building, the following values of the natural periods of vibrations are obtained for the first three mode shapes:

$$T_1 = 1,250 \text{ s}; \quad T_2 = 0,477 \text{ s} \quad \text{и} \quad T_3 = 0,294 \text{ s}$$

and the corresponding eigen vectors are given in the following Table 1.

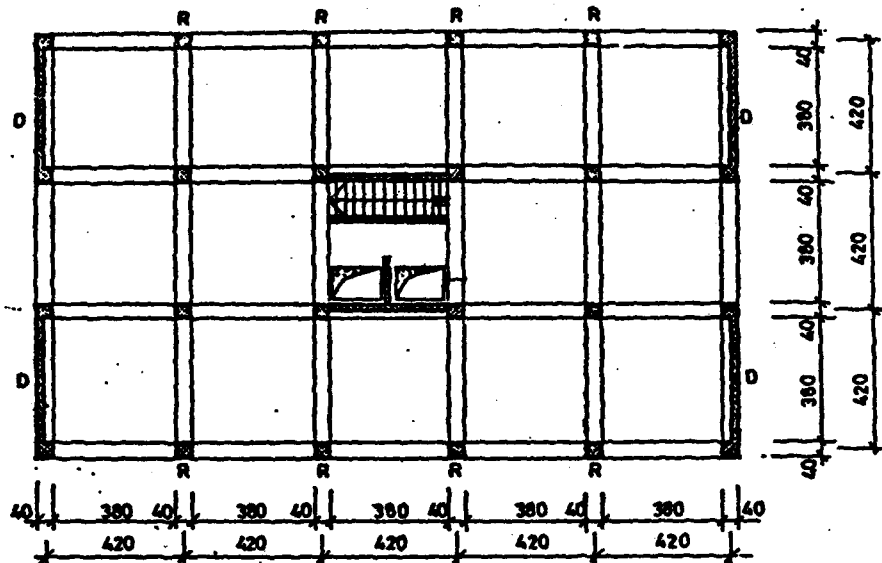


Fig. 4. Characteristic Plan

Considering the fact that under the effect of a real earthquake the foundation accelerations are significantly higher than those defined by the technical regulations, consequently, forces are generated in the structure which are significantly stronger than the normative ones, i.e. those which are determined according to regulations. In order to illustrate this procedure, the proposed structure was tested under the effects of several characteristic earthquakes, recorded in California (USA) and Montenegro (Yugoslavia). For this purpose, selected were the earthquakes of Imperial Valley, El Centro - 1940, SOOE, San Fernando - 1971, 15250 Ventura Blvd. b smth N11F, Montenegro - 1979 - Ulcinj, Albatros and Petrovac, all of them normalized at peak acceleration of 0.35 g. The characteristic acceleration spectra of these earthquakes, for 5% ( $\lambda = 0.05$ ) damping, are given in Fig. 6, normalized in the form of dynamics coefficients " $\beta(T)$ ". The forces generated in the structure depend upon the spectrum of each earthquakes, the peak foundation acceleration and its dynamic characteristics, which is evident from expression (13), i.e. they are determined according to the following expressions:

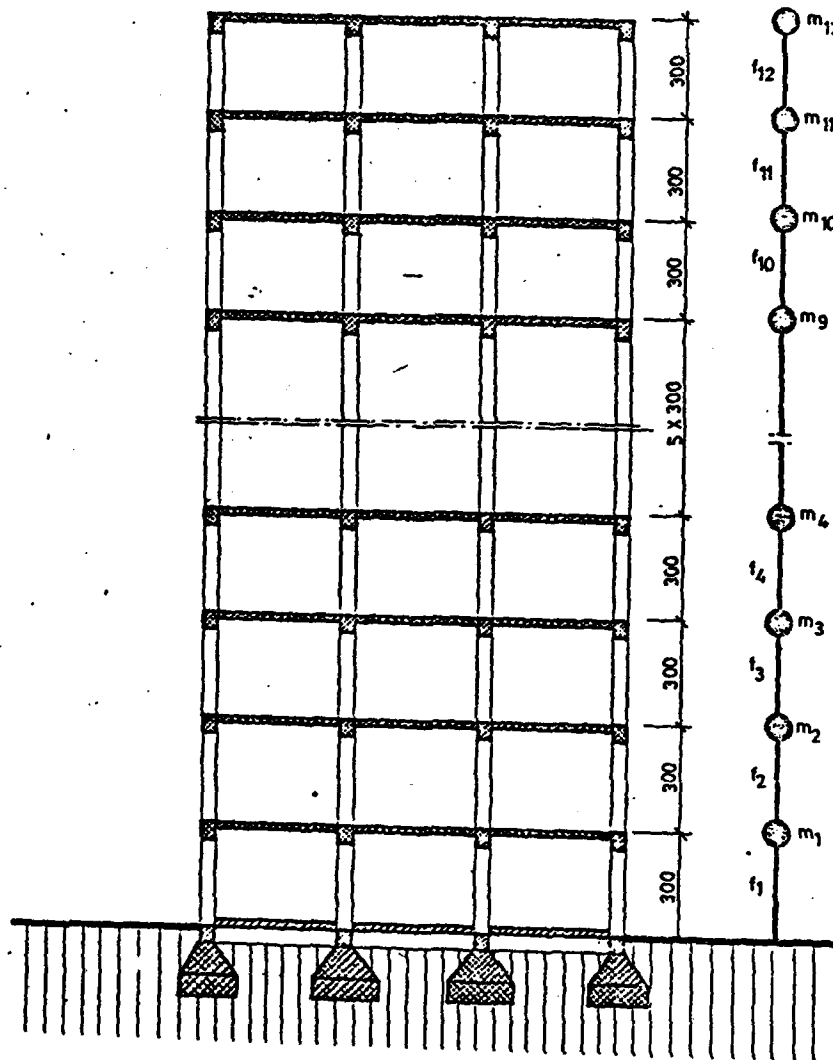


Fig. 5 Vertical Cross-Section

$$S_j = \frac{K_j a_0}{4\pi^2} \left\{ \sum_{i=1}^n [\beta(T_i) T_i^2 \gamma_i \bar{\phi}_{ij}]^2 \right\}^{1/2}$$

$$\gamma_i = \frac{\sum_{j=1}^N m_j \phi_{ij}}{\left( \sum_{j=1}^N m_j \phi_{ij}^2 \right)} = \frac{\sum_{j=1}^n \phi_{ij}}{\sum_{j=1}^N \phi_{ij}^2} \quad (\text{for } m_j = m_k)$$

$$\bar{\phi}_{ij} = \phi_{ij} - \phi_{ij-1}$$

These forces are determined in a tabular way, as shown in Table 2.

## CONCLUSIONS

Based on the developed methodology for calculation and the results obtained for the illustrated example, some points may be emphasized which lead to the following conclusions:

1. The proposed procedure cannot be considered as a thorough replacement of the exact method for calculation of residual structural displacements which is based on a strict solution of the the system of nonlinear differential equations of motion.

2. Definition of the elasticity limit of each storey of the considered building example has been performed in a rather simplified way. In other words, it has been assumed that the reinforcement of the bearing elements be determined on the principle of allowed stresses in the reinforcement ( $\sigma_a = 210$  MPa) under the effect of normative seismic forces, " $F_n$ ", i.e. corresponding transverse forces, " $S_n$ ". Considering the fact that the reinforcement starts yielding under a stress  $\sigma_a = 240$  MPa, the transverse yield stresses " $S_j^*$ " are determined by multiplying the normative " $S_n$ " with the factor  $F = 240/210 = 1.14$  (See Table 1).

3. In order to check the efficiency and usability of this procedure, corresponding inelastic system responses of the example has been calculated by means of step-by-step integration of the differential equations for the effects of the same earthquakes that have been a subject of consideration in the previous pages. The maximum values of the residual interstory drifts obtained in the way, are shifted in Tables 3 and 4 as " $\Delta\delta_j^*$ " - EXACT. By a simple comparison of the corresponding results (column 6 and 7, i.e. 10 and 11), it may be concluded that the values of the corresponding residual displacements determined according to the simplified methodology and according to the exact solution of the differential equations of nonlinear dynamics are rather similar along all storey heights, except for the upper and lower storeys where a slight difference occurs, but in tolerable limits.



## REFERENCES

1. Napetvaridze, Š.G. (1986): "Practical Methods for Considering the Nonlinear Deformations Due to Seismic Effects", Invited Lecture on the Course on Low-Cost Residential Buildings in Seismic Regions, IZIIS, Skopje, Yugoslavia (in Russian).
2. Federal Institute of Standards (1982, 1983): "Regulation Book for the Technical Normatives for Design and Construction of Building Constructions in Seismic Regions" - Official Register of SFRY No. 49/82 and No. 29/83, Belgrade, Yugoslavia (in Serbo-Croatian).
3. Paskalov, T. (1968): "Determinations of Seismic Forces in Building Structural Types", Publication No. 13, IZIIS, Skopje, Yugoslavia (in Macedonian).
4. Paskalov, T. (1982): "Determination of Seismic Effects on Building Constructions", Published by "Tehnika" - "Naše Građevinarstvo" No. 5 and No. 6, Belgrade, Yugoslavia (in Serbo-Croatian).

## **APPENDIX: TABLES AND FIGURES**

Table 1. Rigidity, Dynamic and Elastic-Plastic Characteristics of the System

Storey "i"	Rigid. $K_j$ (kN/cm)	$\phi_1$	$\phi_2$	$\phi_3$	Seis. Force $F_n$	Trans. For $S_n$	Yield. For. $S_j$	$\sigma_j^* = s_j^*/K_j$	$V_j$
12	1720	1,0000	-1,0000	1,0000	546,10	546,10	622,55	0,3619	0,100
11	1780	0,9569	-0,7031	0,2147	233,15	779,25	888,34	0,4991	"
10	1900	0,8751	-0,2145	-0,7070	211,96	991,21	1129,98	0,5707	"
9	2220	0,7686	0,2801	-1,0533	190,76	1181,77	1347,22	0,6067	"
8	2680	0,6480	0,6568	-0,7214	169,56	1351,53	1540,74	0,5749	"
7	3100	0,5299	0,8467	-0,0829	148,37	1499,90	1709,87	0,5516	"
6	3590	0,4151	0,8663	0,5052	127,17	1627,07	1854,86	0,5168	"
5	4200	0,3073	0,7626	0,8230	105,98	1733,05	1975,68	0,4704	"
4	5050	0,2097	0,5812	0,6300	84,78	1817,83	2072,33	0,4104	"
3	6420	0,1254	0,3716	0,6138	63,59	1881,42	2144,82	0,3341	"
2	11780	0,0578	0,1771	0,3146	42,39	1923,81	2193,14	0,1862	"
1	21690	0,0204	0,0634	0,1155	21,20	1945,01	2217,31	0,1022	"

$$Y = 1,3744 \quad 0,5831 \quad 0,3499$$

According to the Book of Regulations (2), the seismic forces are:

$$ES = K_0 \cdot K_s \cdot K_d \cdot K_p \cdot G = 1,0 \times 0,10 \times 0,56 \times (12 \times 2,95 \times 981) = 1945 \text{ kN.}$$

$F_n$  - normative seismic force obtained and distributed according to the Book of Regulations

$S_n$  - corresponding transverse force

$S_n^*$  - transverse force initiating yielding of reinforcement

$\delta_j$  - limit of the elastic interstorey drift

Table 2. Determination of Seismic Forces

Storey "j"	$K_j \frac{a_0}{4 \pi^2}$	$\bar{\phi}_{1j}$	$\bar{\phi}_{2j}$	$\bar{\phi}_{3j}$	El Centro	San Fernando	Petovac	Ulcinj Albatros
1	2	3	4	5	$S_j$	$S_j$	$S_j$	$S_j$
12	14887	0,0431	-0,2969	0,7853	1920	1572	2163	2181
11	15406	0,0818	-0,4886	0,9217	3339	2604	3623	3696
10	17131	0,1065	-0,4946	0,3463	4162	3208	4258	4454
9	19214	0,1206	-0,3767	-0,3319	4658	3827	4249	4853
8	23195	0,1181	-0,1869	-0,6398	5066	4496	4051	5187
7	26830	0,1148	-0,0226	-0,5881	5482	4972	4065	5545
6	31071	0,1078	0,1037	-0,3178	5979	5306	4520	6026
5	36351	0,0976	0,1814	-0,0070	6541	5630	5294	6646
4	43708	0,0843	0,2096	0,2162	7077	5984	6091	7287
3	55565	0,0676	0,1945	0,2992	7459	6268	6673	7766
2	101956	0,0374	0,1137	0,1991	7694	6461	6992	8054
1	187727	0,0204	0,0643	0,1155	7804	6539	7164	8194

Table 3. Ductility Coefficients and Maximum Residual Displacements

"j"	S <sub>j</sub> <sup>*</sup>	δ <sub>j</sub> <sup>*</sup>	El Centro - 1940 Earthquake				Ulcinj-2 - 1979 Earthquake				
			S <sub>j</sub>	μ <sub>j</sub>	Δδ <sub>j</sub> <sup>*</sup>	Δδ <sub>j</sub> <sup>*</sup> exact:	S <sub>j</sub>	μ <sub>j</sub>	Δδ <sub>j</sub> <sup>*</sup>	Δδ <sub>j</sub> <sup>*</sup> exact.	
1	2	3	4	5	6	7	8	9	10	11	
12	623	0,3619	1920	2,8003	0,6515	0,4004	2181	3,2897	0,8286	0,6514	
11	888	0,4991	3339	3,6057	1,3005	0,7009	3696	4,1123	1,5533	1,0009	
10	1130	0,5707	4162	3,5110	1,4330	1,1293	4454	3,8320	1,6162	1,2293	
9	1347	0,6067	4658	3,2385	1,3581	1,0933	4853	3,4129	1,4639	1,0933	
8	1540	0,5749	5066	3,0394	1,1725	1,2251	5187	3,1317	1,2255	0,9251	
7	1709	0,5516	5482	2,9443	1,0736	1,1484	5545	2,9870	1,1,0960	0,8821	
6	1854	0,5168	5979	2,9642	1,0151	1,0832	6026	2,9936	1,0303	0,8832	
5	1976	0,4704	6541	3,0636	0,9707	0,9296	6646	3,1260	1,0001	1,1760	
4	2072	0,4104	7077	3,1878	0,8979	0,8208	7287	3,3090	0,9476	1,2896	
3	2145	0,3341	7459	3,2616	0,7556	0,7016	7766	3,4344	0,7465	1,3364	
2	2193	0,1862	7694	3,2988	0,4280	0,5142	8054	3,4980	0,4651	0,8938	
1	2217	0,1022	7804	3,3128	0,2364	0,3577	8194	3,5267	0,2582	0,5978	

$$\mu_j = 1 + \frac{(1+r_j)(S_j/S_j^*)^2 - 1}{2r_j}^{1/2} - 1; \quad \Delta\delta_j^* = (\mu_j - 1) \delta_j^*$$

Table 4. Ductility Coefficients and Maximum Residual Displacements

Storey "j"	$S_j^*$ (kN)	$\delta_j^*$ (cm)	Petrovac - 1979 Earthquake				San Fernando - 1971 Earthquake			
			$S_j$	$\mu_j$	$\Delta \delta_j^*$	$\Delta \delta_j^*$ exact.	$S_j$	$\mu_j$	$\Delta \delta_j^*$	$\Delta \delta_j^*$ exact.
1	2	3	4	5	6	7	8	9	10	11
12	623	0,3619	2163	3,2550	0,8161	0,6152	1572	2,1982	0,4336	
11	388	0,4991	3623	4,0072	1,5009	1,0009	2604	2,6331	0,8151	
10	1130	0,5707	4258	3,6156	1,4927	1,4293	3206	2,5287	0,8724	
9	1347	0,6057	4249	2,8830	1,1424	1,2933	3827	2,5330	0,9301	
6	1540	0,5749	4051	2,3087	0,7524	0,8251	4496	2,6188	0,9306	
7	1709	0,5516	4065	2,0534	0,5811	0,6484	4972	2,6076	0,8868	
6	1854	0,5168	4520	2,1122	0,5748	0,5168	5306	2,5556	0,8039	
5	1976	0,4704	5294	2,5596	0,6396	0,5174	5630	2,5428	0,7253	
4	2072	0,4104	6091	2,6411	0,6735	0,6896	5984	2,5842	9,6502	
3	2145	0,3341	6673	2,8334	0,6125	0,7659	6268	2,6217	0,5418	
2	2193	0,1662	6992	2,9220	0,3579	0,5958	6461	2,6483	0,3069	
1	2217	0,1022	7164	2,9717	0,2015	0,3978	6539	2,6520	0,1688	

Table 5. Numerical Values of Spectral Dynamics Coefficients

Earthquake	T	0.05	0.10	0.15	0.20	0.25	0.30	0.35	0.40	0.45	0.50	0.55	0.60	0.65	0.70	0.75	0.80
Imperial Valley, El Centro - 1940	$\beta(T)$	1.340	1.628	1.622	1.849	2.531	2.024	1.860	1.766	2.291	2.400	2.633	2.466	2.119	1.786	1.677	1.576
Comp. SCOE $\tau_0 = 341.70$	T	0.85	0.90	0.95	1.00	1.10	1.20	1.30	1.40	1.50	1.60	1.70	1.80	1.90	2.00	2.20	2.40
	$\beta(T)$	1.717	1.547	1.556	1.487	1.111	0.950	0.680	0.520	0.545	0.560	0.537	0.514	0.497	0.511	0.543	0.545
San Fernando, 15250 Ventura Blvd Bunt N11E	T	0.05	0.10	0.15	0.20	0.25	0.30	0.35	0.40	0.45	0.50	0.55	0.60	0.65	0.70	0.75	0.80
$\tau_0 = 479.60$	$\beta(T)$	1.041	1.383	2.330	3.028	3.611	2.624	2.619	2.988	1.371	1.138	1.290	0.996	1.072	0.969	0.996	0.849
	T	0.85	0.90	0.95	1.00	1.10	1.20	1.30	1.40	1.50	1.60	1.70	1.80	1.90	2.00	2.20	2.40
	$\beta(T)$	0.689	0.774	0.778	0.747	0.912	0.778	0.671	0.720	0.912	1.312	1.512	1.325	1.023	0.903	0.836	0.596
Monte Negro, Petrovac - 1979	T	0.05	0.10	0.15	0.20	0.25	0.30	0.35	0.40	0.45	0.50	0.55	0.60	0.65	0.70	0.75	0.80
Comp. N-S $\tau_0 = 427.30$	$\beta(T)$	0.914	1.139	1.199	2.007	2.260	2.168	2.393	3.170	3.661	2.720	2.761	3.007	3.272	2.577	1.892	1.353
	T	0.85	0.90	0.95	1.00	1.10	1.20	1.30	1.40	1.50	1.60	1.70	1.80	1.90	2.00	2.20	2.40
	$\beta(T)$	1.186	1.366	1.401	1.274	0.968	0.586	0.599	0.634	0.552	0.380	0.264	0.256	0.248	0.233	0.223	0.176
Monte Negro, Ulcinj - Albaros 1973	T	0.05	0.10	0.15	0.20	0.25	0.30	0.35	0.40	0.45	0.50	0.55	0.60	0.65	0.70	0.75	0.80
Comp $\tau_0 = 219.10$	$\beta(T)$	0.963	1.498	2.402	1.714	1.936	2.788	2.002	1.970	2.564	2.870	2.748	1.937	1.570	1.156	0.810	0.859
	T	0.85	0.90	0.95	1.00	1.10	1.20	1.30	1.40	1.50	1.60	1.70	1.80	1.90	2.00	2.20	2.40
	$\beta(T)$	0.922	0.792	0.702	0.832	1.138	0.976	0.652	0.621	0.589	0.544	0.504	0.508	0.486	0.454	0.432	0.475

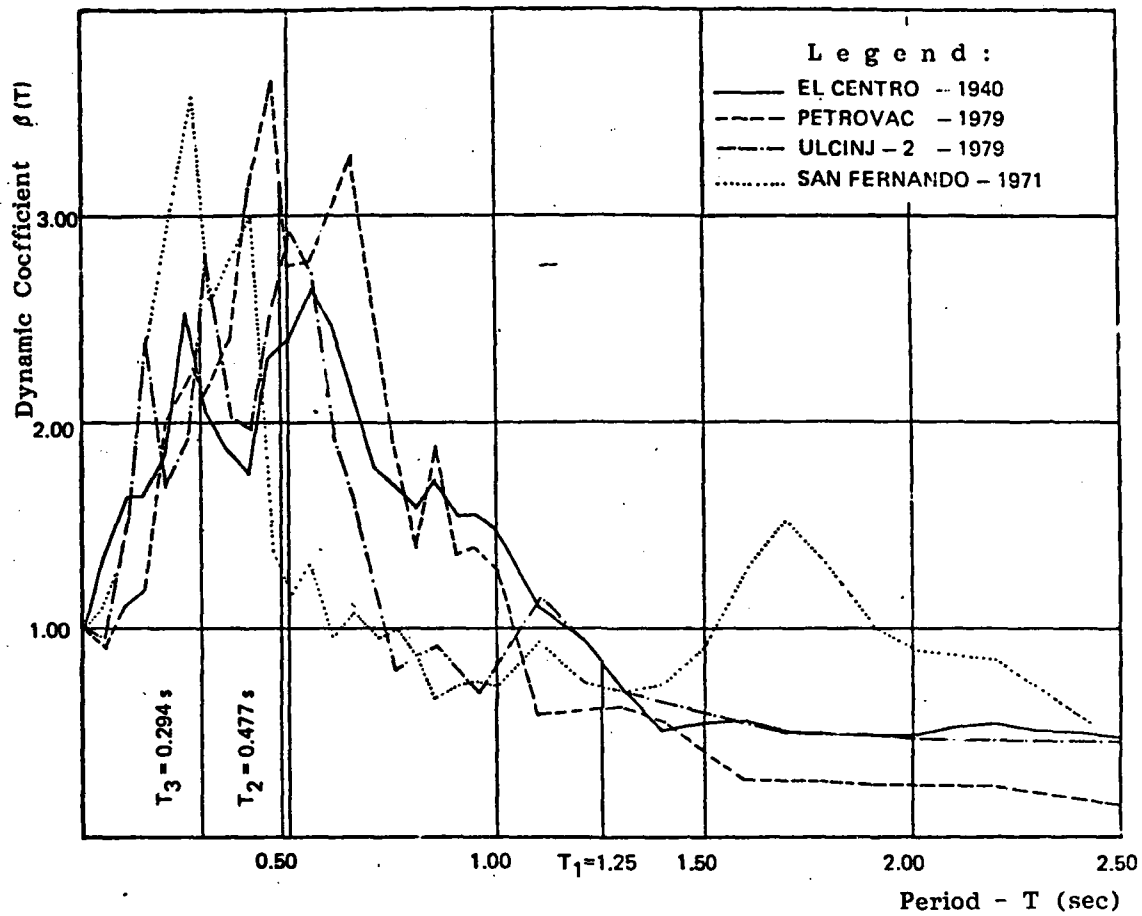


Fig. 6 Response Spectra for Selected Earthquakes

Dynamic Coefficients:

El Centro :  $\beta(T_1) = 0.815$ ,  $\beta(T_2) = 2.350$ ,  $\beta(T_3) = 2.054$

Petrovac :  $\beta(T_1) = 0.593$ ,  $\beta(T_2) = 3.154$ ,  $\beta(T_3) = 2.173$

Ulcinj - 2:  $\beta(T_1) = 0.814$ ,  $\beta(T_2) = 2.729$ ,  $\beta(T_3) = 2.738$

San Fernando:  $\beta(T_1) = 0.725$ ,  $\beta(T_2) = 1.245$ ,  $\beta(T_3) = 2.742$





TURKISH NATIONAL COMMITTEE FOR  
EARTHQUAKE ENGINEERING

THIRTEENTH REGIONAL SEMINAR ON EARTQUAKE ENGINEERING

September 14-24, 1987 - Istanbul - Turkey

FRAMEWORK FOR A FULL SPECIFICATION  
OF SEISMIC DESIGN CONDITIONS

H.Sandi\*

# FRAMEWORK FOR A FULL SPECIFICATION OF SEISMIC DESIGN CONDITIONS

H.Sandi\*

## SUMMARY

The basis for specification of seismic design conditions for structures and for equipment installed on them is analyzed. The necessary prerequisites dealt with in this connection are related to the representation of motion during one event, to the representation of the sequence of expected future events, to some basic relations of structural dynamics (in deterministic and stochastic formulations respectively), to the definition of response spectra with specified non-exceedance probability, to the verification criteria, to the models of ground motion, to the chains of amplification. These prerequisites are then used in order to specify in a consistent manner design conditions for structures and for equipment. Some problems related to the implementation in practice are finally discussed.

## 1. INTRODUCTION

Engineering activities require a specification of seismic conditions leading to adequate control and limitation of seismic risk. This is valid for structures as well as for equipment installed on structures. This general requirement may be fulfilled in various ways, with different degrees of accuracy and certainty. Highly responsible structures will impose, of course, a correspondingly high degree of accuracy and certainty in controlling and limiting risk. The recent years have witnessed therefore a sustained concern of researchers and practitioners for the development of appropriate rules of specification of seismic conditions, especially in relation to the design of potentially highly hazardous structures (the reference case: NPP's). It must be mentioned also that engineering practice requires different approaches for activities related to different categories of structures, but, on the other hand, a common conceptual basis leading to different practical approaches for different practical purposes can be only welcomed.

A consistent control of risk will be based, of course, on the explicit recognition of the random nature of several factors determining structural safety and reliability. According to current concepts, the (implicit) prediction required for protecting structures and equipment against future destructive earthquakes must be made in probabilistic terms. This represents, basically, a consistent extrapolation of the past experience in the future, under the assumption that the general conditions of phenomena and events are characterized by a certain stationarity.

---

\*) INCERC (Building Research Institute), Bucharest

The current state of the art makes it possible to use different alternative representations of entities related to seismic conditions. This refers to the seismic motion of ground, structures, equipment etc. during one event, as well as to the sequence of seismic events. This paper keeps in view these facts and is intended to contribute to the adoption of the most suitable solutions. There is an obvious need of correlation between the representations adopted for the analyses of seismic motion during one event and of sequence of events.

The analysis of risk and, in a complementary sense, of safety and reliability of structures may be carried out, at present, at different levels of application of probabilistic concepts. While the level one approach is currently used in codes and in practice as well, it is desirable to develop formats compatible with the use of higher level approaches. The alternatives from this view point are dealt with too in the paper. The author believes that it has become possible to pass gradually from a methodology based on the use of design spectra (which is compatible with a level one approach) to the use of stochastic representations compatible with a higher level probabilistic approach. The concrete object for which practical steps can be undertaken is represented primarily by NPP's, for which a consistent control of risk is highly enlightened and for which comprehensive data bases as well as resources required by more advanced engineering analyses are available.

## 2. REPRESENTATIONS AND BASIC RELATIONS.

### 2.1. General

The problematique dealt with in this lecture requires a concern for defining some entities, for their appropriate representation and for the presentation of some basic relations. One must consider first in this sense:

- a) the representation of seismic motion (for ground, structures, equipment) during one seismic event and the definition of some corresponding models;
- b) the representation of the sequence of events and the definition of corresponding models;
- c) some basic relations of structural dynamics, in accordance with the representations adopted;
- d) some basic relations concerning the estimate of seismic risk.

### 2.2. Representations of Seismic Motion during one Event

The seismic motion of ground, structures and equipment installed on them, during one event is of random, transient, nature. In order to characterize expected motions, it is necessary, as mentioned to adopt a probabilistic viewpoint. The currently usable representations in this field are:

$A_1$ : stochastic representations, in which the seismic motions are dealt with as random functions of the time variable and are described by correlation functions or their transforms;

$A_2$ : representations in the form of (artificial) accelerograms, which are in fact sample functions of random functions corresponding to representation  $A_1$ ;

$A_3$ : representations by means of design spectra.

The representation  $A_3$  is currently used in engineering practice (it lies among other at the basis of codes). The representation  $A_2$  is increasingly used, especially in connection with computer (non-linear) time history analyses. The representation  $A_1$  is used chiefly in research. Although the frequency of use is as mentioned, the logical sequence is  $A_1$ - $A_2$ - $A_3$ . It is possible and relatively easy to specify, on the basis of representation  $A_1$  the other two representations and, also, to specify on the basis of representation  $A_2$  the representation  $A_3$ . The converse approach is difficult and does not lead to unique solutions.

In case one considers a vectorial random function of time  $W(t)$  (which could represent, e.g. an  $n$ -dimensional accelerogram), its basic characteristic is its (matrix) second order correlation function (or covariance),

$$B^{(n)}[W; t_1, t_2] = W(t_1) \cdot W^T(t_2) \quad (2.1)$$

where the upper index denotes the transposed, and the average is considered for a statistical ensemble. In the particular case of stationary random functions, this function will depend only on the difference  $t_2 - t_1$ ,

$$B^{(n)}[W; t_1, t_2] = B[W; t_2 - t_1] \quad (2.2)$$

A complementary, particularly useful, means for characterization of random functions is represented by their (matrix) spectrum densities. In case of stationary functions the classical spectrum densities  $S[W; \omega_m]$  satisfy the Wiener-Khintchin relations [ 3 ]

$$S[W; \omega_m] = \frac{1}{2\pi} \int_{-\infty}^{\infty} e^{-i\omega_m t_n} B[W; t_n] dt_n \quad (2.3a)$$

$$B[W; t_n] = \int_{-\infty}^{\infty} e^{i\omega_m t_n} S[W; \omega_m] d\omega_m \quad (2.3b)$$

In case of arbitrary (non-stationary) functions one introduces the generalized spectrum density  $S^{(n)}[W; \omega_1, \omega_2]$ , which satisfies the generalized Wiener-Khintchin relations [ 2 ]

$$S^{(n)}[W; \omega_1, \omega_2] = \frac{1}{4\pi^2} \iint_{-\infty}^{\infty} e^{-i\omega_2 t_2 - i\omega_1 t_1} B^{(n)}[W; t_1, t_2] dt_1 dt_2 \quad (2.4a)$$

$$B^{(n)}[W; t_1, t_2] = \iint_{-\infty}^{\infty} e^{i(\omega_2 t_2 - \omega_1 t_1)} S^{(n)}[W; \omega_1, \omega_2] d\omega_1 d\omega_2 \quad (2.4b)$$

Besides the usual representations used, it is useful to consider an alternative approach based on the use of a new system of variables [ 13 ]

$$\begin{aligned} t_m &= (t_1 + t_2)/2 & \omega_m &= (\omega_1 + \omega_2)/2 \\ t_n &= t_2 - t_1 & \omega_n &= \omega_2 - \omega_1 \end{aligned} \quad (2.5)$$

One will introduce in this connection the functions  $B^{(d)}[W; t_m, t_n]$  and  $S^{(d)}[W; \omega_m, \omega_n]$ , which satisfy a couple of relations which are equivalent to (2.4),

$$S^{(d)}[W; \omega_m, \omega_n] = \frac{1}{4\pi^2} \iint_{-\infty}^{\infty} e^{-i(\omega_m t_n + \omega_n t_m)} B^{(d)}[W; t_m, t_n] dt_m dt_n \quad (2.6a)$$

$$B^{(d)}[W; t_m, t_n] = \iint_{-\infty}^{\infty} e^{i(\omega_m t_n + \omega_n t_m)} S^{(d)}[W; \omega_m, \omega_n] d\omega_m d\omega_n \quad (2.6b)$$

In the particular case of stationary random functions the relation (2.2) becomes

$$B^{(d)}[W; t_m, t_n] = B[W; t_n] \quad (2.7)$$

while the two-dimensional spectrum density  $S^{(d)}[W; \omega_m, \omega_n]$  becomes

$$S^{(d)}[W; \omega_m, \omega_n] = \delta(\omega_n) S[W; \omega_m] \quad (2.8)$$

( $\delta(\omega)$ : Dirac's generalized function) and is concentrated along the axis  $\omega_n = 0$ .

The canonic expansion [ 8 ] of non-stationary random function

$$W(t) = \sum_i a_i(t) W_{si}(t) \quad (2.9)$$

is sometimes used, whereby  $a_i(t)$  are (scalar) deterministic envelopes, while  $W_{si}(t)$  are stationary random functions. The function  $B^{(n)}$  will become in this case

$$B^{(n)}[W; t_1, t_2] = \sum_{i,j} a_i(t_1) a_j(t_2) B_{ij}[W; t_2 - t_1] \quad (2.10)$$

whereby  $B_{ij}$  are cross-correlation matrices. The representation (2.9) is a basis for widely used techniques of generation of artificial accelerograms (e.g.: [ 1 ]). The generalized spectrum density matrix  $S^{(d)}[W; \omega_m, \omega_n]$  can be expressed in this case by means of the correlation matrices  $B_{ij}$ ,

$$s^{(d)}[W; \omega_m, \omega_n] = \frac{1}{2\pi} \int_{-\infty}^{\infty} e^{-i\omega_m t_n} \sum_{ij} c_{ij}(\omega_n, t_n) B_{ij}[W; t_n] dt_n \quad (2.11)$$

whereby the correction functions  $c_{ij}(\omega_n, t_n)$  will be

$$c_{ij}(\omega_n, t_n) = \frac{1}{2\pi} \int_{-\infty}^{\infty} e^{-i\omega_n t_m} a_i(t_m - t_n/2) a_j(t_m + t_n/2) dt_m \quad (2.12)$$

The relationship between representations  $A_1$  and  $A_3$  is dealt with in section 2.5.

Any of the representations considered ( $A_1, A_2$  or  $A_3$ ) requires a specification of a model of ground motion as a function of a system of parameters  $s_k$  (this is, desirably, a finite system). The calibration of the values of  $s_k$  will define a ground motion according to this approach.

### 2.3. Representations of Seismicity at a Definite Site

The sequence of seismic events at a site is described, in this frame, by means of the sequence of systems of values of the parameters  $s_k$ . In order to develop operational techniques, it is suitable to adopt a unia amplitude-type parameter  $q$  among the parameters  $s_k$ . This parameter will play the role of a common factor for the amplitude of seismic motion. It is also suitable to adopt, for the remaining parameters  $s_k$ , a discretization, thus defining a finite system of families, or classes, of seismic motions. Motions belonging to a same class will differ in this approach only by the value of  $q$ . It is now possible to use simple probabilistic models in order to characterize the expected frequency of occurrence of seismic events. A most simple model used for describing this expected sequence is poissonian. Alternative models are used too (e.g. [ 5 ]).

The use of a poissonian model leads to the adoption, as a basic parameter, for a class of motions ( $j$ ), of the function  $\bar{N}_j(q, T_d)$ , i.e. the expected number of events exceeding the threshold  $q$ , for a time period  $T_d$ . This function can be expressed as follows:

$$\bar{N}_j(q, T_d) = T_d \int_q^{\infty} \bar{n}_j(q') dq' \quad (2.13)$$

where  $\bar{n}_j(q)$  is a density of expected number of events, for unit time interval. The return period  $\bar{T}_j(q)$  of a value  $q$  can be introduced now, by means of the equation

$$\bar{N}_j(q, \bar{T}_j(q)) = 1 \quad (2.14)$$

with the solution

$$\bar{T}_j(q) = \left[ \int_q^{\infty} \bar{n}_j(q') dq' \right]^{-1} \quad (2.15)$$

The expression (2.13) may be rewritten now,

$$\bar{N}_j(q, T_d) = T_d / \bar{T}_j(q) \quad (2.16)$$

The probability of occurrence of events with amplitudes exceeding  $q$  will be given by a Poisson distribution,

$$G_{mj}(q, T_d) = \frac{[\bar{N}_j(q, T_d)]^m}{m!} \exp[-\bar{N}_j(q, T_d)] \quad (2.17)$$

In particular, the non-exceedance probability will be

$$G_{0j}(q, T_d) = \exp[-\bar{N}_j(q, T_d)] \quad (2.18)$$

#### 2.4. Basic Relations of Linear Structural Dynamics

Some basic relations are given in this section, using mostly the Fourier transforms of functions of time. The Fourier relations between a function of time  $f(t)$  (the original) and its transform  $\tilde{f}(\omega)$  (the image) are

$$\tilde{f}(\omega) = \int_{-\infty}^{\infty} e^{-i\omega t} f(t) dt \quad (2.19a)$$

$$f(t) = \frac{1}{2\pi} \int_{-\infty}^{\infty} e^{i\omega t} \tilde{f}(\omega) d\omega \quad (2.19b)$$

The position of a structure is assumed to be determined by the values of a finite system of parameters, its DOF. It is suitable to consider for a structure in relation to the developments of the lecture, two categories of DOF (fig.2.1):

- the DOF of the interface with the supporting system (in particular: the ground), which determine the vector  $U_g(t)$  of displacements or the vector  $W_g(t)$  of accelerations;
- the DOF of elevated points, which determine a vector of absolute displacements  $U_a(t)$  or a vector of absolute accelerations,  $W_a(t)$ .

A relation

$$\tilde{W}_a(\omega) = \tilde{H}_a(\omega) \tilde{W}_g(\omega) \quad (2.20)$$

exists in general between the vectors referred to, where  $\tilde{H}_a(\omega)$  represents a (matrix) transfer function for accelerations.

It will be assumed that the motion of a structure, subjected to a system of given forces  $F(t)$  is given, for images, by the equation

$$[-\omega^2 M + \tilde{K}(\omega)] \tilde{U}(\omega) = \tilde{F}(\omega) \quad (2.21)$$

where  $M$  is an inertia matrix, while  $\tilde{K}(\omega)$  is the image of a visco-elastic stiffness matrix.

In order to specify the expression of the transfer matrix it is necessary to use the eigenvectors and the natural circular frequencies of the dynamic system corresponding to a structure. One will assume that a classical

eigenvalue problem [ 12 ] leads to the eigenvectors  $V_r$  normalized with respect to the inertia matrix  $M$ ,

$$V_r^T M V_s = \begin{cases} 1 & (r=s) \\ 0 & (r \neq s) \end{cases} \quad (2.22a)$$

$$V_r^T \tilde{K}(\omega) V_s = \begin{cases} \tilde{\omega}_r^2 & (r=s) \\ 0 & (r \neq s) \end{cases} \quad (2.22b)$$

The complex natural circular frequencies (eigenvalues) will be

$$\tilde{\omega}_r^2 = \omega_r^2 + 2in_r \omega_r \omega, \quad (2.23)$$

where  $\omega_r$  are real natural circular frequencies, corresponding to the motion of an ideally elastic system, associated to the structure. One will use also the reduced natural circular frequencies,  $\omega'_r$ ,

$$\omega'_r = \omega_r \sqrt{1-n_r^2} \quad (2.24)$$

One can consider two situations:

- a) the motions of the interface, described by the vector  $U_a(t)$  can be only rigid-body motions;
- b) the motions referred to may be arbitrary. In the first case it makes sense to use, according to tradition, a vector of relative displacements,  $U_{rel}(t)$ , defined by a relation

$$U_{rel}(t) = U_a(t) - G U_g(t) \quad (2.25)$$

where  $G$  is a kinematic matrix, converting the rigid-body motion of the interface into a rigid-body motion of the whole structure.

The transfer matrix will be, in the first case,

$$\tilde{H}_a(\omega) = \sum_r \tilde{h}_{ar}(\omega) V_r V_r^T M G \quad (2.25)$$

In the second case the use of relative displacements becomes a non-sense, while the use of absolute displacements leads to the expression

$$\tilde{H}_a(\omega) = \sum_r \frac{1}{\tilde{\omega}_r^2} \tilde{h}_{ar}(\omega) V_r V_r^T \tilde{R}(\omega) \quad (2.26)$$

whereby  $\tilde{R}(\omega)$  is a cross-impedance matrix, for which one column represents a system of forces (complex amplitudes) acting along the DOF corresponding to the vector  $U_a(t)$  in case when a unit amplitude motion occurs along one DOF corresponding to one component of the vector  $U_g(t)$ .

The modal transfer functions

$$\tilde{h}_{ar}(\omega) = \frac{\tilde{\omega}_r^2}{\tilde{\omega}_r^2 - \omega^2} \quad (2.27)$$



intervene in both relations (2.26) and (2.27). It may be shown that, in the first case dealt with, the expression (2.27) is equivalent to the expression (2.26).

The deterministic relation (2.20) leads to homologous stochastic relations, which can be written for stationary or non-stationary motions. In case of stationary motions, one obtains

$$S[W_a; \omega_m] = \tilde{H}_a^*(\omega_m) S[W_g; \omega_m] \tilde{H}_a^T(\omega_m), \quad (2.29)$$

while for the general case one obtains

$$S^{(n)}[W_a; \omega_1, \omega_2] = \tilde{H}_a^*(\omega_1) S^{(n)}[W_g; \omega_1, \omega_2] \tilde{H}_a^T(\omega_2) \quad (2.30)$$

## 2.5. Response Spectra with Controlled Non-Exceedance Probabilities.

The response spectra concerning various parameters (absolute accelerations, relative velocities, relative pseudo-velocities etc.) are defined, in a classical sense, for one parameter describing the response of a dynamic system and for one fully determined seismic event (as a rule, a recorded accelerogram). The parameter  $u_s(t)$  characterizing the response, the weighting function of the system,  $h_{us}(T, n; t)$  of the system dealt with and the (scalar) accelerogram  $w_g(t)$  intervene in a relation written for original functions (depending on the time variable),

$$u_s(t) = \int_0^t h_{us}(T, n; t-t') w_g(t') dt' \quad (2.31)$$

The response spectrum of the motion  $w_g(t)$ , in connection with the dynamic system and the parameter referred to,  $u_s(t)$ , will be

$$s_u^{(a)}(T, n) = \max_t \left| \int_0^t h_{us}(T, n; t-t') w_g(t') dt' \right| \quad (2.32)$$

The scalar nature of the parameter  $u_s(t)$  is essential for the definition of the response spectrum. The ground motion may be characterized here by a scalar  $w_g(t)$  or a (column) vector  $W_g(t)$ . In the latter case, the function  $h_{us}(T, n; t)$  will be replaced by a row-vector. The dynamic system dealt with is, according to tradition, an SDOF system. One can imagine nevertheless generalizations, in which the parameter  $u_s(t)$  represents a scalar characteristic of an NDOF system (even of equipment installed on a structure). The definition may be extended to non-linear systems too.

The definition of a design spectrum for future events to affect a definite site, changes the data of the problem, since the input function  $w_g(t)$  (or  $W_g(t)$ ) is no longer specified in a classical sense, but is to be predicted. The impossibility of deterministic prediction of the input function makes impossible the determination of calculation of absolute maxima in the classical sense, as in relation

(2.32) and imposes the adoption of a probabilistic standpoint. The spectrum looked for must be defined as a function of  $(T, n)$  characterized by a specified non-exceedance probability. A new definition requires a concern for two fundamental aspects of the random nature of future seismic motions:

a) the random nature of seismic motion during one event, which is specified in a "macroscopic" way (motion of a specified intensity, of a specified predominant frequency etc), by means of specifying the parameters  $s_k$  introduced in sections 2.2 and 2.3;

b) the random nature of the sequence of events during the lifetime of a future structure, represented by the different values that can be taken by the parameters  $s_k$  (in particular, by the intensity or amplitude  $q$ , used in section 2.3).

The design spectra defined in this frame may be determined using two main approaches: use of representations of category  $A_1$  (stochastic representations using second order moments) or of category  $A_2$  (representations by means of systems of sample accelerograms corresponding to a definite stochastic model). The main steps involved by each of the approaches may be briefly examined.

The basic characteristic to be used in connection with the representation  $A_1$  in order to estimate the exceedance probabilities of various (positive) values by the absolute value of a parameter  $u_s(t)$  is the covariance  $b^{(n)}[u_s; t_1, t_2] = b^{(d)}[u_s; t_1, t_2]$ , which may be obtained as a particular case of the definition (2.1). The function  $b^{(n)}[u_s; t, t] = b^{(d)}[u_s; t, 0]$  represents the instantaneous variance of  $u_s(t)$ . The r.m.s. value

$$\sigma[u_s; t] = \{ b^{(n)}[u_s; t, t] \}^{1/2} \quad (2.33)$$

can be determined on this basis and this makes it possible to determine the instantaneous exceedance probabilities of various thresholds (gaussian distribution assumed). The quantity of interest is nevertheless the probability of exceedance of given thresholds at least once during one event (first passage problem). Such probabilities will be of course conditional, upon the values of the parameters  $s_k$  (section 2.2, 2.3), which define in a macroscopic way a motion corresponding to a definite model. In case a definite class of motions is considered, for which a single variable parameter,  $q$ , is to be specified, the covariance  $b^{(n)}[u_s; t_1, t_2]$  will explicitly depend on this parameter. A relation

$$\sigma[u_s; t] = q \sigma[u_{s0}; t], \quad (2.34)$$

where  $u_{s0}(t)$  corresponds to the normalized value  $q=1$ , will be valid. The exceedance probability of a threshold  $u_m$  during one event,  $p^{(-)}(u_m)$ , will be a functional with respect to the r.m.s. value  $u_s^m[t]$ ,

$$p^{(-)}(u_m) = F \{ [u_{so}; t], q/u_m \} \quad (2.35)$$

This functional will depend not only on the ratio  $q/u_m$  as explicitly specified, but also on the time dependence of the r.m.s. value  $\sigma[u_{so}; t]$ , whereby the duration of the event and the predominant oscillation frequency (more precisely their product, which defines the number of loading cycles) will play an important role. It is not possible to derive general expressions for the functional  $F$  (2.35), but it is possible to carry out special studies for definite classes of seismic motions, in order to analyze its dependence on the parameters  $s_k$  defining the motion.

The probability of exceedance of a given threshold  $u_m$  during a specified service period  $T_d$  may be determined by means of appropriate convolutions between the probabilities  $p^{(-)}(u_m)$  (2.35) and the characteristics of seismic activity dealt with in section 2.3. The expected number of cases of exceedance of a threshold  $u_m$  will be

$$\bar{N}^{(-)}(u_m, T_d) = T_d \int_0^\infty p^{(-)}(u_m) \tilde{n}(q) dq \quad (2.36)$$

whereby the subscript  $j$  used in section 2.3, corresponding to definite classes of seismic motions, was omitted. The use of the poissonian model makes it possible to derive relations similar to (2.17) or (2.18) in order to estimate exceedance probabilities. As an example, the probability of exceeding, at least once, a threshold  $u_m$ ,  $P^{(-)}(u_m, T_d)$ , will be given by an expression

$$P^{(-)}(u_m, T_d) = 1 - \exp[-\bar{N}^{(-)}(u_m, T_d)] \quad (2.37)$$

This approach makes it possible to define design spectra with specified non-exceedance probabilities. Such a design spectrum,  $s_u^{(a)}(T, n, P_o^{(-)}, T_d)$ , whereby the arguments  $T$  and  $n$ , characterizing the dynamic system,  $P_o^{(-)}$ , characterizing the exceedance probability and  $T_d$ , characterizing the service duration, occur. The design spectrum will be a solution of the functional equation

$$P^{(-)} \{ s_u^{(a)}(T, n, P_o^{(-)}, T_d), T_d \} = P_o^{(-)} \quad (2.38)$$

whereby  $P_o^{(-)}$  is a suitable exceedance probability.

According to previous remarks, the design spectra with specified non-exceedance probabilities can be derived also on the basis of representation  $A_2$  (i.e. use of systems of sample accelerograms), in case a technique of generation of artificial accelerograms is adopted. A Monte-Carlo analysis of the system of output functions  $u_s(t)$  derived for dynamic systems characterized by various couples  $(T, n)$  makes it possible to estimate on a numerical basis conditional probabilities  $p^{(-)}(u_m)$  (2.35), as functions of the arguments  $(T, n)$ . The use of subsequent relations, (2.36) etc. makes it possible to derive in a similar way design spectra with specified (controlled) non-exceedance probabilities.

## 2.6. Specification of Verification Criteria

The specification of design spectra was considered, in previous section, for an arbitrary parameter  $u_s$ . The parameters to be dealt with in practice are diverse (e.g.: absolute floor acceleration, absolute equipment acceleration, relative displacements of different structural components etc). Moreover, it may be of interest to consider multi-parameter states of stress etc., where appropriate combinations of internal forces, stresses etc. occur.

It is suitable to briefly discuss at this place the case of members subjected to multi-parameter loading, for which some results of rather general interest can be obtained. Consider a member subjected to a multi-parameter loading defined by the quantities  $x$ . (e.g.: bending moment along two orthogonal directions, related to a section of a member). A parameter  $x_\alpha$  used for checking along an oblique direction,  $x_\alpha$  (e.g.: a bending moment) may be determined by means of a relation

$$x_\alpha = \sum_i \alpha_i x_i \quad (2.39)$$

( $\alpha_i$  may be here cosines of a direction). The parameters  $x_i$  may be expressed as

$$x_i = \sum_r y_{ir} q_r, \quad (2.40)$$

whereby  $y_{ir}$  are homologous parameters, corresponding to the normalized eigen vectors  $V_r$  (2.22), while  $q_r$  are normal coordinates. The variance of  $x_\alpha$  will be given by an expression

$$\sigma^2[x_\alpha; t] = \sum_{ijrs} \alpha_i \alpha_j y_{ir} y_{js} q_r(t) q_s(t) \quad (2.41)$$

Its instantaneous values, considered as a function of the cosines  $\alpha_i$ , will determine an ellipse or an ellipsoid etc. (see fig. 2.2. where some vectors  $y_r$  of components  $y_{ir}$  are illustrated too). The condition of verification may be specified as a condition of non-exceedance of a boundary representing a certain limit state. In case one adopts a probabilistic philosophy, ellipses, ellipsoids etc. obtained by multiplying the r.m.s. value of (2.41) by means of a variable factor  $m$ , will correspond to various non-exceedance probabilities, while an exceedance probability related to a specified boundary (corresponding to a definite limit state) will be obtained by means of integrating a multi-dimensional probability density corresponding to the r.m.s. values (2.41) upon the domain lying outside a specified boundary (associated to a limit state dealt with). This is a starting point for determining conditional exceedance probabilities  $p^{(-)}(u_m)$  related to one event and overall exceedance probabilities  $P^{(-)}(u_m, T_d)$  related to a service period. Some more extended developments in this sense are given in [14], where the cases of time dependent masses or intensities of non-seismic loading are dealt with too.

## 2.7. Specification of Ground Motion Models.

The motion of the ground-structure interface, represented by a vector  $W_g(t)$ , was considered in relation (2.20) etc. to be fully specified. That means, more precisely, that the matrix  $B^{(n)}[W_g; t_1, t_2]$  or the spectrum density  $S^{(n)}$  is fully specified. A full specification in this sense requires a concern for ground motion models to make possible a stochastic characterization for each DOF, as well as corresponding cross characterizations. Various DOF, corresponding to linear and angular displacements, must be considered in this connection. Some developments in this sense are given in [ 11 ], [ 14 ]. Some recent data, e.g. the results of processing and interpretation of dense network data [ 7 ] can usefully contribute to the calibration of models referred to.

## 2.8. Amplification Chains

It is possible to meet in practice situations where various distinct parts of structures, dynamically interacting, may be identified. In cases when equipment components installed on structures have small masses as compared to those of the structures, it is possible to neglect dynamic interaction at least for relatively low frequencies and to assume the structural motion to be the same as in the absence of equipment. In such cases the transfer matrices  $\bar{H}(\omega)$  occurring in (2.20) etc. may be specified in a simple way, as products of transfer matrices corresponding to different amplification steps. A common case is that of equipment installed on a structure, for which a transfer matrix  $\bar{H}(\omega)$  will be a product  $\bar{H}_{ag}(\omega) \bar{H}_{eq}(\omega)$ , whereby  $\bar{H}_{ag}(\omega)$  converts the ground-structure interface motion into motion of structure, while  $\bar{H}_{eq}(\omega)$  converts the motion of the structure-equipment interface into motion of the equipment. Some more details in this sense are given e.g. in [ 12 ], [ 16 ].

Previous developments are concerning the case of linear behaviour. The case of non-linear behaviour can be dealt with in the frame of a similar general philosophy, yet the practical approach will require as a rule the use of representations  $A_2$  and of incremental Monte-Carlo analyses (for a sequence of values  $q$  specified previously).

## 3. SOME POSSIBLE WAYS OF SPECIFYING SEISMIC CONDITIONS FOR STRUCTURES AND EQUIPMENT

### 3.1. General

The developments of section 2 put to evidence some main coordinates, or degrees of freedom, that characterize the problem of specifying seismic conditions for structures and equipment. It is suitable to be aware of the alternative possibilities in this field and to develop a flexible approach to the concrete specification, adopting at the same time a consistent philosophy, compatible with

the main goal of controlling seismic risk.

The state of the art of engineering activities and codes is characterized by a level one use of probabilistic concepts. A higher level approach is usable currently primarily in research activities. It is suitable, nevertheless, to adopt for practice formats that make it possible to correlate the standard level one approach with higher level approaches too.

The specification of seismic conditions, first for structures supported by the ground, then for equipment supported by structure, is dealt with in next sections, keeping in view the basic elements discussed in section 2.

### 3.2. Structures Supported by the Ground

Codes used in current practice define seismic design loads by means of expressions relying on model analysis. As an example, the Romanian code [ 20 ] defines conventional seismic forces  $S_{kr}^{(c)}$ , along DOF  $k$ , corresponding to a mode  $r$ , by means of an expression

$$S_{kr}^{(c)} = c_{kr} G_k \quad (3.1)$$

where

$$c_{kr} = k_s \beta_r \psi \eta_{kr} \quad (3.2)$$

The factors of the right members are :

$k_s$  : a seismicity factor corresponding to the design intensity adopted;

$\beta_r$  : a dynamic factor, corresponding to a mode dealt with;

$\psi$  : a factor of reduction of seismic loads keeping in view the post-elastic behaviour, the damping capacity, the strength reserves not accounted for etc.;

$\eta_{kr}$  : a shape factor;

$G_k$  : gravity loads corresponding to the masses that can oscillate along a DOF  $k$ .

The shape factor  $\eta_{kr}$  will be expressed by means of normalized eigenvectors of components  $v_{kr}$ , as

$$\eta_{kr} = v_{kr} \sum_{k',k''} m_{k',k''} v_{k'r} g_{k''} \quad (3.3)$$

where  $m_{k',k''}$  are terms of the inertia matrix  $M$ , while  $g_k$  are components of a column vector  $G$ , that replaces the matrix of relations (2.25) atc., in case one assumes that the vector  $W_g(t)$  may be replaced by one single component of it (assumption on single direction ground motion).

The expression (3.1) is equivalent with an expression concerning conventional absolute accelerations  $w_{kr}^{(c)}$ ,

$$w_{kr}^{(c)} = g k_s \beta_r \gamma_{kr} \quad (3.4)$$

where  $g$  denotes the acceleration of gravity.

Given the developments of section 2.5, it may be stated that, as a first approximation, conventional design accelerations  $w_{kr}$  should be proportional to r.m.s. values determined by means of a stochastic approach. The developments concerning random vibration of structures subjected to earthquake motion make it possible to derive more consistent expressions relying on the use of stochastic concepts. In case one considers a vector  $Q$  of the normal coordinates of absolute accelerations, it is possible to derive for the covariance matrix the expression [ 43 ],

$$b_{rs}^{(n)}[Q; t_1, t_2] = \frac{1}{\omega_r^2 \omega_s^2} \sigma^2[w_g] V_r^T R_0 D_{rs} [W_g^{(o)}; t_1, t_2] \quad (3.5)$$

whereby  $V_r$  are normalized eigenvectors,  $R_0$  is the matrix homologous to  $R(\omega)$ , in case elastic structural behaviour is assumed,  $\sigma^2[w_g]$  is a reference variance of a component of  $W_g(t)$  (say translation along one horizontal direction), and  $D_{rs}^{(n)}[W_g^{(o)}; t_1, t_2]$  is a matrix dynamic factor concerning the non-dimensionalized ground acceleration vector

$$W_g^{(o)}(t) = \frac{1}{\sigma[w_g]} W_g(t) \quad (3.6)$$

The expression of  $D_{rs}^{(n)}[W_g^{(o)}; t_1, t_2]$  is

$$D_{rs}^{(n)}[W_g^{(o)}; t_1, t_2] = \omega_r^2 \omega_s^2 \int_{-\infty}^{\infty} \int_{-\infty}^{\infty} e^{i(\omega_2 t_2 - \omega_1 t_1)} \omega_1^2 \omega_2^2 h_r^*(\omega_1) \cdot h_s(\omega_2) (1 - i\omega_1 T_{ret}) (1 + i\omega_2 T_{ret}) S^{(n)}[W_g^{(o)}; \omega_1, \omega_2] d\omega_1 d\omega_2 \quad (3.7)$$

$T_{ret}$  represents here a rheologic characteristic, the retardation time, which intervenes in a Kelvin-type constitutive relation,

$$\sigma = E(\epsilon + T_{ret} \dot{\epsilon}) \quad (3.8)$$

More expressions like (3.5) and (3.7) are given in [ 13 ] for relative or absolute displacements and accelerations, for stationary and non-stationary models. The full system of expressions (3.7) makes it possible to consider, among other, the correlation of normal coordinates and to generalize on this basis the rule of quadratic summing up of modal effects.

The factor  $\sigma[w_g]$  plays here the role of the product

$g_{kr}$  of (3.4), while the matrix  $D_{rs}^{(0)}[W^{(0)}; t_1, t_2]$  is homologous (in a generalized manner) to the product of the dynamic  $\beta_r$  and of the shape factor  $\gamma_{kr}$  of (3.2) etc. It turns out among other that, in the general case it is no longer possible to replace the matrix  $D_{rs}^{(0)}[W^{(0)}; t_1, t_2]$  by means of a product of factors equivalent to  $\beta_r$  and  $\gamma_{kr}$  respectively.

The basic problem raised by the task of specifying seismic conditions according to the latter relations remains that of specifying the matrix  $S^{(n)}[W_g; \omega_1, \omega_2]$ . Some remarks and recommendations may be presented in this connection, considering the cases of structures supported by a single, rather rigid, foundation and of multi-support structures, respectively. These remarks could be considered, perhaps, rather in relation to the classical spectrum densities  $S_{ij}$  corresponding to the covariance matrices  $B_{ij}$  of (2.11).

In case of structures supported by one connexe foundation that is rather rigid, the dimension of matrices  $S_{ij}^{(n)}$ ,  $B_{ij}$ , etc. will be not larger than  $6 \times 6$ , corresponding to a rigid-body motion of ground-structure interface. A  $6 \times 6$   $S$  - matrix will be diagonal, except perhaps for terms  $S_{ij}$  concerning translation along one horizontal direction and rotation in a corresponding vertical plane (that includes the horizontal direction), that will become non-zero due to ground-structure interaction phenomena. Some isotropy properties of ground motion may be postulated unless firm seismological information supports an opposite conclusion. The isotropy assumption means that terms  $s_{kk}$  corresponding to different horizontal translation directions will be identical, and that terms  $s_{kk}$  corresponding to rotations in different vertical planes are identical too. On the other hand, it may be stated that the diagonal term  $s_{33}$  corresponding to vertical translation will have a different expression as compared with  $s_{11}=s_{22}$  and, in the same way, the diagonal term corresponding to rotation in a horizontal plane could be different as compared to those corresponding to rotation in a vertical plane.

In case of multi-support structures it becomes necessary to consider coherence characteristics for motions along parallel directions at different points. The coherence will be maximum in case of negligible distance between points and will tend to zero in case of increasingly large distances.

Some analytical developments on this subject [ 11 ] put to evidence the importance of two similitude criteria, namely the rotation amplitude criterion

$$s_r = \frac{c \dot{\theta}}{\omega u} \quad (3.9)$$

and the phase lag criterion



$$S_{\Delta\varphi} = \frac{c \Delta\varphi}{\omega d} \quad (3.10)$$

(c : a characteristic wave propagation velocity ;  $\omega$ : circular frequency of spectral component dealt with; d: relative distance; u: amplitude of translation (acceleration) ;  $\dot{\varphi}$ : amplitude of rotation (acceleration);  $\Delta\varphi$ : phase lag for spectral component).

Some developments of section 2.5 were devoted to deriving of design spectra with controlled non-exceedance probabilities on the basis of stochastic models of ground motion. This approach can be considered as a direct approach, leading to design spectra on the basis of spectrum densities, provided the spectrum densities are specified. One can consider, conversely, the problem of deriving spectrum densities compatible with some specified design spectra. The Wiener-Khintchin relations (classical or generalized) make it possible in this case to develop integral equations (Fredholm type) on the basis of which spectrum densities can be derived. This possible approach raises nevertheless difficulties, since the design spectra specified for some given site are to a great extent the outcome of engineering judgement and may lead to funny solutions of integral equations. Some tentative analyses carried out recently in this direction in INCERC, in order to derive design-spectrum-compatible spectrum densities and to generate on this basis artificial accelerograms were nevertheless encouraging, at least in order to derive some first approximations of spectrum densities, that were improved afterwards step-by-step.

A last aspect to be dealt with here is that of different formats, corresponding respectively to different levels of probabilistic approach to risk analysis. The specification of one design spectrum for a definite site will correspond, as mentioned, to a first level approach. A higher level approach will require an explicit concern for specifying characteristics of classes of motions, according to the definitions given in section 2.3. A reference characteristic of expected ground motions, corresponding to an amplitude  $q=1$  should be specified for each class of motions (this could be a response spectrum or, better, a stochastic characteristic corresponding to a definite ground motion model) and, besides this, information on the recurrence characteristics  $\bar{N}(q,T)$  or  $\bar{n}(q)$  should be provided. In case this information is made available, it will be possible to use, alternatively, a first level, or a higher level, approach to risk analysis.

### 3.3. Equipment Installed on a Structure

The approach used as a rule in current practice in order to specify design conditions for equipment installed on structures is that of deriving floor response spectra (FRS). FRS's rely on the same information on ground motion as ground response spectra do, plus on information on the dynamic characteristics of the structure(s) supporting the equipment dealt with.

Techniques developed in order to derive FRS's rely as a rule on the assumption of linear behaviour of structure and equipment both. It must be emphasized, nevertheless, that one must check whether the high, or very high, values, obtained sometimes for FRS's are realistic, in the sense that the structure dealt with is able to transmit, in a linear stage of behaviour, the high accelerations corresponding to linear response spectra. That is in order to avoid unduly conservative design conditions for equipment. There occurred a few cases in INCERC, for which it was obviously necessary to reject results obtained from linear analysis and to derive FRS's on the basis of non-linear analysis of the main structures.

A next problem of first importance is that of specifying appropriate criteria for equipment verification. There will be cases as mentioned, in which criteria are related to absolute acceleration (along what directions ?) or to relative displacements, perhaps between neighbouring structures (again, along what directions ?) etc. Some basic relations, lying at the basis of possible approaches to situations characterized by the use of different criteria were presented in sections 2.4 and 2.5 in this connection.

Engineering activities related to the design of equipment rely generally on a philosophy that will not exceed the level one probabilistic approach. The technical interest of designers will be focused therefore to the use of design spectra (FRS). This approach is in good agreement also with the need of testing of some equipment components in order to obtain a corresponding earthquake qualification. According to the philosophy of current activities, the successive cycles of testing for qualification should be such, as to cover an FRS specified for the equipment dealt with. One must mention here, nevertheless, that any response spectrum (FRS) defined in a classical sense cannot say anything about the simultaneous motion along different directions. The qualification activities will require, therefore, either additional information of this nature, to complete the FRS information or, according to some approaches, a definite increase in the severity of action along one direction, to compensate for neglecting during testing activities the action occurring along other directions.

Various algorithms were developed in literature in relation to FRS analysis. Some data on an algorithm recently developed in INCERC, that may be used in order to derive FRS's related to any type of linear criterion, are given here. The programs developed in this frame were successfully used for some practical purposes. The ground motion is represented by a classical (normalized) spectrum density

$$S_g(\omega) = \frac{2\alpha}{\pi} \frac{\omega^2 + \alpha^2 + \beta^2}{\omega^4 + 2(\alpha^2 - \beta^2)\omega^2 + (\alpha^2 + \beta^2)^2} \quad (3.11)$$

The stationary ground motion is possibly multiplied by a deterministic envelope

$$a(t) = \begin{cases} 0 & (t < t_1) \\ (t-t_1)/(t_2-t_1) & (t_1 \leq t < t_2) \\ 1 & (t_2 \leq t < t_3) \\ (t_4-t)/(t_4-t_3) & (t_3 \leq t < t_4) \\ 0 & (t_4 \leq t) \end{cases} \quad (3.12)$$

to account for the non-stationary character of motion. The ratio  $\alpha/\beta$  for the ground motion is kept constant and relatively low (say, around .1). The variance of acceleration of an SDOF system of characteristics  $(T, n_s)$  to account for the ground response spectrum (GRS) is determined for various values  $T$  and for  $n_s$  corresponding to structural damping, with attention to values  $T \approx 2W/\beta$ , in the neighbourhood of the ground motion spectral peak. The FRS corresponding to a specified criterion and to the same, input values of  $(\alpha, \beta)$  is determined, for  $T = T_s$ , for  $n_s$  as said and for the system of values  $n_s$  of interest for the equipment. The ratio FRS/GRS in the neighbourhood of spectral peak is assumed to be correctly determined for the value  $T = T_s \approx 2W/\beta$  and the FRS values for different values  $n_s$  are derived by multiplying the GRS value with the ratios FRS/GRS. Computation is repeated for values corresponding to the system of values  $T$  of interest for the equipment. The FRS function for various values of  $n_s$  will be determined from envelopes of the system of spectral peaks corresponding to different values  $T = 2W/\beta$ . Computations are particularly fast for a stationary ground motion model (3.11), since exact algebraic relations based on the use of residue techniques [12] are applied. It must be noticed, on the other hand, that the stationarity assumption leads to conservative estimates.

#### 2.4. Some Suggestions Concerning Design Regulations

The current state of the art makes it possible definitely to introduce improvements in the design regulations concerning the specification of seismic conditions. This refers to the conditions for structures supported by the ground as well as for equipment installed on structures. Some main suggestions that may be formulated in connection with the developments of this lecture are:

- a) adoption of a harmonized conceptual basis for the specification of ground and floor design parameters, with an opening towards higher level probabilistic techniques;
- b) providing of full information on the characteristics of the vector  $W(t)$ , including cross-information on its components, for various types of ground-structure interfaces with an opening towards explicit use of stochastic representations;
- c) development of specific criteria for various categories of equipment for the cases of one-point or multi-point supporting systems;
- d) recommendations on techniques of specifying floor design conditions in cases when structures are likely to

perform non-linearly.

#### 4. FINAL REMARKS

The current state of the art makes it possible to introduce significant improvement in the specification of seismic design conditions for structures and equipment both, yet there are some directions in which there is an obvious need for research. Some main aspects of interest are emphasized here in this connection.

1. Models concerning the seismic motion must still be developed at both levels: ground motion during one event and sequence of various seismic events. Such models, basically of probabilistic nature, should depend on a finite system of parameters and extensive work on calibration for specific local conditions should be carried out.

2. Alternative formats for the specification of seismic design conditions in accordance with the requirements of level one, as well as of higher level probabilistic approaches, should be developed for implementation in codes.

3. Work on specific criteria for the verification of various categories of equipment, taking into account the 3D motion of structure and equipment is necessary too. FRS analysis techniques should be made compatible with these criteria.

4. Techniques for deriving GRS-and FRS-type design parameters corresponding to various alternative stochastic models of ground motion and risk analysis philosophies should be further on developed.

#### REFERENCES

1. St. Balan, S. Minea, H. Sandi, G. Serbanescu  
A Model for Simulating Ground Motions.  
Proc. 6 WCEE, New Delhi, 1977
2. T.K. Caughey  
Non Stationary Random Processes. In:  
Random Vibration, Vol. II (editor: S.H. Crandall) - The MIT Press Cambridge, 1963
3. R.W. Clough, J. Penzien  
Dynamics of Structures. Mc Graw Hill, New York, 1975
4. L. Esteva, S.E. Ruiz, A. Reyes  
Response of Multiple-Support Structures  
Proc. 7 WCEE, Istanbul, 1980
5. R. Fregonese, E. Guagenti, V. Petrini, A. Tagliani  
Use of Renewal Process in the Analysis of Seismic Risk: Some Italian Zones (in Italian) Ingegneria Sismica, 2, 1985.
6. C. Lomnitz, E. Rosenblueth, (editors)  
Seismic Risk and Engineering Decisions  
Elsevier, Amsterdam-Oxford-New York, 1976.

- 7.K.Muto,  
T.Ohta,  
H.Yoshida,  
T.Sugano,  
M.Miyamura Time-dependent Variation of Ground Mo-  
tions Observed at Local Seismic Array,  
Proc. 8 ECEE, Lisbon, 1986.
- 8.S.V.Pugachov Theory of Random Functions and its Appli-  
cations to Control Problems (2-nd ed., in  
Russian) GIFML, Moscow, 1960.
- 9.H.Sandi Conventional Seismic Forces Corresponding  
to Non-Synchronous Ground Motion. Proc. 3  
ECEE, Sofia, 1970.
- 10.H.Sandi Design for Spatial Ground Motions,  
Proc. 7 ECEE, Istanbul, 1980.
- 11.H.Sandi Stochastic Models of Spatial Ground Motions  
Proc. 7 ECEE, Athens, 1982.
12. H.Sandi Elements of Structural Dynamics (in Romanian)  
Editura Tehnica, Bucharest, 1983.
- 13.H.Sandi Random Vibrations in Some Structural En-  
gineering Problems. In: Random Vibration-  
Status and Recent Development (The Stephen  
Harry Crandall Festschrift, editors: I.  
Elishakoff, R.H.Lyon) Elsevier, Amsterdam-  
Oxford-New York-Tokyo, 1986.
14. H.Sandi Superposition Rules Recommended as a  
Background for Codified Safety Checking.  
Proc. 8 ECEE, Lisbon, 1986
- 15.M.Shinozuka Digital Simulation of Ground Accelerations,  
Proc. 5 WCEE, Rome, 1973.
- 16.M.P.Singh, A Response Spectrum Approach for Seismic  
R.A.Burdisso Analysis of Multiple Support Secondary  
Systems. Proc. 8 ECEE, Lisbon, 1986
- 17.M.D.Trifunac, Preliminary Empirical Models for Scaling  
J.G.Anderson Relative Velocity Spectra. USC, Los Angeles,  
1978.
- 18.M.Watabe, Simulation of 3 D Earthquake Ground Motions  
R.Iwasaki, along Principal Axes. Proc. 7 WCEE, Istan-  
M.Tohido bul, 1980.
19. ATC Tentative Provisions for the Development  
(Applied of Seismic Regulations for Buildings. ATC  
Technology Publication 3-06, NBS Special Publication  
Council) 510. NSF Publication 78-8, 1978.
- 20.ICCPDC Code for the Earthquake Resistant Design  
of Buildings and Engineering Structures  
(in Romanian). Bul.Constr., 11, 1981.

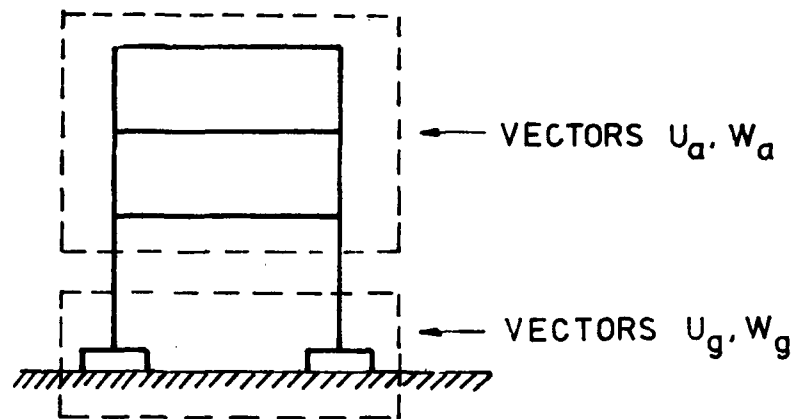


Fig. 2.1.

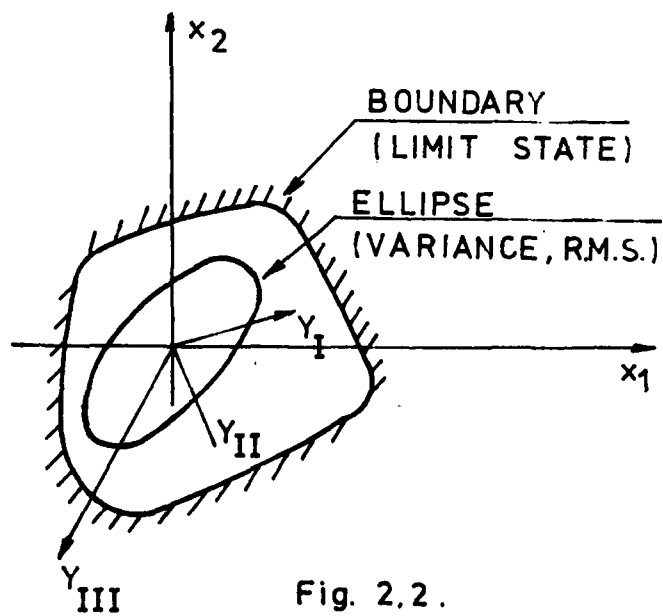
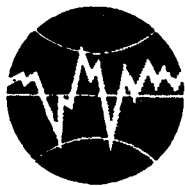


Fig. 2.2.



**TURKISH NATIONAL COMMITTEE FOR  
EARTHQUAKE ENGINEERING**

**THIRTEENTH REGIONAL SEMINAR ON EARTHQUAKE ENGINEERING**

**September 14-24, 1987 - Istanbul - Turkey**

**THE USE OF MASONRY IN SEISMIC ZONES**

**by**

**Artur Ravara (1)**

TURKISH NATIONAL COMMITTEE FOR EARTHQUAKE ENGINEERING

THIRTEEN REGIONAL SEMINAR ON EARTHQUAKE ENGINEERING

September 14-24, 1987 - Istanbul - Turkey

THE USE OF MASONRY IN SEISMIC ZONES

by

Artur Ravara (1)

Summary

Masonry has been traditionally the mostly widely building process used in construction, especially in the mediterranean area, despite its poor behaviour when subjected to strong earthquake ground motion.

After analysing the reasons for such a widely used material, the typical systems of structural masonry are described, and their behaviour under seismic loads discussed. Examples depicted from past earthquakes occurred in the mediterranean area (Agadir 1960, El Asnan 1980, Azores 1980, etc.) illustrate the presentation.

The paper concludes with the main guide-lines towards mitigation of damage in masonry buildings built in zones of moderate and high seismicity. It stresses that it is possible to provide adequate seismic resistance through simple and general code provisions, adapted to local conditions of materials and construction technologies. International cooperation among researchers, designers and the building industry in the mediterranean countries, is also emphasized as an excellent form to mitigate damage in masonry construction in these countries.

- 1) Director LNEC (National Laboratory of Civil Engineering), Lisbon  
President EAEE (European Association of Earthquake Engineering)



## 1. INTRODUCTION

Masonry is extensively used in building construction. In southern Europe, North Africa and Middle East it has been a traditional process over the centuries, even in high seismicity zones, despite its poor behaviour when subjected to strong shocks. Stone, adobe, brick and more recently concrete blocks have been widely used both as a structural or a filling material. In dwelling units and small buildings up to three stories masonry is generally used as a structural element. In tall buildings, masonry (brick or concrete blocks) is mostly used as infill walls built after the main structure is completed.

There are several reasons why masonry construction is so widespread in the mediterranean area. The prime materials are abundant and cheap, easy to obtain, the construction requires simple technologies and is undoubtedly quite suitable to local climate conditions.

However, as far as seismic resistance is concerned, masonry buildings often exhibit a poor performance due to heavy weight, low tensile and shearing resistance, lack of adequate structural connections, poor quality of construction and deterioration of strength with passage of time. They don't have the ductility required to absorb the energy input of strong or even medium earthquakes. As a consequence, the collapse of masonry buildings has certainly been the major source of loss of life and of material damages caused by earthquakes.

Some countries have seriously considered to ban or severely restrict the use of masonry in seismic zones. The progress of earthquake engineering has however provided a comprehensive view of masonry characteristics and shown that it is possible to mitigate the problems of its use as a structural material in seismic areas.

The present notes are intended to review the main aspects of such problems and the solutions that are currently adopted.

## 2. TYPICAL SYSTEMS OF STRUCTURAL MASONRY

Masonry is typically used in one of the following shear wall structural systems:

- Simple, nonreinforced masonry, made of blocks and mortar.
- Reinforced masonry, having steel bars embedded in the mortar, in horizontal and for vertical layers, to provide some ductility and additional resistance.
- Confined (or bounded) masonry, with wall masonry panels bounded by reinforced concrete lintels and columns poured after the masonry panels are assembled, in order to get a good connection between lintels, columns and the masonry itself.
- Infill walls within framed structures. In this case masonry is not considered to make part of the main structure, designed to carry vertical and horizontal loads. However the structural interaction between the framed structure and the infill walls is of great importance as far as seismic actions are concerned and must be taken upon consideration.

Simple, nonreinforced masonry has been largely used, with

poor results, evidenced whenever such constructions are subjected to earthquakes, even of moderate intensity. The material is stiff and can have a considerable resistance under monotonic slow loads but is weak in tension and brittle in compression, with little ductility under dynamic actions and imposed deformations. Therefore it cracks very easily, it loses its cohesion, failing to bear floor and roof loads very quickly.

Experience has clearly shown, very often in dramatic conditions, that simple masonry is not adequate in seismic zones. It should be noted that even in non seismic zones its behaviour as a structural system is poor, due to being very sensible to cracking caused by thermal actions, foundation settlements, etc.

Reinforced masonry is rather used in some countries, namely Italy and New Zealand. The reinforcement can be provided by bars, inside the blocks (vertical), embedded in the horizontal joints or inside the coating mortar, or by welded mesh of small diameter steel embedded in the coating mortar. The reinforcement can be concentrated in local zones (near door and window openings) or uniformly placed.

The structural behaviour of reinforced masonry is much better, than the one of simple masonry. It is not a widely used system in the mediterranean area, possibly due to requiring skilled labour and a construction technology that is considerably different from the traditional one. Also there is lack of basic research and of simple design procedures and codes and standards in this field. It is felt that it should be an important topic of research, since it can provide in several situations better solutions than the ones obtained by the use of confined masonry.

Confined (bounded) masonry is by large the most common process of using resistant masonry in small buildings. It is a traditional method of construction in most mediterranean countries, not only in buildings but also in retaining walls, reservoirs, etc. It does not require very skilled labour or sophisticated mechanical equipment, since floor loads are consecutively carried by the confined masonry. Also it allows to separate the tasks of placing the masonry itself and the confinement, which is very convenient for the construction process.

Confined masonry is currently used in dwelling units and in small buildings up to three stories, even in zones of strong seismicity. Such buildings are considered as non-engineered <sup>(a)</sup> in several codes, such as the 1958 Portuguese Code, presently under revision. In general the codes prescribe maximum general dimensions, distance between resistant walls, vertical and horizontal confinements, mechanical resistance of the masonry and mortar and concrete and steel section of confinement elements.

---

a) The term "non-engineered building" applies to a building whose design for seismic actions is based mostly on a set of specifications derived from observed behaviour of such buildings during past earthquakes using engineering judgment.

### 3 . BEHAVIOUR OF MASONRY DURING EARTHQUAKES

The behaviour of masonry under seismic areas is nowadays well known. The technical literature on earthquake engineering presents very complete information on the subject. Engineering surveys after earthquakes have reported the damage suffered by different types of masonry construction, relating such damage with the characteristics of the ground motion, of the masonry and of the structural systems. Such reports cover seismic activity in the Baalkan countries, Italy, Spain and Portugal, North Africa and many other zones. It is interesting to remind the similarities of masonry construction in all these countries and therefore the common features of earthquake damage pattern.

(Follows 15 min. film about Agadir, Morocco earthquake of 1960 and slides showing damage in masonry after several earthquakes namely in the mediterranean area)

The main conclusions of all such surveys clearly point out as aforesaid that simple nonreinforced masonry is not all adequate and that reinforced and confined masonry, when properly designed and built, are a simple and economic process of providing seismic resistance to small buildings, thus saving human lifes as a primary concern, avoiding collapse and mitigating structural and non-structural damage.

### 4 . DYNAMIC BEHAVIOUR OF MASONRY BUILDINGS

The dynamic behaviour of resistant masonry small buildings is very complex. In fact the high stiffness to horizontal loads originates very high accelerations and inertial forces. Consequently it is not permissible to model floors as rigid diaphragms in their plane as is usually assumed for tall buildings. Also the wall panels should be modelled as plates or as vertical slabs according to the direction of seismic actions being considered. Finally the foundation deformability must be taken in to consideration due to the high stiffness of the superstructure.

However, although the real dynamic behaviour of such structures is very complex, it is not sound to use very sophisticated models for their design, but rather to establish simple provisions, adapted to local materials and construction technologies and based on numerical and experimental studies whose results and conclusions can be settled in codes.

Such studies have been carried out in many research centers, using different types of materials and structural systems. Results are analysed and compared with those obtained by inspection of the behaviour of real structures subjected to earthquakes.

The following slides present some seismic studies performed at LNEC (Lisbon) on traditional and prefabricated shear wall buildings.

As mentioned before, the results obtained in such studies have enabled the progress of code provisions for safer masonry buildings in seismic zones. In Portugal the code for small buildings with

confined brick or concrete block masonry is under revision. The more important provisions of the draft under preparation are presented in the Appendix.

Most of those provisions have already been applied in the reconstruction at the Azores islands affected by a strong earthquake in January 1980.

## 5. FINAL REMARKS

The following general statements and conclusions should be derived from the present notes:

5.1. Small buildings, up to three floors, with resistant masonry are very common in mediterranean countries and therefore of great economic and social impact.

5.2. It is possible to provide adequate seismic resistance for this type of buildings, in zones of moderate or even of strong seismicity, as are the ones in that region.

5.3. As these buildings are usually of non-engineered construction, the best way to provide seismic safety is through simple and general code provisions, adapted to local conditions of materials and construction technologies.

5.4. The similarities of these type of construction in many mediterranean countries should stimulate the international cooperation among researchers, designers and the building industry. The European Association of Earthquake Engineering (EAEE) is willing to pursue its efforts in promoting such a cooperation.

## APPENDIX

Draft of revised Portuguese code provisions for the seismic design of small buildings of confined masonry

### 1. Object and scope of provisions

These provisions apply only to small buildings and enable to part with explicit structural design methods as far as seismic actions are concerned. The characteristics of such small buildings are the following:

- . Buildings with resistant confined masonry of brick or concrete blocks
- . Housing and dwelling buildings where no concentration of people is predictable
- . Maximum floor area 200 sqm
- . Maximum number of stories: two in seismic zones A and B or three in seismic zones C and D (b)
- . Maximum floor height of 3.20 m

### 2. STRUCTURAL CONCEPT

The confined masonry panels must be disposed along two orthogonal directions. Geometrical characteristics and stiffness should be such to avoid or to attenuate assymetry. All panels should be completely confined and interconnected. Spans should be regular along the various floors.

Foundation should be monolithic, acting as a grid in order to confine all the panels base.

### 3. MASONRY CHARACTERISTICS

This section establishes geometric and mechanical characteristics of the masonry - bricks, concrete blocks or even regular stone. In the case of bricks and concrete blocks, the maximum percentage of voids is 0.60. The minimum thickness of the septs is 9 mm for bricks and 25 mm for concrete blocks.

The mortar must have a characteristic compressive resistance at 28 days of 8MPa (80 kgf/cm<sup>2</sup>), determined according to the Portuguese standard.

---

b) The following macrozoning basis has been considered:

- Zone A - Seismic zone of Destruction Risk (MMI IX or more is probable)
- Zone B - Seismic zone of Heavy Damage Risk (MMI VIII is probable)
- Zone C - Seismic zone of Moderate Risk (MMI VII is probable)
- Zone D - Seismic zone of Little Risk (MMI VI or less is probable)

The minimum compression resistance of masonry elements is 2.5 MPA (25 kgf/cm<sup>2</sup>) referred to the apparent external cross section.

The minimum cross section of confined walls at each level and on each main orthogonal direction cannot be less than 0.04 (seismic zones A, B) or 0.03 (zones C, D) of the floor area. In that cross section walls having thickness  $\leq 12$  cm, walls above or below door and window openings should not be considered. All wall zones having ratios length/height smaller than 0.40 should be neglected in the cross area estimation. The same applies to wall zones having horizontal ducts affecting more than 0.20 of the masonry resistance.

#### 4. CONFINEMENTS

The confinements should limit all the wall panels. They are made of reinforced concrete columns and lintels. The materials must follow the general prescriptions of concrete, steel and reinforced concrete. If these elements are used not only as confinement for seismic actions but also to support other types of loads they must be designed accordingly.

Columns should occur at building corners, at the intersection of all resistant masonry panels with a maximum spacing of 5 m.

Lintels should occur at floor levels and at the roof level. Cross sections should have 20 cm minimum height and a minimum width equal to the width of the confined masonry, not less than 15 cm.

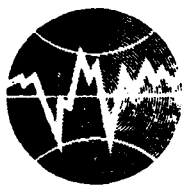
Reinforcement must have a minimum of 4 bars, 10 mm diameter for hard steel A400 or 12 mm for wild steel. Stirrups should have minimum diameters of 6 mm spaced at 15 cm.

#### 5. FLOORS

The draft includes some provisions concerning floors, made of reinforced concrete slabs of several types.

## REFERENCES

- J. Ferry Borges and A. Ravara (1969) "Earthquake Engineering", Course 113, Laboratório Nacional de Engenharia Civil, Lisbon.
- (1980) "Guide-lines for Earthquake Resistant Non-Engineered Construction", International Association for Earthquake Engineering, Committee II, Jacarta.
- E. C. Carvalho, R. T. Duarte and C. S. Oliveira (1985) "Seismic Safety of Non-Engineered Construction", Proceedings 1st National Symposium on Building Materials and Technologies, Instituto Superior Técnico, Lisbon (in portuguese)
- C. S. Oliveira, E. C. Carvalho and A. Ravara (1984) "Reconstruction Policies and Techniques Used in Azores after the January 1st, 1980 Earthquake", Proceedings International Symposium on Earthquake Relief in less Industrialized Areas, Zurich.
- E. C. Carvalho, C. S. Oliveira (1983) "Manual for Earthquake Resistant Non-Engineered Construction". Technical Report, Laboratório Nacional de Engenharia Civil. (in Portuguese)
- (1958) "Earthquake Resistant Code for Non-Engineered Construction", Decree nº 41658 of May, 31, 1958. (in Portuguese)
- M. J. N. Priestley (1987) "Seismic Design Philosophy for Masonry Structures", Course on Recent Advances in Earthquake-Resistant Design, University of California, Berkeley.
- (1984) International Association for Earthquake Engineering, Earthquake Resistant Regulations, A World List - 1984, Gakujutsu Bunken Fukyu-kai, Tokyo.
- (1986) Proceedings of the Meeting of the Working Group of EAEE on "Contemporary Rural Housing in Seismic Areas", Ed. by R. Yazar, Turkish National Committee for Earthquake Engineering, Publication Nº 3, Istanbul.
- S. Di Pasquale, S. Bricoli Bati, M. Paradiso, G. Tempeste and U. Toniatti (1986) "Structural Behaviour of Masonry Structures", Proc. SECEE, Vol. 3, Lisbon.
- A. Giuffré and C. Baggio, (1986) "Design Parameters Calibration for Reinforced Masonry Buildings in Seismic Zones, Proc. SECEE, Vol. 5, Lisbon.



**TURKISH NATIONAL COMMITTEE FOR  
EARTHQUAKE ENGINEERING**

**THIRTEENTH REGIONAL SEMINAR ON EARTHQUAKE ENGINEERING**

**September 14-24, 1987 - Istanbul - Turkey**

**CLAES DYRBYE**

**Department of Structural Engineering  
Technical University of Denmark**

**RESPONSE OF ELASTIC FRAMES TO SEISMIC ACTIONS**



## 1. Introduction

Calculation of the response of structures to seismic actions may be carried out in different ways. One way is to rely upon large computer programs and just provide the structural data and the data of the actions to the computer and then get the response data as output from the computer.

If a program is not available or if there are difficulties in access to a large computer, it may be an advantage to perform the calculations by means of a personal computer.

Also, calculations of simpler systems on a personal computer may be used to check calculations by means of commercially available programs on larger computers. As it may be difficult to estimate if the results are correct, calculations made in quite different ways may be an excellent useful method of checking.

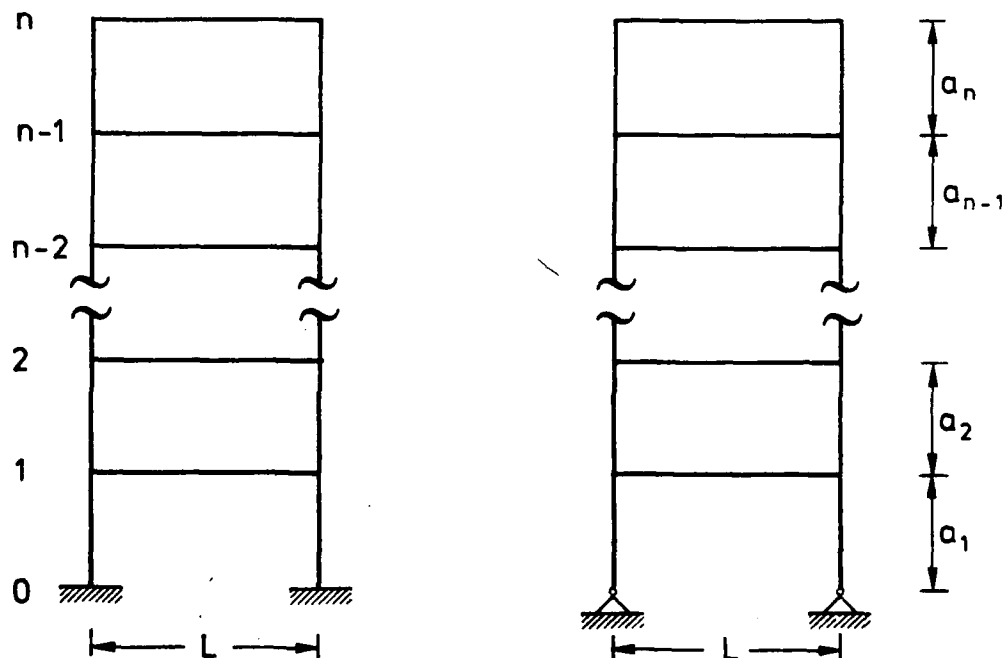


Fig. 1. Frame systems and notations.

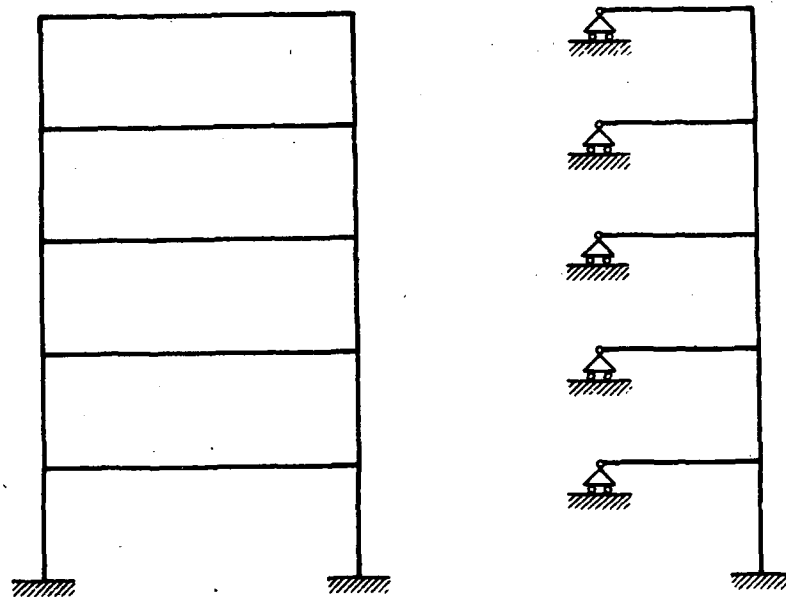


Fig. 2 Clamped frame and calculation model.

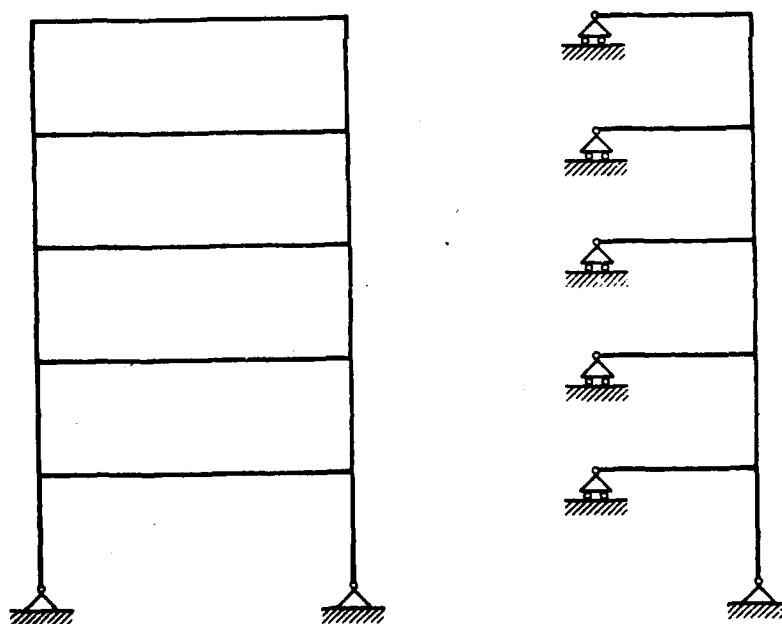


Fig. 3 Hinged frame and calculation model.

This paper describes a method of calculating response of plane frames with two vertical columns connected by horizontal beams, shown in figure 1.

The following assumptions are made:

- 1) The structure is elastic and viscously damped.
- 2) The connections at the joints are rigid meaning that the beam and the column elements have the same deflection and the same rotation at the joints.
- 3) The left column and the right column are identical.
- 4) Each horizontal beam has a constant cross section.
- 5) Between the joints, the columns have a constant cross section.
- 6) The columns are either clamped (zero rotation) or hinged (zero bending moment) at the foundations.
- 7) The seismic actions cause identical horizontal motions of the foundations.

It follows from the assumptions that the motions of the structure will be antisymmetric. This gives rise to important simplifications in the calculations. The midpoint of each horizontal beam then has no vertical motion, and at the midpoint both the normal force and the bending moment are zero. Then the calculation models shown in figs. 2 and 3 are introduced.

With regard to the calculations, some simplifying approximations are made:

- 1) The masses of the columns are concentrated at the joints.

2) The inertial forces resulting from vertical accelerations of the horizontal beams are neglected.

3) Only deformations due to bending moments are taken into account (the Bernouilli-Euler theory).

4) Influence of normal forces upon the bending stiffness is neglected.

In the method described in the following sections, calculations are carried out by a step procedure in space and a step procedure in time.

To some degree, the step procedures in time and in space are interconnected.

Briefly, the procedure can be described as follows:

At a time  $t_r$  all deflections and rotations of the joints and their time derivatives of first and second order are known, and also the shear forces and the bending moments are known.

At the time  $t_{r+1}$  let us assume that we have been able to find the deflections from the bottom and upwards to joint No.  $j-1$ , and that the shear force and the bending moment just above joint  $j-1$  are also determined.

Then it becomes possible to calculate the deflection and rotation in the column just below joint No.  $j$  at time  $t_{r+1}$  and also the bending moment below joint No.  $j$ , see section 4.

From an assumption of constant acceleration during each time step, see section 3, the acceleration and the velocity of joint No.  $j$  at time  $t_{r+1}$  and the rotation velocity at joint No.  $j$  is calculated.

Then from Newton's second law the shear force in the column above joint No.  $j$  at time  $t_{r+1}$  can be calculated. The bending

moment at joint No.  $j$  in the horizontal beam follows from the rotation and the rotation velocity, see section 5, and then from moment equilibrium at joint No.  $j$ . the bending moment above joint No.  $j$  in the column at the time  $t_{r+1}$  is found.

In this way, we have succeeded in climbing one storey upwards. The procedure is repeated until the top of the structure is reached. Here, the shear force and the bending moment above joint No.  $n$  shall both be zero, which determines the conditions at the foundation level. For this reason the structure must be "climbed" twice at each time step, the first time in order to calculate the values at foundation level and the second time to find the state of the structure.

## 2. The column element, part 1.

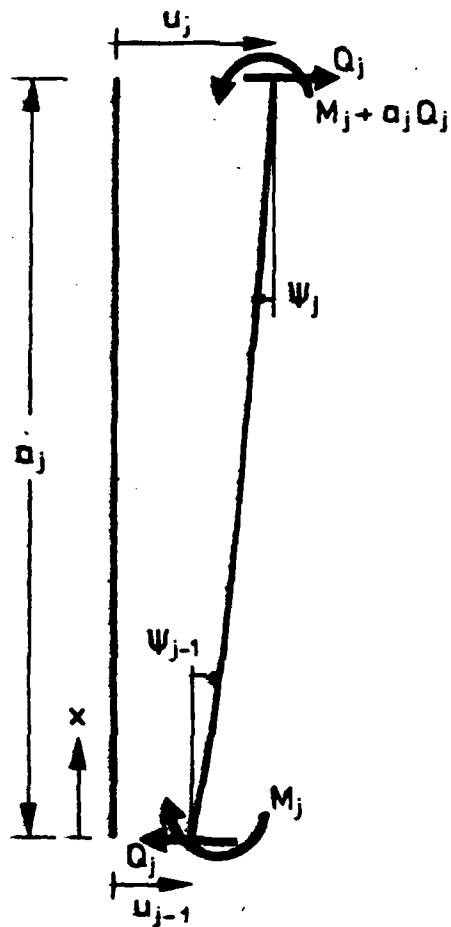


Fig. 4 Notations for a column section.

Assuming that the vertical beam element is unloaded between the horizontal beams, the deflections  $u$  are expressed as a polynomial of the third degree in  $(x/a_j)$ , cf. fig. .

$$u = a + b(x/a_j) + c(x/a_j)^2 + d(x/a_j)^3 \quad (2-1)$$

where  $a$ ,  $b$ ,  $c$  and  $d$  are constants.

The angular rotations  $\psi$  follow from

$$a_j \psi = b + 2c(x/a_j) + 3d(x/a_j)^2 \quad (2-2)$$

The deflections and rotations at the ends of the beam element are

$$\begin{Bmatrix} u_{j-1} \\ a_j \psi_{j-1} \\ u_j \\ a_j \psi_j \end{Bmatrix} = \begin{Bmatrix} 1 & 0 & 0 & 0 \\ 0 & 1 & 0 & 0 \\ 1 & 1 & 1 & 1 \\ 0 & 1 & 2 & 3 \end{Bmatrix} \begin{Bmatrix} a \\ b \\ c \\ d \end{Bmatrix} \quad (2-3)$$

The coefficients are then found as

$$\begin{Bmatrix} a \\ b \\ c \\ d \end{Bmatrix} = \begin{Bmatrix} 1 & 0 & 0 & 0 \\ 0 & 1 & 0 & 0 \\ -3 & -2 & 3 & -1 \\ 2 & 1 & -2 & 1 \end{Bmatrix} \begin{Bmatrix} u_{j-1} \\ a_j \psi_{j-1} \\ u_j \\ a_j \psi_j \end{Bmatrix} \quad (2-4)$$

If it is assumed that the element is elastic, then bending moments  $M$  and shear forces  $Q$  are determined by

$$M = -EI_j \frac{d^2 u}{dx^2} \quad (2-5)$$

$$Q = -EI_j \frac{d^3 u}{dx^3} \quad (2-6)$$

where  $E$  is the modulus of elasticity and  $I_j$  is the moment of inertia of column No.  $j$ .

In particular, we find

$$M_j = -EI_j \frac{d^2 u}{dx^2} \Big|_{x=0} = -\frac{EI_j}{a_j^2} \cdot 2c \quad (2-7)$$

$$Q_j = -EI_j \frac{d^3 u}{dx^3} \Big|_{x=0} = -\frac{EI_j}{a_j^3} \cdot 6d \quad (2-8)$$

and by combining the expressions

$$Q_j = 6 \frac{EI_j}{a_j^3} ((-2u_{j-1} - a_j \psi_{j-1}) + (2u_j - a_j \psi_j)) \quad (2-9)$$

$$M_j = 2 \frac{EI_j}{a_j^2} ((3u_{j-1} + 2a_j \psi_{j-1}) + (-3u_j + a_j \psi_j)) \quad (2-10)$$

The column stiffness  $k_j$  is introduced as

$$k_j = \frac{12EI_j}{a_j^3} \quad (2-11)$$

and we obtain

$$Q_j = k_j ((-u_{j-1} - \frac{1}{2} a_j \psi_{j-1}) + (u_j - \frac{1}{2} a_j \psi_j)) \quad (2-12)$$

$$M_j = a_j k_j ((\frac{1}{2} u_{j-1} + \frac{1}{3} a_j \psi_{j-1}) + (-\frac{1}{2} u_j + \frac{1}{6} a_j \psi_j)) \quad (2-13)$$

When the structure is vibrating, energy will be absorbed by damping. As a reasonable assumption, we shall assume that within each element the damping forces are proportional to the velocities. The contributions from damping to  $Q_j$  and  $M_j$  are found by replacing the deflections and rotations with the rates of deflection and rotation, and by replacing the stiffness  $k_j$  by a damping factor  $c_j$ . In this way,

$$\begin{aligned} Q_j &= k_j ((-u_{j-1} - \frac{1}{2} a_j \psi_{j-1}) + (u_j - \frac{1}{2} a_j \psi_j)) \\ &+ c_j ((-\dot{u}_{j-1} - \frac{1}{2} a_j \dot{\psi}_{j-1}) + (\dot{u}_j - \frac{1}{2} a_j \dot{\psi}_j)) \end{aligned} \quad (2-14)$$



$$\begin{aligned}
M_j &= a_j k_j \left( \left( \frac{1}{2} u_{j-1} + \frac{1}{3} a_j \psi_{j-1} \right) + \left( -\frac{1}{2} u_j + \frac{1}{6} a_j \psi_j \right) \right) \\
&\quad + a_j c_j \left( \left( \frac{1}{2} \dot{u}_{j-1} + \frac{1}{3} a_j \dot{\psi}_{j-1} \right) + \left( -\frac{1}{2} \dot{u}_j + \frac{1}{6} a_j \dot{\psi}_j \right) \right) \quad (2-15)
\end{aligned}$$

### 3. Newmark's $\beta$ -method

In order to solve the dynamic problems, it is necessary to perform some kind of numerical integration in time. This will be done here by the following procedure:

The quantities we are looking for, will only be determined at certain times  $t_0, t_1, t_2, \dots, t_N$ . A time step  $\tau_0$  is chosen, and

$$t_{r+1} - t_r = \tau_0 \quad (3-1)$$

shall be fulfilled for all values of  $r$ . Let  $u_{j,r}$  and  $\psi_{j,r}$  denote the value of the deflection  $u_j$  and the rotation  $\psi_j$  at the time  $t_r$ .

The numerical integration is based upon the approximation that the acceleration  $\ddot{u}_j$  has a constant value in each time interval.

$$\ddot{u}_j(t) = \frac{1}{2} (\ddot{u}_{j,r} + \ddot{u}_{j,r+1}) \quad t_r < t < t_{r+1} \quad (3-2)$$

Integrating (3-2) yields

$$\dot{u}_j(t) = \dot{u}_{j,r} + \frac{1}{2}(t-t_r)(\ddot{u}_{j,r} + \ddot{u}_{j,r+1}) \quad (3-3)$$

and corresponding to  $t=t_{r+1}$

$$\dot{u}_{j,r+1} = \dot{u}_{j,r} + \frac{\tau_0}{2} (\ddot{u}_{j,r} + \ddot{u}_{j,r+1}) \quad (3-4)$$

Integrating (3-3) from  $t_r$  to  $t_{r+1}$

$$u_{j,r+1} = u_{j,r} + \tau_0 \dot{u}_{j,r} + \frac{\tau_0^2}{4} (\ddot{u}_{j,r} + \ddot{u}_{j,r+1}) \quad (3-5)$$

The expressions are rewritten in the form

$$\ddot{u}_{j,r+1} = -\ddot{u}_{j,r} + \frac{4}{\tau_0^2} (u_{j,r+1} - u_{j,r} - \tau_0 \dot{u}_{j,r}) \quad (3-6)$$

$$\dot{u}_{j,r+1} = -\dot{u}_{j,r} + \frac{2}{\tau_0} (u_{j,r+1} - u_{j,r}) \quad (3-7)$$

and correspondingly

$$\ddot{\psi}_{j,r+1} = -\ddot{\psi}_{j,r} + \frac{4}{\tau_0^2} (\psi_{j,r+1} - \psi_{j,r} - \tau_0 \dot{\psi}_{j,r}) \quad (3-8)$$

$$\dot{\psi}_{j,r+1} = -\dot{\psi}_{j,r} + \frac{2}{\tau_0} (\psi_{j,r+1} - \psi_{j,r}) \quad (3-9)$$

The formulas (3-6) to (3-9) are extremely useful, they correspond to Newmark's  $\beta$ -method with  $\beta=1/4$ . Long experience has shown that the method gives a good accuracy when the time step  $\tau_0$  is adequately chosen.

#### 4. The column element, part 2

In section 2, the shearforce  $Q_j$  and the bending moment  $M_j$  were expressed in terms of the deflections  $u_{j-1}$  and  $u_j$  and in terms of the rotations  $\psi_{j-1}$  and  $\psi_j$  and also in terms of the time derivatives of these quantities, formulas (2-14) and (2-15).

These formulas are now rewritten at the time  $t_{r+1}$ , and the formulas (3-7) and (3-9) are used. This leads to

$$\begin{aligned} Q_{j,r+1} = & (k_j + \frac{2c}{\tau_0}) (-u_{j-1,r+1} - \frac{1}{2} a_j \psi_{j-1,r+1} \\ & + u_{j,r+1} - \frac{1}{2} a_j \psi_{j,r+1}) \\ & + c_j (\ddot{u}_{j-1,r} + \frac{1}{2} a_j \ddot{\psi}_{j-1,r} - \ddot{u}_{j,r} + \frac{1}{2} a_j \ddot{\psi}_{j,r}) \\ & + \frac{2c}{\tau_0} (u_{j-1,r} + \frac{1}{2} a_j \psi_{j-1,r} - u_{j,r} + \frac{1}{2} a_j \psi_{j,r}) \end{aligned} \quad (4-1)$$

$$\begin{aligned} \frac{1}{a_j} M_{j,r+1} = & (k_j + \frac{2c}{\tau_0}) (\frac{1}{2} u_{j-1,r+1} + \frac{1}{3} a_j \psi_{j-1,r+1} \\ & - \frac{1}{2} u_{j,r+1} + \frac{1}{6} a_j \psi_{j,r+1}) \\ & + c_j (-\frac{1}{2} \ddot{u}_{j-1,r} - \frac{1}{3} a_j \ddot{\psi}_{j-1,r} + \frac{1}{2} \ddot{u}_{j,r} - \frac{1}{6} a_j \ddot{\psi}_{j,r}) \\ & + \frac{2c}{\tau_0} (-\frac{1}{2} u_{j-1,r} - \frac{1}{3} a_j \psi_{j-1,r} + \frac{1}{2} u_{j,r} - \frac{1}{6} a_j \psi_{j,r}) \end{aligned} \quad (4-2)$$

The equations (4-1) and (4-2) are solved with respect to  $u_{j,r+1}$  and  $\psi_{j,r+1}$ .

$$\begin{aligned}
u_{j,r+1} &= u_{j-1,r+1} + a_j \psi_{j-1,r+1} \\
&+ \frac{1}{k_j + \frac{1}{\tau_0}} \left[ c_j (\dot{u}_{j,r} - \dot{u}_{j-1,r} - a_j \dot{\psi}_{j-1,r}) \right. \\
&+ \frac{2c_j}{\tau_0} (u_{j,r} - u_{j-1,r} - a_j \psi_{j-1,r}) \\
&\left. - 2Q_{j,r+1} - \frac{6}{a_j} M_{j,r+1} \right] \quad (4-3)
\end{aligned}$$

$$\begin{aligned}
\psi_{j,r+1} &= \psi_{j-1,r+1} + \frac{1}{k_j + \frac{1}{\tau_0}} \left[ c_j (\dot{\psi}_{j,r} - \dot{\psi}_{j-1,r}) \right. \\
&+ \frac{2c_j}{\tau_0} (\psi_{j,r} - \psi_{j-1,r}) - \frac{6}{a_j} Q_{j,r+1} - \frac{12}{a_j^2} M_{j,r+1} \left. \right] \quad (4-4)
\end{aligned}$$

These expressions can be found in Dyrbye (1986), but it should be noted that a different definition of shear force and bending moment was used in the paper.

Claes Dyrbye: Dynamic Response of Framed Structures. Earthquake Engineering and Structural Dynamics, Vol.14, p. 487-494, 1986.

## 5. The horizontal beams

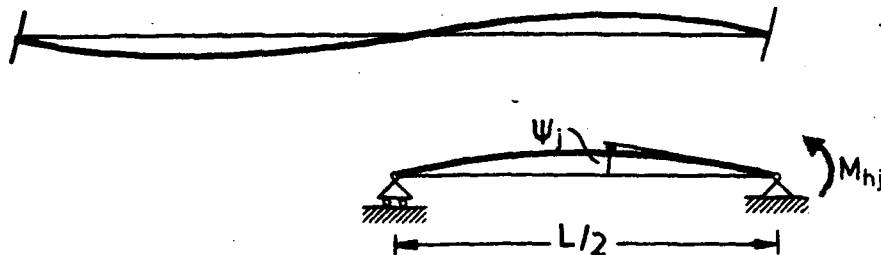


Fig. 5 Model of horizontal beam.

As the structure performs antisymmetrical motions, the center of each horizontal beam has no vertical motion. Furthermore, the normal force and the bending moment are both zero at the center of the beam.

The vertical inertial forces are neglected, and this will usually be a reasonable approximation. If the structure was elastic, the bending moment  $M_{hj}$  in the beam would be

$$M_{hj} = - \frac{3EI_{hj}}{(L/2)} \psi_j \quad (5-1)$$

where  $I_{hj}$  is the inertia moment of the beam. Introducing the stiffness  $k_{hj}$  defined as

$$k_{hj} = \frac{6EI_{hj}}{L} \quad (5-2)$$

we simply find

$$M_{hj} = - k_{hj} \psi_j \quad (5-3)$$

It seems reasonable to assume that some energy may be dissipated from the motion of the horizontal beams, and we shall therefore replace equation (5-3) by

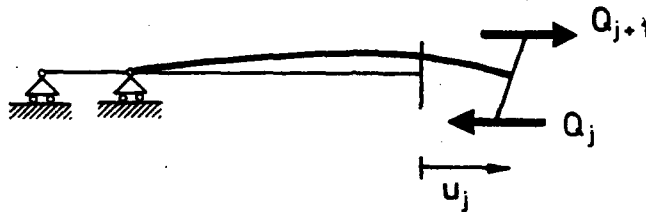


Fig. 6 Forces acting upon horizontal beam.

$$M_{hj} = -k_{hj}\psi_j - c_{hj}\dot{\psi}_j \quad (5-4)$$

where  $c_{hj}$  is a damping coefficient for the horizontal beam No.  $j$ .

It should be noticed that the dimensions of  $k_{hj}$  and  $c_{hj}$  differ from the dimensions of  $k_j$  and  $c_j$  respectively.

The total mass at level  $j$  is called  $m_j$ . Applying Newton's law, see fig. 6, gives

$$\frac{1}{2} m_j \ddot{u}_j = Q_{j+1} - Q_j \quad (5-5)$$

The moments at joint No.  $j$  are shown in fig. 7, from which follows

$$M_{j+1} = M_j + a_j Q_j + M_{hj} \quad (5-6)$$

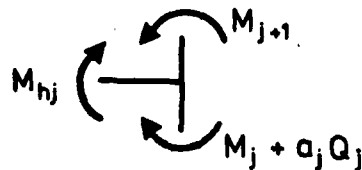


Fig. 7 Moments at joint No.  $j$ .

## 6. Performing a time step

Let everything of importance at the time  $t_r$  be known. Then we shall carry out calculations in order to find out, how the state of the structure will be at the time  $t_{r+1}$ .

Starting with the motions at foundation level, the ground motions will usually be given by the accelerations.

At level 0 we thus know  $u_{0,r}$ ,  $\dot{u}_{0,r}$  and  $\ddot{u}_{0,r}$ , and  $u_{0,r+1}$  follows from the accelerogram. The integration procedure from section 3 is applied, and from the formulas (3-4) and (3-5) we find

$$\dot{u}_{0,r+1} = \dot{u}_{0,r} + \frac{\tau_0}{2} (\ddot{u}_{0,r} + \ddot{u}_{0,r+1}) \quad (6-1)$$

$$u_{0,r+1} = u_{0,r} + \tau_0 \dot{u}_{0,r} + \frac{\tau_0^2}{4} (\ddot{u}_{0,r} + \ddot{u}_{0,r+1}) \quad (6-2)$$

If the structure is clamped at the foundation level, we have  $\psi_{0,r+1} = 0$  and  $\dot{\psi}_{0,r+1} = 0$ . If the structure is hinged at the foundation,  $\psi_{0,r+1}$  and  $\dot{\psi}_{0,r+1}$  must be determined by the method described later, but for the purpose of a more straightforward presentation we shall at present assume these quantities to be known.

The shearforce  $Q_{1,r+1}$  is also unknown, but again let us assume that a value is known.

If the structure is hinged at the foundation level,  $M_{1,r+1}$  is zero, but if the structure is clamped, the value of  $M_{1,r+1}$  is not known, but will be determined in a way which will be described later. For the description of the procedure we assume  $M_{1,r+1}$  known.



Taking  $j = 1$ , all elements on the right hand side of eqs. (4-3) and (4-4) are known, and the equations are used to calculate  $u_{1,r+1}$  and  $\psi_{1,r+1}$ .

From the formulas (3-6), (3-7) and (3-9),  $\dot{u}_{1,r+1}$ ,  $\ddot{u}_{1,r+1}$  and  $\dot{\psi}_{1,r+1}$  are calculated.

As  $\psi_{1,r+1}$  and  $\dot{\psi}_{1,r+1}$  have been found, the bending moment  $M_{h1,r+1}$  in the horizontal beam follows from (5-4),

$$M_{h1,r+1} = -k_{h1}\psi_{1,r+1} - c_{h1}\dot{\psi}_{1,r+1} \quad (6-3)$$

and from equation (5-6) follows

$$M_{2,r+1} = M_{1,r+1} + a_1 Q_{1,r+1} + M_{h1,r+1} \quad (6-4)$$

Finally, the shear force above joint No.  $j$  follows from eq. (5-5) as

$$Q_{2,r+1} = Q_{1,r+1} + \frac{1}{2} m_1 \ddot{u}_{1,r+1} \quad (6-5)$$

Thus it has been described, how the conditions above joint No. 1 could be derived when the conditions above joint No. 0 was known.

The same procedure can now be used upwards, and coming to the top of the structure we finally calculate  $M_{n+1,r+1}$  and  $Q_{n+1,r+1}$  as a bending moment and a shear force which must be applied in order to fulfil the equations of dynamics and of equilibrium.

It is, however, impossible to have forces acting at the top of the structure and consequently we must demand

$$M_{n+1,r+1} = 0 \quad (6-6)$$

$$Q_{n+1,r+1} = 0 \quad (6-7)$$

These equations can be fulfilled, if correct values of the unknown quantities at level 0 are chosen.

### 6.1 Clamped structures

Let us first examine a structure clamped at the foundation level, where the unknown quantities are  $Q_{1,r+1}$  and  $M_{1,r+1}$ . A close examination of the equations used at the calculations show that the problem is linear. Consequently,

$$\begin{Bmatrix} M_{n+1,r+1} \\ Q_{n+1,r+1} \end{Bmatrix} = \begin{Bmatrix} M_{n+1}^m & M_{n+1}^q \\ Q_{n+1}^m & Q_{n+1}^q \end{Bmatrix} \begin{Bmatrix} M_{1,r+1} \\ Q_{1,r+1} \end{Bmatrix} + \begin{Bmatrix} M_{n+1,r+1}^0 \\ Q_{n+1,r+1}^0 \end{Bmatrix} \quad (6-8)$$

$M_{n+1}^m$  and  $Q_{n+1}^m$  are the contributions to  $M_{n+1,r+1}$  and  $Q_{n+1,r+1}$  from  $M_{1,r+1} = 1$  as the only source contributing to deflections, and likewise  $M_{n+1}^q$  and  $Q_{n+1}^q$  are the contributions from  $Q_{1,r+1} = 1$  as the only source.

$M_{n+1,r+1}^0$  and  $Q_{n+1,r+1}^0$  are the bending moment and the shear force above the top of the structure, if we have the correct state of deflections at time  $t_r$  of the ground acceleration and we have chosen  $M_{1,r+1} = 0$  and  $Q_{1,r+1} = 0$ .

The calculation of  $M_{n+1}^m$  and  $Q_{n+1}^m$  will now be shown in detail as it is a very important part of the procedure. We may think of it as a calculation from  $t_0$  to  $t_1$ .

First, let us put all relevant quantities equal to zero at  $t = t_0$ , i.e.

$$\left. \begin{aligned} u_{j,0} &= 0 \\ \dot{u}_{j,0} &= 0 \\ \ddot{u}_{j,0} &= 0 \\ \psi_{j,0} &= 0 \\ \dot{\psi}_{j,0} &= 0 \\ \ddot{\psi}_{j,0} &= 0 \end{aligned} \right\} \quad j = 0 \dots n. \quad (6-9)$$

Furthermore, we shall take

$$\left. \begin{aligned} u_{0,1} &= 0 \\ \psi_{0,1} &= 0 \end{aligned} \right\} \quad (6-10)$$

Finally, we take  $M_{1,1} = 1$  and  $Q_{1,1} = 0$ . Moving from joint No. 0 to joint No. 1, eqs. (4-3) and (4-4) become

$$u_{1,1} = - \frac{1}{k_1 + \frac{1}{\tau_0}} \cdot \frac{6}{a_1} \quad (6-11)$$

$$\psi_{1,1} = - \frac{1}{k_1 + \frac{1}{\tau_0}} \cdot \frac{12}{a_1^2} \quad (6-12)$$

At joint No. 1 we find from the equations (3-6) and (3-9)

$$\ddot{u}_{1,1} = \frac{4}{\tau_0^2} u_{1,1} \quad (6-13)$$

$$\ddot{\psi}_{1,1} = \frac{2}{\tau_0} \psi_{1,1} \quad (6-14)$$

Further at joint No. 1 from eqs. (5-4), (5-6) and (5-5)

$$M_{h1.1} = -k_{h1}\psi_{1.1} - c_{h1}\dot{\psi}_{1.1} \quad (6-15)$$

$$M_{2.1} = 1 + M_{h1.1} \quad (6-16)$$

$$Q_{2.1} = \frac{1}{2} m_1 \ddot{u}_{1.1} \quad (6-17)$$

The following calculations upwards are all based upon the scheme:

$$u_{j.1} = u_{j-1.1} + a_j \psi_{j-1.1} + \frac{1}{k_j + \frac{1}{\tau_0}} (-2Q_{j.1} - \frac{6}{a_j} M_{j.1}) \quad (6-18)$$

$$\psi_{j.1} = \psi_{j-1.1} + \frac{1}{k_j + \frac{1}{\tau_0}} \left[ -\frac{6}{a_j} Q_{j.1} - \frac{12}{a_j} M_{j.1} \right] \quad (6-19)$$

$$\ddot{u}_{j.1} = \frac{4}{\tau_0^2} u_{j.1} \quad (6-20)$$

$$\dot{\psi}_{j.1} = \frac{2}{\tau_0} \psi_{j.1} \quad (6-21)$$

$$M_{hj.1} = -k_{hj}\psi_{j.1} - c_{hj}\dot{\psi}_{j.1} \quad (6-22)$$

$$M_{j+1.1} = M_{j.1} + a_j Q_{j.1} + M_{hj.1} \quad (6-23)$$

$$Q_{j+1.1} = Q_{j.1} + \frac{1}{2} m_j \ddot{u}_{j.1} \quad (6-24)$$

The calculations given by formulas (6-18) to (6-24) are repeated from  $j = 2$  to  $j = n$ .

Finally.

$$M_{n+1}^m = M_{n+1,1} \quad (6-25)$$

$$Q_{n+1}^m = Q_{n+1,1} \quad (6-26)$$

In order to find  $M_{n+1}^q$  and  $Q_{n+1}^q$  a completely analogue method is used, and is only given briefly. We must select  $M_{1,1} = 0$  and  $Q_{1,1} = 1$ .

Eqs. (6-9) and (6-10) are valid. (6-11) and (6-12) shall be replaced by

$$u_{1,1} = -2 \frac{1}{k_1 + \frac{2c_1}{\tau_0}} \quad (6-11a)$$

$$\psi_{1,1} = - \frac{1}{k_1 + \frac{2c_1}{\tau_0}} - \frac{6}{a_1} \quad (6-12a)$$

Eqs. (6-13), (6-14) and (6-15) are valid. (6-16) and (6-17) are replaced by

$$M_{2,1} = M_{h1,1} \quad (6-16a)$$

$$Q_{2,1} = 1 + \frac{1}{2} m_1 u_1 \quad (6-17a)$$

Eqs. (6-18) to (6-24) are valid, finally (6-25) and (6-26) are replaced by

$$M_{n+1}^q = M_{n+1,1} \quad (6-25a)$$

$$Q_{n+1}^q = Q_{n+1,1} \quad (6-26a)$$

The calculation of the matrix

$$\begin{Bmatrix} M_{n+1}^m & M_{n+1}^q \\ Q_{n+1}^m & Q_{n+1}^q \end{Bmatrix}$$

is performed before the calculations of the response to the earthquake motion is carried out.

In the first time step, the initial conditions are given by (6-9). In the following steps, initial conditions are found from the previous calculations. In other words, all quantities with second index named  $r$  will be known before the calculations from time  $t_r$  until time  $t_{r+1}$  are carried out.

It is necessary to perform the calculations twice. In the first calculation,  $M_{1,r+1} = 0$  and  $Q_{1,r+1} = 0$  are chosen, and the calculations are carried out in order to determine  $M_{n+1,r+1}^0$  and  $Q_{n+1,r+1}^0$  appearing in formula (6-8).

Then the values of  $M_{1,r+1}$  and  $Q_{1,r+1}$  are found from Eqs. (6-6), (6-7) and (6-8) and the calculations giving the correct values of the deflections, rotations, shear forces and bending moments and the relevant derivatives are then performed.

In order to illustrate the procedure, a numerical example is given in section 7.

## 6.2 A hinged structure

For the structure hinged at the foundation level, the problem is somewhat different, as we have to find values for  $Q_{1,r+1}$  and for  $\dot{\psi}_{0,r+1}$  and  $\dot{\psi}_{0,r+1}$ . Thus 3 quantities shall be determined but still we only have the two conditions (6-6) and (6-7).

However, looking back at the principles given in section 3 about Newmark's  $\beta$ -method,

$$\dot{\psi}_{0,r+1} = \dot{\psi}_{0,r} + \frac{\tau_0}{2} (\psi_{0,r} + \psi_{0,r+1}) \quad (6-27)$$

$$\psi_{0,r+1} = \psi_{0,r} + \tau_0 \dot{\psi}_{0,r} + \frac{\tau_0^2}{4} (\psi_{0,r} + \psi_{0,r+1}) \quad (6-28)$$

We shall consider the increase in the rate of rotation as the quantity to be determined.

$$\Delta \dot{\psi}_{0,r+1} = \frac{\tau_0}{2} (\psi_{0,r} + \psi_{0,r+1}) \quad (6-29)$$

from which

$$\dot{\psi}_{0,r+1} = \dot{\psi}_{0,r} + \Delta \dot{\psi}_{0,r+1} \quad (6-30)$$

$$\psi_{0,r+1} = \psi_{0,r} + \tau_0 \dot{\psi}_{0,r} + \frac{\tau_0}{2} \Delta \dot{\psi}_{0,r+1} \quad (6-31)$$

The quantities to be determined from the conditions (6-6) and (6-7) are chosen as  $\Delta \dot{\psi}_{0,r+1}$  and  $Q_{1,r+1}$ . Formula (6-8) is replaced by

$$\begin{Bmatrix} M_{n+1,r+1} \\ Q_{n+1,r+1} \end{Bmatrix} = \begin{Bmatrix} M_{n+1}^\psi & M_{n+1}^q \\ Q_{n+1}^\psi & Q_{n+1}^q \end{Bmatrix} \begin{Bmatrix} \Delta \dot{\psi}_{0,r+1} \\ Q_{1,r+1} \end{Bmatrix} + \begin{Bmatrix} M_{n+1,r+1}^0 \\ Q_{n+1,r+1}^0 \end{Bmatrix} \quad (6-32)$$

in which  $M_{n+1}^\psi$  and  $Q_{n+1}^\psi$  are the contributions from  $\Delta \dot{\psi}_{0,r+1} = 1$  as the only action.

Further calculations are made in the same way as calculations for the clamped structure.

## 7. Numerical examples

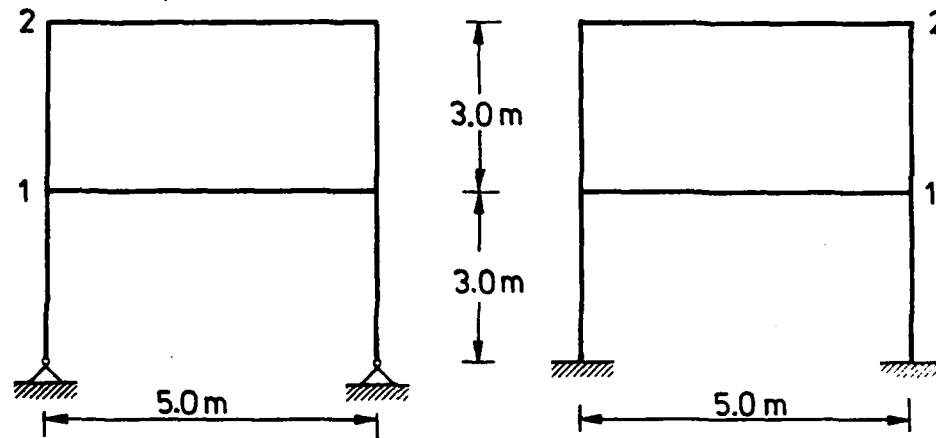


Fig. 8 Two-storey frames.

As an example, the response of 2 frames have been found, when the structures were exposed to ground accelerations shown in fig. 9. The duration of the accelerations is 5 secs.

The frames are identical apart from the supporting conditions, see fig. 8.

The modulus of elasticity is  $E = 2 \cdot 10^{11} \text{ N/m}^2$ . The mass per unit length of a column is 90 kg/m in both storeys, the mass of the beam in storey No. 1 is 1900 kg/m and the mass of the beam in storey No. 2 is 1400 kg/m.

The inertia moment of a column is constant in the entire height  $I_1 = I_2 = 8 \cdot 10^{-5} \text{ m}^4$ . The inertia moments of the beams are  $I_{h1} = 4.5 \cdot 10^{-5} \text{ m}^4$  and  $I_{h2} = 3.5 \cdot 10^{-5} \text{ m}^4$ .

The masses to be used in the calculations are



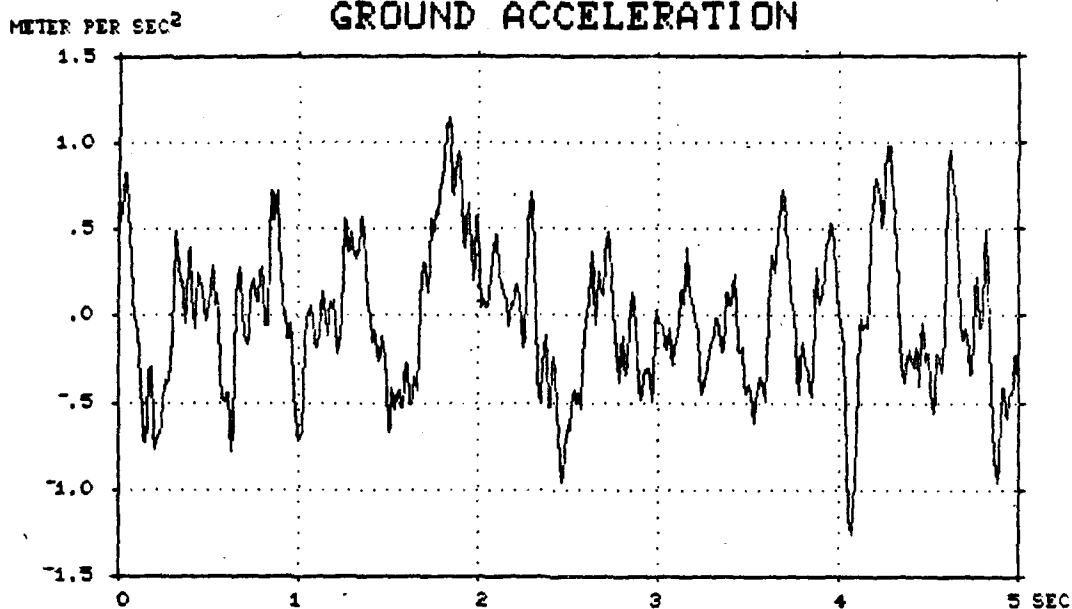


Fig. 9. Ground accelerations.

$$m_1 = 5 \cdot 1900 + 2 \cdot 3.0 \cdot 90 = 10040 \text{ kg}$$

$$m_2 = 5 \cdot 1400 + 2 \cdot 1.5 \cdot 90 = 7270 \text{ kg}$$

The fundamental frequencies of the structures have been calculated as  $f_1 = 1.29 \text{ Hz}$  for the hinged frame and  $f_1 = 2.26 \text{ Hz}$  for the clamped frame.

Values of the damping coefficients should be chosen. As the structure is a steel frame, the damping will be rather moderate, and it is assumed that the damping ratio is  $\zeta_1 = 0.01$  in the fundamental mode of the hinged frame. Further, it is assumed that

$$c_1/k_1 = c_2/k_2 = c_{h1}/k_{h1} = c_{h2}/k_{h2}$$

or that the damping matrix and the stiffness matrices are proportional.

Then if the mode shape vector in the fundamental mode is  $y^1$  and the stiffness and damping matrices are  $K$  and  $C$  resp.,

and  $\underline{y}^1$  is normalized with respect to the mass matrix,

$$\underline{y}^{1T} \underline{K} \underline{y}^1 = (2\pi f_1)^2$$

$$\underline{y}^{1T} \underline{C} \underline{y}^1 = 2(2\pi f_1)\zeta_1$$

From the assumptions follow  $\underline{C} = (c_j/k_j)\underline{K}$ , and

$$(c_j/k_j)(2\pi f_1)^2 = 2 \cdot (2\pi f_1)\zeta_1$$

$$c_j/k_j = \zeta_1/(\pi f_1) = 0.01/(\pi \cdot 1.29) = 0.00247$$

The same values of  $c_j/k_j$  have been chosen for the clamped frame. As the fundamental frequency of this frame is 2.27 Hz, the value of  $\zeta_1$  is  $\zeta_1 = \pi \cdot 2.27 \cdot 0.00247 = 0.018$ .

The shearforces in the hinged frame are shown in fig. 9, and the shear forces in the clamped frame are shown in fig. 10. It should be noted that the force scales are different in the two figures. The bending moments in the clamped frame in column sections above the joints are shown in fig. 11.

Although the ground accelerations are very irregular, the response is highly dominated by vibrations in the fundamental mode, and the phenomenon of beating is also very obvious, especially for the clamped frame.

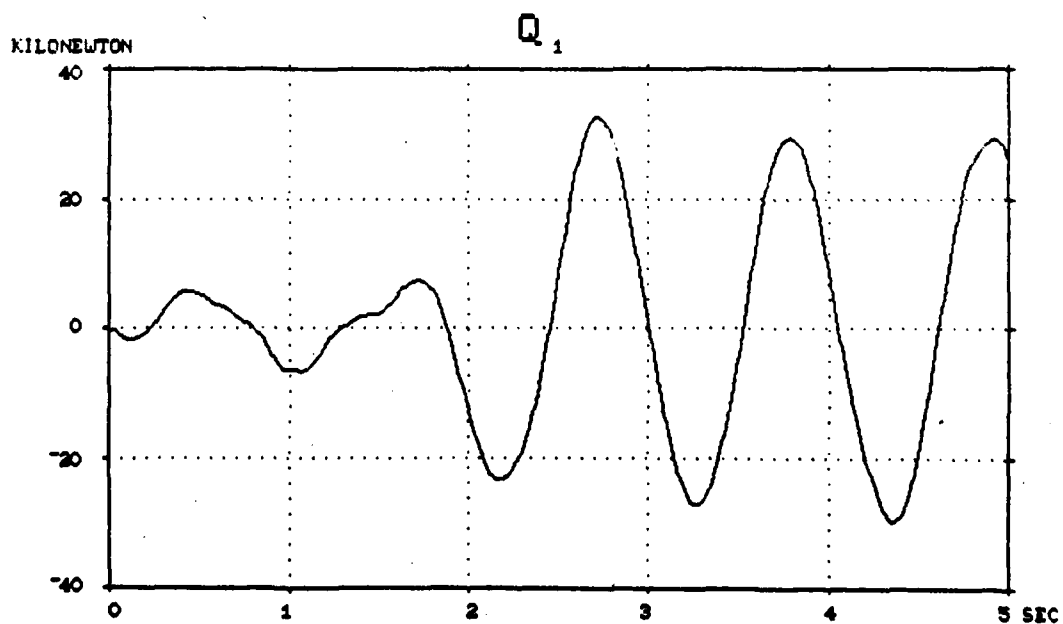
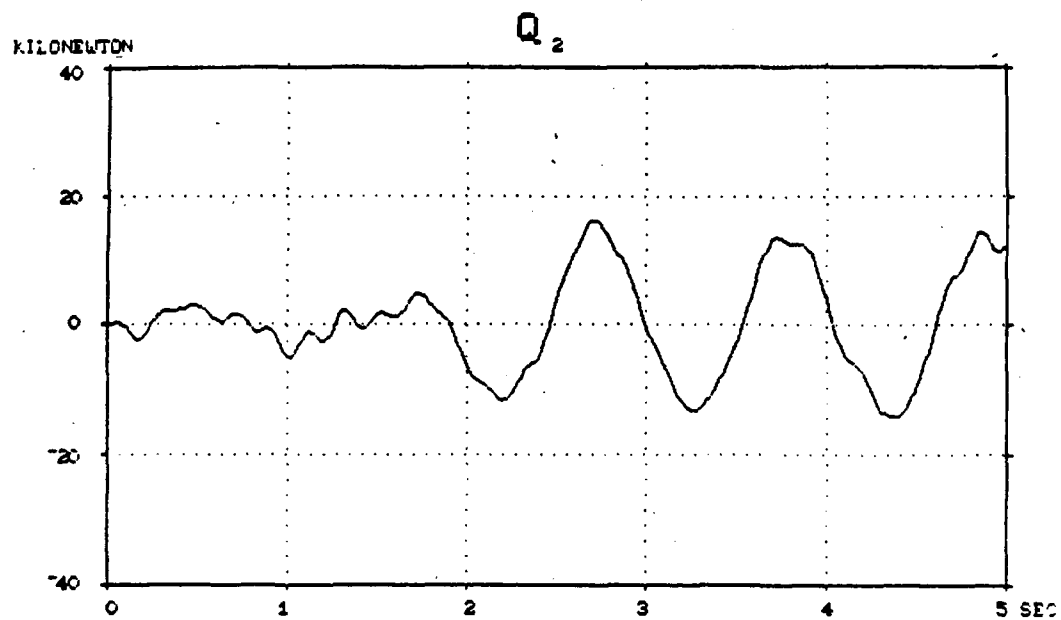


Fig. 10 Shearforces  $Q_1$  and  $Q_2$  in the hinged frame.

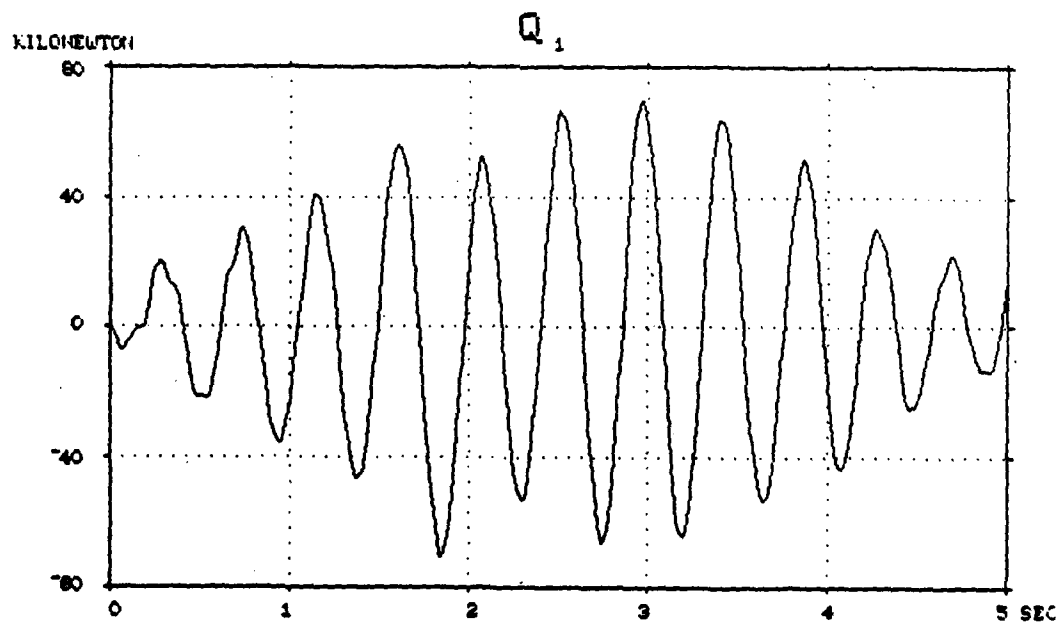
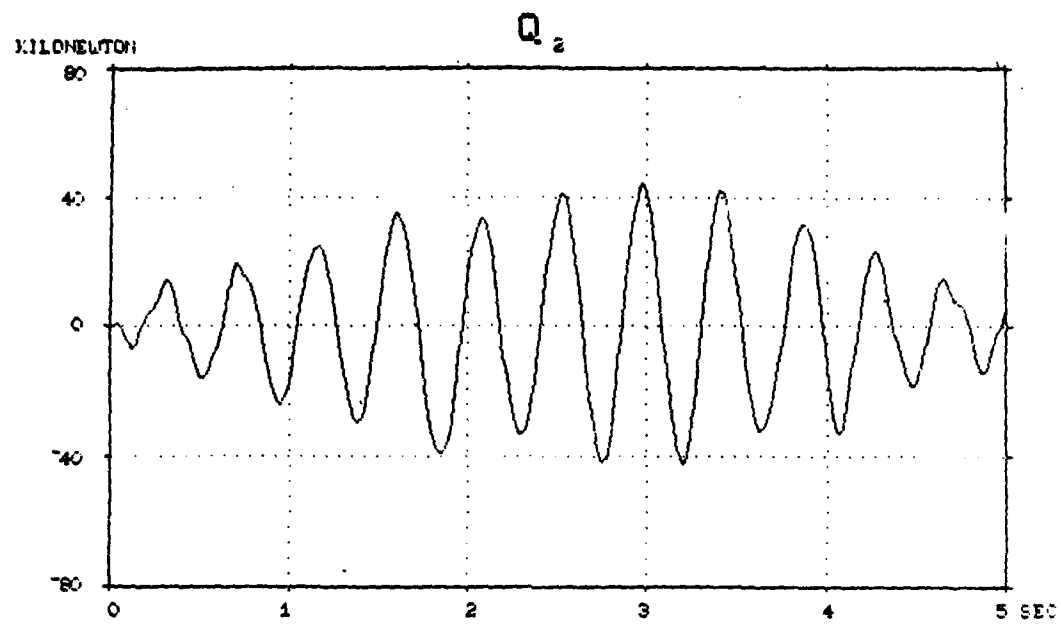


Fig. 11 Shearforces  $Q_1$  and  $Q_2$  in the clamped frame.

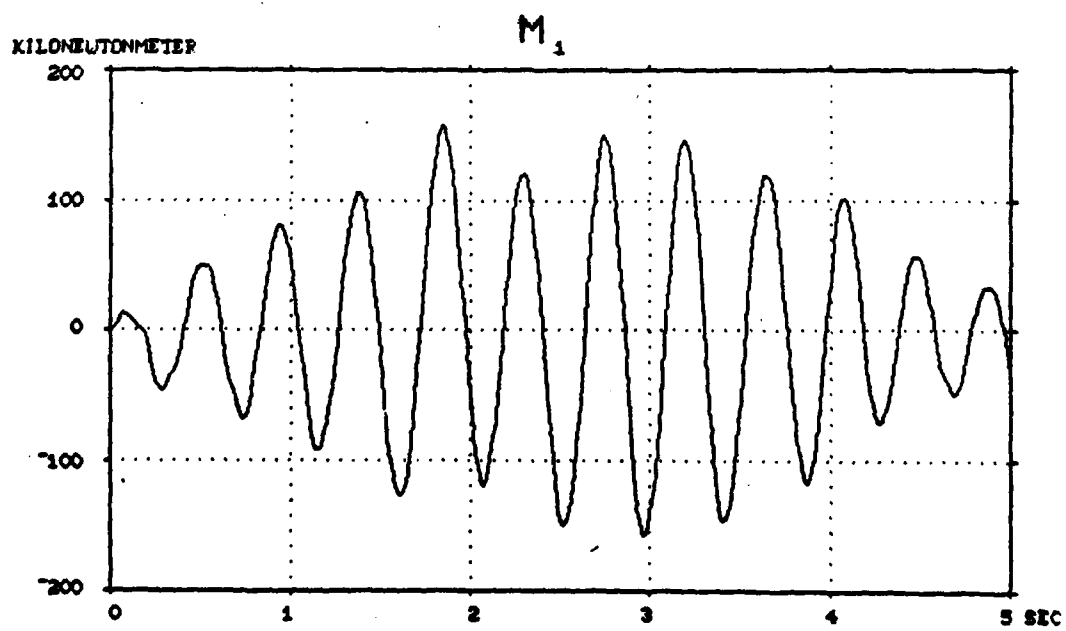
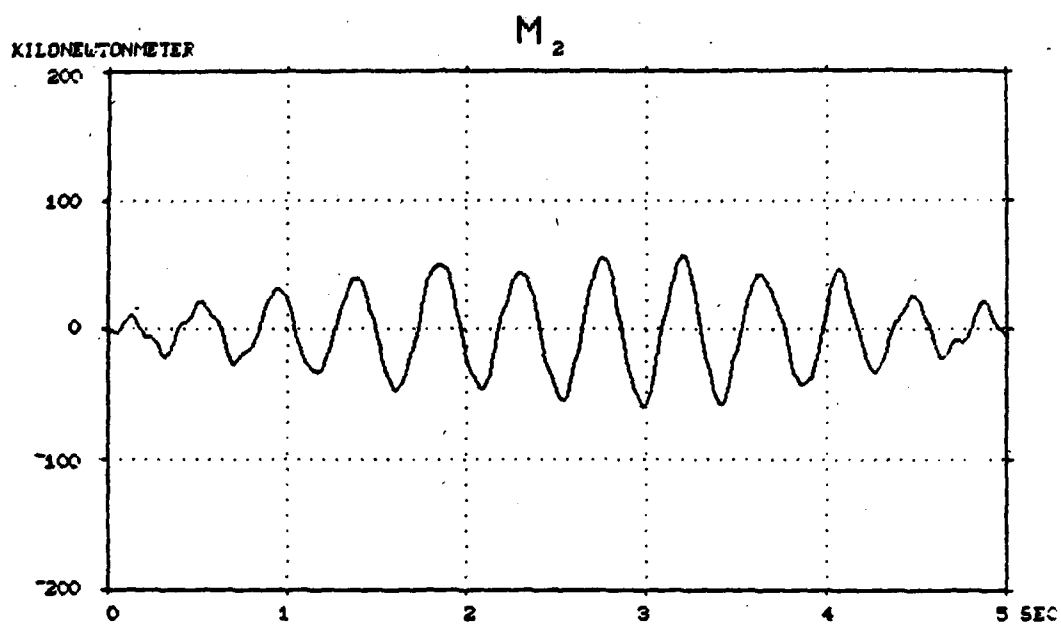
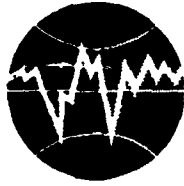


Fig. 12 Bending moments  $M_1$  and  $M_2$  in the clamped frame.



**TURKISH NATIONAL COMMITTEE FOR  
EARTHQUAKE ENGINEERING**

**THIRTEENTH REGIONAL SEMINAR ON EARTQUAKE ENGINEERING**

**September 14-24, 1987 - Istanbul - Turkey**

**SEISMIC RESISTANCE OF HIGH SLENDER STRUCTURES**

**Written by Ondrej FISCHER, Czechoslovak Academy of Sciences, Prague**

## **SEISMIC RESISTANCE OF HIGH SLENDER STRUCTURES**

**Written by Ondrej FISCHER, Czechoslovak Academy of Sciences, Prague**

### **Contents: Foreword**

#### **----- Notation**

- 1. Vibrations of a simple cantilever-beam**
  - 1.1 Natural vibrations**
  - 1.2 Kinematically excited vibrations**
- 2. Natural mode analysis in seismic excitation**
  - 2.1 General remarks**
  - 2.2 Harmonic excitation**
  - 2.3 General deterministic excitation**
  - 2.4 Random excitation**
  - 2.5 Solution using response-spectra curves**
- 3. Construction details**
- 4. Antivibration measures**

#### **References**

**Prague, July 1987**

## FOREWORD

Following text is devoted to the behaviour of high slender structures under seismic excitation. The interpretation has been based predominantly on natural mode analysis, as this approach is quite general and perspicuous. The solution of natural modes can be performed by different methods which are well-known from structural dynamics, and there is no use in arguing, which one is better. The only requirement is to obtain realistic results not only in displacements, but also in bending moments and other stresses, if necessary. The rest depends on the practise of the engineer and on the computer software that he has to his disposal.

In what follows only the solutions of the simplest cases are being presented, on which the fundamental concepts characterising dynamic behaviour of structures, their stresses and possible damages have been recapitulated. Neither the character of seismic shakes, nor the seismic risk are analysed; these are supposed to be given in some way, and several alternatives of shake definitions are concerned. Finally some methods for vibration absorption are presented which could reduce the risk of earthquake damages of slender structures.

## NOTATIONS

A, C - integration constants  
EJ - bending rigidity  
F - frequency function of a beam  
H - frequency characteristic  
M - bending moment  
Q - shear force  
R - response spectrum  
S - power spectral density  
T - period of vibrations  
f - frequency (cps, Hz)  
g - acceleration of gravity  
i - imaginary unit  
j - subscript of j-th natural mode  
k - spring constant (rigidity)  
l - length, span of the beam  
n - mass, number of natural modes  
p - generalised component of the input (loading)  
q - generalised coordinate of the response  
s - position parameter  
t - time  
v - displacement perpendicular to the beam axis z  
z - vertical coordinate (in the axis of the beam)  
 $\alpha$  - parameter  
 $\beta$  - relative damping  
 $\lambda$  - vibrating beam parameter  
 $\mu$  - mass per unit length  
 $\theta$  - rotation of beam element  $dv/dz$   
 $\omega$  - circular frequency (rad/sec)



## 1. VIBRATION OF A SIMPLE CANTILEVER BEAM

Slender structures like towers, antennae, chimneys, high buildings and different structures for technology will mostly be represented -as to their dynamic behaviour- as a cantilever beam fixed at its lower end. To recall the fundamental conceptions let us solve the simplest case - a vertical prismatic cantilever.

### 1.1 Natural modes

The fundamental differential equation for transversal displacement  $v(z, t)$  of a bended prismatic beam without external loading is [1]

$$EJ \frac{\partial^4 v(z, t)}{\partial z^4} + \mu \frac{\partial^2 v(z, t)}{\partial t^2} = 0 \quad /1/$$

Supposing harmonic motion

$$v(z, t) = v(z) \sin \omega t ,$$

$$\frac{\partial^2 v(z, t)}{\partial t^2} = -\omega^2 v(z) \sin \omega t ; \quad \frac{\partial^4 v(z, t)}{\partial z^4} = \frac{d^4 v(z)}{dz^4} \sin \omega t ,$$

the equation /1/ changes into

$$\frac{d^4 v(z)}{dz^4} - \frac{\mu \omega^2}{EJ} v(z) = 0 . \quad /2/$$

This is an equation with constant coefficients, having the solution of the type

$$v(z) = \exp(\alpha z) \quad /3/$$

where the parameter  $\alpha$  is given by characteristic equation

$$\alpha^4 = \mu \omega^2 / EJ$$

with 4 roots

$$\alpha_1 = \sqrt[4]{\mu \omega^2 / EJ} ; \quad \alpha_2 = -\alpha_1 ; \quad \alpha_3 = i \alpha_1 ; \quad \alpha_4 = -i \alpha_1$$

The general solution of /2/ therefore is

$$v(z) = \sum_{k=1}^4 A_k \exp(\alpha_k z) \quad /4/$$

When expressing the exponentials with imaginary argument by means of goniometric, those with real argument by means of hyperbolic functions, we obtain instead of /4/

$$v(z) = C_1 \operatorname{ch} s + C_2 \operatorname{sh} s + C_3 \cos s + C_4 \sin s \quad /5/$$

where for practical reasons the beam parameter  $\lambda$  has been introduced

instead of

$$\lambda = l\alpha = l \sqrt{\omega \sqrt{\mu/EJ}} \quad /6/$$

and the position on the beam was instead of length coordinate  $z$  - defined by the dimensionless parameter

$$s = \lambda z / l \quad /7/$$

$C_1 - C_4$  are integration constants, which will be determined from boundary conditions of the vibrating beam, that means from the types of fixing at its ends (Fig. 1). In order to do it, also the derivatives of /5/ must be expressed, which have the meaning of the tangent to the amplitude curve

$$\dot{v}(z) = dv(z)/dz,$$

of the bending moment

$$M(z) = - EJ d^2 v(z)/dz^2$$

and of the shear force

$$Q(z) = dM/dz = - EJ d^3 v(z)/dz^3.$$

Thus we obtain

$$\begin{aligned} \dot{v}(z) &= \lambda (C_1 \operatorname{sh} s + C_2 \operatorname{ch} s - C_3 \sin s + C_4 \cos s) / l \\ M(z) &= - EJ \lambda^2 (C_1 \operatorname{ch} s + C_2 \operatorname{sh} s - C_3 \cos s - C_4 \sin s) / l^2 \\ Q(z) &= - EJ \lambda^3 (C_1 \operatorname{sh} s + C_2 \operatorname{ch} s + C_3 \sin s - C_4 \cos s) / l \end{aligned} \quad /8/$$

Boundary conditions for the cantilever fixed at one end are

$$\begin{aligned} \text{for } z = s = 0: \quad v(0) &= 0; \quad \dot{v}(0) = 0 \\ z = l \ (s = \lambda): \quad M(l) &= 0; \quad Q(l) = 0 \end{aligned} \quad /9/$$

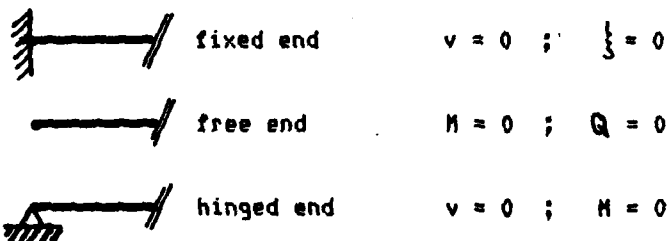


Fig. 1 Boundary conditions for a vibrating beam

Putting /9/ into /5/, /8/ we obtain

$$C_1 + C_3 = 0 \quad C_2 + C_4 = 0$$

$$C_1 \operatorname{ch} \lambda + C_2 \operatorname{sh} \lambda - C_3 \cos \lambda - C_4 \sin \lambda = 0$$

$$C1 \operatorname{sh} \lambda + C2 \operatorname{ch} \lambda + C3 \sin \lambda - C4 \cos \lambda = 0$$

which can be written as

$$C1 (\operatorname{ch} \lambda + \cos \lambda) + C2 (\operatorname{sh} \lambda + \sin \lambda) = 0 \quad /10/$$

$$C1 (\operatorname{sh} \lambda - \sin \lambda) + C2 (\operatorname{ch} \lambda + \cos \lambda) = 0$$

The system has non-zero solution if its determinant equals zero. That leads to the condition

$$1 + \operatorname{ch} \lambda \cos \lambda = 0 \quad /11/$$

Equation /11/ is satisfied for an infinite number of solutions  $\lambda$ , the first three being

$$\lambda_{(1)} = 1.875 ; \lambda_{(2)} = 4.694 ; \lambda_{(3)} = 7.855 \quad /12/$$

The motion without external forces is therefore possible in certain frequencies only. According to /6/ these natural frequencies are

$$f_{(j)} = \frac{\omega_{(j)}}{2\pi} = \frac{\lambda_{(j)}^2}{2\pi} \sqrt{EJ/(\mu l^4)}$$

the first three of which ( $j = 1, 2, 3$ ) are

$$f_{(j)} = 0.560 ; 3.507 ; 9.819 \sqrt{EJ/(\mu l^4)} \quad /13/$$

The integration constants which correspond to these values of the parameter  $\lambda$  can be determined only in the ratios. When choosing the value of the first constant

$$C1 = 0.5$$

we obtain

$$C2 = 0.5 (\sin \lambda_{(j)} - \operatorname{sh} \lambda_{(j)}) / (\operatorname{ch} \lambda_{(j)} + \cos \lambda_{(j)}) \quad /14/$$

$$C3 = -0.5 ; C4 = -C2$$

Putting /14/ into /5/, /8/ we obtain the natural modes (the amplitudes corresponding to vibrations in the above determined frequencies), viz.

$$v_{(j)}(z) = 0.5 (\operatorname{ch} s - \cos s) + (\sin \lambda_{(j)} - \operatorname{sh} \lambda_{(j)}) (\operatorname{sh} s - \sin s) / [2(\operatorname{ch} \lambda_{(j)} + \cos \lambda_{(j)})] \quad /15/$$

where the coordinate on the beam has again been given by the parameter  $s$  according to /7/. The amplitude of bending moment during vibrations in the  $j$ -th mode will be obtained after putting the integration constants /14/ into /8/

$$M_{(j)}(z) = -EJ \lambda_{(j)}^2 [0.5 (\operatorname{ch} s + \cos s) + 0.5 (\sin \lambda_{(j)} - \operatorname{sh} \lambda_{(j)}) (\operatorname{sh} s + \sin s) / (\operatorname{ch} \lambda_{(j)} + \cos \lambda_{(j)})] / l^2$$

similarly also the amplitudes of inclinations  $\theta$  and of shear-forces  $Q$ . First three natural modes are given on Fig.2, all are normalised to the

unitary amplitude on the top of the cantilever, i.e.  
 $v_{(j)}(l) = 1$ , while  $M_{(j)}(0) = -EJ \lambda_{jp}^2 / l^2$ .

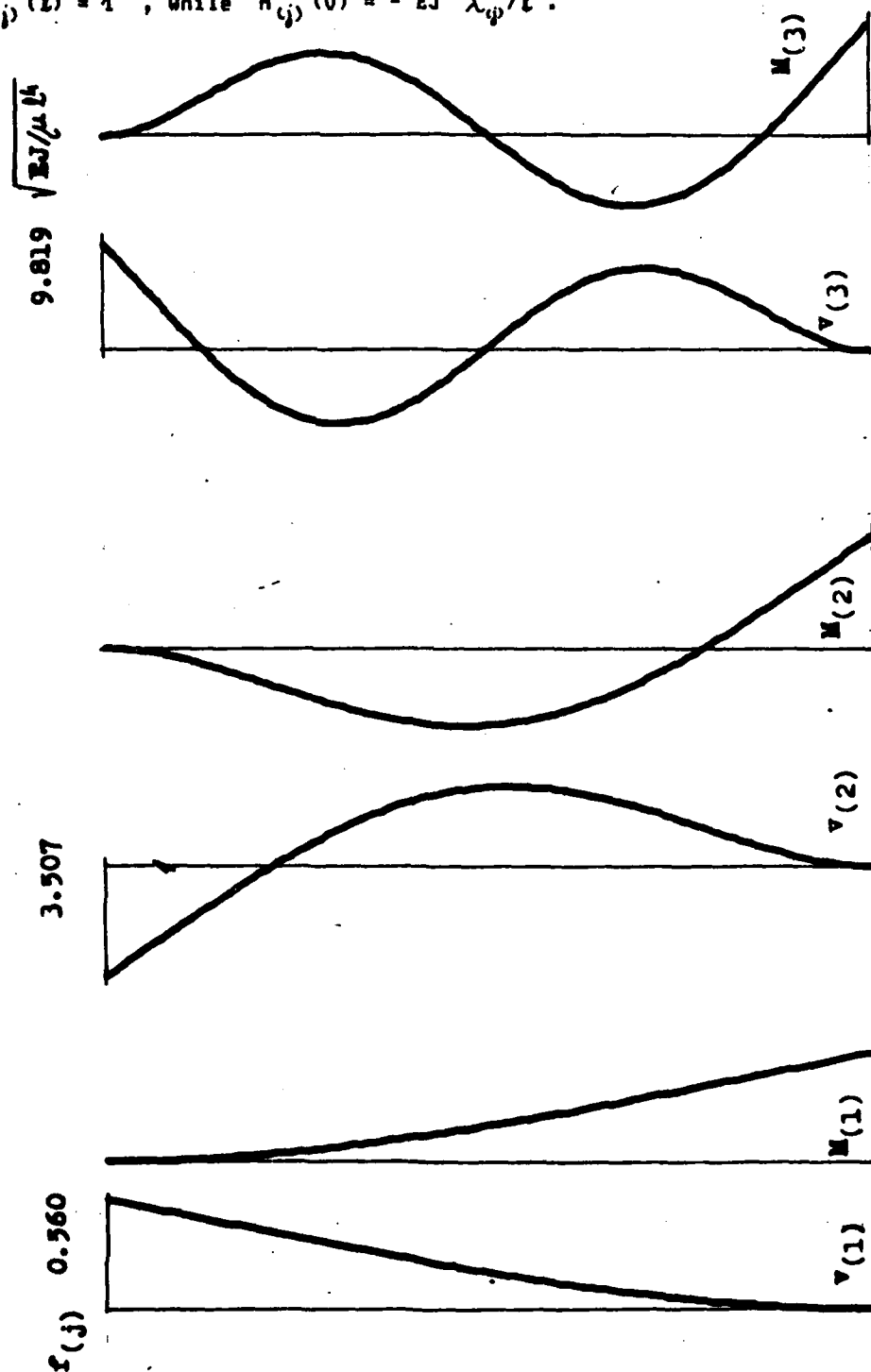


Fig 2. First 3 natural modes of a prismatic cantilever - displacements  $v_{(j)}$  and bending moments  $M_{(j)}$ .

Another important parameter of natural vibrations is the generalised mass

$$m_{(j)} = \int_0^l \mu(z) v_{(j)}^2(z) dz \quad /16/$$

When putting /5/ into /16/ we obtain for prismatic beam

$$\begin{aligned} m_{(j)} = & \{0.5 [\lambda (C1^2 - C2^2 + C3^2 + C4^2) + \operatorname{sh} \lambda \operatorname{ch} \lambda (C1^2 + C2^2) + \\ & + \sin \lambda \cos \lambda (C3^2 - C4^2)] + \\ & + C1 C2 \operatorname{sh}^2 \lambda + C3 C4 \sin^2 \lambda + C1 C4 - C2 C3 + \\ & + \cos \lambda [\operatorname{sh} \lambda (C1 C3 - C2 C4) + \operatorname{ch} \lambda (C2 C3 - C1 C4)] + \\ & + \sin \lambda [\operatorname{ch} \lambda (C1 C3 + C2 C4) + \operatorname{sh} \lambda (C2 C3 + C1 C4)]\} \mu l / \lambda \end{aligned} \quad /17/$$

which, for a prismatic cantilever /14/, /9/, /11/, gives a quite simple result, equal for each natural mode

$$m_{(j)} = \mu l / 4 \quad /18/$$

Fig. 2 reveals evidently the difference between the stresses corresponding to static and dynamic loading. While the first mode shows a little difference in both, displacement and bending moment amplitudes from statical case, with higher modes, which have one or more knots along the height, there are large moments not only near the base, but also in the upper part of the structures. Such vibrations can occur during earthquakes on "favouredly tuned" structures and often cause damages or even breaks just in the higher part.

## 1.2 Kinematically excited vibrations

To make the main principles of kinematic excitation clear let us again solve a prismatic cantilever, the foundation of which moves harmonically; the response too will be considered as stationary harmonic. The fundamental equation has the solution /5/, /8/, but the boundary conditions for the constants  $C1 - C4$  will be different from /9/. If the excitation is unitary translation of the base without rotation with given circular frequency  $\omega$ , viz.

$$\begin{aligned} z = s = 0 : & \quad v(0) = 1 ; \quad \dot{v}(0) = 0 \\ z = l \quad (s = \lambda) : & \quad M(l) = 0 ; \quad Q(l) = 0 \end{aligned} \quad /19/$$

the first equation in /10/ will be

$$C1 + C3 = 1 \quad /20/$$

the other ones remain as in /10/. Such a system of equations has a unique solution for each exciting frequency (for every parameter  $\lambda$  except for values satisfying equ. /11/)

$$C1 = 0.5 + \sin \lambda \operatorname{sh} \lambda / (1 + \cos \lambda \operatorname{ch} \lambda) ; \quad C3 = 1 - C1 \quad /21/$$

$$C2 = - (\operatorname{sh} \lambda \cos \lambda + \operatorname{ch} \lambda \sin \lambda) / (1 + \cos \lambda \operatorname{ch} \lambda) ; \quad C4 = - C2$$

Putting these constants /20/ into the general solutions /5/, /8/, the amplitude of the response (displacement, bending moment) to transitory motion of the basement with given frequency will be obtained. If the amplitude of the excitation is different from unity, the results must be multiplied by its magnitude. For excitation frequencies which are near to natural frequencies /13/, when  $\lambda = \lambda(j)$ , the constants  $C_i$  and the response tends to infinity - in such cases the damping must be taken into consideration [1].

Examples of the response to different excitation frequencies are given in Fig. 3. The excitation is given in ratio vs. the first natural frequency. Considering /13/ one can see the relations

$$f_{(2)} = 6.267 f_{(1)} ; \quad f_{(3)} = 17.548 f_{(1)} .$$

If other types of kinematic excitation are to be considered, the boundary conditions must be modified. If a beam with end points  $g, h$  is forced to vibrate with lower end amplitudes  $v_g, \xi_g$  and upper end amplitudes  $v_h, \xi_h$ , the boundary conditions will be

$$\begin{aligned} z = s = 0 : \quad v(0) = v_g ; \quad \xi(0) = \xi_g \\ z = l \quad (s = \lambda) : \quad v(l) = v_h ; \quad \xi(l) = \xi_h \end{aligned} \quad /22/$$

which, introduced into /5/, /8/ gives corresponding values of  $C$ .

If a cantilever consisting of more prismatic parts or if a more complicated structure (a frame) should be solved, it can be divided into separate beams, each of them being excited by the motions of its ends. Expressing bending moments and shear forces in the end points of each beam and writing equilibrium conditions for moments and forces in each of the joints, we obtain a system of equations for the unknown displacements of the joints  $v, \xi$ . In such a way the amplitudes of a more complicated structure, as well as its natural vibrations can be solved. For details of this dynamic slope-deflection method see ref. [1], [2].

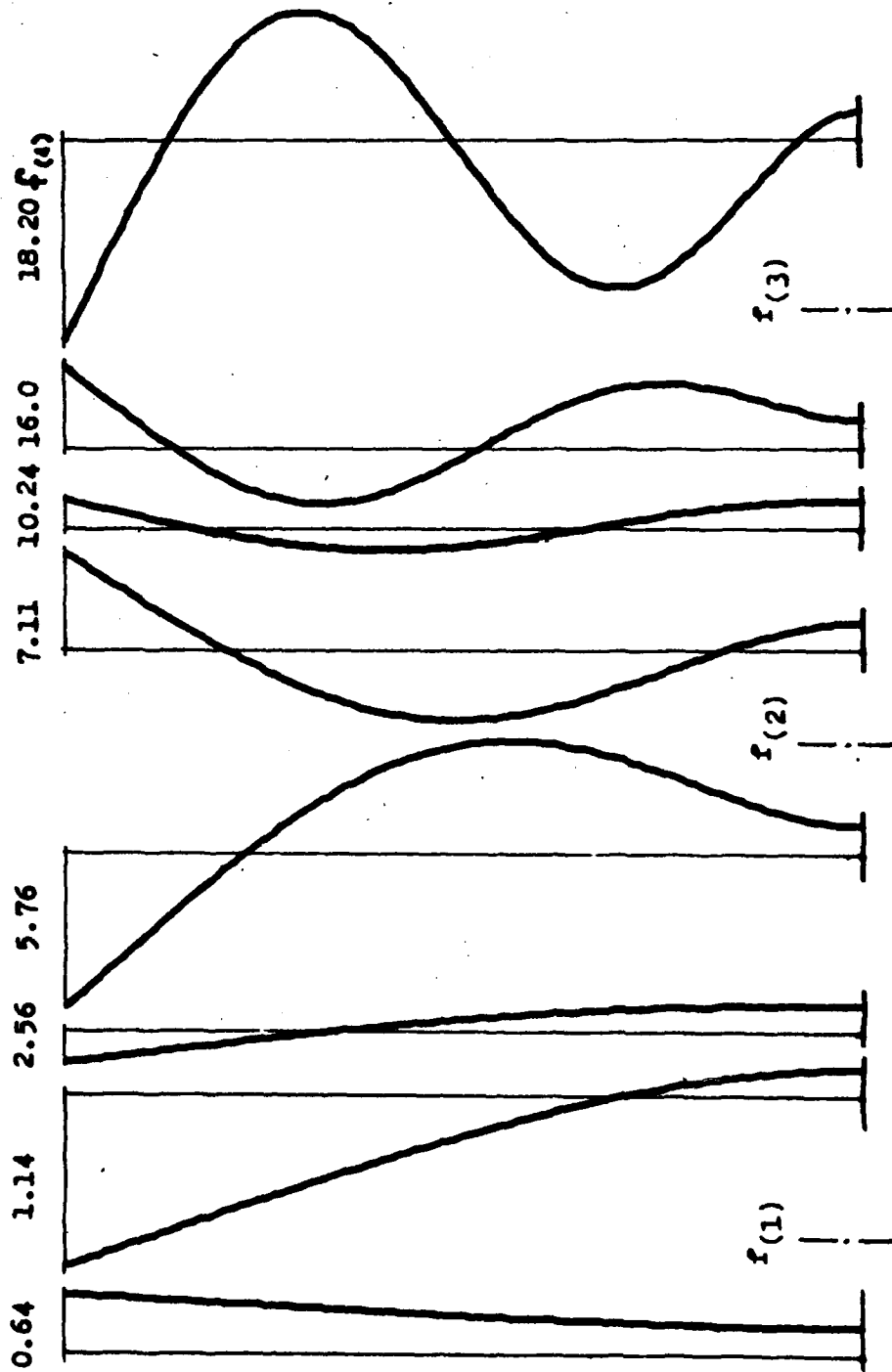


Fig. 3 Displacement amplitude of a cantilever excited by unitary translation of its base with different frequencies

## 2. NATURAL MODE ANALYSIS IN SEISMIC EXCITATION

### 2.1 General remarks

Let us consider an arbitrary structure of cantilever type, whose  $m$  natural modes and frequencies, viz.

$$v_{(j)}(z), f_{(j)}, j = 1, m$$

have already been determined up to the number  $m$ , the corresponding natural frequency of which is greater than the frequency of excitation (with a certain reserve). All natural modes comply with the boundary condition of a fixed lower end

$$z = 0 : v_{(j)}(0) = 0 ; \quad \dot{v}_{(j)}(0) = 0 .$$

The seismic excitation makes the displacement of the basement non-zero, that is why the decomposition of the amplitude into natural modes must be extended by the zero-term. Thus we obtain

$$v(z, t) = v_0(z) q_0(t) + \sum_{j=1}^m v_{(j)}(z) q_{(j)}(t) \quad /24/$$

where  $v_{(j)}(z)$  -  $j$ -th natural mode

$q_{(j)}(t)$  - generalised coordinate of the  $j$ -th natural mode (a time function describing the motion in the  $j$ -th mode, till now unknown)

$v_0(z)$  - amplitude of seismic excitation, namely deflection line caused by unit displacement of the support. For cantilever excited by translation of the foundation  $v_0(z) = 1$ , for rotation of the foundation  $v_0(z) = z$ .

$q_0(t)$  - time function, describing the magnitude and time history of the excitation.

Adding the damping into the beam equation /1/ we obtain

$$\mu \frac{\partial^2 v(z, t)}{\partial t^2} + 2\mu \omega \beta \frac{\partial v(z, t)}{\partial t} + EJ \frac{\partial^4 v(z, t)}{\partial z^4} = 0 \quad /24/$$

where  $\beta$  - relative damping, equal to  $\log. decrement / (2\pi)$ .

Substituting the solution /24/ into /25/, multiplying the whole equation by a certain natural mode  $v_{(k)}(z)$  and integrating each member over the whole beam-length we obtain

$$\ddot{q}_{(j)}(t) + 2\beta \omega_{(j)} \dot{q}_{(j)}(t) + \omega_{(j)}^2 q_{(j)}(t) = - p_{(j)} [\ddot{q}_0(t) + 2\beta \omega_{(j)} \dot{q}_0(t)] \quad /26/$$

where following simplifications were introduced



$$\int_0^L \mu v_{(j)}(z) v_{(k)}(z) dz = 0 \text{ for } k \neq j \text{ (orthogonality of natural modes)}$$

$$= m_{(j)} \text{ for } k = j \text{ (cf. /16/)}$$

$$EJ d^4 v_{(j)}(z)/dz^4 = \mu \omega_{(j)}^2 v_{(j)}(z) \quad (\text{cf. /2/})$$

$$d^4 v_0(z)/dz^4 = 0 \quad (v_0(z) \text{ means deflection line without loading})$$

$$p_{(j)} = \int_0^L \mu v_0(z) v_{(j)}(z) dz / m_{(j)} - \text{generalised component of the excitation relating to the } j\text{-th natural mode.}$$

The second member on the right-hand side of /26/ can be neglected for small damping. The equation /26/ can be written for each of the natural modes and gives the solution for each generalised coordinate separately, depending on the time-history of the ground-acceleration  $\ddot{q}(t)$ .

## 2.2 Harmonic excitation

For harmonic excitation with circular frequency  $\omega$

$$q_0(t) = q_0 \sin(\omega t)$$

the solution of /26/ is

$$q_{(j)}(t) = q_{(j)} \sin(\omega t + \varphi_{(j)}) \quad /27/$$

where the amplitude

$$q_{(j)} = q_0 \omega^2 p_{(j)} / \sqrt{(\omega_{(j)}^2 - \omega^2)^2 + 4\beta^2 \omega_{(j)}^2 \omega^2}$$

and the phase shift against the excitation

$$\varphi_{(j)} = -\arctan[2\beta\omega\omega_{(j)} / (\omega_{(j)}^2 - \omega^2)].$$

This can be simplified in the case far from of resonance ( $\omega \neq \omega_{(j)}$ )

$$q_{(j)} = q_0 p_{(j)} / (\omega_{(j)}^2 / \omega^2 - 1); \quad \varphi_{(j)} = 0; \quad -\pi \quad /28/$$

and near the resonance ( $\omega \approx \omega_{(j)}$ )

$$q_{(j)} = q_0 p_{(j)} / (2\beta); \quad \varphi_{(j)} = -\pi/2 \quad /29/$$

From this generalised coordinate in the  $j$ -th mode we obtain the amplitude of vibrations in this  $j$ -th mode by multiplication this generalised coordinate by the corresponding ordinate of the natural mode. Thus for the displacement we calculate

$$v_j(z, t) = v_{(j)}(z) q_{(j)}(t) \quad /30/$$

for bending moments

$$M_j(z, t) = M_{(j)}(z) q_{(j)}(t), \quad /31/$$

where  $v_{(j)}(z)$ ,  $M_{(j)}(z)$  correspond to the vibration  $j$ -th in natural

mode, for prismatic cantilever see /15/.

Resulting amplitude of the response will be obtained as a sum /24/ namely

$$v(z, t) = v_0(z) q_0 \sin \omega t + v_{(1)}(z) q_{(1)} \sin(\omega_{(1)} t + \varphi_{(1)}) + \\ + v_{(2)}(z) q_{(2)} \sin(\omega_{(2)} t + \varphi_{(2)}) + \dots$$

In the case of moderately damped structures generally only one term prevails in the sum, namely that one, the natural frequency of which is nearest to the frequency of excitation.

### 2.3 General deterministic excitation

If the excitation of the structure is given by means of a certain time function (time-history of the acceleration, a registration of a real previous earthquake or a prescribed artificial earthquake), the equations /26/ will be solved numerically for appropriate number of natural modes. The resulting time-history of the response will be calculated from equ. /24/.

### 2.4 Random excitation

If the foundation acceleration  $\ddot{q}_0(t)$  is a random function described by its power spectral density

$S_{aa}(f)$   
(expressed in cycles per second - Hertz, not  $\omega$  in rad/sec), the variance of the generalised coordinate  $q_{(j)}(t)$  will be

$$\overline{q_{(j)}^2} = \int_0^\infty p_{(j)}^2 S_{aa}(f) |H_{(j)}(if)|^2 df \quad /32/$$

where the absolute value of the complex frequency characteristic (frequency response function, mechanical impedance)  $H(if)$  is according to the equ. /26/

$$|H_{(j)}(if)|^2 = \frac{1}{16\pi^4 f_{(j)}^4 [(1 - (f/f_{(j)})^2)^2 + 4\beta^2 (f/f_{(j)})^2]} \quad /33/$$

In the case that the power spectral density can be considered as white noise (is constant in the vicinity of the natural frequency  $f_{(j)}$ ), having the value of  $S_{aa}$ , the integral /32/, /33/ can be simplified to

$$\overline{q_{(j)}^2} = \frac{p_{(j)}^2 S_{aa} \pi}{16\pi^4 f_{(j)}^3 4\beta} \quad /34/$$

The standard deviation (RMS value) of this coordinate is then given by the square root (Fig. 4)

$$\sigma_{qj} = \sqrt{Q_{jj}} = \frac{P_{(j)}}{4 f_{(j)}^2 \pi^2} \sqrt{\frac{S_{aa} f_{(j)} \pi}{4 \beta}} \quad /35/$$

The back transition from generalised coordinates  $q_{(j)}$  to the response according to /24/ is in principle not so simple with random processes, as variance and spectral densities are quantities of 2nd order and the sum of such quantities contains not only the sum of the squares, but also the mixed products of one quantity with all other ones (cross-spectra). Only in the case of well-separated natural frequencies and small damping of the structure the RMS value of the resulting amplitude at the point  $z$  can be taken as

$$\sigma_{v(z)} = \sqrt{v_o^2(z) \sigma_{qo}^2 + \sum_1^m v_{cj}^2(z) \sigma_{qj}^2} \quad /36/$$

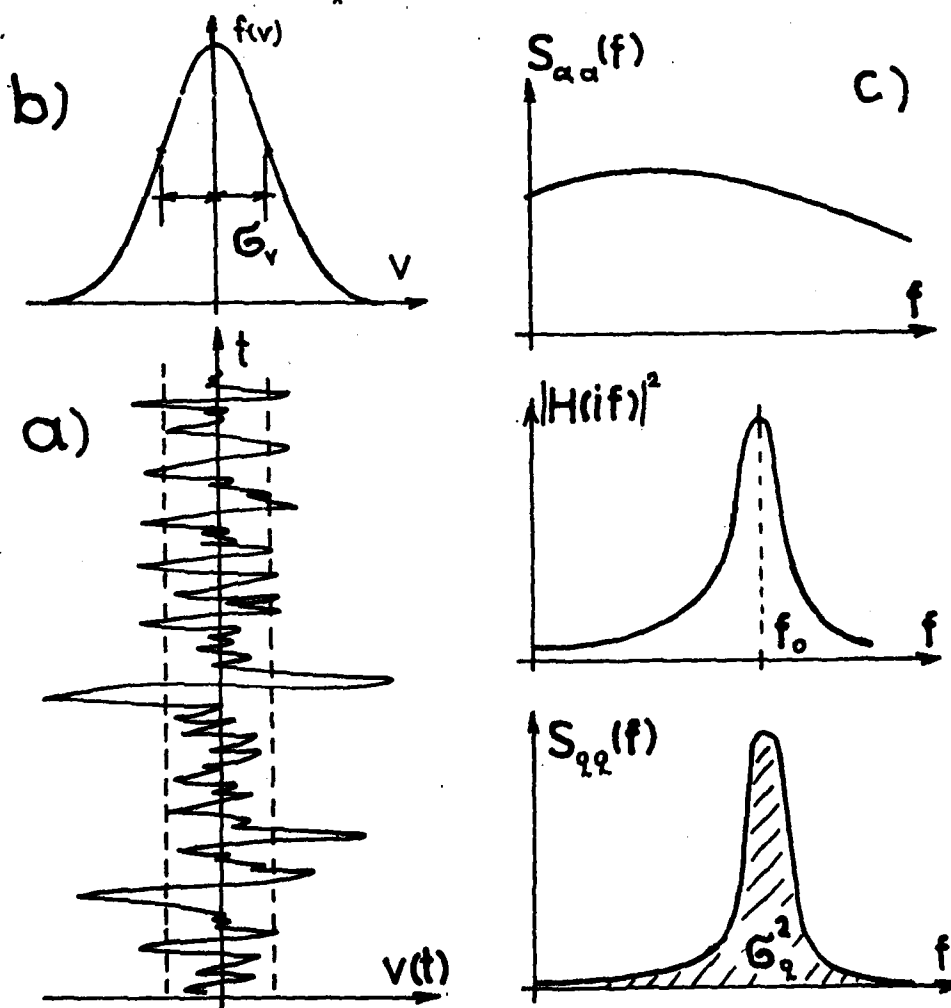


Fig. 4 a) Time history of a displacement  $v(t)$  (random process)  
 b) Probability density of the process  $f(v)$   
 c) Construction of spectral density of the response /32/

## 2.5 Solution using response spectra

If response spectra curves have been used for the description of the earthquake, the contribution of each natural mode will be determined like the response of the system with one degree of freedom. Let us suppose that to the  $j$ -th natural frequency  $f_{(j)}$  (or  $j$ -th natural period  $T_{(j)} = 1/f_{(j)}$ ) and to a given structural damping corresponds the ordinate of response-spectrum curve  $R(f_{(j)})$ , given by a graph, table or formula in the Building Code. This means, that an one degree of freedom system with the natural frequency  $f_{(j)}$  and with the certain damping, subdued to a certain earthquake, will reach the maximum response of magnitude  $R(f_{(j)})$ . In practical cases, the prescribed response-spectrum curve represent either displacement  $R(\text{disp}, f)$ , velocity  $R(\text{vel}, f)$  or acceleration  $R(\text{acc}, f)$ .

According to this definition of response-spectra, the  $j$ -th generalised coordinate will reach during the earthquake its maximum value

$$q_{(j), \max} = p_{(j)} R(\text{disp}, f_{(j)}), \quad /37/$$

the maximum values of the first and second derivatives of this coordinate will be

$$\dot{q}_{(j), \max} = p_{(j)} R(\text{vel}, f_{(j)}), \quad \ddot{q}_{(j), \max} = p_{(j)} R(\text{acc}, f_{(j)})$$

Maximum response in each of these natural modes will be determined independently /30/, /24/

$$v_j(z)_{\max} = v_{(j)}(z) q_{(j), \max} \quad /38/$$

or similarly in velocities and accelerations. All these maxima, belonging to different modes, do not occur simultaneously in the same time and cannot be therefore simply added together. An exact method of superposition of these contributions of individual modes is not possible, the codes can prescribe different ways of combinations, e.g.

$$v(z)_{\max} = \sqrt{\sum_j v_j^2(z)}$$

or

$$v(z)_{\max} = \sqrt{v_{\sup}^2(z) + 0.5 \sum_{j-\sup} v_j^2(z)} \quad /39/$$

where  $v_{\sup}$  is the absolutely greatest value of all response components  $v_j$ ,  
the sum  $j-\sup$  comprehends all members  $v_j$  without the maximum one.

### 3. CONSTRUCTIONAL DETAILS

High slender structures are primarily subdued to the action of wind, which mostly must be considered as a dynamic one. Earthquake evokes dynamic stresses too, but its effect has usually higher frequencies, larger amplitudes and much smaller probability of occurrence. The wind is therefore to be considered as loading causing damages through classic fatigue, the earthquake endangers the structures through low-cycle fatigue. Nevertheless the immediate cause of the damages, viz. the stress concentration, remains the same and should be avoided from both reasons, wind and earthquake. Let us enumerate some important items from this point of view.

a) Large bending moments in the upper part of the structure due to vibrations in higher modes (cf. Fig. 2) cause often damages on chimneys and other structures. The 2nd and 3rd natural frequencies often fall into the frequency band of the earthquake excitation (1 - 8 cps); the corresponding peaks of bending moments along the length of the structure reach nearly the same value as the bending moment at the foundation - this is of course a fundamental difference from the static (and even from the 1st mode dynamic) response to wind loading. Therefore a seismic resistant slender structure must first of all have enough of bearing capacity also in its higher parts; the only increase of design static loading cannot contribute to the seismic safety of structures of this type. High brick-built chimneys and towers should be avoided in seismic regions, concrete structures should have the reinforcement sufficiently strong in their higher parts and also steel structures must be adapted to higher bending moments in the upper half of their height.

b) Most structures have been able to sustain strong earthquakes only thanks to full use of plastic reserve, but this reserve is limited, especially with repeated stresses. To minimize the forming of plastic regions during the normal service of the structure, the stress flow in all parts of the structure must be as smooth as possible and must avoid stress-concentrations. The flanges at the connection between structure and foundation or between different parts of the structure should be well-stiffened with a ring, the concentrated forces of anchor bolts or in attachments of heavy loads or supporting columns should be uniformly dispersed into the structure. The anchor bolts themselves need to be long enough to allow some yielding under the extreme tensile loading. Besides, the plastic reserve cannot be exploited, if buckling effects determine the bearing capacity of the structure. For this reason the stiffeners must not be missing on walls and shells.

c) Appropriate attention should be given to all connections and other details. Welded connections or cut edges should not form notches neither in their design, nor in their workmanship, as such imperfections can cause serious stress concentrations and the initializing of fatigue cracks. Similarly there should be avoided sharp edges, openings without appropriate stiffening etc.

d) Slender structures anchored by the use of guying ropes (guyed masts) require a large site with one foundation block for the mast body and some other blocks for the guys, the distance of these blocks being even several hundreds of meters. If the subsoil under all these blocks is not uniform, different settlements can be expected after an earthquake and the change in horizontal and vertical distances between the blocks can cause additional stresses. Structures of this kind should therefore be built in uniform foundation conditions [3].

#### 4. ANTI-VIBRATION MEASURES

There are several methods of limiting the effects of vibrations in dynamics of structures. When diminishing the amplitudes of stresses the service life of a building and probability of surviving the dynamic loading increases - that is valid for both, for small long-termed service loadings causing fatigue and also for bigger, only several times repeated loadings, causing damage or collapse during earthquakes.

a) Classical method of amplitude reduction by the change in tuning between the natural frequency of the structure and the frequency of excitation will be used only exceptionally, in such localities where the frequency band of seismic action is known reliably enough in advance. In such a case the preliminary dynamic calculus could design the stiffness and mass distribution in such a way, that the natural frequencies do not fall into the interval of earthquake frequency.

The increase of natural frequency of the structure will mostly be reached by strengthening the structure, sometimes also by reducing its mass. The decrease of natural frequency requires the opposite - increase of the mass or decrease of bending rigidity or both. An effective method of softening the structure is to make its foundation elastic, either by making the base-area smaller or by applying elastic bearings from steel or rubber [4] - [7]. All these interventions must of course be done carefully. They must take into consideration not only the first, but also higher natural modes, and besides, they must not affect the static stability or wind-resistance of the wind resistance of the structure.

b) An universal method for reducing dynamic effects is the increase of structural or external damping. Slender structures have in general very small damping (relative damping 0.002 for welded steel, 0.005 are quite realistic values) and this makes them very sensitive to dynamic excitation from both, wind and earthquake.

To increase the damping of an existing structure is usually difficult. Lining or concreting cavities, filling of hollow spaces with sand or some loose material or coating with antivibration plastics could give good results in that case only, that this energy absorbing material is being really deformed together with the bearing construction and that its absorbing capacity is adequate to the mass of the vibrating structure.

Sometimes it could be possible to introduce additional damping from outside; if there is a fixed support available in the vicinity of the object to which a guy or a brace could be attached, or if more objects can be connected together [8]. As damping devices can be used hydraulic shock-absorbers from rail or road vehicles, special elements from suitable plastic materials which are capable to absorb energy by their deformation, or friction elements. Attempts were made to use special plastic pads between the steel smoke-stack and the concrete foundation block [9].

c) Special antiseismic bearings, which are sometimes used for important structures like nuclear reactors or some special buildings, do not seem suitable for antiseismic insulation of high slender structures. These structures are threatened also by wind; antiseismic bearings can lower the horizontal natural frequency under the frequency of seismic action, but then it becomes near to the frequency of wind action. Besides, further lowering of the horizontal rigidity would not be advisable due to static wind resistance too.

d) The last mentioned disadvantage of lack in horizontal stiffness can be suppressed by the use of the system of doubled restrains [10]. One of the restrains is rigid and brittle, the second is soft and ductile (Fig. 5). In ordinary conditions the foundation (or any other structural part) is rigid and the structure sustains service-load, winds and small earthquakes. When the horizontal stress in the foundation reaches a certain limit, the brittle elements break, the structure obtains small rigidity, low natural frequency and can sustain the strong earthquake. After the earthquake the rigid supports must of course be repaired as early as possible.

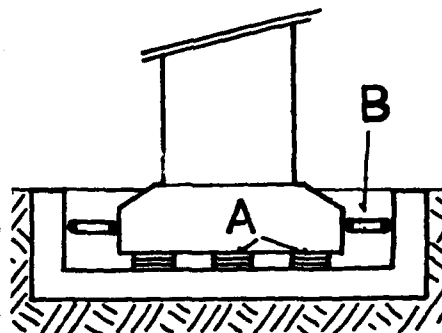


Fig. 5 Foundation block with  
----- doubled restrain  
A - elements with small  
shear rigidity  
B - brittle bracing

e) Vibration absorber represent an additional mass attached to the mass of the structure in a way that makes the two masses free to move relative to one another. A suitable design of the attached mass can ensure that the amplitudes of the structure will grow smaller and that the energy imparted to the structure will manifest itself primarily as a motion of the attached mass. Such absorbers were first used for damping vibrations of machine components, vibrations of electric power transmission lines and finally also for damping vibrations of civil engineering structures.

For the design of a dynamic absorber the structure can be in most cases represented by a system with one degree of freedom, the natural frequency of which corresponds to the most dangerous natural frequency of the structure. Adding one other mass, spring and damping to this system, we obtain a two-mass system according to the Fig. 6, that can be solved for unitary harmonic exciting force. Resulting amplitude of

the main mass is a function of the natural frequency of the absorber (its ratio vs. the natural frequency of the structure) and of the damping. In optimum case the amplitude response curve is flat, without distinct peaks. Roughly speaking, if the absorber mass is about 1/10 of the mass of the equivalent one degree of freedom system, its natural frequency should be slightly smaller than that of the structure and relative damping of the absorber should be of about 0.20. Exact formulae and graphs for the design can be found in [11], some adaptations for civil engineering structures in [12].

For low frequencies (fundamental modes of the structures) will the absorber be mostly constructed as a pendulum, the length of hangers  $l$  determining its natural frequency

$$f_{abs} = \sqrt{g / l} / (2\pi) .$$

For higher natural frequencies the length of pendulum hangers would be too short; in such a case supplementary springs must be used.

Dynamic vibration absorbers are primarily used against stationary excitations, but they are effective also against shocks and transient loadings. As the design of an absorber is in general approximate only, it is recommended to test the structure with the absorber and, if necessary, to adjust its parameter in order to obtain optimum damping efficiency.

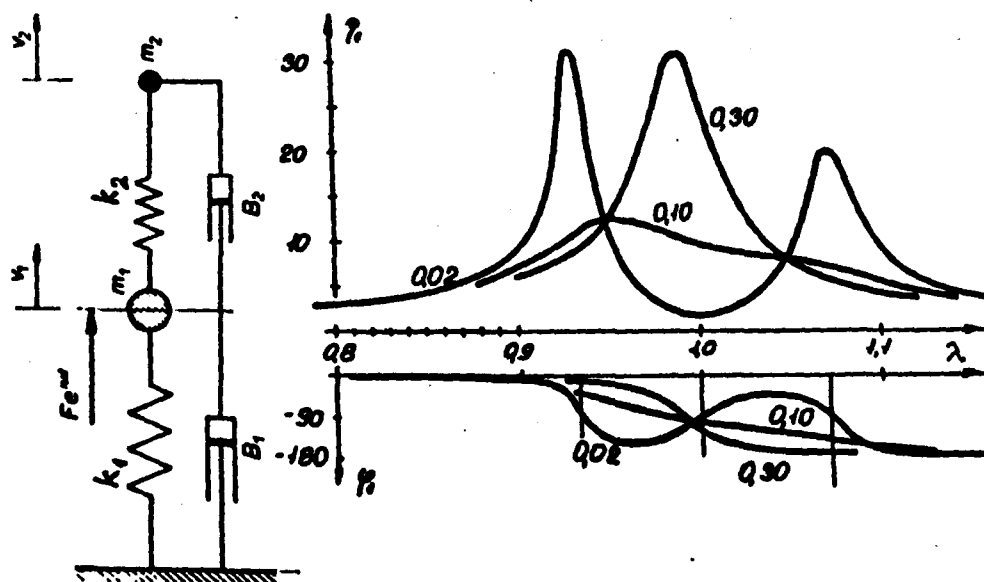


Fig. 6 Scheme of a vibration absorber, resonance curves for different dampings of the absorber mass: main mass amplitude  $\eta_1 = v_1 k_1 / F$  and phase shift  $\varphi$  with respect to the exciting force, plotted versus exciting frequency ratio  $\lambda = f / f_{const}$



# REFERENCES

- [1] KOLOUŠEK V.: Dynamics in engineering structures. Academia, Prague; Butterworths, London 1973
- [2] BAŤA M., PLACHÝ V.: Analysis of dynamic effects on engineering structures. Elsevier, Amsterdam 1987
- [3] FISCHER O.: Seismic behaviour of guyed masts. In: Proc. sem. 'Constructions in seismic zones', Bergamo, May 1978
- [4] Information papers of the house GERB, Essen (FRG)
- [5] Information papers of the house MALAYSIAN RUBBER BUREAU, Washington (USA)
- [6] Information papers of the house SAGA, Milano (Italy)
- [7] Information papers of the house SPIE-BATIGNOLLES, Velizy - Villa Coublay (France)
- [8] DICKEY W.: The design of two electric plants. Trans. ASCE v. 121, 1956, p. 255
- [9] MILSTED M.G.: On the structural response of steel chimneys with added damping. UEROMECH colloquium No 89 on 'Vibration control by damping' at INSA de Lyon, June 1977
- [10] Aizenberg J.M.: Constructions with self-releasing constraints in seismic zones (in Russian). Moskva 1976
- [11] KOLOUŠEK V. et al.: Wind effects on civil engineering structures. Elsevier Amsterdam; Academia Praha, 1983.



**TURKISH NATIONAL COMMITTEE FOR  
EARTHQUAKE ENGINEERING**

**THIRTEENTH REGIONAL SEMINAR ON EARTHQUAKE ENGINEERING**

**September 14-24, 1987 - Istanbul - Turkey**

**STOCHASTIC RESPONSE OF SUSPENSION BRIDGES**

**TO**

**EARTHQUAKE FORCES**

**by**

**A.A. DUMANOGLU and R.T. SEVERN**

STOCHASTIC RESPONSE OF SUSPENSION BRIDGES

TO

EARTHQUAKE FORCES

by

A.A. DUMANOGLU and R.T. SEVERN

University of Bristol

Department of Civil Engineering

University Walk

Queens Building

BRISTOL BS8 1TR

April, 1987.

CONTENTS	Page
1. INTRODUCTION	1
2. RANDOM PROCESS	3
3. STOCHASTIC STRUCTURAL RESPONSE	5
3.1 Mean-Square Response	
3.2 Mean Peak Response	
3.3 Response Spectrum Method For Random Vibration	18
4. STOCHASTIC RESPONSE OF SUSPENSION BRIDGES	22
4.1 The Dolerw Bridge	23
4.2 The Bosporus (Bogazici) Bridge	25
4.3 The Humber Bridge	27
5. CONCLUSION	28
6. REFERENCES	30

## 1. INTRODUCTION

In the design of a structure, the knowledge of the extreme values of the response quantities, that is displacements and internal forces or stresses, under applied load, is of great importance. To obtain the correct extreme values for dynamic excitations, full time histories of structural response quantities have to be determined. This can, however, involve lengthy calculations. Approximate techniques have therefore been developed, such as the response spectrum method, which predicts the extreme response values without performing a full time-history analysis. But because these methods only give instantaneous extreme values which they themselves may not be a proper indication of the damaging potential of dynamic loadings. For design purposes, particularly aspects relating to fatigue, levels of occurrence as well as frequencies of maxima are needed.

For linear structural behaviour resulting from dynamic excitation, a random analysis provides the extreme values of structural response quantities. This analysis, by its nature, is performed in the frequency domain and avoids any calculation in the time domain. The advantages of the random (stochastic) analysis over response spectrum method are that it gives the expected (mean) values of structural response quantities, their probabilities of occurrence for defined limits as well as frequencies of occurrence of peaks.

The theory of the random vibration has a well established background for several years [1, 17, 18], and stochastic dynamic analysis of structural systems based on the random vibration theory, has been matured, especially in the last decade. To this end, the method of analysis is embedded in some well-known general purpose structural analysis computer programs, such as ADINA [19] and STOCAL [12]. More recently, the theory is expanded

to include the stochastic fatigue reliability of offshore structures due to wind and wave forces and a computer program SAPOS was developed [20, 21]. PSAP [25] was developed to carry out a practical stochastic analysis of nuclear power plant piping systems using known power spectrum density functions. The importance of cross-correlations of modal response and cross-correlation of multiple support excitations on the stochastic responses of piping systems were examined.

The objective of the investigation presented here is to study the stochastic response of suspension bridges in particular with box-girder deck inclined hangers and slender towers. These type of bridges are studied in detail by the authors using asynchronous excitation theory for which the travelling ground motion effect is considered [22]. In this study, the effect of cross-correlation of modal response on mean and extreme values of bridge responses are included in the stochastic analysis. A further study was also made of the extreme values of responses obtained by the Complete Quadratic Combination, CQC, method [10, 11] which is based on the random vibration theory, but which made use of the response spectrum method. In both of these methods, either in the stochastic or CQC, the effect of cross-correlation of modal responses on the extreme values is considered.

## 2. RANDOM PROCESS

A random process  $x(t)$ , consists of  $n$  individual functions  $x_1(t), x_2(t), \dots, x_n(t)$   $n \rightarrow \infty$  which are recorded for a physical phenomenon. For a defined time  $t$ , thus  $n$  values of stochastic variable  $x(t)$  are obtained, Fig. (1). The mean (expected) value of this random process is defined as

$$\mu_x = \frac{1}{n} \sum_{i=1}^n x(t) = E[X(t)] \quad n \rightarrow \infty, \quad (2.1)$$

where  $E[\cdot]$  denotes the average or expected value.

The autocorrelation function for a single record is defined as the average value of the product  $x(t) x(t+\tau)$  as

$$R_x(\tau) = E[x(t)x(t+\tau)] \quad (2.2)$$

If the process is stationary, the autocorrelation function will be only the function of the time separation  $\tau$ . When the time interval,  $\tau$ , separating the two measuring points is zero then the autocorrelation function becomes variance as defined by

$$R_x(\tau=0) = E[x(t)^2] = E[x^2] = \sigma_x^2. \quad (2.3)$$

A stationary Gaussian process can also be characterised by its spectral density function,  $S_x(\omega)$ , which will be defined as twice the Fourier transform of  $R_x(\tau)$ ;

$$S_x(\omega) = 2 \int_{-\infty}^{\infty} R_x(\tau) e^{-i\omega\tau} d\tau. \quad (2.4)$$

It can be shown [3, 16] that, substituting equation (2.2) into equation

(2.4)

$$S_x(\omega) = \lim_{T \rightarrow \infty} \frac{1}{n} \sum_{i=1}^n \frac{2 X_i(\omega) X_i^*(\omega)}{T} \quad n \rightarrow \infty, \quad (2.5)$$

is obtained; where  $T$  denotes the duration of the process  $X_i(\omega)$  and  $X_i^*(\omega)$  are the complex conjugates pairs of Fourier transform of  $x(t)$ .  $S_x(\omega)$  is an even function of  $\omega$ . The inverse transform of equation (2.4) gives

$$R_x(\tau) = \frac{1}{4\pi} \int_{-\infty}^{\infty} S_x(\omega) e^{i\omega\tau} d\omega, \quad (2.6)$$

for  $\tau = 0$ ,

$$R_x(0) = \frac{1}{2\pi} \int_{-\infty}^{\infty} S_x(\omega) d\omega. \quad (2.7)$$

It is clear from equation (2.3) and (2.7) that the area of power spectral density function of the response is directly related to mean square response values. This expression is also defined as zeroth spectral moment of the random process.

Once the spectral density  $S_x(\omega)$  of a stationary random process  $x(t)$  has been calculated then it can be used to calculate the mean square value,  $E[x^2]$ , according to equations (2.3) and (2.7). It can also be used to calculate the spectral moments of processes which are obtained by differentiating the autocorrelation function, defined in equation 2.2, with respect to  $\tau$ . In order to do so, each term of the form  $x(t)x(t+\tau)$  in summation has to be differentiated in respect to  $\tau$  while keeping the time,  $t$ , constant.

$$\frac{d}{d\tau} (R_x(\tau)) = E[x(t) \dot{x}(t+\tau)] = E[x(t-\tau) \dot{x}(t)], \quad (2.8)$$

$$\frac{d^2}{d\tau^2} (R_x(\tau)) = -E[\dot{x}(t-\tau) \dot{x}(t)] = -R_{\dot{x}}(\tau). \quad (2.9)$$



Similarly, from the Fourier integral, defined in equation (2.6)

$$\frac{d^2}{d\tau^2} (R_x(\tau)) = \frac{1}{4\pi} \int_{-\infty}^{\infty} \omega^2 S_x e^{i\omega\tau} d\omega. \quad (2.10)$$

or

$$R_{\ddot{x}}(\tau) = \omega^2 R_x(\tau) = \frac{1}{4\pi} \int_{-\infty}^{\infty} \omega^2 S_x e^{i\omega\tau} d\omega. \quad (2.11)$$

If the time interval,  $\tau$ , is zero, then

$$R_{\ddot{x}}(0) = \omega^2 R_x(0) = \frac{1}{4\pi} \int_{-\infty}^{\infty} \omega^2 S_x d\omega. \quad (2.12)$$

This expression is also defined as second spectral moment of the random process.

### 3. STOCHASTIC STRUCTURAL RESPONSE

The dynamic equation of motion of a system with  $N$  degrees of freedom is expressed as

$$[M]\{\ddot{q}\} + [C]\{\dot{q}\} + [K]\{q\} = \{P\}, \quad (3.1)$$

where  $[M]$ ,  $[C]$  and  $[K]$  denote mass damping and stiffness matrices and  $\{q\}$  and  $\{P\}$  are the displacement and load vectors.  $\{q\}$  may be total displacements or displacements relative to base depending on the exciting effects. In a modal formulation, the  $N$  physical coordinates,  $\{q\}$  are expressed as a sum of  $M < N$  modal contribution as

$$\{q\} = [\phi] \{y\} \quad (3.2)$$

where  $[\phi]$  denotes the  $N \times M$  modal matrix containing the first  $M$  eigenvectors,  $\{\phi\}$ ,  $r = 1, 2, \dots, M$  and  $y$  represents the  $M$  modal coordinates. Transformation of (3.1) by means of (3.2) leads to

$$m_r \ddot{y}_r + c_r \dot{y}_r + k_r y_r = p_r \quad (3.3)$$

where,  $\{\phi_r\}$  is the  $r$ th mode of vibration

$$m_r = \{\phi_r\}^T [M] \{\phi_r\} \quad (3.4)$$

$$c_r = \{\phi_r\}^T [C] \{\phi_r\} \quad (3.5)$$

$$k_r = \{\phi_r\}^T [K] \{\phi_r\} \quad (3.6)$$

and

$$p_r = \{\phi_r\}^T \{p\} \quad (3.7)$$

If it is assumed that  $[C]$  becomes a diagonal matrix after transformation, i.e. decouples, then equation (3.3) may be rewritten as

$$\ddot{y}_r + 2 \zeta_r \omega_r \dot{y}_r + \omega_r^2 y_r = \frac{p_r}{m_r} \quad (3.8)$$

where critical damping ratio

$$\zeta_r = \frac{c_r}{2 \sqrt{k_r m_r}} \quad (3.9)$$

and the undamped circular natural frequency

$$\omega_r = \sqrt{\frac{k_r}{m_r}}, \quad (3.10)$$

of the  $r$ th mode. Equation (3.8) may be more simplified if the eigenvectors are mass-normalised as,

$$m_r = 1, \quad r = 1, \dots, M. \quad (3.11)$$

If each value of the modal load,  $P_r$ , defined in equation (3.7) is assumed to represent stationary random process, then taking the Fourier transform of equation (3.7) gives

$$P_r(\omega) = \left\{ \phi_r \right\}^T \left\{ P(\omega) \right\}, \quad (3.12)$$

where  $P_r(\omega)$  and  $\left\{ P(\omega) \right\}$  denote the Fourier transforms of the modal load and of the physical load vector  $p$ , respectively. These Fourier transforms are expressed as

$$P_r(\omega) = \int_0^{\infty} p_r(t) e^{-i\omega t} dt. \quad (3.13)$$

The Fourier transform of the nodal coordinates  $y_r$ , may also be written as

$$Y_r(\omega) = \int_0^{\infty} y_r(t) e^{-i\omega t} dt. \quad (3.14)$$

Substituting equations (3.13) and (3.14) into (3.8) yields

$$(-\omega^2 + 2i\zeta_r\omega_r + \omega_r^2) Y_r(\omega) = P_r(\omega). \quad (3.15)$$

Then, with the complex frequency response function defined as

$$H_r(\omega) = \frac{1}{\omega_r^2 - \omega^2 + 2i\zeta_r\omega_r} \quad (3.16)$$

the relationship between nodal coordinates and forces related to the  $r$ th mode of vibration may then be expressed using equation (3.15) as

$$Y_r(\omega) = H_r(\omega) P_r(\omega). \quad (3.17)$$

It is clear from the definition of the complex frequency response function that it is the response to a unit force. In a matrix notation, for multidegrees of freedom system, Fourier transforms of modal amplitudes may be expressed as from equations (3.17) and (3.12)

$$\{Y(\omega)\} = [H(\omega)] \{\phi\}^T \{P(\omega)\}, \quad (3.18)$$

where,  $\{Y(\omega)\}$ ,  $\{P(\omega)\}$  are Fourier transform of modal coordinates  $y(t)$ , and physical load vector  $\{p\}$ , respectively.  $H_r(\omega)$  is the diagonal matrix of the modal frequency responses as expressed by equation (3.16).

Any structural response quantity,  $q_j(t)$  such as displacement, is obtained from the modal contribution by

$$q_j(t) = \sum_{r=1}^M \bar{\psi}_{jr} y_r(t) = \{\bar{\psi}_j\}^T \{y(t)\}, \quad (3.19)$$

where,  $\bar{\psi}_{jr}$  is the contribution of the  $r$ th mode to  $q_j(t)$  displacement

and  $y_r(t)$  is the  $r$ th modal coordinate. The Fourier transform of equation (3.19) yields,

$$Q_j(\omega) = \{\bar{\psi}_j\}^T \{Y(\omega)\} \quad (3.20)$$

By substituting equation (3.18) into (3.20) the following expression will be obtained

$$Q_j(\omega) = \{\bar{\psi}_j\}^T [\bar{H}(\omega)] [\phi]^T \{P(\omega)\} \quad (3.21)$$

Both the power and cross-spectral density functions,  $S_{ij}^q(\omega)$ , of the process  $q(t)$  and  $q(t)$  may be obtained from the expression defined in equation (2.5)

$$S_{ij}^q(\omega) = \lim_{T \rightarrow \infty} \frac{1}{n} \int \frac{2 Q_{i,k}(\omega) Q_{j,k}^*(\omega)}{T} \quad n \rightarrow \infty \quad (3.22)$$

where  $*$  denotes the complex conjugate and  $T$  is the duration or the period of the process. By substituting equation (3.21) into equation (3.22) then, the following equation is obtained.

$$S_{ij}^q(\omega) = \{\bar{\psi}_i\}^T [\bar{H}(\omega)] [\phi]^T [S^P(\omega)] [\phi] [\bar{H}(\omega)] \{\bar{\psi}_j\} \quad (3.23)$$

where  $[S^P(\omega)]$  is the power and cross-spectral density function of input forces.

This equation can be re-ordered as

$$S_{ij}^q(\omega) = \sum_{r=1}^M \sum_{s=1}^M \bar{\psi}_{ir} \bar{\psi}_{js} H_{ir}(\omega) H_{js}^*(\omega) \sum_{l=1}^N \sum_{m=1}^N \phi_{lr} \phi_{ms} S_{lm}^p(\omega) \quad (3.24)$$

If the elements of the load vector are uncorrelated then  $[S^p(\omega)]$  in equation (3.23) reduces to a diagonal matrix. For  $i = j$  equation (3.24) gives the power spectral density function of  $i$ th displacement output. This equation may be further simplified as

$$S_{ij}^q(\omega) = \sum_{r=1}^M \sum_{s=1}^M \psi_{ir} \psi_{js} H_{ir}(\omega) H_{js}(\omega) S_{p_r p_s}^p(\omega), \quad (3.25)$$

where,

$$S_{p_r p_s}^p(\omega) = \sum_{l=1}^N \sum_{m=1}^N \phi_{lr} \phi_{ms} S_{lm}^p(\omega) = \phi_r^T S_p \phi_s. \quad (3.26)$$

Therefore, the power spectrum density function of any two  $i$  and  $j$  displacements may be further simplified if the elements of load vector are uncorrelated, then

$$S_{p_r p_s}^p(\omega) = 0$$

for  $r \neq s$ .

For the case where a structure subjected to a ground acceleration, then equation (3.1) becomes

$$[M]\{\ddot{q}\} + [C]\{\dot{q}\} + [K]\{q\} = -[M]\{\delta\} \ddot{x}_g(t) \quad (3.27)$$

where  $\{\delta\}$  is the ground acceleration direction vector.

It contains 1's in the direction of the ground acceleration and 0's in all other directions.  $\ddot{x}_g(t)$  ground acceleration time history. Then modal

force defined in equation (3.7) becomes

$$P_r = - \{\phi\}^T [M] \{\delta\} \ddot{a}_g(t) \quad (3.28)$$

and its Fourier transform is

$$P_r(\omega) = \{\phi\}^T [M] \{\delta\} A(\omega) \quad (3.29)$$

By comparing equation (3.29) with equation (3.12) the Fourier transform of modal forces are defined as

$$\{P(\omega)\} = \{\{\phi\}_r^T [M] \{\delta\}\} A(\omega) \quad (3.30)$$

By substituting (3.30) into (3.21) and then using (3.22) the cross spectral density of the output process of the case for which a ground acceleration is used as input may be defined as

$$S_{ij}^q(\omega) = S_{in}^a(\omega) \sum_{r=1}^M \sum_{s=1}^M \psi_{ir} \psi_{js} H_{ir}(\omega) H_{js}^*(\omega) \quad (3.31)$$

The equation (3.31) corresponds to equation (3.23) defined for the case for which forces used as input. In this equation  $S_{in}^a(\omega)$  is the power spectrum density function of input ground acceleration, defined as,

$$S_{in}^a(\omega) = \lim_{T \rightarrow \infty} \frac{1}{n} \sum_{k=1}^n \frac{2 A_{1,k}(\omega) A_{j,k}^*(\omega)}{T} \quad n \rightarrow \infty \quad (3.32)$$

and

$$\psi_{ir} = \bar{\psi}_{ir} \{\phi_r\}^T [M] \{\delta\} \quad (3.33)$$

If the modes are not mass-normalised as in the case of equation (3.11) then  $\psi_{ir}$ 's should be replaced by

$$\psi_{ir} = \bar{\psi}_{ir}(\phi_r)^T \{M\} \{\delta\} / (\phi_r^T) \{M\} \{\phi_r\} \quad (3.34)$$

In equation (3.31)  $S_{ij}^q(\omega)$  is always a real valued as it is  $S_{in}^a(\omega)$ . Because indices  $r$  and  $s$  are switched in complex conjugate expressions, therefore, imaginary terms are lost in the summation.

### 3.1 Mean Square Responses

Of interest to the structural analyst are the zeroth, first and second spectral moments of the response quantity. These spectral moments are defined in terms of the power spectral density function and the frequency by substituting (3.31) into (2.9) and (2.13)

$$\lambda_{mij} = \frac{1}{2\pi} \int_0^\infty \omega^m S_{ij}^q(\omega) d\omega \quad m = 0, 1, 2 \quad (3.36)$$

Substituting (3.31) into (3.36) gives the spectral moments of response in terms of the modal cross-spectral moments as

$$\lambda_{mij} = \sum_{r=1}^M \sum_{s=1}^M \psi_{ir} \psi_{js} \frac{1}{2\pi} \int_0^\infty \omega^m S_{in}^a(\omega) H_{ir}(\omega) H_{jr}^*(\omega) d\omega, \quad (3.37)$$

$m = 0, 1, 2$

or

$$\lambda_{mij} = \sum_{r=1}^M \sum_{s=1}^M \psi_{ir} \psi_{js} \lambda_{m,rs}, \quad (3.38)$$

where,

$$\lambda_{m,rs} = \text{Re} \left[ \frac{1}{2\pi} \int_0^\infty \omega^m S_{in}^a(\omega) H_{ir}(\omega) H_{jr}(\omega) d\omega \right] \quad (3.39)$$



are the cross spectral moments of the normal coordinates associated with modes  $r$  and  $s$ ,  $R_e$  denotes the real part. It is noted that because  $S_{in}^a(\omega)$  is symmetric and has always real-value; therefore only the real parts of the cross-spectral moments are of interest. Introducing coefficients

$$\rho_{m,rs} = \frac{\lambda_{m,rs}}{\sqrt{\lambda_{m,rr} \lambda_{m,ss}}} \quad m = 0, 1, 2, \quad (3.40)$$

equation (3.38) may be re-expressed as,

$$\lambda_{mij} = \sum_{r=1}^M \sum_{s=1}^M \psi_{ir} \psi_{js} \rho_{m,rs} \sqrt{\lambda_{m,rr} \lambda_{m,ss}} \quad m = 0, 1, 2. \quad (3.41)$$

For a particular response value i.e.  $i = j$  and  $i$  and  $j$  indices may be dropped for simplicity. From this expression, the zeroth,  $\lambda_0$  first,  $\lambda_1$  and second,  $\lambda_2$ , spectral moments may be obtained simply by writing  $m = 0, 1, 2$ , respectively. Particularly zeroth and second spectral moments, originally, defined in equations (2.9) and (2.13)

$$\lambda_0 = \sigma_R^2 = E[q(t)^2], \quad (3.42)$$

$$\lambda_2 = \sigma_R^2, \quad (3.43)$$

are the mean square response of  $q(t)$  and its time derivative  $\dot{q}(t)$  respectively, whereas  $\lambda_{0,rr}$  and  $\lambda_{2,rr}$  are the mean squares of the  $r$ th normal coordinates  $y_r(t)$  and its time derivative  $\dot{y}_r(t)$  respectively. These normal coordinates are defined in equation (3.2). Also from the definition of  $\rho_{m,rs}$ , it is clear that  $\rho_{0,rs}$  and  $\rho_{2,rs}$  are cross correlation coefficients between normal coordinates  $y_r(t)$  and  $y_s(t)$  and their time derivatives  $\dot{y}_r(t)$  and  $\dot{y}_s(t)$ .

From the proceeding theory, it is clear that the stochastic dynamic analysis results in the mean square response value in the frequency

domain. To achieve this, modal mean square response value have to be obtained first by the closed form solution of equation (3.39). These solutions for white-noise and filtered white-noise [13] are relatively easier because their power spectral densities are in the form of

$$S(\omega) = S_0 \quad , \quad (3.44)$$

$$S(\omega) = \frac{\omega_g^4 + 4\zeta_g^2 \omega_g^2 \omega^2}{(\omega_g^2 - \omega^2)^2 + 4\zeta_g^2 \omega_g^2 \omega^2} S_0 \quad , \quad (3.45)$$

respectively. Where  $S_0$  is the scale factor and  $\omega_g$  and  $\zeta_g$  are the filter frequency and damping coefficient. It is noted that a filtered white noise with  $\omega_g = 5\pi$  and  $\zeta_g = 0.6$  is commonly used in earthquake engineering to model the ground acceleration process [2, 13].

It was shown by Der Kiureghian [9] that  $\lambda_{m,rs}$  are sensitive to the shape of input power spectral density, whereas the coefficients  $\rho$  remains relatively indifferent for wide-band inputs. It was also proved by the same author that correlation coefficients  $\rho_{m,rs}$  defined in equation (3.40), rapidly diminishes as the two modal frequencies  $\omega_r$  and  $\omega_s$  move apart. Thus, for the wide-band inputs, cross terms in equation (3.41) becomes only significant for modes with closely spaced frequencies. He has suggested the following expressions for correlation coefficients to be used for any arbitrary power spectral density shapes based on first-order approximations [9, 10].

$$\rho_{0,rs} = \frac{2\sqrt{\zeta_r \zeta_s} [(\omega_r + \omega_s)^2 (\zeta_r + \zeta_s) + (\omega_r^2 - \omega_s^2) (\zeta_r - \zeta_s)]}{K_{rs}}$$

$$\rho_{1,rs} = \frac{2\sqrt{\zeta_r \zeta_s} [(\omega_r + \omega_s)^2 (\zeta_r + \zeta_s) - 4(\omega_r - \omega_s)^2 / \pi]}{K_{rs}} \quad , \quad (3.46)$$

$$\rho_{2,rs} = \frac{2\sqrt{\zeta_r \zeta_s} [(\omega_r + \omega_s)^2 (\zeta_r + \zeta_s) - (\omega_r^2 - \omega_s^2) (\zeta_r - \zeta_s)]}{K_{rs}}$$

where .

$$K_{rs} = 4(\omega_r - \omega_s)^2 + (\omega_r + \omega_s)^2 (\zeta_r + \zeta_s)^2 .$$

With the expressions given in equation (3.46), to evaluate equation (3.41) in order to calculate mean-square responses, it is only necessary to compute the spectral moments for individual normal coordinates, expressed by equation (3.39). For  $r = s$ , this equation leads to

$$\lambda_{m,rr} = \frac{1}{2\pi} \int_0^\infty \omega^m S_{1n}^a(\omega) |H_r(\omega)|^2 d\omega \quad m = 0, 1, 2 \quad (3.47)$$

When  $m = 0$ , then equation (3.47) corresponds to the mean square displacement response for the  $r$ th mode. In addition, when  $m = 2$ , the same equation defines the mean square velocity response for a particular mode. Therefore, using equations (3.42) and (3.43) modal, zeroth and second spectral moments are expressed as

$$\lambda_0 = \sigma_R^2 = E [q_r(t)^2] = \lambda_{0,rr} \quad (3.48)$$

$$\lambda_2 = \sigma_{\dot{R}}^2 = E [\dot{q}_r(t)^2] = \lambda_{2,rr} \quad (3.49)$$

### 3.2 Mean Peak Response

In the analysis of structures to dynamic loadings, the parameter of most interest is the expected (mean) peak value of a structural response quantity. This peak value is compared with allowable yield limit which is defined in the code of practice for design purpose.

The mean peak response,  $\mu$ , and its standard deviation,  $\sigma$ , can be expressed in terms of the probability density function  $p(x)$  and the level of variable,  $x$ , as

$$\mu = E[x] = \int_0^\infty x p(x) dx, \quad (3.50)$$

$$\sigma^2 = E[(x^2 - \mu)^2] = \int_0^\infty (x - \mu)^2 p(x) dx \quad (3.51)$$

Probability density function itself is obtained by differentiating the cumulative probability function,  $F(x)$ , as

$$p(x) = \frac{dF(x)}{dx} \quad (3.52)$$

Using equation (3.50) and (3.51) mean and standard deviation of  $x$  may, in general, be written in terms of the root mean square response  $\lambda_0$ ,

$$\mu \approx p \sqrt{\lambda_0} \quad (3.53a)$$

$$\sigma \approx q \sqrt{\lambda_0} \quad (3.53b)$$

where  $p$  and  $q$  are peak factors corresponding to a ground motion duration, and mean zero crossing rate,  $v$ .

Several methods for determining the peak factors have been proposed in the literature. Davenport's [14] suggestion is based on the maximum behaviour on a Poisson 'threshold crossing' model which gives  $p$  and  $q$  peak factors as

$$p = \sqrt{(2 \ln v\tau)} + \frac{0.5772}{\sqrt{(2 \ln v\tau)}} \quad (3.54)$$

$$q = \frac{\pi}{\sqrt{6}} \frac{1}{\sqrt{(2 \ln v\tau)}} \quad (3.55)$$

where

$$v = \frac{1}{4} \sqrt{\frac{\lambda_2}{\lambda_0}}$$

Der Kiureghian [9,10] has shown that Davenport's result tends to overestimate the mean and underestimate the standard deviation since threshold crossings are considered independent in the Poisson model. However, for large values of  $\nu\tau$  ( $\nu\tau > 5000$ ) such as in wind and ocean engineering, Davenport's expressions for peak factors will be used [10]. Kiureghian suggests that in order to account for the dependence between threshold crossings,  $\nu_e$ , which represents an equivalent rate of statistically independent crossing, should be used, in which case,

$$p = \frac{1.2}{\sqrt{2 \ln \nu_e \tau}} + \frac{0.5772}{\sqrt{(2 \ln \nu_e \tau)}} , \quad (3.56)$$

$$q = \frac{1.2}{\sqrt{(2 \ln \nu_e \tau)}} - \frac{5.4}{13 + (2 \ln \nu_e \tau)^{3.2}} , \quad (3.57)$$

where ,

$$\nu_e = \begin{cases} (1.636^{0.45} - 0.38) \nu & \delta < 0.69 , \\ \nu & \delta > 0.69 , \end{cases} \quad (3.58)$$

$$\nu = \frac{\sigma_R}{\pi \sigma_R} = \frac{1}{\pi} \sqrt{\frac{\lambda_2}{\lambda_0}} , \quad (3.59)$$

is the mean zero-crossing rate of the process and

$$\delta = \sqrt{1 - \frac{\lambda_1^2}{\lambda_0 \lambda_2}} , \quad (3.60)$$

is the shape factor for the response power spectral density with a value between zero and unity. (A small value for  $\delta$  denotes a narrow-band process whereas a value near unity denotes a wide-band process [14]). The established values of  $p$  and  $q$  are for  $10 \leq \nu\tau \leq 1000$  and  $0.11 \leq \delta \leq 1$  ,

which are of interest in earthquake engineering [11]. Vanmarcke [12,14] also calculated  $p$  and  $q$  values and derived a cumulative probability distribution function for the first-crossing time of a symmetric barrier

(  $x$  as shown in Fig. 1) for a zero mean stationary Gaussian process. In his formulation the cumulative distribution of the peak absolute response,  $R_T$ , over a duration,  $T$ , defined as

$$R_T = \max_T |R(t)|, \quad (3.61)$$

can be expressed

$$F_{R_T}(r) = \left[ 1 - \exp(-s^2/2) \right] \exp \left[ -v_T \frac{1 - \exp(-\sqrt{(\pi/2)} \delta e^s)}{\exp(s^2/2) - 1} \right]_{x_m > 0} \quad (3.62)$$

in which,

$$v = \frac{x_m}{\sigma_R} = \frac{x_m}{\sqrt{\lambda_0}} \quad (3.62a)$$

is the normalised barrier  $v$  and  $\delta$  are defined in equation (3.59) and (3.60) and  $\delta_e = \delta^{1.2}$ .  $x_m$  is the defined barrier level.

In this analysis, Der Kiureghian's peak factors values and Vanmarcke's cumulative distribution function are used. Furthermore, the parameters defined above,  $v, \delta, p$  and  $q$  are for the  $r$ th normal coordinates. For the simplicity, the indices are dropped.

### 3.3 Response Spectrum Method for Random Vibration

The objective of this section is to explain a procedure for evaluating the response of a multi-degree-of-freedom system when the input is zero-mean wide-band, stationary Gaussian process, specified through its mean response spectrum.

Let  $\bar{S}_r(\omega, \zeta)$  represent the mean value of the maximum absolute response of an oscillator over duration  $\tau$ , of its stationary response to a stationary input excitation  $R(t)$ ; where  $\omega$  and  $\zeta$  are the oscillator frequency and damping coefficient, respectively. Using equation (3.59), the mean zero-crossing rate,  $v_r$ , and the shape factor,  $\delta_r$ , for the  $r$ th mode of vibration may be expressed as

$$v_r = \frac{1}{\pi} \sqrt{\frac{\lambda_{2,rr}}{\lambda_{0,rr}}}, \quad (3.63)$$

$$\delta_r = \sqrt{1 - \frac{\delta_{1,rr}^2}{\lambda_{0,rr} \lambda_{2,rr}}}. \quad (3.64)$$

It was shown by Der Kiureghian [10] that  $v_r$  and  $\delta_r$  are not too sensitive to the shape of the input power spectral density function, provided that the input is wide-band and that the oscillator frequency is not beyond the significant range of input frequencies. For response to a wide-band input with arbitrary power spectral density function, he suggested a more simplified value for  $v_r$  and  $\delta_r$  as

$$v_r \approx \frac{\omega_r}{\pi}, \quad (3.65)$$

$$\delta_r \approx 2 \left( \frac{\zeta_r}{\pi} \right)^{1/2}. \quad (3.66)$$

Once the mean zero-crossing rate,  $v_r$ , and shape factor,  $\delta_r$ , are calculated for a particular mode, then corresponding peak factors, as defined in equations (3.56 - 3.57), may be calculated in terms of frequency contents and the duration of input dynamic effects.

From the definition of the mean response spectrum, it is clear that

$\bar{S}_r(\omega_r, \zeta_r)$  is the mean of the absolute maximum of the  $r$ th normal coordinate,  $y_r(t)$ , defined in equation (3.2). Thus using the equations (3.53) and (3.62a)

$$\bar{S}_r(\omega_r, \zeta_r) = p_r \sqrt{\lambda_{0,rr}} \quad (3.67)$$

may be written, where  $\bar{S}_r(\omega_r, \zeta_r)$  and  $p_r$  are predefined and calculated. In this equation, the only unknown is the zeroth spectral moment which is calculated as

$$\lambda_{0,rr} = \frac{1}{p_r^2} \bar{S}_r^2(\omega_r, \zeta_r) \quad (3.68)$$

Furthermore, using the equations (3.63) and (3.64) together with the equations (3.65, 3.66) then the first and second spectral moments for the  $r$ th normal coordinate are obtained as

$$\lambda_{1,rr} = \frac{\omega_r \sqrt{(1 - 4 \zeta_r / \pi)}}{p_r^2} \bar{S}_r^2(\omega_r, \zeta_r), \quad (3.69)$$

and

$$\lambda_{2,rr} = \frac{\omega_r^2}{p_r^2} \bar{S}_r^2(\omega_r, \zeta_r) \quad (3.70)$$

respectively.

Substituting equations (3.68, 3.69 and 3.70) together with the equations (3.46) in equation (3.41), the spectral moments  $\lambda_0$ ,  $\lambda_1$  and  $\lambda_2$  of the response power spectral density are computed in terms of the response spectrum ordinates. These moments can then be used to calculate the cumulative probability distribution of the peak response and various statistical quantities. In particular the mean maximum response in mode  $r$ , may be expressed as

$$\bar{R}_{r\zeta} = \psi_r \bar{S}_\delta(\omega_r, \zeta_r), \quad (3.71)$$

where,



$\psi$  is the effective modal participation factor defined in equation (3.34). Then utilising equation (3.41) in conjunction with equation (3.36 - 3.70), the root-mean square of response,  $\sigma_R$ , and root-mean square of response rate,  $\sigma_{\dot{R}}$  may be obtained as

$$\sigma_R = \sqrt{\lambda_0} = \left( \sum_r^m \sum_s^m \frac{1}{p_r p_s} \rho_{0,rs} \bar{R}_{rt} \bar{R}_{st} \right)^{1/2}, \quad (3.72)$$

$$\sigma_{\dot{R}} = \sqrt{\lambda_2} = \left( \sum_r^m \sum_s^m \frac{\omega_r \omega_s}{p_r p_s} \rho_{2,rs} \bar{R}_{rt} \bar{R}_{st} \right)^{1/2}. \quad (3.73)$$

Mean of peak response,  $\bar{R}_T$ , and standard deviation of peak response  $\sigma_{R_T}$  may be expressed as,

$$\bar{R}_T = \rho \sigma_R = \left( \sum_r^m \sum_s^m \frac{p^2}{p_r p_s} \rho_{0,rs} \bar{R}_{rt} \bar{R}_{st} \right)^{1/2}, \quad (3.74)$$

$$\sigma_{R_T} = q \sigma_{\dot{R}} = \left( \sum_r^m \sum_s^m \frac{q^2}{p_r p_s} \rho_{0,rs} \bar{R}_{rt} \bar{R}_{st} \right)^{1/2}. \quad (3.75)$$

The response mean frequency, denoted by  $\bar{\omega}$  which may be expressed as

$$\bar{\omega} = \pi \nu = \frac{\sigma_{\dot{R}}}{\sigma} \left[ \frac{\sum_r^m \sum_s^m \frac{\omega_r \omega_s}{p_r p_s} \rho_{2,rs} \bar{R}_{rt} \bar{R}_{st}}{\sum_r^m \sum_s^m \frac{1}{p_r p_s} \rho_{0,rs} \bar{R}_{rt} \bar{R}_{st}} \right]^{1/2}. \quad (3.76)$$

Der Kiurghian [10] have shown that equation (3.74) and (3.76) may be further simplified as

$$\bar{R}_T = \left( \sum_r^m \sum_s^m \rho_{0,rs} \bar{R}_{rt} \bar{R}_{st} \right)^{1/2}, \quad (3.77)$$

$$\bar{\omega} = \left[ \frac{\sum_r^m \sum_s^m \omega_r \omega_s \rho_{2,rs} \bar{R}_{rt} \bar{R}_{st}}{\sum_r^m \sum_s^m \rho_{0,rs} \bar{R}_{rt} \bar{R}_{st}} \right]^{1/2}. \quad (3.78)$$

For structures with well-separated frequencies the cross-correlation coefficients,  $\rho_{m,rs}$ , ( $r \neq s$ ), vanishes. Then only the terms in  $\rho_{m,rs}$  ( $r = s$ ) remains. Since these terms are equal to unity, then, in this particular case, the equation (3.77) reduces to

$$\bar{R}_T = \left( \sum_r \bar{R}_{jT}^2 \right)^{1/2} \quad (3.79)$$

This is however a well known square-root-of-sum of square (SRSS) method.

The response calculation of structural systems to any dynamic loading defined with equation (3.77) is called the complete quadratic combination (CQC) method [11]. The CQC method which is based on the random vibration theory is especially suggested for the structures which have natural frequencies closely spaced. A typical example of such structures are nuclear power plants, building structures with symmetric layout but not in mass and particularly suspension bridges.

The application of the above theories based on the stochastic analysis are demonstrated on different suspension bridges and comparison of results from CQC method and stochastic analysis were carried out.

#### 4. STOCHASTIC RESPONSE OF SUSPENSION BRIDGES

In this section, the stochastic responses of the Dolerw [23], Bosporus [22] and Humber [22] bridges were examined. These bridges cover a large variety particularly in dimensions. The Dolerw bridge, which has only 50 m main span with vertical hangers and concrete deck, forms one extreme size in dimension. Bosporus, with box-girder deck, inclined hangers steel towers, without any side spans supported by cables, has 1074 m main span. There are several suspension bridges with main span around 1000 m long.

The Humber Bridge, however, has the longest main span, 1410 m, in the world

with a total length of 2220 m. The latter may well be accepted as another extreme case in dimension. This bridge has a box girder-deck, inclined hangers, two side spans (280 m and 530 m each length) and concrete towers. With these geometries, the fundamental periods of these chosen bridges vary between 1 - 10 seconds in the vertical plane. The reason for choosing these extremes is to elucidate the applicability of the theory and the verification of assumptions involved in the definitions of peak values.

The above mentioned bridges were first subjected to S16E component of the Pacoima dam record during the San Fernando earthquake in 1971, Fig. 1a. Since the analysis was performed in the vertical plane, the ground motion is also applied in vertical direction and the amplitude of the recorded acceleration values is multiplied by the factor of 2/3. The detail of the considered bridges and their mathematical modelling are given in references [22] and [23] therefore, not repeated here again.

The stochastic analysis was based on the calculated power spectrum density function of the input acceleration which is shown in Fig. 1b.

Maximum values of displacements and forces were calculated using Completed Quadratic Combination (CQC) method. These are then compared with mean peak values obtained by the former method.

#### 4.1 The Dolerw Bridge

The stochastic analysis of the Dolerw Suspension bridge was carried out using the procedure described above. Root-mean-square and mean maximum displacements due to vertical ground motion were shown in Fig. 2. The former one is obtained as a square root of the zeroth spectral moment as defined in equation (3.36). Mean peak values of displacements, were also calculated using equation (3.53). Root-mean-square of displacements at the mid-point of the span is 4.17 cm whereas the maximum of mean peak displacement is 10.7 cm. For the comparison, the maximum displacement

response of the bridge was calculated using CQC method, as described in section 3.3. The displacements were depicted in Fig. 2a.

The average frequencies of occurrence of mean maximum vertical displacements, shown in Fig. 2b, which are larger for the displacements of nodal points nearer to towers than those of the centre. They have the values in the range of 1.89 - 1.2 Hz. The general tendency is that the smaller the displacements the higher the average frequencies of occurrence.

To verify the validity of the results calculated using the stochastic analysis, the time-history analysis of the bridge was performed. From this analysis, the time-history of the vertical displacements of the deck at the mid-point was calculated and shown in Fig. 3. Through the examining of the history record the following conclusions may be drawn.

- a) The displacement time-history does not end as soon as the effect of the earthquake terminates. But the bridge has several peak values with zero crossing within the duration of the earthquake record.
- b) The maximum of displacements is higher than the calculated maximum by the CQC method. This is rather attributable to differences between these two methods of analyses.
- c) The mean peak values obtained by the stochastic analysis is smaller than the maximum values obtained by the CQC method. It may be easily visualised by checking the time history of the displacements, Fig. 3, that the mean peak value being 10.7 cm is a right value. In cases where several peak responses can occur within the duration of an earthquake, the assumption used for the calculation of mean peak values prove to be justified.
- d) The time-history analysis also proves that the average frequency of occurrence being 1.25 second is also right. Due to the

above-mentioned facts, particularly the bridge experiencing several peaks within the duration of the earthquake record, there is no need, however to expand the earthquake record by adding some trailing zero at the end.

The cumulative distribution function (CDF) defined in equation (3.62) of the vertical displacements at the centre is shown in Fig. 4. It is clear from the graph that most of the displacements are accumulated within the range of 7 - 12 cm. The mean (expected) peak value is 57% of its maximum value. In other words, if the mean peak value is assumed to be defined as a barrier level, then the probability of occurrence of displacements below this limit is 57%.

Bending moments and shear forces of the deck by both the stochastic and CQC methods are depicted in Figs. 5 and 6. The former method yields the mean maximum values whereas the latter provides the maximum themselves. The average frequencies of occurrence of bending moments and shear forces are also shown on the same figures. As in the case of displacements, the bigger the internal effects (moments or shear forces) the smaller the frequencies of occurrence are.

#### 4.2 The Bosporus Bridge

Mean peak and root mean square values of displacement response were shown in Fig. 7a. Maximum displacements by the CQC method were also calculated and plotted on the same graph. It is evident from the analysis that the difference between mean peak values and the maximum displacements reaches up to 5 cm at most at the mid point. However, if maximum displacements are calculated by the time-history analysis, the difference reaches up to 15 cm for the same point. To clarify this point further, the time history of the displacement response of the mid-point are plotted and shown in Fig. 8. It is very obvious from the plot that the displacements still

have large values even after the earthquake terminates. Also, the mean peak value, 68 cm, calculated by the stochastic analysis is almost an average value of the two peaks with positive zero crossing on the history plot. This indicates the correctness of stochastic response analysis. The results may be accepted even more reliably bearing the fact in mind that the coefficients relating zeroth spectral moments to mean peak values are themselves based on the same simplifications and prone to error up to 6% [12].

Average frequencies of occurrence of displacements are shown in Fig. 7b. Its lowest value 0.19 Hz ( $T = 5.2$  second) is for the displacements at the mid point. The justification of this value may also be detected through the analysis of the time history plot, in Fig. 8. It is certain that the vertical displacement response will still continue even after the termination of the earthquake input with appreciable amplitude. This reflects itself in the stochastic analysis. If trailing zeros were added after the earthquake record to account for longer duration and for more refined stochastic analysis, root-mean-square of responses and mean peak responses do not diminish rapidly, for the duration of  $\approx 20$  and  $\approx 27$  seconds. The variations of vertical stochastic responses by time are shown in Fig. 9 a and 9 b.

In Fig. 10, root-mean-square, mean peak and maximum of longitudinal displacements are shown. The latest is the largest and obtained by the CQC method. As in the case of the deck, mean peak displacements and maximum displacements have similar values. Fig. 11 and Fig. 12 show mean maximum and maximum bending moments of the European tower and the deck respectively. Bending moments by different methods in both parts of the bridge do not vary significantly.

The cumulative distribution function of the vertical displacements at the mid-point of the deck are shown in Fig. 13. It shows that the probability of occurrence of the mean peak displacement is about 55%.

#### 4.3 The Humber Bridge

Mean (expected) peak and root-mean square values of vertical displacement response of the deck of the Humber bridge were shown in Fig. 14a. The latter is the square-root of the zeroth spectral moments where as the former is calculated by multiplying the square root of zeroth spectral moment by a peak factor as defined in equation 3.53a. The maximum values of vertical displacements of the deck were determined by the CQC method and were depicted on the same graph. These analyses were performed for the duration of 13.5 seconds.

The results show that the mean peak displacement responses are smaller than those of maximum values calculated by the CQC method with the exemption of displacements at the central area of the main span where mean peak responses are slightly bigger. Because of the definition of mean peak displacement response they should not be expected to be bigger than their maxima. There are, however, several factors involved which may cause this error:

- a) The CQC method of analysis itself is prone to error because of numerical procedure involved in calculating the spectral values and in the determination of the contribution of cross-spectral terms to the total displacements. To verify this point a time-history analysis was performed to obtain maximum displacements. In this case, the results seem to be improved and the difference between mean peak and maximum responses are reduced.
- b) The determination peak factors, which relate zeroth spectral moments to mean peak response, is also erroneous. It was reported, however, that up to 6% error will be likely to occur [12].
- c) Perhaps the most important of all is the lack of peak values within

the earthquake duration. An independent time-history analysis of the vertical displacements at the mid-point, Fig. 16, proves that, displacement time-history is almost reaching a peak point just after the earthquake duration is terminated. Based on these time-history records with only a few peaks, to perform a stochastic analysis, however, may not be a very healthy procedure.

- d) If some trailing zeros were added to the end of the earthquake record, mean peak responses become smaller than their maximum values, Figs. 15 and 17. As shown in Fig. 17. A sudden drop in the mean peak values as soon as an earthquake record extends beyond 13.5 seconds is perhaps due to the inclusion of a peak value with a positive zero crossing at 13.5 second.

Average frequencies of occurrence of displacement responses are shown in Fig. 14b with a minimum value of 0.15 Hz. The justification of this value is also noticeable on the time-history plot, Fig. 16.

Longitudinal displacements of the Hesse tower is shown in Fig. 18. The root-mean-square, mean peak and maximum displacement at the top are 3.8, 5.8 and 8 cm respectively. Their expected orderly values may well be explained by the fact that the towers are more rigid than the deck and have higher frequencies which may result in having more peak within the duration of the earthquake record.

Maximum and mean maximum bending moments of the deck and towers are shown in Fig. 19 and 20, respectively. As it is expected mean values are smaller than the maximum ones.

## 5. CONCLUSIONS

1. The stochastic analysis of suspension bridges to earthquake forces generally require a longer input because of lower natural



frequencies of these type of structures.

2. The preceeding analysis shows that the stochastic method may well be performed even moderately during long earthquakes, say up to 15 seconds.
3. Apart from mean peak response and root-mean square of response quantities, their average frequencies of occurrence and probabilities of occurrence may also be obtained by the stochastic analysis.
4. If the aim of analysis is based on the calculation of mean peak responses, the stochastic analysis may be exempted with. In this case, a response spectrum method, CQC, may well be used.

## 6. REFERENCES

- 1) Clough, R.W., Penzien, J. "Dynamics of Structures," McGraw-Hill, 1975.
- 2) Lin, Y.K., "Probabilistic Theory of Structural Dynamics," McGraw-Hill, 1967.
- 3) Hewland, D.E., "An Introduction to Random Vibrations and Spectral Analysis," Longman Group Ltd., 1975.
- 4) Lee, M.C., Penzien, J., "Stochastic Analysis of Structures and Piping Systems Subjected to Stationary, Multiple-Support Excitations," Earthquake Engineering and Structural Dynamics, Vol. 11, 91 - 110 pp, 1983.
- 5) Abdel-Ghaffar, A.M., Rubin, I.I., "Suspension Bridge Response to Multiple Support Excitations," Vol. 108, A.S.C.E., E.M.2, April, 419-434 pp. 1982.
- 6) Abdel-Ghaffar, A.M., Rubin, I.I., "Vertical Seismic Response of Suspension Bridges," Earthquake Engineering and Structural Dynamics, Vol. 11, 1 - 9 pp, 1983.
- 7) Vanmarcke, E.H., "Properties of Spectral Moments With Applications to Random Vibration," A.S.C.E., E.M.2, Vol. 98, April, 425-446 pp, 1971.
- 8) Corotis, R.B., Vanmarcke, E.H., Cornell, C.A., "First Passage of Nonstationary Random Process," A.S.C.E., E.M.2, 401-414 pp, 1972.
- 9) Der Kiureghian, A., "Structural Response to Stationary Excitation," A.S.C.E., E.M.6, Vol. 106, December, 1195 - 1213 pp,

1980.

- 10) Der Kiureghian, A., "A Response Spectrum Method for Random Vibration Analysis of MDF Systems," Earthquake Engineering and Structural Dynamics, Vol. 9, 419-435 pp, 1981.
- 11) Wilson, E.L., Der Kiureghian, A., Bayo, E.P., "Replacement for the SRSS Method in Seismic Analysis," Earthquake Engineering and Structural Dynamics, Vol. 9, 187 - 194 pp, 1981.
- 12) Button, M.R., Der Kiureghian, A., Wilson, E.L., "STOCAL, User Information Manual," EERC, Report No. UCB/SESM-81/02. University of California, Department of Civil Engineering, Berkeley, California, July 1981..
- 13) Kanai, K., "Semi-Empirical Formula for Seismic Characterisation of the Ground," Bulletin of Earthquake Research Institute, University of Tokyo, Japan, Vol. 35, June 1967.
- 14) Vanmarcke, E.H., "On the Distribution of the First-Passage Time for Normal Stationary Random Process." Journal of Applied Mechanics, Vol. 42, March 1975. 215-219 pp.
- 15) Davenport, A.G., The Distribution of Largest Values of Random Function with Application to Gust Loading," Proc. Inst. Civil. Eng., London, Vol. 28, 187-196 pp. 1964.
- 16) Bendat, J.S., Piersal, A.G., "Random Data; Analysis and Measurement Procedures," Wiley-Interscience, 1971.
- 17) Crandall, S.H., Random Vibration, Vol. 12, The M I T Press, 1963.
- 18) Penzien, J., "Application of Random Vibration Theory," Earthquake Engineering, Edited by R. Wiegel, 1970.

- 19) Pfaffinger, D.D., "Probabilistic Dynamic Analysis with ADINA, Computers and Structures, Vol. 13, 1981, 637-646 pp.
- 20) Karadeniz, H., "Spectral Analysis and Stochastic Fatigue Reliability Calculation of Offshore Steel Structures, Delft University of Technology, Department of Civil Engineering, April 1983.
- 21) Karadeniz, H., "Stochastic Analysis Program for Offshore Structures (SAPOS), Delft University of Technology, Department of Civil Engineering, Delft, May 1985.
- 22) Dumanoglu, A.A., Severn, R.T., "Asynchronous Seismic Analysis of Modern Suspension Bridges, Part I, II, III, IV, University of Bristol, Department of Civil Engineering, Research Reports, 1985-86.
- 23) Brownjohn, J., Dumanoglu, A.A., "Theoretical and Experimental Investigation of Dolerw Bridge, University of Bristol, Department of Civil Engineering, Research Report, 1985.
- 24) Bathe, K.J., Wilson, E.L., Peterson, F.E., "SAPIV," A Structural Analysis Program for Static and Dynamic Response of Linear Systems," Earthquake Engineering Research Centre, EERC 73-11, University of California, Berkeley, 1973.
- 25) Lee, M.C., Penzien, J., "PSDGEN/PSAD Stochastic Seismic Analyses of Nuclear Power Plant Structures and Piping Systems Subjected to Multiple-Support Excitations," Earthquake Engineering Research Centre, EERC-80/19, University of California, Berkeley, 1980.

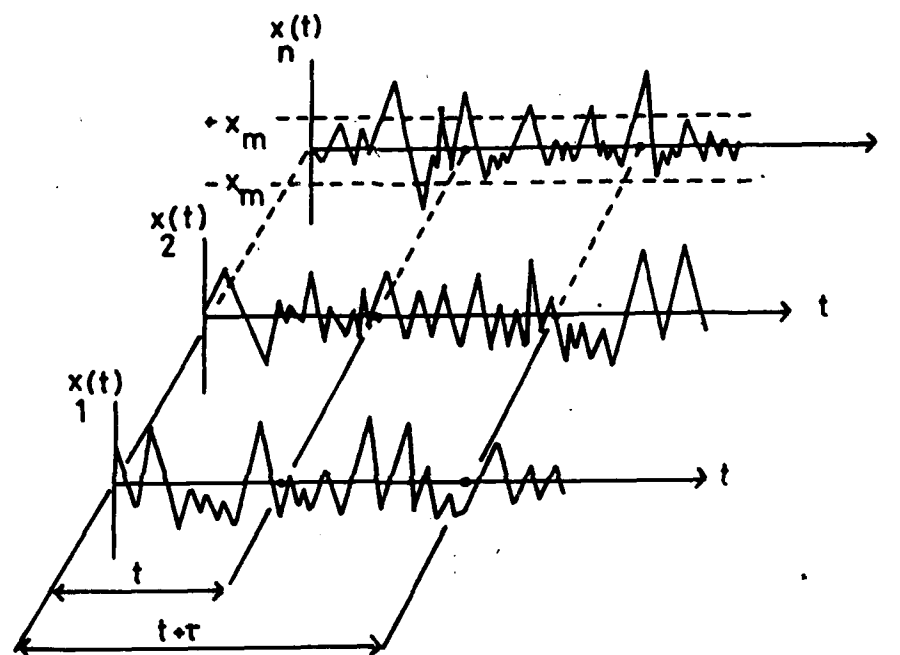


Fig.1 Random process

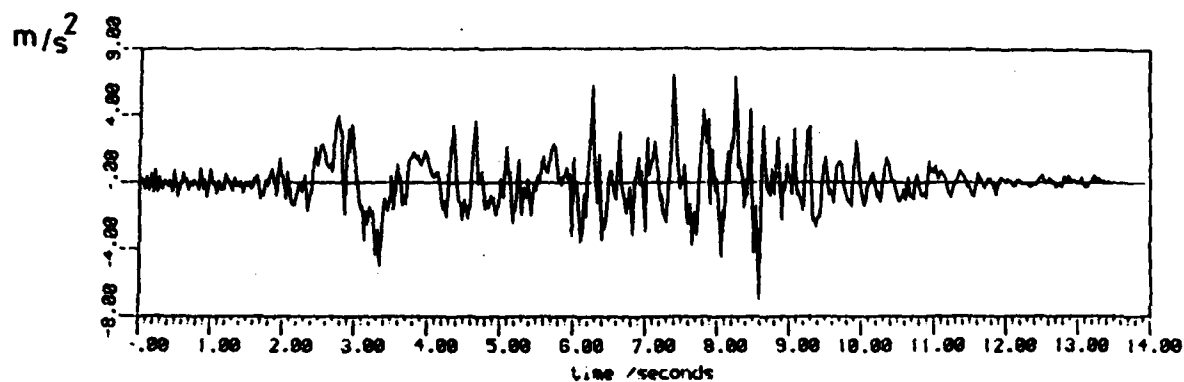


Fig. 1a S16E Component of San Fernando Earthquake( Pacoima Dam record) 1971.

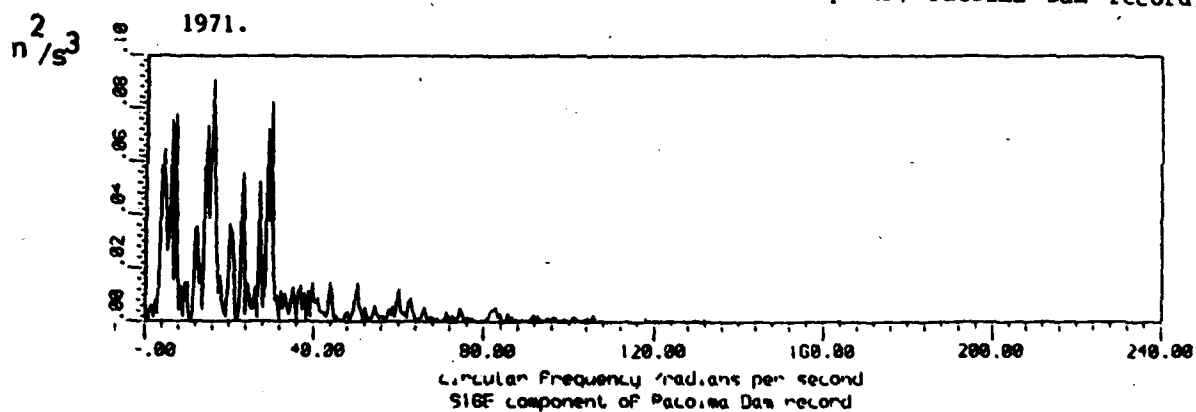


Fig. 1b Power Spectrum Density Function of Pacoima Dam record(S16E Component)

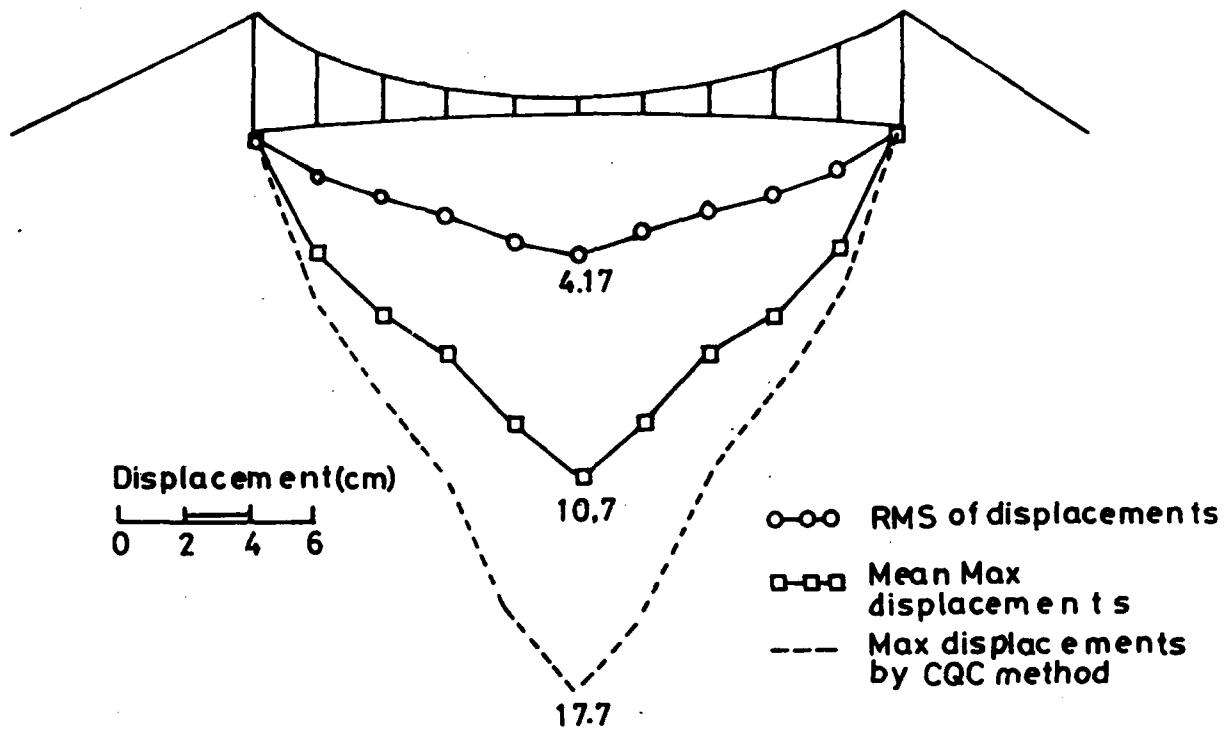


Fig2a Dolerw bridge; vertical displacements of the deck

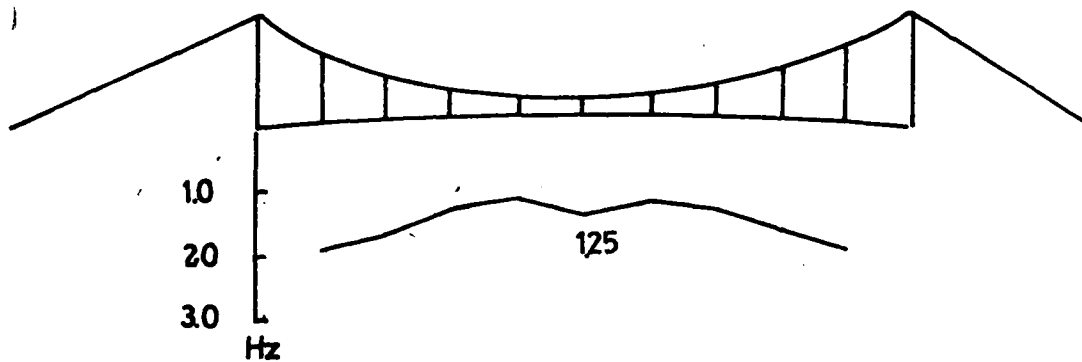


Fig2b Average frequencies of occurrence of vertical displacements of the deck

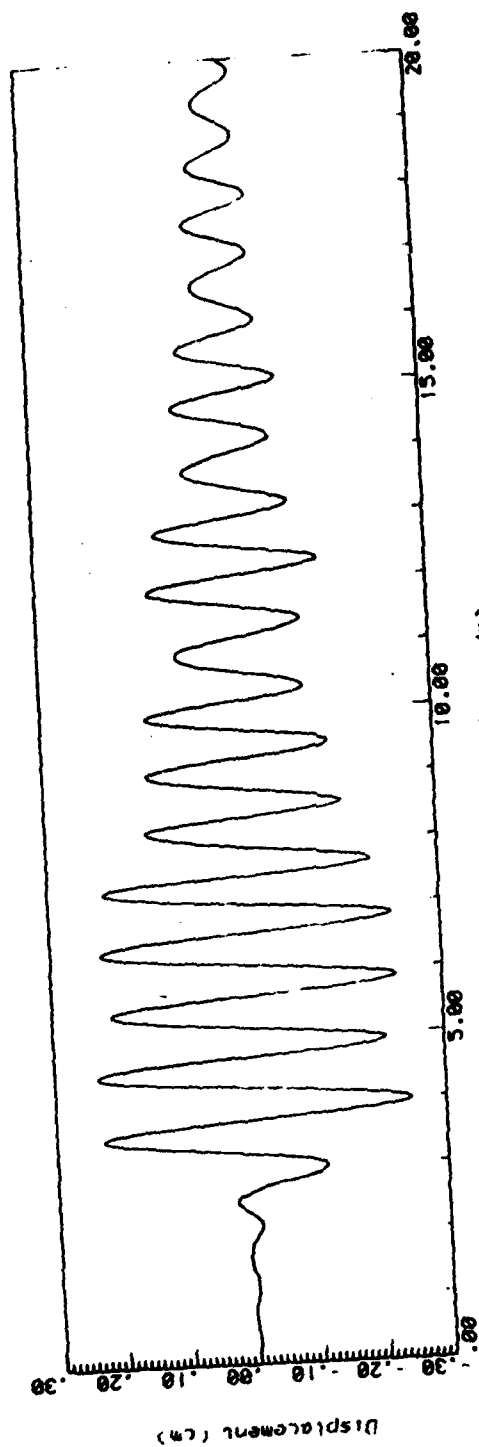


Fig. 3 Dolew Bridge; vertical displacement time-history at mid-span



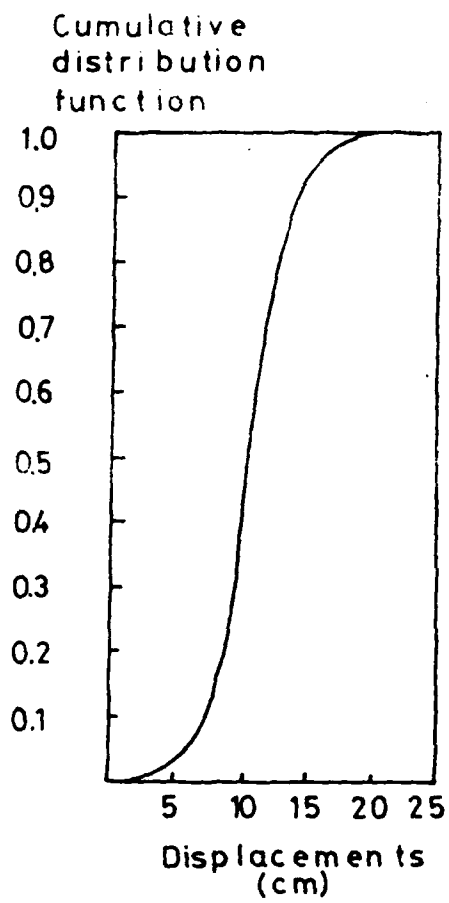


Fig. 4 Dolerw bridge; CDF of vertical displacements at mid-span

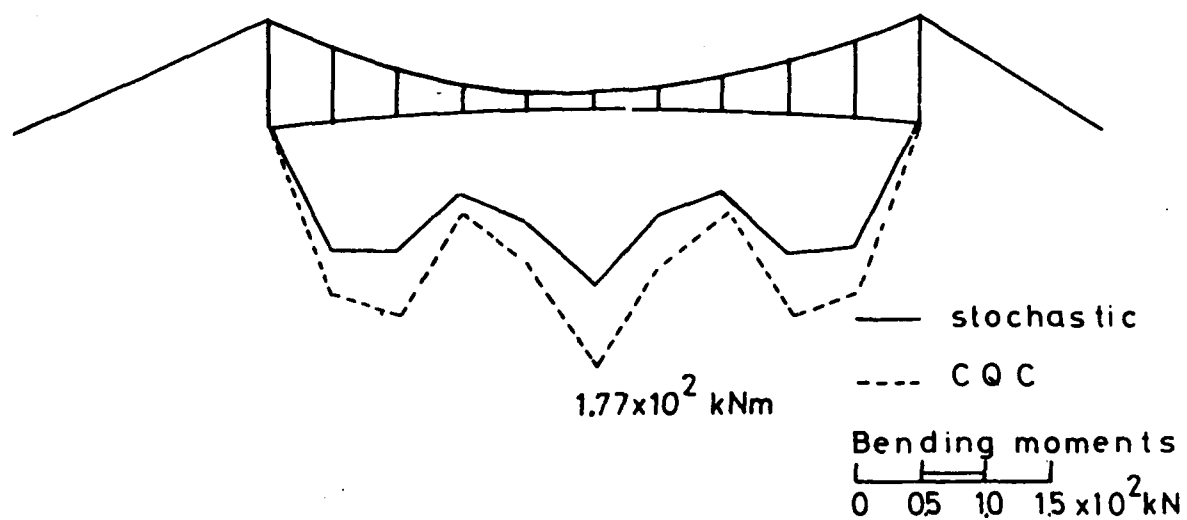


Fig.5a Deck bending moments

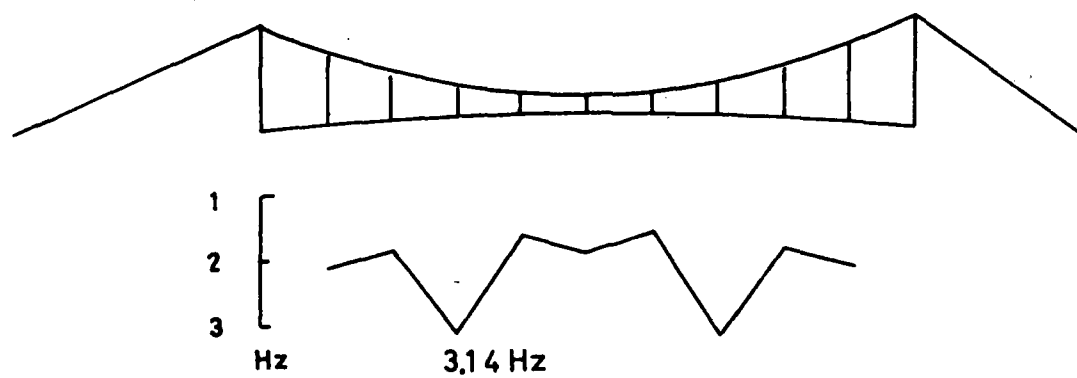


Fig.5b Frequency of occurrence of bending moment

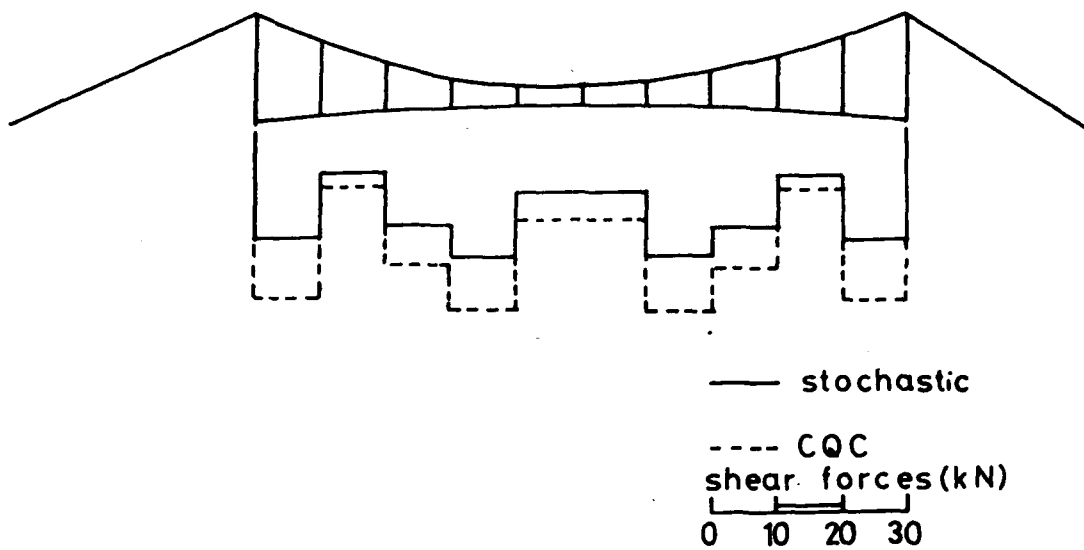


Fig.6a Deck shear forces

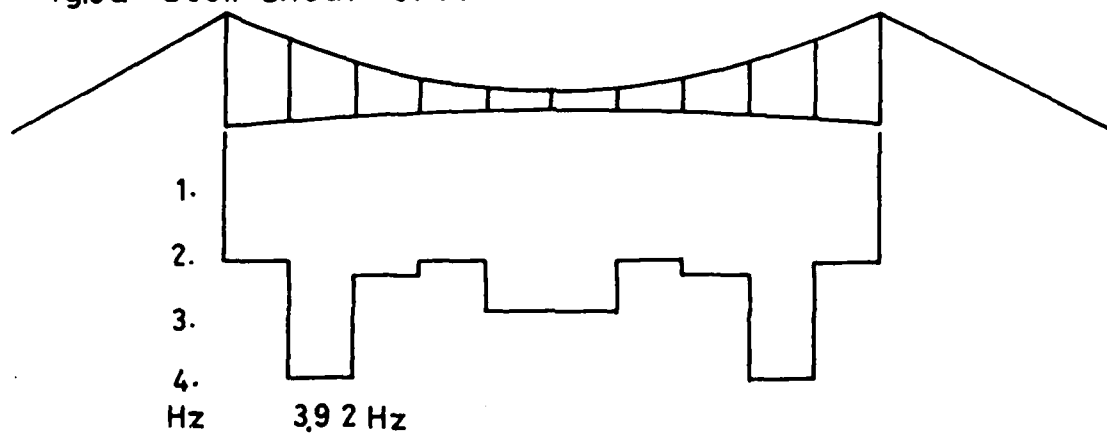


Fig 6b Average frequencies of occurrence of shear forces

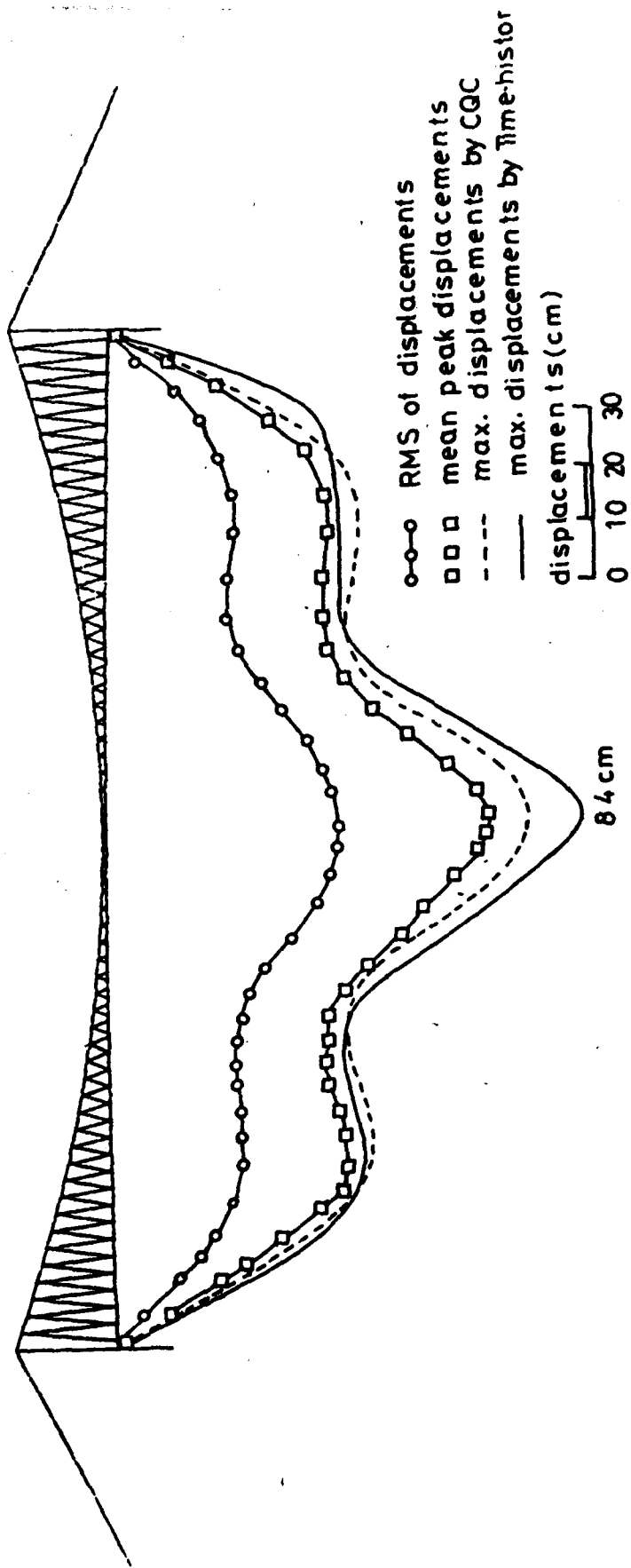


Fig 7a Bosphorus bridge; vertical displacements

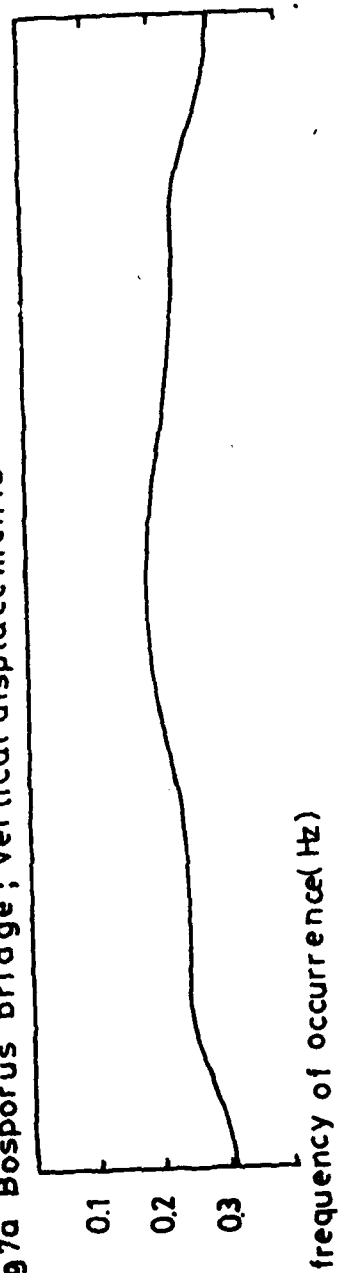


Fig 7b Average frequencies of occurrence of vertical displacements

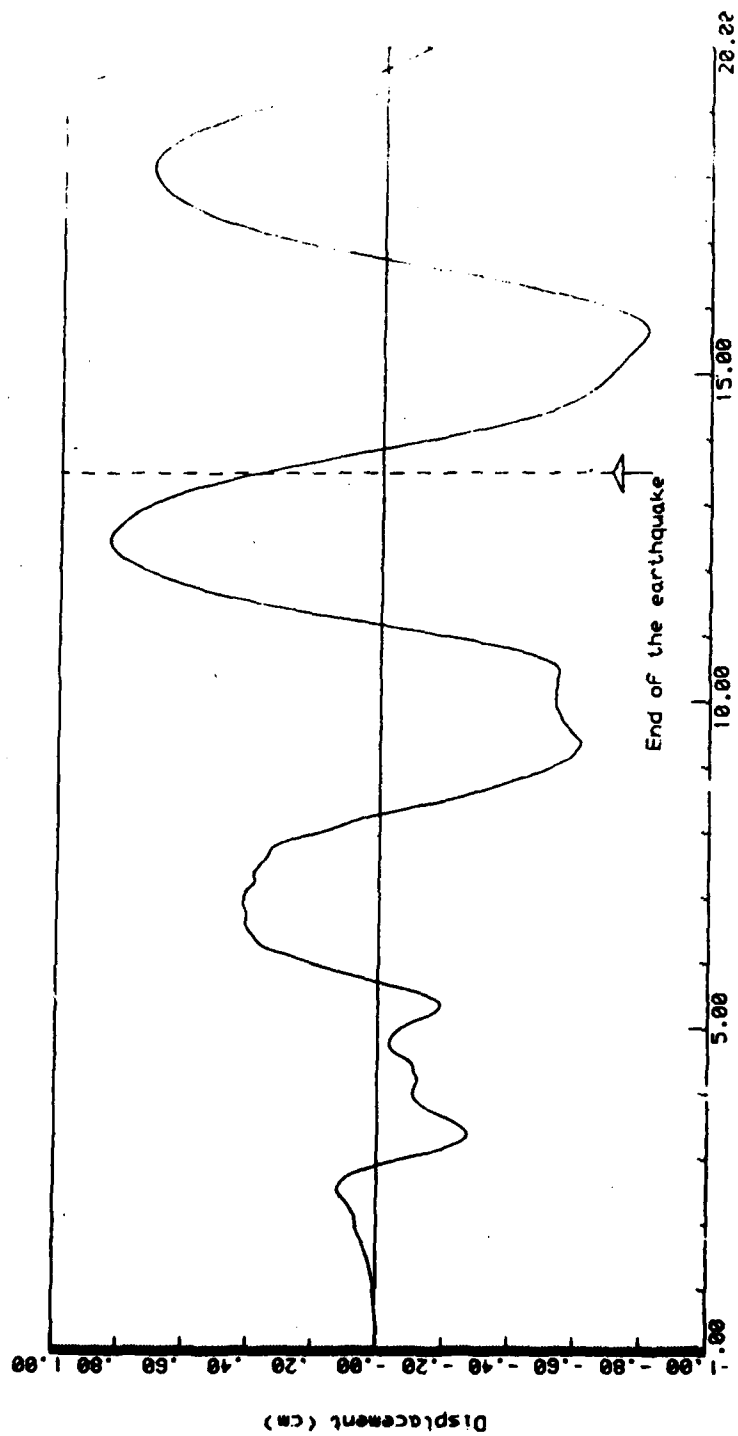


Fig. 8 Bosphorus Bridge; vertical displacement time-history at mid main-span

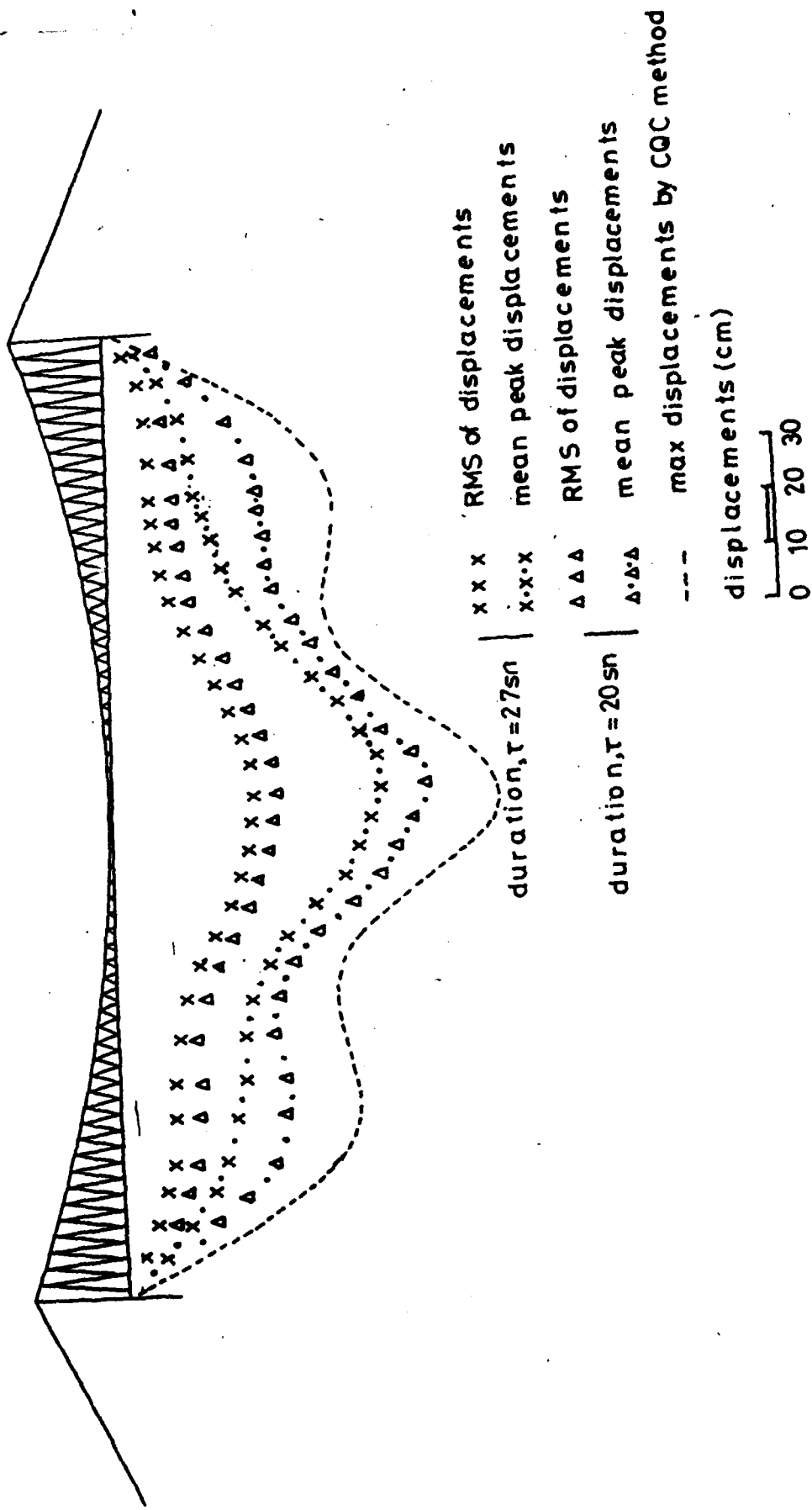


Fig.9- Bosphorus bridge; variation of vertical displacements of the deck

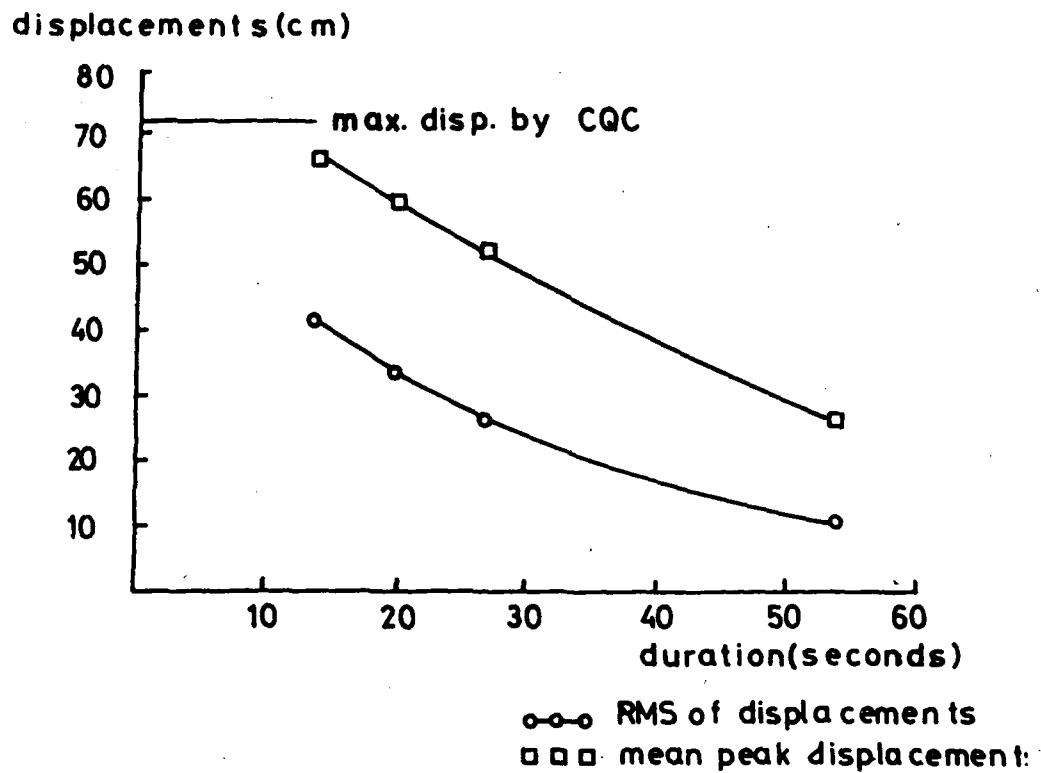


Fig 9b Bosphorus bridge; variation of displacements at the mid-span

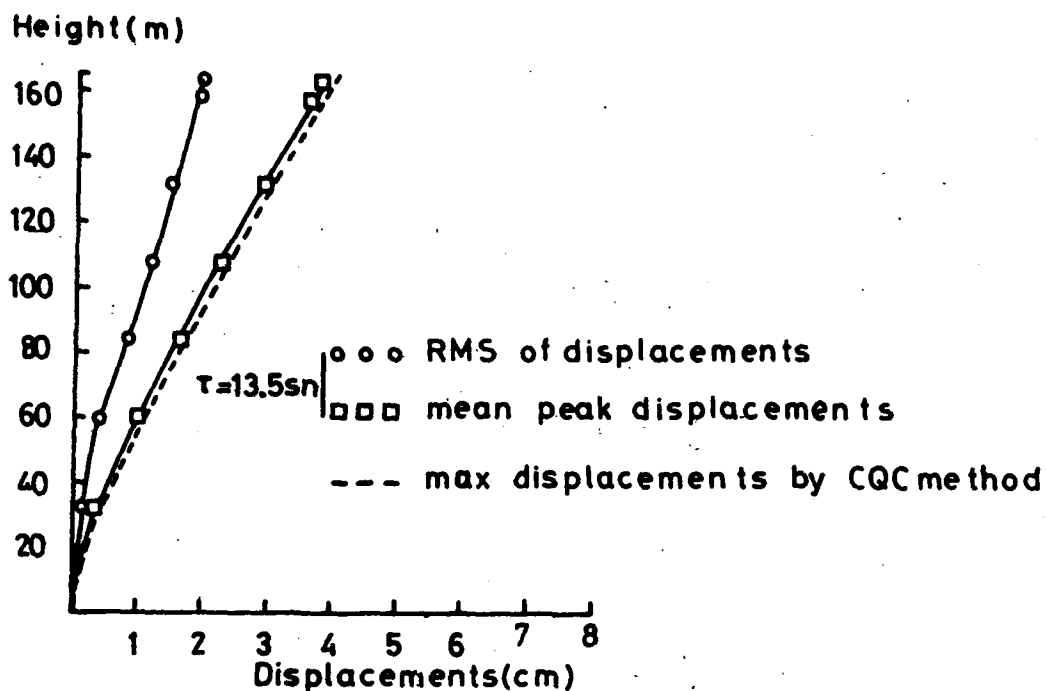


Fig.10 Bosphorus bridge; longitudinal displacements of the European tower.

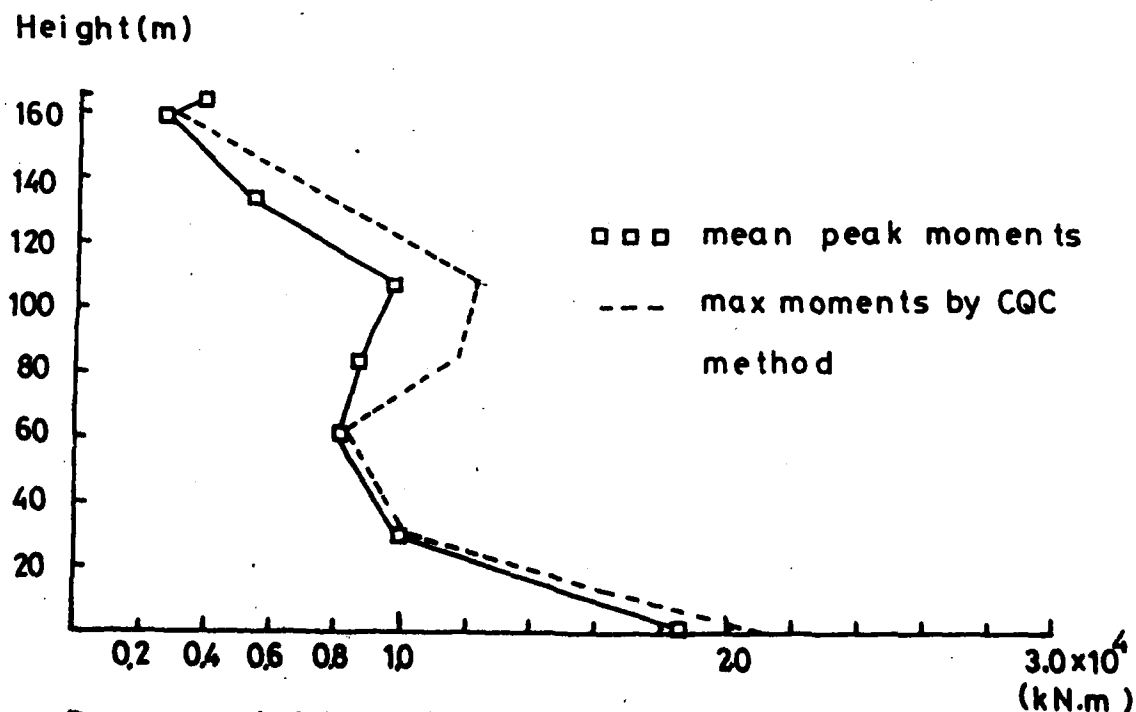


Fig.11 Bosphorus bridge; bending moments of the European tower



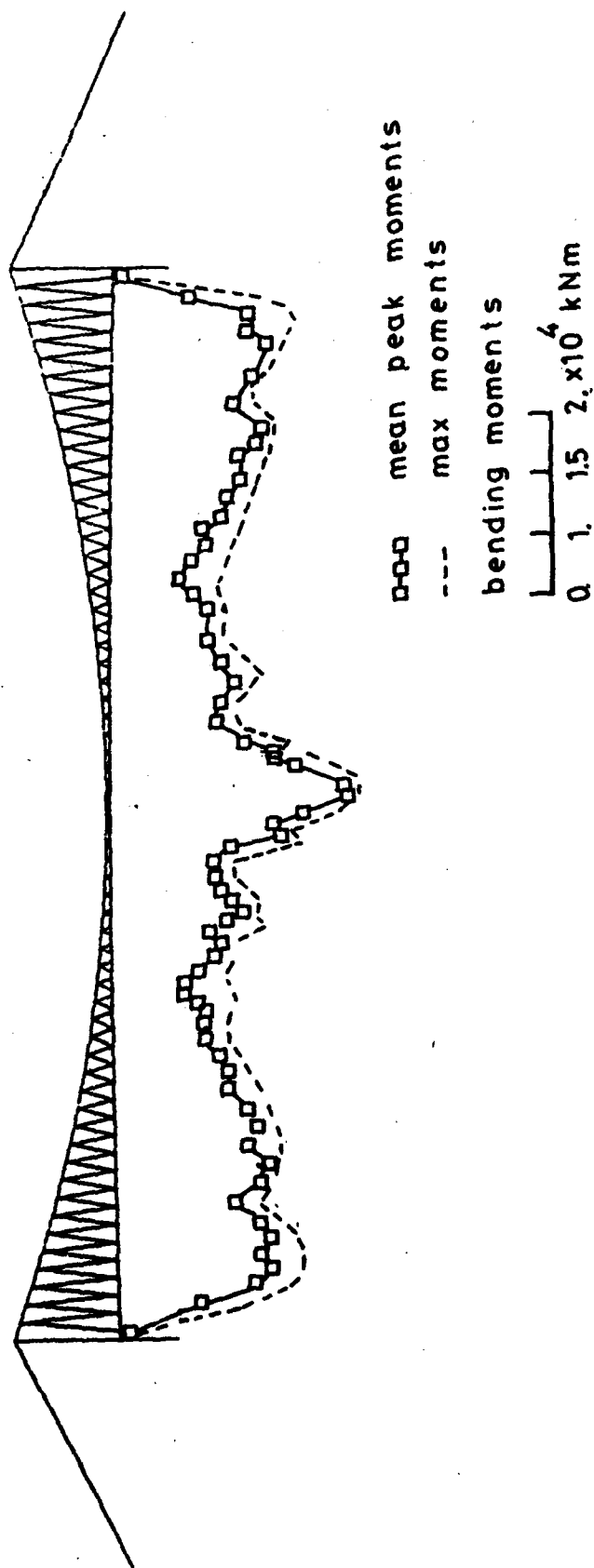


Fig.12 Bosphorus bridge; bending moments

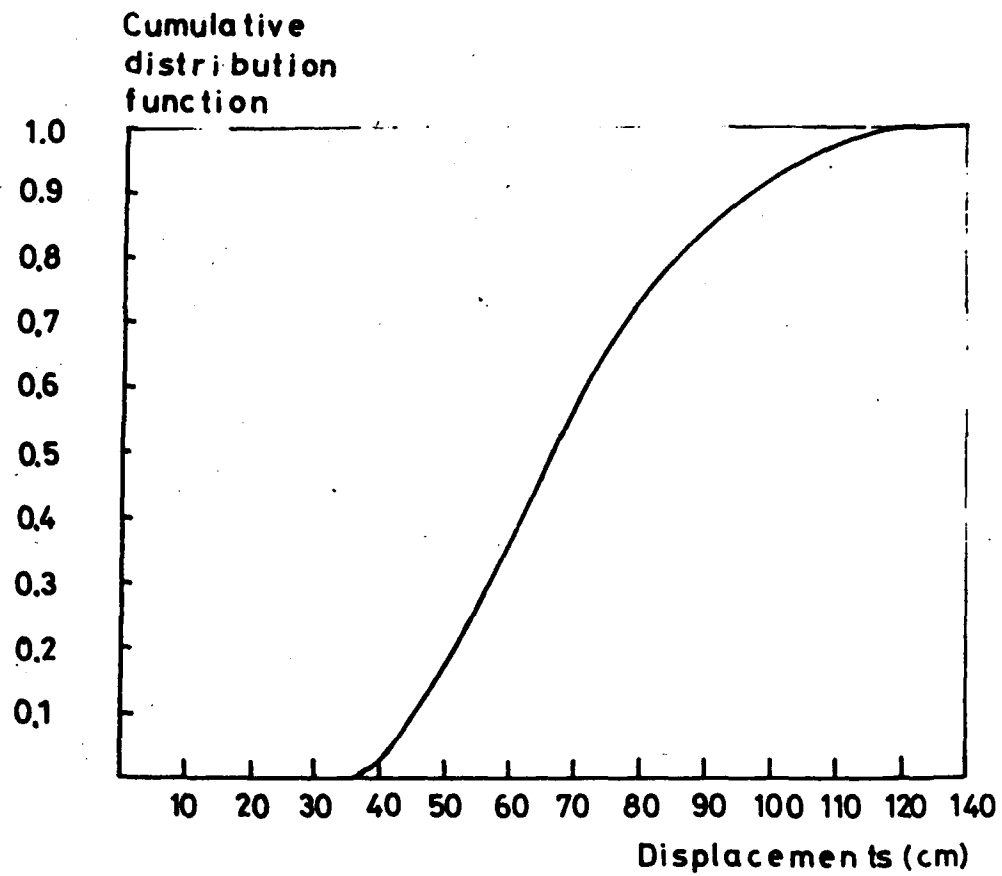


Fig.13 Bosphorus bridge; CDF of vertical displacements at mid-point of the deck.

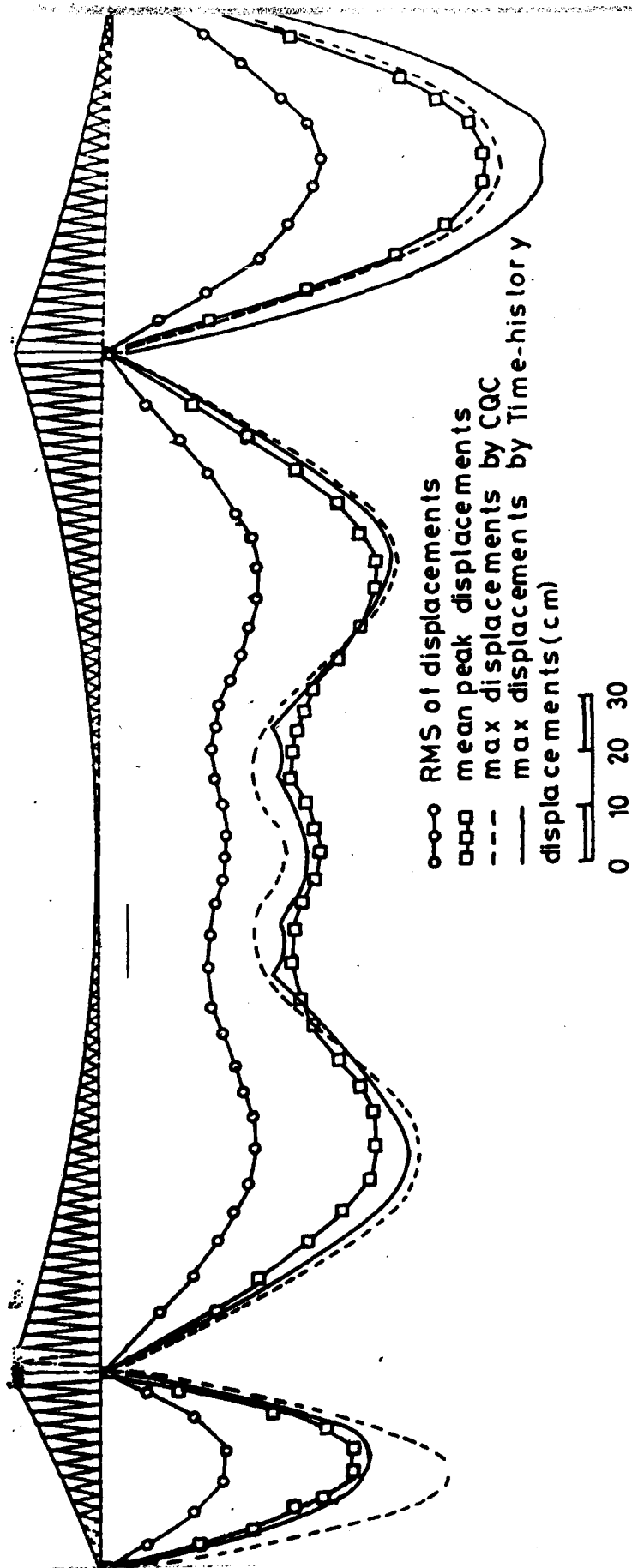


Fig 14a Humber bridge; vertical displacements of the deck

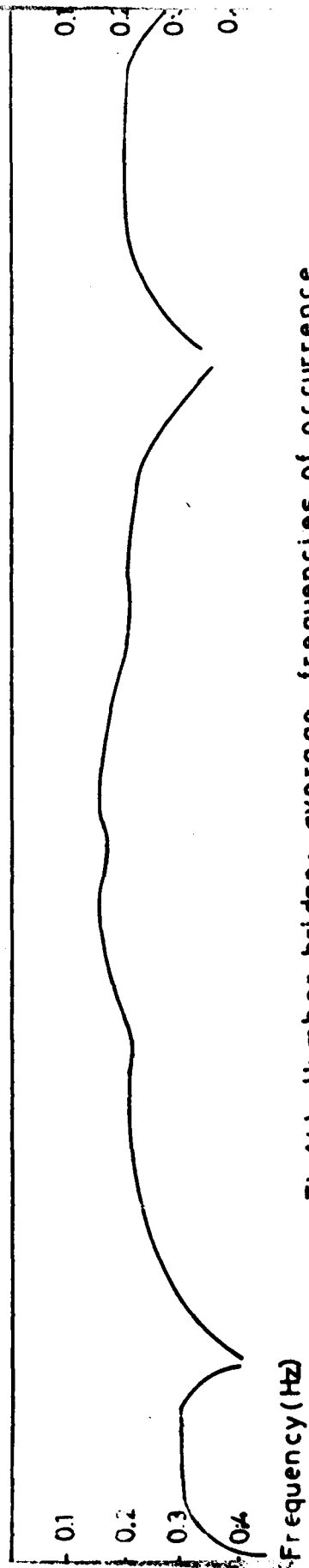


Fig 14b Humber bridge; average frequencies of occurrence

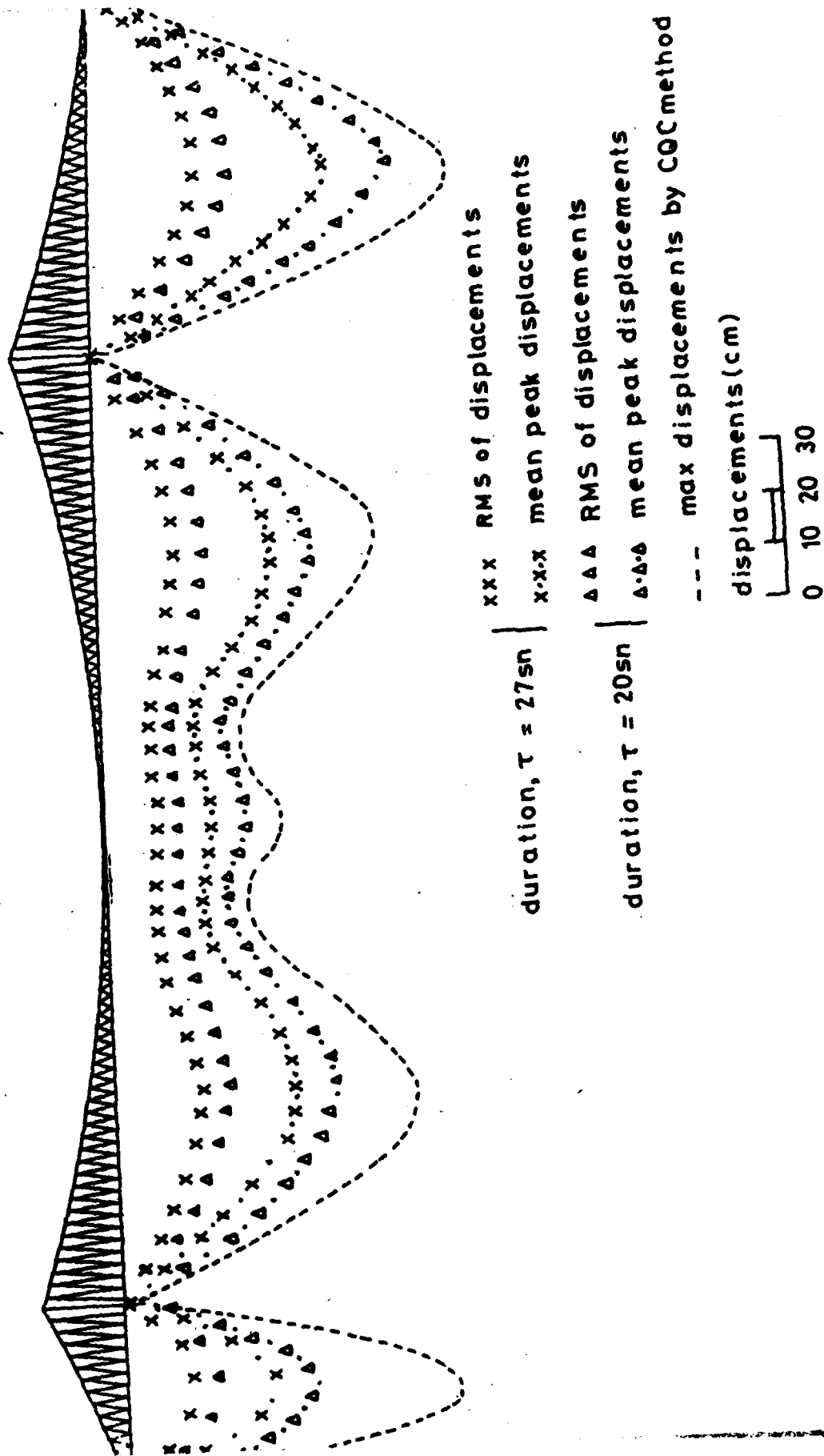


Fig.15 Humber bridge; variation of vertical displacements of the deck

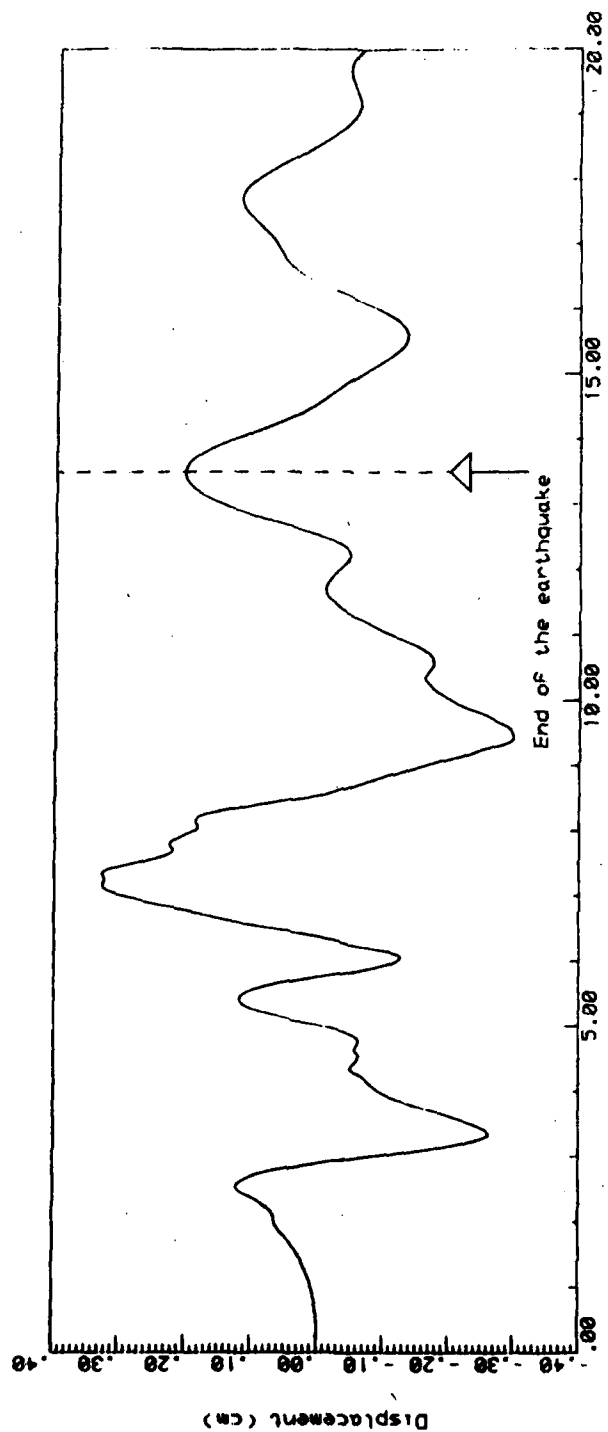


Fig. 16 Humber Bridge; vertical displacement time-history at mid main-span

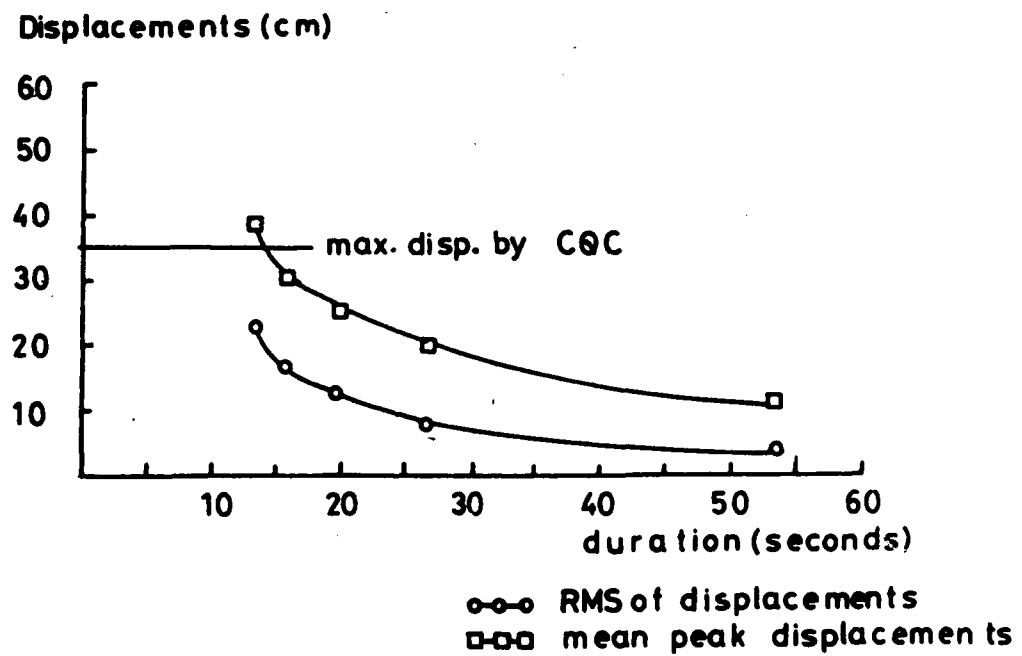


Fig.17 Humber bridge ; variation of displacements at mid main-span

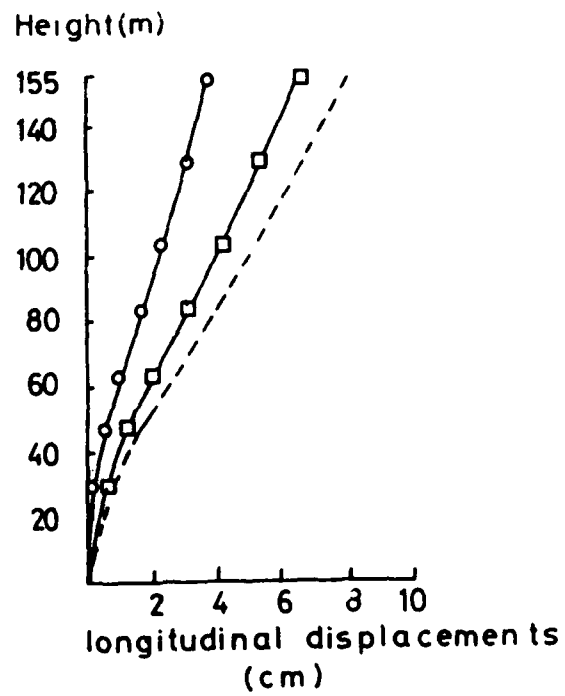


Fig.18 Humber bridge ; Hesse tower

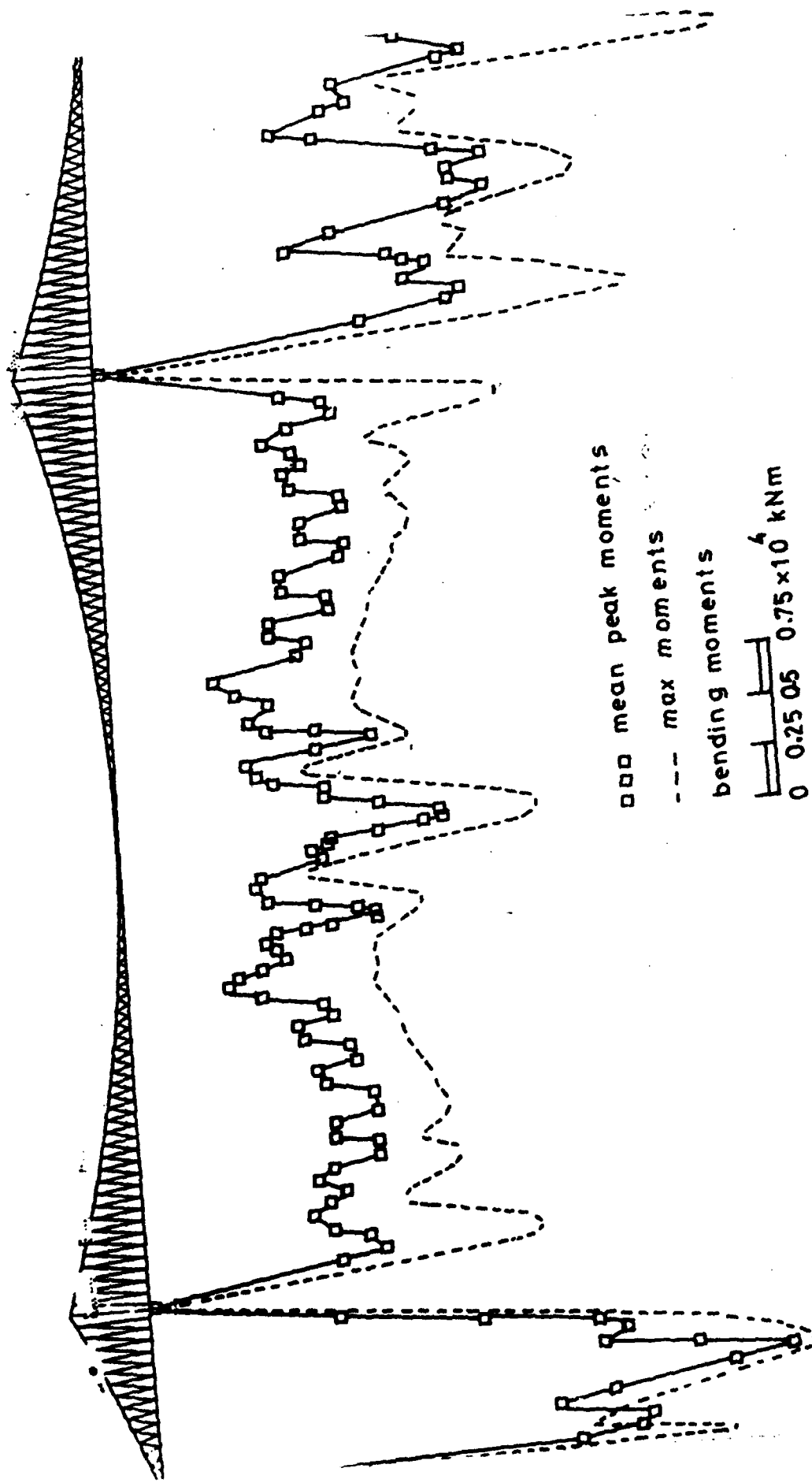
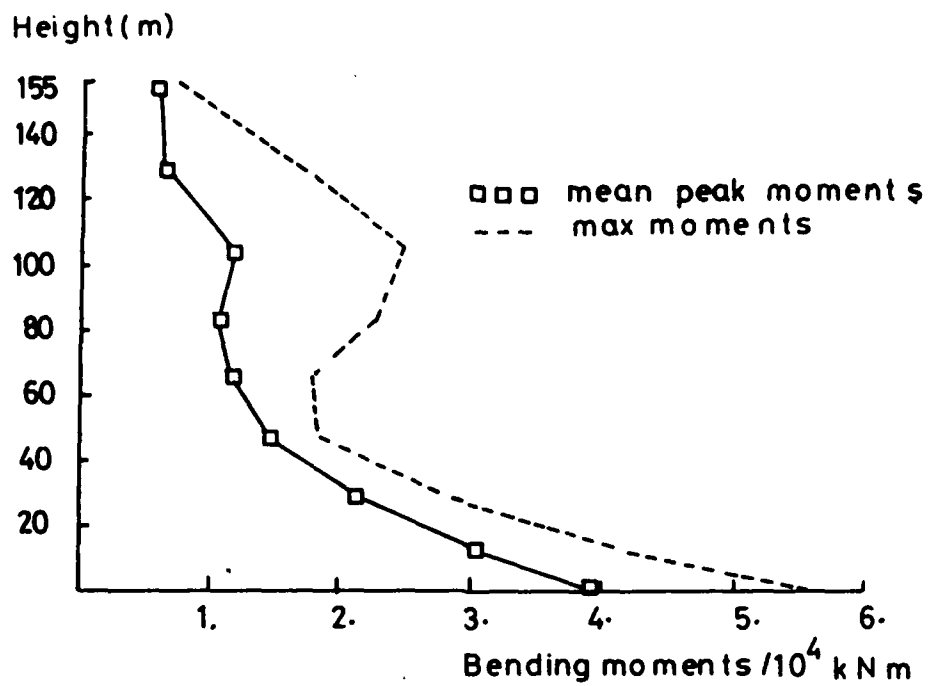
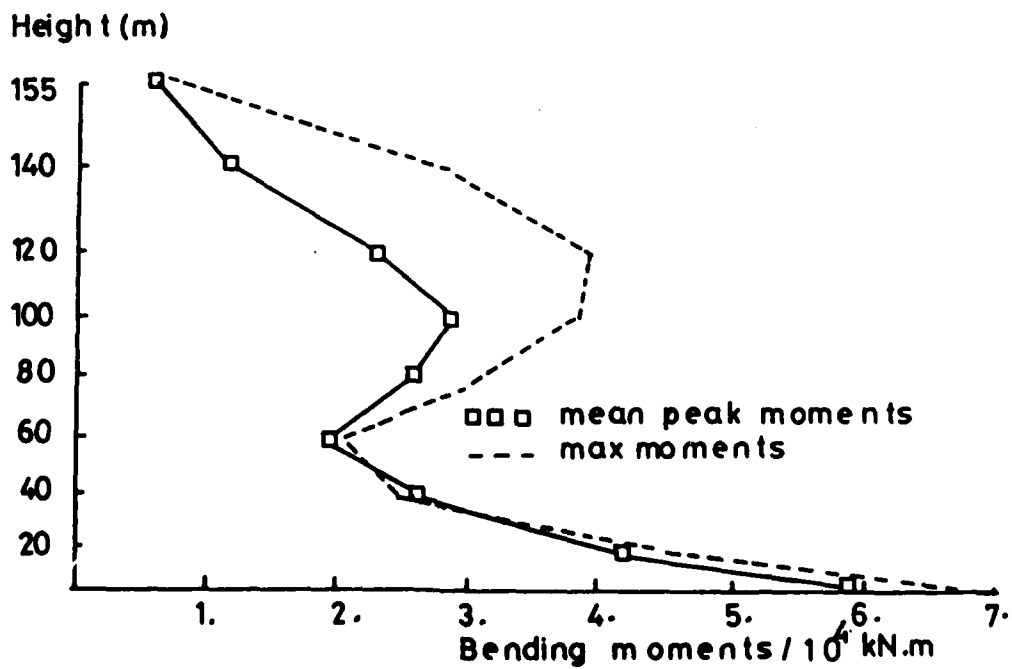


Fig. 19 Humber bridge; bending moments





a) Hessel tower



b) Barton tower

Fig.20 Humber bridge; bending moments of towers

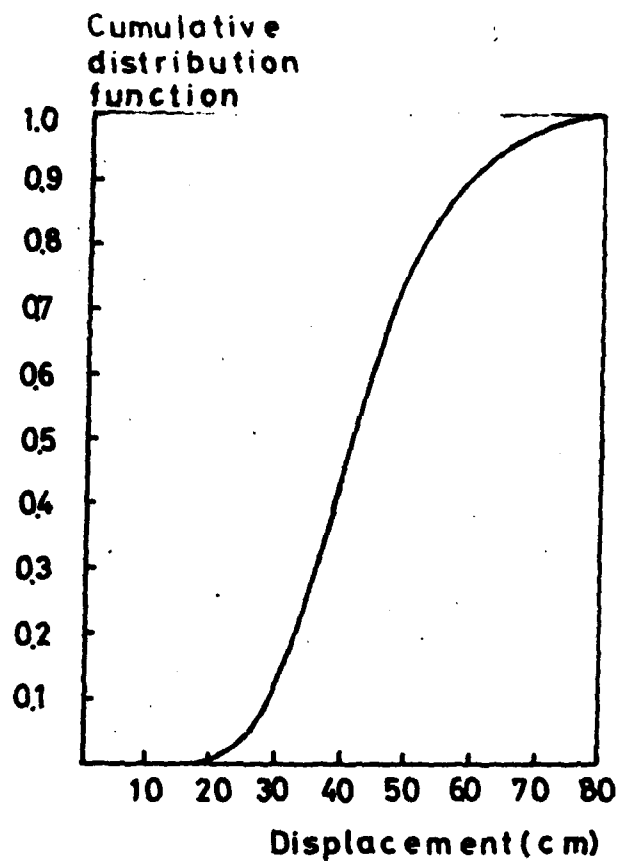
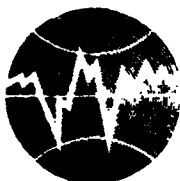


Fig.21 Humber bridge ; CDF of vertical displacements  
at mid-span of the main span



TURKISH NATIONAL COMMITTEE FOR  
EARTHQUAKE ENGINEERING

THIRTEENTH REGIONAL SEMINAR ON EARTHQUAKE ENGINEERING

September 14-24, 1987 - Istanbul - Turkey

A SIMPLE NUMERICAL  
METHOD FOR THE EARTHQUAKE  
RESPONSE OF BRICK MASONRY  
STRUCTURES

METİN AYDOĞAN

Assist.Prof.of Civil Engrg.,  
Civil Engineering Faculty  
Istanbul Technical University  
Maslak, Istanbul-Turkey

ERDOĞAN UZGİDER

Assoc.Prof.of Civil Engrg.,  
Civil Engineering Faculty  
Istanbul Technical University  
Maslak, Istanbul-Turkey

A SIMPLE NUMERICAL  
METHOD FOR THE EARTHQUAKE  
RESPONSE OF BRICK MASONRY  
STRUCTURES

METİN AYDOĞAN  
Assist. Prof. of Civil Engrg.,  
Civil Engineering Faculty  
Istanbul Technical University  
Maslak, Istanbul-Turkey

ERDOĞAN UZGİDER  
Assoc. Prof. of Civil Engrg.,  
Civil Engineering Faculty  
Istanbul Technical University  
Maslak, Istanbul-Turkey

**Abstract:** A simple numerical procedure depending on shear wave propagation concept is proposed in this study which can be employed to obtain earthquake response of brick masonry structures. In order to develop this numerical procedure, brick masonry structures are considered as consisted of series of shear walls with window or door openings. Then, each brick shear wall is considered as a layered elastic media and each layer corresponds to a vertical segment of the brick wall in which the shear stiffness is uniform and there is no strong geometric irregularities such as door and window openings.

In this study, dynamic response of brick masonry structures subject to ground motion is represented by simple wave propagation concept including soil structure effect.

## 1. INTRODUCTION

There have been appeared several numerical or experimental procedures in the literature [1,2,3, ect.] which have been suggested to determine the dynamic response of brick masonry structures subject to ground motions. Some of these studies employ a mathematical model suitable for the finite element representation.

In this study an efficient and very simple numerical procedure developed which is conveniently employed for computing the elastic dynamic response of brick masonry structures subject to ground motion, without any numerical instability problem.

This numerical method is based on simple wave propagation concept. From the point of view of this concept, dynamic response of brick wall structures are the results of imposition of arriving ground waves from the base and already circulating waves due to reflection from heterogeneities and outside boundaries.

Similar simple and efficient numerical method has been produced for the speedy determination of the elastic or elastoplastic dynamic response of orthogonal plane frames, including P-Δ and soil structure interaction effects by UZGIDER, E.A. and AYDOĞAN, M. [4.5]

## 2. MATHEMATICAL FORMULATION

Consider the relation between lateral force  $Q$  applied to the brick masonry wall model shown in Fig. I and corresponding top level lateral displacement  $v$ ,

$$Q = Sv \quad (1)$$

in which  $S$  is the lateral stiffness of brick wall.

For the brick wall model considered herein, the stiffness  $S$  can be given as,

$$S = \frac{GA}{1.2 h} \quad (2)$$

in which  $h$  is the height of the wall,  $G$  is shear modulus of the wall,  $A$  is the cross sectional area of the wall, and  $t$  is the wall thickness.

Actually, a typical load carrying wall of the brick wall structures can be divided into the vertical segments in which the lateral stiffness as well as the weights are uniform.

Then, considering equilibrium condition and equality of lateral displacements and employing the lateral stiffness expression given in Eq.2, one can easily calculate the lateral vertical segment stiffness of a typical brick wall as is shown in Fig.2. This lateral segment stiffness relates the relative lateral segment displacement to the total segment shear.

Now, lateral free vibration of the wall can conveniently be represented by the simple wave propagation concept. In a vertical segment of the wall in which the lateral wall stiffnesses and weights are uniform (Fig.2), the governing differential equations of shear-wave propagation through the structure can be derived.

Consider the  $j$ th uniform vertical segment of the wall shown in Fig.2., in which the mass of each segment is  $m_j$ , the segment stiffness is  $S_j$  and the height of each segment is  $h_j$ . Dynamic equilibrium equation of any brick wall slice (Fig.3) of the segment is

$$m_j \ddot{v} = \Delta Q \quad (3)$$

then the following approximation is reasonable,

$$\Delta v = \frac{\partial v}{\partial x} h_j \quad \Delta Q = \frac{\partial Q}{\partial x} h_j \quad (4)$$

Introducing the first of these into the force deformation relationship given in Eq .1 leads to

$$\frac{\partial v}{\partial x} h_j = \frac{1}{S_j} Q \quad (5)$$

while substituting the second into the dynamic equilibrium equation given in Eq.3

$$m_j \ddot{v} = \frac{\partial Q}{\partial x} h_j \quad (6)$$

Then differentiating Eq.5 with respect to  $x$  and substituting it into the Eq.6, leads to the equation of the shearing vibration of the segment

$$\frac{\partial^2 v}{\partial t^2} = o_j^2 \frac{\partial^2 v}{\partial x^2} \quad (7)$$

in which

$$c_j = h_j \sqrt{S_j / m_j} \quad (8)$$

represents the velocity of shear wave propagation through the  $j$ th uniform vertical segment of the wall.

Consider, for example, the juncture between  $i$ th and  $(i+1)$ th uniform segments shown in Fig.2 and Fig.4. Since, the rigidity or mass values of these two consecutive uniform segments of wall are different from each other, the shear wave velocity defined in Eq.8 are also different for each uniform segment as denoted in Fig.4. As was shown in Eq.9 the general solution of the one dimensional wave equation given in Eq.6 which represents dynamic behaviour of the uniform wall (Fig.1) consists of two arbitrary functions

$$v = \phi(ct+x-h) + \phi(ct-x+h) \quad (9)$$

and shows that the vibration of the wall is produced by two pulses each moving with velocity  $c$  one from the base to the top and the other from the top to the base as is demonstrated in Fig.5

A motion of the ground which will give rise to a motion defined by Eq.9 is obtained by putting  $x=0$  in the above equation. Denoting the motion of the ground by  $v=F(t)$  we have the equation

$$F(t) = \phi(ct-h) + \phi(ct+h) \quad (10)$$

In the case of the ground is fixed

$$\phi(ct-h) = -\phi(ct+h) \quad (10a)$$

Eqs.9,10 and 10a shows that the upwardly propagating waves are reflected at the top of the frame with same sign, on the other hand downwardly propagating wave are reflected at the base with opposite sign. This phenomena are demonstrated in Fig.5. On the other hand upwardly or downwardly propagating waves reflect or refract at the boundaries of uniform segments of the wall due to the different stiffness, mass or shear wave velocities as is shown in Fig.4. This reflection or refraction coefficients can be defined by employing the boundary conditions between to consecutive uniform segments. If upwardly approaching wave to the juncture or boundary between

1<sup>th</sup> and (i+1)<sup>th</sup> uniform segments, the reflected wave and the refracted wave at this boundary are denoted by  $V_i$ ,  $V_{r,i}$  and  $V_{r,i+1}$  respectively. These coefficients are given as below;

$$V_{r,i+1} = \frac{2\alpha_{i,i+1}}{1+\alpha_{i,i+1}} V_i \quad (11)$$

$$V_{r,i} = \frac{\alpha_{i,i+1}-1}{\alpha_{i,i+1}+1} V_i \quad (12)$$

Where

$$\alpha_{i,i+1} = \frac{C_{i+1} S_i h_i}{C_i S_{i+1} h_{i+1}} \quad (13)$$

$$\alpha_{i+1,i} = \frac{1}{\alpha_{i,i+1}} \quad (14)$$

In addition, at the boundary there is following relation between incident or upwardly approaching wave and reflected or refracted waves:

$$V_{r,i+1} = V_i + V_{r,i} \quad (15)$$

### 3. SCHEME OF THE NUMERICAL PROCEDURE

A ground motion which may be defined with arbitrary function, propagates along the structure as is demonstrated in Fig.5. In x,t coordinate system the path of this propagation, reflection or refraction can be represented by a line with slope equal to propagation velocity c. Depending on the time increment, these lines constitute a mesh as is shown in Fig.6. This mesh contains series of node points at the uniform vertical segment boundary levels. At these node points, propagating, reflected or refracted waves cross each other. Then current displacement values at corresponding level can be calculated by employing Eq.15. At each node point there are upwardly coming and reflected parts as is seen in (Fig.7).



Then for each  $\Delta t$  increment, by employing the given ground displacements and following the successive pathes as is denoted by I, II, III, IV and VII in Fig.7., the proposed numerical procedure can be applied in following steps:

- i) Select appropriate  $\Delta t$  time increment consistent with the given ground displacement data.
- ii) Calculate reflection or refraction coefficients for upwardly or downwardly incident wave ordinates for each boundary level and store in memory.
- iii) Start with the far left node point on the ground level and consider the ground displacement value corresponding to the time represented by this node point.
- iv) Following the corresponding characteristic path for the node point considered in step (3) and by employing Eqs. 11,12,13,14 and 15 calculate the current displacement and refracted, reflected part of the incident wave ordinates at the node points on the considered propagation path. These refracted and reflected waves are considered as an upwardly and downwardly incident waves for the nodes crossed by their propagation rays at the boundary levels below or above the considered boundary level respectively.
- v) Then store the reflected and refracted part of the incident wave ordinates calculated for a node point according to the step (4), on appropriate memory locations as an upwardly or downwardly incident waves for the corresponding node points.

#### 4. SOIL STRUCTURE INTERACTION

One of the phenomena with great importance which influence the behaviour of a structure during a ground motion is the soil-structure interaction.

In the analysis of a brick masonry building structure, by considering the soil structure interaction, and employing the numerical procedure proposed in this study, the structure model on a homogenous soil layer under which there is rigid rock (Fig.8) is taken into account. In this model soil deposit or layer between the foundation base and base and base rock, is considered as an additional uniform

segment. The foundation base is considered rigid, rests on the ground and there are no slidings at the foundation-ground interface during the ground motion. However, the proposed method is not able to take into account the effect of the foundation base rotation around the horizontal axis on the soil layer.

### 5. NUMERICAL APPLICATIONS

The numerical procedure proposed in this study has been programmed in Fortran IV language for IBM 4341 type computer and in order to verify the validity of the procedure three numerical results have been produced.

In the first application, single story brick masonry building has been considered. Its plan and elevation is shown in Fig. 9. In all numerical applications, the brick wall thickness used is  $t=24$  cm, and the ratio  $\alpha = \frac{G}{E}$  is assumed as equal to 0.4, modulus of elasticity considered is  $E=120.000 \text{ kg/cm}^2$ . [6]

Then taking into account the all brick walls in the direction of the ground motion and defining the uniform segments for each of them with equal heights, total uniform segment properties were calculated and summarized in Table 1. (Fig.10)

TABLE 1- Uniform Segment Properties

Uniform Segment No:	Height $h_1$ (m)	Mass $m_1$ (tsn <sup>2</sup> /m)	Stiffness $S_1$ (t/m)	Wave Velocity (m/sn)
1	2.20	5.6065	1087893.4	969.10
2	0.60	6.9317	4940535.9	506.55

Depending on this properties, the reflection and refraction coefficients were calculated and given in Table 2.

TABLE 2- Reflection and Refraction Coefficients

Boundary	Reflection Coefficients		Refraction Coefficients	
	Upwardly approaching wave	Downwardly approaching wave.	Upwardly approaching wave	Downwardly approaching wave
1-2	0.40645088	-0.40645088	0.59354912	1.4064509

By employing this data and taking into account the ground motion

$$y_g = 0.01 \sin(4\pi t) \quad (m)$$

acting in the direction shown in Fig. 9a. Dynamic lateral top level response in the considered direction was computed and plotted in Fig.11.

These numerical results can be verified by long hand calculations employing the mode superposition method with selected ground displacements and the corresponding initial conditions as given below

$$v=0, \quad \dot{v}=-0.01\pi \ 4\pi(m/sec.)$$

As a second application, same structural system and ground motion was considered in the first application with 10 m thick single layer hard clay soil deposits between the foundation base and base rock level. Hard clay soil characteristics considered in this application are as follows:

$$\text{Shear wave velocity} = 211 \text{ m/sec}$$

$$\text{Shear Modulus} = 927 \text{ kN/m}^2$$

Dynamic lateral top level response in the ground motion direction was computed and plotted in Fig.12. Finally, the brick wall structures which is composed of two story, each of which has identical properties with the single story building considered in the first application, was subjected to the eight seconds of the N-S component of El-Centro Earthquake ground motion record, between 8 and 16 seconds, and top level response in the ground motion direction was computed and plotted for the first four seconds in Fig.13.

#### ACKNOWLEDGEMENT

The use of the computer facilities at Istanbul Technical University is gratefully acknowledged.

#### REFERENCES

- 1- ÇILLI, F., "Yığma Yapıların Yatay Yüklere Göre Hesabı" Deprem Araştırma Enstitüsü Bülteni, Sayı 22, Temmuz 1978
- 2- MENGI, Y., Mc NIVEN, H., "A Mathematical Model of Masonry for Predicting its Linear Seismic Characteristics", Report No EERC 79/04, University of California, Berkeley 1979.
- 3- YARAR, R., "Behavior of Masonry Brick Walls under Earthquake Loading", 5th Regional Seminar on Earthquake Engrg., Udine (Italy) 1977
- 4- UZGIDER, E., AYDOĞAN, M., "Wave Propagation Approximation for Dynamic Response of Framed Structures Subject to Ground Motion" Regional Seminar on Earthquake Engineering, Istanbul, 1986
- 5- UZGIDER, E., AYDOĞAN, M., "Simple and Efficient Method for the Dynamic Response of 2D Frames Subject to Ground Motions" 8th European Conference on Earthquake Eng. Lisbon (Portugal), 1986, V.3
- 6- BAYÜLKE, N., "Yığma Yapılar", Deprem Araştırma Enstitüsü, Ankara, 1980

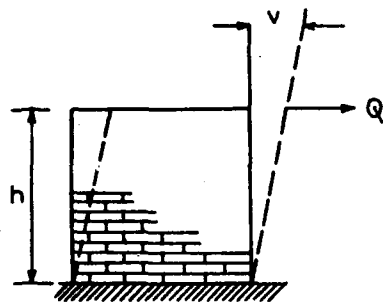


Fig. 1- Brick Masonary Wall

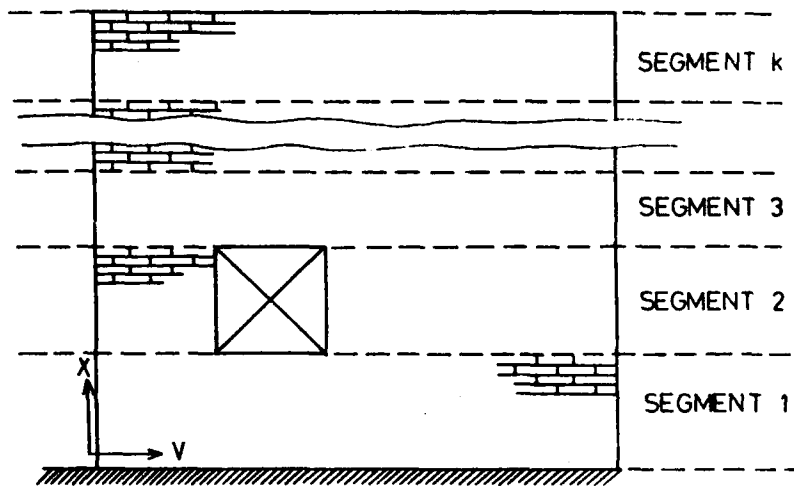


Fig. 2- A Typical Brick Wall

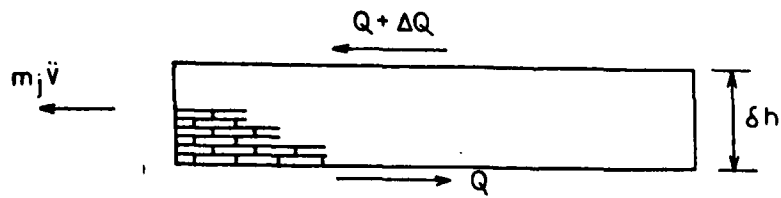
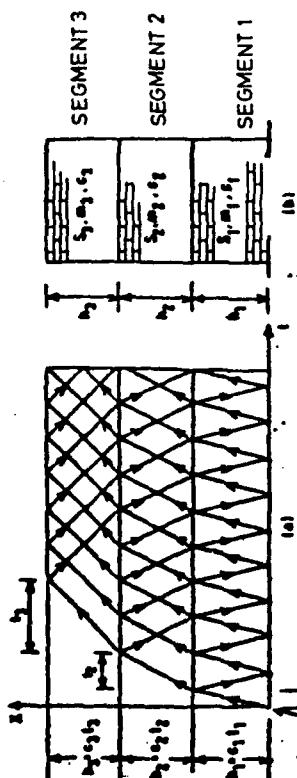
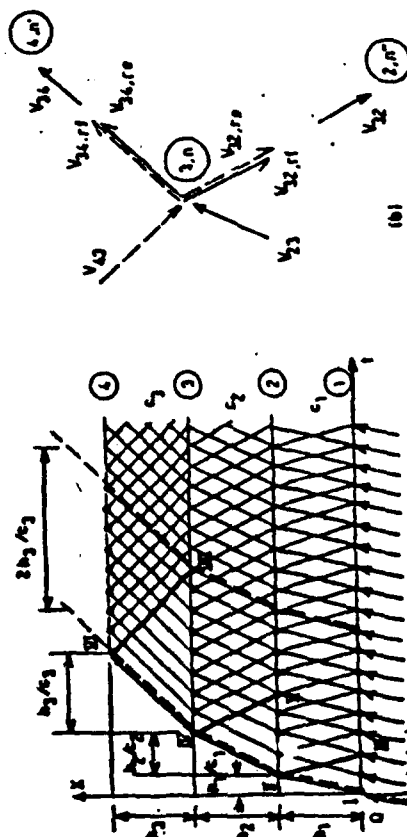


Fig. 3- A Brick Wall Slice



**Figure 6**



**Figure 5**

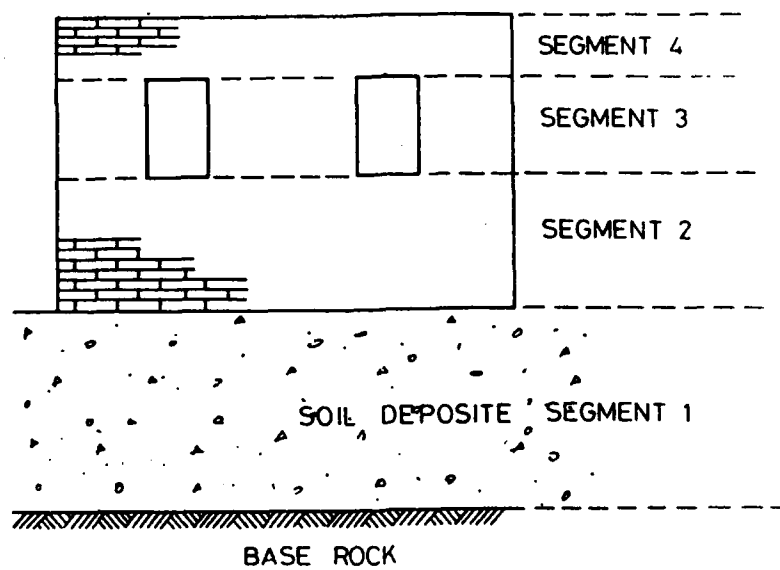


Fig. 8 Soil-Structure Interaction Model

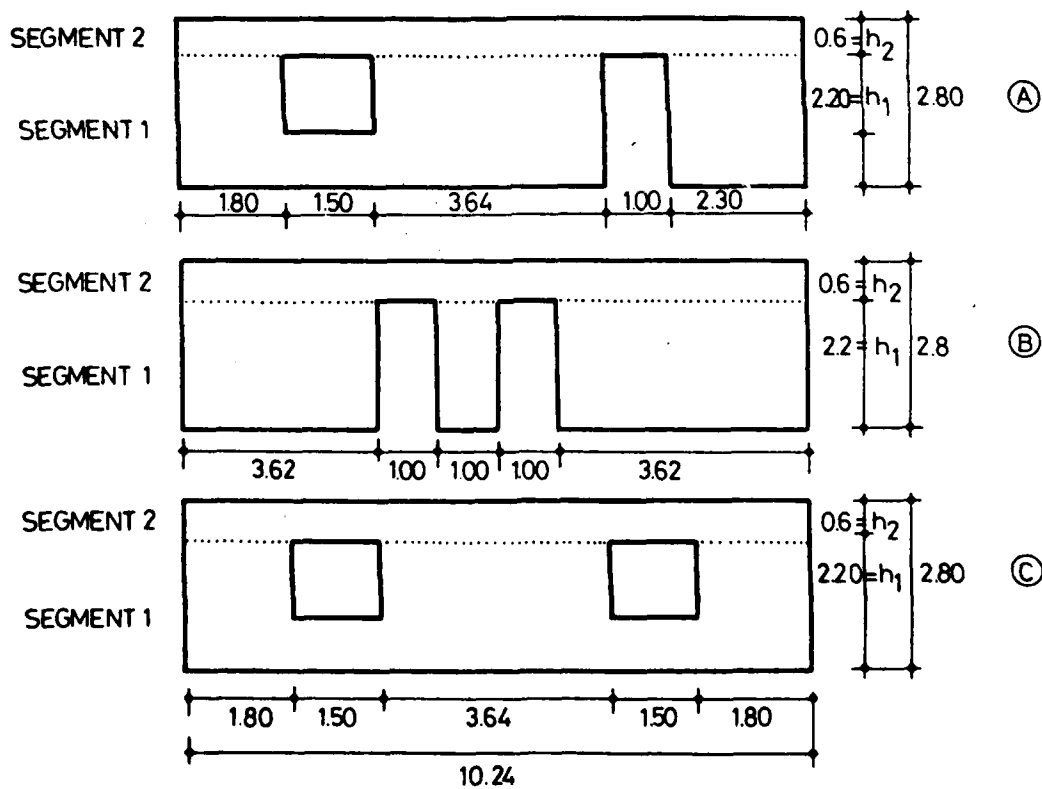


Fig. 10- Vertical Uniform Segments of the Brick Walls.

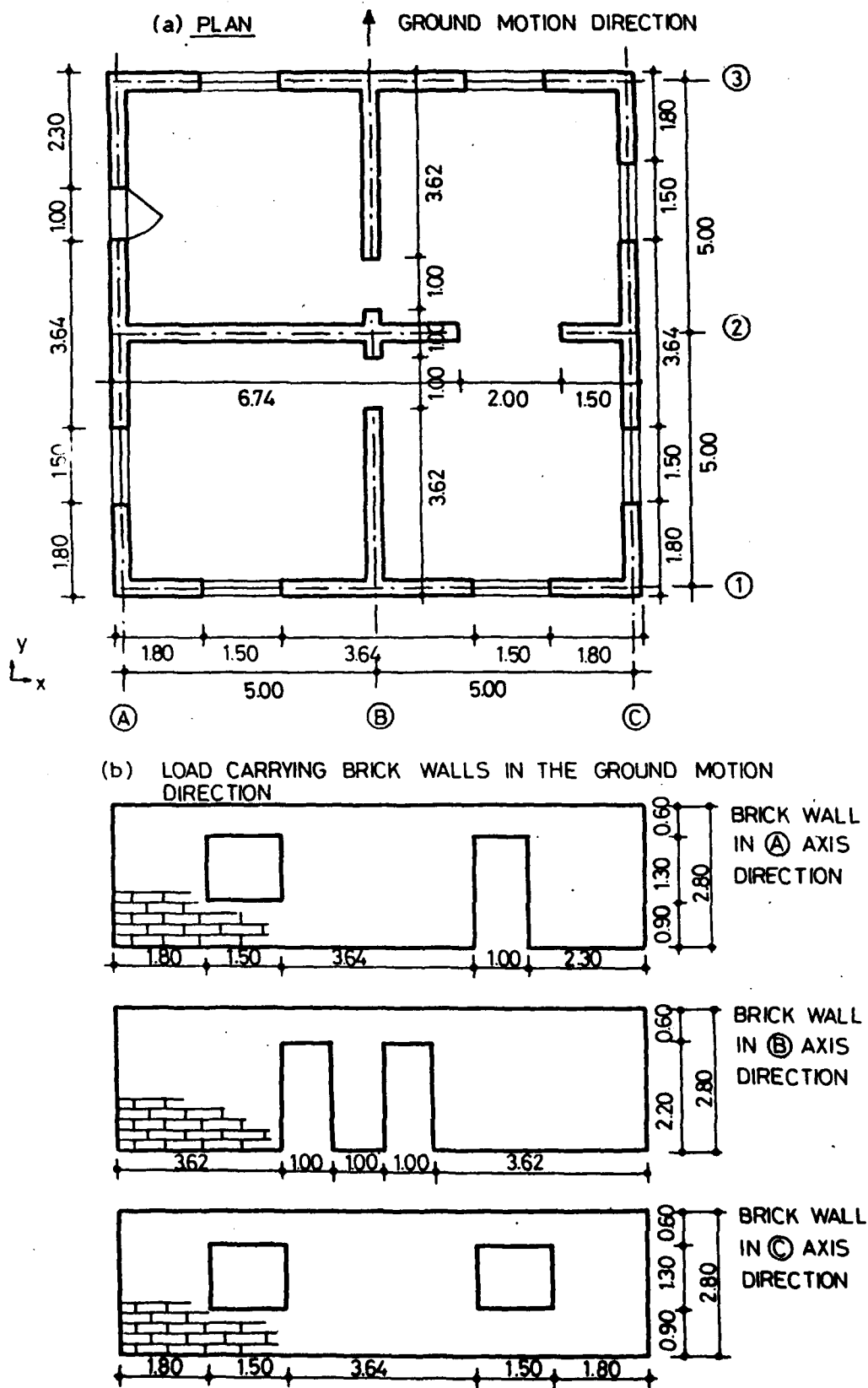


Fig. 9- Plan and Elevation of the Single Story Building



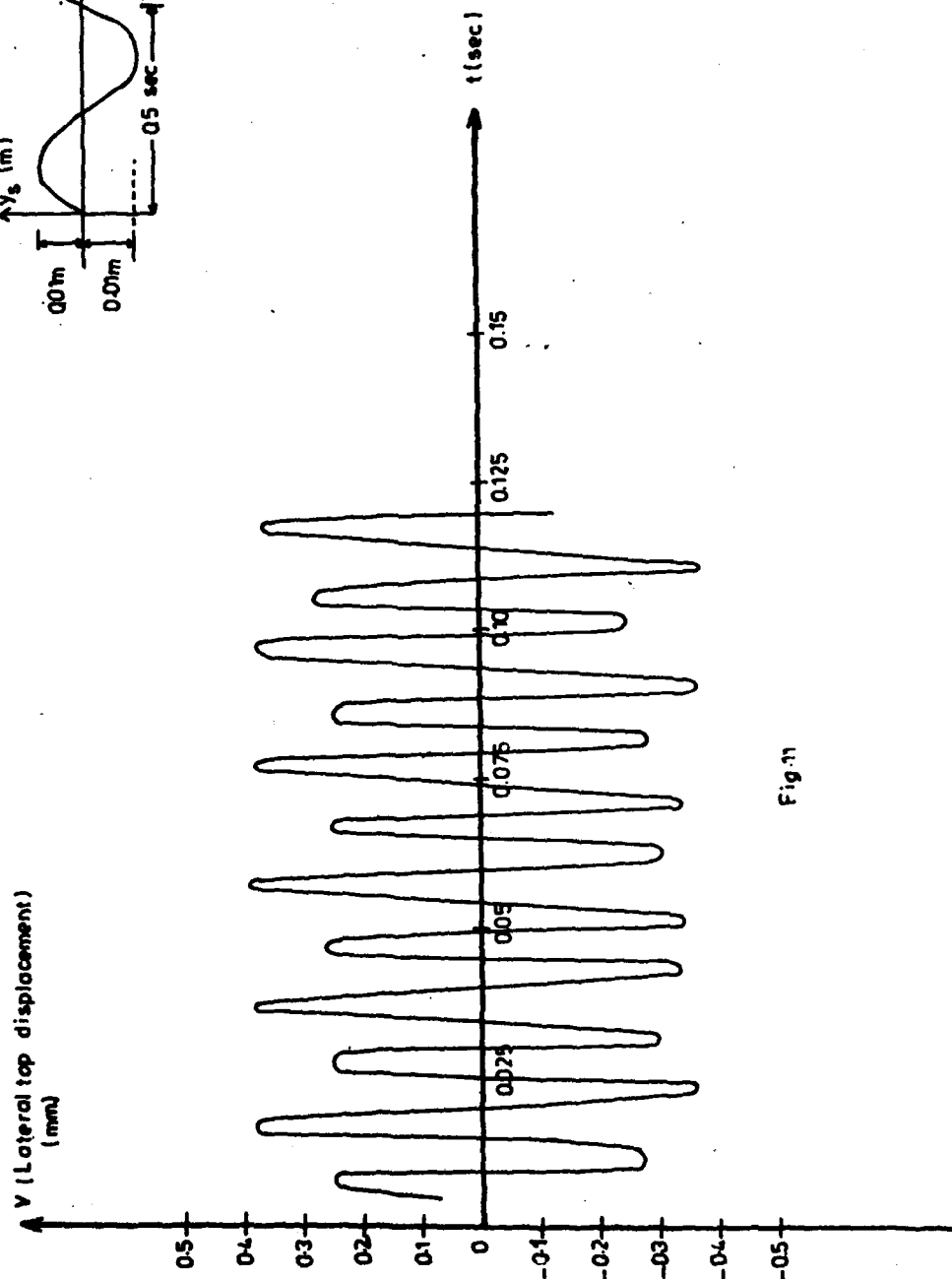
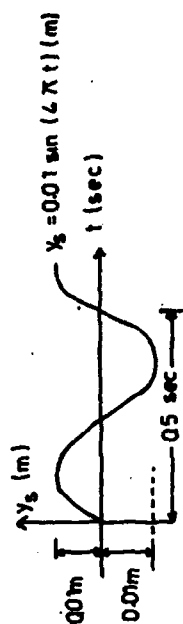


Fig. 11

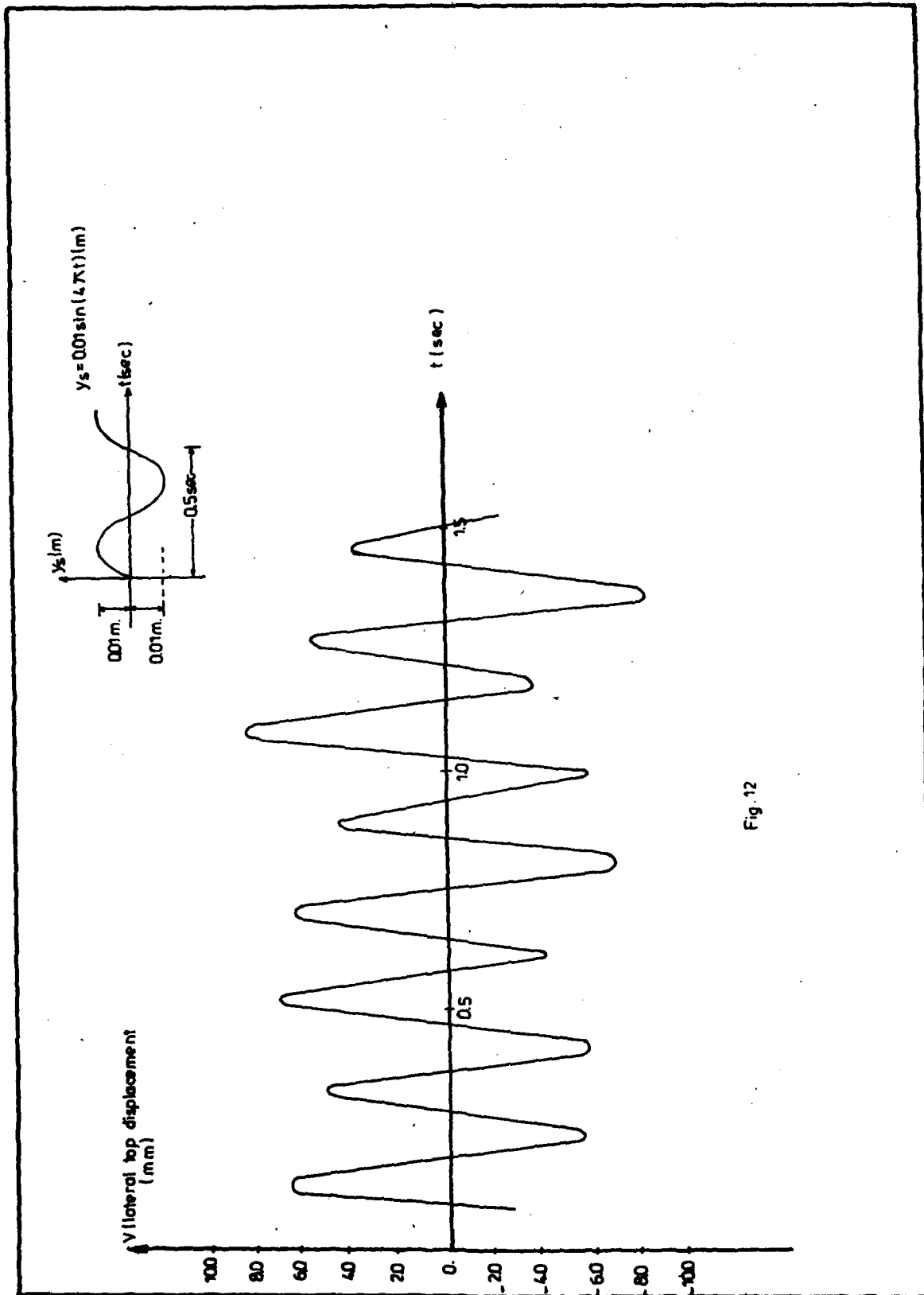


Fig. 12

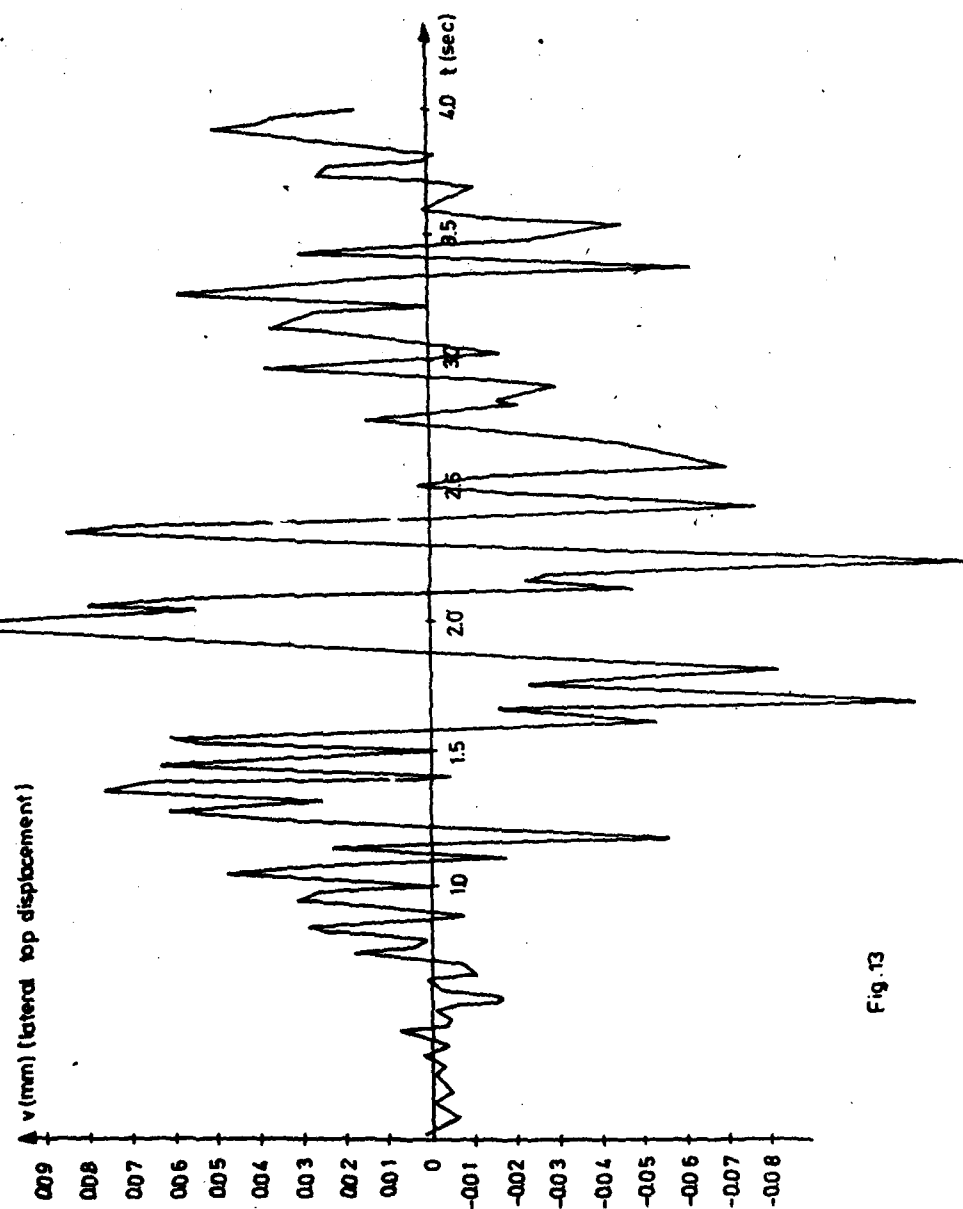
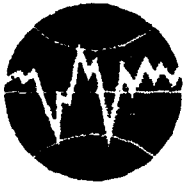


Fig. 13



**TURKISH NATIONAL COMMITTEE FOR  
EARTHQUAKE ENGINEERING**

**THIRTEENTH REGIONAL SEMINAR ON EARTHQUAKE ENGINEERING**

**September 14-24, 1987 - Istanbul - Turkey**

**APPROXIMATE CONSIDERATION OF BEAM STIFFNESSES  
IN SHEAR WALLED STRUCTURES**

**Prof. Dr. Muzaffer Ipek**

## APPROXIMATE CONSIDERATION OF BEAM STIFFNESSES IN SHEAR WALLED STRUCTURES

Prof.Dr. Muzaffer Ipek

### SUMMARY

In this paper a method is presented to obtain approximate solution of shear walled structures considering the stiffnesses of perpendicularly connected beams to shear walls. The basis of the method is the assumption of a beam with elastic hinges at both ends. First of all, the stiffness matrix of an elastically hinged beam is derived. For this matrix, in addition to the beam parameters, the coefficients of two springs which are assumed at both ends of the beam are required. The determination of these two parameters is also discussed.

The numerical analyses performed indicate that the consideration of this kind of wall-beam connections decrease the structural rigidity. Consequently, the vibrational periods, elongate, resulting in the decrease of the design seismic forces. However, structural deformations increase. As a result, especially at lower storeys, significant increases occur in bending moments of shear walls, whereas changes in beam moments depend on the end conditions. The formulation presented can produce more realistic stress distribution in the structure.

### 1. INTRODUCTION

In the lateral load analysis of structures, the omission of beam stiffnesses results in unduly large wall bending moments at lower storeys. The beams, connected to shear walls rigidly at each floor when considered in the analysis resist the deformation of the the structure therefore, decrease the bending moments of the shear wall. In some cases, these beams can rotate the whole section of the wall (Fig. 1). However sometimes, they are connected to some portion of the wall in arbitrary direction. In such a case, they can rotate the beam section only locally (Fig. 2). Hence, when this behaviour is neglected, the moment values differ from the real values.

Rigorous solution of the problem is obtained through 3-dimensional idealization of the shear wall by finite elements, which permit the computation of the local stiffnesses of the shear wall can be computed. Since this solution requires detailed analysis of each wall, it is long and therefore not recommended for practical purposes (Fig. 3).

## 2. BEAM WITH ELASTIC HINGES

In the present analysis, the problem is simulated by using beams having springs with rotatory stiffnesses at both ends (Fig. 4). It is assumed that the whole shear wall section rotates by an angle  $\varphi_A$ , but the beam rotates by an angle  $\varphi_B$  which is larger than  $\varphi_A$ . The angle  $\varphi_B - \varphi_A$  is the rotation taken by the spring.

If the beams are connected to points of low rigidity of shear walls, the bending moments generated at beam ends decrease. The use of beams with elastic hinges in the structure produces similar result. Therefore, if the springs are chosen suitably, the effect of beams in shear walled structures subjected to lateral forces can reasonably be taken into account without performing a detailed rigorous analysis.

## 3. STIFFNESS MATRIX OF BEAM WITH ELASTIC HINGES

In order to solve the problem described above by using beams having springs at both ends, it is necessary to construct, before all, the stiffness matrix of the beam. The stiffness matrix of the beam with constant cross-section shown in Fig. 5 is given by

$$[K_b] = \begin{bmatrix} A & C & B & -C \\ C & D & C & -D \\ B & C & A & -C \\ -C & -D & -C & D \end{bmatrix} \quad (3.1)$$

Where

$$\left. \begin{aligned} A &= \frac{4EJ}{l} \lambda_1, & B &= \frac{2EJ}{l} \lambda_{12} \\ C &= \frac{A+B}{l}, & D &= \frac{2C}{l} \end{aligned} \right\} \quad (3.2)$$

$$\left. \begin{aligned} \lambda_1 &= \frac{3}{4} \epsilon + \frac{1}{4}, & \lambda_{12} &= \frac{3}{2} \epsilon - \frac{1}{2} \\ \epsilon &= 1 / \left[ 1 + \frac{12kEJ}{6I^2F} \right] \end{aligned} \right\} \quad (3.3)$$

$\lambda_1, \lambda_{12}$  are the coefficients which represent the effect of shear deformation (1).  $k$  is a coefficient which depends on the shape of the section. In rectangular sections  $k = 1.2$ .

The beam with elastic hinges is as shown in Fig. 6. The spring coefficients  $R_1$  and  $R_2$  at both ends of the beam are the necessary bending moments to rotate the springs by an angle of one radian.

To obtain the stiffness matrix of this beam, we assume three deformation configurations and solve them to find the rotations at the springs and the generated end forces.

### 3.1 Configuration 1: $\delta_2 = 1$

At this configuration, a unit translation is given to the left end of the beam (Fig. 7). Since the beam has springs at both ends, beam ends do not remain horizontal after the deformation. The left and right ends rotate by angles of  $-\alpha_1$  and  $-\alpha_2$ , respectively. These rotations are determined through the following equations

$$\begin{Bmatrix} M_1 \\ Q_1 \\ M_2 \\ Q_2 \end{Bmatrix} = [K_b] \begin{Bmatrix} -\alpha_1 \\ 1 \\ -\alpha_2 \\ 0 \end{Bmatrix} \quad (3.4)$$

$$M_1 = -A\alpha_1 + C - B\alpha_2 = R_1\alpha_1$$

$$M_2 = -B\alpha_2 + C - A\alpha_1 = R_2\alpha_2$$

$\alpha_1$  and  $\alpha_2$  are solved as follows:

$$\left. \begin{aligned} \alpha_1 &= C(R_2 + A - B)/P \\ \alpha_2 &= C(R_1 + A - B)/P \end{aligned} \right\} \quad (3.5)$$

Where

$$P = (R_1 + A)(R_2 + A) - B^2 \quad (3.6)$$

### 3.2 Configuration 2: $\delta_1 = 1$

At this configuration, a unit rotation is given to the left end of the beam (Fig. 8). To determine the rotations  $\alpha_3$  and  $\alpha_4$  at both ends, we have the equations

$$\begin{Bmatrix} M_1 \\ Q_1 \\ M_2 \\ Q_2 \end{Bmatrix} = [K_b] \begin{Bmatrix} 1 - \alpha_3 \\ 0 \\ -\alpha_4 \\ 0 \end{Bmatrix}$$

$$\begin{aligned} M_1 &= A(1 - \alpha_3) - B\alpha_4 = R_1\alpha_3 \\ M_2 &= B(1 - \alpha_3) - A\alpha_4 = R_2\alpha_4 \end{aligned} \quad (3.7)$$

$\alpha_3$  and  $\alpha_4$  are solved from the above equations

$$\left. \begin{aligned} \alpha_3 &= [A(R_2 + A) - B^2]/P \\ \alpha_4 &= BR_1/P \end{aligned} \right\} \quad (3.8)$$

### 3.3 Configuration 3: $\delta_3 = 1$

At this configuration, a unit rotation is given to the right end of the beam (Fig. 9). The rotations  $\alpha_5$  and  $\alpha_6$  are determined through the following equations

$$\begin{Bmatrix} M_1 \\ Q_1 \\ M_2 \\ Q_2 \end{Bmatrix} = [K_b] \begin{Bmatrix} -\alpha_5 \\ 0 \\ 1 - \alpha_6 \\ 0 \end{Bmatrix} \quad (3.9)$$

$$\begin{aligned} M_1 &= -A\alpha_5 + B(1 - \alpha_6) = R_1\alpha_5 \\ M_2 &= -B\alpha_5 + A(1 - \alpha_6) = R_2\alpha_6 \end{aligned}$$

$\alpha_5$  and  $\alpha_6$  are solved from these equations

$$\left. \begin{aligned} \alpha_5 &= BR_2/P \\ \alpha_6 &= [A(R_1 + A) - B^2]/P \end{aligned} \right\} \quad (3.10)$$

After the determination of the  $\alpha_1 \sim \alpha_6$  values, one has the bending moments  $M_1$  and  $M_2$ . The shear forces  $Q_1$  and  $Q_2$  are obtained through the equilibrium conditions. Finally, one obtains the stiffness matrix of the beam with elastic hinges as

$$[K_b] = \begin{bmatrix} A(1 - \alpha_3) - B\alpha_4 & -A\alpha_1 + C - B\alpha_2 & -A\alpha_5 + B(1 - \alpha_6) & A\alpha_1 + B\alpha_2 - C \\ & -C\alpha_1 + D - C\alpha_2 & -C\alpha_5 + C(1 - \alpha_6) & C\alpha_1 + C\alpha_2 - D \\ & \text{Symmetric} & -B\alpha_5 + A(1 - \alpha_6) & B\alpha_1 + A\alpha_2 - C \\ & & & C\alpha_1 - C\alpha_2 + D \end{bmatrix} \quad (3.11)$$



#### 4. DETERMINATION OF SPRING COEFFICIENTS OF THE BEAM WITH ELASTIC HINGES

As shown in Fig. 10, we assume that the beam is connected to the center of the shear wall and a uniformly distributed moment  $M$  is applied to the wall to rotate the wall section uniformly. The rotations of wall and beam are both equal to  $\varphi_C$ .

Secondly, as shown in Fig 11, we assume that the beam is connected to the shear wall through a spring (for the sake of simplicity in physical representation, a torsion bar is used at the figure) and the same bending moment  $M$  is applied to the wall rotating the wall section uniformly. Let us assume that the shear wall rotates by an angle  $\varphi_A (> \varphi_C)$ . The torsional stiffness of the bar may be selected such that the end of the beam rotates by an angle of  $\varphi_C$ .

If  $B$  is the effective width of the wall when a bending moment is applied at one end

$$\frac{\varphi_C}{\varphi_A} = \frac{b}{B} \quad (4.1)$$

Assume this ratio is known. Since  $\varphi_C / \varphi_A = 1 - \alpha_3$  one obtains

$$\frac{b}{B} = u_1 = \frac{1}{1 - \alpha_3}$$

For the other end of the beam one has

$$u_2 = \frac{1}{1 - \alpha_6} \quad (4.2)$$

In order to compute the effective width  $B$ , in case of a wall with a perpendicular beam, reference is made to a previous paper of the author (2). The result of this paper is summarized in Appendix 1 with a microcomputer program for automatic determination of the width  $B$ .

If  $u_1$  and  $u_2$  values for the two ends of the beam are given,  $\alpha_3$  and  $\alpha_6$  are computed as follows:

$$\left. \begin{aligned} \alpha_3 &= 1 - 1/u_1 \\ \alpha_6 &= 1 - 1/u_2 \end{aligned} \right\} \quad (4.3)$$

After determination of  $\alpha_3$  and  $\alpha_6$ ,  $R_1$  is eliminated between (3.8) and (3.10) to obtain a second order equation,

from where  $R_2$  is solved. Afterwards  $R_1$  is computed.

$$\alpha_6 (R_2 + A)^2 + b_2 (R_2 + A) + c_2 = 0$$

Where

$$\left. \begin{aligned} b_2 &= \frac{B^2}{A} (\alpha_3 - \alpha_6) - A \\ c_2 &= B^2 (1 - \alpha_3) \end{aligned} \right\} \quad (4.4)$$

The expressions of  $R_1$  and  $R_2$  are

$$\left. \begin{aligned} R_2 &= \frac{-b_2 + \sqrt{b_2^2 - 4\alpha_6 c_2}}{2\alpha_6} - A \\ R_1 &= \frac{(R_2 + A)\alpha_6 + b_2 + A}{\alpha_3} - A \end{aligned} \right\} \quad (4.5)$$

## 5. NUMERICAL APPLICATIONS

The effect of the wall-beam connection type on the solution is investigated by applying the presented procedure to a 10-storey shear walled structure. The vertical section and the plan of the structure are shown in Fig. 12 and Fig. 13, respectively. As seen in Fig. 13, every floor has 9 shear walls ( $S_1 \sim S_9$ ) and 16 beams ( $B_1 \sim B_{16}$ ). Wall thickness is 25 cm everywhere. Some beams ( $B_1, B_2, B_7, B_8$ ) are connected to the shear walls at both ends in such a way that they can bend the walls effectively, i.e. beam end moment is capable of rotating the whole wall section uniformly. Some beams ( $B_9, B_{10}, B_{11}, B_{12}, B_{15}, B_{16}$ ) are connected only to one of the shear walls effectively. The other beams ( $B_3, B_4, B_5, B_6, B_{13}, B_{14}$ ) can rotate both shear walls only locally. The  $u_1$  and  $u_2$  values of the beams are shown at beam ends in Fig. 13.

The total weight of the structure is 4018 tons. Firstly, the structure is solved assuming all the wall beam connections as "Rigid" ( $u_1 = u_2 = 1$ ). Second solution is performed assuming "Flexible" wall-beam connections, by using  $u_1$  and  $u_2$  values shown in Fig. 13. In the subsequent figures the results of these two solutions are designated as "R" and "F".

The results of dynamic analysis of the structure are summarized in Table 1. In this table the natural periods of the lower three modes in the x- and y-directions, both for rigid and flexible cases are presented. The period values are longer in the flexible case, however the percentage of elongation is low in the 2nd and in the 3rd mode.

In Table 2 the modal base shears are shown. A quick examination of this table indicates that the base shear of the fundamental mode decreases in the flexible case, whereas

Table 1 Natural Vibration Periods of rigid and flexible structures (secs)

Mode	Direction	Rigid	Flexible	Increase (%)
1	x	0.5833	0.6239	7.0
2	x	0.1701	0.1787	5.0
3	x	0.0847	0.0875	3.3
1	y	0.6689	0.7769	16.1
2	y	0.1816	0.1985	9.3
3	y	0.0851	0.0888	4.3

Table 2 Base shears of rigid and flexible structures (tons)

Mode	Direction	Rigid	Flexible	Increase (%)
1	x	324.8	311.6	-4.1
2	x	70.9	72.8	2.7
3	x	27.0	27.9	3.3
1	y	293.8	265.5	-9.6
2	y	79.7	84.8	6.4
3	y	32.0	34.1	6.6
RMS	x	333.6	321.2	-3.7
RMS	y	306.1	280.8	-8.3

Table 3 Displacements (cm)

Storey	Direction	Rigid	Flexible	Increase (%)
10	x	1.28	1.43	11.7
10	y	1.63	2.08	27.6

the base shears of the 2<sup>nd</sup> and the 3<sup>rd</sup> modes increase. The reason of this discrepancy is perhaps due to the use of Turkish Seismic Code spectrum in the computation of modal seismic forces. However, by the influence of fundamental mode, RMS base shear value is lower in the flexible case.

The top storey displacements of the two cases are shown in Table 3 for purpose of comparison structural deformations. The examination of this table clarifies that inspite of the decrease in seismic forces, the structural deformations increase greatly in the flexible case.

Fig.14 shows the bending moment diagram of S5 under lateral force loading in the x-direction. Although, there are no perceptible changes in the upper storey moment values, significant increases are observed as high as 12.8 % in the bending moments of lower storeys.

In Figs. 15~18 end moments of some typical beams are presented for comparison.

The following conclusions may be drawn by a close examination of these figures:

- a) Due to increase in overall structural deformations in the flexible case, beam end moments where  $u_1=u_2=1$  become slightly larger.
- b) In general, at beams where  $u_1>1$ , and  $u_2>1$  the end moments decrease. If end moments are much greater than unity, the decrease in end moments is higher.
- c) If either of the  $u_1$  or  $u_2$  is unity, it is difficult to guess the direction of change in end moments.

## 6. CONCLUSIONS

The type of shear wall-beam connection in shear walled structures has significant effect on internal force distribution in the structure. It is shown that the use of beam with elastic hinges described in the present paper can represent this behaviour.

Numerical analyses show that the use of shear wall-beam connections with elastic hinges decrease the overall stiffness of the structure. As a result, the displacements and the structural deformations increase, bending moment diagrams of shear walls resemble more to that of a cantilever beam. The moments at beam ends may increase or decrease depending on the values  $u_1$  and  $u_2$  which represent the effectiveness of the wall-beam connection. Therefore, the assumption of rigid wall-beam connection lead to underestimation of the bending moments at some wall and beam sections. The solution based on the assumption of flexible wall-beam connections can give more realistic stress distribution in the structure.

The influence of the formulation presented on the structural cost is not studied, however, the structural safety appears to be significantly improved.

#### REFERENCES

1. Tezcan S.S., "Computer aided analysis of Bar Systems", Publications of the Institute of Computer Sciences, I.T.U., 1970 (in Turkish)

2. Ipek M., "On the Effective Width of Plate in Flat Slab Structures Subjected to Lateral Forces", Publications of the Seismological Institute, I.T.U., No.20, 1964.

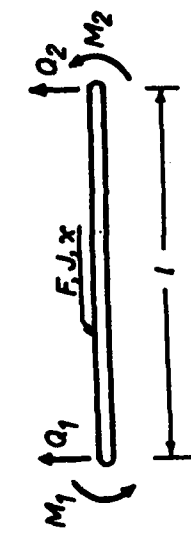


Fig. 5



Fig. 6

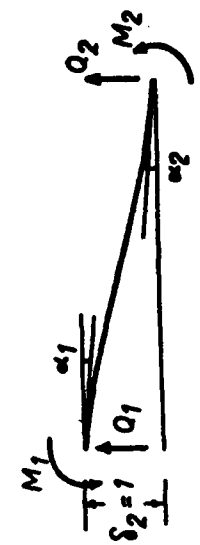


Fig. 7

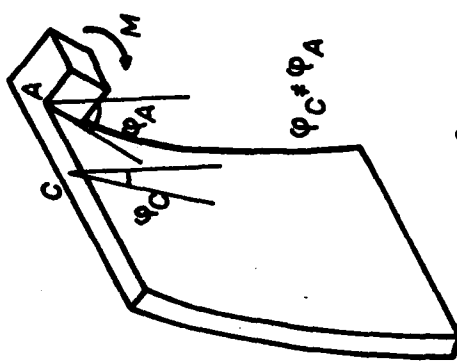


Fig. 2

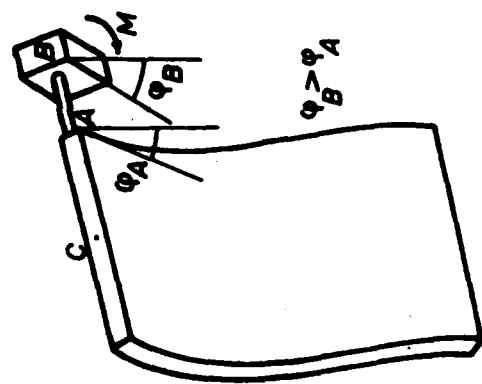


Fig. 4

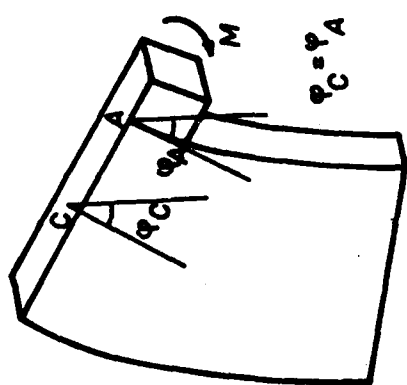


Fig. 1

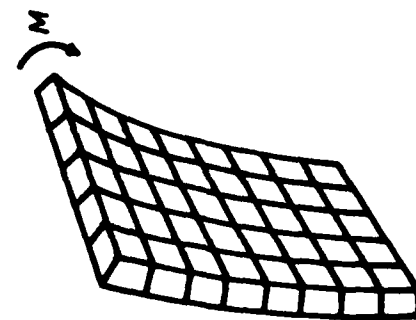


Fig. 3



Fig. 8

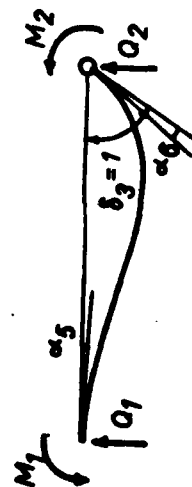


Fig. 9

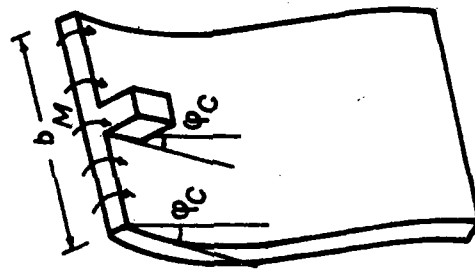


Fig. 10

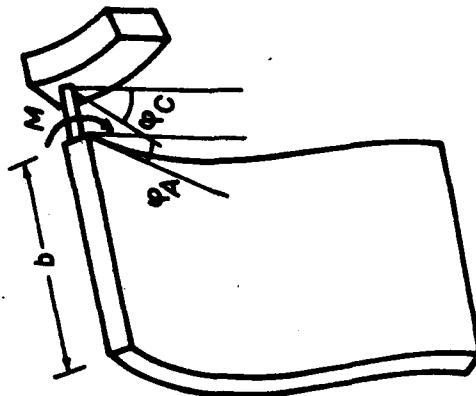


Fig. 11





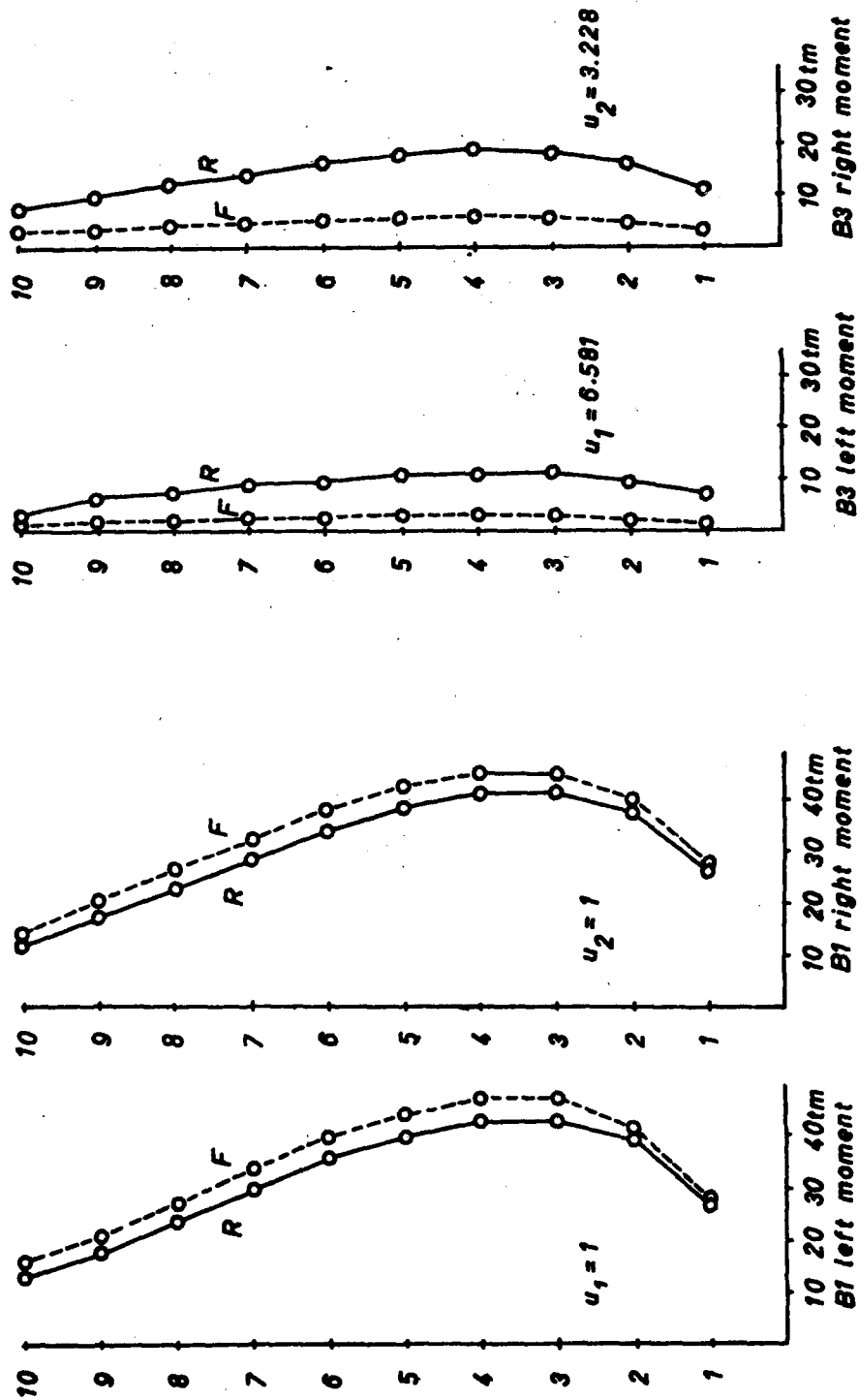


Fig. 15

Fig. 16

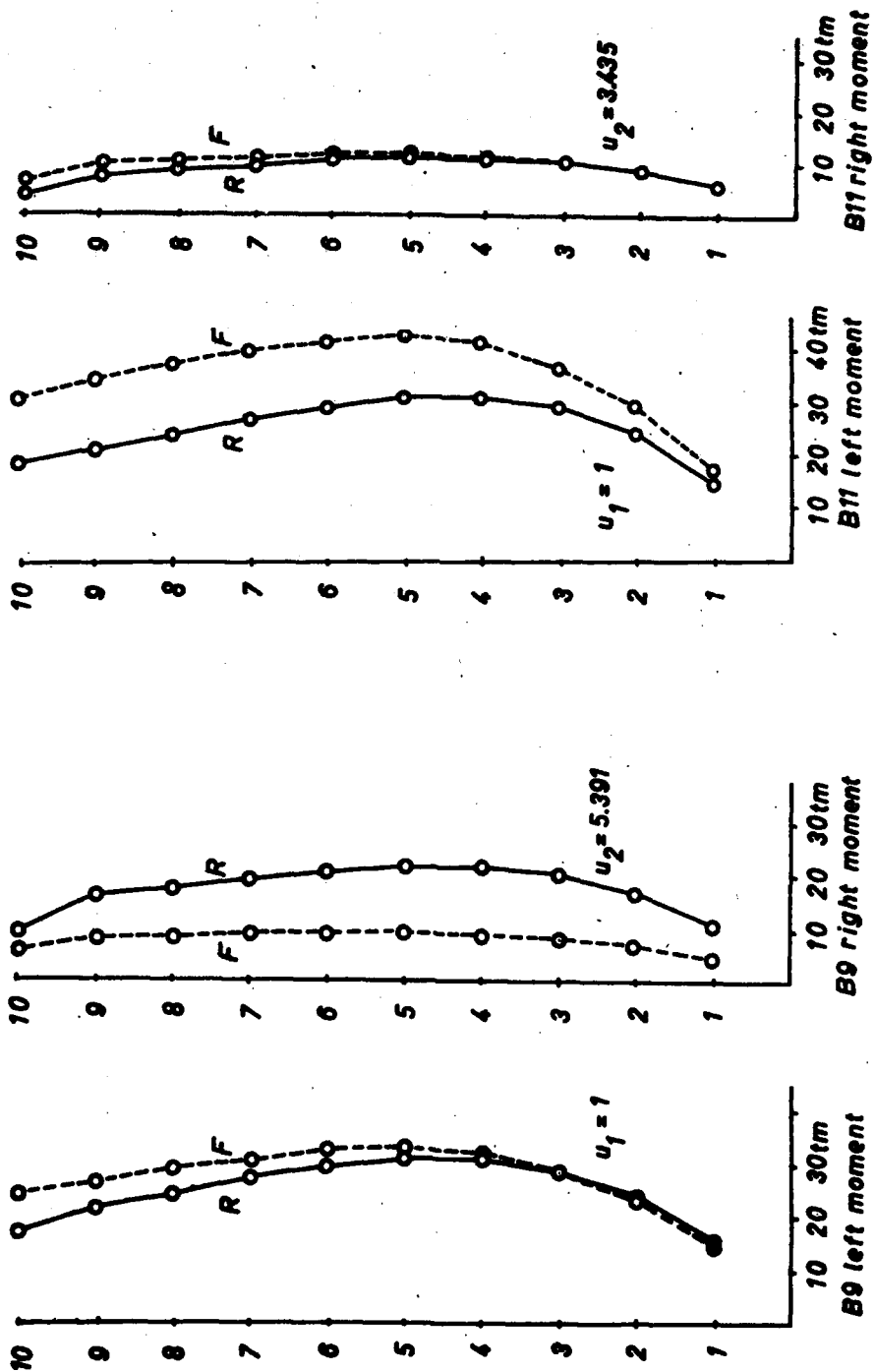


Fig. 18

Fig. 17

## APPENDIX 1

### EFFECTIVE WIDTH OF PLATE IN FLAT SLAB STRUCTURES

Assume that a flat slab is supported by equidistant columns in both directions. Column intervals are "a" in loading direction and "b" in the other direction, column width is "2e" in the transverse direction. Fig. 1 shows such a slab of dimensions axb, where the column is at the center.

When the structure is subjected to lateral loads, bending moments are generated at column heads. The slab sections do not rotate uniformly. Instead, the slab reacts against the external moments, as if it has the stiffness of a plate of width B.

This problem is studied in Ref.2. The result of this paper is summarized herein.

The parameters  $\xi = b/a$ ,  $\alpha = e/b$  define the ratio N between the plate width "b" and the effective width "B". The variation of "N" as a function of  $\xi$  and  $\alpha$  is illustrated in Fig. 2.

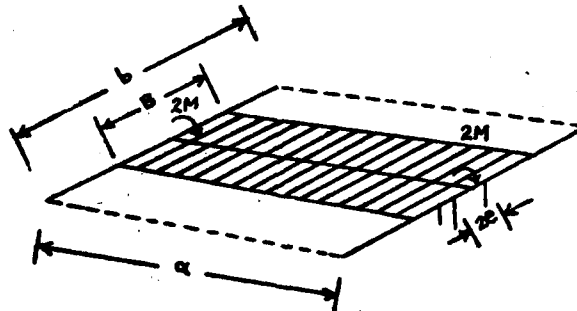


Fig. 1

$$\frac{b}{B} = N = 1 + \frac{8}{4\pi^2} \cdot \frac{b}{a} \cdot \frac{b^3}{e^3} \Sigma$$

$$\Sigma = 4\pi^2 \alpha^2 \left[ -\left( \ln \alpha + \ln 4\pi - \frac{3}{2} \right) + \frac{\pi^2}{9} \alpha^2 + \frac{4\pi^4}{675} \alpha^4 + \frac{16\pi^6}{19845} \alpha^6 + \dots \right]$$

$$- \sin^2 2\pi \alpha \left[ 1 + \frac{\pi}{s} \frac{1}{\operatorname{sh}^2 \frac{\pi}{s}} - \coth \frac{\pi}{s} \right]$$

The analytical formulation is coded in Basic Language and listed below

```

10 'EFFECTIVE WIDTH OF PLATE IN FLAT SLAB STRUCTURES (M.IPEK)
20 PI=3.1415926#
30 P2=PI*PI
40 DP=4*P2
50 P2=PI*PI: DP=4*P2: P4=P2*P2
60 B2=P2/9
70 B4=4*P2*P2/675
80 B6=16*P4*P2/19845
90 B0=LOG(4*PI)-1.5
100 PRINT "      no      a      b      e      b/a      e/b      N=u"
110 PRINT
120 READ NO,A,B,E
130 EPS=B/A
140 ALF=E/B
150 ALF2=ALF*ALF
160 S1=SIN(2*PI*ALF)
170 EX=EXP(PI/EPS)
180 SH=(EX-1/EX)/2
190 TH=(EX-1/EX)/(EX+1/EX)
200 S=DP*ALF2*(-(LOG(ALF)+B0)+ALF2*(B2+ALF2*(B4+ALF2*B6)))
   -S1*S1*(1+PI/EPS/SH/SH-1/TH)
210 N=1+.75*EPS/(P2*PI*ALF2)*S
220 PRINT USING "*****";NO;:PRINT USING "****.***";A;B;E;EPS,
   ALF,N
230 GOTO 120
240 DATA 1, 5, 5.5, .275
250 DATA 2, 5, 6, .15
260 DATA 3, 3.2, 8.48, .24
270 DATA 9, 3.2, 7, .24
280 DATA 11, 3.2, 4.48, .24

```

```

RUN
no      a      b      e      b/a      e/b      N=u
1 5.000 5.500 0.275 1.100 0.050 3.035
2 5.000 6.000 0.150 1.200 0.025 3.995
3 3.200 8.480 0.240 2.650 0.028 6.581
9 3.200 7.000 0.240 2.188 0.034 5.391
11 3.200 4.480 0.240 1.400 0.054 3.435

```

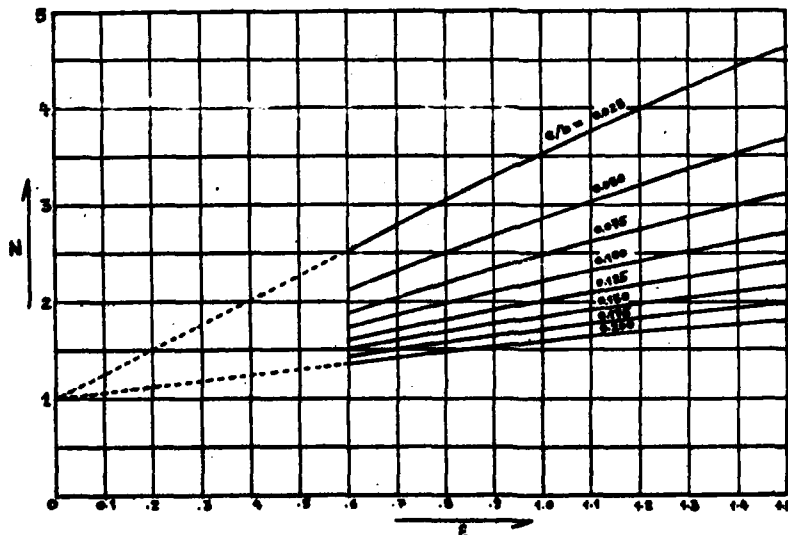
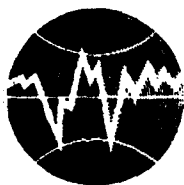


Fig. 2



**TURKISH NATIONAL COMMITTEE FOR  
EARTHQUAKE ENGINEERING**

**THIRTEENTH REGIONAL SEMINAR ON EARTHQUAKE ENGINEERING**

**September 14-24, 1987 - Istanbul - Turkey**

**DYNAMIC TESTS OF LARGE-SCALE MODELS AND FULL-SCALE  
STRUCTURES**

**by**

**Cristian Radu Constantinescu<sup>2</sup>**

# **DYNAMIC TESTS OF LARGE-SCALE MODELS AND FULL-SCALE STRUCTURES**

by

**Cristian Radu Constantinescu<sup>\*</sup>**

## **SUMMARY**

Dynamic tests performed in the Building Research Institute INCERC by the staff on experimental research on structures subjected to earthquake action are presented in this paper as well as the theoretical background, the methodologies and instruments used in this field. Divided in four parts, the first one deals with some elements regarding the role of dynamic tests for the improvement of earthquake-resistant design of structures. The second part presents the theoretical background of dynamic tests, the methods and instrumentation used for dynamic tests. The third part describes the most important types of dynamic tests performed during the last five years in INCERC on large-scale models and full scale structures. Finally, in the fourth part, the paper presents the importance of dynamic tests of structures, giving practical advice and conclusions for the use of experimental results.

## **1. INTRODUCTION**

The problem of the dynamic response of structures to exciting forces requires many quantitative information on dynamic properties of structures as natural periods of vibration, mode shapes of vibration and damping capacity. In design, a lot of idealisations have to be used. If experimental data are available and relevant analyses are performed, their comparison permits to obtain important conclusions regarding the actual response of structures as well as the correctness of the assumed models and the analysis methods. Dynamic tests of full-scale structures or large-scale models are thus a necessity for earthquake-resistant design of structures.

In view of the important advantages offered by dynamic tests, the main objectives of the staff on experimental research on structures subjected to earthquake action from INCERC were to establish a basis for this kind of studies and to obtain experimental data on actual response of structures to different dynamic loads.

The paper presents a review study on the above mentioned problems. The main types of dynamic tests for large-scale models and full-scale structures are described. Each type is discussed, giving specific examples. A special attention is paid to ambient vibration tests of full-scale structures which were highly developed

<sup>\*</sup> Scientific Researcher, Building Research Institute INCERC, Bucharest, ROMANIA

in the last years. The main results obtained in this field and the most important statistical studies carried out are presented. An attempt to correlate experimental data on dynamic characteristics of structures with some parameters that are proper to engineering analyses is also presented.

## 2. CONCEPTUAL AND METHODOLOGICAL ELEMENTS

### 2.1. Theoretical Background

The dynamic tests have to be performed and interpreted by a theoretical background which involves a very well understanding of structural dynamics. The theoretical problems consist in deriving structural properties from experimentally measured parameters. In these cases the theory must be used to obtain the maximum amount of information from the experimental data. As examples, consider different types of dynamic tests and see how the theoretical considerations have to be done.

It is desirable to begin these examples with free vibration tests (initial displacement and initial velocity tests). Because it is not possible to determine analytically the damping ratio  $n$  for a structure, there is of great importance to evaluate it from experiments. The natural period of vibration  $T$  of a one-story structure can also be determined from these experiments. The procedure consists in disturbing the structure from its equilibrium position and record the free vibration of the structure to obtain the displacement-time plot shown in Fig.1. Measured displacements can be used to compute the damping ratio  $n$  by the logarithmic decrement method /4/. The procedure shown above can also be used to compute the damping ratio from acceleration-time records. The natural period of vibration  $T$  (sec.) is the time required for one cycle of free vibration and so it is very easy to be computed.

The second example refers to forced vibration tests. The main types of these tests, as will be discussed in the following part of the paper, are: tests with vibration generators, tests on shaking tables, tests to man-excited vibrations and transient excitation tests (wind excited, blasts excited, natural earthquakes excited and microtremor excited). For each type of these tests the theory must be used. It is well known that the methods of formulating mathematical models of structures and actions have not yet been developed with high accuracy so as to avoid experiments. Hence, it is desirable to combine analytical and experimental studies. For vibration generator tests, the action can be modeled very easy. The more difficult problems consist in modeling structural properties. If large-scale models are tested, additional problems have to be formulated and resolved. In this case a special attention must be paid to the similitude of dynamic phenomena /13/. The same problems have to be considered for shaking table tests. For man-excited vibration

tests, which are in fact resonant vibration tests, the above mentioned theory for free vibration tests can be applied. For transient excitation tests analytical methods have to be used for each type of experiments. In the following, a special attention is paid to microtremor excited vibrations. In this case, the excitation is modeled by a stationary random process with flat frequency spectrum. The structures modeled as multi-degree-of-freedom systems subjected to exciting forces with flat frequency spectrum will respond in a linear combination of all normal modes. It is also assumed that the structures can be modeled by one-dimensional damped systems (usually discrete systems). This assumption is in good agreement with the observation that the floors are stiff enough for the low level of excitation due to microtremors. If the linear model is admitted, the resulting motion can be expressed as a superposition of natural modes of vibration corresponding to the natural frequencies of structure. Using Fourier transforms to analyse low level structural vibrations /2/ it clearly appears how the natural frequencies of structures can be identified.

## **2.2. Classification of Dynamic Tests**

It is very difficult to classify the great number of types of dynamic tests. For the purpose of this paper, it is convenient to use the following classification:

- A. Free vibration tests
- B. Forced vibration tests

The tests from the second category can also be classified in:

- a) Tests with vibration generators
- b) Tests on shaking tables
- c) Tests to man-excited vibrations
- d) Tests to transient excitations as:
  - wind
  - blasts
  - natural earthquakes
  - microtremors

Each of these tests will be discussed in more or less detail, giving examples from the activity of the experimental staff mentioned in the previous part of this paper.

## **2.3. Instrumentation and Measurement Procedures**

A large variety of instrumentation is required by the dynamic tests. Different devices and systems are used to produce dynamic loads and to record structural response. There are three quantities which are of interest in dynamic studies: the displacement, velocity and acceleration of vibration. In order to best utilise the dynamic range of the measuring instrumentation it is preferable to select the parameter which gives the



flattest frequency spectrum. This observation comes from the well known fact that displacement measurements give low frequency components most weight and conversely acceleration measurements give high frequency components most weight.

Appreciable displacements only occur at low frequencies, therefore displacement measurements in mechanical vibrations are of limited value.

Velocity measurements are used for evaluating the severity of vibration, due to the fact that velocity is related to vibratory energy and therefore to the destructive effect of vibration.

Acceleration measurements are used where the frequencies of interest for the research purpose are in high frequency range.

For the free vibration tests presented in the above classification all of the measurement instruments described in this section can be used. In the forced vibration tests the measurement instrumentation have to be used in function of the level of structural response and the frequency range. For the experiments performed in INCERC on large-scale models excited with vibration generators two types of transducers were used: velocity transducers with integration galvanometers and accelerometers. For shaking table tests and quarry blast tests accurate measurements are obtained using accelerometers. Special instrumentation is required for recording structural response due to natural earthquakes. In this connection, it is of great interest to obtain accelerographic data in the basement or foundation of the structure and in upper level positions /18/. The great progress in the electronic equipment field made possible to obtain digital accelerogram records. As an example, many digital records were obtained during the Mexico earthquake of September 1985 /14/. In Romania, many accelerographic records were obtained during the earthquakes of March 1977 and August 1986 /1/, /21/. The records were obtained with Strong Motion Accelerographs (SMA 1 and SMAC).

For man-excited, wind and microtremor vibration tests special instrumentation is required due to the low excitation level and therefore the low response level. The experimental tests performed in INCERC, the results of which will be presented in the following part of the paper, were obtained using seismometers with constant voltage output at all frequencies greater than 1 Hz, signal conditioners to amplify and control seismometer signals and tape recorder systems. The recorded analog signals were analyzed in the frequency domain using an analog-digital converter and a spectrum analyzer. The data obtained were plotted on a X-Y recorder. When measuring ambient vibrations and man-excited vibrations of the buildings, it is of interest to identify the dynamic properties of structures. The modal frequencies were obtained by placing seismometers at the top level of buildings. Special placements of seismometers are made for obtaining

torsional frequencies /2/. The mode shapes of structures were obtained by placing seismometers at different levels of the building. In this connection, many examples are given in the following part of this paper.

### 3. DYNAMIC TESTS CARRIED OUT AND RESULTS OBTAINED BY THE INGERO STAFF ON EXPERIMENTAL RESEARCH ON STRUCTURES SUBJECTED TO EARTHQUAKE ACTION

#### 3.1. Dynamic Tests on Free Vibration Response of Structures

The free vibration tests are very simple and consist in recording the vibrations of a structure about its static equilibrium position, after the deformation caused by pulling with a horizontal (or inclined) force or by an impact with a pendulum that can strike horizontal blow. By recording the amplitudes of structural vibrations vs. time, the natural period can be directly identified and the damping ratio can be easily evaluated (see paragraph 2.1.) An application of the pulling technique was performed on some low-rise building with wood structures.

An interesting example can be discussed as an impulsive test. A reinforced concrete structure with eight levels was struck by a pendulum and the structural response to this "initial-velocity" excitation was recorded. The results are plotted in Fig. 2. The data obtained from these tests were compared with ambient vibration studies. In connection with the natural periods of vibration the results from both studies showed good agreement.

#### 3.2. Dynamic Tests on Forced Vibration Response of Structures

##### 3.2.1. Tests with vibration generators

Tests with eccentric weight exciters were performed on large-scale models. The vibration generator used have two baskets which can rotate about a vertical axis. The magnitude of the unbalanced weights can be altered so as to produce different alternating forces. The maximum moment of eccentric weights is approx. 22 kgm which leads to a maximum force of approx. 90 kN at 10 Hz. This force is too small for exciting full-scale structures and therefore only models were tested.

An example of a recent investigation of the dynamic behaviour of a R.C. frame structure (model at 1:4 scale) is presented in the following. The scheme of the model is shown in Fig. 3. The acceleration and velocity transducers were placed at different levels of the structure, as shown in the same figure. The model was tested at four levels of excitation, corresponding to maximum forces of approx. 56 kN, 62 kN, 68 kN and 90 kN (at 10 Hz). The resonant curves for each level of excitation are plotted in Fig. 4. It can be clearly seen that the model has non-linear resonance curves (the natural period decreases with the increase of the exciting force). The responses of

structure at different levels were recorded so as to derive the natural periods and modeshapes. The experimental mode shapes are plotted in Fig. 5. In order to compare experimental results with analytical evaluations some theoretical analyses were performed. The mathematical model of the frame structure is shown in Fig. 6. It can be seen that the 11-story structure was modeled as a 13-degree-of-freedom system (11 DOF for each concentrated mass and 2 DOF for the foundation). The stiffness properties of the structure are characterized by the lateral stiffness of individual stories. The schematic deformation of the frame structure is shown in Fig. 7 and the ecological model is plotted in Fig. 8. Using this model, the modal analysis and the response of structure to dynamic loads were performed. The evaluations were made for different values of stiffness so as to obtain a good agreement with experimental results. The analytical mode shapes are plotted in Fig. 9. Using similitude criteria, the results obtained on the large-scale model were transposed to the prototype. Taking into consideration these criteria the natural frequencies, the stiffness properties, the maximum response in accelerations were evaluated. Important conclusions for the design of R.C. frame structures were obtained.

### 3.2.2. Tests on Shaking Tables

The same type of large-scale models as described above were tested on a shaking table in order to compare the results. The testing were performed in the laboratories of the Jassy Branch of the Central Institute for Research, Design and Guidance in Civil Engineering (ICGPDC). Since the shaking tables of the seismic testing station which will be built in INCERC are planned to function in 1988, no other aspects on shaking table tests are presented in this paper.

### 3.2.3. Tests to Man-Excited Vibrations

As shown in the previous part of this paper, man-excited vibration tests are simple tests of resonant vibration of structures. Using the movement back and forth of two or three persons in synchronism with the natural period of the structure, it is possible to excite structural vibrations with amplitudes higher than those excited by ambient vibrations. The resonance testing is easier to be done if the persons who are moving to excite the structure are watching on a monitor so that to follow the resonant tendency of structure. Vibration records obtained in this way in a multi-story reinforced concrete building are plotted in Fig. 10. In this way, both the natural periods and the damping ratios can be determined. Of course such tests with their low amplitudes of vibration can't substitute more complex investigations on dynamic behaviour of structures. However, this method offers useful data in many cases for which no other dynamic tests can be carried out.

### 3.2.4. Tests to Transient Excitations

#### 3.2.4.1. Tests to Wind-Excited Vibrations

Buildings are exposed to a wide range of aerodynamic effects. The wind effect to a given building depends on the structural type and characteristics. Only the dynamic effect which causes building oscillations is presented here. The wind exciting forces are a stationary random process with flat frequency spectrum. Therefore the assumptions made in chapter 2 of this paper may be used. The wind induced vibrations of a high-rise building having steel structure are described in the following. The overall floor dimensions and the height of the building are shown in Fig. 11 and 12. Measurements of wind induced vibrations were performed at different levels of the building and the results were compared with those obtained to microtremor tests. Figures 13 and 14 represent structural oscillations at the 9th level of building in these two situations mentioned above. The Fig. 13 refers to transverse oscillations and Fig. 14 to longitudinal oscillations. It can be observed how the amplitude of vibration increase when the building is subjected to wind excitation. The same observation can be made in connection with Fig. 15 in which vibrations of building in floor plan are plotted. It must be mentioned here that the wind speed during the measurements was approx. 25 m/sec. Because of the low level of excitation and the complex nature of the exciting force, data analysis based on autocorrelation techniques has been applied. In Fig. 16 the autocorrelation function of oscillations at basement is plotted. It can be observed that the function is typical for wide band excitations /3/. Conversely, the autocorrelation functions for the oscillations recorded at upper levels of the building are typical for narrow band stationary random process /3/. These functions are plotted in Fig. 17 and 18. Using autocorrelation technique and other types of data analysis suitable for low level excitations, the dynamic properties of the building were obtained. The natural periods of vibrations were:

- in the transverse direction:  $T_I = 1.20 \text{ sec.}$   
 $T_{II} = 0.40 \text{ sec.}$
- in the longitudinal direction:  $T_I = 1.10 \text{ sec.}$   
 $T_{II} = 0.50 \text{ sec.}$

The damping ratios obtained were:

- in the transverse direction:  $\alpha_I = 0.04$
- in the longitudinal direction:  $\alpha_I = 0.02$

The results indicate how the building excited to wind forces responds in the fundamental and the second mode of vibration. The second mode has a rarer occurrence but it could be identified.

1

The natural periods obtained from wind-excitation tests show good agreement with microtremor tests.

#### 3.2.4.2. Quarry Blast Tests

The blasting is widely used in mine work, when great weight explosive charges are used to dislocate the minerals. These explosions cause seismic vibrations which can be dangerous for the buildings located near the blasting centre. It has been found that large quarry blasts generate ground accelerations in their immediate vicinity, that are comparable to earthquake ground motions, the buildings being subjected to high level excitation /12/. In this connection, the staff on experimental research from INCERC performed many tests on structures located near blasting centres and subjected to quarry blast loads. The main results are presented in the following.

Fig. 19 represents the acceleration-time plot of seismic oscillations caused by a blast operation. It can be observed the envelope of amplitudes of vibrations which is typical for blasts. Time acceleration records and Fourier spectra of these records are shown in Fig. 20. Many building were tested to microtremors and blast excitation in order to compare the responses. Different Fourier spectra for building oscillations due to microtremors in different years are shown in Fig. 21. It was observed that after many blasts the natural periods of buildings increase (see Fig. 22) and consequently the stiffness of structures decreases. This observation is due to the fact that cumulative damages appear after blasting operations which cause building vibrations.

The results obtained in this field allowed to create a base of data very useful for the evaluation of existing buildings in blasting areas and the design of new buildings near mining enterprises. It was observed that the spectral composition of oscillations during explosions is narrower than that of earthquakes. There are no long periods of oscillation and therefore the effect of blast operations on flexible structures is not dangerous when compared to earthquakes. The dynamic amplification of structures subjected to blast excitation (the ratio of the vibration amplitudes at the top to its base) is less than it is when subjected to earthquakes due to the lesser duration of oscillations during the explosions.

From the results of the data concerning the blasting operations affecting several buildings, a technical prescription for the design of buildings in mining zones was elaborated.

#### 3.2.4.3. Tests to Natural Earthquakes

A strong earthquake can be considered a great dynamic test for full-scale structures. In this connection many pre-earthquake research activities are necessary.

In order to better know the seismic action, the network of seismic accelerographs is of inestimable importance. Also the structural response records are of great importance for structure engineers. Consequently, after the 1977 earthquake, this field was highly developed in INCHERG and many instrumental data were obtained during the 1986 earthquake. The analysis of the records and the data interpretation are not detailed in this paper.

#### 3.2.4.4. Microtremor Tests

There are many small earthquakes and there is a continuous ground motion of low level due to microseismic activity and to different activities such as traffic, industrial vibrations etc. The response of structures subjected to microtremors can be recorded and analyzed so as to identify their structural properties in the linear range /2/.

The ambient vibration tests of full-scale structures offer not only an efficient way of studying the linear response of structures but an instrument for identifying building damage after strong earthquakes /7/. Because of the very low level of vibrations, special methods and adequate instrumentation are required. A general scheme of the data processing and instrumentation required for ambient vibration tests is shown in Fig. 23.

Dynamic properties of structures can be identified using different methods of data analysis such as those presented in the following.

Many types of structures were tested to ambient vibrations in order to identify their dynamic properties. The most important characteristics that can be identified are the natural periods of vibration. For determining the translational and the torsional natural periods the seismometers are located at different levels of the buildings. A typical record of the response of structure at the top level is plotted in Fig. 24. The corresponding Fourier spectra of structural oscillations are shown in Fig. 25 and the corresponding autocorrelation functions are shown in Fig. 26. Using the sum and the difference of seismometer signals at each floor level, translational and torsional modal information can be obtained. In this way natural periods and mode shapes are identified.

For more important structures some biographical studies were performed in order to identify changes in structural stiffness. As an example, a test on a large-span structure is described below. The floor plan and the section of the structure are shown in Fig. 27. The natural periods of vibrations for each mode were determined at different periods of time. The results are shown in Fig. 28.

Ambient vibration tests were performed on some special structures such as towers and pylons.

Dynamic characteristics of a control tower are discussed in the following. The tower is more than 50 m height and has a cross section as shown in Fig. 29.

A representative sample of structural response at + 82.50 m level and its corresponding Fourier spectrum are shown in Fig. 30. The mode shapes of vibration are shown in Fig. 31.

The natural periods of vibration were:

- in the transverse direction  $T_I = 0.90$  sec.
- in the longitudinal direction  $T_I = 0.64$  sec.

Important results were obtained on large capacity gylas structures. The seismometers were placed as shown in Fig. 32. Typical oscillations of this kind of structures are plotted in Fig. 33.

Dynamic tests to microtremor excitation were also performed during the translations of some important monuments which were replaced in the urban area. The translation displacement vs. time and the structural oscillations are plotted in Fig. 34 and 35. It can be seen that in the first case (Fig. 34) the speed of translation is not so uniform and therefore the structural oscillations are due to microtremors and shocks. In the second case (Fig. 35) the uniformity of translation speed (due to the running in of the mechanical system of translation), is obvious and therefore the oscillations are due only to microtremors.

Important tests were carried out on a residential building on which the response at the top level was recorded during the 1977 earthquake. The floor plan of the building is shown in Fig. 36. In order to compare the structural response with the strong motion acceleration, Fig. 37 shows acceleration vs. time records. In Fig. 37a the N-S component of the accelerogram recorded during the 4 March 1977 earthquake is plotted. In Fig. 37b the response of structure in the normal directions A and B (the main record directions of the strong motion accelerograph) is represented. The response of structure in the main directions of the building (transverse and longitudinal) is plotted in Fig. 37c. The biographical evolution of the natural periods of vibration is shown in Fig. 38.

With the great number of experimental data on existing buildings, a lot of statistical studies were possible. These studies took into consideration all the available data concerning the dynamic characteristics of different types of buildings.

A first attempt was made to correlate the fundamental natural periods (as a function of the number of building levels) and the observed damage of buildings. The results are presented in Fig. 39.

An other attempt was made to check the efficiency of strengthening works carried out after the 1977 earthquake by means of the changes in natural periods of buildings pre and post-strengthening works (see Fig. 40).

Other types of correlations such as the increase of natural periods vs. damage degree of building were also carried out /21/.

#### 4. FINAL REMARKS

The paper presented a review of the main activities carried out by the staff on experimental research on structures subjected to earthquake action from INGERC. There are, of course, many things omitted or insufficiently developed but the most important aspects concerning dynamic tests on large-scale models and full-scale structures were presented.

It clearly appeared the importance of the dynamic tests on structures for the development of earthquake engineering field. It was also shown that experimental studies have to be performed in correlation with theoretical analyses.

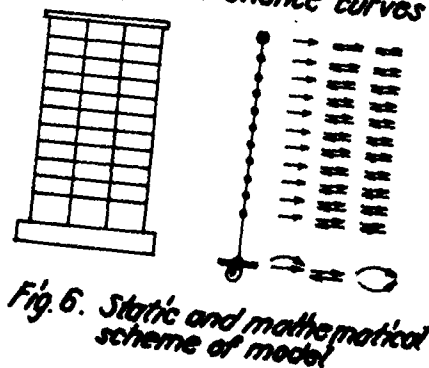
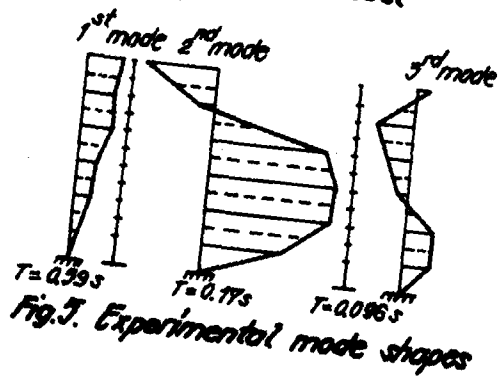
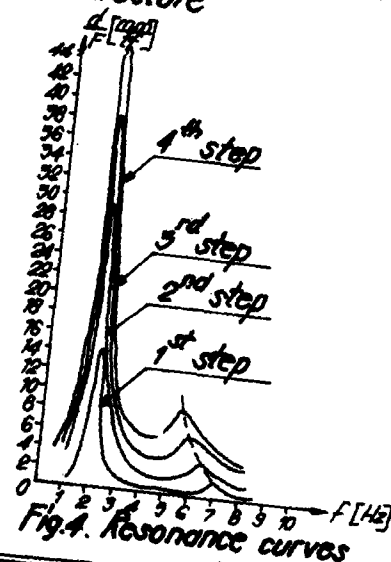
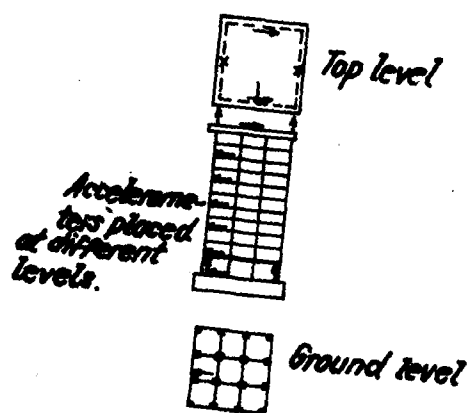
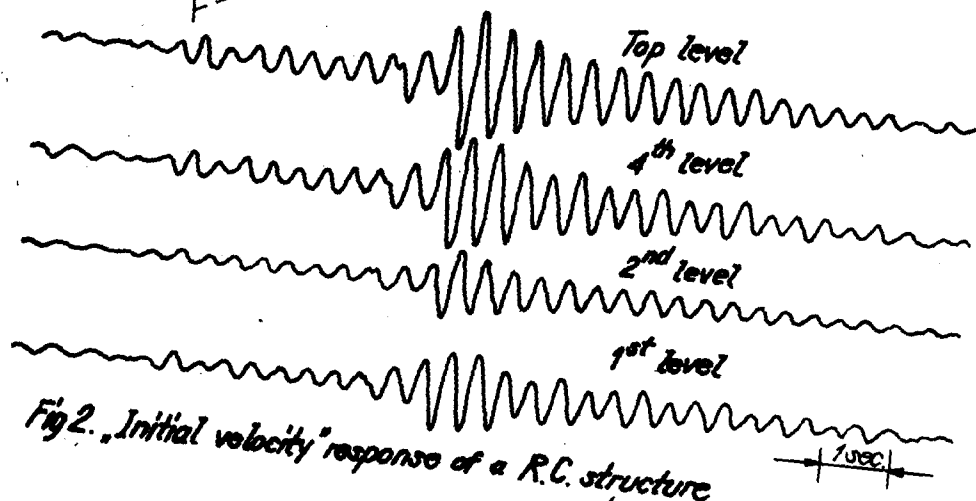
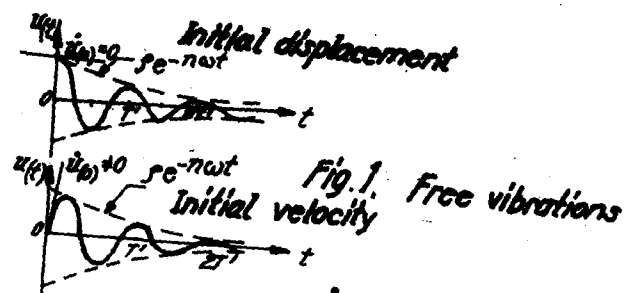
The author considers that the efforts for experimental investigations mentioned above must be continued and increased, because the dynamic testing of structures has made a great progress in the past years and this progress has to be accelerated.



## REFERENCES

1. Bilan, St., Cristescu, V. and Gernea, I. (editors): *Cutremurul de pământ din România de la 4 martie 1977*. Editura Academiei R.S.R., Buc., 1983
2. Bouwhamp, J.G., Kolleger, J.P. and Stephen, R.M.: *Dynamic Properties of a Twelve-Story Prefabricated Panel Building*. REPORT NO. UMR/NERC-80/29, Oct., 1980
3. Brech, J.T.: *Mechanical Vibration and Shock Measurements*. Bröel & Kjaer, Oct. 1980
4. Chopra, A.K.: *Dynamics of Structure*. EERI, Dec., 1980
5. Clough, R.W. and Pensen, J.: *Dynamics of Structure*. Mc. Graw Hill, 1975
6. Constantinescu, C.R. and Stancu, M.: *Dynamic Analyses of the Control Tower. "Portile de Fier"*. National Conference "Design, Construction and Assessment of Structures in Seismic Zones", Jassy, 13-14 Mai, 1983.
7. Constantinescu, C.R. and Stancu, M.: *Statistical Studies for the Prediction of Seismic Damage of R.C. Structures*. Proceedings-Eighth European Conference on Earthquake Engineering, Lisboa, 1986.
8. Crandall, S.H.: *Random Vibrations*. Prentice Hall, 1963.
9. Harris, C.M. and Crede, C.E. (editors): *Shock and Vibration Handbook* (translated into Romanian), Editura Tehnică, Buc., 1968.
10. Hudson, D., Keightley, W. and Nielsen, N.: *A New Method for the Measurement of the Natural Periods of Buildings*.
11. Ifrim, M.: *Dinamica structurilor și inginerie seismică*. Editura Didactică și Pedagogică, Buc., 1984.
12. Medvedev, S.V.: *Evaluation of Seismic Safety during Blasting Operations in Mines*. Bulletin of the ERI, Vol. 46, 1968.
13. Sandi, H.: *Elemente de dinamica structurilor*. Editura Tehnică, Buc., 1983
14. Sandi, H.: *UNIDO Report on the Mission to Mexico* (SI/MEX/85/8e4), 1986
15. Shah, P.C. and Udvardi, F.E.: *A Methodology for Optimal Sensor Locations for Identification of Dynamic Systems*. Transactions of the ASME, Vol. 45, 1978
16. Udvardi, F.E. and Jerath, N.: *Time Variations of Structural Properties during Strong Ground Shaking*. Journal of the Engineering Mechanics Division, 1980.
17. Vértess, G.: *Structural Dynamics*. Elsevier Science Publishers, Vol. 11 in the series of "Developments in Civil Engineering", 1985.

18. Wiegel, R.L.(coordinating editor); Earthquake Engineering. Prentice-Hall, Inc., Englewood Cliffs, N.J., 1970.
19. Yamahara, H.: The Dynamic Properties of Soil and Interaction Problems between Soil and Structure. Tokyo Japan, 1969
20. x x x Studii privind conlucrarea elementelor structurale și nestructurale. Experimentări. INCERC, Oct., 1984
21. x x x Studii privind comportarea diferitelor tipuri de construcții la acțiuni seismice, INCERC, June, 1987.



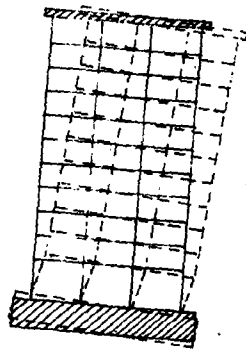


Fig. 7. Structural deflection of the model

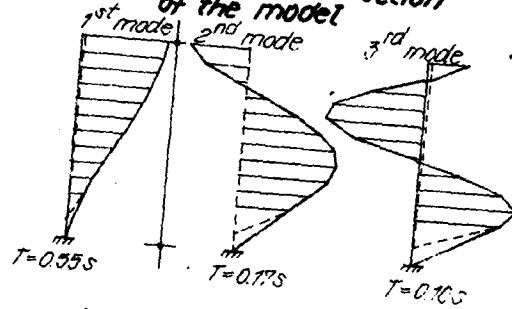


Fig. 9. Analytical mode shapes

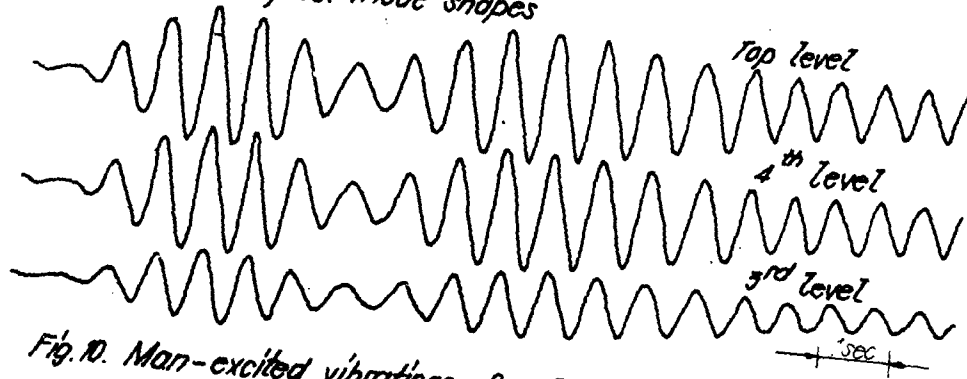


Fig. 10. Man-excited vibrations of a R.C. structure

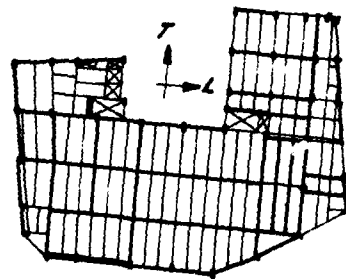


Fig. 11. Typical floor plan

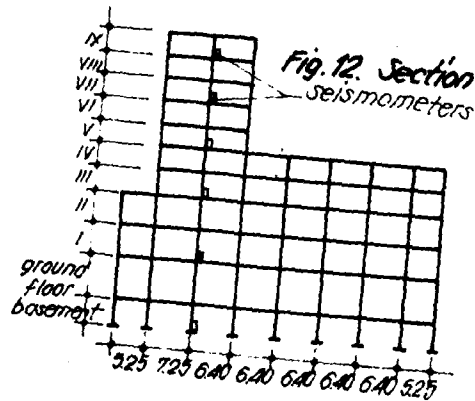


Fig. 12. Section

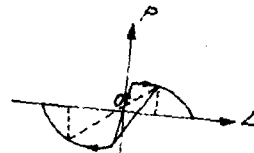
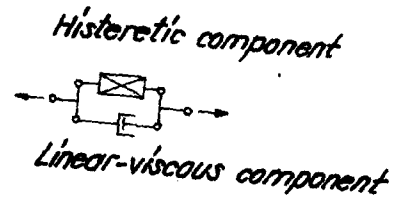


Fig. 8. Reological model assumed

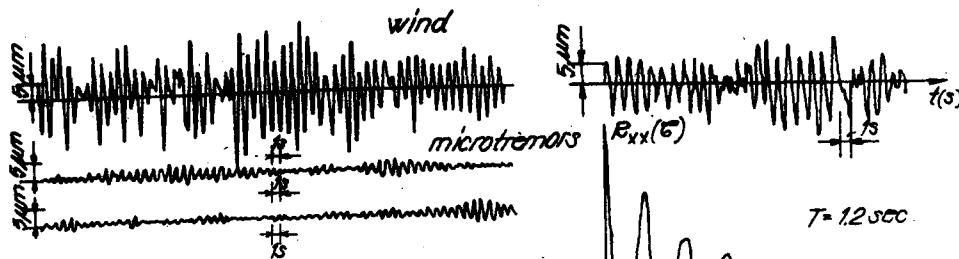


Fig. 13. Structural response due to wind and microtremors (transverse)

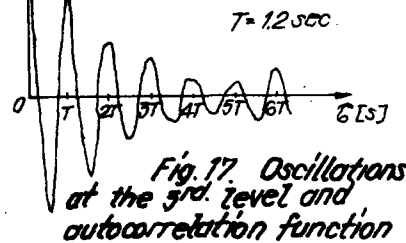


Fig. 17. Oscillations at the 1st level and autocorrelation function

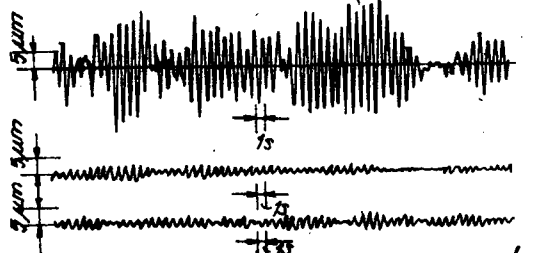


Fig. 14. Structural response due to wind and microtremors (longitudinal)

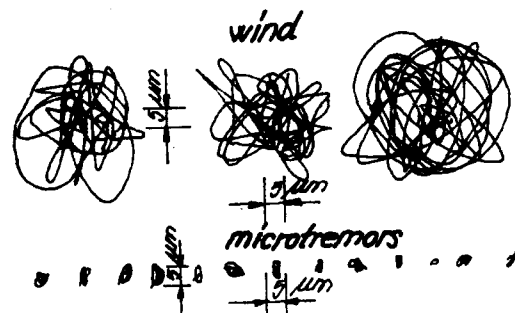


Fig. 15. Oscillations in horizontal plan

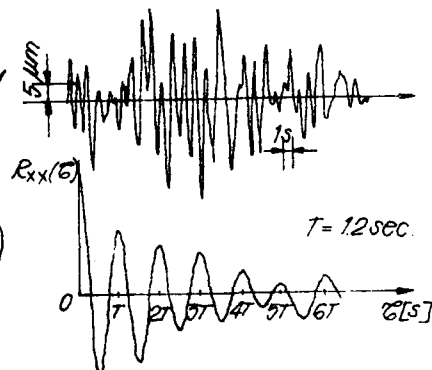


Fig. 18. Oscillations at the 5th level and autocorrelation function

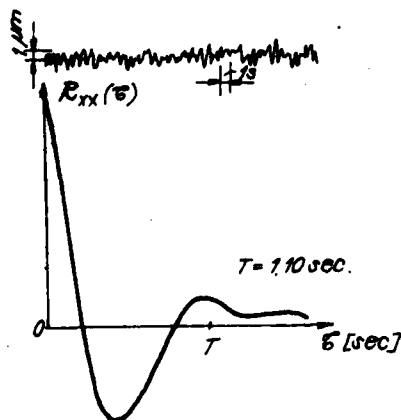
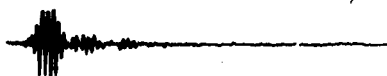


Fig. 16. Oscillations recorded at basement and autocorrelation function

Predominant excitation: air pressure



0 2 4 6 8 10 12 sec

Predominant excitation: ground motion

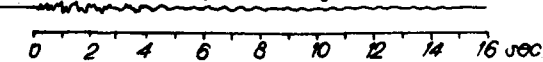


Fig. 19. Structural oscillations due to quarry blasts

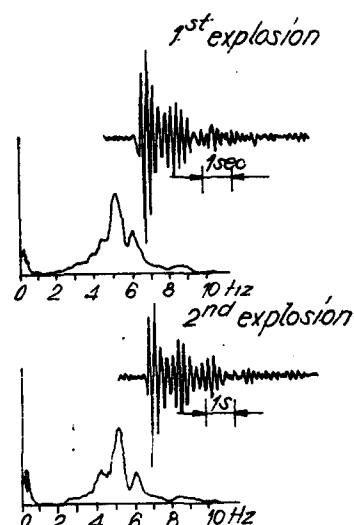


Fig. 20. Oscillations due to quarry blasts and Fourier spectra

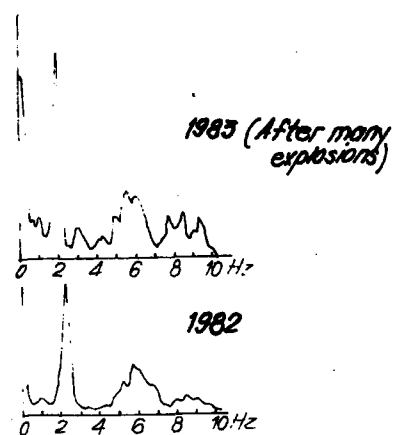


Fig. 21. Fourier spectra of oscillations due to microtremors

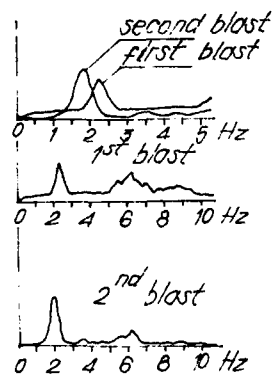


Fig. 22. Fourier spectra of oscillations due to quarry blasts

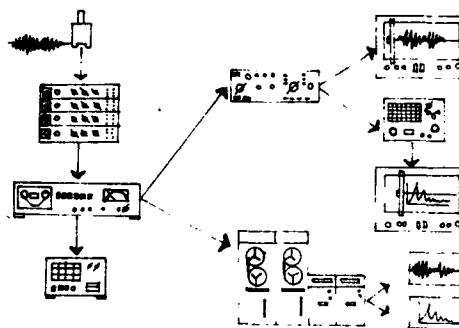


Fig. 23. Measurement set-up for ambient vibration tests.

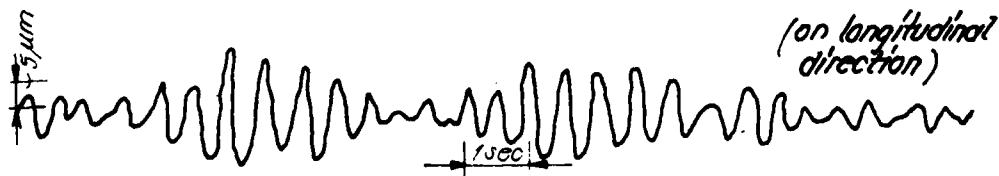
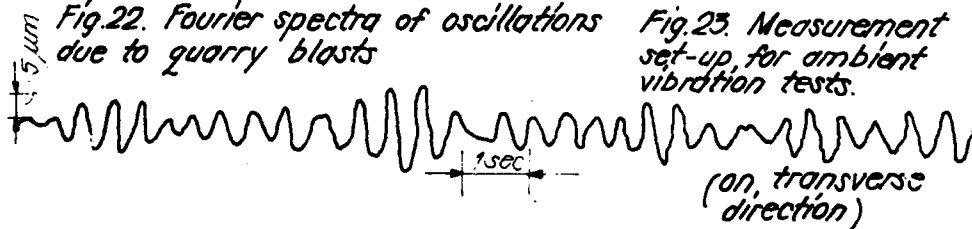


Fig. 24. Typical oscillations of a R.C. structure subjected to microtremors.

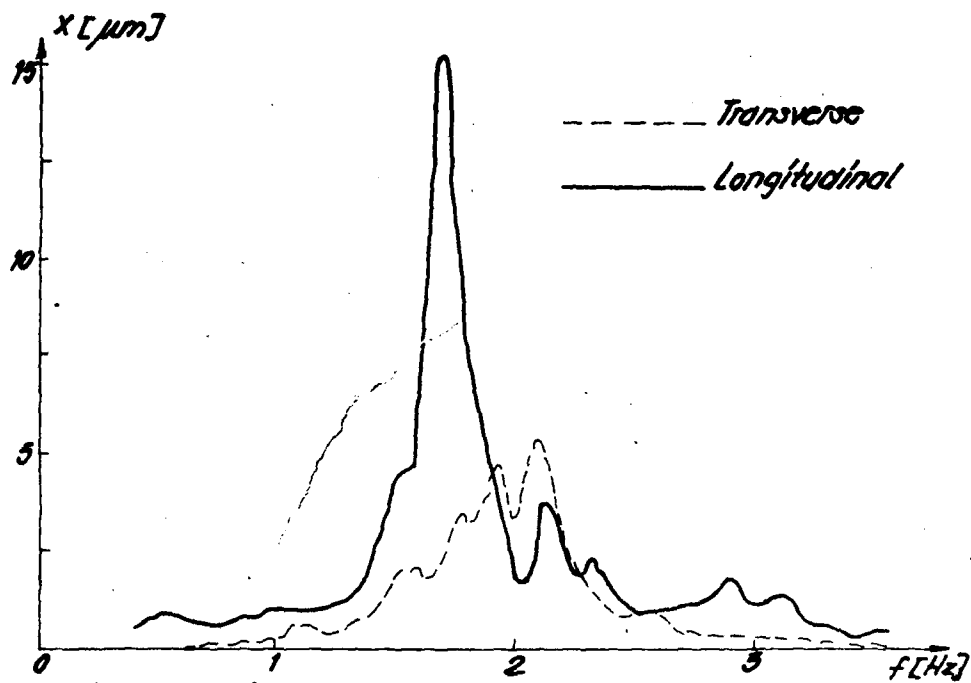


Fig. 25. Fourier spectra of structural oscillations

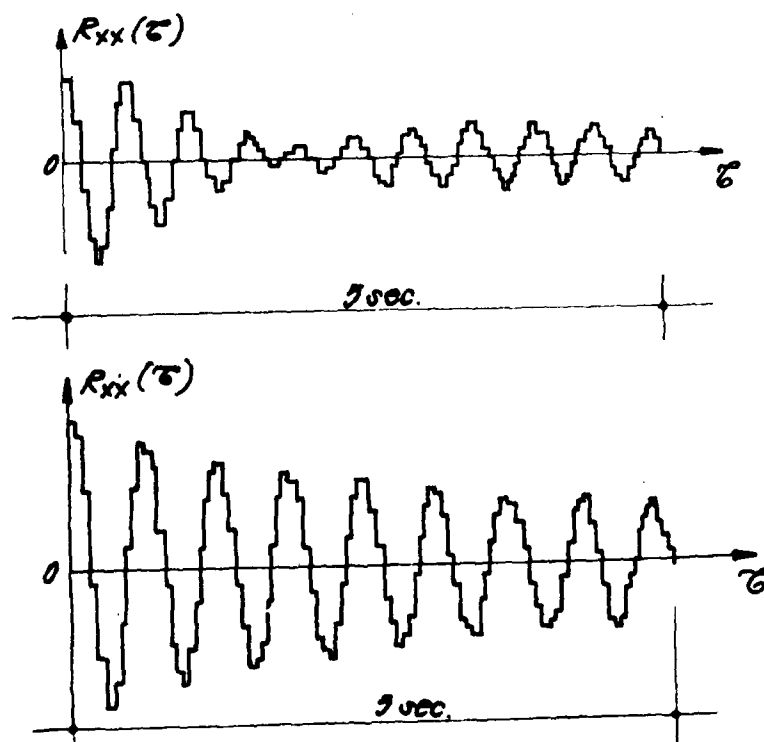


Fig. 26. Autocorrelation functions for the top level transverse and longitudinal oscillations.

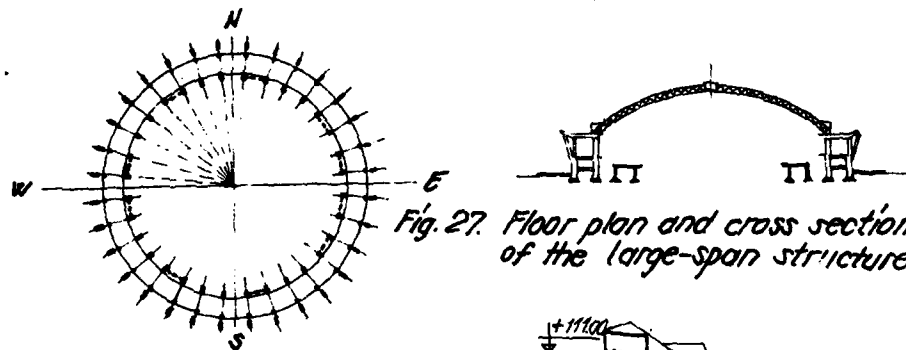


Fig. 27. Floor plan and cross section of the large-span structure

No	Test date	Natural periods (sec)			
		N-S	E-W	transverse	longitudinal
1	July 1976	0.60	0.60	0.41	0.35
2	March 1977	1.08	0.98	0.94	0.36
3	April 1977	0.78	0.74	0.48	0.37
4	Sept. 1982	0.77	0.72	0.48	0.37
5	July 1984	0.55	0.52	0.43	0.34
6	Sept. 1986	0.65	0.65	0.52	0.39

Fig. 28. Natural periods of the large-span structure

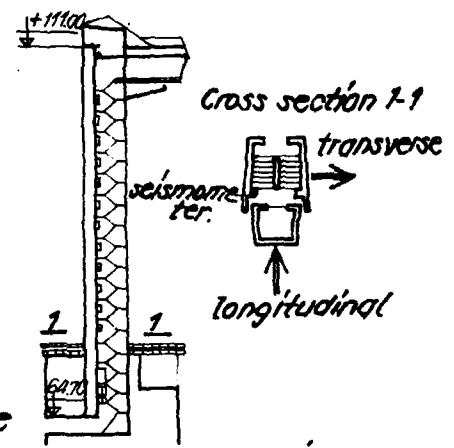


Fig. 29. Location of seismometers on "Portle de Fier" tower

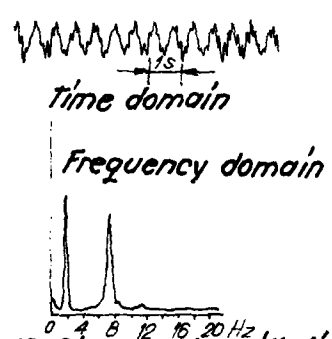


Fig. 30. Structural oscillations of the tower and Fourier spectrum.

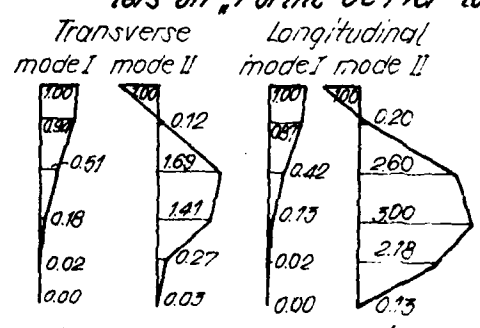


Fig. 31. Mode shapes of vibration (for the tower)

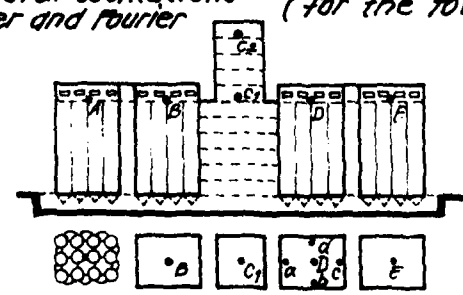


Fig. 32. Location of seismometers on a large capacity sylos



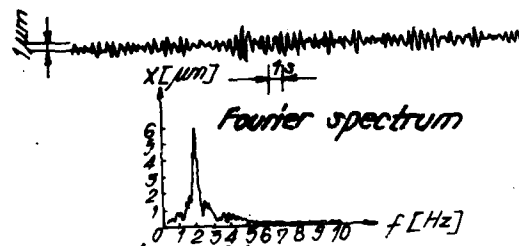


Fig. 33. Structural response of the system to microtremors

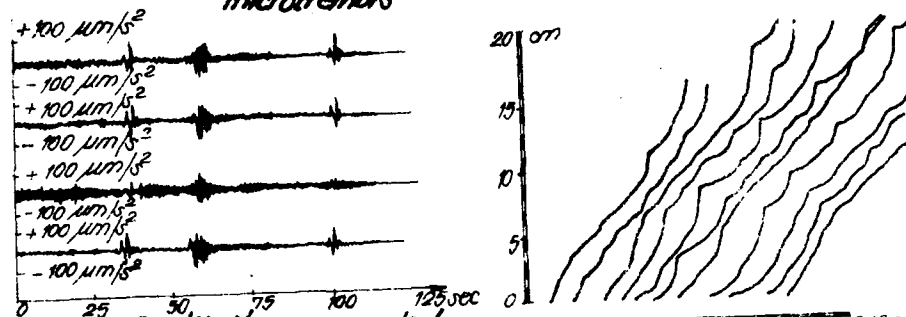


Fig. 34. Oscillations recorded during the translation (1<sup>st</sup> monument) and displacement vs. time record.

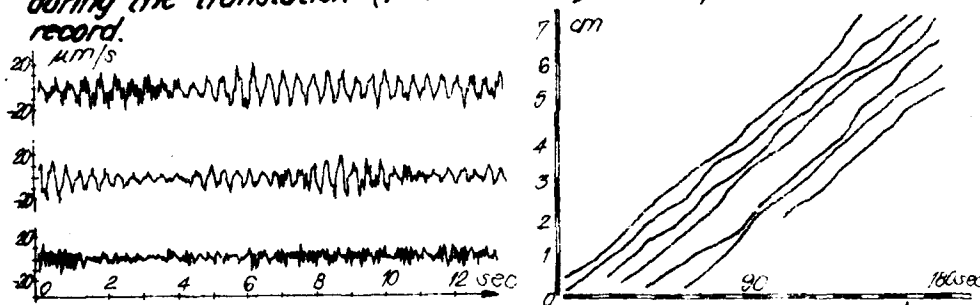


Fig. 35. Oscillations recorded during the translation (2<sup>nd</sup> monument) and displacement vs. time.

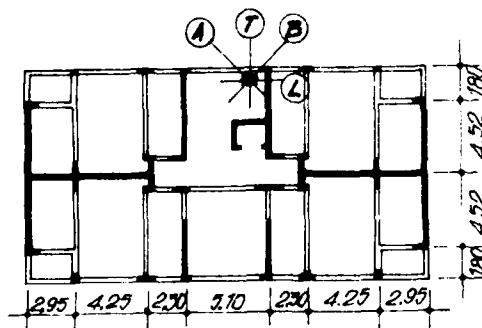


Fig. 36. Floor plan of a residential building



Fig. 37a. 4 March 1977 accelerogram (N-S component)

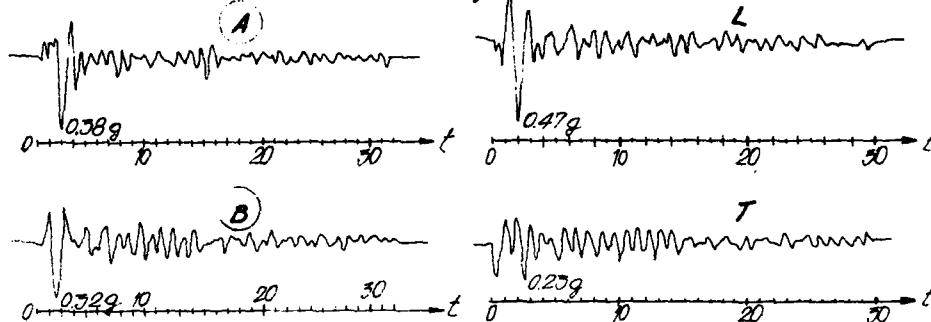


Fig. 37b. Response of structure at the top level.

Fig. 37c. Response of structure at the top level.

No	Excitation type	Natural periods (sec)	
		T	L
1	Microtremors before 4.03.77	0.53	0.43
2	4.03.77 Earthquake	0.90	0.82
3	Microtremors after 4.03.77	0.59	0.49
4	Microtremor after 31.08.86	0.60	0.52

Fig. 38. Natural periods of the building.

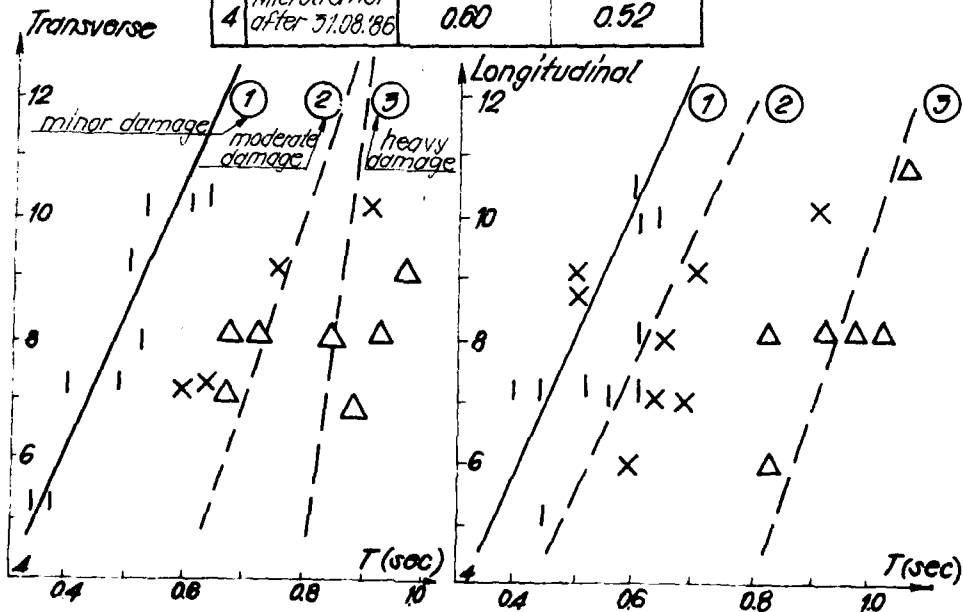


Fig. 39. Correlations between experimental data and observed damage

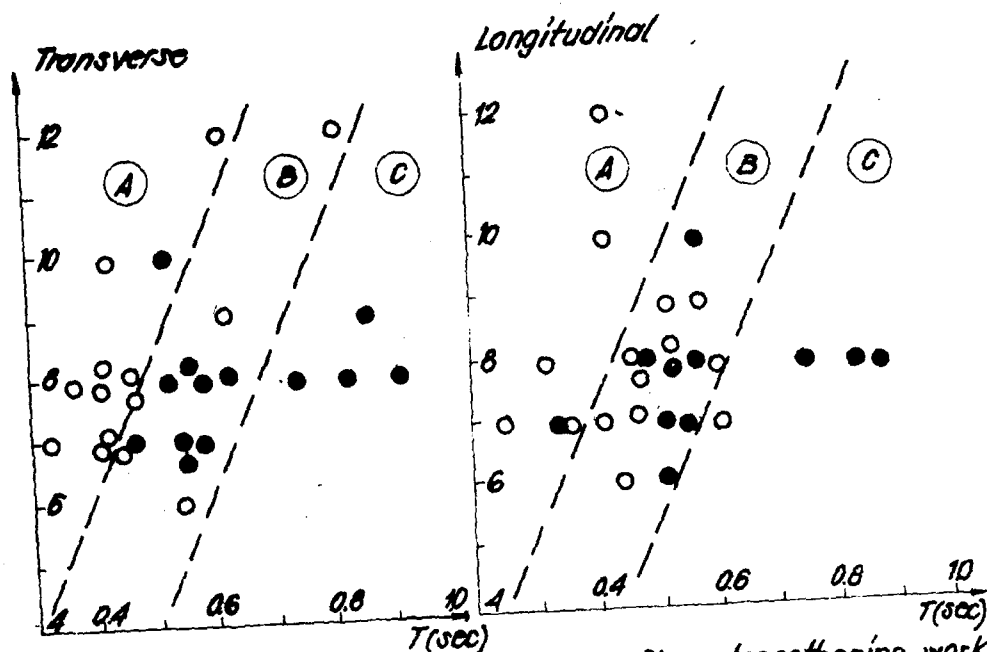


Fig. 40. Experimental data before and after strengthening works

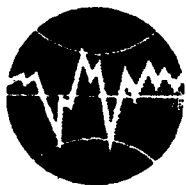
A - minor damage

B - moderate damage

C - heavy damage

● T before strengthening

○ T after strengthening



**TURKISH NATIONAL COMMITTEE FOR  
EARTHQUAKE ENGINEERING**

**THIRTEENTH REGIONAL SEMINAR ON EARTQUAKE ENGINEERING**

**September 14-24, 1987 - Istanbul - Turkey**

**United Nations Centre for Regional Development**

**Director  
Hidehiko Sazanani**

**Regional Development Planning for Disaster Prevention  
and International Cooperation**

**United Nations Centre for Regional Development**

**Director  
Hidehiko Sazanani**

## 1. Foreword

Human history has recorded many cases of natural disasters such as earthquakes, floods, high winds, volcanic eruptions, and the like, the consequence of which have sometimes been extremely serious, especially in urban areas with high population densities. In recent years, the general public has become increasingly concerned with this matter. It is high time, for both developing and developed nations, to start working to formulate more positive disaster prevention measures which consist not only of relief action but also of disaster prevention and mitigation considerations. Moreover, there is a rising interest among policymakers and planners regarding disaster prevention measures to be considered in the context of regional development planning and management. For this purpose, study and research concerning regional development planning focusing on disaster prevention and an introduction to new technology are essential. Particularly, there is a need to reconsider the existing legal and institutional aspects of disaster prevention, to analyse the principal measures concerning disaster prevention and relief actions within the policies of each nation, to study the methods and mechanisms of including disaster prevention in the process of regional development, and to seek for the possible measures to construct a human living environment more resilient to natural disasters. Presently, several international organizations are beginning work on such study and research work in respect to the prevention of natural disasters. In this regard, the United Nations Centre for Regional Development held an International Seminar on Regional Development Planning for Disaster Prevention, in September 1986.

Let me give you a brief introduction to the United Nations Centre for Regional Development (UNCRD). The Centre was created in 1971 as a field project of the United Nations, to promote regional development planning in developing countries.

The UNCRD's aims are: to serve as a training and research centre in regional development planning and related fields for developing countries who may wish to avail themselves of its services; to provide advisory services in regional development planning and related fields at the request of developing countries; to assist developing countries in promoting the exchange of data in regional development planning and related fields; and to assist and cooperate with other international organizations concerned with regional development planning and related fields. Throughout the sixteen years of UNCRD's existence, these aims have remained constant.

UNCRD's current projects are concentrated in the following areas: 1) Urban housing development (focusing on development strategies for metropolitan areas and on the strengthening of living environment management); 2) Regional management (focusing principally the strengthening of regional planning and management by legal autonomous governments); 3) Environmental management (focusing on the prevention of environmental degradation with reference to inland water management); 4) Regional disaster prevention (focusing on the strengthening of

local communities' capacity for disaster prevention); 5) Social development (focusing on the strengthening of social, economical, and administrative assistance to the poor); 6) Information system planning (focusing on the development of information systems for the regional community and the strengthening of planning and management systems); 7) Industry involvement and energy development (focusing on the improvement of local industry and its sustainability).

Among the seven areas listed above, item four, disaster prevention, constitutes an important domain in which our research and studies fully embody the Centre's objectives, as outlined previously.

The roving International Seminar on Regional Development Planning for Disaster Prevention was held in Nagoya, Shizuoka, and Tokyo, with each venue averaging an attendance of 250 participants. I would like to provide an outline of the major features of this Seminar in the following sections.

## 2. The International Seminar on Regional Development Planning for Disaster Prevention

### (1) The Background And Main Objectives of the Seminar

As mentioned in the previous chapter, the necessity of including disaster prevention and mitigation considerations in regional planning has become increasingly recognized in many countries, especially in the developing countries. Accordingly, the need to formulate development policies which are more responsive to disaster prevention and mitigation considerations, is gaining recognition. In disaster-prone countries, the integration of disaster prevention measures into comprehensive regional planning and resource management is desperately needed. The incorporation of disaster prevention measures into regional planning practices is intended to promote safer local communities. A philosophy of safety and securing is the fundamental prerequisite for maintaining and promoting communities development, as well as international peace.

It is worthwhile noting that in this respect, the International Seminar was held to commemorate both the United Nations International Year of Peace, and the fifteenth anniversary for the United Nations Centre for Regional Development.

The Seminar's objectives were to:

- 1) Serve as a forum for exchange of relevant experiences and ideas among policymakers, scholars, and planners, who are engaged in regional development planning for disaster prevention, and to promote greater understanding of common problems;

- 2) Review current approaches and practices in selected countries for promoting disaster prevention in the context of regional development planning management;

- 3) Investigate the ways in which regional development planning can contribute to disaster prevention and post-disaster rehabilitation/reconstruction;

- 4) Delineate, on the basis of seminar discussions, the policy issues as well as some prospective strategies for creating

urban and rural communities which are more resilient to disasters; and

5) Discuss future alternative approaches to regional development planning that will incorporate the need for comprehensive resource management and disaster prevention.

This Seminar was organized by UNCRD in collaboration with other UN organizations such as the United Nations Department of Technical Cooperation for Development (UNDTCD), the World Meteorological Organization, Food and Agriculture Organization of the United Nations, United Nations Educational, Scientific and Cultural Organization, United Nations Office of the Disaster Relief Coordinator, and the United Nations Centre for Human Settlements (HABITAT). Other collaborating agencies and organizations from Japan included the Ministry of Foreign Affairs, eleven other government organizations, five local government bodies, and two nongovernmental organizations.

## (2) Organization of the Seminar

The International Seminar on Regional Development Planning for Disaster Prevention had three plenary sessions held, respectively, in Nagoya, Shizuoka, and Tokyo, and three ancillary programmes (workshop, citizen's forum, and special programme) held in Tokyo. At each plenary session, a theme was allocated in view of the feature characterizing each region.

In Nagoya, the first plenary session was held under the theme of "Planning and Management for the Prevention and Mitigation from Flood and High Wind Disasters," as the Nagoya area is prone to serious damage of this type. Various disaster prevention measures, especially those to combat high tide have been implemented by national and local government in response to typhoons and high winds. The plenary session held at the Shizuoka part of the Seminar was held under the theme of "Planning and Mitigation for the Prevention and Mitigation from Earthquake Disasters" in view of the fact that various countermeasures for the potential Tokai Earthquake, including earthquake prediction measures, are currently being implemented because of the area's high hazard risk.

In Tokyo, the theme was "Planning and Management for the Prevention and Mitigation from Natural Disasters in Metropolises." Tokyo has suffered repeated damage from strong earthquakes, and is a high risk area where a strong earthquake is likely. There are many problems in the restructuring of Tokyo to transform it into a metropolis which is resistant to urban hazards. Various organizations are making endeavours which are worth examining. On the last day of the Seminar in Tokyo, a summary and a set of recommendations, synthesizing the findings from all three venues, were presented for discussion, and a declaration and a framework for action were presented. The declaration makes reference to the role of individual international organizations in the context of international collaboration in disaster prevention, and this paper will present the details.

In Tokyo, three ancillary programmes were held besides the plenary seminar: the Workshop, the Citizen's forum, and the



Special programme. In the Workshop, the professionals, specialists and allied experts who attended the seminar were given an opportunity to discuss disaster prevention and mitigation measures in the context of regional planning in depth. Three workshops were conducted on the themes which corresponded with the sessions in Nagoya, Shizuoka, and Tokyo. About 70 persons attended those workshops.

At the Citizen's Forum, under the assumption that an earthquake with an intensity of 6 has occurred in Tokyo, "Community and Disaster Prevention" was discussed with reference to reports from the public sector, the business sector and the private sector. Approximately 250 people attended.

Lastly, the Special Programme focused on Mexico and Colombia which suffered great damage as a result of disasters in 1985. With the attendance of several experts from both countries, the rehabilitation and reconstruction programmes and relief activities following earthquake disaster in Mexico, and the flood disaster following the volcanic eruption in Colombia, as well as potential problems arising from such disasters were discussed along with the presentation of detailed reports. About 200 persons attended this programme.

### (3) Contents of the Seminar

As to the detailed contents of the Seminar reference should be made to the summary of the proceedings already published, (Footnote 1). This paper will detail the contents of the discussions with respect to planning and management for the prevention and mitigation from natural disasters. The summary of the discussion was made with an emphasis on four broad action areas, (data base preparation, research, education and training, and implementation strategies).

#### 1) Data Base Preparation

Data is available through various means, but increased importance should be given to the effective and appropriate process and utilizing such collected data. Accordingly, it is necessary to identify existing data sources, analyse their content, and to fill in any gaps which may exist. Such data should take into account situation, specificity of type of disaster and hazard, the nature of the location, cultural factors which distinguish disasters, from one context to another. Such collected data should be viewed as a broad concept which embodies more than an accumulation of statistics and digital data. The past records of disasters, for instance, constitute a source of data both relevant and important for future disaster prevention. The collected data should be made available, at an affordable cost, to the countries in need of them, and then disseminated through mass media. In addition, it is necessary to prepare a widely accepted and understood set of terms for practical usage, which could be adapted to different languages. This would facilitate making the best use of available information on a shared basis. Also, in metropolitan areas, it was seen as vital to set up continual disaster warning systems and a mechanism for communicating information to users.

## 2) Research

The most important criterion for conducting research in any area should be its relevance to citizens' needs. There is a need to establish close cooperation and mutually supportive relations between producers and users of technological expertise. Also required are improved interdisciplinary relations and a close examination of regional and local conditions. As one means toward that goal, it is necessary to clarify terminology in related fields of natural disasters.

## 3) Training and Education

Training and education should be directed not only at researchers, scientists, and allied specialists to disseminate new methods and techniques, but also at politicians, planners, community leaders, and architects. It is necessary to anticipate the requirement for disseminating information to the public and to support the activities of universities and research institutes.

## 4) Implementation

In implementing effective data base construction, research, training and education programmes, international cooperation, both bilateral and multilateral, is necessary. Particularly required is the collaboration between the developing and the developed countries in working towards the development of new technologies which are both inexpensive and appropriate. Through dissemination of data and research, the developed countries should support the developing countries in reinforcing their technological and economical foundations towards disaster prevention. In implementing disaster prevention programmes, it is necessary to firstly understand the fact that an acceptable level of risk in any society is essentially a political decision, and then secondly, to work within these parameters.

To summarize, it was pointed out that further efforts are needed from UNCRD and other United Nations International Organizations, international organizations, and participating countries regarding how to integrate such disaster-related subjects as rescue, relief, rehabilitation, reconstruction and so forth into regional development planning. Also required are the collaboration and sharing of the burden on the public sector by private sector and voluntary organization, technological exchange through increase international collaboration between the developed and the developing countries. Moreover, it is vital for developing countries to share their experiences with each other.

## (3) Recommendations from the Workshop Sessions

The followings are the six recommendations which were extracted from the discussions during the Workshop Sessions.

1) It is important to promote international exchange and the sharing of information and experience. In this regard, it is proposed that an international network of institutions be established to facilitate definition of terms for mutual understanding; development of a data base; regular convening of

study meetings; and strengthening of international cooperation in disaster prevention and post-disaster rehabilitation and reconstruction.

2) An international centre needs to be established to promote research and development in the systems of disaster prevention and post-disaster rehabilitation and reconstruction.

3) In considering the problems and issues of disaster prevention, due attention should be paid to the cultural background of each region concerned. Past experiences for both success and failure should be fully taken note of in creating communities which are resilient to disaster and can recover speedily from their aftermath.

4) Dissemination of information, training, and education constitute an important area of policy action for ensuring that the public is well prepared in the event of disasters. In this connection, the collaboration of the mass media to facilitate fuller understanding of disasters and their impact is particularly called for.

5) Planning for disaster prevention with a balanced mix of amenity and safety factors needs to pay due consideration to cultural and social elements. Careful consideration is needed to ensure the smooth introduction and dissemination of new technologies in disaster prevention planning.

6) It is proposed that a specific year should be designated as the "International Year for Disaster Preparedness." This could be an integral part of the programme proposed for an "International Decade of Hazard Reduction."

#### (4) Recommendations

As a summary of the whole Seminar, a set of recommendations and a framework for action were presented. The recommendations are briefly outlined below:

1) the participants in the Seminar request that strong emphasis be given to the following points:

<1> There exists an urgent need to improve disaster mitigation and prevention in the context of post-disaster reconstruction, regional planning, urbanization, and economic development programmes;

<2> It is essential to harness the capabilities of science and technology to the task of mitigating and preventing natural disasters;

<3> To achieve the goals of disaster mitigation and prevention it is necessary to organize and support international collaboration among and between the producers and users of scientific and technical expertise, including the development and dissemination of appropriate technologies for disaster prevention and hazard reduction.

2) the concerned national governments are called upon to:

<1> Take steps to include disaster prevention components and actions in programmes of regional development;

<2> Promote the development and use of hazard assessment.

<3> Encourage the preparation and dissemination of public

disaster awareness information by the mass media and the educational institutions;

<4> Support the development of research and monitoring technology necessary for the attainment of disaster prevention goals;

<5> Prepare topographic maps for disaster-prone areas;

<6> Support and participate in the International Decade of Hazard Reduction (I.D.H.R.)

3) International organizations such as UNCRD are required to assist in the efforts towards disaster prevention in the following ways;

<1> To support the establishment of regional centres for training, research and development as well as extend and strengthen the existing centres;

<2> To ensure that adequate resources are available to assist nations in taking improved disaster prevention and mitigation measures as well as long-term reconstruction and recovery in the wake of major natural disasters;

<3> To support and assist the holding of regular international seminars to disseminate information about natural hazard prevention and to exchange experience and views on regional development planning for disaster prevention.

4) Scientific and professional organizations are required to work in the following ways;

<1> Develop systems for the sharing and supporting of data.

<2> Support and participate in assessments of natural hazard risk and vulnerability.

<3> Address more intensively the subjects of costs, benefits, and socioeconomic implications for hazard prevention and mitigation measures.

<4> Clarify terminology in natural disaster related fields and prepare guidelines for a more standardized vocabulary.

### 3. An International Decade of Hazard Reduction

#### (1) IDHR programmes.

An International Decade of Hazard Reduction was proposed by Dr. Press, Chairman of the U.S. National Research Council in his keynote address given at the eighth World Earthquake Engineering Conference held in San Francisco in July 1984. It is an international collaboration programme designed to mitigate the damage from natural disasters. At the International Seminar on Regional Development Planning for Disaster Prevention to which reference was made in the previous chapter, Professor James K. Mitchell of Rutgers University described the main points of the programme. In the declaration presented at the Seminar, national governments were called upon to support and participate in the IDHR programmes.

The programme's primary goal is to reduce future losses of life and property by encouraging the use of the best available hazard reduction information in decisions that affect areas at risk and to mitigate from the effects of damage caused by natural disasters during the last decade of the 20th century designated as an International Decade of Hazard Reduction.

The essential significance of the programme lies in the development of scientific and technological knowledge concerning natural disasters and their mitigation, and in the fostering of close collaboration and mutually supportive relationships among users. Accordingly, the focus of the programme is on the development and use of procedures for incorporating information about natural hazards into decisions about major investments in hazard-prone areas and especially in developing countries that have rapidly growing populations.

The proposed programme has four interrelated goals:

- 1) To increase awareness of natural hazards and of available means for hazard reduction among the populations of hazard-prone areas;
- 2) To increase knowledge about natural hazards and natural hazard reduction within the global scientific and engineering community;
- 3) To improve the exchange of information about natural hazard reduction among scientists, engineers, governmental bodies, developers, investors, public and private organizations responsible for hazard management, and the populations of hazard-prone areas;
- 4) To promote the use of hazard reduction measures and the evaluation of their effectiveness.

Some suggestions are offered concerning the first steps that should be taken in the development of this programme. Foremost among these are:

- 1) the suggestion that the programme might initially concentrate on the incorporation of information about natural hazards into major investment decisions in hazard-prone areas with rapidly growing populations; and
- 2) the suggestion that initial focus might be on the vulnerability of such rapid-onset events, such as earthquakes, floods, landslides, and severe windstorms.

Moreover, in launching the programme, two important tasks are required:

- 1) documenting and assessing existing collections of data that describe the global distribution of natural hazard exposure, vulnerability, and losses; and
- 2) collecting and evaluating existing information about past experience with loss reduction measures.

These tasks can be accomplished through the combination of research activities, the convening of workshops, conferences, and symposiums.

As previously mentioned, the International seminar on Regional Development Planning for Disaster Prevention extensively dealt with the above important subjects, and called upon national governments to promote the IDHR programme. In this respect, the Seminar may be regarded as the first international meeting which plays a role of disseminating IDHR on a global scale.

## (2) Japan's Role in the IDHR

In the wake of Dr. Press's proposal, a few individuals in Japan were sufficiently motivated to seek the ways of promoting the IDHR specifically within the realm of earthquake engineering.

Afterwards, the Disaster Engineering Research and Liaison Committee of Japan Scientific Council resolved to support the IDHR, which coincided with recognition of the importance of the IDHR proposal by the General Scientific Research Group for Natural Disasters organized by researchers into natural disasters. The parties collaborated in the establishment of a Japan IDHR Committee which intended to promote the IDHR programme in Japan.

In this regard, the IDHR is still confined to the academic sphere with little real discussions taking place or considerations being made about the IDHR among government organizations and other concerned organizations. At present, an investigation committee set up by the National Land Agency has started operation.

The IDHR related programmes in Japan are the following:

- 1) To invite Dr. Press, the proposer of the IDHR and to hold a seminar of administrators responsible for hazard management and researchers concerned with natural hazard reduction.

- 2) To establish a council comprised of national and local government bodies, research organizations, private corporations, and academic societies in order to unify connections and consultations concerning natural disasters.

- 3) To educate foreign students who are majoring in natural hazard study at research /educational organizations, and provide training to personnel at national and local government bodies and to administrators from abroad who are responsible for natural hazard reduction management.

- 4) To establish a standign international rescue organization for purposes of post-disaster rescue operation and reconstruction.

- 5) To promote the improvement of hazard related research and education and to extend and strengthen organizations in that connection.

- 6) To hold a regular national and international symposium for natural hazard reduction.

- 7) To construct a data base on an international scale concerning refernces and statistics regarding natural hazards.

- 8) To promote technological assistance with regard to natural disaster prevention and mitigation at an international level.

- 9) To apply high technology to disaster preveniton and develop its use for that purpose.

- 10) To promote international collaborative study of natural disasters with the consideration of specifying the type of disaster and the conditions in the respective country.

As for the first of the above items, UNCRD in collaboration with the oreviously mentioned Japan IDHR Committee is scheduled to invite Dr. Press to hold a roving lecture meeting on IDHR in Tokyo, Nagoya, and Osaka in October of this year.

In this connection, the International Research and Training Seminar on Regional Development Planning for Disaster Prevention is also scheduled to be held in October to coincide with Dr. Press's visit. There will be 15 administrators and researchers

concerned with disaster prevention participating in the seminar from abroad, and additional participants from concerned UN organizations are expected. This seminar is expected to be held annually so as to have discussions on various aspects of regional planning and disaster prevention.

### (3) The Role of U.N. Organizations

There are many U.N. organizations concerned with natural disaster problems. Accordingly, presented here are the major organizations and so of their activities regarding disaster prevention and roles in the promotion of IDHR.

a) As for UNCRD, its disaster prevention activities were mentioned in the first chapter of this paper. Its role in connection with IDHR are as follows.

- 1) To give priority to disaster mitigation in regional development planning;
- 2) To include disaster mitigation measures in medium and long-term comprehensive regional development planning;
- 3) To call to public attention in disaster-prone countries to the need for disaster mitigation measures;
- 4) To hold an international conference under the theme of regional planning for disaster prevention;
- 5) To conduct training programmes for disaster mitigation in regional development planning.

During the period of IDHR, promoted within the context of the United Nations, UNCRD will act as a participating organization, and particularly where developing countries are concerned in IDHR promotion, the Centre is expected to play a major role.

b) The disaster related activities of UNDP (United Nations Development Planning) are to be found in emergency assistance of a short-term perspective, and reconstruction of a long-term perspective. It will play the following roles in the context of the IDHR.

- 1) To call for the participation of participation of countries in the various IDHR programmes;
- 2) To develop and promote projects with feasibility for disaster mitigation in IDHR.
- 3) To establish a special fund for proliferating disaster mitigation projects during the IDHR.

In addition, UNDP will play somewhat similar roles to those of UNCRD's item 1-5. It will act as a leading organization in promoting IDHR within the realm of the United Nations.

c) UNEP (United Nations Environment Programme) is concerned with problems of desertification and floods in connection with disaster prevention, with an emphasis on man-made disaster rather than on natural disaster owing to its orientation around environmental planning. Besides playing a similar role to UNCRD, it works to raise funds in support of projects connected with mitigation within the context of the United Nations in promotion of IDHR.

d) UNCHS (United Nations Centre for Human Settlements) has, as one of its major projects, the matter of disaster prevention in the context of human settlements problems, and holds international conferences under such a theme. In supporting IDHR as a U.N. organization, it is expected to play a leading part in conjunction with UNDP while within the IDHR context, it plays a similar role to UNEP.

e) UNDRD (Office of the United Nations Disaster Relief Coordinator) is a major organization which takes charge of disaster relief in the system of the United Nations. The followings are its duties in IDHR.

1> To promote IDHR through international meetings and trainign courses;

2> To decide and link different UN strategies in disaster mitigation;

3> To establish a fund for a disaster mitigation trainings;

4> To proliferate an awareness of the need for including disaster prevention activities in regional development planning.

Hence it is expected to play the leading role in promoting IDHR within the United Nations, but its range of activities and funds are limited.

f) FAO (Food and Agriculture Organization of the United Nations) is concerned with disaster prevention from the viewpoint of disaster mitigation and rehabilitation in agriculture, and it develops and carries out a variety of projects in early disaster warning and mitigation. Accordingly, it is developing different types of disaster mitigation projects, operates an emergency relief programme and holds training courses which will be confined to the spheres of agriculture while participating in the U.N. promotion of the IDHR.

g) UNESCO (United Nations Educational Scientific and Cultural Organization) practices such disaster related activities as: building inspection of educational facilities in disaster-prone countries; holding of training courses supporting international meetings for and exchange of disaster-related information; and preservation of constructions of historical value. In the IDHR programme, it plays a similar role as UNDP, and in the UN, it is a leading organization in promoting IDHR.

h) The World Bank' primary role is to financially assist in various disaster prevention programmes. Within IDHR, it is expected to endeavour to reduce the debt burden of the disaster-prone countries, and to assist in providing opportunities for technological assistance in the integration of disaster mitigation measures into regional development planning when working as a part of the United Nations.

i) WMO (World Meteorological Organization), though not directly involved in the matter of disaster mitigation, is expected to make a contribution in technical improvement in the areas of disaster forecasting and prediction. It is as important



as UNEP in the IDHR programme and its promotion by the United Nations.

#### 4. International Cooperation: the present situation and future perspectives

##### (1) Emergency Relief System

Presently, an emergency relief system is being organized among international organizations and national governments of the developed and developing nations so as to facilitate the rescue and relief operations immediately after a disaster has occurred. Among the international organizations, the International Red Cross Society assists in the medical field, and among the U.N. organizations, UNDRD leads such activities. In addition, in different countries, emergency rescue groups are organized by experts from such institution as the fire services, the police, and medical agencies, and thence dispatched to the disaster stricken country.

Japan has an international emergency rescue system for which groundwork for its legal improvement is underway. It will enable experts to be sent to disaster afflicted countries through the Japan International Cooperation Association. It has performed nine rescue operations since the Mexico earthquake disaster which was the original stimulus for its organization.

##### (2) International Conferences

An international conference is a form of international cooperation. At the International seminar on Regional Development Planning for Disaster Prevention held by UNCRD to which references were made in Chapter 2, there was participation not only of professionals and experts from developed and developing countries, but also of administrators from national governments. The Seminar made a contribution in disseminating information concerning disaster prevention and promoting the exchange and sharing of knowledge and experiences of each participating country.

In Japan, the International Meeting on Volcanoes is scheduled to be held in Kagoshima, in July 1988, and in August of the same year, the World Earthquake Engineering Society is planning to hold its general meeting in Japan. Both conferences concern topics in which Japan has made significant advances in terms of its being a disaster prone country with a well-prepared anti-disaster system. This will therefore be an excellent opportunity to disseminate Japan's knowledge and to share experience concerning these areas. As for developing countries which have densely populated cities, an international meeting focused on urban disaster prevention measures (such as ways for a disaster-prone metropolis to implement its disaster prevention provisions) is being planned. Additionally, information presented at the abovementioned meetings focusing on different phenomena of disasters will be disseminated to a wider audience.

##### (3) International Training

International Training Courses are of necessity designed for the education of specialists in developing countries, and are

provided by UN organizations and other institutions. The Asian Disaster Preparedness Center at the Asian Institute of Technology (AIT) in Bangkok provides training for Asian countries in disaster management. Similar programmes are provided at the Cranfield Institute of Technology, England for African countries. In Japan, JICA training courses incorporate disaster-related activities as a Disaster Prevention Technology Seminar (held at the National Disaster Prevention Scientific Technology Centre) and seminars on seismology and earthquake engineering with respect to earthquake prevention (at the Construction Research Institute).

#### (4) The Future Activities of UNCRD

As a follow-up to the previously discussed Declaration and Framework for Action presented at the International Seminar on Regional Development for Disaster Prevention, the UNCRD Advisory Committee on Regional Development for Disaster Prevention was organized by the professionals who attended the Seminar, in order to seek ways of developing and implementing the abovementioned results. At present, UNCRD is working on the following areas:

- Preparatory work for the International Research and Training Seminar on Regional Development for Disaster Prevention which is aimed at realizing the results of research and study on disaster prevention in the form of human resource production;
- Groundwork for establishing the International Center of Regional Development for Disaster Prevention where training courses as well as data bank formulation and research would be carried out;
- Arrangement for annual experts' meetings to be held to complement the international seminar which is to be held quarterly;
- Supporting the promotion of IDHR in Japan and the developing countries;
- Cooperating with other international conferences held in Japan which deal with disaster prevention; and actively supporting the training courses and ongoing research projects with regard to disaster prevention.

In sum, UNCRD intends to positively cooperate with the Japanese government and other developing countries in the wide field of disaster prevention activities.

#### (5) Postscript

The rapid population increase and resulting influx into large cities in the developing countries is drastically increasing the risk to human life which natural disasters such as earthquakes, floods, high winds, volcanic eruptions, and the like constitute. The consequences of such natural catastrophes are particularly serious in the developing countries as was observed in the case of Agadir, Morocco, several years ago, and in the recent case of the Mexico City earthquake, or the mud flood disaster caused by the eruption of Nevado del Ruiz in Colombia. The international response to such natural disasters has been focused primarily on

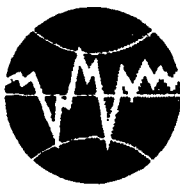
relief actions, the examples of which were seen in the responsive actions of Japan and other countries following the abovementioned disasters.

Nevertheless, complete prevention of disasters would seem impossible at present for the current state of science and technology, hence it has become widely understood that more importance must be attached to creating a system which will restrict damage and loss of life to a minimum in the event of a disaster. In addition, post-disaster rehabilitation and reconstruction measures are increasingly being seen as constituting preventative measures in the event of future disasters. Hence disaster prevention measures which incorporate rehabilitation and reconstruction are important tasks for all countries, both developing and developed.

Japan has become well-prepared in the event of natural disasters due to its repeated affliction by natural disasters since prehistoric times. It is therefore Japan's responsibility to offer and to share its accumulated knowledge of disaster prevention with other disaster-prone countries, particularly the developing countries with limited resources. This can be performed through the training of specialists and the reliable supply of essential materials.

#### References:

1. Report and Summary of the Proceedings of the UNCRD International Seminar on Regional Development Planning for Disaster Prevention, (UNCRD, 1987)
2. Fifteen Years' Progress in Regional Development, (UNCRD, 1986)
3. Basic Knowledge on the United Nations (Sekai-no-Ugoki-sha), (Dec. 1986)
4. On the International Decade of Hazard Reduction, (IDHR Committee, 1986)
5. The People of the UN System and the Decade (Advisory Committee for IDHR, 1987)



**TURKISH NATIONAL COMMITTEE FOR  
EARTHQUAKE ENGINEERING**

**THIRTEENTH REGIONAL SEMINAR ON EARTHQUAKE ENGINEERING**

**September 14-24, 1987 - Istanbul - Turkey**

**DAMAGING AND RETORING PROCESSES IN AN EARTHQUAKE: EVALUATION  
OF TIME-VARING EFFECT UPON HOUSEHOLD**

**Yutaka OHTA**

DAMAGING AND RESTORING PROCESSES IN AN EARTHQUAKE: EVALUATION  
OF TIME-VARING EFFECT UPON HOUSEHOLD

Yutaka OHTA

1. INTRODUCTION

In spite of recent development in regional seismic risk assessment, it is still far insufficient in several points. First, the disaster aspects or events considered are rather confined in the structural and other engineering facilities and are treated as if they are isolated. Second, most of the assessment has no clarity of description in which time phase risk evaluation was made. They are more or less "static". Numbers of published papers which concern the time-sequential changes of earthquake disaster aspects are made mostly in scenario writing method and thus far conceptual than our expectation. There are a few papers which study quantitatively the temporal changes of damaging or restoring events. The conducted are, however, at most on earthquake fire spreadings and life-line systems recoveries, and comprehensive consideration inclusive of all of major processes in an earthquake has never been made until now. As we have demonstrated in other papers all the phenomena in an earthquake are seamlessly linked and are ceaselessly changed. Our desire in seismic risk assessment is to estimate such causal and dynamic characteristics of earthquake disasters in an area and to connect to betterment of areal counter measures against earthquakes.

Desired ways of developing the areal seismic risk assessment in this point of view are to develop a methodology by which i) major damaging and restoring processes can be simultaneously treated, ii) descriptions can be made in dynamical (time-dependent) manner and evaluations are capable in quantitative manner. We attempt in this paper to explore such methodology, through an actual evaluation of "seismic effect upon household".

Incidentally, the seismic effects upon a household are innumerable and are incapable of counting all of them. So, an alternative and easy-capable method should be introduced. What we tried was to integrate various effects into one characteristic index in terms of "time-varying household's living standards". In this paper, after a brief explanation about a basic framework of approach, a provisional methodology for that objective is explained in relation with existing empirical relations and field data. In the latter part a case study for a hypothetical urban city in Japan, with a population of 1 million, are demonstrated.

-----  
Professor of Engineering Seismology and Earthquake Disaster  
Prevention Planning, Faculty of Engineering, Hokkaido University,  
Sapporo 060, JAPAN

## 2. METHODOLOGY AND BACK DATA

### 1) Conceptual understanding

Disaster aspects in an significant earthquake changes time-sequentially from damaging to restoring processes while giving various impacts on regional society, as shown schematically in Fig. 1. A household( equivalently to family ) is a socially fundamental unit in which people lives their life as a minimum community. In such a sense it is important to know how an earthquake affects upon a household. But, up to now no good way is developed among earthquake engineers, probably because of the difficulty and multiplicity in the problem.

In the field of sociology a term of "Living Standards of household" has frequently been used as an integrated and effective index for expressing in which state people are and for sounding the way of developing the family life. According to their explanation, it is composed of two major parts. One is the essential part for maintaining the minimal life of a family and the other the part for acquiring the better life. An earthquake, if occurred, may affect both of the above elements. But, in emergency case as an earthquake takes place, one can probably neglect the better life and the importance would be more on the maintenance of essential life of family members. From this point of view we pay much attention to the fundamental lives and attempt to measure the time-varying features of the fundamental living standards.

As for essential needs for such minimum maintenance of family life we consider four major factors. They are physical, commodity, family and economic factors. Damage to housing and life line systems are major items in the physical factors. Commodity factor relates to the shortage of foods and other daily goods. Most serious items in family factor are casualties in the members. Among various components of economic factor, various and extraordinary expenses would be of primary importance. In understanding that an earthquake all of these factors are more or less suffered, we attempt to measure them in quantitative ways. For that we should, first of all, frame a causal relation among the factors. Fig. 2 represents a short scenario adopted in this study. It is as follows; an earthquake, its severity being measured in terms of the seismic intensity, attacks an area and, bring various damage to dwelling houses, life line and other physical systems, while accelerating disasters by spreading fires, which cause human casualties on one side and shortage of commodities on the other side. Shifting from damaging stage to restoring stage it changes from physical to socio-economical features as rise of prices and extraordinary expenses for medical care and housing restoration etc. What we attempt first is to measure them in quantitative way and in a certain severity of seismic input, and second is to summarize all of them into an integrated index of living standards of the average household in the suffered area.

## 2) Quantitative evaluation of various factors

### a) Seismic intensity distribution in an area

A simple assumption is introduced that seismic intensity distribution in an area is mostly controlled by the ground soil types in the manner as shown in Fig. 3. It is to assume that there are 'm' soil types and each distribution in one soil type is approximated by an error function with the center intensity at  $[I_{in} + \Delta I_i]$  and with the standard deviation of  $[\sigma_i]$ , and to assume that the total distribution in an area is obtained as a summation of those of all soils. Here,  $I_{in}$  is the intensity on the reference soil. In the middle figure a schematic chart is illustrated for three soils. Provisional values are to be estimated in reference with the field data as shown in the bottom figure. One example is  $\Delta I = 0.8$  and  $\sigma = 0.25$  for deep alluvial soil,  $\Delta I = 0.4$  and  $\sigma = 0.25$  for thin alluvial soil in regard with the reference diluvial soil.

### b) Temporal characteristics of damaging and restoring processes

Preceded to the evaluation details of various factors it seems necessary to make clear the time-dependent characteristics of earthquake disasters and impacts. As has been known well, most of the physical damages as to dwelling houses and life line systems occur during seismic shaking or immediately after an quake and primary casualties follow, and continuously fire breaks may occur to spreading and to secondary casualties. Shortage of daily commodities, rise of prices and income cut etc are late coming ones. The latest impact is, within the scope of this study, the effect on the household economy. Time-dependent characteristic of all of them are briefly approximated by a simple curve starting from zero at a certain time delay from the earthquake occurrence, increasing toward the maximum value and decreasing toward zero gradually. From this consideration we assume the functional forms as shown in Fig. 4. The upper one is an equation for momentary damaging( or impacting ) rates and the lower one for cumulative rates. Corresponding curves are also in the figure. The constants, the delay time and the time toward the maximum( in momentary equation ) are adjusted in reference with the empirical data.

Also, we adopt the similar equations for restoring( or recovering ) processes in general. The significant difference from the damaging processes is the more importance of the delay time in the restoring processes. It is a matter of special mentioning that the delay time and consequently the time toward the maximum are heavily correlated with the disaster features as larger in severer situation. Time-dependent characteristics of each factor will be estimated in view of these general trends in damaging and restoring processes.

### c) Evaluation of physical factor

Considered items in this factor are damages to dwelling houses(

inclusive of household contents ) and life line systems, earthquake fires and so forth.

Dwelling houses We introduce a drastic simplification that the vulnerability characteristic of a house is, in relation of earthquake motions expressed in terms of seismic intensity,  $I$ , approximated by an error distribution function as

$$F(I; S_0, \alpha) = \frac{1}{\sqrt{2\pi}\alpha} \int_0^I \exp\left[-\frac{(I-S_0)^2}{2\alpha^2}\right] dI,$$

where  $F$  measures the severity of structural damage from 'no damage' ( $F = 0.0$ ) to 'collapse' ( $F = 1.0$ ), and  $S_0$  the structural strength at which  $F$  becomes 0.5 (moderate damage) and the nonuniformity of a structure by which the ductility characteristic would be evaluated. Since the most popular houses in Japan are of wooden frame and detached type, no other structural types are considered for simplicity. Based on the vulnerability curves in Fig. 5, Nos. of houses in classified damage levels can be estimated under a given seismic intensity distribution, by defining that collapse for  $1.0 > F > 0.8$ , heavy damage for  $0.8 > F > 0.4$ , partial damage for  $0.4 > F > 0.2$  and no damage for  $0.2 > F$ . No significant time delay is necessary to be introduced. The time toward the maximum would be enough at most 1 to 3 min.

The restoration details seem more complicated. According to our field survey (See Fig. 6) the delay and associated characteristic times are closely related with damage details such as the degree of damage and the total number of damaged houses in an area and etc, as being delayed in concordance to the severity of damage total in the area. Parameters controlling such delay should be incorporated in equations for restoring processes.

Life line systems Considered are interruption rates of Electricity, Water and City Gas supply systems. In this paper a rough translation of observed damaging rates of system itself to interruption rates of household is made. Fig. 7 shows a result of such translation. An inequality relation of Gas > Water > Electricity in the vulnerability characteristic seems plausible. Actual estimation of the interruption rates of the life line systems is to be made in corporation with the derived intensity distribution in the area. Damage to life line systems occur almost instantly. In contrast, the restoring processes are rather complicated. The delay and associated times toward the maximum are longest in Gas, medium in Water and shortest in Electricity and in 1 to several weeks. A field data from Sendai city (I<sub>JMA</sub> : 5.0 or higher) in 1978 Miyagi-ken-oki, north-eastern Japan, is referred in Fig. 8.

Earthquake fires If fires follow an earthquake the damaging processes change to the most serious and complicated ones in Japan. An empirical equation to describe No. of burnt houses



$$B = 0.0001 \times H^2 \times ( \rho / \rho_m )^a$$

is used. Hence B and H are Nos. of burnt and collapsed houses, and  $\rho$  and  $\rho_m$  are population densities of the suffered area and of the nationwide area respectively. The exponent 'a' is between 1/3 - 1/1.5 depending on several conditions. The delay and associated times seem to change from several min. to several hrs in relation with damaged area size and meteorological and other conditions. Fig. 9 is rare data in 1923 Kanto earthquake in Japan which shows a distribution of times until fire breaks. Restorations of burnt houses can be dealt similarly with those of collapsed houses.

#### d) Evaluation of family factor

One of the most serious earthquake disaster is doubtlessly to find injured and/or killed people in a family. Considered from this point are casualty occurrence and recovery by medical cares.

Casualty occurrence There are various empirical equations describing casualty occurrences in Japan. No. of deaths in collapsed houses is

$$D = ( 1/30 - 1/100 ) \times H$$

known as for an approximate estimation. Scatter of coefficients is mostly due to the various situation under which an earthquake attacks. No. of deaths in collapses and spreading fires is evaluated as

$$D = 0.5 \times H^{0.62} \times B^{0.34}.$$

Most simple relation of injuries vs. deaths is

$$D = ( 1 - 1/100 ) \times W.$$

Hence D, W, H and B are Nos. of deaths, injuries, collapsed and burnt houses respectively.

As for time dependency of casualty occurrence there are two aspects. One is the primary casualty due to structural and other mechanical damages. In this case casualties may occur almost instantly, although the time toward the maximum seems slightly longer than that of structural damaging process. The other one is that due to spreading fires. The secondary casualty occurrence process may go in parallel with that of fires and the delay and associated times as well. Fig. 10 is a good example to see how people were killed in an earthquake with large scale spreading fires. This is again the data from 1923 Kanto earthquake in Japan.

As for deaths there is no recovery at all in physical sense. A very limited treatment which can be done is to bury the bodies. Therefore for a family in which one or more members were taken off there might be no remedy, but we would like to believe a

mental recovery in a certain length of time. There is no longer delay time than several hrs for medical cares, but the necessary periods for recovery are aware of 1 - 2 weeks for light injuries and 1 - 3 months even in the moderate situation.

e)Evaluation of commodity factor

According to the field data in Japan the damaging details are roughly in parallel to that of structures, but the recovery for resupply of foods and other daily goods are much faster than in structural restorations. We take account of such characters into the equations for damaging and recovering process of commodities.

f)Evaluation of economic factor

There are so many items which may affect upon household economy. Some are income cut, rise of prices, extraordinary expenses for medical cares and housing and associated restorations. However, in Japan we know that the former two are not so serious even under the worst situation as in 1923 Kanto earthquake. Then the latter two are considered to be accounted for. Fundamental idea to evaluate economic factor is, after recounting them into monthly installment manner, to compare the extra ordinary expenses with the household's average salary.

Medical care etc For deaths the expenses for burial treatment should be prepared in the early stage after an earthquake. The cost would be around ¥500,000( \$3,300 ). Medical expenses and associated payment periods differ depending on the severity of injuries( or diseases ). For heavy injuries it may cost around ¥300,000( \$2,000 ) and 1 - 3 months, for light injuries around ¥50,000( \$330 ) and 1 - 2 weeks. We assume at calculation that the payments are to be made monthly in the period when the medical care continues.

Restoration of houses( inclusive of household contents) Similarly to the previous case the restoration costs and the necessary periods are closely dependent on the degree of structural damages and payment would be made by monthly installment system. It costs around ¥500,000( \$3,300 ) within 1 yr installment for partial repair, ¥2,000,000( \$13,300 ) by monthly installment in 5 - 10 yrs and ¥5,000,000( \$33,300 ) by monthly installment in 10 - 20 yrs. It is necessary to keep in mind that monthly installment in long period is to be computed at compound interest. Fig. 11 indicates a case study in 1983 Central Japan Sea earthquake on how much they payed for the restoration of houses.

3)Integration to fundamental living standards

In order to fulfill the major objective in this paper we attempt an integration of the above individual factors into one representative index. For that a consideration is necessary for weighting of all the evaluations of physical, commodity, family and economic factors. But in the present no objective method is established nor no consensus is existing on how to weight them.

So, in this paper an apriori assignment for weighting is made, which gives largest weight on physical factor, then moderate weight on family and economic factors, and smallest weight on commodity factor. Consequently, the fundamental living standards[ FLS ] we define is

$$\begin{aligned}
 [ \text{FLS} ] &= 1.0 - 0.3 \times [ \text{House} ] \\
 &\quad - 0.1 \times [ \text{Water} + 0.5 \times \text{Electricity} + \text{Gas} ] \\
 &\quad - 0.05 \times [ \text{Commodity} ] \\
 &\quad - 0.2 \times [ \text{Family} ] \\
 &\quad - 0.2 \times [ \text{Economy} ].
 \end{aligned}$$

### 3. EXECUTION OF TEST RUN

A test run was made for a hypothetical urban city in Japan, in order to examine the validity of the methodology and the derived sets of equations for damaging and restoring process and, if valid, to have a comprehensive understanding of seismic effects upon a household.

#### 1) Areal data and assumptions

Natural and social data on a hypothetical area are summarized in Fig. 12. In Japan urban cities with a population larger than 1 million are around 10 in number. So, the test run is for one of the major urban cities in Japan. Readers are requested to accept that, in order to avoid useless difficulties, an oversimplification is introduced in this test run, as all the dwelling houses are of wooden-framed structure and are homogeneously distribute in the whole area, and no areal distribution is considered except for soils, nor any effect from neighbouring areas is accounted for. Seismic input is measured in terms of JMA intensity with 2-3 significant figures and ranges I = 5.00 - 7.00.

#### 2) Evaluation of individual factors

##### a) Physical factor

Dwelling houses In Fig. 13 time-varying characteristics of damaging and restoring processes of dwelling houses are shown. The upper set of curves are for momentary numbers of [ collapsed + burnt - restored ] houses and the lower set for cumulative numbers. As is seen in these figures, the housing situation in an earthquake changes with the elapsed time following an earthquake occurrence. During shaking and immediately after a quake the collapsed houses increase rather explosively then in input intensities higher than 5.5 continues to be burnt out. Two peaks in the early stage in momentary curves express well such temporal variation. Dotted curves in the momentary figure show

the restoration processes. A general trend that the increasing number of damaged houses enlarge the time necessary for the restoration completion. Cumulative curves in the lower figure reflect well such restoration details. Cumulative curves in Fig. 14 were made to see the differences depending on the degree of structural damages. Partial or heavy damaged houses at  $I_{in} \approx 6.0$  are rather small in number in comparison with those at  $I_{in} = 5.75$ . Such is mostly due to if there occur large scale fire spreads or not. The bottom figure is for an integration of all the dwelling damages. This was made adopting a summation of

$$\begin{aligned} \text{Total damage} = & [ \text{collapsed} + \text{burnt houses} ] \\ & + 1/2 \times [ \text{heavily damaged houses} ] \\ & + 1/4 \times [ \text{partially damaged houses} ], \end{aligned}$$

and will be a principal part of evaluation of the living standards.

Life line systems Three sets of figures in Figs. 15 - 17 are results for electricity, water and gas supply interruption and their restoration. The general tendencies are similar to those in dwelling houses, except that latter being much quicker. Here, no consideration of effects due to fires was taken into account. Fig. 18 is illustrated for integrating the effect of individual supply systems. The adopted relation is

$$\text{Total effect} = 1/2 \times [ \text{Electricity} ] + [ \text{Water} ] + [ \text{Gas} ],$$

which suggests less effectiveness of the electricity interruption on the household.

Casualties Fig. 18 shows time-varying features of death occurrence. Deaths are dominant in spreading fires at higher intensities than 5.5. In this figure a apparent recovery is considered from mental point, but we must keep in mind that physically there is no recovery at all. An example of summation procedure at  $I_{in} = 6.0$  is shown in Fig. 19 among different degree of casualties. The weighting relation is again

$$\begin{aligned} \text{Total casualty} = & 1/4 \times [ \text{Light injury} ] + 1/2 \times [ \text{Heavy injury} ] \\ & + [ \text{death} ]. \end{aligned}$$

Commodities and extra expenses Effect on commodities shown in Fig. 21 was calculated in an assumption that the damaging process is in proportion to that of dwelling houses but restoring process is much quicker. The lower figures are for extra expenses. It is well seen that expenses for housing restoration are larger and continue longer until several or more yrs. The total in extra expenses is a simply summation between medical care and housing restoration.

3) Integration toward the fundamental living standards

Living standards in general Based on the previously derived weighting relation an integration toward the time-varying evaluation of the fundamental living standards was conducted. Fig. 22 is an example at intensity 6.0. The upper five curves are for physical( housing and life line systems ), family , commodity, economic factors, and the lowest curve is the one which we wanted to arrive at. The derived living standards are interpreted as the ones for the average household in the suffered area. Fig. 23 summarizes the total features of the living standards in an input intensity range of 5.0 - 7.0. By taking a look at this we understand easily how the living standards in household unit changes temporally as a sharp drop immediately after an earthquake and very slow recovery toward the prior level and as strong dependency on the severity of seismic input as well as areal and social conditions under which people live. A significant gap between 5.75 - 6.0 correlate well with the additional disasters due to earthquake fires. Earthquake fires become dominant above 6.0 in the intensity. It seems to take at least a time length of several yrs to regain the living standards before earthquake.

Simple parameter analysis A few sensitivity analyses were made to see what factors affect significantly on the living standards. Examined are the structural strength of dwelling houses and the population density in the area. Fig. 24 shows the results for various structural strengths in 6.0 - 6.5. The top figure is for the damaging and restoring process of houses in different strengths and the middle one for the deaths. The bottom one illustrates the development of the living standards with increasing structural strengths. These are the case at input intensity 6.0. As far as these figures concern the seismic reduction seems remarkable. Another case examined is to change the population density( See Fig. 25 ). The originally adopted density of 5000 persons / km<sup>2</sup> is an average in major cities in Japan. It was decreased in this parameter analysis down to the average density, 300 persons / km<sup>2</sup>, of the whole Japan. There seems significant changes in disaster features below 3000 persons / km<sup>2</sup>. To consider that the parameter of population density is employed as a good substitute for the concentration rate of dwelling houses, one can understand that seismic reduction with decreasing densities results from lesser probability of fire spreads in an earthquake. In Japan this would be very important, because many of dwelling houses are wooden-made. From this kind of analysis we may explore better countermeasures for diminishing earthquake disasters.

#### 4. CONCLUDING REMARKS

In this paper we attempted to develop a way of describing in the time domain the damaging and restoring processes in an earthquake, paying a special attention to disclose the seismic effect upon household. The obtained results and the issues that follow are summarized.

1. Time-varying characteristics of the fundamental living standards of household was evaluated in simultaneous consideration of damaging and restoring processes. Results that seismic impacts on household continue longer than several yrs suggest the necessity of paying more attention to socio-economic aspects of earthquake disasters. Estimation of areal activity standards might be an important problem to be made in the next.

2. A case study in this papers is for Japan. Similar but more advanced test runs are recommended to be performed in every earthquake country, since disaster sequences after an earthquake are different from Japan and since we believe that understanding of seismic effects in this approach will be sure to give fresh ideas for earthquake disaster reduction policies.

3. Methodology introduced here is so simple that more development is necessary. One probable way is to revise this so as to fit for "Urban System Dynamics", primarily proposed by Forester of MIT. Another importance is to conduct long-term field surveys as well as immediate reconnaissances in suffered areas due to an earthquake.

Finally, I would like to express my sincere thanks to the members of the Chair for Engineering Seismology and Earthquake Disaster Prevention Planning, Dept. of Architectural Engineering, Hokkaido University, Japan, who assisted me very much in the course of this study.

#### 5. REFERENCES

- [1] Bolin, R. C., 1982, Long-term family recovery from disaster, Inst. Behavioral Sci., Univ. of Colorado.
- [2] Ohta, Y., 1985, An evaluation of regional seismic risk potential in Japan as emphasized on disaster sequences, Natural Disaster Science, 7, 95-111.
- [3] Ohta, Y., 1986, Earthquake casualty in rural houses: mechanism and assessment, Proc. Earthern and Low-strength Masonry Bldg in Seismic Areas, 681-699, Ankara, Turkey.
- [4] Coburn, A. W., 1986, Relative vulnerability assessment, submitted to Proc. for 8th European Conf. Earthq. Engr., Lisbon, Portugal.
- [5] Kawasumi, H., 1954, Intensity and magnitude of shallow earthquake, Bureau Central Seism. Intern., Ser. A, Trav., Sci., 19, 99-114.
- [6] Ohta, Y., 1983, An empirical construction of equations for estimating number of victims as an earthquake, Bull. Seism. Soc. Japan, Ser. II, 36, 463-466.
- [7] Ohashi, H. and Y. Ohta, 1985, A household survey on damaging and restoring processes due to the 1983 Central Japan Sea earthquake, Bull. Seism. Soc. Japan, Ser. II, 40, 39-50.
- [8] Okada, S. and Y. Ohta, 1986, Factor analysis on earthquake disasters and restorations in municipal unit, Jour. Struct. and Constr. Engr., 361, 60-67.

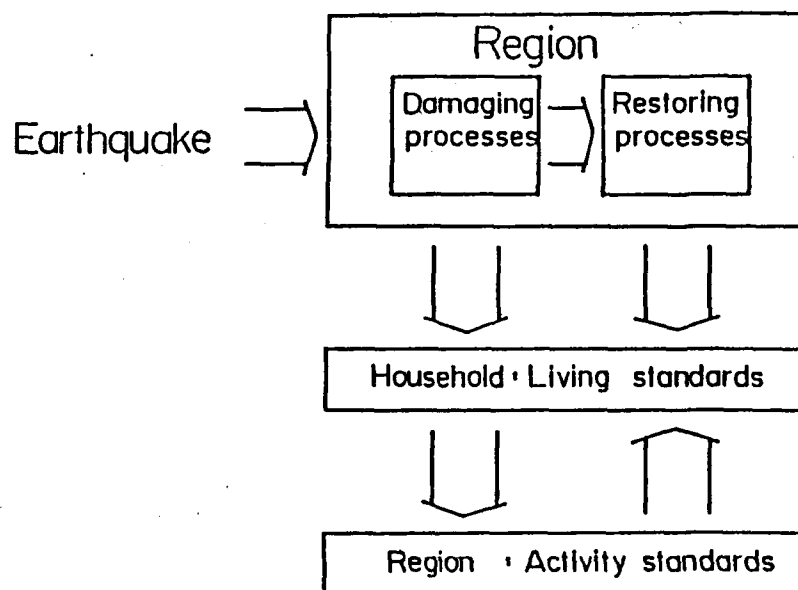


Fig. 1 Schematic diagram showing seismic effects on a region.

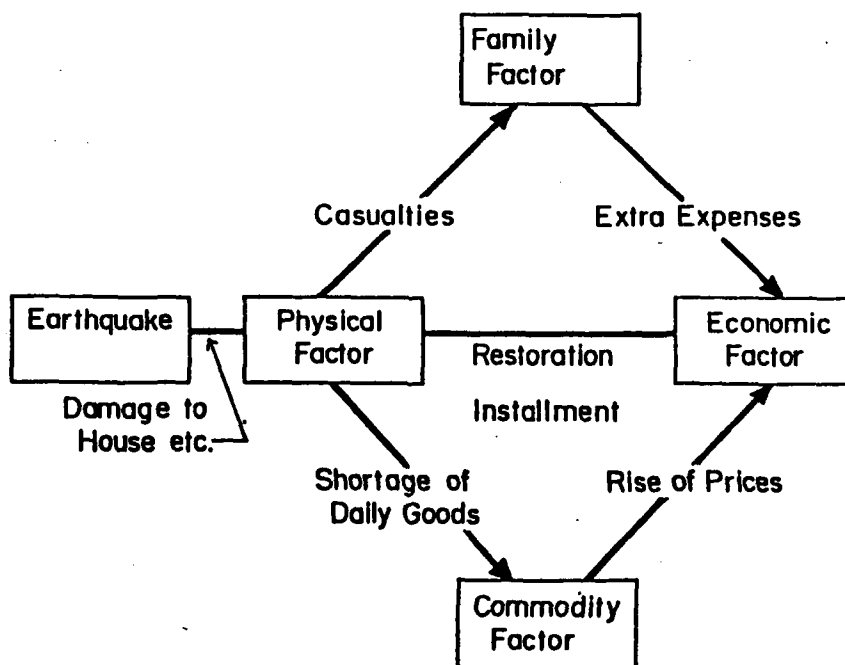
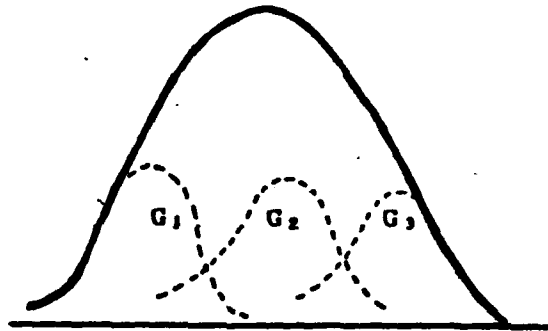


Fig. 2 Controlling factors on household's living standards and their causal relation.

Given intensity =  $I_0$  on reference soil  $G_1$

Soil type		$G_1$	$G_2 \dots$	$G_1$	.....	$G_n$
Intensity	Increment	$\Delta I_1$	$\Delta I_2$	0	.....	$\Delta I_n$
	Standard deviat.	$\sigma_1$	$\sigma_2$	$\sigma_1$	.....	$\sigma_n$



Seismic Intensity

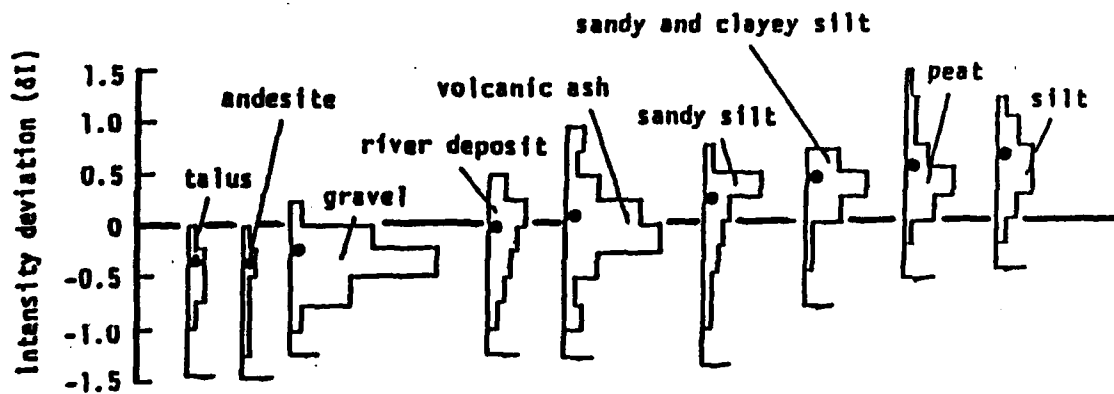


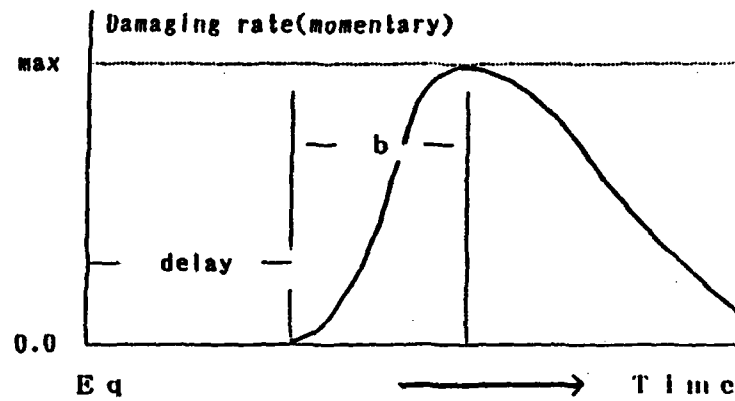
Fig. 3 A simple evaluation of seismic intensity distribution in an area.



Functional form in general: damaging processes

1) Momentary equation:

$$P_m = \text{const} \cdot t \cdot \exp[-t/b]$$



2) Cumulative equation:

$$P_c = \text{const} \cdot \int_0^t t \cdot \exp[-t/b] dt$$

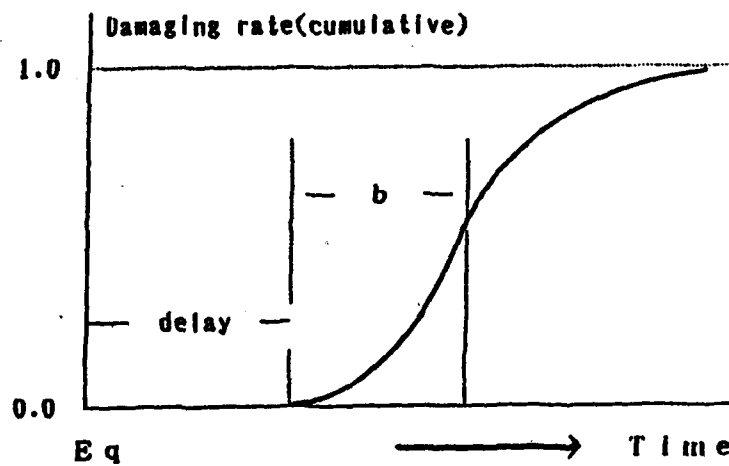


Fig. 4 Functional forms for describing damaging processes.

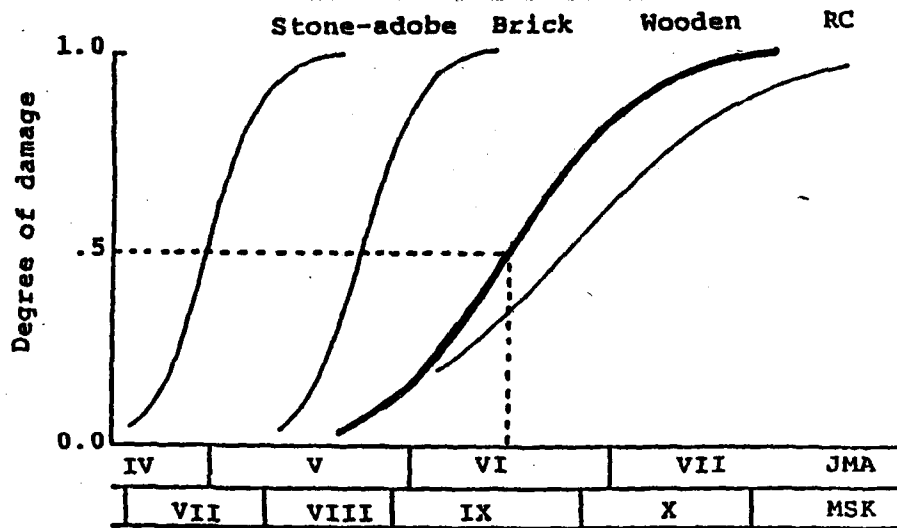


Fig. 5 Vulnerability function of wooden structure (other structural types are referred for comparison).

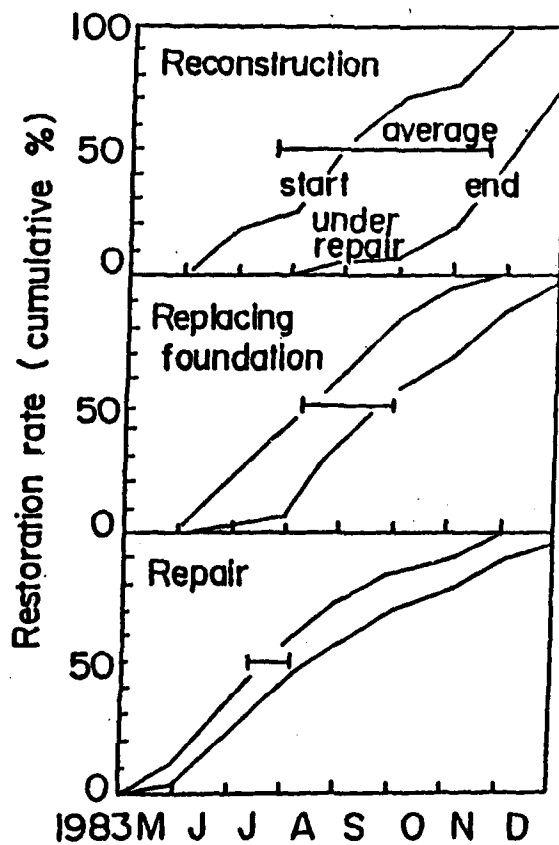


Fig. 6 Field data showing restoring processes of dwelling houses.

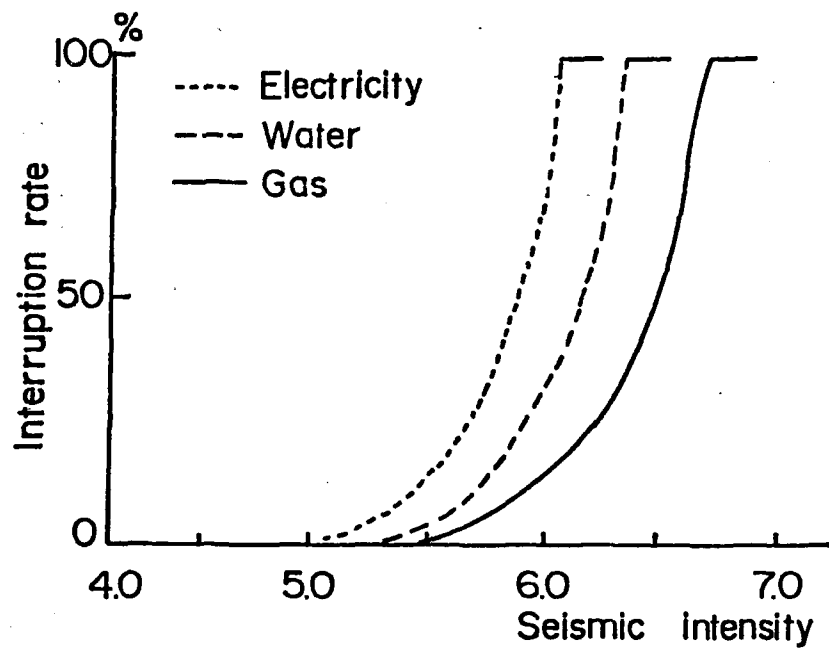


Fig. 7 Vulnerability functions of life line systems in terms of interruption rates.

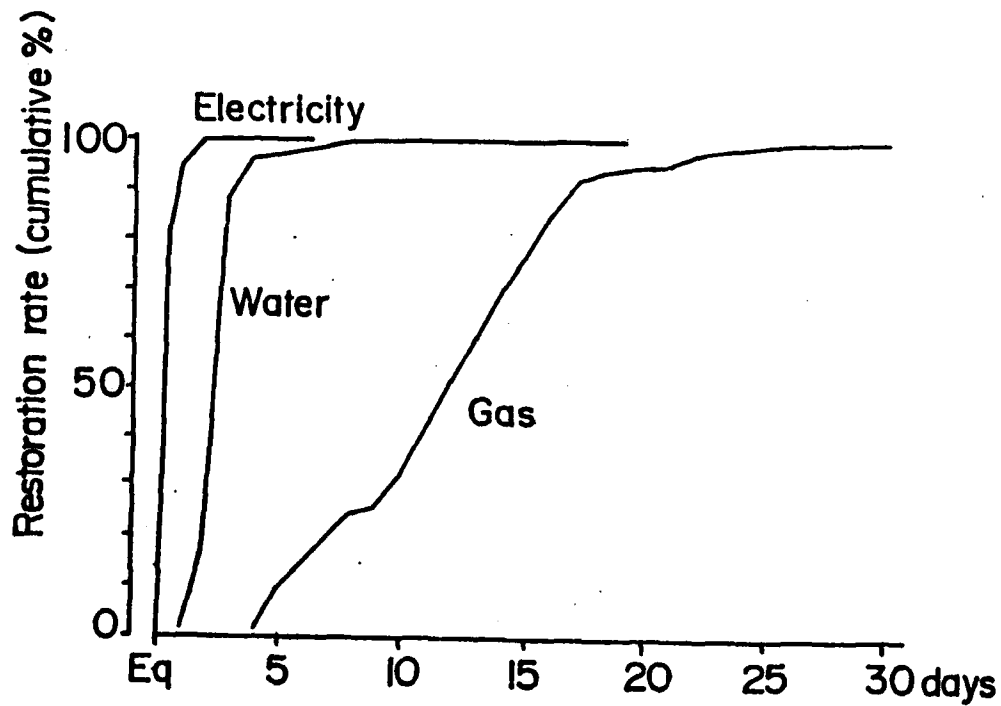


Fig. 8 Field data showing restoring processes of life line systems.

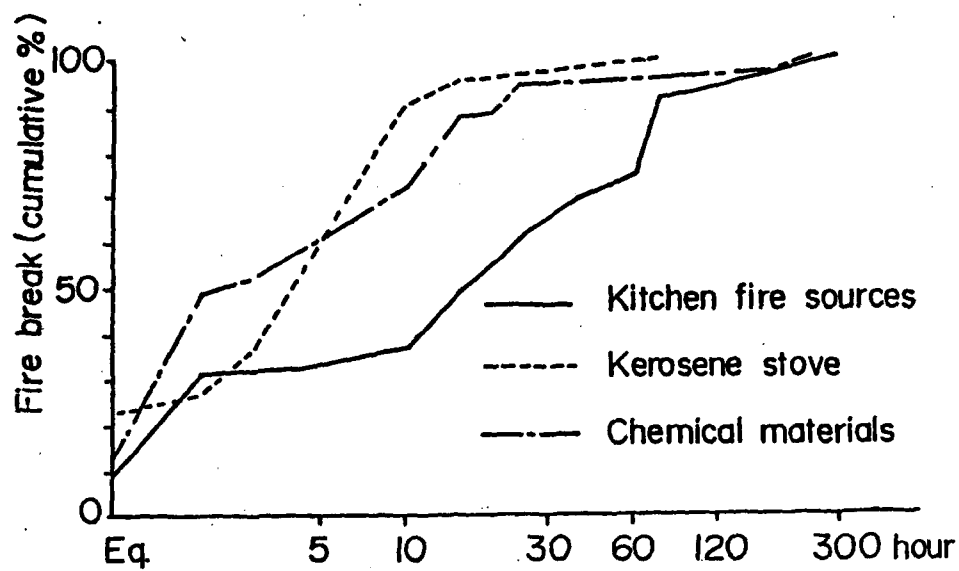


Fig. 9 Field data showing fire breaks by different sources.

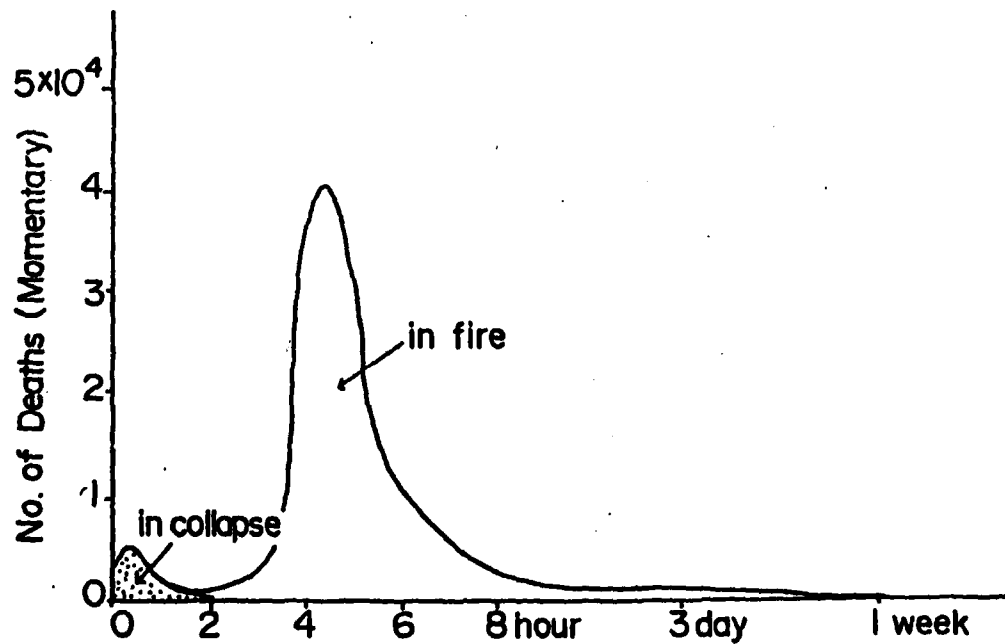


Fig. 10 Field data showing time-varying occurrence of deaths in an earthquake with large scale fires.

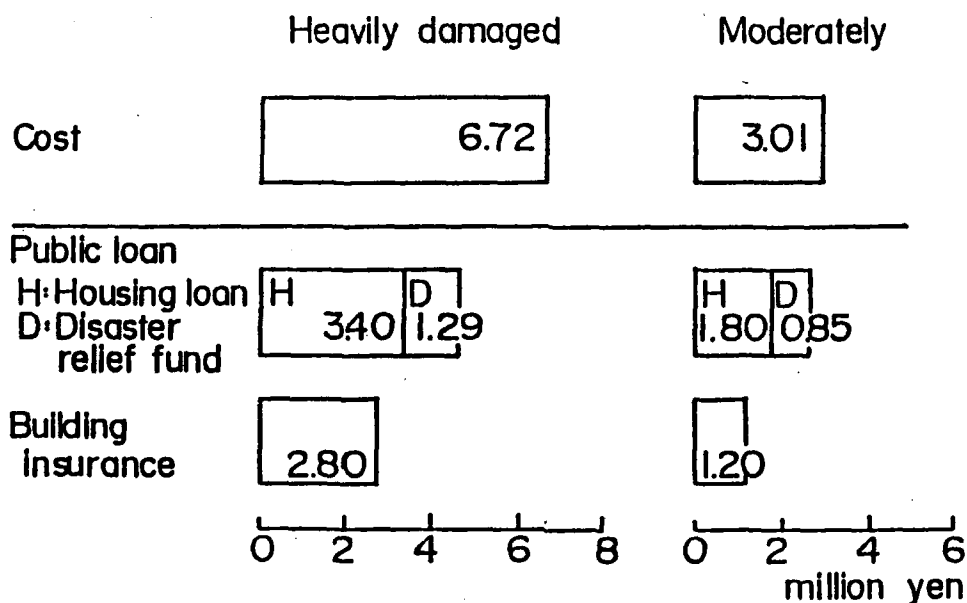


Fig. 11 Field data showing monetary balance in regard with restoration of dwelling houses.

## Hypothetical Area

### Medium-size urban city

Population :  $1 \times 10^6$   
 No. of household :  $200 \times 10^3$   
 Density :  $5 \times 10^3$  persons / km<sup>2</sup>

### Soil condition

Diluvial zone : 30%  
 Alluvial zone : 30%  
 Thick alluvial + reclaimed zone : 40%

### Dwelling houses

Wooden-framed structure with average strength  $S_0 = 6.0$

### Seismic input

5.0–7.0 (JMA Intensity)

Fig. 12 Natural and social data of a hypothetical urban area.

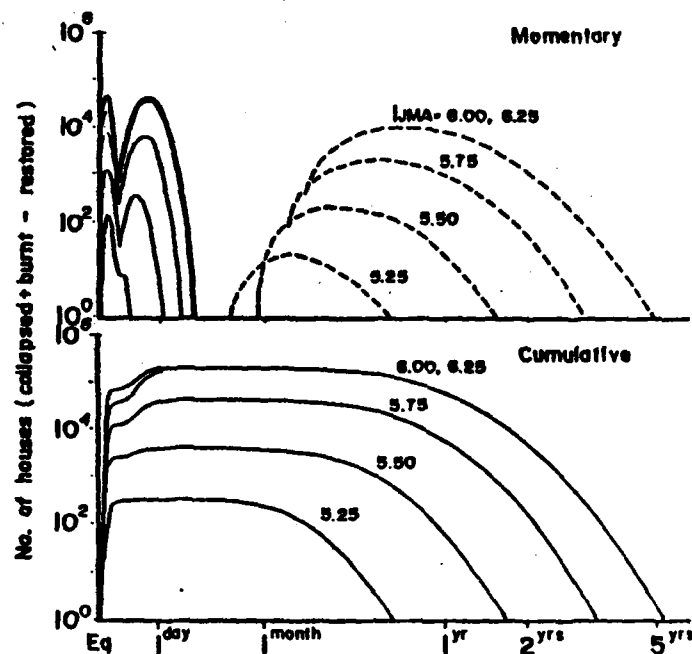


Fig. 13 Time-varying features of dwelling houses from collapsing and burning to restoring (momentary and cumulative).

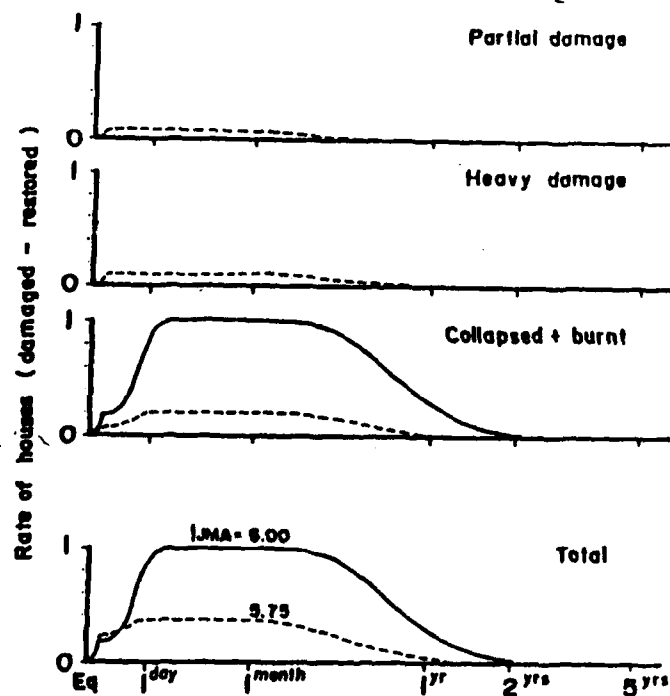


Fig. 14 A summation of damaging and restoring processes of dwelling houses.

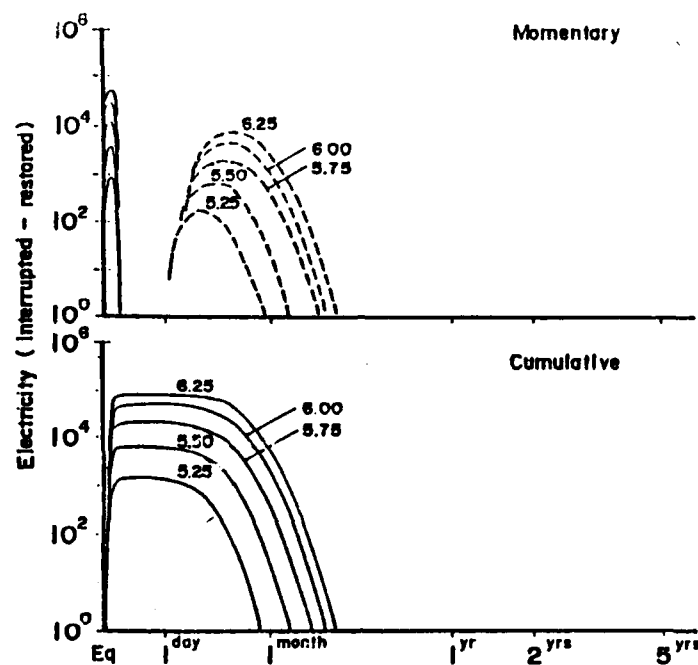


Fig. 15 Time-varying features of life line systems (electricity).

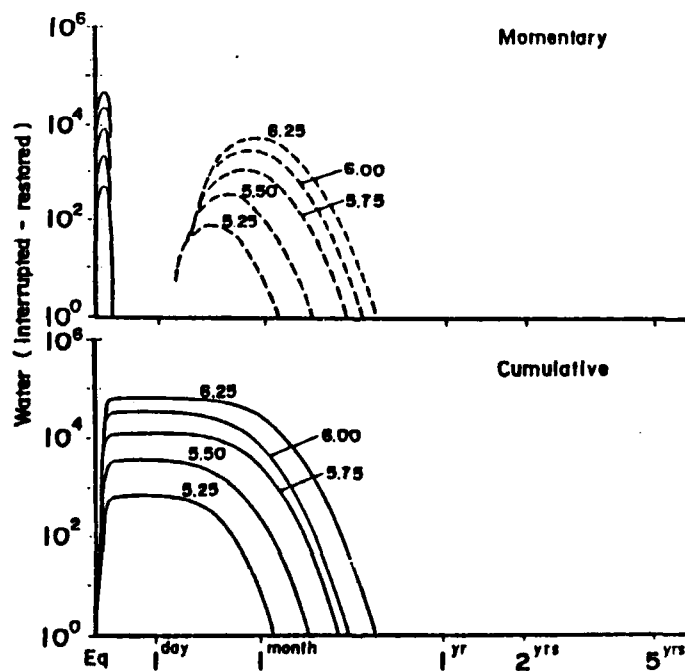


Fig. 16 Time-varying features of life line systems (water).

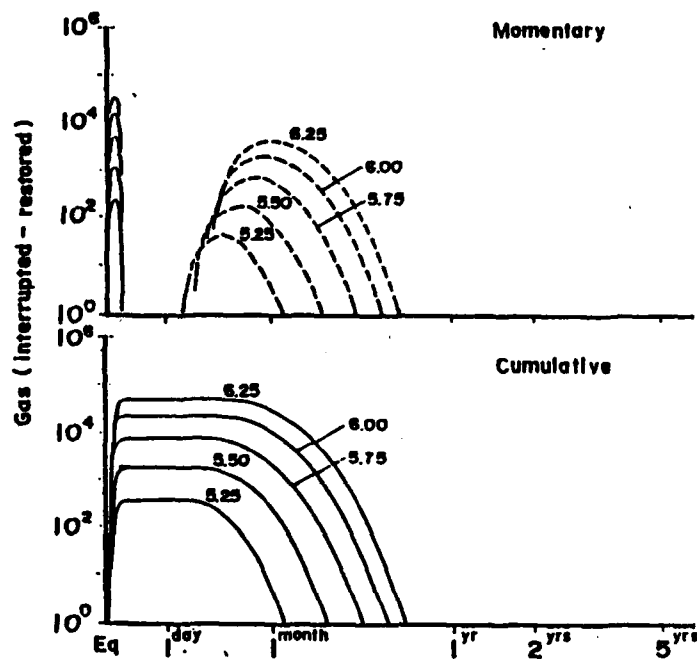


Fig. 17 Time-varying features of life line systems (gas).

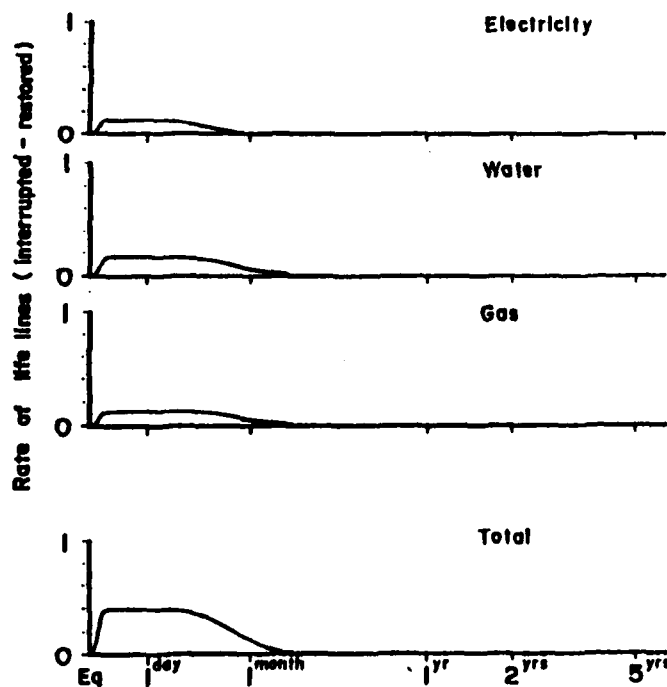


Fig. 18 A summation of damaging and restoring processes of life line systems.



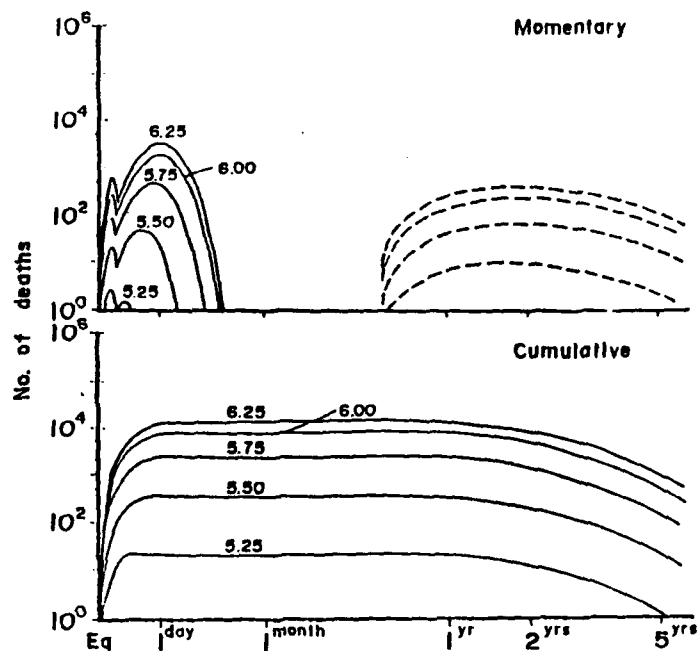


Fig. 19 Time-varying features of deaths (momentary and cumulative).

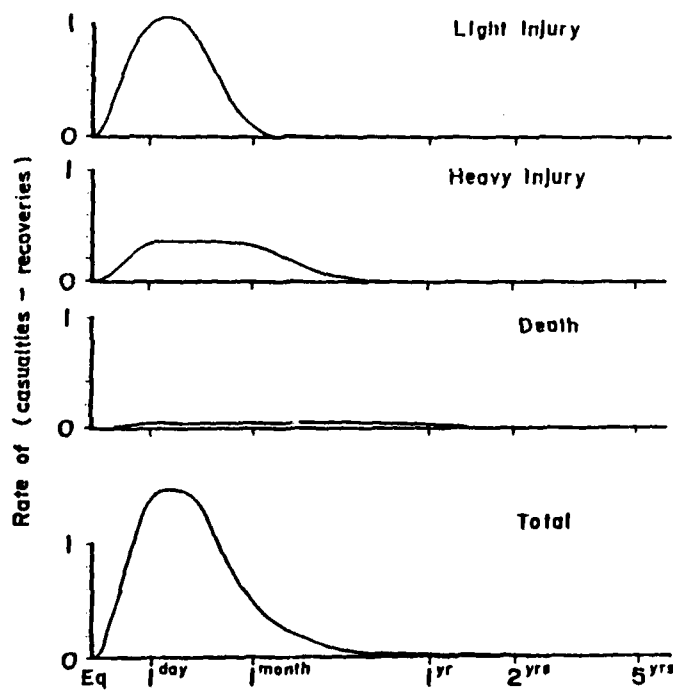


Fig. 20 A summation of casualties and recoveries.

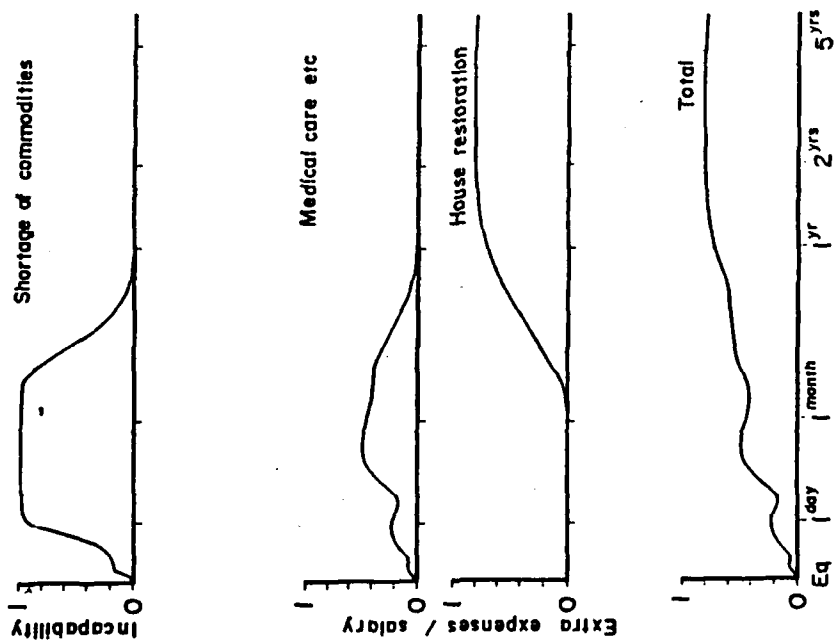


Fig. 21 Time-varying features of daily commodities (top figure) and time-varying extra expenses.

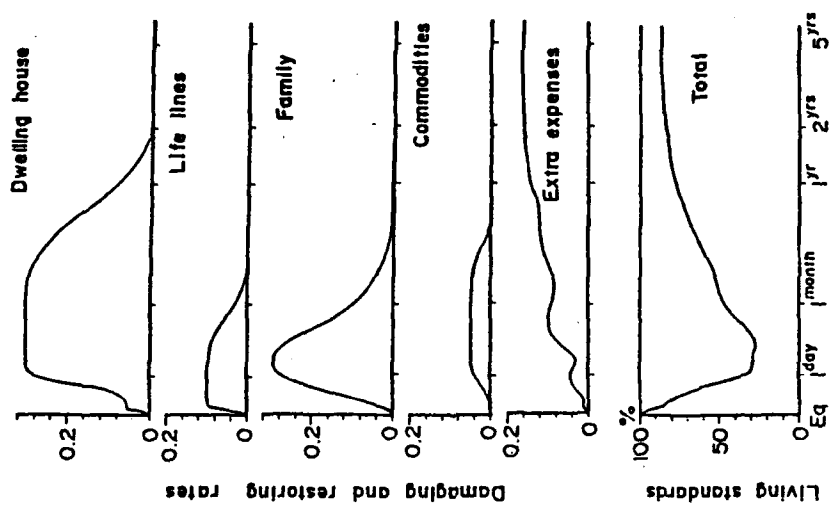


Fig. 22 An integration to household's living standards.

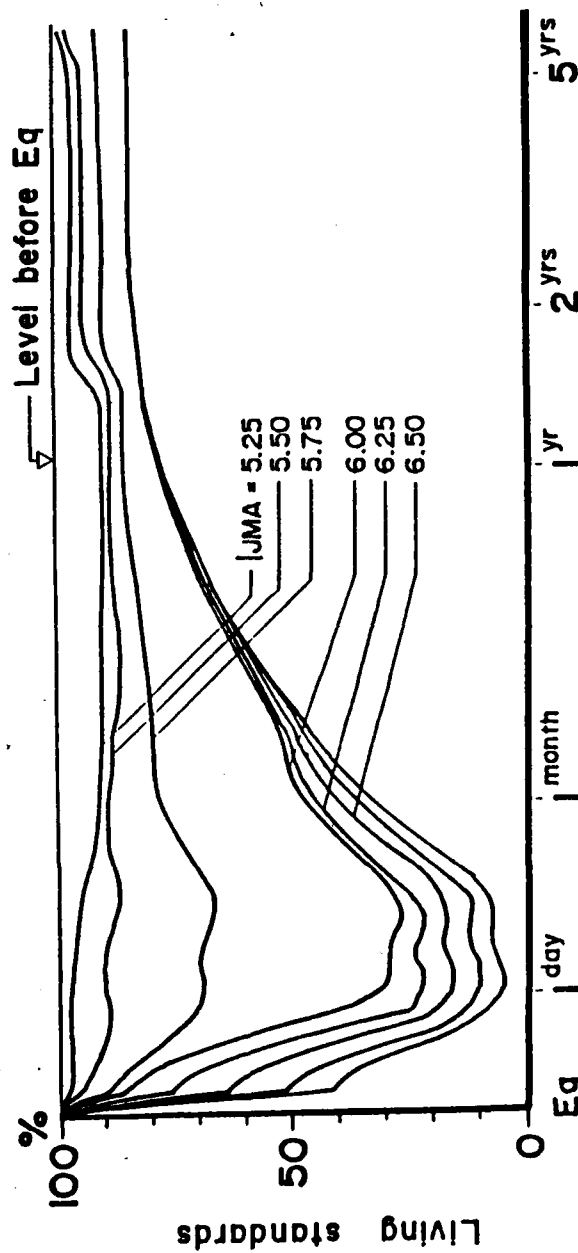


Fig. 23 Derived time-varying living standards in regards with seismic intensities.

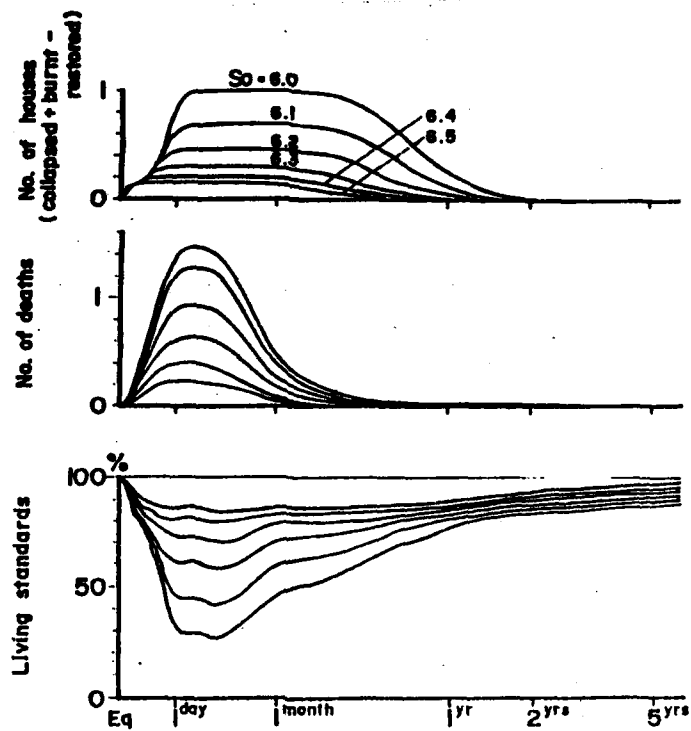


Fig. 24 Living standards in relation with strength of dwelling houses.

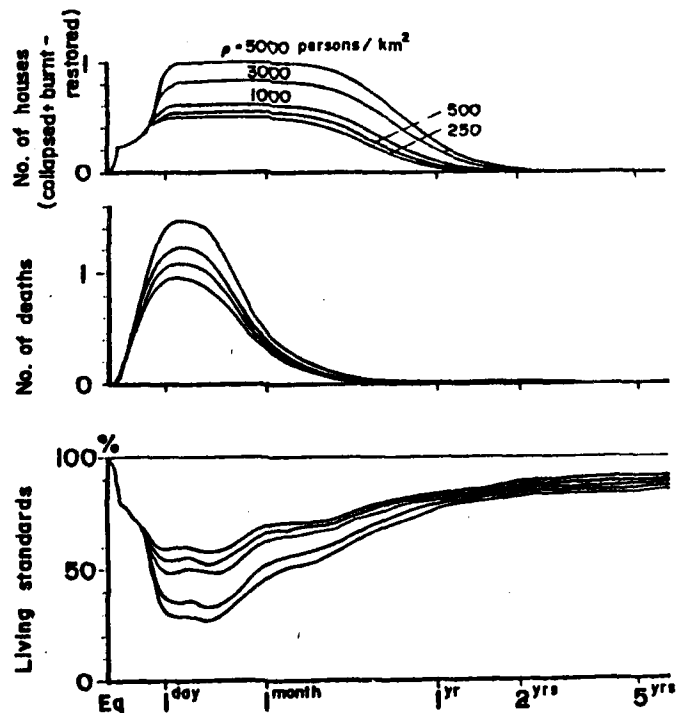


Fig. 25 Living standards in relation with population densities.



**TURKISH NATIONAL COMMITTEE FOR  
EARTHQUAKE ENGINEERING**

**THIRTEENTH REGIONAL SEMINAR ON EARTHQUAKE ENGINEERING**

**September 14-24, 1987 - Istanbul - Turkey**

**PRESENT ASPECTS OF THE ASEISMIC PROTECTION  
OF RURAL BUILDINGS IN ROMANIA**

**Eng. Emil-Sever Georgescu  
Structural Engineer  
Scientific Researcher**

**Earthquake Engineering and Structural Dynamics Division  
INCERC, Bucharest, ROMANIA**

MINISTRY OF INDUSTRIAL CONSTRUCTION  
CENTRAL INSTITUTE FOR RESEARCH, DESIGN AND GUIDANCE IN  
CIVIL ENGINEERING - ICCPDC  
BUILDING RESEARCH INSTITUTE  
INCERC

PRESENT ASPECTS OF THE ASEISMIC PROTECTION  
OF RURAL BUILDINGS IN ROMANIA

Eng. Emil-Sever Georgescu  
Structural Engineer  
Scientific Researcher  
Earthquake Engineering and Structural Dynamics Division  
INCERC, Bucharest, ROMANIA

Paper prepared for the session of the Working Group of the  
European Association of Earthquake Engineering - EAEE - "Low-  
Cost Rural Housing In Seismic Areas" - in the frame of the  
13th Regional Seminar of Earthquake Engineering organized by  
the Turkish National Committee on Earthquake Engineering

14 - 24 September 1987

Istanbul - ATAKÖY

TURKEY

PRESENT ASPECTS OF THE ASEISMIC  
PROTECTION OF RURAL BUILDINGS IN ROMANIA

Emil-Sever Georgescu<sup>1)</sup>

ABSTRACT

The paper deals with the following aspects:

- the seismicity of the territory and the overall effects of past strong motions that affected rural areas;
- the structure of population and rural settlements subjected to seismic risk;
- types and classification of traditional rural structures in seismic areas;
- intuitive aseismic protection, design and rehabilitation - strengthening measures for rural structures;
- statistical aspects on the losses during earthquakes in rural construction;
- the specific earthquake behaviour of various types of rural structures;
- aseismic planning and rehabilitation procedures and measures used in rural areas of our country during the continuous urbanization;
- technical and economical aspects of the aseismic protection referring to rural areas;
- conclusions.

1. INTRODUCTION

The Thirteenth Regional Seminar on Earthquake Engineering organized by the Turkish National Committee for Earthquake Engineering, sponsored by the European Association of Earthquake Engineering provided the opportunity of attending the special session of the Working group of the Association on "Contemporary Rural Buildings in Seismic Zones" dealing with "Low Cost Rural Housing in Seismic Areas".

The presence of this subject on the agenda of the European Association underlines the importance of this problem for the countries with large rural zones out of the seismic zones on the earth.

The South-East European and Mediteranean areas provides specific examples for the state-of-the-art and the possible measures for the mitigation of the seismic risk for several rural houses.

The present state-of-the-art of rural housing in Romania connected with the severe seismicity of the ground

1) Scientific Researcher, Building Research Institute-INCERC  
Sos.Pantelimon 266, Sector 2, Cod 79614, Bucharest - ROMANIA

provides the information necessary for the mutual exchange of data in the frame of the Working Group and of the Regional Seminar that is held in Istanbul, in September 14-24, 1987.

Several questions are being raised and the answers given by the paper or by the discussions of the working group are as follows:

- what does the 'low cost housing' mean and what are the causes that generate, at present, the building of low-cost rural housing and what is the state-of-the-art in Romania?
- what are the minimum cost price levels for the types of structures and what are their correlations with the strength level of the rural houses during an earthquake?
- what are the materials and traditional and modern building technologies available in the rural areas and what is the aseismic resistance they provide?
- what are the general social and economic factors that influence at present the development of rural areas?
- what is the nature of the effects and what are the measures taken after the previous earthquakes?
- what does the urban planning of rural areas look like and what is its correlation with the type of house, and with the value and earthquake resistance?
- what are the new elements provided by the building research for the foregoing problems?

## 2. GENERAL DATA ON ROMANIA (Geography, geology and seismicity)

Romania /1/ is located at the curvature area of the Carpathian Mountains, downstream the Danube, in the area of the Black Sea along the 45° parallel, northern latitude and has a balanced distribution of the relief: in the South and West there are plains (33%), in the middle of the country and in the East there are hills and plateau (36%), in the middle, in the East and in the West there are the Carpathian Mountains (31%), and in the East the Danube Delta.

The seismicity of Romania is related to many epicentral zones, among which Vrancea subduction zone (at the South-East Carpathian curvature) is the most important. The depth of the foci varies between 70-170 km, the motions are of the multi-shock type and have a large area of microseismic effects of an elliptical shape, elongated on the NE-SW direction (strong earthquakes: 10.XI.1940, 4.III.1977), and a relative reduced return period (30-40 years)/Fig.1/.

The fundamental oscillation periods of Vrancea strong motions in the southern plain are long (1.5-1.8 sec.) due in the main to the deep sedimentary deposits. During the earthquake of 31 august 1986 (M=6.8) INCERC obtained also strong motion records with higher frequencies content. In all other



epicentral zones of the country the earthquakes are of the normal type, connected to the intraincrustation cracks, with depth of 5 to 30 km, with a reduced released energy and the high return periods (of 100 years) /2/. For these types of earthquakes, short natural oscillation periods can be expected, e.g. Tulcea Earthquake of 13 November 1981. It is worth mentioning the fact that half of the territory of the country may be subjected to seismic intensities of minimum VII MSK (MM), the most important zone being the S-E zone. The seismicity degree of VI requires important aseismic constructive measures, too /2/. The geography, geology and seismicity strongly influence the construction types designed and built by people in various zones of the country. Localities and inhabitants from the rural area of Romania are exposed to risk due to the foregoing natural hazards. Additionally, the present state of these elements and the implications of the environment, social and economical, demographic, historical and political factors are complex and require a thorough analysis.

### 3. RURAL POPULATION OF ROMANIA

Romania has a population of 22,624,505 inhabitants (1984) and a surface of 237,500 km<sup>2</sup>, including 237 towns only of which 56 municipalities, 2,705 communes including 135 suburban communes and 13,123 villages. As compared with the year 1948 the population of the country increased with almost 7 million inhabitants /3/. At present 49.2% of the whole population live in municipalities and towns, 3.1% in suburban communes and 47.8% in communes.

The population density represents at present an average of 95.3% inhabitants/km<sup>2</sup> (1984), this value varying between minimum values of 31.5 inhabitants per km<sup>2</sup> (Tulcea county) and maximum values of 182.9 inhabitants per km<sup>2</sup> (Prahova county). Contemporary rural settlements have between 2,000 and 4,999 inhabitants (1,690 communes comprising 50.9% of the rural population) together with the localities that have between 5,000-9,999 inhabitants (739 communes comprising 41.5% of the rural population) /3,11/. The development of rural settlements is controlled by land planning laws and regulations concerning height, layout, position, that are compulsory for obtaining construction permit

### 4. TRADITIONAL RURAL SETTLEMENTS AND STRUCTURES

#### 4.1. CLASSIFICATION AND CHARACTERISTIC OF TRADITIONAL ROMANIAN RURAL SETTLEMENTS

Rural settlements were the main living area from old times, especially due to the fact that the soil was good for agriculture, for breeding cattle and for wood industry. All these activities were specific to the Romanian territory.

The varied relief (mountains, hills, plateaux, river valleys, plains, meadows) and a varied climate demanded various types of specific Romanian constructions and houses. The economical, geographical and demographical factors gradually lead to the increase of the density of localities. In Wallachia although there were quite a lot of fortresses, they were just an alternative for the defense of the country against the enemies and not a permanent residential locality. As far as villages are concerned, specialists consider that very important were three types of villages: the first with longdistanced houses, the second with houses that bordered the roads, and the third one, the so-called compact village with houses very close to each other.

There is another classification for villages, too, according to the area they are located: the valley village and the road village.

Each of these types were determined by the geographical, climatic and economic conditions specific to each zone.

The scattered village is specific to the mountain areas with isolated and long-distanced houses and with no streets. The peasants own the land (the hills, mountains, woods and hayfields) that is in the neighbourhood of their houses and another main concern is the breeding of cattles, growing hay and cultivating agriculture on a reduced scale, namely on terraces. This type of village is widespread in west and north-west parts of the country and in a very short time it will no longer exist.

The dispersed houses villages is the second type of village and is specific to the hill areas. It has long and irregular traced streets, the houses are bordering the roads with a small cultivated land round the house and another land outside the village/5/.

The compact village has houses very close to each other and this type of village is specific for the plain area but it may also be found in the hill or mountain area. The streets (lanes) network is irregular and the houses are very close to each other because they try to save the agricultural ground and to build their houses on valleys or near water sources. Nevertheless, the yards are larger, the houses have flowers and vegetables gardens and orchards/5/. In the Romanian villages the house is separated from other household constructions such as the stable, hen coops, granary, store rooms. The houses have all around a fence.

As the Romanian territory was not very large, with maximum dimensions of about 500-700 Km, and had always a dense population, the historical, social and economical evolution led to the foundation of commercial or military localities that were relatively close to each other (at about 100 Km) that would become towns in the time evolution.

In the 19<sup>th</sup> century a large number of rural localities were developed (especially in agriculture areas, or on meadows), streets were designed and peasants and free handicraftmen were appropriated land to. Later on, several localities on this type become important local towns (e.g. Alexandria town in

the Danube plain).

In the modern development of rural areas the most impact elements are the historical and political events:

- the land reforms of 1864 and 1921;
- the development of industry after 1878;
- the development of modern capitalist industry (1920-1938);
- land reform of 1945;
- industry nationalization (1948);
- agricultural cooperativization, started after 1950.

These events led gradually to the foundation of new rural localities, especially in the plain area, to the increase of the economical power of the peasants, provided new building materials and caused the migration of the manpower to towns.

The strongest impact on the rural area started after 1944 and later on in 1965 when Romania changed its statute from an eminently agricultural country (80% of the whole population lived in rural area areas in 1930) to that of a country with a complex industry and a modern agriculture.

As positive effects of the industrial and urban planning evolution of rural areas in Romania one may remark the followings:

- preservation of several traditional and architectural types in less industrialized zones;
- the development of rural localities in the industrialized zones where running shuttle service was possible;
- people migration to urban areas took place at the same time with the building of residential houses in those towns, trying to avoid the occurrence of temporary buildings as it had happened between the two world wars.

In the Romanian rural zones, the term of "low-cost rural housing" is tightly connected to the available low-cost materials in the area and used by the majority of people as traditional building materials. Only the rich used to build their houses using building materials and technologies that were not specific to the respective zone (for example burnt bricks, stone a.s.o.).

In the suburban zones the term of low-cost rural housing is closer to its economic meaning because the workers coming up to town, having low income and no local tradition, needed a shelter no matter what living conditions they were provided with.

Some of the building technologies were taken from the rural zones but the shortage of materials led to the use of the less difficult to be found building technologies (such as the common earth instead of clay).

Nowadays, in the urban zones such types of buildings are no longer of present interest because of the state control and the reconstruction of the peripheral zones.

In the rural zones, due to the increase of the inhabitants' income, both the traditional materials and the modern ones have been used.

#### 4. TYPES, CLASSIFICATION AND DESCRIPTION OF TRADITIONAL STRUCTURES AND MATERIALS FOR RURAL BUILDINGS IN ROMANIA

##### A. Timber structures (block structures)

Foundation: - thick wooden beams under external and main transversal walls and stone boulders below.

Walls: - horizontal wooden beams or planks; keys at half section, nut and father or dowel joints; walls are sometimes plastered for protection.

Floors: - collar, main and secondary beams, ceiling.

Roof: - wooden structure with round wood, in 2 - 4 slopes, rafters and purlins joined with superior collar beams; cantilever eaves; roofing with wooden tiles, straws or reed.

Layout: - rectangle, symmetrical for single story houses; asymmetrical for two storied houses when first floor is usually with stone walls.

Location: - mountain, hill and plateau villages.

##### B. Masonry structures

###### B.1. Stone masonry

Foundation: stone plates walled with clay or lime mortar or in dry masonry.

Walls: - walled stone plates (40 - 50 cm wall thickness) wooden lintels; lime or mud mortar.

Floors: - vaults in old buildings basement; wooden floor over first story.

Roof: - in 2 - 4 slopes, wooden structure with round wood rafters and purlins; cantilever eaves; roofing with wooden tiles, straw, reed, tiles; local roofing with stone plates (5 cm) out in tuffa, limestone, a.s.o.

Layout: - rectangular, symmetrical for single story houses; /fig. 2/

Location: - mountain, hill and plateau villages.

###### B.2. Adobe masonry (unburnt brick masonry)

Foundation: - river stones compacted clay in a reduced foundation trench;

Walls: - adobe masonry with heavy solid unburnt brick made of clay with vegetal admixtures (straws) and clay-sand mortar; wooden lintels; clay-sand or lime-sand plastering.

Floors: - round or wooden beams, timber or reed ceiling, plastered;

Roof: - in 2-4 slopes with simple structures directly or on collar beams supported on walls; cantilever eaves; roofing with straws, reed, tiles.

Layout: - rectangular

Location: - hill, plain, meadow villages in East, West and South of the country.

#### B.3. Kiln brick masonry

Foundation: brick or stone with lime mortar; basement on masonry vaults in old buildings.

Walls: - masonry in kiln brick and lime mortar (clay-sand mortar in poor houses); wooden lintels or arches for openings.

Floors: - wooden beams and timber ceiling; masonry vaults in old monumental buildings.

Roof: - in 2-4 slopes with wooden structure, with round wood rafters and purlins; cantilever eaves; roofing tiles, lead or copper sheets.

Layout: - rectangle, T or L; 1-3 stories with towers, external stairs, balconies.

Location: - towns, landlord mansions, religious buildings in XIV - XX centuries situated mainly in hill and plain zones; well built houses in villages after 1926's.

#### B.4. Compacted clay structures

Foundation: - 30-50 cm height in compacted clay, compacted river stones or walled quarry stones; in foundation trench.

Walls: - solid walls, 40-60 cm. thickness built in wet state in two variants;

I variant: - compacted clay wall made of clay, long boulders walled in wet state; horizontal thin wooden beams (tree branches) connections at corners and over openings added in order to increase the strength;

II variant: compacted clay wall using sliding forms; - material with sandy clay (25% clay) in a reduced humidity state;

- 30-40 cm thickness layers compacted; opening for doors and windows are cut in dry wall afterwards by saw;

Floors: - wooden beams, timber or reed ceiling, plastered;

Roof: - in 2-4 slopes, wooden simple structures; roofing with straws, reed, tiles;

Layout: rectangular, symmetric;

Location: - plain and meadow villages in East, South and West country. There are villages where buildings

are compacted clay structures.

C. Framed wall structures

C.1. Timber frame structures with infilling materials  
(paddle or trellis work)

Foundation: - sometimes river stone boulders below the wooden beams at the wall base in the foundation trench;

Walls: - timber frames with corner columns and opening bordering posts as well as horizontal beams, sometimes horizontal wattled tree branches; inclined bracings; infilling in the timber frame with: mud, clay brick and clay, stones and clay a.s.o.; plastering with clay or lime sand mortar;

Floors: - wooden collar beams and main beams connected plastered timber or tree branches ceiling;

Roof: - in 2-4 slopes; structures connected with frames and collar beams; roofing with wooden tiles, galvanized sheets;

Layout: - rectangle, symmetric;

Location: - plain, hill, mountain villages in specific forms for South, East, Center and North-West of the country.

C.2. Plated timber frame structures

Foundation: - riverstones; wooden beams at wall base;

Walls: - timber frames with corner columns and opening bordering posts as well as horizontal beams;  
- external and internal plating using inclined thin planks nailed on frame followed by external and internal plastering.

Floors: - main and secondary beams, timber ceiling.

Roof: - in 2-4 slopes (usually very inclined) using wooden structure joined with frames and superior collar beams; roofing with wooden tiles, galvanized sheets.

Layout: - rectangle, L, T, towards external stairs;

Location: - hill, mountain villages.

5. LESSONS FROM THE EARTHQUAKE BEHAVIOUR OF TRADITIONAL RURAL BUILDINGS IN ROMANIA

The development of structural engineering led to a certain lack of interest about traditional buildings. The behaviour of some old, dilapidated houses gave the false impression that rural buildings are completely unproper for seismic zones. Nevertheless, the comparisons with other buildings erected sometimes by engineers and architects do not give us the right to afford this conclusion.

5.1. Behaviour of traditional of rural structures during Vrancea 1977, 1986 and Tulcea 1981 earthquakes

Timber structures (A) withstand earthquakes without collapse or major damage. Several nonstructural damage occurred (plaster and chimneys failure). Stone structures (B.1) presented cracks and partial failure due to bad mortar quality or poor workship. Cut stone is more adequate for seismic zones. Adobe structures (B.2) presented local increasing in old buildings. Masonry structures (B.3) presented damage by wall corners and crossings cracking, diagonal cracking, local failure of untied walls. The quality of mortar and brick, the overall layout and conception of the building played an important role. Compacted clay of structures (B. 4) suffered heavy damage only by wall crossings large cracking and displacement of entire panels; sliding and collapse of roofs insufficiently connected to the walls a.s.o. One can remark anyway, enough cases when behaviour was better than masonry. This unusual damage pattern was commented in papers /4,5,7,8,10/. Timber frame structures with infilling or timber plated (C<sub>1</sub> and C<sub>2</sub>) behaved better than masonry. Nonstructural damage by plaster falling and lintels cracking were often observed. The spatial braced wooden frame (if the building age did not lead to weak points) makes this type of structure proper for seismic zones.

As a consequence of this analysis results the main quality of Romanian rural structures: even in case of heavy damage (at VII-VIII MSK or MM intensities) the safe evacuation of inhabitants is possible. It is true record, if data about other countries are used for comparison. This fact is due to the intuitive aseismic construction methods based on the historical seismic experience of the Romanian people/2, 4,5,7,10,11,12/.

The architectural and constructive elements that ensure this essential quality are as follows /4,5,6,10/:

- reduced dimensions of Romanian rural buildings and a relatively simple layout;
- a relatively light roof, in 2-4 slopes having a structure well tight with the masonry and the walls;
- the room floors are built with dense beams tightly connected with the masonry walls;
- the height of only 1-2 levels; the floor being made of lighter materials (such as wood, trellis work);
- the existence of a sufficient number of elements that take the horizontal loads (columns, masonry walls, wooden walls with corner joints, bracings a.s.o.);
- a relative symmetry of the building layout and a symmetrical distribution of the doors and windows openings;
- the pressure of certain elements that provide the spatial interaction: wooden horizontal elements at corners in the earthen walls a.s.o.;
- a relatively large time interval between the Vrancea

earthquakes;

- the seldom use of gable walls;
- the rigidity specific to rural buildings made of earth and masonry that under the earthquakes with long vibration period given by the Vrancea focus did not lead to resonance;
- the proper granulometry of the soil used in walls avoiding shrinkage and long-term degradation. For instance the analysis of the earth used for compacted clay buildings in Tulcea County indicates the following content:
  - clay,  $d < 0.005$  mm - 25 - 33%
  - dust,  $d = 0.005$  mm -  $0.05$  mm - 53 - 57%
  - sand,  $d = 0.05$  -  $2.0$  mm - 10 - 20%

This composition should be related to a good behaviour of local rural buildings in that zone.

#### 5.2. Repair and strengthening of traditional structures

Masonry structures (B.1., B.2., B.3.) have been strengthened and repaired by rebuilding of fallen portions, by mortar grouting, plating and jacketing with wire mesh plastered with cement mortar, addition of new horizontal tensioned steel bars a.s.o. Nevertheless, the sole steel mesh on the wall sides can rather difficult recover the bearing capacity of the wall, therefore it is mainly a method of repair. The intervention may be considered as strengthening only if these operations lead to a spatial behaviour of structure by the proper connections of walls, roof and foundation. These technologies requires a careful work.

Compacted clay structures (B.4.) cannot be in most of the cases easily recovered if corner cracking and displacements of detached wall panels are larger than 1 - 2 cm. The jacketing using wire mesh and concreting or cement grout plastering will be in most cases too expensive as related to the building replacement cost and the obtained safety. In specific cases, if considered efficient (having in mind the fact that entire wall portions remain undamaged after earthquake) the introduction of several perimetral tendons over the lintels level could be beneficial. A new perimetral basement socket and a good connection of roof structure to the walls could be a variant to increase the seismic safety. Grouting should be considered with care of compatibility between basic and added material.

Timber frame structures (C<sub>1</sub> and C<sub>2</sub>) require sometimes after shaking new plaster or infilling repair. For new structures this operations are sufficient. It can be concluded that the basic requirement for a nonengineered rural building should be the life safety of the inhabitant although the damage cannot be avoided. The second requirement must be the possibility to perform certain repair works in order to recover this basic quality.

#### 5.3. Comparison of earthquake effects on rural buildings and inhabitants in Romania and in other countries



The violence of the Vrancea earthquake produces always great damage but in a specific way. Thus, following the earthquakes of 23 and 29 XI, 1829 (I = 9 MM) 80% of structures were damaged but only 3% were destroyed. The earthquake of 1838 produced the collapse of only 35 of 10,000 rural buildings. In Bucharest while other monumental buildings failed. The earthquake of 10.XI.1940 (M = 7.4; I = 9 MM) destroyed 90-95% of 1,000 rural houses in the small rural town Panciu (near Vrancea epicentral zone) but led only to 22 loss of life. The earthquake of 4.III.1977 (M = 7.2; I = VIII MSK) damaged in Vrancea zone only 5.1% of rural buildings. Only 1% of buildings were destroyed and 10% damaged in the South of Romania. It is frequently mentioned the case of town Zimnicea (on the Danube), a small rural like town, with 14,000 inhabitants living in rural type houses. The town was destroyed 80%, heavy damage representing 20% and other damage 50%.

The building stock was not ever recovered (the town being reconstructed under new urban concepts) but the loss of life reached only 4 persons. In the neighbouring town Alexandria collapses represent 3.85%, damage 30%, but only 3 victims were recorded. Similar remarks relies on the 1977 earthquake effects on wood and clay buildings of Jassy in N-E of the country. In the Danube plain (Teleorman and Ilfov counties) the bulk of rural compacted clay, masonry, adobe, paddle work buildings is greater. In Teleorman County a dwelling stock of ca. 130,000 dwellings, 19,900 houses were damaged in villages (20%) but 14,500 of urban stock (52,5%). It should be noted that rural buildings stock was usually rebuilt in a faster rhythm than in towns. In the urban stock, buildings of Zimnicea town (destroyed 80%) as well as those of Alexandria (an old town, too) were included. In Ilfov County the percentage of 4.75% represents 9,848 one storey buildings (adobe, brick, compacted clay and infilled frames). The Prahova County (North of Bucharest) the 14.5% rural stock damage must be understood related to the high intensity of the motion (VIII - IX degrees MSK) as well as to the positive presence of mixed rural buildings having the first story of stone and the second of timber. In the Dolj County (S-W) the percentage of 30% damage refers to the whole amount of rural households receiving insurance indemnities.

For comparison one can mention the following cases in cases in some Middle East Countries /4,14,15/:

- 3,840 loss of life/9,232 collapses and heavy damage in Caldiran Earthquake Turkey, 24 November 1976, in a prominent rural zone;

- 60,000 loss of life/100,000 destroyed buildings in rural zones of Iran due to earthquakes of Buin Zahra (1962), Dasht-e-Biaz (1969), Qir (1972), Tabas (1978), Golbaf (1981) (cumulated effects);

- 1,155 loss of life/3,007 destroyed rural buildings in Erzurum and Kars zones due to the earthquake of 30<sup>th</sup> November 1983 in Erzurum, Turkey.

The excessive weight of the flat roof, the lack of lateral strength of adobe walls within the context of the regional seismicity are the main reasons of these disasters.

In Mediterranean zone the situation of casualties is different:

- 35 loss of life/9,816 destroyed houses many of them of rural type reported in Albania, during Montenegro earthquake of April 15<sup>th</sup> 1979;

- 94 loss of life/9,968 destroyed buildings, many of them of rural type or of urban type but with rural materials (stone, clay, wood, a.s.o.), in Yugoslavia, during Montenegro earthquake of April 15<sup>th</sup>, 1979.

## 6. CONTEMPORARY RURAL SETTLEMENTS AND STRUCTURES

### 6.1. RURAL DWELLING STOCK EVOLUTION

Over 5,000,000 dwelling have been built between 1951-1986 in the whole country, including 2,220,000 rural buildings/4/. Under this development ca. 80% of country population lives now in a new house./10/. Due to the specific of local needs, about 91% of this amount have been built with private funding./4/.

Between 1956-1960 and 1961-1965 maximum figures of 550,000 dwellings per each five years were built, but in the present the rate is of 70,000-80,000 dwellings per five years. There are enough localities where the number of rooms or even of dwellings are exceeding the demand because the new generation prefers to learn and then to work in urban activities. However, the families build large houses as for all members. In such conditions, new buildings are erected mostly for the comfort improvement. Another reason of reduced living density in some villages is the traditional architecture influence. At least from the last century, the most common type of rural house has three rooms: one as bedroom and dinner room, another - great too - for guests and clothes, and another, intermediate, narrow, lobby, serving as entrance, kitchen, a.s.o.

As a matter of fact, statistics indicate that the ratio of 3 room dwellings exceeds with 50% the actual similar ratio among state built apartments.

### 6.2. RURAL INFRASTRUCTURES

Romanian villages are power supplied from the national power network. In oil-bearing zones the natural gas supply is usual. Water supply relies on private or public fountains, running water is under development but is not very installed.

The railways represents a rich network, the public roads and bridges have modern structure, the bus transportation is organized by state companies.

Private cars are utilized in all the villages, but on rocky mountain roads the carriage transportation using animals is more appropriate.

### 6.3. RURAL SUPRASTRUCTURES

Romanian villages are organized as communes, on a radius of 4-10 km around the most developed settlement. The local administration belongs to a Peoples Council. For the whole country, the Committee of Peoples Council acts as a Ministry,

coordinating the councils activity. Councils administrate an own budget integrated in five years and yearly plans of the country.

At present, in all communes there are at least a school, shops, hospital, mail office, culture house, movie and library. Radio sets and television sets are used all over the country (3,300,000 TV sets in the country except Bucharest).

#### 6.4. PRESENT AND PROSPECTIVE PRINCIPLES IN SETTLEMENTS DEVELOPMENT AND PLANNING

The entire social and economic development of the country is state planned every 5 years.

Starting with 1974, new prospect principles of an unified and harmonic development of villages and towns were applied, in order to obtain:

- equal life conditions in town and villages;
- full utilization of local resurces;
- protection of the environment;
- reduction of built areas;
- rational organizing of transportation network;
- obtaining of an optimal density of buildings;
- gradual transformation of rural settlements in developed towns;
- development of 300-400 new towns as gravity centers for villages;
- each town or commune should become a strong economical and administrative center.

Between 1976 - 1990 will be erected ca. 3,000,000 new dwellings in the country (2,500,000 in urban zones).

In 1979, the XII-th Congress discussed a large PROGRAM-DIRECTION ON THE ECONOMICAL AND SOCIAL DEVELOPMENT OF ROMANIAN TERRITORY BETWEEN 1981-1985, including:-

- development of industrial and agricultural production of each county;
- increasing the degree of employment on local scale;
- increasing the wealth by construction of new social and cultural endowments.

At present, a NATIONAL PROGRAM FOR LAND PLANNING is applied for:

- transformation of 140 communes in small agricultural-industrial towns;
- increasing of urban population: 54,5% in 1985 with trends towards 57-58% in 1990;
- presence of 9 urban centers in each county, with 4 - 6 communes for a town, with a radius of influence of 15 - 20 km;
- erection of 1 - 2 stories (sometimes 4 stories)

dwellings in small towns;

- development of buildings more related to the local architecture pattern using typified projects and local materials.

In 1984, the XIII-th Congress established the erection of 750,000 dwellings in 1986-1990, including 50,000 rural dwellings.

Towards the years 2,000 it is planned to provide for each inhabitant of the country a mean living area of 14 sq.m. and 18-20 sq.m. if householders facilities are considered.

Recently, in September 1985, the Congress of Peoples Councils established new measures to increase the density of rural buildings using 2-3 storied buildings.

According to the rules in force, any further development of a settlement will not exceed the present local limits.

The provisions stated in the building authorization concerning height, layout, position, should be respected by owner and builder.

#### 6.5. CONSTRUCTION INDUSTRY AND BUILDING MATERIALS INDUSTRY

A number of 64 building material factories exist in all country counties. These large enterprises produce cement, lime, glass, brick, ceramic blocks, concrete blocks, roofing materials, a.s.o. 40 of these 64 factories produce precast elements. Other local, small factories produce: brick, lime, timber planks, river aggregates, a.s.o. In the mountain or hilly zones village masters produce for local consumption: hand-made brick, lime, timber, woodentiles, etc.

The construction industry works for state investments in large development projects, urban construction, a.s.o.

#### 6.6. RURAL CONSTRUCTION

Tendencies which are new real in the modern rural housing presents the following characteristics:

First of all, one can mention the buildings erected accordingly to a design provided by private sources or from catalogues given to local councils. This drawing are compulsory in order to obtain the erection permit. However, the checking points refers mainly to the architectural aspect, the minimum height, distance to the streets, a.s.o. The structural detailing remains a problem of professional conscience, competence as well as of acceptance or rejection of some requirements. As a matter of fact, builders make "simpler" detailing looking too complicate, and the local control cannot provide a proper quality.

The local builder perform the erection works gradually, first of all the structure and then the finishing works. One can remark the tendency of the owner to spend much more money for modern endowments and finishing works, although the cost control is almost impossible. However, this way is considered the "cheaper". On the other hand, there are cases when cooperatives or small enterprises try to comply with the typified

project, but the competence of the staff is limited, the control is not sufficient, therefore the seismic risk increase in some cases. This way is considered by the owner could due to the necessity to pay in advance the costs.

Taking into account the coexistence of both technologies for a while, the study of "non-engineered inovations in rural construction" will be beneficial for seismic risk reduction.

ICCPDC is a coordinator of a selection study of the most representatives traditional rural dwellings, in order to provide the local specific in catalogs.

A first group of 1,000 types of rural traditional houses will be published as an album to be used by the designers of typified structures.

.-.-.

## 6.7. TYPES OF CONTEMPORARY RURAL STRUCTURES, MATERIALS AND TECHNOLOGIES IN ROMANIA

In the last decades new characteristics in rural construction occurred mainly due to the following reasons:

- the need to improve the durability and fire resistance, the comfort, living space utilization etc;
- the shortage of traditional materials and introduction of industrial materials;
- the change in the styl- of-life, modernization of building sector, urban influence concerning the architecture and aspect;
- new official regulations concerning the buildings height, and the erection permit, use of typified projects.

Because the traditional buildings classification already mentioned remains valid we should point out only some new elements, including the new technological problems, too /11/.

### A.a. Timber structures

Foundation :- ground floor is often in stone and brick ;  
fou dation in stone or plain concrete or hollow blocks.

Walls, - similar to the A type, sometimes r.c.slab over basement or ground- floor.

Floors :

Roof: - galvanized sheets and asbestocement plates.

Layout : - urban influence in room distribution ; balconies.

Technology: - new elements only for r.c. members.

### B.1.a. Stone masonry structures

Stone is used mainly for ground-floor erection and for external plating because of its insulation and finishing qualities, in mountain zones. New houses include r.c. collar beams and floors, balconies and villas architecture. New technological elements occurred only for r.c. members.

### B.2.a. Abohe masonry structures

Foundation :- plain concrete, raw stone, concrete hollow blocks.

Walls:/ - wire mesh nailed on walls sides for plaster durability.

Floors: - r.c. collar beams and linels are often provided.

Roofs: - bitumated sheets, asbestocement plates, galvanized sheets, tiles.

Layout : - rectangle, L.T., with veranda.

Technology: - new elements only for r.c. members and plastering.

### B.3.a. Brick, concrete block, ytong block masonry structures

- Foundation:- plain concrete or concrete hollow blocks.
- Walls: - similar to B.3. but masonry made of:pressed brick (factory brick), hollow brick, concrete hollow blocks, ytong blocks (autoclaved lightweight concrete), for 2-3 storied houses r.c. columns and collar beams are added, r.c. lintels.
- Floors: - sometimes r.c. slabs for 2-3 storied houses for roof terrace.
- Roof: - wooden structures, new forms with r.c. slab roof, roofing made of galvanized sheets, tiles, asbestocement plates.
- Layout: - L,T, balconies and towers. Fig. 5,6,7,8
- Technology:- new elements for r.c. members and masonry works with ytong blocks requiring a proper mortar mixture, wetting of blocks, adequate bonding, etc.

#### B.4.a. Compacted clay structures

- Foundation:- river stone, plain concrete.
- Walls: - similar to B.4.  
- innovations: two stories compacted clay structures with reinforced concrete slabs and lintels.
- Floors: - reinforced concrete slabs (innovative solutions).
- Roof: - wooden structure;  
- roofing: galvanized sheets, tiles, bitumated cartoon.
- Layout: - similar to B.3.a.
- Technology:- as for reinforced concrete elements (foundation and slabs).  
- sliding forms for two storied compacted clay walls.

#### C.a. Timber frame structures

- Foundation:- ground-floor is erected in stone or masonry with plain concrete foundation.
- Walls: - finishing works in stucco.
- Technology:- new elements for reinforced concrete elements.

#### D. Brick masonry and reinforced concrete frame structures

- Foundation:- plain concrete sometimes with reinforced concrete perimetral beam.
- Walls: - reinforced concrete frames or reinforced concrete skeleton (no moment resisting).  
- masonry bordered by r.c. columns and collar beams.
- Floors: - r.c. precast hollow strips or monolithical slabs.
- Roof: - in 2-4 slopes or flat terrace, tiles or galvanized sheets.
- Layout: - villa type, duplex, 2-4 stories in urbanized centers.
- Technology:- urban type for r.c. and masonry techniques, some mounting devices are necessary for 2-4 storied houses.

In this framework we should point out that the use

of typified projects are mostly in force for new rural civic center buildings. For residential buildings, the land planning law requirements concerning the existence of a project and the erection permit are controlled mainly in view of external aspect, architecture, minimum height a.s.o. In fact local builders make "innovations" when they use catalogue projects according to their own experience, under the tradition influence.

#### 7. IMPROVEMENT OF EARTHQUAKE BEHAVIOUR OF NEW TYPES OF RURAL BUILDINGS IN ROMANIA.

##### 7.1. Earthquake behaviour of existing new types of rural buildings.

Besides the general increase in production construction materials in the last decades, rural construction used an original combination of local and modern materials.

Engineered contemporary rural buildings performed well during earthquakes due to the aseismic conception, the good quality of factory materials and the state control.

Contemporary rural buildings erected with some modern materials but without aseismic design suffered effects of recent earthquakes. After Vrancea intermediate earthquake of 4.03.1977 and Tulcea shallow earthquake of 13.11.1981 several conclusions were evident /2, 4,5,11/.

- damage pattern similar to point 5.1 were recorded but in all cases at a more reduced scale;

- stone masonry structures whose foundation was walled with cement mortars behaved better than dry stone masonry;

- adobe masonry structures (besides the brittleness of the material) behaved much better if r.c. foundation and collar beams have been provided.

The mesh for plastering improve the durability and the strength;

- brick, concrete blocks and ytong blocks masonry structures performed better in the presence of concrete foundations and collar beams. Combination of heavy and light-weight materials in structure must be properly done; innovative structural systems use monolithical beam-lintels as a second collar beam;

- compacted clay structures behaved well if a horizontal reinforcement ( $\varnothing$  6 mm steel bars or  $\varnothing$  3-4 mm wire, even barbed wire) has been provided in walls. Especially the corners reinforcement could provide a work as for plain concrete shear walls. Two storied compacted clay structures with concrete foundation and reinforced concrete floor slabs withstand without damage 1981 Tulcea earthquake (M=5.3);



- reinforced concrete frame structures (complying generally with an engineering design) should be carefully used in rural settlements controlling the quality of works in order to avoid damage.

For the improvement of earthquake behaviour of new types of rural buildings, several research studies were performed by INCERC.

7.2. INCERC research on the building materials and on the detailing and protection of stabilized earthen buildings.

Since 1979 research works have been performed at INCERC on the increased efficient use of loamy and stabilized earthen houses. Based on these research, technical recommendations concerning the following materials used for rural houses and agrozootechnical constructions have been drawn up. In 1982 experiments were performed on:

1. New materials for soil stabilizing using local materials;
2. New reinforcing methods for corners and wall crossings;
3. New solutions for plastering the walls.

During the experiments, the earth was used from the outskirts of Bucharest having the following compositions:

- a) -clay (  $d \leq 0.005$  mm) = 47%  
-dust (  $d = 0.005-0.05$  mm) = 49%  
-sand (  $d = 0.5 - 2$  mm) = 4%  
-density = 2650 kgm<sup>3</sup>
- b) -clay = 43%  
-dust = 45%  
-sand = 12%  
-density = 2650 kg/m<sup>3</sup>

.Five formulae including different stabilizers were experimented according to table I. The compression strength were determined on cubes of 14 cm for the A.B.C. and D solutions and on cubes of 20 cm for the E solution. Fig.4 gives the tests results. It can be stated that the A formula provides the best results. Formulae C and D have led to penetrating cracks in the built wall samples.

.Wall sections and intersections were experimented by reproducing parts of a building, window opening a.s.o. The followings have been used:

- wooden formworks (h=70 cm, width 25 and 35 cm);
- steel walking formworks (adopted from the industrial construction technology).

Inside the steel walking formworks earth layers (prepared according to the formulae included in table I) of 12-14 cm were laid by compaction up to thickness of 6-7 cm and the height of 1 m daily and let to dry after removing

the walking formwork. Structural and reinforcing details of corners and crossings are presented in Fig.3. The method based on steel walking formworks has been proved to be more rapid, but it requires large investments for its application in rural areas.

. The following finishing solutions were experimented by plastering (2 cm thickness):

\* On clayey soils with sand admixtures:

- mortar plastering of cement-sand-lime (1:3:0.3) on a galvanized wire mesh hammered with nails;
- similar plasterings (ratio 1:2:5:0.3) on a horizontal reed support hammered in nails on a galvanized wire mesh;
- similar plasterings on a support made of brick pieces inserted in clay mortar;
- plasterings made of gypsum-cement-sand and chemical agents (GIF type-INCERC patent).

\* On clayey soils with admixtures of sand and fly ash interior plastering made of clay and sand and then painted with hydrated lime (12) has been applied.

After three years of specimens exposure the followings could be stated:

- the plastered zones behave very well;
- the unprotected zones are eroded due to the atmospheric agents (rain, frost and thaw);
- plasterings performed on a reed support have a proper adherence (7-8 daN/cm<sup>2</sup>);
- plasterings on brick pieces have a higher adherence (8-10 daN/cm<sup>2</sup>) confirming the intuitive use of that technique in the rural area;
- the interior clay mortar plasterings applied on earthen walls confer a "warm" sensation as compared with the plasterings made of lime and cement.

The INCERC results are compared with data provided by the papers /18,19/ and show the followings:

- the obtained strength is satisfactory, The composition of the earth used is very important and if the clay quantity is too large contractions and low resistance may occur (a big difference should be observed between the clay ratio in the Tulcea and Bucharest soils, clearly underlined by the behaviour of rural buildings, too);
- strength obtained by stabilizing with cement as in Pakistan /18/: the natural strength of earthen cubes is doubled by adding 5% cement, 30% sand and 14% water;
- strength obtained by stabilizing with gypsum as in Turkey /19/: strength of 20-45 kg/cm<sup>2</sup> may be obtained by adding 10 % gypsum.

Table II shows that traditional rural low-rise

houses have a better behaviour when built of compacted earth than of masonry in zones of seismic intensities of 7 and 8. A permanent mortar strength of 10-25 daN/cm<sup>2</sup> under rural conditions is not often possible while strength given by the compaction works (sometimes of 10-15 daN/cm<sup>2</sup>, without stabilizers) are very frequently obtained in the East and South of Romania.

7.3. Repair, strengthening methods for the rehabilitation or recovery of contemporary rural buildings made of earth and masonry.

The relatively new rural buildings made of good quality materials, even without specialized technical assistance, but provided with modern facilities (running water, sewage, power and finishes), justify important intervention works aiming to prevent damage (rehabilitation or to recover the building after the earthquake. If the post-seismic damage degree is not high the structure will present certain general aseismic qualities for the respective seismic intensity. With a view to bring the building to its initial state, measures should be applied from paragraph 5.2 entitled "repair works".

Contemporary rural buildings that present a certain technical influence show favourable premises for ensuring a safety degree at severe strong motions (if one estimates that during the rural building life such a strong motion should be possible).

The purpose of the strengthening works refer to the increase of the structure strength and its rigidity, to the increase of ductility and energy dissipating capacity by adding vertical and horizontal reinforcement. The foregoing strengthening works may become efficient when reinforcing bars could be anchored at the foundation level and at the level of the collar beam. During the strengthening works, when there are no collar beams, and according to the requirements, reinforced concrete base-plinth and collar beams are to be cast after the mechanical anchorage of the vertical reinforcing bars.

With a view to perform the strengthening works the followings should be provided:

- 4-8 vertical bars  $\varnothing$  8-10 mm at corners (ends of shear walls) anchored at the lower and upper parts by welding or by screw nut connection. A certain pretensioning degree is very useful. From place to place the bars are connected with the walls by means of hooks in order to avoid their buckling during compression and are plastered with cement mortar;

- strengthening works similar to those mentioned at point 5.2 thus:

- \* welded meshes  $\varnothing$  4/10 cm applied on both sides of the masonry, tied with hooks that penetrate the walls;

- \* mortar injected into cracks and joints;

\* a 3-4 cm thick plaster using cement-sand mortar (ratio 1:3), ensuring the joints and walls cleaning for an adequate adherence.

The tests performed by INCERC specialists /13/ show the efficiency of the suggested methods. In special cases, together with the foregoing solutions, other solutions of the type given below should be taken into consideration as follows:

- concrete buttresses at corners or wall crossings;
- steel profile members acting as collar beams;
- framing the masonry by casting reinforced concrete columns in vertical slittings, and casting collar beams and base plinth (underpinning and overconcreting) as well.

For rehabilitation works (pre-seismic) similar strengthening measures should be used by introducing members of the collar beam and base-plinth types a.s.o. whether the technical and economical analysis shows the efficiency of the respective measures.

## 8. CONCLUSIONS

1. The rural housing existent in seismic areas in Romania are characterized by a steadiness of the traditional elements mingled with the existence of the modern building materials and technologies under the influence of the general industrialization and the urban planning of the localities.

The knowledge experienced from previous earthquakes has proved that although several damages and material losses have been recorded, no significant life losses have been recorded in the affected rural zones.

2. The characterization of rural housing from the value viewpoint - low or high cost does not depend so much upon the inhabitant's income, but also upon the available local materials such as manual labour, local and regional tradition as well as the urban planning degree of the localities. The value of the dwelling increases due both to the strength degree given by the modern material and technologies (very often intuitively applied) and to the endowments of the dwelling inside (such as running water, electricity, sewerage system, central heating a.s.o.).

Another tendency that has to be carefully controlled is that of the inhabitant's attention to the finishing and installation works instead of the structural control when one is building his own house.

3. The development of rural zones is done at present according to the approved designs using, in many cases, structures included in catalogues or approved typified projects

for which the aseismic protection is controlled. Naturally a thorough and competent local control for the whole rural area is still difficult to be achieved at present.

4. With a view to reduce the seismic risk in rural zones a number of measures are necessary as follows:

- the inventory of old buildings, damaged by the previous earthquakes, in even locality, controlling the strengthening and reconstruction works, showing the owners simple methods but possible to be applied, and providing technical and material support according to the methods applied after the previous earthquakes;

- the analysis of the building technologies, used by the inhabitants for building with their own means, concerning various types of structures and materials used in different zones of the county. It will be taken into account that the increase in height, floor number, and room dimensions as compared with the traditional house will have direct consequence on the spatial behaviour of rural buildings;

- the adequate application of principles and measures included in the official regulations concerning the rural planning and taking into account the positive local experience and conclusions on the effects of the previous earthquakes;

- the aseismic education in zones where people built on a large scale using their own means in order to avoid the incorrect usage of new industrial materials and the inadequate material mixtures and to pay the adequate attention to the aseismic resistance according to the modern knowledge in the field;

- the performance of sociological study in order to establish to what extent the typified rural catalogue buildings fulfil the requirements of the customers and ensure, according to the seismic risk mitigation necessities, the renewing of the housing stock in seismic rural zones.

#### REFERENCES

1. BONIFACIU, S., Romania, Ghid turistic, Editura Sport-Coordinator Turism, Bucuresti 1983
2. BALAN, St., Cutremurul de pamint din Romania de la  
CRISTESCU, V., 4 martie 1977-Editura Academiei RSR,  
CORNEA, I., Bucuresti 1982  
coordinators
3. \* \* \* Anuarul Statistic al RSR 1985. Directia Centrala de Statistica Bucuresti 1986
4. GEORGESCU, E.S. Low-cost traditional dwellings for rural  
CRAINICESCU, M.M. areas in Romania. Structural systems and their performance during the Vrancea March 4, 1977 earthquake  
7th Regional Seminar on Earthquake En-

5. GEORGESCU, E.S.  
et al. Seismological and engineering aspects of 13 November 1981 Tulcea, Romania earthquake-9th Regional Seminar on Earthquake Engineering, September 7-17 1982, Istanbul
6. YARAR, R. Rural Dwellings in Earthquake Areas in Turkey, TNCEE, Istanbul, 1985.
7. TEZCAN, S.,  
YERLICI, V.,  
DURGUNOGLU, H.I. Romanian Earthquake of March 4th, 1977, June 1977, Bebek, Istanbul Turkey.
8. MOINFAR, A.A. The Romania Earthquake of March 1977, Publication no. 77 January 1978. Technical Research and Standard Bureau, Plan and Budget Organization, IRAN.
9. ARIOGLU, E., Response of rural dwellings to recent destructive earthquake in Turkey (1967-1977) Proc. International Conference on Disaster Area Housing-Sept. 4-10, 1977, Istanbul, Turkey.
10. OHTA, Y. A Comprehensive Study on Earthquake Disasters in Turkey in View of Seismic Risk Reduction-Hokkaido University, Sapporo, Japan, 1983.
11. GEORGESCU, E.S. Contemporary rural buildings in seismic zones of Romania. Turkish National Seminar on Earth. Eng. October 1985, Istanbul, Turkey.
12. GEORGESCU, E.S. State of the art of the earthquake behaviour specific to several types of traditional and new rural buildings in Southern Romania. 8th ECEE Lisbon, Portugal, 7-12 September 1986.
13. SIMONICI, M. Research on strengthening methods for earthquake damaged masonry. Proc. Seminar Romano-American on Earthquake Behaviour and Energy Problems, INCERC, Bucharest, Romania. Sept. 1985.
14. JAVAHERI, H.J. Contemporary rural housing in seismic areas of Iran. Proc. Seminar TNCEE October 1985, Istanbul, Turkey.
15. CETINKALE, Y. After an earthquake. Proc. Seminar TNCEE, October 1985, Istanbul Turkey.
16. STANESCU, M.  
OLARU, V. Tests concerning the execution of stabilized soil walls using sliding formworks (in Romanian), Internal Report INCERC, 1982.
17. STANESCU, M.  
GHEORGHIU, FI.,  
OLARU, V. Long term behaviour of compacted stabilized soil plastered in different variants (in Romanian). Internal Report INCERC, 1982.

18. AHMAD, S. N., Soil stabilized housing for flood affected villages in Pakistan.  
Proc. Int. Conf. on Disaster Area Housing,  
Sept. 1977, Istanbul, Turkey.
19. KAFESCIOGLU, R., ALKER-Adobe stabilized with gypsum.  
GURDAL, E., Seminar TNCEE Sept. 1985, Istanbul, Turkey.  
KARAGULER, M. E.

LEGEND

6....9 MSK ZONING  
DEGREES  
ACCORDINGLY  
TO STANDARD  
11.100 / 1977

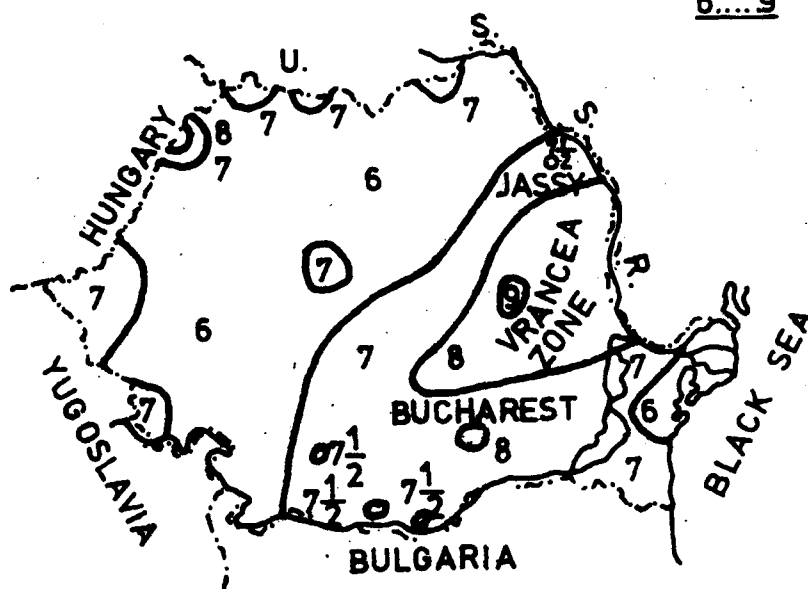


Fig.1. Seismic zoning map of Romania



Fig.2. Stone and timber rural traditional building.  
The light material is used for upper story.



Table I

Mixing formulae with earth stabilizers tested in  
Building Research Institute - INCERC Bucharest, Romania

Formula	Clayey earth kg / m <sup>3</sup>	Sand kg / m <sup>3</sup>	Stablilizers (kg / m <sup>3</sup> )				Water l / m <sup>3</sup>	Density ( kg / m <sup>3</sup> )			$\lambda$ $\frac{\text{kcal}}{\text{m h deg.}}$
			Cement	Lime	Ash	Straw		Wet state	After 28 days	Dry state	
A	850	550	100				30	2 250	1970	-	0,378
B	1050	700	50				130	2 190	1870	1730	0,378
C	850	550		50			130	2050	1870	1800	0,402
D	700	350		50	250		130	1700	1580	1520	0,319
E	850	600				25	130	2125	1900	1812	0,385

The image contains two technical drawings of a composite wall section, labeled B-B and A-A.

**Top Drawing (B-B):** This is a lateral view of the wall section. It shows a cross-section with a vertical rib on the left and a horizontal rib on the top. The wall is supported by a foundation. The dimensions are given as  $b_l = 25 - 45 \text{ cm}$  and  $b_e = 35 - 50 \text{ cm}$ . The label "LATERAL SIDE" is written above the wall. The section is labeled "B - B" on the left.

**Bottom Drawing (A-A):** This is a vertical view of the wall section. It shows a cross-section with a vertical rib on the left and a horizontal rib on the top. The wall is supported by a foundation. The dimensions are given as  $b = 25 - 50 \text{ cm}$ . The label "VERTICAL RIB" is written above the wall. The section is labeled "A - A" on the left.

**Fig 3. COMPACTED CLAY WALLS DETAILING AND TECHNOLOGY**

Table II

Correlation of building height, brick and mortar marks in seismic zones according to Romanian code P2-85 for masonry buildings

Building height H	No. of stories	Seismic zoning (MSK)							
		6		7		8		9	
		Brick mark	Mortar mark	Brick mark	Mortar mark	Brick mark	Mortar mark	Brick mortar	Mortar mark
H < 4m	1	50	10	50	10	50	25	75	50
4 - 9m	3	75	25	75	25	75	50	100	50
9 - 12m	4	75	25	100	25	100	50	-	-
12 - 15m	5	100	25	100	50	-	-	-	-

NOTE: marks are given in daN/cm<sup>2</sup>

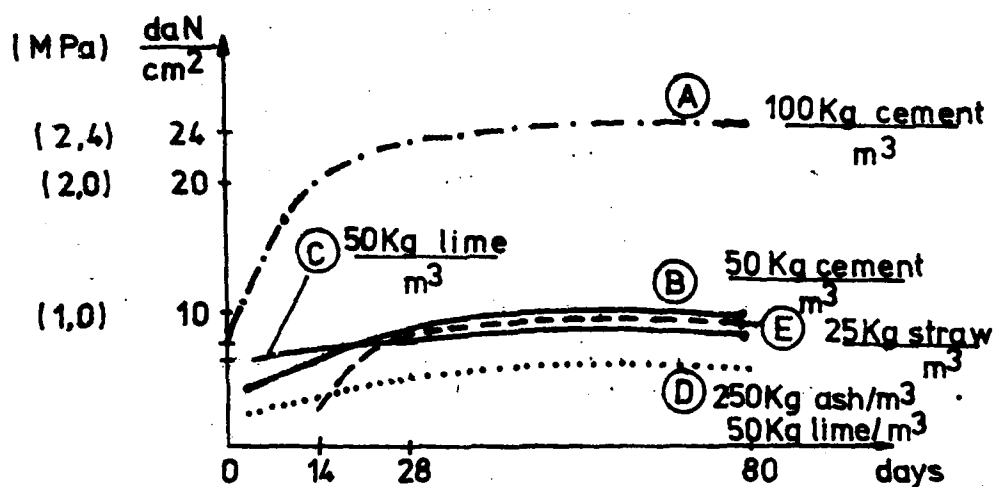


Fig. 4. Increase of cube strength of stabilized soil samples for different stabilizers and admixture ratio

(Building Research Institute Bucharest, Romania, 1982)



Fig.5. - Contemporary rural building before finishing works.  
Walls:ytong blocks framed by cast in place r.c. columns lintels and slabs.  
Stone foundation.3 stories.Upper story in timber.Seismic zone:VIII degrees MSK.Stone and timber available in the region.Materials and workmanship quality: medium.



Fig.6. Contemporary rural building before finishing works.  
Walls:kiln brick masonry.R.C. slabs and lintels. Stone foundation.3 stories.  
Materials and workmanship quality: very good.Seismic zone:VIII degrees MSK.

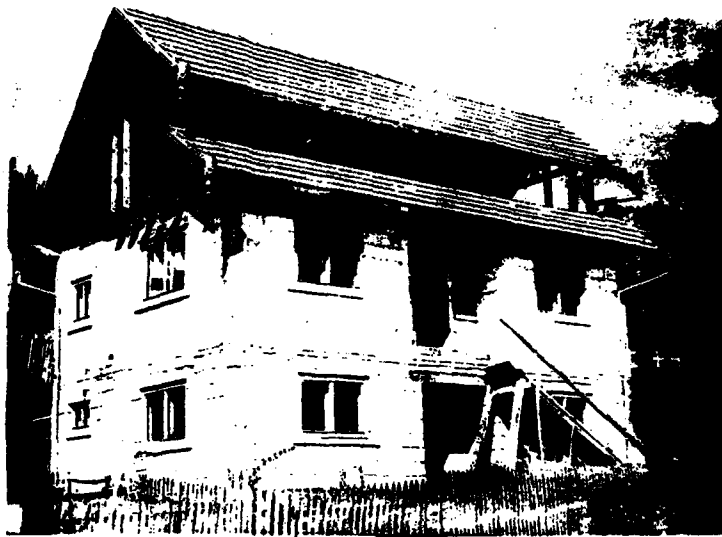


Fig.7. Contemporary rural building during construction works. Walls:ytong blocks framed by cast in place r.c. columns, collar beams, lintels. Stone foundation. Seismic zone:VIII degrees MSK. Upper story in timber. Materials and workmanship quality:very good.



Fig.8. Contemporary rural building: before finishing works. Walls:concrete hollow blocks (1 st. story), ytong blocks (2nd story) and timber (3rd story). Masonry framed by cast in place r.c. columns, collar beams-lintels, slabs. Stone foundation.Seismic zone: VIII degrees MSK. Materials and workmanship quality:very good.



Fig.9. Walling of the ytong blocks masonry on the stone foundation. The owner's family members help the skilled master.



Fig.10. Contemporary rural building after finishing works. First story in masonry, second story in timber. Seismic zone: VIII degrees MSK.



Fig. 11. Contemporary three storied rural building after finishing works. Upper story in timber.



Fig.12. Nonengineered contemporary rural hous- in ytong blocks and reinforced concrete members. Note the r.c. window beam lintel parallel

to the collar beam and floor slab, acting as a frame with the columns. Foundation is made of concrete. Remark new architectural aspect.



Fig.13. Contemporary, nonengineered rural two storied brick masonry building with embeded r.c. columns and r.c. slabs. Note the tendency to use the collar beam as a frame beam with positive effects on the earthquake behaviour (Seismic zoning in 7th degree MSK).

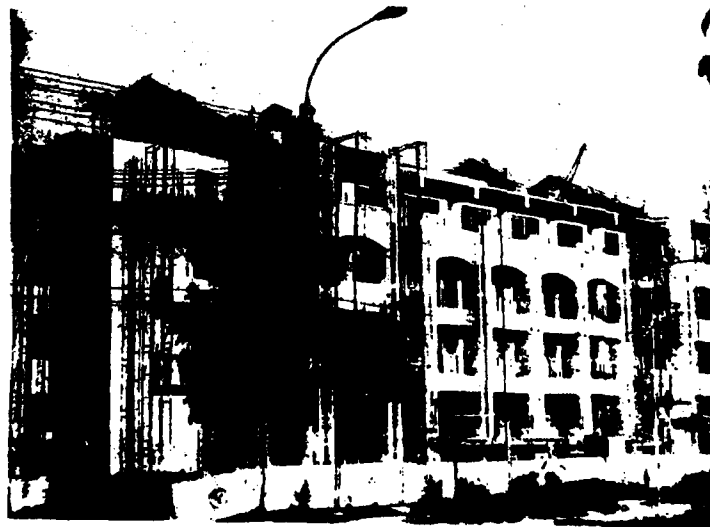
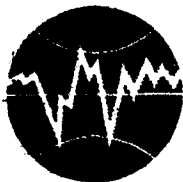


Fig.14. Four storied standard buildings for rural zones using precast members, erected by a specialized construction company near a city. Seismic zone: VII degrees MSK.





**TURKISH NATIONAL COMMITTEE FOR  
EARTHQUAKE ENGINEERING**

**THIRTEENTH REGIONAL SEMINAR ON EARTHQUAKE ENGINEERING**

**September 14-24, 1987 - Istanbul - Turkey**

**PRINCIPLES FOR THE ELABORATION OF NATIONAL SEISMIC CODES -  
NATIONAL AND INTERNATIONAL TRENDS**

=====

**R. G. Flesch<sup>1)</sup>, C. Unger<sup>2)</sup>**

PRINCIPLES FOR THE ELABORATION OF NATIONAL SEISMIC CODES -  
NATIONAL AND INTERNATIONAL TRENDS

=====

R. G. Flesch<sup>1)</sup>, C. Unger<sup>2)</sup>

Summary

-----

The harmonization of national seismic codes is preceding very slowly. Results of research in structural dynamics are often inadequately adapted for practical use. First, basic rules given by modern safety concepts and earthquake engineering monographs are discussed. Then the methods for the earthquake resistant design are summarized. The state of the art of harmonization is discussed focusing the uncertainties and open problems. Then the concept of the new Austrian seismic code is presented. As the degree of vulnerability of a building by vibrations is a central problem, criteria for the classification will be elaborated. Results of first sensitivity investigations of design actions on local differences between assumed and actual stiffness and masses are given.

1) Head of department of Structural Dynamics/BVFA-Vienna  
2) Research assistant/BVFA-Vienna

## 1. Scope

---

The methods in Earthquake Engineering (EE) were developed during the last thirty years. Modern computers and measuring devices are powerful means for the improvement of the methods. For the greater part of all structures seismic codes are used for the earthquake resistant design. Most national seismic codes prescribe quasistatic or response spectrum calculations. Attempts for harmonization of codes are undertaken but the progress is very slow. Many national codes are a mixture of several codes resulting sometimes in unrealistic models and values. Results of research in structural dynamics are mainly known by few specialists but are often inadequately adapted for practical use. Hence, it is necessary to elaborate codes compatible with latest results of research and easy to use by the practical engineer.

The accuracy of structural models can be further improved but many uncertainties are inherent in the assumptions of earthquake loads and local soil properties. Therefore upper quality limits for earthquake resistant designs exist which cannot be overcome by a further improvement of the structural model.

After a great number of earthquakes damage observations were carried out by international specialists. From many damages fundamental rules of earthquake engineering could be obtained which are given in the literature, e.g. /1,3/. The most important rules concern the ratio of main dimensions, permissible differences of mass and stiffness of adjacent stories etc. The earthquake resistance of a structure can be significantly increased by the consideration of the fundamental rules during planning and construction.

Codes should prescribe more complicated calculations only in situations promising an increased quality of the earthquake design. The more fundamental rules of earthquake resistant design are considered, the easier the calculation should be.

## 2. Basic concepts of seismic codes

---

### 2.1 General principles on reliability of structures

---

During the last years an increased number of investigations of the reliability of structures was carried out using probabilistic methods. The procedures are often too complicated for real structures but semiprobabilistic concepts are a useful basis for uniform safety specifications for civil engineering structures. In Austria the code ÖNORM B 4040 is prepared which will be the future basis for preparation and review of specific building standards. This code is based on the latest international and national drafts or standards on reliability, especially ISO 2394 and takes also into account Eurocode no. 1. Hence, codes on the reliability of structures will have an important influence on the development of seismic codes.

The standards on reliability specify general principles for the verification of reliability of structures to known or foreseeable loads. Reliability is considered in relation to the performance of the structure throughout its intended life. The principles must be in accordance with technical and economic facts.

It is important to recognize that structural safety is an overall concept comprising models for describing loads, design rules, safety elements, workmanship, quality control procedures, maintenance and repair and national requirements all of which are mutually dependent. This philosophy is new and unusual for the practical engineer. The concept seems to be good but practical application is often not easy. Following the concept, modifications of any one factor should be accompanied by a study of the implications involved in relation to the overall concept of safety.

Structures and structural elements should fulfill the following performance requirements:

- \* they should withstand all normal actions imposed upon them during their construction and anticipated use.
- \* they should in general, retain sufficient integrity to withstand local failures and specified accidental events.
- \* structures and structural elements should perform adequately under normal use.

Deterioration of material properties should not lead to an unacceptable probability of failure. Further the design solutions should be economical in their utilization of materials, energy, financial resources etc.

The structural performance of a whole structure or part of it should be described with reference to a specified set of limit states beyond which the structure no longer satisfies the design requirements. The limit states are divided into the following two categories:

- \* the ultimate limit state which generally correspond to the maximum load carrying capacity (safety related).
- \* the serviceability limit state which correspond to the criteria governing function related normal use.

The choice of the various levels of reliability should take into account the possible consequences of failure in terms of risk to human life or injury, the potential economic losses and the degree of social inconvenience. According to the consequences, structures are often classified as follows:

- \* risk to life negligible and economic and/or social consequences small or negligible (safety class 1 of draft ÖNORM B 4040).
- \* risk to life exists, economic and/or social consequences considerable (safety class 2 of draft ÖNORM B 4040).
- \* risk to life great, economic and/or social consequences very great (safety class 3 of draft ÖNORM B 4040).

For any structure it is generally necessary to consider several distinct design situations. Corresponding to each of these design situations, there may be different structural systems, different reliability requirements, different design values, different environmental conditions. Separate reliability checking is required for each design situation with due regard to different consequences of failure.

The design situations may be classified as:

- \* persistent situations, having a duration of the same order as the life of the structures.
- \* transient situations, having a shorter duration and a high probability of occurrence.
- \* accidental situations, normally of short duration and low probability of occurrence.

The actions (or loads) are divided - according to their variation in time - into:

- \* permanent actions which are likely to act throughout a given design situation and for which variations in magnitude with time are negligible in relation to the mean value.
- \* variable actions which are unlikely to act throughout a given design situation or for which variations in magnitude with time are not monotonic and not negligible in relation to the mean value.
- \* accidental actions, the occurrence of which, with a significant value, is unlikely on a given structure over the period of time under consideration and also in most cases is of short duration. The occurrence of an accidental action could in many cases be expected to cause severe consequences unless special measures are taken.

For practical applications e.g. in the draft ÖNORM B 4040 the following condition must be satisfied:

$$R^* \geq S^* \quad (1)$$

with  $R^*$  ... design resistance  
 $S^*$  ... design action effect

$S^*$  is given by

$$S^* = L \cdot \gamma_{\text{red}} \cdot \gamma_{\text{cont}} \cdot \gamma_n \quad (2)$$

For the ultimate limit state  $L$  is given by

$$L = \gamma_s \cdot G + \gamma_s^a \cdot Q_1 + \gamma_s^a \sum_{i=2}^n \psi_{\phi,i} \cdot Q_i + F_{\text{ex}} \quad (3)$$

with  $G$  ... permanent actions  
 $Q_1$  ... most important of variable actions  
 $Q_i$  ... additional variable actions, simultaneous with  $Q_1$   
 $\psi_{\phi,i}$  ... action - combination coefficient  
 $\gamma_s, \gamma_{\text{red}}, \gamma_{\text{cont}}, \gamma_n$  ... partial factors, reflecting the following influences:

- \*  $\gamma_s$  reflects the uncertainties of the characteristic values and of the stochastic model of the actions:
- \*  $\gamma_{\text{red}}$  reflects the simplifications due to structural modelling
- \*  $\gamma_{\text{control}}$  takes into account the influence of an independent quality control on safety
- \*  $\gamma_n$  is used to take into account the actual safety class

For the serviceability limit state the following formulas are given:

for infrequent combinations:

$$L = G + Q_1 + \sum_{i=2}^n \psi_{\phi,i} \cdot Q_i \quad (4)$$

for frequent combinations:

$$L = G + \psi_1 Q_1 + \sum_{i=2}^n \psi_{2,i} \cdot Q_i \quad (5)$$

and for quasi - permanent combinations:

$$L = G + \sum_{i=2}^n \psi_{2,i} \cdot Q_i \quad (6)$$

with  $\psi_1$  and  $\psi_{2,i}$  ... actions - combination coefficients

The partial factors for calculating the design action effect and the action - combination coefficients are given in the draft ÖNORM B 4040.

The design resistance  $R^*$  is found from

$$R^* = \frac{R}{\gamma_R} \quad (7)$$

with  $R$  ... characteristic value of resistance  
and  $\gamma_R$  ... partial factor reflecting the uncertainties of the characteristic values of the resistance.

## 2.2 Basic statements from IAEE - Monographs

### 2.2.1 Introduction

In earthquake engineering investigations can be carried out at different levels of accuracy. In principle, for each dynamic investigation the modelling of the excitation and of the structure is necessary. The dynamic response of a structure depends strongly on the layout and the construction. The more regular the buildings are, the simpler the structural model can be and a less sophisticated design procedure will be adequate.

Basic concepts of seismic codes are given in /1,2/ or in ISO/DIS 3010. Further, for the countries of European Community the draft of Eurocode no.8 was elaborated as a basis for the harmonization of seismic codes.

In part 1 of /1/ seismic zoning for building codes is discussed. Seismic zoning and earthquake parameters are not discussed in this paper, detailed information can be found elsewhere, e.g. /1,3/.

Part 2 of /1/ deals with the basic concepts for non engineered constructions. Most of the loss of life in the past earthquakes has occurred due to the collapse of buildings, constructed in traditional materials like stone, brick, adobe and wood, which were not particularly engineered to be earthquake resistant. In view of the continued use of such buildings in most countries of the world, especially in areas with low standard of living and heavy earthquakes, it is essential to introduce earthquake resistance features in their construction. Further in /1,3/ basic rules are given. The consideration of these rules during planning and construction will significantly increase the earthquake resistance of the structures.

In /2/ the basic concepts for engineered constructions are presented. For arriving at an economical solution to the earthquake protection problem, the level of desired protection must be specified. While theoretically it may be possible to construct buildings which can withstand the effects of earthquake without damage, where availability of suitable building materials may not pose a serious problem, it will generally not be feasible to do so due to very high costs involved /1/. From the safety view point, the safety of human lives is the primary concern and the functioning of the buildings has lower priority except the buildings required for the emergency, e.g. hospitals etc. The above aims could be met, if a building is designed and constructed such that in the event of the probable maximum earthquake intensity in the region

- \* the building should not suffer total or partial collapse
- \* it should not suffer such irreparable damage which would require demolishing and rebuilding
- \* although it may sustain such damage which could be repaired quickly and the building put back to its usual functions

### 2.2.2 Structural model

Seismic design regulations shall state criteria for idealizing structural systems. Quasistatic methods can be adopted when stiffness and mass vary gradually throughout the structure.

The seismic behaviour of a structure is to a large extent determined by its capacity to dissipate energy through ductile deformation.

Linear models can be used in conjunction with response spectra reduced to account for ductility, when dealing with regular elasto-plastic systems having gradual variations of the ratio of the strength available to that requires at critical sections. For irregular systems only a smaller load reduction through ductility can be used or local corrective factors are necessary. Irregular systems tend to local brittle failure or to the accumulation of plastic deformations at some locations of the system with pronounced variations in strength. Hence, to predict ductility demands of irregular systems, nonlinear methods of response analysis must be used.

Structural models must include the stiffness of all elements that may influence their response, including the so - called non - structural elements. Non - structural elements were often neglected in the past leading to unrealistic models and structural damage during earthquakes. It is often difficult to model accurately the possible interaction between structure and non - structure or to isolate non - structural elements from the structure. In many cases it will be convenient to carry out a double structural analysis, with and without non - structural elements.

Non - linear models shall also account for P -  $\Delta$  effects and specify the locations where non - linear material behaviour may occur. To obtain accurate results when carrying out step - by - step non - linear response analyses significant components of the ground motion must be treated simultaneously.

### 2.2.3 System requirements

System requirements define the conditions that a system is expected to satisfy in accordance with its intended use. For structural systems these requirements are grouped as follows:

- \* safety
- \* serviceability
- \* durability
- \* appearance

/2/ deals with the first two groups.

Safety requirements should state bounds to the probability of failure of a system for given time intervals. The influence of cumulative damage and degradation of mechanical properties should be taken into account. The reliability of a complex system depends on the reliabilities of the individual members and on the way they are interconnected. Hence, it is difficult to state a system reliability from the reliability of the single members. The safety requirements for structural members assumed to contribute to earthquake resistance must refer to the earthquake intensity that corresponds to a given return period.

Structural elements assumed not to contribute to earthquake resistance should maintain, with an adequate reliability, their integrity during and after the occurrence of seismic actions, and should not adversely affect the behaviour of the structure.

Non - structural members and their fastenings to the structural system should provide adequate safety against local damage and collapse during and after earthquake and should not adversely affect the behaviour of the structure. They should not create serious life hazards during and after earthquake.

Serviceability requirements for structures and structural elements should state the limit states e.g. excessive residual deflections, cracking or loss of stiffness. It is often advantageous to accept significant local damage to dissipate energy and prevent more dangerous failure modes, but repair work should be easy and reliable and should be undertaken immediately after damage takes place. It may even be advisable to place some structural elements destined to fail and be replaced.

#### 2.2.4 Performance criteria

Performance criteria are statements about the required properties of structures and structural members so that they will satisfy the assumptions of structural analysis and design. These rules cover the following properties:

- \* strength
- \* stiffness
- \* ductility

Strength performance rules should include statements about minimum and maximum acceptable values, in order to ensure that the system as whole is not weaker than intended and that no unforeseen behaviour problems will occur by the presence of members stronger than assumed. These rules should also include specifications about the acceptable relative values of the capacities of members and sub - assemblages in different failure modes.

Stiffness performance criteria should include statements about minimum and maximum acceptable values, in order to ensure that the system is not more flexible than intended and that no unfavourable distribution of internal forces will result from deviations of member stiffness with respect to those assumed.

Performance rules relative to ductility should state minimum values of that variable, as well as the number of alternating load cycles for which each member or subassemblage should be able to reach a specified deformation without significant reduction in strength or energy dissipation capacity.

### 3. Methods for the earthquake resistant design

#### 3.1 Layout and constructions according to basic rules

After many heavy earthquakes damage observations were carried out by international specialists. In many cases damage was caused by bad workmanship, especially in the area of joints. From other damages fundamental rules were obtained. Results are given in the literature, e.g. /1,3,4/. The most important rules concern the ratio of main dimensions, permissible differences of mass and stiffness of adjacent stories, eccentricities between the center of mass and stiffness, etc. Some examples are given in fig. 1-3. The earthquake resistance of a structure can be significantly increased by the consideration of the rules during planning and construction.



### 3.2 Concepts for the reduction of seismic forces

In principle, for sites with soft soil earthquake components with lower frequencies and for rock with higher frequencies are predominant. Hence, it is a basic rule to build soft buildings on rock and stiff buildings on soft soil to avoid resonances. Soft buildings are storey frames but the stiffness of non structure must be taken into account, which is often not easy. Stiff buildings are shear wall buildings and corewall buildings, having the disadvantage of a lower available ductility, which is difficult to predict. In addition, for heavy buildings on soft soil the soil - structure interaction has to be considered. In practical design situations it is often difficult to follow the rule mentioned above.

Following another basic principle, only negligible damages should occur during medium earthquakes. The structural elements should be stressed only in the linear range. For earthquakes of high intensity plastic hinging will start but it must not result in structural collapse.

Fig. 4 shows two principle hinging mechanism. Normally the beam-sidesway mechanism is preferred because greater ductility ratios can be obtained and the danger of structural collapse is minimized. A special detailing is necessary to ensure the development of hinges in the right areas. Some examples for steel structures are shown in fig. 5. Disregarded and unforeseen influences could reduce the effectiveness of the hinging concept during real earthquakes.

Using another concept, structural response can be reduced by dampers which are activated by relative movements between adjacent storeys. One possible variant is the use of dampers incorporated into diagonal stiffening members. Some examples are shown in fig. 6.

Further, base isolation can be used to reduce structural response. Using elastomere bearings the natural frequency of the structure can be decreased to about 0,5 Hz. If equation (8) is valid

$$f_n \leq \frac{f_{g,max}}{\sqrt{2}} \quad (8)$$

with  $f_n$  ... natural frequency of the structure with base isolation  
 $f_{g,max}$  ... lowest dominant frequency of earthquake spectrum

a significant reduction of the response can be obtained. Sometimes the damping of the bearings is increased by lead cores.

Base isolation reduces the acceleration within the structure but increases the displacements at the base to about 10 - 20 cm. Often problems with basement detailing and the connections of gas-, water- and sewage pipes arise. Further, the overturning moments and the long - term behaviour can cause problems. The low natural frequency of a base isolated structure can be excited by ambient vibrations. As these vibrations can cause kinetosis (motion sickness) of the inhabitants, base isolated systems are often blocked for small amplitude excitation and start operation at earthquake levels.

### 3.3 Dynamic calculations prescribed in codes

Dynamic calculations can be carried out at different levels of accuracy. Both the dynamic load and the structure must be modelled as accurate as necessary for the problem.

The following methods can be used:

- \* pseudo - static method
- \* response - spectrum method
- \* time - history analysis (modal superposition method and step - by - step integration)
- \* methods in the frequency domain
- \* stochastic methods

The methods are described well in literature, e.g. /5,6/.

The International Association for Earthquake Engineering (IAEE) brings out the latest collection of national seismic codes once every four years at the time of the World Conference on Earthquake Engineering.

Most national seismic codes prescribe pseudo - static and response spectrum calculations. The basic quantity used in the greater part of all codes is the base shear calculated from the total mass and a seismic coefficient, which is the product of several partial factors. Depending on the method used, the distribution of the design action over the height of the building is carried out more or less accurate.

Only short comments on the use of more sophisticated methods can be found in some codes.

#### 4. Trends in the harmonization of codes

-----

##### 4.1 State of the art

-----

In the greater part of all seismic codes quasistatic or response spectrum methods are used. The increased possibilities of computers encourage some engineers to use sophisticated programs, but many input data are uncertain. Therefore, the questions arises, whether the quality of the earthquake resistant design can be really increased. It must be the aim to elaborate more realistic codes in the future. More sophisticated methods should be used only in situations promising an increased quality.

It is assumed that also in the future for the greater part of structures quasistatic- or response spectrum methods are sufficient.

Most codes take into account the basic statements of EE - monographs but more principles on the reliability should be fitted in. Some important problems of code-procedures are discussed in what follows:

- \* global earthquake parameters can be estimated well, but assumptions about the frequency content for a special site are often unrealistic. The influence of local soil dynamics is very important but information for the practical design situation is available only at a relatively high cost level. Quick and unexpensive experimental methods would be necessary.  
For the today - situation the question arises, how accurate the calculation of modal frequencies of the structure must be.
- \* the field of applicability is not defined uniformly in all codes. Some codes principally exclude bridges, dams, nuclear facilities and structures with the potential danger of secondary disasters such as fire, leakage of hazardous material, etc. In general, also for these structures code procedures could be used to a certain extent, but the codes should state the limits of applicability. e.g. small bridges can be designed well using a quasistatic method while for a long span bridge with multipoint excitation a more sophisticated method will be adequate.

- \* in urban areas there are often ensembles of adjacent buildings built without adequate isolation gaps between them. Damping contact often occurs during severe earthquakes, especially if buildings have different heights. New buildings are often fitted in without adequate gaps to preserve the townscape. The problem is difficult, but solutions should be elaborated.
- \* there is no doubt that quasistatic or simplified response spectrum methods give good results in the case of regular structures. Due to the uncertainties inherent in response spectra the fundamental frequency can be calculated well using simplified formulas. Also the assumed distribution over the height will be realistic.

If irregular buildings are treated as regular buildings the wrong distribution of the design action will introduce greater errors than inaccurate modal frequencies.

Several codes give rules to distinguish between regular and irregular structures but the values are very different. Attempts for a harmonization are reported in chapter 6.

- \* separate calculations are carried out for two horizontal directions. There is no agreement between the codes if some percentage of the design action of the second direction should be taken into account when designing the first direction. No statement on that point was found in the reliability concepts. Some codes prescribe also a design in vertical direction for special structures or members. Near epicentres vertical excitation can be non - negligible but statements are missed in the codes.
- \* when modal responses in a particular direction can be regarded as independent of each other, the combination may be generally performed according to

$$S = \sqrt{\sum S_i^2} \quad (9)$$

where  $S$  ... is the response quantity under consideration  
 $S_i$  ... is the response quantity in the  $i$ -th mode of vibration

If modes with close spaced frequencies occur more sophisticated combination rules should be used, e.g. /7/.

- \* while actions from medium earthquakes are normally resisted in a linear way a ductile behaviour is necessary for extreme earthquakes. A good review of the problem and of ductility factors is given in /8/. One must be very careful to obtain an adequate ratio between ultimate deformation capacity and nonlinear design deformation all over the structure to avoid unforeseen hinging.
- \* damping strongly influences the magnitude of the design actions. Several damping mechanisms act within a structure, which are understood not very well at the moment. Damping is taken into account via a equivalent damping ratio. More research is necessary for a better modelling.

For a better harmonization the following points should be considered:

- \* uniform criteria for seismic zoning
- \* uniform criteria for the elaboration of maximum values of ground acceleration etc.
- \* use of an uniform normalized response spectrum
- \* uniform safety concept and rules for the combination of actions
- \* use of an improved ductility concept, giving rules avoiding adverse discontinuities in strength and ductile behaviour in vertical direction. Elaboration of more realistic ductility factors
- \* uniform maximum values of interstorey drift, especially to limit damage of non - structural elements

"Trends in harmonization of codes" is the name of one topic at many conferences on EE. The literature was reviewed starting with the 6. ECEE, Dubrovnik, 1978. Most papers present new national codes or compare different codes but few real harmonization concepts are discussed.

In /9/ the partial factors used in several European codes for the calculation of the base shear are compared.

In /10/ the comparison is carried out for non - European countries. Formulas and values of comparable factors are listed, easy to survey.

From the results of /11/ it is evident that seismic forces calculated by Balkan countries codes are 10-50 % smaller than the forces from USA-ATC-78.

The new earthquake resistant regulations for buildings in Japan are presented in /12/. This paper seems to be a good help for the revision of codes because it comes from a country with great practical experience in EE. For most buildings the Japanese code prescribes a design for the ultimate limit state as well as for the serviceability limit state.

In /13/ some of the more significant underlying assumptions and experiences introduced into the seismic provisions of the Uniform Building Code over many years are discussed.

In /14/ information on sources of fatal weakness in the designer - contractor - user system and on the distribution of error source in design/construction of R/C structures is given. More investigations of that kind will be necessary to follow the principles stated in chapter 2.1.

In /15/ the outline of the Yugoslav code is given, especially smoothed and normalized response spectra are presented covering American-, Yugoslavian- and Italian earthquakes.

The philosophy of the new Swiss earthquake regulations is given in /16/. The draft prescribes a quasistatic analysis. A construction factor is introduced, serving for two different purposes:

- \* reduction of the elastic equivalent static forces by allowing plastic deformations
- \* taking account of the difference between the design values and the effective values (resistance and deformations) which determine the behaviour (using specific damage patterns assigned to structural classes)

During the development of the new Swiss seismic design code, several comparative analysis studies have been performed especially with drafts of CEB, Eurocode no. 8, ATC-3. Results are given in /17,18,19/.

A typical example from /18/ is given in fig. 7. The design base shear for a warehouse was calculated using 8 different codes. A maximum difference of 500 % between the results of the Indian and the Japanese code was obtained.

Very interesting results are presented in /19/. Deformations, moments and shear were calculated for 3 different buildings, using the Swiss draft (SIA), ATC-3, the code of Baden-Württemberg (RL-TW) and a response spectrum calculation (ASM) using a spectrum obtained from the Friulian earthquakes. The results are shown in fig. 8.

The main conclusions are:

- \* the codes underestimate the maximum bending moment strongly for buildings with a fundamental frequency  $> \sim 1$  Hz. The calculated maximum moment is only 12 - 60 % of the moment obtained by the response spectrum method.

- \* for buildings with a fundamental frequency  $< \sim 0,5$  Hz the bending moments are underestimated in the upper parts and overestimated in the lower parts by the code procedures (see fig. 9). This is especially true if also higher modes are excited.

In /20/ the use of ductility to reduce the strength demanded by linear elastic response through the use of response reduction factors is examined. The rationale for these factors and for the values recommended by ATC and SEAOC is discussed in light of recent earthquakes and research results.

In /21/ a procedure is shown to limit the potential damage of buildings to a tolerable level. The procedure is based on a damage model, in which structural damage is expressed as a function of the maximum deformation and dissipated hysteretic energy.

#### 4.2 Draft of international standard ISO/DIS 3010

This draft is an important basis for the harmonization of codes. The seismic actions described are fundamentally compatible with the general principles on reliability (ISO 2394).

The draft specifies methods of evaluating seismic actions for the earthquake resistant design of buildings, towers, chimneys and similar structures. Most of the principles are applicable also to structures such as bridges, dams, harbour installations, tunnels, fuel storage tanks, chemical plants, conventional power plants, etc. Nuclear power plants are not covered by this code.

The basic philosophy is:

- \* to prevent human injury
- \* to ensure continuity of vital services
- \* to minimize damage to property

Seismic actions shall be taken either as accidental actions or variable actions. For accidental actions the structure has to be designed for the ultimate limit state. It is assumed that the serviceability limit state is verified indirectly in that case.

For variable actions the structure has to be designed for the serviceability limit state.

The draft prescribes an equivalent static analysis or a dynamic analysis. For the dynamic analysis only few general statements are given.

Using the equivalent static method, for the ultimate limit state the seismic design action for the  $i$ -th level of a structure is given by

$$F_{ia} = \alpha \beta \gamma_a \delta \eta \phi_i G \quad (10)$$

where

- $\alpha$ ... is the importance factor as related to the use of structure
- $\beta$ ... is the seismic hazard zoning coefficient to be specified in the national code
- $\gamma_a$ ... is the standard base shear coefficient for the accidental seismic action to be specified in the national code
- $\delta$ ... is the structural coefficient to be specified for various structural systems according to their ductility
- $\eta$ ... is the dynamic coefficient as related to the response spectrum considering the effect of soil conditions and damping property of the structure

$\phi_i$  ... is the coefficient which characterizes the distribution of seismic forces in elevation, where  $\phi_i$  satisfies the condition

$G$  ... is the gravity load of structure

For the serviceability limit state the design action is given by

$$F_{i,v} = \alpha \beta \gamma_v g \phi_i G \quad (11)$$

where  $\gamma_v$  is the standard base shear coefficient for variable seismic action to be specified in the national code.

The structure has to be designed according to the orthogonal axes x-y. The total design seismic action,  $E$ , to be considered usually consists of the following two combinations of  $E_x$  and  $E_y$

$$E = E_x + \lambda E_y \quad (12)$$

$$E = \lambda E_x + E_y \quad (13)$$

where

$E_x$  ... seismic design action in x - direction  
 $E_y$  ... seismic design action in y - direction  
 $\lambda$  ... coefficient to be specified in the national code  
 e.g.  $\lambda = 0,3$

The vertical component  $E_z$  is usually not considered explicitly. It is, however, taken into account with its most unfavourable value, for example in the following cases:

- prestressed structures
- horizontal structural members with clear spans of more than 20 m
- constructions with high arching forces
- cantilever members
- concrete columns and shear walls subjected to high shear forces, especially at construction interfaces

Two different kinds of deformations of the structure have to be controlled:

- \* the inter - story drift should be limited to restrict damage to non - structural elements such as glass panels, curtain walls, etc. for moderate earthquakes and to control against fracture of structural elements and instability of the structure for severe earthquakes
- \* the control of the total displacement is concerned with the reduction of panic or discomfort for moderate earthquakes and with sufficient separations of two adjoining structures to avoid damaging contact for severe earthquakes. For severe earthquakes  $\rho - \Delta$  - effects must be taken into account.

The torsional moment of the i-th level of the structure,  $M_i$ , may be determined by

$$M_i = Q_i e_i \quad (14)$$

where  $Q_i$  is the seismic shear force of the i-th level:

$$Q_i = \sum_{j=1}^n F_j \quad (15)$$

$e_i$  is one of the following two values, whichever is the most unfavourable for the structural element under consideration.

- \* the actual eccentricity between centres of mass and rigidity, multiplied by a dynamic magnification factor representing the coupling of transverse and torsional vibrations, and by adding the incidental eccentricity of the i-th level
- \* the actual eccentricity between the centres of mass and rigidity, diminished by subtracting the incidental eccentricity

The dynamic magnification factor will be specified in the national code. For example, this value may be taken as around 1,5.

In addition to equ. (9) for the combination of the modal responses the equation (16) is given:

$$S = \sqrt{S_{max}^2 + \sigma \sum S_i^2} \quad (16)$$

where  $S_{max}$  is the maximum value of  $S_i$  and  $\sigma$  may be taken as 0,5 for example.

It can be concluded, that ISO/DIS 3010 is an excellent basis for the elaboration of seismic codes, giving the important points in a clear and effective way. The code is material independent. No constructive rules are given.

#### 4.3 Draft of Eurocode no. 8

At the moment the draft is not so well elaborated as ISO/DIS 3010. In the future this code will be very important for the European countries, among them Austria.

In principle, the code can be used for dwelling - office - and industrial houses. The use for other structures can be prescribed by the authorities except for extraordinary structures and structures with a potential danger of secondary disasters. The seismic actions are classified as accidental actions.

The code does not directly state a design for an ultimate limit state or a serviceability limit state.

At the moment two response spectra are given, but only the second one is necessary. This design spectrum is given in fig. 10.

The code gives statements on time history analysis, complete and simplified response spectrum method and a quasistatic method. For the simplified response spectrum method formulas for the fundamental period and the distribution of the design actions over the height are given.

Using the equivalent static method, the design action for the  $i$ -th level is given by

$$F_i = A R(T) W_i / q \quad (17)$$

where

$A$  ... maximum ground acceleration  
 $R(T)$  ... ordinate of the design spectrum  
 $q$  ... ductility factor  
 $W_i$  ... gravity load of the  $i$ -th level

The code uses also equ. (12,13) for the combination of the two horizontal design actions.

For the evaluation of torsional moments, some advanced formulas for the eccentricities are given.

For the combination of the modal responses equ. (9) is prescribed.

Some basic rules of EE are stated in the code. A third part of the code is under elaboration at the moment, containing constructive rules and material demands for foundations, concrete-, steel-, composite-, timber-, masonry- and mixed structures.



## 5. Concepts and methods for the improvement of seismic codes

---

### 5.1 General aspects

---

In EE the following methods are used

- \* dynamic calculations
- \* dynamic in-situ tests
- \* dynamic model tests
- \* elaboration of dynamic structural models from earthquake responses recorded in instrumented structures

Each method has advantages, disadvantages and limitations. By an optimum combination of these methods progress can be obtained. In principle, in EE to less work is done to adapt results for practical use. Recent approaches are discussed in chapter 6.

### 5.2 Concept of the new Austrian seismic code (ÖNORM B 4015)

---

The Austrian committee for the revision of the seismic code tries to find a solution between a code containing the latest international results and a code which can be easily used by the practical engineer. The code should give realistic results. More complicated calculations will be prescribed only in situations promising an increased quality of the design. The code will include a pseudostatic and a response spectrum procedure.

The method to be used (quasi - static, response spectrum or more sophisticated calculation) will depend on the following factors:

- \* earthquake risk at the site
- \* safety class of the building (e.g. life line character)
- \* degree of vulnerability of the building by vibrations

From tab. 1 a parameter giving a "combined hazard" of earthquake damages as a function of the seismic zone and the safety class can be obtained. The values are a first proposal and need a review by people working on reliability of structures.

The degree of the vulnerability of a building is strongly influenced by its structural irregularities. A lot of criteria for classification were found in several national codes and in literature. The values often differ drastically. In tab. 2 some first estimates are compiled, which will be the basis for a more detailed elaboration. It is assumed that not all criteria will have the same importance and hence the number can be reduced.

The following groups are used:

- N ... low vulnerability
- R ... medium vulnerability, but relatively regular buildings
- U ... medium vulnerability, but irregular buildings
- S ... high vulnerability

The method to be used follows from tab. 3 as a function of the "vulnerability - group" and the "combined hazard".

The following design method can result from tab. 3:

- NK ... no consideration of earthquake forces. The necessary horizontal resistance is provided by the design prescribed in the material codes
- K ... no dynamic calculation necessary if fundamental rules of EE are considered
- Q ... quasistatic method

- A ... response spectrum method
- D ... a more sophisticated dynamic analysis by a specialist is necessary, the code procedure is not sufficient in this case.

Hence, in the best case for the designer (lowest danger of earthquake damage) no special seismic design will be necessary. In the worst case which can be treated by the code, a response spectrum method will be prescribed. For a hospital, for example, in an area of high seismic risk which is strongly vulnerable a more sophisticated design will be necessary.

The classification given in tab. 3 is a first assumption and will be elaborated in the research project discussed in chapter 6.

The first draft of the new ÖNORM B 4015 was elaborated 4 years ago. The idea of introducing tab. 1 and tab. 3 is basically new.

Procedures mainly given in ATC-3 were chosen as the backbone for the calculations planned. In the research project all equations and values should be elaborated finally. The text is now very long and should be reduced on the basis of the research project as much as possible looking at the excellent compact format of ISO/DIS 3010.

Further, some demands from the superior reliability concept must be fitted in.

Seismic actions will be classified as accidental actions and the structure will be normally designed for the ultimate limit state. The statement of ISO/DIS 3010 that serviceability is verified indirectly when designing for ultimate limit state seems to be doubtful. Therefore, for lifeline structures serviceability will have to be verified in addition.

To have a modern code the following input must be contributed from the superior reliability concept (for Austrian from ÖNORM B 4040):

- \* partial factor  $\gamma_n$ , equation (2)
- \* partial factor  $\gamma_{contr}$ , equation (2) alternatively to be fixed by seismic code committee
- \* rules defining quality of workmanship, control procedure, maintenance
- \* action - combination coefficients in equation (3,4,5,6)
- \* combination coefficient for dead masses and live masses

The following points are not included in reliability concepts and have to be discussed with the specialists:

- \* "combined hazard" according to tab. 1
- \* combination of two horizontal orthogonal actions by a factor  $\lambda$  in equation (12,13)

The following points should be fixed by the seismic code committee:

- \* partial factor  $\gamma_{contr}$ , equation (2), eventually
- \* partial factor  $\gamma_{mod}$ , equation (2)
- \* method to be used as a function of "combined hazard" and "vulnerability - group", tab. 3
- \* dynamic magnification factor in  $e_i$  (equation 14)
- \* factor  $\sigma$  in equation (16)

The partial factor  $\gamma_A$  (equation 7) will be in the responsibility of the material code committees.

## 6. Research project for the elaboration of the code

---

### 6.1 Program of investigations

---

The degree of the vulnerability of a building must be known before the necessary design method can be found from tab. 3.

The degree of the vulnerability is strongly influenced by the main dimensions and the structural irregularities. Starting from the values in tab. 2 the most important criteria will be elaborated. Sensitivity investigations will be carried out, first results are given in chapter 6.2. In addition, the limits of the applicability of the different methods, resulting in the final edition of tab. 3, will be obtained.

The second aim of the project is a rational further improvement of structural modelling, especially a better consideration of influences of the non - structural elements. For several types of buildings in-situ tests combined with calculations are planned at different phases of the construction.

### 6.2 Sensitivity of seismic design actions on the distribution of mass and stiffness

---

#### 6.2.1 Results for a storey frame buildings

---

To elaborate the sensitivity of the design actions on the distribution of mass and stiffness, the example of a storey frame given in /5/ was chosen. The layout of the building is given in fig. 11. The numbers of storeys was increased to five. A response spectrum analysis was carried out for y-direction, using the spectrum given in DIN 4149. The resulting bending moments for the inner columns of one of the 9 equal frames are also given in fig. 11. In tab. 4 the different steps of the investigation are listed. Differences of the bending moments due to a variation of mass or stiffness at certain locations of the structure are given in fig. 13 - 14. Only a part of the calculations is finished at the moment. A detailed discussion of the results will be given in forthcoming papers.

#### 6.2.2 Results for a shear wall building

---

For the investigations example 2 given in /5/ was used.

The cross section of the normal storey is given in fig. 12. The building has 11 storeys. The structure was idealized using an equivalent beam model, with one lumped mass per storey. The normal storey height is 2,75 m. The height of the base storey was increased to obtain the same modal frequencies as in example 2. The equivalent moments of inertia and the masses were taken from example 2 in /5/. The procedure to calculate equivalent moments of inertia which approximately consider shear- and normal - force - deformations is discussed in /5/. A response spectrum calculation was carried out for y-direction using the response spectrum for soft soil and 5 % of critical damping given in /22/. The resulting bending moments are also given in fig. 12. Differences of the bending moments due to  $\pm 50$  % variations of mass or stiffness at certain levels of the structure are given in fig. 15 - 16. Only a part of the calculations is finished at the moment. A detailed discussion of the results will be given in forthcoming papers.

## 7. Conclusion

The Austrian committee for the revision of the seismic code is elaborating a new seismic standard. The code should be compatible with basic requirements of structural safety and of earthquake engineering. The code must be easily practicable by engineers and must be up to date with recent results of EE research. Only quasistatic - and response spectrum procedures can be given in codes, but the code must contain criteria concerning the limits of these methods. More complicated calculations should be prescribed only in situations promising an increased quality of the design. Starting from a relatively complicated first draft of the new ÖNORM B 4015 which was strongly influenced by ATC-3, the excellent compact format of ISO/DIS 3010 should be approached.

For each design situation an adequate idealization should be used. The degree of the vulnerability of a building is a central parameter for this demand. Rational criteria for classification are necessary. Some results of sensitivity investigations reported in chapter 6 are very promising. A lot of further work will be necessary.

## 8. References

-----

1. Basic Concepts of Seismic Codes. Vol. 1 Monograph of IAEE, Tokyo, 1980.
2. Basic Concepts of Seismic Codes. Vol. 2 Monograph of IAEE, Tokyo, 1982.
3. Dowrick D. J.: Earthquake Resistant Design. John Wiley & Sons, 1977.
4. Flesch R.: Grundlagen des erdbebensicheren Konstruierens. ÖIAZ, 131.Jg. Heft 9/1986.
5. Müller F. P., Keintzel E.: Erdbebensicherung von Hochbauten. Wilhelm Ernst & Sohn, 2. Auflage, Berlin - München
6. Cough R. W., Penzien J.: Dynamics of Structures. New York, Mc Graw Hill 1975.
7. Gupta A. K.: Modal combination in response spectrum method. 8. WCEE, Vol. 4, San Francisco, 1984.
8. Structures of limited ductility. Bulletin of New Zealand Nat. Soc.f.EE Vol. 19, No. 4, Dec. 1986.
9. Demir H., Bazyar T.: The comparative study of the earthquake resistance regulation of European countries. 6. ECEE, Dubrovnik, 1978.
10. Demir H., Polat Z.: A comparative study of the earthquake resistance regulations of non - European countries. 7. ECEE, Athens, 1982.
11. Agent R., et.al.: New Romanian Code for the aseismic design of multistory building shear - wall structures. 7. ECEE, Athens, 1982.
12. Umemura H., et.al.: Follow - up of new earthquake resistant regulations for buildings in Japan. 8. WCEE, San Francisco, 1984.
13. Hadjian A. H.: A calibration of the lateral force requirements of the UBC. 8. WCEE, San Francisco, 1984.
14. Moncarz P. D., Ross B.: Structural failures and the side benefits of seismic codes. 8. WCEE, San Francisco, 1984.
15. Zelenovich V., Paskalov T.: Yugoslav code for aseismic design and analysis of engineering structures in seismic regions. 8. ECEE, Lisbon, 1986.
16. Bachmann H.: The philosophy of the new Swiss earthquake regulations. 8. ECEE, Lisbon, 1986.

17. Amman W. J., et.al.: A comparison of the seismic design forces due to the Swiss draft with other codes and analysis procedures. 8. ECEE, Lisbon, 1986.
18. Bachmann H., Wieland H.: Erdbebensicherung von Bauwerken. Vorlesungsskriptum, ETH - Zürich, 1979.
19. Ammann H., Bachmann H.: Erdbebenbeanspruchung von Hochbauten nach verschiedenen Normen und Berechnungsverfahren. Bericht 110, Inst. f. Baustatik u.- Konstr., ETH - Zürich, 1981.
20. Bertero V. V.: Evaluation of response reduction factors recommended by ATC and SEAOC. 3. US-Nat. Conf. on EE, Charleston, 1986.
21. Park Y. J., et.al.: Damage - limiting aseismic design of buildings. 3. US-Nat. Conf. on EE, Charleston, 1986.
22. Grossmayer R. L., Fritz R.: Design Response Spectra for Central Europe. Vol. 2. Proceedings 8. WCEE, San Francisco, 1984.

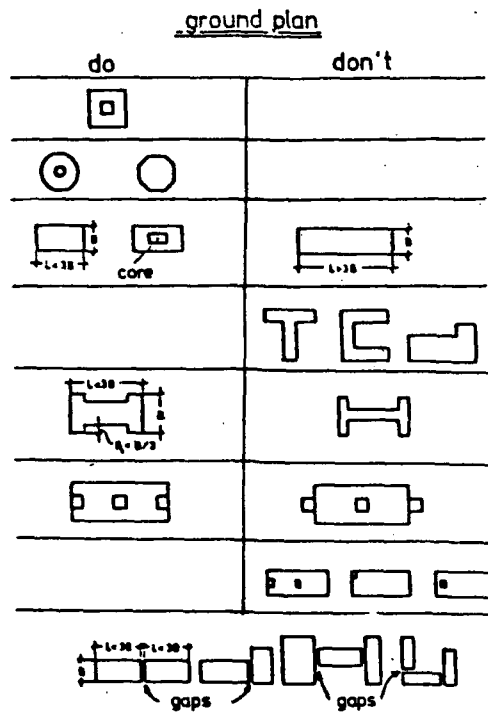


fig.1 Earthquake resistant layout of groundplan

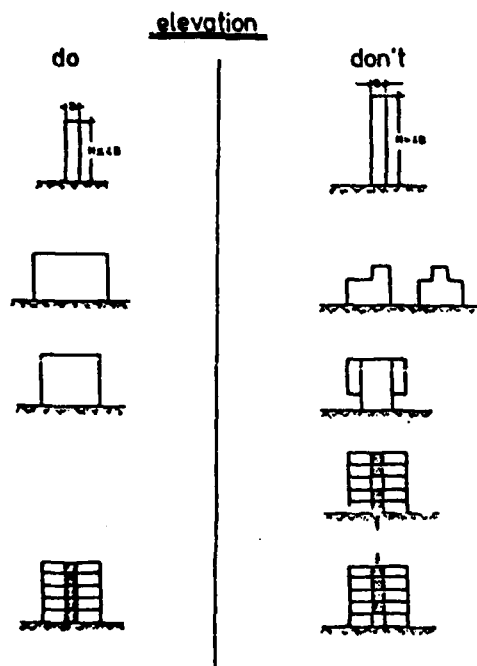
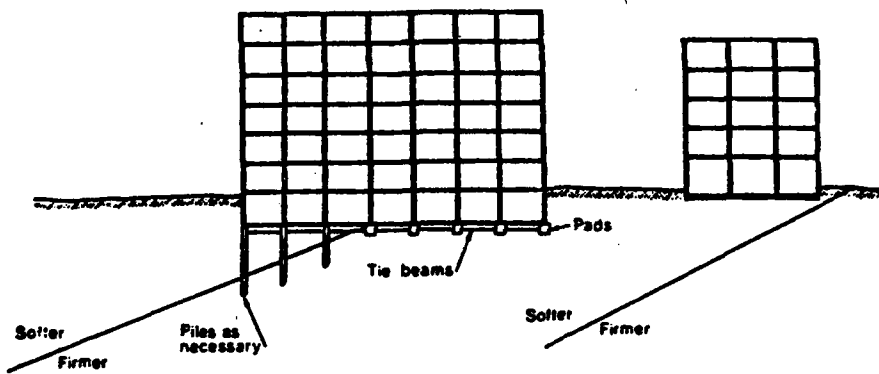
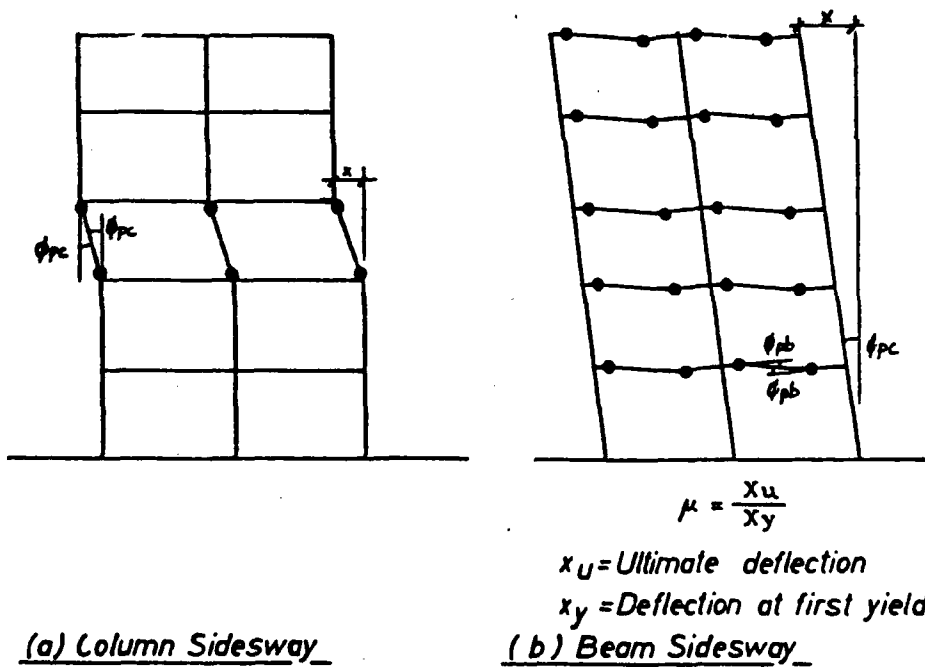


fig.2 Earthquake resistant layout of elevation

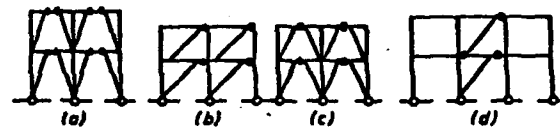


**fig.3** Earthquake resistant layout of foundation

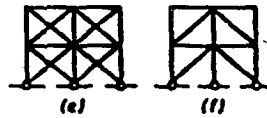


**fig.4** Hinge mechanisms for multi storey frames



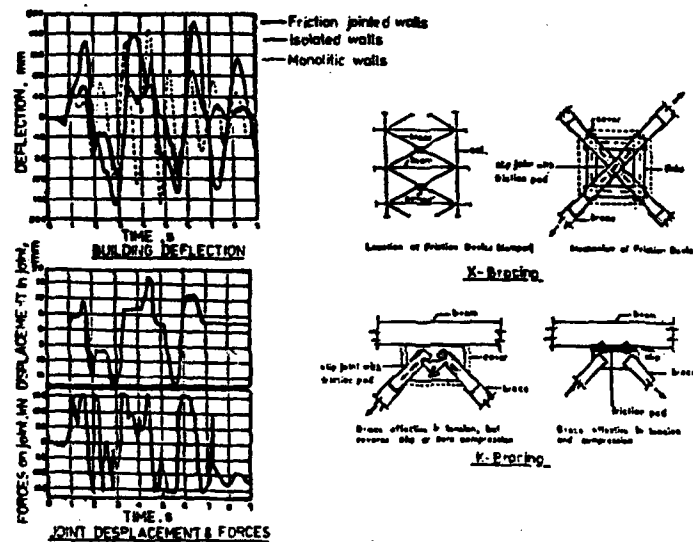


Eccentrically braced frames - Plastic yielding in flexure or shear



Concentrically braced frames - Plastic yielding in tension and compression

fig.5 Mechanisms of inelastic deformation of braced frames



Time-Histories at Top of 20 Story Wall

fig.6 Typical friction devices for frames (from A.S.Pall, Proc.SWCEE, vol.V)

	seismischer Faktor	regionale Seismizität	dynamischer Faktor	Konstruktionsart (Multipl.)	Risikofaktor	Deutungsanlass	Verform-Gründungs-Interaktion	Periode T	Produkt der Koeffizienten	base shear
	Z	Z <sub>r</sub>	S	K	R-I	F	I	T		h (m)
Schweiz	0.05	-	-	-	-	-	-	0.05	410	
Frankreich	1.00	-	0.13	-	-	1.15	0.28	0.15	920	
Baden-Württemberg	0.065	-	1.50	-	0.8	1.20	0.10	0.08	320	
Richtlinie	0.05	-	3.00	1.00	1.00	1.00	-	0.05	920	
USA	1.00	-	0.12	0.80	1.00	1.50	0.30	0.14	1140	
Japan	0.20	0.80	1.00	In F	1.20	0.80	0.24	0.17	1220	
Indien	0.20	-	0.18	0.80	1.00	1.00	0.40	0.03	270	
Neuseeland	In S	-	0.125	0.80	1.00	In S	-	0.10	810	

fig.7 Design base shear for a warehouse calculated after different codes (from /18/)

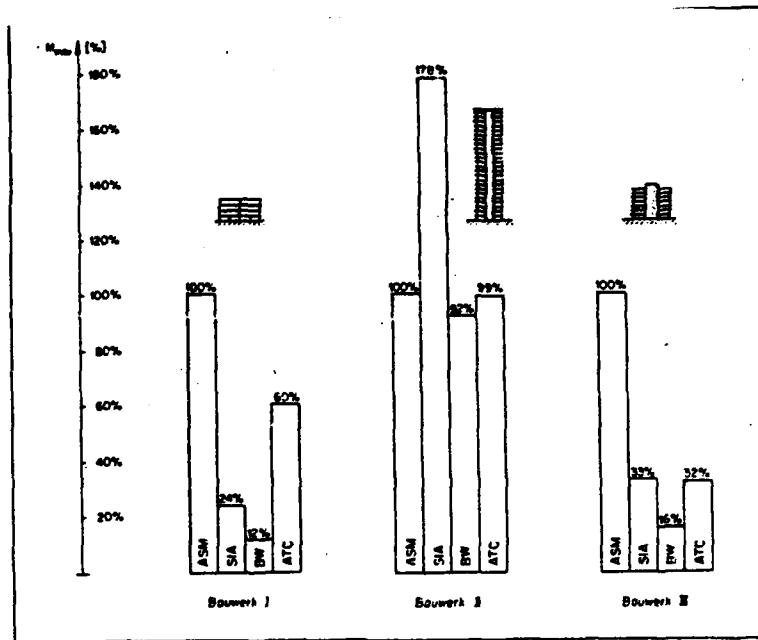


**fig.8** Comparison of maximum bending moment calculated by different methods (from /19/)

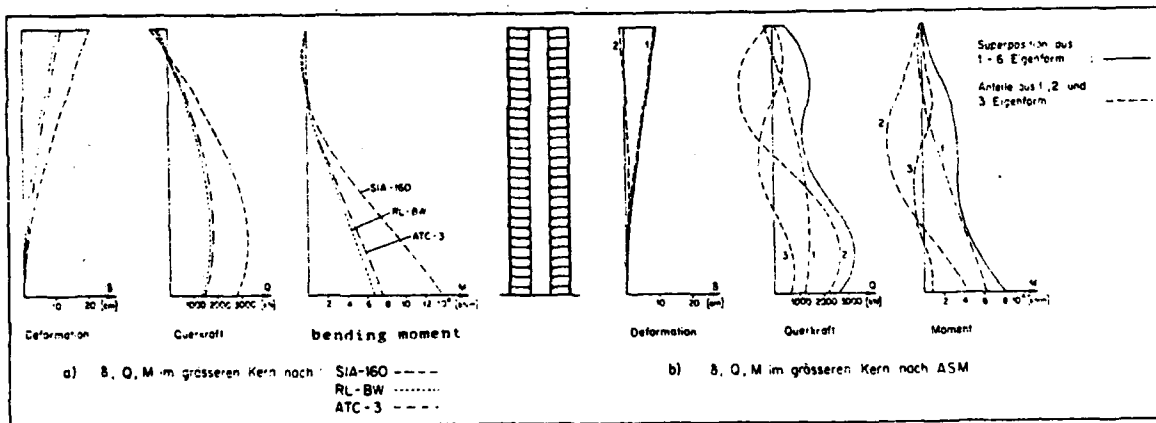


**fig.9** Comparison of vertical distribution of bending moments calculated by different methods (from /19/)

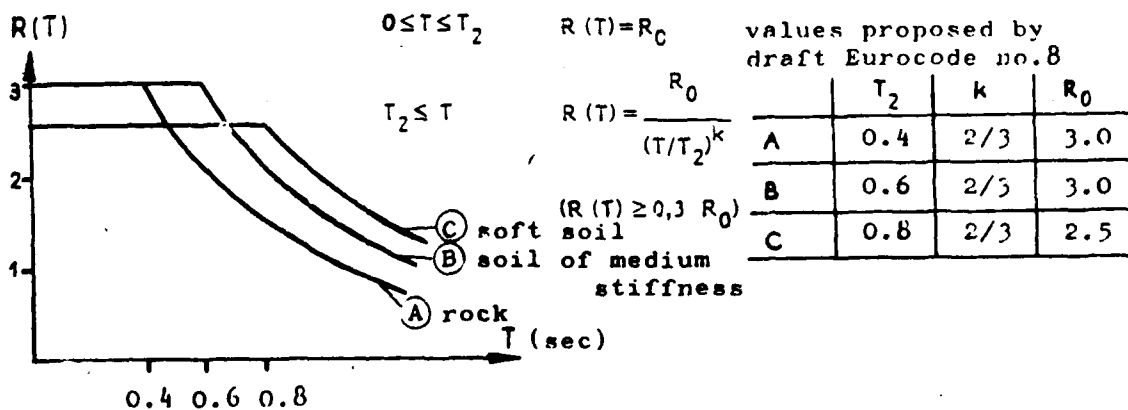


**fig.10** Design response spectrum from Eurocode no.8

degree of vulnerability				N	R	U	S
$h$	( m )	< 12	12 bis 50	> 50 bis 100	> 100		
$h/b_1$	( - )	< 2	2 bis 4	> 4 bis 6	> 6		
$l/b_1$	( - )	< 2	2 bis 3	> 3 bis 5	> 5		
$a_1/b_1$	( % )	< 25	25 bis 30	> 30 bis 50	> 50		
$a_2/b_1$	( % )	< 15	15 bis 20	> 20 bis 25	> 25		
$a_3/b_3$	( % )	< 10	10 bis 15	> 15 bis 20	> 20		
$a_4..a_6/b$	( % )	< 15	15 bis 20	> 20 bis 25	> 25		
$\Delta m_{max}$	( % )	< 20	20 bis 30	> 30 bis 40	> 40		
$\Delta k_{max}$	( % )	< 20	20 bis 30	> 30 bis 40	> 40		
$e/l$	( % )	< 5	5 bis 10	> 10 bis 15	> 15		
$f$	( Hz )	> 2	> 1,5 bis 2	1 bis 1,5	< 1		
$f_b/f_t$	( - )	?	?	?	...	?	

$\Delta m$ ....relative mass difference of adjacent storeys

$\Delta k$ ....relative stiffness difference of adjacent storeys

$e$ ....maximum of eccentricity between centres of mass and rigidity

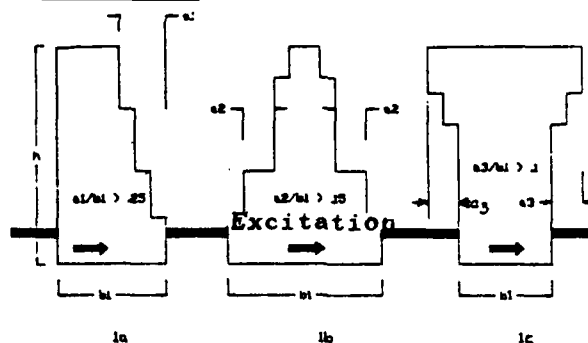
$f$ ....fundamental frequency

$f_b$ ....lowest bending eigenfrequency

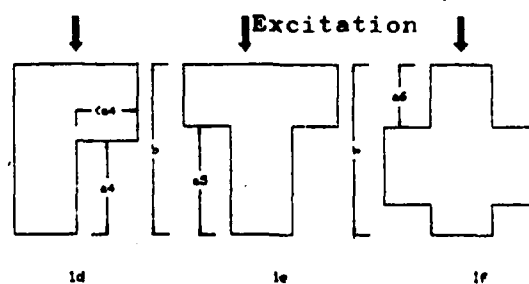
$f_t$ ....lowest torsional eigenfrequency

tab.2 Criteria for classification of the vulnerability of buildings

#### ELEVATION



#### GROUNDPLAN



		seismic zone				
		0	1	2	3	4
safety class	1	1	1	2	3	4
	2	1	2	3	4	5
	3	2	3	4	5	5

tab.1 "Combined hazard" as a function of seismic zone and safety class

		"combined hazard"				
		1	2	3	4	5
degree of vulnerability	N	NK	NK	K	K	Q
	R	K	Q	Q	Q	Q
	U	Q	Q	A	A	A
	S	A	A	D	D	D

tab.3 The necessary method as a function of the "vulnerability - group" and the "Combined hazard"

	column no.	mass no.	variation	$\Delta f_1$ [Hz]	$\Delta f_2$ [Hz]	$\Delta f_3$ [Hz]
1	-	m2	+30%	-0.041	-0.069	-0.092
2	-	m2	-30%	<u>+0.049</u>	+0.000	+0.160
3	-	m11	+30%	-0.010	-0.114	-0.026
4	-	m11	-30%	+0.011	<u>+0.143</u>	+0.035
5	-	m14	+30%	-0.002	-0.048	-0.169
6	-	m14	-30%	+0.002	+0.047	<u>+0.179</u>
7	3,8,13	-	+30%	+0.003	+0.003	+0.045
8	3,8,13	-	-30%	-0.012	-0.036	-0.133
9	5,10,15	-	+30%	+0.014	+0.057	+0.090
10	5,10,15	-	-30%	-0.021	-0.084	-0.128

tab.4 Steps of investigations in example 1

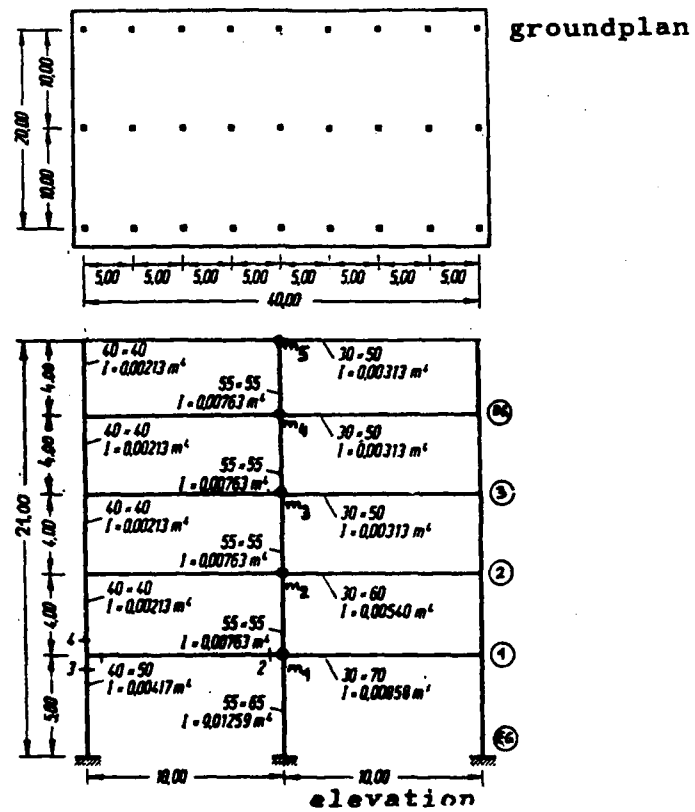


fig.11 Example 1 - multistorey frame

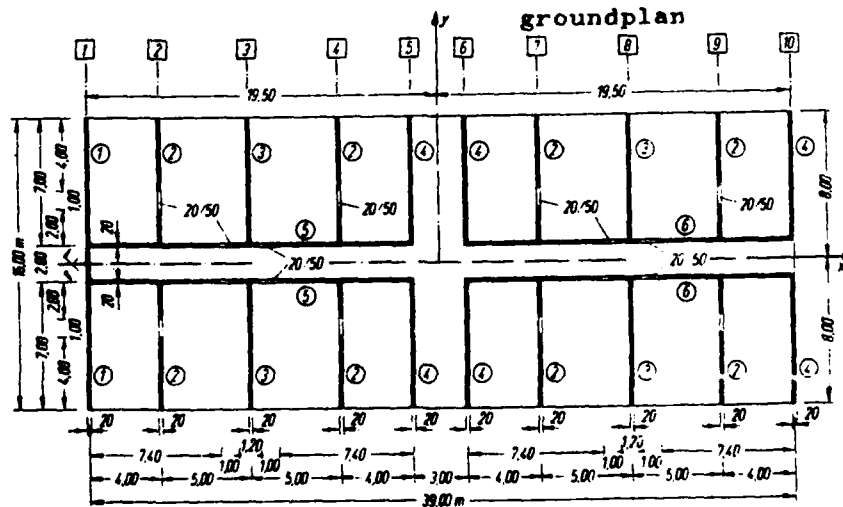


fig.12 Example 2 - shear wall building

Sensitivity of bending moment  
to  $\pm 30\%$  variation of storey-mass at different levels

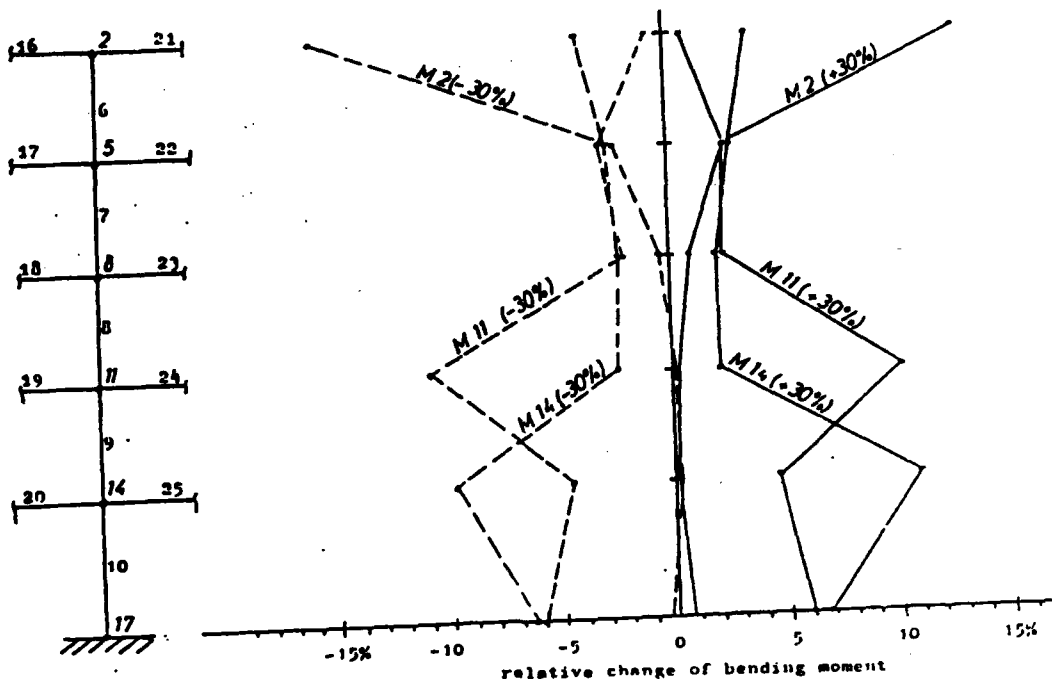


fig.13 Results for the storey frame building (example 1)

Sensitivity of bending moment  
to  $\pm 30\%$  variation of column stiffnesses at different levels

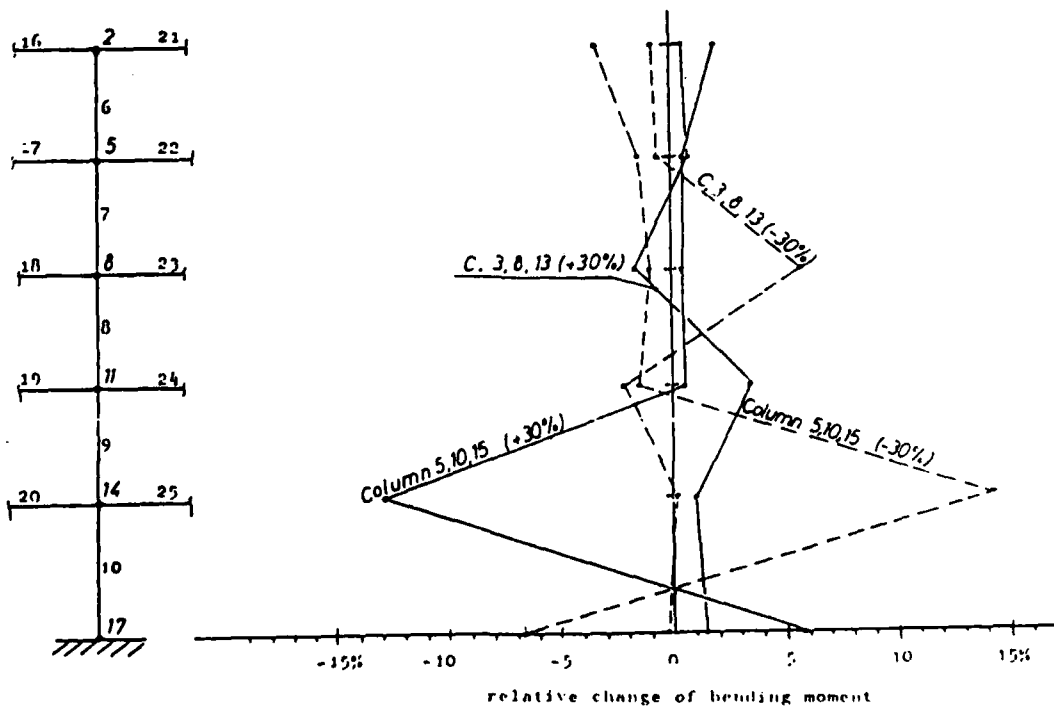


fig.14 Results for the storey frame building (example 1)

Sensitivity of bending moment  
to  $\pm 50\%$  variation of storey mass at different levels

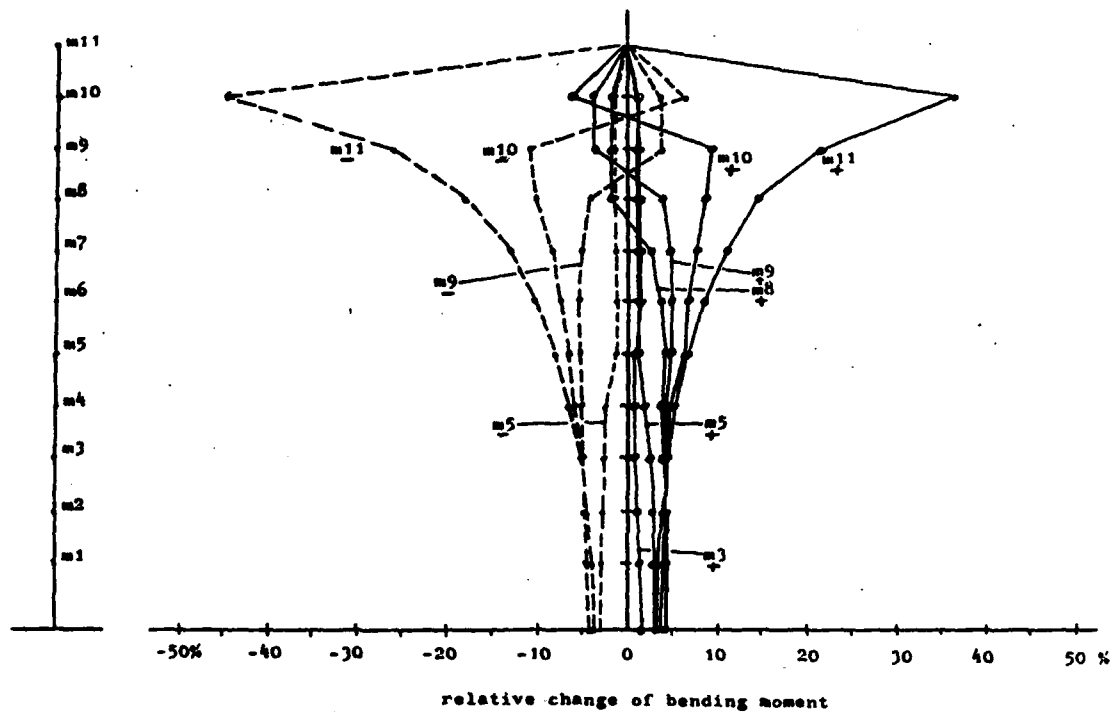


fig.15 Results for the shear wall building (example 2)

Sensitivity of bending moment  
to  $\pm 50\%$  variation of storey stiffness at different levels

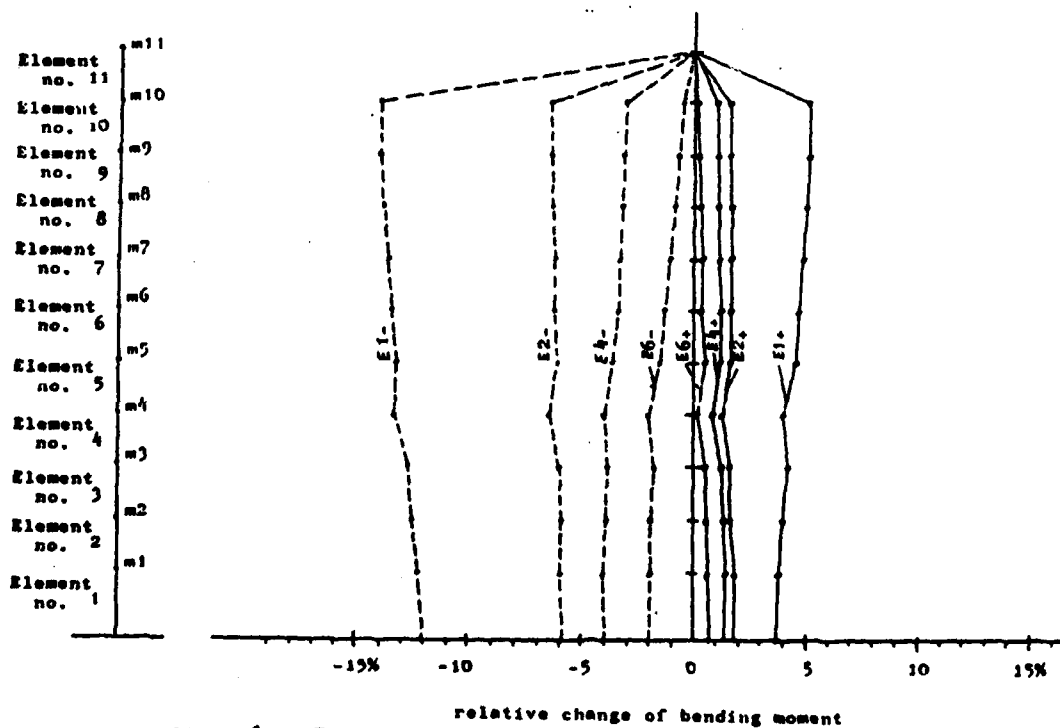
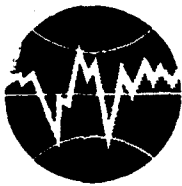


fig.16 Results for the shear wall building (example 2)



**TURKISH NATIONAL COMMITTEE FOR  
EARTHQUAKE ENGINEERING**

**THIRTEENTH REGIONAL SEMINAR ON EARTHQUAKE ENGINEERING**

**September 14-24, 1987 - Istanbul - Turkey**

**SOME NORMATIVE REQUIREMENTS FOR DESIGN AND CONSTRUCTION  
OF LARGE-PANEL BUILDINGS IN SEISMIC REGIONS**

**D. Nenov<sup>\*</sup>**



# SOME NORMATIVE REQUIREMENTS FOR DESIGN AND CONSTRUCTION OF LARGE-PANEL BUILDINGS IN SEISMIC REGIONS

D. Nenov<sup>\*</sup>

## SUMMARY

The present lecture treats first of all the necessity of consideration the problem and indicates its up-to-date importance. Farther are examined two kinds of requirements for construction of large-panel buildings in seismic regions : general requirements valid also for all other types of buildings and specific requirements valid for large-panel buildings only. Additionally there is presented the method of calculation of the bearing capacity of some of the connections.

### 1. INTRODUCTION

From historical point of view the large-panel buildings are a new type of construction. They came into the practice as late as several years after the end of World War II.

Nowadays the mass-scale construction of large-panel residential buildings is performed in more than 20 European countries.

In Europe, except the USSR there are now functioning more than 320 industrial enterprises for construction of large-panel buildings producing annually more than 600 thousand flats. This type of construction is developed widely in GDR, Poland, Hungary and Czechoslovakia where its relative portion of the whole construction is 50 to 75%.

The first large-panel building has been built in the USSR in the period 1947-1948. Afterwards, in many towns of the USSR started the experimental construction. In 1981 the construction of large-panel buildings is realized by 472 enterprises having a total production capacity of about 58 million  $m^2$  /i.e., about 900 thousand flats annually assuming 65  $m^2$  as the average floorage of a flat/. In some cities as Moscow, Leningrade, Kiev, Tashkent and others the relative portion of this type of construction is more than 75%.

---

\* Prof., Dr., Director, Central Laboratory for Seismic Mechanics and Earthquake Engineering, Bulgarian Academy of Sciences, Sofia, Bulgaria

According to the Soviet specialists the large-panel buildings construction in seismic regions has many advantages in comparison to the brick masonry construction : reduction of labour expenses with 35 to 40%, price reduction average of 6%, shortening of construction deadlines 1,5 to 2 times. Thanks to its advantages and its high reliability this type of construction takes more than 60% of the total volume of construction in the seismic regions of the USSR.

France is one of the first West European countries applying the large-panel construction. The first large-panel buildings have been built in 1949 and further on this type of construction gradually has obtained a mass character.

Since 1960 the large-panel buildings construction has been applied also in Czechoslovakia. In 1975 the relative portion of the large-panel construction is about 75% of the total volume of the mass residential construction.

In the German Democratic Republic the large-panel construction begins in 1958 and becomes quickly a mass type of construction.

In Poland, in a short period of time and particularly during the last decade was developed a strong large-panel production industry. In 1969 have been built 27 thousand large-panel flats and in 1978 their number is already 180 thousand.

The majority of the Balkan countries paid an interest to the large-panel construction long ago.

In Yugoslavia the experimental construction with large-panel elements began in 1955. After the Skopje earthquake in 1963 large-panel buildings continued to be built in several cities in this country. Since 1964 in Skopje the construction of earthquake resistant large-panel buildings up to 5 storey has started. In New Belgrade for seismicity 7 according to the MSK scale, 21-storey large-panel buildings were built in 1974, their first 5 storeys in cast in-situ reinforced concrete walls. Before the Montenegro earthquake in 1979 several large-panel buildings up to 6-7 storeys were built in the town of Bar and their behaviour during the strong earthquake in 1979 was satisfactory. Since 1976 mass construction of large-panel buildings was applied in New Belgrade with height up to 16 storeys.

The large-panel structures for multistorey residential buildings have been used in Romania since the end of the 'fifties as an efficient and rapid solution of the housing shortage problem of the country. Considering the system's multiple advantages, the number of large-panel buildings built every year has continuously increased, so that today about 60% of the total number of flats are built with large panels. There are factories for industrial production of prefabricated panels all over the

country.

The first one-storey large-panel building was built in Bulgaria in 1956-1957 and the first four-storey residential building was built in Sofia in 1958. The first complex of many large-panel buildings was built in 1959-1960. Gradually this type of construction obtained a mass character. Now in Sofia and in the majority of the districts' capital cities are functioning plants for industrial production of prefabricated panels with a total capacity of 45 thousand flats annually.

In the most of European countries non mentioned herein large-panel buildings are also being built intended preferably for dwellings.

In some European countries are used large-panel systems with wider purposes. Thus, in Italy the Peruggia University and the construction company "Elcom System" have worked out the structural system GN/PI for construction of residential, public, educational, and similar buildings up to several storeys. The special feature of this system is the use of prestressed reinforced concrete panels.

The large-panel buildings construction is applied also overseas. For example, this type of buildings have a wider application in seismic regions of the Chinese People's Republic particularly after the strong earthquake in 1976 in Tanshan. The volume of the large-panel buildings construction in USA is comparatively small. Usually large-panel buildings with shear bearing walls and hollow slabs elements concreted along their edges are built. A considerable number of large-panel buildings is performed in Japan, their height limited prior up to two storeys and later up to 4-5 storeys, designed for seismic intensity 9 according to MSK-64 scale.

The brief survey above shows that the large-panel buildings are widely applied in the majority of European countries either in seismic or in non-seismic regions. That is why the respective countries are obliged to work out for this type of construction such requirements which could assure the buildings for expected seismic excitations.

## 2. BASIC STRUCTURAL CONFIGURATIONS OF LARGE-PANEL SYSTEMS

There exist in the literature some distinctions in the description of the different basic structural configurations for construction of large-panel buildings. In the present lecture we stand by preferably to the description given in "Design and Construction of Prefabricated Reinforced Concrete Building Systems, UNDP/UNIDO Project RER/79/015, Vol.2, Vienna, 1985".

Prefabricated large-panel systems are used mainly for residential buildings. The designation "large-panel system" is applied to structures composed of large concrete panels which are connected in the vertical and horizontal direc-

tions so that the wall panels enclose appropriate size spaces for the rooms of the building. The panels form the structural system. Prefabricated wall panels are usually one-storey in height and in general both horizontal and vertical joints exist between the panels. The horizontal floor and roof panels usually consist either of one-way spanning prefabricated slab elements or of two-way spanning elements of the size of the relevant room. When properly connected together the horizontal elements act as diaphragms, transferring the earthquake loads to the walls, in addition to resisting the gravity loads.

Three basic configurations are used for large-panel buildings:

- a) Cross-Wall System. The walls bearing the gravity loads in the cross-wall system are placed perpendicular to the longitudinal axis of the building (Fig.1a). These cross-walls provide resistance to horizontal seismic loads in their direction and support the gravity loads from one-way spanning floor and roof elements. Walls not bearing gravity loads are placed parallel to the longitudinal axis of the building to provide resistance to horizontal seismic loads in that direction.
- b) Long-Wall System. The walls bearing gravity loads in the long-wall system are placed parallel to the longitudinal axis of the building (Fig.1b). The long walls provide resistance to horizontal seismic loads in their direction and support the gravity loads from one-way spanning floor or roof elements. Walls not bearing gravity loads are placed perpendicular to the longitudinal axis of the building to provide resistance to horizontal seismic loads in that direction.
- c) Two-Way System. The walls bearing gravity loads in the two-way system are placed both perpendicular and parallel to the longitudinal axis of the building (Fig.1c). These walls provide resistance to horizontal seismic loads in both directions and support the gravity loads from two-way spanning floor or roof elements.

Nowadays in the mass construction of the majority of the European countries is applied predominantly the configuration (a), as well as the configuration (c). The most wide-spread distances between the bearing transverse walls are 3 and 3,6 m.

The buildings constructed by the mentioned mass-applied structural systems represent rigid space structures capable to bear different static and dynamic loads. That is why such buildings are successfully applied in complex geological conditions and in regions of 7,8 and 9 MSK seismicity.

### 3. MORE IMPORTANT GENERAL REQUIREMENTS FOR CONSTRUCTION OF BUILDINGS IN SEISMIC REGIONS VALID ALSO FOR CONSTRUCTION OF LARGE-PANEL BUILDINGS

The majority of seismic building codes including the standards adopted by CEB[1] do not provide particular requirements for panel structures' design and building. They are treated in the same way as the other contemporary reinforced concrete buildings and have to comply with the general requirements for the reinforced concrete buildings with shear walls though in these requirements the characteristic features of the large-panel buildings are not taken into account. According to these general design requirements the lay-out of the structures as well as the positioning of the load bearing walls should comply with the following provisions :

a) In the town planning and architectural planning buildings with simple configuration in plan (square, rectangular, multiangular, round, etc.) should be provided.

b) The mass- and stiffness distribution should be uniform. The centre of masses to coincide with or to be with minimal deviation towards the stiffness centre of the vertical diaphragms.

c) The gravity load of the buildings to be decreased inclusively by application of light effective materials. Heavy roofs, cornices, etc. causing mass increase in the higher parts of the building should be avoided.

Aseismic joints are provided with the purpose of separating various parts of the building with different dynamic characteristics in order to allow them to oscillate independently when excited by seismic ground motion. The width of the joints has to be established stipulating that during the earthquake the building parts separated by the joints do not affect each other by collision during the out-of-phase oscillations.

For example, the Bulgarian code prescribes :

a) When the floor structures of the separate building parts are designed on different levels it is necessary aseismic joints to be provided.

b) The maximal length of a block, if no special additional requirements, is limited:

- for normal ground conditions - not more than the length of three sections but no more than 60 m;
- for loess and other weak soils - not more than the length of two sections but not more than 40 m.

c) The width of the aseismic joint is accepted as  $1/250$  part of the building height but not less than 3 cm.

d) The aseismic joints should start from the upper edge of the foundation and proceed along the whole height of the building. If the aseismic joint coincides with the dilatational one it should pass also through the foundations.

The Soviet code [13] prescribes the following :

a) Buildings and structures are separated by aseismic joints when having complex configuration in plan or when the separate adjoining parts of the building have a difference in height 5 m or more. No aseismic joints are necessary for one-storey buildings in seismic regions of seismicity 7.

b) The distances between the aseismic joints for large-panel buildings should not exceed 80 m in regions of seismicity 7 and 8 and 60 m in regions of seismicity 9.

c) The width of the joints is determined by calculation but minimal recommended values are : not less than 30 m for buildings up to 5 m height and additionally 20 mm for every additional 5 m in height.

The Romanian code [5] prescribes :

a) As a rule the aseismic joints should separate :  
- parts of the building with considerable height-mass- or stiffness differences;  
- parts of the building with different floor level;  
- parts of the building with excentric relative position being thus stressed unfavourably during the out-of-phase oscillations.

b) The joint width has to be calculated according to the code in force (formula is given) but it should not be smaller than 4 cm for a superstructure and 2 cm for a substructure.

#### 4. MORE IMPORTANT SPECIFIC REQUIREMENTS FOR DESIGN AND CONSTRUCTION OF LARGE-PANEL BUILDINGS IN SEISMIC REGIONS

In addition to the general requirements some of the seismic building codes provide specific requirements for the large-panel buildings taking into account their specific peculiarities. They are given hereafter.

The building must have sufficient number of panel elements capable to bear the horizontal loadings in both orthogonal directions. There is often a case in panel structures when the number of panels in transverse direction is sufficient while the number of longitudinal panels is not; this is a frequent case in panel buildings where facade elements are not bearing ones.

Panels must extend along the height of the building uninterruptedly. Substitution of panel elements by columns on certain storeys is prohibited. A tendency exists among architects to free the ground floor and/or the basement of the unwanted panels and substitute them by column elements since different functions are assigned to these spaces as compared with the higher storeys. Such a substitution may be tolerated if the remaining panels are able to bear the total seismic loading and if their stiffness is satisfactory. Special attention should be paid to columns taking the places of panels since they may be acted upon by highly

unfavourable loads. However, it is a very dangerous practice to replace all panel elements by columns in one-storey and it should not be approved.

The most responsible details of the large-panel buildings are the connections of the panels. They are performed along the horizontal and the vertical joints between the panels. They had their way of development depending on the experience accumulated during the assemblage and exploitation of the buildings as well as on the results of research work.

The main purpose of the connections between the prefabricated elements of the large-panel structures is that their structural elements (i.e. bearing walls and horizontal diaphragms built up from individual panels) should achieve as nearly as possible a monolithic behaviour. That is why the specialists of each country where large-panel buildings are built in seismic regions pay particular attention to the design and performance of the connections. As an illustration some generalized recommendations by Romanian specialists are given hereafter :

a) The connections must be of the "wet" type by casting in situ concrete within the joints between the prefabricated panels.

b) The connections should be detailed as to be able to support all the internal forces obtained in the respective regions from the structural analysis.

c) The transmission of the internal forces from one panel to the other through the joint must be distributed along the whole connection, avoiding the concentration of stresses that could have undesirable effects during seismic movement.

d) The vertical connections (monolithic concrete is cast into the vertical space between the wall panels) should provide horizontal links between the wall panels.

e) The horizontal connections (concrete is cast in situ into the horizontal space between panels) must provide vertical links between slab panels and final connection between the bearing walls and the horizontal diaphragms of the structure.

f) Subjected to shear forces, the joints should have an elastoplastic behaviour allowing, before failure, relative large displacement between the two panels without an important loss of shear strength. Under the design shear forces the joints should have an elastic behaviour.

g) Since the connections between the prefabricated panels are undoubtedly the regions of greatest seismic difficulties, the design forces transferred through the joints should be determined using greater safety coefficients than for the rest of the structure.

A lot of other specialists from the European countries have drawn similar conclusions concerning the connections in the large-panel buildings.

Having in mind the importance of the connections for the large-panel buildings special instructions [15] for

their design are in force in Bulgaria. As an illustration in Appendix 1 is given the method for calculation of the connections along the horizontal joints of vertical diaphragms. An other method [18] is given in Appendix 2.

Other specific requirements according to the codes of some countries are given hereafter.

#### Bulgaria

According to the Bulgarian codes [10, 11] the more important specific requirements are :

1. It is recommended the vertical diaphragms to be constructed so that the ratio of their maximal rigidity to the minimal one to be not more than 2.

2. The height of the large-panel buildings for the seismicity of the respective region has to be determined by calculation on the basis of bearing capacity and deformations.

3. When checking the deformations it is recommended the calculated horizontal displacement of the building at the upper/roof/ slab level to be not more than  $1/750$  part of the building height. The maximal relative floor deviation should not exceed  $1/500$  part of the floor height.

4. In large-panel buildings with bearing facade walls it is prohibited to design stores and other public premises if it causes change of the structural scheme or leads to changes in configuration of vertical of horizontal bearing structures.

5. Partial or full elimination of suspended facade panels in one or more storeys is permitted.

6. Special attention should be paid to the design of blind walls since they are loaded by the floor structures on one side only. Except the connections of wall panels along the height it is compulsory to perform also a reliable tie between the blind wall elements and the floor structure elements at every storey. Such a tie should be provided also between the blind walls and the walls in the other direction of the building.

7. The width of openings in blind walls /windows, etc/ should not exceed  $1/2$  of the panel width.

8. The reinforcement of vertical panels for taking out the lateral earthquake loading should proceed uninterruptedly throughout the whole height of the building and through the basement walls up to the lower end of the strip foundations or foundation plate.

9. When designing floor structures it is necessary to keep the following :

- to avoid weakening of slab diaphragm by openings or cuttings /for staircases, etc./ exceeding 50% of the diaphragm cross section;

- the floor panels to be designed with maximal dimensions complied with the transport and assemblage possi-



bilities. Their width is recommended to be not less than 14 cm;

- the assemblage and the connection of the floor panels should lead to an integrated rigid floor diaphragm. The bearing capacity of the floor panel connections in the weakened section of the floor diaphragm should be proved by calculation;

- in regions of seismicity 8 and 9 it is recommended the floor diaphragms to be fenced along the contour by continuous steel ties passing through the floor panels.

10. Special attention should be paid to the design of welding. When calculating the welding of elements the determined earthquake inner forces must be increased by 25%. Design of connections the weldings of which are loaded in tension perpendicular to the joint length is not allowed.

In 1985 was completed the work on the new Code for construction in earthquake regions [12]. It came into force in the beginning of 1987.

While keeping the requirements of the 1964 Code and the additional 1972 Instructions, the new Code contains also some new principles and requirements for large-panel buildings. Some of them are :

1. The maximal accepted height of the buildings in regions of seismicity 7, 8 and 9 is respectively 12 storeys /39 m/, 9 storeys /30 m/ and 9 storeys /30 m/.

2. In order a high quality of the connections between the elements to be assured it is recommended for them to be approved by a report signed by the chief technical manager of the construction site and the representative of the investor's control. The connections could be covered only after completing this procedure.

3. The cantilever protruding of floor- and roof structures when they are on one and the same level with the floor- or roof structures /except the oriels/ should not exceed 1,80 m. for regions of seismicity 7 and 1,50 m. - of seismicity 8 and 9.

4. If the cantilever protruding parts and the floor- or roof structures are at different levels the maximal acceptable protruding is 1,20 m.

5. Oriel protrudings are allowed up to 1 m.

#### Czechoslovakia

The Czechoslovak standard CSN.730036 [3] does not comprise any specific clauses concerning structures erected of large precast panels.

#### Romania

According to the Romanian code [6,7] some of the specific requirements are :

1. The number of overground levels of buildings with

structures made of large panels should be limited as follows :

- for regions of seismicity 6, 7 and 8 - maximum 9 levels (GF+8F);
- for regions of seismicity 9 - maximum 5 levels (GF+4F).

These limits could be reduced according to the specific local conditions (nature of ground, etc.).

2. The stiffness of the structure along the longitudinal and transversal axes of the buildings must be as close as possible, leading to close natural periods of vibrations and to similar behaviour along the both axes.

3. The arrangement of the bearing walls of different stiffness degrees should be as symmetric as possible in order to minimize the general torsional response of the buildings.

4. The bearing walls must be continuous along the height of the building, directly transmitting the vertical loads to the foundations.

5. The wall openings (typical for doors and windows) must be arranged in rows along the height of the diaphragms.

6. The shear walls must be stiffened by the connection with the floor diaphragms forming T, L elements in order to delimitate the buckling effect of the free edges where there may appear strong compressions due to the combined action of the horizontal and gravity loads.

7. The lay-out of the floor diaphragms must be carried out considering the following requirements :

- the gravity loads must be transmitted as directly as possible to the structural walls;
- the floors of the structure must act as rigid in-plane floor diaphragms able to transmit and distribute the seismic inertia forces;
- the openings into the floors for elevator- and staircases should not affect essentially the rigidity and the strength of the floor diaphragms.

8. The shear walls should be continuous along the whole length and width of the transom between two joints. In this way the rigidity and the strength of the building are increased.

9. The distance between shear walls should not exceed 7,20 m in any direction.

10. All panels of bearing walls and floors as well as the joints must be manufactured of the same type of concrete (normal concrete or lightweight concrete with granulated aggregates) ensuring thus the homogeneity of the material the shear walls are made of. Use of different type of concrete could be allowed to maximum five-storey buildings and only after having performed all the necessary lab tests and calculations.

11. Taking into account the important role of lintels

when taking over efforts resulted out of seismic stresses and when dissipating energy, the internal wall panels with openings for doors should be provided with lintels properly reinforced.

#### USSR

In the operative now Soviet codes for construction in seismic regions are given also recommendations related only to large-panel buildings. They are as follows:

1. For construction in seismic regions of seismicity 7, 8 and 9 are permitted the following respective heights: 14 storeys (45 m), 12 storeys (39 m), and 9 storeys (30 m).

2. Large-panel buildings should be designed with longitudinal and transversal panels joined one another and with the floor structure so as to perform a whole space system taking up the seismic loads.

3. Special attention is paid by the codes also to the obtaining of the necessary stiffness of floor- and roof structures. It is recommended to do it by respective connections between the elements of the floor (or roof) structure and pouring cement grout in the joints between elements. The lateral surfaces of floor- and roof elements should not be flat but roughed accordingly and there should be provided the necessary steel bonds to tie up all adjoining elements in a whole rigid structure.

4. As a rule the wall- and floor elements should be room sized. The connections between the walls and between the floor elements should be performed by welding the steel bars sticking out of the panels and anchoring details, as well by filling the vertical and horizontal contours of the elements by fine-grain concrete of reduced drying-up. In the sticking areas of the floor elements and outer walls of the building it is required to perform connections by welding the steel bars sticking out of the floor elements and the vertical reinforcement of wall elements.

5. The design of the horizontal connections should assure the taking up of the respective inner forces. The necessary cross section of the metal bonds in the places between the panels is determined by calculation but it has to be at least  $1 \text{ cm}^2$  for each meter of the horizontal joint. A cross section of not less than  $0,5 \text{ cm}^2$  for each meter is permitted for buildings of 5 or less storeys in regions of seismicity 7 and 8.

6. The wall panels reinforcement should be performed as space skeletons or as welded reinforced nets.

7. For the non-bearing elements such as partition panels it is recommended for them to be light and as a rule - large panels joining with the bearing vertical elements (walls, columns) and if longer than 3 m - with the floor elements. Application of non-bearing partitions of hand-made brick masonry in buildings taller than 5 storeys is not permitted.

8. In cases of sandwich outer walls the thickness of

the inner bearing concrete layer has to be not less than 100 mm.

9. Also, the walls should be continuous along the whole width and length of the building.

10. Loggias should, as a rule, be fitted into the outline of the building, not sticking out and their length being equal to the distance between the adjacent walls. Reinforced concrete frames should be performed in the facade plane.

11. Performance of oriels is not allowed.

#### Standard documents in other countries

We had not the opportunity to make acquainted with standard documents of other countries related entirely to the large-panel building construction in seismic regions. But, there exist some individual documents giving instructions only on some of the problems of large-panel building construction in such regions. For example, in [17] a Guide Text for Proportioning of Horizontal and Vertical Joints is given. It comprises some recommendations with respective formulae mainly for design of connections under the action of different forces.

#### 5. CONCLUSION

The first large-panel buildings in seismic regions have been designed and constructed mainly on the basis of the general codes for construction in seismic regions and thanks to the initial pioneer investigations of the specialists in different countries. Now there are already in some countries special standard documents assuring the seismic resistance of large-panel buildings. Some more important general as well as specific requirements and regulations of these documents are given in these lecture notes.

Special attention in the design and construction of large-panel buildings in seismic regions should be paid to the connections since they are very important for the assurance of the necessary seismic resistance.

The fast development of the large-panel building construction in seismic regions up to now was related as a necessity to an intensive theoretical-experimental research. Many of the results obtained reflected in the standard documents and the others helped the solution of a lot of particular design and construction problems. This activity is to be continued.

The most significant contribution to the development of the large-panel construction in seismic regions is due to the efforts of the specialists of every individual country. There has been realized also bilateral or multilateral cooperation in different forms. It will be desirable this international cooperation to be furthered along with the furthering the activities of the EAEE.

# CALCULATION OF CONNECTIONS ALONG THE HORIZONTAL JOINTS OF VERTICAL DIA- PHRAGMS [13]

In structural aspect the building is regarded as a combination of vertical and horizontal diaphragms (fig.2). The most frequent cases of elastic connections application will be considered (fig.3).

The dowels (connections) calculation is performed for efforts caused by bending moments  $M$ , normal forces  $N$  and shear forces  $Q$ , acting on the respective horizontal joint.

Depending on the place of the dowels (connections) in the horizontal joints the following three cases of loading are possible (fig.4): pure shear, shearing and pressure, and shearing and tension. For these three cases the calculation of one separate dowel (fig.5) is performed as follows

## a) Pure shear

In this case the calculation is performed by the formula:

$$Q_o \leq [Q_o] = \sqrt{R_{pr}} \left( 1.7bl + 80F_a \frac{6}{6+\mu} \right) \cos \alpha, \quad (1)$$

where  $Q_o$  is the shear force, in daN, acting on the dowel in absence of normal forces;

$[Q_o]$  - shear force, in daN, that the dowel could bear in absence of normal forces;

$R_{pr}$  - prismatic pressure strength of the concrete filled in the dowel, in daN/cm<sup>2</sup>;

$b$  and  $l$  - width and length of the dowel, in cm;

$F_a$  - cross section of the choosed reinforcement of the dowel, in cm<sup>2</sup> (it is related to a reinforcement of bars with round section placed perpendicularly to the shear force  $Q_o$ );

- reinforcement percentage

$$\mu = \frac{F_a}{bl} 100 \leq 5\%; \quad \cos \alpha = \frac{l}{\sqrt{l^2 + 4e_o^2}};$$

$2e_o$  - distance, in cm, between the edges of the connected panels.

## b) Shearing and pressure

In this case the following formula is used:

$$Q_p \leq [Q_p] = [Q_o] + 4 \frac{N_p}{\sqrt{R_{pr}}} \cdot \frac{1}{1+0.5\mu} \leq 1.4 [Q_o], \quad (2)$$

where  $Q_p$  is the shear force, in daN, acting on the dowel in presence of normal pressure forces;

$[Q_p]$  - shear force, in daN, that the dowel could bear in presence of normal pressure forces;

$N_p$  - pressure force, in daN, acting on the dowel.

c) Shearing and tension

In this case the following formula is used:

$$Q_{tr} \leq [Q_{tr}] = [Q_0] \cdot \left\{ 1 - \left( \frac{N_{tr}}{F_a R_a} \right)^2 \right\} \geq 0, \quad (3)$$

where  $Q_{tr}$  is the shear force, in daN, acting on the dowel in presence of normal tension forces;  
 $[Q_{tr}]$  - shear force, in daN, that the dowel could bear in presence of normal tension forces;  
 $N_{tr}$  - tension force, in daN, acting on the dowel;  
 $R_a$  - tension strength of the reinforcement, in daN/cm<sup>2</sup>.

The formulae (1) and (2) are valid when the dowel reinforcement is anchored in the panels not less than 30d, and the formula (3) - when the reinforcement bearing the tension forces passes along the entire height of the vertical diaphragms and is reliably anchored in the foundation.

For determining  $N_p$  by the formula (2) and  $N_{tr}$  by the formula (3) the following expression is used (fig. 5):

$$N_i = \frac{N}{n} \pm \frac{a_i}{\sum_{m=1}^n a_m^2} M, \quad (4)$$

where  $N_i$  is the pressure force  $N_p$  or tension force  $N_{tr}$  of the i-th dowel;  
 $M$  and  $N$  - bending moment and normal force acting on the given section of the diaphragm;  
 $a_i, a_m$  - distance from the i-th and the m-th dowels to the central axis of the section;  
 $n$  - number of dowels in the given diaphragm section.

The expression (4) is used when  $M < 0,3h N$ . When  $M \geq 0,3h N$  other more complicated expressions are used for determining  $N_i$ . Owing to the limited space these expressions are not given in this lecture.

## APPENDIX 2

### SOME REQUIREMENTS FOR THE CONNECTIONS OF LARGE-PANEL BUILDINGS CONSTRUCTED IN SEISMIC REGIONS 18

Although this document is only a project, it contains several interesting requirements attracting the specialists' attention. We shall consider hereafter only some of them.

1. In principle the connections should be of dowel type (continuous or discontinuous). Exception is allowed only for connections along the horizontal joints if they are entirely pressed. It is recommended however a transversal reinforcement to be assured in all cases.

2. The minimum reinforcement quality for walls with horizontal connections entirely pressed is 0,1% and if partly pressed - 0,25% of the wall cross section respectively.

3. The reinforcement anchorage length should be increased with 50% as compared to construction in nonseismic regions.

4. The floor slabs should be connected with reinforcement passing through continuously over the supports. The reinforcement percentage is not fixed.

5. The filling concrete can be of one grade lower than that of the connecting elements.

6. The design of the connections is performed by the formula:

$$R_{jE} = \lambda \cdot R_{jv} \cdot \frac{1}{\gamma_{d1}}$$

where  $R_{jE}$  is the shear strength for construction in seismic regions;

$R_{jv}$  - the shear strength given by the respective formula for construction in nonseismic zones;

$\gamma_{d1}$  - the additional safety coefficient. It is accepted of value 1,15 for vertical connections and for horizontal completely pressed ones, and of 1,40 for horizontal partly pressed connections;

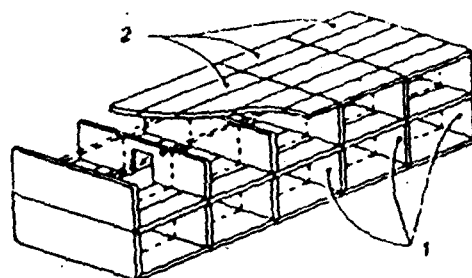
$\lambda$  - a coefficient depending on the place and the supposed work of the connection during earthquakes. For connections located outside the supposed local plastification zones  $\lambda = 0,8$  and for those located in such zones  $\lambda \leq 0,8$ . A formula for determining this coefficient is given.

As it is seen the design strengths of connections in earthquake conditions are considerably lower than those for normal exploitation in nonseismic regions

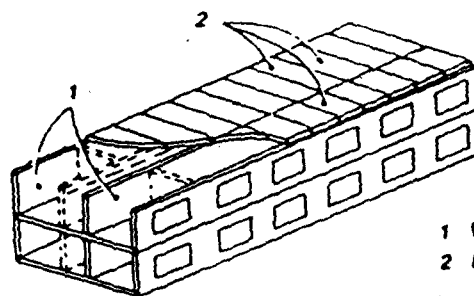
## REFERENCES

1. Bulletin d'information No 160, Comité Euro-International du Béton, Oct.83/Mars 1984, Paris.
2. Czechoslovak standard CSN 730032 "Design of Building Structures Loaded by the Dynamic Effects of Machines".
3. Czechoslovak standard CSN 730036 "Seismic Loads of Buildings", Nov., 1973.
4. Czechoslovak standard CSN 732044 "Dynamic Tests of Building Structures".
5. Standard for Aseismic Design of Dwellings, Social-Cultural, Agro-Zootechnical and Industrial Buildings, P100-81/1982, Romania.
6. Technical Instructions for Design of Large-Panel Buildings P.101-78/1979, I.P.C.T., Romania.
7. Technical Instructions for Designing Buildings with Concrete Diaphragms - I.P.C.T., I.C.B., P.85-82/1982, Romania.
8. Tentative Provisions for the Development of Seismic Regulations for Buildings, Yugoslavia.
9. Yugoslav Code of Technical Regulations for the Design and Construction of Building in Seismic Regions.
10. Code for Construction in Earthquake Regions, 1964, Amendments, 1972, Bulgaria (in Bulgarian).
11. Instructions for Design and Construction of Residential and Public Buildings in Earthquake Regions, 1977 (in Bulgarian).
12. Norms for Design of Buildings and Structures in Earthquake Regions, 1987, Sofia (in Bulgarian).
13. Construction in Seismic Regions, SN-P II-7-81, Moscow, 1982 (in Russian).
14. Instructions for Design of Large-Panel Buildings in Seismic Regions, SN 328-65, Gosstrojizdat, Moscow, 1966 (in Russian).
15. Instructions for Design of Connections in Large-Panel Buildings, Bulletin for Construction and Architecture, Sofia, 1981 (in Bulgarian).
16. Prefabricated Large-Panel Buildings in Seismic Regions, Working Group 3, 8-th European Conference on Earthquake Engineering, Lisbon, 1986.
17. Seismic Design Codes of the Balkan Region, Building Construction under Seismic Conditions in the Balkan Region, UNDP/UNIDO Project RER/79/015, Vol.7, Vienna, 1985.
18. Draft Guide for the design of precast wall connections, CEB, Bulletin d'Information No 169. April, 1985.





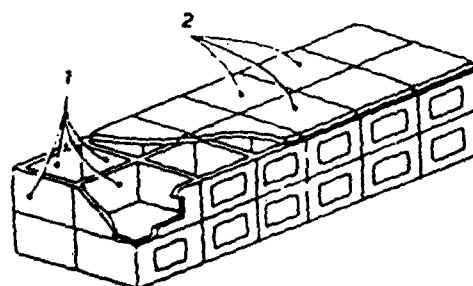
(a) Cross-Wall System



(b) Long-Wall System

1 Wall panel  
2 Floor panel

(dashed lines indicate walls  
not bearing gravity loads)



(c) Two-Way System

Fig. 1 Basic Structural Configurations of Large Panel Systems

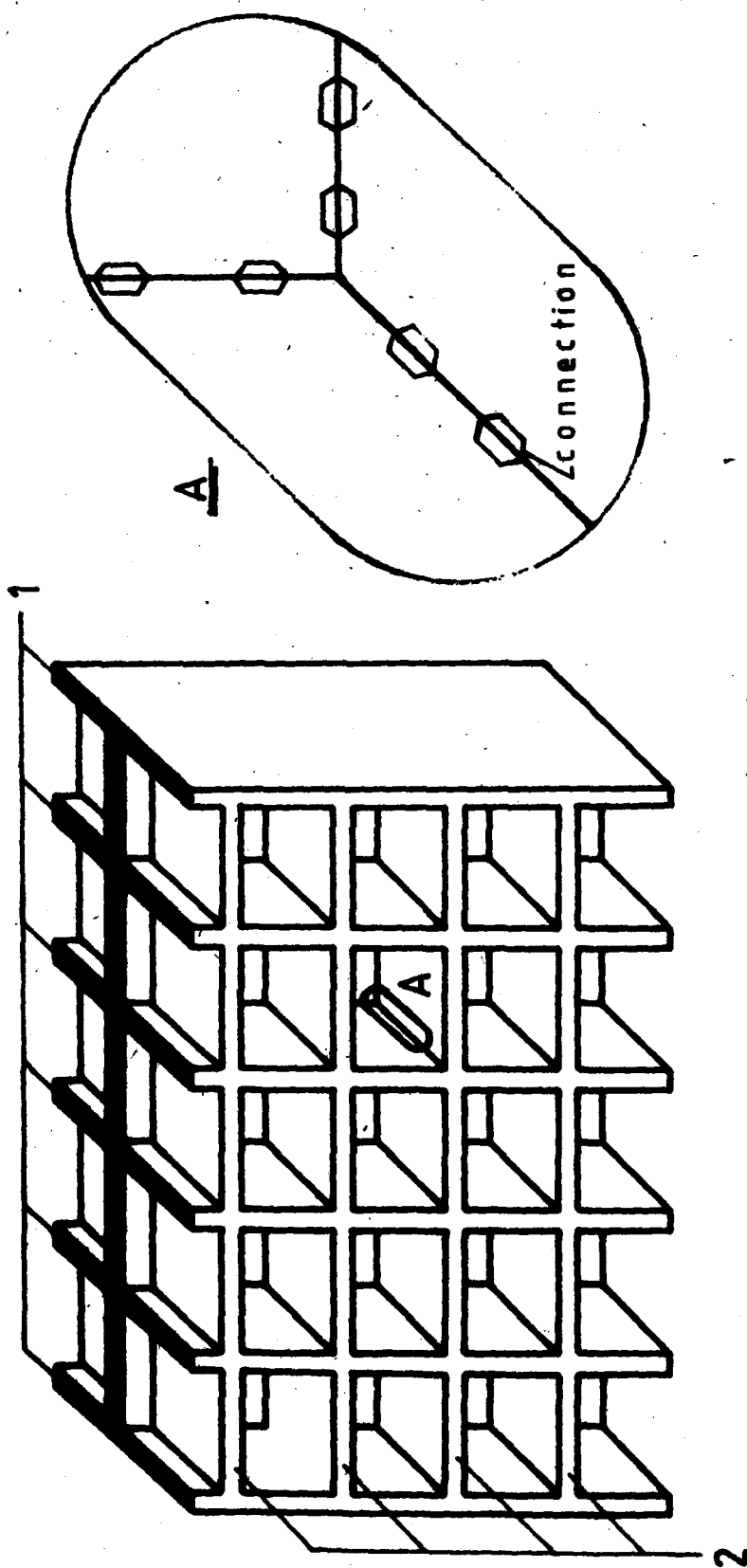


Fig.2  
 1-Vertical diaphragms  
 2-Horizontal diaphragms

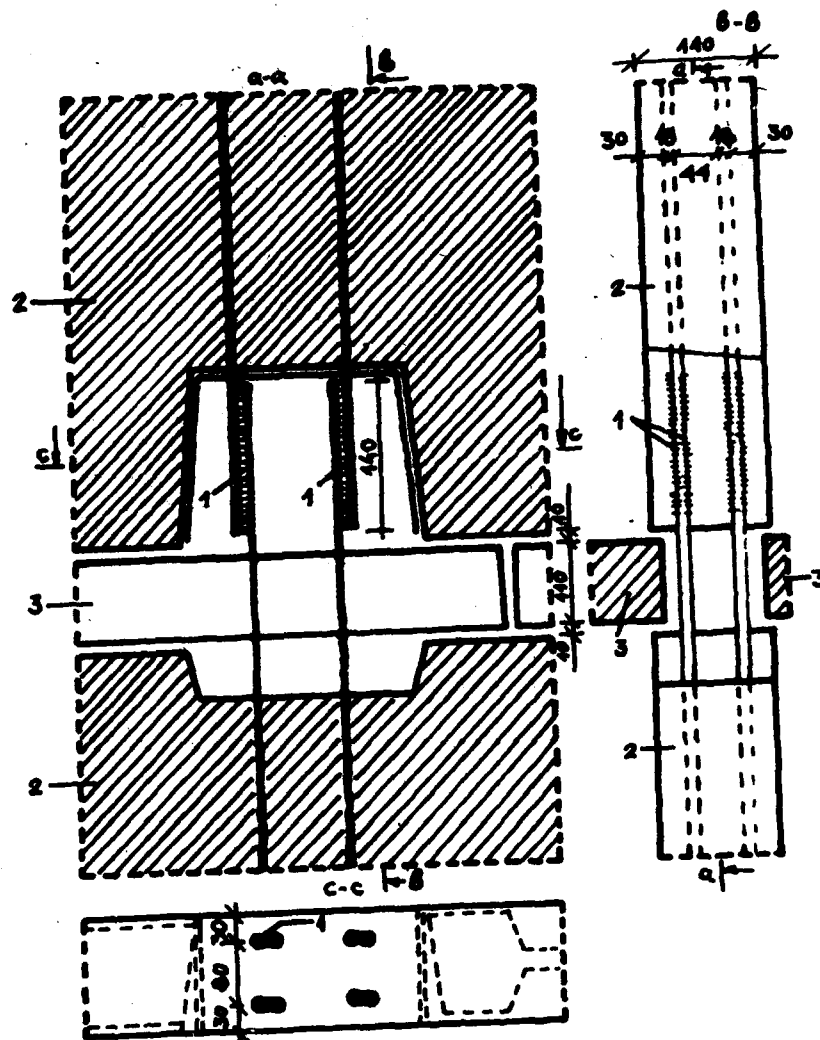


Fig. 3  
Elastic Connection Between Wall  
Pannels  
1- Welds      2-Wall Pannel      3-Floor Pannel

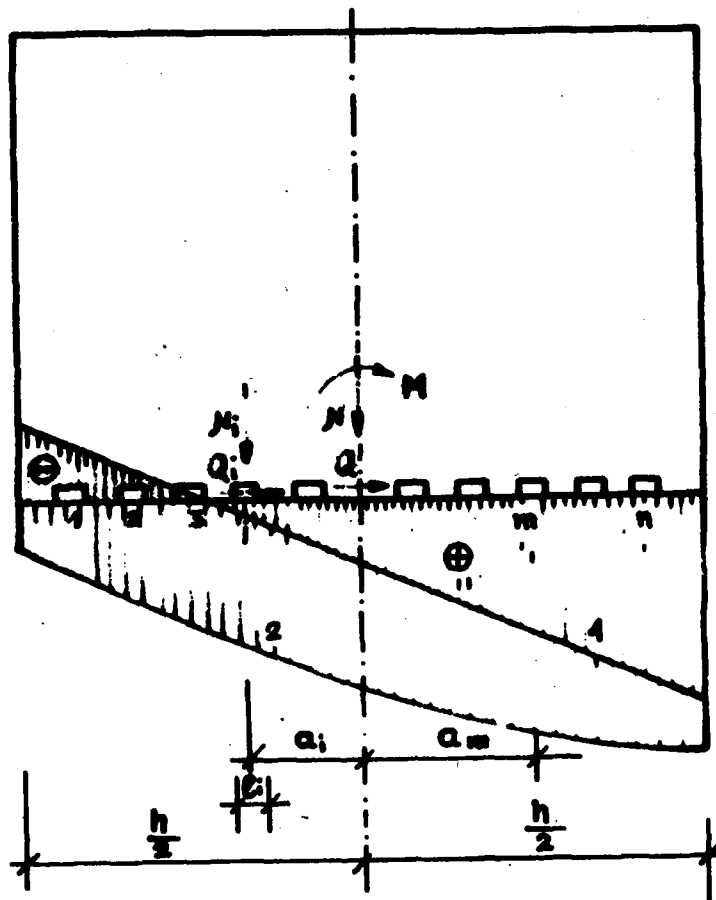


Fig. 4

1-Distribution of  $N_i$   
 2-Distribution of  $Q_i$

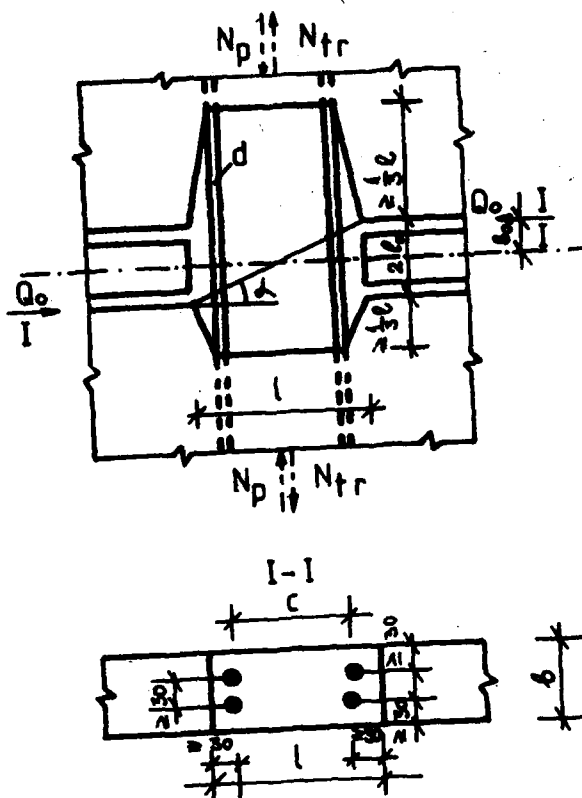


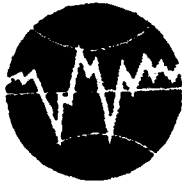
Fig. 5  
Design Diagram of a connection

- a) pure shear  
 $Q_0 = [Q_0] = R_{pr} (1,7 bl + 80 F_a \frac{6}{6 + M}) \cos \alpha \quad (1)$
- b) shearing and pressure  
 $Q_p = [Q_p] = [Q_0] + 4 \frac{N_p}{\sqrt{R_{pr}}} \frac{1}{1 + 0,5 M} = 1,4 [Q_0] \quad (2)$
- c) shearing and tension  
 $Q_{tr} = [Q_{tr}] = [Q_0] \left\{ 1 - \left( \frac{N_{tr}}{R_a F_a} \right)^2 \right\} = 0 \quad (3)$

$$N_i = \left\{ \frac{N_p}{N_{tr}} \right\} = \frac{N}{n} \pm \frac{a_i}{\sum_{m=1}^n a_m^2} M \quad (4)$$

*LIMITATIONS  
OF FLOORS NUMBER AND HEIGHT OF THE  
LARGE PANEL BUILDINGS ACCORDING TO SOME CODES*

COUNTRY	INTENSITY (MSK)					
	VII		VIII		IX	
	FLOORS NUMBER	HEIGHT	FLOORS NUMBER	HEIGHT	FLOORS NUMBER	HEIGHT
BULGARIA { UP TO 1986 SINCE 1987	THE HEIGHT HAS TO BE PROVED BY CALCULATION ON THE BASIS OF BEARING CAPACITY AND ALLOWABLE DE- FORMATIONS					
	12	39	9	30	9	30
ROUMANIA	9	-	9	-	5	-
USSR	14	45	12	39	9	30



**TURKISH NATIONAL COMMITTEE FOR  
EARTHQUAKE ENGINEERING**

**THIRTEENTH REGIONAL SEMINAR ON EARTQUAKE ENGINEERING**

**September 14-24, 1987 - Istanbul - Turkey**

**RESPONSE OF FRAMED STRUCTURES  
TO SEISMIC ACTIONS**

**Class Dyrbye<sup>I)</sup>  
Gylfi Magnusson<sup>II)</sup>**

## RESPONSE OF FRAMED STRUCTURES TO SEISMIC ACTIONS

Claes Dyrbye<sup>I)</sup>  
Gylfi Magnusson<sup>II)</sup>

### SUMMARY

Holzer's method and Holzer-Myklestad's method have been very useful, when response to harmonic loads should be calculated. When the basic principles of these methods are combined with the basic principles of Newmark's  $\beta$ -method corresponding to constant acceleration, a simple method is established, which permits earthquake response calculations to be carried out on microcomputers. Mass-eccentricities are taken into account.

Using the method, computer programmes are not very difficult to formulate, and the need for computer space is rather limited. It is easy to follow the calculations, since the shear forces and the moments are currently calculated.

### INTRODUCTION

The impact of mass eccentricities upon the forces in structures subjected to seismic actions is generally recognized, and modern codes present rules concerned with this problem, see e.g. the draft proposal of Eurocode 8 [1].

For certain types of structures with eccentric masses, Holzer's method has been shown to be suitable, when free vibrations or response to harmonic loading or harmonic ground motion should be calculated, Dyrbye [2]. In Holzer's method two kinds of equations are used:

- 1) The deflections of story No.  $j$  equal the deflections of story No.  $(j-1)$  plus a flexibility matrix times the sectional forces between the two stories.
- 2) The sectional forces above story No.  $j$  equal the sectional forces below story No.  $j$  plus the mass matrix times the accelerations of the story.

When the system performs harmonic vibrations, the accelerations are proportional to the deflections and this is essential to Holzer's method.

When a structure is subjected to an earthquake, the ground motion is not harmonic, and quite complicated motions will take place, and it then becomes logical to find the motions by some kind of numerical integration. An attractive method in this respect is Newmark's  $\beta$ -method, Newmark [3], by which the motions are calculated at times  $\dots t_{r-1}, t_r, t_{r+1}, \dots$ , with constant time intervals  $t_0 = t_r - t_{r-1}$ .

In Newmark's method, assumptions are made about the variation of accelerations in the time intervals  $t_{r-1} < t < t_r$ . It has been shown by Dyrbye [4] that for a framed structure with central mass distribution and the assumption of constant acceleration in each time interval, it becomes possible to perform the calculations using almost the same types of equations as were used in

- 
- I) Assoc.Professor, dr.techn., Department of Structural Engineering, Technical University of Denmark.
  - II) M.Sc. in Civil Engineering, Department of Structural Engineering, Technical University of Denmark.



Holzer's method, and that the accuracy of the calculations is satisfactory. The same principles have been extended to frames with eccentricities in the mass distribution, Magnusson [5].

The paper describes the calculation principles and some results for 3 and 6 story buildings subjected to a simulated ground motion are presented.

#### GROUND MOTION

In the examples presented, the ground acceleration  $a(t)$  is a realization of a stochastic process with the spectral density given by

$$S_a(\omega) = \frac{(\omega/\omega_0)^4}{1+(\omega/\omega_0)^4} S_T(\omega) \quad (1)$$

where  $S_T(\omega)$  is an approximation to the Tajimi spectrum,

$$S_T(\omega) = \frac{2\tau_0}{\pi} \frac{(1-\cos\omega\tau_0)^2}{(\omega\tau_0)^4} \frac{1+4\zeta_g^2(\omega/\omega_g)^2}{(1-(\omega/\omega_g)^2)^2 + 4\zeta_g^2(\omega/\omega_g)^2} \quad (2)$$

$\omega$  is the angular frequency,  $\omega = 2\pi f$ ,  $f$  is the frequency in Hz.  $\tau_0$  is the time step,  $\omega_g$  and  $\omega_0$  are frequencies and  $\zeta_g$  is a damping ratio.  $S_g(\omega)$  is preferred in order to avoid troubles with low frequency contents of the spectrum.

In the examples, the following values are chosen

$$\tau_0 = 0.01 \text{ sec}, \omega_g = 16 \text{ sec}^{-1}, \omega_0 = 0.9 \text{ sec}^{-1}, \zeta_g = 0.6.$$

The spectrum corresponding to the parameters is shown in fig. 1.

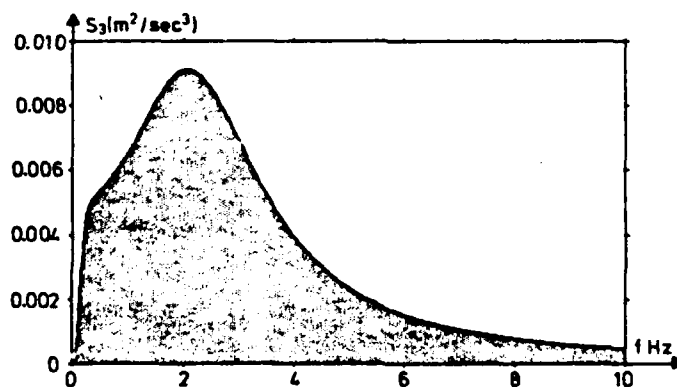


Figure 1. Idealized spectrum of ground motion.

For further information about the simulation technique, reference is made to Dyrbye [6].

Four earthquakes of 15 sec duration were used, the mean value  $m_a$ , the standard deviation  $s_a$  and the maximum value  $a_{max}$  are given in table I.

Table I. Earthquake characteristics. Units:  $m/sec^2$ .

Earthq. No.	$m_a$	$s_a$	$a_{max}$
1	0.000	0.388	1.256
2	0.002	0.404	1.218
3	0.007	0.360	1.214
4	-0.001	0.381	1.367

#### RESPONSE CALCULATION

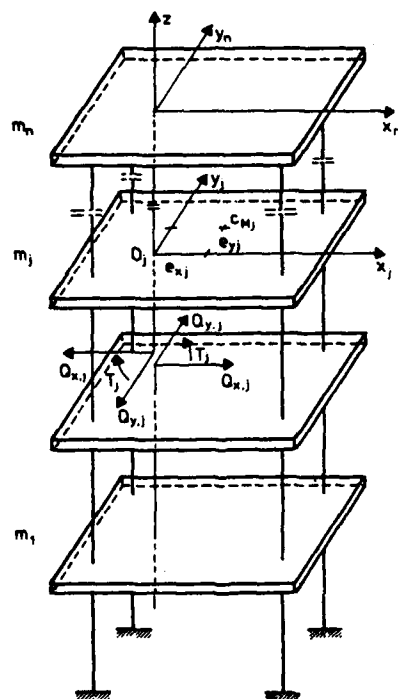


Figure 2. Nomenclature.

At story No.  $j$  the deflection vector at time  $t$  is called  $u_j$ . The 3 components of the vector are the deflections in direction of the  $x$ -axis and  $y$ -axis and the rotation about the  $z$ -axis, the deflections concern the intersection of the  $z$ -axis with the story.

The mass matrix  $M_j$  is, cf. Dyrbye [2],

$$M_j = \begin{bmatrix} m_j & 0 & -m_j e_{yj} \\ 0 & m_j & m_j e_{xj} \\ -m_j e_{yj} & m_j e_{xj} & I_{Mj} + m_j (e_{xj}^2 + e_{yj}^2) \end{bmatrix} \quad (1)$$

where  $I_{Mj}$  is the massmoment of inertia about the masscentre  $C_{Mj}$ .

The sectional force vector  $\underline{S}_{j,r}$  at time  $t_r$  between storys Nos.  $(j-1)$  and  $j$  is defined

$$\underline{S}_{j,r} = \begin{Bmatrix} Q_{xj,r} \\ Q_{yj,r} \\ T_{j,r} \end{Bmatrix} \quad (2)$$

It is assumed that the acceleration during the time interval  $t_r < t < t_{r+1}$  can be expressed as

$$\ddot{u}_j = \frac{1}{2} (\ddot{u}_{j,r} + \ddot{u}_{j,r+1}) \quad (3)$$

and from this follows, cf. Dyrbye [4]

$$\dot{u}_{j,r+1} = -\dot{u}_{j,r} + \frac{2}{\tau_0} (u_{j,r+1} - u_{j,r}) \quad (4)$$

$$\ddot{u}_{j,r+1} = -\ddot{u}_{j,r} + \frac{4}{\tau_0^2} (u_{j,r+1} - u_{j,r} - \tau_0 \dot{u}_{j,r}) \quad (5)$$

This means that the velocities and accelerations at the time  $t_{r+1}$  can be expressed by the quantities at the time  $t_r$  and by the deflections at the time  $t_{r+1}$ .

Dealing with response to seismic actions, it becomes necessary to take damping into account, and viscous damping is assumed. The stiffness and damping matrices  $\underline{K}_j$  and  $\underline{C}_j$  are introduced, and at time  $t_{r+1}$

$$\underline{S}_{j,r+1} = \underline{K}_j (u_{j,r+1} - u_{j-1,r+1}) + \underline{C}_j (\dot{u}_{j,r+1} - \dot{u}_{j-1,r+1}) \quad (6)$$

The equation No. (6) is used together with equation (4) to express  $u_{j,r+1}$ :

$$\begin{aligned} u_{j,r+1} = & u_{j-1,r+1} + (\underline{K}_j + \frac{2}{\tau_0} \underline{C}_j)^{-1} \underline{S}_{j,r+1} \\ & + (\underline{K}_j + \frac{2}{\tau_0} \underline{C}_j)^{-1} \underline{C}_j (\dot{u}_{j,r} - \dot{u}_{j-1,r} + \frac{2}{\tau_0} (u_{j,r} - u_{j-1,r})) \end{aligned} \quad (7)$$

Newton's second law at story No.  $j$  at the time  $t_{r+1}$  gives

$$\underline{S}_{j+1,r+1} = \underline{S}_{j,r+1} + M_j \ddot{u}_{j,r+1} \quad (8)$$

and from (5) this is changed into

$$\underline{S}_{j+1,r+1} = \underline{S}_{j,r+1} + M_j (-\ddot{u}_{j,r} + \frac{4}{\tau_0^2} (u_{j,r+1} - u_{j,r} - \tau_0 \dot{u}_{j,r})) \quad (9)$$

Let  $u_{j,r}$ ,  $\dot{u}_{j,r}$  and  $\ddot{u}_{j,r}$  be known for  $j = 1, 2 \dots n$ .

Put  $\underline{S}_{1,r+1} = 0$  as a first choice. With  $j = 1$ ,  $u_{1,r+1}$  is calculated by (7), and then  $\dot{u}_{2,r+1}$  is found from (9). Then  $u_{2,r+1}$  is found from (7),  $\dot{u}_{3,r+1}$  from (9) and so on, until  $\underline{S}_{n+1,r+1} = \underline{S}_{\text{top}}$  is found from (9).

If all deflections, velocities and accelerations were 0 at the time  $t_0$ , and we also put  $u_{0,1}$  and  $\dot{u}_{0,1}$  equal to 0, then we are able to find the contribution from  $\underline{S}_{1,r+1}$  to the sectional forces  $\underline{S}_{n+1,r+1}$ , cf. Dyrbye [2] and [4], and it may be written  $\underline{D} \underline{S}_{1,r+1}$ .

As no external forces act upon the top of the structure,  $\underline{S}_{1,r+1}$  is determined by

$$\tilde{S}_{1,r+1} = -\tilde{p}^{-1} \tilde{S}_{top} \quad (10)$$

Using this value of  $\tilde{S}_{1,r+1}$ , the sectional forces and the deflections of the structure at time  $t_{r+1}$  are calculated by alternately use of eqs. (7) and (9), and then velocities and accelerations at time  $t_{r+1}$  are found from the equations (4) and (5).

#### NUMERICAL EXAMPLES

3 different structures are considered, 2 of them are 3 story buildings (examples 1 and 2) and 1 is a 6 story building (example 3). Each structure is subjected to 4 simulated earthquakes, cf. sect. 2, with the motion in the x-direction.

The x- and y-axis are main axis for the stiffness, which in all the examples has the same value in all storys, and at each story the damping is assumed proportional to the stiffness.

For each story, the stiffness against translation is 30 MN/m, and against rotation it is 900 MNm/rad. The damping coefficients are 0.2 MN/(m/sec) against deflection and 6 MNm/(rad/sec) against rotation.

At each example, the eccentricities  $e_{xj}$  are all 0, the eccentricities  $e_{yj}$  are identical at all storys varying between 0 and 1 m. In the 3-story buildings  $e_{yj}$  takes the values 0, 0.2, 0.4, 0.6, 0.8 and 1.0 m, in the 6 story building only values 0, 0.5 and 1.0 m are chosen.

Maximum values of shear forces  $Q_{xj}$  and of torsional moments  $T_j$  are calculated corresponding to the 4 artificial earthquakes mentioned in the section ground motion. Results are presented corresponding to the mean value plus or minus the standard deviation.

Example 1. The building has 3 storys. All  $m_j = 5 \cdot 10^4$  kg and all  $I_{Mj} = 5.6 \cdot 10^5$  kgm. The natural frequencies are 1.73 Hz, 4.86 Hz and 7.03 Hz.

The maximum response values are given in Table II.

Table II. Maximum response. Units kN and kNm.

$e_{yj}$ (m)	0.0	0.2	0.4	0.6	0.8	1.0
$Q_{x1}$	307-375	306-374	304-374	300-374	296-376	307-377
$Q_{x2}$	236-306	234-306	231-305	229-305	228-304	237-303
$Q_{x3}$	137-173	136-173	135-173	131-173	131-173	140-172
$T_1$	0	97-141	195-279	293-415	389-545	483-667
$T_2$	0	77-115	152-226	234-316	306-430	382-524
$T_3$	0	45-65	90-128	136-178	178-238	222-284

The shearforces  $Q_{xj}$  are almost independent of the eccentricity, whereas the torsional moment is nearly proportional to the eccentricity, see fig. 3.

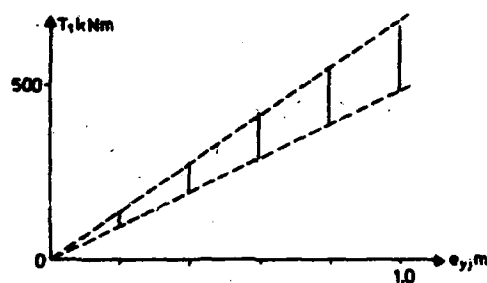


Figure 3. 3-story building with identical masses. Torsional moment in the bottom story.

Example 2. The building has 3 stories.  $m_1 = m_2 = 5 \cdot 10^4$  kg,  $m_3 = 2.5 \cdot 10^4$  kg,  $I_{M_1} = I_{M_2} = 5.6 \cdot 10^5$  kgm,  $I_{M_3} = 2.8 \cdot 10^5$  kgm. The natural frequencies are  $f_1 = 2.02$  Hz,  $f_2 = 5.51$  Hz,  $f_3 = 7.53$  Hz.

The maximum response values are given in table III.

Table III. Maximum response. Units kN and kNm.

$e_{y,j}$ (m)	0.0	0.2	0.4	0.6	0.8	1.0
$Q_{x1}$	350-416	351-415	352-408	353-397	353-383	352-366
$Q_{x2}$	245-303	246-302	247-299	248-292	248-284	248-272
$Q_{x3}$	89-113	89-113	89-111	91-109	90-106	91-103
$T_1$	0	112-150	221-297	325-439	419-563	514-656
$T_2$	0	81-109	160-214	238-314	313-401	388-468
$T_3$	0	30-40	59-79	88-114	115-147	147-173

In this example, the standard deviation of the shear forces has decreased as the eccentricity increases and also the mean values are decreasing, but only slightly.

The torsional moments increase with the eccentricity, but not proportional to the eccentricity, see fig. 4.

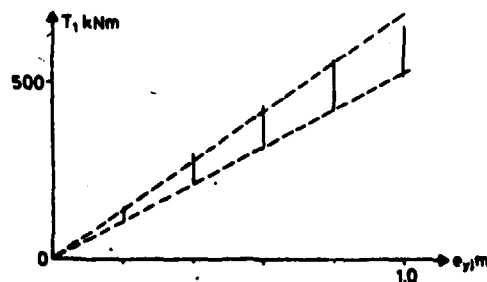


Figure 4. Example 2. Torsional moment in the bottom story.

Example 3. The building has 6 storys. All  $m_j = 5 \cdot 10^4$  kg and all  $I_{M_j} = 5.6 \cdot 10^5$  kgm. The first 3 natural frequencies are  $f_1 = 0.94$  Hz,  $f_2 = 2.76$  Hz,  $f_3 = 4.43$  Hz.

The maximum values of the response are given in table IV.

Table IV. Maximum response. Units kN and kNm.

$e_{y_j}$ (m)	0	0.5	1.0
$Q_{x1}$	410-536	398-533	402-522
$Q_{x2}$	375-499	364-498	387-481
$Q_{x3}$	343-429	328-430	333-441
$Q_{x4}$	293-351	279-353	264-376
$Q_{x5}$	227-269	216-270	206-274
$Q_{x6}$	126-150	119-151	116-150
$T_1$	0	350-520	730-934
$T_2$	0	322-488	701-879
$T_3$	0	299-423	625-783
$T_4$	0	278-334	517-647
$T_5$	0	216-236	406-468
$T_6$	0	118-128	225-249

#### CONCLUSION

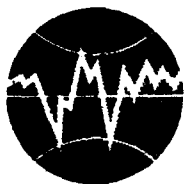
The response to seismic actions of framed structures with eccentricities in the mass distribution has been calculated using a microcomputer only. The ground motion was found by a simulation technique.

Numerical examples demonstrate that shear forces are rather insensitive to the eccentricity, and also that torsional moments may be rather important in case of eccentric mass distribution.

#### REFERENCES

- (1) Commission of the European Communities, (ed. H. Bossenmayer et al.): Draft Eurocode No. 8, Common Unified Rules for Structures in Seismic Regions, 1984.
- (2) C. Dyrbye: Harmonische Schwingungen von Geschossbauten, Bauingenieur, 59, p. 127-130, 1984.
- (3) H. M. Newmark: A Method of Computation for Structural Dynamics, Proc. A.S.C.E., Journ. Eng. Mech. Div., 85, EM3, p. 67-94, 1959.
- (4) Claes Dyrbye: Dynamic response of framed structures. Accepted for publication in Earthquake Engineering and Structural Dynamics.

- (5) Gylfi Magnusson: Seismic actions on buildings with eccentrical mass distribution (in Danish). M.Sc. Thesis, Dept. of Struct. Eng., Techn. Univ. of Denmark, 1985.
- (6) Claes Dyrbye: Simulation of Earthquake Ground Motion on a Microcomputer. Dept. of Struct. Eng., Techn. Univ. of Denmark, Report No. 197, 1985.



**TURKISH NATIONAL COMMITTEE FOR  
EARTHQUAKE ENGINEERING**

**THIRTEENTH REGIONAL SEMINAR ON EARTHQUAKE ENGINEERING**

**September 14-24, 1987 - Istanbul - Turkey**

**TOPOGRAPHICAL AND GEOLOGICAL AMPLIFICATIONS  
DETERMINED FROM STRONG-MOTION AND AFTERSHOCK  
RECORDS OF THE 3 MARCH 1985 CHILE EARTHQUAKE**

**By M. ÇELEBI**



## TOPOGRAPHICAL AND GEOLOGICAL AMPLIFICATIONS DETERMINED FROM STRONG-MOTION AND AFTERSHOCK RECORDS OF THE 3 MARCH 1985 CHILE EARTHQUAKE

By M. ÇELEBI

### ABSTRACT

Site-response experiments were performed 5 months after the  $M_s = 7.8$  central Chile earthquake of 3 March 1985 to identify amplification due to topography and geology.

Topographical amplification at Canal Beagle, a subdivision of Viña del Mar, was hypothesized immediately after the main event, when extensive damage was observed on the ridges of Canal Beagle. Using frequency-dependent spectral ratios of aftershock data obtained from a temporarily established dense array, it is shown that there is substantial amplification of motions at the ridges of Canal Beagle. The data set constitutes the first such set depicting topographical amplification at a heavily populated region and correlates well with the damage distribution observed during the main event.

Dense arrays established in Viña del Mar also yielded extensive data which are quantified to show that, in the range of frequencies of engineering interest, there was substantial amplification at different sites of different geological formations. To substantiate this, spectral ratios developed from the strong-motion records of the main event are used to show the extensive degree of amplification at an alluvial site as compared to a rock site. Similarly, spectral ratios developed from aftershocks recorded at comparable stations qualitatively confirm that the frequency ranges for which the amplification of motions occur are quite similar to those from strong-motion records. In case of weak motions, the denser arrays established temporarily as described herein can be used to identify the frequency ranges for which amplification occurs, to quantify the degree of frequency-dependent amplification and used in microzonation of closely spaced localities.

### INTRODUCTION

The 3 March 1985 Central Chile earthquake ( $M_s = 7.8$ ) caused a variety of damages to structures in the townships of San Antonio, Melipilla, Valparaíso, and Viña del Mar as well as the capital, Santiago. The general location of the epicenter of the main shock and some of the important aftershocks and heavily affected areas are depicted in Figure 1.

At the coastal town of Viña del Mar, some engineered structures with unique architectural features suffered extensive damage. And at Canal Beagle, a subdivision of Viña del Mar, the damages inflicted on the three distinctive types of buildings, situated on a hilltop crowned by ridges and canyons, indicated specific ridge effects as a result of the earthquake. While the four-story buildings in the canyon did not suffer any damage and only two of the many single- and two-story buildings on top of the hill suffered minor damage, on the ridges all of the four- and five-story buildings were extensively damaged, some beyond repair. In Figure 2, a general location map of Viña del Mar, Canal Beagle and surroundings, latitudes and longitudes, as well as general topography and geology are shown.

The purpose of this paper is to present results related to topographical and geological amplifications using selected sets of aftershock data obtained from dense arrays established temporarily at Viña del Mar and its subdivision, Canal Beagle,

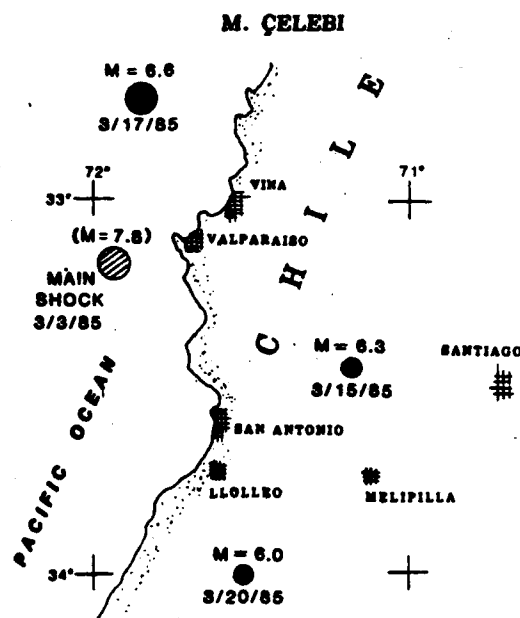


FIG. 1. Main population centers affected by the main shock and aftershock of the 3 March 1985 Chile earthquakes.

approximately 5 months after the main event. The data set from Canal Beagle represents the first such set of data depicting topographical amplification in a heavily populated area. The findings correlate well with the damage distribution observed after the main event. The scope of the paper includes description of the site-response experiments, the data obtained, and the identification of the topographical and geological amplifications as a function of frequency. The discussion of the geological amplification is further substantiated by using the spectra obtained from the strong-motion records of the Chilean strong-motion network (Saragoni *et al.*, 1985).

Previous theoretical and experimental studies on ridge effects were performed by a number of authors including Boore (1972, 1973), Davis and West (1983), and Bard and Tucker (1985). Shiga *et al.* (1979) have performed theoretical studies on effects of irregular geophysical features on seismic ground motions. The results of their study of the features, particularly of hills, display various degrees of frequency-dependent amplification of motion. Ridge effects have been observed in many hill towns of southern Italy during postearthquake studies of the Campania-Basilicata (Italy) earthquake of 1980 (Lagorio and Lager, 1981; Alexander, 1986). Steinbrugge, (1986, private communication) and Donovan (1986) have observed topographical effects in other parts of the world. The use of spectral ratios in describing amplification of ground motions at different sites is discussed by Gibbs and Borchardt (1974) and Rogers *et al.* (1984).

Structural damage surveys related to the 3 March 1985 Chile earthquake is not intended herein. Detailed information on structural damage surveys have been documented by Çelebi (1985), Wyllie *et al.* (1986), and Monge *et al.* (1986). It is not intended to include extensive data sets related to the experiments either. These have been documented elsewhere (Çelebi, 1986).

In the site-response studies presented herein, the General Earthquake Observation System recorders and related peripherals were used. The General Earthquake Observation System is discussed in detail by Borchardt *et al.* (1985). During the

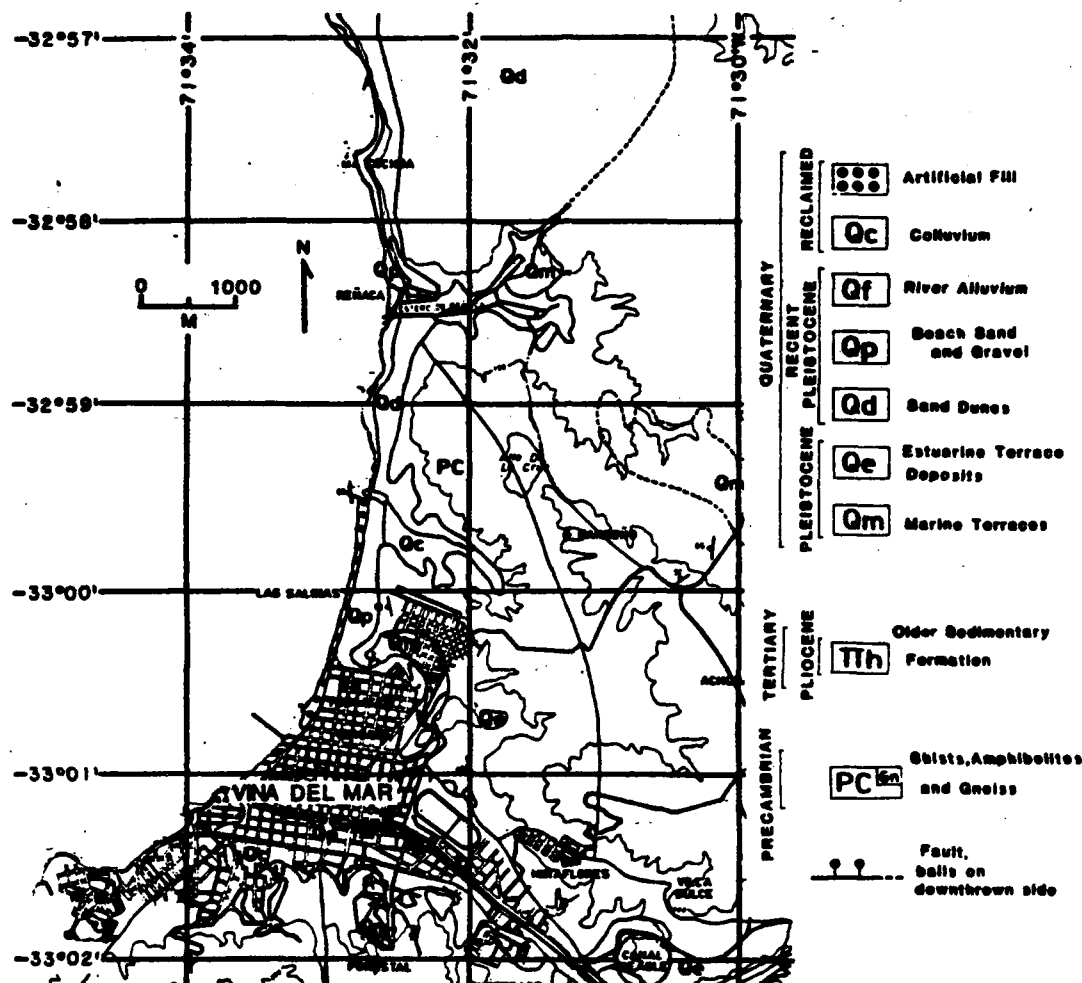


FIG. 2. General geology, topography, and coordinates of Viña del Mar, Canal Beagle, and Renecá on the central coast of Chile. Canal Beagle is circled.

course of these experiments, the three-component package Mark\* Products L22-three-dimensional velocity transducers and the three-component package Kinematics\* FBA-13 acceleration transducers were used.

#### ORGANIZATION OF THE PAPER

Since important results of two separate experiments are discussed in this paper, the manuscript will be divided into two parts: Part I will be devoted to topographical amplification at Canal Beagle, and Part II will be devoted to geological amplification at Viña del Mar.

#### PART I: TOPOGRAPHICAL AMPLIFICATION AT CANAL BEAGLE

Between 26 July and 10 August 1985, several aftershocks were recorded simultaneously in most of the stations established at Canal Beagle, as well as at two reference stations (MUN and VAL) in downtown Viña del Mar (an alluvial site)

\* These are commercial names of instruments used only and do not constitute endorsement of these products.

and at Valparaiso (an amphibolite gneiss rock site), respectively. Both reference stations were in the vicinity of the Chilean Strong-Motion Network stations. In Figure 3, the general layout of the Canal Beagle subdivision is shown; the three types of buildings and their locations are indicated. Also indicated in this figure are the ridges and the stations. In Figure 4, detailed topography and the locations of the stations (CBA-CBG) established at Canal Beagle are depicted. In Figure 5, location of reference station VAL is shown. The Canal Beagle subdivision stations (CBA-CBG) were all sited on alluvial deposits and decomposed granite (locally known as Maicillo). In selecting the particular sites of stations, care was taken to have representative ridge, canyon, and main hilltop locations in order to be able to distinguish the ridge effect. One of the ridges and the structures on it, as well as the geology, are depicted in Figure 6. A typical damaged structure and details of damage to structural components are shown in Figure 7. Typical profiles of the Canal Beagle area are shown in Figure 8. These profiles will be used in future work to perform theoretical studies of amplification of these ridges.

For the sake of brevity, only one typical set of velocity seismograms of one event at selected stations of Canal Beagle as well as the reference rock station, VAL, is provided in Figure 9. Referring even only to these seismograms whose components are plotted to the same scale, it is possible to distinguish that the ridges are subjected to amplified motions as compared to the canyon and reference rock station, VAL. Since the Canal Beagle stations are further away from the epicenter than the reference rock station, VAL, conservatively, the distance effect can be neglected; therefore, the spectral ratios of stations CBA/VAL provided in Figure 10 display the frequency-dependent geological amplification at Canal Beagle relative to the rock station in Valparaiso. On the other hand, since Canal Beagle stations are close to one another (see Figure 4 for scale) and all are sited on similar geology, the

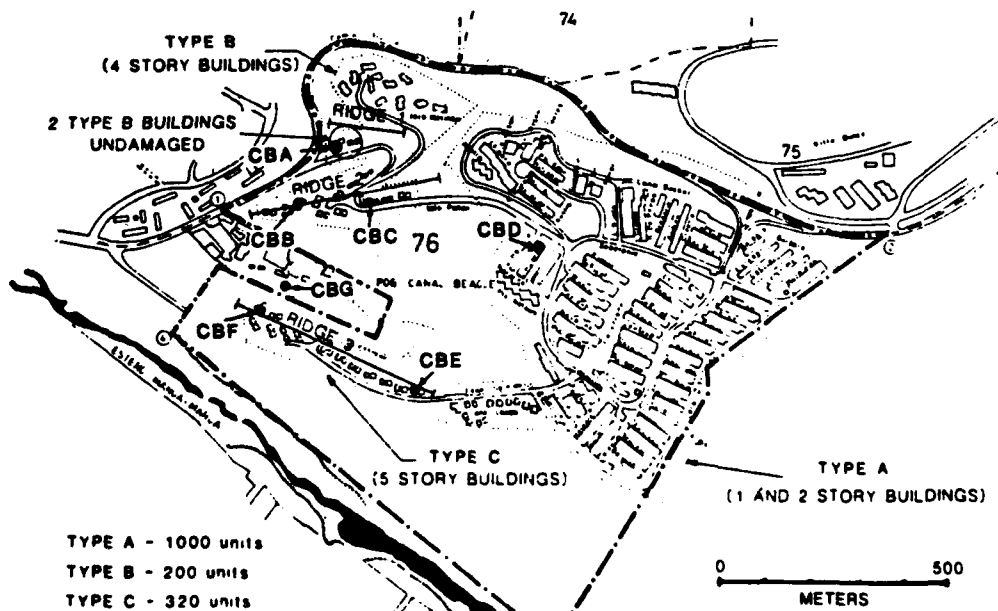


FIG. 3. General layout of the Canal Beagle subdivision. Types of buildings and their locations are indicated. Also, the locations of the temporary seismograph stations are shown.

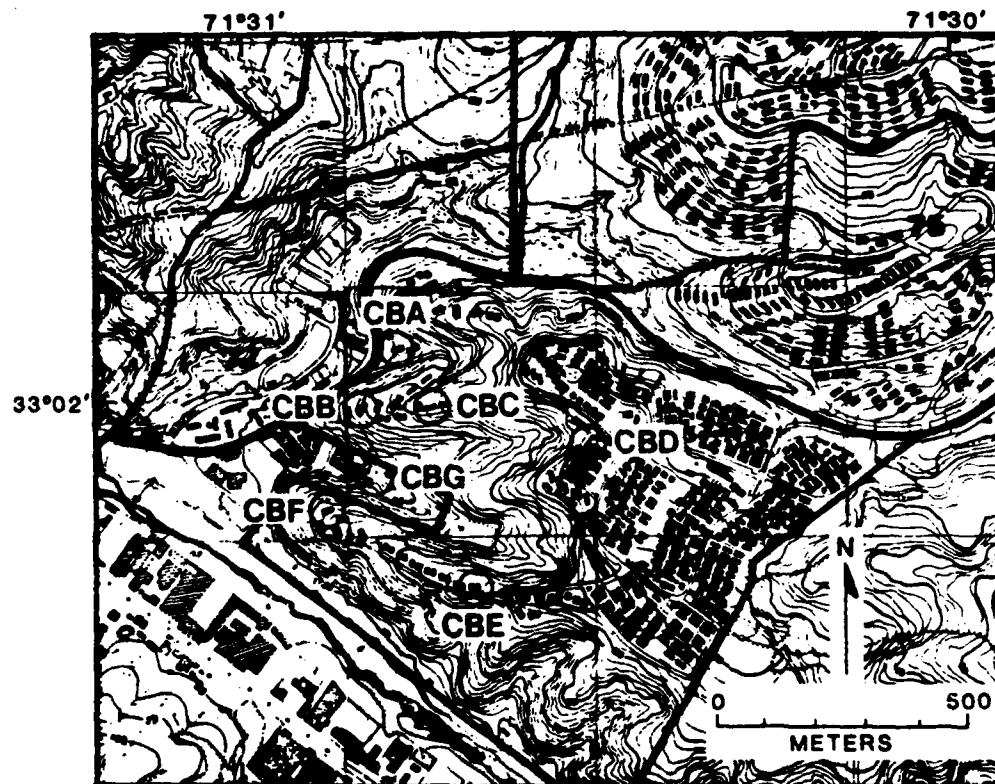


FIG. 4. Detailed topography of Canal Beagle. The ridge and the buildings on them as well as the stations established for aftershock studies are indicated. Details of contour lines are shown in Figure 8.

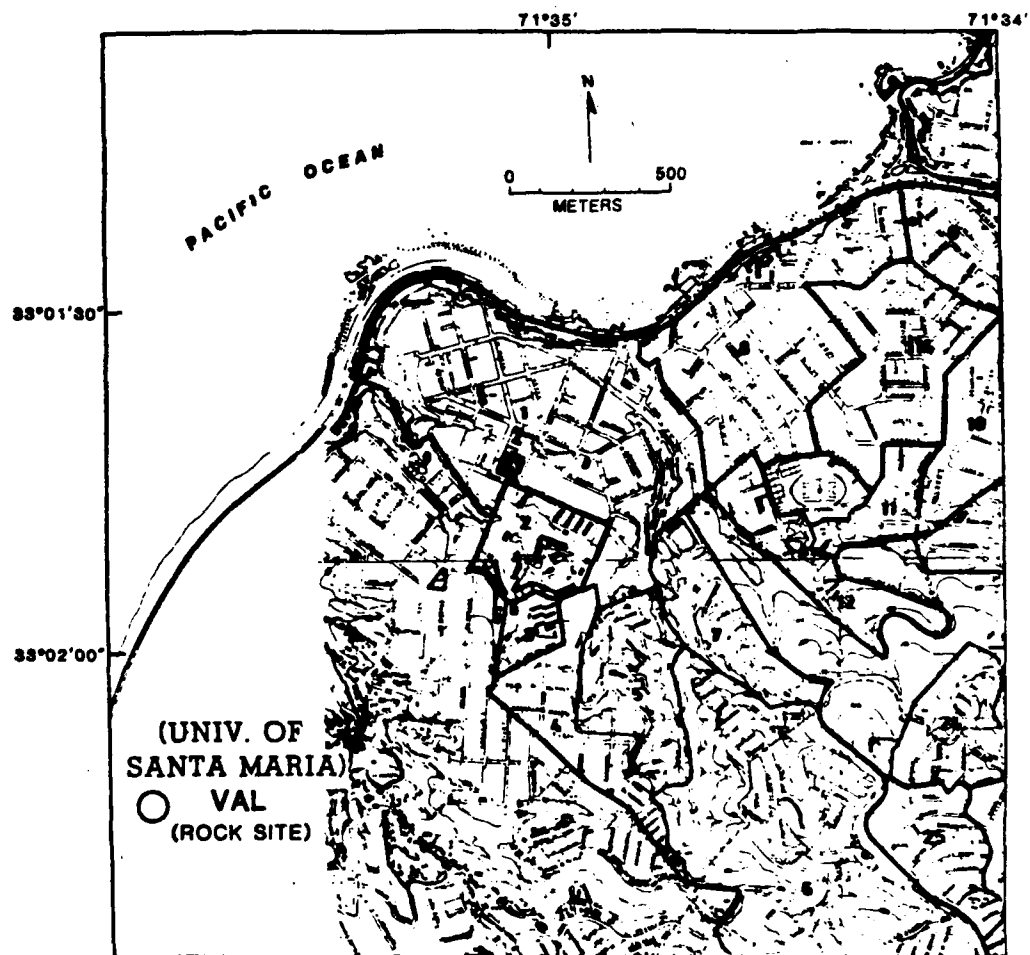


FIG. 5. Location of reference station VAL (same site of the accelerograph station of Chilean Strong-Motion Network).



FIG. 6. One of the ridges of Canal Beagle and structures on it. The alluvial deposits of the ridge can be seen in this figure.

spectral ratio of motions at a ridge station with respect to the station CBA at the canyon represents the topographical amplification function,  $T_i(\omega)$

$$T_i(\omega) = \frac{A_i(\omega)}{A_1(\omega)}$$

where  $A_i(\omega)$  is the Fourier amplitude spectrum at station  $i$ . In Figure 11 (a to d), then, the frequency-dependent topographical amplification is clearly depicted in the spectral ratio plots (between 0 to 10 Hz) of stations on the ridges with respect to station CBA, which is in the canyon.

In general, the spectral ratios show that the frequency ranges for which horizontal amplification of motion occurs are 4 to 8 Hz for the canyon relative to the rock site (Figure 10) and 2 to 4 Hz as well as 8 Hz for the ridges of Canal Beagle relative to the canyon (Figure 11). The frequency range of 2 to 4 Hz is well within the fundamental frequencies of the four- and five-story buildings observed to be heavily damaged during the main event of 3 March 1985. On the other hand, the frequencies of the 2 four-story undamaged buildings in the canyon are outside the frequencies (4 to 8 Hz) for which amplification occurred in the canyon relative to the rock site. These spectral ratios (as well as others to follow) were smoothed with a triangular weighting function with width of 0.15 Hz. Other sets of velocity seismograms and spectral ratios related to topography of Canal Beagle are documented elsewhere (Çelebi, 1986). The spectral ratios of other events corresponding to each station indicate similarities and show repeatability of frequency-dependent amplification. This is clearly depicted in the superimposed spectral ratios from two or three events (as available) presented in Figure 12.



FIG. 7. (a) A typical damaged four-story building on a ridge and (b) close-up of damage to structural components.



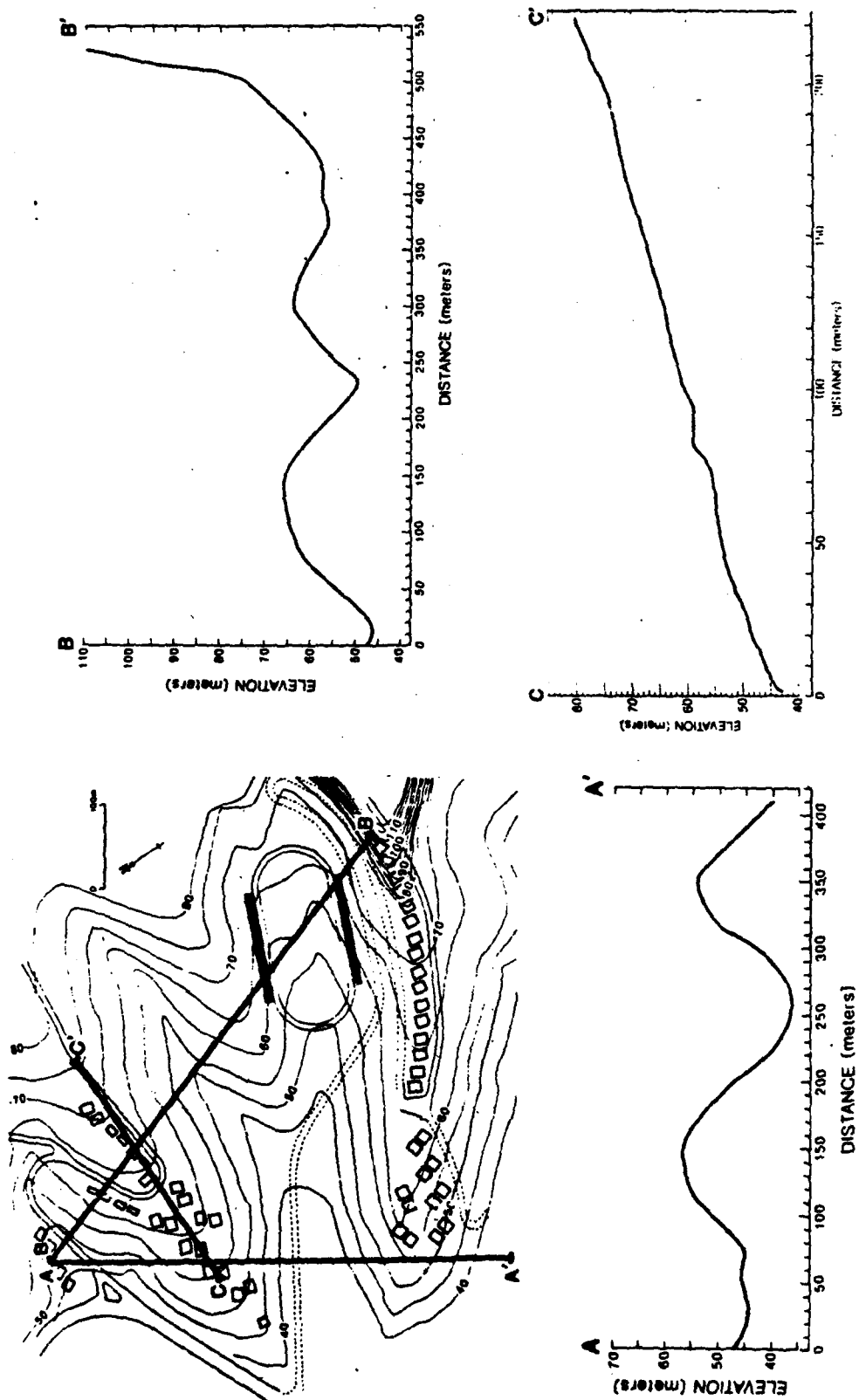
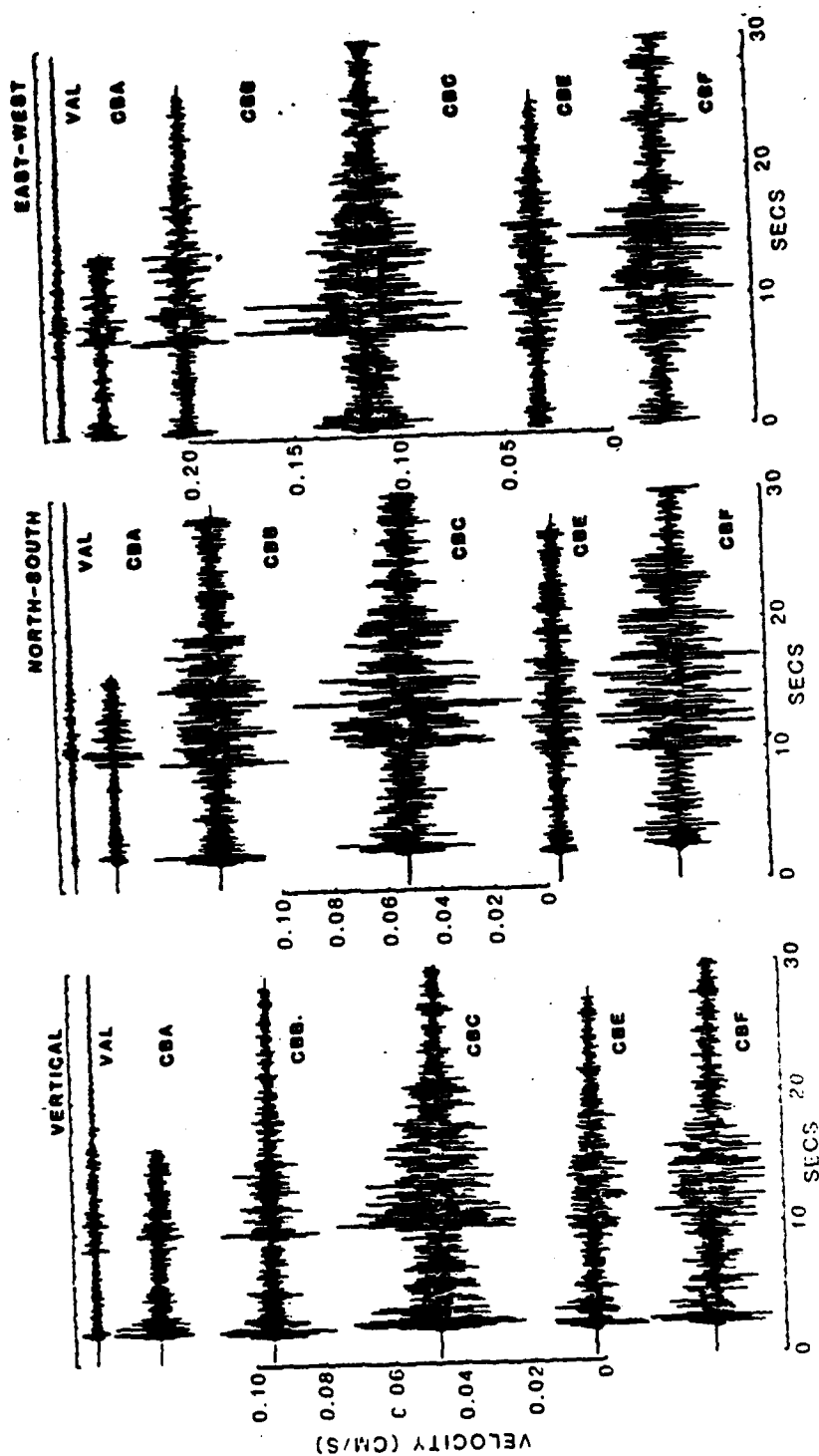


FIG. 8. Typical topography and profiles of Canal Beagle. Contour lines are provided in the general layout depicting the ridges and buildings.



EVENT 2100652

FIG. 9. A typical set of scaled velocity seismograms—event 2100652 corresponding to Julian 210 (29 July 1985) at 08:52 UTC—for the vertical and horizontal components, respectively, from the reference station VAL and Canal Beagle stations CBA, CBB, CBC, CBE, and CBF. Stations CBB, CBF, CBE, and CBF are on the ridges.

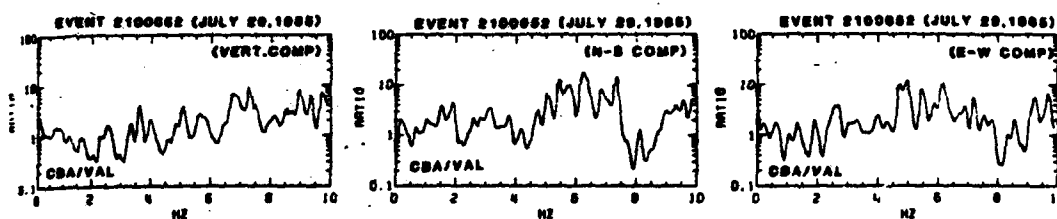


FIG. 10. Spectral ratios of event on 29 July 1985 (Julian 210) at 06:52 UTC for the vertical and horizontal components (N-S and E-W), respectively, of stations CBA/VAL.

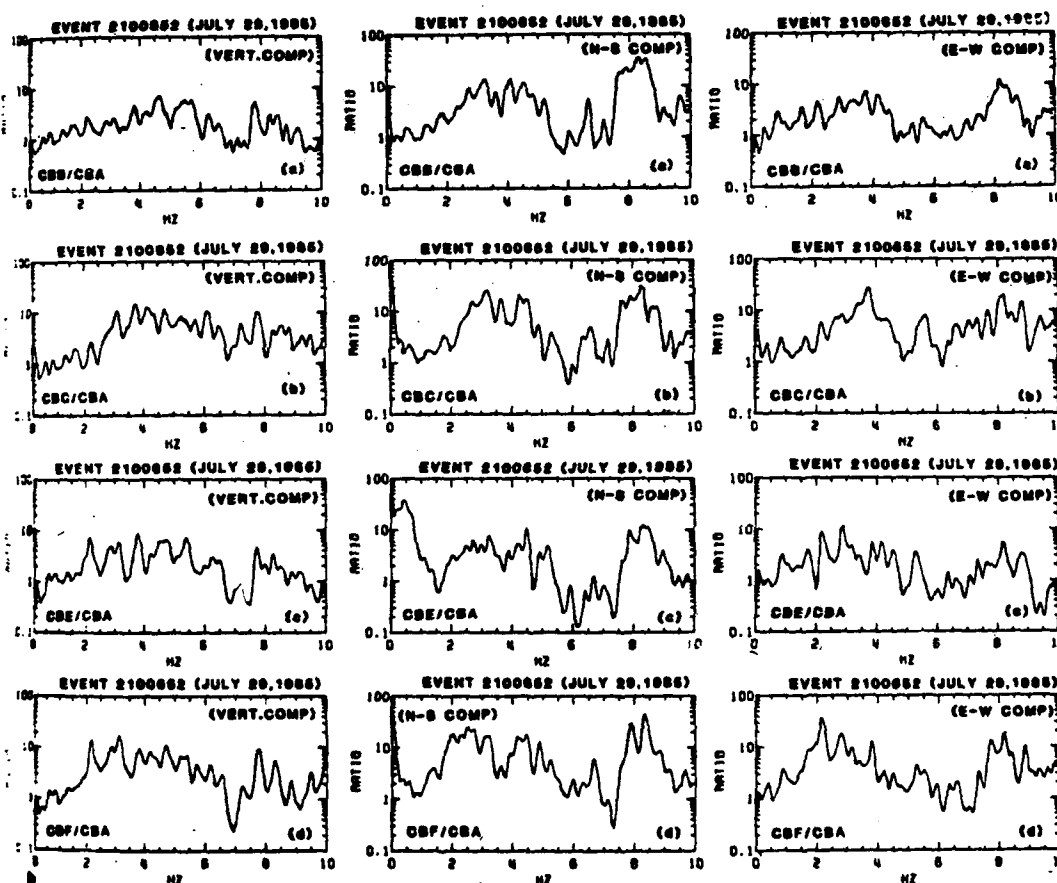


FIG. 11. (a) Spectral ratios of event on 29 July 1985 (Julian 210) at 06:52 UTC for the vertical and horizontal components (N-S and E-W), respectively, of stations CBB/CBA. Station CBB is on one of the ridges, and station CBA is in the canyon. Spectral ratios of event on 29 July 1985 (Julian 210) at 06:52 UTC for the vertical and horizontal components (N-S and E-W), respectively, of stations (b) CBC/CBA, (c) CBE/CBA, and (d) CBF/CBA. Stations CBC, CBE, and CBF are on the ridges.

Of particular interest are the spectral ratios in Figure 13 of the ridge stations relative to the rock site (VAL) station. These spectral ratios depict higher ordinates (amplification) due to the fact that they contain both topographical and geological effects while those spectral ratios in Figure 11 contain only topographical effects (ridge versus canyon). Qualitatively, the ridge versus rock station spectral ratios

(Figure 13) show peaks of horizontal amplification of motion around 3 Hz (as in Figure 11).

Ultimately, the spectral ratios can be used in microzonation of these sites or of similar sites with ridges. One such similar site in Viña del Mar is the subdivision of Gomez Carreño, which also suffered considerable damage during the 3 March 1985 event. Another site recently visited by the author is the La Foresta development in Santiago (approximately 120 km from the epicenter), where the homes on the ridges were damaged during the same event, while others on the flat areas were not.

## PART II: GEOLOGICAL AND TOPOGRAPHICAL AMPLIFICATIONS IN VIÑA DEL MAR

Stations established in Viña del Mar are shown in Figures 14 and 15. The stations EAC, REN, and TRA were established at basements of three significant buildings (Edificio Acapulco, Edificio El Faro, and Edificio de Miramar), respectively, founded on sand (on the coast). Of these, Edificio Acapulco and Edificio El Faro were severely and extensively damaged during the main event. Edificio El Faro, built on sand dune hills of Renecá, had tilted due to crushing of first-floor shear walls and

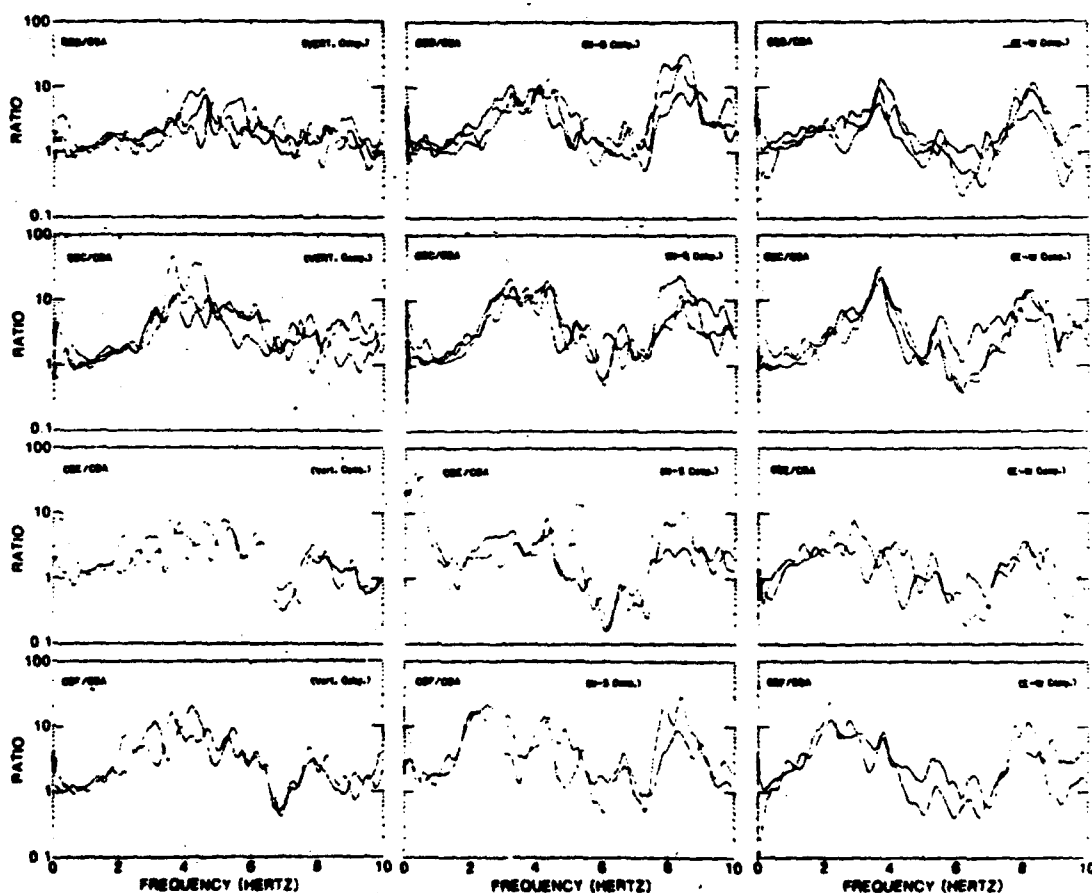


FIG. 12. Superimposed spectral ratios of two or three events (as available) at stations identified.

was later dynamited. Edificio de Miramar was not damaged. Alluvial-site station MUN (also a reference station) was located at the basement of the Municipality Building. Detailed pictures and descriptions of structural damages are documented elsewhere by Çelebi (1985, 1986), and Wyllie *et al.* (1986).

Figure 16 provides velocity seismograms (plotted to the same scale for each component) of a single event recorded at the stations mentioned above. These seismograms also show considerable amplification of motion at nonrock sites compared to the rock site (VAL). Figure 17 (a to d) show spectral ratio plots (between 0 to 10 Hz) of one event at each one of the stations listed above with respect to station VAL, respectively. Again, considerable frequency-dependent amplification of motions (particularly for frequencies of 1 to 4 Hz) at the sand and alluvial sites are displayed in these figures. Spectral ratios of stations REN/VAL reflect both geological and topographical effects and the others reflect only geological effects.

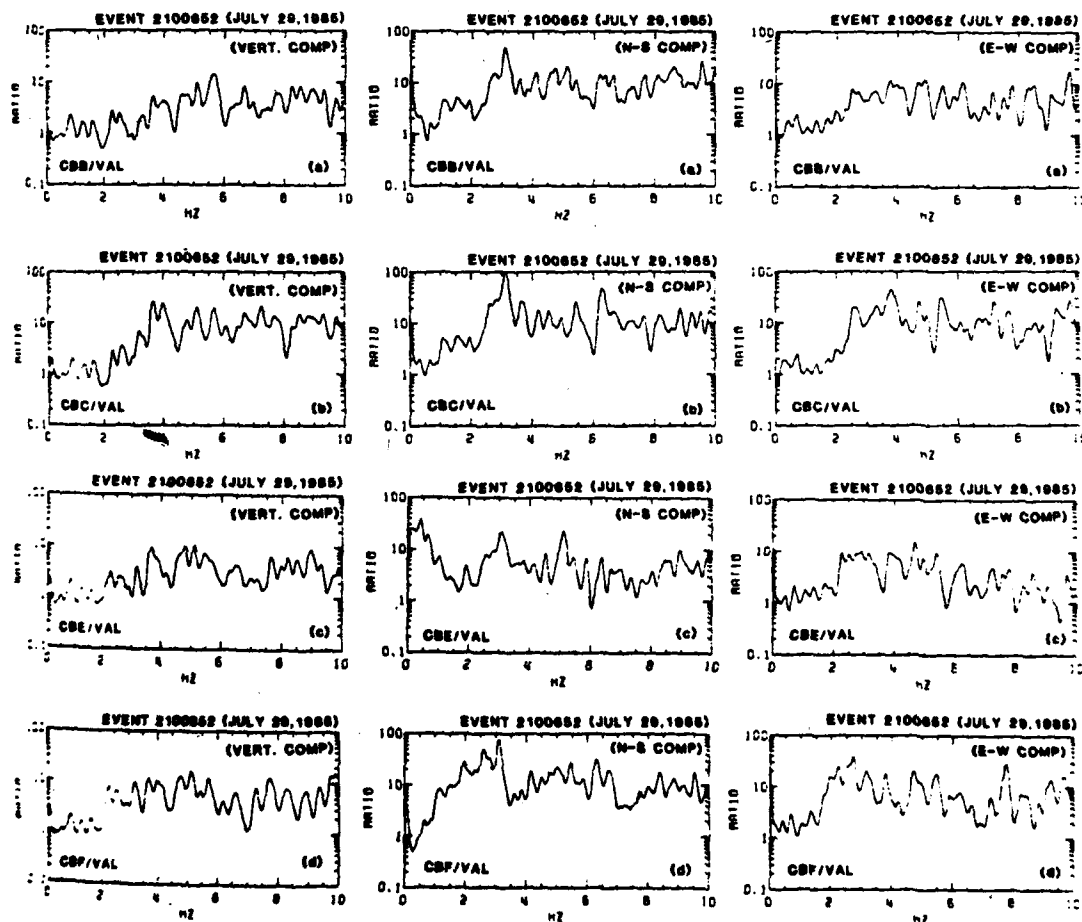


FIG. 13. Spectral ratios of events on 29 July 1985 (Julian 210) at 06:52 UTC for the vertical and horizontal components (N-S and E-W), respectively, of stations: (a) CBB/VAL; (b) CBC/VAL; (c) CBE/VAL; and (d) CBF/VAL.

### AMPLIFICATION QUANTIFIED FROM THE STRONG-MOTION RECORDS OF 3 MARCH 1985

In Figure 18, the (vertical, N-S, and E-W components) spectral ratios developed from the main shock records of 3 March 1985 are shown for stations in Valparaiso (University of Santa Maria—a gneiss amphibolite rock site) and in Viña del Mar (an alluvial site). Only these two stations correspond to the dense array stations established temporarily for recording the aftershocks described earlier. The strong-motion data used to obtain the Fourier spectra and the spectral ratios have been obtained and digitized by the Chilean Strong-Motion Network operated by Saragoni *et al.* (1985). The seismogram and spectral ratio plots dramatically display the amplification of three-component motions at an alluvial site (near station MUN) with respect to a rock site (same as VAL) during the main strong-motion event and show peaks in the range of 0.5 to 1.5 sec. This same trend is exhibited in the weak-

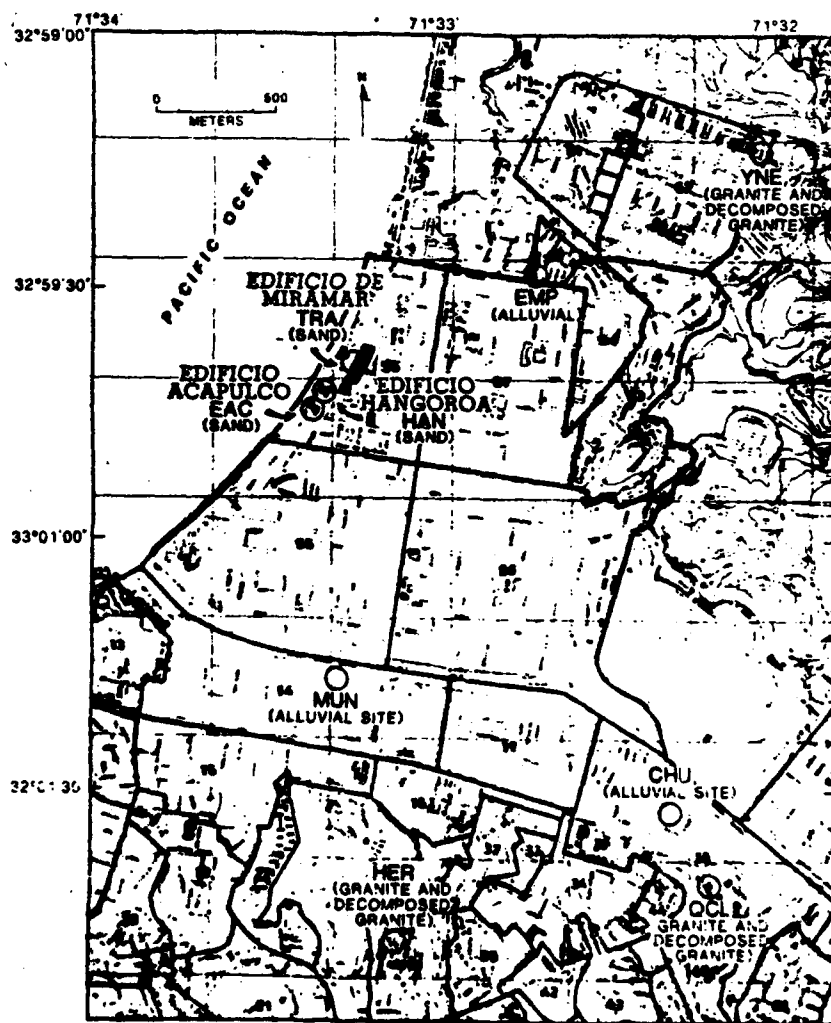


FIG. 14. Location of stations in Viña del Mar.

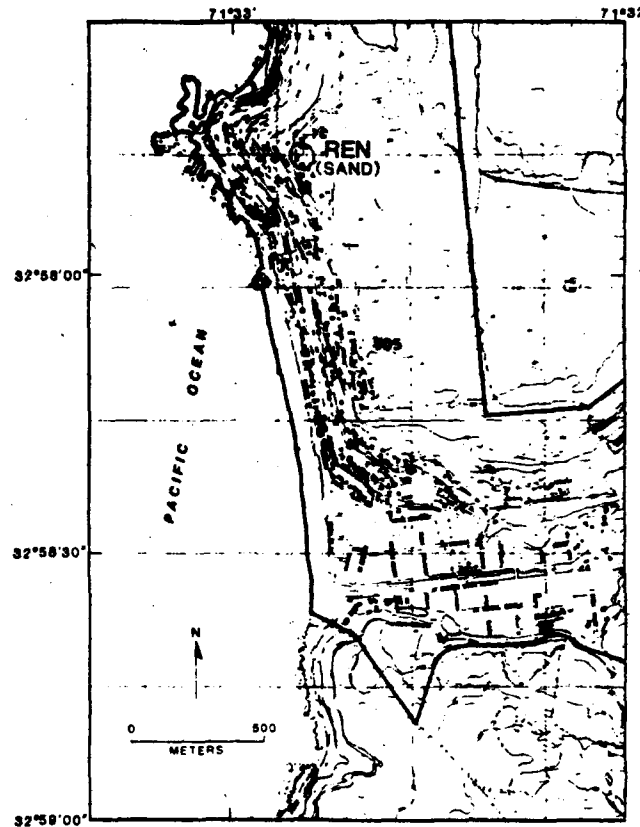
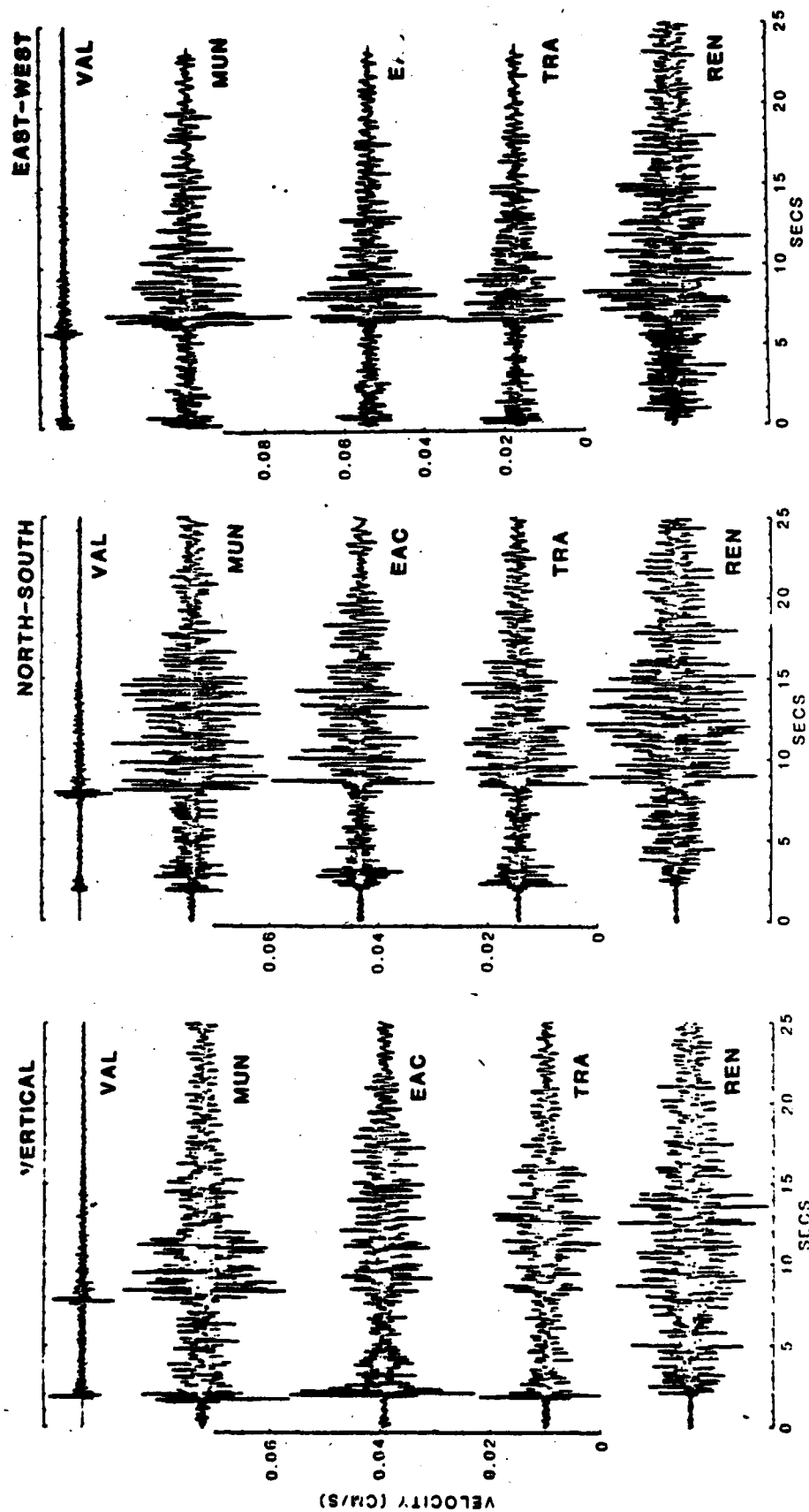


FIG. 15. Location of station REN in Renecá, a suburb of Viña del Mar.

motion spectral ratios corresponding to stations MUN/VAL presented in Figure 17d. Comparison of Figure 17d (weak-motion spectral ratios) and Figure 18 (strong-motion spectral ratios), at a minimum, qualitatively indicates that the weak-motion spectral ratios exhibit much greater amplification than the strong-motion spectral ratios. On the other hand, the frequency-dependent amplification of motions at Viña del Mar with respect to Valparaiso show amplification in similar frequency ranges for either strong or weak motions. However, any differences should be attributed to: (a) the Viña del Mar strong-motion data station is approximately 100 m from the weak-motion data station and therefore there is possibility of change of soil profile; (b) acceleration records of strong-motion data and velocity records of weak-motion data are used to obtain spectral ratios; (c) there was no time synchronization of the strong-motion data from Valparaiso and Viña del Mar and, therefore, the 77 sec of the strong-motion data used to obtain the spectral ratios provide only a qualitative spectral ratio and not an exact comparison; (d) the horizontal components of the strong-motion data have been rotated from their actual orientations to N-S and E-W directions to provide the comparison with the aftershock data; and (e) effect of possible nonlinear response of soil.

In addition, Figures 19 and 20 provide the relative velocity and absolute acceleration response spectra traced from plots of Saragoni *et al.* (1985) (only the 0 per cent damping spectra are traced for comparison purposes). Since the spectral ratios



EVENT 2161857

FIG. 16. A typical set of scaled velocity seismograms - event 2161857 corresponding to Julian 216 (4 August 1985) at 18:57 UTC—for the vertical and horizontal components, respectively, from reference stations VAL and MUN and stations EAC, TRA, and REN.



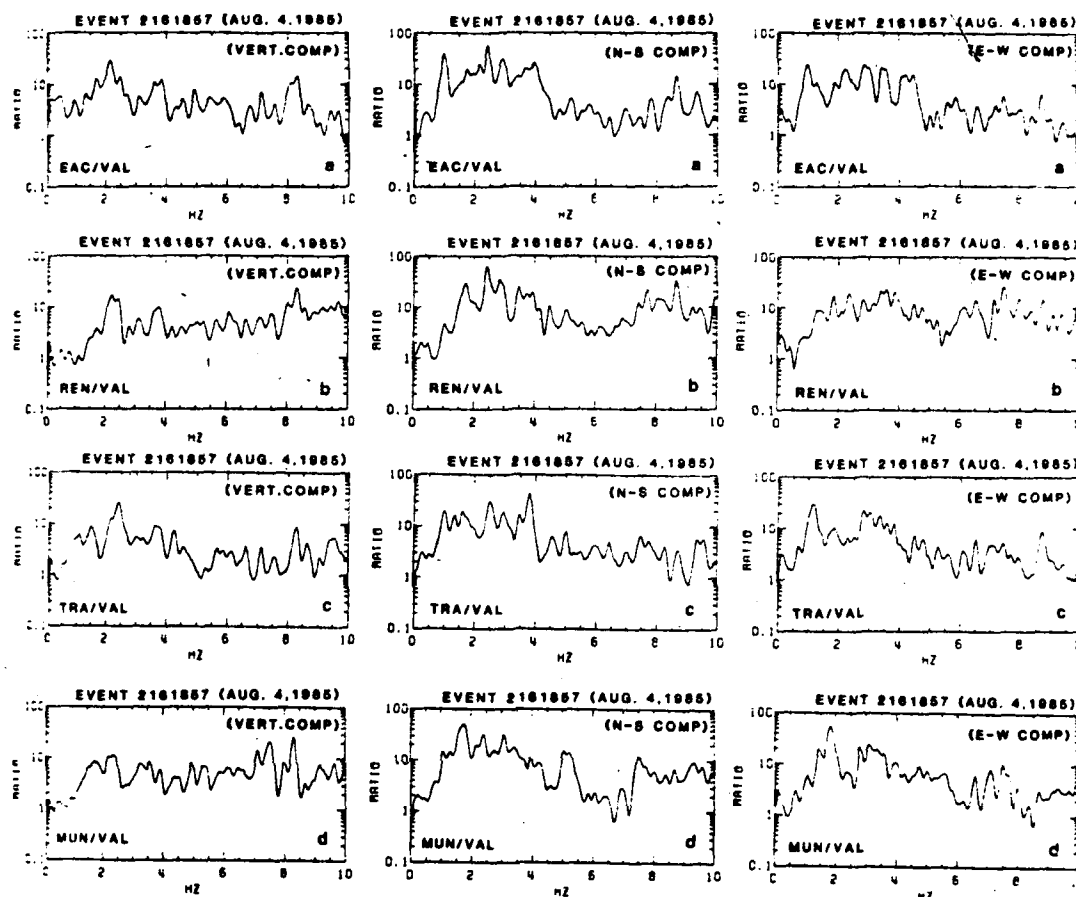


FIG. 17. (a) Spectral ratios of event on 4 August 1985 (Julian 216) at 18:57 UTC for the vertical and horizontal components (N-S and E-W), respectively, of stations EAC/VAL. (b) Spectral ratios of event on 4 August 1985 (Julian 216) at 18:57 UTC for the vertical and horizontal components (N-S and E-W), respectively, of stations REN/VAL. (c) Spectral ratios of event on 4 August 1985 (Julian 216) at 18:57 UTC for the vertical and horizontal components (N-S and E-W), respectively, of stations TRA/VAL. (d) Spectral ratios of event on 4 August 1985 (Julian 216) at 18:57 UTC for the vertical and horizontal components (N-S and E-W), respectively, of stations MUN/VAL.

from the weak-motion as well as the strong-motion data and the response spectra from the strong-motion data indicate the same trend of the frequency-dependent amplification at Viña del Mar with respect to Valparaíso, there is sufficient evidence to indicate that the spectral ratios from weak motions at other localities are valid just as well to identify those frequency ranges for which amplification of motions should be expected during strong-motion events. This point is further justified by the superimposed weak-motion spectral ratios of the ridges (Figure 12) which show good repeatability.

### CONCLUSIONS

The objective of this paper is to demonstrate quantitatively and qualitatively the frequency-dependent amplification at sites with different geology and topography. By using the spectral ratios of motions obtained from aftershocks recorded at ridges and sites of differing geology, it can be asserted that amplification did take place

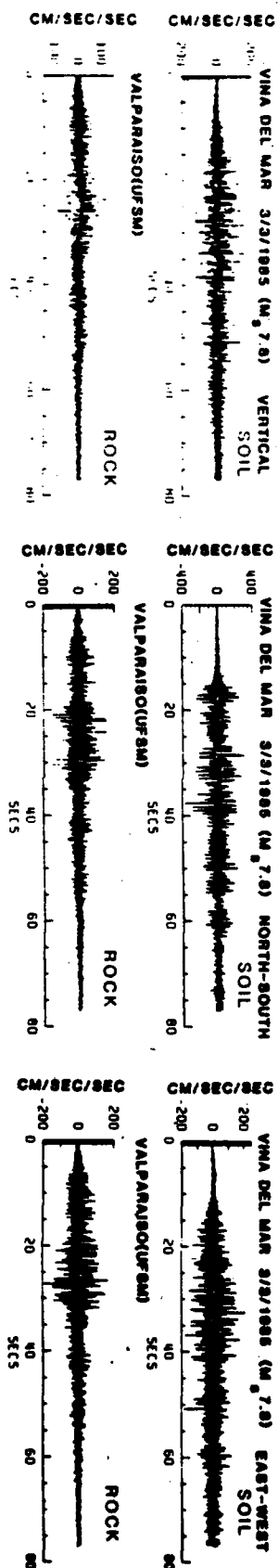


Fig. 18. Acceleration time histories (77 sec duration) and spectral ratios from records of the main event of 3 March 1985 ( $M_s = 7.8$ ) for the vertical and horizontal (N-S and E-W) components, respectively, of stations Vina del Mar and Valparaiso (UFSM). The Valparaiso strong-motion station (rock site) is the same station as the temporary station established (VAL). The Vina del Mar strong-motion station is only one block (approximately 100 m) from the temporary station (MUIN). Comparison of these spectral ratios with those of MUIN/VAL (Figure 17d) qualitatively show amplification, particularly in low frequencies as determined from both strong-motion and weak-motion data.

during the occurrence of aftershocks as well as during the main shock. It must be remembered that observations of distribution of damage to structures on the ridges and at soft soil sites during the main event were the primary reason to look into the problems of amplification of motions in central Chile. This has been accomplished by recording the aftershocks and obtaining the spectral ratios. It is believed

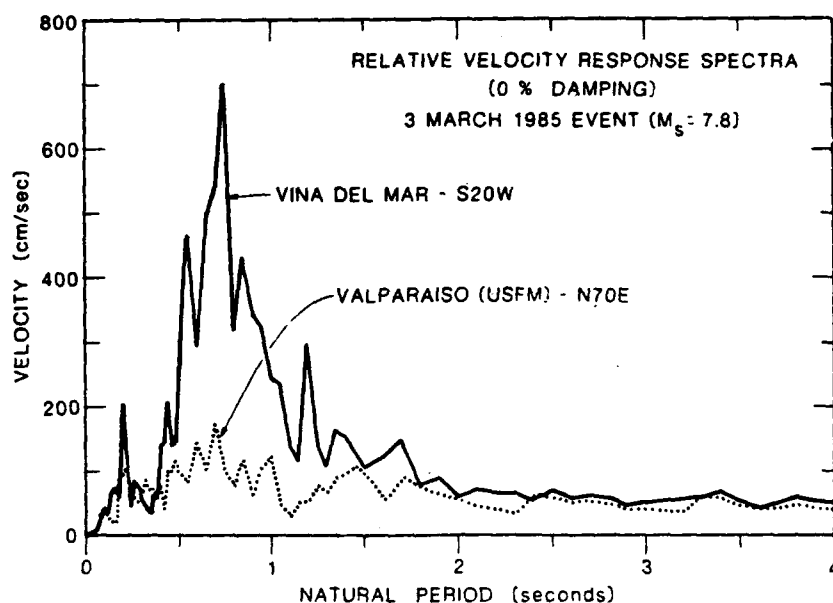


FIG. 19. Relative velocity (horizontal) response spectra (0 per cent damping) of records obtained at Valparaiso (rock site) and Viña del Mar (alluvial site) during the main event of 3 March 1985 ( $M_s = 7.8$ ) (from Saragoni *et al.*, 1985).

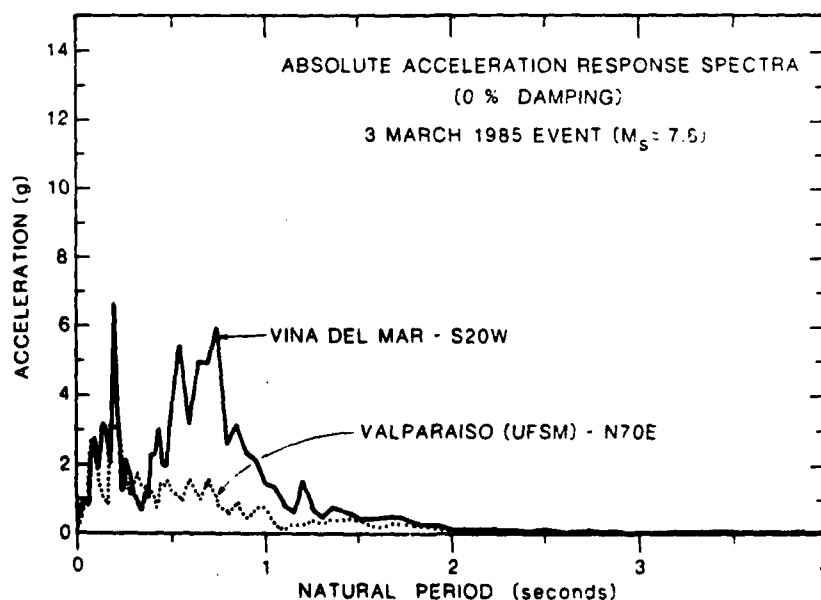


FIG. 20. Absolute acceleration (horizontal) spectra (0 per cent damping) of records obtained at Valparaiso (rock site) and Viña del Mar (alluvial site) during the main event of 3 March 1985 ( $M_s = 7.8$ ) (from Saragoni *et al.*, 1985).

that the spectral ratios presented herein serve the purpose well by qualitatively identifying the frequency ranges for which amplification of motion takes place in different localities of different topography and geology. The user of these results should be careful not to generalize these phenomena to all sites without careful evaluation and correlation with the similarities of the sites in question. Furthermore, the user should always note that while these results can be used to increase seismic design forces in one way or another, it is just as important to provide adequate quality control into the details of design and construction practices. In other words, frequency-dependent amplification, while influencing the performance of structures in central Chile during the 3 March 1985 event, should not be taken as the sole contributor to the damages and destruction experienced and observed.

#### ACKNOWLEDGMENTS

The field work portion of the study presented herein was performed with partial financial support of the Office of Foreign Disaster Assistance of the Agency for International Development. Dr. S. T. Algermissen, U.S. Geological Survey, administered the funding and provided valuable advice and consultation throughout the project. The project was mutually initiated by the Municipality of Viña del Mar and the U.S. Geological Survey. The Mayor of Viña del Mar, Madame Eugenia Garrido, provided invaluable assistance through her offices and her staff, L. F. Baeza, H. Balbontin, and M. Mayo. Professors R. Saragoni and P. Bonelli, respectively, of the University of Chile, Santiago and the University of Santa Maria, Valparaiso, contributed during the several states of discussion and organization of the project. E. Sembera and C. Dietel worked late hours to successfully perform field work. C. Mueller assisted in supervision of data processing using his computer programs, and R. Eis and L. Hollis drafted the majority of the figures. I would also like to express my gratitude to W. Joyner and E. Safak for their helpful review comments. B. Gessner typed several drafts, and C. Sullivan typed the final version of the manuscript.

#### REFERENCES

- Bard, P. Y. and B. E. Tucker (1985). Underground and ridge site effects: a comparison of observation and theory, *Bull. Seism. Soc. Am.* **75**, 905-922.
- Boore, D. M. (1972). A note on the effect of simple topography on seismic SH waves, *Bull. Seism. Soc. Am.* **62**, 275-284.
- Boore, D. M. (1973). The effect of simple topography on seismic waves: implications for the accelerations recorded at Pacoima Dam, San Fernando Valley, California, *Bull. Seism. Soc. Am.* **63**, 1603-1609.
- Borcherdt, R. D., J. B. Fletcher, E. G. Jensen, G. L. Maxwell, E. Cramswick, J. R. VanSchaack, and R. E. Warrick (1985). A General Earthquake Observation System (GEOS), *Bull. Seism. Soc. Am.* **75**, 1783-1825.
- Çelebi, M. (1985). Preliminary evaluations of performance of structures, in *Preliminary Report of Investigations of the Central Chile Earthquake of March 3, 1985*, S. T. Algermissen, Editor, U.S. Geol. Surv., Open-File Rept. 85-542.
- Çelebi, M. (Editor) (1986). Seismic site-response experiments following the March 3, 1985, central Chile earthquake, U.S. Geol. Surv., Open-File Rept. 86-90.
- Davis, L. L. and L. R. West (1983). Observed effects of topography on ground motion, *Bull. Seism. Soc. Am.* **63**, 283-298.
- Donovan, N. (1986). Ground attenuation relationship and response spectra, or do witch doctors know more than we do?, in *Learning from Earthquakes*, Structural Engineers Association of Northern California (from *Seminar Lectures of 1977*), San Francisco, California, 3-26.
- Gibbs, J. F. and R. D. Borcherdt (1974). Effects of local geology on ground motion in the San Francisco Bay region, California—A continued study, U.S. Geol. Surv., Open-File Rept. 74-222.
- Lagorio, H. J. and G. C. Mader (1981). Earthquake in Campania-Basilicata, Italy, November 23, 1983, *Architectural and Planning Aspects*, EERI Publication, July.
- Monge, J. E., et al. (1986). El Sismo de Marzo 1985, Chile, *Special Publication of Acero Comercial S.A.*
- Rogers, A. M., R. D. Borcherdt, P. A. Covington, and D. M. Perkins (1984). A comparative ground response study near Los Angeles using recordings of Nevada nuclear tests and the 1971 San Fernando earthquake, *Bull. Seism. Soc. Am.* **74**, 1925-1949.

- Saragoni, R. H., M. B. Fresard, and S. Gonzalez (1985). Analisis de Los Acelerogramas del Terremoto del 3 de Marzo de 1985, I Parte, in *Publicacion SES 14/1985 (199)*, University of Chile, December.
- Shiga, T. A., A. Shibata, J. Shibuya, and R. Minami (1979). Effects of irregular geophysical features on seismic ground motions, in *The Architectural Reports of the Tohoku University*, Department of Architecture, Tohoku University, Sendai, Japan.
- Wyllie, L., *et al.* (1986). The Chile earthquake of March 3, 1985, in a special issue of *Spectra* (a publication of *EERI*), February.

U.S. GEOLOGICAL SURVEY  
345 MIDDLEFIELD ROAD  
MENLO PARK, CALIFORNIA 94025

Manuscript received 19 June 1986